5
BRAIN-0960
Brain Course

Pursuit of Relevant Preclinical Studies of Stroke in Rodent Models Brain Course

Modeling common stroke morbidities and their impact on stroke outcome

A. Denes[1]
[1]*Laboratory of Neuroimmunology, Institute of Experimental Medicine, Budapest, Hungary*

Common risk factors for stroke such as old age, atherosclerosis, hypertension, diabetes, obesity or infection promote the occurrence of acute cerebrovascular events and impact negatively on outcome. Although the development of vascular diseases usually precedes stroke by several years or decades, mechanisms how these conditions contribute to brain injury are improperly understood. Recent data indicate that stroke comorbidities commonly involve systemic inflammation, which is associated with the development of inflammatory alterations in the brain prior to any acute cerebrovascular event takes place. Experimental data show that immune cells and inflammatory mediators contribute to brain injury after stroke. Dysregulation of systemic inflammatory processes is observed in common risk factors for stroke and elevated systemic inflammatory burden before or after stroke is associated with worse outcome in both patients and experimental models. Recent preclinical studies show that therapeutic blockade of key inflammatory pathways reduces brain injury and improves outcome in comorbid animal models of stroke. One major challenge is to establish appropriate animal models that allow the understanding of how inflammatory mechanisms and vascular risk factors contribute to stroke outcome and translate these results to clinical benefit. In spite of the good representation of disease mechanisms by several animal models of comorbidities, their limitations must be understood. Development of new imaging technologies, transgenic models, and appropriate biomarkers will greatly improve the translational value of preclinical models in brain diseases.

6
BRAIN-0979
Brain Course

Pursuit of Relevant Preclinical Studies of Stroke in Rodent Models Brain Course

Design and interpretation of appropriate behavioral analysis

D. Corbett[1]
[1]*Cellular & Molecular Medicine, University of Ottawa, Ottawa, Canada*

BEHAVIOURAL OUTCOME MEASURES IN PRECLINICAL MODELS OF STROKE-PITFALLS IN EXPERIMENTAL DESIGN AND DATA INTERPRETATION

While animal models of stroke will never perfectly capture all the elements of the human condition it is essential that key clinical features be incorporated wherever possible. For example, animal models should reflect the most common brain regions and relative injury sizes that are observed clinically. Knowledge about the fundamental characteristics of human stroke (e.g. specific functional deficits, chronicity of impairments, etc.) should be part of new investigators' training prior to designing experiments. For these reasons, this workshop will emphasize a “bedside to bench” approach instead of the universal “bench to bedside” line of thinking that characterizes and undoubtedly hampers current preclinical stroke research.

The first question to be addressed is: What is one trying to model? When using rodent stroke models it seems obvious that the model should be relevant to the clinical problem being investigated but this is often not the case. Accordingly, a brief but critical review of commonly used rat and mouse stroke models will be presented highlighting the similarity and differences to stroke in humans.

While histological outcome measures (e.g. infarct volumes and cell counts) provide valuable information, behaviour is the most important clinical outcome measure. Consequently, investigators need to select a battery of tests that are not simply convenient or easy, but instead appropriate for the specific type of stroke being modeled. The time

course of injury progression is an important variable that can affect interpretation of both neuroprotective or neurorecovery interventions. The choice of behavioural tests can ultimately determine the "apparent" level of neuroprotection or functional recovery so a number of widely used sensory-motor and cognitive tests will be discussed and critically evaluated with regard to their sensitivity and relevance to human stroke. Differences in the timing and repetition of behavioural testing can also markedly affect outcome and illustrative examples will be provided. Special consideration will be given to use of appropriate control groups used to assess new treatments. Another issue of considerable importance is the extent to which improvement in post-stroke performance reflects true recovery or instead is partly or entirely the result of compensatory strategies.

At the conclusion of the workshop attendees will have acquired new knowledge that will help them approach and design more thoughtful and valid experiments that better mimic the clinical condition of interest. In so doing, there is a greater likelihood that results from the laboratory will be successfully translated to the clinic.

11
BRAIN-0983
Brain Course

CBF/Neurovascular Unit Brain Course

Neurogenic and astrogliogenic perturbation of local CBF

K. Masamoto[1], *I. Kanno*[2]
[1]*Brain Science Inspired Life Support Research Center, Univ. of Electro-Communications, Tokyo, Japan*
[2]*Molecular Imaging Center, National Institute of Radiological Sciences, Chiba, Japan*

Cerebral blood flow (CBF) is maintained globally at constant, whereas local blood velocity and volume in cerebral microcirculation was found to fluctuate continuously. The cerebral microcirculation is maintained by regional interactions between vascular cells (i.e., vascular endothelial cells, pericytes, and smooth muscle cells) and brain cells (i.e., neurons and glial cells). In this talk, we will focus on the role of the neurons and astrocytes on a perturbation of the cerebral microcirculation. First, we study the anatomical features of the cellular communications between the vascular and brain cells. Because the neurons and astrocytes reside with variable densities across the cortical layers and areas, this causes a region-dependent variation in the vascular actions. Secondly, we look at the mode of transmission from the neurons/astrocytes to the vascular cells, including a diffusion process of transmitters and mediators. Those signaling mode confines a spatial extent of the blood velocity/volume changes and their propagations. Finally, we examine the vascular targets via neurogenic and astrogliogenic perturbations, and discuss the importance of the dual control of local CBF in view of the pathogenesis of neurodegenerative disorders.

12
BRAIN-0975
Brain Course

CBF/Neurovascular Unit Brain Course

Quantitative optogenetic interaction

A. Vazquez[1]
[1]*Radiology, University of Pittsburgh, Pittsburgh, USA*

Optogenetics has emerged as a powerful tool to precisely modulate neuronal activity. This course will describe technical and physiological considerations for the investigation and quantification of neuro-vascular (and neuro-metabolic) interactions using optogenetic approaches. The advantages and disadvantages of several different optogenetic models that target Channelrhodopsin expression in cortical neurons will be discussed. Quantification of spatial and temporal neuro-vascular relationships will be discussed as well. Finally, a summary of important findings and frontiers will be overviewed.

13
BRAIN-0966
Brain Course

CBF/Neurovascular Unit Brain Course

Metabolic balance of neurons, glia, and vessels

S. Takahashi[1]
[1]*Department of Neurology,*
Keio University School of Medicine, Tokyo, Japan

Astroglia play a pivotal role in the brain metabolism as well as in the regulation of cerebral blood flow. In particular, the astroglial metabolic compartment exerts supportive roles in making neurons dedicated to generating action potentials and protects them against oxidative stress associated with high energy consumption. Thus, the metabolic responses of the astroglia in the normal physiological state would possibly be neuro-protective. Under ischemia, numerous metabolic derangements occur, resulting in irreversible neuronal damage. The neurovascular unit (NVU) is a conceptual framework used to better understand the pathophysiology of cerebral ischemia. The major components of the NVU are neurons, microvessels and the astroglia that are interposed between the neuronal synapses and the microvasculature. Therefore, the metabolic responses of the astroglia in the early stage of ischemia could be either protective or deleterious. In this review, I focus on three major metabolic compartments: the 1) glucose, 2) fatty acid and 3) amino acid, especially D-/L-serine, compartments. Both the beneficial and detrimental roles of the metabolic responses induced in the astroglia will be discussed. A better understanding of the astroglial metabolic response in normal physiological state may be expected to lead to the development of a novel strategy in stroke therapy.

References:

Takahashi S, et al: Roles and regulation of ketogenesis in cultured astroglia and neurons under hypoxia and hypoglycemia. ASN Neuro.2014;6(5). pii: 1759091414550997.

Abe T, et al: Cellular origin and regulation of D- and L-serine in in vitro and in vivo models of cerebral ischemia. J Cereb Blood Flow Metab. 2014;34(12):1928-35.

Takahashi S, et al: Roles of metabolic compartmentalization by astrocytes and neurons in the pathophysiology and treatment of Parkinson's disease. Brain Nerve. 2013;65(12):1497-508.

Takahashi S, et al: Astroglial pentose phosphate pathway rates in response to high-glucose environments. ASN Neuro. 2012 Mar 22;4(2).pii: e00078.

Takahashi S, et al: Astrogliopathy as a loss of astroglial protective function against glycoxidative stress under hyperglycemia. Rinsho Shinkeigaku. 2012;52(1):41-51.

16
BRAIN-0953
BrainPET Course

Morning Session: Basics of PET Imaging BrainPET Course

Fundamentals of the PET signal: Scanners, signal detection & reconstruction

R. Boellaard[1]
[1]*Radiology & Nuclear Medicine,*
VU University Medical Centre, Amsterdam, Netherlands

PET is a molecular imaging technique allowing to quantitatively measure the distribution of a molecule (radiotracer) labelled with a positron emitting isotope, such as ^{18}F, ^{11}C or ^{15}O. By using different radiotracers information on various molecular or functional processes can be obtained, such as (changes in) receptor density, metabolism or perfusion.
PET is based on the simultaneous detection of 2 annihilation photons that are generated upon emission of a positron (from the radiotracer). The positron travels a short distance (a few mm) in tissue and, when its kinetic energy is sufficiently reduced, annihilates with an electron thereby generating two 511 keV photons that are emitted in (near) opposite

directions. A PET system consists of thousands small detectors allowing to detect these photons. When these 2 photons are detected simultaneously, i.e. typically within 4 to 6 ns, the PET systems registers a coincidence detection. The line connecting these 2 detectors is called a line of response (LOR). However, some of the emitted photons may be deflected from its original direction due to (Compton) scatter resulting in a dislocation of the LOR. In addition, 2 photons from uncorrelated positron emissions at different locations may be detected at the same time as well. This so-called accidental or random coincidence detection is an invalid LOR and should be corrected for. Finally, the patient itself attenuates the emitted photons. As a consequence only a few percent of all positron emissions are being detected. In order to quantitatively measure the distribution of the radiotracer *in vivo* accurately, corrections for randoms, scatter and attenuation need to be applied.
Upon data collection all coincidences are stored in list mode or sinograms and represent the projection data. The projection data are then reconstructed into an image representing the activity (radiotracer) distribution in the patient. Corrections for randoms, scatter and attenuation are applied during this process. Various different reconstruction methods are available such as filtered back projection and various iterative methods. In addition, during image reconstruction time of flight information and the PET system resolution characteristics can be included to enhance the quality of the reconstructed PET image. During this presentation the principles of positron emission tomography (PET) data acquisition and image reconstruction will be addressed and the impact of acquisition and reconstruction settings on image quality will be discussed.

17
BRAIN-0958
BrainPET Course

Morning Session: Basics of PET Imaging BrainPET Course

Fundamentals of PET radiochemistry: Radionuclides, radiolabeling techniques, and radioligand synthesis

C. Halldin[1]
[1]*Department of Clinical Neuroscience, Karolinska Institute, Stockholm, Sweden*

PET provides a new way to image the function of a target in a translational way from mouse to man, and by elevating the mass, to pharmacologically modify the function of the target. The main applications of radioligands in brain research concern human neuropsychopharmacology and the discovery and development of novel drugs to be used in the therapy of psychiatric and neurological disorders. A basic problem in the discovery and development of novel drugs is the absence of relevant *in vitro* or *in vivo* animal models that can yield results to be extrapolated to man. Unlike MRI or CT which mainly provide details about the anatomy, PET can measure chemical changes that occur before macroscopic anatomical indications of a disease may be observed. A basic problem in PET brain receptor studies is the lack of useful radioligands with ideal binding characteristics.

Prerequisite criteria,such as high affinity and selectivity etc, need to be satisfied for a radioligand to reveal target binding sites *in vivo*. Molecular biological techniques have now revealed the existence of hundreds of novel targets for which little or no prior pharmacological or functional data existed. The development of synthetic strategies for the synthesis of novel positron-emitting molecules is, however, not trivial. This talk review key aspects of radionuclides, radiolabeling strategies, and radioligand synthesis of PET radioligands with short-lived positron emitting radionuclides such as carbon-11 and fluorine-18 with emphasis both on classical but also the most recent labeling strategies.

19
BRAIN-0987
BrainPET Course

Morning Session: Basics of PET Imaging BrainPET Course

Quantification of PET signal: Biological parameters derived from the physical signal

E. Morris[1]
[1]*Yale University PET Center,*
Yale University PET Center, New Haven CT, USA

This presentation will introduce basic concepts underlying quantitative analysis of PET data. It will explain the standard study endpoints for receptor-ligand imaging and compare the standard study designs that produce those endpoints. The endpoints are physiological parameters of interest. Unavoidable ambiguities in interpretation of the common endpoints will be discussed. The presentation will develop modeling and analysis concepts in qualitative but intuitive ways. It will conclude with designs and results of different study types drawing examples from ongoing receptor-imaging studies of addiction and cancer at the Yale PET Center.

PET is a powerful high resolution *in vivo* imaging technique with unparalleled molecular specificity. The high resolution owes much to the physics of PET and the specificity derives from PET chemistry. But the full power of PET would remain unrealized were it not for proper kinetic modeling of the emission images to yield “images of physiology”.

The talk is appropriate for anyone who has struggled to read a PET paper, contemplated acquiring some PET data of their own … or seeks greater insight into the data they already have.

22
BRAIN-0959
Brain Course

Optogenetics Brain Course

Optogenetic agents introduction and application for studies of sleep

A. Adamantidis[1]
[1]*Dept of Neurology, University of bern, Bern, Switzerland*

While the functions of sleep are still a matter of debate and may include memory consolidation and plasticity, the neural substrates of sleep and wake states are the subject of intense study. Successive sleep-wake cycles rely on an appropriate balance between sleep-promoting nuclei of the brain located in the anterior hypothalamus and, arousal-promoting nuclei from the posterior hypothalamus and the brainstem including the dopamine, norepinephrine, serotonin systems. We have investigated some of the neural substrates of arousal and REM sleep using a combination of electrophysiology and optogenetics in freely-moving mice. We recently demonstrated that a subset of hypothalamic cells expressing the peptide melanin-concentrating hormone (MCH) are both sufficient for the induction of rapid-eye movement (REM) sleep (or paradoxical sleep), and required for theta rhythm stability during REM sleep. We further identified a subset of inhibitory cells from the same hypothalamus area that directly control the activity of the reticular thalamus nuclei and induce arousal through feed-forward disinhibition of thalami-cortical loop during NREM, but not REM sleep. This lecture will present these recent work and proposed an integrated model of hypothalamic regulation of sleep-wake states, as well as consciousness.

23
BRAIN-0972
Brain Course

Optogenetics Brain Course

Recombinant sensor development for the neurovascular unit, second messenger and calcium dependent reporters

R. Srinivasan[1], A.D. Johnston[1], H. Chai[1], B.S. Khakh[1]
[1]Physiology, University of California Los Angeles, Los Angeles, USA

Intracellular Ca^{2+} signaling is considered important for multiple astrocyte functions in neural circuits. However, resolving role(s) of astrocyte calcium signaling in the CNS will require a more complete morphological and functional description of astrocyte signals in brain slices and *in vivo*. To address this issue, we developed a set of sensitive tools that can report calcium signals with high spatial and temporal precision. Our tools include: (1) newly engineered adeno-associated viruses (AAVs) expressing the latest genetically encoded calcium indicator (GECI), GCaMP6f, under control of an astrocyte-specific promoter, $GfaABC_1D$, (2) a semi-automated image analysis program, GECIquant, that can demarcate and quantify a large number of calcium signals with subcellular resolution and (3) confocal and 2-photon imaging methods to study astrocyte function in live brain slices and *in vivo*.

We employed our tools and techniques to address an unresolved question in the field. Mice devoid of inositol triphosphate type 2 receptors (IP3R2) reportedly lack all astrocyte Ca^{2+} signals, but display no behavioral, neuronal or neurovascular deficits, implying that astrocyte Ca^{2+} signals play no role(s) in these processes. An invariable assumption has been that loss of somatic Ca^{2+} signals also reflects similar loss in astrocyte territories. We tested this assumption using our newly developed tools and found diverse types of Ca^{2+} signals within astrocytes, with most signals occurring within processes rather than in somata. These signals were preserved in $IP3R2^{-/-}$ mice in brain slices and *in vivo,* were increased by G-protein-coupled receptor activation and by startle-induced neuromodulatory responses. In addition, we identified in astrocyte territories a delayed Ca^{2+} response to *in vivo* startle that was independent of both IP3R2- and GPCR-mediated pathways. Our data revealed enduring novel Ca^{2+} signals within astrocyte territories and highlight limitations of studies that used $IP3R2^{-/-}$ mice to evaluate astrocyte contributions to neural circuit function and plasticity.

We have recently expanded our tools to include knock in mice with a loxP flanked STOP cassette that will drive GCaMP6f or membrane targeted Lck-GCaMP6f in an inducible manner when the mice are crossed with appropriate mouse lines expressing cre recombinase. Double transgenic mice derived from crosses of knock in and Cre/ERT2 mouse lines enabled us to study and directly compare astrocyte calcium signals from multiple brain regions.

Funding: Supported by NINDS and NIMH

28
BRAIN-0971
Brain Course

miRNA in Brain Injury and Repair Brain Course

miRNA and ischemic neuroprotection

R. Giffard[1], Y. Ouyang[1], X. Sun[1], X. Xiong[2], L. Xu[1]
[1]Anesthesiology, Stanford University, Palo Alto, USA
[2]Neurosurgery, Stanford University, Palo Alto, USA

ALTERING microRNA LEVELS AS A WAY TO PROTECT FROM STROKE AND FOREBRAIN ISCHEMIA

Objectives: Stroke is a major cause of death and long term neurological disability world wide. Despite many years of research, the development of effective clinical treatments other than thrombolysis has been elusive. Similarly, brain injury induced by cardiac arrest also has few treatment options. miRNA are now appreciated to play a role in ischemic brain injury, as well as in normal brain function and the immune response. One important aspect of the regulation of gene expression by miRNAs is that a single miRNA may target multiple mRNAs and thus reduce expression of multiple proteins. Further, in the progression of stroke and recovery, it is likely that different miRNAs may be relevant at different times. We altered levels of miRNAs and tested whether

altering levels of individual miRNAs could alter the outcome from stroke or forebrain ischemia using rodent models.

Methods: The mouse model of transient middle cerebral artery occlusion (MCAO) was used (1), and outcome evaluated by assessment of infarct volume using TTC or cresyl violet staining, and neuroscore. For animals allowed to survive to 1 month, rotarod was used to assess outcome (2). For forebrain ischemia a rat model of transient bilateral carotid occlusion and hypotension was used (3). Immunohistological staining was performed to evaluate expression of relevant proteins and identify cells. Alteration of miRNA levels was achieved using commercially available mimic, inhibitor and antagomir, administered intracerebroventricularly or intravenously. RT-qPCR wa used to evaluate levels of miRNA and mRNA.

Results: We investigated the effects of several different miRNAs. miR-181 contributes to injury, and reducing levels of miR-181 were protective, when lowered prior to MCAO or prior to forebrain ischemia. Pretreatment resulted in reduced infarct size and improved neuroscore. We also tested the effect of reducing miR-181a levels after focal ischemia, and found this could still reduce infarct volume at 24 hr reperfusion, and this treatment resulted in long lasting improvement in rotarod performance out to 1 month. There are multiple potential targets of miR-181 that might be relevant to ischemic outcome. We validated Bcl-2, XIAP with post-treatment, and GRP78 and Bcl-2 with pretreatment. Astrocytes are known to play a central role in forebrain ischemia, and increasing miR29, a miRNA known to be highly expressed in astrocytes, provided protection from forebrain ischemia (4).

Conclusions: It is possible to both increase and decrease miRNA levels in brain. Depending on the target of the miRNA, appropriate changes can lead to protection, which can be long lasting. Due to their ability to target multiple mRNAs the prospect for developing new treatments for stroke that may be effects, both early and late, is an exciting possibility.

References:

1. Ouyang YB, et al. *Neurobiology of Disease* 45: 555–563, 2012.

2. Xu LJ, et al. *Experimental Neurology* 264: 1-7, 2015.

3. Moon JM, et al. *Journal of Cerebral Blood Flow and Metabolism,* 33(12): 1976-82, 2013.

4. Ouyang YB, et al. *Glia,* 61(11):1784-1794, 2013

29
BRAIN-0951
Brain Course

miRNA in Brain Injury and Repair Brain Course

lnc RNA

R. Vemuganti[1]
[1]*Neurological Surgery,*
University of Wisconsin School of Medicine and Public Health, Madison, USA

By definition, a non-coding RNA (ncRNA) is a functional RNA molecule that is not translated into a protein. In mammals, >98% of the RNAs transcribed are ncRNAs that belong to many functional classes. The ncRNAs can be small (~20 nucleotides; e.g. microRNAs) to very big (~10,000 nucleotides; e.g. long noncoding RNAs). The precise functional significance of various classes of ncRNAs is still being evaluated, but many of them are thought to regulate chromatin function, transcription and translation to maintain genome fitness and function. CNS is known to have a very high level of ncRNA expression that might be essential for maintaining the complex brain functions. Many recent studies show that chronic and acute insults to CNS alter the expression profiles of ncRNAs with functional impact on the disease outcome. Emerging evidence also indicate that modulation of ncRNAs can be therapeutically beneficial. The long non-coding RNAs (lncRNAs; lincRNAs) have recently emerged as one of the epigenetic modulators of cells under physiological and pathological conditions. These gigantic RNAs (typically ~1-10 kB) are expressed through development and adulthood in a stage and cell-

specific manner. Several recent studies have suggested that lncRNAs may provide a missing link between DNA, histones and chromatin modifying proteins (CMPs), either acting as structural scaffolding or directly recruiting epigenetic factors to chromatin. LncRNAs have been shown to interact with a litany of epigenetic factors, including the polycomb repressive complex 2 (PRC2), heterogeneous nuclear ribonucleoprotein K (hnRNP-K), lysine (K)-specific demethylase and euchromatic histone-lysine N-methyltransferase-2 and thus regulate the epigenetic processes such as chromatin remodeling and chromosome inactivation. The basis of lncRNA action, however, remains poorly understood at the molecular level. Perturbations in lncRNA expression have been implicated in a variety of human diseases including Alzheimer's disease, myocardial infarction and multiple forms of cancer. However, very little is known about the dynamics of lncRNAs following acute insults to the CNS. Recent studies showed that the expression profiles of cerebral lncRNAs are altered temporally after stroke. In this lecture, I will discuss the functional significance and mechanism of action of certain lncRNAs in post-stroke pathophysiology. I will then give examples and modalities of how to use them to design and test lncRNA-based therapies for minimizing post-stroke brain damage.

30
BRAIN-0991
Brain Course

miRNA in Brain Injury and Repair Brain Course

miRNA and AVM

G. Yang[1]
[1]*Neuroscience and Neuroengineering Research Center , Med-X Research Institute and School of Biomedical Engineering Shanghai Jiao Tong University, Shanghai, China*

Small noncoding microRNAs play critical roles in biological and pathological processes including human brain arteriovenous malformations (BAVMs). In this course, BAVM associated microRNAs regulated downstream mRNAs and proteins were explored. We established microRNA profile in human BAVM tissue and circulating blood. We discussed the difference of microRNAs expression between BAVM and the brain vascular tumor. Using BAVM smooth muscle cells, we further showed how microRNAs regulate the BAVM smooth muscle cell proliferation, migration and tube-formation. This information provided valuable clue on the identification of microRNAs function in cerebrovascular pathologic processes.

31
BRAIN-0952
Brain Course

miRNA in Brain Injury and Repair Brain Course

Treatment of stroke and Neural Injury with Exosomes and miRNA cargo

M. Chopp[1]
[1]*Neurology, Henry Ford Health System, Detroit, USA*

Traditionally, treatment of neural injury (e.g. stroke, traumatic brain injury neurodegenerative disease) has focused on reduction of the lesion, with, as of now, little translational benefit to humans. A more effective and viable translational approach for the effective treatment of neural injury may reside in stimulating and amplifying endogenous restorative mechanism. Thus, we redirect the focus of therapy from the lesion (i.e. neuroprotection) to the intact central nervous system (CNS) (neurorestoration), to remodel the CNS. In this presentation, data will be presented illustrating robust post neural injury plasticity, and coupling of neurovascular restorative processes. I will describe ways by which we may amplify these processes by both cellular and pharmacological means to promote neurological recovery. Molecular underpinnings of these restorative events will be described, e.g., where the developmental morphogen, sonic hedgehog (Shh) is activated by effective neurorestorative treatments of neural injury. Delving deeper into the molecular targets of recovery, I discuss how restorative therapies, such as cell-based therapies, which amplify neurological recovery and stimulate remodeling of tissues, communicate with and alter their environment. I will describe the essential roles of microRNAs, master molecular switches-that regulate gene translation and subsequently many biological processes, in promoting neurological recovery. I will demonstrate that stem-like cells act as "factories" to

produce tiny lipid particles, exosomes (~40-100nm). Exosomes encapsulate proteins, mRNAs, and miRNAs within. Stem-like cells, and many others, generate these exosomes, and thereby transfer key genetic regulatory instructions to tissue adjacent to and remote from the administered stem cells. These exosomes may be employed without their mother-cells as a monotherapy for the treatment of stroke and neural injury. In addition, I will describe how the cargo of the cell generated exosomes may be tailored to contain specific miRNA to promote neurite outgrowth. This exosome/miRNA communication network underlies a vast arena of biological processes and may be employed to promote recovery post stroke and neural injury.

36
BRAIN-0963
BrainPET Course

Afternoon Session: Applications of PET Imaging
BrainPET Course - Contd.

Positron Emission Tomography of Human Brain can Monitor Neuroinflammation and cAMP Signaling: Applications to Alzheimer's Disease and Depression

R. Innis[1]
[1]*Chief Molecular Imaging Branch NIMH, NIH, Bathesda, USA*

Positron Emission Tomography of Human Brain can Monitor Neuroinflammation and cAMP Signaling: Applications to Alzheimer's Disease and Depression

I will overview studies in my laboratory on two targets: 1) translocator protein (TSPO), a putative marker of neuroinflammation and 2) phosphodiesterase4 (PDE4), the major enzyme in brain to metabolize the second messenger cAMP.

TSPO. We developed the PET radioligand [^{11}C]PBR28, which has high affinity and high specific binding to TSPO. Increased uptake of the radioligand can identify localized areas of inflammation in human brain associated with stroke, epilepsy, and neurocysticercosis, a worm infection of the brain. We recently found that patients with Alzheimer's disease, but not those with the precursor syndrome of mild cognitive impairment, have globally increased uptake of this radioligand. In contrast to the amount of amyloid in brain, the brain uptake of this marker of neuroinflammation correlated with disease severity. This radioligand can now be used in longitudinal studies to examine the pathophysiological role of neuroinflammation in Alzheimer's disease. Expressed more simply, does neuroinflammation cause the conversion from mild cognitive impairment to Alzheimer's disease?

PDE4. The second part of my talk will review PET imaging of PDE4 using [^{11}C]rolipram. The purposes were to examine the "cAMP theory of depression" (i.e., cAMP signaling is decreased in depression) and the "cAMP theory of antidepressants" (i.e., that numerous antidepressant treatments upregulate cAMP signaling after several weeks of administration). In fact, our published study in unmedicated depressed patients showed decreased radioligand binding, consistent with decreased signaling via cAMP cascade. In addition, an interim analysis of an on-going study shows that antidepressants reverse this downregulation.

38
BRAIN-0990
BrainPET Course

Afternoon Session: Applications of PET Imaging
BrainPET Course - Contd.

Application of PET imaging in CNS drug development

R. Gunn[1]
[1]*Imaging, Imanova Ltd, London, United Kingdom*

The discovery and development of central nervous system (CNS) drugs is a complex task that requires large investments of time and money with no guarantee of success. Currently it is estimated that it costs around $2 billion to bring each successful drug to market. Imaging techniques, such as positron emission tomography (PET), can provide important information by taking direct biological measurements in tissues of interest in preclinical and clinical species in vivo. These measurements can be divided into three types:

1. Biodistribution - Direct radiolabelling of the drug candidate itself with a positron emitter does not

change the properties of the drug and allows for direct measurements of the drugs concentration in tissues of interest. These studies can provide confidence that the drug is crossing the blood brain barrier in humans.

2. Target Engagement - Radiolabelling of the drug target with a probe that provides a specific signal allows for the assessment of whether a cold drug candidate interacts with the target. Such studies, often referred to as occupancy studies, provide valuable information on dose selection early in Phase 1.

3. Measuring Downstream Responses – By employing radiolabelled probes that directly measure physiological or biochemical processes, it is possible measured to measure the downstream impact of drugs on these key biological processes in the body.

48
BRAIN-0968
Special Symposium

Presidential Symposium

Bright and dark sides of innate immunity in stroke and dementia

C. Iadecola[1]
[1]*Brain and Mind Research Institute, Weill Cornell Medical College, New York, USA*

Owing to the blood-brain barrier,the brain was traditionally considered an “immune privileged” organ, nearly impenetrableto immune cells. However, a growing body of evidence indicates that cells ofthe immune system traffic in and out of the brain, and, while preserving brainhealth in the normal state, they can also cause brain damage in disease. Thislecture will highlight these double-edged roles of the immune system in twomajor brain diseases: stroke and dementia. Whereas innate and adaptive immunitycontribute to the acute phase of the tissue damage associated with experimentalcerebral ischemia, immune cells protect the brain from impending damage inmodels of preconditioning, and contribute to tissue repair in the late phasesof ischemic injury. In addition, immune cells play a critical role in conditionsassociated with cognitive impairment, such as Alzheimer’s disease and vasculardementia. Thus, innate immunity cells and their receptors contribute to the neurovasculardysfunction associated with amyloid-beta, a key pathogenic factor inAlzheimer’s disease, or with hypertension, a major risk factor for vascularcognitive impairment. The realization that the immune system is critically involvedin the pathobiology of major brain diseases, provides the opportunity tomodulate immune function to reset the balance between its detrimental andbeneficial effects on the brain, and to develop new approaches for thetreatment of stroke and dementia.

51
BRAIN-0973
Symposium

Signaling mechanisms in local control of cerebral blood flow

Role of astrocyte in cerebral autoregulation

J. Filosa[1], *K.J. Kim*[1], *J.A. Iddings*[1], *J.E. Stern*[1], *S.A. Kirov*[2], *V.M. Blanco*[3], *D. Croom*[2]
[1]*Physiology, Georgia Regents University, Augusta, USA*
[2]*Brain and Behavior Discovery Institute, Georgia Regents University, Augusta, USA*
[3]*Internal Medicine, University of Cincinnati, Cincinnati, USA*

Basal and activity-dependent cerebral blood flow changes are tightly coordinated by processes including cerebral autoregulation, endothelial-mediated signaling and neurovascular coupling. The cellular mechanisms underlying these events are incompletely understood. Objectives: The aim of our study was to determine astrocytes contribution to flow/pressure-evoked changes in parenchymal arteriole (PA) vascular tone. Methods: Astrocyte contribution to cortical PA vascular responses was measured using an *in vitro* rat/mouse brain slice model of perfused/pressurized PA in combination with confocal astrocyte Ca^{2+} imaging. *In vitro,* PA diameter changes were measured following increased in lumen flow rate (and concomitant increases in pressure). Astrocyte Ca^{2+} responses to flow/pressure-evoked changes in vascular

reactivity were measured in brain slices loaded with the Ca^{2+} indicator dye Fluo4. Astrocyte responses to changes in systemic arterial pressure were corroborated *in vivo* following a tail vein injection of phenylephrine. Results: By measuring concomitant changes in vascular smooth muscle cell and astrocytic Ca^{2+} activity in brain slices, we demonstrate that astrocytes are activated by flow/pressure-evoked changes PA diameter changes. Increased PA lumen flow/pressure constricted arterioles by ~20% from baseline. Flow/pressure-evoked changes in vascular diameter were followed by an increased in astrocytic Ca^{2+} activity. While the magnitude of the flow/pressure-evoked PA vasoconstriction was unchanged, when the astrocytic syncytium was loaded with Ca^{2+} chelator BAPTA, a significant decreased in the maintenance of PA vascular tone was observed suggesting astrocytes contribute to the sustained component of PA myogenic responses. While the cellular mechanisms underlying vessel-to-astrocyte signaling are yet to be determined we found expression of mechanosensitive TRPV4 channels to be restricted to astrocytic endfeet processes and not PA endothelial cells. Furthermore, we showed that bath application of the TRPV4 channel blocker HC067047 significantly blunted flow/pressure-evoked vasoconstriction and diminished flow/pressure-evoked astrocyte Ca^{2+} increases. Corroborating these findings, studies conducted in $TRPV4^{-/-}$ mice also resulted in diminished flow/pressure evoked astrocyte Ca^{2+} responses both *in vivo* and *in vitro*. Conclusions: Taken together, our results support a novel bidirectional signaling modality within the neurovascular unit in which the astrocyte serves as a mechanosensory system to dynamically modulate steady-state vascular responses. References: Kim, KJ., Iddings, JA., Stern, JE., Blanco, V.M., Kirov, SA., Croom, D., Filosa, JA. Astrocyte contribution to flow/pressure-evoked parenchymal arteriole vasoconstriction. ***Journal of Neuroscience*** (*In press*.)

52
BRAIN-0012
Symposium

Signaling mechanisms in local control of cerebral blood flow

Cerebral blood flow modulation can occur independently of large cytosolic Ca2+ signaling in astrocytes

H. Hirase[1]
[1]*Brain Science Institute, RIKEN, Wakoshi, Japan*

Activation of the nucleus basalis of Meynert (NBM), the primary source of cholinergic projection to the cerebral cortex, has been reported to cause significant changes in cerebral cortical blood flow (CBF) in rodents. The NBM-driven increase of CBF has been described to be dependent in part on muscarinic acetylcholine receptors (mAChRs). Lately, several groups reported that astrocytes modulate local CBF via intracellular Ca^{2+} signaling. Considering that cortical astrocytes express mAChRs and *in vivo* activation of NBM leads to mAChR-dependent Ca^{2+} surges in astrocytes, cholinergic modulation of CBF via astrocytic Ca^{2+} surges is conceivable. We find that a brief stimulation of the NBM induces a biphasic CBF response as measured by laser Doppler flowmetry in the somatosensory cortex of C57BL/6J mice. This response consists of a rapid increase, followed by an overshooting slower decrease that goes back to baseline within a minute. The stNBM-induced CBF response was sensitive to the mAChR antagonist atropine. Surprisingly, we find that IP_3R2 knockout mice, which lack cytosolic Ca^{2+} surges in astrocytes, show a similar CBF response to stNBM. Moreover, whisker stimulation resulted in similar degrees of CBF increase in IP_3R2 knockout mice and the background strain C57BL/6J. Our results show that neural activity-driven CBF modulation can occur without large cytosolic Ca^{2+} increases in astrocytes. We are currently investigating cerebral vessel diameter change in response to optical activation of G-protein

53
BRAIN-0989
Symposium

Signaling mechanisms in local control of cerebral blood flow

The basis of vascular reactions during spreading depression and astroglial calcium waves

L. Khennouf[1], J. Fordsmann[1], C. Cai[1], A. Brazhe[1], C. Mathiesen[1], B.V. Gesslein[1], I. Søndergaard Rasmussen[1], K. Kucharz[1]
[1]Neuroscience and Pharmacology, Panum University of Copenhagen, Copenhagen, Denmark

Cortical spreading depression (CSD) is a transient depolarization wave that pervades cerebral grey matter. CSD is associated with large scale changes of cerebral blood flow (CBF) and oxygen consumption ($CMRO_2$) and followed by prolonged reduction in CBF accompanied by persistent rise in $CMRO_2$. The overall decrease of vascular reactivity after CSD explains in part the accompanying impairment of neurovascular coupling. Numerous factors contribute to the rise in CBF during the initial 1-2 minutes of CSD and it is unclear whether a single substance plays a key role. After CSD, the vasoconstrictor 20-HETE accumulates and blockade of 20-HETE synthesis ameliorates the hypoperfusion after CSD, but not the reduced vascular reactivity. In comparison, L-arginine, the substrate for NO synthesis and blockade of the mitochondrial permeability transition pore ameliorates both the reduced CBF and the reduced vascular reactivity. Astroglial calcium waves (AGCW) enable astroglial cells to communicate, but our knowledge of AGCW in disease models is incomplete. AGCWs propagate 20-50 µm from the initiation site and are rarely observed in young healthy mice, but AGCWs may accompany CSD. The incidence is increased in aging rodents, in hypoxia and in Alzheimer's disease. AGCWs are distinct from CSD by being restricted in the extent of propagation and by being strictly astroglial. AGCWs are accompanied by slight rises in oxygen use and in a low proportion of cases AGCW induce capillary constriction, but not vasodilation. Both CSD and AGCW may contribute to the changes of CBF and CMRO2 in patients with migraine or acute brain injury.

55
BRAIN-0670
Symposium

Blood-Brain Barrier and the Immunology of Stroke

Macrophages Prevent Hemorrhagic Transformation following Stroke

S. Jander[1], M. Gliem[1]
[1]Neurology, Heinrich-Heine-University, Düsseldorf, Germany

Objectives

Macrophages (MP) and their circulating monocyte (MO) precursors are key players in the innate immune response to ischemic stroke. However, their functional role was so far poorly understood. Basic immunological work has identified distinct subpopulations of inflammatory and non-inflammatory MO/MP. Goal of our study is to delineate the temporal pattern, mechanism and function of hematogenous MO/MP recruitment in stroke-induced neuroinflammation.

Methods

We addressed the role of bone-marrow-derived MO/MP in mouse models of permanent and transient focal brain ischemia using a combined cell-specific depletion, chemokine receptor knock-out, bone marrow chimeric, and pharmacological approach.

Results

Inflammatory $Ly6c^{hi}/CCR2^{+}$ monocytes infiltrated into the infarct borderzone within 24 h of stroke onset and subsequently differentiated into mature $Ly6c^{lo}/CX3CR1^{+}$ phagocytes within the CNS compartment. Functional studies revealed a critical role of the hematogenous MO/MP response for infarct demarcation and neovessel stabilization via a transforming growth factor (TGF)-β1-dependent mechanism. Accordingly, early depletion of circulating MO/MP precursors caused delayed clinical deterioration and hemorrhagic conversion of the

infarctions. MO/MP recruitment and subsequent differentiation towards a non-inflammatory phenotype proved also essential in order to prevent secondary intracerebral hemorrhage (sICH) after stroke in orally anticoagulated mice. Clinically relevant risk factors such as diabetes interfered with appropriate MO/MP differentiation, impaired their repair function, and increased the rate of sICH. Further studies revealed a role of MO/MP-specific PPARγ activation for neurovascular repair after ischemic stroke.

Conclusions

Our study elucidated an essential repair function of hematogenous MO/MP and identified targets for novel therapies preventing secondary infarct bleeding after ischemic stroke.

References

Gliem M, Mausberg AK, Lee JI, Simiantonakis I, van Rooijen N, Hartung HP, Jander S (2012) Macrophages prevent hemorrhagic infarct transformation in murine stroke models. Ann Neurol 71:743-752.

Gliem M, Hermsen D, van Rooijen N, Hartung HP, Jander S (2012) Secondary intracerebral hemorrhage due to early initiation of oral anticoagulation after ischemic stroke: an experimental study in mice. Stroke 43:3352-3357.

56
BRAIN-0992
Symposium

Blood-Brain Barrier and the Immunology of Stroke

Leukocyte mRNA Predict Hemorrhagic Transformation following Stroke

G. Jickling[1]
[1]*Neurology, University of California Davis, Sacramento, USA*

Background: Hemorrhagic transformation (HT) is a major complication of ischemic stroke that worsens outcomes and increases mortality. Disruption of the blood brain barrier is a central feature to HT pathogenesis, and leukocytes may contribute to this process. We sought to determine whether ischemic strokes that develop HT have differences in RNA expression in blood within 3 hours of stroke onset prior to treatment with thrombolytic therapy.

Methods: Stroke patient blood samples were obtained prior to treatment with thrombolysis, and leukocyte RNA assessed by microarray analysis. Strokes that developed HT (n=11) were compared to strokes without HT (n=33) and controls (n=14). Genes were identified (corrected p-value <0.05, fold change $\geq |1.2|$) and functional analysis performed. RNA prediction of HT in stroke was evaluated using cross-validation, and in a second stroke cohort (n=52).

Results: Ischemic strokes that developed HT had differential expression of 29 genes in circulating leukocytes prior to treatment with thrombolytic therapy. A panel of 6 genes could predict strokes that later developed HT with 80% sensitivity and 70.2% specificity. Key pathways involved in HT of human stroke are described, including amphiregulin, a growth factor that regulates matrix metalloproteinase-9; a shift in transforming growth factor-beta signaling involving SMAD4, INPP5D and IRAK3; and a disruption of coagulation factors V and VIII.

Conclusions: Identified genes correspond to differences in inflammation and coagulation that may predispose to HT in ischemic stroke. Given the adverse impact of HT on stroke outcomes, further evaluation of the identified genes and pathways is warranted to determine their potential as therapeutic targets to reduce HT and as markers of HT risk.

57
BRAIN-0965
Symposium

Blood-Brain Barrier and the Immunology of Stroke

Regulatory B Cells in Experimental Stroke

H. Offner[1]
[1]*Neurology and Anesthesiology and Perioperative Medicine, Oregon Health & Science University, Portland, USA*

It is now increasingly clear that human stroke creates not just a single organ insult, but a complex interaction between two physiological systems: the CNS and the peripheral immune system. Until recently, the events behind how stroke induces pathology in distant immune organs (e.g. spleen and thymus) has been relatively unstudied. Furthermore, the significance of, and mechanisms underlying, cerebral ischemia-induced immune dysfunction remain poorly understood. However, using animal and cell models, we have observed that systemic immunopathology evolves in tandem with the maturing central cerebral infarct. I will present evidence from our work, characterizing the systemic immune response after experimental stroke, the cell players, and their interactions with the injured brain.

The implications of brain-spleen injury cycling for future immunotherapy will be presented. MCAO triggers early signaling from the ischemic brain to spleen, resulting in a massive production of inflammatory factors and transmigration of splenocytes to the circulation and brain. Whereas inflammatory cells from the periphery have now been shown to contribute to CNS damage and cell death, other regulatory immune cells can reduce inflammation and limit damage within the brain. A major conundrum in the immunology of stroke is how to enhance the early immunoregulation that limits CNS inflammation while preventing excessive systemic suppression. We evaluated the ability of regulatory B-cells from the peripheral immune system to exert immunosuppressive effects, diminish stroke lesion size and protect from neurological damage. Recent evidence demonstrated that absence of B-cells led to larger infarct volumes and CNS damage after middle cerebral artery occlusion (MCAO) that could be prevented by transfer of IL-10$^+$ B-cells. Our study demonstrated beneficial immunoregulatory effects on MCAO of the IL-10$^+$ B-cell subpopulation in the B-cell-sufficient mice. CNS inflammation and infarct volumes were evaluated in male C57BL/6J mice that received either RPMI or IL-10$^+$ B-cells and underwent 60 min of middle cerebral artery occlusion followed by 96 hours of reperfusion. Transfer of IL-10$^+$ B-cells markedly reduced infarct volume in WT recipient mice when given 24 hours prior to or 4 and 24 hours after MCAO. B-cell protected MCAO mice had increased regulatory subpopulations in the periphery, reduced numbers of activated, inflammatory T-cells, decreased infiltration of T-cells and a less inflammatory milieu in the ischemic hemispheres of the IL-10$^+$ B-cell-treated group. Moreover, transfer of IL-10$^+$ B-cells 24 hours before MCAO led to a significant preservation of regulatory immune subsets in the IL-10$^+$ B-cell protected group presumably indicating their role in immunomodulatory mechanisms, post-stroke. These novel observations demonstrated the previously unrecognized activity of B-cells to limit infarct volume and functional neurological deficits as well as to inhibit activation and recruitment of inflammatory T-cells, macrophages and microglia into the growing CNS infarct after experimental stroke in mice. A key function of B-cells is their secretion of IL-10, an anti-inflammatory cytokine that has been studied extensively in stroke. Taken together, these findings suggest that local secretion of IL-10 by circulating or CNS-infiltrating B-cells may be preferable to systemic delivery.

This work was supported by
NIH/NINDS 1RO1NS075887.

58
BRAIN-0906
Symposium

Blood-Brain Barrier and the Immunology of Stroke

Inflammation affects cerebral perfusion in Ischemic Stroke.

M. Zhang[1], Q. Zhao[1], J. Lao[1], Y.U.N. Xu[1]
[1]Neurology,
Affiliated Drum Tower hospital of Nanjing University medical school, Nanjing, China

Inflammation and immune modulation of ischemic stroke

Objectives: Inflammation has been shown to be an important player in the progression of ischemic brain damage. Cerebral inflammation is characterized by the activation of microglia, the accumulation of inflammatory cells and production inflammatory mediators. Our group devoted to detailing the pathological characterization of inflammation in ischemic stroke and finding out potential neuroprotectants reversing these deleterious events.

Methods: In clinic, we enrolled 30 ischemic stroke patients and 40 moyamoya patients with acute cerebrovascular event episode. Cerebral parenchymal edema were measured the by MRI Flare image. Serum inflammatory mediators and clinic neurological deficits were calculated by ELISA and NIHSS scale respectively. In animal studies, we applied mouse middle artery occlusion model (MCAO) model to test the inflammatory mediators in the ischemic tissue, in the peripheral blood and spleen by Q-PCR, western blotting and ELISA. CD4+/CD8+ ratio, Treg cell were determined by flow cytometric analysis. Infarcted size, neurological function, cell apoptosis were tested by TTC, NSS scale, TUNEL stain. In vitro studies, BV2 cells exposure to oxygen-glucose deprivation and LPS were used to mimic microglia activation.

Results: In clinic, elevation of serum IL-6、IL-10、IL-12、TNF-α and VEGF were observed in moyamoya patients. In stroke patients, serum TNF-α and 1L-1 were positively related with the NIHSS scale and parenchymal edema size. Administration of human urinary kallidinogenase (HUK) to stroke patients was able to inhibit parenchymal edema. In animal studies, regarding the T cells, a substantial increase in CD4+/CD8+ ratio at 24 h was observed in blood of MCAO mice, while, a remarkable decline of spleen CD4+/CD8+ ratio was measured at 96 h. Th1/Th2 ratio from blood of MCAO mice was markedly increased at 24 h, while slightly reduced by 96 h. An increased percentage of Treg cell in MCAO mice was observed at both 24 and 96 h. Modulating post-stroke immune responses by cocaine-and amphetamine-regulated transcript (CART) exerted a neuroprotective effect in experimental stroke. Additionally, FasL mutation also caused T lymphocyte subsets reprogramming, characterized by a reduction of $CD3^+CD8^+$ T cells and a skew of Th1/Th2 balance towards Th2 in the brain and blood plasma, resulting in neurological improvements. Regarding the microglia, exposing BV2 cells to LPS or OGD increased the expression of inflammatory cytokines including 1L-1β, TNF-α, iNOS, COX-2, MCP-1. Our study demonstrated that chemicals-Hydroxysafflor yellow A and Dalesconols B could decrease these inflammatory reactions. Microglia has two different phenotypes regarding activation status, M1 (pro-inflammation) and M2 (anti-inflammation). Decreased cortex mRNA expression of M1 markers (TNF-α, iNOS, IL-1, IL-6, MCP-1) and increased M2 markers (CD206, YM-1, IL-10, TGF-β) were detected in the Malibatol A group compared to the vehicle group after reperfusion.

Conclusions: Inflammatory and immune responses are complicated in ischemic stroke. Targeting different mechanisms, we found that HUK, CART, Hydroxysafflor yellow A, Dalesconols B, Malibatol A could be potential medications in modulating inflammatory responses and protecting against ischemic injury.

61
BRAIN-0837
BrainPET

BrainPET Oral Session: Novel Tracer Evaluation, Data Acquisition & Analysis

FROM MOLECULE TO MAN: DEVELOPMENT OF NOVEL AGONIST PET RADIOTRACERS FOR IMAGING THE KAPPA OPIOID RECEPTOR IN VIVO

S. Li[1], M. Zheng[1], N. Nabulsi[1], M. Naganawa[1], D. Holden[1], S. Lin[1], H. Gao[1], T. Lara-Jaime[1], M. Kapinos[1], J. Ropchan[1], R. Carson[1], Y. Huang[1]
[1]PET Center Department of Diagnostic Radiology, Yale University, New Haven, USA

Objectives: The kappa opioid receptor (KOR) is an important target for the investigation of stress-related disorders and for drug development in depression and alcoholism. We have developed a pair of KOR agonist and antagonist radiotracers for PET imaging (1, 2). Nonetheless, the agonist radiotracer ^{11}C-GR103545 displays slow tissue kinetics in human, and thus is not ideal for the imaging and quantification of KOR *in vivo*. We embarked on a novel radiotracer discovery program to develop KOR agonist radiotracers with more favorable pharmacokinetic and imaging characteristics.

Methods: Novel compounds based on the structure of the prototypical ligand GR103545 were synthesized and assayed for binding affinities in radioligand competition experiments with cloned human opioid receptors. Candidate ligands with appropriate binding affinity and selectivity were then radiolabeled for evaluation in rhesus monkeys. Baseline and blocking scans with opioid ligands were conducted on a Focus-220 scanner to assess the ligands' pharmacokinetics and *in vivo* binding characteristics. Metabolite-corrected arterial activity curves were measured and used as input functions in the analysis of brain time-activity curves and calculation of binding parameters with kinetic models. Best performing radioligands were finally advanced to PET imaging evaluation in humans using the HRRT scanner.

Results: Two ligands, EKAP and FEKAP, emerged from our ligand discovery programs with high KOR binding affinity (K_i = 0.28 and 0.43 nM, respectively) and selectivity, and were chosen for comprehensive evaluation in rhesus monkeys. Both ^{11}C-EKAP and ^{11}C-FEKAP were prepared in high specific activity and radiochemical purity. In monkeys, both tracers metabolized fairly quickly with ~30% of parent fraction at 30 min post-injection. In the brain, they exhibited fast and reversible kinetics with peak uptake time of <20 min. Pre-treatment with the non-selective opioid antagonist naloxone (1 mg/kg) decreased uptake in high binding regions to the level of cerebellum, and the selective KOR antagonist LY2456302 (0.02-0.1 mg/kg) reduced ^{11}C-EKAP and ^{11}C-FEKAP specific binding in a dose-dependent manner. Mean binding potential (BP_{ND}) values derived from multilinear analysis (MA1) were higher for ^{11}C-FEKAP than ^{11}C-EKAP, with values of 2.22 (1.73), 1.84 (1.43), 1.08 (0.76), 1.28 (0.81), respectively, for the cingulate cortex, insula, putamen and frontal cortex (n=5-6). PET scans in a female human subject found that ^{11}C-EKAP had higher brain uptake (peak SUV of 3-4 vs. 2-2.6 for ^{11}C-FEKAP), higher plasma free fraction (24% vs. 6%) and faster tissue kinetics. Higher regional distribution volumes (V_T) were also seen for ^{11}C-EKAP. Specific binding signals, however, were the same for the two radiotracers, and similar to those of ^{11}C-GR103545, based on comparative analysis of regional V_T values (3).

Conclusions: We discovered two KOR agonist radiotracers with the dual attractive properties of fast tissue kinetics and high specific binding as demonstrated in imaging studies in rhesus monkeys. First-in-human evaluation indicated that both ^{11}C-EKAP and ^{11}C-FEKAP exhibited specific binding signals comparable to those of ^{11}C-GR103545, but with faster tissue kinetics.

Research support: NIH R21/R33 MH092664

References:
1. Naganawa M. *et al*. *Neuroimage* 2014; 99:69.
2. Naganawa M. et al. *JCBFM* 2014, 34:1818. 3. Qi G *et al*. *JCBFM* 2014; 34:1162

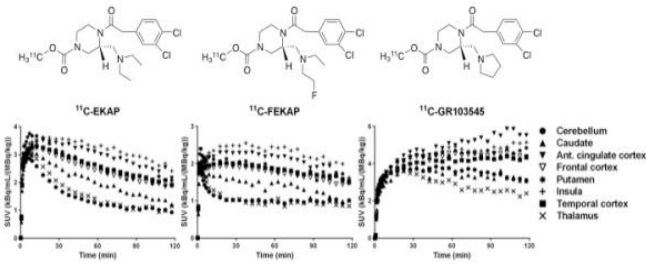

Figure 1: Top: Chemical structures of ^{11}C-EKAP, ^{11}C-FEKAP and ^{11}C-GR103545; Bottom: Time-activity curves (TACs) of ^{11}C-EKAP and ^{11}C-FEKAP in the brain of a female human subject, along with composite TACs of ^{11}C-GR103545 from n = 22 human subjects.

62
BRAIN-0303
BrainPET

BrainPET Oral Session: Novel Tracer Evaluation, Data Acquisition & Analysis

VERMIS – TO EXCLUDE OR NOT EXCLUDE? DEFINING A PROPER REFERENCE REGION FOR PET MODELLING OF THE SEROTONIN SYSTEM

M. Ganz[1], H.D. Hansen[1], V. Beliveau[1], L. Feng[1], C. Svarer[1], G.M. Knudsen[1]
[1]Neurobiology Research Unit and Center for Integrate d Molecular Brain Imaging, Rigshospitalet, Copenhagen, Denmark

Objectives:

Reference-Tissue modelling (RTM) necessitates a proper reference region and for that purpose cerebellum is most commonly used. The cerebellum can, however, be subdivided into sub-regions that may vary in terms of their suitability as reference tissue. We investigate regional differences in binding within the grey matter of the cerebellar hemispheres (CH) and the cerebellar vermis (CV) for PET radioligands targeting the serotonin system.

Methods:

The following PET scans were available for analysis: 5-HT_{1A}R ([^{11}C]CUMI, n=8), 5-HT_{1B}R ([^{11}C]AZ10419369, n=12), 5-HT_{2A}R ([^{18}F]Altanserin, n=7) and ([^{11}C]Cimbi-36, n=29), 5-HT_4R ([^{11}C]SB207145, n=51), and 5-HTT ([^{11}C]DASB, n=63). All subjects were scanned on a HRRT scanner and corresponding T1-weighted MRI scans were also available. We employed the software packages SUIT [1] to segment CV and FreeSurfer [2] to delineate CH. We used mean standardized uptake values (SUV) weighted by frame-length as a measure of brain uptake. SUV is defined as the time-activity-curve in the region-of-interests divided by injected dose per kg bodyweight. Statistical difference was assessed with paired two-tailed t-tests.

Results:

Figure 1 shows the ratio (CV/CH) in mean SUV between CV and CH. A significant ($p<0.001$) difference between CH and CV was found for [^{11}C]CUMI, [^{11}C]AZ10419369 and [^{11}C]SB207145. No significant difference was found between CH and CV with the antagonist Altanserin, but uptake was significantly lower ($p<0.001$) in CV with the agonist [^{11}C]Cimbi-36. We found no significant difference between CH and CV for [^{11}C]DASB. All these data are consistent with the available literature on human post-mortem autoradiography [3][4][5][6], with the exception of 5-HT_4R, where Hall et al [7] reported no evidence for specific binding to 5-HT_4R in cerebellum.

Conclusions:

We demonstrate radioligand specific regional differences in cerebellar uptake, of relevance for its use as a reference region in PET imaging. These differences may be ascribed to differences in concentration of the receptor or transporter in question in CV vs. CH, could reflect off-target binding of the radioligands or – less likely – differences in the non-displaceable binding in the two tissue types. There is evidence from post-mortem autoradiography of the presence of 5-HT_{1A}Rs in CV [3] and we observe a significantly higher [^{11}C]CUMI uptake in the CV compared to CH. We also found significantly higher uptake of [^{11}C]AZ10419369 in CH compared to CV, which is consistent with an autoradiographic study showing presence of 5-HT_{1B}Rs in CH [6]. Additionally, we observed a CH-CV difference between the 5-HT_{2A}R agonist [^{11}C]Cimbi-36 and the 5-HT_{2A}R antagonist [^{18}F]Altanserin. Our data highlight the importance of validating each radioligand carefully with regard to the suitability of including or excluding CV in the reference region definition. Additionally, we recommend the use of automatic segmentation software based on

individual structural MRIs to accurately delineate cerebellum subregions.

References:

[1] Diedrichsen, J. *Neuroimage* 33. (2006):127-138.

[2] Fischl, B. *Neuroimage* 62. (2012):774-781.

[3] Parsey, RV., et al. *J Cereb Blood Flow Metab* 25. (2005):785-793

[4] Varnäs, K, et al. *Brain research* 915. (2001):47-57.

[5] Varnäs, K, et al. *European Neuropsychopharmacology* 13.4(2003):228-234

[6] Varnäs, K,et al. *Human Brain Mapping* 22.3(2004):246-260.

[7] Hall, H, et al. *Synapse* 38.4(2000):421-431.

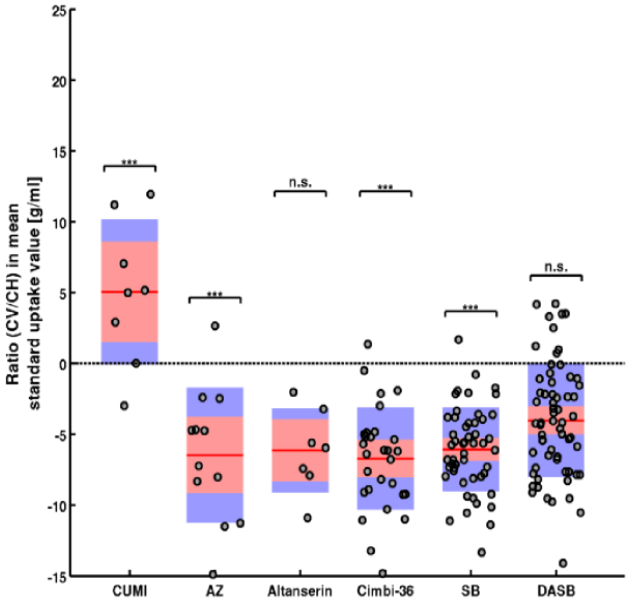

Figure1: Ratio (CV/CH) between mean standard uptake value in CV and CH

63
BRAIN-0637
BrainPET

BrainPET Oral Session: Novel Tracer Evaluation, Data Acquisition & Analysis

TRACER KINETIC ANALYSIS OF [18F](S)-THK5117 AS A PET TRACER FOR TAU PATHOLOGY

M. Lubberink[1], M. Jonasson[1], A. Wall[1], K. Chiotis[2], L. Saint-Aubert[2], J. Eriksson[1], J. Sörensen[1], N. Okamura[3], G. Antoni[4], A. Nordberg[2]

[1]Nuclear medicine & PET, Uppsala University, Uppsala, Sweden

[2]Translational Alzheimer Neurobiology, Karolinska Institutet, Stockholm, Sweden

[3]Pharmacology, Tohoku University School of Medicine, Sendai, Japan

[4]Pre-clinical PET platform, Uppsala University, Uppsala, Sweden

Objectives: There is an increasing interest in developing PET tracers that bind specifically to tau protein since tau pathology is hypothesized to correlate to clinical symptoms in Alzheimer's disease (AD)[1]. The aim of this study is to evaluate tracer kinetic models for quantitative analysis and generation of parametric images of the novel tau ligand [^{18}F]*(S)*-THK5117[2].

Methods: 15 subjects (5 AD, 4 mild cognitive impairment (MCI), one non-AD dementia, 5 healthy controls (HC)) received a 90 min dynamic [^{18}F]*(S)*-THK5117 PET scan. In dementia and MCI patients, arterial blood was sampled for measurement of blood radioactivity and metabolite analysis. All subjects underwent a T1-MRI for segmentation (SPM8) and definition of volumes of interest (VOIs) using a probabilistic template (PVElab[3]). VOI-based analysis was performed using plasma-input models (single-tissue 1T and two-tissue 2T compartment models; plasma-input Logan) and reference tissue models (SRTM, reference Logan, and SUV ratio). Cerebellum gray matter was used as reference region. In addition to 90 min, initial 40 and 60 min data were analysed. Voxel-level analysis was performed using basis function implementations of SRTM (RPM, RPM$_2$), reference Logan and SUV ratio. Regionally averaged voxel values were compared to

VOI-based values from the optimal reference tissue model. Simulations were performed to assess accuracy and precision.

Results: Plasma-input Logan DVR-1 agreed well with 2T DVR-1 (R^2=0.99, slope=0.99). SRTM BP_{ND} and reference Logan DVR-1 showed high correlation to plasma-input Logan DVR-1 (R^2[3]0.99, slope=0.98-0.99) while SUVr-1 values overestimated binding (R^2=0.92, slope=1.6). SRTM BP_{ND} and reference Logan DVR-1 values were not affected by a 60 min scan duration, whereas SUVr-1 values decreased for shorter scan durations. Figure 1 shows parametric images. Agreement between parametric methods and SRTM was best for reference Logan (R^2=0.99, slope=1.01). In white matter, SUVr-1 values were 2.6 times higher than DVR-1 values, compared to 1.6 times in grey matter, resulting in a considerably higher relative white matter signal in SUVr-1 images than in DVR-1 images. Simulations showed a lower accuracy and precision for SUVr-1 values compared to other reference methods.

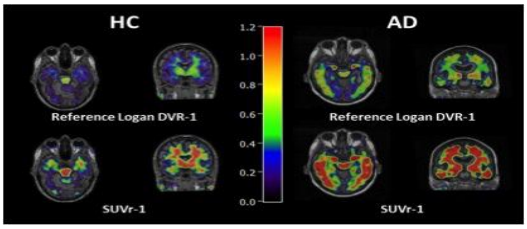

Figure 1: *Parametric [^{18}F](S)-THK5117 images of reference Logan DVR-1 and SUVr-1 in a typical healthy control (HC) and AD patient.*

Conclusions: SRTM BP_{ND} and reference Logan DVR-1 showed high correlation to plasma-input Logan DVR-1 and robust results of VOI-based and parametric data analyses were found for scan durations of 60 min. Reference Logan was able to generate quantitative [^{18}F]*(S)*-THK5117 DVR-1 parametric images with the highest accuracy and precision, and with a lower white matter signal than SUVr-1 images.

References:

[1]Okamura *et al*, Curr Neurol Neurosci Rep 2014
[2]Okamura *et al*, J Nucl Med 2013
[3]Svarer *et al*, Neuroimage 2005

64
BRAIN-0791
BrainPET

BrainPET Oral Session: Novel Tracer Evaluation, Data Acquisition & Analysis

REALISING THE BINDING POTENTIAL DIRECTLY AND INDIRECTLY

G.E. Searle[1], *C. Coello*[1], *R.N. Gunn*[1]
[1]*Modelling and Analysis,*
Imanova Centre for Imaging Sciences, London, United Kingdom

Objectives

The two tissue compartment model (2TCM) is often identified as the optimal model for quantifying PET radioligand binding. 2TCM quantification produces estimates of rate constants as well as the equilibrium partition coefficient V_T. When a reference region exists, the binding potential BP_{ND} can be calculated directly (from k_3 and k_4) or indirectly (via V_T data). It has previously been observed [1] that the estimation of microparameters (k_2, k_3, k_4) is often poor, whilst the macroparameters (V_T, K_1) are robustly estimated. Despite this, direct calculation of BP_{ND} as k_3/k_4 continues to appear in the literature.

The objective of the work presented here is to investigate the performance of direct and indirect 2TCM methods to estimate BP_{ND} from human PET data.

Methods

Three methods to estimate BP_{ND} were investigated:

- **Indirect:** V_T calculated in target and reference region from 2TCM; BP_{ND} calculated as $(V_T - V_T^{REF})/V_T^{REF}$.
- **Direct I:** BP_{ND} calculated as k_3/k_4 from 2TCM.
- **Direct II:** 2TCM fitted to a set of regions with a common V_{ND}. BP_{ND} calculated as k_3/k_4 [2].

The Indirect method is considered the gold standard, but requires a reference region. Estimates of BP_{ND} from Direct I & II were compared with the Indirect

method for 15 PET scans (7 [^{11}C]-IMA107; 8 [^{11}C]-PHNO) in 7 brain regions.

Results

BP_{ND} values calculated using Direct I & II are plotted against the Indirect Method in Figure 1. For [^{11}C]-IMA107 and [^{11}C]-PHNO, Direct I produces very poor correspondence to the Indirect method. For Direct II the correlation is better, but a significant bias still remains. The quality of model fits to the time-activity curves was markedly poorer for Direct II as compared to the Indirect Method, (AIC: Indirect: -49, Direct II: -1).

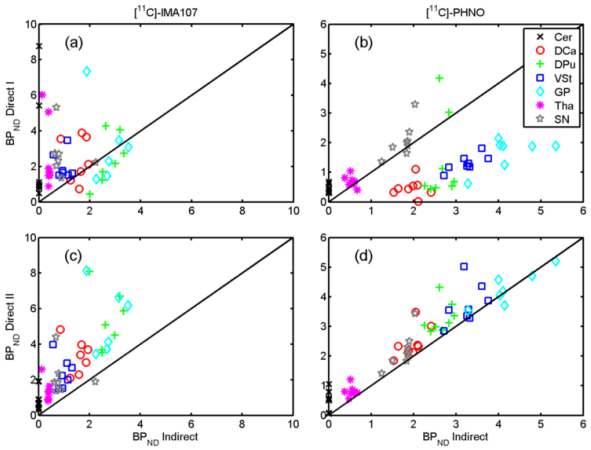

Figure 1: BP_{ND} estimated via Direct I & II plotted against Method 1.

Conclusions

Direct methods to quantify specific binding in the absence of a reference region suffer from significant bias and variance when evaluated on measured PET data. Caution should be used when validating methods to estimate the binding potential using only idealised 2TCM simulated data that does not reflect the real world situation.

Whilst the 2TCM structure suggests a direct relationship between the partitioning of kinetic components of the PET signal and the underlying biology in terms of the specific and non-displaceable compartments, in practice this is not the case. There are many more complexities to the data including tissue heterogeneity, non-equilibrium of non-specific binding, imperfections in scatter, attenuation, subject motion as well as partial volume and finally noise that compromise the interpretation of the 2TCM derived microparameters. Thus, the ratio k_3 to k_4 is not a good unbiased and low variance estimator of the binding potential. When no reference region is available it may be more appropriate to limit one's endpoints to the outcome measure V_T and derivatives thereof.

References

1. Parsey, R.V., et al., JCBFM, 2000. **20**(7): p. 1111-33.

2. Todd Ogden, et al., Neuroimage, 2014. **108C**: p. 234-242.

65
BRAIN-0731
BrainPET

BrainPET Oral Session: Novel Tracer Evaluation, Data Acquisition & Analysis

PHARMACOKINETIC EVALUATION OF THE TAU RADIOTRACER [18F]T807 WITH ARTERIAL KINETIC ANALYSIS

D. Wooten[1], N. Guehl[1], D. Yokell[1], T. Shoup[1], N. Zubcevik[2], R. Zafonte[2], K. Johnson[3], G. El Fakhri[1], M. Normandin[1]
[1]CAMIS/Radiology, Massachusetts General Hospital and Harvard Medical School, Boston, USA
[2]Physical Medicine and Rehabilitation, Spaulding Rehabilitation Hospital, Boston, USA
[3]Radiology, Massachusetts General Hospital and Harvard Medical School, Boston, USA

Objectives: [^{18}F]T807 was developed for PET imaging of tau protein aggregates which are implicated in a wide range of neuropathologies including Alzheimer's disease and traumatic brain injury (TBI). The goal of this work was to provide an initial characterization of [^{18}F]T807 pharmacokinetics including arterial plasma and metabolite analysis and compartmental modeling.

Methods: Five subjects (1 control, 1 MCI, 3 TBI) underwent [^{18}F]T807 PET scans. Collection of

dynamic PET data was initiated for 120 minutes following the bolus injection of [^{18}F]T807. Arterial blood sampling was acquired rapidly immediately after injection and was reduced in frequency to every 15 minutes toward the end of the scan. Venous blood samples were acquired in a subset of the subjects receiving arterial sampling to allow comparison of time courses. [^{18}F]T807 blood radiometabolite analysis was performed using our column switching radioHPLC. Dynamic PET images were warped to a standardized space using the subject's T1 MEMPRAGE MRI. Total volume of distribution (V_T) was estimated using the Logan graphical method and one- (1CM) and two- (2CM) tissue compartment models.

Results: Whole blood:plasma ratio was close to unity by 1 minute (range: 0.75-1.1). Plasma parent fraction followed a single exponential ($T_{1/2}$: 14.2 ± 2.7 min) resulting in primarily polar metabolites as observed on HPLC. Metabolite corrected plasma activity fit a bi-exponential (time > 5 minutes: $T_{1/2}$: 165 ± 90; 3.4 ± 0.67 min). Plasma clearance was 170 ± 54 ml/kg/hr. By 15 minutes, venous matched arterial concentrations within ~10%. [^{18}F]T807 in gray matter peaked quickly (SUV > 2 at ~5 minutes). Logan plots became linear no later than 30 min and voxelwise analysis gave high quality results. Compartmental models gave good fits but preferred model varied by region. V_T was higher in the occipital lobe of the MCI subject (6.1) compared to control (4.4). The occipital lobe preferred a 2CM as opposed to the cerebellum that preferred a 1CM. High focal uptake was found in the corpus callosum of the acute head injury subject compared to control (V_T =5.3 vs. 4.6).

Conclusions: [^{18}F]T807 showed rapid clearance from plasma and properties suitable for tau quantification with PET. Initial studies suggest that graphical and compartmental techniques are suitable for quantification. Future [^{18}F]T807 scans with arterial sampling are scheduled and will provide a more thorough assessment of [^{18}F]T807 kinetics.

Research Support: R01MH068376, R01MH095809, T32EB013180

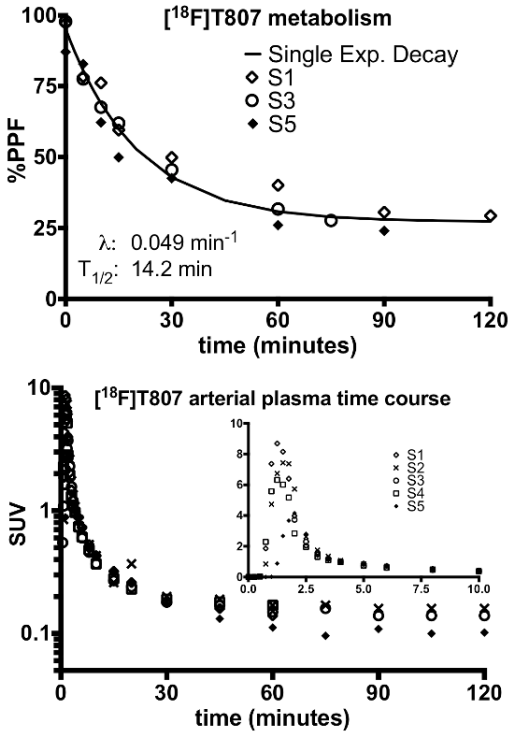

Figure 1: [^{18}F]T807 arterial kinetics. (Top) %PPF and (Bottom) [^{18}F]T807 arterial time course.

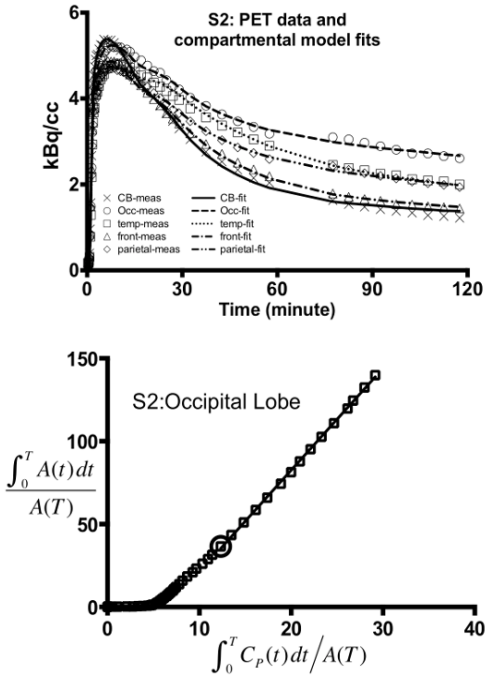

Figure 2: (Bottom) Logan regression plot and (Top) compartmental model fits to measured PET data (cerebellum, occipital lobe, temporal lobe, frontal lobe, parietal lobe).

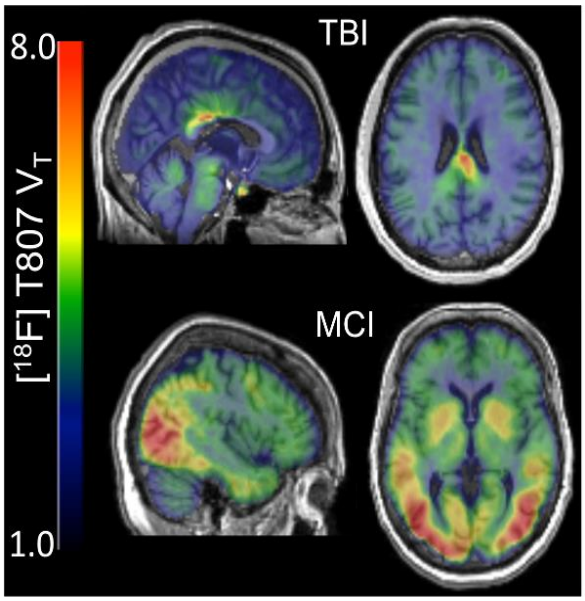

Figure 3: Logan DV images in a subject with TBI and a subject with MCI.

66
BRAIN-0457
BrainPET

BrainPET Oral Session: Novel Tracer Evaluation, Data Acquisition & Analysis

THE USE OF PET DISPLACEMENT STUDIES AS AN INDIRECT MEASURE OF BRAIN PENETRATION OF ANTIEPILEPTIC DRUGS

J. Mercier[1], S.J. Finnema[2], D. Holden[2], S. Kervyn[3], K. Fowles[2], J.M. Nicolas[3], N. Nabulsi[2], Y. Huang[2], J. D'Souza[4], R.E. Carson[2], J. Hannestad[5]
[1]Medicinal Chemistry, UCB Pharma, Braine l'Alleud, Belgium
[2]Yale PET Center, Yale University, New Haven, USA
[3]Non Clinical Development, UCB Pharma, Braine l'Alleud, Belgium
[4]Clinical Pharmacology, UCB Pharma, Smyrna, USA
[5]Global Exploratory Development, UCB Pharma, Braine l'Alleud, Belgium

OBJECTIVES: Levetiracetam (LEV) is an antiepileptic drug that binds to synaptic vesicle glycoprotein 2A (SV2A). Preclinical data suggest that brivaracetam (BRV) – an SV2A antiepileptic drug in Phase 3 development – has higher brain permeability than LEV.[1] Here we evaluated the use of PET displacement studies in nonhuman primates to measure the brain entry rates of these two drugs.

METHODS: Using the SV2A PET tracer [^{11}C]UCB-J,[2,3] four blocking studies and four displacement studies were performed in rhesus monkeys after approval by the Institutional Animal Care and Use Committee. Care/handling of animals was in accordance with NIH guidelines. In the blocking studies, BRV (4 mg/kg) or LEV (30 mg/kg) was given intravenously (IV) 15 min before tracer injection. Receptor occupancy was determined using occupancy plots. In the displacement studies, BRV (5 mg/kg) or LEV (30 mg/kg) was given IV 45 min after tracer administration. Displacement halftime was defined as the time it takes from drug administration until 50% of maximal tracer displacement is achieved. Displacement halftimes were estimated using average standardized uptake values (SUV) from baseline and displacement experiments. The difference in SUV (ΔSUV) between conditions over time was plotted and fitted to the following model:

$$\Delta SUV = A(1-\exp(-\beta(t-t_0)))$$

where β is the clearance rate of tracer from the brain, which can be attributed to the entry of the drug. The estimate of β was then converted to a displacement halftime. Because displacement requires BRV or LEV entry *and* tracer exit, we estimated the halftime of BRV or LEV entry by subtracting the tracer clearance halftime from the displacement halftime. A conservative estimate of the tracer clearance halftime was calculated from the tracer's k_2, ($k_2 = K_1 / V_{ND}$).

RESULTS: The estimated displacement halftimes were 10 min for BRV and 30 min for LEV. The tracer k_2 was 0.1 min^{-1}, which gives a tracer clearance halftime of ~7 min. Thus, in a theoretical displacement study in which all specific binding sites were occupied instantaneously, the displacement halftime would be 7 min. Therefore, the entry speed of BRV is very fast, since the tracer clears almost as fast as its theoretical maximum (10 vs. 7 min). If we subtract the tracer clearance halftime from the displacement halftimes, the drug entry halftimes would be 3 min for BRV and 23 min for LEV, respectively. Preliminary data indicate that the [^{11}C]UCB-J clearance halftime in

humans is ~13 min, suggesting that a similar study would be feasible in humans.

CONCLUSIONS: PET data in rhesus monkeys confirmed the faster brain entry of BRV vs. LEV, which is consistent with rodent efficacy data. It also shows that using a tracer with fast kinetics, a PET displacement study can be used to estimate a drug's speed of entry into the brain.

REFERENCES:

1. Gillard M, et al. Eur J Pharmacol 2011;664:36-44.

2. Huang Y, *et al.* Development of a PET tracer for imaging synaptic vesicle glycoprotein 2A (SV2A) *NeuroReceptor Mapping Meeting.* Amsterdam 2014.

3. Mercier J, *et al*. ChemMedChem 2014;9:693-698.

69
BRAIN-0146
Brain Oral Communication

Oral Session: Neurovascular Coupling: Physiology

ARTERIOLE DILATION TO SYNAPTIC ACTIVATION THAT IS SUB-THRESHOLD TO ASTROCYTE ENDFOOT CA2+ TRANSIENTS

A. Institoris[1], *D. Rosenegger*[1], *G.R. Gordon*[1]
[1]*Department of Physiology and Pharmacology, Hotchkiss Brain Institute, Calgary, Canada*

Ca^{2+} dependent pathways in neurons and astrocyte endfeet can initiate arteriole diameter changes to control local brain blood flow. Discrepancies between the clear involvement of Ca^{2+} transients in astrocyte endfeet in brain slices versus controversial endfeet signals *in vivo* during functional hyperemia, prompted us to determine whether there exists an activity threshold in which neurons control arteriole diameter independent of astrocyte endfeet. We used two-photon fluorescence imaging of acute brain slices of the sensory-motor cortex from Sprague-Dawley rats to examine both synthetic (Rhod-2/AM) and genetically encoded Ca^{2+} indicator signals. We systematically examined different imaging planes and used various rates of data acquisition (1Hz and 30Hz) during a range of electrical evoked vasodilations.

Ramping stimulation (0.9-1.8V, 50Hz, 1s) at a particular intensity triggered a time-locked, uniformly spreading neuropil (relative fluorescence change: $\Delta F/F=21\pm7\%$) and neuron somata Ca^{2+} signals ($\Delta F/F=252\pm87\%$)(Fig.1D) encompassing the arteriole prior to vasodilation (4.0±0.5%)(Fig.1A-C) with no appearance of astrocyte somata ($\Delta F/F=3\pm2\%$) or endfeet ($\Delta F/F=1\pm1\%$) Ca^{2+} transients (n=6; * labels spontaneous Ca^{2+} signals). When imaging in additional image planes around the vessel, the same stimulation failed to trigger endfeet Ca^{2+} transients despite clear neuropil and neuron somata Ca^{2+} transients (Fig.1E). Blocking voltage-gated sodium channels with tetrodotoxin (500nM) eliminated arteriole dilation (0.3±0.4%), neuropil ($\Delta F/F=2\pm1\%$) and neuronal somata ($\Delta F/F=2\pm1\%$) Ca^{2+} signals (n=6)(Fig.1C-D). To potentially detect a fast astrocyte Ca^{2+} signal, we next imaged neuropil and endfeet apposed to the region of peak vasodilation at 30Hz. The neuropil Ca^{2+} signal was again reliably evoked ($\Delta F/F=43\pm10\%$), but without endfoot Ca^{2+} transients (n=6, $\Delta F/F=7\pm2\%$)(Fig.1E). When a different pattern of afferent fiber activity was evoked (20Hz, 5s stimulation), it still failed to trigger reliable astrocyte somata ($\Delta F/F$ 3±2%) or endfeet Ca^{2+} transients ($\Delta F/F=0\pm1\%$) preceding arteriole dilation (5.7±0.6%; n=6)(Fig.1F). Since ambient O_2 concentration can influence vasodilation and vasoconstriction pathways, we confirmed that bubbling with 30% O_2 evoked larger vasodilation (7.5±0.9%, n=7, $P<0.05$)(Fig.1F) than standard, 95% O_2 in response to 50Hz 1s stimulation, with a clear neuropil Ca^{2+} signal ($\Delta F/F=24\pm4\%$) and a lack of endfoot activity ($\Delta F/F=4\pm1\%$).

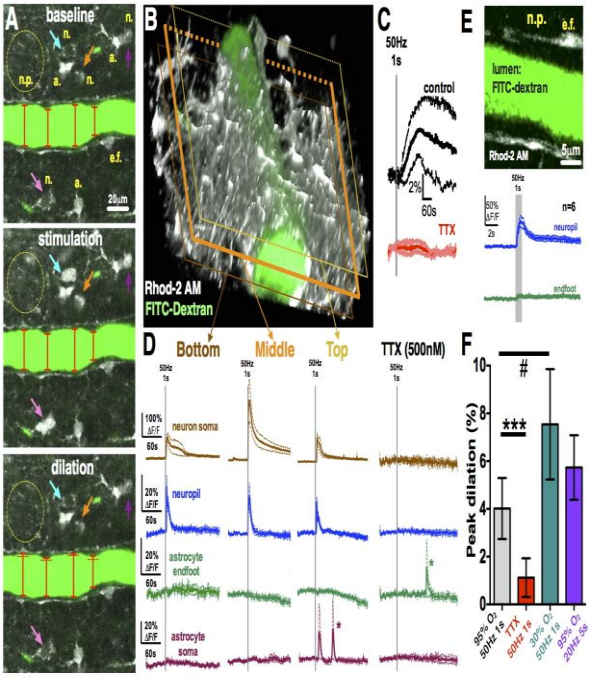

In contrast, higher stimulation voltages crossed a threshold for astrocyte activation (supra-threshold), where we detected consistent Ca^{2+} transients in astrocyte somata (ΔF/F=117±44%) and endfeet (ΔF/F=42±19%), which preceded vasodilation that was of similar magnitude to respective sub-threshold dilation (sub=4.5±0.8% vs. supra=5.0±0.4%, n=7)(Fig.2A-B). Next, we employed a GFAP-controlled genetic Ca^{2+} indicator to enable astrocyte-specific Ca^{2+} measurements using AAV2/5-gfaABC1D-cyto-GCaMP3 (Fig.2C-D). We could elicit vasodilation (6.5±1.1%, n=6) in the absence of Ca^{2+} transients in astrocyte processes (ΔF/F=5±3%, n=6) and in endfeet in multiple imaging planes (central: ΔF/F=4±2%, superficial: ΔF/F=5±0.1%, n=3; deeper: ΔF/F 5±2%, n=3)(Fig.2E). 30Hz image acquisition using GCaMP3 did also not detect a reliable endfoot Ca^{2+} transient (ΔF/F=6.7±5%)(Fig.2F). Notably, supra-threshold stimulation activated astrocyte processes (ΔF/F=125±46%) and endfeet (ΔF/F=102±57%) as well as caused vasodilation (3.6±0.5%, n=4)(Fig.2E).

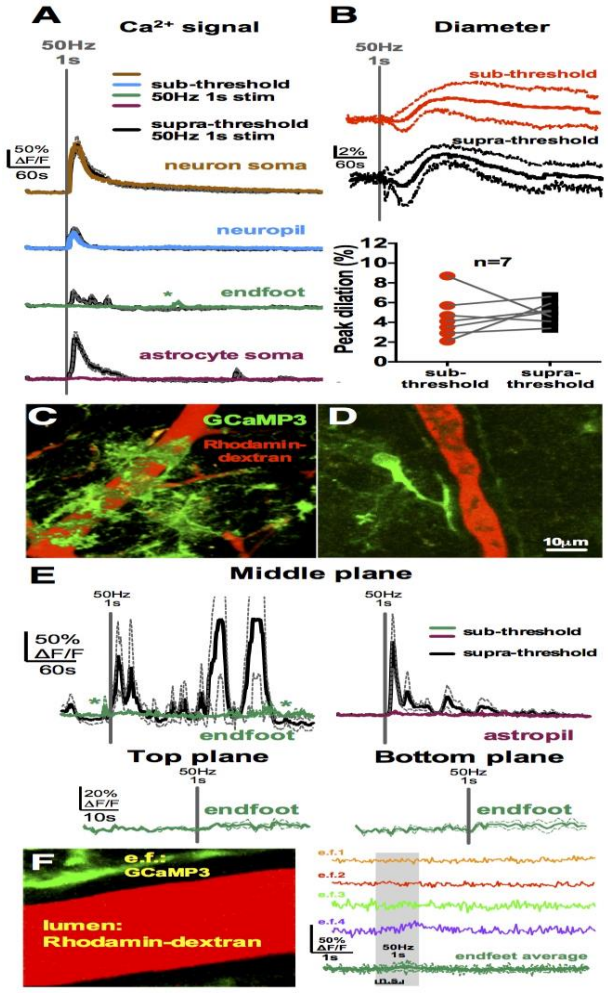

These data demonstrate that neuronal control of hyperemia can be functionally separated from astrocytes, and below a certain threshold of neuronal activity, endfoot Ca^{2+} transients are not an essential initiation signal for activity-dependent vasodilation in acute brain slices.

70
BRAIN-0709
Brain Oral Communication

Oral Session: Neurovascular Coupling: Physiology

SPONTANEOUS CALCIUM TRANSIENTS PRECEDE HEMODYNAMIC ACTIVITY AND SHOW HOMOTOPIC FUNCTIONAL CONNECTIVITY PATTERNS

P. Wright[1], A. Bauer[2], J. Culver[2]
[1]Biomedical Engineering,
Washington University in Saint Louis, Saint Louis, USA
[2]Radiology, Washington University in Saint Louis, Saint Louis, USA

Objectives: Brain dynamics are most commonly recorded using imaging contrasts that depend on changes in local concentrations of hemoglobin, such as functional MRI or optical intrinsic signal (OIS) imaging [1-2]. However, hemodynamic fluctuations are an indirect report of brain function; driven by electrical and metabolic activity through neurovascular coupling and are sensitive to diseases that impact it [3]. Here we extend functional connectivity (FC) imaging, a method to map functional relationships within brain networks using low frequency (0.009-0.08 Hz) spontaneous brain activity, and frequency-domain analysis methods beyond hemodynamic contrasts to Ca^{2+} transients. These Ca^{2+} dynamics should not only be temporally distinct due to their dependence on synaptic potential-dependent Ca^{2+} concentration changes but also predictive of the slower, downstream hemodynamic response.

Methods: Five transgenic mice expressing a fluorescent calcium indicator (GCAMP3 [4]) driven by the *Emx1* promoter in glutamatergic neurons and glia in the cortex and hippocampus were anesthetized using ketaminze/xylazine and imaged transcranially through implanted chronic imaging windows. Sequential LED illumination enabled simultaneous imaging of both GCAMP3 fluorescence emission (excitation at λ=470nm) and hemodynamics (using λ=530nm, 590nm, 625nm for oximetry). Somatosensory responses were evoked using an electrical hindpaw block paradigm that consisted of 0.5mA pulses at 2Hz for 4 seconds. FC patterns of low (0.009-0.08Hz) and high (0.2-2Hz) frequency spontaneous brain activity were quantified through analysis of spatio-temporal correlations in time series brain imaging data. Cross-correlation analysis was used to determine time delays between time series. The Fast Fourier Transform was used to examine frequency spectra and used in all subsequent frequency-domain analysis.

Results: Following electrical hindpaw stimulation, GCAMP3 provided an evoked response time course that was sensitive to individual high frequency (2Hz) pulse presentations, whereas the OIS trace followed the stereotypical hemodynamic response function independent of pulse frequency (**Fig. 1A**). This evoked GCAMP3 response preceded the OIS response by approximately 1.5 seconds (**Fig 1B**). Within the high-frequency band, pixelwise cross-correlation analysis of spontaneous data revealed that GCAMP3 again preceded OIS by approximately 1.5 seconds across the brain (**Fig 1C&D**). Furthermore, bilateral homotopic FC maps, created using eight bilateral canonical seeds, remained intact in higher frequency bands (>=2.0Hz) relative to OIS maps (**Fig. 1E**), but had analogous structure overall.

Conclusions: Using Ca^{2+} as a target for functional neuroimaging has provided evidence that organized temporal coherence in cortical activity across the brain is not exclusive to hemodynamics, providing an alternate view of neuronal mechanisms underlying disease. Moreover, this fast Ca^{2+} signal is more directly coupled to activity at the neuronal level and provides causal information predictive of the downstream hemodynamic response. Combined Ca^{2+} and OIS imaging will enable the dissociation of changes in ionic and metabolic networks from altered neurovascular coupling, providing a framework for subsequent studies of neurological disease (e.g. stroke).

References:

[1]. Biswal, B., et al. 1995. Magnetic Resonance in Medicine. 34(4):537-41.

[2]. White, B.R., et al. 2011. PLoS One 6(1):e16322.

[3]. Bauer, A.Q., et al. 2014. Neuroimage 99:388-401.

[4]. Tian L., et al. 2009. Nature Methods 6(1):875-81.

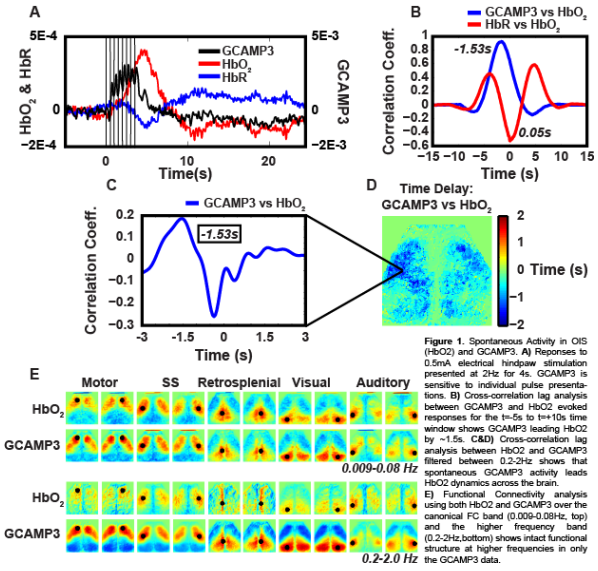

Figure 1. Spontaneous Activity in OIS (HbO2) and GCAMP3. **A)** Reponses to 0.5mA electrical hindpaw stimulation presented at 2Hz for 4s. GCAMP3 is sensitive to individual pulse presentations. **B)** Cross-correlation lag analysis between GCAMP3 and HbO2 evoked responses for the t=-5s to t=+10s time window shows GCAMP3 leading HbO2 by ~1.5s. **C&D)** Cross-correlation lag analysis between HbO2 and GCAMP3 filtered between 0.2-2Hz shows that spontaneous GCAMP3 activity leads HbO2 dynamics across the brain. **E)** Functional Connectivity analysis using both HbO2 and GCAMP3 over the canonical FC band (0.009-0.08Hz, top) and the higher frequency band (0.2-2Hz,bottom) shows intact functional structure at higher frequencies in only the GCAMP3 data.

71
BRAIN-0681
Brain Oral Communication

Oral Session: Neurovascular Coupling: Physiology

ODOR-EVOKED FMRI MAPS ARE COUPLED TO CALCIUM-SENSITIVE DYE IMAGING PATTERNS OF INPUT ACTIVITY IN THE OLFACTORY BULB

B. Sanganahalli[1], M. Rebello[2], P. Herman[1], G. Shepherd[3], X. Papademetris[1], J. Verhagen[2], F. Hyder[1]
[1]Diagnostic Radiology, Yale School of Medicine, New Haven, USA
[2]The John B. Pierce Laboratory, Yale School of Medicine, New Haven, USA
[3]Neurobiology, Yale School of Medicine, New Haven, USA

OBJECTIVES: To improve functional understanding of odor-evoked glomerular activity patterns revealed by BOLD signal and to relate how input activities of glomeruli reflected by calcium imaging relate to bulk neuropil activity of fMRI, we designed a study to image the same rats with fMRI first and then with calcium imaging.

METHODS: ***Animal preparation:*** Male Sprague-Dawley rats (250-350 g; Charles River, Wilmington, MA) were anesthetized with urethane (1.3 g/kg, intraperitoneal). **fMRI** (n=6): The fMRI data were obtained on a modified 9.4T system with Varian (Agilent Technologies, Santa Clara, CA) spectrometer using a custom-built 1^H surface coil. The neuroanatomy was imaged using fast spin echo with multi slice (fSEMS) sequence. For functional imaging of the dorsal bulb we used FLASH contrast: TR = 312 ms; TE = 12 ms; FOV = 1.56×1.56 cm^2; image matrix = 64×64; number of slices = 5; slice thickness = 300 µm [1]. Odor delivery was precisely time-locked to fMRI acquisition in a block design experiment (3-min OFF, 2-min ON, 3-min OFF) and was controlled through Spike-2 software. **Calcium imaging** (n=6): Three days after fMRI rats recovered, olfactory receptor neurons in the dorsal recess of the nasal cavity of rats were loaded bilaterally with dextan-conjugated calcium sensitive dye (Oregon Green BAPTA 488-1 dextran) using a well-established protocol [2]. Odorant evoked calcium signals were imaged across the dorsal bulb during the presentation of odors, at 256x256 pixels and 25 fps. Raw images were converted to images representing the relative change in fluorescence (%DF/F) in each pixel and frame after stimulus application. **Co-registration**: Using Bioimage suite (www.bioimagesuite.org) and MATLAB, co-registered all of the images by maximizing the similarity between the optical anatomical image and the MRI anatomical image.

RESULTS: Figure shows the bulbar responses (calcium maps and fMRI activity) of a subject exposed to two different odors. Odor evoked calcium maps show strong specificity for methyl valerate and ethyl butyrate. fMRI activation maps revealed similar activation patterns for both the odors. Similar regions in anterior OB were significantly activated under both imaging modalities (dotted circle). Excellent correspondence between odor-evoked fMRI and calcium maps was observed across trials and subjects for each imaging modality. Our results show strong correspondence between odor-evoked fMRI and calcium maps, confirming the strong relationship between the bulk neuropil and presynaptic activities. These in vivo results are in good agreement with an energy budget of glomerular activity, as the activated state is dominated by energy demands of action

potential propagation in afferent olfactory sensory neurons and their synaptic input to dendritic tufts, whereas subsequent dendritic potentials and dendrodendritic transmission contribute only a minor share of energy costs [3]

CONCLUSION: Multi-modal functional imaging of rat olfactory bulb with odorant stimulation provides new opportunities for gaining insights of complexities of neuropilar activities.

REFERENCES:

[1] Xu et al., (2000) Proc Natl Acad Sci U S A 97:10601-10606.

[2] Wachowiak and Cohen. (2003) J Neurophysiol 89:1623-1639.

[3] Nawroth JC et al (2007) J Neurosci. 27:9790-9800

ACKNOWLEDGEMENTS: Supported by NIH (R01 DC-011286, P30 NS-52519).

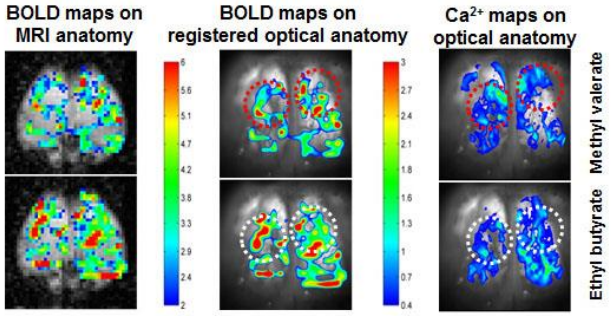

72
BRAIN-0306
Brain Oral Communication

Oral Session: Neurovascular Coupling: Physiology

LONGITUDINAL TWO-PHOTON IMAGING OF CORTICAL MICROVESSELS AND NEURAL ACTIVATION IN AWAKE MARMOSET MONKEYS

T. Santisakultarm[1], C. Kersbergen[1], D. Bandy[2], D. Ide[2], S. Choi[1], A. Silva[1]

[1]National Institute of Neurological Disorders and Stroke, National Institutes of Health, Bethesda, USA

[2]National Institute of Mental Health, National Institutes of Health, Bethesda, USA

Objectives: Two-photon microscopy (2PM) is a nonlinear optical imaging technique that allows visualization of cellular structure and function deep within the cortex, and followed longitudinally over days to months. Recently, transgenic marmoset models of Parkinson's disease, Alzheimer's disease, amyotrophic lateral sclerosis, and schizophrenia have been successfully produced, providing a research biological model that closely mirrors human conditions. In the present work, we aim to develop a longitudinal approach to quantify cerebral microvessels dynamics and neural activity in awake marmosets with 2PM.

Methods: Adult marmosets were gradually acclimated to a custom-designed body and head restraint system in the sphinx position for up to two hours. Following behavioral training, a 10-mm diameter polyetheretherketone cranial chamber was implanted over Broadman Area 3b, along with a headpost at the medioposterior skull to stabilize imaging. To visualize neuronal activity, AAV1-GCaMP5G virus was injected into the somatosensory cortex. This genetically encoded calcium indicator enables neuronal fluorescence changes during activation.

Results: After 14 days of recovery, 2PM of intravenously labeled blood plasma revealed vascular topology and enabled linescan measurement of red blood cell motion in microvessels 500 µm below the cortical surface in awake marmosets (Figure 1). 29% of GCaMP5G-labelled neurons were responsive to electrical stimulation of the wrist and showed fluorescence increase (Figure 2). Capillary density was 6,695 capillaries/mm3 with a median diameter of 6.4 µm, segment length of 67 µm, and tortuosity of 1.2 (arc-chord ratio). The median number of capillaries connecting penetrating arterioles to ascending venules was 8 branches. These vascular structures were similar to a control animal. Behavioral assessment before/after cranial chamber implantation demonstrates no significant impact on cognitive and motor functions (Figure 3). During awake imaging, 99.5% of capillaries had blood flow, indicating a robust cortical perfusion. When comparing isoflurane-anesthetized and awake imaging of the same animal, surface arterioles dilated by 16%, and decreased flow speed by 24%. After 139 days, image quality deteriorated to 150 µm of optical

penetration. GCaMP5G-labelled neurons were responsive at 135 days after viral delivery. Post-mortem immunohistochemistry confirmed ~3-mm diameter of GCaMP5G expression and astrocyte activation in the cortex.

Conclusions: These results demonstrate the capability to perform longitudinal 2PM imaging of cerebral microcirculation and neuronal activity in awake marmosets. This work provides a novel and insightful imaging technique to assess neurovascular coupling at the spatial resolution of the neurovascular unit, and allows for investigation of critical mechanisms in many neurological disorders.

Figure 1:

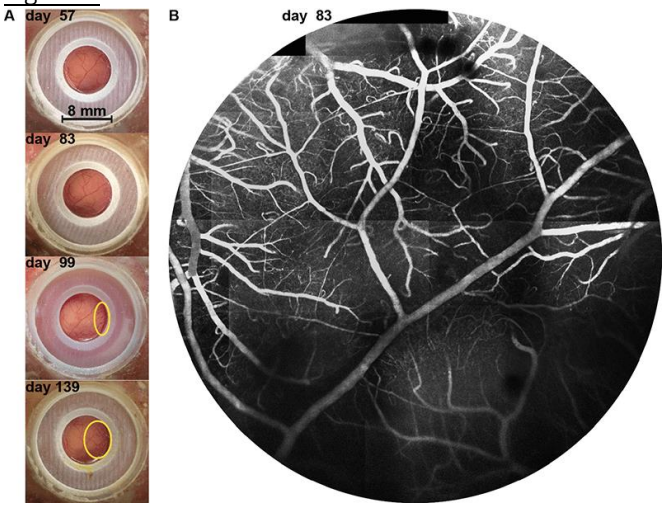

Figure 2:

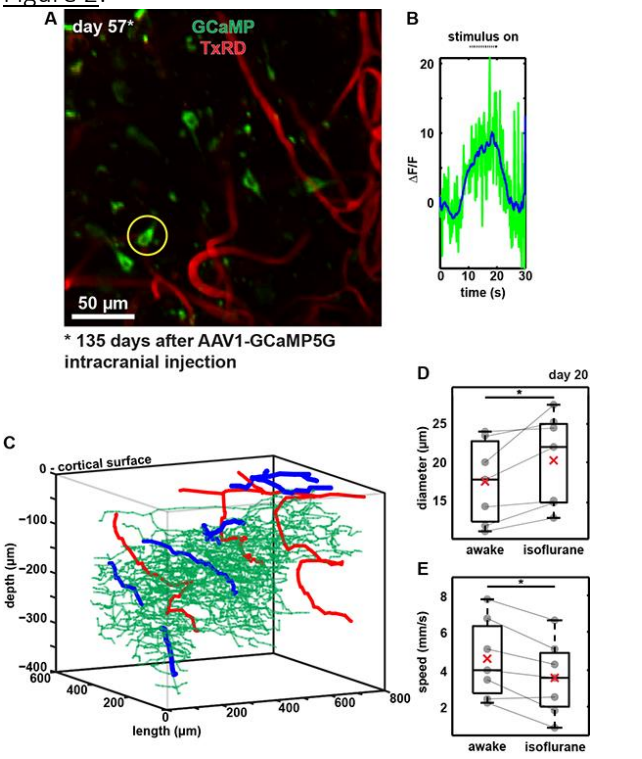

Figure 3:

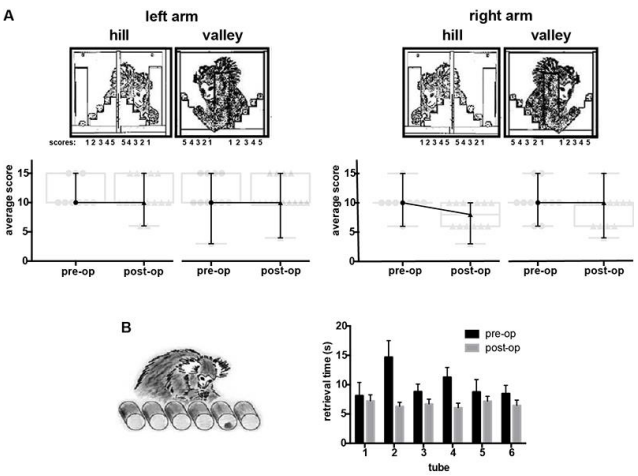

73
BRAIN-0765
Brain Oral Communication

Oral Session: Neurovascular Coupling: Physiology

ROLE OF INHIBITORY NEURON ACTIVITY ON VASCULAR REGULATION AND HEMODYNAMIC RESPONSES

A. Vazquez[1], *M. Fukuda*[1], *S.G. Kim*[1]
[1]*Radiology, University of Pittsburgh, Pittsburgh, USA*

Introduction

The role of inhibitory neuron activity on vascular regulation have been difficult to determine because it is difficult to stimulate and isolate inhibitory neuron activity in vivo, particularly in cortex. Recent advances in optogenetics allow for the selective stimulation of cortical inhibitory neurons. The goal of this work is to use this optogenetic model to investigate the contributions of inhibitory neuron activity, including g-aminobutyric acid (GABA) neurotransmission, on vascular regulation and hemodynamic signals.

Methods

Transgenic mice expressing Channelrhodopsin-2 (ChR2) under the control of the vesicular GABA transporter (VGAT) promoter were obtained from the Jackson Laboratory (Bar Harbour, ME) for experimentation. Mice were induced using ketamine and xylazine and placed in a stereo-taxic frame. An acrylic well was placed over the somato-sensory cortex and a craniotomy was performed. A fiber optic (125µm), electrode (to measure LFP and MUA) and laser Doppler flowmetry (LDF) probe (sensitive to CBF) were placed in the forelimb area. Different photo-stimulation parameters were tested using a 473nm laser light source. Photo-stimuli delivered for 4-sec at a frequency of 5-Hz were repeated every 60-sec for a total of 10 times. Experiments were performed under three conditions: control, glutamate receptor blockade (GRB) and GABA-and-glutamate receptor blockade (GGRB). The GRB condition was established by intra-cortical administration of ionotropic glutamate receptor antagonists APV (50mM) and NBQX (5mM) to block excitatory input to excitatory and inhibitory neurons while sparing GABA neurotransmission. Recent studies have found that inhibitory neuron activity can not only dampen excitatory activity, but also increase excitatory activity via inhibitory-to-inhibitory connections that disinhibit excitatory neurons. The GGRB condition was established by the administration of APV (50mM), NBQX (5mM) and BMI (0.5mM; a $GABA_A$ receptor antagonist) to isolate pre-synaptic inhibitory activity. Forelimb stimulation experiments were performed for comparison (1mA, 0.5ms pulses).

Results and Discussion

Photo-stimulation of inhibitory neurons under control conditions generated LFP and MUA responses that were effectively modulated by the photo-stimulus duration (Figure 1). More importantly, the evoked hemodynamic responses were much larger than those evoked by forelimb stimulation and they were also slower (longer time-to-peak; Figure 2). Inspection of the evoked LFP activity shows prolonged features similar to that of excitatory activity generated by forelimb stimulation. Preliminary experiments using two-photon calcium imaging were performed to visualize neuronal activity, inhibitory and excitatory. YFP-positive inhibitory neurons as well as many other cells, showed increases in neuronal activity (data not shown). These preliminary experiments suggest that the activity of inhibitory and excitatory neurons increases with inhibitory photo-stimulation under control conditions. Experiments were performed under GRB conditions show robust but slightly reduced MUA and hemodynamic responses relative to control (Figure 3). This condition is not sufficient to determine if GABA release plays a significant role in vascular regulation since post-synaptic inhibitory neuron activity is not blocked. Experiments were also performed under the GGRB condition. Electrophysiology experiments showed temporal narrowing of the LFP and significantly reduced hemodynamic responses (Figure 3). In summary, increasing inhibitory activity has a profound impact on vascular regulation and the hemodynamic response.

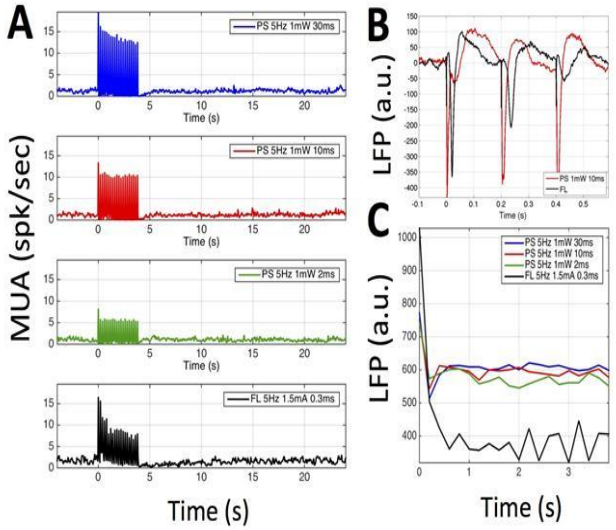

Figure-1.

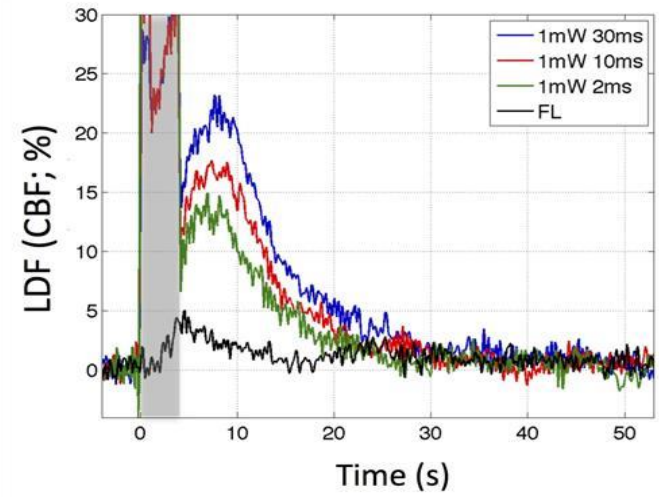

Figure-2.

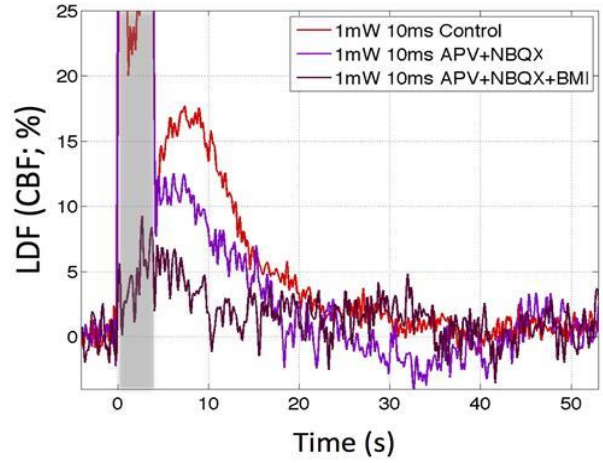

Figure-3.

74
BRAIN-0716
Brain Oral Communication

Oral Session: Neurovascular Coupling: Physiology

ASTROCYTIC DEPOLARIZATION INDUCED RAPID AND BROAD INCREASE IN CBF IN IN VIVO MOUSE CORTEX

K. Masamoto[1], M. Unekawa[2], T. Watanabe[3], H. Toriumi[2], H. Takuwa[4], H. Kawaguchi[4], I. Kanno[4], K. Matsui[5], K. Tanaka[6], Y. Tomita[2], N. Suzuki[2]
[1]Brain Science Inspired Life Support Research Center, Univ. of Electro-Communications, Tokyo, Japan
[2]Department of Neurology, Keio University School of Medicine, Tokyo, Japan
[3]Faculty of Informatics and Engineering, University of Electro-Communications, Tokyo, Japan
[4]Molecular Imaging Center, National Institute of Radiological Sciences, Chiba, Japan
[5]Division of Interdisciplinary Medical Science, Tohoku University Graduate School of Medicine, Sendai, Japan
[6]Department of Neuropsychiatry, Keio University School of Medicine, Tokyo, Japan

[Objectives] To examine the astrocytic role on the neurovascular coupling, specific manipulation of astrocytic activity is required. We introduced a recently developed mouse with genetically targeted expression of a light-gated cation channel, channelrhodopsin-2 (ChR2), in astrocytes. In this model, photo-stimulation to the ChR2-expressing astrocyte was shown to induce a transient depolarization of the astrocytic membrane potential depending on an irradiated light power and duration [1,2]. Here, we tested whether photo-stimulation to the ChR2-expressing astrocytes causes a local change in cerebral blood flow (CBF) in *in vivo* mouse cortex.

[Methods] A total of twenty-one Mlc1-tTA::tetO-ChR2(C128S)-EYFP double transgenic mice (10-30 weeks) were used for the experiments. ChR2(C128S) is opened by a blue light, and it requires an yellow/orange light to close. Thus, photo-stimulation was delivered with a 488-nm argon laser followed by a brief irradiation with 595-nm LED light. The irradiation spot evoked with the blue laser was a center of the parietal bone (0.5 mm in diameter), and the irradiation power (0.1-3.3 mW) and duration (0.5-3.0 sec) were varied to test the irradiation-dependences of the CBF. A skull over the somatomotor cortex of both hemispheres was exposed under urethane anesthesia, and a spatiotemporal dynamic CBF response to photo-stimulation was measured using laser speckle flowgraphy. Additionally, a pharmacological test was performed after the skull and dura were removed and topical application of drugs were conducted. The CBF responses to photo-stimulation were further compared between pre- and post-treatment in the same hemisphere.

[Results] A brief photo-stimulation induced a fast and transient increase in CBF (20-60% relative to the baseline), and the response magnitude relied on the irradiated laser power and duration. The evoked

response was reproducible for repeated photo-stimulation. An onset time of the CBF was 0.6 sec at the response foci where the blue laser was irradiated, while this CBF response spread widely (3.4 ± 2.2 mm^2) from the irradiation spot. Pharmacological manipulation further showed that a topical administration of either $BaCl_2$ (0.5 mM) or 4-aminopyridine (1 mM), known as potent inhibitors of K^+ channel activities, significantly reduced the CBF response to the ChR2-activation. However, topical administration of indomethacin (a non-selective cyclooxygenase inhibitor), tetrodotoxin (a sodium channel inhibitor), and MPEP (metabotropic glutamate receptor antagonist) had negligible effects on the CBF response to the ChR2-activation. These findings therefore indicate that the ChR2-evoked depolarization of astrocyte may induce K^+ signaling to the vascular smooth muscle cells.

[Conclusion] The ChR2-evoked depolarization of astrocytes may directly induce K+ signaling to the vascular smooth muscle cells. Thus, the optogenetic mouse model with ChR2-expressing astrocytes is a powerful tool for exploring a role of the cortical astrocytes in the neurovascular coupling.

References:

[1] Tanaka, K. F. et al. Cell. Rep. 2, 397-406 (2012).

[2] Sasaki, T. et al. Proc. Natl. Acad. Sci. U. S. A. 109, 20720-20725 (2012).

77
BRAIN-0740
Brain Oral Communication

Oral Session: Cellular Pathways of Ischemic Injury

THE NEURONAL ENDOPLASMIC RETICULUM (ER) UNDERGOES RAPID AND REVERSIBLE FISSION IN VIVO. THE ER FISSION-FUSION CORRELATES WITH CHANGES IN NEURONAL ACTIVITY FOLOWING CORTICAL SPREADING DEPRESSION.

K. Kucharz[1], *M. Lauritzen*[1]
[1]*Department of Healthy Ageing, University of Copenhagen, Copenhagen, Denmark*

BACKGROUND: The neuronal endoplasmic reticulum (ER) is the major intracellular Ca2+ store that modulates synaptic transmission and plasticity. The ER lumen maintains continuity through all neuronal compartments allowing ER to act as a signal integrating organelle for spatially separated events: synaptic activity and gene expression. Here, we reveal the occurrence and characterise the spatio-temporal properties of a transient rapid neuronal ER fission (=fragmentation) in vivo and correlate the phenomenon with changes in neuronal electrophysiology.

MATERIALS AND METHODS: The 2-photon microscopy was used to assess the neuronal ER structure in anesthetized transgenic mice expressing EGFP targeted to ER lumen. A custom-developed ER profile plot intensity variance (ER_{var}) analysis and fluorescence recovery after photobleaching (FRAP) was used to quantify the degree of ER fragmentation. The NMDAR hyperactivity, previously described to cause the ER structure alteration in neuronal cultures and organotypic slices, was induced using experimental model of cortical spreading depression (CSD). The intracellular Ca^{2+} was monitored with Asante Calcium Red (ACR), a novel red-shifted Ca^{2+} indicator. Simultaneously with imaging, we performed the electrophysiological assessment of direct current (DC) and local field potentials (LFPs) that reflect neuronal/synaptic activity. All experiments were approved by the Danish National Ethics committee.

RESULTS: The ER in its basal state appeared continuous with clear spine-ER morphology. The ER 3D reconstructions delineated the dendritic tree up to 450 μm below the brain surface. With the onset of CSD, in all investigated animals, the ER underwent rapid (~10s) fission, assuming the form of small, numerous and seemingly isolated fragments. With the recovery from DC tough, the ER regained its pre-CSD morphology within ~2-3min after the fission, as assessed optically and by ER_{var}. There was a high inverse correlation between DC change and the degree of ER fragmentation (DC vs. ER_{var}; Pearson's correlation; $r=-0.7791$; $p<0.001$; $n_{animals}=4$; $n_{neurons}=32$). Noteworthy, the cycle of ER fission-fusion could be induced multiple times within the same neuron in a train of evoked CSDs. The spatio-

temporal assessment of ER in relation to Ca^{2+} signal demonstrated that the ER fission is a highly localized process and the degree of ER fragmentation correlates with the amount of intracellular Ca^{2+} (ACR_{Ca2+} vs. ER_{var}; r=0.6609; p<0.001; $n_{animals}$=4; $n_{neurons}$=32). Interestingly, although ER appeared fused after the DC shift, the FRAP analysis revealed the existence of a neuronal ER fraction that remained isolated even ~2h after the onset of CSD. The initial increase and decline in the amount of non-continuous ER (measured with FRAP) corresponded to the loss and regain of neuronal activity expressed as the average of absolute LFPs ($ER\_FRAP_{immbobile\_fraction}$, $ER\_FRAP_{half\text{-}time}$ vs. $avgLFP_{abs}$; r=-0.8865, r=-0.8872, respectively; p<0.05; $n_{animals}$=5; $n_{neurons}$=14).

CONCLUSIONS: The neuronal ER can rapidly, reversibly and repeatedly alter its continuity in vivo. The phenomenon coincides with intracellular Ca2+ increase and the post-CSD recovery of neuronal activity correlates with the regain of neuronal ER continuity. The ER fission-fusion may be of relevance since the alteration of ER lumen continuity, even if transient, may have far reaching impact on Ca2+ signaling, homeostasis, synaptic activity and thus on many vital aspects of neuronal function.

78
BRAIN-0719
Brain Oral Communication

Oral Session: Cellular Pathways of Ischemic Injury

NOVEL DANGER SIGNALING MOLECULE PEROXIREDOXIN-1 INDUCES NEUROTOXIC MICROGLIAL ACTIVATION AFTER EXPERIMENTAL CARDIAC ARREST

I.P. Koerner[1], *S. Mader*[1], *M. Ikeda*[1]
[1]*Anesthesiology & Perioperative Medicine, Oregon Health & Science University, Portland, USA*

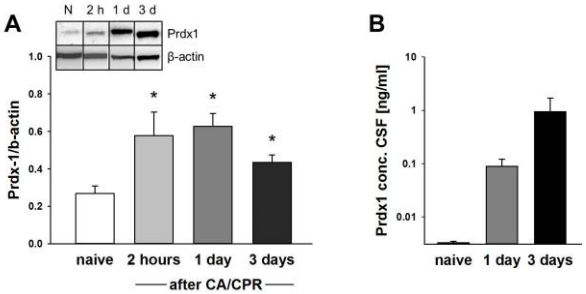

Objectives: Ischemic heart disease frequently manifests as cardiac arrest (CA). While recent advances in cardiopulmonary resuscitation (CPR) and critical care have improved survival after CA, brain injury that leads to long-term cognitive dysfunction remains a common problem among survivors. CA causes wide spread inflammation and activation of microglia, the brain resident immune cells, followed by neuronal death in ischemia-sensitive brain regions [1]. We hypothesized that injured neurons release a danger signaling molecule after CA, which activates microglia to a neurotoxic phenotype, and that neurotoxic microglia exacerbate neuronal death and functional deficit after CA. We tested whether the antioxidant protein Peroxiredoxin-1 (Prx1) acts as a danger signaling molecule after experimental CA.

Methods: In vivo: CA was induced in anesthetized and intubated male adult C57BL/6 mice by injection of potassium chloride. CPR was initiated after 10 min of CA. Hippocampal tissue was harvested and cerebrospinal fluid (CSF) collected 1 or 3 days after CA/CPR for quantification of Prx1 by immunoblot (tissue) or ELISA (CSF). Recombinant Prx1 was injected into the hippocampus of additional mice and microglial activation assessed by immunohistochemistry using Iba1 antibody 1 day later. In vitro: Primary cultured mouse neurons were exposed to oxygen-glucose deprivation (OGD) to simulate ischemia, and cell death assessed 1 day later. Neurotoxicity of primary mouse microglia was assessed by measuring neuronal death in microglia-neuronal co-cultures after OGD. Microglial release of cytokines was quantified by ELISA. Group differences were evaluated using ANOVA or Student's t-test, as appropriate. Results are mean±SEM.

Results: Prx1 protein was upregulated in mouse hippocampus within 2 hrs after CA/CPR (Fig. 1A) and released into the CSF. Prx1 was absent in CSF of

control mice, but readily detectable by ELISA on the first day after CA/CPR (Fig. 1B). Similarly, cultured neurons released Prx1 into the medium after OGD. This neuron-conditioned medium (NCM) induced a pro-inflammatory phenotype in cultured microglia, characterized by release of TNF-α (104±31 pg/10^5 cells vs 0.8±0.4 pg/10^5 untreated cells) and IL-β (11.4±6.5 vs 0±0 untreated). Similar release of pro-inflammatory cytokines was induced when microglia were treated with recombinant Prx1 (TNFα 1482±798, IL-1β 8.0±5), while depletion of Prx1 from neuron-conditioned medium by immunoprecipitation abolished the cytokine release. Microglia activated by NCM or recombinant Prx1 significantly increased neuronal cell death after OGD, compared to untreated microglia (NCM 37±6% death, Prx1 34±3%, untreated 25±5%, P<0.05). Finally, injection of recombinant Prx1 into the hippocampus caused morphologic activation of microglia that mimicked activation after cardiac arrest.

Conclusions: We identified Prx1 as a novel danger signaling molecule that is released by ischemia-injured neurons and activates microglia to a pro-inflammatory and neurotoxic phenotype, which exacerbates neuronal death. As Prx1 release after CA/CPR precedes microglial activation, it provides a promising new target for interventions aimed at reducing brain injury and subsequent dysfunction after CA/CPR by blocking inflammation and microglial neurotoxicity.

Reference: [1] Wang J J Cereb Blood Flow Metab. 2013 Oct;33(10):1574-81

79
BRAIN-0212
Brain Oral Communication

Oral Session: Cellular Pathways of Ischemic Injury

MIRNA PROFILING AND MODULATION FOLLOWING ISCHAEMIC STROKE

E.N.J. Ord[1], E.L. Low[1], S.L. Finnie[1], C. McDonald[1], M.A. Hamid[1], C. McCabe[2], J.D. McClure[1], I.M. Macrae[2], L.M. Work[1]
[1]Institute of Cardiovascular and Medical Sciences, University of Glasgow, Glasgow, United Kingdom
[2]Institute of Neuroscience & Psychology, University of Glasgow, Glasgow, United Kingdom

Objective: MicroRNAs (miRNAs), small non-coding RNA molecules (20-24 nucleotides), function to inhibit mRNA translation. They have key roles in normal CNS development and function, and have specific effecter roles in both pathogenesis and endogenous repair mechanisms following stroke. We aimed to profile miRNA changes in evolving and final peri-infarct tissue to explore the potential for therapeutic modulation.
Methods: To identify miRNAs with potential for therapeutic modulation, we profiled miRNA expression from the evolving (24h) and final (72h) peri-infarct tissue of adult spontaneously hypertensive stroke-prone rats (SHRSP) following 45min transient middle cerebral artery occlusion (tMCAO) using Openarray® rodent miRNA microarray cards v3.0 (Applied Biosystems). T_2-weighted magnetic resonance imaging allowed accurate dissection of peri-infarct tissue, with equivalent brain regions taken from time-matched shams (n=6/group). Validation of miRNA changes was performed using Taqman™ qRT-PCR with specific miRNA probes (n=9/group). To determine whether modulation of selected miRNAs could influence deleterious mechanisms in the ischaemic cascade, *in vitro* studies were performed on rat neuronal cell line B50 and rat glial cell line B92 subjected to 9hr hypoxia (1% O_2) and serum starvation with 24h reoxygenation in complete media±miRNA modulation (transfection using siPORT±miR*Vana* mimics or inhibitors). For *in vivo* miRNA modulation, miRNA mimic was delivered (complexed with 5% (v/v) Invivofectamine) stereotactically into the cortex (from bregma 1st injection: AP -2.4 mm, ML +4 mm, DV -1.5 mm; 2nd injection: AP +1.4 mm, ML +4 mm, DV -1.5 mm) or intranasally to naïve SHRSP (n=3/group) and animals sacrificed 7 days later.
Results: Out of 754 miRNAs evaluated, 89 were differentially regulated following tMCAO. Twenty two miRNAs underwent Taqman™ qRT-PCR validation using specific probes (n=9/group). Five miRNAs were significantly altered including miR-34b and miR-520b which were selected as "miRNAs of interest" due to their novelty, time-point of endogenous upregulation and targets. Upregulation of either miRNA in B50 cells demonstrated a

reduction in hypoxia-induced apoptosis, assessed qualitatively by Caspase-3 immunocytochemistry and quantitatively by cell death detection ELISA ($p<0.01$ vs hypoxic non-treated cells (NTC)). Upregulation of either miRNA in B92 cells significantly reduced superoxide production, assessed by electron paramagnetic resonance spectroscopy ($p<0.001$ vs hypoxic NTC). MiR-520b significantly lowered levels of lipid peroxidation in B92 cells, assessed by malondialdehyde assay ($p<0.01$ vs hypoxic NTC), and both were significantly effective in B50 cells ($p<0.01$ vs hypoxic NTC). Delivery of miRNA mimic into cortex (500 pmol/L; 11.7 µg/kg) or intranasally (9.6 nmol/L; 224 µg/kg) did not induce significant modulation of miRNA expression determined by Taqman™ qRT-PCR in naïve SHRSP brain tissue 7 days after delivery. Extracellular vesicles (EVs), isolated from SHRSP brain homogenates, were loaded with miRNA by electroporation. Delivery of miRNA–loaded EVs to B50 cells induced a marked and significant modulation of miRNA expression determined by Taqman qRT-PCR ($p<0.001$ vs NTC).

Conclusion: Taken together these data suggest miR-34b and -520b upregulation ameliorates damage following hypoxia/reoxygenation in neuronal and glial cell lines. Future studies will assess the effect of modulating these miRNAs *in vivo*.

Acknowledgements: We thank the Medical Research Council and British Heart Foundation for funding.

80
BRAIN-0512
Brain Oral Communication

Oral Session: Cellular Pathways of Ischemic Injury

AMNIOTIC MESENCHYMAL STROMAL CELL SECRETOME INDUCES PROTECTION AFTER BRAIN ISCHEMIA

F. Pischiutta[1], P. Romele[2], F. Marchesi[1], G. Cermisoni[1], E. Sammali[1], L. Brunelli[3], R. Pastorelli[3], M.G. De Simoni[1], O. Parolini[2], E.R. Zanier[1]
[1]Neuroscience, IRCCS - Mario Negri Institute for Pharmacological Research, Milano, Italy
[2]Centro di Ricerca E. Menni, Fondazione Poliambulanza, Brescia, Italy
[3]Environmental Health Sciences, IRCCS - Mario Negri Institute for Pharmacological Research, Milano, Italy

Objectives. Mesenchymal stromal cell (MSC) paracrine action now stands as the main driver of protection after acute brain injury, suggesting the potential for a cell-free therapeutic strategy. It is still debated, whether MSC neuroprotective effectors are secreted in response to an ischemic environment or also in unchallenged conditions. In this work we tested the effects of human amniotic-derived MSC (hAMSC) versus their secretome in an *in vitro* model of brain ischemia.

Methods. hAMSC were obtained from amnion of human term placentas[1] after informed consent. The conditioned medium (CM) containing the secretome was obtained culturing 10^6 hAMSC in 1ml serum-free medium for 5days[1]. Procedures involving animals were conducted in conformity with national and international laws and policies for ethical animal treatment. Cortical organotypic brain slices (200µm) from prefrontal cortex of C57BL/6 mouse (P1-3) were maintained in NB/B27 medium (Neurobasal, B27 1:50, P/S 1:100, L-glut 1:100) for 1week. Slices were subjected to oxygen-glucose deprivation (OGD) for 2h (hypoxic chamber: N_2=95%,CO_2=5%,O_2=0.1%,37°C; DMEM without glucose) to model ischemic injury. One hour after OGD, slices were cultured with: 1)NB/B27, 2)CM, 3)hAMSC (60000/cm^2) in a transwell system allowing only paracrine events. Cell death was evaluated by propidium iodide (PI) incorporation at 24 and 48h. Gene expression analysis was performed at 48h. Data analysis: one-way ANOVA, Tukey post-hoc test.

Results. A similar protection on organotypic brain slices was observed by CM or hAMSC post-OGD treatment as revealed by the decreased PI incorporation at 24h (mean±SD: CM:-40±27%, hAMSC:-25±24%) and 48h (CM:-48±30%, hAMC:-54±22%) after OGD. Gene expression analysis revealed that OGD reduced the neuronal marker MAP2 compared to controls and that CM and hAMSC treatments produced a significant rescue effect (CTRL:1.02±0.19%, OGD:0.25±0.07%, OGD+CM:0.48±0.21%, OGD+hAMSC:0.51±0.15%). Furthermore, protective conditions were associated with an increased expression of the microglial pan-

marker CD11b (CTRL:1.00±0.18, OGD:1.28±0.49, OGD+CM:2.88±0.64, OGD+hAMSC:3.35±0.85) and of the M2 protective marker Ym1[2] (OGD:0.87±0.63, OGD+CM:3.21±1.96, OGD+hAMSC:4.46±1.37) compared to OGD alone. CM, but not hAMSC treatment, induced a significant increase of the endothelial marker CD31 (CTRL:1.15±0.66, OGD:0.61±0.29, OGD+CM:2.93±1.02, OGD+hAMSC:1.06±0.40) and significantly attenuated the OGD induced down-regulation of BDNF (CTRL:1.05±0.32, OGD:0.14±0.05, OGD+CM:0.43±0.25, OGD+hAMSC:0.29±0.06) and VEGF (CTRL:1.00±0.20, OGD:0.18±0.02, OGD+CM:0.29±0.09, OGD+hAMSC:0.25±0.05).

In order to characterize the nature of the protective bioactive components contained in the hAMSC secretome, we first heat-treated CM (80°C, 30 min) and tested its efficacy on organotypic slices exposed to OGD at 48h. Heat-treated CM reduced PI incorporation after OGD with similar effects compared to unheated CM (CTRL:0.84±0.35%, OGD:100±39.48%, OGD+CM:24.44±8.19%, OGD+CM heat-treated:26.92±9.17%) suggesting that the protective effectors are not proteins with secondary structures. We then fractionated CM with vivaspin-column with a 2kDa cut-off. CM fraction <2kDa, but not >2kDa, induced a protective effect on organotypic slices 48h after OGD (CTRL:1.52±0.80%, OGD:100±59.34%, OGD+CM:42.52±28.13%, OGD+CM<2kDa:44.67±0.27%, OGD+CM>2kDa:106.42±41.33%) indicating that protective effectors have small molecular weight.

Conclusions. Our data show that hAMSC bioactive effectors are small molecules that protect the ischemic brain tissue by rescuing neurons and promoting M2 microglia polarization and trophic events. The definition of the protective cocktail secreted by hAMSC may open new therapeutic cell-free approaches for acute brain injury.

References.

[1]Rossi D, PlosOne.2012;7(10):e46956

[2]Zanier ER, Neurotherapeutics.2014;11(3):679-95

81
BRAIN-0449
Brain Oral Communication

Oral Session: Cellular Pathways of Ischemic Injury

INVESTIGATION OF THE ASSOCIATION OF THE EARLY RECOVERY OF CYTOCHROME-C-OXIDASE REDOX STATE WITH INJURY SEVERITY FOLLOWING HYPOXIA-ISCHEMIA IN THE NEONATAL PIG

P. Kaynezhad[1], A. Bainbridge[2], D. Price[2], G. Kawano[3], M. Ezzati[3], J. Rostami[3], K.D. Broad[3], L. Beichert[1], E. Rocha Ferreira[3], I. Fierens[3], A. Oliver-Taylor[3], X. Golay[4], N.J. Robertson[3], I. Tachtsidis[1]
[1]Medical Physics and Biomedical Engineering, University College London (UCL), London WC1E 6BT, United Kingdom
[2]Medical Physics and Bioengineering, UCLH NHS Foundation Trust, London NW1 2BU, United Kingdom
[3]Institute for Women's Health, University College London (UCL), London WC1E 6AU, United Kingdom
[4]Institute of Neurology, University College London (UCL), London WC1N 3BG, United Kingdom

Introduction: Broadband near-infrared spectroscopy (NIRS) offers the ability to measure the changes in brain tissue oxygenation, haemodynamics and the oxidation state of cytochrome-c-oxidase (oxCCO) non-invasively. Our group previously described the integration of broadband NIRS with Phosphorous Magnetic Resonance Spectroscopy (31P-MRS) to investigate Hypoxia-Ischaemia (HI) in new-born pigs and discussed the physiological/biochemical dynamic relationships of these measurements (A Bainbridge, 2014). We also recently demonstrated the use of broadband NIRS in the neonatal intensive care unit (G. Bale, 2014). The aim of this study is to investigate the correlations between the early recovery fractions of our broadband NIRS measurements with injury severity as assessed by 31P-MRS and systemic measurements, following HI in new-born pigs.

Methods: Experiments were under UK Home Office guidelines. 24 piglets (aged<24h) were subjected to transient HI (inspired oxygen fraction 9% and bilateral carotid artery occlusion for ~20 min).

Broadband NIRS and whole-brain 31P-MRS were acquired synchronously with the systemic data. Head transmission NIRS spectra (650-980nm) were collected and absolute changes in oxyhaemoglobin (Δ[HbO2]), deoxyhaemoglobin (Δ[HHb]) and cytochrome-c-oxidase oxidation state (Δ[oxCCO]) were measured; concentration changes in total haemoglobin (blood volume, Δ[HbT]=Δ[HbO2]+Δ[HHb]) and haemoglobin difference (blood oxygenation, Δ[Hbdiff]=Δ[HbO2]-Δ[HHb]) were then derived. 31P-MRS measurements of Inorganic phosphate (Pi)/epp, phosphocreatine(PCr)/epp, and total nucleotide triphosphate (NTP)/epp were measured and used as indicators of metabolic recovery following HI. NIRS, 31P-MRS and systemic data were used to estimate recovery fractions at the end of 1hour recovery period after HI based on the following formula:

Recovery-Fraction=([5min average at the end of recovery period]-[Nadir during HI])/([5min average at the end of baseline period]-[Nadir during HI])*100%

Pearson's correlation analysis was carried out (significance threshold $p<0.05$) between the recovery fractions of NIRS and 31P-MRS markers as well as the physiological data including heart rate and mean blood pressure.

Results: The recovery fractions of Δ[oxCCO] had a highly significant strong correlation with the recovery fractions of NTP/epp ($r= 0.83, p<0.000001$) and Pi/epp ($r= 0.85, p<0.000001$)(Fig.a,b). There was also a significant moderate relationship between the recovery fractions of Δ[HbT] with NTP/epp and Pi/epp ($r=0.48$ and $r=0.47$ respectively and $p<0.05$ for both). However, the recovery fraction of Δ[HbDiff] had no significant association with any of the MRS injury biomarkers (NTP/epp,$r= 0.32$ and Pi/epp,$r=0.31$, $p>0.1$). Only the recovery fraction of Δ[HbDiff] showed a moderate correlation with the recovery fraction of heart rate ($r=0.49$, $p<0.05$).

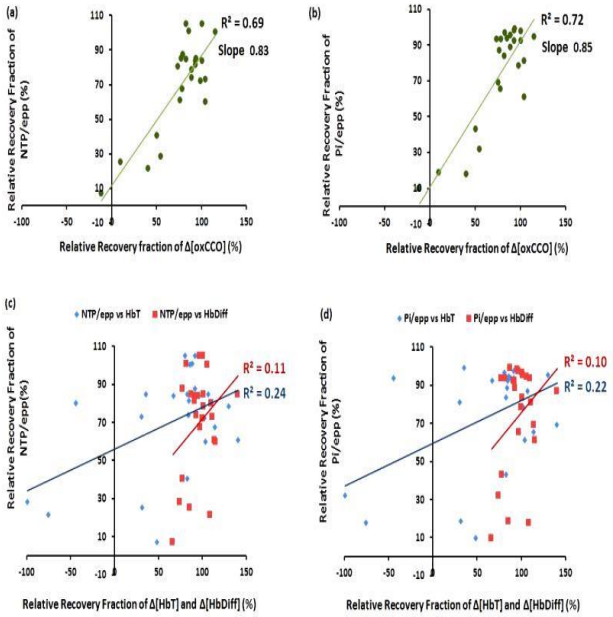

Figure: Recovery fractions of MRS metabolites against NIRS measures following HI- a&b: NTP/epp &Pi/epp vs Δ[oxCCO] - c&d: NTP/epp and pi/epp against Δ[HbT] and Δ[HbDiff]

Conclusions: The early recovery fraction of the broadband NIRS measurement of Δ[oxCCO] was strongly correlated with the recovery fractions of the 31P-MRS metabolic indicators following HI. This suggests that the recovery fraction of Δ[oxCCO] might be used as an indicator of early injury severity.

References:

[1]Bainbridge A. et al. NeuroImage. 15(102), 173-183 (2014)

[2]Bale G. et.al. Biomedical Optics Express, 5 (10), 3450-3466 (2014)

82
BRAIN-0542
Brain Oral Communication

Oral Session: Cellular Pathways of Ischemic Injury

DISRUPTING MAPK/CX43 INTERACTION REDUCES NEURONAL ISCHEMIC DAMAGE

M. Freitas-Andrade[1], J. Bechberger[1], D. Lu-Cleary[1], A. Williams[2], P.D. Lampe[3], C.C. Naus[1]
[1]Cellular and Physiological Sciences, Life Sciences Insitute, Vancouver, Canada
[2]Molecular Genetics and Microbiology, University of Toronto, Toronto, Canada
[3]Public Health Sciences Division, Fred Hutchinson Cancer Research Center, Seattle, USA

Objectives: In astrocytes, gap junction (GJ) channels are composed primarily of the channel protein, Connexin43 (Cx43). Cx43 GJ channels directly bridge the cytoplasm between coupled astrocytes and have been implicated in spatial buffering in stroke, contributing to neuroprotection. In contrast, Cx43 channels also exist on their own as single membrane hemichannels that directly connect the cell cytoplasm to the extracellular milieu. Hemichannel activity has been linked with deleterious outcome in stroke. The cytoplasmic C-terminus (CT) region of Cx43 has been shown to be critical for the regulation of GJ channel and hemichannel activity. Several lines of evidence indicate that mitogen-activated protein kinase (MAPK) phosphorylation of Cx43 can occur at specific CT residues (1). With regard to models of cerebral ischemia, several reports have demonstrated that Cx43 is an important factor in neuroprotection, specifically the CT (2). We investigated whether disrupting MAPK interaction with Cx43 CT affects neuronal survival in mice subjected to permanent middle cerebral artery occlusion (pMCAO).

Methods: We subjected wild-type (WT) and novel knock-in mice containing Cx43-MAPK null phosphorylation (Ser > Ala mutation, $Cx43^{S255/262/279/282A}$) mutant (MK4) to pMCAO. After 4 days of recovery, brain sections were histologically evaluated for infarct volume. Immunofluorescent analysis of astrocyte reactivity, microglial activation, Cx43 expression, vascular elements and apoptosis were also performed. *In vitro* Cx43 coupling and hemichannel activity was assessed in WT and MK4 astrocytes. In both *in vitro* ischemic astrocyte cultures and *in vivo* infarct mice, Cx43 protein expression was analyzed.

Results: We show that MK4 mice are associated with significantly reduced infarct injury after pMCAO. No significant differences in the cerebrovascular architecture were measured in both genotypes. In the penumbra, an increase in astrocyte reactivity was observed in the MK4 mice, compared with WT mice. Consistent with the infarct volume data, a significant reduction in cell death was also observed in MK4 mice. While no differences in GJ coupling were measured between WT and MK4 astrocytes, preliminary studies show a reduction in Cx43 hemichannel activity in MK4 astrocytes. In addition, an overall reduction in Cx43 protein levels was exhibited both in MK4 ischemic mice and in ischemic MK4 astrocytes.

Conclusion: These results suggest that specifically inhibiting MAPK phosphorylation of Cx43 provides neuroprotection in ischemic conditions. This may be mediated by reduced Cx43 hemichannel expression and activity in MK4 mice.

Supported by grants from the National Institutes of Health (GM55632) (PDL) and Heart & Stroke Foundation of Canada Fellowship (MFA). CCN holds a Canada Research Chair.

Reference:

1. Johnstone SR, Kroncke BM, Straub AC, Best AK, Dunn CA, Mitchell LA, Peskova Y, Nakamoto RK, Koval M, Lo CW, Lampe PD, Columbus L, Isakson BE. MAPK phosphorylation of connexin 43 promotes binding of cyclin E and smooth muscle cell proliferation. Circ Res. 2012 Jul 6;111(2):201-11.

2. Kozoriz, M. G., Bechberger, J. F., Bechberger, G. R., Suen, M. W., Moreno, A. P., Maass, K., Willecke, K. and Naus, C. C. The connexin43 C-terminal region mediates neuroprotection during stroke. J Neuropathol Exp Neurol 69(2): 196-206

85
BRAIN-0840
BrainPET

BrainPET Oral Session: Preclinical Imaging

EFFECTS OF FORMULATION VEHICLES ON PET TRACERS BRAIN UPTAKE IN DRUG STUDIES

C.C. Constantinescu[1], A. Tavares[1], O. Barret[1], D. Alagille[1], T. Morley[1], C. Papin[1], Y. Zhang[1], N. Twardy[1], G. Kudej[1], A. Vaughan[1], G. McLane[1], J.P. Seibyl[1], G.D. Tamagnan[1]
[1]Chemistry, Molecular NeuroImaging, New Haven, USA

Objectives: In PET drug blockade or displacement studies, several excipients often compose the vehicle used to formulate the drug under study, where it is assumed that the administration of these excipients do not modify the PET tracer brain uptake. However, we have found that such an excipient, solutol, led to a large increase of [^{18}F]FE-SPA-RQ brain uptake (> 5 times) compared to baseline and we have subsequently performed several PET experiments in non-human primates (NHP) to study the effect of different drug vehicles on the brain uptake of 4 PET radioligands: [^{18}F]MNI-444 (A2A receptor) , [^{18}F]MNI-659 (PDE10A), [^{18}F]FPEB (mGluR5 receptor), and [^{18}F]FE-SPA-RQ (Neurokinin 1).

Methods: Several formulations were tested: 20% solutol, 10% ETOH in saline (vehicle 1) against [^{18}F]MNI-444, [^{18}F]FPEB and [^{18}F]FE-SPA-RQ, 33% polyethylene glycol 400 (PEG400) in saline (vehicle 2) and 20% Hydroxypropyl beta-Cyclodextrin (HPbCD) 10% ETOH in acetate buffer 4.5 pH (vehicle 3) against [^{18}F]FE-SPA-RQ, and 30% PEG400 50% propylene glycol in acetate buffer 4.5 pH (vehicle 4) against [^{18}F]MNI-659. PET tracers were delivered either as a bolus followed by a constant infusion (B/I) ([^{18}F]MNI-444, [^{18}F]MNI-659 and [^{18}F]FPEB), or as a bolus ([^{18}F]FE-SPA-RQ) in baboon (*Papio anubis*) or rhesus macaque (Macaca mulatta). For the B/I studies, the vehicles (15-30 ml) were infused over 5-15 minute at 120 min post injection of the tracer (displacement study conditions), and for the PET tracer bolus studies the vehicles were infused during the whole study, starting at 60 min before tracer administration (blockade study conditions). Dynamic images were acquired over 210-240 min for B/I and 180 min for bolus studies. Blood samples were collected throughout and tissue time-activity curves together with metabolite-corrected plasma activity were used to compute steady-state distribution volumes (V_T) before and after vehicle administration.

Results: Following administration of vehicle 1 (post-tracer injection), [^{18}F]MNI-444 V_T increased by 26-30% in high binding regions (putamen, caudate) and by 57-71% in low binding regions, whereas [^{18}F]FPEB V_T change was low (~3 ± 4%) across all brain regions. For [^{18}F]FE-SPA-RQ, administration of vehicle 1 (pre-tracer injection) led to an increase of V_T in putamen of 750%, whereas vehicles 2 and 3 caused more moderate changes of 10% and -18%, respectively. For [^{18}F]MNI-659, administration of vehicle 4 induced a V_T increase of ~6% in high binding regions (putamen) and ~30% in low binding regions (cortex).

Conclusions: These results demonstrated that the vehicle used to formulate a drug can affect the PET tracer brain uptake and that this effect, which can be subtle or dramatic, is PET tracer and vehicle dependent. This is of particular importance in that it may affect drug occupancy estimates, and validation studies for a particular vehicle with a particular tracer may have to be considered prior to a dose occupancy study.

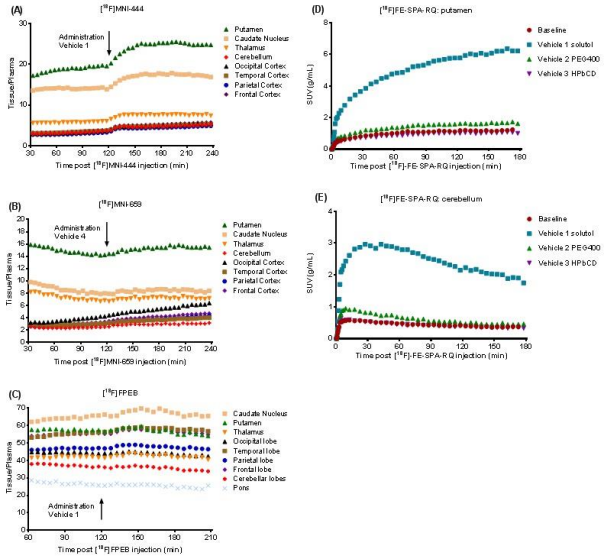

Figure 1. B/I studies : tissue to metabolite corrected plasma activity of (A) [^{18}F]MNI-444, (B) [^{18}F]MNI-659, and (C) [^{18}F]FPEB. Bolus studies: standard uptake

value (SUV) curves of [^{18}F]FE-SPA-RQ in (D) putamen, and (E) cerebellum at baseline and post-administration of vehicles 1-3.

86
BRAIN-0481
BrainPET

BrainPET Oral Session: Preclinical Imaging

PET IMAGING OF THE ALPHA-7 NICOTINIC ACETYLCHOLINE RECEPTOR WITH 18F-ASEM AND 18F-DBT-10 IN THE NONHUMAN PRIMATE: A COMPARATIVE STUDY.

A.T. Hillmer[1], M.Q. Zheng[1], D. Holden[1], M. Scheunemann[2], S. Li[1], S. Lin[1], D. Labaree[1], W. Deuther-Conrad[2], R. Teodoro[2], R.E. Carson[1], P. Brust[2], Y. Huang[1]
[1]PET Center, Yale University, New Haven, USA
[2]Neuroradiopharmacy, Helmholtz-Zentrum Dresden-Rossendorf, Leipzig, Germany

Objectives: The homomeric α7 subtype of nicotinic acetylcholine receptors (nAChRS) is an important target for the investigation of schizophrenia, Alzheimer's disease, and substance dependence. ^{18}F-ASEM is an α7-nAChR specific PET radioligand previously characterized in both nonhuman primates[1] and humans[2], while ^{18}F-DBT-10 is a recently developed candidate radioligand for the same site[3]. This work directly compares the pharmacokinetic and imaging properties of ^{18}F-ASEM and ^{18}F-DBT-10 in nonhuman primates.

Methods: ^{18}F-ASEM and ^{18}F-DBT-10 were prepared by nucleophilic substitution of their respective precursor with K^{18}F/Kryptofix$_{222}$. Imaging experiments were carried out on a Focus-220 scanner. Arterial blood samples were obtained for metabolite analysis and generation of input function. First scans consisted of high specific activity radiotracer administered as a bolus followed by 240 min PET data acquisition in two rhesus monkeys. After at least two weeks, additional PET scans administered unlabeled ASEM prior to radiotracer as blocking studies to assess the extent of specific binding. Data were analyzed with the one- and two-tissue compartment models (1TCM & 2TCM) to determine regional distribution volumes (V_T). Lassen plots were used to assess receptor occupancy.

Results: Both ^{18}F-ASEM and ^{18}F-DBT-10 were produced in high specific activity and radiochemical purity. The metabolism rates differed between subjects with the same rank order, yielding a higher parent fraction at 120 min postinjection of ^{18}F-DBT-10 (M1=15%; M2=54%) compared to ^{18}F-ASEM (M1=6%; M2=35%). Greater plasma free fractions were also observed for ^{18}F-DBT-10 (18±2%) than ^{18}F-ASEM (13±3%). Tissue kinetics was faster for ^{18}F-ASEM. The 2TCM better described the PET data for both radiotracers. Slightly greater V_T values were measured for ^{18}F-DBT-10 (35-58 mL/cm^3) than ^{18}F-ASEM (32-53 mL/cm^3). Regional V_T values followed the same rank order for both tracers: thalamus > frontal cortex > striatum = temporal cortex > hippocampus > occipital cortex > cerebellum. Blocking with cold ASEM decreased V_T/f_P from baseline levels in a dose-dependent manner (^{18}F-ASEM: 39% occupancy for 0.9 mg/kg ASEM dose; ^{18}F-DBT-10: 30% occupancy for 0.7 mg/kg, and 64% occupancy for 1.2 mg/kg) throughout the brain, demonstrating binding specificity of both radiotracers and indicating no suitable reference region in rhesus monkeys.

Conclusions: Both ^{18}F-ASEM and ^{18}F-DBT-10 have suitable properties to image α_7 nAChRs with PET in nonhuman primates.

References:

[1]Horti AG, et al. *J Nucl. Med.* 2014; 55:672-677.
[2]Wong DF, et al. *Mol. Imaging Biol.* 2014; 16:730-738.
[3]Kranz M, et al. *J. Nucl. Med.* 2014; 55 (Supplement 1):1143.

87
BRAIN-0624
BrainPET

BrainPET Oral Session: Preclinical Imaging

OPEN FIELD PET: A SYSTEM FOR SIMULTANEOUS BRAIN PET AND BEHAVIORAL RESPONSE MEASUREMENTS IN FREELY MOVING RATS

A. Kyme[1], J. Eisenhuth[1], G. Angelis[1], R. Fulton[1], V. Zhou[1], K. Popovic[1], K. Clemens[2], A. Parmar[3], M. Akhtar[4], G. Pascali[3], G. Hart[1], S. Meikle[1]
[1]Brain and Mind Research Institute, University of Sydney, Sydney, Australia
[2]School of Psychology, University of New South Wales, Sydney, Australia
[3]Division of LifeSciences, Australian Nuclear Science and Technology Organisation, Sydney, Australia
[4]University of Sydney, Brain and Mind Research Institute, Sydney, Australia

Objectives:

Small animal PET has the potential to play an important role in understanding the molecular pathways regulating decision-making and behavior under normal and pathological conditions. However, the use of anaesthesia precludes the study of behavioral responses to sensory stimuli and/or drug administration during PET studies. We have developed Open Field PET for imaging awake, unrestrained rats in a conventional microPET scanner while simultaneously recording behavioral outputs following the delivery of controlled stimuli. Here we present the system design, data acquisition and processing methodologies and initial animal studies demonstrating its capabilities.

Methods:

The animal is placed in a 20x12cm^2 chamber constructed from lightweight 3D printed materials. The chamber is positioned within the field of view (FoV) of a microPET Focus 220 scanner (Siemens Healthcare Molecular Imaging, USA) and attached to a 6-axis robot (Seiko Corp., Japan) adjacent to the scanner. The changing pose of the animal's head is measured at up to 24Hz using two MicronTracker stereo-optical motion tracking systems (Claron Technology Inc., Canada) positioned on either side of the PET scanner (Kyme et al, 2011) while the animal moves freely within the chamber. Pose data are used to smoothly adjust the position of the chamber within the PET FoV (Zhou et al., 2013) and to correct coincidence events for motion within a list mode MLEM reconstruction algorithm (Rahmim et al., 2008).

Two adult male Sprague-Dawley rats were administered 45MBq (<1 nmol) [^{11}C]raclopride via an indwelling jugular vein catheter and imaged in the Open Field system for 50min. One animal was administered 2 mg.kg^{-1} of unlabelled raclopride (D2 antagonist) and the other animal 1 mg.kg^{-1} of sumanirole (full D2 agonist) 20 minutes after tracer injection. Dynamic PET data were analysed by least squares fitting striatal and cerebellar time-activity curves with the lp-ntPET ligand displacement model (Normandin et al., 2012). The posterior probability distributions of displacement parameters were further analysed using an Automated Bayesian Computation rejection algorithm (Marin et al., 2011). Behavioral data were analysed by measuring absolute head displacement as a proxy for locomotor activity before and after drug injection and compared with the timing and magnitude of [^{11}C]raclopride displacement.

Results:

Both drugs caused a measurable displacement of [^{11}C]raclopride which corresponded to their injection times, i.e. approximately 20min (figure 1). In the case of sumanirole the displacement also correlated with increased locomotor activity (492%), consistent with agonist effects on the indirect thalamo-striatal dopaminergic pathway. The displacement was similar in magnitude ($k_{2a}(t)$ = 1.5-2x baseline) for the two studies but more prolonged in the case of raclopride than sumanirole.

Conclusions:

The Open Field PET technique thus allows simultaneous measurements of PET derived changes in regional receptor binding and behavioral

responses due to controlled stimuli in conscious unrestrained animals.

References:

1. Kyme et al., PLoS ONE doi:10.1371/journal.pone.0021727, 2011.

2. Zhou et al., IEEE Trans Nucl Sci 60:3423-3431, 2013.

3. A. Rahmim et al., IEEE Trans Med Imag 27:1018-1033, 2008.

4. M.D. Normandin et al., NeuroImage 59: 2689–2699, 2012.

5. J-M. Marin et al., arXiv:1101.0955v2 [stat.CO], 27 May 2011.

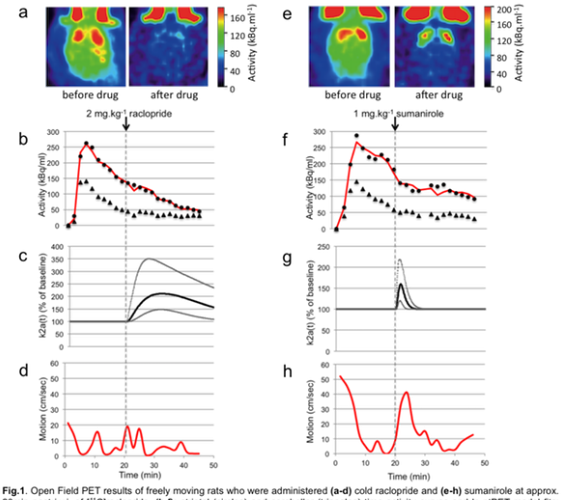

Fig.1. Open Field PET results of freely moving rats who were administered **(a-d)** cold raclopride and **(e-h)** sumanirole at approx. 20min post i.v.i. of [^{11}C]raclopride. **(b,f):** striatal (circles) and cerebellar (triangles) time-activity curves and Ip-ntPET model fits; **(c,g)**: model predicted displacement curves (bold curve=median, dashed curve=+/-1 quartile); **(d,h):** locomotor activity.

88
BRAIN-0478
BrainPET

BrainPET Oral Session: Preclinical Imaging

UNCOUPLING BETWEEN STRIATAL DOPAMINE TRANSPORTER AND GLUCOSE METABOLISM IN DIET INDUCED OBESITY

C. Malbert[1], *N. Coquery*[2]
[1]*Dept of Human Medecine, Ani-Scans, St Gilles, France*
[2]*Dept of Human Medecine, Ani-Scans and ADNC, St Gilles, France*

Introduction: Dopamine receptor was down regulated in obese animals and humans brain (Nummennmaa et al, 2012). Data are conflicting about the density of dopamine transporter in obese striatum. Furthermore, while striatal D2R availability is negatively associated with frontocortical glucose metabolism in obese patient (Volkow et al, 2004), the impact of obesity on striatal metabolism is unknown. Methods: Fourteen adults mini-pigs were imaged for dopamine transporter and glucose metabolism in lean and obese conditions. Obesity was induced by high fat, high glucose diet supplied at 200% metabolic requirement (measured by indirect calorimetry) during 3 months. Brain glucose metabolism was obtained using PET imaging (HR+ Siemens) after the IV injection of 250 MBq FDG (IBA). The density of dopamine transporter was evaluated using SPECT imaging (Millenium, GE) after the IV injection of 180 MBq DatScan (GE). Sinograms were corrected for attenuation using STIR software. FDG images were coregistered against a PET template (n=20 animals) obtained using the same machine and identical pig breed in our laboratory. DATScan images were also coregistered using a DATscan template (n=10 animals). Both templates were within the same tridimensionnal reference i.e. a pig brain atlas consisting in 70 paired structures and 30 unpaired ones (Saikali et al, 2010). Coregistration was achieved using FNIRT from FSL software. The amount of radioactivity in specific areas was obtained using Pmod software adapted to our pig brain atlas with SVC applied. Data afte normalisation were also analysed without apriori using SPM8 software. Results: The animals almost doubled their weight during the three months high calorie, high fat/glucose diet (87 ± 4.4 versus 36 ± 3.9 Kg). Striatal dopamine transporter density expressed as the ratio between striatum vs occipital cortex was significantly less in the obese than in lean situation (1.8 ± 0.04 vs 1.6 ± 0.02, $p<0.01$). Inversely, the striatal glucose metabolism expressed as the ratio between striatum vs cerebellum was significantly greater in the obese than in the lean condition (1.4 ± 0.02 vs 2.3 ± 0.02, $p<0.01$). Identical figures were obtained with statistical parameter mapping analyses. Conclusions: Our results demonstrated clearly a reduced density of striatal dopamine transporter in morbid obese animal. This was associated with an

increased striatal metabolism that might compensate for changes in synaptic dopamine availability. This uncoupling might a critical mechanism to explain overeating in obesity.
Figure 1 - Statistical image showing the decreased dopamine transporter density in obese compared to lean condition (shades of blues mean that the radioactivty is less in obese than in lean condition whereas shades of red mean that the radioactivity is more in obese than in lean condition) at the striatal level. The striatum is highlighted in white underlined with orange line for comprehension. It is visible arround the most intense blue spot

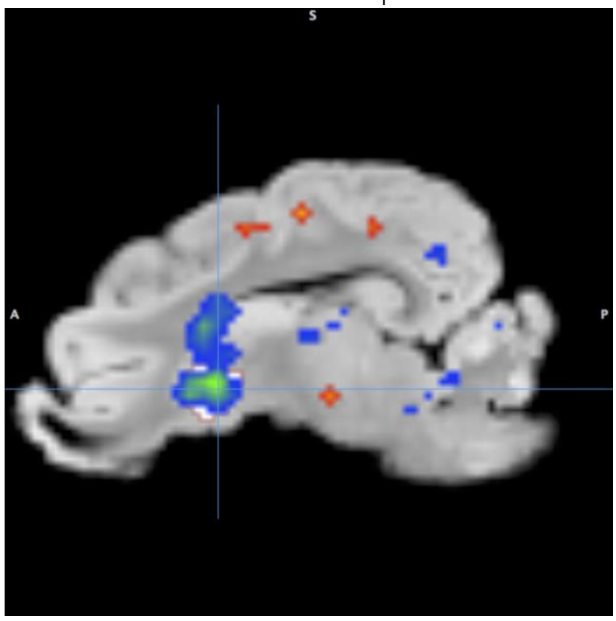

89
BRAIN-0786
BrainPET

BrainPET Oral Session: Preclinical Imaging

TSPO AVAILABILITY IS A ROBUST MEASURE OF SEVERITY IN A RAT MODEL OF MULTIPLE SCLEROSIS

A. Kesingland[1], E. Browne[2], C. Coello[1], S.P. Tang[1], N. Matusiak[1], N. Keat[1], B. Nuesslein-Hildesheim[3], R. Reynolds[2], L. Wells[1]
[1]Radiochemical Sciences, Imanova Centre for Imaging Sciences, London, United Kingdom
[2]Division of Brain Sciences, Imperial College London, London, United Kingdom
[3]Autoimmunity Transplantation & Inflammation Disease Area, Novartis Institutes for BioMedical Research, Basel, Switzerland

Objectives

Increased expression of 18kDa translocator protein (TSPO) by activated glia in the CNS has been reported in various neuroinflammatory conditions[1,2]. Positron emission tomography (PET) with the new generation TSPO radioligands may provide a sensitive and non-invasive approach for quantifying inflammatory processes *in vivo.* Myelin oligodendrocyte glycoprotein (MOG)-induced experimental autoimmume encephalomyelitis (EAE) is an established preclinical model of multiple sclerosis. We investigated whether the change in TSPO availability induced in the EAE model can be detected *in vivo* using the TSPO ligand [^{11}C]PBR28.

Methods

All procedures were carried out in accordance with the UK Home Office Animal (Scientific Procedures) Acts 1986. Recombinant MOG corresponding to the N-terminal extracellular domain of mouse (rmMOG,1–116a.a.) was administered intradermally in the dorsal aspect of the tail base of Female Dark Agouti (DA) rats. Animals were weighed and scored daily for clinical signs of EAE[3]. On the study day, anaesthetised rats received an intravenous administration of 15.4±11MBq of [^{11}C]PBR28. After 60mins, the spinal cord was removed, divided into sections from cervical to sacral and the radioactivity associated with each section (SUV) determined by gamma counting. Seven of the rats also underwent a 60min dynamic PET-CT scan. The PET data were reconstructed (2D FBP with scatter and CT attenuation correction), regions of interest were drawn on the sacral and cervical spinal cord areas and the uptake of radioligand (SUV) determined.

Results

A heterogeneous uptake of [^{11}C]PBR28 was observed in the spinal cord of rats in which EAE clinical signs were observed. The peak tissue uptake of [^{11}C]PBR28, measured by *ex vivo* gamma counting, was significantly higher in rats in which EAE clinical symptoms were observed compared with rats that

did not exhibit any clinical signs (mean SUV_{PEAK}, 4.8±2 vs 2.5±1 respectively, t-test, $P<0.05$). [^{11}C]PBR28 uptake was positively correlated with the degree of clinical severity observed (SUV_{PEAK} compared with Clinical $Score_{PEAK}$ Pearson R^2= 0.64, $P<0.05$; SUV_{PEAK} compared with Clinical $Score_{MEAN}$ Pearson R^2=0.70, $P<0.05$; **Figure 1**). Image derived SUVs were generated for the cervical and lower-lumbar to sacral spinal regions, but not other spinal areas due to significant spillover effects from radioactivity in the lung and liver. The PET image derived SUVs correlated well with the associated SUV determined by tissue gamma counting (Cervical $SUV_{PETvsTissue}$ Pearson R^2=0.88, Sacral $SUV_{PETvsTissue}$ Pearson R^2=0.70, Spinal cord $SUV_{PETvsTissue}$ Pearson R^2=0.75).

Conclusions

The uptake of [^{11}C]PBR28 was robustly correlated with the clinical severity of EAE observed in rats treated with rmMOG. Preclinical [^{11}C]PBR28 PET can be used as a measure of severity in longitudinal studies for focal EAE models targeting the sacral or cervical spinal areas. Further, *in vitro* work correlating the increase in [^{11}C]PBR28 uptake to an increase in neuroinflammation and spinal lesions is on-going.

References

[1] Abourbeh G et al., J NeuroSci, 2012;32:5728-36

[2] Xie L et al, J Neuroimmune Pharmacol 2012;7:231-42

[3] Papadopoulos *et al*. J Neurosci Res, 2010; 88:346-59

Correlation of the peak uptake of [^{11}C]PBR28 in the spinal cord of rats treated with rmMOG with the average clinical severity score.

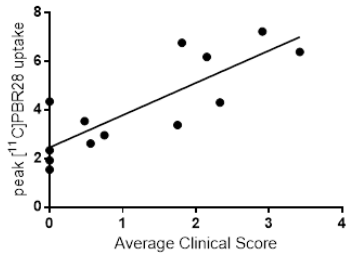

90
BRAIN-0454
BrainPET

BrainPET Oral Session: Preclinical Imaging

[18F]DPA-714 PET IMAGING IN PRE-CLINICAL MODELS OF HUMAN GLIOMAS

H. Pigeon[1], R. Boisgard[1], F. Caillé[1], F. Dollé[1], A.H. Jacobs[2], A. Winkeler[1]
[1]Inserm / CEA / Université Paris Sud UMR 1023 – ERL 9218 CNRS IMIV, CEA, Orsay, France
[2]European Institute for Molecular Imaging, Westfälische Wilhelms University Münster, Münster, Germany

Objectives

The 18 kDa translocator protein (TSPO) is a protein of the outer mitochondrial membrane widely expressed in peripheral organs. TSPO expression in the brain is low but its expression is dramatically increased after glial cell activation and has become a well-characterized marker for neuroinflammation. Moreover, TSPO expression has also been shown in some cancers including gliomas. TSPO imaging can be performed using positron emission tomography (PET) with the specific radioligand [^{18}F]DPA-714. As demonstrated in a rat glioma model, TSPO imaging in glioma monitors TSPO-positive neoplastic and to a lesser amount TSPO-positive inflammatory cells (Winkeler et al., 2012). To study a) the use of [^{18}F]DPA-714 PET imaging in human gliomas and b) the impact of the tumor microenvironment, in particular glioma-associated inflammation, we have started to characterize an angiogenic and an invasive human glioma model for in vivo imaging using [^{18}F]DPA-714 PET as well as immunohistochemistry (IHC) with dedicated human and murine TSPO antibodies.

Methods

$2x10^5$ human glioma cells (angiogenic, U87dEGFR or infiltrative) were stereotactically implanted in the striatum of nude mice (n=4 or n=6, respectively). To monitor tumor growth, 30 minutes [^{18}F]DPA-714 PET scans were acquired 10 days (U87dEGFR) or 1, 3, 5, 7 and 9 weeks (infiltrative) post-inoculation. Validation

of PET findings was done by *ex vivo* autoradiography and IHC using specific human and murine TSPO antibodies.

Results

Ten days after cell implantation significantly higher uptake of [^{18}F]DPA-714 has been demonstrated in human U87dEGFR tumors as compared to the contralateral brain (%ID/cc: 0.9 ± 0.1 and 0.4 ± 0.; p < 0.01) with a tumor-to-brain ratio of 2.2 ± 0.1. Furthermore, immunohistochemistry confirmed TSPO expression within the tumor. IHC using human and mouse specific TSPO antibodies allowed distinction between tumoral and stromal TSPO, indicating the presence of TSPO-positive stromal cells within the glioma (see Figure). In contrast tumor-to-contralateral-brain ratios in the invasive model ranged from 1.2 to 1.7, with a significantly higher uptake in the tumor only after 9 weeks post implantation (p<0.05), which was confirmed by *ex-vivo* autoradiography (p< 0.0001).

Conclusion

First results demonstrate that imaging of TSPO expression *in vivo* using [^{18}F]DPA-714 PET is feasible in the human U87dEGFR glioma model. Distinction between tumoral and stromal TSPO could be achieved by *ex vivo* IHC, which will be of use to help studying changes of tumoral and stromal TSPO expression during tumor progression and therapy. However, kinetics of TSPO imaging in the infiltrative glioma model have to be further investigated and compared with *ex vivo* IHC and autoradiography at earlier time points.

This work was supported by the European Union's Seventh Framework Programme [FP7/2007-2013] INMiND (Grant agreement no. 278850)

References

Winkeler, A. et al., 2012. Eur J Nucl Med Mol Imaging.

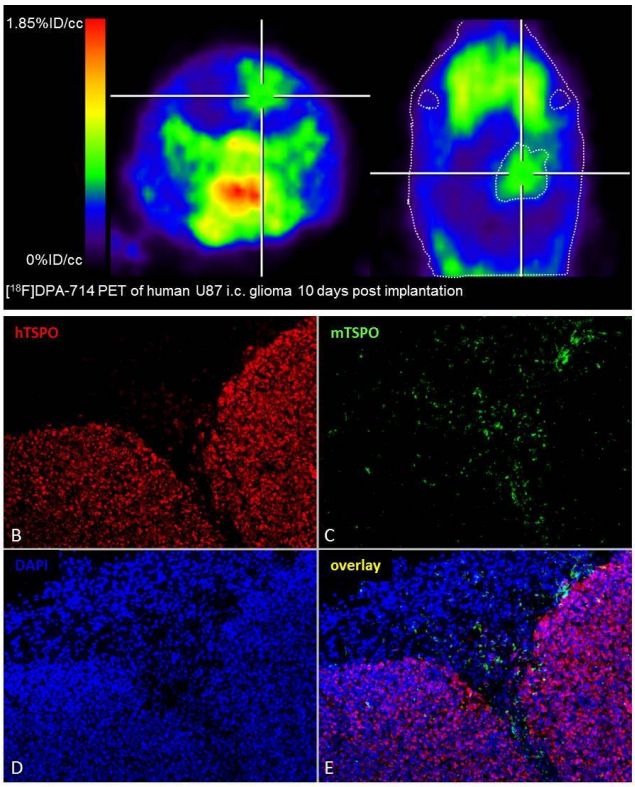

Figure: PET imaging of intracranial human U87dEGFR glioma using the specific TSPO radioligand [^{18}F]DPA-714. A volume-of-interest analysis indicated a tumor-to-contralateral ratio of 2.2±0.1 (**A**). Immunohistochemistry of whole coronal brain sections from the same animal demonstrated tumoral (**human, B**) and stromal (**mouse, C**) TSPO expression.

93
BRAIN-0964
BrainPET Symposium

Frontiers in Brain PET Imaging

Advances in MR/PET for studies in brain Function

B. Rosen[1]
[1]*q, Harvard, Boston, USA*

The simultaneous acquisition of both positron emission tomography (PET) and magnetic resonance imaging (MRI) data offers an exciting opportunity to merge anatomical, physiological, metabolic, and molecular information in a single examination setting. This is especially relevant in studies of the brain, where many fundamental questions remain on the linkage between structure and function, and where even basic principals of the interactions between physiological changes such as cerebral blood flow, neuronal "activity", and neuroreceptor function are yet to be fully elucidated. This talk will first describe the technological principals

underpinning such combined instruments, including changes in both the PET and MRI architectures which allow such instruments to be cross-compatible. The talk will then discuss how combining information from both modalities can be used to explore structure/function relationships, and how the simultaneous acquisition of data can provide information that is difficult to obtain using sequential acquisitions. Finally, some clinically relevant examples will be presented to highlight the future potential of this tool for advanced diagnostic evaluation of neurolopsychiatric diseases.

94
BRAIN-0961
BrainPET Symposium

Frontiers in Brain PET Imaging

Molecular tools for imaging misfolded proteins

C.A. Mathis[1]
[1]*Radiology, University of Pittsburgh, Pittsburgh, USA*

A variety of neurodegenerative diseases are pathologically characterized by the aggregation of specific proteins, such as extracellular aggregates of amyloid-β in senile plaques and intracellular aggregates of hyperphosphorylated tau in neurofibrillary tangles observed in Alzheimer's disease or intracellular aggregates of α-synuclein in Lewy bodies and Lewy neurites in Parkinson's disease. The utilization of positron emission tomography (PET) radioligands for the in vivo characterization of these aggregated proteins likely will play a critical role in defining pathological processes and guiding therapeutic treatment of these diseases and others characterized by abnormal protein aggregations. [C-11]-Labelled Pittsburgh compound B (PiB) was the first successful PET imaging agent to selectively target one of these aggregated proteins (amyloid-β), and selective targeting is important because many neurodegenerative diseases contain two or more different types of aggregated proteins. Worldwide investigations using PiB and four closely related F-18 analogues, now numbering in the tens of thousands, have helped identify the time course and pattern of amyloid-β plaque deposition characteristic of Alzheimer's disease a decade or more before the clinical symptoms of dementia. While recent progress has been realized in developing selective and potent tau PET tracers, efforts to develop selective α-synuclein radioligands remain a work in progress. The talk will highlight the considerations and challenges of designing PET radioligands for advancing scientific knowledge of the role aggregated proteins play in neurodegenerative diseases.

95
BRAIN-0982
BrainPET Symposium

Frontiers in Brain PET Imaging

Beyond a single target: Multi-modal & neural pathway imaging

D. Martinez[1], *M. Slifstein*[1], *N. Nablusi*[2], *M.Q. Zheng*[2], *J. Ropchan*[2], *N. Urban*[2], *R.E. Carson*[2], *Y.Y. Huang*[2]
[1]*Psychiatry, NYSPI/Columbia UNiversity, New York, USA*
[2]*Yale University School of Medicine, Yale PET Center, New Haven, USA*

The goal of this study was to use Positron Emission Tomography (PET) to investigate the neurobiology of cocaine addiction using the radiotracer [11C]GR103545 (1) to detect changes in the kappa opioid receptor (KOR) dynorphin system in cocaine abuse, based on animal experiments showing that binge cocaine administration significantly increases levels of endogenous dynorphin.

Cocaine abusers and matched control subjects were scanned with the radiotracer [11C]GR103545, in order to compare kappa receptor availability between groups. In addition to this baseline scan, the cocaine abusers underwent PET scans following three days of binge smoked cocaine (300 mg/day), to investigate effect of cocaine on brain dynorphin levels. We also investigated the association between kappa receptor binding and stress-induced cocaine self-administration using the cold-pressor test. In these sessions, cocaine abusing subjects were allowed to chose between smoked cocaine and an alternative reinforcer (money) following a stress.

Data are available now for 14 cocaine abusers and 10 controls. The cocaine abusers were heavy, chronic users of smoked cocaine, and the controls were matched for age, gender, ethnicity, and cigarette smoking. The outcome measure for the PET scans was the volume of distribution (VT) of the regions of interest, which included the striatum (and its subdivisions), cortical regions (including prefrontal cortex), and medial temporal structures. The results were as follows: 1) No difference in [^{11}C]GR103545 VT in any of the regions of interest was seen between the cocaine abusers and controls. 2) A positive correlation was seen between kappa receptor binding in the striatum and stress-induced cocaine self-administration: higher values of VT were associated with more choices for cocaine following the cold pressor test (Spearman correlation coefficient of 0.53, p = 0.03). 3) In the cocaine dependent subjects, a significant decrease (-17.7% ± 2.3%) in VT was measured in the stratum when comparing the baseline and post-binge scans, and similar decreases were seen in other brain regions (-12.9% ± 5.1%).

There was no between-group difference in kappa receptor VT in the baseline condition. However, there was a positive correlation between striatal kappa receptor VT and cold-pressor induced cocaine self-administration, showing that higher kappa receptor binding is associated with a greater vulnerability to stress induced choices for cocaine. The decrease in [^{11}C]GR103545 VT seen following binge dosing of cocaine suggests that levels of dynorphin might be significantly upregulated, which replicates in humans the finding that cocaine increases brain levels of dynorphin. These data indicate that altered the kappa receptor/dynorphin system is significantly altered in the human brain in response to cocaine exposure.

Supported by NIDA 1R01 DA027777

1. Naganawa M, Jacobsen LK, Zheng MQ, et al. Evaluation of the agonist PET radioligand [(1)(1)C]GR103545 to image kappa opioid receptor in humans: kinetic model selection, test-retest reproducibility and receptor occupancy by the antagonist PF-04455242. *Neuroimage.* 2014;99:69-79.

96
BRAIN-0957
BrainPET Symposium

Frontiers in Brain PET Imaging

Awake animal imaging

H. Tuskada[1]
[1]*Central Research Laboratory, Hamamatsu Photonics, Hamamatsu, Japan*

Objectives; In PET imaging with experimental animals, anesthetics are indispensable to fix animals during data acquisition. However, anesthetics have been reported to affect the brain function [1], kinetics of PET probes [2], and pharmacological effects of drugs [2, 3], which may humper PET brain imaging research. To solve the problem, we developed a unique PET scanner, which can tilt its gantry up to 90 degrees [4]. This PET scanner allowed us to measure monkey brain function in conscious condition. In the presentstudy, we applied it to develop the novel PET probes for mitochondria complex-I (MC-I) to evaluate the brain aging. We previously demonstrated that Ischemic neuronal damage in the brains of rat [5] and monkey[6] could be detected using ^{18}F-BCPP-EF 7 days post ischemic insul, twhen ^{18}F-FDG could not do because of neuroinflammation with activated microglia [5, 6].

Methods; We conducted medicinal chemistry research based on BMS-747158 as a lead compound [7], developed ^{18}F-BCPP-EF [5], and evaluated its specificity and affinity for MC-1 in the living monkey brain [8]. Then, PETscans using ^{11}C-PIB for amyloid-β (Aβ) deposition,^{11}C-DPA-713 for translocator protein (TSPO) activity as an inflammatory index, ^{18}F-FDG for regional cerebral metabolism of glucose (rCMRglc), and ^{18}F-BCPP-EF for MC-1 were performed in young and aged monkeys (*Macaca mulatta*) in conscious condition [9].

Results; Since isoflurane anesthesia affected rCMRglc and standard uptake value (SUV) of ^{11}C-DPA-713, not total distribution volume (V_T) of ^{18}F-BCPP-EF and SUV ratio (SUVR) of ^{11}C-PIB, the following analyses including rCMRglc and ^{11}C-DPA-713 were conducted using data obtained in conscious condition only. When plotted V_T of ^{18}F-BCPP-EF against SUVR of ^{11}C-

PIB in the cerebral cortical regions, it showed a significant negative correlation between them. Plotting of SUV of ^{11}C-DPA-713 against SUVR of ^{11}C-PIB resulted in a significant positive correlation, suggesting that Aβ deposition-induced inflammatory effects with microglial activation. In contrast, plotting of rCMRglc against SUVR of ^{11}C-PIB did not reach statistically significant level because of unexpected ^{18}F-FDG uptake into the activated microglia.

Conclusions; The present study demonstrated that anesthesia and neuroinflammation significantly affected rCMRglc as measured by ^{18}F-FDG. In contrast, ^{18}F-BCPP-EFcould be a potential PET probe for quantitative imaging of age-related neurodegenerative alterations as a change in MC-1 activity in the living brain without being disturbed by anesthesia and neuroinflammation.

References; [1] Noda A, et al., *J Cereb Blood Flow Metab* 2003;23:1441-1447 [2] Tsukada H, et al., *Synapse* 2002;45: 207-212 [3] Tsukada H, et al., *Brain Res* 1999;849: 85-96 [4] Watanabe M, et al., *IEEE Trans Nucl Sci* 1997;44:1277-1282 [5] Tsukada H, et al., *J Nucl Med* 2014;55:473-480 [6] Tsukada H, et al., *J Cereb Blood FlowMetab* 2014;34:708-714 [7] Yalamanchili P, et al., *J Nucl Cardiol* 2007;14:782-788 [8] Tsukada H, et al., *Eur J Nucl Med Mol Imaging* 2014;41:755-763 [9] Tsukada H, et al., *Eur J Nucl Med Mol Imaging* 2014;41:2127-2136.

98
BRAIN-0955
Symposium

Pericytes in the Neurovascular Unit and During Neurovascular Coupling

Potential role of pluripotent fat pericytes in cell replacement in neurodegenerative disease

P. Dore-Duffy[1], N. Esen[1]
[1]Neurology,
Wayne State University School of Medicine,
Detroit Michigan, USA

Adult stem cells (somatic cells) are undifferentiated cells found throughout the body after development. They have the potential to self renew and multiply indefinitely and have primary responsibility to maintain and repair the tissue of origin. The identity of the adult undifferentiated pluripotent stem cell is not known. Most experimental data has been gleaned from progenitor populations with limited ability to differentiate and an inherent genetic imprinting, or from differentiated adult cells induced to be pluripotent by the insertion of four embryonic genes (induced pluripotent cells [IPS]). The use of these cells seemed a promising answer to the debates over embryonic-stem-cell research. However IPS as well as progenitors have limited replicative ability and have early genetic senescence compared with embryonic stem cell derived tissue. This points to the continuing need to study true quiescent resting pluripotent cells of adult origin. We have identified an NG2+/nestin+/PDGFbR+ adult stem cell population within the CNS as well as other capillary networks (pericyte). CNS pericytes express all four embryonic antigens and are pluripotent having both neural and mesenchymal stem cell potential and can be isolated and expanded from brain capillaries. CNS pericytes as well as pericytes from many different organs have now been shown to be pluripotent and have the ability to form tissue specific progenitors. We have developed techniques to isolate human fat pericytes and pre-adipocyte progenitor cells and developed human cell lines that self renew and have pluripotent capacity. Two of these lines have been in culture for 8 months. Human populations retain pluripotent stem cell activity and self renew. Fat stem cells are easily obtained and expanded and can be frozen and thawed. Pericyte fat stem cell populations have been tested in an animal model of the human CNS degenerative disease multiple sclerosis to determine the potential therapeutic usefulness of human fat stem cells in cell replacement therapies for this disease.

100
BRAIN-0949
Symposium

Pericytes in the Neurovascular Unit and During Neurovascular Coupling

Pericyte regulation of the blood-brain barrier

R. Daneman[1]
[1]*Pharmacology and Neuroscience, UCSD, San Diego, USA*

Vascular endothelial cells in the central nervous system (CNS) form a barrier that restricts the movement of molecules and ions between the blood and the brain. This blood-brain barrier (BBB) is crucial to ensure proper neuronal function and protect the CNS from injury and disease. Although the properties of the BBB are manifested in the endothelial cells, transplantation studies have demonstrated that the BBB is not intrinsic to the endothelial cells, but is induced by interactions with the neural cells. Here we use a genomic, genetic and molecular approach to elucidate the cellular and molecular mechanisms that regulate the formation of the BBB. We have identified a critical role for pericytes in regulating the permeability of CNS vessels by inhibiting the properties that make endothelial cells leaky. In particular pericytes limit the rate of transcytosis through endothelial cells as well as the expression of leukocyte adhesion molecules in CNS endothelial cells, which limits CNS immune infiltration. Furthermore, we have developed methods to highly purify and gene profile endothelial cells from different tissues, and by comparing the transcriptional profile of brain endothelial cells with those purified from the liver and lung, we have generated a comprehensive resource of transcripts that are specific to the BBB forming endothelial cells of the brain. We have further examined the profile of CNS endothelial cells following injury and disease and have identified molecular mechanisms by which pericytes control BBB formation, which are then disrupted during neurological disease leading to BBB dysfunction.

101
BRAIN-0948
Symposium

Pericytes in the Neurovascular Unit and During Neurovascular Coupling

Control of blood flow by capillary pericytes and the origin of BOLD fMRI signals

D. Attwell[1]
[1]*NPP, UCL, London, United Kingdom*

Brain blood flow is regulated to ensure adequate power for neuronal computation. Blood flow is increased to areas where neurons are active, and this increase underlies non-invasive brain imaging using BOLD fMRI. Blood flow is controlled at the arteriole level by smooth muscle, but there is controversy over whether it is also regulated by pericytes at the capillary level. I will demonstrate that neuronal activity and the excitatory neurotransmitter glutamate evoke an outward membrane current in pericytes and dilate capillaries, and that this dilation is caused by active relaxation of pericytes rather than a passive expansion of capillaries downstream of arteriole relaxation. Glutamate-evoked dilation is mediated by prostaglandin E_2, but requires nitric oxide release to suppress synthesis of the vasoconstrictor 20-HETE. *In vivo*, when sensory input to the neocortex releases glutamate and increases blood flow, capillaries dilate first, followed by arterioles. Capillary dilation is estimated to generate ~80% of the increase of blood flow occurring. Capillaries also have a role in pathology. Ischaemia was previously shown to lead to a contraction of pericytes. I will report that this is followed by their death, which is expected to produce an irreversible constriction of capillaries. Pericyte death is reduced by block of glutamate receptors or calcium removal, and increases with reperfusion, but is not blocked by scavenging of reactive oxygen species. These data establish, for the first time, pericytes as major regulators of cerebral blood flow, and initiators of the BOLD fMRI response. They also focus attention on prevention of pericyte death as a therapeutic strategy to reduce the long-lasting blood flow decrease which contributes to neuronal death after stroke.

104
BRAIN-0431
Brain Oral Communication

Oral Session: Energy metabolism in health and disease

LOCAL NEURONAL AND GLIAL OXIDATIVE METABOLISM DURING FOCAL CORTICAL ACTIVITY

S. Sonnay[1], N. Just[2], R. Gruetter[1], J.M.N. Duarte[1]
[1]Laboratory for Functional and Metabolic Imaging (LI FMET), Ecole polytechnique fédérale de Lausanne, Lausanne, Switzerland
[2]Centre d'Imagerie Biomédicale – Animal and Technol ogy Core (CIBM-AIT),
Ecole polytechnique fédérale de Lausanne, Lausanne, Switzerland

Objective: Brain energy metabolism results from coordinate interaction between neurons and astrocytes. Although both cell types modulate synaptic transmission via the glutamate-glutamine cycle, the metabolic involvement of glia during brain activity is still not fully understood [1]. The aim of the study was to measure the relative contribution of glial and neuronal metabolic fluxes by direct ^{13}C MRS *in vivo* during prolonged cortical activation.

Materials and Methods: Sprague Dawley rats under α-chloralose anesthesia were fixed in a homebuilt holder. Electrical stimulation was achieved through stainless steel electrodes inserted between the digits of both hind- and forepaws. Square pulses (0.5 ms width) were delivered at constant current (2.5 and 3 mA for the fore- and hindpaws, respectively) and variable frequency (2-3 Hz) [2]. The stimulation paradigm was 30 s ON - 10 s OFF repeated for 4 h, switching the frequency every 5 minutes. Cortical activation was confirmed by blood oxygenation level-dependent functional magnetic resonance imaging (BOLD fMRI). Localized ^{1}H and ^{13}C MRS [3] were performed at 14.1 T from a 94 µL volume in the activated cortex during infusion of [1,6-^{13}C]glucose. Data were analysed with LCModel [4] and fitted to a two-compartment model of energy metabolism previously described [5].

Results: Prolonged and localized BOLD response following the applied paradigm was detected over 4 h in the cortex prior to ^{13}C MRS experiments [2]. The relative activated volume confirmed by BOLD fMRI was large enough to detect FE curves of aliphatic carbons of glutamate, glutamine, and aspartate with a temporal resolution of 11 minutes. Rats under stimulated brain activity (n=7) showed faster neuronal oxidative metabolism compared to rest (n=8). More precisely, intermittent focal brain activity resulted in an increase in neurotransmission rate (V_{NT} +58%), neuronal and glial TCA cycles rates (+4% V_{TCA}^{n} and +18% V_{TCA}^{g}, respectively), glutamine synthetase rate (V_{GS}, +30%) and cerebral metabolic rate of glucose oxidation ($CMR_{glc(ox)}$, +8%).

Conclusion: The present results indicate that the neuron-glia interactions adapt to different brain activity states in such a way that focal cortical activity increases neuronal and glial oxidative metabolism to produce energy for neurotransmission support, namely glutamate clearance and conversion to electrophysiologically inactive glutamine.

References: [1] Lanz et al, (2013) Front Endocrinol 4:156 [2] Sonnay *et al.* (2015) NMRBiomed in press [3] Henry *et al*. (2003) MRM 50:684 [4] Henry *et al*. (2003) NMR Biomed 16:400. [5] Duarte *et al*. (2011) Front Neuroenergetics,3:3

This work was supported by Swiss National Science Foundation (#148250), Centre d'Imagerie BioMédicale and National Competence Center in Biomedical Imaging.

105
BRAIN-0856
Brain Oral Communication

Oral Session: Energy metabolism in health and disease

GLUCOSE CONSUMPTION ASSOCIATED WITH RESTING STATE FMRI ACTIVITY IN HUMAN BRAIN

B. Dietz[1], N. Benbrahim[1], R.S. Menon[1]
[1]Robarts Research Institute, Western University, London, Canada

Objectives: The energy demand of the human brain is primarily met by ATP derived from the oxidation of glucose. An energy audit (1), the Magistretti model (2) and 13C-MRS results (3) support the hypothesis that the metabolic steps involved in neurotransmitter

cycling consume 5–10% of the total energy used by the brain (4). At 'rest" brain metabolism consists of a tonic component and a temporally varying (on the scale of seconds to minutes) component which likely supports the fluctuations responsible for the resting state functional magnetic resonance imaging (rs-fMRI) signal. The objective of this study was to determine the fraction of brain glucose consumption that supports the rs-fMRI signal.

Methods: We used data from 9 subjects in the ADNI database. All participants were required to have had at least one FDG-PET scan, one structural MRI scan and one rs-fMRI scan. The FDG-PET scans were acquired on a single Phillips scanner. All MRI images were preprocessed using FSL (5). Each PET image was processed using the recommended ADNI processing stream (6). PET and rs-fMRI images were registered to each other in MNI space after registering each to their respective structural MRI. Each subject's BOLD time-series underwent ICA using MELODIC, followed by denoising by discarding artifactual components. The remaining fMRI signal was expected to be neuronal in origin and was characterized by its temporal variance on a voxel-vise basis. A joint-histogram analysis compared this voxel-wise rs-fMRI variance with the FDG-PET derived glucose consumption.
Results: The joint histogram for one subject is shown in Fig. 1. All 9 subjects looked similar and a group analysis was also performed. These joint histograms (JH) demonstrate that the glucose consumption associated with the rs-fMRI signal fluctuations was 5-10% of the total glucose consumption (see y-intercept), in line with prior estimates for task based fMRI (4). Furthermore, by mapping back the voxels in the far right of the JH (high FDG/high BOLD variance), we were able to show that these voxels corresponded to rich hubs (network hubs with high connectivity - Fig. 2). The JH approach allows the metabolic cost of each resting state network to be measured and compared as a fraction of total brain FDG consumption and to each other.

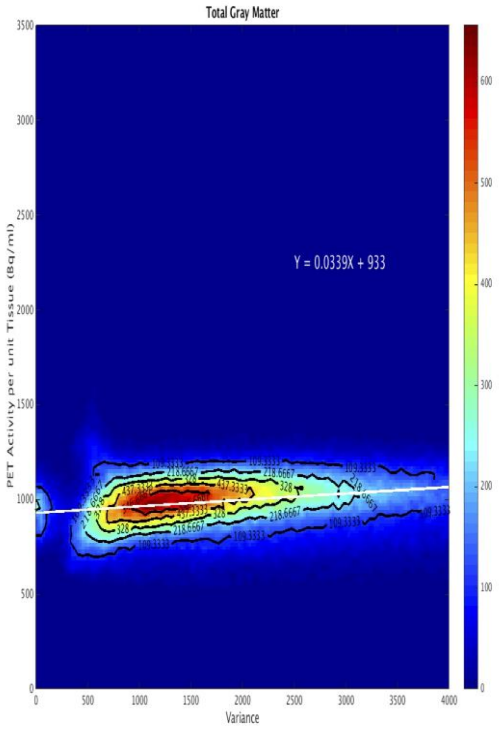

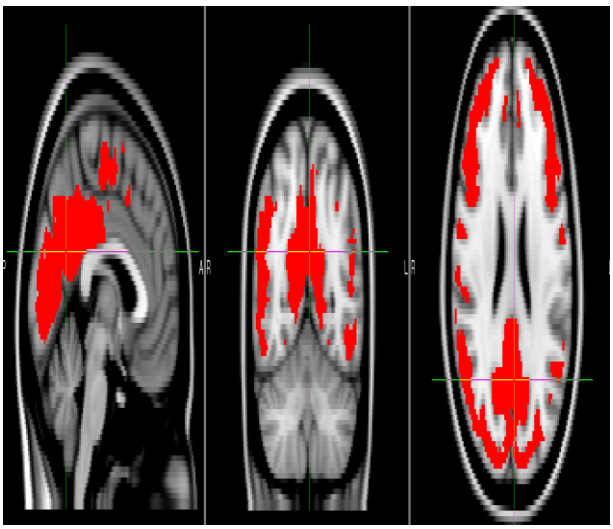

Conclusions: Our JH analysis demonstrated that the metabolic cost of the rs-fMRI signal represents about 5-10% of the total metabolism of the brain. Regions of high rs-fMRI variance correspond to the rich hubs in the brain. Furthermore, the linear relationship between rs-fMRI variance and FSG-PET suggests that fMRI variance associated with the sum of the resting state networks can be used as a surrogate for FDG-PET of neural activity.

References

(1) Attwell D, Laughlin SB (2001) J Cereb Blood Flow Metab 21:1133–1145.

(2) Pellerin, L. and Magistretti, P.J. (1994) Proc. Natl. Acad. Sci. U. S. A. 91, 10625–10629.

(3) Sibson, N.R. et al. (1998) Proc. Natl. Acad. Sci. U. S. A. 95, 316–321.

(4) Shulman, RG, Rothman, DL, Behar, KL and Hyder, F (2004) Trends in Neurosci. 27: 489-495.

(5) http://fsl.fmrib.ox.ac.uk/fsl/fslwiki

(6) http://adni.loni.usc.edu/methods/pet-analysis/pre-processing/

106
BRAIN-0562
Brain Oral Communication

Oral Session: Energy metabolism in health and disease

RESTING-STATE BRAIN ENERGY METABOLISM PREDICTS LEVEL AND CONTENT OF CONSCIOUSNESS AFTER SEVERE BRAIN INJURY

J. Stender[1], K. Nygaard Mortensen[1], R. Kupers[1], A. Thibaut[2], S. Darkner[3], S. Laureys[2], A. Gjedde[1]
[1]Department of Neuroscience and Pharmacology, University of Copenhagen, Copenhagen, Denmark
[2]Cyclotron Research Unit and Department of Neurology, University of Liège, Liège, Belgium
[3]Department of Computer Science, University of Copenhagen, Copenhagen, Denmark

Objectives
Differential diagnosis between the minimally conscious and vegetative states (MCS, VS) remains an unresolved clinical challenge with important ethical and therapeutic implications. Current research addresses physiological correlates of perceptual awareness in these patients (1).

Assessment of cerebral glucose metabolism with fluorodeoxyglucose in positron emission tomograms (FDG-PET) serves as a diagnostic tool in disorders of consciousness (2). Here, we present a novel method of FDG-uptake normalization to non-cerebral tissue, which solves the issue of FDG-PET quantification in severely injured brains. We hypothesize that baseline metabolism predicts the level of consciousness, while regional variations relative to the baseline reflect preservation of specific functions, such as vision and language comprehension (3).

Methods
We included 138 patients clinically diagnosed with VS (n=49), MCS (n=65) or emergence from MCS (EMCS; n=17), and 28 healthy control subjects. We obtained one-year outcome (conscious/unconscious) for all patients.

All subjects had FDG-PET. Regions of interest were chosen as Brodmann areas and combined to cortical masks for each hemisphere. We normalized images by fitting the intensity distributions of extracerebral cranial tissue of individual patients to that of healthy subjects. A scaling parameter was found by minimizing the Jensen-Shannon divergence between the distributions. We used the average metabolic index of the least affected hemisphere as diagnostic marker, validated against behavioral diagnosis and outcome. Classification accuracy between VS and MCS was assessed by receiver operating characteristic (ROC) analysis. Brainwide interregional variability was assessed by the coefficient of variance (CV; std/mean). Following further scaling of the images to the global mean, we tested Pearson correlations between relative metabolic activity in visual cortex and language-related areas with visual responsiveness and command following capacity, respectively.

Results
Area under the ROC curve was 0.89 (0.82-0.96). The optimal classification threshold that distinguished MCS from VS was 41% of normal metabolism, which diagnosed 88% of the patients correctly, with 95% sensitivity and 78% specificity to MCS. All EMCS and healthy subjects were identified as conscious. The model predicted 86% of known outcomes in MCS and VS, with 97% sensitivity and 70% specificity to consciousness at follow-up. Notably, 8 out of 9 recoveries from VS were associated with above-threshold metabolism (Figure 1). No individual regions provided diagnostic classification superior to

the hemisphere mean value. Interregional variance was 0.03 CV in VS, 0.093 in MCS, 0.097 in EMCS and 0.11 in controls. Relative metabolism in the visual cortex correlated with visual responsiveness (R=0.2443, p=0.0028), whereas relative metabolism in language-related areas correlated with command following capacity (R=0.486, p<0.0001).

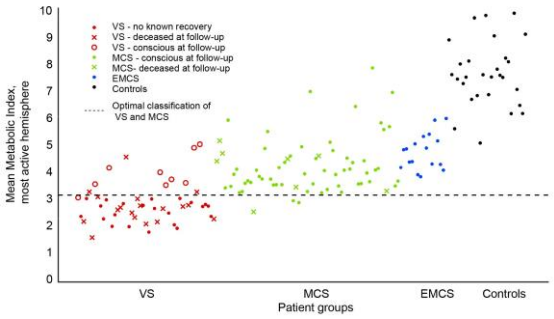

Conclusion

Global resting-state brain metabolism accurately predicted levels of consciousness. Regional metabolic variations relative to the baseline are characteristic of the conscious state and reflect perceptual contents. The metabolic level accounted for either the presence or imminent rise of consciousness in 95% of the patients. The results suggest that disorders of consciousness can be understood as abnormal neuroenergetic states and provides a unifying pathophysiological basis for these syndromes.

References

1. Giacino et. al. Nat Rev Neurol 2014;10:99-114.
2. Stender et. al. The Lancet 2014;384:514-22.
3. Shulman et. al. PNAS 2009;106:11096–101.

107

BRAIN-0510

Brain Oral Communication

Oral Session: Energy metabolism in health and disease

METABOLIC CHANGES IN EARLY POST STATUS EPILEPTICUS MEASURED BY MR SPECTROSCOPY IN RATS

Y.J. Wu[1], P.S. Pierce[2], T.K. Hitchens[3], A. Rapuano[4], N. de Lanerolle[4], J.W. Pan[2]

[1]Developmental Biology, University of Pittsburgh, Pittsburgh, USA

[2]Neurology, University of Pittsburgh, Pittsburgh, USA

[3]Biology, Carnegie Mellon University, Pittsburgh, USA

[4]Neurosurgery, Yale University, New Haven, USA

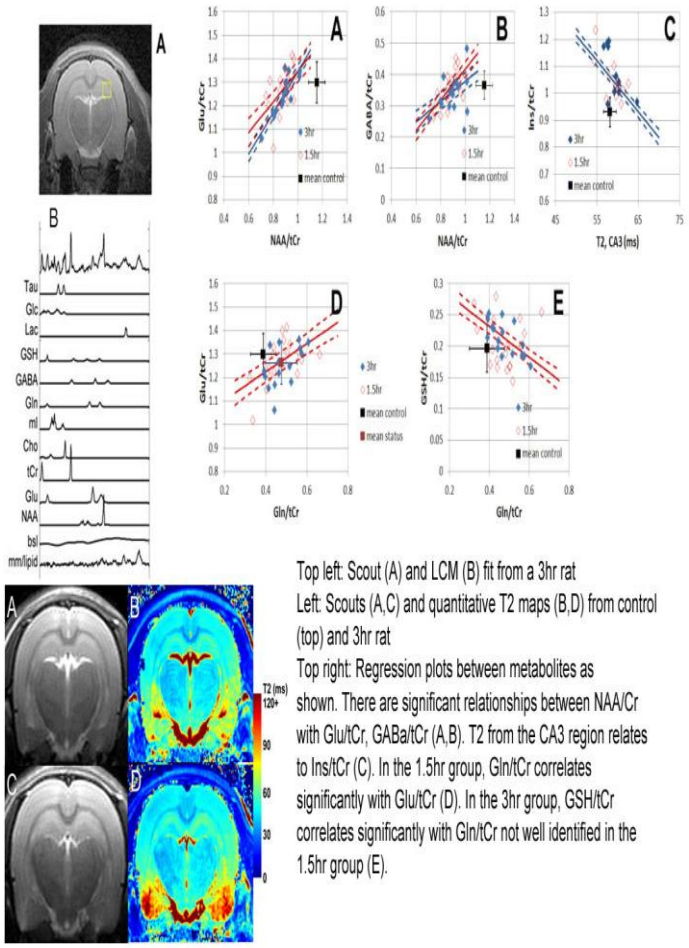

Top left: Scout (A) and LCM (B) fit from a 3hr rat
Left: Scouts (A,C) and quantitative T2 maps (B,D) from control (top) and 3hr rat
Top right: Regression plots between metabolites as shown. There are significant relationships between NAA/Cr with Glu/tCr, GABa/tCr (A,B). T2 from the CA3 region relates to Ins/tCr (C). In the 1.5hr group, Gln/tCr correlates significantly with Glu/tCr (D). In the 3hr group, GSH/tCr correlates significantly with Gln/tCr not well identified in the 1.5hr group (E).

OBJECTIVES: The development of spontaneous recurrent seizures (epilepsy) is a complex process that commonly ensues after an initial cerebral insult. While variation in seizure duration in human epilepsy is known to influence the likelihood of development of recurrent seizures, there is little experimental in vivo data on how duration of seizure injury influences metabolic injury. The goal of this study is to access the variability of metabolic injury in experimental status epilepticus (SE) model in the post-status early epileptogenesis time period using magnetic resonance studies.

METHODS *Animal model:* The Hellier Dudek model (1) was used with male Sprague Dawley rats (190±20g), treated with multiple low doses of intraperitoneal kainate (KA) to generate two durations of status epilepticus (SE), 1.5hr (n=9) or 3hr (n=8). Diazepam (10 mg/kg) was used to terminate behavioral

seizures. In the two groups, the KA dose was 19.4±2.7mg/kg and 23.1±4.2mg/kg respectively. Sham controls (n=10) received equivalent volumes of saline.

MR assessment: 3days after status, animals underwent MRI (Bruker Biospec 7T) for localized ^{1}H spectroscopy and imaging. Localized single-voxel ($8mm^3$) PRESS spectroscopic acquisitions at TE=10ms and TE=40ms were performed separately over the left and right hippocampus (Figure, top left). T_2 relaxometry (Figure, bottom left) was performed with a multi-slice-multi-spin-echo sequence with a monoexponential least squares fit. Metabolites (including N-acetyl aspartate NAA, glutamate Glu, GABA, glutamine Gln, myo-inositol Ins, glutathione GSH, lactate Lac) were analyzed as a ratio to total creatine using a LCM analysis with inclusion of data if the Cramer Rao values were

RESULTS The status injury resulted in decreased NAA/tCr and increased Ins/tCr and Gln/tCr, increased quantitative T2 and significant declines in Neu-N stained neuronal counts. For both the 1.5hr and 3hr groups, several regressions were identified between metabolites (Figure, top right). NAA/tCr and Glu/tCr, NAA/tCr and GABA/tCr were significantly correlated, consistent with a synchronous loss of neuronal mitochondrial, glutamatergic and GABAergic function in the 3day post-status epilepticus period. Ins/tCr increased in both groups and correlated significantly with quantitative T2 in the CA3 region, consistent with the homeostatic response to seizure induced edema. In the 1.5hr group, a significant positive correlation between Gln/tCr and Glu/tCr was identified, with a weaker but similar correlation seen in the 3hr group. A negative correlation between increased GSH/tCr with decreased Gln/tCr was seen in the 3hr group (R = -0.66 p

CONCLUSIONS: These data provide evidence for neuronal injury and astrocytic reaction after status epilepticus in both the short and long status duration groups. The elevation in Gln/tCr and its relationship to Glu/tCr is consistent with increased glutamine synthetase activity occurring early in the status epilepticus injury trajectory and is consistent with literature (2). The 3hr status group displayed changes in GSH/tCr that were not identified in the 1.5hr status group, which is hypothesized to represent a maturation of injury and anti-oxidant response in the more severely injured animals.

REFERENCES

1. Hellier JL, Dudek FE. Curr Protoc Neurosci 2005 9:9–19.
2. Hammer, Alvestad et al. Glia 2008 56(8):8560868.

108

BRAIN-0096

Brain Oral Communication

Oral Session: Energy metabolism in health and disease

NEURO-PROTECTIVE ROLE OF ASTROGLIA IN PARKINSON'S DISEASE ARISING FROM A REDUCTION IN OXYGEN STRESS THROUGH THE DOPAMINE-INDUCED ACTIVATION OF THE PENTOSE-PHOSPHATE PATHWAY

K. Mashima[1], S. Takahashi[1], T. Iizumi[1], T. Abe[1], N. Suzuki[1]
[1]Department of Neurology,
Keio University School of Medicine, Tokyo, Japan

Objectives

Oxygen stress plays an important role in the onset and progression of Parkinson's disease (PD). Mitochondrial overload induced by the pace-making activity of dopaminergic neurons to maintain an optimal dopamine (DA) concentration in the striatum (tonic release) might be a major cause of oxygen stress.[1] Dopaminergic neurons also release additional DA as the need arises (phasic release). Another source of oxygen stress seems to be DA *per se*, since DA is auto-oxidized to form dopamine quinone, resulting in reactive oxygen species (ROS) production.[1] Therefore, reducing oxygen stress seems to be an important strategy for the treatment of PD. Especially, the neuro-protective roles of astroglia have been recognized.[1,2] Although most of the released DA is collected by dopaminergic neurons themselves, a part of DA is presumed to be collected by astroglia.[3] DA may activate astroglial glucose metabolism via a mechanism similar to that induced by glutamate[1-3] and may contribute to the reduction of oxygen stress. The present study examined DA-induced astroglial protective function

through the activation of the pentose-phosphate pathway (PPP) to reduce ROS.

Methods

In vitro experiments were performed using striatal neurons and cortical or striatal astroglia prepared from Sprague-Dawley rats. The rates of glucose phosphorylation in astroglia were evaluated using a modification[4] of the [^{14}C]deoxyglucose method. PPP activity was measured using a modification[4] of the method described by Hothersall et al.[5] based on the determination of the difference in $^{14}CO_2$ production from [1-^{14}C]glucose and from [6-^{14}C]glucose after acute (60 min) or chronic (15 hours) exposure to different concentrations of DA (10, 100 µM). ROS production was measured using H_2DCFDA. The involvement of the Keap1/Nrf2 system was evaluated using immunohistochemistry.

Results

Acute exposure to DA (10, 100 µM) elicited increases in astroglial glucose consumption (123.3±6.0,108% and 130.4±11.5, 115%, respectively) with lactate release, indicating an enhancement of glycolysis probably because of Na^+-dependent DA uptake by a norepinephrine transporter. PPP activity in astroglia was enhanced robustly (2.9±0.4, 166% and 120.7±3.4, 6873%, respectively). In contrast, chronic exposure to DA induced moderate increases in PPP activity (2.0±0.1, 118% and 2.7±0.1, 163%, respectively). Chronic exposure to DA induced Nrf2 translocation to the nucleus in astroglia, indicating the Nrf2-dependent transcriptional up-regulation of G6PDH, a rate limiting enzyme of PPP. ROS production induced by DA in the absence of astroglia increased gradually over 12 hours, whereas it decreased in the presence of astroglia (86% and 75%, respectively).

Conclusions

DA released from dopaminergic neurons enhanced astroglial PPP activity in both an acute and a chronic manner, which may reduce neuronal oxygen stress and play an important role in preventing the onset and progression of PD. Further enhancement of the protective roles of astroglia could lead to an important therapeutic strategy for the treatment of PD.

References

1. Takahashi S, et al. Brain Nerve 2013; 65:1497-508.
2. Takahashi S, et al. Rinsho Shinkeigaku 2012; 52:41-51.
3. Semenoff D and Kimelberg HK, Brain Res 1985; 348:125-136.
4. Takahashi S, et al. ASN Neuro 2012; 4(2).pii: e00078.
5. Hothersall JS, et al. Arch Biochem Biophys 1979; 198:478–492.

109
BRAIN-0772
Brain Oral Communication

Oral Session: Energy metabolism in health and disease

AN ALZHEIMER-LIKE PATTERN OF LOW BRAIN GLUCOSE UPTAKE ASSOCIATED WITH MILD INSULIN RESISTANCE IN YOUNG WOMEN WITH POLYCYSTIC OVARY SYNDROME: AN FDG PET/MRI STUDY

C.A. Castellano[1], J.P. Baillargeon[2], S. Nugent[1], S. Tremblay[3], M. Fortier[1], H. Imbeault[4], E. Turcotte[5], S.C. Cunnane[1]
[1]Clinical Axis, Research Centre on Aging, Sherbrooke, Canada
[2]Endocrinology, Université de Sherbrooke, Sherbrooke, Canada
[3]Sherbrooke Molecular Imaging Center, Université de Sherbrooke, Sherbrooke, Canada
[4]Memory Clinic, Health and Social Sciences Center - Geriatrics Institute , Sherbrooke, Canada
[5]Nuclear Medicine and Radiobiology, Université de Sherbrooke, Sherbrooke, Canada

Introduction: Polycystic ovary syndrome (PCOS) is commonly associated with insulin resistance (1). Insulin resistance is associated with regional brain glucose hypometabolism and may contribute to the risk of Alzheimer's disease (AD) in elderly pre-diabetes (2). PCOS provides an opportunity to studying the influence of insulin resistance on brain glucose metabolism independently of age.

Objective: To determine whether regional cerebral metabolic rate of glucose (CMRglu) is altered in young adults with PCOS.

Methods: Healthy age-matched controls (n=11, age 24 ± 3 y) were compared to patients with PCOS (n=7, age 25 ± 6 y). All participants underwent structural 1.5T MR and quantitative PET imaging with ^{18}F-FDG. Dynamic PET images were co-registered to MR images and corrected for partial volume effect and atrophy. CMRglu (µmol/100 g/min) and brain volumes were calculated as previously described (3). Blood biochemistry parameters including an index of insulin resistance (HOMA2-IR) were also obtained for all participants. A cognitive battery was also administered to the PCOS group and compared to age-matched reference values. Group differences were examined using Mann–Whitney U-tests with a multiple comparison (FDR) correction set at 0.05.

Results: Fasting plasma glucose and HOMA2-IR was significantly higher in the PCOS group compared to the controls ($p \leq 0.04$). PCOS patients also showed 10-17% lower brain volume mainly in fronto-parietal cortical regions and in the caudate ($p \leq 0.03$ FDR corrected). CMRglu in the PCOS group was 11-14% lower mainly in temporo-parietal regions and in the cuneus ($p \leq 0.03$ FDR corrected). When data from controls and PCOS were combined, an inverse linear regression between the HOMA2-IR and CMRglu was observed for the temporo-parietal regions, the hippocampus and the amygdala ($p \leq 0.03$). In the PCOS group results of the cognitive tests were within the normal range but 5/7 had a low score for working memory (PASAT).

Conclusions: Our results suggest that PCOS is associated with a pattern of lower regional brain volume and CMRglu that has a certain resemblance to that seen in the early stage of Alzheimer's disease. The mild insulin resistance is probably a significant factor in this Alzheimer-like pattern given that the PCOS group was metabolically well-matched to the controls. We show that insulin resistance can be associated with brain glucose hypometabolism and regional brain atrophy even in a young adult population.

References: (1) Dunaif (1997) Endocr Rev. 18(6); (2) Baker et al. (2011) Arch Neurol. 68(1) ; (3) Nugent et al. (2014) Am J Physiol Endocrinol Metab. 306 (11).

Acknowledgements: Éric Lavallée and the clinical PET group (CIMS). Funded by CIHR, CFI, CRC, FRQS, Université de Sherbrooke Research Chair (SCC).

112
BRAIN-0967
Symposium

Targeting spreading depolarizations in injured brain: triggers, modulators and causation

Supply-demand mismatch transients trigger spreading depolarizations within penumbral hot-zones

C. Ayata[1]
[1]*Neurology and Radiology, Massachusetts General Hospital, Charlestown MA, USA*

Peri-infarct depolarizations (PIDs) are seemingly spontaneous spreading depression-like waves that negatively impact tissue outcome in both experimental and human stroke. Factors triggering PIDs are unknown. Here, we show that somatosensory activation of peri-infarct cortex triggers PIDs when the activated cortex is within a critical range of ischemia. We show that the mechanism involves increased oxygen utilization within the activated cortex, worsening the supply-demand mismatch. We support the concept by clinical data showing that mismatch predisposes stroke patients to PIDs as well. Conversely, transient worsening of mismatch by episodic hypoxemia or hypotension also reproducibly triggers PIDs. Therefore, PIDs are triggered upon supply-demand mismatch transients in metastable peri-infarct hot zones due to increased demand or reduced supply. Based on the data, we propose that minimizing sensory stimulation and hypoxic or hypotensive transients in stroke and brain injury would reduce PID incidence and their adverse impact on outcome.

113
BRAIN-0013
Symposium

Targeting spreading depolarizations in injured brain: triggers, modulators and causation

Does age have an impact on spreading depolarization?

E. Farkas[1], *F. Bari*[1]
[1]*Department of Medical Physics and Informatics, University of Szeged, Szeged, Hungary*

Waves of spreading depolarization (SD) spontaneously occur minutes after the onset of ischemia in the brain, and keep generating for a number of days to follow. It has become widely accepted that ischemia-related SDs are part of the pathophysiology of cerebrovascular diseases and predict worse outcome. SDs may exacerbate ischemic injury via related atypical hemodynamic responses. Aging is the most important risk factor for the incidence of cerebral ischemic stroke; yet, the effect of aging on the evolution of SDs and related hemodynamic responses has remained largely unexplored. Our recent investigations have aimed to identify the impact of aging on the elicitation threshold, duration, and propagation of SD, and the typical features of the related neurovascular coupling during ischemia. We have shown that the electric threshold to trigger SDs increases with progressing life time. Likewise, spontaneous SDs occur at lower frequency in the ischemic brain of aged animals, as compared with their young counterparts. However, once elicited, SDs tend to be persistent in the aged brain (as compared with predominantly transient SDs in the young brain), and their long duration may indicate metabolic crisis. While ischemia clearly compromises the kinetics of the SD-associated cerebral blood flow response (i.e. lower magnitude and longer duration of the distinct elements of the response), age exerts an additional shift to injurious CBF response types, especially inverse neurovascular coupling. We propose that an age-specific pattern of the SD-associated hemodynamic response must be involved in augmenting the expansion of ischemic brain damage in the elderly, and that structural and functional (mal)adaptation of the cerebrovascular system with aging serves as a potential basis for compromised vascular reactivity and subsequent tissue damage.

115
BRAIN-0024

Symposium

Targeting spreading depolarizations in injured brain: triggers, modulators and causation

Spreading depolarizations in human brain trauma: a causal pathomechanism?

J. Hartings[1]
[1]*Neurosurgery, University of Cincinnati, Cincinnati, USA*

Excitotoxicity and loss of ion homeostasis are well established as key mediators of secondary injury and lesion development after traumatic brain injury (TBI). Recent experimental evidence, however, suggests that these processes are actively induced and propagated in mass tissue events known as spreading depolarizations (SD), providing a novel basis for patient monitoring and therapeutic targeting. While SD scarcely occurs in rodent models of TBI, clinical studies now show that SD is a dominant pathophysiologic mechanism in many patients with severe TBI. Surgical patients monitored with subdural electrode strips have a 55% incidence of SD, and patterns vary widely from occasional events to continuous, repetitive events lasting hours to days. The basis of this heterogeneity is largely unknown, as the occurrence or severity of SD is not predicted by other clinical variables. Patients with and without SD are similar in terms of classical prognostic factors, indicators of injury severity, and pathoanatomic subtypes of TBI. Furthermore, the occurrence of SDs is largely independent of other physiologic 'secondary insults' such as hypotension or intracranial hypertension. Nonetheless, the occurrence of SD carries a significant and substantial increased risk for worse outcome, with estimated odds ratios in the range of 1.4 to 2.5. The risk is higher yet for patients with more severe SD patterns. A causal adverse impact of SD on injury progression is evidenced more directly by real-time monitoring. In some patients, SDs induce a persistent isoelectric "flatline" of cortical activity, analogous to the ischemic penumbra, lasting hours to days. Furthermore, simultaneous monitoring of local cerebral blood flow has shown that SDs can induce a spreading hypoperfusion, which limits delivery of metabolic substrates at a time of maximal metabolic demand. Together, these data suggest that SD as a

sequela of TBI is not simply a marker of injury severity or other known pathologic processes, but is an independent factor with adverse impact on TBI recovery. As the first method to assess a heterogeneous mechanism in individual patients, monitoring of SD may allow for novel clinical trials based on selective inclusion, mechanistic targeting, and tailored therapeutic dosing.

116
BRAIN-0097
Symposium

Targeting spreading depolarizations in injured brain: triggers, modulators and causation

The stroke-migraine depolarization continuum
J.P. Dreier[1]
[1]*Center for Stroke Research Berlin, Charité University Medicine Berlin, Berlin, Germany*

The term spreading depolarization describes a mechanism of abrupt, near-complete ion translocation between neurons and the interstitial space which leads to a cytotoxic edema in the gray matter of the brain above the thalamic/hypothalamic boundary zone. In energy compromised tissue, spreading depolarization is preceded by a non-spreading silencing (depression of spontaneous activity) because of a neuronal hyperpolarization. By contrast, in non-energy compromised tissue, spreading depolarization causes spreading silencing (spreading depression) of spontaneous activity by a depolarization block. It is assumed that the non-spreading silencing translates into the initial clinical symptoms of ischemic stroke and the spreading silencing (spreading depression) into the symptoms of migraine aura. In energy compromised tissue, spreading depolarization is long-lasting and facilitates neuronal death whereas, in healthy tissue, it is short-lasting and relatively innocuous. Therapies targeting spreading depolarization in metabolically compromised tissue may potentially treat conditions of acute cerebral injury such as aneurysmal subarachnoid hemorrhage, ischemic stroke and traumatic brain injury. Moreover, neuromonitoring of spreading depolarizations has increasingly become routine practice in neurointensive care as it may offer unprecedented opportunities for treatment stratification.

119
BRAIN-0984
Symposium

Energetic basis of resting function in the human brain

Neurophysiological basis of spontaneous fluctuations in BOLD signal: Correlations of non-linear couplings between bands of the local-field potentials
A. Shmuel[1]
[1]*McConnell Brain Imaging Centre, Montreal Neurological Institute McGill University, Montreal, Canada*

Experimental evidence (Shmuel and Leopold, 2008) suggests that spontaneous blood oxygenation signals correlate with slow local fluctuations in amplitude of the gamma-band (30-100 Hz) local field potentials (LFP). In contrast, blood-oxygenation-based inter-areal correlations are associated with correlations of low-frequency rhythms of <20 Hz (Lu et al, 2007).

Phase-Amplitude coupling (PAC), in which the phase of a low-frequency rhythm modulates the amplitude of a higher frequency rhythm, has been proposed as the mechanism linking these two phenomena. However, it remains unclear how the various spontaneous rhythms interact and whether their interactions predict spontaneous fluctuations in blood oxygenation. Here we investigated intra- and inter-laminar PAC during spontaneous activity, and its correlation with cortical blood oxygenation. To this end, we simultaneously recorded spontaneous LFP using laminar probes and optical imaging signals (OIS) in the forelimb representation of area S1 in anesthetized rats.

We observed both intra- and inter-laminar spontaneous PAC in a cortical column, with the highest measures of interaction obtained for the 2 pairs of delta/fast-gamma and theta/fast-gamma bands. Intra- and inter-laminar PACs involving layers 2/3–5a were higher than those involving layer 6. Current sinks (sources) in the delta band were associated with increased (decreased) amplitudes of high-frequency signals in the beta to fast gamma

bands throughout layers 2/3–6. Spontaneous sinks (sources) of the theta and alpha bands in layers 2/3 to 5a were on average linked to dipoles completed by sources (sinks) in layer 6, associated with high (low) amplitudes of the faster rhythms in the entire cortical column.

To determine whether PAC predicts spontaneous fluctuations in blood oxygenation, linear and nonlinear correlation between band-limited-amplitude and OIS and separately between PAC and OIS were then computed. For the majority of frequency-band combinations, PAC is positively correlated with spontaneous fluctuations in blood oxygenation, with the highest correlation values found between phases of delta to beta and amplitudes of low - and middle-gamma. Furthermore, nonlinear models of PAC are better predictors of OIS than linear models of band-limited-amplitude, although worse than nonlinear models of band-limited-amplitude.

Our study links recent theories on the involvement of PAC in resting-state functional connectivity with previous work that revealed lamina-specific thalamo-cortico-cortical anatomical connections. Our results highlight the importance of nonlinear mechanisms in the generation of spontaneous fluctuations in blood oxygenation.

120
BRAIN-0978
Symposium

Energetic basis of resting function in the human brain

Principles of energy demand in gray and white matter of the human brain

Y. Yu[1]
[1]*Physiology and Biophysics, Fudan University, Shanghai, China*

The mammalian brain is organized on multiple scales of network connections and functionally dependent regions for sensory and cognitive functions. Normal mammalian brain functions are mainly supported by high ATP yield from glucose oxidation ($CMR_{glc(ox)}$). How the metabolic energy used at the subcellular level is related to the large swathes within the brain are still not well-known yet. We created a comprehensive $CMR_{glc(ox)}$-derived energy budget for gray and white matter from the bottom-up, using biophysical properties of neurons and glia in conjunction with species-specific electrophysiological and morphological data. Comparing metabolic measurements by PET, ^{13}C MRS, and autoradiography in rat and human brain with budget-derived $CMR_{glc(ox)}$ revealed conserved properties. Signaling events (e.g., synaptic transmission, propagation of action potentials, glutamate recycling) in gray and white matter respectively demanded ~65% and ~25% of awake state $CMR_{glc(ox)}$ values in the respective tissues, whereas remaining portions were used for nonsignaling functions (e.g., resting membrane potential, housekeeping). GABAergic neurons and glia each demanded ×5 less energy than glutamatergic neurons. Although rat brain possesses smaller cells, due to higher firing rates in rat brain their functions demand 15-20% greater energy than their human brain counterparts. While neuronal energetics was governed by events associated with synaptic transmission and propagation of action potentials, glial energetics was dominated by nonsignaling needs. Then, we feed the energy budget calculations of individual neurons and glias into a 3-D human brain cell density map calculated based on BigBrain cell-stained histological data, formulating a 3-D brain energy map with energy calculations in unit of either glucose in micromole/min/gram or ATP/min/gram in order to compare with PET measurement of actual brain. The quantitative comparison demonstrated a perfect match, indicating a first successful reconstruction of brain energy map fully consistent with PET glucose imaging measurement. Human brain $CMR_{glc(ox)}$ maps assembled using the budget with BigBrain cell-stained histological data showed voxel-wise correspondence with $CMR_{glc(ox)}$ maps measured (by PET, awake state) across large swathes of gray and white matter, requiring 0.5-1.5 Hz firing rates across the entire cerebrum. A validated bottom-up energy budget of heterogeneous cellular functions spanning gray and white matter of healthy human brain can provide opportunities to reveal testable microscopic-level anomalies underlying metabolic neuroimaging of brain diseases and disorders.

121
BRAIN-0985
Symposium

Energetic basis of resting function in the human brain

Blood flow & oxidative metabolism coupling in the awake and resting human brain: On the signaling roles of aerobic glycolysis and lactate

A. Gjedde[1]
[1]*Dept Neuroscience and Pharmacology, University of Copenhagen, Copenhagen DK-2200, Denmark*

Lactate appears to serve several roles as a signal in mammalian brain (Gjedde &Magistretti 2010, Bergersen & Gjedde 2012). Recent data suggests that lactate is a signal responsible in part or in whole for the coupling of blood flow to oxidative metabolism. In addition, there is emerging evidence that lactate also serves as a volume transmitter engaged, among other effects, in memory consolidation by interaction with the lactate receptor GBR81. Lactate is the product of aerobic glycolysis when oxygen tensions in the tissue are adequate for complete oxidation of glucose to CO_2. Aerobic glycolysis, also known as the Warburg Effect, results in values of the Oxygen-Glucose Index (OGI) that are significantly less than 6. Conversely, when OGI values exceed 6, the phenomenon sometimes is referred to as the Inverse Warburg Effect. Recent evidence shows that OGI values change as function of age, rising from 4 or less during childhood to 7 or more in old age (Goyal et al, 2014). The consequences of this change are disputed, but here we claim that the change reflects evolving functions of lactate as a volume transmitter involved in learning in mammalian brain.

The theory of lactate as a volume transmitter claims that the presence of lactate in the tissue at certain concentrations imparts information to the regulatory mechanisms of the tissue. By consideration of the steady- and non-steady-states that brain tissue metabolism may occupy, we describe the processes of release of lactate to the tissue as tonic during steady-state and as phasic during non-steady-states, respectively, when temporary increases of the concentration of lactate occur, in keeping with the terminology used for the monoaminergic volume transmitters.

Lactate is the product of aerobic glycolysis in response to glutamate uptake into astrocytes in the steady-state and glycogenolysis in response to noradrenaline (NA) acting on beta 2 receptors in astrocytes in non-steady-states. The role of NA in the breakdown of glycogen suggests that this monoamine plays a special role in the phasic release of lactate. This role is reminiscent of NA's role in working memory and memory consolidation by interaction with alpha2 adrenoceptors that limit cAMP formation. Lactate similarly interacts with the GPR81 (or HCA1) G-protein receptor that also mediates an inhibition of cAMP formation. These actions imply that NA and lactate collaborate in second-messenger effects associated with working memory and memory consolidation. Further evidence for this control comes from actions of lactate in gene expression that are related to its positive modulatory effect on NMDA signaling in neurons (may be related also to the limitation of cAMP formation). The putative tonic and phasic release patterns of lactate further suggest that lactate concentrations in brain could reflect the memory and learning loads that brains face in different states.

In this context it is remarkable that OGI and OEF measurements together with measures of glucose and oxygen consumption rates as functions of age predict that lactate concentrations in brain tissue are particularly high during childhood (0-15 years) and low above the age of 60, in keeping with the memory, learning and plasticity loads that characterize these ages.

122
BRAIN-0986
Symposium

Energetic basis of resting function in the human brain

Glucose oxidation in normal human brain across different resting states

F. Hyder[1]
[1]*Departments of Diagnostic Radiology & Biomedical E ngineering,*
Magnetic Resonance Research Center Yale University, New Haven CT, USA

Pioneering efforts in the past decades with PET and fMRI have laid strong foundations for network mapping in the human brain. Early PET work concentrated on quantitative imaging of resting state blood flow and metabolism. By the 1990s fMRI became popular because it was possible to conduct repeated mapping in the same session, where the functional hyperemic changes provided the contrast. In this presentation I will focus on two specific issues of network mapping by fMRI and PET (Hyder et al, 2013) that impact interpretations of what networks mean.

First, recent proposals that certain resting-state fMRI networks have higher rates of glycolysis imply regional variation of ATP regeneration rates. Furthermore, if regional glucose utilization is mismatched with oxygen delivery, then those areas can have impaired ATP production. These predictions are testable by measured differences between the oxygen to glucose index (OGI) and the oxygen extraction fraction (OEF). We used quantitative PET measurements of blood flow and rates of oxygen and glucose consumption in normal human brain (resting awake, eyes closed) to test whether values of OEF and OGI differ regionally. Similar OEF and OGI values and patterns prevailed as networks regardless of their size, location, and origin showed OEF and OGI values that matched the gray matter means. The excellent spatial agreement between oxygen transport and glucose metabolism in normal human gray matter suggests that no specific region is preferentially vulnerable to impaired ATP production. In normal human gray matter, uniform OGI and OEF sustained globally high total ATP turnover rates, with less than 1% contribution of total ATP from non-oxidative glycolysis. We conclude that the intrinsic network activity in healthy human brain covers the entire gray matter with ubiquitously high-energy demands met by glucose oxidation.

Second, human neuroimaging studies aim to isolate brain networks that differ between health and disease. But network differences revealed by methods that utilize global mean normalization remain difficult to interpret because it is unknown what fraction of total metabolic (or neuronal) activity the state-dependent variations reflect. To quantitatively characterize global vs. regional metabolic variations from a control state of awake with eyes closed, we examined PET-measured glucose consumption (CMR_{glc}) in other states. The different states included awake with eyes open, awake but congenitally blind, healthy but sedated with anesthetics, and patients with disorders of consciousness. In relation to the control state, quantified CMR_{glc} maps for all states (except congenitally blind) revealed significant global changes, ranging from +10% with eyes open, -20% with sedation, and -60% with disorders of consciousness. Statistical t-maps with quantified CMR_{glc} data for each state (vs. control) revealed globally unidirectional metabolic changes. In contrast global mean normalized CMR_{glc} t-maps exposed regionally bidirectional metabolic effects across different states. These results suggest that the hypothesized confounding effects from the global signal, in fact, contains metabolic information that depicts brain-wide deviations that are state-dependent.

In summary, quantitative metabolic mapping can be used to advance disease biomarker in human neuroimaging studies.

125
BRAIN-0261
Brain Oral Communication

Oral Session: Cerebral Hemorrhage and Related Pathologies

INHIBITION OF BOTH THE ACTIVATED MICROGLIA/MACROPHAGE AND THE INFILTRATED NEUTROPHILS ATTENUATES BRAIN INJURY AND IMPROVES OUTCOMES FOLLOWING INTRACEREBRAL HEMORRHAGE

W. Chen[1], X. Li[1], Y. Li[1], X. Li[1], Y. Fang[1], J. Fang[1], L. Jiang[1], R. Huang[1], M. Liu[1], Y. SUN[1], V.W. Yong[2], M. Xue[1]
[1]Neurology,
The First Affiliated Hospital of Henan University, Kaifeng, China
[2]Clinical Neurosciences and Hotchkiss Brain Institute, University of Calgary, Calgary, Canada

OBJECTIVES: Microglia become activated following intracerebral hemorrhage (ICH). Monocytes from the circulation migrate into areas of CNS injury to become macrophages. These activated cells are often called 'microglia/macrophage" since it is difficult to differentiate between them. The neutrophils also infiltrate into the injured brain after ICH. Activated microglia/microphages and the infiltrated neutrophils are capable of releasing numerous detrimental mediators such as matrix metalloproteinases, free radicals, chemokines and cytokines, but they can also produce neurotrophic factors. We tested the hypothesis that the activation of microglia/macrophage and the infiltrated neutrophils promote brain injury in the acute period after ICH and that inhibition both of the activated microglia/macrophage and the infiltrated neutrophils attenuates brain injury and improves outcomes following ICH.

METHODS: 10-µl of autologous blood obtained from tail was introduced into the right striatum of adult male mice (7-9 weeks old) to produce ICH injury. C57/B6 wildtype mice were used to evaluate the time course of brain injury from 1-7 day(s). We determined the area of brain damage, the extent of neuronal death, the number of infiltrated neutrophils and microglia/macrophage activity. We also used transgenic CD11b thymidine kinase (CD11b-TK) mice where proliferating microglia/macrophage were removed by ganciclovir treatment. Functional grade purified anti-mouse Ly6G/Gr-1 antibodies or isotype-matched control antibodies were used to reduce the neutrophil infiltration. Wildtype and CD11b-TK mice were randomized into sham, injured treated, or controls and received either 4 mg/kg intraperitoneal injections of anti-LyG6/Gr-1 antibodies or isotype control at 2 and 24 h after SCI. Groups of CD11b-TK mice were treated with ganciclovir and/or anti-mouse Ly6G/Gr-1 antibodies. These mice were killed at 3 days after ICH injury and brain sections were stained for various parameters.

RESULTS: We found that ICH injury resulted in activation of microglia/macrophages through 1-7 days of brain insult. The area of brain damage peaked at 2-3 days; the number of dying neurons peaked at 1-3 days, the number of infiltrated neutrophils peaked at 1-3 days, while the activation of microglia/macrophages peaked at days 3-4. These findings led us to choose day 3 for further studies. We found that the activation of microglia/macrophage was significantly reduced in CD11b-TK transgenic mice with ganciclovir treatment after ICH compared to various injury control groups, including wildtype mice with ganciclovir treatment after ICH. The numbers of infiltrated neutrophils were significantly reduced in the group with anti-mouse Ly6G/Gr-1 antibodies treatment after ICH compared to various injury control groups, including wildtype mice with isotype treatment after ICH. Correspondingly, the area of brain damage and the extent of neuronal death were minimal in CD11b-TK mice with ganciclovir and anti-LyG6/Gr-1 antibodies treatment after ICH compared to all other groups.

CONCLUSIONS: Both activated microglia/macrophages and the infiltrated neutrophils in the early periods after ICH promote brain injury. Thus inhibition of their activities attenuates brain injury following ICH. These results shed light on the advent of new medications for ICH patients, including microglia deactivators and the antibodies to alleviate neutrophil infiltration.

126
BRAIN-0294
Brain Oral Communication

Oral Session: Cerebral Hemorrhage and Related Pathologies

A NEW ANTIFIBRINOLYTIC, CM352, MEDIATES REDUCTION OF HEMATOMA VOLUME AND IMPROVES FUNCTIONAL RECOVERY IN EXPERIMENTAL INTRACEREBRAL HEMORRHAGE.

T. Sobrino[1], J.A. Rodríguez[2], A. Vieites-Prado[3], E. López-Arias[3], R. Iglesias[3], Y. Oyarzabal[4], J. Orbe[2], J.A. Páramo[2], J. Castillo[3], F. Campos[3]
[1]Clinical Neurosciences Research Laboratory, Heath Research Institute of Santiago de Compostela (IDIS), Santiago de Compostela, Spain
[2]Atherosclerosis Research Laboratory, Center for Applied Medical Research (CIMA), Pamplona, Spain
[3]Clinical Neurosciences Research Laboratory, Health Research Institute of Santiago de Compostela (IDIS), Santiago de Compostela, Spain
[4]Small Molecule Discovery Platform, Center for Applied Medical Research (CIMA), Pamplona, Spain

Objective: Intracerebral hemorrhage (ICH) represents 10% to 15% of all strokes. Early mortality ranging between 32%-52% within the first 30 days, and only 20 % of patients live independently at six months. Despite being the most severe cerebral vascular disease, there is no specific pharmacological treatment and the role of surgical treatment is not well established. Hematoma expansion is one of the factors more associated to poor outcome in ICH patients. Therefore, our aim was to study the effectiveness of a novel antifibrinolytic agent, CM352, a short half-life (1.4 h) MMP inhibitor, to achieve early hemostasis and improve functional outcome in a rat model of collagenase-induced ICH.

Methods: We used SD rats (350-375 g) (n=12) subjected to collagenase-induced ICH. Rats were randomized into 2 experimental groups (each of n=6) treated with: 1) control group (1 mL PBS); 2) CM-352 (1 mg/kg). All treatments were intravenously administered at 1 hour after collagenase injection. Hematoma volume was measured on T2-weighted magnetic resonance images (MRI) at 1, 3 and 24 hours, and at day 14 after ICH. Neurological and functional recovery was assessed by Bederson and cylinder tests, respectively, at baseline and at 24 hours and day 14 after ICH.

Results: CM352 mediated a reduction of hematoma expansion at 3 hours (310 ± 62 *vs.* 200 ± 86%; p<0.01) and, more significantly, at 24 hours (305 ± 51 *vs.* 133 ± 63%; p<0.001). This reduction of early hematoma expansion by CM352 was associated to smaller lesion volume at 14 days (27.8 ± 4.1 *vs.* 14.4 ± 2.4 mm3; p<0.001) **(Figure 1)**. On the other hand, CM352 reduced sensorimotor impairment after ICH in rats from 73% to 16% (p<0.01) at 24 hours, and from 49% to 6% (p<0.01) at day 14 after ICH. Likewise, CM352 also attenuated neurological deficit at 24 hours (71 *vs.* 14%; p<0.01) and at 14 days (43 *vs.* 0%; p<0.01).

Conclusions: CM352 reduces hematoma growth and lesion size, and induces a better functional and neurological recovery, in a rat model of collagenase-induced ICH. Future preclinical studies are needed to validate CM352 as a promising drug to be used in clinical trials in ICH.

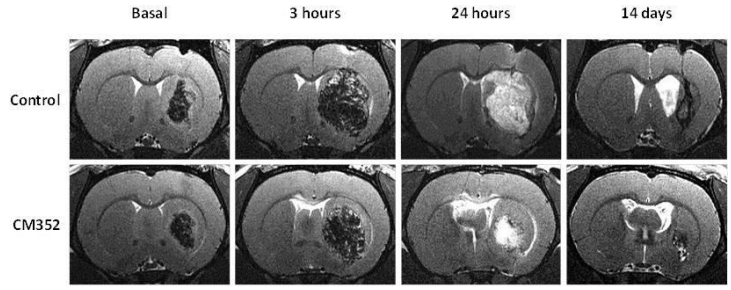

Figure 1: Hematoma and lesion volumes were assessed by means of magnetic resonance imaging (MRI). T2-weighted images were acquired at 1, 3, and 24 hours and at day 14 after ICH onset. T2-weighted images on each row correspond to one of 2D slices of the same animals within each group at different time points.

127
BRAIN-0640
Brain Oral Communication

Oral Session: Cerebral Hemorrhage and Related Pathologies

RED BLOOD CELL-DERIVED MICROPARTICLES FOR THE TREATMENT OF INTRACEREBRAL HEMORRHAGE.

V. Shukla[1], S. Koch[1], I. Saul[1], C. Bidot Jr.[2], A. Liu[1], M.A. Perez-Pinzon[1], W. Jy[2], Y.S. Ahn[2], K.R. Dave[1]
[1]Department of Neurology, University of Miami Miller School of Medicine, Miami, USA
[2]Division of Hematology/Oncology Department of Medicine, University of Miami Miller School of Medicine, Miami, USA

Objectives: Spontaneous intracerebral hemorrhage (SICH), although less common than ischemic stroke, is the most devastating form of stroke. Morbidity and mortality are high. No effective treatment is available so far. Preventing hematoma extension, and/or prevention of continued bleeding in SICH have been attractive therapeutic targets. It has been shown *in vitro* that red blood cell-derived microparticles (RMP) enhance platelet function as well as accelerate coagulation, augmenting both primary and secondary hemostasis[1]. In the present study we determined the efficacy of RMP in reducing hematoma expansion in a rat model of SICH.

Methods: RMPs were prepared from human RBCs using a high-pressure extrusion method[1]. SICH was induced in male Sprague Dawley rats by injection of 0.17U of collagenase into the left striatum. Rats were randomly divided into two groups (a) Placebo (vehicle-treated) group, n=9; and (b) RMP-treated group, n=10. RMP were injected via femoral vein at 1 hour and again at 2 hours post-SICH, at $3x10^9$ particles / kg per injection. At ~24 hours post-collagenase injection, neurological scores were evaluated[2,3], rats were sacrificed and the hematoma areas on images of brain sections were measured. Induction of SICH and evaluation of hematoma area and neurological score was carried out by an investigator blinded to the experimental conditions.

Results: (i) The effect of RMP treatment on hematoma area: A significant ($p < 0.05$) 31% reduction in hematoma area was observed in RMP-treated group; i.e. 72 ± 9 mm^2 (mean ±SEM) compared to placebo group (105 ± 13 mm^2) at ~24 hr post-collagenase injection. (ii) Brain hemoglobin level: For placebo-treated rats, 315 mg Hb / g protein. For RMP-treated rats, a small but significant ($p<0.001$) decrease in hemoglobin level was observed (275 mg Hb / g protein). (iii) Mortality and morbidity: At ~24 hr post-SICH, one vehicle-treated rat died, group while no mortality was observed in the RMP-treated group. No significant difference in neurological score was observed at ~24hr post-SICH.

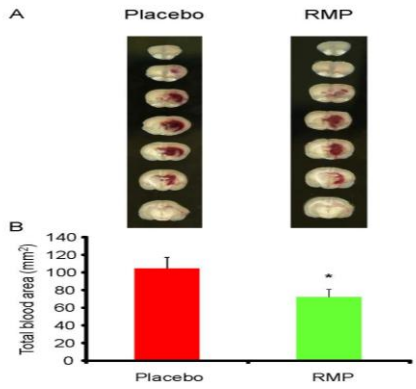

Figure: The effect of RMP therapy on hematoma area following collagenase-induced SICH. *, $p < 0.05$ placebo vs. RMP.

Conclusions: Our results demonstrate that RMPs have the potential to arrest or limit hematoma growth in SICH. These preliminary results are promising, but need future investigation. Also, a modified dosage regimen might improve efficacy since we have previously observed that continuous infusion of RMPs is more effective than bolus. If further work confirms and improves this benefit, RMP treatment could save many lives.

Acknowledgement: This study is supported by the Wallace Coulter Foundation and an internal grant from the University of Miami.

References: 1) Thrombosis & Haemostais, 2013; 110:751-760; 2) Stroke. 1986; 17:472-476; 3) Stroke. 1989; 20:1383-1390

128
BRAIN-0310
Brain Oral Communication

Oral Session: Cerebral Hemorrhage and Related Pathologies

EXPRESSION AND FUNCTION OF MICRORNAS IN HUMAN BRAIN ARTERIOVENOUS MALFORMATION

J. huang[1], W. zhu[2], J. song[2], M. qu[3], Y. wang[3], Z. zhang[1], Y. wang[1], G.Y. yang[1]
[1]Neuroscience and Neuroengineering Research Center , Med-X Research Institute, Shanghai, China
[2]Department of Neurosurgery, Hua Shan Hospital, Shanghai, China
[3]Department of Neurology, Ruijin Hospital, Shanghai, China

Objectives: Small noncoding microRNAs (miRNAs) modulates vascular development and angiogenesis [1-2]. The expression and function of miRNAs in human brain arteriovenous malformations (BAVMs) are largely unknown. In present study, we aim to investigate the miRNAs signature in human BAVMs to identify key miRNAs and down stream proteins that relate to vascular malformation. In addition, to identify potential biomarkers for human BAVMs in the peripheral circulation.

Methods: Total RNA from the surgical specimen of human BAVMs (n=6), hemangioblastoma (n=5), and epileptic brain vascular tissue (as a control, n=5) were isolated and assessed using a RT-PCR assay. 739 miRNAs were validated with quantitative RT-PCR analysis to establish the miRNAs expression signature. Potential miRNAs targets and their functions were predicted via ingenuity pathway analysis. Human BAVM vascular smooth muscle cells(AVM-SMCs) were identified, and the proliferation, migration and tube formation of these cells were examined *in vitro*. miRNAs identified in the previous steps were overexpressed in the AVM-SMCs by transfected mimics and downstream target proteins were quantified by proteomics assay. Finally, 21 miRNAs were validated using RT-PCR on an independent set of expression in the blood of human BAVMs (n=43) and the controls (n=43).

Results: Twenty-one miRNAs were identified to be significantly differently expressed among human BAVMs, hemangioblastoma, and control vascular tissue. Cell proliferation, migration and tube formationwere greatly enhanced in the AVM-SMCs compared to the controls both *in vitro* and *in vivo* (*pp*

Conclusions: Our study identified a distinct miRNAs expression signature in human brain vascular diseases. Specifically, miRNA-137or miRNA-195* were down-regulated in human AVM-SMCs, which could up-regulate associated proteins and lead to enhanced vascular smooth muscle cell proliferation, migration, and tube formation. Our findings provide valuable clue on the identification of miRNAs function in cerebrovascular pathologic processes.

References:

1. Small EM, Olson EN. Nature. 2011 Jan 20;469(7330):336-342.
2. Andreas Schober, etl. Nature Medicine. 2014 Apr;20(4):368-376.

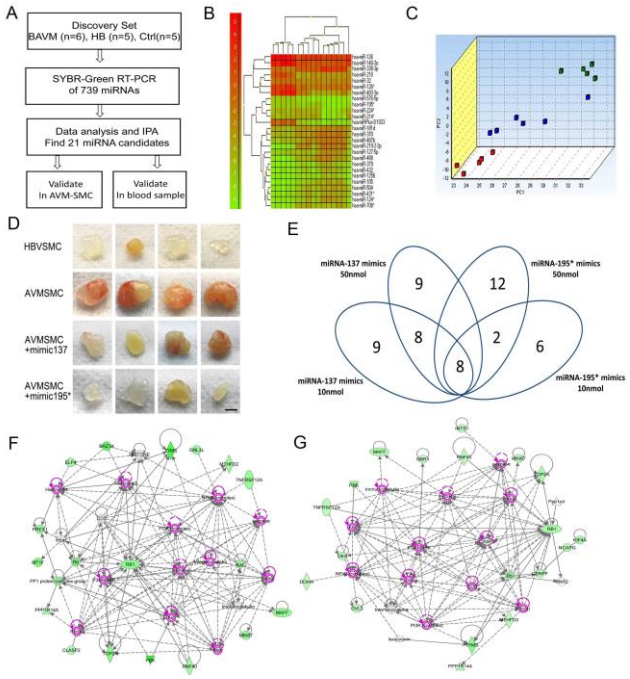

Figure. A, Workflow of the experiment. B, Heatmap ofthe significant differently expressed miRNAs in the discovery set. C, Principalcomponent analysis plots of all the 739

miRNAs. Green square=HB samples. Bluesquare=AVM samples. Red square=Ctrl samples. D, Overexpression of miRNA-137 ormiRNA-195* inhibited the AVM-SMC vasculogenesis. Scle bar=3mm. E, Overlapof proteins identified in the down regulated protein after the miRNA-137 ormiRNA-195* mimics transfered into the AVM-SMC. F, IPA predited regulatory mainnetwork of miRNA-137 down regulated proteins. G, IPA predited regulatorymain network of miRNA-195* down regulated proteins.

129
BRAIN-0455
Brain Oral Communication

Oral Session: Cerebral Hemorrhage and Related Pathologies

HISTOPATHOLOGICAL INVESTIGATION OF INTRACRANIAL ARTERIAL DISSECTIONS

H. Ono[1], H. Nakatomi[1], H. Imai[1], N. Saito[1]
[1]Department of Neurosurgery,
The University of Tokyo, Tokyo, Japan

[Objectives]

Intracranial arterial dissections (IAD) are mainly divided into hemorrhagic and non-hemorrhagic ones, the former is subarachnoid hemorrhage (SAH) and the latter are headaches or ischemic stroke. For patients with non-hemorrhagic IAD, conservative treatments has been advocated, while early repair of the affected vessels by open surgery or endovascular technique tends to be performed for SAH patients. Recently as the endovascular techniques advance, open surgery gradually decreased, and the chance of histopathological examination of the IAD gets rare. In this study, we conducted a histopathological investigation of intracranial arterial dissections.

[Methods]

From April 1980 to December 2000, 143 patients were diagnosed with acute IADs at our institutions. All cases satisfied one of the three diagnostic criteria for acute IAD: 1) the typical pearl and string or double lumen sign at a non-branching site of the intracranial cerebral arteries on angiography; 2) fusiform dilatation with retention of contrast medium or angiographic steno-occlusive lesions accompanied by intramural hemorrhage detected on MRI at the same region; or 3) histopathologically confirmed IAD. Among these cases, we obtained the tissue samples of IAD vessels from 13 patients at various intervals from onset and conducted histopathological investigation.

[Results]

17 pathological specimens were obtained from 13 IAD patients. 14 speciemens were hemorrhagic and 3 were non-hemorrhagic. The time to histological examination from the initial onset varied from 0 days to 8 months. Four characteristic features were identified: 1) internal elastic layer (IEL) disruption and intramural hemorrhage (IMH) causing additional medial disruption; 2) replacement of IMH within the pseudolumen by granulation tissue; 3) reactive intimal thickening around the pseudolumen; and 4) recanalizing vessel formation in the thickened intima. Disruption of the IEL and media were found in all cases. Replacement of IMH within the pseudolumen by granulation tissue was observed in all 6 samples obtained more than 14 days after onset. In addition, intimal thickening was observed in 4 samples obtained 26 days from onset. Recanalizing vessel formation within the thickened intima was observed in the 2 samples obtained more than 30 days after onset. Three IADs presenting with cerebral ischemia but showing aneurysmal enlargement demonstrated subintimal hemorrhage, medial disruption, and subadventitial hemorrhage.

[Conclusions]

Based on the results, we propose the following hypothesis for the mechanism of IAD. The first change in IAD seems to be IEL and medial disruption. The earliest repair process seems to be replacement of intramural hemorrhage within the pseudolumen by granulation tissue, which is rapidly followed by intimal hyperplasia. When intimal thickening reaches a sufficient level, neovascularization within the thickened intima seems to start. The new vessels within the intima seem to be fragile and cause

repetitive intramural hemorrhage leading to dolichoectatic aneurysm. Although further studies are needed to confirm this hypothesis, knowledge of this possible mechanism of formation, repair, and recurrence of IAD would help understand the clinical features of IAD at different stages and would also help determine the appropriate treatment strategy.

[Reference]

Ono H, Nakatomi H, et al. Stroke. 2013 Jan;44(1):126-31

130
BRAIN-0696
Brain Oral Communication

Oral Session: Cerebral Hemorrhage and Related Pathologies

INVOLVMENT OF BLOOD CONSTITUENTS ON LESION DEVELOPMENT AFTER ACUTE SUBDURAL HEMORRHAGE IN RATS

O. Kempski[1], S. Saeed[1], D. Jussen[2], B.E.A.T. Alesssandri[1]
[1]Inst. Neurosurgical Pathophysiology, University Medical Center, Mainz, Germany
[2]Dept. Neurosurgery, Horst-Schmidt Clinic, Wiesbaden, Germany

Objective: Intracranial hemorrhages are a frequent complication of traumatic brain injury. Especially acute subdural hematomas (ASDH) worsen outcome dramatically. Despite evacuation of the subdural blood clot early after an incidence 30% of these patients still die. The extravasated blood causes an increase of the intracranial pressure (ICP), a decrease of the cerebral perfusion pressure and the local cerebral blood flow (CBF). Replacement of subdural blood by an inert substance in an animal model of ASDH induces similar ICP, CPP and CBF changes, but a much smaller damage (1,2). Thus, it is speculated that substances from the extravasated blood (e.g. thrombin, potassium) contribute largely to the developing lesion (1). The goal of the presented study was to investigate the potential role of various blood constituents for the ASDH-induced brain damage.

Methods: Male Sprague-Dawley rats were anesthetized using chloral hydrate and mechanically ventilated during surgery, induction of the ASDH and 1-hour monitoring. They were monitored for mean arterial blood pressure (MAP) and ipsilateral CBF (Laser-Doppler probe). After a survival period of 48h brains were removed carefully for histological analysis of lesion volume. Functional outcome was assessed using neuronal (neuroscore) and motor function tests (beam walk, beam balance,) before and on day 2 post-injury. Rats were randomly assigned to two experimental series. The first series consisted of groups subdurally infused with 300 µl freshly drawn blood (whole blood, n=10), whole blood lysed with ultrasound (lysed blood, n=9) or washed erythrocytes from whole blood (erythrocytes, n=9). The second series consisted of groups receiving plasma (n=9), plasma mixed with Argatroban (10µl/500µL whole blood; anticoagulated plasma, n=10) or a physiological ionic solution (ion solution, n=9). All infused solutions were prepared immediately before injury induction.

Results:The two groups injected with whole blood or lysed blood showed a Cushing reflex of MAP and a long-lasting reduction of CBF (>60%). Infusion of erythrocytes induced a drop of 20%. No significant Cushing reflex and CBF change was observed in all other groups. Lesion volumes of the experimental series 1 were 21,33±6,47 mm^3 (whole blood), 17,32±13,01 mm^3 (lysed blood) and 0,45±0,10 mm^3 (erythrocyte),respectively ($p<0.05$ vs. erythrocytes). In series 2 infusion of plasma, anticoagulated plasma and physiological ion solution induced lesion volumes of 1,59±0,68 mm^3, 1,36±0,92 mm^3 and 1,10±0,56 mm^3, respectively (n.s. for all comparisons). Only the two groups with largest lesions had significant behavioral deficits.

Conclusion: Blood constituents such as plasma, anticoagulated plasma, pure erythrocytes and ionic components contribute only slightly on the lesion development after ASDH. Even the intracellular content of erythrocytes from lysed whole blood (e.g. 80 mM potassium) did not augment the whole blood-induced lesion volume. Thus, the combination of various intra- and extracellular blood components - possibly in combination with elevated ICP - appears

to be necessary for the devastating effects of acute subdural hemorrhage.

References:

1 Baechli et al. (2010) Blood constituents trigger brain swelling, tissue death, and reduction of glucose metabolism early after acute subdural hematoma in rats. J Cereb Blood Flow Metab 30:576-585.

2 Kuroda et al. (1992) Transient glucose hypermetabolism after acute subdural hematoma in the rat. J Neurosurg 76:471-477.

133
BRAIN-0084
Brain Oral Communication

Oral Session: Neurological Diseases: Animal Studies

DISRUPTION OF CAVEOLIN-1 FUNCTION COMPROMISES NEURAL PROGENITOR CELL REPONSE TO STROKE: IMPLICATIONS FOR THE DEVELOPMENT OF COGNITIVE DEFICITS.

O. Lazarov[1], J. Bonds[1], R. Minshall[2], D. Pelligrino[3]
[1]Anatomy and Cell Biology,
University of Illinois at Chicago, Chicago, USA
[2]Pharmacology and Anesthesiology,
University of Illinois at Chicago, Chicago, USA
[3]Anesthesiology, University of Illinois at Chicago, Chicago, USA

Objectives: Stroke patients are at risk for the development of cognitive deficits and Alzheimer's disease. However, the vascular component underlying lack of brain repair and cognitive deterioration is unknown. Neural progenitor cells have the capacity to replace dying neurons and support brain repair following stroke, but they fail to do so. Neural progenitor cells play a role in learning and memory and in the maintenance of brain plasticity. The neurogenic niche greatly depends on brain vasculature and angiogenesis. Endothelial cells intimately interact with neural stem cells and their progeny in vascular foci termed "hot spots". Caveolin-1 (Cav-1) is a cholesterol binding protein, which plays a major role in endothelial cell function. Cav-1 knockout mice exhibit oxidative stress, greater susceptibility to stroke, as well as enhanced aging and Alzheimer's disease-like neuropathology. The objective of this study is to examine the role of Cav-1 in the neurogenic response to stroke.

Methods: Extent of neurogenesis was assessed in Cav-1 knockout mice (Cav-$1^{-/-}$). Expression of Cav-1 and neurogenic response following stroke were examined in adult mice following middle cerebral artery occlusion.

Results: We observed that Cav-1 expression is downregulated in adulthood as a function of age. Further, neurogenesis is altered in Cav-1 knockout mice (Cav-$1^{-/-}$). In addition, lack of Cav-1 induces upregulation of amyloid precursor protein (APP). Mutations in *APP* cause familial Alzheimer's disease. Intriguingly, the expression of Cav-1 is reduced in the neurogenic microenvironment following cerebral ischemia (MCAO) in adult mice. Lastly, we show that hypoxic conditions induce Cav-1 degradation.

Conclusions: These results suggest that following stroke Cav-1 function in endothelial cells is disrupted, leading to compromised vascular neurogenic niche and may underlie, at least in part, the failure of neurogenesis to support brain repair.

134
BRAIN-0350
Brain Oral Communication

Oral Session: Neurological Diseases: Animal Studies

CALORIC RESTRICTION INCREASES KETONE BODIES METABOLISM AND PRESERVES BLOOD FLOW IN AGING BRAIN

A. Lin[1], W. Zhang[2], X. Gao[3]
[1]Sanders-Brown Center on Aging,
University of Kentucky, Lexington, USA
[2]Research Imaging Institute,
University of Texas Health Science Center at San Antonio, San Antonio, USA
[3]Institutional Mass Spectrometry Laboratory,
University of Texas Health Science Center at San Antonio, San Antonio, USA

Objectives: Caloric restriction (CR) has been shown to increase the lifespan and healthspan of a broad range of species. However, CR effects on in vivo brain

functions are far from explored. In the study, our goal was to identify CR effects on cerebral metabolism and blood flow in aging rats. We used multi-metric neuroimaging methods and mass spectroscopy to characterize the CR-induced changes of brain metabolic and vascular functions.

Methods: Experiments were conducted using male Fischer 344 Brown-Norway F1 (F344BNF1) rats. Young control (5 months, N = 6), old control, and old calorie-restricted rats (24 months, N= 6 for each group) were obtained from the NIA Caloric Restricted Colony. Cerebral metabolic rate of glucose (CMR_{Glc}) was measured using ^{18}FDG PET with 0.5 mCi of ^{18}FDG dissolved in 1mL of physiologic saline solution injected through the tail vein. CMR_{Glc} was determined using the mean standardized uptake value equation. Cerebral blood flow (CBF) was measured using MRI-based arterial spin labeling. The rats were scarified after MRI scans. We used high-performance liquid chromatography-electrospray ionization-mass spectrometry to measure brain metabolites in the cortex and hippocampus, including Glucose 1-Phosphate/D-Fructose 6-Phosphate (G1P-F6P), lactate, ketone bodies (β-Hydroxybutyrate; BHB). We used one-way, repeated measures ANOVA to determine the difference of the measured indices between the three groups. Post-hoc testing was performed by Newman-Keuls test.

Results: We found that old control rats had significantly lower CMR_{Glc} in the whole brain compared to the young controls; the old CR had significantly lower global CMR_{Glc} relative to both control groups. Similar observations were also found in cortex, hippocampus and hypothalamus. This suggests that CMR_{Glc} declines with age, and CR further reduces glucose utilization in aging. Old control rats overall had significantly lower CBF than that of the young controls. However, old CR rats had indistinguishable CBF compared to the young controls. Similar CBF patterns were also found in cortex, hippocampus and hypothalamus. This indicates that CBF reduces with age, but CR is able to impede the decline. In the brain tissue, we observed significantly reduced G1P-F6P and lactate concentrations, two glycolytic metabolites, in the old CR rats compared to the age-matched controls. In contrast, ketone bodies (BHB) were significantly elevated in the old CR group. Taken together, we found that CR reduces glycolysis, increases ketone bodies level and preserves cerebral blood flow in aging F344BNF1 rats.

Conclusion: We demonstrated that CR shifts brain metabolism from glucose to ketone bodies metabolism, and preserves CBF in aging brain. These changes may play a crucial role in preserving neuronal healthspan under CR. Our results are consistent with previous findings that CR impedes age-related decline in mitochondrial functions and neuronal activity (1) and thus preserve memory in aging F344BNF1 rats (2). These results provide a rationale for CR-induced sustenance of brain health with extended lifespan. Understanding nutritional effects on brain function may have profound implications in human aging and other age-related neurodegenerative disorders.

References:
(1) Lin et al., JCBFM, 34:1440-1443; (2) Markowska and Savonenko, NBA, 23:75-86.

135
BRAIN-0445
Brain Oral Communication

Oral Session: Neurological Diseases: Animal Studies

SPONTANEOUS WHITE MATTER DAMAGE, COGNITIVE DECLINE AND NEUROINFLAMMATION IN MIDDLE-AGED HYPERTENSIVE RATS: AN ANIMAL MODEL OF EARLY-STAGE CEREBRAL SMALL VESSEL DISEASE

D. Kaiser[1], G. Weise[1], K. Möller[1], J. Scheibe[1], C. Pösel[1], S. Baasch[1], M. Gawlitza[2], D. Lobsien[3], K. Diederich[4], J. Minnerup[4], A. Kranz[1], J. Boltze[1], D.C. Wagner[1]
[1]Department of Cell Therapy, Fraunhofer Institute for Cell Therapy and Immunology , Leipzig, Germany
[2]Department of Radiology, University Hospital University of Leipzig, Leipzig, Germany
[3]Department of Neuroradiology, University Hospital University of Leipzig, Leipzig, Germany
[4]Department of Neurology, University of Münster, Münster, Germany

Objectives

Cerebral small vessel disease (cSVD) is one of the most prevalent neurological disorders. The progressive remodeling of brain microvessels due to arterial hypertension or other vascular risk factors causes subtle but constant cognitive decline and substantially increases the risk for stroke. Preliminary evidence suggests a contribution of the immune system to disease initiation and progression. Since most cSVD animal models are biased towards the hemorrhagic component of the disease[1], a more detailed understanding is currently impaired by the unavailability of appropriate animal models. Here, we investigated the spontaneously hypertensive rat (SHR) as a possible model for early onset cSVD.

Methods

Male SHR and normotensive Wistar Kyoto rats (WKY, n=16 each, 11 weeks at enrolment) were used in this study. Animals were assigned to four experimental groups (Fig. 1). In group 1 (n=3/3), blood brain barrier (BBB) integrity was assessed by FITC-lectin and Evans Blue at 24 weeks. A brain tissue leukocyte profile of was obtained from group 2 (n=3/3) by fluorescence activated cell sorting (FACS) in week 35. In groups 3 and 4 (n=5/5 each), blood pressure was measured biweekly from week 12 to 22. Animals were further subjected to the novel object recognition (week 30) and Morris Water Maze (week 34) tests. Total brain, ventricle and corpus callosum (CC) volumes were determined by cerebral T2 MRI (3T) in week 35. Postmortem analyses included detailed cerebrospinal fluid, peripheral blood analysis by FACS and gene expression studies (laser microdissection and PCR), as well as detailed brain histology (neural cells, white matter density (Luxol Fast Blue), vessels and macro-/microglia).

Results

Blood pressure in SHR was significantly higher and increased over time ($p<0.01$ each). In contrast to age-matched normotensive WKY, SHR exhibited non-spatial memory deficits ($p<0.01$). MRI showed brain atrophy (increased ventricle volumes and decreased CC/brain volumes; $p<0.01$). An increased myelin index, indicating myelin loss in SHR ($p<0.01$; Fig. 2). Histological analyses confirmed white matter demyelination and unveiled a circumscribed BBB dysfunction in conjunction with micro- and macrogliosis in deep cortical regions (DCR; $p<0.05$ or below; Fig. 3). FACS and histological analyses further revealed substantial disparities in cerebral $CD45^{high}$ leukocyte counts and distribution patterns between SHR and WKY. SHR showed lower T cells counts in the choroid plexus and meningeal spaces as well as decreased interleukin-10 levels in the cerebrospinal fluid ($p<0.05$ or lower). Moreover, both T and NK cells were significantly augmented in the SHR brain microvasculature.

Conclusions

Our results indicate that SHR share behavioral and neuropathological characteristics with human cSVD patients and further undergird the relevance of immune responses for the initiation and progression of cSVD[2].

References

1. Schreiber et al. (2012); J Cereb Blood Flow Metab. 32(2):278-290.

2. Kaiser et al. (2104); Acta Neuropathol Commun. 2(1):169.

Fig. 1: Experimental setup.

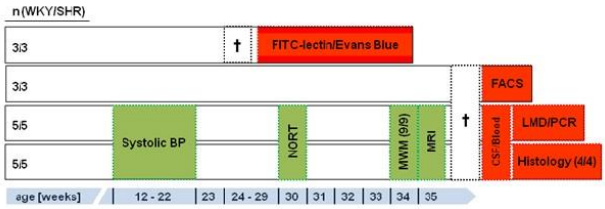

Fig. 2: SHR exhibited increased ventricle (A), decreased CC and brain volumes (B, C), and a higher

myelin index (D) indicating white matter loss.

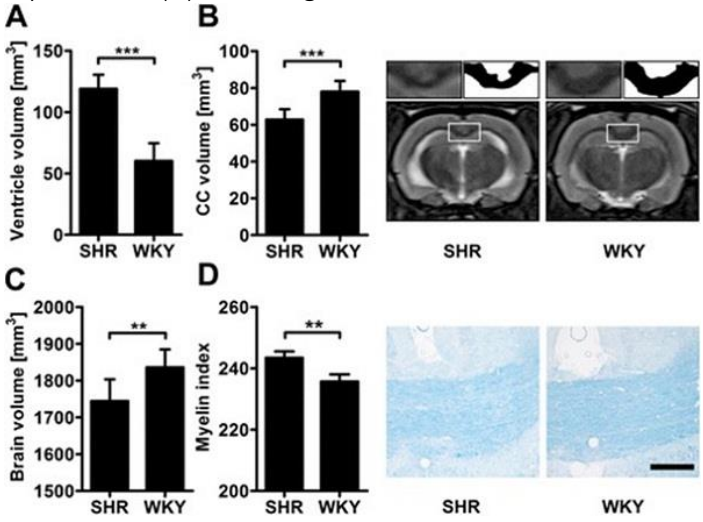

Fig. 3: Circumscribed BBB integrity loss in DCRs and activated astroglia.

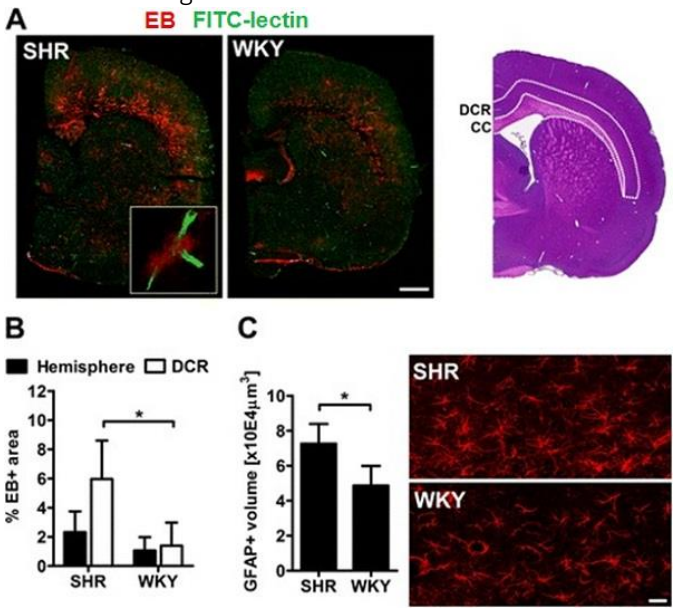

136
BRAIN-0549
Brain Oral Communication

Oral Session: Neurological Diseases: Animal Studies

CEREBRAL SMALL VESSEL DISEASE, OBSTRUCTIVE SLEEP APNEA, AND GUT DYSBIOSIS

B. Bryan[1], *D. Durgan*[1], *E. lloyd*[1]
[1]*Anesthesiology, Baylor College of Medicine, Houston, USA*

Individuals suffering from obstructive sleep apnea (OSA), a condition where the upper airway repeatedly collapses during sleep to produce apnea, are at risk for either developing cerebrovascular diseases or accelerating their progression. One of these cerebrovascular diseases, cerebral small vessel disease (CSVD), involves pathological alterations to the small vessels of the brain. CSVD produces cognitive impairment, resulting from damage to cerebral white and deep grey matter. In the present study we tested the hypothesis that CSVD is accelerated by pathological alterations to the gut microbiome (i.e., dysbiosis) resulting from OSA. 15 to 20 week old spontaneously hypertensive stroke prone rats (SHRSP), an animal model for CSVD, were chronically instrumented with a tracheal balloon that could be remotely inflated. Rats were randomly assigned to an OSA group, where the balloon was inflated 60 times/hr for 10 sec to produce apneas (corresponding to severe OSA in humans) or to a sham control group that were instrumented with a tracheal balloon but were not subjected to apneas. In the OSA group, apneas continued each day for 8 hr during the sleep cycle for 2 weeks. Analysis of the gut microbiome, through sequencing of the bacterial 16s rRNA gene in fecal samples, revealed a significant shift in the Bacteroidetes:Firmicutes ratio (from 0.76 to 0.48, $p=0.046$) indicating dysbiosis. Systolic blood pressure was significantly increased ($n=7$-10, $p<0.05$) in SHRSP with OSA by 20 ± 4 mm Hg above the sham rats. Blood brain barrier permeability, as assessed by IgG extravasation, was significantly increased ($n=6$, $p<0.05$) in small vessels of the OSA group compared to sham controls. Activation of microglia, the resident immune cells in brain was significantly greater (as determined by morphometric analysis) in the OSA group compared to sham controls ($n=6$,$p<0.05$). When pretreating the SHRSP OSA group with antibiotics (ampicillin [1gm/L] and neomycin [0.5 gm/L] in drinking water), which almost abolished the Firmicutes, OSA had no significant effect on the systolic blood pressure ($n=4$-9,$p=0.478$), damage to the blood brain barrier ($n=4$-9, $p=0.015$) was reduced, and activation of microglia was attenuated ($n=4$-9, $p=0.001$). Our studies link gut dysbiosis, occurring as a result of OSA, to hypertension, blood-brain barrier integrity, and activation of resident immunity in the brain. Our study further suggests that bacteriotherapy could

possibly blunt some of the pathological consequences of OSA.

137
BRAIN-0508
Brain Oral Communication

Oral Session: Neurological Diseases: Animal Studies

INSULIN REGULATED AMINOPEPTIDASE: A POTENTIAL CEREBROVASCULAR AND NEUROPROTECTIVE MECHANISM IN A MOUSE MODEL OF ALZHEIMER'S DISEASE

J. Royea[1], L. Zhang[2], S. Ozcelik[1], X.K. Tong[1], E. Hamel[1]
[1]Laboratory of Cerebrovascular Research, Montreal Neurological Institute McGill University, Montreal, Canada
[2]Department of Human Anatomy, Nanjing Medical University, Nanjing, China

Background: We recently found that the angiotensin II (AngII) type 1 receptor (AT1R) antagonist losartan restored cerebrovascular and cognitive deficits in an Alzheimer's disease (AD) mouse model[1]. The mechanism underlying these beneficial effects remains unknown. Yet, blockade of the AT1R is suggested to favour conversion of AngII to angiotensin IV (AngIV)[2]. AngIV interacts with insulin regulated aminopeptidase (IRAP), an enzyme which has been linked with improved cognitive performance in rats whereas IRAP gene knockout mice have spatial and short term memory deficits[3,4].

Objective: We investigated whether IRAP was involved in the benefits of chronic losartan treatment in transgenic mice overexpressing the Swedish and Indiana mutations of the human amyloid precursor protein (APP mice, line 20).

Methods: APP mice and wild-type controls (2-3 months old) received losartan (10 mg/kg/day, in the drinking water, 4 months). Blood pressure was monitored monthly by non-invasive tail-cuff plethysmography. Following 3 months of losartan treatment, a Morris water maze (MWM)[5] was performed to assess the effects of treatment on spatial learning and memory retention. Subsequently, intracerebroventricular administration of artificial CSF (control) or divalinal (~1 nmol/day), an IRAP blocker, was combined with losartan treatment using osmotic minipumps during the last month of treatment. A second MWM consisting of hidden platform testing and a probe trial was conducted after 1 month of combined treatment. Evaluation of neurovascular coupling was conducted by laser Doppler flowmetry to measure changes in blood flow evoked by whisker stimulation followed by experiments to measure cerebral vasodilatory function.

Results: Divalinal countered losartan's capacity to rescue spatial learning and memory retention. Additionally, divalinal reversed losartan's benefits on the neurovascular coupling response to sensory stimulation. Divalinal also blocked losartan's capacity to rescue dilatations of cerebral arteries to acetylcholine, calcitonin gene-related peptide and the transient receptor potential vanilloid 4 (TRPV4) channel opener GSK1016790A, as well as the baseline production of nitric oxide measured by incubating vessel segments with N^{ω}-nitro-$_{L}$-arginine. However, divalinal did not rescue the dilatory response to the ATP-sensitive potassium (KATP) channels. Neither losartan nor divalinal altered arterial blood pressure or amyloid-β pathology.

Conclusions: Since the beneficial effects of losartan on cerebrovascular and cognitive function could be reverted by concurrent intracerebral blockade of IRAP, we conclude that the AngIV/IRAP cascade likely mediates the positive benefits of the AT1R blockade observed in APP mice. This mechanism may represent a new therapeutic target in AD and may explain the reported decreased incidence of AD in hypertensive patients treated by AT1R blockers[6].

References: 1. Ongali B et al., Neurobiol Dis, 2014, 68: 126-136; 2. Braszko JJ et al., JRAAS, 2006, 7(3): 168-174; 3. Braszko JJ et al., J Neurosci, 1988, 27(3): 777-783; 4. Albiston AL et al., Neurobiol Learn Mem, 2010, 93(1): 19-30; 5. Deipolyi AR et al., *Neurobiol. of Aging, 2008, 29: 253-66.* 6. Wolozin B et al., Alzheimers Dement, 2008, 4: T118.

Acknowledgements: Supported by grants from the Canadian Institutes of Health Research (MOP-126001) and the Heart and Stroke Foundation of Canada.

138
BRAIN-0836
Brain Oral Communication

Oral Session: Neurological Diseases: Animal Studies

TOR-DEPENDENT NEUROVASCULAR DYSFUNCTION IN ALZHEIMER'S AND RELATED DEMENTIAS

V. Galvan[1], N. Sayre[2], J. Cirrito[3], J. Jahrling[4], A.L. Lin[5], S. Hussong[4], N. DeRosa[4], S. Austad[6], K.E. Fischer[6], R. Asmis[7]
[1]Barshop Institute/Physiology, University of Texas Health Science Center, San Antonio, USA
[2]Cellular and Structural Biology, University of Texas Health Science Center, San Antonio, USA
[3]Neurology, Washington University in St Louis School of Medicine, St Louis, USA
[4]Barshop Institute/Physiology, University of Texas Health Science Center at San Antonio, San Antonio, USA
[5]College of Medicine, University of Kentucky, Lexington, USA
[6]Biology, University of Alabama at Birmingham, Birmingham, USA
[7]Biochemistry, University of Texas Health Science Center at San Antonio, San Antonio, USA

We recently showed that chronic treatment with the target-of-rapamycin (TOR) inhibitor rapamycin, a drug that extends lifespan and delays aging in mice, halted and even reversed Alzheimer's (AD)-like memory deficits and reduced Aβ accumulation in brains of hAPP(J20) mice modeling the disease. Using multi-metric imaging we showed that attenuating TOR activity restored cerebral blood flow (CBF) and vascular density (VD) via eNOS activation in brain vascular endothelium, reduced CAA and microhemorrhages, and reestablished blood-brain barrier (BBB) integrity. As expected from the critical role of BBB in the clearance of Aβ peptide from brain, *in vivo* brain microdialysis studies showed that chronic TOR attenuation with rapamycin reduced the half-life of interstitial Aβ peptide in pre-plaque hAPP(J20) mice. Reducing TOR activity also restored cognitive function, CBF and VD in mice modelling atherosclerosis, as well as in aged rats, in which reduced TOR activity was associated with a complete recovery of cortical network activation and functional hyperemia evoked by somatosensory stimulation. Further, we showed that acute *in vivo* mTOR attenuation elicited endothelium-dependent NO-mediated vasodilation, and that endothelium-dependent NO release was required for the restoration of CBF and VD in AD mice. Taken together, our data suggest that TOR-dependent mechanisms of neurovascular dysfunction may be common to different age-associated neurological diseases and to brain aging, and single out endothelium-dependent NO release as a critical mechanism by which chronic TOR attenuation restores neurovascular competence and blocks age-related brain dysfunction or disease in rodent models. Thus, relieving mTOR-dependent inhibition of NO release may be a critical mechanism by which chronic rapamycin preserves brain vascular integrity and function during aging and in models of age-associated brain disease.

141
BRAIN-0293
Brain Oral Communication

Oral Session: Cerebral Ischemia: Functional Recovery

RAGE IS A KEY RECEPTOR MEDIATING PERIPHERAL IMMUNE ALTERATIONS AFTER STROKE

S. Roth[1], V. Singh[1], A. Geerlof[2], G. Huber[2], A. Liesz[1]
[1]Institute for Stroke and Dementia Research (ISD), Klinikum der Universität München, München, Germany
[2]German Research Center for Environmental Health, Helmholtz Zentrum München, München, Germany

Objectives: Acute brain injuries, including stroke, induce a neuroinflammatory reaction to the lesioned brain as well as systemic immune alterations. We have recently demonstrated that damage associated molecular patterns (DAMPs) passively released from the necrotic brain tissue to the circulation are key effector molecules in brain-immune communication. In this study, we investigated DAMP receptors in the systemic immune system as druggable target molecules, mediating peripheral immunomodulation induced by circulating DAMPs after stroke. Particularly, we have focused on the function of the receptor of advanced glycation endproducts (RAGE),

which is a key DAMP receptor on peripheral immune cells.

Methods: We used the transient middle cerebral artery occlusion model (MCAO) in C57BL6/J and RAGE-/- mice for induction of experimental brain ischemia. Mice received either intraperitoneal injections of soluble RAGE (sRAGE) or antibodies for cytokine neutralization (anti-IL-1β, anti-TNF-α and anti-IL6), respectively. Plasma levels of cytokines and immune cell subpopulations in peripheral tissues were analyzed by ELISA and flow cytometric analysis. Neurological deficits were assessed by a series of behavioral tests for sensorimotor focal deficits, motivation, anxiety, circadian rhythm and mobility. In order to analyze the *in vivo* ligands of sRAGE, sRAGE-ligand complexes were purified from mouse plasma by antibody immobilization, separated by gel electrophoresis and detected by mass spectrometry.

Results: We detected an increased humoral immune response after stroke measuring pro-inflammatory IL-6 plasma levels 24h after MCAO (MCAO: 456±190.87 pg/mL; Sham: 221±56.61 pg/mL; n=5, $p<0.05$). Moreover, flow cytometric analysis revealed an expansion of immature monocytes in the spleen characterized as CD11b+Ly6C+MHCII$_{low}$ cells while total spleen cellularity was decreased. In order to correlate immunological alteration, we analyzed a set of behavioral tests, which are indicative of cytokine-induced sickness behavior (CISB). We detected a significant improvement in overall activity and locomotion in RAGE-/- mice compared to WT mice, indicating ameliorated CISB under RAGE-deficiency. In contrast, tests for focal sensorimotor function were not altered in RAGE-/- compared to WT mice, confirming the role of RAGE-mediated peripheral inflammation independent of effects on primary cerebral outcome. Consequently, we used the decoy receptor sRAGE as a treatment paradigm and confirmed a comparable improvement of markers for CISB but not for focal deficits as in RAGE-deficient animals. We administered cytokine-neutralizing antibodies in order to test the role of pro-inflammatory cytokines as the effector molecules of the RAGE-pathway in mediating the behavioral alterations. Indeed, blocking circulating IL-1β, TNF-α and IL-6 had a comparable treatment pattern in reducing post-stroke CISB as blocking the RAGE-pathway, supporting the key role of circulating pro-inflammatory cytokines as crucial mediators of acute sickness behavior after brain injury. Moreover, sRAGE treatment reduced bone marrow-release of immature monocytes and splenic expansion of this cell population.

Conclusion: We have identified a key role for the RAGE-pathway in the systemic inflammatory response after stroke which is encompassed by a pronounced 'cytokine storm" and subsequent behavioral deficits characterized as cytokine-induced sickness behavior. We have identified DAMPs released from the necrotic brain tissue as ligands of the RAGE-mediated immune cascade, which can be antagonized using sRAGE as a potent decoy receptor.

142
BRAIN-0546
Brain Oral Communication

Oral Session: Cerebral Ischemia: Functional Recovery

GENETIC ENGINEERING OF PRIMARY GLIAL RESTRICTED PROGENITORS FOR IMPROVED INTRAARTERIAL TARGETING TO THE ISCHEMIC BRAIN

A. Jablonska[1], D.J. Shea[2], A. Arnold[1], J.W. Bulte[1], M. Janowski[1], K. Konstantopoulos[2], P. Walczak[1]
[1]Radiology, Johns Hopkins School of Medicine, Baltimore, USA
[2]Department of Chemical & Biomolecular Engineering , Johns Hopkins School of Medicine, Baltimore, USA

Objectives: Stroke is a leading cause of severe, long-term disability and it lacks effective therapy. Stem cells transplantation is an attractive strategy to repair damage following ischemia. In our model of mild stroke we observed loss of oligodendrocytes, while the integrity of axons was still retained. It provides rationale for treatment using glial restricted precursors (GRPs) to prevent delayed axonal degeneration. Our earlier work indicates positive effect of GRPs transplantation in rat models of transverse myelitis and dysmyelinated mice. However, clinical translation lacks methodology facilitating efficient targeting and broad cell distribution in the lesion. Local injections, effective in small animals, failed in several clinical trials. Intraarterial route may result in efficient distribution

of cells within the lesioned area; however, it requires diapedesis. Studies with immortalized GRPs showed that overexpression of VLA4 adhesion molecule results in their capture on activated brain endothelium in rats. Though immortalized cells are relatively easy to transfect they are not suitable for clinical applications.

Methods: Primary glial restricted progenitor cells were genetically engineered to transiently overexpress VLA4 and functionality of the transgene has been assessed *in vitro* using microfluidic adhesion assays and *in vivo* following intraarterial injection in MCAO mouse model of stroke. Moreover, dynamics of oligodendrocyte damage following stroke has been assessed in PLP-GFP reporter mice using intravital two-photon microscopy

Results: Transfection efficiency with DNA plasmids for integrin α4 and β1 optimized for the primary GRPs reached 60%. Functionality of the transgene was tested in microfluidic adhesion assays. Perfusion of VLA4^{+}GRPs through microfluidic channels coated with VCAM1 protein showed their slowed rolling compared to naïve GRPs. Adhesion experiment with brain endothelial cells coated channels revealed higher number of VLA4^{+}GRPs binding to endothelial cells activated with TNFα. Based on these data we initiated animal studies with assessing endothelial capture and diapedesis in rodent model of stroke using intravital multi-photon microscopy. Using time-lapse multi-photon microscopy and immunohistochemistry we have shown that degradation of oligodendrocytes starts within minutes after ischemia as evidenced by loss of green fluorescence in transgenic PLP-GFP mice, leaving surviving axons denuded for extended periods after stroke. With immunohistochemistry we demonstrate degradation of basic myelin protein (MBP) as early as 24 hours after stroke and this effect was amplified over time. Moreover, using time-laps 2-photon microscopy with visualization of brain vasculature based on systemic injection of TxRed Dextran® (Life Technologies) we demonstrated that intraarterially injected VLA4+GRPs effectively bind to endothelial cells and extravasate (Fig. 1). Ex vivo analysis of brain slices 3 hours after transplantation showed significantly greater number of arrested mouse GRPs transfected with VLA4 compared to naïve GRPs.

Conclusions: We demonstrated that overexpression of VLA4 in primary GRPs results in their improved adhesion to endothelium both *in vitro* and *in vivo*. We also provided evidence that intra-arterially delivered GRPs are indeed capable of extravasation.

143
BRAIN-0539
Brain Oral Communication

Oral Session: Cerebral Ischemia: Functional Recovery

NEUROGENESIS MANIPULATION AFTER STROKE CAN AFFECT A PREVIOUS ACQUIRED MEMORY

M.I. Cuartero[1], J. de la Parra[1], A. Pérez-Ruiz[1], I. Bravo-Ferrer[1], A. Moraga[1], A. García-Culebras[1], J.M. Pradillo[1], I. Lizasoain[1], M.A. Moro[1]
[1]Pharmacology, Complutense University of Madrid, Madrid, Spain

Background: The contribution of hippocampal neurogenesis to the recovery of cognitive function after stroke has been previously evaluated through different pharmacological or genetic tools[1-4]. Interestingly, the experimental design used in the aforementioned studies consists of manipulating neurogenesis before or just after cerebral ischemia induction and then, days or weeks later, the ability to form new hippocampus-dependent memories is evaluated. The main conclusion is that ablating neurogenesis after ischemia impedes cognitive recovery after stroke. Recent studies in adult mice under physiological conditions suggest that increasing neurogenesis after the formation of a memory was sufficient to induce forgetting by remodeling the pre-existing hippocampal circuits[5]. With this background, we asked whether ischemia-induced adult hippocampal neurogenesis or experimental interventions directed to manipulate neurogenesis could have a retrograde effect.

Methods: Permanent middle cerebral artery occlusion (MCAO) was performed by the ligature model in P60 C57BL/6J male mice. To check hippocampal-dependent tasks after MCAO and/or after neurogenesis intervention, animals were trained in the contextual fear conditioning and the Barnes maze 7d after MCAO. To increase adult neurogenesis after the formation of a memory in

ischemic mice, mice were allowed access to a running wheel for 28d. To suppress adult neurogenesis, mice were treated with temozolomide (TMZ; 25mg/Kg) for 4-weeks starting at day 7. Coronal fixed sections from ischemic and sham mice were stained for Ki67, DCX, Casp-3, BrdU and NeuN to determine the levels of neurogenesis. Quantification was performed using an Olympus microscope or serial Z-stack images were acquired with LSM-710 Confocal microscope.

Results: First, our data demonstrate that both Ki67 and DCX increased bilaterally in the SGZ of ischemic mice. Next, we assessed hippocampal memory persistence in sham and ischemic mice. For this, mice trained in the contextual fear conditioning were tested at 1 and 24h, and 7, 14, 21 and 28 days later. In the retrieval test, cerebral ischemia significantly reduced the freezing response and the activity suppression in comparison with the sham group in both short-term and long-term retrieval test (n=9-10, $p<0.05$), suggesting that after ischemia hippocampal-dependent function is impaired. Given that memory impairment persists long-term after ischemia, we chose the longer retention time to evaluate our hypothesis. First, pharmacological increase of neurogenesis by voluntary running starting 7d after MCAO increased neurogenesis, reduced freezing response in the contextual fear memory and impaired performance in the Barnes maze (n=10-15; $p<0.05$). On the contrary, and confirming our results, reducing neurogenesis by TMZ treatment after training improved contextual fear retrieval in ischemic mice (n=10-15; $p<0.05$).

Conclusions: Experimental interventions directed to manipulate neurogenesis after the formation of a post-stroke memory could have a retrograde effect.

References

1. Wang X et al. *PLoS One*. 2012;7:e38932

2. Jin K et al. *Proc Natl Acad Sci U S A*. 2010;107:7993-7998

3. Sun C et al. *J Neurosci*. 2013;33:17314-17325

4. Arvidsson A et al. *Nat Med*. 2002;8:963-970

5. Akers KG et al. *Science*. 2014;344:598-602

144
BRAIN-0509
Brain Oral Communication

Oral Session: Cerebral Ischemia: Functional Recovery

PURKINJE CELL DEATH AND CEREBELLAR DEFICITS RESULTING FROM EXPERIMENTAL CARDIAC ARREST AND CARDIOPULMONARY RESUSCITATION

N. Quillinan[1], G. Deng[2], M. Moreno[1], R.J. Traystman[2], P.S. Herson[1]
[1]Anesthesiology, University of Colorado, Denver, USA
[2]Pharmacology, University of Colorado, Denver, USA

Objectives: Purkinje cell death in the cerebellum is a well-accepted consequence of global cerebral ischemia resulting from cardiac arrest and cardiopulmonary resuscitation (CA/CPR). However, the mechanisms of injury and consequences of Purkinje cell loss are poorly understood. The goal of this study was to assess Purkinje cell injury and cerebellar function in adult and pediatric mice following cardiac arrest and cardiopulmonary resuscitation. We also tested the hypothesis that calcium/calmodulin-dependent kinase (CAMKII) activation contributes to Purkinje cell death in pediatric and adult mice.

Methods: Pediatric (21-25 day old) and adult (8-12 week) male mice were subjected to 8 minutes cardiac arrest followed by cardiopulmonary resuscitation or sham surgery. Purkinje cells were labeled using anti-calbindin antibody and cell density was analyzed to examine neuronal injury. To examine synaptic function, whole-cell voltage clamp recording on acute cerebellar slices was performed at 1 and 7 days after CA/CPR or sham surgery. Excitatory postsynaptic currents (EPSCs) resulting from parallel (PF) or climbing fiber (CF) stimulation were recorded. To assess motor function rotarod and gait analysis was performed. Long-term depression (LTD), a form of synaptic plasticity that underlies aspects of motor learning, was induced by simultaneous parallel and climbing fiber stimulation (1 Hz, 5 min).

Results: At 7 days following CA/CPR, Purkinje cell loss was observed in pediatric (24% cell loss) and adult (32% cell loss) mice. Administration of the novel CAMKII peptide inhibitor, tat-CN19o, provided significant protection against Purkinje cell loss in adults and pediatric mice compared to vehicle controls. In adult mice, latency to fall on rotarod testing was significantly faster following CA/CPR, demonstrating motor coordination impairments. Similarly, gait abnormalities were observed in adult and pediatric mice at 7 days after CA/CPR. Long-term depression, a characteristic reduction of synaptic strength of PF EPSCs, was observed in adult and pediatric sham controls following PF+CF stimulation (46.6 ± 10% of baseline n=5 and 55.4 ± 6.1% n=3, respectively). LTD was absent in pediatric and adult mice at 24 hours after CA/CPR (96.1 ± 5.2% n=6 and 89.4 ± 4.5% n=2, respectively). At 7 after CA/CPR LTD was absent in adult mice (81.6 ± 10.8% n=6 and 86.5 ± 8.9% n=4) but had returned in pediatric mice at 7 days after CA/CPR (70 ± 5.4% n=3).

Conclusions: The results of this study suggest that CA/CPR results in significant Purkinje cell loss in pediatric and adult mice and that CAMKII activation contributes to cell death. Motor coordination impairments were observed in adult and pediatric mice following cardiac arrest and these impairments likely correlate with Purkinje cell death. In contrast, differences were observed in synaptic plasticity with pediatric mice showing enhanced recovery of LTD compared to adult mice. Therefore, future studies will be aimed at determining whether there are motor learning impairments that recover in pediatric, but not adult mice.

145
BRAIN-0676
Brain Oral Communication

Oral Session: Cerebral Ischemia: Functional Recovery

SENSORY DEPRIVATION FOLLOWING CORTICAL FOCAL ISCHEMIA FACILITATES REMAPPING AND ACCELERATES BEHAVIORAL RECOVERY

A.W. Kraft[1], A.Q. Bauer[2], K.P. Smith[1], J.P. Culver[3], J.M. Lee[4]
[1]Neurology, Washington University, St. Louis, USA
[2]Radiology, Washington University, St. Louis, USA
[3]Radiology Physics Biomedical Engineering, Washington University, St. Louis, USA
[4]Neurology Radiology Biomedical Engineering, Washington University, St. Louis, USA

Objective: Ischemic stroke is the leading cause of disability in the developed world [1]. The spontaneous behavioral recovery that does occur, while often unpredictable and incomplete, is associated with functional remapping of infarcted representations to cortical regions adjacent to the lesion [2,3,4]. This suggests that remapping may be an important therapeutic target for stroke recovery. However, the molecular mechanisms underlying remapping have not been investigated, and it is unclear if remapping can be modified to alter behavioral recovery outcomes. Using photothrombosis to ablate the forepaw somatosensory representation (S1FP) in mice, we sought to determine if remapping could be accelerated by depriving the unaffected perilesional whisker barrel cortex of sensory input (via chronic whisker trimming) and if this would impact sensorimotor behavioral recovery. In addition, by applying the S1FP photothrombosis to deficient for Arc, a gene critical for synaptic plasticity and learning[5], we sought to determine the role of activity-dependent synaptic plasticity in remapping and behavioral recovery.

Methods: Three cohorts of mice were subjected to photothrombosis of the right S1FP cortex (right forepaw, left cerebral cortex): 1) C57bl6 mice (control, n=11); 2) C57bl6 mice subjected to chronic whisker trimming (sensory deprivation, n=9); and 3) C57bl6 mice with Arc gene deletion (Arc-/-, n=7). S1fp remapping was assessed by electrical forepaw stimulation with optical intrinsic signal (OIS) imaging through the intact skull prior to, and 1, 4, and 8 weeks following photothrombosis. Somatosensory recovery was measured using the cylinder rearing test at 1, 3, 5, and 7 weeks after photothrombosis. ANOVA with repeated measures and Newman–Keuls' multiple comparisons was used to compare each timepoint to baseline.

Results: Photothrombosis reproducibly infarcted S1fp in all cohorts, resulting in absent S1fp activation maps and reduced right forepaw use (30% more left

paw use than right P≤0.001 in all groups) at wk1 post-photothrombosis. Left S1FP and Right Hindpaw representations were not affected demonstrating lesion selectively. In control mice, S1fp remapping was first observed at wk8 anterior to the original S1FP territory, and symmetric forepaw use improved along a similar time-course (26% asymmetry at wk3, P≤0.01; 17% asymmetry at week 5, P≤0.05; 7% at wk7, P=n.s. compared to baseline). Sensory deprivation induced earlier remapping into the barrel cortex (wk4), and behavioral recovery (symmetric limb use) also occurred by wk3 (9% asymmetry, P= n.s.). Arc$^{-/-}$ mice showed no S1fp remapping and limb asymmetry persisted for the entire recovery time course (31% at wk3, 29% at wk5, and 27% at wk7, P≤0.01).

Conclusion: The results demonstrate that functional remapping following cortical stroke can be redirected to targeted regions by focal sensory deprivation, resulting in accelerated remapping and recovery. These recovery processes are dependent on Arc, which plays an important role in activity-dependent synaptic plasticity. Further characterization of the mechanisms involved in remapping may lead to additional approaches that accelerate remapping and recovery.

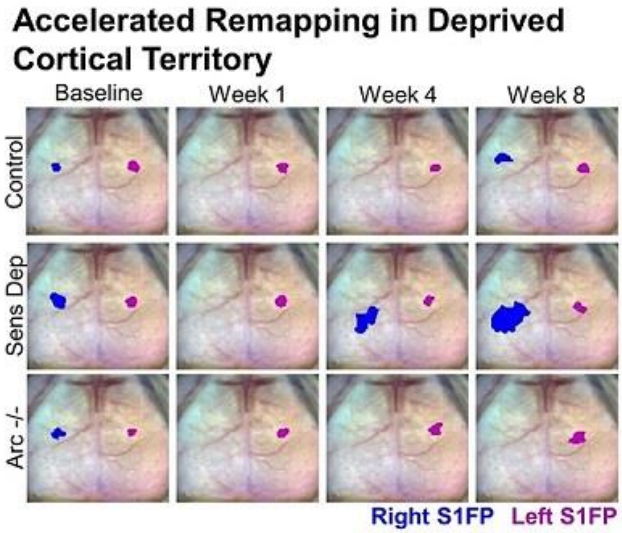

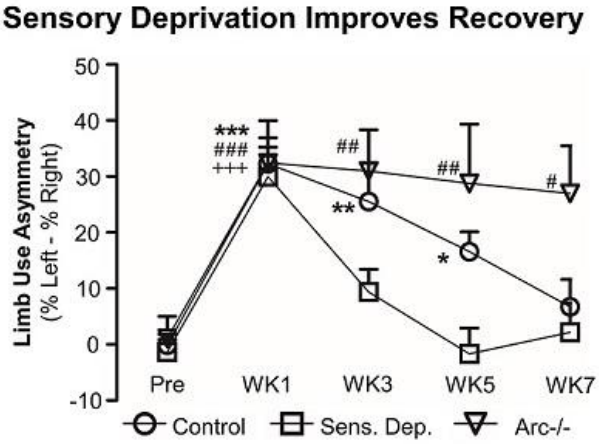

References:

1. AHA(2008)

2. Duncan et al., *Stroke.* 23(8):1084-1089(1992)

3. Nudo et al., *Science.* 272(5269):1791-1794(1996)

4. Rossini et al., *Neuroreport*. 9:2141–2146(1998)

5. Plath et al., *Neuron, 52*(3), 437-444(2006)

146
BRAIN-0867
Brain Oral Communication

Oral Session: Cerebral Ischemia: Functional Recovery

CONCURRENT ASSESSMENT OF FORELIMB FUNCTION AND MESOSCOPIC CORTICAL NETWORKS IN MOUSE STROKE MODELS

G. Silasi[1], *M. Vanni*[1], *F. Bolanos*[1], *J.D. Boyd*[1], *S.H. Scott*[2], *T.H. Murphy*[1]
[1]*Department of Psychiatry, University of British Columbia, Vancouver, BC, Canada*
[2]*Department of Biomedical and Molecular Sciences, Queen's University, Kingston, ON, Canada*

Introduction:
The need for reliable animal models of small vessel disease is great, as the vascular and neuronal changes that produce this condition in humans are difficult to study in patient populations. Our approach here was to first develop and characterize

a mouse model of diffuse microinfarction that produces occlusions in penetrating arterioles throughout the brain. We then developed an automated forelimb motor task that allows us to perform simultaneous imaging of brain activity using the GCaMP6 calcium indicator, and behavioural assessment. We validate this approach in a longitudinal study where we assess brain activity and behavioural performance after recovery from focal ischemia.

Methods:
To assess the structural impact of micro-occlusions, ~20µm fluorescent microspheres were injected in the common carotid artery of Thy1-GFP transgenic mice and histological sections were examined at 9-day survival. In parallel experiments we developed a forelimb functional assessment tool that requires head-fixed mice to pull and hold a lever to receive a water reward. The task was designed to be compatible with wide-filed imaging in GCaMP6 transgenic mice, thus allowing longitudinal monitoring of cortical activity during stroke recovery. Imaging was performed transcranially through a chronic window that did not require removal or thinning of the skull.

Results:
We found that injecting ~2,000 microspheres produces 423±218 micro-occlusions per brain, with the majority located in the cortex (34%±5.6) or thalamus (31%±5.7; N=6 mice). Although the cortex contained more occlusions than other structures, labeled layer 5 neurons were resistant to structural damage, with < 2% of the lodged microspheres producing obvious neuronal damage. The mean diameter for blocked vessels was 12.36±0.5 µm in the cortex, 11.04±0.2 µm in the striatum and 10.26±0.1 µm in the thalamus, consistent with measures of penetrating arteriole diameter in vivo. Mice trained on the lever-pulling task completed an average of 128±27 successful lever pulls per session (N=7 mice). Calcium imaging revealed a time-locked increase in activity of the forelimb sensorimotor region (8.5% ΔF/F) while barrel cortex and other unrelated sensory areas showed much less activity (1.8% ΔF/F) during pulling. After a 1mm diameter photothrombotic stroke in the forelimb sensorimotor cortex, successful pulls decreased significantly during the first week (48% of baseline, p=0.022), indicating that motor cortex at least in part contributes to task performance. The calcium activity within the forelimb region was substantially diminished during the first post-stroke week (1.5% ΔF/F), however peri-infarct motor regions such as the rostral forelimb area maintained their baseline level of activity (5% ΔF/F).

Conclusions:
Our results demonstrate that endovascular injection of fluorescent microspheres produces identifiable microinfarcts throughout the brain, thus opening the possibility of assessing the functional impact of this form of stroke. To this end, we describe a novel method of wide-field imaging of cortical activity during a simple forelimb motor task and quantify deficits in both behaviour and cortical activity after a relatively small focal ischemic stroke. Future studies will apply these tools to assess deficits in motor function after diffuse microinfarction.

149
BRAIN-0813
BrainPET

BrainPET Oral Session: Modeling and Methods

MEASUREMENT OF DOPAMINE RELEASE WITH PET/FMRI

N. Guehl[1], W. Wooten[1], G. El Fakhri[1], N. Alpert[1], M. Normandin[1]
[1]Radiology,
Massachusetts General Hospital Harvard Medical School, Boston, USA

Objectives: We evaluate a new kinetic model for the estimation of spatiotemporal patterns of dopamine (DA) signaling in the brain. The model simultaneously analyzes dynamic positron emission tomography (PET) data and cerebral blood volume (CBV) changes measured by functional magnetic resonance imaging (fMRI). The model was characterized with simulated data and its application was demonstrated in experimental data.

Methods: Two kinetic models have recently been developed to characterize the transient aspect of neurotransmission - neurotransmitter PET (ntPET) (1,2) and an fMRI model based on DA receptor

signaling which was shown to reconcile inconstencies in CBV responses between species and across different dose ranges (3). We integrated these two models into a unified mathematical framework to improve our ability to measure endogenous DA release. A simulation study tested the ability of the proposed model to recover characteristics of DA profile curves. Noisy CBV-fMRI and PET data sets were generated to mimic pharmacological challenge experiments in non-human primates (NHP) and rats, then analyzed with the proposed PET-fMRI model. The model was also applied to PET/fMRI data simultaneously acquired in two rhesus monkeys that received [^{11}C]raclopride and amphetamine challenge.

Results: In the simulation studies, the unified model performed well at recovering the DA release timing and magnitude, and estimated PET tracer kinetic parameters with minimal bias and good precision. In NHP simulation, the onset of the DA response and time at which DA concentration peaked were estimated with bias±s.d. of 0.27±0.21 minutes and 0.14±0.71 minutes, respectively. The magnitude of the DA curve was estimated in absolute units with low bias (mean less than 3%) and coefficient of variation better than 20%. Similar performance was found in rat simulations. In experimental rhesus data, the unified model provided good fits to both PET time activity curve and CBV-fMRI measurements suggesting that the model correctly describes the physiological processes involved. The affinity of DA for D2-like receptors was estimated to be greater than for D1-like (K_D ratio=7±3), in line with *in vitro* studies (4) and prior theoretical predictions (3). Moreover, the model estimated DA release profiles and receptor occupancies consistent with expectations.

Conclusions: We developed and assessed a unified kinetic model that simultaneously analyzes dynamic PET and fMRI data. Our results suggest that the technique is promising for non-invasive mapping of dopamine neurotransmission.

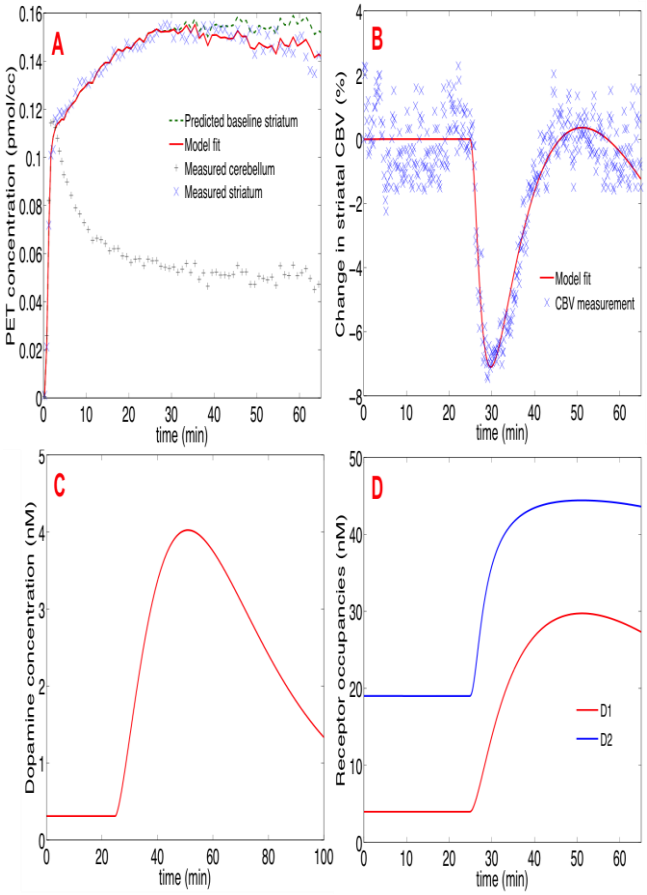

(A,B) Unified PET-fMRI model fit to experimental rhesus data. [^{11}C]Raclopride was administered by bolus-plus-infusion (Kbol=50 min) and i.v. amphetamine (0.15 mg/kg) was injected at 25 minutes. Predicted baseline PET curve is obtained using cerebellar input and estimated parameters to extrapolate to later time points in absence of DA increase. Dopamine release profile (C) and receptor occupancies at D1-like and D2-like receptors (D) estimated by the model.

References

1. Morris ED et al., *Molecular Imaging*, 4(4):47, 2005.
2. Normandin MD, Morris ED, *NeuroImage*, 39(3):1162-79, 2008
3. Mandeville JB et al., *NeuroImage*, 75:46-57, 2013
4. Marcellino D et al. *Synapse* 66:196-203, 2012

150
BRAIN-0488
BrainPET

BrainPET Oral Session: Modeling and Methods

CATEGORIZING NETWORKS OF VOXELS INTO BRAIN STATES BASED ON SEGMENTATION OF DOPAMINE LATENCY IMAGES

S. Wang[1], A. Vijay[2], K.P. Cosgrove[3], E.D. Morris[2]
[1]Biomedical Engineering, Yale University, New Haven, USA
[2]Diagnostic Radiology, Yale University, New Haven, USA
[3]Psychiatry, Yale University, New Haven, USA

Objectives: We have recently introduced a new analysis technique, 'lp-ntPET', that can extract voxel-wise dopamine time-courses from PET data in the presence of a stimulus[1,2]. We applied lp-ntPET to male and female smokers smoking cigarettes in the PET scanner. The goals of this project were (1) to identify unique brain networks by virtue of the timing of their respective dopamine responses to smoking and (2) to identify differences between male and female smokers.

Methods: Dynamic 11C-raclopride PET data were acquired in 16 smokers according to the protocol published in Cosgrove et al., 2014[1]. The lp-ntPET model was fitted to the time activity curve (TAC) at each voxel in a precommissural striatal mask. 'Latency" (the 'take-off" time of DA activation relative to the start of smoking) was estimated at each voxel. Each 'Latency" map was thresholded into 3 binarized masks describing 3 different states, 'Expectation state" (Latency<0), 'Drug state" (0≤Latency<9), or 'Slow modulatory state" (Latency>9). The masks were summed up by sex and divided by the number of subjects. These brain state images represent the probability of dopamine activation at a given voxel within a given time window. They were further thresholded at 3/8, i.e. in every retained voxel at least 3 of the 8 subjects were classified into the same brain state. The ratio of the number of voxels in the 'Drug state" over that in the 'Slow modulatory state" was calculated by region for M and F separately. The statistical significance of this ratio was assessed with a permutation test (100,000 re-samples).

Results: From the brain state images, it appears that the male response to cigarette smoking is dominated by the 'Drug state" whereas the response of the women is not. The ratio of activation (voxels of drug state : voxels of slow modulatory state) in males was 16.33, significantly higher than the results in random samples from the combined male and female data (p=0.03) by the permutation test. The ratio in females was 0.86. (Fig. 1)

Conclusions: Transient dopamine responses produced by lp-ntPET can be segmented by time to identify distinct networks of brain states elicited by cigarette smoking. A comparison of these new 'brain state" images suggests that activation in the right ventral striatum in men occurs primarily immediately following the cigarette - which could be thought of as a drug response. This temporal segmentation of the parametric images generated by lpntPET into brain states may be a useful way to identify sex differences in response to stimuli.

References: [1] Cosgrove KP, Wang S, Kim SJ et al., J Neurosci 2014 [2] Kim SJ, Sullivan JM, Wang S et al., Hum Brain Mapp 2014

Research support: R21DA032791, P50DA033945, K02DA031750

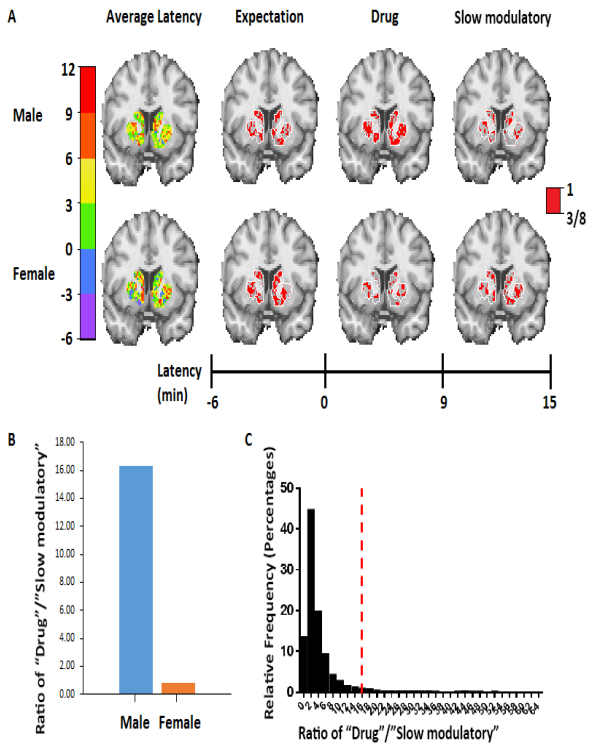

Figure 1. A. Overall 'Latency" maps averaged across subjects and Brain State images segmented by time. **B.** Ratio of the number of voxels in 'Drug state" over "Slow modulatory state" for Male and Female in the rVS. **C.** Histogram of ratios of 'Drug state"/"Slow modulatory state" in the rVS from 100,000 random samples of 8 out of the 16 subjects.

151
BRAIN-0662
BrainPET

BrainPET Oral Session: Modeling and Methods

INVESTIGATION OF THE VARIABILITY OF THE TSPO RADIOLIGAND [11C]PBR28 IN HUMAN BRAIN

Q. Guo[1], D.R. Owen[2], N.J. Kalk[2], E.A. Rabiner[1], R.N. Gunn[1]
[1]Imanova Centre for Imaging Sciences, Imanova Ltd, London, United Kingdom
[2]Division of Brain Sciences, Imperial College London, London, United Kingdom

Objectives

[^{11}C]PBR28 is a 2nd generation Translocator Protein (TSPO) radioligand for imaging neuroinflammation. Although [^{11}C]PBR28 has demonstrated good radioligand properties, the variability in total volume of distribution (V_T) and standardized uptake value (SUV) is high. Demonstration of the rs6971 single nucleotide polymorphism (SNP)[1] has accounted for a large component of this variability, but the remaining variability is still higher than expected from a 'well behaved' reversible ligand. Here, we investigate the inter- and intra-subject variability in a range of outcome measures and explore the contributions from blood and tissue.

Methods

Dynamic [^{11}C]PBR28 PET scans from 34 healthy volunteers (19 HABs, 10 MABs and 5 LABs) with arterial sampling were analysed. 5 HABs and 3 MABs received a second scan approximately 3 months after baseline.

Inter- and intra-subject variability was investigated for 4 outcome measures across regions: I) V_T using a 2-tissue compartmental model (2-TCM) with parent plasma input; II) distribution volume ratio (DVR) from 2-TCM V_T with cortical grey matter as pseudo reference; III) SUV between 60-90 min (SUV_{60-90}) and IV) SUVR derived as the ratio of SUV_{60-90} in tissue and cortical grey matter.

Individual variability in blood and tissue data was investigated. Plasma over blood ratios (pob) were fitted to an exponential plus constant model while controlling for the SNP, and cluster analysis was employed to investigate heterogeneity in tissue time activity data.

Results

In HABs, the inter-subject variability was 28.2% in V_T, 1.0 % in DVR, 24.3% in SUV_{60-90} and 1.2% in SUVR in brain. The intra-subject variability was 19.8±14.0% in V_T, 0.9±0.4% in DVR, 7.9±4.9% in SUV_{60-90}, and 0.6±0.3% in SUVR (Figure 1A). The variability of $AUC_{0-90min}$ in total plasma for HABs was 21.2%/21.9% (Inter/Intra), 17.7%/18.8% in parent plasma, 18.2%/18.0% in whole blood, and 21.8%/13.8% in

parent fraction. This suggests that ~63% of the variability in total V_T could be attributed to blood.

The pob curves were significantly different by genotype (Figure 1B) suggesting that access of [^{11}C]PBR28 to blood cells was mediated by the affinity for TSPO. The tissue delivery of [^{11}C]PBR28 (2-TCM) also varies across genotypes, with K_1=0.17±0.05 in HABs, 0.11±0.03 in MABs and 0.09±0.02 mL/cm^3/min in LABs.

Within HABs, two distinct tissue kinetic classes were observed with significant difference in K_1 (0.23±0.05 vs. 0.18±0.05 mL/cm^3/min, p<0.05) and V_T (7.19±1.06 vs. 4.66±1.01 mL/cm^3, p<0.001)(Figure 1C&D).

Conclusions

[^{11}C]PBR28 variability in blood and tissue leads to the high variability observed for V_T and SUV as compared to DVR and SUVR. Similar variability has been observed for other TSPO ligands (e.g. [^{11}C](R)PK11195[2] and [^{18}F]PBR111[3]) implicating unaccounted factors in TSPO biology rather than individual radioligand characteristics.

Our data highlights the challenges with identifying the correct input function, the existence of distinct kinetic tissue classes beyond the rs6971 SNP and opens the question of whether TSPO acts as a transporter for PET radioligands into cells.

References

[1] Owen et al. *J Cereb Blood Flow Metab.*2012;32:1-5.

[2] Jucaite et al. *EJNMMI Research*.2012;2:15

[3] Guo et al. *J Nucl Med*.2013;54:1915-1923

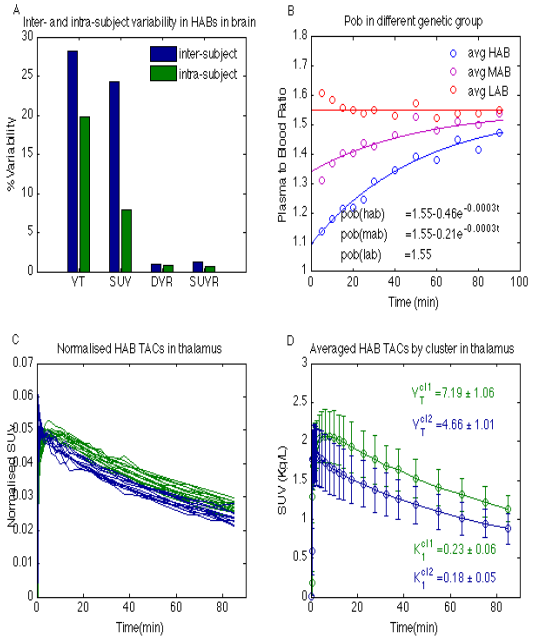

152
BRAIN-0848
BrainPET

BrainPET Oral Session: Modeling and Methods

REFERENCE TISSUE-BASED KINETIC EVALUATION OF [F-18]AV-1451 IN AGING AND DEMENTIA

S. Baker[1], J.C. Price[2], S.N. Lockhart[3], D. Schonhaut[4], J. Faria[1], G. Rabinovici[4], W.J. Jagust[3]
[1]Radiotracer development and imaging technology, Lawrence Berkeley National Laboratory, Berkeley, USA
[2]Radiology, University of Pittsburgh, Pittsburgh, USA
[3]Helen Wills Neuroscience Institute, University of California Berkeley, Berkeley, USA
[4]Memory and Aging Center, University of California San Francisco, San Francisco, USA

Objectives: To evaluate the in vivo kinetics of the novel tau-specific PET radioligand, [F-18]AV-1451 (AV-1451) [1], in cognitively normal healthy control (HC) and Alzheimer's disease (AD) subjects, using reference region analyses.

Methods: AV-1451 PET imaging was performed on 34 subjects (2 young controls (YC); 19 elderly HC; 13

AD). Data were collected from 0-150 minutes post-injection, with a break from 100-120 minutes. T1-weighted MRIs were collected and segmented using Freesurfer to create 14 bilateral regions-of-interest. In all analyses, cerebellar gray matter was used as the reference region. Binding potential values (BPs) were determined using the simplified reference tissue model without (SRTM) and with median k2' clearance constraints (SRTM2) [2-3]. Logan distribution volume ratios (DVR) [4] and standardized uptake value ratios (SUVR) were determined for 40-70 minute, 70-100 minute, 120-150 minute, and 40-150 minute intervals. Pearson correlations were used to compare BP, DVR and SUVR.

Results: Figure 1 shows a comparison between HC and AD of BP from SRTM and SRTM2, DVR40-150, and SUVR40-150 values in putamen and temporal cortex. There was a significant difference (Welch's T-test) between HC and AD in all measurements in the temporal cortex, no difference in the putamen.

Figure 1 Tau AV1451 Values from BP-SRTM, BP-SRTM2, DVR and SUVR

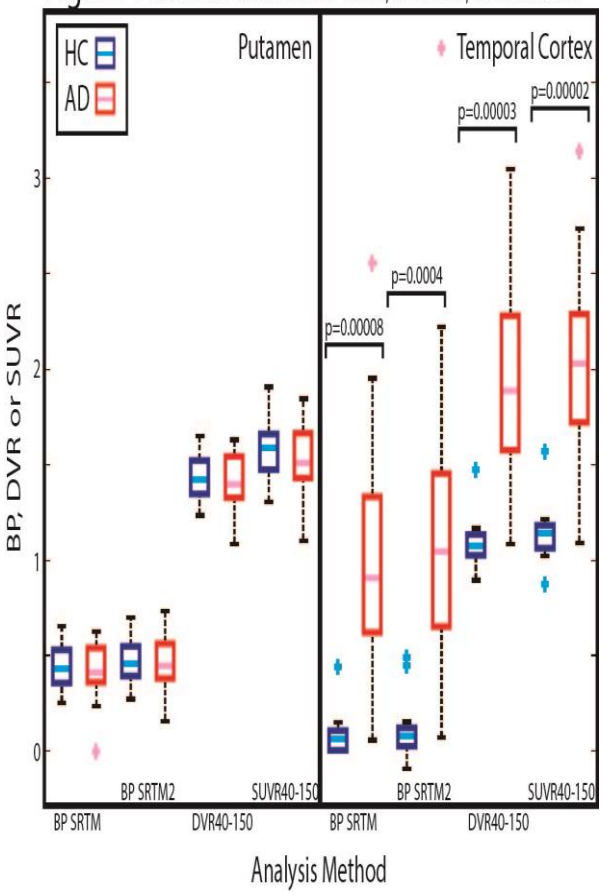

SRTM produced unrealistically large BPs (>15) or failed to converge for brainstem (n=28), entorhinal cortex (n=13), caudate (n=12), occipital (n=9), and anterior cingulate (n=6). The k2 values were higher in subcortical regions and lower in cortical. SRTM2 yielded reasonable values across all subjects and regions. DVR and SUVR values continued to increase over time (Figure 2) in cortical regions known to accumulate aggregated tau (temporal, parietal, occipital and frontal) in AD subjects, without plateau within the 150 minute scan.

Figure 2 DVR and SUVR values in Temporal Cortex

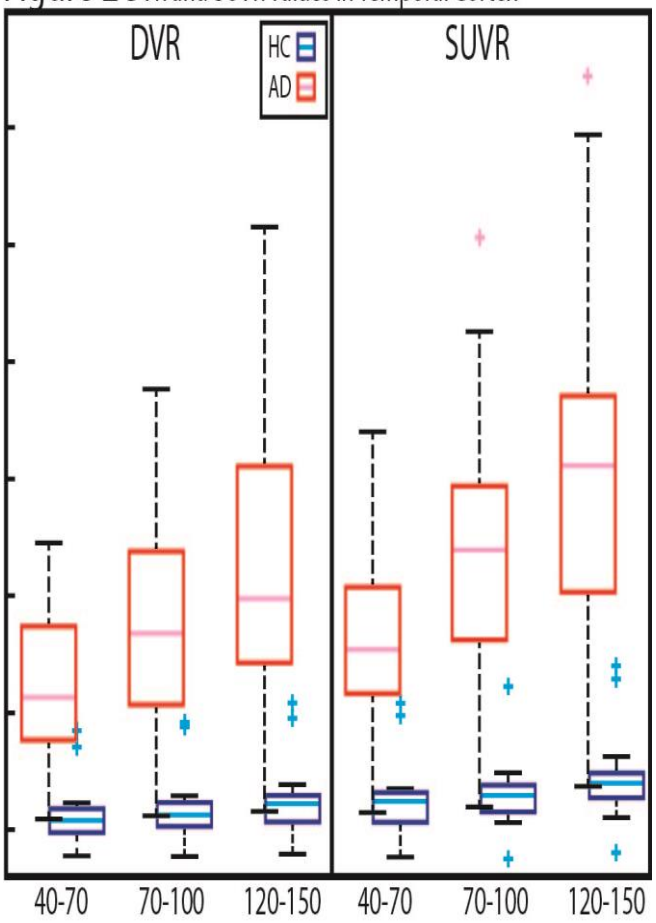

Subcortical regions (putamen, thalamus, caudate, and pallidum), assumed to exhibit off-target binding, showed a decrease in SUVR and DVR values over time and faster tracer washout relative to the reference region. Intermediate kinetics were observed in medial regions (hippocampus, precuneus, anterior and posterior cingulate). Linear Correlations: Using SRTM2 BP as the gold standard, we investigated which time window best satisfied BP=DVR-1 for all subjects and regions. DVR120-150 yielded the slope closest to 1 (0.93, relative to 0.56 for DVR40-70 and 0.76 for DVR70-100), all had an intercept of 1.02. Correlations improved with time

(r^2=0.86, 0.94, 0.95 for DVR40-70, DVR70-100, DVR120-150). Examination of BP versus SUVR yielded SUVR slopes/intercepts of 0.65/1.09 (SUVR40-70), 0.93/1.10 (SUVR70-100) and 1.15/1.06 (SUVR120-150). Correlation between BP and SUVR was best for SUVR70-100 (r^2=0.90) and SUVR120-150 (r^2=0.89), in comparison to SUVR40-70 (r^2=0.83).

Conclusion: Different regions exhibited different tracer kinetics, making it difficult to establish a consistent time interval for stable DVR and SUVR determination for bias minimization. SRTM2 yields stable BPs that are most highly correlated to DVR120-150. With regard to patient burden and study feasibility, the next best option would be SUVR70-100 or SUVR120-150.

Support: NIA, Tau Consortium

References: [1] Xia et al. (2013) Alzheimers Dement 9:666-76; [2] Lammertsma and Hume (1996) Neuroimage **4**:153-8; [3] Wu and Carson (2002) J Cereb Blood Flow; [4] Logan et al. (1996) J Cereb Blood Flow Metab **16** 834-40.

153
BRAIN-0587
BrainPET

BrainPET Oral Session: Modeling and Methods

MODEL TO DESCRIBE THE SPATIOTEMPORAL DISTRIBUTION OF MISFOLDED PROTEINS IN ALZHEIMER'S DISEASE

A. Whittington[1], Y. Iturria-Medina[2], A. Evans[2], D.J. Sharp[1], R.N. Gunn[1]
[1]Brain Sciences, Imperial College London, London, United Kingdom
[2]McConnell Brain Imaging Centre, Montreal Neurological Institute, Montreal, Canada

Introduction

The accumulation of misfolded proteins (β-amyloid and tau) in Alzheimer's Disease (AD) follows a stereotypical pattern. We introduce a model to describe the spatiotemporal distribution of misfolded proteins and apply it to cross-sectional β-amyloid data obtained from the Alzheimer's Disease Neuroimaging Initiative (ADNI).

Method

The brain is parcellated into regions that contain local production and clearance of misfolded protein. Distal spreading is incorporated using a weighted graph determined from white matter connectivity (obtained from deterministic DTI). This leads to a system of ordinary differential equations describing the misfolded protein concentration time course in each region,

$$\frac{dP_i(t)}{dt} = v_i - k_i P_i(t) + s\left[\left(\sum_{j\in G} c_{i,j} P_j(t)\right) - \deg(i)\, P_i(t)\right]$$

where $P_i(t)$ is the concentration of misfolded protein in region i, v_i and k_i are the production and clearance rates in region i respectively, s is the global coefficient for distal spreading, $c_{i,j}$ is the connection strength between region i and j, deg(i) is the degree of region i (the sum of all connection strengths connected to region i) and G is the set of all regions. An analytical solution was calculated from the state space representation. Here, we hypothesise that each region has an individual production rate, each subject has a parameter, t* which determines at what age production begins and a constant clearance rate across all regions. The model was applied to β-amyloid data both with and without (s=0) distal spreading. Regional SUVr values were derived, using whole cerebellum as a reference region, from 76 cortical regions in 733 subjects (HC[193], EMCI[233], LMCI[196], AD[111]) obtained from the ADNI database. The model was implemented in Matlab and nonlinear parameter optimisation was achieved using Levenberg-Marquardt.

Results

The model provided good fits to the cross-sectional data (see Figure 1) both with and without spreading. The decrease in the residual sum of squares with distal spreading was -0.1% with a similar AIC for both models indicating that spreading is minimal.

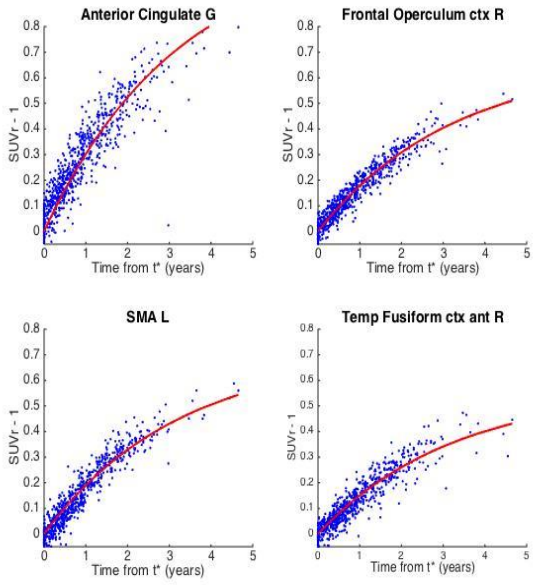

Figure 1: Spatiotemporal model (without spreading) fit to β-amyloid data from 733 subjects (4 of 76 cortical regions displayed).

The predicted regional production rates varied across regions, v_i=0.2±0.05 years^{-1} [range:0.03-0.35] and the clearance rate was 0.31 years^{-1}. The estimated parameter t*, ranged between 46.3 and 91.4 (72.0±7.7) years. Estimated values of T (= age at time of scan – t*) for the 4 groups are given in Table 1 along with results from an SUVr in anterior cingulate gyrus.

Clinical Diagnosis	T (years)	Effect size using T	SUVr in anterior cingulate gyrus	Effect size using SUVr from anterior cingulate gyrus
HC	1.2±1.21	na	1.2±0.15	na
EMCI	1.4±1.16	0.19	1.2±0.16	0.23
LMCI	2.0±1.52	0.33	1.3±0.19	0.37
AD	2.6±1.51	0.53	1.4±0.19	0.40

Table 1: The table shows the mean and standard deviation of T and anterior cingulate gyrus SUVr. Effect sizes are between a group and the group in the row above.

Conclusion

The presented model accurately describes β-amyloid data taken from ADNI. Inclusion of distal spreading did not significantly improve the performance suggesting that the behaviour is governed by local production and clearance. Future studies will investigate longitudinal data and application to tau where spreading may play a greater role.

154
BRAIN-0584
BrainPET

BrainPET Oral Session: Modeling and Methods

SPECTRAL ANALYSIS OF [18F]FLUTEMETAMOL GREY AND WHITE MATTER KINETICS

K. Heurling[1], C. Buckley[2], K. Van Laere[3], R. Vandenberghe[4], M. Lubberink[1]
[1]Nuclear Medicine and PET, Uppsala University, Uppsala, Sweden
[2]Life Sciences, GE Healthcare, Amersham, United Kingdom
[3]Nuclear Medicine & Molecular Imaging, KU Leuven Hospital, Leuven, Belgium
[4]Experimental Neurology, KU Leuven Hospital, Leuven, Belgium

Objectives

Most amyloid imaging PET tracers exhibit high uptake in the white matter (WM) to different degrees in spite of absence of fibrillar β-amyloid which is the intended target of the tracers. Although WM uptake has been hypothesized to be non-specific binding of equal magnitude in amyloid positive and negative subjects, recent studies suggest that the uptake of the amyloid imaging agent [^{11}C]PiB in WM is due to specific binding to myelin basic protein β-sheet structures[1,2], and as such could be useful for identifying WM lesions[3]. The aim of this study was to investigate kinetics of the uptake of the amyloid

imaging agent [^{18}F]flutemetamol in the WM in comparison with grey matter (GM).

Methods

Dynamic [^{18}F]flutemetamol PET scans were performed in three elderly healthy volunteers (HV) and three patients with probable Alzheimer's disease (AD) between 0-90 min, together with arterial blood sampling. Subjects underwent T1 MRI which was used to segment the image data into GM and WM. The data was analyzed with and without correction for partial volume effects (PVE) and time activity curves for total WM and GM of the whole brain were extracted. Kinetic components of total WM and GM uptake were identified using spectral analysis enabling analysis without a pre-defined assumption of the number of compartments and compared to the total volume of distribution (V_T).

Results

Three categories of exponential components were identified in GM and two in WM. The slowest component was detected in both GM and WM; the average contribution to V_T of this was 35%(±25) in GM and 77%(±6) in WM when the data was uncorrected for PVE. After correction, the average contribution to V_T was 16%(±18) in GM and 90%(±4) in WM. Two of the HV subjects and one AD subject had zero contribution of the slow component in GM, whereas in the remaining HV and two AD subjects, visually recognized as amyloid positive, 21-42% of V_T was attributable to the slowest component.

The intermediate of the three components, contributing on average 40%(±16) to the V_T in GM, was not detected in WM. The fastest component had an average contribution to the V_T of 43%(±9) in GM and 10%(±4) in WM.

Conclusions

Spectral analysis indicated the presence of a dominating slow binding process of [^{18}F]flutemetamol in the WM, much less prominent in GM uptake and following PVE correction completely absent in the GM in amyloid negative brains. Kinetic properties of GM and WM are thus easily distinguishable, but further studies are needed in order to identify the exact mechanism of the WM binding. If WM lesions alter tracer binding and the potential use of [^{18}F]flutemetamol as a marker for WM injury remains to be investigated.

References

1. Stankoff, B. *et al*. Ann Neurology 2011, 69(4), 673–680.

2. De Paula Faria, D. *et al*. EJNMMI 2014, 41(5), 995–1003.

3. Glodzik, L. *et al*. EJNMMI 2015, 42(1), 97–102.

157
BRAIN-0969
Symposium

Neurovascular pathways to cognitive dysfunction and neurodegeneration

Neurovascular coupling in health and disease: the next chapter

C. Iadecola[1]
[1]*Brain and Mind Research Institute, Weill Cornell Medical College, New York, USA*

Brain function requires a finely regulated homeostatic balance between delivery of nutrients and clearance of waste products through blood flow. If the blood flow delivery does not match the dynamic energy requirements imposed by neural activity, brain dysfunction and damage may ensue. The mechanisms of the increase in blood flow evoked by neural activity have been the subject of extensive investigation over the past two centuries, and our appreciation of their complexity has increased dramatically over the time. Whereas early models emphasized direct metabolic or synaptic interactions between neurons on cerebral blood vessels, current constructs have evolved towards a coordinated interaction among multiple cell types, neurons, astrocytes, vascular-perivascular cells, etc., converging on the microvasculature to regulate flow. These cells, collectively termed the "neurovascular unit", work in concert to implement the changes in

microvascular network resistance underlying the temporally and spatially focused increases in cerebral blood flow triggered by neural activation. Increasing evidence implicates neurovascular unit dysfunction in brain diseases associated with cognitive deficits. Although cognitive dysfunction caused by vascular factors (vascular cognitive impairment) or neurodegeneration (Alzheimer's disease, AD) have traditionally been considered distinct, recent data suggest that alterations in cerebral blood vessels play a role in both. In addition to blood flow, alterations in cerebral blood vessel ultrastructure resulting in disruption of the blood-brain barrier may also play a role, particularly in AD, vascular dementia due to hypertension, and frontotemporal dementia, the major cause of dementia in the middle aged. These observations, collectively, indicate that neurovascular dysfunction is involved in a wide variety of diseases affecting cognitive function and support the use of approaches to safeguard cerebrovascular health in their prevention. At the same time, research efforts need to continue to unravel the cellular basis of the hemodynamic response induced by activation and gain a better insight into how its dysfunction leads to the synaptic alterations underlying cognitive impairment.

158
BRAIN-0988
Symposium

Neurovascular pathways to cognitive dysfunction and neurodegeneration

Blood brain barrier alterations in neurodegenerative diseases: towards a molecular understanding

B. Zlokovic[1]
[1]*Keck School of Medicine,*
Zilkha Neurogenetic Institute, Los Angeles, USA

Blood vessels in the brain are organized with surprising precision, patterned in parallel with the major brain circuits tasked with sensation, memory and motion. This tight interrelationship may reflect key functional roles in neuronal normal function, disease and brain aging. I will discuss the cellular and molecular mechanisms within the neurovascular unit and the blood-brain barrier (BBB) including aberrant pericyte-endothelial and pericyte-astrocyte signal transduction that can lead to BBB breakdown, dysregulated and reduced cerebral blood flow responses, diminished oxygen and glucose supply leading to cerebral microvascular degenerative changes and causing secondary neuronal injury, neurodegeneration, loss of connectivity and neuronal loss. Examples in animal models and human studies using molecular and imaging biomarkers of neurovascular and brain functions will be provided. I will also discuss how highly validated genetic risk factors for late onset Alzheimer's disease (*APOE4, PICALM*) and early autosomal Alzheimer's disease (*PSEN1*) affect the neurovascular unit and BBB functions and brain function and structure.

159
BRAIN-0980
Symposium

Neurovascular pathways to cognitive dysfunction and neurodegeneration

Neurovascular and cognitive failure in Alzheimer's disease

E. Hamel[1]
[1]*McGill University, Montreal Neurological Institute, Montréal QC, Canada*

Background: Alzheimer's disease (AD) patients and animal models display altered cerebrovascular and neuronal function that together contribute to the cognitive failure. We and others previously found that mice that overexpress a mutated form of the human amyloid precursor protein (APP mice) display impaired neurovascular coupling responses and dilatory capacity, together with reduced cholinergic innervation and protein levels of memory-related immediate early genes (IEGs) such as c-Fos and Erg-1 (Zif 268) (1), or the angiotensin IV receptor (AT4R) (2) that has been involved in facilitating learning and memory.

Objectives: In this presentation, we will explore the effects of drugs commonly used to treat hypercholesterolemia or hypertension, two major risk factors for developing AD with increasing age, on cerebrovascular and neuronal failure as a function age in APP mice.

Methods: Adult or aged APP mice and age-matched wild-type (WT) littermate controls were treated with the cholesterol-lowering drug simvastatin (SV, 3 months) or the anti-hypertensive drug losartan (LO, 3-10 months). Animals were tested for spatial learning and memory (Morris water maze), cerebrovascular function (neurovascular coupling and cerebrovascular reactivity), and protein levels of IEGs, AT4Rs and other markers of synaptic function or brain homeostasis.
Results: SV and LO, irrespective of age of the APP mice, successfully restored neurovascular coupling and dilatory function, including signaling at KATP and TRPV4 channels (1-3). Despite some positive effects of LO on long-term memory in elderly APP mice, spatial learning and memory could only be fully rescued in adult or aged APP treated either with SV or LO (1,2). Similarly, only SV-treated adult APP mice with restored cognitive performance displayed normalized c-Fos and Erg-1 levels in hippocampal CA1 neurons, and improved neuronal maturation of granule cells in the dentate gyrus (4). Both adult and aged mice APP mice exhibited reduced AT4R protein levels that were reinstated to WT levels by LO administered either as a preventive (adult) or rescuing (aged) therapy. All benefits were independent from reducing effects on the amyloid pathology and were unrelated to cholesterol lowering (SV) or antihypertensive (LO) effects.

Conclusion: Our results indicate that normalization of cerebrovascular function in APP mice can occur independently from cognitive rescue, suggesting that cerebrovascular deficits cannot be imputed, at least in the late stage of the disease, for the neuronal dysfunction that results in memory failure. Further, the results indicate that early intervention with drugs designed for treating cardiovascular diseases can protect from the deleterious effects of the amyloid pathology on neuronal pathways related to learning and memory formation. Together these findings strongly support early pharmacological intervention in patients at risk for developing AD with increasing age, and demonstrate clear benefits on the cerebral circulation.

References: (1) Tong XK, et al. 2012, J Neuroscience 32:4705 **(2)** Ongli B et al., 2014, Neurobiol Dis 68: 126 **(3)** Royea J et al., Brain 2015, Abstract #0508 **(4)** Tong XK and Hamel E, Brain 2015, Abstract #0505.

Acknowledgements: Supported by the Canadian Institutes of Health Research and the Heart and Stroke Foundation of Québec.

163
BRAIN-0738
Brain Oral Communication

Oral Session: Imaging: pre-clinical – new tool development

IN SILICO INVESTIGATION OF REGIONAL CEREBRAL BLOOD FLOW TO ACCOUNT FOR THE DISCREPANCY AMONG MEASURES BY DIFFERENT PERFUSION IMAGING METHODS

T. Ku[1], *C. Choi*[1]
[1]*Department of Bio and Brain Engineering, Korea Advanced Institute of Science and Technology, Daejeon, Korea*

Objectives: Calculations of regional cerebral blood flow (rCBF) by perfusion imaging techniques have been developed based on substantial theories. However, different methods, devices or software frequently fail to give concordant results. Here we demonstrate that the microvascular simulation technique helps us understand the complex nature of rCBF. We also address the issues related to the discrepancy by current perfusion imaging methods such as water PET, perfusion CT, DSC-MRI and optical imaging.

Methods: We modeled a three-dimensional microvascular network obtained from anesthetized mouse brain with multi-photon microscopy. We simulated blood flow and time-course distribution of $H_2{}^{15}O$ and non-diffusible tracers (NDTs) given to the virtual tissue. The rCBFs of virtual voxels were estimated using four perfusion imaging methods including one-compartment modeling (F_{1C}) for $H_2{}^{15}O$ and mean transit time (F_{MTT}), deconvolution technique (F_{DT}) and blood flow index (F_{BFI}) for NDTs. We compared the estimates to the true blood flow with tuning tissue conditions and voxel size and location.

Results: F_{1C} and F_{BFI} were proportional to the voxel volume but not the sum of penetrating inflows; whereas F_{DT} showed proportionalities to the voxel surface area and the sum. F_{1C} and F_{BFI} did not linearly respond to the reduction in the amount of blood supply. K_1 in one-compartment modeling was not a direct index of blood flow because it was contaminated by vascular permeability. The presence of multiple feeding arterioles resulted in incorrect rCBF quantification using NDTs. Specifically, non-synchronous tracer arrival at the arterioles and changes in the arteriolar flow ratio disturbed the precise quantification. These features comprehensively caused the perfusion alterations after changes in the hemodynamic status of a voxel to be over- or underestimated in physiological conditions.

Conclusions: Current high-resolution perfusion imaging methods might have fundamental limitation in quantifying rCBF. Moreover, they might measure rCBF in different definitions, and using rCBF in the volume-normalized unit (ml/min/100g) could not be valid for certain methods. We should be cautious when we compare and interpret perfusion images obtained by different techniques or rCBF values measured at different study levels such as microvascular computational study and clinical imaging study.

164
BRAIN-0355
Brain Oral Communication

Oral Session: Imaging: pre-clinical – new tool development

LONGITUDINAL MONITORING OF MICROGLIAL ACTIVATION AFTER STROKE WITH A NOVEL SPION-ENHANCED MRI METHOD IN A RAT MCAO MODEL

L. Sillerud[1], Y.R. Yang[2], J. Thompson[1], V. Salayandia[1], Y. Yang[1]
[1]Neurology, University of New Mexico, Albuquerque, USA
[2]College of Pharmacy, University of New Mexico, Albuquerque, USA

Objectives: Neuroinflammation, one of the important early contributors to brain injury after a stroke, also plays a key role in neurovascular remodeling during recovery. These two distinct processes are denoted M1 for the early pro-inflammatory phase, and M2 for the later anti-inflammatory/repair phase. Microglia are the brain-resident macrophages which form the first line of defense and control the inflammatory response in the brain. We previously demonstrated that the switch in microglial activation from the M1 state to the M2 state is involved in blood-brain-barrier (BBB) remodeling after stroke. This switch of microglial activity to the M2 state promotes neurovascular remodeling, and is therefore an attractive therapeutic target (*Yang, Y., et al. JCBFM, 2013; 33:1104, Yang, YR., et al. JNI, 2015, in pressing*). Prior studies have demonstrated that our antibody-conjugated superparamagnetic iron oxide nanoparticles (SPIONs), penetrate the BBB, and serve as an *in vivo* agent for the specific MRI detection of amyloid-β plaques in mice with Alzheimer's disease (*Sillerud, L.O., et al. JAD, 2013; 34, 349*). The focus of this study is to apply this novel technique to the MRI detection of microglial-targeted SPIONs in rat brain to evaluate the alteration of microglia functional activation during stroke recovery.

Methods: Adult spontaneously hypertensive rats had a 90 min transient middle cerebral artery occlusion (MCAO) followed by reperfusion. Iron-platinum (FePt) nanoparticles, synthesized and conjugated with anti-Iba-1 antibodies (anti-Iba-1-FePtNs), were used to label microglia/macrophages via i.v. injection 24 h before an MRI scan. T_2*-weighted MRI scans, and immunohistochemistry, were used to detect the FePtNs and to measure the temporal profile of microglial activation in the brain at multiple times up to 4 weeks.

Results: We found that Iba-1-positive microglia/macrophages were seen in ischemic hemispheres as early as 24 h after reperfusion and reached a peak at 1 week that extended to 4 weeks. The switch to the M2 phase was shown by the co-localization of Iba-1 with YM1 at 4 weeks. MRI data showed the presence of the anti-Iba-1-FePtNs in the ischemic hemisphere surrounding the peri-I at 1, 2 and 4 weeks, which was confirmed by H & E and Perl's prussian blue stains. The histological staining showed that the Perl-positive cells were seen in the lesion area, where the infarct lesion was detected in

a T_2w image and the FePtNs were detected in a T_2*w image. Perl-positive cells was also seen around vessels in the peri-infarct areas. No Perl-positive cells were seen in the nonischemic hemisphere.

Conclusion: Our data suggest that: 1) with the enhancement provided by the anti-Iba-1-FePtNs, imaging of active microglia in living rat brains can be obtained using T_2*-weighted MRI scans; 2) these non-toxic nanoparticles have the potential to measure stroke-induced inflammation in an animal model, and later in patients.

165
BRAIN-0796
Brain Oral Communication

Oral Session: Imaging: pre-clinical – new tool development

LABEL-FREE OPTICALLY QUANTIFIED CORTICAL METABOLIC RATE OF OXYGEN CONSUMPTION

V. Srinivasan[1], C. Merkle[1], S. Chong[1], H. Radhakrishnan[1], C. Leahy[1]
[1]Biomedical Engineering, University of California Davis, Davis, USA

Objectives

Positron emission tomography (PET) with the $^{15}0$ labeled gas tracer $0^{15}0$, while technically complex, remains the gold standard measure of oxygen consumption[1]. Here, we present a new all-optical method of measuring mouse cortical cerebral oxygen metabolism ($CMRO_2$) quantitatively that uses measurements of three key parameters: cortical cerebral blood flow (CBF), arteriovenous oxygen saturation difference (Y_a-Y_v), and hematocrit ($[Hb_{total}]$). This method involves scanning a visible light beam of a few milliwatts average power (the same as a laser pointer) on the sample, and does not require an exogenous oxygen probe.

Methods

A visible light Optical Coherence Tomography (OCT) system was constructed to image the mouse cerebral cortex. Individual measurements were performed using Doppler[2] and Spectroscopic[3] algorithms through a thinned skull cranial window[4]. Detailed and systematic *ex vivo* validation of saturation and hematocrit measurements were performed, demonstrating the capability to quantify both. A series of *in vivo* experiments were performed to verify that $CMRO_2$, saturation, and hemoglobin concentrations behaved as expected under a range of physiological manipulations including modulation of the fraction of inspired oxygen (FiO_2), modulation of the fraction of inspired carbon dioxide ($FiCO_2$), and cardiac arrest.

Results

Baseline metabolic measurements in mice are shown to be consistent with literature values (~100-300 µmol/100g/min). $CMRO_2$, as measured using our method, does not change during minor variations in FiO_2 and $FiCO_2$, in spite of much larger changes in oxygen saturation and flow. In particular, the figure shows that during mild hypoxia (FiO_2=16%), saturation drops in both arteries and veins (A). Overall, there is a slight increase in oxygen extraction during mild hypoxia (B). However, there also is a slight decrease in blood flow during mild hypoxia (C). These results are consistent with the assertion that $CMRO_2$ remains constant during mild hypoxia. During mild hypercapnia, vessels dilate and flow increases. Accordingly, the venous saturation increases considerably due to the lower tissue oxygen extraction (D), consistent with the assertion that $CMRO_2$ remains unchanged. Complete conversion of oxy-hemoglobin to deoxy-hemoglobin after loss of brain blood flow upon cardiac arrest was also verified.

Conclusions

In conclusion, a method of measuring $CMRO_2$ using three optical measurements of cortical blood flow, arteriovenous oxygen saturation difference, and hematocrit using a single instrument was presented. Several key validation experiments were performed. To provide further methodological validation, these methods will be compared against

gold standard measurements such as PET in the future.

References

1. Mintun, M.A., Raichle, M.E., Martin, W.R. & Herscovitch, P. Brain oxygen utilization measured with O-15 radiotracers and positron emission tomography. *Journal of nuclear medicine : official publication, Society of Nuclear Medicine* **25**, 177-187 (1984).

2. Srinivasan, V.J. et al. Multiparametric, longitudinal optical coherence tomography imaging reveals acute injury and chronic recovery in experimental ischemic stroke. *PloS one* **8**, e71478 (2013).

3. Yi, J., Wei, Q., Liu, W., Backman, V. & Zhang, H.F. Visible-light optical coherence tomography for retinal oximetry. *Optics letters* **38**, 1796-1798 (2013).

4. Drew, P.J. et al. Chronic optical access through a polished and reinforced thinned skull. *Nature methods* **7**, 981-984 (2010).

Figure

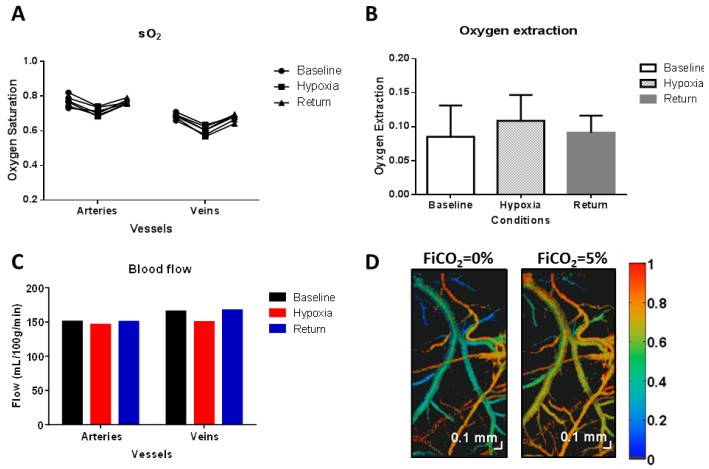

166
BRAIN-0141
Brain Oral Communication

Oral Session: Imaging: pre-clinical – new tool development

MAGNETIC RESONANCE ADVECTION IMAGING (MRAI): SENSITIVITY TO PULSATILE FLOW

H.U. Voss[1], J.P. Dyke[1], K. Tabelow[2], D.J. Ballon[1], N.D. Schiff[3]

[1]Radiology, Weill Cornell Medical College, New York, USA

[2]Stochastic Algorithms and Nonparametric Statistics, WIAS, Berlin, Germany

[3]Neurology, Weill Cornell Medical College, New York, USA

Objectives

Magnetic Resonance Advection Imaging (MRAI, [1]) is an imaging modality to obtain velocity vector maps related to vascular dynamics directly from spatiotemporal differential modeling of EPI data. It has the potential to provide precisely localized, in relation to BOLD-EPI data, information about vascular dynamics, which might aid the interpretation of (resting state) functional MRI experiments affected by vascular anatomy [2, 3]. Up to now, the biophysical origins of the estimated velocity vectors were unknown. Here we provide evidence that for a certain spatiotemporal scale MRAI maps depict areas affected by pulsatile flow [4].

Methods

It is assumed that the BOLD signal $\rho(\mathbf{r},t)$ obeys the continuity equation [5]

$$\partial\rho(\mathbf{r},t)/\partial t + \mathrm{div}\, \mathbf{j}(\mathbf{r},t) = 0,$$

with the flux having only an advective component, i.e., $\mathbf{j}(\mathbf{r},t) = \mathbf{u}\,\rho(\mathbf{r},t)$, where $\mathbf{u}$ is the local velocity vector, approximated to be constant and divergence-free. Direct substitution yields the advection equation

$$\partial\rho(\mathbf{r},t)/\partial t + \mathbf{u} \bullet \mathrm{grad}\, \rho(\mathbf{r},t) = 0.$$

Parameters such as the velocity can be estimated from spatiotemporal data by multiple regression [6], in this case from

$$Y = \text{const} + u_x X_1 + u_y X_2 + u_z X_3 + \varepsilon,$$

with $Y = \partial\rho(\mathbf{r}, t)/\partial t$, $X_1 = -\partial\rho(\mathbf{r}, t)/\partial x$, $X_2 = -\partial\rho(\mathbf{r}, t)/\partial y$, $X_3 = -\partial\rho(\mathbf{r}, t)/\partial z$ estimated from data by finite differencing.

In order to compute coherence between the cardiac cycle and estimated velocities for each voxel in the brain, pulse-oximetry data, pulse(t), was recorded from the left hand of an adult male volunteer (rest, eyes closed) during a multiband-EPI acquisition [7] on a 3.0 T MRI scanner (TR = 187 ms, 2 mm isotropic resolution, 1000 repetitions, scan time 3:07 min).

Results

MRAI maps of estimated average velocities showed venous, arterial, and CSF components that correspond to anatomy visible in a time-of-flight (TOF) angiogram of the same subject (see Figure). A map displaying max[coherence(pulse(t), ρ(**r**,t))] resembled the MRAI map but was less specific with respect to the precise location of blood vessel anatomy. The coherence map histogram peaked at a frequency corresponding to the average pulse frequency obtained from pulse oximetry.

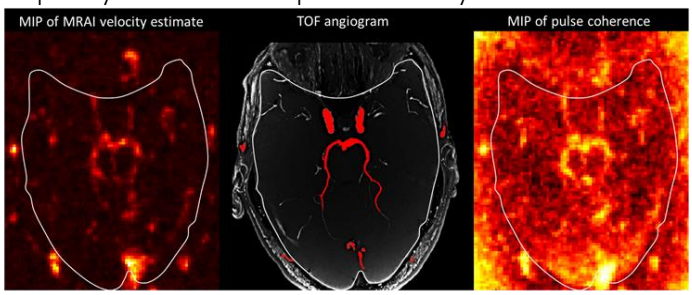

Figure: Magnetic Resonance Advection Imaging (MRAI) compared with pulse coherence
Left: Maximum intensity projection (MIP) of MRAI velocities (hot color = high velocity estimates)
Middle: TOF angiogram with some blood vessels highlighted in red for clarity
Right: MIP of the maximum coherence between the BOLD signal and pulse oximetry data
(EPI based images manually corrected for geometric distortions against the TOF)

Conclusions

MRAI partially reproduces vascular anatomy. For the chosen temporal and spatial resolution, the observed MRAI maps are mainly affected by pulsatile flow components but are more specific to vascular anatomy than maps correlating pulse with voxel intensity; the latter one probably picking up motion in adjacent tissue as well. We believe that MRAI at this spatiotemporal scale can contribute to the modeling of the cerebrovascular system with potential for application as a biomarker for cerebrovascular disease.

References

[1] H. U. Voss *et al.*, Submitted to OHBM - Human Brain Mapping (2015).
[2] J. T. Webb *et al.*, PloS one **8** (2013).
[3] R. M. Birn, NeuroImage **62** (2012).
[4] M. S. Dagli, J. E. Ingeholm, and J. V. Haxby, NeuroImage **9** (1999).
[5] H. U. Voss, and N. D. Schiff, Entropy **16** (2014).
[6] H. U. Voss *et al.*, Phys Rev Lett **83** (1999).
[7] S. Moeller *et al.*, Magn Reson Med **63** (2010).

167
BRAIN-0543
Brain Oral Communication

Oral Session: Imaging: pre-clinical – new tool development

MULTI-EXPOSURE, CONTINUOUS LASER SPECKLE CONTRAST IMAGING OF MOUSE BRAIN ENABLED BY A NOVEL SINGLE PHOTON AVALANCHE DIODE (SPAD) ARRAY

T. Dragojević[1], D. Bronzi[2], H.M. Varma[1], C.P. Valdes[1], C. Castellvi[3], A. Tosi[2], F. Zappa[2], C. Justicia[3], T. Durduran[1]
[1]Medical Optics, ICFO-Institut de Ciencies Fotonique, Castelldefels, Spain
[2]Dip. Elettronica Informazione e Bioingegneria, POLIMI-Politecnico di Milano, Milano, Italy
[3]Department of Brain Ischemia and Neurodegenerati on Institute for Biomedical Research (IIBB) Spanich Co uncil Research (CSIC),
IDIBAPS - Institut d´Investigacions Biomediques Augus t Pi i Sunyer, Barcelona, Spain

Objectives: Multi-exposure laser speckle contrast imaging (MESI) measures absolute microvascular blood flow by using the speckle contrast data acquired sequentially, at a wide range of exposure times[1]. To minimize the sensitivity to physiological changes, there is a need for fast data acquisition.

Here we present a new single shot multi-exposure laser speckle contrast imaging approach on the mouse brain enabled by a novel, high frame-rate single-photon avalanche diode (SPAD) array. The method provides sensitive, robust data acquisition compared to conventional laser speckle imaging and hence is suitable for longitudinal studies.

Methods: SPAD array is a high frame rate (up to 100000 fps) imager with single-photon counting sensitivity [2]. There is no readout noise and, therefore, it is possible to acquire a continuous stream of very short frames and to estimate all exposure times for single-shot MESI by summation of the acquired frames, instead of performing different set of acquisitions for each exposure time. In these experiments, full-field illumination was achieved with a continuous-wave laser diode (785 nm). Three month old male mice (C57/BL6, 30g) were placed on a stereotaxic frame, anesthetized with isoflurane, and scalp was removed. Hypercapnia ($20\%O_2+75\%N_2O+5\%CO_2$) and hyperoxia ($100\%\ O_2$) were utilized to cause bulk changes in the brain for validation followed by sacrifice [3]. First single-shot MESI data was acquired, followed by standard approach.

Results: The speckle contrast was calculated for both single-shot and standard methods. The decorrelation time (τ_C) was obtained by fitting the data against a theoretical model [1]. Blood flow was assumed to be inversely proportional to τ_C and relative blood flow was used to compare two approaches as shown in Table 1. The standard and continuous methods are in agreement in absolute values as well as in changes.

Conclusion: We have introduced a new laser speckle contrast imaging approach enabled by a novel SPAD array that is able to provide multi-exposure data in a fast single-shot acquisition. To validate the approach, measurement of absolute and relative blood flow during baseline, hypercapnia and hyperoxia in the mouse brain were utilized showing close agreement between the two methods. This high performance method will be further demonstrated during functional activation of the whisker barrel cortex. Future potential for this technology will be discussed.

The project was funded by Fundació Cellex Barcelona, LlumMedBCN (La Caixa), Ministerio de Economía y Competitividad (PHOTOSTROKE) and LASERLAB-EUROPE.

References:

[1] A. B. Parthasarathy, et al. Biomed. Opt. Express 1, 246–259 (2010).
[2] D. Bronzi, et al. Selected Topics in Quantum Electronics, IEEE Journal of, Vol. 20 (6), 1-10, (2014).
[3] C.Ayata, et al. Jorunal of Cerebral Blood Flow & Metabolism, 24:744-755 (2004)

Table 1: Fitted values of τ_C and changes of cerebral blood flow for each challenge

Challenge	τ_c *(sec)*		Relative blood flow (%)	
	Single-shot	Standard	Single-shot	Standard
Baseline	$(3.8\pm0.4)10^{-4}$	$(3.41\pm0.32)10^{-4}$	100	100
CO_2	$(3.10\pm0.29)10^{-4}$	$(3.04\pm0.26)10^{-4}$	121.6±2.0	112.1±4.6
Recovery	$(3.17\pm0.33)10^{-4}$	$(3.10\pm0.23)10^{-4}$	118.9±1.6	109.7±3.6
O_2	$(3.23\pm0.33)10^{-4}$	$(3.24\pm0.24)10^{-4}$	98.3±4.0	95.8±4.7
Recovery	$(2.83\pm0.26)10^{-4}$	$(2.89\pm0.24)10^{-4}$	112.0±3.3	107.5±4.3
Biological Zero (post mortem)	$(259\pm4)10^{-4}$	$(519\pm89)10^{-4}$	0	0

170
BRAIN-0611
BrainPET

BrainPET Oral Session: Neurotransmitter System Evaluation

ENDOTOXIN ENHANCES METHYLPHENIDATE-INDUCED DOPAMINE RELEASE MEASURED WITH [11C]-RACLOPRIDE PET

J. Petrulli[1], H. Gao[2], J. Ropchan[2], B. Kalish[3], Y. Huang[2], J. Hannestad[4], E. Morris[1]
[1]Biomedical Engineering,
Yale University School of Engineering Arts and Science s, New Haven, USA
[2]Chemistry, Yale PET Center, New Haven, USA
[3]Research Coordination, Yale PET Center, New Haven, USA
[4]Clinical Neuroscience,
Yale University School of Medicine, New Haven, USA

OBJECTIVES

It is known that the brain monitors inflammatory signals from the periphery, but details on how the brain incorporates and uses this information is lacking. Endotoxin-induced systemic inflammation in rodents causes an increase in striatal dopamine (DA). Here, we used methylphenidate to induce DA release and [11C]-raclopride PET to measure it in the human striatum. The *change* in DA release in the presence of endotoxin was the primary outcome measure.

METHODS

Five healthy subjects received [11C]-raclopride PET scans in 2 conditions: methylphenidate (MP) alone and methylphenidate plus endotoxin (MP+E). MP (40 mg) was given 60 minutes before tracer administration in each condition, and endotoxin (0.8 ng/kg) was given intravenously 30 minutes before tracer administration in the MP+E condition. Each condition was performed on a separate day, and each drug scan followed a baseline scan (total of 4 scans per subject). PET images were obtained on a Siemens HR+ and corrected for motion, scatter, randoms, and dead time. Modeling of regional PET time activity curves was performed using the Simplified Reference Tissue Model with the cerebellum as the reference region to obtain regional non-displaceable binding potential (BP_{ND} abbreviated here as BP). DA release was measured as percent change of BP from baseline (ΔBP) and was calculated as:

$$\Delta BP = (BP_{baseline} - BP_{condition}) / (BP_{baseline}) * 100$$

Subjective sickness symptom ratings (0-4 from negligible to severe) were recorded for each subject in each scan every 30 minutes. Levels of peripheral inflammatory cytokines were measured from blood plasma every 30 minutes in drug scans.

RESULTS

Striatal regions displayed high test-retest reliability based on a comparison of each subject's two separate baseline scans (intraclass correlation coefficient = 0.97, fitted linear slope = 0.95, r^2 = 0.96). Whole striatum mean ΔBP was 13.9% +/- 1.3% in the MP+E condition compared to 3.5% +/- 1.5% in the MP condition. The MP+E condition displayed significantly greater mean ΔBP in whole striatum ($p<0.005$), caudate ($p<0.005$), and right putamen ($p<0.05$) as compared to the MP condition. As expected, endotoxin produced mild sickness symptoms and a robust increase in blood levels of inflammatory cytokines.

CONCLUSIONS

This study shows for the first time that acute systemic inflammation induced by endotoxin enhances MP-induced synaptic DA levels in the human striatum, a finding that is consistent with rodent studies and with the fact that striatal dopamine release can signal both rewarding and

aversive stimuli.

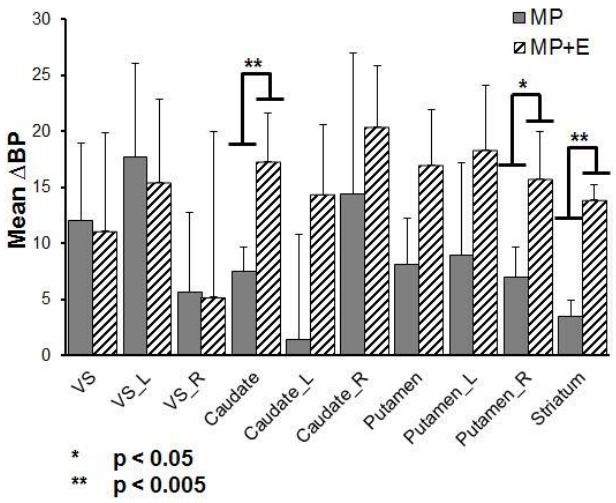

171
BRAIN-0477
BrainPET

BrainPET Oral Session: Neurotransmitter System Evaluation

DETECTING DOPAMINERGIC MODULATION INDUCED CAMP CHANGES IN MONKEY BRAIN BY PDE10A PET IMAGING

K.C. Yang[1], S. Grimwood[2], J. Nielsen[3], B. Bang-Andersen[4], V. Stepanov[1], N. Amini[1], S. Martinsson[1], A. Takano[1], C. Halldin[1], L. Farde[1], S.J. Finnema[1]
[1]Department of Clinical Neuroscience, Karolinska Institutet, Stockholm, Sweden
[2]Neuroscience Research Unit, Pfizer Inc., Cambridge MA, USA
[3]Division of Synaptic Transmission, H. Lundbeck A/S, Valby, Denmark
[4]Division of Discovery Chemistry and DMPK, H. Lundbeck A/S, Valby, Denmark

Objectives: Phosphodiesterase 10A (PDE10A) plays a key role in modulating central 3',5'-cyclic adenosine monophosphate (cAMP) levels, especially in the striatum, globus pallidus (GP) and substantia nigra (SN) [1]. Several PET radioligands have recently been reported for the PDE10A, including [^{11}C]Lu AE92686. [^{11}C]Lu AE92686 has high affinity for PDE10A and quantification of the radioligand has already been validated in humans [2]. Based on a competition model, alterations in cAMP levels may induce changes in PDE10A radioligand binding. It has been demonstrated that activating dopamine D_1 receptors increases cAMP levels and stimulating dopamine D_2 receptors decreases cAMP levels [1]. The aim of this study was to evaluate dopaminergic modulation induced cAMP changes in the monkey brain by PET imaging with [^{11}C]Lu AE92686.

Methods: A total of 30 HRRT PET measurements (10 for test-retest and 20 for dopaminergic modulation challenge studies) were performed in 5 cynomolgus monkeys. During each study day (n=15), after a baseline PET measurement, a second measurement was performed with (n=10) or without (n=5) drug pretreatment. The pretreatment regimes designed to decrease cAMP were SCH 23390 (2.0 mg/kg) with (n=5) or without apomorphine (1.0 mg/kg; n=3). cAMP was increased with haloperidol (0.05 mg/kg) with (n=1) or without *D*-amphetamine (1.0 mg/kg; n=1). Five target regions: putamen (PUT), caudate nucleus (CN), ventral striatum (VS), GP and SN and the cerebellum (CB) as reference region were delineated on MRI. Binding potential (BP_{ND}) values were determined with the simplified reference tissue model (SRTM) for 63 min of PET data. Statistical analysis was performed using paired *t*-tests ($p<0.05$).

Results: The absolute variability in the test-retest studies ranged from 6.1±6.6% in VS to 16±6.0% in SN (mean±SD). Pretreatment with SCH23390 significantly decreased BP_{ND} in PUT (-21±2.0%) and CN (-23±1.5%). Administration of SCH23390 and apomorphine also decreased BP_{ND} in PUT (-13±5.4%), CN (-20±5.2%) and VS (-15±3.5%), but increased BP_{ND} in the SN (22±14%) (see also Figure). Pretreatment with haloperidol with and without amphetamine induced only equivocal changes in BP_{ND} across regions (-17% to 7.9%).

Conclusions: PET imaging with [^{11}C]Lu AE92686 could detect dopaminergic modulation induced cAMP changes in the monkey brain. The mechanisms for the unexpected direction of changes of [^{11}C]Lu AE92686 binding in striatum and the specific role of dopamine D_1 and D_2 receptors in the regional differences of change in [^{11}C]Lu AE92686 binding warrant further evaluation.

References: [1] Nishi et al. 2011, [2] Kehler et al. 2014.

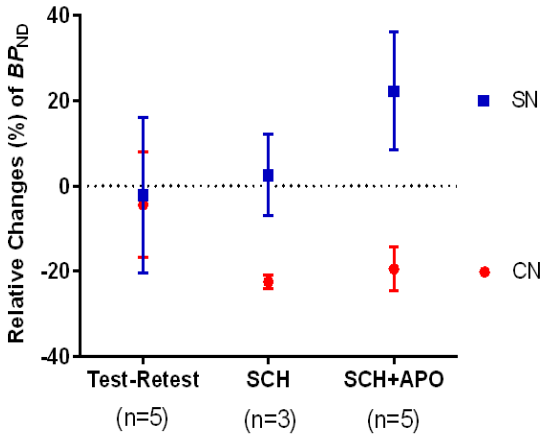

Figure: Different patterns of relative change in BP_{ND} after dopaminergic modulation between substantia nigra (SN) and caudate nucleus (CN).

172
BRAIN-0365
BrainPET

BrainPET Oral Session: Neurotransmitter System Evaluation

CEREBRAL SEROTONIN 4 RECEPTOR BINDING IS NEGATIVELY ASSOCIATED WITH THE CORTISOL AWAKENING RESPONSE IN HEALTHY VOLUNTEERS

G. Jacobsen[1], P. Fisher[1], B. McMahon[1], P. Jensen[1], G. Knudsen[1], V. Frokjaer[1]
[1]Neurobiology Research Unit, Copenhagen University Hospital Rigshospitalet, Copenhagen, Denmark

Objectives

Serotonin signaling is considered critical for an appropriate adaptation to stress. Previously we have shown that prefrontal serotonin transporter (SERT) binding is positively associated with hypothalamic-pituitary-adrenal (HPA)-axis output as indexed by cortisol awakening response (CAR) (Frokjaer V.G. et al. 2013). This implies that prefrontal SERT, which regulates synaptic serotonin, is coupled to CAR. However, it remains elusive if the coupling is mediated through synaptic serotonin. CAR is a distinct feature of the HPA-axis output and reflects both the increase in response to awakening and the following decrease due to inhibitory feedback regulation. CAR is thus considered an index of HPA-axis reactivity and its response to, e.g., psychosocial stressors; CAR has for example been found blunted in mood disorders (Fries E. et al. 2009). Cerebral serotonin 4 (5-HT_4) receptor binding as measured with [^{11}C]SB207145 PET has in preclinical and clinical studies recently been shown to index serotonin levels (Haarh M.E. et al 2014). Here, we investigated in healthy individuals if cerebral 5-HT_4 receptor binding - as a probe for serotonin levels – is associated with CAR.

Methods

Thirty healthy volunteers (25 male, 5 female, age range 20 to 56 years) underwent PET imaging with [^{11}C]-SB207145, genotyping of the serotonin-transporter-linked polymorphic region (5-HTTLPR), and performed serial home sampling of saliva to assess CAR, defined as the area under curve with respect to increase from baseline from 0-60 minutes after awakening (unit: nmol/l*min). The association was tested in a multiple linear regression model. The primary model included CAR as the predictor, 5-HT_4 binding (BPnd) as the outcome, and adjusted for age and 5-HTTLPR genotype. Three regions of interest (ROIs) were defined a priori: prefrontal cortex, anterior cingulate cortex and pallidostriatum.

Results

CAR was negatively associated with 5-HT_4 receptor binding in pallidostriatum (p=0.01), frontal cortex (p=0.03) and anterior cingulate cortex (p=0.002) with parameter estimates of -3.28, -14.6, and -12.4 nmol/l*min per 0.01 BPnd, respectively. The 5-HTTLPR status did not show a main effect on CAR, nor did it moderate the association between CAR and 5-HT_4 binding as tested in an interaction analysis. The CAR association with 5-HT_4 proved robust, remaining significant in age-restricted subsamples (<40 years) and when taking into account other potentially relevant covariates (sex, BMI, Cohen's perceived stress scale, Neuroticism, absolute cortisol concentrations at wake-up or sleep length on the day of the samples).

Conclusions

In healthy volunteers, we find a robust negative association between CAR and 5-HT_4 receptor binding

in prefrontal and anterior cingulate cortex, and pallidostriatum. We speculate that high synaptic serotonin, as indexed by low 5-HT_4 binding, is of importance to maintain HPA-axis dynamics, i.e. a robust CAR. Future studies with experimental manipulation of synaptic serotonin must elucidate if acute and/or subacute changes in serotonergic tone affect CAR and, further, if direct 5-HT_4 receptor signaling plays a role in HPA-axis regulation including in relevant clinical populations, e.g. major depression.

173
BRAIN-0578
BrainPET

BrainPET Oral Session: Neurotransmitter System Evaluation

SIMULTANEOUS PET/MRI MEASUREMENTS OF HEMODYNAMIC RESPONSE TO μ-OPIOID RECEPTOR OCCUPANCY

H. Wey[1], J. Hooker[1], M. Placzek[1], B. Rosen[1], J. Mandeville[1]
[1]Department of Radiology, Massachusetts General Hospital Harvard Medical School, Charlestown, USA

Objectives

The molecular mechanisms underlying the development of opioid addiction remain incompletely understood. Interaction between the brain's opioid and dopamine systems has been highlighted as potentially pivotal in opioid addiction. Simultaneous PET/MRI could be used to investigate inter-related receptor system interactions and to dissect complex fMRI signals into neurochemical constituents. In this study, we measure the relationship between μ-opioid receptor occupancy and fMRI response, and to examine how different receptor systems contribute to a composite fMRI signal.

Methods

Ten PET/MRI scans were acquired on two macaques (male, ~12 kg). Animals were anesthetized with isoflurane and ventilated. Images were acquired on a 3T Siemens BrainPET with an 8-channel coil. PET/MRI scans were acquired from each animal using a μ-opioid selective radiotracer (~10 mCi [^{11}C]carfentanil) given as a bolus-infusion. PET data were stored in list mode and binned into 1-min frames. CBV-fMRI data were obtained following an iron oxide (Feraheme, 10 ug/kg, i.v.)[1-3] injection. Graded doses of an opioid receptor antagonist, naloxone (baseline, 0.01, 0.03, and 0.05 mg/kg) were given intravenously at 35 min post radiotracer bolus injection. In addition, one dose of a potent μ-opioid agonist, remifentanil (10 μg/kg) was used as the challenging drug. PET data was analyzed for binding potentials referenced to a non-displaceable compartment (BP_{ND}) using the simplified reference tissue model[4]. A gamma-variant function was used to model the PET and fMRI temporal response to drug challenge. Changes in fMRI signal were converted to CBV changes[1-3].

Results

Baseline PET BP_{ND} maps showed a high-level of specific binding in the thalamus, caudate, putamen, frontal cortex, which corresponded well to known distribution of μ-opioid receptors in NHPs (Figure). μ-Opioid receptor BP_{ND} and percent CBV reduced in a dose-depended manner to naloxone challenges (Figure). A dose of 0.05 mg/kg naloxone achieved >90% receptor occupancy. The largest BP_{ND} reductions were observed in the thalamus and caudate, while the largest CBV changes were observed in the putamen (Figure). Regional analysis of the BP_{ND} and CBV data revealed a 2nd-order polynomial coupling relationship. Naloxone induced a negative CBV response, which could be due to activating the inhibitory neurotransmitter (GABA) and/or its downstream effects (i.e. GABA depletes basal level of dopamine in the basal ganglia). At a given receptor occupancy, the ratio of putamen:caudate %CBV change was ~1.7, implying the possibility that the CBV responses observed in the basal ganglia are dominated by the indirect opioid-dopamine mechanism[1,2]. Remifentanil challenge showed the opposite sustained CBV-fMRI responses[3]. Future pharmacological studies modulating the GABA and dopamine systems are needed to confirm the opioid direct vs. indirect modulations on the fMRI signals

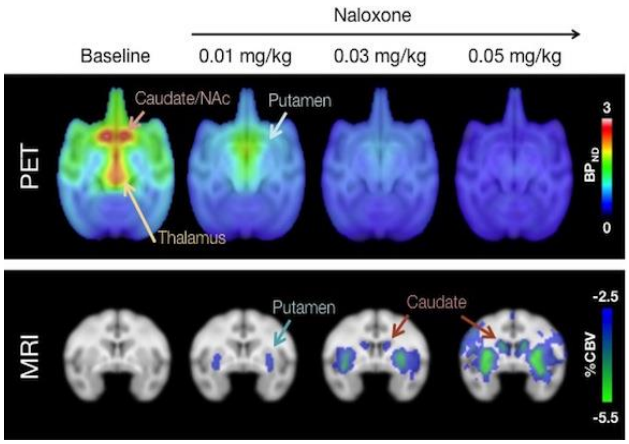

Conclusions

Using simultaneous PET/MRI with pharmacological challenges in NHPs, we determined the engagement of the opioid system and the resulting CBV-fMRI implicated a dopaminergic component in limbic basal ganglia. Simultaneous PET/MRI provides the unique opportunity to directly relate neurochemical events to functional responses and has great potential to facilitate drug development.

References: 1. Mandeville JB, NeuroImage, 2013. 2. Sander CY, et al., PNAS, 2013. 3. Wey et al., ISMRM 2014. 4. Lammertsma, NeuroImage, 1996.

174
BRAIN-0742
BrainPET

BrainPET Oral Session: Neurotransmitter System Evaluation

BLOCKADE OF TRANSLOCATOR PROTEIN (TSPO) BY XBD173 TO MEASURE SPECIFIC BINDING OF 11C-(R)-PK 11195 IN HUMAN BRAIN: AN ONGOING STUDY

M. Kobayashi[1], K.J. Jenko[1], S.S. Zoghbi[1], C. Morse[1], D. Rallis-Frutos[1], E. Page[1], T.G. Lohith[1], M. Ikawa[1], T. Jiang[1], J. Hong[1], V.W. Pike[1], R.B. Innis[1], M. Fujita[1]
[1]National Institute of Mental Health, National Institutes of Health, Bethesda, USA

Objectives: Although ^{11}C-(*R*)-PK 11195 has been widely used for three decades to image translocator protein (TSPO), controversyremains about the percentage of its uptake in human brain that is specifically bound to translocator protein (TSPO) and whether its in vivo binding is affected by the co-dominantly expressed single nucleotide polymorphism rs6971. The purpose of this study was to measure binding potential (BP_{ND}, the ratio of specific to non-displaceable uptake) of ^{11}C-(*R*)-PK 11195 in human brain after partial blockade of TSPO by XBD173, a TSPO agonist, in each of the three genotypes.

Methods: Eight healthy humans (4 high- (HABs), 2 mixed- (MABs), and 2 low-affinity binders (LABs)) had two ^{11}C-(*R*)-PK 11195 scans with arterial sampling: baseline and blocked at 1.5 – 2 hours after oral administration of XBD173 (45 mg for 3 HABs, 2 MABs, and 1 LAB; and 90 mg for 1 HAB and 1 LAB). Total distribution volume (V_T) was measured by Logan plot in each scan, and nondisplaceable distribution volume (V_{ND}) was measured by the Lassen plot using V_T in baseline and blocked scans. Binding potential (BP_{ND}) was calculated for each subject from V_T of the baseline scans and V_{ND}. Plasma free fraction (f_P) of ^{11}C-(*R*)-PK 11195 was measured in each scan.

Results: V_T of the baseline scans was similar among the three genotypes: 0.72 (HABs), 0.73 (MABs), and 0.70 (LABs). After XBD173 administration, V_T decreased by about 14% in both HABs and MABs, but was unchanged in LABs. In HABs, Lassen plot determined V_{ND} as 0.54 from the x-intercept of the linear regression. V_{ND} was identified in all HABs with an average 95% confidence interval (CI) of -0.37 – 1.06. However, in MABs, Lassen plot was unable to determine V_{ND} due to a large CI ranging from minus infinity to 3.24. In HABs, BP_{ND} was 0.38. XBD173 increased f_P of radioligand by an average of 19% in HABs. By correcting for f_P in each scan, the changes in V_T after XBD173 administration became bigger, and BP_{ND} increased ~120% in HABs from average 0.38 to 0.86. In HABs, V_{ND}/f_P was identified with a similar confidence interval as V_{ND}. In MABs, V_{ND}/f_P was not identifiable.

Conclusions: Depending on whether the imaging results are corrected for the increase of f_P apparently caused by XBD173, the BP_{ND} of ^{11}C-(*R*)-PK11195 in human brain of HABs was either low (~0.6 without correction) or moderate (~1.2 with correction). The cause of the poor identifiability of the V_{ND} in Lassen

plot for MABs is not clear. Because an in vitro study showed that the binding of XBD173 is affected by the genotype [1], the higher dose of 90 mg may allow greater binding blockade and measurement of V_{ND} in MABs. Therefore, 90 mg XBD173 is being administered in the ongoing study. The effect of genotype to the binding of ^{11}C-(*R*)-PK 11195 will need to be carefully evaluated because the in vivo binding of XBD173 may also be affected by the genotype.

[1]Owen et al. Synapse 2011; 65:257-9.

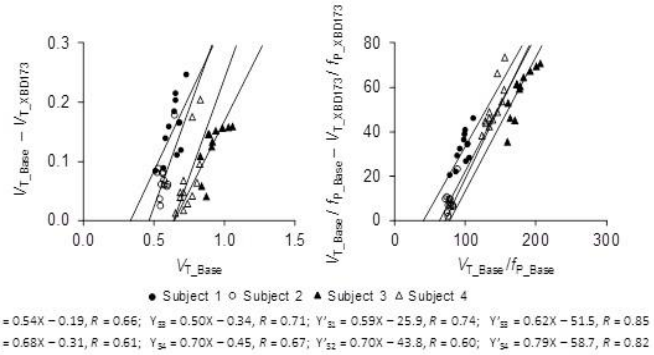

Figure: Lassen plots with V_T and V_T/f_P on HABs

175
BRAIN-0702
BrainPET

BrainPET Oral Session: Neurotransmitter System Evaluation

PK-PD ANALYSIS OF OCCUPANCY-CONCENTRATION-TIME CHARACTERISTICS OF A NOVEL GLYCINE TRANSPORTER-1 (GLYT1) INHIBITOR EXHIBITING PHARMACOLOGICAL HYSTERESIS IN NON-HUMAN PRIMATES AND HUMANS USING [18F]CFPYPB

R. Rajagovindan[1], R. Carr[1], M. Voorbach[1], J. Wang[1], A. Tovcimak[1], D. Reuter[1], A. Giamis[1], P. Jacobson[1], B. Behl[2], E. van der Kam[2], B. Rendenbach-Mueller[2], A. Basso[1], E. Bain[1], J. Beaver[1]
[1]., AbbVie Inc., North Chicago, USA
[2]., AbbVie Deutschland GmbH & Co KG, Ludwigshafen, Germany

Objective: The glycine transporter-1 (GlyT1) has been implicated in the pathophysiology of schizophrenia and is pursued as a target for therapeutic drug development. The purpose of this study was to model the receptor occupancy-concentration-time relationship of a novel GlyT1 inhibitor in non-human primates and in human volunteers.

Methods: [18F]CFPyPB [1] dynamic PET data were collected in 3 cynomologus monkeys (cynos), 4 baboons and 9 healthy volunteers with arterial sampling prior to and at multiple time points (0h-32h) post administration of a novel GlyT1 inhibitor at varying dose levels. The 3 cynos received test-retest scans separated by 1-3 weeks. Subject-space atlas based on anatomical MRI was coregistered to PET images of each animal to derive regional time activity curves for high binding regions: brainstem, pons, midbrain, thalamus, cerebellum and low binding regions: frontal, temporal and occipital cortex. Volume of distribution (VT) values were derived using both Logan and 2TCM+Vb models. Receptor occupancy was determined using Lassen occupancy plot [2] and pseudo reference tissue method [3] using occipital and whole cortex as the pseudo reference region in primates and humans respectively. The occupancy-concentration-time relationship were modeled using a population based biophase model [4] and an indirect model [5]. The model relationship derived from primate data was applied to human PK time course to predict the human occupancy time course and confirmed with observed human occupancy. The model was then fit to human data to estimate the half-life, kon, koff and Kd at the effect site.

Results: Logan and 2TCM+Vb methods were able to fit the data well. The test-retest variability of VT across all regions were 6%, 8% and 20% in the 3 cynos tested. The VT (ml/cm3) ranged between 3-14 in cynos, 2-14 in baboons and 2-9 in humans. Dose-dependent receptor occupancy was observed following different doses of the GlyT1 inhibitor. Hysteresis was observed in the plasma concentration-occupancy relationship. The indirect model and the biophase model with a semi-mechanistic effect-site compartment fit the data well.

Conclusion: Dose-dependent and time-variant GlyT1 receptor occupancy was successfully modeled. Such PK-PD modeling approach can be leveraged to

predict human occupancy time course from preclinical species and to predict repeat-dose occupancy using occupancy data obtained after administration of a single dose [5].

References:

1. Hamill TG et al., Synapse (2011) 65:261-270
2. Cunningham VJ et al., JCBFM (2010) 30:46-50
3. Gunn R et al., Synapse (2011) 65:1319-1332
4. Kim E et al., JCBFM (2012) 32:759-768
5. Abanades S et al., JCBFM (2011) 31:944–952

Disclosures: All authors are employees of AbbVie. The design, study conduct, and financial support for this research were provided by AbbVie. AbbVie participated in the interpretation of data, review, and approval of the publication.

178
BRAIN-0533
Brain Oral Communication

Oral Session: Focal Ischemia: Reperfusion Therapies

CD69 PLAYS A BENEFICIAL ROLE IN ISCHEMIC STROKE POTENTIALLY VIA THE MODULATION OF LEUKOCYTE RECRUITMENT AND SECONDARY MICROTHROMBOSIS

V.H. Brait[1], F. Miró[1], I. Pérez-de-Puig[1], M. Ferrer-Ferrer[1], B. Hurtado[1], A. Salas-Perdomo[1], J. Monteagudo[2], L. Notario[3], P. Garcia de Frutos[1], P. Lauzurica[3], A.M. Planas[1]
[1]Institut d'Investigacions Biomèdiques de Barcelona (I IBB), Consejo Superior de Investigaciones Científicas (CSIC) Institut d'Investigacions Biomèdiques August Pi i Suny er (IDIBAPS), BARCELONA, Spain
[2]Hemotherapy and Haemostasis Service, Hospital Clinic, BARCELONA, Spain
[3]Grupo de Activación Inmunológica Centro Nacional d e Microbiología, Instituto de Salud Carlos III (ISCIII), MADRID, Spain

Objectives: Expression of CD69 is a hallmark of lymphocyte activation and the majority of research on CD69 has focused on its effects on the immune system. Several lines of evidence support that inflammatory and immune responses are involved in stroke brain damage. The aim of this study was to examine whether CD69 plays a role in stroke outcome and to investigate the underlying mechanisms.

Methods: Cerebral ischemia was produced by 45-min intraluminal middle cerebral artery occlusion (tMCAo) followed by reperfusion in male CD69 KO (n=56) and Wt (n=68) mice. In addition, permanent distal MCAo (pMCAo) was induced in male CD69 KO (n=28) and Wt (n=41) mice and in $Rag2^{-/-}$ $CD69^{-/-}$ (n=27) and $Rag2^{-/-}$ $CD69^{+/+}$ (n=31) mice. Neurological impairment was assessed and brain infarct and edema volume were measured using MRI (T2 maps). Flow cytometry was used to measure changes in immune cell populations in the brain, spleen, cervical lymph nodes (CLNs) and the blood. PCR was performed to measure changes in inflammatory gene expression in the brain. Circulating von Willebrand factor (vWF) levels (ELISA) and function (Collagen Binding Assay) were studied in plasma, and fibrin(ogen) deposition was also studied in cerebral blood vessels (Western Blot). In other mice, we performed the tail-bleeding test. Animal work was carried out in compliance with Spanish law and with approval of the Ethics Committee (CEEA) of the University of Barcelona.

Results: CD69 KO mice had a significantly larger infarct volume compared to Wt mice at 24 and 72h after tMCAo ($P<0.05$). Also, CD69 deficiency increased infarct volume 24h after pMCAo ($P<0.05$). Following tMCAo, CD69 KO mice were more functionally impaired using a neurological score and tape test than the Wt mice. 96h after tMCAo, CD69 KO mice had a greater percentage of T cells ($CD45^{hi}$ $CD3^{+}$) in the CLNs, spleen and brain compared to WT mice and less B cells ($CD45^{+}$ $CD45R^{+}$) in the CLNs. There was also a greater number of neutrophils ($CD11b^{+}$ $Ly6G^{+}$) in the brain. To test whether the absence of CD69 in lymphocytes was responsible for the observed effects, we carried out pMCAo in lymphocyte deficient $Rag2^{-/-}$ mice. $Rag2^{-/-}$ mice showed smaller infarct volumes than the Wt mice ($P<0.001$) and CD69 deficiency in $Rag2^{-/-}$ mice increased infarct volume ($P<0.001$) demonstrating that the absence of CD69 in cells other than lymphocytes was playing a role. In addition to lymphocytes, CD69 is expressed in platelets, which led us to hypothesize that CD69 deficiency might

affect thrombosis. Preliminary findings in the tail-bleeding test showed a trend for less total bleeding time and less re-bleeds in the CD69 KO mice compared to the Wt mice. In the plasma, the concentration and activity of vWF was higher 6h after pMCAo in CD69 KO mice compared to Wt mice ($P<0.05$). In cerebral blood vessels, CD69 deficiency enhanced vWF expression and fibrin(ogen) deposition after ischemia.

Conclusions: Our results suggest that CD69 may play a beneficial role in cerebral ischemia by regulating leukocyte recruitment and secondary local microthrombosis.

Funding: Supported by the Spanish Ministry of Economy (SAF2011-30492).

179
BRAIN-0065
Brain Oral Communication

Oral Session: Focal Ischemia: Reperfusion Therapies

INCREASED TONE OF BRAIN PARENCHYMAL ARTERIOLES DURING EARLY POST-ISCHEMIC REPERFUSION IS ASSOCIATED WITH INCOMPLETE REPERFUSION AND GREATER INFARCTION

M.J. Cipolla[1], *K. Chan*[1], *J. Sweet*[1]
[1]*Neurological Sciences,*
University of Vermont College of Medicine,
Burlington, USA

Objectives: Brain parenchymal arterioles (PAs) are high resistance vessels in the brain that connect pial vessels to the capillary network.[1] We previously showed that PAs undergo vasoconstriction and increased myogenic tone after exposure to 2 hours ischemia and 30 min reperfusion.[2] Here, we measured PA tone and parenchymal cerebral blood flow (CBF) during ischemia and reperfusion to determine if vasoconstriction of PAs was associated with incomplete reperfusion. In addition, we determined if transient middle cerebral artery occlusion (tMCAO) promoted accumulation of intravascular polymorphonuclear leukocytes (PMNs) that may also contribute to incomplete reperfusion.

Methods: Male Wistar rats (~380g; n=6) underwent tMCAO by filament occlusion for 2 hrs with 30 min reperfusion or sham surgery. PAs were dissected from within the MCA territory, mounted on glass cannulas in an arteriograph chamber and myogenic tone measured at 40 mmHg. Brain tissue from just below the PAs were fixed for immunohistochemical staining of myeloperoxidase (MPO) and collagen IV. The presence of intravascular PMNs was assessed morphometrically. In a separate group of rats (n=6), H_2 clearance was used to measure brain parenchymal CBF from the tissue desaturation of inhaled H_2 gas during tMCAO. Briefly, rats were anesthetized with chloral hydrate and mechanically ventilated to maintain blood gases and pH within physiologic ranges. A 50 µm diameter glass H_2 probe (recording and reference electrodes are together) was placed 2 mm into the peri-infarct region of the MCA territory (Figure 1A). CBF was measured at baseline, during MCAO for 2 hrs, and up to 90 min of reperfusion. Brains were removed and infarct volume measured using 2,3,5-triphenyltetrazolium chloride (TTC) as a percentage of contralateral.

Results: PAs developed myogenic tone that was significantly increased after tMCAO (38±4% for Sham vs. 50±2% for tMCAO; $p<0.05$). The number of total intravascular PMNs was 0.00±0.00/mm^2 for Sham vs.0.59±0.26/mm^2 for tMCAO ($p>0.05$). Baseline CBF prior to filament occlusion was 116±9 mL/100g/min that dropped to 19±3 mL/100g/min after 60 min tMCAO. When the filament was withdrawn for reperfusion, none of the animals completely reperfused with the majority below baseline at 90 min. Reperfusion CBF at 15, 60 and 90 min was: 53±20, 27±6 and 46±19 mL/100g/min ($p<0.01$ vs. baseline for all; Figure 1B). Incomplete reperfusion correlated with infarct size such that the less reperfusion the greater infarct ($R^2=0.65$, $p<0.05$; Figure 1C).

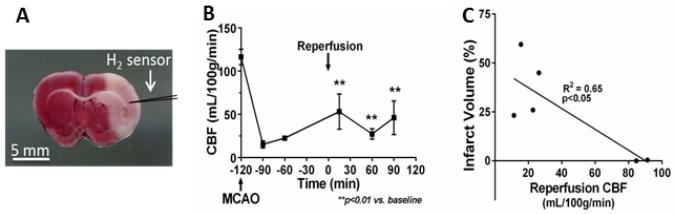

Conclusions: Incomplete reperfusion occurs at early time periods of reperfusion that is associated with PA vasoconstriction and to a lesser extent intravascular PMNs that may impede capillary flow. Strategies to alleviate PA vasoconstriction and decrease small vessel resistance during reperfusion may improve outcome from acute stroke.

References: 1. Nishimura N, et al., PNAS 2007. 2.Cipolla M, et al., Stroke 2014

180
BRAIN-0237
Brain Oral Communication

Oral Session: Focal Ischemia: Reperfusion Therapies

PREDICTORS OF MORTALITY IN ACUTE ISCHEMIC STROKE INTERVENTION: ANALYSIS OF THE NASA REGISTRY

I. Linfante[1], G.R. Walker[2], A.K. Starosciak[3], G. Dabus[1], A.J. Yoo[4], G.W. Britz[5], A. Abou-Chebl[6], A.C. Castonguay[7], A. Alvarez[1], R. Gupta[8], N. Mueller-Kronast[9], J.D. English[10], T.W. Malisch[11], A. Xavier[12], A.T. Rai[13], M.T. Froehler[14], T.N. Nguyen[15], R. Novakovic[16], R.G. Nogueira[8], O.O. Zaidat[7]
[1]Miami Cardiac & Vascular Institute, Baptist Health South Florida, Miami, USA
[2]Center for Research & Grants, Baptist Health South Florida, Miami, USA
[3]Neuroscience Center, Baptist Health South Florida, Miami, USA
[4]Radiology Division of Diagnostic & Interventional Ne uroradiology, Massachusetts General Hospital, Boston, USA
[5]Neurosurgery, Methodist Neurological Institute, Houston, USA
[6]Neurology, Baptist Health Louisville, Louisville KY, USA
[7]Neurology, Medical College of Wisconsin/Froedtert Hospital, Milwaukee WI, USA
[8]Neurology, Emory University School of Medicine, Atlanta, USA
[9]Neurology, Delray Medical Center, Delray Beach FL, USA
[10]Neurointerventional Services, California Pacific Medical Center, San Francisco, USA
[11], Alexian Brothers Medical Center, Elk Grove Village IL, USA
[12]Neurology, Wayne State University School of Medicine, Detroit, USA
[13]Radiology, West Virginia University Hospital, Morgantown WV, USA
[14]Neurology Neurosurgery and Radiology, Vanderbilt University Medical Center, Nashville, USA
[15]Neurology Neurosurgery and Radiology, Boston Medical Center, Boston, USA
[16]Radiology and Neurology, UT Southwestern Medical Center, Dallas, USA

In acute ischemic stroke from large vessel occlusion (LVO), failure to recanalize strongly predicts mortality. We used the retrospective North American Solitaire Acute Stroke (NASA) registry (approved by each entity's Institutional Review Board with waiver of consent) to investigate baseline characteristics, recanalization parameters, and symptomatic intracranial hemorrhage (sICH) in association with mortality (90-day mRS=6).

Fisher's exact test compared 90-day mortality between patients with successful and failed recanalization. In successfully recanalized patients (TICI≥2b), logistic regression evaluated baseline characteristics and recanalization outcomes for association with 90-day mortality. A multivariable model was developed based on backwards selection with retention criteria of $p<0.05$ from factors with at least marginal significance ($p\leq0.10$) on univariate analysis. This model was refit to minimize the number of excluded cases; the c-statistic was used as a measure of predictive power.

Patients who were successfully recanalized had lower mortality compared to those whose recanalization failed [25.2% (59/234) vs. 46.9% (38/81) $p<0.001$], but there was no difference in the incidence of sICH between groups [9% (21/234) vs. 14% (11/79), $p=0.205$]. However, mortality was significantly higher in patients with sICH compared to those without [72% (23/32) vs. 26% (73/281), $p<0.001$]. In successfully recanalized patients, univariate analysis identified increased risk of mortality for: proximal occlusion (ICA or vertebrobasilar), initial NIHSS≥18, use of rescue therapy ($p<0.05$), final TICI 2b and 3+ passes ($p<0.10$). In the multivariate model with good

predictive power (c-index=0.72), proximal occlusion, initial NIHSS≥18 and use of rescue therapy were significant independent predictors of 90-day mortality.

In the NASA registry, failure to recanalize and presence of sICH resulted in increased mortality. Furthermore, despite successful recanalization, proximal occlusion, severe neurological deficit at stroke onset, and need for rescue therapy were predictors of mortality.

181
BRAIN-0328
Brain Oral Communication

Oral Session: Focal Ischemia: Reperfusion Therapies

NEUROPROTECTIVE ROLE OF CARBON MONOXIDE RELEASE FROM CELL-FREE PEGYLATED HEMOGLOBIN DURING REPERFUSION FROM TRANSIENT FOCAL CEREBRAL ISCHEMIA

X. Lui[1], H. Kwansa[1], E. Kulikowicz[1], J. Armstrong[1], D. Spicer[1], R. Koehler[1]
[1]Department of Anesthesiology and Critical Care Medi cine, Johns Hopkins University, Baltimore, USA

Objective: Early transfusion of carbon monoxide-bound PEGylated hemoglobin (PEG-COHb) helps to maintain pial arteries in a dilated state and reduces infarct volume when transfused at 20 min of a 2-h period of middle cerebral artery occlusion (MCAO)(1). The CO is quickly released from the Hb, which is converted into an oxygen carrier. Because PEG-COHb was superior to PEG-Hb without CO, the small amount of released CO provides additional protection. Here, our first objective was to determine whether transfusion of PEG-COHb during MCAO reduces the upregulation of hif1alpha, a marker of tissue hypoxia. Our second objective was to determine if delaying transfusion until after reperfusion also is protective by a mechanism dependent on CO and suppression of pro-inflammatory cytokines. To assess the role of CO, groups were also treated with PEG-Hb without CO and with CO-releasing molecule-3 (CORM3).

Methods: Male rats weighing~300 g were subjected to 2 h of MCAO by the filament technique and were treated with iv 10 ml/kg of saline, 4% PEG-COHb or 4% PEG-Hb without CO. Some groupswere treated with iv 6.6 mg/kg CORM3. In the first experiment, hif1alpha was measured at 2 h in ischemic hemisphere by Western blot. In the second experiment, infarct volume was measured at 2 days of reperfusion by TTC staining. In the third experiment, gene expression of TNFalpha and IL-1beta was measured at 1 day of reperfusion in cortex by RT-PCR.

Results: Transfusion of PEG-COHb at 20 min of MCAO reduced hif1alpha abundance by 82±14% (±SE, n=5) at 2 h MCAO. Infarct volume in cerebral cortex (% of ipsilateral structure) was significantly decreased from 36.1±5.1% (SE; n=12) in a saline-treated control group to 16.7±6.2% in a group transfused with PEG-COHb at 20 min (n=13), to 14.9±4.6% in a group transfused at 2 h of MCAO (onset of reperfusion; n=10), and to 17.4±4.9% in a group transfused at 4 h of MCAO (2 h of reperfusion; n=11). Infarct volume was also reduced to 15.7±5.9% (n=9) in a group injected with CORM3 at 2 h of MCAO, but not by infusion of PEGHb without CO at 2 h (38.1±7.3%; n=8). Infarct volume in striatum also was significantly in the 2-h PEG-COHb- and CORM3-treated groups. Relative to sham controls, the median [interquartilerange]-fold increase in gene expression for TNFalpha in the saline group (5.6[4.0-11.3]; n=8) and IL-1beta (10.9[4.3-26.7]) at 1 day was significantly attenuated in the 2-h PEG-COHb group (1.5[1.3-3.6]; 2.5[2.3-6.0]; n=7) and CORM3 group(1.7[0.3-2.3]; 1.9[0.5-3.9]; n=8) but not in the PEG-Hb-treated group (6.4[3.1-9.9]; 4.9[1.1-13.3], respectively; n=9).

Conclusions: These data indicate a significant therapeutic time window for transfusion of small amounts of PEG-COHb after ischemic stroke. For early intraischemic infusion, release of CO appears to increase tissue oxygenation as reflected by decreased hif1alpha. For infusion after reperfusion, release of CO may act by reducing pro-inflammatory cytokines. The lack of an augmentation of pro-inflammatory cytokines by PEG-Hb without CO suggests a lack of toxicity of the PEG-Hb, per se.

Reference: 1. Zhang et al. J Appl Physiol 2012; 113:1709

182
BRAIN-0118
Brain Oral Communication

Oral Session: Focal Ischemia: Reperfusion Therapies

EFFECT OF NEURONAL NO SYNTHASE INHIBITION BY 7-NI IN A JUVENILE CEREBRAL ISCHEMIC MODEL: PENUMBRAL REPERFUSION IMPROVEMENT

P. LEGER[1], P. BONNIN[2], R. MORETTI[3], S. RENOLLEAU[4], O. BAUD[5], C. CHARRIAUT-MARLANGUE[3]
[1]PICU- Armand-Trousseau, AP-HP, PARIS, France
[2]Physiology unit- Lariboisière, AP-HP, PARIS, France
[3]U1141, INSERM, PARIS, France
[4]PICU- Necker, AP-HP, PARIS, France
[5]PICU- Robert Debré, AP-HP, PARIS, France

Objectives – One of the main goals of hemodynamic support is to preserve microvascular perfusion by collateral recruitment in the penumbral tissue after acute arterial occlusion, but microcirculation is not well defined in experimental models. We studied the dynamic macro- and microcirculation after ischemia-reperfusion in the juvenile rat brain and evaluated the impact of neuronal nitric oxide synthase (nNOS) on collateral flow and ischemic lesion.

Methods – All animal procedures complied with the ethical guidelines of the Robert Debre´ Hospital Research Council Review Board (A75-19-01), and the INSERM, and the ARRIVE guidelines. P15 (15 day-old) rats were subjected to ischemia-reperfusion, which received either PBS or 7-nitroindazole (7-NI, a nNOS inhibitor, 25 mg/kg) before ischemia. Arterial blood flow was measured using 2D-color-coded pulsed ultrasound imaging. Laser speckle contrast imaging and side-stream dark-field videomicroscopy were used to measure cortical and microvascular blood flow, respectively. Two investigators blind to the treatment group determined the size of the lesion in each animal at 48 hours after ischemia.

Results – On ischemia, increased mean blood-flow velocities in the basilar trunk under both PBS and 7-NI demonstrated the establishment of collateral support and patency. On re-flow, blood flow immediately recovered to basal values in the internal carotid arteries in both conditions. Surprisingly, 7-NI improved intra-ischemic collateral flow in the penumbral tissue at early re-flow as compared to PBS (Fig. 1). The proportion of perfused capillaries was significantly increased under 7-NI (67.0±3.9 *versus* 46.8±8.8, $p<0.01$) that led to a significantly reduced (by 43%) brain injury after 48 hours by comparison to PBS.

Conclusions – Neuronal NOS inhibition maintained collateral support initiated during ischemia, and sustained it during early re-flow by increasing the density of perfused capillaries in the penumbra, thus preserving tissue in the juvenile rat brain.

183
BRAIN-0693
Brain Oral Communication

Oral Session: Focal Ischemia: Reperfusion Therapies

IN VIVO IMAGING OF COLLATERAL BLOOD PERFUSION DYNAMICS DURING FOCAL STROKE

U. Baran[1], Y. Yuandong Li[1], R.K. Wang[1]
[1]Bioengineering, University of Washington, Seattle, USA

BACKGROUND AND OBJECTIVE

Changes in blood perfusion in highly interconnected pial arterioles provide important insights about hemodynamic homeostasis at the ischemic region in brain. Penetrating arterioles are other important components of blood flow regulation, as they play an essential role in delivering blood from a highly collateralized pial arteriole network to capillaries in cerebral cortex. In case of stroke, the source of blood to these vital pathways to penumbra is regulated by pial arterioles. Within the highly collateralized pial arteriole network, major cerebral arteries, such as middle cerebral artery and anterior cerebral artery, are interconnected by arteriolo-arteriolar anastomoses (AAAs), with penetrating arterioles attaching to them as T-junctions. Here, we evaluate vessel diameter, red blood cell (RBC) velocity, and total flow changes in significant number of pial and penetrating arterioles in relation with AAA to provide an insight about AAA's role in active hemodynamic regulation during focal stroke.

METHODS

A fiber-based spectral domain optical coherence tomography system[1] is used in this study to acquire volumetric images of mouse cerebral cortex *in vivo* through a cranial window. The system operates on a central wavelength of 1340 nm with an A-line rate of 92 kHz, and provides ~7 µm axial and ~10 µm lateral resolution with 0.12 mm depth of field. We apply optical microangiography (OMAG) techniques[1,2] to evaluate vessel diameter and RBC velocity changes in a large number of pial and penetrating arterioles within AAA abundant and AAA scarce regions overlie the stroke penumbra in the parietal cortex after middle cerebral artery occlusion (MCAO). In contrast to other techniques, our methods make it possible to image a larger set of vessels with a high resolution in a short imaging time without administering exogenous contrast agents during a time-constrained MCAO experiment.

RESULTS

We evaluated diameter and flow fluctuations in total 143 surface and 127 penetrating arterioles overlie stroke penumbra on four mice during MCAO. Three main findings are highlighted: (1) Flow reversals occur in pial arterioles through anastomosis, and ACA takes over blood supply to the penetrating arterioles attaching to MCA side. (2) Penetrating arterioles dilate near strong AAAs, and sufficiently restore flow to the ischemic region. (3) The flow compensation grows weaker as getting further away from AAA, resulting in poorly recovered penetrating arterioles residing further from AAA connections during reperfusion.

CONCLUSIONS

Thanks to the high sensitivity and the large field of view provided by OMAG, we compare areas in mouse cerebral cortex closer to, or further away from AAAs during MCAO in mouse cerebral cortex after focal stroke. The results suggest that AAA plays a major role in active regulation of the pial arterioles during stroke, providing blood flow for active dilation of penetrating arterioles to rescue stroke penumbra.

REFERENCES

[1] Li Y., Baran U., Wang R.K. "Application of Thinned-Skull Cranial Window to Mouse Cerebral Blood Flow Imaging Using Optical Microangiography" PLoS ONE (2014).

[2] L. An, J. Qin, and R. K. Wang, "Ultrahigh sensitive optical microangiography for in vivo imaging of microcirculations within human skin tissue beds," Opt. Express (2010).

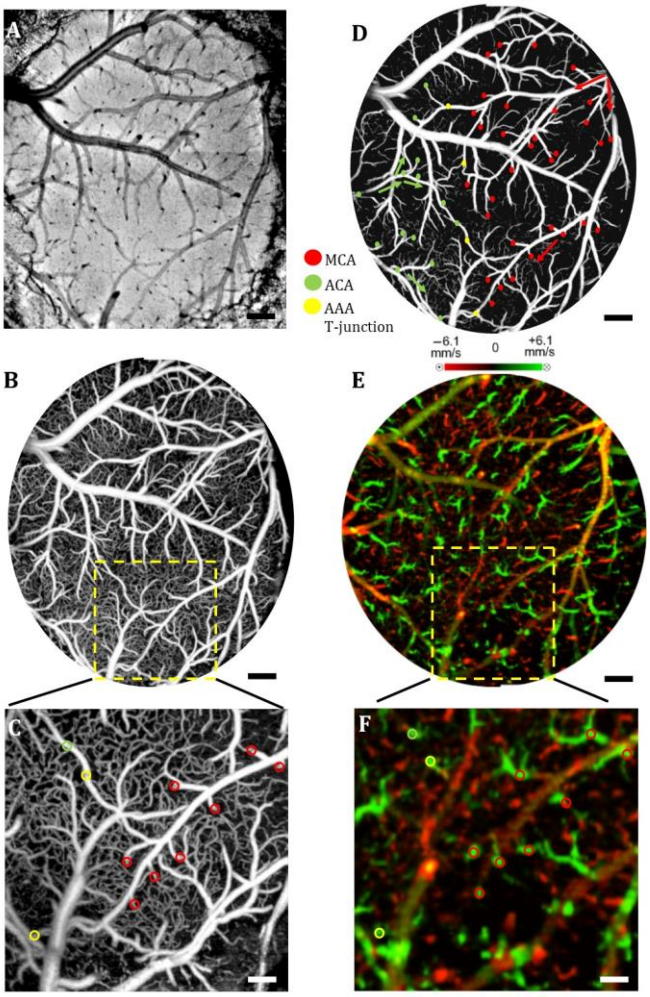

186
BRAIN-0710
Brain Oral Communication

Oral Session: Imaging: Pre-Clinical – Applications

INFLAMMATORY AND ANGIOGENIC RESPONSE TO CHRONIC HYPOXIA IN MOUSE BRAIN EVALUATED BY POSITRON EMISSION TOMOGRAPHY AND HISTOLOGICAL STUDIES

I. Kanno[1], C. Seki[1], H. Takuwa[1], Z.H. Jin[1], D. Boturyn[2], P. Dumy[3], T. Furukawa[1], T. Saga[1], H. Ito[1], K. Masamoto[4]
[1]Molecular Imaging Center, National Institute of Radiological Sciences, Chiba, Japan
[2]Département de Chimie Moléculaire, CNRS-Université Joseph Fourier, Grenoble, France
[3]Institut des Biomolécules Max Mousseron, UMR 5247 École Nationale Supérieure de Chimie de Montpellier, Montpellier, France
[4]Brain Science Inspired Life Support Research Centre, University of Electro-Communications, Chofu, Japan

[Objectives] We reported morphological and functional changes in cerebral vascular system in mice induced by chronic hypoxia (Takuwa 2013, Masamoto 2014, Sekiguchi 2014). The present study aims to evaluate the occurrence of chronic hypoxia-induced inflammatory and angiogenic responses in mouse brain using positron emission tomography (PET) and histological studies.

[Methods] Thirty-five mice, 8 to 12 weeks of age, kept in hypoxic chamber with 8-9% oxygen concentration for 0, 4, 7 and 14 days, were used for the subsequent assays. Firstly, the in vivo expression of translocator protein 18 kDa (TSPO), a known biomarker of brain inflammation, was examined by dynamic PET scans with ^{11}C-PK11195. In vitro autoradiography (ARG) studies were performed to evaluate the specific binding of ^{11}C-PK11195 and the distribution of TSPO in brain tissues. Up-regulated Iba1 expression in activated microglia, as a sign of inflammation, was examined by immunohistofluorescence staining. Secondly, the expression of $\alpha_V\beta_3$ integrin, a known angiogenesis biomarker, was examined by PET imaging and ex vivo ARG using the $\alpha_V\beta_3$ integrin-specific radiotracer ^{64}Cu-cyclam-RAFT-c(-RGDfK-)$_4$ (Jin 2012). Double immunohistofluorescence staining of the pan-endothelial cell marker CD31 and the mouse β_3 integrin subunit CD61 was conducted to determine the hypoxia-induced changes in microvasculature and $\alpha_V\beta_3$ integrin expression in mouse brain.

[Results] Standardized uptake value (SUV) of ^{11}C-PK11195 PET revealed chronologically 50 % higher at 4 days than others at 0, 7 and 14 days, and anatomically uniform across brain regions within +/-10%. These were supported by in vitro ARG of ^{11}C-PK11195 with 2.5 times higher in the specific binding at 4 days, and by Iba1 immunofluorescence with the highest staining at 4 days. It is considered that homogeneous microglia activation precedes vascular remodeling, which we observed at 7 days or after the chronic hypoxia (Yoshihara, 2013). Regarding the angiogenesis study in mouse brain, ^{64}Cu-cyclam-RAFT-c(-RGDfK-)$_4$ PET and ARG studies did not show distinctive tracer uptake except for the ventricles in all the mice studied. This is corresponded with the weak or negative expression of β_3 integrin on CD31-stained brain microvessels. The lack of detectable expression of vascular $\alpha_V\beta_3$ integrin is consistent with our previous measurement of low frequency of the vascular sprouting with less than 30 vessels per mm^3 (0.02% of microvessels) in the mouse cortex after exposure to chronic hypoxia (Masamoto, 2013). Therefore, it is estimated that the vascular remodeling under chronic hypoxia was achieved mostly by vascular morphological changes and very little by the vascular sprouting based on $\alpha_V\beta_3$ integrin expression.

[Conclusion] In chronic hypoxia mouse brain, homogenous inflammation occurred at 4 days after induction of hypoxia, indicating a transient microglial activation prior to the vascular remodeling, with very little angiogenesis.

[References]
1. Sekiguchi Y, et al. JCBFM. 2014, 34: 1761-70.
2. Masamoto K, et al. JCBFM. 2014 34: 325-31.
3. Takuwa H, et al. JCBFM. 2013 33: 774-9.
4. Masamoto K, et al. Adv Exp Med Biol. 2013 789: 15-20.
5. Yoshihara K, et al. Adv Exp Med Biol. 2013 765: 357-63.

6. Jin ZH, et al. Angiogenesis. 2012 15: 569-80.

187
BRAIN-0759
Brain Oral Communication

Oral Session: Imaging: Pre-Clinical – Applications

GLASGOW OXYGEN LEVEL DEPENDENT (GOLD) TECHNOLOGY AS A NOVEL THERANOSTIC IN ACUTE ISCHEMIC STROKE

G. Deuchar[1], D. Brennan[2], W.M. Holmes[1], I.M. Macrae[1], K.W. Muir[1], C. Santosh[2]
[1]Institute of Neuroscience & Psychology, University of Glasgow, Glasgow, United Kingdom
[2]Institute of Neurological Sciences, NHS Greater Glasgow & Clyde, Glasgow, United Kingdom

Background: Thrombolysis remains the only approved acute ischaemic stroke (AIS) therapy. Only ~5-10% of patients are treated due to risk of haemorrhage, highlighting the need for novel therapeutic options. The introduction of accurate techniques to identify the therapeutic target, potentially salvageable ischaemic penumbra, would lead to improved treatment decisions, potentially extending thrombolysis to more patients.

A potential solution to this unmet medical need is Glasgow-Oxygen-Level-Dependent (GOLD) technology, a novel stroke management product. GOLD offers unique theranostic benefits through simultaneous diagnostic and therapeutic applications. Diagnostic: two complementary MRI-based techniques are combined with intravenous perfluorocarbon (Oxycyte®) and an oxygen challenge (OC, through increased inspired oxygen) to identify ischaemic penumbra. Technique-1utilises a T_2* signal[1] based on the different magnetic properties of deoxy- and oxyhaemoglobin in blood, while technique-2 uses Lactate Change (LC) Imaging[2], which differentiates between anaerobic/aerobic metabolism[2]. Diagnostic proof-of-concept was established using 100%O_2 alone in rodent stroke models with T2*OC translated to 3T clinical scanners and tested in healthy volunteers and stroke patients[3]. However both techniques were subject to limitations (poor signal-to-noise, artefacts related to 100% O_2 on T2*scans and long scan times for LC) which were overcome with the addition of Oxycyte. Therapeutic: Oxygen-carrying perfluorocarbon particles (ca. 200nm) enable enhanced oxygen transport through the microcirculation via any remaining plasma flow, improving oxygen levels in penumbra and limiting damage.

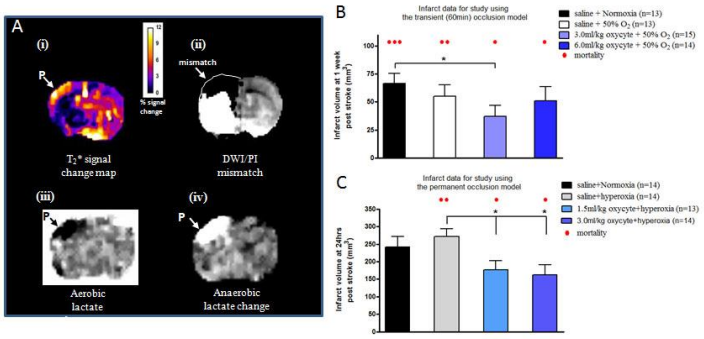

Figure demonstrating GOLD theranostic properties (A) Illustrates both T_2*OC and lactate change diagnostic techniques working concurrently in permanent stroke model following administartion of Oxycyte (4.5ml/kg). (i) T2* signal change map to 50%OC at ~2.5hrs post stroke. (ii) corresponding time matched DWI/PI mismatch. (iii) Aerobic lactate change map in response to hyperoxia at ~3hrs post stroke (black region indicates decrease in lactate) and (iv) anaerobic lactate change mao in response to returning to normoxic ventialtion at ~3hrs post stroke (white region indicates increase in lactate). P; indicates penumbra detected by GOLD techniques. **(B)** Graph showing a significant reduction in infarct size at 7-days post stroke in transient rat stroke model treated with 3ml/kg Oxycyte + hyperoxia where treatment was initiated 50-min following stroke onset (10-min prior to reperfusion) **(C)** Graph showing a significant reduction in infarct size at 24-hrs post stroke in permanent rat stroke model treated with both 1.5ml/kg and 3ml/kg Oxycyte + hyperoxia where treatment was delayed until 1 hour following stroke onset. Data presented as mean ± SEM. *P<0.05.

Methods and Results: GOLD's theranostic potential in AIS has been evaluated using permanent and transient intraluminal filament occlusion (MCAO) in SD rats (in accordance with Animals (Scientific Procedures) Act 1986). Intravenous oxygen-carrier Oxycyte®, is administered before OC to overcome limitations in both diagnostic techniques and increase oxygen delivery to penumbra.

Study design: serial scanning (Bruker 7T Biospec) included diffusion-, perfusion-weighted imaging, T_2*OC & LC imaging following permanent MCAO (n=9). Results confirmed previous findings[4] that Oxycyte (4.5ml/kg, i.v) combined with 40-50%O_2 resulted in a strong T2*OC signal within penumbra (Figure A.i). In all animals increased lactate levels detected within the penumbral zone decreased in response to hyperoxia+Oxycyte® (Figure A.iii). On returning to normoxia, lactate increased within this tissue (Figure A.iv). The addition of Oxycyte® improved sensitivity to detect LC to OC, when compared to hyperoxia (100%O_2) alone[2]. Terminal [^{14}C]2-deoxyglucose (2-DG) autoradiography confirmed ongoing glucose metabolism in tissue identified as penumbra.

Serial diffusion-weighted MRI, acutely following permanent MCAO (30mins-4hrs post-stroke),

revealed less lesion growth in rats administered 3ml/kg Oxycyte®+hyperoxia compared to normoxia or hyperoxia alone controls. In neuroprotection studies Oxycyte®+hyperoxia reduced infarct size and improved functional outcome following transient and permanent MCAO (Figure B,C).

Conclusion: GOLD has the potential to transform acute stroke patient management. Diagnostically, it will provide clinicians with a single stratified measure of tissue viability through two complementary MRI-based metabolic imaging techniques while therapeutically supporting survival of salvageable penumbra by improving oxygen delivery to penumbra using the injectable oxygen carrier Oxycyte® with 40-50%O_2.

References:

1. Santosh C, et al. *JCBFM* 2008;28:1742-53.
2. Holmes WM, et al. *NMR Biomed* 2012;25:295-304.
3. Dani KA, et al. *Ann Neurol* 2010;68(1):37-47
4. Deuchar GA, et al. *JCBFM* 2013;33(9):1422-8.

Oxycyte® provided by Tenax Therapeutics Inc. (Morrisville, NC, USA).

188
BRAIN-0594
Brain Oral Communication

Oral Session: Imaging: Pre-Clinical – Applications

QUANTITATIVE BETA MAPPING FOR HIGH-FIELD CALIBRATED FMRI IN RAT BRAIN

C. Shu[1], D. Rothman[1], B. Sanganahalli[2], D. Coman[2], P. Herman[2], F. Hyder[1]
[1]Biomedical Engineering, Yale University, New Haven, USA
[2]Diagnostic Radiology, Yale University, New Haven, USA

OBJECTIVES: The BOLD signal is derived from the relaxation rate of tissue water (R_2') that depends on deoxyhemoglobin-based susceptibility[1]. R_2' is related to the susceptibility of deoxyhemoglobin by a power-law relationship containing the scaling exponent β[1,3], where $R_2' \propto$ (susceptibility of deoxyhemoglobin) $^{\beta}$. Since deoxyhemoglobin-based susceptibility depends on the interaction between cerebral blood flow (CBF) and cerebral metabolic rate of oxygen (CMR_{O2}), β is the basis of calibrated fMRI[2,3]. As β is not yet determined in vivo, it is common to use a value of 1.5 determined by simulations from behavior of water molecules within blood vessels at 2T[1]. Because R_2' is dependent on the subject's physiological conditions and the field strength of the magnet, there is a need for measuring β in vivo for calibrated fMRI in clinical settings. This study proposes an experimental approach to measure β in vivo. We enhanced susceptibility through injecting multiple doses of a superparamagnetic contrast agent and assumed that susceptibility of blood is proportional to the amount of contrast agent. We measured R_2' as a function of the contrast agent concentration (C), and β was determined from linearizing the power-law relationship between R_2' and concentration of contrast agent. Since we used Feraheme (i.e., an FDA-approved contrast agent), this method can be translated to humans[4].

METHODS: Sprague-Dawley rats were anesthetized with α-chloralose. fMRI data were obtained on a 9.4T spectrometer. Feraheme was injected intravenously three times, each at a dose of 3.5 mg/kg. Following each injection, multi-slice R_2^{GE} and R_2^{SE} images were acquired with gradient echo and spin echo sequences. R_2' images were calculated from the R_2^{GE} and R_2^{SE} difference. β was fitted according to $\beta = \text{Ln}(R_2'/R_2'_0) / \text{Ln}(C/C_0)$, where 0 represents the initial conditions. A template containing 22 regions of interest (ROIs) was used to calculate mean across regions.

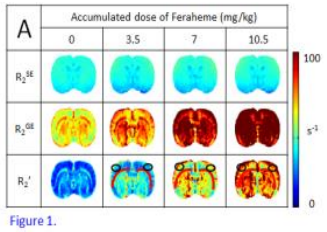

Figure 1.

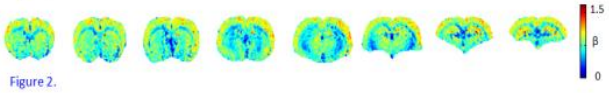
Figure 2.

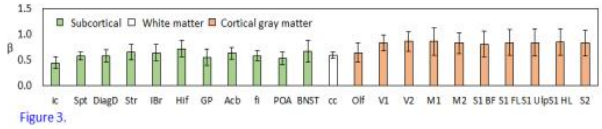

Figure 3.

RESULTS: In Figure 1(A), as more contrast agent exists in the blood, R_2^{GE} and R_2' increased significantly while R_2^{SE} changes were small. Figure 1(B) shows that linear

fits give a higher slope for cortical ROI than white matter ROI. In Figure 2., β across ROIs are consistently uniform in the cortical regions. Mean values of β for each ROI are shown in Figure 3. Similarly here, β in the cortical regions are generally uniform, with mean values around 0.8 and standard deviations 24% of mean. In white matter β is about 0.6. Otherwise, β values are between 0.4 and 0.7.

CONCLUSIONS: The β values measured are lower than simulation results, reducing the BOLD signal's dependencies on CBF and CMR_{O2}[2,3]. β's heterogeneities across regions emphasize the need for calibrated fMRI studies to measure β directly. Finally, because data fitting is based on the ratios of concentration, dose of Feraheme can be within FDA regulation for human studies.

REFERENCES:

1. Kennan RP et al (1994) *Magn Reson Med.* 31:9-21.
2. Kida I et al (2000) *J Cereb Blood Flow Metab*. 20:847-860
3. Davis TL et al (1998) *Proc. Natl. Acad. Sci*. 95:1834-1839.
4. Christen T et al (2013) *Magn Reson Med*. 70:705-710.

189
BRAIN-0682
Brain Oral Communication

Oral Session: Imaging: Pre-Clinical – Applications

FUNCTIONAL CONNECTIVITY IN THE MOUSE BRAIN DURING TRANSITIONS FROM AWAKE TO DEEP ANESTHESIA

A.Q. Bauer[1], *P.W. Wright*[2], *G. Baxter*[1], *A. Bice*[1], *M.D. Reisman*[3], *B. Palanca*[4], *J.P. Culver*[1]
[1]*Radiology, Washington University in Saint Louis, Saint Louis, USA*
[2]*Biomedical Imaging, Washington University in Saint Louis, Saint Louis, USA*
[3]*Physics, Washington University in Saint Louis, Saint Louis, USA*
[4]*Anesthesiology, Washington University in Saint Louis, Saint Louis, USA*

Objectives: Resting-state functional magnetic resonance imaging studies have shown spatiotemporal correlations in spontaneous activity among functionally-related brain regions[1]. Recent human studies have investigated the significance of intrinsic brain activity to explain altered states of consciousness. Loss of consciousness during general anesthesia is thought to be due to reductions in network functional connectivity [2], network specialization[3] or brain integration[4]. While burst-suppression in electroencephalogram (EEG) activity is a clinical indicator of unconsciousness, several distinct spontaneous coherent networks were identified in primates deeply anesthetized by isoflurane[5]. This finding suggests that coherent networks persist even in the unconscious brain, and may represent a fundamental and intrinsic property of functional brain organization. In order to understand how spontaneous hemodynamic fluctuations evolve in the mouse brain from an awake state to deep anesthesia, we developed a new technique combining resting-state functional connectivity (fc) mapping and optical intrinsic signal (OIS) imaging for application in awake-behaving mice.

Methods: An "awake" mouse preparation allows mice to walk on a levitating Styrofoam ball during imaging sessions (Fig. 1A) by securing the head to a bracket (Fig. 1B). Following scalp retraction, small screws for EEG recordings are placed laterally, and a Plexiglas cranial window is installed over the intact skull and secured with dental cement. Once recovered, mice are trained to become behaviorally acclimated to the imaging system over a period of 5 days. OIS imaging was performed in 5 mice in order to record spontaneous activity in the brain as mice transitioned from an awake state through increasing levels of isoflurane anesthesia (0-2%, Fig. 1C). We quantified the extent of motor movement, spectral content in concurrently-recorded EEG, and the presence/absence of electrical burst-suppression to compare how those observations relate to changes in network functional connectivity (Fig. 1D, E).

Results: Awake mice exhibit strong, bilaterally-symmetric fc patterns. With increasing anesthetic dose, we observe a progressive, regional reduction in the magnitude and coherence of spontaneous activity over the cortex(Fig. 1C). While deep

anesthesia was found to ablate fc globally over the brain, activity in some networks (e.g., somatosensory) persisted longer than others with increasing anesthesia (Fig. 1D). Disruption in functional connectivity magnitude and brain-wide hemodynamic activity appear commensurate with reduced EEG spectral power over the functional connectivity band (Fig. 1E).

Conclusions: Extensive reduction of neural activity by anesthetics is evidenced by burst-suppression (using EEG) that may increase mortality risk for critically-ill patients[6], but the corresponding features of network topology during anesthetic transition remain unclear. Results from measuring fc under state transitions could shed light on the functional significance of intrinsic brain activity, and the role of fc as a correlate of anesthetic depth.

References

[1]. Biswal et al., *Magn Reson Med.*, 34(4), pp. 537-41 (1995)
[2]. Boveroux, et al., *Anesthesiology*. 113(5), pp 1038-1053 (2010)
[3]. Alkire, et al., *Science*, 322, pp.876-880 (2008)
[4]. Schrouff, et al., *NeuroImage*, 57, pp. 198-205 (2011)
[5]. Vincent et al., *Nature* 447, pp. 83-86 (2007)
[6]. Watson et al., *Crit Care Med.*; 36(12), pp. 3171–3177 (2008)

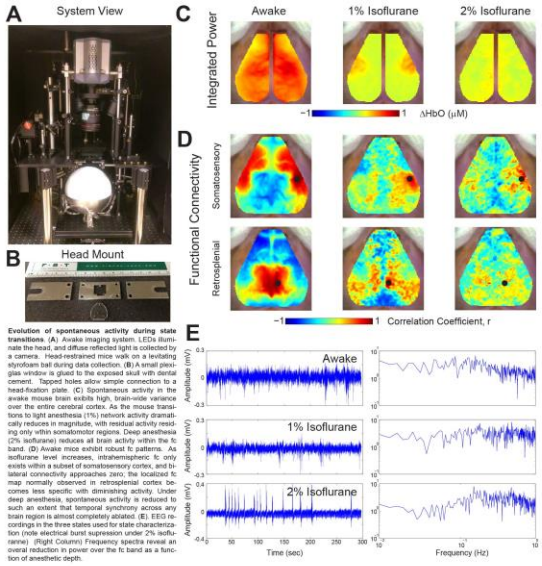

190
BRAIN-0172
Brain Oral Communication

Oral Session: Imaging: Pre-Clinical – Applications

MONITORING THE FUNCTIONAL PARCELLATION AND TOPOGRAPHY WITH MESOSCOPIC CALCIUM IMAGING OF RESTING STATE CORTICAL ACTIVITITY IN MICE

M. Vanni[1], A. Chan[1], D. Xiao[1], G. Silasi[1], M. Moshevand[1], J. Ledue[1], T. Murphy[1]
[1]Psychiatry, UBC, VANCOUVER, Canada

Objectives:

Strong reciprocal connections exist between the primary (S1) and secondary somatosensory cortex (S2) and primary motor cortex (area M1) within and between both hemispheres. These areas are organized in somatotopic maps of the body. In this study, the topology of functional connections between these areas was explored by using wide field calcium imaging in Emx1-cre X R26-GCaMP3 or CaMK2-tTA/TIGRE-GCaMP6 mice expressing the genetically encoded calcium indicator GCaMP3 in excitatory neurons.

Methods:

Wide field green fluorescence imaging measured cortical calcium responses in anesthetized and awake mice. Spontaneous activity was recorded to establish connectivity relations between arbitrary cortical points using a 'seed pixel" approach.

Results:

During sequences of spontaneous activity, calcium signals recorded of each location of the area S1 were correlated with localized activity in region of homotopic contralateral area S1, ipsilateral area S2 and bilateral areas of M1. Comparably, activity within each location of area S2 was correlated with activity localized in ipsilateral area S1 and M1. Activity within each location of area M1 was correlated with localized activity in region of homotopic contralateral area M1, bilateral areas of S1, and ipsilateral area S2.

The K-means clustering revealed 3 mains clusters of brain areas corresponding to locomotion (sensorimotor regions of hindlimb and forelimb), oro-facial activity (e.g. somatosensory and motor barrel cortex) and vision. By increasing the number of cluster, the symmetries existing between area S1 and M1 was clearly revealed. These results are consistent with this idea that connections between areas of the somatomotor cortex link similar somatotopic regions and that these maps are reflected across the cortex and hemispheres as mirror images of each other that flipped in orientation and scaled in size.

Conclusions:

This study demonstrated that several degrees of imbricated mesoscopic cortical functional organization co-exist and should have a major contribution in the spatial component of neural coding. We anticipate that calcium imaging of functional connections using spontaneous activity will enable longitudinal studies during plasticity paradigms or after models of CNS disease such as stroke where the weighting within these connectivity maps could be altered.

191
BRAIN-0806

Brain Oral Communication

Oral Session: Imaging: Pre-Clinical – Applications

CHANGES IN FUNCTIONAL CONNECTIVITY OF THE CONTRALESIONAL SENSORIMOTOR SYSTEM IN RATS RECOVERING FROM UNILATERAL STROKE TO THE MOTOR CORTEX

G.A.F. van Tilborg[1], G. Sarolidou[1], P. Yanev[1], T. Wieloch[2], C. Sjölund[2], W.M. Otte[1], A. van der Toorn[1], R.M. Dijkhuizen[1]
[1]Biomedical MR Imaging and Spectroscopy Group, University Medical Center Utrecht, Utrecht, Netherlands
[2]Laboratory for Experimental Brain Research, Lund University, Lund, Sweden

Objectives: Reorganization of intact ipsi- and contralesional neural networks may critically contribute to functional recovery after unilateral stroke. Partial restoration of sensory and motor functions is still possible, even when ischemic infarction involves large parts of primary sensorimotor cortical regions, which may strongly rely on functional remodeling of the undamaged contralesional sensorimotor system. We tested the hypothesis that functional connectivity of the contralesional primary motor cortex with other sensorimotor areas increases during recovery from unilateral infarction of the primary sensorimotor cortex.

Methods: Photothrombotic stroke was induced in the right sensorimotor cortex of male adult Sprague Dawley rats.[1] Serial MRI (9.4T) was conducted at 3, 8 and 60 days after stroke (n=4). During MRI, rats were anesthetized and mechanically ventilated with 1.5% isoflurane in air/O_2 (2:1). Temperature was maintained at 37.0±0.5°C. MRI included high-resolution anatomical imaging (bSSFP, 125µm isotropic voxels), and resting-state functional MRI (rs-fMRI) (3D gradient echo EPI (800 images, TR/TE=26.1/15ms, flip angle=13°; 600µm isotropic voxels). Sensorimotor function was assessed with a cylinder test (n=3).[2] For MRI analysis, a reference image matched to a 3D-model of Paxinos' stereotaxic rat brain atlas was registered to the anatomical and functional images. Regions-of-interest (ROIs) included the primary and secondary motor cortices

(M1 and M2), forelimb region of the primary somatosensory cortex (S1FL), caudate putamen (CPU) and thalamus (Th) in the contralesional hemisphere (Figure A). Functional connectivity between contralesional M1 and other contralesional ROIs was calculated as Fisher-transformed correlation (z') between low-frequency BOLD fluctuations as described previously.[3] Repeated measures ANOVA with Tukey's post-hoc testing and FDR correction was applied for statistical analyses.

Results: The photothrombotic lesion, which included ipsilesional S1FL, M1 and M2, was clearly identified on the anatomical images (figure A). Unilateral sensorimotor dysfunction was evident from forelimb use asymmetry in the cylinder test (58±8% at day 8), which partly recovered towards the chronic stage (38±19% at day 60) (figure B). This was accompanied by increased functional connectivity of contralesional M1 with contralesional S1FL, CPU and Th from days 3 and 8, towards day 60 after stroke ($p<0.05$) (figure C).

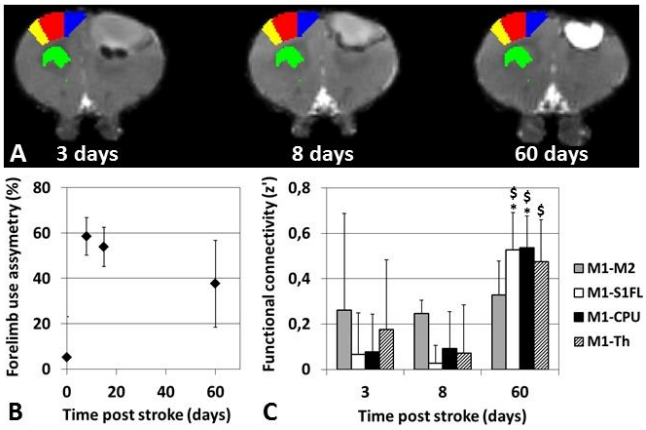

Figure: A. Anatomical MR images at 3, 8 and 60 days after photothrombotic stroke. ROIs in the contralesional hemisphere, i.e. M1 (red), M2 (blue), S1FL (yellow) and CPU (green), are overlaid on the anatomical images. B. Forelimb use asymmetry before, and up to 60 days after stroke. C. Functional connectivity (z') between contralesional M1 and contralesional M2, S1FL, CPU and Th at 3, 8 and 60 days after stroke ($p<0.05$ vs. 3 days* or 8 days$^{\$}$ post-stroke).

Conclusions: Our study suggests that enhancement of functional connectivity in the contralesional sensorimotor system may be critical for recovery of sensorimotor functions when the primary sensorimotor cortex in the ipsilesional hemisphere is largely infarcted. To what extent these plastic changes relate to actual functional recovery of the affected limb(s) or to compensatory overuse of the nonaffected limb(s) remains to be further investigated.

References:

[1]Madinier et al., Behav Brain Res. 2014;261:282-8
[2]Hua et al., Stroke. 2002;33:2478-84
[3]Van Meer et al., J Neurosci. 2012;32:4495-507

194
BRAIN-0634
BrainPET

BrainPET Oral Session: Neurological Disorders

ALPHA SYNUCLEIN MODEL OF PARKINSON'S DISEASE DISPLAYS SYNAPTIC DISRUPTION

J. Phan[1], K. Stockholm[1], S. Jakobsen[1], K. Vang[1], A. Gjedde[2], A.M. Landau[1], M. Romero-Ramos[3]
[1]Department of Nuclear Medicine and PET centre, Aarhus University Hospital, Aarhus, Denmark
[2]Department of Neuroscience and Pharmacology, University of Copenhagen, Copenhagen, Denmark
[3]Department of Biomedicine, Aarhus University, Aarhus, Denmark

Objectives

Investigation of the pathogenesis of Parkinson's disease (PD) has extensively progressed through the development of gene modification techniques in order to reproduce features of PD in animal models. The misfolding and aggregation of the alpha synuclein protein is linked to both sporadic and familial PD, and multiplication of the alpha synuclein gene is identified in families with an autosomal dominant presentation. The aim of this study is to apply PET imaging with [^{11}C]DTBZ, the radioligand of the vesicular monoamine transporter (VMAT-2), to detect disrupted synaptic function in rat models of PD that overexpress alpha synuclein in nigrostriatal dopaminergic projections. In order to support the in vivo findings, we included in vitro autoradiography and immunohistochemistry.

Methods

PD was reproduced in female Sprague Dawley rats by unilateral intranigral injection of recombinant adeno-associated viral vectors, engineered to overexpress the human wild type alpha synuclein gene. The control group received a viral vector designed to overexpress green fluorescent protein (GFP). We performed 90 minute dynamic [^{11}C]DTBZ tomography at 12 weeks after gene transduction using the MEDISO nanoScan PET/MRI imaging system,. Binding potentials (BP_{ND}) in left and right striatum were quantified by Logan plot using cerebellum as input function. To support the in vivo findings, in vitro autoradiography with tritium labeled DTBZ was performed on post-mortem brains at the coronal level -0.3 mm from bregma. Total binding was determined by incubation with [^{3}H]DTBZ and nonspecific binding was obtained by co-incubation with non-radioactive DTBZ.

Results

Immunohistochemical staining confirmed the sustained unilateral expression of alpha synuclein and GFP expression at 12 weeks after transduction (**Figure 1**). Furthermore, pathological accumulation of alpha-synuclein was obvious in the dopaminergic terminals of the ipsilateral striatum, but not in the contralateral side or the GFP animals. Ipsilateral VMAT expression significantly declined at 12 weeks in the alpha synuclein overexpressing animals, but not in the GFP counterparts, as detected with in vivo PET and in vitro autoradiography **(Figures 2A-B)**. As presented in **Figures 3A,** quantification of binding in PD animals revealed a significant reduction of [^{11}C]DTBZ BP_{ND} in response to alpha synuclein overexpression, but not in response to GFP (two-way ANOVA, Tukey post hoc test). Equivalent results were found with [^{3}H]DTBZ autoradiography, as presented in **Figure 3B**. A robust correlation (r^2=0.87) was found between in vivo PET and in vitro autoradiography in animals that underwent both PET and autoradiography, as shown in **Figure 3C**.

Conclusions

Our data indicate that alpha synuclein overexpression induces toxicity and disrupts the integrity of dopaminergic axonal projections in an adult trangenic rat model of PD. In agreement with recent investigations in human,[1] and other VMAT studies in rodent models of PD,[2-4] our data indicate that [^{11}C]DTBZ is powerful marker for monitoring early degenerative processes. This is beneficial for future investigations of the dynamics of alpha synuclein pathology in PD as well in evaluating response to treatment.

References

1. Hsiao et al. JAMA neurology 2014;71:758-66.
2. Strome et al. Molecular imaging and biology 2006;8:292-9.
3. Sossi et al. Journal of cerebral blood flow and metabolism 2007;27:1407-15.
4. Mackey et al. Experimental neurology 2013;247:19-24.

Figure 1

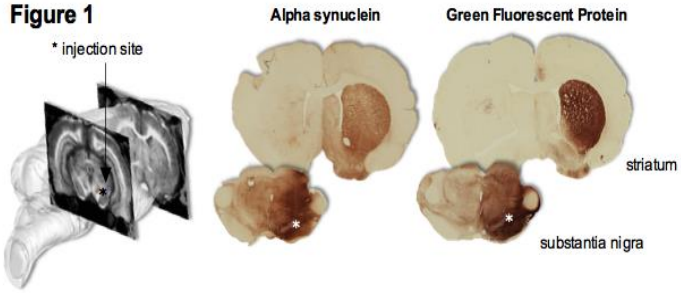

Figure 2

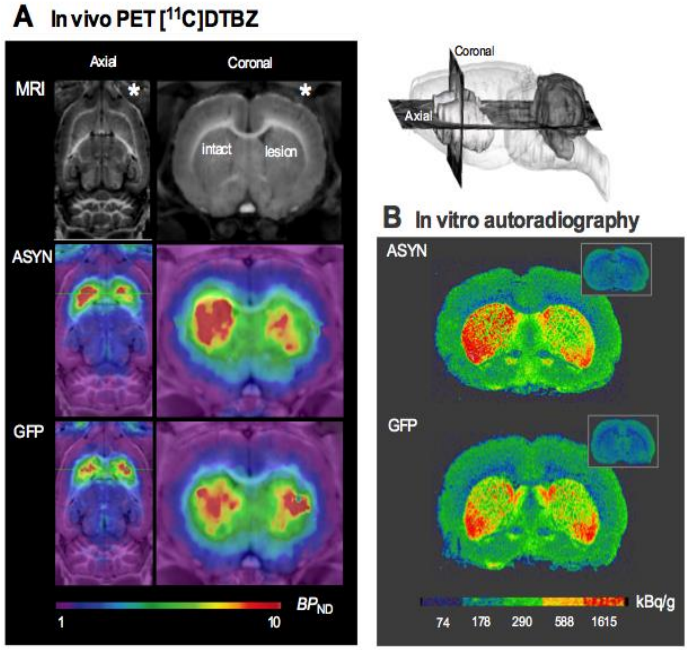

Figure 3

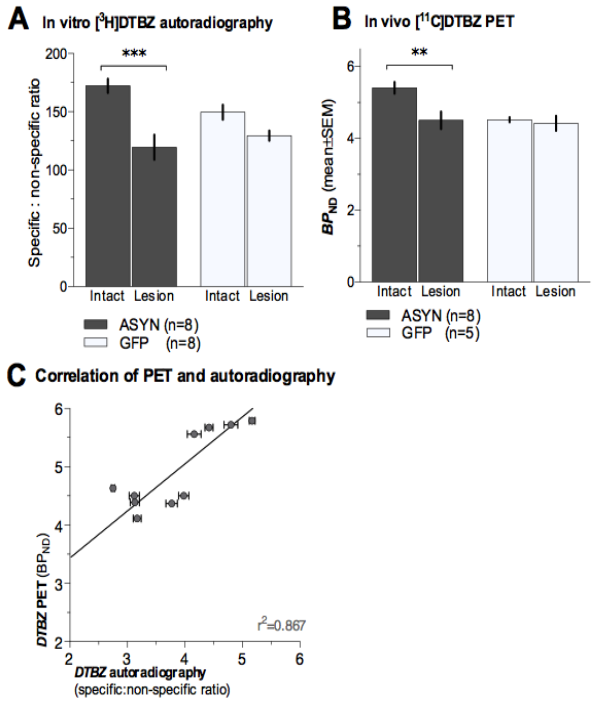

195
BRAIN-0372
BrainPET

BrainPET Oral Session: Neurological Disorders

LOSS OF PHOSPHODIESTERASE 10A SIGNALLING IS ASSOCIATED WITH PROGRESSION AND SEVERITY IN PATIENTS WITH PARKINSON'S DISEASE

F. Niccolini[1], T. Foltynie[2], T. Reis Marques[3], S. Natesan[3], S. Kapur[3], N. Mulhert[4], G.E. Searle[5], A.C. Tzortzi[5], E.A. Rabiner[5], R.N. Gunn[5], P. Piccini[6], P. Marios[1]

[1]Department of Basic & Clinical Neuroscience, King's College London, London, United Kingdom
[2]Sobell Department of Motor Neuroscience, UCL Institute of Neurology, London, United Kingdom
[3]Department of Psychosis Studies, King's College London, London, United Kingdom
[4]School of Psychology, Cardiff University, London, United Kingdom
[5]Centre for Imaging Sciences, Imanova, London, United Kingdom
[6]Division of Brain Sciences, Imperial College London, London, United Kingdom

OBJECTIVES

To assess the availability of phosphodiesterase 10A (PDE-10A) *in vivo* in Parkinson's disease (PD) patients, using [^{11}C]IMA107 PET.

BACKGROUND

PDE-10A is a dual substrate enzyme highly expressed in the striatal medium spiny neurons, where it regulates cAMP/cGMP signaling cascades, thus having a key role in the regulation of the striatal output pathways, and in promoting neuronal survival.

METHODS

We have quantified the availability of PDE-10A in 24 patients with levodopa-treated PD (13 males, mean-age: 67 years, mean-PD-duration: 9.7 years, H&Y range: 1-4, UPDRS-III: 36.2) and compared to a group of 12 healthy controls. Parametric images of [^{11}C]IMA107 binding potential relative to non-displaceable binding (BP_{ND}) were generated from the dynamic [^{11}C]IMA107 scans using implementation of the simplified reference tissue model with the cerebellum as the reference tissue. To facilitate anatomical delineation of regions of interest (ROIs), PET images were co-registered and resliced to the corresponding volumetric MRI using the Mutual Information Registration algorithm in SPM8. Striatum (caudate and putamen) and globus pallidus ROIs were manually delineated on the co-registered MRIs using ANALYZE11.

RESULTS

PD patients had significantly lower mean [^{11}C]IMA107 BP_{ND} in the caudate (28.4%; P<0.001), putamen (25.5%; P<0.001) and globus pallidus (14.2%; P<0.05) compared to healthy controls. Longer PD duration correlated with lower [^{11}C]IMA107 BP_{ND} in caudate (r=-0.65; P<0.01;), putamen (r=-0.51; P<0.01), and globus pallidus (r=-0.47; P<0.05;). Higher UPDRS-III scores correlated with lower [^{11}C]IMA107 BP_{ND} in caudate (r=-0.54; P<0.05), putamen (r=-0.48; P<0.05), and globus pallidus (r=-0.70; P<0.001;). Higher UDysRS scores in those Parkinson's patients with levodopa-induced dyskinesias (n=12), correlated with lower [^{11}C]IMA107 BP_{ND} in caudate (r=-0.73; P<0.05) and putamen (r=-0.74; P<0.05).

CONCLUSIONS

Our findings suggest loss of PDE-10A signalling in PD, which is associated with the progression and severity of the disease. [^{11}C]IMA107 PET may provide a valuable tool to understand the pathophysiology of PD. PDE-10A is an enzyme that could be targeted with novel pharmacotherapy, which may help to alleviate PD symptoms and complications.

FIGURE LEGEND

Axial summed [^{11}C]IMA107 PET images for the striatum of a healthy male showing normal striatum [^{11}C]IMA107 binding (BP_{ND} = 2.24) (top); a Parkinson's disease male patient (disease duration: 16 years; H&Y: 4; UPDRS-III: 64) showing decreases in striatal [^{11}C]IMA107 binding (BP_{ND} = 1.09) (bottom).

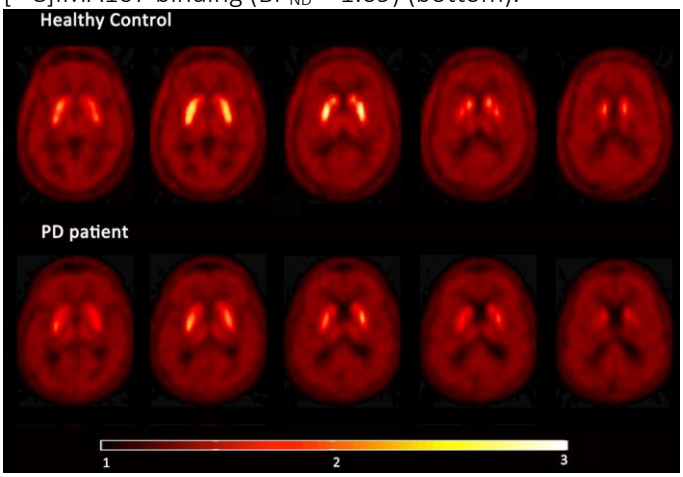

196
BRAIN-0750
BrainPET

BrainPET Oral Session: Neurological Disorders

GRAY MATTER VOLUME ASSOCIATIONS WITH AMYLOID-BETA DEPOSITION AND AGE IN DOWN SYNDROME

P.J. Lao[1], T.J. Betthauser[1], A.T. Hillmer[1], D.L. Tudarascu[2], J.C. Price[3], W.E. Klunk[4], I. Mihaila[5], A.T. Higgins[5], P.D. Bulova[6], S.L. Hartley[5], R.V. Tumuluru[4], D. Murali[1], C.A. Mathis[3], A.D. Cohen[4], T.E. Barnhart[1], D.A. Devenny[7], M.R. Mailick[5], S.C. Johnson[8], B.L. Handen[4], B.T. Christian[1]
[1]Medical Physics, University of Wisconsin-Madison, Madison, USA

[2]*Biostatistics, University of Pittsburgh, Pittsburgh, USA*
[3]*Radiology, University of Pittsburgh, Pittsburgh, USA*
[4]*Psychiatry, University of Pittsburgh, Pittsburgh, USA*
[5]*Waisman Center, University of Wisconsin-Madison, Madison, USA*
[6]*Internal Medicine, University of Pittsburgh, Pittsburgh, USA*
[7]*Psychology,*
New York Institute for Basic Research in Developmental Disabilities, Albany, USA
[8]*Medicine-Geriatrics, University of Wisconsin-Madison, Madison, USA*

Objectives: Young adults with Down syndrome (DS) are predisposed to early development of Alzheimer-like pathology (amyloid-β plaques and neurofibrillary tangles). Stages of Alzheimer disease (AD) pathogenesis can be described by the amyloid cascade hypothesis, in which various biomarkers undergo a sigmoidal increase. The goal of this work is to assess the earliest stage of AD pathogenesis in the DS population and interrogate the complex association between amyloid-β deposition and gray matter atrophy along the course of normal aging.

Methods: 68 nondemented adults (30-53yrs) with DS underwent dynamic [^{11}C]PiB PET scans. SUVR images were created using 40-70 min post-injection data and cerebellum as reference region. A global mean SUVR was calculated from six regions: frontal cortex, anterior cingulate, parietal cortex, precuneus, striatum, and temporal cortex. Modulated gray matter (GM) probability maps were segmented from T1wMRI scans using a modified mixture cluster algorithm, normalized to a study specific template, and smoothed with a 12mm isotropic Gaussian kernel in SPM12. Linear regression models assessed the association of GM volume with age or global mean SUVR. Two sample t-tests checked for unadjusted mean differences in the GM between PiB(+) and PiB(-). Sparse k-means clustering determined PiB status. Furthermore, a multiple linear regression model assessed the effect of age, PiB status and their interactions on GM volume. A FWE correction ($p< 0.05$) was used for statistical significance with a minimum cluster size of 5 voxels.

Results: A statistically significant negative association was found between GM volume and age as well as between GM volume and PiB SUVR in the striatum and thalamus. The GM volume association with age was limited to the putamen and caudate tail, while the GM volume association with SUVR extended throughout the putamen and caudate tail and moderately into the caudate head. However, no significant association of GM volume and age was detected when correcting for SUVR, or of GM volume and SUVR when correcting for age. The two-sample t-test showed that the PiB(-) group had significantly more GM volume in the striatum than the PiB(+) group. This group difference did not survive after adjusting for age. No significant interactions were detected between PiB status and age.

Conclusions: In the DS population, there exists significant negative associations of GM volume with age and of GM volume with SUVR in the striatum, regardless of PiB status. The PiB(-) group had a significantly larger GM volume in the striatum than the PiB(+) group; however the associations of GM volume and age ceased to be significant within groups. A multiple linear regression model could not separate group difference due specifically to amyloid-β or simply to age. Further analysis will be required, perhaps in a larger cohort, to determine if age is truly a confounder of the association between GM and amyloid-β deposition in the striatum.
Research Support: R01AG031110 and P30 HD03352

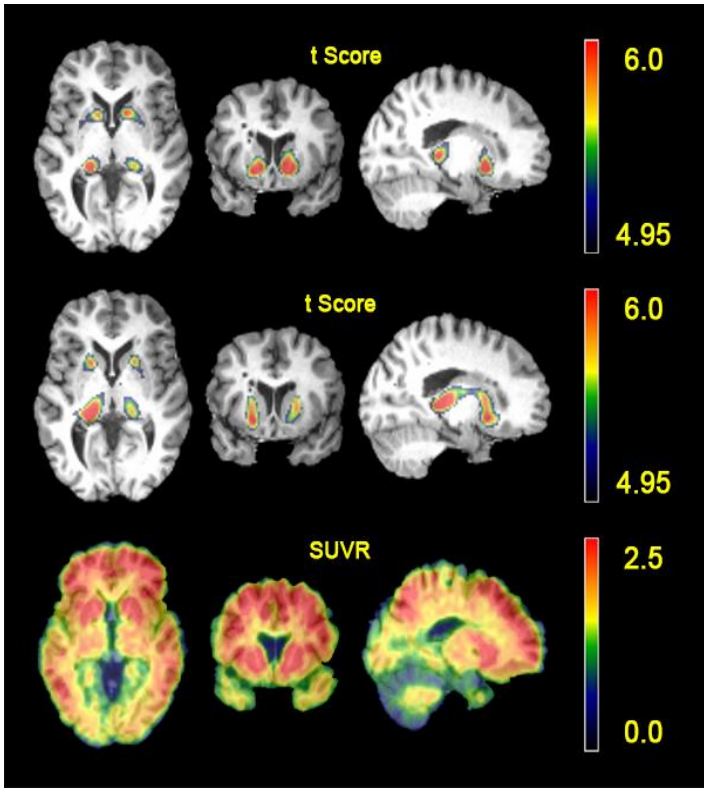

Figure1. Clusters of significant negative association between GM volume and age (top row) and between GM volume and SUVR (middle row) regardless of PiB status, alongside a PiB(+) SUVR image (bottom row).

197
BRAIN-0383
BrainPET

BrainPET Oral Session: Neurological Disorders

EVIDENCE FOR EXACERBATED NEUROINFLAMMATION FOLLOWING AN INFLAMMATORY TRIGGER IN THE G2019S LRRK2 RAT MODEL USING LONGITUDINAL PET IMAGING

V. Sossi[1], M. Walker[1], K. Dinelle[1], A. Schildt[3], R. Kornelsen[2], Q. Miao[3], C. Takhar[3], D. Bannon[4], M. Mejias[4], D. Doudet[3], M. Farrer[5]
[1]PHAS, University of British Columbia, Vancouver, Canada
[2]PPRC, University of British Columbia, Vancouver, Canada
[3]UBC/TRIUMF, University of British Columbia/TRIUMF, Vancouver, Canada
[4]Neuroscience, University of British Columbia, Vancouver, Canada
[5]Medical Genetics, University of British Columbia, Vancouver, Canada

OBJECTIVES. The G2019S LRRK2 mutation is the most common mutation associated with an increased risk of Parkinson's disease (PD); the related pathogenic mechanisms are however still not well understood. Here we test the hypothesis that increased risk could be mediated by an exaggerated neuroinflammatory response to an inflammatory trigger, ultimately resulting in selective degeneration of the dopaminergic system.

METHODS. 11 male wild-type (WT) and 13 male LRRK2 G2019S (BAC) transgenic (TG) littermates [1] were scanned at baseline (4 month of age) with ^{11}C-PBR28, a marker of microglia activation, and ^{11}C-DTBZ, a marker of VMAT2 density, an indicator of dopaminergic integrity. Each group was then divided into two subgroups; approximately half of the animals in each group were administered 3mg/kg of LPS i.p., while the other half was given saline. Animals were rescanned at 1, 6 and 12 weeks and 6 and 10 months post-LPS administration. Logan derived tissue input binding potential (BP_{ND}) was the primary outcome variable for DTBZ, while standard uptake values (SUV), previously validated against 2-

compartment based total distribution volume (DV), were used to quantify ^{11}C-PBR binding. Behavioural tests were administered at 4-6 months post-LPS administration.

RESULTS. No difference in any of the markers was observed at baseline. Likewise the acute response to LPS was similar in the two LPS-treated groups. ^{11}C-PBR binding was similar in the four groups up to the 12 weeks time point. At 6 months post LPS a significant interaction between genotype and treatment was observed (p=0.02), with the LPS-TG group showing the highest ^{11}C-PBR28 binding reflecting a higher degree of neuroinflammation. Preliminary data indicate such effect to persist at 10 months, while no difference in dopaminergic integrity is being observed. The only relevant outcome of the behavioral studies was an almost significant (p=0.07) genotype effect for the time spent on the rotarod consistent with earlier observations[1].

CONCLUSION. The results of this longitudinal in-vivo study seem to support the hypothesis that the G2019S LRKK2 mutation mediates an exacerbated response to an inflammatory trigger, consistent with what was observed in cross-sectional studies in a mutant alpha-synuclein overexpression mice model [2]. These preliminary results however do not provide evidence for selective dopaminergic deficit following an acute inflammatory insult, as previously observed in [2]. Further studies should explore effects of repeated rather than single acute insults and possible effects on other systems other than the dopaminergic.

REFRENCES

1. Walker, M.D., et al., J Parkinsons Dis, 2014. **4**(3): p. 483-98.

2. Gao, H.M., et al., Environ Health Perspect, 2011. **119**(6): p. 807-14.

198
BRAIN-0516
BrainPET

BrainPET Oral Session: Neurological Disorders

SPECT-IMAGING OF DISTURBED BRAIN FUNCTIONS IN DEMENTIA USING A LIPOPHILIC CHELATE COMPLEX OF THE K+-PROBE 201THALLIUM

A.M. Oelschlegel[1], F. Stöber[2], T. Stöter[3], I. Apostolova[2], H. Scheich[4], H. Amthauer[2], K.G. Reymann[1], J. Goldschmidt[5]
[1]PG Neuropharmacology, Leibniz Institute for Neurobiology, Magdeburg, Germany
[2]Department of Radiology and Nuclear Medicine, University Hospital Magdeburg, Magdeburg, Germany
[3]Special Lab Non-Invasive Brain Imaging, Leibniz Institute for Neurobiology, Magdeburg, Germany
[4]Emeritus Group Lifelong Learning, Leibniz Institute for Neurobiology, Magdeburg, Germany
[5]Department Systemphysiology, Leibniz Institute for Neurobiology, Magdeburg, Germany

Objectives: Chronically altered spatial patterns of neuronal activity are hallmarks of dementia. These alterations are accompanied by up- or down-regulations of neuronal Na,K-ATPase activities, transmembrane potassium (K^+)-turnover rates and membrane potentials. Thus, K^+-probes, such as thallium (Tl^+) could be of high interest, for imaging chronically disturbed patterns of neuronal activity in dementia, but their poor blood-brain-barrier (BBB) permeability had limited their use for imaging brain K^+-metabolism.
We have previously shown that the CNS K^+-metabolism can be studied using thallium diethyldithiocarbamate (TlDDC) (Stöber et al. 2014). TlDDC is a lipophilic chelate complex that crosses the BBB. After crossing the BBB, Tl^+ is released from TlDDC.
When animals are intravenously injected with TlDDC, neurons in the CNS take up Tl^+ in an activity-dependent manner from the extracellular space. With increasing Tl^+-uptake, Tl^+-efflux increases in

return and Tl^+ redistributes over time. When Tl^+-influx and –efflux equilibrate, the intra- to extracellular Tl^+-gradients are related to the intra- to extracellular K^+-gradients and to the membrane potentials.
We here tested, whether dynamic single-photon emission computed tomography (SPECT) imaging after a single intravenous injection of ^{201}TlDDC could be used to detect in vivo alterations in ^{201}Tl-uptake patterns and redistribution kinetics in mouse models of dementia.

Methods: Mice (5xFAD or TBA2.1 and their respective controls) were imaged repeatedly 20 minutes, 3 hours, 6 hours and 22 hours after a single intravenous injection of ^{201}TlDDC.

Results: Tl^+-uptake patterns and redistribution kinetics differ in mouse models of dementia. Differences in $^{201}Tl^+$-redistribution kinetics are shown exemplarily for TBA2.1 mice in the figure below. Compared to control mice, TBA2.1 mice (10 to 11 weeks old) show faster $^{201}Tl^+$-wash-out within the posterior cingulate cortex and slower $^{201}Tl^+$-wash-out within the amygdala.

Conclusions: Dynamic SPECT-imaging of ^{201}Tl-redistribution kinetics after a single intravenous injection of ^{201}TlDDC is a novel approach for analyzing in vivo spatial patterns of disturbed brain functions in mouse models of dementia. Our results indicate that the technique is a sensitive tool for monitoring disease progression in preclinical studies and suggest testing the approach for clinical use.

References:
Stöber F et al. Single-cell resolution mapping of neuronal damage in acute focal cerebral ischemia using thallium autometallography. J Cereb Blood Flow Metab. 2014; 34(1):144-52

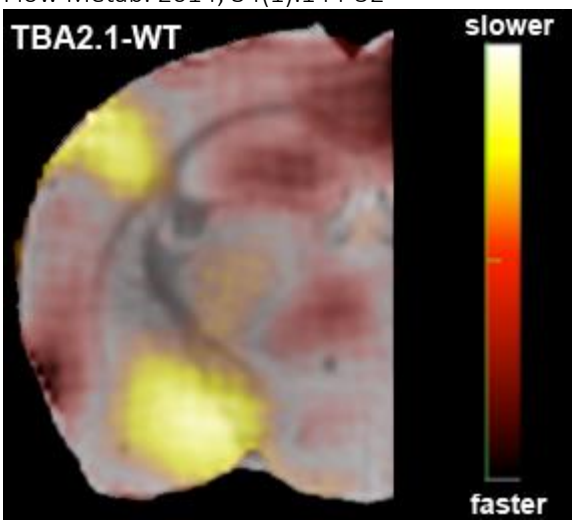

Figure: Map of differences in $^{201}Tl^+$-redistribution kinetics (TBA2.1 minus WT) laid over a standard-MRI for reference. When compared with wild-type mice, TBA2.1 mice show faster $^{201}Tl^+$-wash-out within the posterior cingulate cortex and slower $^{201}Tl^+$-wash-out within the amygdala; MRI grey level, SPECT image pseudo colored.

199
BRAIN-0511
BrainPET

BrainPET Oral Session: Neurological Disorders

LONGITUDINAL 6-[18F]FLUORO-L-M-TYROSINEPET IMAGING OF DOPAMINE FUNCTION FOLLOWING ADMINISTRATION OF OXB-102, AN ENHANCED GENE THERAPY FOR PARKINSON'S DISEASE

N. Van Camp[1], R. Aron Badin[1], K. Binley[2], C. Jan[1], Y. Bramoulle[1], H. Steward[2], S. Ralph[2], Y. Lad[2], S. Naylor[2], K. Hosomi[3], S. Palfi[3], P. Hantraye[1], K. Mitrophanous[2]
[1]Commissariat à l'Energie Atomique et aux Energies Alternatives (CEA), Département des Sciences du Vivant (DSV) Institut d'Imagerie Biomédicale (I2BM) MIRCen Centre National de la Recherche Scientifique (CNRS) Université Paris-Sud Université Paris-Saclay UMR 9199 Neurodegenerative Diseases Laboratory, Fontenay-aux-Roses, France
[2]Oxford BioMedica, (UK) Ltd, Oxford, United Kingdom
[3]Commissariat à l'Energie Atomique et aux Energies Alternatives (CEA),

Département des Sciences du Vivant (DSV) Institut d'I magerie Biomédicale (I2BM) MIRCen Neurosurgery H enri Mondor Hospital APHPInstitut Mondor de Recher che Biomédicale (IMRB) INSERM/Université Paris Est Creteil (UPEC), Fontenay-aux-Roses / Créteil, France

Introduction: Dopamine (DA) depletion in the sensorimotor area of the putamen accounts for the motor symptoms in Parkinsonian patients such as akinesia, tremor and postural rigidity. Recently a phase I/II clinical trial with a lentiviral vector-based gene therapy for Parkinson's disease (ProSavin®) has been reported (Palfi, Lancet 2014), demonstrating the long-term safety and tolerability of ProSavin®, injected in the motor striatum of patients with advanced Parkinson's disease. An improvement in the motor UPDRS score (OFF) was observed in all patients relative to baseline. Oxford BioMedica is now developing OXB-102, an improved version of ProSavin®, that expresses the same enzymes but with an increased DA production per genetically modified cell.

Objectives: To evaluate therapeutic efficacy of OXB-102 compared to ProSavin® in a NHP model of PD using a longitudinal Positron Emission Tomography study with ^{18}F-FMT, a specific radiotracer of the aromatic acid decarboxylase (AADC) enzyme.

Material & Methods: Sixteen Parkinsonian macaques received stereotactic intra-putaminal administration of ProSavin® (n=4), OXB-102 at a high (n=4) or low dose (n=4) and control (n=4) lentiviral vectors. PET imaging using ^{18}F- FMT was performed at baseline, after MPTP intoxication, and 3 and 6 months post-vector administration using a FOCUS220 PET scanner, under propofol anesthesia. Thirty minutes prior to PET examination NHPs were pretreated with 2.5 mg/kg benserazide. Parametric Ki images were calculated according to the graphical method of Patlak using the occipital cortex as a reference region. Parametric images were then coregistered to individual T_2-weighted images, acquired on a 7T Varian, to allow precise segmentation around the injection area as visualized by the needle tract. In parallel to PET imaging the NHPs were rated using a clinical rating scale. At the end of the study animals were sacrificed and brains were histologically processed to evaluate the level ofAADC/CH1 immunostaining. A PET histological comparative study is ongoing to correlate PET data with viral vector expression.

Results: All NHPs displayed a significantly reduced Ki in the caudate and putamen following MPTP intoxication. At 3 months post-injection (PI), an increase in the Ki value was observed in the putamen of all OXB-102 and ProSavin® treated animals but not the controls, as compared to the levels after MPTP intoxication. At 6 months PI, the Ki value was significantly increased in the putamen of OXB-102 low and high dose treatment groups, compared to the ProSavin® and control group animals. No significant increase in Ki was observed at any timepoint in the non-treated caudate nucleus. A significant negative correlation was observed between Ki values and clinical scores. Histological analysis is still ongoing but preliminary results suggest a more important AADC imuno-staining in OXB-102-treated animals compared to the ProSavin®-treated primates, which might correlate with the ^{18}F-FMT PET findings.

Discussion & Conclusion: Longitudinal PET imaging with ^{18}F-FMT was used to compare the functional efficacy of two dopamine replacement gene therapy strategies in Parkinsonian primates. An enhanced AADC activity was observed with OXB-102 compared to ProSavin®. Ki data were correlated to behavioral data and will be confirmed by preliminary post-mortem analyses.

202
BRAIN-0977
Symposium

Early Career Symposium

Everything you need to know about behavioral testing in rodent models of stroke.

R. Trueman[1]
[1]*School of Life Science, Univeristy of Nottingham, Nottingham, United Kingdom*

Or, What I learnt moving from behavioural assessment in Huntington's disease to Stroke.

In order to test whether therapeutics will be beneficial for stroke functional assessments are required. I will discuss how behavioural assessment of models of other basal ganglia disorders, such as Parkinson's and Huntington's disease can be utilized to assess the MCAO model of stroke. This will included a discussion of the pit falls of the functional tests, and how some of these can be overcome. We assessed 14 different behavioural tests in the rat filament model to establish which provides the most robust and reliable method for assessing long term functional impairments in the model. In the majority of commonly used tests deficits are not maintained over the 2 months following stroke, rendering them unsuitable for assessments of therapeutics. However, a number of tests are robust and therefore suitable for assessing treatments over the long term; these included skilled reaching behaviour, assessment of response to whisker stimulation and lateralised stepping. Using data from stroke and examples from other disease, I will also talk about how these tests can inform us about the disease process and treatment strategies, and how we can develop more reliable and relevant tests of function.

203
BRAIN-0093
Symposium

Early Career Symposium

FXII INHIBITION PROTECTS FROM EXPERIMENTAL BRAIN TRAUMA BY REDUCING THROMBUS FORMATION

S. Hopp[1], C. Albert-Weissenberger[1], M.W. Nolte[2], S. Mencl[1], A.L. Sirén[3], C. Kleinschnitz[1]
[1]Neurology, University Hospital Würzburg, Würzburg, Germany
[2]Pharmacology and Toxicology, CSL Behring GmbH, Marburg, Germany
[3]Neurosurgery, University Hospital Würzburg, Würzburg, Germany

Objective:

Traumatic brain injury (TBI) is a result of an outside force causing mechanical disruption of brain tissue. In addition, delayed pathogenic events occur, which collectively exacerbate the injury. Although TBI is a devastating neurological condition and a frequent cause of permanent disability in young adults, causal treatment options are lacking. Recent studies indicate that thrombus formation in the brain microvasculature is an important pathologic feature of TBI, probably contributing to the immediate decline in regional cerebral blood flow that can also affect remote brain areas. Thrombus formation may be triggered either by the tissue factor-driven extrinsic coagulation pathway or by the coagulation factor XII (FXII)-driven intrinsic coagulation pathway. We examined the pathophysiological role and drugability of FXII in different mouse models of brain trauma.

Methods:

Male C57Bl/6 wild-type mice (wt), FXII-deficient mice ($FXII^{-/-}$), and $FXII^{-/-}$ mice reconstituted with human FXII ($FXII^{-/-}$/hFXII) were subjected to cortical cryolesion or weight drop injury resulting in focal or diffuse TBI, respectively. Pharmacological inhibition of activated FXII (FXIIa) was achieved by intravenous application of 200mg/kg recombinant human albumin-fused Infestin-4 (rHA-Infestin-4; provided by CSL Behring GmbH, Marburg) 1 hour after trauma. Neurological recovery after brain trauma was assessed by the neurological severity score and lesion size was calculated by volumetry from brain slices stained with 2,3,5-triphenyltetrazolium chloride. The extent of microvascular thrombosis was quantified from H&E stained brain sections and Western Blot against the platelet surface marker glycoprotein Ib. Animal experiments were approved by legal state authorities (Government of Lower Franconia) and conducted in accordance with the recommendations of the European Convention for the Protection of Vertebrate Animals used for Experimentation.

Results:

Genetic deficiency of FXII was protective after focal TBI. Male $FXII^{-/-}$ mice subjected to cryolesion showed significantly reduced lesion volumes on day 1 when compared with wt mice or $FXII^{-/-}$/hFXII mice. This protective effect was preserved in female mice and at later stages of trauma (day 3). Reduced microthrombus formation in the brains of $FXII^{-/-}$ mice could be identified as underlying mechanisms. Similar

results could be observed in the weight drop model or following pharmacological inhibition of FXIIa with rHA-Infestin-4 1 hour after induction of TBI in both animal models. Importantly, blocking of FXII did not increase the risk of intracranial bleeding after TBI as assessed by serial magnetic resonance imaging (MRI).

Conclusion:

We here for the first time describe a prominent role of the intrinsic coagulation cascade during TBI. Blocking of FXII effectively reduced thrombotic processes in the injured brain and this was not accompanied by an increased bleeding risk. Hence, targeted interference with the intrinsic coagulation cascade might become an effective and safe strategy to treat TBI and other neurological disorders associated with increased cerebrovascular thrombosis.

204
BRAIN-0976
Symposium

Early Career Symposium

Elevated intracranial pressure following stroke: there's more to the story than cerebral oedema.

D.D. McLeod[1], L.A. Murtha[1], D.J. Beard[1], R.J. Hood[1], C.L. Logan[1], D. Pepperall[1], N.J. Spratt[1]
[1]School of Biomedical Sciences & Pharmacy, The University of Newcastle and Hunter Medical Research Institute, Callaghan, Australia

Background: It has largely been assumed that cerebral oedema is the primary cause of intracranial pressure (ICP) elevation after large hemispheric stroke, and that more oedema equates to higher ICP. Our studies suggest that ICP elevation occurs after both small and large ischaemic infarcts and that cerebral oedema may not be the sole cause. Recent advanced imaging studies in stroke patients indicate that delayed infarct expansion most commonly occurs around 24 h post-stroke[1], and is associated with 'failure' of collateral blood flow. In a series of studies we investigated potential mechanisms of ICP elevation after ischaemic stroke, and its potential role in late infarct expansion.

Methods: Experiments were conducted in three different strains of adult male rats under isoflurane anaesthesia. The intraluminal middle cerebral artery occlusion (MCAo) model was modified to produce either small or large cerebral infarcts by maintaining patency or occluding an important internal collateral artery[2]. Monitored physiological parameters included ICP, arterial pressure, rectal temperature and arterial blood gases. Cerebral oedema was quantified with wet-weight-dry-weight, or via histology and/or MRI. The effects of whole body hypothermia on ICP, cerebral oedema and infarct volume after stroke was performed in a series of experiments[3,4]. To investigate the role of cerebrospinal fluid (CSF) in ICP elevation after stroke, a CSF transfusion assay was developed. The effect of elevated ICP on collateral blood flow to the ischaemic penumbra was assessed with a novel method of leptomeningeal collateral blood flow quantification[5].

Results: In five separate studies (three rat strains), there was dramatic and transient ICP elevation at 24 h after both small and large ischaemic infarcts in rats; mean ΔICP (24 h peak – baseline) was 32.1 mmHg[3, 4]. A short-duration (2.5 h) of moderate (33°C)[3,4] or mild (35°C)[4] whole body hypothermia prevented ICP elevation at 24 h after MCAo. Importantly, there was no correlation between ΔICP and oedema or infarct volume[4]. CSF collected from rats 6 h after MCAo and transfused into the cerebral ventricles of naïve rats resulted in significant ICP elevation, 24 h after the MCAo induction time-point. Artificial ICP elevation significantly reduced collateral blood flow to the ischaemic penumbra after MCAo[5].

Conclusions: The data indicates that ICP elevation at approximately 24 h after ischaemic stroke is oedema-independent and is triggered by molecules found within the CSF after stroke. ICP elevation is a potential cause for collateral failure and delayed infarct expansion after ischaemic stroke.

References:

1. Coutts S et al., *Stroke* 2012; 43, 1013-1017.
2. McLeod DD et al., *PLoS One* 2013; **8**(9): e75779.
3. Murtha LA et al. *Int J Stroke* 2014; **9**: 553–559.
4. Murtha LA et al. *J Cereb Blood Flow Metab* 2014; doi: 10.1038/jcbfm.2014.230.

5. Beard DJ et al. *J Cereb Blood Flow Metab* 2015; doi: 10.1038/jcbfm.2015.2.

205
BRAIN-0009
Symposium

Early Career Symposium

The role of Src family kinases in traumatic and hemorrhagic brain injury

D. Liu[1], K. Van[2], H. Hull[1], B. Ander[1], J. Lin[2], G. Jickling[1], X. Zhan[1], C. Dykstra-Aiello[1], B. Stamova[1], B. Lyeth[2], F. Sharp[1]
[1]Neurology, University of California at Davis, Sacramento, USA
[2]Neurosurgery, University of California at Davis, Sacramento, USA

Objectives: Traumatic brain injury (TBI) is often associated with intracranial hemorrhage[1-3]. An initial tissue response to bleeding involves activation of the coagulation cascade, where thrombin is released and blood clot formation limits bleeding. Apart from serving as a clotting factor[1,2], thrombin mediates brain injury by acting on endogenous receptors (protease-activated receptors, PARs)[4]. However, PAR inhibitors may not be good treatment targets since they could affect the clotting function of thrombin and cause catastrophic brain hemorrhage post-TBI[5]. This led us to consider an approach that would target downstream molecules of PAR, such as Src family kinases (SFKs) that are not involved in hemostasis process[6]. Since inhibiting SFKs is able to block toxic signaling of PARs, we hypothesized that SFK inhibitors can attenuate brain injury following TBI.

Methods: Using moderate lateral fluid percussion (LFP)-induced TBI model in rats, we examine the time course of thrombin (indicator for blood clotting), oxyhemoglobin (indicator for blood lysis) in cerebrospinal fluid (CSF) and SFKs kinase activity in ipsilateral hippocampus after TBI. Based on the time courses of thrombin concentration and SFKs acidity post-TBI, we design acute administration of SFK inhibitors (PP2, or nanoparticle-siRNA to Fyn and c-Src) to test whether inhibiting SFKs decreases damage to hippocampal neurons and attenuates cognitive deficits following TBI.

Results: The data shows that thrombin and oxyhemoglobin in CSF and Fyn (one SFKs family member) activity in ipsilateral hippocampus are increased significantly at 0.5 hr and decrease gradually post-TBI. Moreover, a non-specific SFK inhibitor PP2 protects hippocampal neurons and improves spatial memory cognitive function post-TBI. In addition, nanoparticle based siRNA to SFK family members Fyn and c-Src *in vivo*, but not either one alone, produces similar protection as PP2 does.

Conclusions: The approach to inhibit SFK subtypes (e.g. c-Src, Fyn) using SFK inhibitors or the in vivo nanoparticle-siRNA method, can be readily translated to humans, since SFK antagonists have been tested in clinical trials for cancer therapy, and in vivo nanoparticle delivery methods are FDA approved for human use.

Acknowledgements: This study was supported by supported by AHA Beginning Grant-in-Aid (12BGIA12060381 (DZL) and NIH grant R01NS066845 (FRS).

References:

1. Gaetz, M. The neurophysiology of brain injury. *Clin Neurophysiol* **115**, 4-18 (2004).

2. Keep, R. F., Hua, Y. & Xi, G. Intracerebral haemorrhage: mechanisms of injury and therapeutic targets. *Lancet Neurol* **11**, 720-731 (2012).

3. Liu, D. *et al.* Inhibition of Src Family Kinases Protects Hippocampal Neurons and Improves Cognitive Function after Traumatic Brain Injury. *Journal of neurotrauma* **31**, 1268-1276, (2014).

4. Vu, T. K., Hung, D. T., Wheaton, V. I. & Coughlin, S. R. Molecular cloning of a functional thrombin receptor reveals a novel proteolytic mechanism of receptor activation. *Cell* **64**, 1057-1068 (1991).

5. Garber, S. T., Sivakumar, W. & Schmidt, R. H. Neurosurgical complications of direct thrombin inhibitors--catastrophic hemorrhage after mild traumatic brain injury in a patient receiving dabigatran. *J Neurosurg* **116**, 1093-1096 (2012).

6. Thomas, S. M. & Brugge, J. S. Cellular functions regulated by Src family kinases. *Annu Rev Cell Dev Biol* **13**, 513-609 (1997).

206
BRAIN-0954
Symposium

Early Career Symposium

Investigating capillary dynamics with aging

F. Lesage[1]
[1]*Génie Biomédical, École Polytechnique Montréal, Montreal, Canada*

Using various optical techniques: intrinsic imaging, optical coherence tomography and two photon microscopy, we investigate changes in the brain functional response with age and its relation to microvasculature. We identify brain vessel pulsatility as a contributor to flow mediated dilation and investigate the consequences of these changes on brain oxygenation. Finally, a model of the BOLD response is built from first principles to translate these results to the macroscopic world.

209
BRAIN-0164
Brain Oral Communication

Oral session: Cerebrovascular Regulation

MULTIMODAL PERCEPTION OF SUGAR MODULATES CEREBRAL BLOOD FLOW IN THE HEDONIC CIRCUIT DIFFERENTLY THAN INDEPENDENT ORAL OR INTESTINAL PERCEPTION

D. VAL-LAILLET[1], *C. CLOUARD*[1], *M.C. MEUNIER-SALAUN*[2], *P. MEURICE*[1], *C.H. MALBERT*[3]
[1]*UR1341 ADNC, INRA, St Gilles, France*
[2]*UMR1348 PEGASE, INRA, St Gilles, France*
[3]*US1395 Ani-Scans, INRA, St Gilles, France*

Objectives

The characterization of brain networks contributing to the processing of oral and/or intestinal sugar signals in a relevant animal model might help to understand the neural mechanisms related to the control of food intake in humans and suggest potential causes for impaired eating behaviours. The aims of this study were 1) to investigate whether the combination or dissociation between oral and post-oral sucrose perception influence the brain activity in reward-related brain structures, and 2) to determine whether duodenal infusion of sucrose in the absence of sweet taste, and conversely, induce specific activity in the brain reward circuit.

Methods

Seven growing pigs underwent four brain single photon emission computed tomography to assess cerebral blood flow (CBF) modifications further to oral stimulation with neutral or sucrose artificial saliva paired with saline or sucrose infusion in the duodenum. For each brain imaging session, animals were anaesthetised after an overnight fasting and the injection of ^{99}Tc-HMPAO (740 MBq) was synchronized with the oral stimulation, 50 min after the duodenal infusion (timeline corresponding to the peak of glycemia after sucrose duodenal infusion). CBF changes were investigated *via* SVC analyses using SPM8 in several regions of interest including cortical and subcortical areas of the hedonic/limbic circuit. An uncorrected value of P=0.01 was set as threshold for the clusters' peak and clusters comprising a minimum of 25 contiguous voxels were considered significant.

Results

Oral and/or duodenal sucrose sensing induced differential CBF changes in brain regions known to be involved in memory, reward processes and hedonic (i.e. pleasure) evaluation of sensory stimuli, including the dorsal striatum, prefrontal cortex, cingulate cortex, insular cortex, hippocampus, and parahippocampus cortex. Sucrose duodenal infusion only and combined sucrose stimulation induced similar activity patterns in the putamen, ventral anterior cingulate cortex and hippocampus. Some brain deactivations in the prefrontal and insular cortices were only detected in the presence of oral sucrose stimulation. Finally, activation of the right insular cortex was only induced by combined oral and duodenal sucrose stimulation, while specific activity patterns were detected in the hippocampus and

parahippocampal cortex with oral sucrose dissociated from caloric load.

Conclusions

We demonstrated that oral, duodenal and the bimodal perception of sucrose induced different patterns of brain metabolism in structures involved in memory, reward processes and hedonic evaluation of sensory stimuli. Using controlled conditions in a pertinent animal model for human nutrition and nutrient sensing, we managed to demonstrate that some CBF changes are specific to oral or duodenal sucrose sensing, and that bimodal sucrose stimulation can even have a synergetic effect in some brain areas. We identified brain areas that are probably involved in the congruence between the sweet oral perception and internal state. All these results have important implications for discussions related to caloric *vs*. non-caloric sweeteners consumption and impact of sugars on the brain hedonic circuits and motivational processes.

References

Clouard C, Meunier-Salaün MC, Meurice P, Malbert CH, Val-Laillet D 2014. Combined compared to dissociated oral and intestinal sucrose stimuli induce different brain hedonic processes. *Frontiers in Psychology*, 5:Article 861.

210
BRAIN-0315
Brain Oral Communication

Oral session: Cerebrovascular Regulation

OBSTRUCTIVE SLEEP APNEA ATTENUATES THE CEREBROVASCULAR CIRCADIAN CLOCK AND RHYTHMS IN VASCULAR FUNCTION

D. Durgan[1], *E. Lloyd*[1], *R. Bryan Jr.*[1]
[1]*Anesthesiology, Baylor College of Medicine, Houston, USA*

Objectives: Molecular circadian clock components oscillate in cells of the cardiovascular system. These clocks allow the cell to respond to a stimulus with proper timing and magnitude. Alterations in these rhythms are associated with and/or contribute to various cardiovascular diseases. We tested the hypothesis that obstructive sleep apnea (OSA) disrupts the normal rhythms of the cerebrovascular circadian clock and vascular function.

Methods: OSA was produced in rats by remotely inflating a balloon placed in the trachea. Unanesthetized rats underwent 60 apneas/ hour for 8 hours/ day (sleep phase). Following 2 weeks of sham or OSA, cerebral arteries were isolated at; the transition from dark-to-light (i.e., zeitgeber time (ZT) 0), 6, 12, or 18, for mRNA and functional analysis.

Results: We identified significant diurnal rhythms in mRNA expression levels of the circadian clock genes period 1 (*per1*), period 2 (*per2*), and the clock controlled gene albumin d-site binding protein (*dbp*) in cerebral vessels of sham rats, which were significantly attenuated following OSA ($p<0.05$ for each). Perfused posterior cerebral arteries (PCA) from sham rats exhibited a significant diurnal rhythm in the sensitivity to ATP induced vasodilation, that was most responsive at the beginning of the awake phase ($p<0.05$). This rhythm was abolished in OSA arteries, which exhibited diminished ATP sensitivity independent of the time-of-day (see Figure; $p<0.05$). In the presence of L-NAME the diurnal rhythm in ATP sensitivity was abolished in sham vessels and not different from OSA.

Conclusions: Cerebral arteries possess a functional circadian clock and exhibit a diurnal rhythm in nitric oxide induced vasodilation. In our model of OSA, 2 weeks of apnea significantly attenuates the diurnal rhythms of the cerebrovascular circadian clock and vascular function.

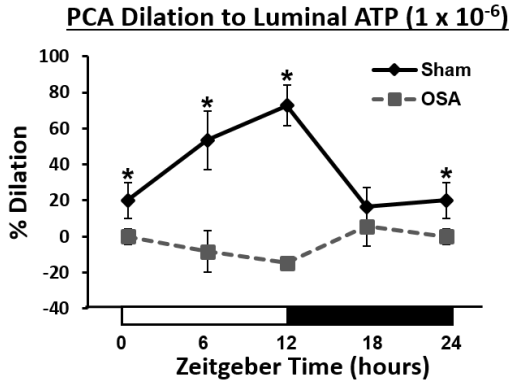

211
BRAIN-0329
Brain Oral Communication

Oral session: Cerebrovascular Regulation

MODELLING THE FLOW IN CEREBRAL CAPILLARY NETWORKS WITH DISCRETE RBC TRACKING

F. Schmid[1], *P. Jenny*[1], *B. Weber*[2]
[1]*Institute of Fluid Dynamics, Swiss Federal Institute of Technology, Zurich, Switzerland*
[2]*Institute of Pharmacology and Toxicology, University of Zurich, Zurich, Switzerland*

A profound understanding of the distribution of red blood cells (RBCs) in the cerebral microvasculature is crucial to analyze oxygen delivery in the microcirculation and the capabilities of the vasculature to locally up-regulate the oxygen supply. It is well established that neuronal activation leads to dilations of penetrating arterioles. However, the regulation mechanisms at smaller scales are still fairly unknown. Recently, evidence was found that pericytes can alter the diameter of capillaries [1]. Our work focuses on investigating the role of capillary dilation in microvascular networks.

We developed a numerical model, which simulates blood flow in the microcirculation with discrete RBC tracking [2]. It accounts for three well-known hemodynamic effects: Fahraeus-, Fahraeus-Lindqvist and phase-separation effect [3]. Furthermore, transient effects are captured and due to discrete RBC tracking we are able to comment on phenomena such as transit time heterogeneity.

First we studied the impact of RBCs on flow in artificial capillary networks. We showed that the interaction of RBCs and flow promotes well-balanced divergent bifurcations (bulk flow velocities in the outflow branches are equalized). Furthermore, our results suggest that at well-balanced bifurcations capillary dilation leads to an accumulation of RBCs in the dilated branch without significantly influencing the flow rates [4]. For example, in a hexagonal network the dilation of a 40 µm long segment by 15% increases the number of RBCs on average by 32%. Hence, we postulate that capillary dilation is an effective mechanism to locally alter the distribution of RBCs.

To confirm our results in realistic cerebral networks, appropriate boundary conditions need to be defined. This constitutes a major challenge for flow simulations in realistic networks. We present a new approach to define boundary conditions: the realistic network is implanted in a large artificial vascular bed. A Kirchhoff-simulation (without RBC tracking) is performed to obtain boundary conditions for the simulations with discrete RBC tracking (Figure 1). We validated the method by comparing the resulting boundary conditions computed from different artificial vascular networks and different locations for the realistic implant.

We could confirm that the presence of RBCs increases the number of well-balanced divergent capillary bifurcations. Whereas in networks without RBCs only 23% of divergent capillary bifurcations are well-balanced, for networks with an inflow tube hematocrit of 0.2 (0.3) 31% (34%) are well-balanced. As shown for the artificial network, capillary dilation leads to an increased number of RBCs in the dilated branch for all investigated cases. However, the changes in flow rate are more complex in the realistic networks and need to be investigated in more detail. All in all, this supports our hypothesis that capillary dilation may play an important role in neurovascular-coupling on the small scale.

Currently, we are working on analyzing capillary transit time heterogeneity and on deriving mechanisms to explain the homogenization of hematocrit during activation.

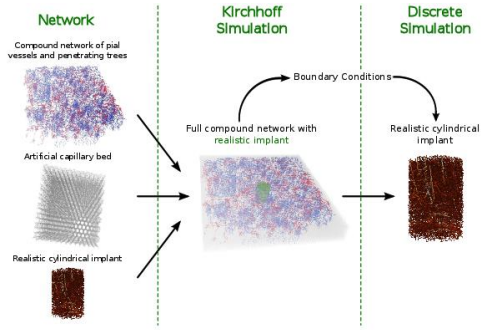

Figure 1 Definition of boundary conditions.

[1] Hall et al., Nature, 508:55-60, 2014
[2] Obrist et al., Phil.Trans.R.Soc.A, 368(1921):2897-2918, 2010
[3] Pries et al., Am.J.Physiol.Heart.Circ.Physiol, 289(6):H2657 – H2664, 2005.
[4] Schmid et al., Am.J.Physiol.Heart.Circ.Physiol, DOI:10.1152/ajpheart.00335.2014, 2015

212
BRAIN-0690
Brain Oral Communication

Oral session: Cerebrovascular Regulation

TEMPORAL DIAMETRIC CHANGE OF INTRACORTICAL PENETRATING ARTERIES IN RESPONSE TO CORTICAL SPREADING DEPRESSION OBSERVED WITH TWO-PHOTON MICROSCOPY IN ANESTHETIZED MICE

M. Unekawa[1], Y. Tomita[1], H. Toriumi[1], T. Osada[1], K. Masamoto[2], I. Kannno[3], N. Suzuki[1]
[1]Neurology, Keio University School of Medicine, Tokyo, Japan
[2]Brain Science Inspired Life Support Research Center, University of Electro-Communications, Chofu, Japan
[3]Molecular Imaging Center, National Institute of Radiological Sciences, Chiba, Japan

[Objective] Cortical spreading depression (CSD) is a parenchymally propagating mass depolarization of neuronal and glial cells, followed by sustained suppression of spontaneous neuronal activity. CSD induces at least three vasomotor elements, vasoconstrictive tone, profound hyperemia and long-lasting hypoemia(1). We observed marked constriction, followed by dilation and subsequent mild constriction in pial arteries, and the vasoreactivity was diminished with subsequent CSD passage in spite of the constant response of marked hyperperfusion(2). To further understand the microcirculatory responses associated with CSD, we examined the temporal diametric changes and its relationship with baseline diameter of intracortical penetrating arteries associated with KCl-induced CSD in mice.

[Methods] Male Tie2-green fluorescent protein transgenic mice, in which fluorescent vascular endothelial cells can be specifically identified, were used (n=11). Under urethane-anesthesia and artificial ventilation, intracortical images were obtained with a two-photon microscope through a cranial window made on the parieto-temporal cortex. After acquisition of volume images up to 350 μm from the cortical surface with a z-step size of 5 μm, a region of interest was selected to follow a single penetrating artery. Sequential images at three depths (0, 150, 300 μm) were acquired every 6 sec with continuous recording of DC potential during passage of subsequent CSD induced by application of KCl. Vessel diameter was measured with Image Pro®. Regional cerebral blood flow (rCBF) was measured with laser Doppler flowmetry during subsequent CSD.

[Results] Passage of CSD could be identified by a rapid fall of intracortical background intensity of the images. First CSD elicited rapid and marked constriction throughout the arteries (mean of maximum response; 0 μm, -21.1±24.3%; 150 μm, -22.2±19.9%; 300 μm, -14.7±13.8%) with subsequent dilation (0 μm, 30.5±15.8%; 150 μm, 14.4±16.4%; 300 μm, 8.3±12.5%) (Figure Aa). Second or later CSD elicited smaller or no constriction followed by marked dilation at any depth (23.7 to 41.8%) (Figure Ab). Slight dilation preceded the transient constriction throughout the arteries, suggesting that transient vasoconstriction might counteract lasting vasodilation. Vasodilation and the decrease of intracortical background intensity temporally corresponded to the change of rCBF and the DC potential deflection, respectively (Figure B), suggesting that dilation of penetrating arteries may provoke rCBF increase, while the decrease of background intensity may be related to parenchymal cellular activity. Furthermore, first CSD-induced initial constriction and subsequent dilation of the entrance of the penetrating artery were well correlated with the basal diameter (r=0.581 and r=-0.558, respectively). Second or later CSD-induced dilation was also well correlated with the basal diameter throughout the arteries (r=-0.538 to -0.867). This correlation indicates that smaller arteries showed higher vasoreactivity.

[Conclusion] These results indicate that CSD-induced rCBF changes mainly reflect changes of the diameter of intracortical arteries, and the effect seems to be higher in smaller arteries.

[References] (1) Ayata, C. Stroke 2013:44:S87-89. (2) Unekawa, M., *et. al.*, J Cereb Blood Flow Metab, in press (doi:10.1038/jcbfm.2014.250).

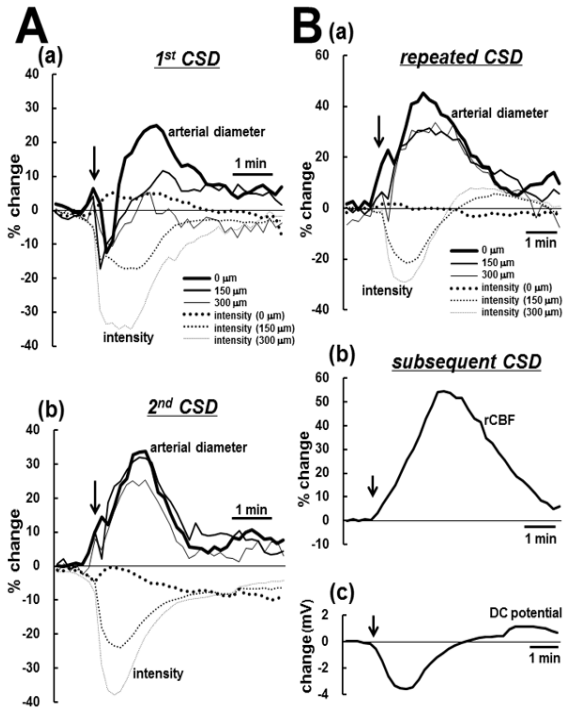

Figure. (A) Temporal average of diameter of penetrating artery and background intensity associated with the passage of first (a) and second CSD (b). (B) Temporal comparison of changes of diameter of penetrating artery (a) with rCBF (b) and DC potential (c) recorded during subsequent CSD. Arrows indicate the times at which intracortical background intensity, rCBF and DC potential began to change.

213
BRAIN-0843
Brain Oral Communication

Oral session: Cerebrovascular Regulation

EFFECT OF ELECTRICAL FOREPAW STIMULATION ON CAPILLARY TRANSIT TIME HEREOGENEITY

E. Gutierrez[1], P.M. Rassmussen[1], C. Cai[1], K. Mouridsen[1], S.N. Jespersen[1], I.K. Mikkelsen[1], H. Angleys[1], N.K. Iversen[1], J. Lee[2], S. Sakadzic[2], L. Østergaard[1]
[1]CFIN, Aarhus University Hospital, Aarhus C, Denmark
[2]Optics Division,
Martinos Center for Biomedical Imaging MGH /Harvard Medical School, Charlestown, USA

Introduction:

Reduction of capillary transit time heterogeneity (CTH) was recently shown to counteract the inherent reduction in oxygen extraction efficacy as CBF increases.[1] Indeed, it may be an intrinsic property of passive microvascular networks that CTH falls in proportion to the mean capillary transit time (MTT) during functional hyperemia[2]. In this study we adapted a method for CTH estimation[3] for use with bolus tracking by two-photon microscopy (TPM)[4] to quantify changes in plasma MTT and CTH during forepaw stimulation in mice.

Methods:

Mice were anesthetized with Isofluorane and femoral catheters were placed to monitor blood gases and for bolus injection of intravascular dye (30 µl, Texas-Red dextran). Mice were mechanically ventilated and TPM of the somatosensory cortex through a cranial window. Feeding and draining vessels were then defined based on a dye bolus, and line-scan positions defined. Line-scans during additional dye injections were acquired in each vessel during rest and forepaw stimulation (6 trials per subject). Arteries and veins, as well as their closest arteriole and venule, were identified by vessel segmentation. For these corresponding inputs and outputs, we estimated the distribution of capillary transit times by fitting to a gamma distribution [2]. MTT and CTH were then determined as the mean and standard deviation of the distribution. Red blood cell velocities (RBCv) and flux (RBCf) were measured to confirm the area of neuronal activation. We also analyzed the relative dispersion, CTH:MTT (CoV), to examine whether transit time homogenization occurred beyond that expected as a result of hyperemia.This study were approved by the Danish Animal Experiments Inspectorate (Dyreforsøgstilsynet), and handling of the animals was performed following the guidelines for ethical animal treatment.

Results:

1. Neuronal activation produced an increase on RBCv and RBCf of 29.5 % ± 8.3 ($p<0.001$) and 15.9% ± 1.7% ($p<0.001$) on 295 capillaries in 8 mice.

2. Electrical forepaw stimulation produced a 16.0% ± 1.6% (s.e) reduction of MTT ($p<0.001$) and 24.6 % ± 4.0% reduction of CTH ($p<0.001$) throughout all segments. Thus, CoV fell by 14.3% ± 3.5% ($p<0.001$).

3. From artery to vein, MTT and CTH showed significant reductions of 15.6% ± 2.7% (p=0.001) and 15.4 ± 7.8% (p<0.001), respectively. However, no CoV changes were observed. From arteriole to venule, MTT fell by 13.7% ± 3.7% (p=0.012) and CTH by 38.4% ± 3.6% (p<0.001). This corresponded to a significant reduction in CoV (20.3% ± 5.8%, p=0.021).

Conclusions:

MTT and CTH decreased by the electrical forepaw stimulus, in agreement with earlier observations[5]. When combined with the Jespersen-Østegaard model, our results suggest that CTH indeed co-vary with MTT to maintain efficient oxygen extraction in the brain. The decrease on CoV by neuronal activation suggests homogenization beyond that expected by a passive microvascular network. Our results suggest that active reduction of CTH occurs between arterioles to venules, consistent with active pericyte dilation[6].

214
BRAIN-0871
Brain Oral Communication

Oral session: Cerebrovascular Regulation

Investigating the Spatiotemporal Characteristics of the BOLD and the Non-BOLD Response Across Cortical Layers in Awake Marmosets

C. Yen[1], *D. Papoti*[1], *A. Silva*[1]
[1]*NINDS, National Institutes of Health, Bethesda, USA*

Blood oxygenation level dependent (BOLD) functional magnetic resonance imaging (fMRI) has a strong prognostic potential in ischemic stroke due to its non-invasive nature, high spatial resolution in differentiating cortical layers, and high sensitivity to changes in hemodynamics. However, reports of the spatiotemporal characteristics of the cortical fMRI response are non-conclusive. For instance, there is no consensus on onset time (OT) values of the BOLD fMRI response across each cortical layer. One source of contamination to BOLD fMRI is the inflow effect, which may contribute differently at the pial surface versus parenchyma due to the different orientation of tangential pial vessels and penetrating cortical vessels.
To address these concerns, we adopted a dual-echo sequence to separate the fMRI signal into pure-BOLD (deoxyhemoglobin-related) component and non-BOLD component, including inflow effect and partial volume effect from the cerebrospinal fluid, and used it to map laminar BOLD responses with high spatiotemporal resolution in awake marmosets, a small New World non-human primate model. Four adult male marmosets were acclimated to head restraint by custom-built helmets in the sphinx position (as shown in figure 1) inside a horizontal 7T MRI spectrometer. High-resolution BOLD functional images were obtained every 200ms using a dual-echo EPI sequence from a single coronal slice. The median nerve was stimulated by pairs of electrode pads placed across both wrists. The stimulus paradigm was 4s of pulse train with 50Hz of pulse frequency, 0.4ms of pulse duration and 1.5mA of stimulus intensity. AFNI and Matlab were used to process the data.

In one representative animal shown in figure 2, robust BOLD responses were bilaterally detected in primary somatosensory area (S1), secondary somatosensory area and caudate nucleus, in support of previous work [Liu et al Neuroimage 2013]. In S1, Laminar OT values were determined to be 1.4s in layers 1 to 3, 1.2s in layer 4 and 1.6s in layers 5 to 6, which was consistent with the order previously reported in rodents [Silva et al PNAA 2002]. Robust pure-BOLD responses were observed across all layers except layers 1 and 2, which showed an insignificant pure-BOLD response but a strong and delayed non-BOLD response.

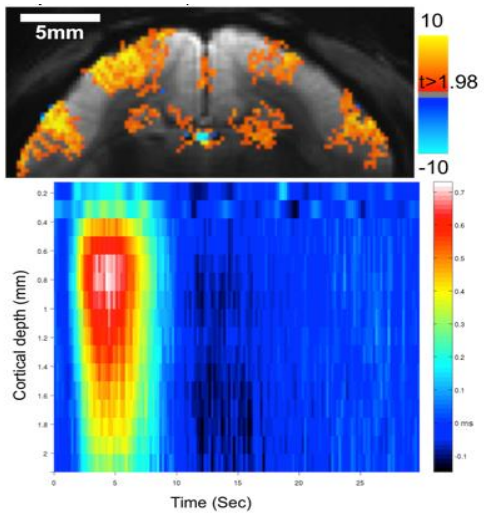

We have demonstrated the feasibility of measuring the dynamics of pure-BOLD and non-BOLD changes across the cortical layers of awake marmosets. A significant contribution of the non-BOLD component was found on the superficial layers, which may be attributed to the inflow effect from pial vessels running perpendicular to the imaging plane. Therefore, caution should be exercised when measuring the laminar onset time of BOLD fMRI.

217
BRAIN-0783
BrainPET

BrainPET Oral Session: Psychiatric and Other Diseases

EFFECT OF MODAFINIL ON THE DOPAMINE TRANSPORTER AND ITS CLINICAL EFFECTIVENESS IN COCAINE DEPENDENT PATIENTS: A PET STUDY

M. Dubol[1], E. Artiges[1], C. Leroy[2], C. Trichard[1], A. Mabondo[1], C. Marill[3], A. Dubois[4], N. Bordas[1], R. Maroy[5], F. Dollé[2], C. Comtat[2], P. Gervais[2], M. Reynaud[3], J.L. Martinot[1], L. Karila[3]
[1]UMR 1000 Research Unit "Neuroimaging & Psychiatry", INSERM Paris Sud University Paris Descartes University, Orsay, France
[2]Laboratoire Imagerie Moléculaire In Vivo (IMIV), INSERM CEA CNRS Paris Sud University, Orsay, France
[3]Addictology Department, Paul Brousse Hospital AP-HP, Villejuif, France
[4]UMR 8165 Laboratoire Imagerie et Modélisation en Neurobiologie et Cancérologie, CNRS Paris Sud University Paris Diderot University, Orsay, France
[5]Service Hospitalier Frédéric Joliot, CEA I2BM, Orsay, France

Although Modafinil has shown promise in the treatment of cocaine dependence, its mechanism of action remains to be elucidated. Recently, PET studies confirmed that it produces a significant level of dopamine transporter (DAT) blockade in healthy humans. Cocaine acts as a dopamine reuptake inhibitor and its action on the DAT is usually considered critical for its psychoactive effects and the establishment of an addiction. Thus, the potential therapeutic effect of modafinil in cocaine users could be mediated by its pharmacological mechanism. So far, the DAT blockade produced by modafinil has never been directly studied in cocaine-dependent patients. The main aims of our study were to evaluate the level of the DAT occupancy produced by therapeutic dosage of modafinil in cocaine users and to examine if this blockade was correlated with the clinical outcome of the patients.
Thirty treatment seeking cocaine-dependent patients recently abstinent were hospitalized for seventeen days within the framework of a three-month longitudinal randomized modafinil vs placebo controlled study. Cerebral DAT availability was investigated using high resolution PET imaging (HRRT) and a specific DAT radioligand, [11C]-PE2I, before (PET1) and after (PET2) two weeks of treatment. Neuropsychological tests and clinical measures as craving, depression rates and urinary cocaine amount were carried out during and after hospitalization. Voxel-wise analyses were performed using Statistical Parametric Mapping (SPM8).
Analysis of the [11C]-PE2I binding potential indicated a significant interaction between time and group factors. Modafinil-treated patients showed a significant decrease of the [11C]-PE2I binding after two weeks of treatment in regions that are known to have high DAT density levels whereas no significant difference was found in the placebo-treated group. Additionally, a positive correlation has been found between a risk-taking behavior and DAT availability of these cocaine-dependent patients. During hospitalization, a significant time effect showing an improvement in clinical outcomes was displayed for both modafinil and placebo groups. Nevertheless, the outpatients' follow-up displayed more therapeutic failures in the modafinil-treated patients than in the placebo-treated patients beyond hospitalization.
For the first time in cocaine outpatients, we confirm the high level of DAT occupancy by therapeutic dosage of modafinil, previously reported in healthy subjects. However, despite its pharmacological effect on DAT, modafinil did not improve the clinical outcome of the patients.
Acknowledgments: PHRC 2007 - French ministry of health; MILDT/INCa Inserm 2006
Dackis et al. A double-blind, placebo-controlled trial of modafinil for cocaine dependence. J Subst Abuse Treat. 2012; 43(3):303-12
Kim et al. In vivo activity of modafinil on dopamine

transporter measured with PET and [18F]FE-PE2I. Int J Neuropsychopharmacol. 2014; 17(5): 697-703
Volkow et al. Effects of Modafinil on Dopamine and Dopamine Transporters in the Male Human Brain: Clinical Implications. JAMA. 2009; 301(11): 1148-1154

218
BRAIN-0326
BrainPET

BrainPET Oral Session: Psychiatric and Other Diseases

SEASONAL VARIATION OF MONOAMINE OXIDASE A QUANTIFIED WITH [11C]HARMINE AND POPULATION-BASED INPUT FUNCTIONS

A. Hahn[1], D. Winkler[1], C. Vraka[2], L. Nics[2], C. Philippe[2], G.M. James[1], G. Gryglewski[1], M. Hienert[1], P. Baldinger[1], A. Kautzky[1], M. Spies[1], A. Komorowski[1], T. Vanicek[1], E. Winkler-Pjrek[1], T. Traub-Weidinger[2], W. Wadsak[2], M. Mitterhauser[2], M. Hacker[2], S. Kasper[1], R. Lanzenberger[1]
[1]Department of Psychiatry and Psychotherapy, Medical University of Vienna, Vienna, Austria
[2]Department of Biomedical Imaging and Image-guided Therapy Division of Nuclear Medicine, Medical University of Vienna, Vienna, Austria

OBJECTIVES

Monoamine oxidase A (MAO-A) is responsible for the degradation of various neurotransmitters, hence, it plays an important role in mood disorders [1]. However, potentially relevant seasonal variations, such as of the serotonin transporter [2], have not yet been evaluated. On the other hand, quantification of MAO-A requires an arterial input function (AIF) due to lack of a reference region. Therefore, the aims of this study were to investigate the seasonal variation of MAO-A and an alternative quantification with population-based input functions (PBIF).

METHODS

15 healthy subjects (35.4±10.3 years, 10 females) underwent a single 90min PET scan with [^{11}C]Harmine for PBIF evaluation. Another 12 subjects (partly overlapping, 35.7±10.7, 10 females) were scanned two times, once during the summer and once in early (November, n=6) or late winter season (February, n=6). Arterial blood sampling was done automatically for 10min and manually thereafter (5, 10, 20, 30, 45, 60, 80min). For AIFs, whole blood activity was corrected for plasma-to-whole blood ratio and radioactive metabolites [3]. To construct PBIFs, AIFs were normalized by injected dose/kg, shifted in time that maxima coincide and averaged with a leave-one-out procedure. PBIFs were scaled with the average of 10min and 60min samples as this showed highest correlation with AIF area under the curve (r=0.99). For the evaluation of seasonal effects, PBIFs were applied prospectively. Quantification of total volume of distribution (V_T) was carried out with the two-tissue compartment model (2TCM) with K1/k2 coupled across regions as well as the Logan plot [3] for 12 regions of interest (frontal, temporal, parietal, occipital, cingulate, insulary cortices, amygdala-hippocampus complex, thalamus, striatum, midbrain, cerebellar gray and white matter).
The study was approved by the ethics committee of the Medical University of Vienna, Austria, and all participants provided written informed consent.

RESULTS

Comparison between AIF and PBIF showed good agreement for Logan V_T (r=0.95, slope=0.86, intercept=1.95, Fig 1a), which was slightly reduced for 2TCM V_T (r=0.90, slope=0.85, intercept=2.17). Assessment of MAO-A seasonal variations with the Logan plot showed significant main effects of the factors summer/winter scan (F=86.5) and early/late winter (F=48.8) as well as an interaction between summer/winter scan * early/late winter across all regions (F=98.4, all p<0.001). The same result was observed when using PBIFs (summer/winter scan F=163.8, early/late winter F=58.0, summer/winter * early/late F=80.0, all p<0.001) and for the 2TCM independent of the input function (all p<0.001). Post-hoc evaluation revealed that MAO-A V_T increased throughout the year from late winter to summer and from summer to early winter (Fig 1b).

CONCLUSIONS

MAO-A of healthy individuals is subject to substantial changes throughout the year, which might have potential implications in mood disorders [1, 2]. Although some individual variability remains, PBIFs seem to be able to capture these seasonal changes,

hence, they may represent a promising alternative for quantification [4].

REFERENCES
[1] Meyer J. 2009. Arch Gen Psych 66:1304.
[2] Praschak-Rieder N. 2008. Arch Gen Psych 65:1072.
[3] Ginovart N. 2006. JCBFM 26:330.
[4] Zanotti-Fregonara P. 2014. Nucl Med Commun 35:1254.

DISCLOSURE
The study was supported by a grant from the Austrian Science Fund (FWF 24359) to D. Winkler.

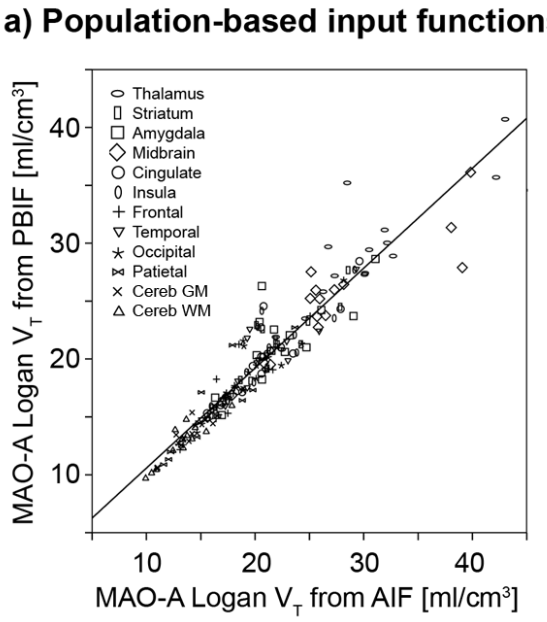

Fig 1a: Quantification of monoamine oxidase A (MAO-A) with [^{11}C]Harmine and population-based input functions (PBIF). Comparison between arterial (AIF) and population-based input functions showed good agreement for V_T when using the Logan plot (r=0.95).

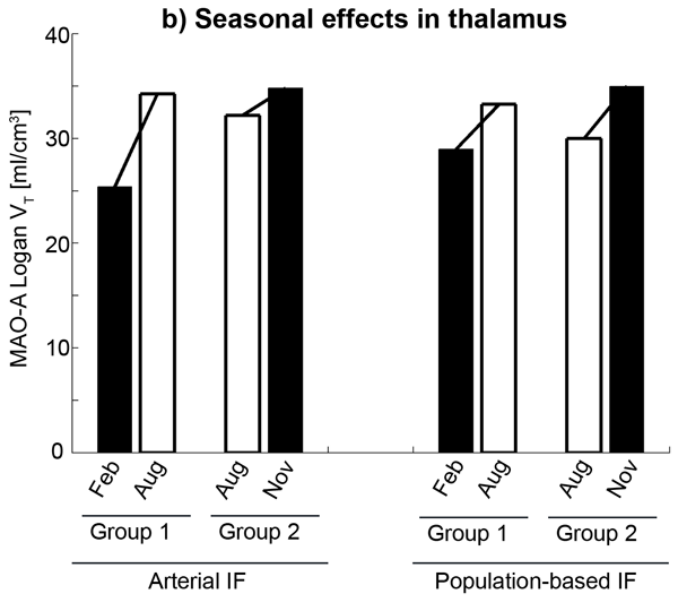

Fig 1b: Monoamine oxidase A (MAO-A) V_T increased from late winter to summer and further increased until early winter in the thalamus. The same pattern was observed for all other regions, independent of the input function (arterial or population-based) and model (two-tissue compartment model or Logan plot).

219
BRAIN-0699
BrainPET

BrainPET Oral Session: Psychiatric and Other Diseases

TREATMENT RESPONSE EVALUATION USING 18F-FET PET IN GLIOBLASTOMA PATIENTS AT FIRST RECURRENCE TREATED WITH A COMBINATION OF BEVACIZUMAB PLUS LOMUSTINE

N. Galldiks[1], V. Dunkl[1], G. Stoffels[2], C. Filss[2], C. Tscherpel[1], G. Ceccon[1], I. Law[3], M. Schmidt[4], G.R. Fink[1], N.J. Shah[2], K.J. Langen[2]
[1]Dept. of Neurology, University of Cologne, Cologne, Germany
[2]Inst. of Neurosciene and Medicine, Research Center Juelich, Juelich, Germany
[3]Dept. of Clinical Physiology Nuclear Medicine & PET, Rigshospitalet Copenhagen, Copenhagen, Denmark
[4]Dept. of Nuclear Medicine, University of Cologne, Cologne, Germany

Objectives:

The recent BELOB trial suggests that the combination of bevacizumab plus lomustine (BEV/LOM) is a valuable treatment option for glioblastoma patients at first recurrence (1).

The objective of this study was to prospectively compare MRI response assessment based on RANO criteria (2) with metabolic *O*-(2-^{18}F-fluoroethyl)-L-tyrosine (FET) PET response evaluation during BEV/LOM treatment in glioblastoma patients at first recurrence.

Methods:

Fifteen patients (median age, 55 years; range, 34-75 years) with a first recurrence of a primary glioblastoma (MGMT promoter not methylated in 87% , unmutated IDH status in 100%) after radiotherapy with concomitant and adjuvant temozolomide chemotherapy were treated with LOM 90 mg/m² every 6 weeks and BEV 10 mg/kg every 2 weeks. Additionally, 5 patients (33%) underwent surgery at time of first recurrence.

Dynamic FET PET and standard MRI scans were performed immediately before BEV/LOM treatment and after 10 weeks. FET PET metabolic tumor volumes (MTV), maximum and mean tumor/brain ratios (TBR_{max}, TBR_{mean}) as well as dynamic FET PET parameters such as time-to-peak (TTP) and curve pattern of FET uptake were obtained.

The predictive abilitiy of FET PET parameters and standard MRI on treatment response assessment was evaluated with regard to the disease-free survival (DFS), defined as time between first glioblastoma recurrence and clinical deterioration / palliative care.

Using receiver-operating characteristic (ROC) curve analyses, threshold values for FET PET parameter changes between baseline and follow-up imaging were obtained. For MRI changes, the RANO criteria for “Stable Disease”, “Partial Response” and “Complete Response” were considered as treatment response. Subsequently, Kaplan-Meier survival analyses were performed to assess their predictive power for DFS.

Results:

At the time of data evaluation, 12 of 15 patients (80%) expirienced clinical deterioration / needed palliative care (median DFS, 5 months; range, 2-13 months), while the remaining 3 patiens were disease-free (median follow-up, 7 months; range, 4-8 months).

Treatment response as assessed by standard MRI based on RANO criteria was not predictive for a significant longer DFS. Responders on MRI had a 1.2 times longer DFS (6 months vs. 5 months; $P = 0.17$) than nonresponders (8 patients vs. 7 patients, respectively).

In contrast, the FET PET parameters MTV (MTV decrease > 30%) and TBR_{max} (TBR_{max} decrease > 12%) were predictive for treatment response to BEV/LOM. Changes of MTV predicted best a longer DFS. Responders with a MTV decrease > 30% had a 1.6 times longer DFS (8 months vs. 5 months; $P = 0.008$) than nonresponders (7 patients vs. 8 patients, respectively).

However, both TBR_{mean} and dynamic FET PET parameters were not predictive for treatment response.

Conclusions:

FET PET appears to be helpful to identify treatment responders to BEV/LOM early after initiation of treatment.

References:

(1) Taal et al., 2014 *Lancet Oncol*

(2) Wen et al., 2010 *J Clin Oncol*

220
BRAIN-0817
BrainPET

BrainPET Oral Session: Psychiatric and Other Diseases

DECREASED DOPAMINE TRANSPORTER EXPRESSION IN MAJOR DEPRESSIVE DISORDER MEASURED WITH [11C]ALTROPANE PET

M.D. Normandin[1], D.W. Wooten[1], F. Goer[2], M. Beltzer[2], G. Vitaliano[3], B. Brennan[4], N. Brooks[2], D. Crowley[2], N.M. Alpert[1], G. El Fakhri[1], D.A. Pizzagalli[5]
[1]Center for Advanced Medical Imaging Sciences & De partment of Radiology, Massachusetts General Hospital & Harvard Medical S chool, Boston, USA
[2]Center for Depression Anxiety and Stress Research, McLean Hospital, Belmont, USA
[3]McLean Imaging Center, McLean Hospital & Harvard Medical School, Belmont, USA
[4]Biological Psychiatry Laboratory, McLean Hospital & Harvard Medical School, Belmont, USA
[5]Center for Depression Anxiety and Stress Research & McLean Imaging Center, McLean Hospital & Harvard Medical School, Belmont, USA

Introduction: Dopamine (DA) plays an important role in learning and motivation. These functions are impaired in major depressive disorder (MDD), highlighting possible DA abnormalities in MDD. The DA transporter (DAT) terminates DA signaling by reuptake of synaptic DA. Post-mortem studies have found decreased DAT in MDD, which has been interpreted as a compensatory down-regulation due to low DA levels; SPECT and PET studies have, however, been inconclusive. Therefore, the aim of this study was to compare striatal DAT expression in individuals with MDD and healthy controls (HCs) using the PET radiotracer [^{11}C]altropane which has high selectivity for DAT binding sites.

Methods: After slow bolus administration of [^{11}C]altropane, dynamic PET data were acquired for 60 min in 25 unmedicated adults with MDD and 23 HCs using an ECAT HR+ scanner. Reconstructed PET images were corrected for motion by inter-frame registration and rigidly aligned to the subject's structural magnetic resonance image, which was in turn warped to an anatomical template where standardized regions of interest were delineated. Regional estimates of binding potential relative to nondisplaceable uptake (BP_{ND}) were generated using MRTM2 for the caudate (CAU), putamen (PUT), nucleus accumbens (NAc) and ventral tegmental area (VTA) in each hemisphere. The reference input function was extracted from a region defined by the cerebellum excluding the vermis.

Results: A *Group* (controls, MDD) x *Region* (caudate, putamen, nucleus accumbens) x *Hemisphere* (left, right) multivariate analysis of covariance (covariate: age) indicated a significant *Group x Region* interaction ($p < 0.03$). MDD subjects had decreased DAT density evidenced by reduced [^{11}C]altropane BP_{ND} in the left and right putamen as compared to healthy controls ($p < 0.03$). Similarly, MDD subjects had lower BP_{ND} than healthy controls in the ventral tegmental area ($p < 0.02$). These effects were specific to the VTA and putamen, as similar analysis on the substantia nigra found no effects (all ps > 0.05). For both the putamen (r = -0.36) and VTA (r = -0.36), mean [^{11}C]altropane BP_{ND} was negatively correlated with the number of prior major depressive episodes ($p < 0.01$). Additionally, duration of current major depressive episode was negatively correlated with mean BP_{ND} in both the putamen (r= -0.41) and caudate (r = -0.43; $p < 0.05$).

Conclusion: Results indicate decreased DAT expression in the striatum and VTA in MDD. The specificity of this finding highlights the significance of mesolimbic over nigrostriatal pathways in the pathophysiology of MDD. Decreased DAT in MDD may be explained as a compensatory down-regulation due to chronic low DA signaling. This is further supported by the finding that [^{11}C]altropane BP_{ND} was negatively correlated with number of previous major depressive episodes,suggesting a progression of DAT down-regulation as episodes accumulate. These findings have promising implications for understanding the physiological processes underlying MDD as well as potential for interventions.

Research Support: R01MH068376, R01MH095809, T32EB013180

221
BRAIN-0077
BrainPET

BrainPET Oral Session: Psychiatric and Other Diseases

REDUCED INSULIN SENSITIVITY IS RELATED TO LESS ENDOGENOUS DOPAMINE AT D2/3 RECEPTORS IN THE VENTRAL STRIATUM OF HEALTHY NON-OBESE HUMANS

F. Caravaggio[1], C. Borlido[1], M. Hahn[1], Z. Feng[1], G. Fervaha[1], P. Gerretsen[1], S. Nakajima[1], E. Plitman[1], J. Chung[1], Y. Iwata[1], A. Wilson[1], G. Remington[1], A. Graff-Guerrero[1]
[1]Research Imaging Centre, Centre for Addiction and Mental Health, Toronto, Canada

REDUCED INSULIN SENSITIVITY IS RELATED TO LESS ENDOGENOUS DOPAMINE AT $D_{2/3}$ RECEPTORS IN THE VENTRAL STRIATUM OF HEALTHY NON-OBESE HUMANS

Objectives: Food addiction is a debated topic in neuroscience (Volkow et al., 2013; Ziauddeen et al., 2012). Evidence suggests diabetes is related to reduced basal dopamine (DA) levels in the nucleus accumbens, similar to persons with drug addiction (Murzi et al., 1996; O'Dell et al., 2014). It is unknown whether insulin sensitivity (IS) is related to endogenous DA levels in the ventral striatum (VS) of humans. We examined this using the agonist DA $D_{2/3}$ receptor ($D_{2/3}$R) radiotracer [^{11}C]-(+)-PHNO and an acute DA depletion challenge. In a separate sample of healthy persons, we examined whether DA depletion could alter IS.

Methods: IS was estimated for each subject from fasting plasma glucose and insulin using the Homeostasis Model Assessment II. Eleven healthy non-obese and non-diabetic persons (3 female) provided a baseline [^{11}C]-(+)-PHNO scan, 9 of which provided a scan under DA depletion, allowing estimates of endogenous DA at $D_{2/3}$R. DA depletion was achieved via alpha-methyl-para-tyrosine (64mg/kg, P.O.). In 25 healthy persons (9 female), fasting plasma and glucose was acquired before and after DA depletion.

Results: Endogenous DA at VS $D_{2/3}$R was positively correlated with IS ($r(7)=.84$, $p=.005$), and negatively correlated with insulin levels ($r(7)=-.85$, $p=.004$). Glucose levels were not correlated with endogenous DA at VS $D_{2/3}$R ($r(7)=-.49$, $p=.18$). Consistently, acute DA depletion in healthy persons significantly decreased IS ($t(24)=2.82$, $p=.01$), increased insulin levels ($t(24)=-2.62$, $p=.01$), and did not change glucose levels ($t(24)=-0.93$, $p=.36$).

Conclusions: In healthy individuals, diminished IS is related to less endogenous DA at $D_{2/3}$R in the VS. Moreover, acute DA depletion reduces IS. These findings may have important implications for neuropsychiatric populations with metabolic abnormalities.

References:

Murzi E, Contreras Q, Teneud L, Valecillos B*, et al.* (1996). Diabetes decreases limbic extracellular dopamine in rats. *Neurosci Lett,* **202**(3): 141-144.
O'Dell LE, Natividad LA, Pipkin JA, Roman F*, et al.* (2014). Enhanced nicotine self-administration and suppressed dopaminergic systems in a rat model of diabetes. *Addict Biol,* **19**(6): 1006-1019.
Volkow ND, Wang GJ, Tomasi D, Baler RD (2013). The addictive dimensionality of obesity. *Biol Psychiatry,* **73**(9): 811-818.
Ziauddeen H, Farooqi IS, Fletcher PC (2012). Obesity and the brain: how convincing is the addiction model? *Nat Rev Neurosci,* **13**(4): 279-286.

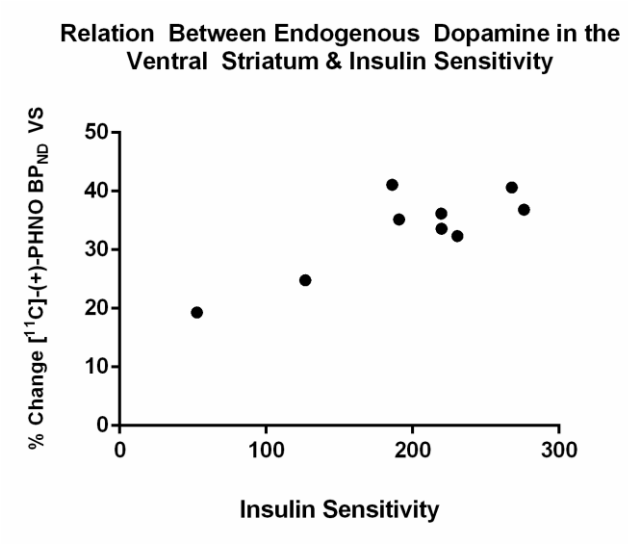

222
BRAIN-0215
BrainPET

BrainPET Oral Session: Psychiatric and Other Diseases

KINETIC ANALYSES OF 11C-PIB WITH 3 COMPARTMENTAL MODEL IN PATIENTS WITH SYMPTOMATIC SMALL VESSEL DISEASE: PET STUDIES

T. Hashimoto[1], C. Yokota[1], K. Koshino[2], R. Shimomura[1], T. Uehara[1], N. Morita[3], N. Funatsu[1], T. Hino[1], J. Nakagawara[4], K. Minematsu[1], H. Iida[2], K. Toyoda[1]

[1]Department of Cerebrovascular Medicine, National Cerebral and Cardiovascular Center, Suita, Japan

[2]Department of Investigative Radiology, National Cerebral and Cardiovascular Center, Suita, Japan

[3]Department of Radiology, National Cerebral and Cardiovascular Center, Suita, Japan

[4]Department of Integrative Stroke Imaging Center, National Cerebral and Cardiovascular Center, Suita, Japan

Objectives: Amyloid-β (Aβ) deposition is not only observed in pathologic conditions, such as Alzheimer disease (AD) or cerebral amyloid angiopathy, but also in normal aging. Pittsburgh Compound-B (^{11}C-PiB) positron emission tomography (PET) enabled us to visualize and quantify the Aβ deposition in the brain. Although the retention of ^{11}C-PiB to the gray matter has been well demonstrated in patients with AD, the nature of retention of ^{11}C-PiB to the white matter has not been clarified. The aim of this study was to determine the kinetics of ^{11}C-PiB in relation with cerebral blood flow (CBF) in different regions of the brain in patients with symptomatic small vessel disease.

Methods: Subjects were 19 patients who had past history of non-cardioembolic stroke without major cerebral arterial stenosis (69±7 years, 9 women). No patients were diagnosed as having AD. All patients underwent brain magnetic resonance (MR) imaging, ^{11}C-PiB PET and ^{15}O-gas PET with a rapid technique[1)]. In ^{11}C-PiB PET, we derived input function from the arterial plasma radioactivity and metabolite correction, and analyzed the kinetics of ^{11}C-PiB with 3 compartmental model, defined by K1, k2, k3, k4 (K1: a constant of transition from blood to tissues, k2: an index of clearance, k3/k4: an index of binding capacity)[2)]. Brain MR and CBF images of ^{15}O-gas PET were superimposed on ^{11}C-PiB PET image. On the brain MR image, we set regions of interest (ROIs) in the cortex-subcortex regions (C), basal ganglia (B) and centrum semiovale (CS). We calculated distribution volume (DV) of ^{11}C-PiB, K1, k2, k3/k4 and CBF in each region.

Results: DV of ^{11}C-PiB increased significantly in the order of C (2.19±0.31), B (2.60±0.31) and CS (3.05±0.33) ($p<0.0001$). K1 decreased significantly in the order of B (0.200±0.048/min), C (0.191±0.053/min) and CS (0.114±0.029/min) ($p<0.0001$). As for k2, there were no significant differences among the 3 regions ($p=0.0747$). k3/k4 increased significantly in the order of C (0.900±0.230), B (1.115±0.281) and CS (3.220±1.038) ($p<0.0001$). There was no relationship between k3/k4 and CBF in each region.

Conclusions: Higher ^{11}C-PiB retention in the centrum semiovale was associated with ischemia indicated by the low CBF, but not with a slower clearance of the radiotracer shown by k2. Higher ^{11}C-PiB retention in the centrum semiovale would be attributable to the higher binding capacity of the tracer in this region.

References:

1. Kudomi N, et al : J Cereb Blood Flow Metab 25 : 1209-1224, 2005
2. Price JC, et al : J Cereb Blood Flow Metab 25 : 1528-1547, 2005

225
BRAIN-0950
Journal Highlights

Journal of Cerebral Blood Flow and Metabolism: Highlights

Bone-marrow derived endothelial progenitor cells protect postischemic axons after traumatic brain injury

K. Park[1], E. Park[2], E. Liu[2], A.J. Baker[3]
[1]Neurovascular group, Create Fertility Research, Toronto, Canada
[2]Critical Care and Anaesthesia St Michael's Hospital, Keenan Research Centre Li Ka Shing Knowledge Institute, Toronto, Canada
[3]Critical Care and Anaesthesia St Michael's Hospital, University of Toronto, Toronto, Canada

White matter sparing after traumatic brain injury (TBI) is an important predictor of survival and outcome. Blood vessels and axons are intimately associated anatomically and developmentally. Neural input is required for appropriate vascular patterning, and vascular signaling is important for neuron development and axon growth. Owing to this co-dependence between vascular cells and axons during development and the contribution of endothelial progenitor cells (EPCs) in ischemic injury, we hypothesized that EPCs are important in axonal survival after TBI. We examined the effects of allogenic-cultured EPCs on white matter protection and microvascular maintenance after fluid percussion injury in adult Sprague-Dawley rats. We used two *in vitro* models of injury, mechanical stretch and oxygen-glucose deprivation (OGD), to examine the effects of EPCs on the mechanical and ischemic components of brain trauma, respectively. Our results indicate that EPCs improve white matter integrity and decrease capillary breakdown after injury. Cultured cortical neurons exposed to OGD had less axon degeneration when treated with EPC-conditioned media, whereas no effect was seen in axons injured by mechanical stretch. The results indicate that EPCs are important for the protection of white matter after trauma and represent a potential avenue for therapy.

228
BRAIN-0956
Journal Highlights

Journal of Cerebral Blood Flow and Metabolism: Highlights

Pathophysiology of vascular cognitive impairment: From animal models to patients

G.A. Rosenberg[1]
[1]Neurology, University of New Mexico, Albuquerque, USA

Pathophysiology of vascular cognitive impairment: From animal models to patents

Gary A. Rosenberg, MD, Professor and Chair of Neurology, University of New Mexico Health Sciences Center, Albuquerque, NM

Abstract:

Vascular cognitive impairment (VCI) is the diagnostic term used to describe a heterogeneous group of sporadic and hereditary diseases of the large and small blood vessels.[1] Subcortical small vessel disease (SVD) leads to lacunar infarcts and progressive damage to the white matter. Patients with progressive damage to the white matter, referred to as Binswanger's disease (BD), constitute a spectrum from pure vascular disease to a mixture with neurodegenerative changes.[2] BD patients are a relatively homogeneous subgroup with hypoxic hypoperfusion lacunar infarcts and inflammation that act synergistically to disrupt the blood-brain barrier and break down myelin. Identification of this subgroup can be facilitated by multimodal disease markers obtained from clinical, CSF, neuropsychological, and imaging studies. Spontaneously hypertensive stroke prone rat (SHR/SP) is an animal model for BD that has been

used to test treatments. We showed that hypoxia measured with electron paramagnetic resonance triggered an inflammatory response that damaged the white matter as shown on MRI,[3] and that the anti-inflammatory tetracycline derivative, minocycline, reduced the white matter injury.[4] A pilot clinical trial to demonstrate the effect of minocycline on the blood-brain barrier has been started, demonstrating the translation of results from animal studies into patients.

REFERENCES

1. Gorelick PB, Scuteri A, Black SE, Decarli C, Greenberg SM, Iadecola C, et al. Vascular Contributions to Cognitive Impairment and Dementia: A Statement for Healthcare Professionals From the American Heart Association/American Stroke Association. Stroke; a journal of cerebral circulation 2011;42:2672-2713.
2. Rosenberg GA, Bjerke M, Wallin A. Multimodal Markers of Inflammation in the Subcortical Ischemic Vascular Disease Type of Vascular Cognitive Impairment. Stroke; a journal of cerebral circulation 2014.
3. Weaver J, Jalal FY, Yang Y, Thompson J, Rosenberg GA, Liu KJ. Tissue oxygen is reduced in white matter of spontaneously hypertensive-stroke prone rats: a longitudinal study with electron paramagnetic resonance. J Cereb Blood Flow Metab 2014;34:890-896.
4. Jalal FY, Yang Y, Thompson JF, Roitbak T, Rosenberg GA. Hypoxia-induced neuroinflammatory white-matter injury reduced by minocycline in SHR/SP. J Cereb Blood Flow Metab 2015.

231
BRAIN-0666
Niels Lassen Award

The Niels Lassen Award Session

ASSESSING RECEPTOR DESENSITIZATION AND INTERNALIZATION PARAMETERS WITH SIMULTANEOUS PET/FMRI

C.Y. Sander[1], J.M. Hooker[1], C. Catana[1], B.R. Rosen[1], J.B. Mandeville[1]
[1]A. A. Martinos Center for Biomedical Imaging, Massachusetts General Hospital, Charlestown, USA

Objectives: Receptor desensitization and internalization (RDI) are synaptic mechanisms that modulate downstream cellular activity in response to receptor activation by agonist. RDI has been demonstrated in vitro[1], and in vivo results have indirectly implicated effects of RDI[2]. Despite its importance in optimizing drug dosing and minimizing side effects, methods for assessing RDI non-invasively are currently unavailable. Together with simultaneous PET/fMRI and a model of RDI, we show how RDI can affect amplitudes and timing of functional signaling, thereby indicating a method to measure RDI rates in vivo.

Methods: A neurovascular coupling model that relates dynamic receptor occupancy to changes in hemodynamics, was extended to include RDI. The model allows for prediction of ligand properties (signal magnitudes, RDI rates). To test the model, we acquired simultaneous PET/fMRI in anesthetized non-human primates with the radiotracer [^{11}C]raclopride and D2/D3 pharmacological challenges: high-affinity agonist quinpirole (0.1, 0.2, 0.3 mg/kg), lower-affinity agonist ropinirole (0.1, 0.3 mg/kg), and antagonist prochlorperazine (0.1 mg/kg). fMRI data were analyzed with the GLM to yield changes in cerebral blood volume (CBV). PET kinetic modeling was performed with SRTM2[3] using a time-dependent $k_{2a}(t)$ term[4], from which temporal indices of occupancy were derived.

Results: Simulations: The classical model without RDI predicted roughly linear and dose-dependent CBV magnitude increases with occupancy for agonists and antagonists, albeit with different CBV signs. Peak

occupancies of 80% evoked a CBV^{peak} of -45% without internalization, based upon prior antagonist studies[5] and assuming ~20% basal DA occupancy. In simulations with RDI, shorter internalization time constants consistently reduced CBV amplitudes at all occupancy levels. Peak CBV amplitudes decreased to -39% and -25% with RDI time constants of 30 and 5 min, respectively. Experimental measurements: Figure 1A-C shows representative timecourses of CBV and occupancy for each injected pharmacological challenge. The agonist quinpirole shows a CBV^{peak} signal at -5% whereas the less potent agonist ropinirole displays a CBV^{peak} signal of -8.5% at lower occupancy. The antagonist prochlorperazine resulted in the largest CBV^{peak} amplitudes of 14.4% at 88% occupancy. Agonist, but not antagonist, challenges show a pronounced temporal dissociation between CBV and occupancy. Fitting our model to the data, we estimated RDI time constants as 5±1 min for quinpirole and 8.5±2.1 min for ropinirole.

Conclusions: Our model of RDI conformed to our experimental data that showed a reduction in amplitude and a shortened fMRI response as an index of RDI. These results show that amplitude and duration of dynamic function-occupancy measurements can be used to assess and estimate RDI rates in vivo, thereby giving access to a new biological parameter. In addition, novel agonist drugs can be evaluated and classified according to their potency using these measures. Further studies, using targeted drugs that exhibit biased agonism and selectively activate the b-arrestin pathway, can give further insight into biological mechanisms and consequences of RDI in vivo, which will be especially important for improving antipsychotic drug treatment.

References: [1]Guo et al. *Neuropsychopharmacology* (2009). [2]Skinbjerg et al. *NeuroImage* (2010). [3]Ichise et al. *JCBFM* (2003). [4]Normandin et al. *NeuroImage* (2012). [5]Sander et al. *PNAS* (2013).

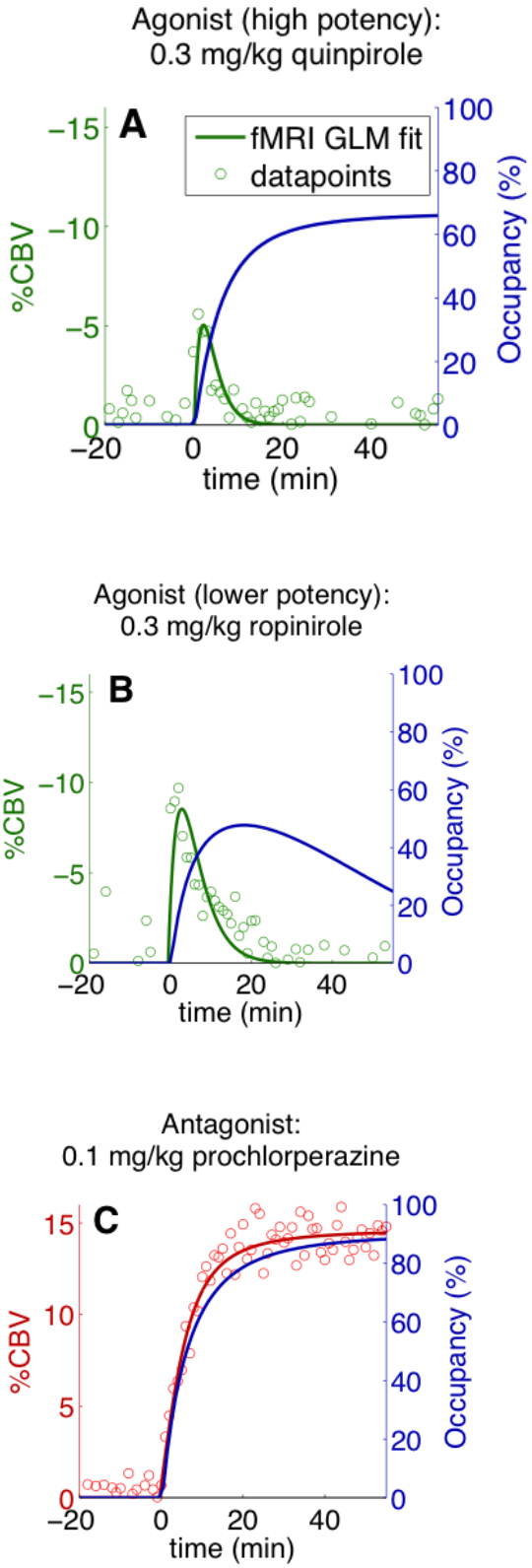

232
BRAIN-0174
Niels Lassen Award

The Niels Lassen Award Session

ENDOTHELIAL CYTOSKELETAL REORGANIZATION CONTRIBUTES TO SURPRISINGLY EARLY BLOOD-BRAIN BARRIER DISRUPTION AND PERMANENT ISCHEMIC/REPERFUSION BRAIN INJURY

Y. Shi[1], L. Zhang[1], L. Mao[1], H. Pu[1], X. Hu[1], R. Stetler[1], Y. Gao[1], R. Leak[2], R. Keep[3], J. Chen[1]
[1]Neurology, University of Pittsburgh, Pittsburgh, USA
[2]Mylan School of Pharmacy, Duquesne University, Pittsburgh, USA
[3]Neurosurgery, University of Michigan, Ann Arbor, USA

Objectives: The mechanisms of permanent neurovascular damage after stroke are still poorly understood. In this study, we identified an early breach of the blood-brain barrier (BBB) within 30 minutes after cerebral ischemic/reperfusion (I/R) injury and investigated the accompanying changes in brain microvascular endothelial cells (BMECs). We targeted these early structural changes within BMECs with molecular tools to brake the progression of permanent neurovascular damage and improve long-term functional outcomes after I/R injury.

Methods: Animals were randomly assigned to groups and all measurements were made by investigators blinded to experimental groups. Transient focal cerebral ischemia (tFCI) was induced in mice by 60-min middle cerebral artery occlusion and reperfusion. BBB breakdown was characterized by the extravasation of injected tracers from peripheral circulation into the brain parenchyma. The underlying mechanism was investigated in an *in vitro* BBB model comprised of BMECs and astrocytes. Changes in EC structures were examined by immunostaining and subcellular fractionation followed by Western blotting. EC-specific transgenic mice were generated to abolish EC structural alterations *in vivo*, and their neurovascular damage, neuroinflammation, as well as functional outcomes were evaluated for up to 28 days after tFCI.

Results: Both *in vivo* and *in vitro* I/R injury induced early (<30 min), subtle leakage of small tracers (≤3kDa) through the BBB that was independent of matrix metalloproteinases (MMPs). This early breach slowly evolved into late-onset MMP-dependent BBB breakdown. Early loss of BBB integrity was not mediated by significant degradation of tight junctional and adherens junctional proteins. Rather, persistent actin polymerization (shown by a 2.04-fold increase of the F/G-actin ratio within 1 h), and formation of F-actin$^+$ stress fibers in BMECs increased cell centripetal tension and disassembled junctional proteins (*e.g.* occludin, claudin, VE-cadherin). Consequently, junctional proteins redistributed from cell membrane to the actin cytoskeletal fraction, increasing BBB permeability and allowing the leakage of small macromolecules (≤3kDa). The weakened BBB permitted the infiltration of peripheral immune cells, including MMP9-producing neutrophils which further damage the BBB (1). Actin depolymerizing factor (ADF), a major endogenous inhibitor of actin polymerization, was rapidly inactivated after I/R, contributing to sustained actin polymerization in BMECs. Lentivirus-mediated overexpression of a constitutively-active mutant ADF (ADFm) reduced actin polymerization within BMECs and prevented junctional protein redistribution. Furthermore, overexpression of ADFm in EC-targeted transgenic mice attenuated BBB disruption at both early (1h) and late (24h) reperfusion stages ($p<0.01$). ADFm overexpression reduced neutrophil infiltration by 70.4% and downregulated 11 proinflammatory cytokines tested ($p<0.05$) at 24 h, thereby alleviating secondary tissue injury. Brain infarct was reduced by 45% at 48 hours, and sensorimotor ($p<0.01$ in the cylinder and corner tests) and cognitive functions ($p<0.05$ in the water maze test) were robustly improved in ADFm overexpressors up to 28 days after tFCI.

Conclusions: This study identifies an important new role for early BBB disruption in permanent neurovascular damage and long-term stroke outcomes. Inhibition of MMPs fails to provide long-term neurological and histological protection. In contrast, prevention of early cytoskeletal changes in BMECs offers long-lasting neurovascular protection after stroke.

References:

1. Li *et al.* (2013) *Ann Neurol* 74(3):458.

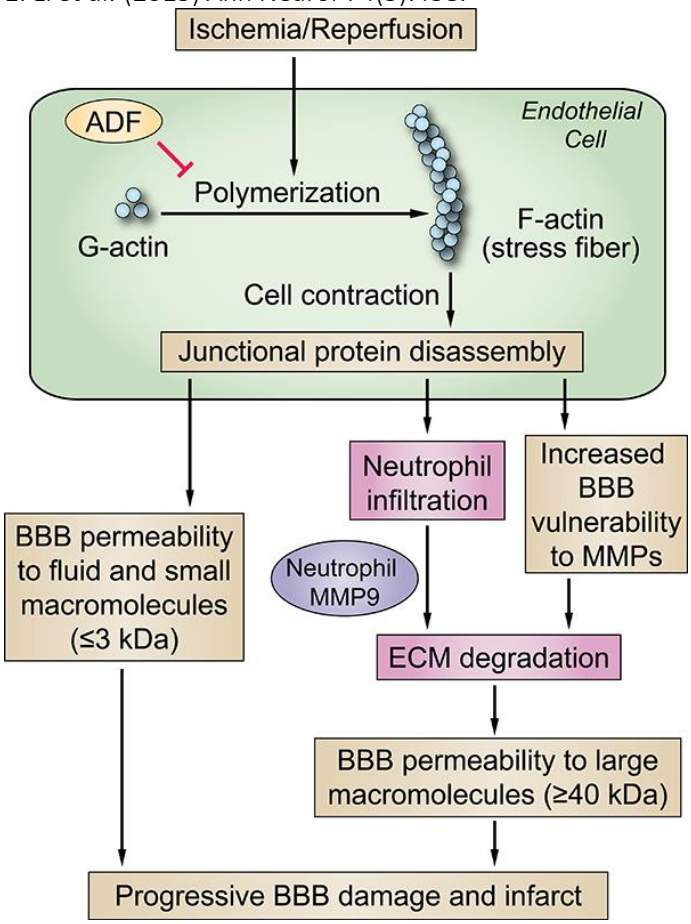

233
BRAIN-0297
Niels Lassen Award

The Niels Lassen Award Session

RESULTS OF THE FIRST PRECLINICAL MULTICENTER TRIAL: ANTI-CD49D TREATMENT IN ACUTE BRAIN ISCHEMIA

A. Liesz[1], *A.M. Planas*[2], *M.G. De Simoni*[3], *N. Plesnila*[1], *D. Vivien*[4], *U. Dirnagl*[5]
[1]*Institute for Stroke and Dementia Research, Klinikum der Universität München, Munich, Germany*
[2]*Department of Brain Ischemia and Neurodegeneration, IDIBAPS, Barcelona, Spain*
[3]*Neuroscience Department, Mario Negri Institute, Milan, Italy*
[4]*GIP Cyceron, INSERM UMR-S U919, Caen, France*
[5]*Center for Stroke Research Berlin, Charité Universitätsmedizin Berlin, Berlin, Germany*

Objective. Numerous experimental approaches have been investigated to treat stroke but all have failed in clinical translation and novel study rationales are sought after to enhance predictability of drug efficacies from bench to bedside. The design of pre-clinical randomized, controlled multicenter trials (pRCTs) has been proposed as a powerful tool aiming to bridge the gap between experimental and clinical research. Thus, this study aimed to test the feasibility of such a “preclinical phase III trial”. Blocking cerebral leukocyte migration by anti-CD49d antibodies has been chosen as the treatment paradigm due to the prototypical controversy in this field raised by the initiation of a premature clinical phase II trial despite inconsistent preclinical results.

Methods. Six independent European centers have investigated in two different murine stroke models with a total animal number of 315 mice the efficacy of anti-CD49d treatment in a centrally coordinated multicenter, randomized and blinded approach. Infarct volumes of pooled samples 7d after distal, permanent MCA occlusion (cMCAo) or 4d after transient, proximal MCAo (fMCAo) was determined as the primary outcome. Secondary outcomes included behavioral deficits, cerebral leukocyte invasion and physiological parameters. Cerebral CD45+ leukocytes were detected

immunohistologically. Behavioral deficits were tested by the Rotarod test and adhesive removal test after cMCAO and by a composite Neuroscore after fMCAO, respectively. Rigorous guidelines were preset for sample size calculation and statistical testing. The full original data set of this study is accessible at Figshare repository (http://dx.doi.org/10.6084/m9.figshare.1289824).

Results. The results from pooled centers revealed that administration of CD49d-specific antibodies significantly reduced the infarct volume one week after permanent ischemia, which results in cortical infarcts (anti-CD49d 8.9mm^3, control: 7.2mm^3, effect size d: 0.56, p=0.027), but not after transient ischemia, which produces more extensive hemispheric lesions. Interestingly, treatment effect was statistically overt only in pooled data sets but not in the analysis of individual center results. Moreover, cerebral invasion of leukocytes was significantly reduced after anti-CD49d treatment compared to control in the cMCAO model. In contrast, leukocyte counts were overall substantially lower after fMCAO and a treatment effect was not detected. Anti-CD49d treatment had no effect on secondary outcome parameters – neither for individual centers nor in the pooled analysis – including the behavioral tests and physiological parameters.

Due to the unprecedented sample size from 6 leading stroke research centers, this study enabled additionally to objectively review the performance of widely used methods in experimental stroke research. Major methodological difficulties were identified including the operational complexity to harmonize experimental methods across centers, the exceedingly high variability of the fMCAO model, differences in mortality between centers and surprisingly low sensitivity of common behavior tests.

Conclusions. This study clearly demonstrates the feasibility of conducting “pre-clinical Phase III” trials, which we propose as a novel and useful tool in biomedical research. Our results on one side confirmed efficacy of anti-CD49d treatment in one stroke model - supporting currently taken efforts to test CD49d inhibition for stroke patients - but also indicates that patients may need to be better stratified to optimally benefit from immune-targeted approaches.

234
BRAIN-0522
Niels Lassen Award

The Niels Lassen Award Session

EVALUATION OF [11C]UCB-J AS A NOVEL PET RADIOLIGAND FOR IMAGING SYNAPTIC VESICLE GLYCOPROTEIN 2A (SV2A) IN THE HUMAN BRAIN

S.J. Finnema[1], N. Nabulsi[1], J. Mercier[2], S. Lin[1], S. Najafzadeh[1], J. Ropchan[1], J. Hannestad[3], T. Eid[4], K. Detyniecki[5], R.E. Carson[1], Y. Huang[1]
[1]Department of Diagnostic Radiology, Yale University, New Haven, USA
[2]Medicinal Chemistry, UCB Pharma S.A., Braine-l’Alleud, Belgium
[3]Global Exploratory Development, UCB Pharma S.A., Braine-l’Alleud, Belgium
[4]Department of Laboratory Medicine, Yale University, New Haven, USA
[5]Department of Neurology, Yale University, New Haven, USA

Objectives: Synaptic vesicle glycoprotein 2A (SV2A) is an essential protein with ubiquitous expression in the CNS, and the site of action for antiepileptic drug levetiracetam. As animal and clinical studies have shown decreased SV2A density in the epileptogenic zone, SV2A may serve as an important biomarker in epilepsy. We recently reported [^{11}C]UCB-J as a novel PET radioligand for imaging of SV2A in non-human primates [1]. Here we report a test-retest reliability evaluation of [^{11}C]UCB-J binding in humans, and the first PET scan with [^{11}C]UCB-J in a patient with temporal lobe epilepsy.

Methods: A total of 9 PET measurements were conducted on the HRRT scanner after injection of ~15 mCi of [^{11}C]UCB-J. Four healthy male subjects (age: 33-55 years) were scanned twice on the same day. The epilepsy patient, with right mesial temporal sclerosis (MTS) seen on MRI, was scanned once. Arterial blood samples were collected for measurement of radiometabolites and free fraction (f_p) in plasma using HPLC and ultrafiltration methods, respectively. Regional time-activity curves (TACs)

were analyzed with 1- and 2-tissue compartment models (1TC & 2TC) to estimate volumes of distribution (V_T) using the metabolite-corrected arterial input function. Parametric V_T maps were generated using the 1TC model.

Results: [^{11}C]UCB-J metabolized fairly quickly, with parent fraction of 28±7% at 60 min post-injection. Plasma free fraction was 32±1%. Brain uptake of [^{11}C]UCB-J was very high. Regional TACs displayed rapid kinetics and were well described by 1TC, with no improvement in fitting with 2TC. 1TC V_T values were highest in striatum and cortex (20±3 mL/cm^3), moderate in cerebellum and thalamus (15±1 mL/cm^3) and lowest in centrum semiovale (6±1 mL/cm^3). V_T values estimated with 2TC were similar to those from 1TC (R^2>0.95). The mean % difference in V_T between test and retest measurements ranged from -3% to 2% across regions. The mean of the absolute differences was <5% for all brain regions. Parametric maps were of high quality and V_T values correlated well with ROI-based estimates (R^2>0.99). Shortening of acquisition time to 60 min altered V_T values by <5% across regions. Evaluation of the epilepsy patient indicated a significant reduction of [^{11}C]UCB-J binding in the right mesial temporal lobe co-localized with MTS seen on MRI.

Conclusions: The novel radioligand [^{11}C]UCB-J exhibits excellent characteristics as a PET imaging tracer in humans. PET measurement in an epilepsy patient confirmed a decrease in SV2A binding in the epileptogenic zone and suggests that [^{11}C]UCB-J may be a suitable biomarker in epilepsy. This radioligand may also have the potential to be a general-purpose tool for measuring synaptic vesicle density in neurodegenerative disorders.

References: Nabulsi et al, 2014, JNM 55:S1:355.

Research Support: UCB Pharma S.A.

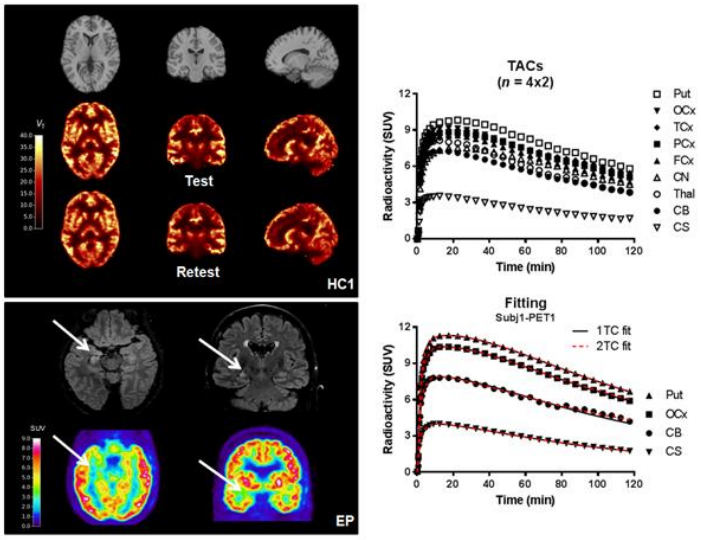

Figure: (Left top) Parametric V_T maps of test and retest PET measurement with [^{11}C]UCB-J in a healthy subject. (Left bottom) PET summation images (40-60 min) post [^{11}C]UCB-J injection in epilepsy patient, with arrows indicating areas with reduced binding in the right mesial temporal lobe. (Right top) Mean regional time activity-curves of [^{11}C]UCB-J. (Right bottom) Fitting of regional time activity-curves using 1TC and 2TC models.

239
BRAIN-0018
Symposium

The cerebral microcirculation in disease

Capillary flow patterns and cerebral oxygenation

L. Østergaard[1], S.N. Jespersen[2]
[1]Center of Functionally Integrative Neuroscience, Institute of Clinical Medicine Aarhus University Denmark, Aarhus, Denmark
[2]Center of Functionally Integrative Neuroscience, Institute of Clinical Medicine and Institute of Physics and Astronomy Aarhus University Denmark, Aarhus, Denmark

A recent reanalysis of the classical flow-diffusion equation shows that brain oxygenation depends not only on CBF, but also on the capillary distribution of blood: If capillary transit times for blood are short, then its oxygen cannot be efficiently extracted by the tissue [1]. This property forces us to consider whether

the vascular system may interfere with tissue function in two different ways: By limiting blood supply (ischemia) *or* by limiting the extraction efficacy of its oxygen (capillary dysfunction) [2].

Neurovascular coupling mechanisms are expected to adjust CBF according to the metabolic needs of the tissue - and in doing so, presumably also to adjust for the CTH-dependent oxygen extraction efficacy. In disease, where capillary morphology and function may be severely disturbed, CBF could therefore be profoundly affected by parallel capillary dysfunction. Recent reviews of the possible effects of capillary dysfunction on the relation between CBF and tissue metabolism in ischemia-reperfusion injury [3], delayed ischemia after subarachnoid hemorrhage (SAH)[4] , and traumatic brain injury (TBI) [5] indeed suggest that capillary constriction, capillary compression, or changes in blood rheology may be important sources of tissue injury in these conditions.

(1) Jespersen,Østergaard. The Roles of Cerebral Blood Flow, Capillary Transit Time Heterogeneity and Oxygen Tension in Brain Oxygenation and Metabolism. JCBFM 2012;32:264-277.

(2) Østergaard, Aamand, et al. The capillary dysfunction hypothesis of Alzheimer's disease.Neurobiol Aging . 2013;34:1018-31.

(3) Østergaard, Jespersen, et al. The extended Penumbra Model. JCBFM. 2013;33:635-648.

(4) Østergaard, Aamand, et al. The role of the microcirculation in delayed cerebral ischemia and chronic degenerative changes after subarachnoid hemorrhage. JCBFM. 2013;33:1825-1837.

(5) Østergaard L, Engedal TS, et al. Capillary transit time heterogeneity (CTH) and flow-metabolism coupling after traumatic brain injury (TBI). JCBFM. 2014;34:1585-1598.

240
BRAIN-0185
Symposium

The cerebral microcirculation in disease

The effects of elevated intracranial pressure on capillary perfusion patterns

E. Nemoto[1], D. Bagin[1], H. Yonas[1]
[1]Neurosurgery, University of New Mexico, Albuquerque, USA

Despite considerable evidence for the existence of microvascular shunts (MVS) in the brain, few investigators acknowledged their existence: “Red veins” in contused brains; “shunt peaks” in cerebral blood flow (CBF) measurements; and hyperemia in infarcted brain. In 1972 Miller et al (Prog Brain Res. 1972; 35: 411-432) reported that increasing intracranial pressure (ICP) decreased the critical CPP from 60 to 30 mmHg. The reason for this decrease in critical CPP was unknown. We hypothesized that it was due to an elevated CBF due to MVS. We tested this hypothesis using two-photon laser scanning microscopy (2PLSM) studying brain microvascular flow in rats during progressive decrease in CPP by either reducing arterial pressure or by increasing ICP. Reduction of CPP by decreasing arterial pressure reduced flow in all microvessels whereas by increasing ICP compromised capillary flow and increased flow in microvessels >8-25 um diameter at flow rates > 1.0 mm/s; consistent with of microvascular shunt flow (Bragin et al, J Neurotrauma. 2011 May;28(5):775-85.). For the first time we showed a graded transition from capillary (CAP) to MVS flow. We also showed that increasing CPP delayed the conversion to MVS at high ICP (Bragin et al, Stroke. 2013 Jan; 44(1): 177-81). Using this same high ICP model with microvascular shunting, we showed that *passive pressure* as compared to *dynamic pressure* measurement of the critical CPP threshold of CBF autoregulation failed at high ICP (Bragin et al, Crit Care Med. 2014 Dec; 42(12): 2582-90). These observations on capillary flow transitions to MVS can be used to study its relationship to the loss of CBF autoregulation clinically and in laboratory animals (Nemoto et al, Acta Neurochir Suppl. 2013; 118:205-9).

241
BRAIN-0415
Symposium

The cerebral microcirculation in disease

Capillary perfusion patterns during cortical spreading depressions

N. Suzuki[1]
[1]*Department of Neurology,*
Keio University School of Medicine, Tokyo, Japan

Red blood cell (RBC) behaviour in capillariesis important, since RBCs are the predominant oxygen carrier from lung to brain tissue. However, the dimensions of RBCs in bloodare of the same order as the diameter of capillaries, so RBCs do not behavelike solutes, but their passage is constrained by local changes in extracellular environment, viscosity, morphological transformation and other factors. Cortical spreading depression (CSD) is a mass depolarization of neurons and excitationof glial cells, followed by sustained suppression of spontaneous neuronal activity, characterized by suppression of electrical activity, negative deflection of direct current (DC) potential and redistribution of ions between extracellular and intracellular compartments. We examined microcirculatory changes, including RBC movements, associated with neuronal dysfunction during CSD with ahigh-speed camera laser-scanning confocal fluorescence microscope system, as well as a two photon microscope,in anesthetized animals. Application of KCl ontothe surface of rat brain elicited concentrically propagating CSD, accompanied with a biphasic response of regional cerebral blood flow (rCBF), namely initial oligemia with capillary flow cessation followed by hyperemia(1). Rapid and prominent constriction of pial arteries propagated in the distal direction with transmission of the CSD wave. RBCs flowing in intraparenchyal capillaries were globally decelerated during passage of CSD, but a small population of RBCs was remarkablyaccelerated(2). The decrease of RBC velocity corresponded temporallyto DC potential deflection and a transient fall of rCBF. Since pial arteriesand intracortical penetrating arteries exhibited prominent constriction followedby slight dilation during first CSD passage in mice(3), the RBC slowdown might be due, at least in part, to the arterial behavior. Diametric changes of pial veins and parenchymal capillaries were much smaller and were heterogeneous. Vasoconstriction of both pial and penetrating arteries was considerably diminished and prominent vasodilation of intracortical penetrating arteries was elicited by repeated CSD. RBC velocity was generally high and stable during repeated passage of CSD, in spite of neuronal depolarization and metabolic enhancement. On the other hand, RBC flow in single capillaries fluctuated constantly and the changes associated withCSD were heterogeneous(4). Unpredictable redistribution of RBCs at branches of capillaries was commonly observed, even though nochange in diameteror arteriolar-venule pressure difference was apparent. Sluggish movements of RBCs in capillaries and occasional full stops or evenbackflow were observed. Local changes, such as morphological changes of astroglial endfeet, swelling of neurons and contraction of pericytes may play a role in this phenomenon. Thus, CSD-induced global activation of neurons and glia might alter adjacent capillary resistance through a physical and/or hemorheological mechanism, so-called neuro-capillarycoupling(4).

[References] (1)Tomita M, et al., J Cereb Blood Flow Metab 25:742-7:2005. (2) Unekawa M, etal., Microcirculation 19:166-74:2012. (3) Unekawa, M., et. al., J Cereb BloodFlow Metab, in press (doi:10.1038/jcbfm.2014.250). (4) Tomita M, et al.,NeuroImage 56:1001-10:2011.

242
BRAIN-0974
Symposium

The cerebral microcirculation in disease

The role of pericytes in incomplete microcirculatory reperfusion in the brain and retina

T. Dalkara[1]
[1]*Institute of Neurological Sciences and Psychiatry,*
Hacettepe University, Ankara, Turkey

Increasing evidence shows that re-opening of the occluded artery within the accepted therapeutic time window does not ensure a good outcome without achieving microvascular reperfusion. Unlike other

parts of the circulation, pericyte density is high in retina and CNS microvessels in line with their role in maintenance of the blood-brain/retina barrier (BBB) and fine control of local microcirculatory blood flow in these tissues. Capillary pericytes dilate or contract in response to physiological stimuli and vasoactive agents. Ischemia induces persistent contraction of microvascular pericytes in the brain and retina in vivo within two hours, which persists after recanalization. Capillary pericytes are particularly vulnerable to disturbances in calcium homeostasis compared to upstream pericytes or smooth muscle cells. Subtle luminal diameter decreases due to pericyte contractions disrupts tissue oxygenation by restricting capillary transit of erythrocytes. Increased capillary transit time heterogeneity can catastrophically impair tissue oxygenation and promote tissue lactic acidosis and infarction. In addition to the pericyte contraction, astrocytic end-feet and endothelial swelling can also contribute to incomplete microcirculatory reflow and BBB dysfunction after ischemia. Restoring pericyte function and reducing swelling of end-feet and endothelia may then favorably impact the outcome of recanalization therapies in stroke by improving microcirculatory blood flow and BBB integrity. Indeed, we have recently shown that sustained release of adenosine to circulation from squalenoyladenosine nanoparticles reduced ischemia-induced erythrocyte entrapment and improved microcirculatory reflow by relaxing contracted pericytes after 2 hours of MCA occlusion. Adenosine also reversed the retinal no-reflow 2 hours after ischemia before irreversible injury to pericytes. These developments bring about the exciting possibility that effective prevention of the injury to neurovascular unit during pharmacological or interventional re-opening of the occluded artery may significantly improve the outcome of recanalization therapies by promoting microcirculatory reflow. They also point to the critical (but partly neglected) importance of the microcirculation in neuroprotection.

243
BRAIN-0962
Symposium

The cerebral microcirculation in disease

IMAGING THE CEREBRAL MICROCIRCULATION AND OXYGENATION

S. Sakadzic[1]
[1]*Martinos Center Optics Division, Massachusetts General Hospital and Harvard Medical School, Charlestown, USA*

Objectives

The global architecture of the blood supply to the cortex consists of a planar mesh of pial arteries and veins that dive into the cortex supplying the complex microvascular network and draining the blood back to the surface. However, in spite of extensive efforts in brain and in other organs, the detailed intravascular oxygen distribution along the microvascular paths that connect pial arteries and veins remains largely unknown. Therefore, we have limited knowledge about the mechanisms that secure sufficient oxygen delivery in microvascular domains during brain activation, and provide some metabolic reserve capacity in diseases that affect either microvascular networks or the regulation of cerebral blood flow (CBF). Such information is therefore critical for our understanding of not only normal brain physiology, but also the relation between progression of microvascular dysfunction and neurodegeneration in various brain diseases, and for attempts to develop a quantitative interpretation of existing and emerging brain imaging modalities.

Methods

To start addressing these questions, we used Two-Photon Microscopy (Sakadžić et al., 2010; Lecoq et al., 2011) to measure PO_2 in a large subset of arterioles, venules, and capillaries at different levels of CBF, and to obtain microvascular morphology. We exploited a Doppler Optical Coherence Tomography to acquire CBF in penetrating arterioles and surfacing venules. The measurements were combined with a detailed analysis of the microvascular morphology and with computation of oxygen delivery from an

anatomical vascular model under different levels of oxygen metabolism.

Results and Conclusions

We have found that arterioles are responsible for 50% of the extracted O_2 at baseline activity (Sakadžić et al., 2014). Most of the remaining O_2 exchange is taking place at the level of the first few capillary branches after precapillary arterioles, while majority of the capillaries (those of higher branching orders) on average release little O_2 at rest. Our measurements and modeling results support this finding showing that high branching order capillaries may act as a dynamic O_2 reserve that is recruited on demand to ensure adequate tissue oxygenation during increased neuronal activity or decreased blood flow. Our results challenge the common perception that O_2 is almost exclusively released from the capillaries and provide a novel understanding of the distribution and dynamics of O_2 extraction along the capillary paths in the cortex.

References

Lecoq, J., et al., 2011. Simultaneous two-photon imaging of oxygen and blood flow in deep cerebral vessels. Nat. Med. 17, 893–898.

Sakadžić, S., et al., 2014. Large arteriolar component of oxygen delivery implies a safe margin of oxygen supply to cerebral tissue. Nat. Commun. 5.

Sakadžić, S., et al., 2010. Two-photon high-resolution measurement of partial pressure of oxygen in cerebral vasculature and tissue. Nat. Methods 7, 755–759.

246
BRAIN-0330
Symposium

Metabolic pathways for ischemic tolerance

Mechanisms of intrinsic ischemic tolerance in the arctic ground squirrels

K.L. Drew[1], T.J. Jinka[2]
[1]Institute of Arctic Biology,
University of Alaska Fairbanks, Fairbanks Alaska, USA
[2]Department of Emergency Medicine,
University of Michigan Medical School,
Ann Arbor Michigan, USA

Objectives: Hibernating species exhibit unparalleled resistance to brain injury including ischemia/reperfusion. This resistance is enhanced by cold during torpor and restorative processes ensue upon rewarming[1, 2]. Animals enter hibernation, in part, by suppressing thermogenesis which conserves energy and allows body temperature (T_b) to approach ambient temperature (T_a). Activation of A_1 adenosine receptors (A_1AR) in the CNS induces hibernation in hibernating species and a hibernation-like state in rats, principally by attenuating shivering and nonshivering thermogenesis[3-5]. However, with systemic drug administration direct effects of A_1AR agonists on the heart may produce unwanted bradycardia. Thus, we tested the hypothesis that central A_1AR could be targeted by combined drug administration.

Methods: We targeted A_1AR within the CNS by IP delivery of the A_1AR agonist ^{6}N-cyclohexyladenosine (CHA) along with 8-(p-Sulfophenyl) theophylline (8-SPT), a non-specific adenosine receptor antagonist with poor blood brain barrier permeability. After 8 min of asphyxial cardiac arrest animals that were resuscitated within 120 sec and met additional inclusion criteria were randomly allocated to therapeutic hypothermia (TH) or normothermia control (NC). Treatment commenced 70 min after ROSC. Animals assigned to the TH group were moved to 16°C and CHA and 8-SPT delivered every 4h for 24h. Animals assigned to the NC group were moved to a neonatal incubator at 29°C and vehicles delivered in the same manner as CHA and 8-SPT. At the end of 24h, all rats were housed at 20°C for 7

days until tissue collection. Body temperature was monitored throughout treatment and daily thereafter using subcutaneous IPTT-300 transponders.

Results: CHA (1mg/kg, IP every 4 hours for 20 hours at T_a of 16°C) with 8-SPT induced and maintained T_b between 29-31°C for 24 h in both naïve rats and rats subjected to 8 minutes of asphyxial cardiac arrest. More stable hypothermia was achieved by continuous infusion of CHA delivered subcutaneously via iPRECIO® minipumps. 8-SPT (25mg/kg,IP) produced a T_b dependent increase in heart rate without affecting T_b. Animals subjected to cardiac arrest and cooled by CHA survived better and showed less neuronal cell death than controls where the highest T_b recorded was 37.1°C.

Conclusions: Systemic administration of 8-SPT reverses A_1AR agonist and cooling-induced bradycardia without interfering with hypothermia. Depth and rate of cooling is easily controlled by the temperature gradient. A_1AR agonists show promise as effective pharmacological adjuncts for therapeutic hypothermia.

References

1. Peretti D., et al. Nature. 2015. epub 2015/01/22.

2. Zhou F., et al. Hibernation, a model of neuroprotection. Am J Pathol. 2001; **158**(6): 2145-51.

3. Muzzi M, et al. AMP-dependent hypothermia affords protection from ischemic brain injury. J Cereb Blood Flow Metab. 2013; **33**(2): 171-4.

4. Jinka TR, et al. Season primes the brain in an arctic hibernator to facilitate entrance into torpor mediated by adenosine A(1) receptors. J Neurosci. 2011; **31**(30): 10752-8.

5. Tupone D, et al. Central Activation of the A1 Adenosine Receptor (A1AR) Induces a Hypothermic, Torpor-Like State in the Rat. J Neurosci. 2013; **33**(36): 14512-25.

247
BRAIN-0947
Symposium

Metabolic pathways for ischemic tolerance

SUMO2/3 conjugation as an endogenous neuroprotective mechanism.

C. Harms[1], G. Lättig-Tünnemann[1], A.L. Datwyler[1], B. Brommer[2], J. Schwab[2], C.J. Hoffmann[1], F. Yildirim[3], P. Euskirchen[2]
[1]Department of Experimental Neurology, Center for Stroke Research Berlin (CSB) Charité-Universitätsmedizin, Berlin, Germany
[2]Department of Experimental Neurology, Clinic for Neurology Charité-Universitätsmedizin, Berlin, Germany
[3]Department of Experimental Neurology, Cluster of Excellence NeuroCure Charité-Universitätsmedizin, Berlin, Germany

SUMO2/3 conjugation as an endogenous neuroprotective mechanism

- Objectives

Small ubiquitin-like modifier (SUMO) conjugation to a broad range of target proteins was identified in animal models of hibernation and ischemia as an endogenous brain protective mechanism (Lee et al., 2007; Yang et al., 2008). SUMOylation predominantly targets chromatin-associated transcription factors and epigenetic modifiers and thereby changes transcriptional profiles (Nayak & Müller, 2014). The maintenance of SUMO-conjugation levels in post-mitotic neurons during the course of multiple and multicellular damaging cascades following an ischemic insult may therefore increase the survival rate of neurons and improve the outcome after stroke. Ischemic tolerance might be induced by inhibition of SUMO specific proteases (sentrin-specific isopeptidase; SENP).

- Methods

We investigated the vulnerability of mouse cortical neurons to combined oxygen-glucose deprivation (OGD) after RNA interference with SUMO2/3 (Datwyler et al., 2011) or SENP7 using neuronal-

specific lentiviral gene delivery. We applied RNA sequencing in conditions of SENP7 loss of function at baseline and early after OGD and assessed intracellular localizations and kinetics of SUMO species upon various SENP7 mutations. Finally, we addressed neurite outgrowth after SENP7 depletion in retina explants as a model of regeneration.

- Results

The loss of free SUMO2/3 in cortical neurons reduced cell viability and survival already in case of sub-threshold OGD were almost all control neurons maintained healthy morphology. While SENP7 depletion in cortical neurons improved their survival during OGD, the number of neurites and the length of neurite outgrowth was reduced in retina explants.

- Conclusions

SUMO2/3 conjugation to nuclear proteins is an important mechanism to modify cellular transcriptional activities. Insufficient amounts of SUMO2/3 limit the cellular stress tolerance of cortical neurons to OGD. However, maintenance of the pool of SENP7-cleavable SUMO2/3 conjugation levels enhances survival after OGD. Loss of SENP7 had a detrimental effect in a neurite outgrowth assay in retina explants. This illustrates the complex and intricate interplay between endogenous neuroprotection and endogenous regeneration and recovery after stroke.

Datwyler AL, Lättig-Tünnemann G, Yang W, Paschen W, Lee SL, Dirnagl U, Endres M, Harms C (2011). SUMO2/3 conjugation is an endogenous neuroprotective mechanism. J Cereb Blood Flow Metab. 31(11):2152-9.
Lee YH, Miyake S, Wakita H, McMullen DC, Azuma Y, Auh S, Hallenbeck JM (2007). Protein SUMOylation is massively increased in hibernation topor and is critical for the cytoprotection provided by ischemic preconditioning and hypothermia in SHSY5Y cells. J Cereb Blood Flow Metab. 27 (5):950-62.
Nayak A, Müller S (2014). SUMO-specific proteases/isopeptidases: SENPs and beyond. Genome Biol. 15(7):422.
Yang W, Sheng H, Warner DS, Paschen W (2008). Transient focal cerebral ischemia induces a dramatic activation of small ubiquitin-like modifier conjugation. J Cereb Blood Flow Metab. 28 (5):892-6.

248
BRAIN-0981
Symposium

Metabolic pathways for ischemic tolerance

Non-Coding RNAs in Neuroprotection

J. Saugstad[1]
[1]*Anesthesiology & Perioperative Medicine, Oregon Health & Science University, Portland, USA*

- Objectives: There has been intense interest in delineating the molecular and cellular mechanisms initiated by preconditioning that lead to endogenous neuroprotection (tolerance). In ischemic preconditioning, induction of tolerance requires new protein synthesis, yet the prominent signature of tolerance is repressed gene expression. One of our objectives was to delineate the role of non-coding RNAs[1], specifically microRNAs (miRNA), as potential contributors to post-transcriptional gene expression and new protein synthesis that is necessary for ischemic tolerance. We have also examined miRNA expression responses to ischemia is male and female brain, to identify targets that contribute to sex differences in responses to ischemia.
- Methods: RT-qPCR assays were used to profile the expression of miRNAs in preconditioned and ischemic rodent brain. These studies were followed by experiments to assess the expression of predicted novel target proteins that may serve a role in the induction of tolerance.
- Results: Our studies revealed that there is differential regulation of miRNAs in preconditioned versus ischemic brain[2]. We also found that the protein expression of predicted targets of regulated miRNAs are changed in preconditioned brain. The proteins of interest include transcriptional regulators, which may serve in the subsequent repression in gene expression that is a feature of tolerance. One target of

the regulated miRNAs is MeCP2, whose protein expression is increased in tolerant cortex[2]. MeCP2 are not able to form tolerance, and show increased sensitivity to ischemia. Experimental manipulation of miRNAs and/or their targets has also been shown to induce neuroprotection[1].

- Conclusions: Evidence supports that mechanisms of ischemic tolerance include the regulation of miRNAs that may alter the expression of transcription proteins. Subsequent studies provide accumulating evidence for important roles of miRNAs and other non-coding RNAs is ischemia and neuroprotection.
- References: (1) Saugstad JA, Non-Coding RNAs in Stroke and Neuroprotection. *Frontiers in Neurology* 2015 Mar 13;6:50 PMID:25821444; (2) Lusardi T, Farr CD, Faulkner CL, Pignataro G, Yang T, Lan JQ, Simon RP, Saugstad JA (2010) Ischemic preconditioning regulates expression of microRNAs and a predicted target, MeCP2, in mouse cortex, *Journal of Cerebral Blood Flow and Metabolism,* 30(4):744-56, PMID: 20010955.

249
BRAIN-0010
Symposium

Metabolic pathways for ischemic tolerance

Ischemic pre-condiitioning alters cerebral microRNA that are upstream to neuroprotective signaling pathways

A. Dharap[1], R. Vemuganti[1]
[1]Neurological Surgery,
University of Wisconsin School of Medicine and Public Health, Madison, USA

Cerebral gene expression is known to be significantly influenced by a sublethal ischemic event (preconditioning; PC) that induces tolerance to future damaging ischemic events. Small non-coding RNAs known as microRNAs (miRNAs) were recently shown to control the mRNA translation. We currently profiled cerebral miRNAs in the cerebral cortex of rats subjected to PC. The miRNAome reacted quickly and by 6h following PC, levels of 51 miRNAs were altered (26 up- and 25 downregulated; >1.5 fold change). 20 of these stayed at the altered level even at 3 days after PC. At least 9 miRNAs showed >5 fold change at one or more time points between 6h to 3 days after PC compared to sham. Bioinformatics analysis showed 2007 common targets of the miRNAs that were up-regulated and 459 common targets of the miRNAs that were down-regulated after PC. Pathways analysis showed that MAP-kinase and mTOR signaling are the top 2 KEGG pathways targeted by the upregulated miRNAs, and Wnt and GnRH signaling are the top 2 KEGG pathways targeted by the down-regulated miRNAs after PC. We hypothesize that alterations in miRNAs and their down-stream mRNAs of signaling pathways might play a role in the induction of ischemic tolerance.

252
BRAIN-0408
Brain Oral Communication

Oral Session: Neuroinflammation

EFFECT OF B2 LYMPHOCYTE DEFICIENCY ON OUTCOME AFTER TRANSIENT FOCAL ISCHEMIA IN MICE

H.X. Chu[1], T. Kyaw[2], B.H. Toh[3], A. Bobik[2], D.R. Grant[1], C.G. Sobey[1]
[1]Department of Pharmacology, Monash University, Melbourne, Australia
[2]Vascular Biology and Atherosclerosis Laboratory, Baker IDI Heart and Diabetes Research Institute, Melbourne, Australia
[3]Department of Medicine,
Centre for Inflammatory Diseases Monash University, Melbourne, Australia

Objectives: B cells are thought to influence neuroinflammatory conditions such as stroke. B cell deficiency is reported to worsen stroke outcome due to the lack of a subset of B cells which secrete IL-10[1]. Two major subtypes of B cells are involved in inflammation, namely B1a and B2, which comprise ~10% and ~90% of B cells, respectively. Recent studies have identified distinct roles of B1a and B2 cells in atherosclerosis[2]. Our study aimed to

investigate the importance of B2 lymphocytes in acute stroke outcome using BAFFR$^{-/-}$ mice in a model of transient cerebral ischemia.

Methods: Focal ischemia was induced in 8-12 week-old male wild-type (C57Bl6/J, n=40) or BAFFR$^{-/-}$ (n=21) mice by middle cerebral artery occlusion (MCAO, 1 h) followed by 23 h or 47 h reperfusion. Functional tests (neurological deficit score; hanging wire latency; parallel rod floor test) were performed at the end of the experiment. Infarct volumes were estimated using thoinin-stained brain sections. Brain, blood, spleen and peritoneal fluid were collected for flow cytometry.

Results: B2 lymphocytes were markedly reduced in number in blood (by ~92%), spleen (by ~95%) and peritoneal fluid (~98%) of BAFFR$^{-/-}$ mice compared to wild-type mice. Plasma levels of IgG and IgM were also ~70% and ~64% lower, respectively, in BAFFR$^{-/-}$ mice. In wild-type mice, the number of B cells infiltrating the brain was increased by ~4-fold after MCAO and appeared to be maximal by 24 h. By contrast, the number of B cells present in the ischemic brains of BAFFR$^{-/-}$ mice was ~15% of those in wild-type animals. Furthermore, numbers of other infiltrating immune cells, including T cells, neutrophils, macrophages and monocytes, did not differ significantly between wild-type and BAFFR$^{-/-}$ mice after stroke. Despite these selective effects on B cell populations, functional and histological data revealed that deficiency of B2 lymphocytes in BAFFR$^{-/-}$ mice had no effect on functional outcomes or infarct volume.

Conclusion: Our data suggest that B2 lymphocytes, which represent 90% of B cells, have no significant role in stroke outcome after transient focal ischemia.

References:

1. Ren X, Akiyoshi K, Dziennis S, Vandenbark AA, Herson PS, Hurn PD, et al. Regulatory B cells limit CNS inflammation and neurologic deficits in murine experimental stroke. *J Neurosci* 2011; **31**: 8556-8563.
2. Kyaw T, Tay C, Hosseini H, Kanellakis P, Gadowski T, MacKay F, et al. Depletion of B2 but not B1a B cells in BAFF receptor-deficient ApoE mice attenuates atherosclerosis by potently ameliorating arterial inflammation. *PLoS One* 2012; **7**: e29371.

253
BRAIN-0446
Brain Oral Communication

Oral Session: Neuroinflammation

AIM2 AND NLRC4 INFLAMMASOMES CONTRIBUTE WITH ASC TO ACUTE BRAIN INJURY INDEPENDENTLY OF NLRP3

S.M. Allan[1], A. Denes[2], G. Coutts[1], N. Lenart[2], S.M. Cruickshank[1], P. Pelegrin[3], J. Skinner[1], N.J. Rothwell[1], D. Brough[1]
[1]Faculty of Life Sciences, University of Manchester, Manchester, United Kingdom
[2]Laboratory of Molecular Neuroendocrinology, Institute of Experimental Medicine, Budapest, Hungary
[3]Inflammation and Experimental Surgery Unit, Murcia Biohealth Research Institute, Murcia, Spain

Objectives: Inflammation that contributes to acute cerebrovascular disease is driven by the pro-inflammatory cytokine interleukin-1 (IL-1) and is known to exacerbate resulting injury [1]. Multi-molecular protein complexes called inflammasomes, which are activated in a diverse range of diseases, regulate IL-1 activity [2]. However, the nature of the inflammasomes involved in brain injury is currently unknown, and we set out here to test this using mice deficient ($^{-/-}$) in specific inflammasome components.

Methods: Experiments were carried out in 12-16 week old male mice (n=71), all on a C57BL/6 background (WT, NLRP3$^{-/-}$, NOD2$^{-/-}$, ASC$^{-/-}$, NLRC4$^{-/-}$, AIM2-/-). Cerebral ischemia was induced via transient (45min) middle cerebral artery occlusion (tMCAo), followed by 24h reperfusion. Neurological deficit was assessed using the Bederson score [3], with subsequent post-mortem measurement of infarct volume (cresyl-violet) and neuroinflammation (IL-1 (α and β) expression, microglial (Iba1, CD45) and vascular activation (tomato lectin)) on coronal brain sections.

Results: ASC$^{-/-}$, AIM2$^{-/-}$ and NLRC4$^{-/-}$ mice showed significantly reduced (~50% for all) ischemic injury when compared to WT, whereas there was no difference in mice with deletion of NLRP3 or NOD2. Reductions in ischemic injury were accompanied by

improved behavioural outcomes. Microglial activation and leukocyte recruitment were also reduced in the brains of $ASC^{-/-}$, $AIM2^{-/-}$ and $NLRC4^{-/-}$ mice, though numbers of microglial expression IL-1α and IL-1β were similar across all strains.

Conclusions: These data identify the NLRC4 and AIM2 inflammasomes as new potential therapeutic targets for stroke, and provide new insights into how the inflammatory response is regulated after an acute injury to the brain.

References

1. Denes et al (2011) Interleukin-1 and stroke: biomarker, harbinger of damage, and therapeutic target. *Cerebrovasc Dis* 32:517-27
2. Latz et al (2013) Activation and regulation of the inflammasomes. *Nat Rev Immunol* 13:397-411
3. Bederson et al (1986) Rat middle cerebral artery occlusion: evaluation of the model and development of a neurologic examination. *Stroke* 17:472-476

254
BRAIN-0569
Brain Oral Communication

Oral Session: Neuroinflammation

SHAPE DESCRIPTORS AS TOOLS TO INVESTIGATE THE FUNCTIONAL COMMITMENT OF MYELOID CELLS IN ACUTE BRAIN INJURY MODELS

S. Fumagalli[1], E.R. Zanier[1], C. Perego[1], E. Carlino[1], F. Orsini[1], F. Pischiutta[1], M.G. De Simoni[1]
[1]Department of Neuroscience, IRCCS - Istituto di Ricerche Farmacologiche Mario Negri, Milan, Italy

Objectives

Myeloid cells in the brain (microglia and macrophage) respond to acute injury developing either harmful or beneficial functions, making their manipulation an attractive tool to define novel therapeutic strategies. Morphological changes can provide information on microglia/macrophage functional commitment. A morphological description is thus a priority to clarify the specific functional significance of these cells in brain pathology. Here we identified quantitative morphological parameters that can be used to explore myeloid cell functions in acute brain injury.

Methods

Procedures involving animals and their care were conducted in conformity with the institutional guidelines that are in compliance with national and international laws and policies for ethical animal treatment. We used three different clinically relevant murine models of focal injury, namely controlled cortical impact brain injury (TBI), transient and permanent occlusion of middle cerebral artery (tMCAo and pMCAo, respectively). Twenty four hours after injury, myeloid cells were labeled by CD11b, CD45 or CD68 and 40x photomicrographs were acquired by unbiased sampling of the lesion core using a motorized stage microscope[1]. CD45 staining can distinguish between microglia (faint expression and ramified cells, $CD45^{low}$) and infiltrated leukocytes (strong labeling and round cells, $CD45^{high}$), therefore it was employed for a differential count. Images were processed with Fiji software to obtain shape descriptors.

Results

We validated several parameters, including area, perimeter, Feret's diameter (caliper), circularity, aspect ratio and solidity on CD11b-stained sections, providing quantitative information on myeloid cell morphology over wide tissue portions[2]. We showed that the shape descriptors that best represent ramification/elongation are area and perimeter, while circularity and solidity provide information on the ameboid shape. We also provide evidence of the involvement of different populations in local inflammatory events, with macrophages replacing microglia into the lesion core when reperfusion does not occur. Increasing the duration of transient ischemia from 30 to 60 minutes of occlusion caused a larger ischemic damage as expected. In the ischemic territory (striatum) after 60 minute-tMCAo, myeloid cells had increased round-shape parameters (circularity and solidity), larger cell area and caliper than after 30 minute-tMCAo. This indicates a reactive ameboid phenotype with massive leukocyte infiltration after 60 minute-tMCAo, as confirmed by increased CD68 expression (lysosomial marker) and

larger amount of infiltrated CD45^{high} cells than after 30 minute-tMCAo.

Conclusions

We have defined specific morphological features that myeloid cells acquire in response to different acute insults by applying a sensitive and readily applicable approach to cell morphological analysis in the brain tissue. These morphologies were associated with specific functions, e.g. phagocytic behavior, that define the myeloid cell commitment. Potential application of this method can be extended to all cell types able to change shape following activation, e.g. astrocytes, or to different disease states, including chronic pathologies.

References

1. Perego C et al., *Journal of Neuroinflammation* 2011
2. Zanier ER, Fumagalli S, *Intensive Care Medicine Experimental* In Press
SF is funded by Fondazione Cariplo, project 2012-0590.

255
BRAIN-0747
Brain Oral Communication

Oral Session: Neuroinflammation

BRAIN INFLAMMATION DURING ANGIOTENSIN II-INDUCED HYPERTENSION

S. Chrissobolis[1], N.D.D. Ranasinghe[1], Q.N. Dinh[1], C.T. Chan[1], A. Vinh[1], H.X. Chu[1], G.R. Drummond[1], C.G. Sobey[1]
[1]Pharmacology, Monash University, Clayton, Australia

Objectives: Hypertension is a major risk factor for stroke, and is associated with Nox2 oxidase-mediated oxidative stress and inflammation. The aims of this study were to characterize inflammatory cell types in the brain during hypertension involving elevated angiotensin II (Ang II), and to test whether Nox2 deletion attenuates this inflammation.

Methods: Male mice (8-12 weeks old) were used. C57Bl/6 (wild-type) and Nox2-deficient mice were infused with saline (vehicle) or Ang II (0.7mg/kg/d, *s.c.*) for 14 days using osmotic minipumps. Systolic blood pressure (SBP) was measured using tail-cuff plethysmography. Inflammatory cell numbers were quantified using flow cytometry and levels of inflammatory cell markers in the brain were assessed using quantitative PCR. All protocols and procedures were approved by the Animal Ethics Committee at Monash University.

Results: In Ang II-infused wild-type mice, SBP was elevated (150±4mmHg, n=20) when compared to vehicle-treated mice (118±4mmHg, n=17; P<0.0001). Similarly, Ang II increased SBP in Nox2-deficient mice (157±7mmHg, n=11) when compared with vehicle treatment (113±7mmHg, n=9; P<0.005). Flow cytometric analysis of brain cell suspensions indicated an increase of microglia (CD45^{lo} CD11b^{+} F4/80^{+}; 2.1-fold), total leukocytes (CD45^{hi}; 3.9-fold) and leukocyte subsets including total monocytes (CD45^{hi} Ly6C^{+}; 2.2-fold), neutrophils (CD45^{hi} Ly6G^{+}; 3.9-fold) and T cells (CD45^{hi} CD11b^{-} CD3^{+}; 3.0-fold) in Ang II-infused wild-type mice compared to vehicle (n=12-19; all P<0.05). The Ang II-induced increases in microglia, total leukocytes and neutrophils were attenuated in Nox2-deficient mice (n=9-11). Quantitative PCR analysis indicated no effect of Ang II on mRNA expression of interleukin-6, chemokine (C-C motif) receptor 2, and interleukin-10, in the brains of wild-type mice compared to vehicle treatment (n=8, all P>0.05).

Conclusions: Ang II-induced hypertension is associated with increased numbers of inflammatory cells in the brain. Nox2 oxidase appears to mediate this increase in a SBP-independent manner. Overall, these findings suggest that Nox2 oxidase inhibition may reduce brain inflammation during Ang II-dependent hypertension. Such a therapy could mitigate the increased clinical stroke risk due to chronic brain inflammation.

256
BRAIN-0596
Brain Oral Communication

Oral Session: Neuroinflammation

SYSTEMIC IMMUNE CHALLENGE WITH ENDOTOXIN INDUCES A ROBUST INCREASE IN BRAIN MICROGLIAL ACTIVATION: A C-11 PBR28 PET STUDY IN HUMANS

C.M. Sandiego[1], J.D. Gallezot[2], J. Ropchan[2], S.F. Lin[2], L. Rodriguez[1], B. Pittman[1], L. Devine[3], K. O'Connor[4], Y. Huang[2], J. Hannestad[5], R.E. Carson[2], K.P. Cosgrove[1]
[1]Psychiatry, Yale University, New Haven, USA
[2]Diagnostic Radiology, Yale University, New Haven, USA
[3]Laboratory Medicine, Yale University, New Haven, USA
[4]Neurology, Yale University, New Haven, USA
[5]CNS Molecular Translational Medicine, UCB Pharma SA, Braine-l'Alleud, Belgium

Objectives: Neuroinflammation is associated with the brain and behavioral changes that underlie the pathology of a broad spectrum of neurodegenerative diseases. Microglia, the primary immune cells of the CNS, are responsible for mounting the neuroinflammatory response to pathogens. Endotoxin has been used to challenge the immune system in rodent models to study sickness symptoms and depressive-like behaviors brought on by peripheral inflammation and microglial activation. We previously demonstrated in baboons with [^{11}C]PBR28 PET that a systemic endotoxin challenge increases brain microglial activation, mediated by peripheral inflammatory cytokines [1]. The aim of this study was to measure in humans the effects of systemic endotoxin administration on microglial activation, peripheral inflammation and self-reported sickness symptoms.
Methods: Eight healthy male subjects (25±6 y.o., 88±12 kg) were scanned on the HRRT with [^{11}C]PBR28 before and 180 min after endotoxin administration (1.0 ng/kg, i.v.). Each scan was 120 min, and both scans were performed on the same day. Subjects were genotyped for TSPO binding status, and only high-affinity (n=3) and mixed-affinity (n=5) binders were included [2]. Peripheral inflammatory cytokine concentrations were measured in serum and subjects were asked to report sickness levels from 0 (least) to 4 (most) at -10, 60, 90, 120, 180, and 240 min relative to endotoxin administration (t=0 min). Volume of distribution (V_T) was estimated with the 2-tissue compartmental model in several brain regions. The change in V_T from baseline was computed as $\%\Delta V_T=[(V_T(\text{endotoxin}) / V_T(\text{baseline}) - 1]*100$, averaged across brain regions.
Results: Endotoxin significantly increased [^{11}C]PBR28 V_T by 47±18% throughout the brain ($p < 0.001$, 1-tailed, paired t-test), with no significant difference in $\%\Delta V_T$ between high-affinity (41±21%) and mixed-affinity binders (50±17%). Endotoxin also significantly increased peripheral inflammatory cytokine concentrations and self-reported sickness symptom levels (Fig. 1).
Conclusions: These data are the first in humans to demonstrate that a systemic endotoxin challenge induced robust increases in microglial activation, systemic inflammation and sickness symptoms. This paradigm to measure brain microglial activation, with [^{11}C]PBR28 PET, and the association to peripheral inflammation provides a novel approach to test the efficacy of neuroprotective and anti-inflammatory drugs.

Research Support: UCB, K02DA031750

References: [1] Hannestad J, Gallezot JD, Schafbauer T *et al.* Endotoxin-induced systemic inflammation activates microglia: [(1)(1)C]PBR28 positron emission tomography in nonhuman primates. *NeuroImage* 2012; 63(1): 232-9. [2] Owen DR, Yeo AJ, Gunn RN *et al.* An 18-kDa translocator protein (TSPO) polymorphism explains differences in binding affinity of the PET radioligand PBR28. *J Cereb Blood Flow Metab* 2012; 32(1): 1-5.

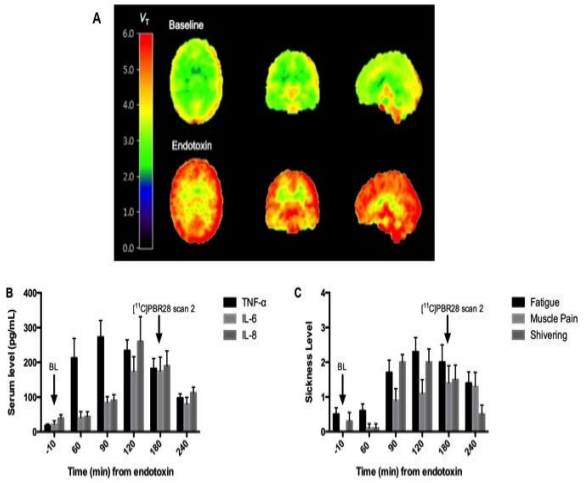

Figure 1 Endotoxin significantly increases microglial activation, peripheral inflammation, and sickness symptoms from baseline (BL) shown with A) mean [^{11}C]PBR28 V_T images, B) serum inflammatory cytokines and C) sickness symptom levels. Time in B) and C) are relative to endotoxin administration at t=0 min with baseline levels at t=-10 min. [^{11}C]PBR28 scan 2 started 180 min after endotoxin was given. Error bars are SEM.

257
BRAIN-0645
Brain Oral Communication

Oral Session: Neuroinflammation

IN VIVO KINETIC ANALYSIS FOR WM LESIONS IN MULTIPLE SCLEROSIS WITH [11C]-PK11195

K. Yeona[1], M. Elizabeth[2], V. Shankar[1], M. Paul D.[1], G. Susan A.[2]
[1]Radiology, Weill Cornell Medical College, New York, USA
[2]Neurology, Weill Cornell Medical College, New York, USA

Objectives: The inflammation associated with Multiple Sclerosis (MS) results in a distribution of activated microglia and macrophages within the demyelinating lesions linked with the disease. PET imaging using [^{11}C]-PK11195, which is known to bind to the Translocator protein (TSPO) expressed on the surface of activated microglia and macrophages, can be used to visualize and quantify activation of the innate immune response in vivo. The objective of this study is to evaluate whether TSPO imaging could be used to study regional kinetic differences within the white matter of patients with MS using the distribution volume (VT) and influx rate, K1, with image-derived input function (IDIF).

Methods: Nineteen patients with MS (female:13, male:6, age:38±12 years) had brain MRI (3T GE, HDxt 16.0). [^{11}C]-PK11195 PET imaging was started simultaneously with the intravenous bolus injection of the radioligand and all PET images were co-registered with the MR images. White matter (WM) segmentation was completed with FreeSurfer and a semi-automated T2 lesion mapping method was applied on all the acquired T1 and T2 data to create normal appearing white matter (NAWM) and WM T2 lesion masks. All the images were linearly aligned onto the T1 FreeSurfer volume. The distribution volume (VT) related to TSPO binding of [^{11}C]-PK11195 was calculated using the Logan graphical method as well as 2-compartment model with IDIF. K1 values were generated by a 2-compartment model with IDIF. For metabolite correction, we applied previously published data [1].

Results: We confirmed that early uptake in the lesions was significantly lower, compared to the segmented NAWM in MS patients. K1 for NAWM was 0.35±0.16 and for lesions was 0.23±0.12. The Logan-VT values in MS patients did not show less significant difference between NAWM (0.89±0.17) and lesion (0.94±0.23). Given the low K1 of lesions, the Logan-VT values may be underestimated, therefore a 2-compartment model was applied to our data, which demonstrated a significant difference between NAWM (0.97±0.28) and lesions (1.13±0.43). In addition, for NAWM and WM lesion, Logan-VT and 2comp-VT were highly correlated (R^2=0.93 (NAWM); R^2=0.85 (WM lesion), p<0.01).

Conclusions: In this study, we demonstrate that K1 in the MS lesions is lower as compared to NAWM, which may represent of hypoperfusion within demyelinating lesions and suggests vascular damage as a result of the demyelinating event. A lower K1 within a specific tissue is known to under-estimate Logan-VT, therefore given our finding within MS lesions, likely lesion Logan-VT is estimated. A 2-compartment model, felt to be more applicable to disease such as MS, showed an increase in [^{11}C]-PK11195 binding globally within MS lesions, which suggests the presence chronically activated microglia throughout known regions of demyelination. Our study demonstrates the unique advantage of PET [^{11}C]-PK11195, wherein both disease-related

hemodynamic changes and innate immune inflammatory activity can be evaluated in MS patients and the relationship further explored.

Reference:

[1] Roivainen A et al., Eur J Nucl Med Mol Imaging. 2009; 36:671-682

[2] Yuichi K. et al., Annals of Nuclear Medicine, 2007; 21:1-8

260
BRAIN-0555
Brain Oral Communication

Oral Session: Blood-Brain Barrier

PILOCARPINE ACTS ON DISTINCT MUSCARINIC ACETYLCHOLINE RECEPTORS EXPRESSED IN BRAIN MICROVASCULAR ENDOTHELIAL CELLS AND ALTERS BBB FUNCTIONALITY. A NEW PARADIGM IN EPILEPTOGENESIS

B.M. Radu[1], M. Radu[1], A. Banciu[2], F. Merigo[1], C. Tognoli[1], M. Di Chio[3], D.D. Banciu[2], G. Constantin[4], S. Fucile[5], G. Bertini[1], P.F. Fabene[1]
[1]Department of Neurological and Movement Sciences , University of Verona, Verona, Italy
[2]Department of Anatomy Animal Physiology and Biophysics, University of Bucharest, Bucharest, Romania
[3]Department of Public Health and Community Medicine, University of Verona, Verona, Italy
[4]Department of Pathology and Diagnostics, University of Verona, Verona, Italy
[5]Department of Physiology and Pharmacology, Sapienza University of Rome, Rome, Italy

Objective

Blood brain barrier (BBB) alterations play an essential role in epilepsy and there is a pathogenetic link between leukocyte-vascular interactions, BBB damage and seizure generation [1,2]. Considering the pilocarpine-induced mice epilepsy model, in our study we aim to highlight the role of brain microvascular endothelial cells as the primary site of pilocarpine action in epileptogenesis.

Methods

Male Balb/c mice (6 weeks old, 25±5 g; Harlan-Nossan, Italy) were used in accordance to international animal welfare guidelines. Patch-clamp recordings on hippocampal transverse slices were performed in the absence/presence of pilocarpine.

Primary brain microvascular endothelial cells (BMVEC) and bEnd.3 (ATCC) cells have been used in control conditions and upon pilocarpine treatment. qRT-PCR was used to quantify *chrm*1-5 gene expression, and immunofluorescence (IF) to evaluate mAChR and tight junctions proteins (claudin-5 and ZO-1) expression after pilocarpine treatment. The pharmacological response evaluation of endothelial cells upon treatment with acetylcholine (ACh), pilocarpine, M1R antagonists (telenzepine, VU-0255035) and M3R antagonists (J104129-fumarate, 4-DAMP) was done by Fura-2-based calcium imaging assay. Pilocarpine-induced cytokine production (IL-1β, IL-6, TNF-α, CCL2, CXCL1) was evaluated by Luminex xMAP Technology, and the endothelial–leukocyte adhesion (ICAM-1, VCAM-1, P-selectin and E-selectin) expression changes were monitored by IF and flow-cytometry.

Results

The application of pilocarpine (10μM, 200μM) on whole-cell voltage-clamped CA3 hippocampal pyramidal neurons in slices produced a 2-fold enhancement of the mean frequency of spontaneous excitatory (sEPSCs) and inhibitory (sIPSCs) postsynaptic currents, without changes in amplitude or without eliciting any paroxysmal depolarization or other epileptiform activity.

qRT-PCR analysis indicated the ranking expression: *chrm3 > chrm4 > chrm5 > chrm2 > chrm1* in BMVECs and bEnd.3 cells. ACh induces a concentration-dependent increase in peak-amplitude cytosolic calcium transients, with EC_{50} 0.21μM (BMVECs) and 0.29μM (bEnd.3). mAChR antagonists have the binding characteristics IC_{50}(nM) and Ka (nM), respectively: telenzepine (4.13±1.02; 0.69), VU-0255035 (48.19±7.11; 8.56), J104129-fumarate (33.81±3.8; 6.00) and 4-DAMP (1.96±0.48; 0.42), correlating with high M3R and low M1R expression.

Pilocarpine triggers cytosolic calcium transients in 13% (10µM) and 19% (100µM) of BMVECs. Pilocarpine (15µM; 2hrs, 6hrs) upregulates ICAM-1, VCAM-1 expression (leukocyte adhesion involvement) and slightly upregulates P-selectin expression (neutrophils adhesion involvement) in BMVECs, similarly to *in vivo* preclinical and clinical epilepsy data [2]. Pilocarpine (100µM; 2hrs, 6 hrs, 24hrs) significantly upregulates M1R, M3R, *chrm1*, *chrm3* expression, slightly downregulates claudin-5 and ZO-1 expression, and decreases CXCL1, CCL2 production in BMVECs.

Conclusion

Pilocarpine acts on the brain endothelium by complex mechanisms: (i) activation of mAChR triggers cytosolic calcium signaling, (ii) adhesion molecules increased expression (probably correlated with leukocyte recruitment), (iii) modulation of tight junctions proteins expression, (iv) cytokine release. In conclusion, we might hypothesise that pilocarpine triggers BBB permeabilisation mechanisms, the primary event in pilocarpine-induced epileptogenesis model being its direct action on brain endothelium and the neuronal epileptiform activity being a secondary event.

References

[1] Bertini G. et al. (2013) *Neurochemistry International* 63(7):652-7.

[2] Fabene PF. et al. (2008) *Nature Medicine* 14(12):1377-83.

Acknowledgements. This work is supported by EpimiRNA grant.

261
BRAIN-0708
Brain Oral Communication

Oral Session: Blood-Brain Barrier

DRUG METABOLIZING ENZYMES P450S AND NUCLEAR RECEPTORS IN HUMAN EPILEPTIC BRAIN: IMPORTANT THERAPEUTIC TARGET TO TACKLE DRUG RESISTANCE

C. Ghosh[1], M. Hossain[1], N. Marchi[2], D. Janigro[1]
[1]Biomedical Engineering,
Cleveland Clinic Lerner Research Institute, Cleveland, USA
[2]Department of Neuroscience,
Institute of Functional Genomics CNRS, Montpellier, France

Objective: Nuclear receptors (NRs) and cytochrome P450 (CYP) together regulates majority of drugs in the liver. In past years, we found a significant contribution of P450s to drug metabolism in human epileptic blood-brain barrier (BBB). In the present study, we explored whether nuclear receptors (NRs) such as pregnane X (PXR), constitutive androstane (CAR) and glucocorticoid (GR) receptors, all involved in the control of P450 expression in the liver are also responsible for abnormal expression of P450 enzymes in human epileptic brain.

Methods: Surgical brain specimens were obtained from drug resistant epileptic subjects undergone temporal lobectomies (according to IRB guidelines). Primary cultures of patient derived epileptic brain microvascular endothelial cells (EPI-EC, n=8), control brain microvascular endothelial cells (HBMEC, n=8, commercially procured) and hepatocytes (n=3) were used. Nuclear receptor mRNA levels were assessed by cDNA microarrays. The expression of nuclear receptors, PXR, CAR and GR was also evaluated by western blotting and pattern of CYP and NRs in drug resistant epileptic brains is determined by immunohistochemistry. PXR and key drug regulated CYPs (CYP3A4, 2C9, 2C19, 2D6 and 2E1) involved in hepatic AED metabolism were studied by western blot and siRNA approaches.

Results: Increased mRNA levels of nuclear receptors (NR) were found in epileptic brain endothelial cells compared to control. CYP3A4, 2C9, 2E1 were

overexpressed in majority of EPI-ECs compared to control; in contrast, CYP2D6, 2C19 were down-regulated or absent in EPI-EC. Increased PXR and GR expression were found in EPI-ECs (*p<0.05) whereas CAR expression were variable across the samples. Hepatocytes consistently showed an elevated levels of PXR, CAR and GR (*p<0.01). The levels of CYPs directly correlated with PXR and GR expression in EPI-ECs and controls, although such effect could not be demonstrated for CAR. Co-localization and increased CYP-NR expression was found in EC, glia and neurons predominantly in the region with reactive gliosis. Levels of PXR were positively correlated with CYP3A4 and CYP2E1 whereas CYP2C9 remained unaltered when PXR was silenced.

Conclusions: The study suggests that at steady-state PXR transcriptional activity is elevated in drug resistant epileptic BBB cells; this is supported by increased expression of PXR regulated CYP. Among other nuclear receptors GR followed a similar trend as PXR in EPI-EC whereas CAR did not, thereby suggesting a different pattern of P450-nuclear receptor regulation in brain of drug resistant epileptics.

Acknowledgement: This work is supported by R01NS078307 (awarded to DJ and NM), R01NS43284, R41MH093302, R21NS077236, R2MH093302, UH3TR000491, and R21HD057256 awarded to DJ. NARSAD Brain and Behavior Foundation and National Center Scientist Development Grant (13SDG13950015) from American Heart Association awarded to CG.

262
BRAIN-0171
Brain Oral Communication

Oral Session: Blood-Brain Barrier

IDENTIFICATION OF P-GLYCOPROTEIN CO-FRACTIONATING PROTEINS AND BINDING PARTNERS IN RAT BRAIN MICROVESSELS SUGGESTING POTENTIAL REGULATORY MECHANISMS

M.E. Tome[1], J.M. Herndon[1], Y. Zhang[1], C.P. Schaefer[1], L.M. Jacobs[1], F.O. Matty[1], T. Davis[1]
[1]Pharmacology, University of Arizona, Tucson, USA

One of the most difficult clinical challenges for treatment of pathologies with a CNS component is drug delivery across the blood brain barrier (BBB). The endothelial cells of the BBB provide a physical and biochemical barrier between the blood and the CNS. The barrier function is required to prevent CNS infection and toxicity; however, it must be selectively modulated to allow for effective CNS drug delivery. P-glycoprotein (PgP), a transmembrane ATP-driven efflux pump, is a major biochemical component of the BBB. PgP extrudes a wide range of substrates, including toxins and drugs, from the cytoplasm and lipid bilayer into the blood, effectively blocking CNS uptake of the major portion of these compounds. Agents that directly inhibit PgP activity have not proven clinically viable. Alternative strategies to selectively modulate PgP activity at the level of the BBB are needed to facilitate targeted drug delivery to the CNS.

Previously, we found that in response to an acute pain stimulus, increased PgP activity is accompanied by a redistribution of PgP in BBB endothelial membrane fractions and disassembly of high molecular weight PgP-containing complexes. These data suggest that post-translational regulation of PgP activity can occur via modulation of PgP-containing protein complexes and trafficking.

Objectives: The long-term goal of our research is to identify PgP regulatory pathways that could be modulated to increase drug delivery to the brain for the treatment of CNS pathologies. The objective of

this project was to identify proteins *in vivo* that co-fractionate with PgP in rat brain microvessels.

Methods: We enriched for proteins that are located in the same membrane fractions as PgP using density gradients of lysed freshly isolated rat microvessels (IACUC protocols approved). We identified proteins in the PgP-containing fractions by 2D gel electrophoresis followed by LC-MS/MS. We verified the identified proteins co-fractionated with PgP via immunoblots, co-localized with PgP via immunofluorescence or bound PgP by co-immunoprecipitation.

Results: We found that PgP was located in two unique pools with different densities in membrane fractions. Each pool contained caveolar constituents: caveolin1, cavin1 and cavin 2. A chaperone (Hsc71), a thiol oxidoreductase (protein disulfide isomerase/PDI), plasma membrane-located ATP synthase β subunit and endosomal/lysosomal sorting proteins (Rab5, Rab11a) co-fractionated with PgP. Hsc71 and PDI bound PgP.

Conclusions and implications: Identification of PgP co-fractionating proteins allows us to suggest potential PgP-regulatory pathways. Our data indicate that there are two pools of PgP in caveolae with different characteristics. The presence of PDI in a complex with PgP suggests this protein could be responsible for disulfide bond rearrangement during the activation of PgP. The presence of ATP synthase β subunit suggests that purinergic signaling could occur in membranes containing PgP. Co-fractionation of PgP with the Rab proteins indicates that the endosomal/lysosomal trafficking pathways may contribute to the redistribution of PgP during the pain stimulus. These data provide the basis for testing whether the suggested pathways impact PgP activation during a pain stimulus. Funding: (NIH: DA 011271; NS 042652)

References:

McCaffrey et al. 2012. J. Neurochem. 122:962.

Seelbach et al. 2007. J. Neurochem. 102:1677.

263
BRAIN-0349
Brain Oral Communication

Oral Session: Blood-Brain Barrier

THE AQUAPORIN-MEDIATED MOLECULAR MECHANISMS OF MANNITOL IN BRAIN OEDEMA AND CEREBRAL WATER FLOW

M. Salman[1], *A. Conner*[2], *M. Conner*[1]
[1]*Biosciences, BMRC/ Sheffield Hallam University, Sheffield, United Kingdom*
[2]*School of Clinical and Experimental Medicine, University of Birmingham, Birmingham, United Kingdom*

Objective:

Elucidating the molecular mechanisms of mannitol action/resistance that could lead to an improvement in its effect as an osmotherapeutic agent in treating cerebral oedema and enhancing cerebral water flow. This will be achieved through the understanding of the functional and expressional profile of cerebral AQPs and their distribution in astrocytes.

Methods:

An osmotic swelling assay has been used to investigate the effects of mannitol on astrocytes by studying the effects of four different mannitol incubation times including mannitol effective half-life incubation period on the cross-sectional diameter of U373 MG astrocytes and primary rat astrocytes in response to hypotonic stress.

Real-time PCR has been used to assess the expression level of natively expressed cerebral AQPs in primary rat astrocytes under nomoxic and hypoxic conditions as experienced following traumatic brain injury (TBI). These data have been used as a platform to investigate the effects of different clinically used mannitol concentrations on the expression of cerebral AQPs.

Western blotting analysis has been used to investigate the translation capacity of the expressed mRNAs and cell surface biotinylation has been used

to determine the membrane localisation of investigated AQPs.

Plasmid DNA encoding AQP 1, 4, 5 and 9-GFP fusion protein-was transfected into HEK293 cell line and also into a more physiologically relevant cell line of U373 MG astrocytes. The translocation responses of these AQP-GFPs were visualised following hypotonic stimulation using confocal microscopy.

Results:

Our data suggest the possible protective effect of mannitol following sudden hypotonic stress conditions that experimentally mimic those occurring in an acute brain oedema.

Primary rat astrocytes were shown to endogenously express all of the investigated cerebral AQPs but at different levels. The changes that happen following mannitol incubation could indicate the possible involvement of cerebral AQPs in the mannitol mechanism of action and/or loss of its initial effect.

In our study, AQP-GFPs undergo rapid and reversible trafficking to the cell membrane in HEK293 and show changes in the distribution profiles in U373 astrocytes following hypotonic stress.

Conclusions:

Mannitol is a cornerstone therapy in the treatment of acute brain oedema. Part of its initial mechanism of action could be related to AQP1&4. The upregulation of AQP9; which is permeable to mannitol, under the stressful conditions seen in brain oedema such as hypoxic stress and lack of nutrients could have a role in mediating the resistance to mannitol that is seen 48-72 h following treatment. Hypotonicity has been shown to regulate the translocation of AQP1, 4, 5 and 9 within a time-scale of seconds. Applying these findings together with the possible protective role of mannitol on astrocytic swelling following hypotonic stimuli could help in the discovery of targeted pharmacological modulation of water and solute transport using AQPs that would appear to provide novel opportunities for therapeutic interventions in a variety of human disorders.

REFERENCES

1. A. S. Verkman, *J Exp Biol* **212**, 1707 (2009).

2. M. T. Conner, A. C. Conner, J. E. Brown, R. M. Bill, *Biochemistry* **49**, 821 (2010).

3. M. T. Conner *et al.*, *J Biol Chem* (2012).

264
BRAIN-0151
Brain Oral Communication

Oral Session: Blood-Brain Barrier

THE BLOOD-BRAIN BARRIER AFTER STROKE: STRUCTURAL STUDIES AND THE ROLE OF CAVEOLAE IN TRANSCELLULAR PERMEABILITY

M.J. Haley[1], C.B. Lawrence[1]
[1]Faculty of Life Sciences, University of Manchester, Manchester, United Kingdom

Objectives: Disruption of the blood-brain barrier (BBB) is an important complication of cerebral ischaemia as the resulting uncontrolled entry of molecules and cells into the brain worsens ischaemic damage. However, the exact processes occurring *in vivo* that allow molecules to pass through the BBB during ischaemia are unclear. Here, we investigated how structural changes to the microvasculature associated with stroke related to BBB permeability, and specifically assessed potential mediators of transcellular and paracellular permeability.

Methods: Obese (*ob/ob)* mice were used as a model of enhanced BBB breakdown after ischaemia, and underwent middle cerebral artery occlusion (MCAO) alongside control (*ob/-*) littermates, followed by 4 or 24 hours reperfusion. BBB integrity was assessed by the presence of tracers in the parenchyma, including endogenous IgG and intravenously injected horse-radish peroxidase (HRP). The structure of the BBB in capillaries after stroke was assessed using both 2D and 3D electron microscopy (EM). Expression of tight junction proteins was assessed by Western blot of isolated microvessel homogenates.

Results: BBB permeability to IgG and HRP was increased in obese mice, and was greatest at 4 hours

post-MCAO. Stroke had a pronounced effect on the structure of the BBB at 4 and 24 hours post-MCAO, featuring an increase in the number of endothelial caveolae (vesicles) and swelling of astrocyte end-feet. Furthermore, more caveolae were found in obese animals in areas with more severe BBB breakdown. However, the severity of astrocytic swelling did not correlate with ischaemic outcome, though 3D rendering of vessels demonstrated swelling was compressing the vessel lumen. No effect of stroke was found on tight junction expression or structure.

Conclusion: Overall, an increase in the number of endothelial caveolae was the best indicator of BBB breakdown, correlating spatially and temporally with BBB breakdown severity. These data suggest that transcellular pathways have been underappreciated in their role in mediating BBB breakdown after cerebral ischaemia.

265
BRAIN-0565
Brain Oral Communication

Oral Session: Blood-Brain Barrier

REGULATING THE BLOOD BRAIN BARRIER AFTER STROKE WITH TPA INHIBITORS

E.J. Su[1], L. Fredriksson[2], M. Warnock[3], D. Bushart[3], D.A. Lawrence[3]
[1]Internal Medicine, University of Michigan, Ann Arbor, USA
[2]Vascular Biology, Karolinska Institutet, Stockholm, Sweden
[3]Internal Medicine, Unversity of Michigan, Ann Arbor, USA

Stroke is a leading cause of morbidity and the third leading cause of mortality in the United States. Treatment of acute ischemic stroke with the thrombolytic agent tissue plasminogen activator (tPA) can improve patient outcomes. However, the number of patients receiving tPA is limited due to the association of thrombolytic therapy with a significant risk of intra-cerebral hemorrhage (ICH). Recently, we demonstrated that tPA in the neurovascular unit (NVU) can exacerbate blood brain barrier (BBB) leakage and promote ICH via activation of latent platelet derived growth factor CC (PDGF-CC) in a plasminogen independent manner. This is in contrast to blood where the primary tPA substrate is plasminogen, and suggests that the regulation of tPA activity may be different in CNS than it is in the blood. This compartmentalization of tPA activity suggests that regulators of tPA activities may have different functions depending on which side of the NVU they reside. Since it is well established that in the blood tPA activity is controlled by plasminogen activator inhibitor 1 (PAI-1) whereas in the CNS it has been suggested that the related inhibitor, neuroserpin, regulates tPA activity, we have investigated if modulating the level of these two inhibitors either genetically or pharmacologically promotes different outcomes after middle cerebral artery occlusion (MCAO) in mice. Our results showed that infarct volume, BBB permeability, and ICH were exacerbated in $Ns^{-/-}$ mice compared to wild type mice after MCAO, whereas in PAI-$1^{-/-}$ mice, infarct volume was reduced but BBB permeability was not worsened, suggesting differential roles for these two tPA inhibitors in stroke. These studies suggest that tPA has opposing activities in the cerebrovasculature, promoting both fibrinolysis and BBB permeability, and that these two activities overlap in complex ways that have made the practical application thrombolytic therapy in stroke difficult. Our data also support the concept that promoting the fibrinolysis in the vessel lumen while limiting tPAs activity in the brain can be beneficial in ischemic stroke.

268
BRAIN-0811
Brain Oral Communication

Oral Session: Neurological Diseases: Human Studies

AGING IS ASSOCIATED WITH IMPAIRED CEREBRAL ENDOTHELIAL FUNCTION THAT IS GREATER IN MEN THAN WOMEN

L.A. Reyes[1], F.A. Sorond[2], L.A. Lipsitz[3], J.M. Serrador[1]
[1]War Related Illness and Injury Study Center, New Jeresy VA Hospital, East Orange, USA
[2]Neurology, Brigham and Women's Hospital, Boston, USA
[3]Gerontology, Beth Israel Deaconess Medical Center, Boston, USA

Objectives: Aging is associated with peripheralvascular changes such as stiffening of vessels and impairments in endothelialfunction. Despite this, cerebral autoregulation remains intact and is better infemales than males. While animal models demonstrate some impairment ofcerebrovascular endothelial function with aging, it is unclear if this is truein humans. We also do not know if males are different than females, similar towhat we see in cerebral autoregulation. This study was designed to determine if cerebrovascular responseto the vasodilator, CO_2, would differ in elderly men and women.Since endothelial function is essential for proper vasodilation in response toCO_2, impaired vasodilator response would be indicative of possible endothelialdysfunction.

Methods: Weused TCD to evaluate cerebrovascular reactivity in 419 (186 males) subjectsover the age of 70 recruited as part of the MOBILIZE Boston study (MBS). TheMBS is a prospective cohort study of a unique set of risk factors for falls inseniors in the Boston area. We assessed CO_2 vasoreactivity duringboth hypercapnia (8% inspired CO_2) and hypocapnia (mildhyperventilation) as well as cerebral autoregulation (sit to stand maneuver).

Results: Malesubjects had significantly lower CO_2 vasoreactivity (Males: 2.8±0.7,Females: 3.1±0.8 %/mmHg CO_2, $p<0.001$) as we have previouslyreported. Examination of their response to reduced end tidal CO2 (hypocapnia)found that there was no difference in the reduction of cerebral flow velocityor vasoconstrictor response (Males: 3.7±3.7, Females: 3.5±4.0 %/mmHg CO_2,$p=0.6$). In contrast, while both sexes had an impaired ability to vasodilate toCO_2, males demonstrated an even greater impairment than females(Males: 0.0±1.3, Females: 0.5±2.1 %/mmHg CO_2, $p<0.006$). Interestingly,there was no correlation between the vasodilatory or vasoconstrictor responseand measures of cerebral autoregulation. In addition, controlling for diabetes,hyperlipidaemia or hypertension did not change the results.

Conclusion: Thesedata demonstrate that aging is associated with impaired cerebral endothelialfunction, confirming findings from animal models, as demonstrated by a reducedvasodilator response but intact vasoconstrictor response to CO_2. Inaddition, this endothelial impairment is worse in males then females. Thesedata in combination with our previous findings of intact autoregulation in aginghighlight that different pathways are involved in these two mechanisms. Whilecerebral smooth muscle function controlling autoregulation remains intact withaging, cerebral endothelial function is impaired, similar to what is seen in peripheralvessels.

References: Deegan etal, Stroke. 2011 Jul;42(7):1988-93

269
BRAIN-0145
Brain Oral Communication

Oral Session: Neurological Diseases: Human Studies

PERIVASCULAR AQUAPORIN-4 POLARIZATION IS COMPROMISED IN THE AGING HUMAN BRAIN AND ASSOCIATED WITH AMYLOID BETA PLAQUE DEPOSITION

D. Zeppenfeld[1], J. Haswell[1], M. Grafe[2], R. Woltjer[2], J. Iliff[1]
[1]Department of Anesthesiology and Perioperative Medicine, OHSU, Portland, USA
[2]Department of Pathology, OHSU, Portland, USA

Objectives: Advanced age is the strongest risk factor for the development of chronic neurodegenerative disorders including Alzheimer's disease (AD) and cerebral amyloid angiopathy (CAA). A common feature of these disorders is the deposition of aberrant proteins throughout the brain, yet the factors that render the aged brain susceptible to protein aggregation and the development of dementia are poorly understood[1]. In recent studies, we demonstrated that clearance of soluble amyloid β protein (Aβ) along the brain-wide 'glymphatic' pathway relies on aquaporin-4 (AQP4) expression that is localized specifically to perivascular astrocytic endfeet[2]. This perivascular localization is lost during aging in rodents and is associated with the failure of glymphatic function and the slowed clearance of Aβ[3]. We sought to define the pattern of AQP4 expression in the cortex of patients with AD, CAA, or cognitively healthy aging controls.

Methods: Sections of the frontal cortex from cognitively-healthy adults aged 20-45, 60-85, and >85 years and from AD patients aged 60-85 and >85 years were obtained from the Oregon Brain Bank and immunostained for $A\beta_{1-42}$, $A\beta_{1-40}$, AQP4, and GFAP. Wide field montages of the cortex were acquired by confocal microscopy. Individual vessels were characterized as plaque-bearing or plaque-spared and AQP4 density surrounding the perivascular space was quantified and characterized as polarized or non-polarized.

Results: Perivascular AQP4 polarization in the frontal cortex declined significantly as a function of subject age, and loss of perivascular polarization was associated with both greater Aβ plaque burden and neurofibrillary tangle pathology. Vascular Aβ deposits (CAA) were associated only with perivascular spaces featuring low AQP4 expression. In a subpopulation of cognitively-intact "super-agers" over the age of 85, perivascular AQP4 polarization was preserved and indeed was preserved to levels seen in young adults.

Conclusions: Loss of perivascular AQP4 polarization is a feature of the aging human brain and is associated with Aβ plaque burden. This suggests that loss of AQP4 localization may be one of the events that render the aging human brain vulnerable to neurodegeneration. The association of the loss of perivascular localization with vascular Aβ deposits in subjects exhibiting CAA suggests that AQP4 mis-localization may promote the deposition of $A\beta_{1-40}$ into paravascular plaques.

References:
1. Thies, W. and Bleiler, L. (2013). 2013 Alzheimer's disease facts and figures. *Alzheimer's & Dementia : The Journal of the Alzheimer's Association*, *9*(2), 208–45.
2. Iliff, J. J. et al. (2012). A paravascular pathway facilitates CSF flow through the brain parenchyma and the clearance of interstitial solutes, including amyloid β. *Science Translational Medicine*, *4*(147), 2012.
3. Kress, B. T., Iliff, J. J., et al. (2014). Impairment of paravascular clearance pathways in the aging brain. *Annals of Neurology*, *76*(6), 845–61.

270
BRAIN-0803
Brain Oral Communication

Oral Session: Neurological Diseases: Human Studies

DEPLETION OF MEMORY B CELLS IN THE CSF IS ASSOCIATED WITH DYSREGULATION OF AB CLEARANCE IN SUBJECTS WITH AMNESTIC MILD COGNITIVE IMPAIRMENT

A.M. Stowe[1], S.B. Ortega[1], S.J. Ireland[1], D. Chen[1], R.M. Huebinger[2], C.M. Cullum[1], B.M. Greenberg[1], T. Harris[3], N.L. Monson[1], R. Zhang[3]
[1]Neurology & Neurotherapeutics, University of Texas Southwestern Medical Center, Dallas, USA
[2]Surgery, University of Texas Southwestern Medical Center, Dallas, USA
[3]Institute for Exercise & Environmental Medicine, Texas Health Presbyterian Hospital, Dallas, USA

Objectives: Mechanisms contributing to the progression of Alzheimer's disease (AD) remain unclear, though AD onset is heavily influenced by risk factors, including the ε4 allele of the apolipoprotein gene (APOε4), which is the greatest risk factor after age. We previously identified increased inflammatory markers in subjects with amnestic mild cognitive impairment (aMCI), prodromal for AD [1]. aMCI subjects exhibited elevated lymphocytes, innate cells, and pro-inflammatory cytokines in the cerebrospinal fluid (CSF), to levels indistinguishable from subjects with multiple sclerosis (MS), an inflammatory CNS disease. To determine the potential contribution of central and peripheral inflammation to the development of AD pathology, we analyzed within-subject leukocyte populations and correlated these measures with brain amyloid (Aβ) burden, quantified by PET imaging at time of CSF and blood collection.

Methods: Fifteen confirmed aMCI subjects (55-76 yr old) and/or their study partners signed written informed consent approved by the Institutional Review Boards of the UT Southwestern Medical Center and Texas Health Presbyterian Hospital of Dallas. Banked CSF samples from a healthy donor (HD) cohort were obtained from the UTSW Biorepository. CSF and peripheral blood (PBL)

leukocytes were collected for immune profiling and immediately processed by flow cytometry. Cytokine and Aβ levels were quantified in banked CSF and PBL using standard ELISA techniques. Cortical Aβ depositions were measured by ^{18}F-florbetapir positron emission tomography (PET) and expressed as standardized uptake value ratio (SUVR) relative to the cerebellar uptake. APOe genotype was determined using standard SNP analysis.

Results: Quantification of soluble Aβ levels in the CSF showed decreased soluble $A\beta_{42}$ in aMCI subjects compared to HD ($p<0.0001$). This decrease in soluble CSF $A\beta_{42}$ associated with a concomitant loss of memory B cells ($CD19^{+}CD138^{-}CD27^{+}$) in the CSF of APOe3 carriers ($R^2=0.75$; $p=0.03$). A smaller cohort (n=4) of $APOe4^{+}$ aMCI subjects exhibited lower soluble CSF $A\beta_{42}$ ($p<0.01$ vs. APOe3) which also associated with a loss of memory B cells in the CSF ($R^2=0.84$; $p=0.08$). Increased Aβ PET SUVR during aMCI correlated with elevated peripheral memory B cell and CD8 T cell populations, and decreased CD4 T cell populations in the PBL (all $p<0.05$). These changes were independent of patient age.

Conclusions: These data indicate a reduction in memory B cells in the CSF that associates with increased brain Aβ deposition in older adults at-risk for AD. The predominant immunogenic Aβ peptide sequence for Aβ immunotherapy is directed to a B cell epitope [2]. Thus it is imperative to determine if a loss of these adaptive immune mediators could affect efficacy of central plasmablast induction by active Aβ immunotherapy, which could contribute to the mixed success of anti-Aβ clinical trials.

References:

1.Monson, N.L., et al., *Elevated CNS inflammation in patients with preclinical Alzheimer's disease.* J Cereb Blood Flow Metab, 2014. 34(1): p. 30-3.

2.Wisniewski, T., et al., *Immunotherapy for Alzheimer's disease.* Biochem Pharmacol, 2014. 88(4): p. 499-507.

271
BRAIN-0385
Brain Oral Communication

Oral Session: Neurological Diseases: Human Studies

INFLAMMATORY BLOOD-BRAIN BARRIER DISRUPTION IN PATIENTS WITH SUBCORTICAL ISCHEMIC VASCULAR DISEASE OF THE BINSWANGER TYPE

B.N. Huisa[1], A. Caprihan[2], G.A. Rosenberg[1]
[1]Neurology, University of New Mexico, Albququerque, USA
[2]Translational Science, MIND Research Network, Albququerque, USA

Objectives: Small vessel disease leads to white matter hyperintensities (WMHs) that are associated with vascular cognitive impairment (VCI). The blood brain-barrier (BBB) is disrupted in VCI patients with large WMHs. BBB disruption has been implicated in the pathophysiology and progression of the WMHs. However, the relationship of WMHs and regional BBB permeability changes has not been studied. We hypothesized that BBB disruption occurs in different regions over time with increased permeability in normal appearing WM (NAWM) and regions near the formation of new WMHs. To test the hypothesis we repeated BBB permeability measurements over one to two years in patients with extensive WMHs related to subcortical ischemic vascular disease of the Binswanger type (SIVD-BT).

Methods: We studied 22 patients with SIVD-BT that were part of a long-term study of VCI in which they had multiple disease markers collected at entry to the study and were followed up for several years to confirm the diagnosis. BBB permeability was measured using dynamic contrast-enhanced MRI (DCEMRI) with Gd-DTPA and the Patlak graphical method of transfer constant calculation. Thresholds for abnormal permeability were measured in 12 controls. Permeability maps were created from all pixels in the white matter with values above the thresholds. First and second scans were compared. Total white matter was divided into 3 regions; 1) NAWM, 2) WMH ring, 3) WMH core. The ring was defined as 2mm inside and outside the WMH border.

Results: Total permeability was significantly higher in subjects than controls (p<0.001). WM regions of high permeability had minimal overlap between first and second scan. There was no correlation between WMHs and total permeability. Regional permeability showed 9% of the total permeability within the WMHs, 49% within the NAWM, and 52% within the WMH ring (p<0.001; ANOVA).

Conclusions: Increased permeability fluctuated between the two scans with very little overlap. The NAWM and the ring around the WMHs rim contained the greatest number of pixels with increased permeability. The fluctuations in locations and the clustering of permeability at the WMH borders suggest an inflammatory etiology rather than a series of small strokes.

Acknowledgements: Supported by grants from the NIH (RO1 NS052305-08) and from the US-Israel Biennial Foundation to GAR, and by the National Center for Research Resources and the National Center for Advancing Translational Sciences of the NIH through Grant Number 8UL1TR000041, UNM Clinical and Translational Science Center.

272
BRAIN-0544
Brain Oral Communication

Oral Session: Neurological Diseases: Human Studies

A COMPARATIVE METABOLIC PET AND PERFUSION MRI STUDY FOR ASSESSING ABNORMAL METABOLIC NETWORK ACTIVITY IN PATIENTS WITH MULTIPLE SYSTEM ATROPHY

J. Ge[1], S. Peng[2], P. Wu[1], J. Wang[3], D. Eidelberg[2], Y. Ma[2], C. Zuo[1]
[1]PET center, Huashan Hospital, Shanghai, China
[2]Center for Neurosciences, Feinstein Institute for Medical Research, Manhasset New York, USA
[3]Department of Neurology, Huashan Hospital, Shanghai, China

Objectives:

Multiple system atrophy (MSA) is one of the most common atypical parkinsonism which is associated with a disease-related metabolic brain network (MSARP). Network activity of MSARP was found to be elevated in patients with MSA relative to healthy controls as well as patients with Parkinson's disease (PD), suggesting that it can assist in differential diagnosis of parkinsonism [1-2]. In this study we compared the metabolic network activity in MSA patients using FDG PET images and cerebral blood flow images acquired with perfusion MRI.

Methods:

A Chinese cohort of 12 MSA patients (age 59.8 ± 9.0 years) and 14 healthy control subjects (age 60.5 ± 6.0 years) underwent FDG PET and perfusion MRI with arterial spin labeling (ASL). All subjects signed written informed consent for the study which was approved by the IRB. Network scores were computed using MSARP identified in a Chinese cohort of 10 MSA patients and 10 healthy controls. The computation was performed for both types of images as described previously [3-4]. The network scores were compared between the groups for each imaging measure and correlated between two modalities.

Results:

MSARP was characterized by covarying metabolic decreases in the putamen, thalamus, midbrain, pons, occipital regions and cerebellum, covarying with metabolic increases in the precuneus, cingulate, insular and temporal areas. MSARP scores were significantly elevated (P < 0.001; unpaired t-test) in the patients relative to the controls in the derivation cohort. Individual scores of MSARP measured prospectively in both FDG PET and ASL MRI were higher (P < 0.002) in the MSA patients than in the controls. Of note, MSARP network activities obtained from both imaging modalities were comparable (P = 0.37; paired t-test) and correlated significantly (R = 0.728, P <0.001) in the combined cohort.

Conclusions:

Network activity of MSARP can be quantified using FDG PET and ASL MRI to differentiate MSA patients from normal controls, very similar to the analogous findings reported in patients with PD using the PD-related pattern [4]. These results further suggest that

images of cerebral blood flow and glucose metabolism are comparable for assessing abnormal metabolic network activity as well as for deriving disease-related brain networks [5]. Both measures may provide viable markers to discriminate MSA patients in differential diagnosis of parkinsonism.

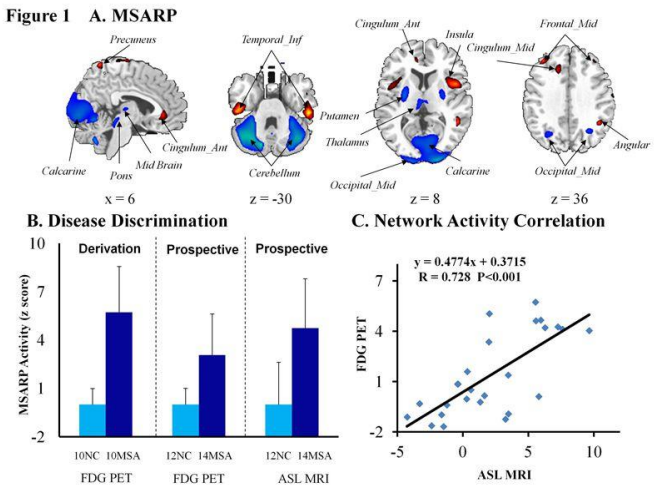

References:

1. Poston KL, Tang CC, Eckert T, et al. Network correlates of disease severity in multiple system atrophy. Neurology 2012; 78: 1237-1244.

2. Eckert T, Tang C, Ma Y, et al. Abnormal metabolic networks in atypical parkinsonism. Mov Disord 2008; 23: 727-733.

3. Wu P, Yu H, Peng S et al. Consistent abnormalities in metabolic network activity in idiopathic rapid eye movement sleep behaviour disorder. Brain 2014; 137: 3122-3128.

4. Ma Y, Huang C, Dyke JP, et al. Parkinson's disease spatial covariance pattern: noninvasive quantification with perfusion MRI. J Cereb Blood Flow Metab 2010; 30: 505-509

5. Melzer TR, Watts R, MacAskill MR, et al. Arterial spin labelling reveals an abnormal cerebral perfusion pattern in Parkinson's disease. Brain 2011; 134: 845-855.

273
BRAIN-0768
Brain Oral Communication

Oral Session: Neurological Diseases: Human Studies

FADD PHOSPHORYLATION LINKS TO ABNORMAL MITOCHONDRION PROLIFERATION IN MITOCHONDRIAL ENCEPHALOMYOPATHY

F. Niu[1], H. Wu[1], Q. Zhang[1], X. Li[2], S. Wang[2], Y. Xu[2]
[1]Pathology Department,
Affiliated Drum Tower Hospital of Nanjing University Medical School, Nanjing, China
[2]Neurology Department,
Affiliated Drum Tower Hospital of Nanjing University Medical School, Nanjing, China

Objectives:

Mitochondrial encephalomyopathy(ME) is a group of metabolic neuromuscular diseases that are mainly involved in skeletal muscle. Mitochondrial proliferation is the most important pathological change of these diseases [1]. Fas-associated protein with death domain (FADD) is a critical adaptor protein for Fas induced apoptosis. Recently, FADD has been found to participate in non-apoptotic activities, such as modulation of cell proliferation and cycle progression [2]. However, the influence of FADD on mitochondrial metabolic disorders, especially in mitochondrial encephalomyopathy, has not been evaluated to date. This study elucidates a previously unexplored role of FADD in mitochondrial diseases that were independent of its well-known effect in triggering apoptosis.

Methods:

Patients: We recruited 16 patients with definite mitochondrial encephalomyopathy by gene mutation and muscle biopsy. Common symptoms were muscle weakness, exercise intolerance, and/or muscular atrophy, as well as other secondary manifestations including numbness, bulbar palsy, intention tremor, depression, ataxia, and cardiac conduction defects cardiomyopathy. The average age was 27.6±1.4 years (range from 6 to 54 years).

Analysis: The quadriceps femoris muscle (vastus lateralis) was chosen as the most suitable muscle for biopsy. Serial cryostat sections of fresh frozen tissue were stained with routine histochemical reactions, including HE, MGT, PAS, NADH-TR, COX, and SDH. Real-time PCR (qPCR) was used to detect mRNA expressions of FADD. Protein levels of FADD and p-FADD were detected by western blot. Immunostaining were used to observe the co-expression of p-FADD in pathological mitochondrial proliferation .

Results: 1) The mRNA expressions of FADD were significantly increased in ME patients. Similarly, mitochondrial related protein of DRP1 (dynamic related protein 1), and MFN2 (Mitofusin 2) mRNA were also dramatically elevated (Fig 1). 2) Investigations on western blot revealed that, patients with mitochondrial diseases had increased p-FADD levels compared with healthy controls in muscle biopsy (Fig 2). 3) The abnormal mitochondrial changes included the appearance of ragged-red fibers (RRFs). The reason for pathological RRFs was an abundance of proliferated mitochondrial. Immunostaining showed p-FADD were mainly localized on the RRFs (Fig 3).

Conclusions: In the current study, our findings strongly suggest that FADD is an important player in the pathological process of mitochondrial encephalomyopathy due to its phosphorylation to provoke abnormal mitochondrial proliferation.

Keywords: mitochondrial encephalomyopathy, FADD phosphorylation, muscle biopsy, abnormal mitochondrial proliferation, ragged-red fibers

Reference:

1. Sarnat, H.B. and J. Marin-Garcia, *Pathology of mitochondrial encephalomyopathies.* Can J Neurol Sci, 2005. **32**(2): p. 152-66.

2. Yao, C., et al., *Role of Fas-associated death domain-containing protein (FADD) phosphorylation in regulating glucose homeostasis: from proteomic discovery to physiological validation.* Mol Cell Proteomics, 2013. **12**(10): p. 2689-700.

Fig1

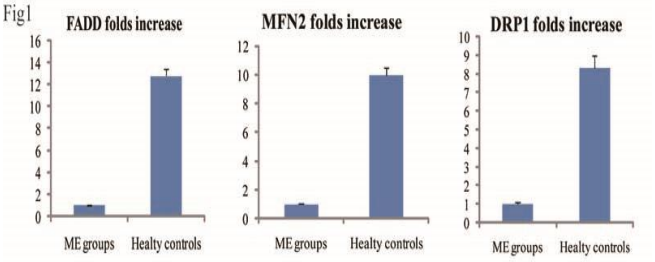

Fig2

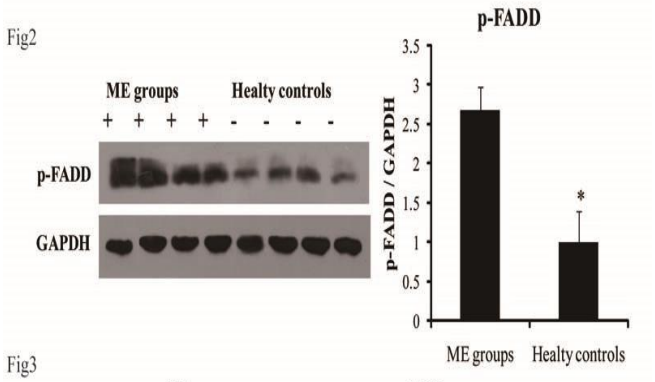

Fig3

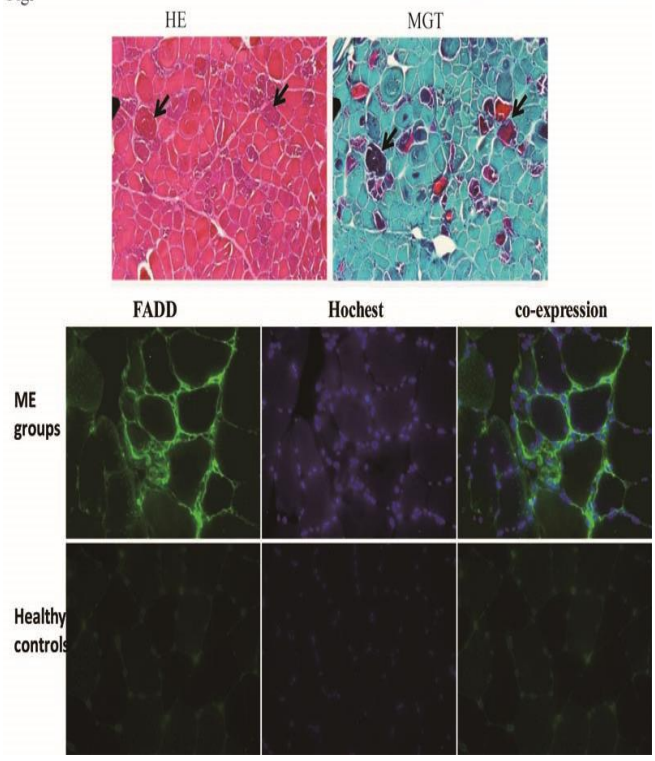

276
BRAIN-0866
Brain Oral Communication

Oral Session: Neurovascular Coupling: Pathophysiology

DRAG REDUCING POLYMERS IMPROVE MICROVASCULAR PERFUSION IN THE TRAUMATIZED BRAIN WITH HIGH INTRACRANIAL PRESSURE

D. Bragin[1], S. Thomson[1], O. Bragina[1], G. Statom[1], M.V. Kamenava[2], E.M. Nemoto[1]
[1]Department of Neurosurgery, University of New Mexico School of Medicine, Albuquerque, NM, USA
[2]McGowan Institute for Regenerative Medicine University of Pittsburgh, Pittsburgh, PA, USA

Objectives: High intracranial pressure (ICP) is a frequent complication of traumatic brain injury (TBI) which, as we previously shown in the healthy brain, compromised capillary (CAP) flow and increased non-nutritive microvascular shunt (MVS) flow, associated with ischemia, edema and blood brain barrier (BBB) damage (Bragin et al, J Neurotrauma, 2011). Therapies for TBI with high ICP have not explored methods aimed to improve cerebral microvascular circulation. Nanomolar intravenous concentrations of linear, blood-soluble drag-reducing polymers (DRP) have been shown to improve circulation and survival in animal models of the ischemic myocardium and limbs, but not yet in the brain. Recently, we have demonstrated that DRP enhanced hemodynamics and tissue oxygenation in the healthy rat brain. Here we examined the effects of DRP on microcirculation in traumatized rat brain with high ICP.

Methods: Two models were employed: 1) intracranial pressure (ICP) increased by artificial cerebrospinal fluid reservoir connected to the cisterna magna; 2) TBI resulting in an increase in ICP, by fluid percussion injury (FPI) with a custom built gas-driven device (1.5 ATA, 100 ms pulse). Using in vivo 2-photo laser scanning microscopy over the rat parietal cortex, we studied the effects of DRP on microvascular blood flow velocity, tissue oxygenation (NADH) and BBB permeability at elevated ICP or post-TBI. DRP solution (2 µg/ml blood) was injected i.v. at 30 minutes after raising ICP or TBI. Doppler cortical flow, rectal and cranial temperatures, intracranial and arterial pressures, blood gases and electrolytes were monitored.

Results: DRP applied at high ICP model (40 mmHg) enhanced capillary flow and reduced MVS flow, reflected by a decrease in the MVS/CAP ratio from 1.07 ± 0.22 to 0.68 ± 0.17 (Mean ± SEM, n=5, P<0.01) compared to a baseline ratio of 0.43 ± 0.16 at an ICP of 10 mmHg. The relative change in NADH autofluorescence (ΔF/Fo(ICP 10 mmHg)) at an ICP of 40 mmHg decreased from 0.17 ± 0.03 to 0.13 ± 0.01 after DRP injection, reflecting improved tissue oxygenation (P<0.05). The TBI increased ICP to 30.8 ± 4.7 mmHg (n=8, p<0.05), and increased the MVS/CAP ratio from 0.43 ± 0.09 before injury to 0.92 ± 0.25, 0.96 ± 0.21, 1.18 ± 0.26, 1.32 ± 0.20 and 1.39 ± 0.23 at 0, 1, 2, 3 and 4 hours after injury, respectively (P<0.01). The increase in the MVS/CAP ratio was associated with an increase in NADH (ΔF/Fo=0.59 ± 0.06, P<0.01), reflecting reduced tissue oxygenation. DRP reduced ICP to 24.6 ± 5.6 mmHg, restored flow in collapsed capillaries and decreased MVS/CAP ratio to 0.67 ± 0.22 (p<0.05). Improved capillary flow mitigated tissue hypoxia, as reflected by a decrease in NADH (ΔF/Fo=0.24 ± 0.05, p<0.05) and reduced BBB degradation.

Conclusions: DRP enhanced and restored capillary flow, decreased MVS flow, reduced tissue hypoxia and BBB degradation after FPI induced TBI with a high ICP. DRP might be effective in improving cerebral microvascular flow and an invaluable therapeutic intervention for the treatment of high ICP after TBI.

277
BRAIN-0434
Brain Oral Communication

Oral Session: Neurovascular Coupling: Pathophysiology

ASTROCYTE ACTIVATION BY BRAIN METASTASES ALTERS NEUROVASCULAR COUPLING

S. Serres[1], M. Sarmiento Soto[1], J.R. Larkin[1], J.A. Meakin[2], A.A. Khrapitchev[1], C. Escartin[3], G. Bonvento[3], N.R. Sibson[1]
[1]CRUK and MRC Oxford Institute for Radiation Oncolo

gy Department of Oncology, University of Oxford, Oxford, United Kingdom
[2]FMRIB Centre Nuffield Department of Clinical Neuros ciences John Radcliffe Hospital, University of Oxford, Oxford, United Kingdom
[3]MIRcen UMR9199 CEA CNRS, University of Paris Sud, Fontenay-aux-Roses, France

Objectives: Astrocytes have been suggested to play a central role in neurovascular coupling between local neural activity and associated changes in cerebral blood flow (CBF). Astrocyte activation is associated with many neurological diseases, which may have significant consequences for cerebrovascular function. We have recently demonstrated marked astrocyte activation in association with secondary tumours (metastases) in the brain. The aim of this study, therefore, was to determine the effects of astrocyte activation on both basal CBF, and the CBF response to either stimulation of the whisker-barrel pathway or hypercapnic challenge in rat brain using laser speckle contrast imaging (LSCI), arterial spin labelling magnetic resonance imaging (ASL-MRI) and local field potential (LFP) measurement.
Methods: Two cohorts of BD-IX rats were injected intracortically in one node of the whisker barrel cortex pathway (the barrel field somatosensory cortex) with either (i) a lentivirus expressing ciliary neurotrophic factor (Lv-CNTF) known to switch astrocytic phenotype to an activated state, or (ii) a metastatic N-ethyl-N-nitrosourea-induced mammary adenocarcinoma cell line (ENU1546). Lv-CNTF injected animals were studied 6 weeks after intracortical injection, and ENU1546 injected animals were studied 1 week after injection. All animals underwent multiphase pseudo Continuous Arterial Spin Labelling (pCASL) imaging to measure basal CBF and LSCI to measure the CBF response, to both electrical stimulation of the whisker pad and hypercapnic (CO2) challenge. LFP measurements of neuronal responses to electrical stimulation of the whisker pad were acquired from the same animals. Histological assessment of metastatic burden, astrocyte activation and neuronal death was performed post-mortem.
Results: In both cohorts, persistent activation of astrocytes, revealed by strong upregulation of GFAP, was observed in the injected cortex, which was not associated with neuronal damage. Basal CBF was decreased (~30%) in the injected cortex compared to the non-injected cortex, for both Lv-CNTF and ENU1546 injected animals. Notably, in the ENU1546 injected rats, the area of metastasis was considerably more restricted than the area of altered CBF, whilst the area of astrocyte activation correlated closely with the area of reduced CBF. CBF responses to whisker pad stimulation or CO2 challenge were greatly reduced (~50%) in the injected cortex compared to the non-injected cortex for both Lv-CNTF and ENU1546 injected animals (Fig 1). Interestingly, LFP responses to whisker pad stimulation were not reduced in either cohort compared to the control contralateral cortex, indicating modulation of neurovascular coupling.
Conclusion: Our findings suggest that astrocyte activation occurring in brain metastasis is the major cause of both decreased basal CBF and altered neurovascular coupling. Our findings also provide evidence to suggest that astrocytes play an important role in the physiological control of CBF. Together these findings support the concept that astrocytes are key mediators of cerebrovascular function and that reactive astrocytes are unable to perform this function in brain metastasis.

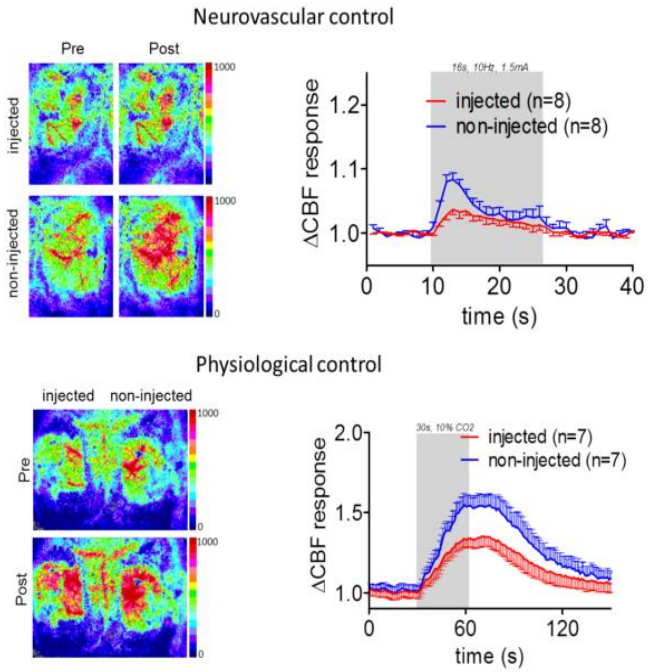

Figure 1 - Both neurovascular and physiological coupling is reduced in brain metastasis as demonstrated by LSCI.

278
BRAIN-0441
Brain Oral Communication

Oral Session: Neurovascular Coupling: Pathophysiology

TIME COURSE OF PERICYTE CONSTRICTION OF CAPILLARIES FOLLOWING TRANSIENT MIDDLE CEREBRAL ARTERY OCCLUSION

B.A. Sutherland[1], C.N. Hall[2], F.M. O'Farrell[3], A.A. Neuhaus[1], A.M. Buchan[1], D. Attwell[3]
[1]Acute Stroke Programme Radcliffe Department of Medicine, University of Oxford, Oxford, United Kingdom
[2]School of Psychology, University of Sussex, Brighton, United Kingdom
[3]Department of Neuroscience Physiology & Pharmacology, University College London, London, United Kingdom

Objectives

Pericytes, located on the extra-luminal surface of brain capillaries, regulate cerebral blood flow (CBF), blood-brain barrier integrity and vascular stability. After stroke, recanalisation of an artery does not necessarily lead to reperfusion of the brain parenchyma, which could be explained by capillary narrowing[1], caused by pericyte contraction[2,3] and their subsequent death in rigor[2]. We wished to determine the time course of capillary constriction after stroke and whether this narrowing was due to pericyte contraction.

Methods

All procedures were in accordance with the Animal (Scientific Procedures) Act, 1986 (UK). Adult male Sprague-Dawley rats (250-330g) were subjected to 90 minutes middle cerebral artery occlusion (MCAO) using an intraluminal filament. CBF was monitored using laser Doppler flowmetry. At various times after recanalisation, rats underwent a gel-filling procedure[4] to determine capillary diameter and define perfused regions of the brain. This involved intra-aortic perfusion of 0.5% FITC-albumin in 5% gelatin in PBS, and solidifying the gelatin *in situ* on ice. Brains were sectioned into 200µm slices and labelled with propidium iodide (for cell death) and Alexa 647-isolectin B_4 (vessel basement membrane marker for pericyte identification[2]). Slices were subsequently fixed, and imaged using confocal microscopy. Capillary diameter was determined at regions adjacent to and distant from pericytes. For each image, non-perfused regions and pericyte death were also quantified. Sham MCAO (with no change in blood flow) or naïve animals were used as controls. All imaging analysis was conducted in the striatum and cortex, where ischaemia occurs during MCAO.

Results

Throughout MCAO, CBF decreased to 30% of pre-MCAO levels and returned to approximately 70% upon filament retraction, indicating hypoperfusion even though full recanalisation had occurred. CBF did not change from baseline in sham animals. Within 5 mins of recanalisation after MCAO, there was no change in capillary diameters in the ipsilateral striatum and cortex compared to controls. At 1.5 h following recanalisation, capillary diameters were significantly (p<0.001) reduced in both the ipsilateral striatum and cortex compared to controls, with a significantly (p=0.035) greater constriction at pericyte locations. The length of non-perfused regions in the ipsilateral cortex and striatum increased (p=0.001) following MCAO compared to controls. At these early timepoints, there was very little cell death in pericytes (8%) compared to 24 h following 1.5 h MCAO (70%)[2].

Conclusions

These results show that at 1.5 h post-recanalisation (but not immediately after MCAO), pericytes constrict capillaries, presumably leading to no reflow and post-ischaemic hypoperfusion. Therefore, there is a time window of less than 1.5 h after recanalisation to pharmacologically prevent pericyte constriction of capillaries and improve perfusion to the brain after ischaemia, but pharmacological reversal of constriction once it has occurred may be efficacious at later times, before the pericytes die.

References

1. Hauck EF *et al*. 2004. JCBFM. 24:383-91
2. Hall CN *et al*. 2014. Nature. 508:55-60
3. Yemisci M *et al*. 2009. Nat Med. 15:1031-7

4. Blinder P *et al*. 2013. Nat Neurosci. 16:889-97
Supported by the Fondation Leducq, ERC, MRC, Wellcome Trust, Henry Smith Charity and Rosetrees Trust.

279
BRAIN-0307
Brain Oral Communication

Oral Session: Neurovascular Coupling: Pathophysiology

INTERNEURON DEFICIT LINKS ATTENUATED NETWORK SYNCHRONIZATION TO MISMATCH OF ENERGY SUPPLY AND DEMAND IN AGING

S. Jessen[1], C. Mathiesen[2], B. Lind[2], M. Lauritzen[3]
[1]Neuroscience and Pharmacology & Center for Health y Aging, University of Copenhagen, Copenhagen, Denmark
[2]Neuroscience and Pharmacology, University of Copenhagen, Copenhagen, Denmark
[3]Neuroscience and Pharmacology and Clinical Neurop hysiology, University of Copenhagen and Glostrup Hospital, Copenhagen, Denmark

During aging global cerebral blood flow (CBF) is reduced, while the cerebral metabolic rate of oxygen ($CMRO_2$) is relatively preserved in humans. The neuronal substrate for this change in function is incompletely understood. We here examined the hypothesis that an overall reduction in activity of cortical interneurons explained the decline in CBF and $CMRO_2$. We focused on parvalbumin positive (PV) interneurons, which are fast spiking and induce neuronal network oscillations in the gamma frequency range. Gamma oscillations correlate strongly with hemodynamic responses in both humans and rodents and evoke large increases in $CMRO_2$. Gamma oscillations are believed to underlie higher cognitive functions and disruptions in gamma rhythm and function of parvalbumin positive interneurons are associated with cognitive decline seen in CNS disorders, such as schizophrenia and Alzheimer's disease.

Using 2-photon microscopy, we examined PV interneuronal Ca^{2+} signals *in vivo* in relation to CBF and $CMRO_2$ in adult and aged mice. We report, that evoked CBF responses, synaptic activity and gamma oscillations decreased in old mice as compared to adult mice. The decline in gamma activity was consistent with a decrease in Ca^{2+} activity in PV perisomatic boutons, and in neurons receiving PV perisomatic innervation in old as compared to adult mice. In comparison, the stimulation-induced rise in $CMRO_2$ became larger; suggesting that the metabolic costs of evoked synaptic activity was increased in old animals.

These results suggest that PV interneurons are selectively affected by aging and that changes in function of PV interneurons may be lead to frailty and cognitive decline. The age-dependent increase in energetic costs of synaptic activity is consistent with a decline in energetic reserve capacity with age and disrupted network deficiency leading to age-related cognitive decline.

280
BRAIN-0506
Brain Oral Communication

Oral Session: Neurovascular Coupling: Pathophysiology

INTERRELATIONSHIP BETWEEN NIRS MEASUREMENTS OF CEREBRAL CYTOCHROME-C-OXIDASE AND SYSTEMIC CHANGES INDICATES INJURY SEVERITY IN NEONATAL ENCEPHALOPATHY

G. Bale[1], S. Mitra[2], M. Chan[1], I. de Roever[1], J. Meek[2], N. Robertson[2], I. Tachtsidis[1]
[1]Medical Physics and Biomedical Engineering, University College London, London, United Kingdom
[2]Institute for Women's Health, University College London, London, United Kingdom

Objectives: Perinatal hypoxic ischaemic encephalopathy (HIE) is associated with severe neurodevelopment problems and mortality. There is an urgent need for techniques which can provide cotside assessment of the injury extent. This study aims to use non-invasive cerebral near-infrared spectroscopy (NIRS) in combination with physiological parameters to assess the severity of HIE injury. Broadband NIRS is used to detect changes in the oxidation state of cytochrome-c-oxidase (CCO), a

measure of cerebral metabolism. We use canonical correlation analysis (CCA), a multivariate statistical technique that measures the relationship between two groups of variables, to test the dependency of cerebral CCO on systemic physiological changes [1].

Methods: Term neonates with suspected HIE were monitored with a broadband NIRS system [2] over the frontal lobe for three hours on day 3 of life. All infants were therapeutically cooled during the measurement. Changes in the concentration of cerebral oxygenated- (HbO_2) and deoxygenated-haemoglobin (HHb), and CCO were measured. Systemic signals, including arterial blood pressure (BP), oxygen saturation (SpO_2), heart rate (HR), respiration rate (RR), partial pressures of carbon dioxide ($PaCO_2$) and oxygen (PaO_2) were recorded simultaneously. Signals were synchronised at 1Hz and artefacts were removed. The signals were grouped into 'cerebral' (HbO_2, HHb and CCO) and 'systemic' (BP, SpO_2, HR, RR, $PaCO_2$ and PaO_2). CCA was used to assess the dependency of the cerebral signals on the systemic signals. This gives a score that varies from 0 to 1, where 0 indicates no dependency and 1 indicates total dependency. CCA results were compared with the severity of the injury which was assessed by Sarnat scoring and magnetic resonance spectroscopy (MRS) measured lactate to NAA ratio (Lac/NAA) on days 5-14 of life. Lac/NAA is the most sensitive biomarker of outcome [3].

Results: Preliminary analysis was performed on 9 subjects with varying degrees of HIE: severe injury n=4, moderate injury n=2, mild injury n=3. CCA showed that there is a higher canonical correlation between cerebral metabolism (CCO) and the systemic signals in severe brain injury. Figure 1 shows that the CCA score of the relationship between CCO and systemic variables increases with Sarnat graded-injury severity. This difference was not seen in the CCA scores between the cerebral haemodynamics (HbO_2 and HHb) and the systemic signals. The infants with predicted poor outcome (with a Lac/NAA of 0.3 or greater) had CCA scores of 0.74 or greater.

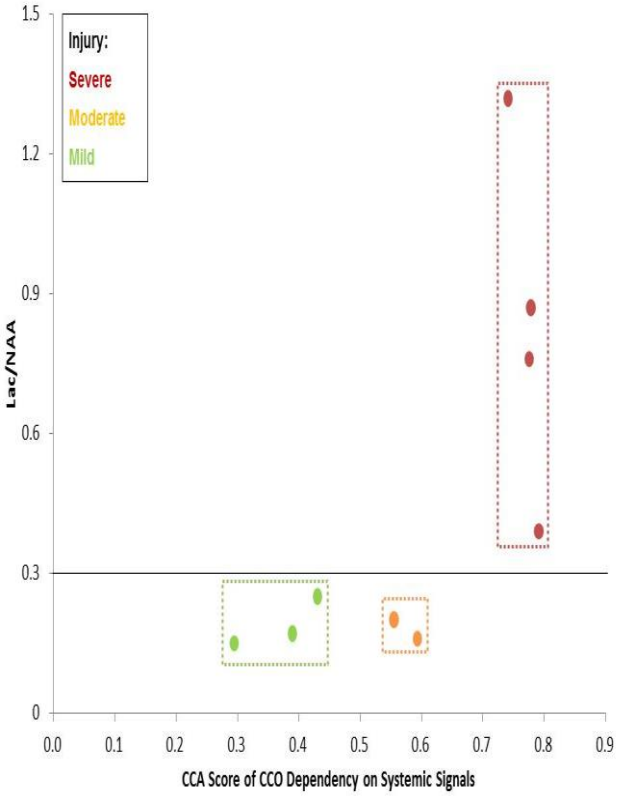

Figure 1: CCA score of CCO dependency on the systemic signals plotted against MRS measured Lac/NAA per subject. A Lac/NAA ratio of greater than 0.3 indicates severe injury (black line). Dotted boxes show injury groupings.

Conclusions: The dependency of the cerebral metabolism, measured with broadband NIRS, to changes in systemic physiology increases with injury severity, suggesting perhaps impairment in cerebral vascular reactivity of the more injured brain. Preliminary analysis suggests broadband NIRS has the potential to provide an early cotside biomarker of outcome.

References:

[1] Caicedo et al. Adv Exp Med Biol, 765:23-29 (2013)
[2] Bale et al. Biomed Opt Express, 5(10):3450-3466 (2014)
[3] Thayyil et al. Pediatrics, 125(2):382-395 (2010)

281
BRAIN-0665
Brain Oral Communication

Oral Session: Neurovascular Coupling: Pathophysiology

PERIOPERATIVE CEREBRAL HEMODYNAMICS AND METABOLISM IN NEONATES WITH SINGLE-VENTRICLE PHYSIOLOGY

M. Dehaes[1], H. Cheng[2], S. Ferradal[1], E. Buckley[3], P. Lin[3], R. Vyas[1], K. Hagan[1], D. Wigmore[2], E. McDavitt[2], A. Fenoglio[1], D.A. Boas[3], J. Soul[4], M.A. Franceschini[3], J.W. Newburger[2], P.E. Grant[1]
[1]Medicine,
Boston Children's Hospital/Harvard Medical School, Boston, USA
[2]Cardiology,
Boston Children's Hospital/Harvard Medical School, Boston, USA
[3]Radiology,
Athinoula A. Martinos Center for Biomedical Imaging Massachusetts General Hospital/Harvard Medical School, Charlestown, USA
[4]Neurology,
Boston Children's Hospital/Harvard Medical School, Boston, USA

Objectives

Newborns with congenital heart disease have brains that are different than controls possibly due to impaired *in utero* cerebral perfusion and oxygen delivery leading to impaired cerebral maturation.[1] Our goal was to characterize preoperative brain hemodynamics in neonates with single-ventricle (SV) physiology compared to normal neonates by measuring cerebral blood volume (CBV), indices of cerebral blood flow (CBF_i) and cerebral metabolic rate of oxygen consumption ($CMRO_{2i}$) using near infrared spectroscopy (NIRS) techniques. We also sought to measure these parameters postoperatively to determine if they provide additional information compared to NIRS measures of cerebral oxygen extraction fraction (OEF) and cerebral hemoglobin oxygen saturation (SO_2).

Methods

Frequency-domain NIRS and Diffuse Correlation Spectroscopy were used to quantify CBV and CBF_i, respectively, and to derive $CMRO_{2i}$. Measurements were made preoperatively and postoperatively until discharge in 11 neonates with SV defects (Stage I with Blalock-Taussig shunt or Sano modification). Median age at surgery was 4 days, median gestational age was 39 weeks, and median length of stay in the Hospital was 31 days including 15 days (median) in the Cardiac Intensive Care Unit (CICU). No patients experienced significant adverse events. Preoperative measurements in SV patients were compared to normals (N=20, median gestational age: 39.9 weeks). Relative changes in CBV, CBF_i, and $CMRO_{2i}$ as well as OEF and SO_2 were calculated by dividing postoperative by preoperative values. Relative changes when neonates were critically ill with vasoactive scores[2] (VAS≥10) and when well (after discharge from CICU and VAS<10) were compared. Relative changes were also correlated with temperature.

Results

Preoperatively, SV patients had significantly lower $CMRO_{2i}$ and CBF_i and higher OEF compared to normals (Fig 1). SO_2 was also lower (p<0.001). Relative changes in $CMRO_{2i}$, CBF_i and OEF were lower when patients were sick compared to well (Fig 2). However, no differences were found in cerebral SO_2 and CBV. Only when patients were well did changes in $CMRO_{2i}$ and CBF_i positively correlate with temperature whereas OEF and SO_2 did not correlate with temperature in either sick or well neonates (see Fig 3).

Conclusions

If baseline $CMRO_{2i}$ is dominated by synaptic density,[3] lower $CMRO_{2i}$ in SV patients compared to normals suggests impaired *in utero* synaptic development, consistent with other studies.[4] The lower baseline CBF_i suggests that *in utero* the brain is in a flow limited state that is not completely compensated by the increased OEF. $CMRO_{2i}$, CBF_i, and cerebral OEF became significantly reduced when patients were sick, however SO_2 was not significantly different suggesting that our additional measures provide complimentary information. The lack of temperature correlation with $CMRO_2$ in sick unlike well neonates, suggests other factors dominate neuronal metabolism in sick neonates. Thus, our measures

provide additional new information about cerebral hemodynamics not provided by SO_2 that may in future prove useful in monitoring neonatal CICU course in congenital heart disease.

References

[1]McQuillen P.S. and Miller S.P., Ann NY Acad Sci, 2010.
[2]Gaies M.G. et al., Pediatr Crit Care Med, 2010.
[3]Bourgeois J.P. et al., Proc Natl Acad Sci USA, 1989.
[4]Dimitropoulos A. et al., Neurology, 2013.

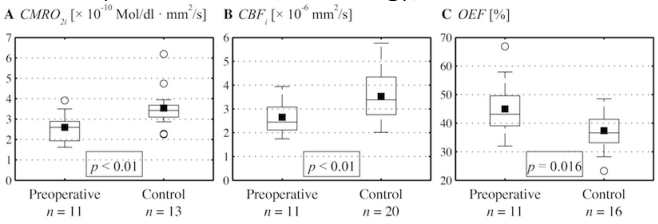

Fig. 1: Preoperative (A) cerebral metabolic rate of oxygen ($CMRO_{2i}$), (B) cerebral blood flow (CBF_i) and (C) cerebral oxygen extraction fraction (OEF). Preoperative variables are compared with age-matched normal controls, with indication of *p*-values. Numbers (*n*) represent the number of neonates.

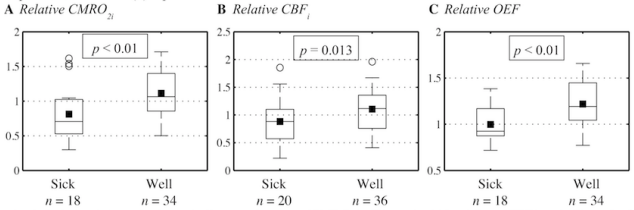

Fig. 2: Relative (A) cerebral metabolic rate of oxygen ($CMRO_{2i}$), (B) cerebral blood flow (CBF_i) and (C) cerebral oxygen extraction fraction (OEF) with reference to preoperative values. Relative variables are compared when neonates were sick (i.e. vasoactive scores ≥ 10) and when they were well (i.e. after discharge from the Cardiac Intensive Care Unit and vasoactive scores < 10), with indication of *p*-values. Numbers (*n*) represent the number of measurements.

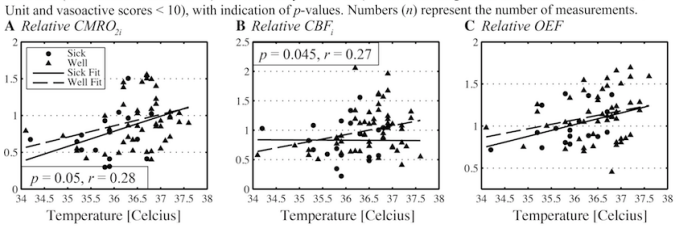

Fig. 3: Relative (A) cerebral metabolic rate of oxygen ($CMRO_{2i}$), (B) cerebral blood flow (CBF_i) and (C) cerebral oxygen extraction fraction (OEF) with reference to preoperative values. Relative variables in neonates when they are sick (black circles) and well (black triangles) are correlated againts temperature (in Celcius) at time of measurement. *p*-values and Pearson's correlation coefficients (*r*) were significant in neonates when they were well (A and B). All other correlations were not significant.

285
BRAIN-0014
Symposium

Exploring the dynamics of brain energy metabolism

Investigating cerebral energy metabolism in vivo using two-photon imaging and FRET nanosensors

B. Weber[1]
[1]*Institute of Pharmacology and Toxicology, University of Zurich, Zurich, Switzerland*

The lack of adequate methods to investigate brain energy metabolism with the required spatio-temporal resolution in the intact organism has hampered significant advances in the field. Förster resonance energy transfer (FRET) sensors specific for energy substrates, such as glucose, lactate and pyruvate have been developed and successfully used in cultured cells and in brain slices. A major advantage of these FRET sensors is that they do not interfere with the intrinsic metabolite concentrations and pathways. In addition to unsurpassed spatial resolution, FRET microscopy can also detect fast metabolic dynamics. Furthermore, these sensors have great potential for *in vivo* studies in combination with two-photon microscopy.

We present here first results using the genetically encoded FRET sensors for glucose, lactate and pyruvate *in vivo*. Recombinant adeno-associated virus (AAV) was used with appropriate promoters to express the sensors in astrocytes and neurons. Experiments were carried out under anesthesia and in awake, head-fixed mice. Various pharmacological interventions were developed and applied to compare the basal concentration and transients of energy substrates in single cells. We demonstrate that FRET sensors for energy substrates are powerful tools for *in vivo* investigations of the cellular compartmentalization of energy metabolism. We will present novel evidence for a significant lactate concentration gradient from astrocytes to neurons. This gradient is in support of a vectorial flux of lactate from astrocytes to neurons, as suggested by the astrocyte-neuron lactate shuttle hypothesis.

286
BRAIN-0032
Symposium

Exploring the dynamics of brain energy metabolism

Contribution of oligodendrocytes to brain energy metabolism assessed by genetically encoded sensors for metabolites

J. Hirrlinger[1,2], A. Trevisiol[2], A.S. Saab[3], K.A. Nave[2]
[1]Carl-Ludwig-Institute for Physiolgy, University of Leipzig, Leipzig, Germany
[2]Dept. of Neurogenetics, Max-Planck-Institute for Experimental Medicine, Göttingen, Germany
[3]Institute of Pharmacology & Toxicology, University of Zurich, Zurich, Switzerland

Metabolic cooperation between different types of brain cells has been a major topic of research in brain energy metabolism for many years. However, this research has mainly focussed on astrocytes and neurons for a long time and only recently oligodendrocytes have entered the stage provoked by some seminal discoveries. This includes for example the finding that oligodendrocytes lacking functional mitochondria are still able to support the axons enwrapped by their myelin sheaths, most likely via release of metabolites via MCT1. Nevertheless, the precise pathways of metabolic support of oligodendrocytes to axons as well as its regulation and physiological impact are still to be elucidated. To further address this contribution of oligodendrocytes to brain metabolism, genetically encoded fluorescent sensors for metabolites like ATP and glucose were used to image these metabolites and their dynamics both in cultured primary cells and tissue preparations. Intracellular glucose concentrations in oligodendrocytes were found to be regulated by neurotransmitters by direct action on receptors present on oligodendrocytes. Using novel transgenic mice expressing a fluorescent ATP sensor in neurons in combination with a setup allowing simultaneous confocal imaging of axons as well as electrophysiological recordings of compound action potentials in ex vivo optic nerves, ATP content was assessed in myelinated axons. We found that ATP content in axons is indeed subject to fast and reversible changes during physiological activity, which are modulated by neighbouring oligodendrocytes. Therefore, genetically encoded fluorescent biosensors for metabolites will contribute to a detailed understanding of brain energy metabolism as well as of the pivotal involvement of oligodendrocytes.

287
BRAIN-0017
Symposium

Exploring the dynamics of brain energy metabolism

Measuring brain oxygen consumption with a micron-scale resolution

S. Charpak[1], D. Lyons[1]
[1]Laboratory of Neurophysiology and new microscopies, Inserm U1128, paris, France

The brain is extremely sensitive to hypoxia. Yet, the physiological values of oxygen concentration in the brain remain elusive because resolute measurements have only been performed during anesthesia, which affects two main parameters modulating tissue oxygenation, i.e. neuronal activity and blood flow. Using the recent finding that measurements of capillary erythrocyte-associated transients (EATs), i.e. fluctuations of oxygen partial pressure (Po_2) associated with individual erythrocytes, can be used to infer Po_2 in the nearby neuropil, we report the first non-invasive micron-scale mapping of Po_2 in the brain of awake resting mice. We find that within two brain regions, the olfactory bulb and the somato-sensory cortex, tissue Po_2 is about half of that under mild isoflurane anesthesia, ranges from very low values, few mm Hg, up to 50 mm Hg, and displays regional layer-specificity. Our study stresses the importance of measuring energy parameters non-invasively in physiological conditions to precisely quantify and model brain metabolism.

292
BRAIN-0970
Symposium

Novel approaches to neuroprotection

Novel Animal Models to Mechanistically Link SUMOylation to Neuroprotection

W. Yang[1], L. Wang[1], H. Sheng[1], W. Paschen[1]
[1]Anesthesiology, Duke University Medical Center, Durham, USA

Impairment of brain functions due to cerebral ischemia is associated with many pathological states of high clinical significance including stroke, cardiac arrest following resuscitation, and various surgical procedures involving cardiopulmonary bypass. New pharmacological tools are still urgently needed to increase the resistance of the brain to transient ischemia. Neuroprotective pathways that are activated under ischemic conditions could be promising targets for novel therapeutic strategies. One such promising target is the small-ubiquitin-like modifier (SUMO1-3) pathway, which is massively activated after ischemia (1). SUMO conjugation (SUMOylation), a post-translational modification, modulates almost all major cellular processes. Mounting evidence from *in vitro* and *in vivo* studies suggests that increased global SUMOylation protects the brain against ischemic damage. To explore the potential for manipulating SUMOylation for preventive and therapeutic purposes, a better understanding of this pathway and its impact on ischemic outcome is important. To facilitate this line of research, we have created several genetically modified mouse models that will allow us to investigate the mechanisms that link SUMOylation to neuroprotection. First, to study the effect of SUMOylation by all 3 SUMO isoforms (SUMO1-3), we have generated a novel SUMO transgenic mouse (Sumo-KD) in which a Thy1 promoter drives expression of 3 distinct microRNAs to silence *Sumo*1–3 expression, specifically in neurons (2). The Sumo-KD mouse line 27 shows widespread transgene expression of *Sumo*1–3 microRNAs and a corresponding marked decrease in levels of SUMO1 and SUMO2/3 protein in neurons of the cerebral cortex, hippocampus, and amygdala, as well as in isolated motor neurons of the spinal cord. To clarify the role of individual SUMO isoforms in pathological states, SUMO knockout mice are preferred. Two groups have generated SUMO1 knockout mice, and found that they are viable and lack any overt phenotype, since SUMO2/3 provides functional compensation. We, therefore, generated SUMO2 and SUMO3 knockout mice (3). While SUMO3 knockout mice are healthy, deletion of SUMO2 is embryonic lethal. Currently, we are in the process of generating conditional SUMO2 knockout mice. To uncover the mechanisms that link SUMOylation to neuroprotection, we must identify proteins that are SUMOylated in post-ischemic brains. Profiling the SUMO-modified proteome is, however, still challenging because the levels of SUMOylated proteins are low. To overcome this challenge, we have generated a novel conditional SUMO transgenic mouse model (CAG-SUMO) expressing all 3 SUMO isoforms with different epitope tags to enable efficient enrichment of SUMOylated proteins from mouse tissue samples. Using these mice and proteomics techniques, we have characterized the SUMO3-modified proteome regulated by brain ischemia, and have identified putative protective proteins and pathways in post-ischemic brains (4). Thus, this novel mouse model will be an invaluable tool for in-depth analysis of the SUMO-modified proteome associated with pathological states. In summary, our new SUMO mouse models are important experimental tools for unraveling the mechanisms that link SUMOylation to a pathological state under investigation.

References: 1. Yang et al., J Cereb Blood Flow Metabol 28:892-896; 2. Wang et al., J Psychiatry Neurosci 39:259-266; 3. Wang et al., EMBO Rep 15:878-885; 4. Yang et al., Stroke 45:1115-1122.

294
BRAIN-0222
Symposium

Novel approaches to neuroprotection

Docosanoid-mediated neuroprotection for stroke: underlying mechanisms and clinical translation

L. Belayev[1], L. Khoutorova[2], S.H. Hong[2], A. Obenaus[3], N.G. Bazan[2]
[1]Neurosurgery and Neuroscience, LSUHSC,

New Orleans, USA
[2]Neuroscience, LSUHSC, New Orleans, USA
[3]Pediatrics, Loma Linda, Loma Linda, USA

INTRODUCTION: Ischemic stroke triggers lipid peroxidation and neuronal injury. Brains undergoing ischemia-reperfusion generate a series of novel compounds derived from docosahexaenoic acid (DHA) and eicosapentaenoic acid (EPA). Neuroprotectin D1 (NPD1), a derivative of DHA, has been shown to reduce polymorphonuclear lymphocyte infiltration, regulate apoptosis, and attenuate infarct size after middle cerebral artery occlusion (MCAo) in mice. Omega-3 fatty acid-derived resolvins from DHA (RvD2) and EPA (RvE1) has been shown to promote inflammation resolution in murine models of acute inflammation. We used magnetic resonance imaging (MRI) and mass spectrometry in conjunction with behavioral assessment and immunohistochemistry to expand our understanding of this novel therapeutic approach.

METHODS: Physiologically-controlled male SD rats received 2 h MCAo. DHA (5 mg/kg; n=10) or vehicle (saline; n=9) was administered i.v. at 3 h after onset of MCAo. *In behavioral studies,* the composite 12-point neuroscore, rota-rod, Y-maze and beam walking test were conducted 1, 2 and 3 weeks after MCAo. *Ex vivo* imaging of the brains and histopathology were carried out on day 21. *In blood-brain barrier (BBB) studies,* fluorometric quantitation of Evans Blue (EB) was performed in six brain regions at 6, 24 or 72 h after stroke. FITC dextran leakage was analyzed on day 3 after MCAo. *In lipid mediator studies*, rats were treated with NPD1, RvD2 or RvE1 [LRR1] (2µg per day during 7 days) or CSF by ICV infusion at 1 h after MCAo. Behavioral tests, *ex vivo* MRI, lipidomic analysis and immunohistochemistry were conducted.

RESULTS: Physiological variables were stable and showed no significant differences between groups. DHA treatment significantly improved the 12-point neuroscore compared to vehicle on day 1 (by 16%), day 2 (by 19%), day 3 (by 22%), week 1 (by 20%), week 2 (by 22%) and week 3 (by 33%) respectively. Treatment with DHA prolonged latency time in the rota-rod test on weeks 1-3 (by 44-68%), enhanced the score in the balance beam (by 29%) and improved Y-maze performance by 19% compared to the saline group. DHA decreased EB extravasation in the posterior ischemic hemisphere at 6 h (by 34%), 24 h (by 42%) and 72 h (by 38%). EB extravasation was decreased by DHA in the cortex and total hemisphere as well. FITC dextran leakage was reduced by DHA treatment on day 3 by 68% compared to the saline group. Treatment with NPD1, RvD2 and RvE1 significantly improved behavioral score (days 1, 3 and 7) and reduced total lesion volumes computed from T2WI images on day 7. Lipidomic analysis showed that DHA potentiates NPD1 synthesis in the penumbra 3 days after MCAo.

CONCLUSIONS: We have shown that administration of the DHA, novel docosanoids and pro-resolving mediators provide neurobehavioral recovery, diminish BBB damage, reduce brain infarction and brain edema, activate docosanoids synthesis in the penumbra and promote cell survival. These treatments might provide the basis for future therapeutics for patients suffering from ischemic stroke.

[LRR1]See previous comment.

295
BRAIN-0090
Symposium

Novel approaches to neuroprotection

OMEGA-3 FATTY ACIDS IN NEURODEGENERATIVE DISEASES: FOCUS ON MITOCHONDRIA

G. Eckert[1], S. Afshordel[1], S. Hagl[1], D. Werner[1], N. Röhner[2], D. Kögel[2], N.G. Bazan[3]
[1]Pharmacology, Nutritional Neuroscience Group, Frankfurt, Germany
[2]Neuroscience Center, Experimental Neurosurgery, Frankfurt, Germany
[3]LSU Neuroscience Center, Ophthalmology, New Orleans, USA

Objectives: The present study investigated the effects of orally administered long chain omega-3 polyunsaturated fatty acids (PUFA) on mitochondrial function and processing of the amyloid precursor protein (APP) in brains of young (3 months old) and

aged (24 months old) NMRI-mice.
Methods: Neuroprotective properties of fish oil (FO) (1,7 ml/kg p.o) were assessed ex vivo after 21 days in dissociated brain cells (DBC) and isolated mitochondria.
Results: Docosahexaenoic acid (DHA) levels were significantly lower in blood and brains of aged mice which was compensated by FO administration. Isolated DBC and mitochondria from aged mice showed significantly lower adenosine triphosphate (ATP) levels and reduced activity of complex I+II and IV of the mitochondrial respiration system, respectively. FO restored the age-related decrease in respiration and improved ATP production. Moreover, FO increased the levels of the anti-apoptotic Bcl-2 protein. Cell membrane fractions isolated from the brain of aged mice exhibited lower membrane fluidity, which was partially improved under FO treatment. In comparison to young animals, levels of neuroprotective sAPPα were significantly lower in the brain of aged mice. However, levels of sAPPα, Aβ and C-terminal APP fragments (CTF) were largely unchanged after FO treatment in aged mice. Neuroprotectin D-1 (NPD-1) represents a neuroprotective compound that is derived from unesterified DHA. Levels of NPD1-like metabolites (NPD1-like) and of unesterified DHA were significantly increased in brains of aged mice. FO treatment further strongly increased NPD1-like levels indicating an accelerated conversion rate of free DHA to NPD1-like.
Conclusions: Our findings provide new mechanisms underlying the neuroprotective actions of omega-3 PUFA and identified FO as promising nutraceutical to delay age-related mitochondrial dysfunction in the brain.
Reference: Afshordel S. et al. Prostaglandins Leukot Essent Fatty Acids (doi: 10.1016/j.plefa.2014.05.008)

298
BRAIN-0818
Brain Oral Communication

Oral Session: Imaging: Clinical

HEMODYNAMIC CHARACTERISTICS OF CEREBRAL ARTERIOVENOUS MALFORMATION FEEDER VESSELS WITH AND WITHOUT ANEURYSMS.

S.F. Shakur[1], S. Amin-Hanjani[1], H. Mostafa[1], F.T. Charbel[1], A. Alaraj[1]
[1]Neurosurgery, University of Illinois at Chicago, Chicago, USA

Objectives: Cerebral arteriovenous malformation (AVM) feeder aneurysm pathogenesis is poorly understood. Its association with high-flow states is largely based on anecdotal evidence of the high occurrence of aneurysms with AVMs and aneurysm regression following AVM obliteration.[1,2] Here, we measure flow, vessel diameter, and wall shear stress (WSS) in arterial feeders of AVMs with and without feeder aneurysms using quantitative magnetic resonance angiography (QMRA).

Methods: Records of patients with cerebral AVMs evaluated at our institution between 2007-2014 and with flow, vessel diameter, and WSS obtained before treatment using QMRA were retrospectively reviewed. AVMs were classified into groups with and without feeder aneurysms, defined as aneurysms arising from arteries supplying the AVM (A1, M1, or P1 segments). Flow, vessel diameter, and WSS were calculated for each arterial feeder and then compared between the two groups.

Results: 51 patients had AVMs without feeder aneurysms (76 arterial feeders) and 11 patients had AVMs with 12 feeder aneurysms (12 arterial feeders). Cohort characteristics are summarized in the Table. Mean AVM volume was higher among AVMs with feeder aneurysms but not significantly (16.7 vs. 11.5 mL, P=0.30). Absolute mean feeder artery flow (500.5 vs. 323.1 mL/min, P=0.02) and WSS (95.7 vs. 34.3 dynes/cm^2, P<0.001) were significantly higher in feeders with aneurysms. However, vessel diameter was similar between the two groups (3.9 vs. 3.7 mm, P=0.48). Multivariate analysis showed that WSS (P=0.004), but not flow (P=0.49) or diameter

(P=0.67), is predictive of presence of a feeder aneurysm. Linear regression demonstrated that higher flows were significantly associated with larger vessel diameter in AVM feeders with (R^2=0.63, P=0.004) and without aneurysms (R^2=0.67, P<0.001), and importantly, at most flow rates AVM feeders with aneurysms had smaller vessel diameters and subsequently higher WSS.

Conclusions: Arterial flow and WSS are significantly higher among cerebral AVM feeders with aneurysms, and so AVM feeder vessels with and without aneurysms are hemodynamically different. Despite the higher flows, feeder artery diameter was similar between the two groups, suggesting that AVM feeders with aneurysms are a subgroup in which vessel remodeling cannot compensate for increased blood flow.

References:

1. Redekop G, TerBrugge K, Montanera W, Willinsky R. Arterial aneurysms associated with cerebral arteriovenous malformations: classification, incidence, and risk of hemorrhage. *J Neurosurg*. 1998;89:539-546.
2. Kondziolka D, Nixon BJ, Lasjaunias P, Tucker WS, TerBrugge K, Spiegel SM. Cerebral arteriovenous malformations with associated arterial aneurysms: hemodynamic and therapeutic considerations. *Can J Neurol Sci*. 1988;15:130-134.

Table. Clinical and anatomical characteristics of AVMs with and without feeder aneurysms.

	Feeder aneurysms absent (51 patients)	**Feeder aneurysms present** (11 patients)
Clinical characteristics		
Mean age, years (range)	36 (16-70)	45 (25-72)
Hemorrhagic presentation (%)	25.5	9.1
Anatomical features		
Spetzler-Martin grade (% of cohort)	1 (18) 2 (39) 3 (23) 4 (12) 5 (8)	1 (37) 2 (27) 3 (18) 4 (9) 5 (9)
Mean volume, mL (range)	11.5 ± 14.6 (0.2-62.8)	16.7 ± 17.7 (0.9-54.0)

299
BRAIN-0588
Brain Oral Communication

Oral Session: Imaging: Clinical

DOES EXTREME PREMATURITY AFFECT ADULT BRAIN VESSEL COMPLIANCE? A PRELIMINARY MRI STUDY.

I. Huen[1], J. Beckmann[2], Y. Suzuki[3], M.A. Zuluaga[4], A. Melbourne[4], M.J.P. van Osch[5], D. Atkinson[6], S. Ourselin[4], N. Marlow[2], X. Golay[1]
[1]Institute of Neurology, University College London, London, United Kingdom
[2]Institute for Women's Health, University College London, London, United Kingdom
[3]Philips Medical Systems, Philips, Tokyo, Japan
[4]Centre for Medical Image Computing, University College London, London, United Kingdom
[5]C.J. Gorter Center for High Field MRI, Leiden University Medical Center, London, United Kingdom
[6]Centre for Medical Imaging, University College London, London, United Kingdom

Objectives: Elastin is a protein that increases blood vessel elasticity. Since elastin is deposited late in gestation, subjects born at extreme prematurity are thought to lack elastin in large arterial walls[1], leading to elevated blood pressure[2]. Would this be true in

the brain, longer lasting effects might include predisposition for neurovascular events or other small vessel disease-related problems. Therefore, the objective of this preliminary study was to investigate the hypothesis that adult preterm subjects have shorter blood arrival times from their neck to their brain than control subjects via magnetic resonance angiography of the Circle of Willis (CoW).

Methods: 5 preterm (3M/2F) (born <25 weeks completed gestation) and 5 age-matched term-born subjects (2M/3F) were scanned as part of the EPICure study[3] using a modified ECG-triggered CINEMA-STAR[4] sequence (12min) on a Philips 3T Achieva. All subjects were 19 years old. A slab 20mm inferior to the CoW was labelled using a STAR[5] labelling. Blood arrival was then monitored by TFEPI acquisition of 16 phases of 3D volumes spaced by 65ms.

Image processing was based on CoW angiography analysis by van Osch *et al.*[6]. Control volumes were subtracted from label volumes for all 16 phases. These were then corrected for label T_1 decay. For visualization of volumes, a 2D maximum intensity projection was taken in the axial plane for all 16 phases. For each pixel, the blood arrival time was defined as the phase at which signal increased most rapidly. Finally, non-vessel regions were removed from these blood arrival time maps using a vessel extraction method by Zuluaga *et al.*[7], limited to a single image modality.

In each subject, mean blood arrival times were measured in a region of interest drawn on the bilateral M1 and M2 segments of the medial cerebral artery, terminating at its bifurcation.

Results and Discussion: Blood arrival times are shown in the axial plane (Fig 1) for term and preterm subjects. Mean blood arrival times were significantly shorter (p = 0.044, t-test) in preterms (208ms ± 27ms) than terms (283ms ± 59ms) at the level considered. There was no significant difference (p = 0.43, t-test) between male (261ms ± 66ms) and female (229ms ± 52ms) subjects.

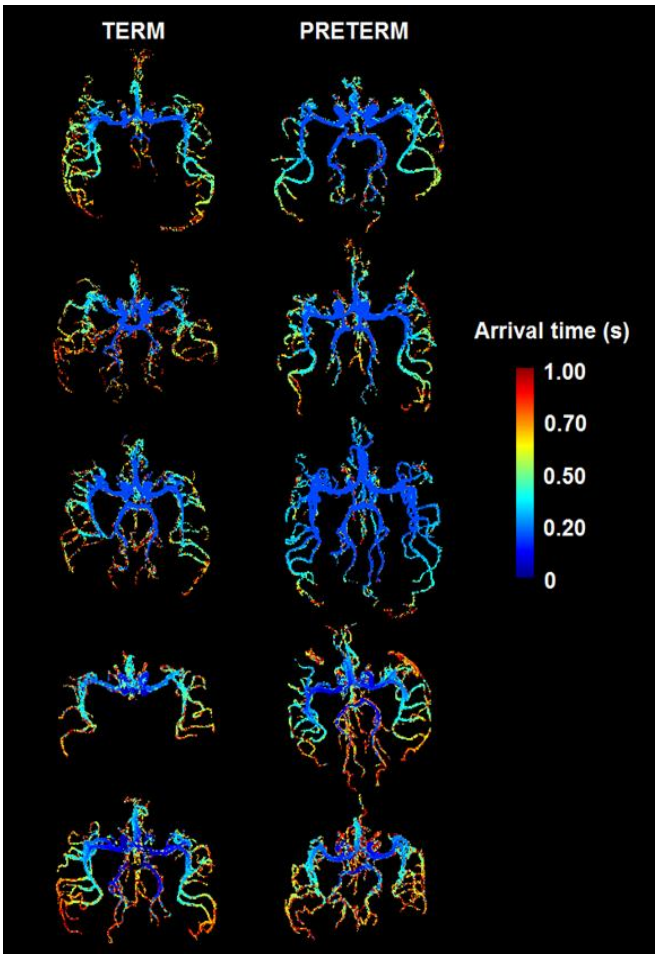

Figure 1. Blood arrival times (seconds) for each subject in axial MI projection.

Conclusions:

In this small group, cerebral blood arrival times have been found to be significantly shorter in preterm-born adults compared to terms. This is consistent with cerebral hypertension and reduced brain vessel compliance in this population, which may affect health outcomes. It also suggests that prematurity-induced reductions in compliance are not rectified at adulthood. Further studies with larger sample sizes would need to be undertaken to confirm these results.

References:

1. Bolton, C. E, et al.(2012). J. Pediatr. **161**(4):595-601.e592.
2. Martyn, C. N, et al.(1997). Lancet 350(9082):953-955.

3. Costeloe, K, et al.(2000). Pediatrics **106**(4):659-671.
4. Nakamura M, et al.(2011). Proc. ISMRM 19.
5. Edelman, R.R, et al.(1998). MRM **40**(6):800-805.
6. van Osch, M.J.P, et al.(2006). Medical Image Analysis **10**(1):59-70.
7. Zuluaga, M., et al.(2014). MICCAI 2014. **8674:**651-658.

300

BRAIN-0420

Brain Oral Communication

Oral Session: Imaging: Clinical

DEFINING THE ISCHAEMIC PENUMBRA WITH COMBINED METABOLIC AND PERFUSION MR IMAGING

G. Harston[1], P. Mathieson[2], I. Reckless[2], U. Schulz[2], K. Shah[2], Y.K. Tee[3], N. Blockley[4], T. Okell[4], F. Sheerin[5], S. Payne[3], P. Jezzard[4], M. Chappell[3], J. Kennedy[1]
[1]Radcliffe Department of Medicine, Oxford University, Oxford, United Kingdom
[2]Acute Stroke Service, Oxford University Hospitals NHS Trust, Oxford, United Kingdom
[3]Department of Engineering, Oxford University, Oxford, United Kingdom
[4]Nuffield Department of Clinical Neurosciences, Oxford University, Oxford, United Kingdom
[5]Department of Neuroradiology, Oxford University Hospitals NHS Trust, Oxford, United Kingdom

Objectives

The original description of the ischaemic penumbra asserted that both cerebral blood flow (CBF) and metabolism would be required to monitor therapeutic intervention in acute stroke (Astrup *et al* 1981). However, investigation of the ischaemic penumbra in patients has generally relied on perfusion-weighted imaging alone. pH-weighted imaging has aided the preclinical definition of the penumbra (Sun *et al* 2007), with proof of principle of this approach recently demonstrated in man (Harston *et al* 2015). The aim of this clinical MRI study was to use serial measurements of pH-weighted imaging, in addition to CBF, to improve the understanding of tissue outcome in patients with acute stroke.

Methods

Patients with non-lacunar ischaemic stroke underwent serial MRI over 1 month. The imaging protocol included single slice pH-weighted imaging (quantified using amide proton transfer ratio, APTR*), and vessel-encoded pseudocontinuous arterial spin labeling (ASL) to quantify CBF. Repeatability measures were quantified in healthy volunteers using coefficients of variation. Diffusion-weighted imaging, T1-weighted structural and FLAIR imaging were used to define the tissue outcome in grey and white matter: ischaemic core, infarct growth, and oligaemic tissue that survived. Images and masks were registered to native image spaces for voxelwise and patient-level serial analyses. Thresholds were calculated using ROC curve and Youden analyses.

Results

30 patients and 6 volunteers were included in this analysis. The repeatability of both CBF and APTR* demonstrated significant variation between healthy individuals ($p<0.0001$, $p=0.002$ respectively). Repeatability between time points was variable for CBF ($p<0.0001$), but not APTR* ($p=0.3$). Variability of CBF was within the accepted limits for ASL (<20%).

In the voxelwise analyses, the degrees of both hypoperfusion and acidosis were associated with tissue outcome in patients (<6hrs, ANOVA, $p<0.0001$). Presenting grey matter CBF predicted tissue at risk with an optimum threshold of 26ml/100g/min (AUC=0.70, sensitivity=73%, specificity=61%), and 24ml/100g/min for predicting acute infarction (AUC=0.74, sensitivity=77%, specificity=61%). The relationship between acidosis and tissue outcome was similar in grey and white matter.

In the patient-level analyses, neither hypoperfusion nor acidosis was significantly associated with tissue outcome ($p=0.1$, $p=0.07$ respectively). Patterns of serial CBF values within individuals were independent of tissue outcome. However, serial pH-weighted

imaging was most severely acidotic in the infarct core acutely, remaining abnormal at 24 hours. Infarct growth demonstrated acidosis acutely, and both acidosis and alkalosis at 24 hours. Oligaemic regions that survived all had normal pH by 24 hours. Dynamics of intracellular pH were not related to reperfusion status.

Conclusions

Both sequences generated data in voxelwise analysis consistent with preclinical data, demonstrating thresholds associated with tissue outcome. However, following patient-level analysis, issues of sequence repeatability and the diversity of an individual's response to ischaemia exposed the flaw of relying on a single parameter to define the ischaemic penumbra. These data strongly support Astrup's contention of the need to combine CBF and metabolic measures, in this case pH, to define the ischaemic penumbra in the clinical setting, and, hence, opportunities for therapeutic intervention.

References

Astrup (1981).*Stroke* 12:723-5
Harston (2015).*Brain* 138:36-42
Sun PZ (2007).*J Cereb Blood Flow Metab* 27:1129-36

301
BRAIN-0826
Brain Oral Communication

Oral Session: Imaging: Clinical

DETECTING FUNCTIONAL ACTIVATION SEPARATED BY PERIODS UP TO 4 WEEKS BY ARTERIAL SPIN LABELING

T. Ssali[1], U. Anazodo[1], Y. Bureau[1], J. Butler[1], M. Günther[2], K. St Lawrence[1]
[1]Imaging Program, Lawson Health Research Institute, London, Canada
[2], Fraunhofer Institute for Medical Image Computing M EVIS, London, Germany

Introduction: The ability of arterial spin labeling (ASL) to measure cerebral blood flow (CBF) independent of task frequency makes it attractive for longitudinal studies to follow disease progression or track treatment response[1]. However, ASL's poor spatial resolution and low signal-to-noise ratio makes image alignment from separate sessions difficult. Registration errors will reduce sensitivity by increasing variance and Type I errors. Variations in basal CBF can further reduce reproducibility over longer periods of time[2]. The aim of this study was to quantify between-session variance and demonstrate that with the appropriate steps, ASL can detect activation-induced changes in regional CBF over periods extending up to a month.

Methods: Seven right-handed volunteers (22.7 ± 1.3 years, 2 male) were scanned during three sessions separated by a week and a month. Registration errors between sessions were minimized by creating an immobilizing head mold for each subject during the first session, which was reused in the following sessions to replicate head position. Each session consisted of two sets of rest and sequential finger tapping task epochs (6 min, 48 label/control pairs). pCASL GRASE[3] images (1.5s label duration, 1.2s post-label delay, 24 axial slices, matrix = 64 x 64, FOV = 24cm) were acquired on a Siemens 3.0T Biograph system. Data were processed using SPM8 (UCL, London, UK). Variability and reproducibility of CBF were assessed using within-session coefficient of variance (wsCV) and intra-class correlation coefficient (ICC), respectively. In addition, statistical parametric maps were created from rest and task data acquired in the same session and from data acquired in different sessions (i.e. task and rest periods separated by a week and a month). To remove the variability in basal CBF, data were scaled by their respective resting grey-matter CBF. Areas of activation were identified after correction for multiple comparisons using the family-wise error rate ($p < 0.05$).

Results: ICC for within and between-session was 0.86 and 0.62, respectively, and wsCV was 9.1% and 10.0% respectively (Fig 1). Removing variability in basal CBF increased the within and between-session ICC to 0.873 and 0.781, and decreased the wsCV to 4.71% and 5.74% respectively. Absolute and normalized gray matter CBF activation maps from within and between-session analyses are shown in

Figure 2.

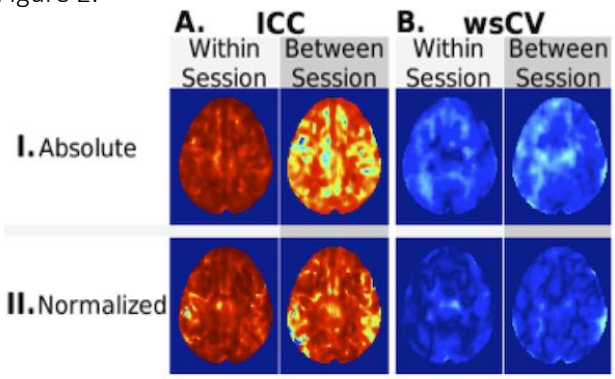

Figure 1: Within and between session (a) reliability and (b) variance in (i) absolute CBF and (ii) CBF normalized by resting grey matter flow.

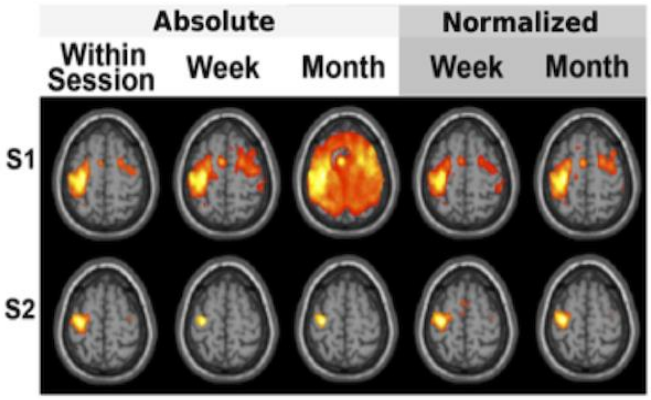

Figure 2: Within and between-session motor activation with absolute and normalized CBF

Discussion: Variance and ICC values were similar to other studies[4]. wsCV images showed some regional heterogeneity, but only a marginal increase when compared to between-session images. This is reflected in the comparison of activation maps generated from rest and activation images from the same session and from data acquired on separate days. The remarkable similarity in these maps after removing the variability in resting CBF indicates that registration errors between sessions were minimal. These results demonstrate the feasibility of conducting voxel-wise analysis of CBF images acquired on different days (in this case, a month apart) and highlight the potential of this technique for longitudinal studies.

[1] Borogovac. *J Cereb Blood Flow Metab* 2010:30;1721
[2] Chen *J Magn Reson Imaging* 2011;33:940
[3] Günther *Magn Reson Med* 2005;54:491
[4] Mezue *J Cereb Blood Flow Metab* 2014;163:1

302
BRAIN-0627
Brain Oral Communication

Oral Session: Imaging: Clinical

FUNCTIONAL HYPEREMIA OF THE VISUAL CORTEX IN EARLY STAGE ALZHEIMER'S DISEASE

R. Janik[1], S. Chaudhary[1], A. Dorr[2], A. Scouten[1], G. Schwindt[1], M. Masellis[3], G.J. Stanis[1], S.E. Black[4], B. Stefanovic[1]
[1]Medical Biophysics, University of Toronto, Toronto, Canada
[2]Imaging Research, Sunnybrook Research Institute, Toronto, Canada
[3]Institute of Medical Sciences, University of Toronto, Toronto, Canada
[4]Neurology, Sunnybrook Health Sciences Centre, Toronto, Canada

Objectives There is increased recognition of the importance of cerebrovascular impairment in the etiology and progression of Alzheimer's disease; however, early stage impairment in the stimulation-induced increase in focal cerebral blood flow, or functional hyperemia, is still incompletely understood, especially in the context of pharmacological interventions. While regional hypometabolism and hypoperfusion are frequently observed in AD patients, both potentiated and attenuated BOLD responses to functional stimulation have been reported. To elucidate the changes in the functional reactivity of the microvasculature, we examined the functional stimulation elicited changes in perfusion before and during treatment with cholinesterase inhibitors in early AD patients and healthy controls. We focused on examining the vascular function in the absence of neuronal impairment, thus interrogating the hemodynamic responses in the primary visual cortex, a region spared by the early AD pathology.

Methods Using pseudo continuous arterial spin labeling (PCASL) MRI, we conducted quantitative 3D mapping of both resting perfusion and visual stimulation elicited changes in cerebral blood flow

and BOLD fMRI signal in a cohort of early stage AD patients immediately prior to, 6-months post, and 12-months post commencement of open label cholinesterase inhibitor (ChEI) treatment. Their data were contrasted to those of age-, education-, and gender-matched healthy volunteers imaged over the same observation interval.

Results Prior to treatment, patients exhibited normal BOLD responses and resting perfusion, but visual stimulation elicited CBF response was decreased in the patients relative to controls (patients: 38±3 ml/100g/min; controls: 48±5 ml/100g/min; p<1e-3). Figure 1 displays stimulation-induced change in the absolute perfusion, in ml blood/100g of tissue/minute, overlaid on the corresponding T1-weighted anatomical scan in a healthy control (A) and an early stage AD patient (B) along with the corresponding perfusion time courses (C) and (D). Over the 12-months of ChEI treatment, the BOLD and resting perfusion remained unchanged, whereas the perfusion response declined in patients (-9.5±2.4 ml/100g/min/year; p<1e-3) but not in controls (p~0.06). The decrease in the perfusion response argues against a floor effect in the patients. This decline was not secondary to grey matter atrophy, drop in the activated tissue volume nor was it associated with a deterioration in cognitive performance, as assessed using ADAS-Cog error rates.

Conclusion This study represents the first step in disentangling the effects of AD pathology *vs.* those of cholinesterase inhibitors on vascular injury. The findings suggest that MRI-based measurements of functional hyperemia through absolute quantification of the visual stimulation-elicited perfusion response offer a robust and sensitive marker of the hemodynamic compromise in early stage AD which extends to regions conventionally considered as spared of the disease process.

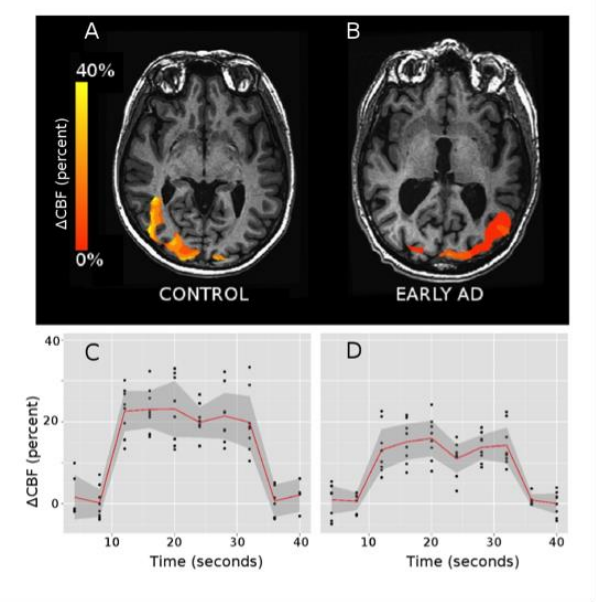

303
BRAIN-0035
Poster Session

Aging

DYSFUNCTION OF MOUSE CEREBRAL ARTERIES DURING EARLY AGING

M. Balbi[1], M. Ghosh[1], T.A. Longden[2], M. Jativa[3], B. Gesierich[1], F. Hellal[1], A. Lourbopoulos[1], M.T. Nelson[2], N. Plesnila[1]
[1]Institute for stroke and dementia (ISD), LMU, Munich, Germany
[2]Department of Pharmacology, University of Vermont, Burlington, USA
[3]Graduate School of Systemic Neuroscience (GSN), LMU, Munich, Germany

Objectives: Aging leads to a gradual decline in the fidelity of cerebral blood flow (CBF) responses to neuronal activation, resulting in an increased risk for stroke and dementia. However, it is currently unknown when age-related cerebrovascular dysfunction (ACD) starts or which vascular components and functions are first affected. The aim of this study was to examine the function of microcirculation throughout aging in mice.

Methods: Microcirculation was challenged by inhalation of 5 and 10% CO_2 or by forepaw

stimulation in six week-, 8 month-, and 12 month-old male FVB/N mice. The resulting dilation of pial vessels and increase in CBF was measured by intravital fluorescence microscopy and laser-Doppler fluxmetry, respectively. Neurovascular coupling and astrocytic end-foot Ca^{2+} were measured in acute brain slices from 18 month-old mice.

Results: We did not reveal any vascular dysfunction up to an age of 12 months. However, direct visualization of pial vessels by in vivo microscopy showed a significant, age-dependent loss of CO_2 reactivity and neurovascular coupling starting at 8 months.

Conclusion: These results suggest that aging does not affect cerebral vessels simultaneously, but starts in pial microvessels months before changes in CBF are detectable.

304
BRAIN-0452
Poster Session

Aging

DYNAMIC MAGNETISATION TRANSFER MRI: CARDIAC PULSATION IN AGING BRAIN TISSUE

D. López[1], E. Kehoe[1], D. Farrel[1], J. McNulty[2], P. Mullins[3], S. Joseph[1], A. Bodke[1], S. O'Mara[1], C.M. Kerskens[1]
[1]Lloyds Institute of Neuroscience, Trinity College Dublin, Dublin, Ireland
[2]School of Medicine & Medical Science, University College Dublin, Dublin, Ireland
[3]School of Psychology, Bangor University, Wales, United Kingdom

Objectives

The aging process profoundly impacts the brain and the heart at multiple levels, ranging from sub-cellular to macro-structural [1, 2]. In the brain, aging causes deterioration of neuronal and mitochondrial membranes, which leads to the loss of cellular integrity and impaired neuronal function [3]. At the same time, the cardiac dynamics are altered, which influences the brain metabolism. Here, we want to study the interplay between heart and brain in a new fashion. Our hypothesis is that using our method of ultrafast magnetisation transfer MR [4] we can measure water dynamics changes in brain tissue which depend on cell integrity and on cardiac pulsation.

Methods

The MRI sequence consists of a magnetisation transfer (MT) preparation phase followed by single-slice echo-planar imaging sequence. MT effect was introduced by a negative (-5236.8 ± 894.18 Hz) and a positive off frequency (6982.5 ± 894.18 Hz) RF pulse. Imaging parameters were voxel size of 3.5 x 3.5 x 3 mm, TR = 60 ms, TE = 18 ms, FA = 35 degrees and 3000 repetitions.

48 subjects (25 between 18 and 29 years old, and 23 over 65 years old) were scanned with the protocols approved by the local ethics committee.

Results

A comparison between the time series for both age groups is shown in figure 1a-b. In both cases, the time series of all the voxels across the slice were averaged to showcase the difference between populations. Strong cardiac constant peaks are resolved only for the young subjects while for the older subjects the strong cardiac peaks are diminished. The Fourier Transform of the time series was calculated in each case (Figure 1c-d). The frequency spectra for the young group present strong cardiac frequencies. However, the spectra for the older group show stronger harmonics or envelope waves or both, in addition to the weaker cardiac frequencies. The envelope waves have a beat frequency of the (cardiac frequency)/n, where n takes values of (2,3,4,6,9 ...). These results are consistent over all subjects.

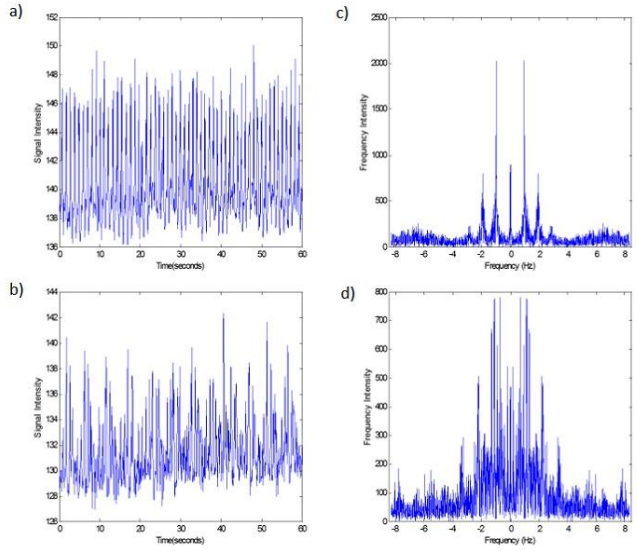

[Figure] Time series and frequency spectra for a young (a and c) and an old (b and d) subjects.

Conclusions

To our knowledge, the observation of a cardiac related MT change and its variation with aging has not yet been reported. Most likely, as the brain ages the deterioration of the cellular membranes lowers the magnitude of the exchange between the pool of free water and the macromolecules. Since the pressure wave is thought to interrupt this exchange [4], the effect of the pressure wave in the old age population diminishes. Taken together with the additional variation of the cardiac dynamics, the shape and number of frequencies in the spectra change between age groups. It is our understanding that using this method we can increase our knowledge of the interplay between heart and brain in aging.

References

[1] Allen, J.S., et al. *Neurobiol. Aging*. 2005; 26(9):1245-60.
[2] Salat, D.H. et al. *Cereb Cortex*. 2004; 14(7):721-30.
[3] Solsona-Sancho, C., et al. *Rev Neurol.* 1999; 29(11):1083-8.
[4] López, D., et al. *Brain & BrainPET2015.*

305
BRAIN-0153
Poster Session

Aging

REVERSAL OF BETA-AMYLOID-INDUCED NEUROTOXICITY IN PC12 CELLS BY CURCUMIN, THE IMPORTANT ROLE OF ROS-MEDIATED SIGNALING AND ERK PATHWAY

S. Zhang[1], K. Wang[2], Y. Hou[1], M. Yang[1], J. Sun[3], C. Fan[1], X. Fu[3], B. Sun[1]
[1]Key Lab of Cerebral Microcirculation in Universities of Shandong, Taishan Medical University, Taian, China
[2]Nursing Department, Taishan Vocational College of Nursing, Taian, China
[3]School of Basic Medicine, Taishan Medical University, Taian, China

Objectives: Progressive accumulation of beta-amyloid (Aβ) will form the senile plaques, caused oxidative damage and neuronal cell death, which was accepted as the major pathological mechanism to the Alzheimer's disease (AD). Hence, inhibition of Aβ-induced oxidative damage and neuronal cell apoptosis by agents with potential antioxidant properities represents one of the most effective strategies in combating human AD. Curcumin (Cur) a natural extraction from curcuma longa has potential of pharmacological efficacy, including the benefit to antagonize Aβ-induced neurotoxicity. However, the molecular mechanism remains elusive. The present study aim to evaluate the protective effect of curcumin against Aβ-induced cytotoxicity and apoptosis in PC12 cells and investigate the underlying mechanism.

Methods: Several methods of cell biology and molecular biology *in vitro* were employed.

Results: The results showed that curcumin markedly reduced Aβ-induced cytotoxicity by inhibition of mitochondria-mediated apoptosis through regulation of Bcl-2 family. The PARP cleavage, caspases activation and ROS-mediated DNA damage induced by Aβ were all significantly

blocked by curcumin. Moreover, regulation of p38MAPK and AKT pathways both contributed to this protective potency.

Conclusions: Our findings suggested that curcumin could effectively suppressed Aβ-induced cytotoxicity and apoptosis by inhibition of ROS-mediated oxidative damage and regulation of ERK pathway, which validated its therapeutic potential in chemoprevention and chemotherapy of Aβ-induced neurotoxicity.

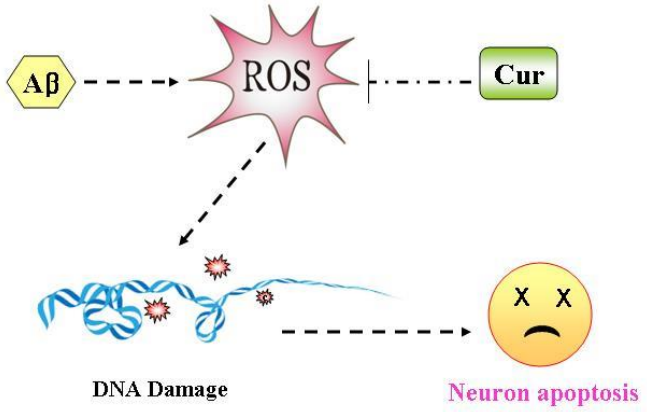

TOC Graphic: Oxidative stress signaling. Aβ triggered DNA damage and induced neuron apoptosis through ROS overproduction. However, curcumin rescued Aβ-induced DNA damage and neuron apoptosis by inhibition of ROS generation.

References:

1. Huang, H.C., Jiang, Z.F. Accumulated amyloid-beta peptide and hyperphosphorylated tau protein: relationship and links in Alzheimer's disease. J. Alzheimers. Dis. 2009, 16, 15-27.
2. Pagani, L., Eckert, A. Amyloid-Beta interaction with mitochondria. Int. J. Alzheimers. Dis. 2011, 925050.
The study was supported by the National Natural Science Foundation of China No.81471212, 81271275, 81070947, 30770759 to B.-L. Sun; Natural Science Foundation of Shandong No. ZR2012HZ006 to B.-L. Sun.
***Corresponding author**: Cun-dong Fan, Xiao-yan Fu, Bao-liang Sun, Tel: +86-538-6230027, E-mail: tsmc_nks@tsmc.edu.cn; blsun@tsmc.edu.cn; xyfu@tsmc.edu.cn

306
BRAIN-0436
Poster Session

Aging

ELICITATION THRESHOLD OF CORTICAL SPREADING DEPOLARIZATION INCREASES WITH BRAIN MATURATION AND ISCHEMIA

P. Hertelendy[1], *A. Menyhárt*[1], *T. Kiss*[1], *G. Tóth*[1], *Z. Ungvári*[2], *F. Bari*[1], *E. Farkas*[1]
[1]*Department of Medical Physics and Informatics F aculty of Medicine & Faculty of Science and Infor matics, University of Szeged, Szeged, Hungary*
[2]*Donald W. Reynolds Department of Geriatric Med icine Reynolds Oklahoma Center on Aging, University of Oklahoma Health Sciences Center, Oklahoma City, USA*

Objectives

Spreading depolarization (SD) is a wave of synchronized depolarization of neurons and glia cells, which propagates across the cerebral gray matter at a rate of 2–5 mm/min. SD is rapidly followed by a local hemodynamic response, the kinetics of which is characteristic of the metabolic state of the tissue. SD is associated with migraine aura, and also occurs in the vicinity of ischemic brain lesions, where it is considered to aggravate the initial damage. Even though age is a highly significant predictor of both migraine and stroke, very few studies investigated whether aging has an impact on SD evolution.

The major goal of this study was to determine the electric threshold of SD elicitation before and during incomplete forebrain ischemia in rats of various age groups of early adulthood.

Methods

Animal procedures were approved by the Ethical Committee for Animal Care of the University of Szeged adhering to national regulation. Male Sprague-Dawley rats (n=37, age groups: 7, 8, 9, 10, 12, 16 and 30 week-old) were anesthetized with isoflurane in N_2O:O_2. Both common carotid arteries were dissected for the latter induction of

incomplete forebrain ischemia by occlusion of the vessels (2VO). Two, separate craniotomies were created on the right parietal bone for SD elicitation and data acquisition. SDs were triggered by cathodal direct current stimulation of the dura, allowing the calculation of the exact amount of current delivered. To determine the threshold of an SD, the current was elevated stepwise, until SD was detected. SDs were identified using DC-and local-field potentials. SD related hemodynamic changes were recorded by Laser-Doppler flowmetry. In order to discriminate between the non-ischemic and ischemic threshold of SD elicitation, 3 SDs were elicited prior ischemia induction. Three additional SDs were elicited following 2VO.

Results

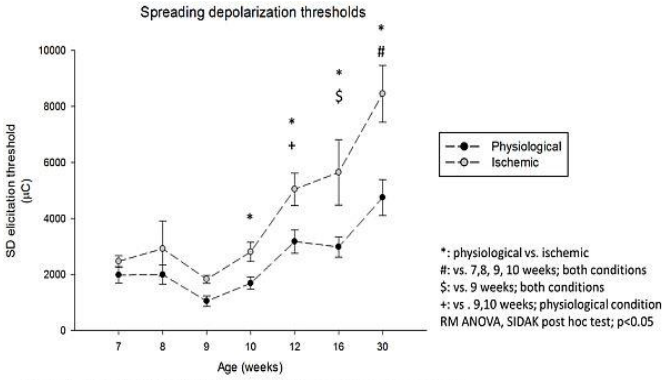

Figure 1.: Electrical threshold of SD elicitation in different age groups. Data are presented as mean±SEM.

The threshold of SD elicitation was higher during ischemia as compared with the non-ischemic condition in all age groups studied; statistical significance was found in the 10-30 week-groups. The threshold proved to be the lowest in the 9-week-old group, both for non-ischemic and ischemic SDs, being significantly lower than in the 12-30-week-old groups.

Conclusions

Our data demonstrate that the threshold to trigger SDs increases with progressing life time, as described previously in brain slices.[1] The susceptibility of the brain to SD may be determined by the gray matter's biochemistry and cytoarchitecture (e.g. density of dendritic spines, volume of extracellular space) that undergo adaptational changes with maturation. The threshold of SD elicitation also increased during ischemia, coinciding with earlier findings. [2] Since decreasing pH has been known to hinder SD evolution, acidosis created by ischemia is suggested to inhibit SD elicitation.

References

1. Maslarova, A., et al., *Chronically epileptic human and rat neocortex display a similar resistance against spreading depolarization in vitro.* Stroke, 2011. **42**(10): p. 2917-22.

2. Farkas, E., et al., *Effects of early aging and cerebral hypoperfusion on spreading depression in rats.* Neurobiol Aging, 2011. **32**(9): p. 1707-15.

Grant support: János Bolyai Research Scholarship of the Hungarian Academy of Sciences and The Hungarian Scientific Research Fund: OTKA K111923

307
BRAIN-0182
Poster Session

Aging

AGE-ASSOCIATED ALTERATIONS OF ANTIOXIDANT STATUS, CALCIUM HOMEOSTASIS AND GLUCOSE TRANSPORTER IN FEMALE RAT BRAIN: NEUROPROTECTIVE ROLE OF ESTRADIOL

P. Kumar[1], *R. Kale*[1], *N. Baquer*[1]
[1]*School of Life Sciences,*
Jawaharlal Nehru University, New Delhi, India

During normal aging, brain experiences structural, molecular, and functional alterations. Aging in females and males is considered as the end of natural protection against age related diseases like osteoporosis, coronary heart disease, diabetes, Alzheimer's disease and Parkinson's disease. Protection from age-related disorders is provided by several factors, including estrogens. These changes increase during menopausal condition in females when the level of estradiol is decreased. The objective of this study was to observe the changes in activities of superoxide

dismutase (SOD), glutathione S-transferase (GST), Ca^{2+}ATPase, intracellular calcium levels, DNA degradation and glucose transporter 4 (GLUT4) occurring in brains of female albino Wistar rats of 3 months (young), 12 months (adult) and 24 months (old) age groups, and to see whether these changes are restored to normal levels after exogenous administration of estradiol (0.1 µg/gm body weight for one month). The results obtained in the present work revealed that normal aging was associated with significant decrease in the activities of SOD, GST, Ca^{2+}ATPase and GLUT4 levels in the brains of aging female rats, and an increase in DNA degradation and intracellular calcium levels. Administration of E2 brought these changes to near normalcy. It can therefore be concluded that E2's beneficial effects seemed to arise from its antioxidant and antilipidperoxidative effects, implying an overall neuroprotective and anti-aging action. The results of this study will be useful for pharmacological modification of the aging process and applying new strategies for control of age related disorders.

308
BRAIN-0245
Poster Session

Aging

DELAYED INTRACRANIAL PRESSURE ELEVATION FOLLOWING ISCHEMIC STROKE IS PREVENTED BY EARLY AND SHORT HYPOTHERMIA TREATMENT IN AGED RATS

L. Murtha[1], R. Hood[1], D. Beard[1], D. Pepperall[1], D. McLeod[1], N. Spratt[1]
[1]School of Biomedical Sciences and Pharmacy, University of Newcastle, Newcastle, Australia

Objectives: Stroke is predominantly a senescent disease, yet the majority of preclinical studies investigate treatment on young animals. Intracranial pressure (ICP) is known to be a detrimental secondary complication of large 'malignant' stroke, however little is known about ICP regulation following small stroke. It is generally accepted that cerebral edema is the primary cause of ICP elevation. We recently demonstrated, however, that a significant ICP rise occurs despite small stroke and edema volumes in young rats, suggesting another mechanism is at play. Treatment options for ICP elevation are limited. Our studies demonstrated that a short duration of hypothermia-treatment completely prevented ICP elevation. Here, our aim was to investigate whether a similar ICP rise occurs in aged rats and determine whether short-duration hypothermia is an effective treatment in this cohort. Methods: Experimental stroke was performed on male Wistar rats aged 19-20 months. Shortly after stroke, rats were randomized to 2.5 hours hypothermia-treatment (32.5°C) or normothermia (37°C); n=6/group. ICP was monitored throughout and at 24 hours post-stroke. Results: ICP at baseline was 9.6 ± 3.8 mmHg and 11.8 ± 3.1 mmHg in the normothermic and hypothermia-treated group, respectively. ICP was significantly higher in normothermic animals compared to hypothermia-treated animals at 24 hours post-stroke, 24.8 ± 17.4 mmHg versus 8.0 ± 5.0 mmHg, p=0.05. Conclusions: These data confirm that this newly discovered phenomenon of ICP elevation at 24 hours post-stroke and the significant response to hypothermia is not restricted to young animals. We have also recently discovered that this ICP elevation results in a dramatic reduction in collateral blood flow, potentially worsening patient outcome. Consequently, these findings may have important implications for the use of hypothermia in clinical trials of aged stroke patients.

309
BRAIN-0160
Poster Session

Aging

AGING-ASSOCIATED INFLAMMATION IN THE VISCERAL ADIPOSE TISSUE AND THE BRAIN ARE REDUCED BY RESVERATROL

S.I. Jeong[1], J.A. Shin[1], E.M. Park[1]
[1]Pharmacology,
Ewha Womans University College of Medicine, Seoul, Korea

Objectives: We previously reported that resveratrol increased tight junction (TJ) protein levels in the blood-brain barrier (BBB) and reduced BBB breakdown after an ischemic insult in ovariectomized young female mice (Shin et al., *in press*). However, the protective effects of resveratrol should be verified in gonadally intact female animals during natural reproductive senescence. In addition to estrogen deficiency, one of aging signs is expansion of visceral adipose tissue with its inflammation that is linked with several metabolic diseases and cerebrovascular diseases (Farooqui et al., 2012). It has been reported that resveratrol reduces dysregulated inflammatory responses in adipose tissue, and thereby improves metabolic dysfunction (Siriwardhana et al., 2013). This study was performed to define resveratrol effects on inflammation of the visceral adipose tissue and ischemic brain damage in aged female mice.

Methods: Female C57BL/6 mice (20 months) were randomly divided into vehicle (0.2% ethanol) and resveratrol (0.1 mg/kg) treatment groups, and treated orally by gavage for 10 days starting 7 days before transient middle cerebral artery occlusion (MCAO). Behavioral tests (neurological score, hanging wire test and grip strength test) were performed before and 3 days after MCAO, and infarct volumes were measured 3 days after MCAO. Expression levels of Protein (SIRT1, PGC1α, claudin-5, occludin, CD86 and TNF-α) and mRNA (SIRT1, PGC1α, SOD, UCP2, IL-1β, IL-6 and TNF-α) in parametrial fat and the cortex of the brain were analyzed by Western blot and real-time PCR, respectively.

Results: Resveratrol increased the levels of SIRT1, PGC1α, SOD and UCP2 but decreased pro-inflammatory cytokines and activated macrophage M1 phenotype marker CD86 in visceral fat compared with vehicle. Also in the brain before ischemic insult, SIRT1, PGC1α, and TJ protein levels were increased while pro-inflammatory cytokines were decreased by resveratrol. Three days after MCAO, resveratrol reduced infarct volumes with better neurological outcomes, and pro-inflammatory cytokine levels in the visceral fat and the brain were decreased in resveratrol-treated mice compared with vehicle.

Conclusions: The findings showed that resveratrol ameliorated inflammatory responses in aged visceral adipose tissues and the ischemic brain. These beneficial effects of resveratrol might be mediated by activation of SIRT1 signaling pathway. The data suggest that resveratrol is useful in prevention and treatment for diseases implicated in aging processes in aged females.

Acknowledgements: This research was supported by the National Research Foundation of Korea (NRF) grant funded by the Ministry of Science, ICT & Future Planning (2010-0027945 and 2011-0015923).

References:

Farooqui AA, Farooqui T, Panza F, Frisardi V. Metabolic syndrome as a risk factor for neurological disorders. Cell Mol Life Sci. 69(5):741-62, 2012.

Siriwardhana N, Kalupahana NS, Cekanova M, LeMieux M, Greer B, Moustaid-Moussa N. Modulation of adipose tissue inflammation by bioactive food compounds. J Nutr Biochem. 24(4):613-23, 2013.

Shin JA, Oh S, Ahn JH, Park EM. Estrogen receptor-mediated resveratrol actions on blood-brain barrier of ovariectomized mice. Neurobiol Aging, *in press*.

310

BRAIN-0515

Poster Session

Aging

HUMAN ADIPOSE-DERIVED MESENCHYMAL STROMAL CELL ADMINISTRATION IMPROVES OUTCOME IN AGED STROKE MICE

E. Sammali[1], G. Boncoraglio[2], G. Cermisoni[1], F. Marchesi[1], F. Pischiutta[1], E. Parati[2], M.G. De Simoni[1], E.R. Zanier[1]

[1]Neuroscience, IRCCS - Istituto di Ricerche Farmacologiche Mario Negri, Milan, Italy

[2]Cerebrovascular Diseases,

Fondazione IRCCS Istituto Neurologico Carlo Besta , Milan, Italy

Objectives: Aging is a major risk factor for stroke incidence, post-ischemic mortality and severe and long-term disability. Mesenchymal stromal cells have been shown to improve functional outcome in young rodents after stroke, however data on aged ischemic rodents are extremely limited and controversial. Human adipose mesenchymal stromal cells (hADMSC) are a promising source for cell therapy and they can be easily harvested from patients by a simple and minimally invasive method. Studies in young rodents have shown that these cells improve functional outcome after stroke however their effect in aged mice has not been assessed so far. In this study we examined the effect of hADMSC, isolated from abdominal fat of patients, on aged mice after ischemic stroke.

Methods: Procedures involving animals and their care were conducted in conformity with the institutional guidelines that are in compliance with national and international laws and policies for ethical animal treatment. Aged C57Bl/6 male mice (12 months) were subjected to right transient middle cerebral artery occlusion (tMCAo, 30 min)[1]. PBS (control) or hADMSC ($1x10^6$ cells/300uL) were administered intravenously 24h after surgery. No animal died in either experimental groups for the whole duration of the experiment. Sensorimotor deficits were assessed weekly up to 4 weeks post-injury by composite neuroscore (NS) and rotarod, exploratory behavior was assessed at 3 weeks by open field test. Anatomical damage was assessed at 4 weeks. At the same time point the effects of hADMSC on non-neuronal cells was evaluated by quantification of the expression of GFAP for astrocytes, CD11b for microglia/macrophages and CD31 for endothelial cells.

Results: hADMSC significantly improved neurological function as shown by neuroscore (4 weeks, mean±SD: hADMSC 10.8±1.2, PBS 13.1±1.3, p<0.001) and rotarod (4 weeks: hADMSC 92.7±4.1%, PBS 76.6±11.2%, p<0.001) tests, with no difference in exploratory behavior. hADMSC induced a significant rescue effect on ipsilateral vs contralateral cortical neurons assessed by cresyl violet staining (neuronal count: hADMSC 95.4±7.6%, PBS 76.6±11.9%, p<0.01). No major effect on atrophy was detected by conventional histology. A selective increase in GFAP stained area in the ipsilateral cortex (hADMSC 1.5±0.4%,PBS 0.6±0.3%, p<0.01) and striatum (hADMSC 7.5±0.6%, PBS 5.3±0.9%, p<0.001), compared to PBS was observed, with no differences on the other examined cell populations.

Conclusions: hADMSC, administered 24h after injury, significantly improve functional deficits and histological damage in aged stroke mice. hADMSC induced reactive astrocytosis may contribute to the observed protection by improving post-ischemic healing thus limiting neuronal loss in the perinfarct area.

References:

1. Zanier ER et al., CNS Neurosci Ther. 2013.

311
BRAIN-0657
Poster Session

Aging

LONG-TERM RELATIONSHIP OF SERUM BRAIN-DERIVED NEUROTROPHIC FACTOR WITH CEREBRAL BLOOD FLOW AND COGNITION IN COGNITIVELY NORMAL ELDERS

C. Sarles[1], H. Aizenstein[2], C. O'Hare[3], A. Rosso[1], L. Launer[4], S. Kritchevsky[5], K. Yaffe[6], A. Newman[1], C. Rosano[1]
[1]Epidemiology,
University of Pittsburgh Graduate School of Public Health, Pittsburgh, USA
[2]Psychiatry, University of Pittsburgh, Pittsburgh, USA
[3]Medical Gerontology, Trinity College Dublin, Dublin, Ireland
[4]Neuroepidemiology Section,
National Institute on Aging, Bethesda, USA
[5]Sticht Center on Aging,
Wake Forest School of Medicine, Winston-Salem,

USA
[6]Psychiatry, University of California San Francisco, San Francisco, USA

OBJECTIVES: Among older adults, lower brain-derived neurotrophic factor (BDNF) is associated with poorer visuospatial memory and executive function and with stroke, transient ischemic attack, and greater white matter hyperintensity volume. However, most existing studies examining cerebral blood flow (CBF) report cross-sectional or short-term relationships for adults with a range of cognitive impairment. We assess the long-term relationship of BDNF with resting cerebral perfusion among cognitively normal older adults. We hypothesized that lower serum BDNF is associated with poorer performance on cognitive tests of spatial memory and executive function and with lower CBF, as measured by arterial spin labeling (ASL).

METHODS: This study was approved by the Institutional Review Board, and all participants signed written informed consent. Complete data on BDNF in 1999-2000 and magnetic resonance imaging with ASL and cognitive testing in 2006-08 were obtained in 21 participants in the Health, Aging, and Body Composition study who were free of prevalent stroke and of cognitive impairment or dementia at time of MRI (mean age=83, 68% women, 47% black). Delayed recall of the modified Rey-Osterrieth figure and Trails B completion time were used to evaluate performance in spatial memory and executive function. ASL was obtained as averages from regions known to be vulnerable to lower perfusion and/or related to performance in spatial memory and executive function: fronto-parietal (dorsolateral prefrontal cortex, superior parietal lobule) and subcortical networks (hippocampal formation, amygdala, cingulate cortex, basal ganglia). Correlations of BDNF with CBF and cognition were adjusted for gender and gray matter atrophy.

RESULTS: Lower BDNF was associated with longer time to complete Trails B (rho= -0.77; p<0.001), but was not significantly associated with the Rey figure delayed recall. Higher BDNF was associated with lower CBF in subcortical regions: posterior cingulate cortex bilaterally; insula, putamen, thalamus and amygdala in the left hemisphere; and dorsal cingulate cortex in the right hemisphere (Table 1). Associations with cortical regions and hippocampal formation were not significant.

CONCLUSIONS: In cognitively normal elders, poorer Trails B performance and higher CBF in predominantly subcortical regions associated with executive control function and memory are correlated with lower BDNF levels nine years prior. The negative correlations of BDNF with CBF run counter to our hypothesis. Because BDNF helps to maintain homeostasis in the neurovascular unit, it is possible that increased levels of BDNF are marshaled to maintain neural functioning in the face of lower CBF that can accompany aging. It is also possible that those elders who survived to study entry and follow-up assessment despite low BDNF levels are those who are remarkably resilient as marked by high CBF years later. Thus, future work should evaluate survivor bias and incorporate repeated measures to assess change over time.

Table 1. Brain regions with significant correlations of brain-derived neurotrophic factor and resting cerebral blood flow.

Region	Correlation	P-value
Posterior cingulate (left)	-0.54	0.02
Posterior cingulate (right)	-0.59	0.01
Insula (left)	-0.48	0.04
Putamen (left)	-0.47	0.04
Thalamus (left)	-0.46	<0.05
Amygdala (left)	-0.49	0.03
Dorsal cingulate cortex (right)	-0.51	0.03

Note: Correlations adjusted for gender and gray matter atrophy.

312
BRAIN-0711
Poster Session

Aging

CHARACTERIZATION OF AGE-RELATED CHANGES IN MICROGLIA/MACROPHAGE POLARIZATION AND FUNCTIONAL OUTCOMES IN A MOUSE MODEL OF ISCHEMIC STROKE

J. Suenaga[1], X. Hu[1], H. Pu[1], S.H. Hassan[1], J. Chen[1]
[1]Neurology,
Department of Neurology University of Pittsburgh, Pittsburgh, USA

Objectives;

One reason for thefailure of translating the successes in stroke models to the clinical applications is that themajority of experimental stroke studies have used young adult animals, whilestroke in humans mainly afflicts the elderly. It is therefore necessary toinvestigate the different pathological changes after stroke in young and oldanimals, and elucidate how these differences contribute to stroke outcomes. Inthe present study, we investigated the difference between aged and young micein their responses to ischemic challenge, focusing on infarct volume, long termfunctional outcomes, and M1-M2 polarization of microglia/macrophage.

Methods;

Young (2 monthold) or aged (18 month old) male mice were subjected to permanent tandemocclusion of left distal middle cerebral artery (dMCAO) and ipsilateral commoncarotid artery (CCA). Sensorimotor and cognitive behavioral tests wereperformed up to 35d after stroke. Infarct volumes were quantified at 2d afterstroke. The expression of M1 (CD16 and CD32) and M2 (CD206 and Arg1) markers wasexamined by immunohistochemical stainings and reverse-transcriptase polymerasechain reaction (RT-PCR) at 1, 3,7, 14 and 35d after stroke.

Results;

Brain infarct at2d after stroke was significantly larger in aged mice as compared to youngadults (young 15.6±2.3 vs aged 20.7±1.8%, $p<0.01$). Remarkably, aged miceexhibited more severe long-term sensorimotor deficits, as manifested bydeteriorated performance in rotarod and hang wire tests up to 35d stroke. The agedmice also showed significantly worse long-term cognitive deficits as measured byMorris water maze test at 21d after stroke. RT-PCRand immunohistochemistry staining of M2 or M1 markers revealed a similar trendof change in microglia/macrophage polarity after stroke between young and agedmice. The expression of M2 markers peaked around 7d after stroke and theexpression of M1 markers peaked later around 14-21d after stroke, suggesting aM2-to-M1 phenotype shift with the progress of stroke. Interestingly, the agedmice exhibited a trend of reduced extent of M2 polarization after stroke ascompared to young adults.

Conclusions;

This distal MCAOmodel of stroke consistently result in ischemic brain injury with very lowmortality and long-term behavioral deficits, and therefore is suitable for theevaluation of long term stroke outcome. The aged mouse exhibits deterioratedfunctional outcome after stroke, which might associated with reduced M2microglia/macrophage polarization.

313
BRAIN-0684
Poster Session

Neurodegeneration

CARRIER MEDIATED DELIVERY SYSTEM BEARING DOPAMINE FOR EFFECTIVE MANAGEMENT OF PARKINSONISM

S. Bhargava[1], V. Bhargava[2]
[1]Department of Pharmacy,
Manav Bharti University, Kanpur, India
[2]R&D, KRV Hospitals Pvt. Ltd., Kanpur, India

Delivery of drug and sustaining it in effective concentration in brain is challenging due to blood brain barrier. In the present investigation, amino acid coupled liposomes bearing dopamine-HCl were prepared to deliver drug to the brain utilizing receptor-mediated transcytosis for effective management of parkinsonism.

L-lysine stearylamine conjugate (LSC) was synthesized & LSC coupled liposomes bearing dopamine HCl was prepared by lipid cast film method. Formulations were analyzed for average vesicle size, drug entrapment, *in-vitro* drug release and *in-vivo* efficacy of the formulations was assessed by measuring the reduction in the degree of drug induced catatonia in albino rats.

Average particle size was found in the range of 1.92-0.80 mm. There was increase in the size for coupled liposomes due to the inclusion of LSC in liposomal bilayers. The percent encapsulation efficiency decreased from 46.82±2.17% in uncoupled to 38.13±1.18% in coupled liposomes. The *in-vitro* drug release after 24hrs was 58.9±2.94% with uncoupled while the coupled liposomes showed 43.7±2.18% drug release. The lower value for coupled formulation could be due to the retardation of drug release caused due to the incorporation of LSC in the liposomal bilayers, which enhanced the structural integrity of the bilayer. *In-vivo* study reveals that the animals receiving uncoupled liposomes showed partial reduction and animals that received coupled liposomes showed almost complete reduction in catatonia.

Fluoresence study clearly indicates the uptake of 6-CF in blood vessels and accumulated in brain. This could be due to enhanced uptake of Lysine coupled liposomes through amino acid transporters present at BBB surface.

314
BRAIN-0142
Poster Session

Neurodegeneration

ALTERATIONS OF BRAIN MORPHOLOGY AND ENERGY METABOLISM UNDERLYING MEMORY DETERIORATION IN INSULIN-RESISTANT GOTO-KAKIZAKI RATS

F.M. Girault[1], R. Gruetter[1], J.M.N. Duarte[1]
[1]Laboratoire d'imagerie fonctionnelle et métaboliq ue, Ecole polytechnique fédérale de Lausanne, Lausanne, Switzerland

Objectives: Impaired insulin signalling in diabetes deteriorates brain structure and function leading to cognitive deficits. While the neurodegeneration process has been largely studied in diabetes, early metabolic modifications associated to such events remain to be elucidated. Aiming at identifying early biomarkers of diabetic encephalopathy, we performed a multimodal magnetic resonance imaging (MRI) and spectroscopy (MRS) study in insulin-resistant Goto-Kakizaki (GK) and Wistar rats.

Methods: After assessing spatial memory performance by measuring spontaneous alternation in a Y-maze [1], T_2-weighted MRI and ^{1}H MRS were performed as previously [2] in the brain of GK (n=8) and Wistar (n=12) rats anesthetised with isoflurane (1-2% in O_2) at 2, 4 and 6 months of age, on a 14.1 T spectrometer with a ^{1}H quadrature surface coil. At 6 months, ^{13}C MRS was acquired under α-chloralose anaesthesia, during [1,6-^{13}C]glucose infusion, with a ^{1}H quadrature coupled to a ^{13}C single loop surface coil [3]. ^{13}C spectra were acquired using semi-adiabatic DEPT combined with ^{1}H localization [4].

Results: Compared to controls, GK rats displayed smaller hippocampus (-19±1%, P<0.0001), cortex (-10±2%, P<0.0001) and whole brain (-10±1%, P<0.0001), at all ages. In contrast, the ventricular volume in GK rats was larger than controls and increased strongly with age (from +45±9% to +92±6%, P<0.0001). Hippocampal and cortical

neurochemical profiles were affected by insulin resistance: out of 20 metabolite concentrations, GK rats displayed significantly higher taurine (+13±3%, P<0.0001) and ascorbate (+44±8%, P<0.0001), and reduced glutamine (-23±5%, P<0.0001), choline (-14±5%, P<0.0001), phosphorylethanolamine (-19±5%, P<0.0001), *myo*-inositol (-7±2%, P<0.01), alanine (-24±7%, P<0.001), and *N*-acetylaspartylglutamate (-12±5%, P<0.01) in the hippocampus; and higher taurine (+9±6%, P<0.05), and reduced glutamine (-20±3%, P<0.0001), choline (-19±5%, P<0.0001), phosphorylethanolamine (-21±8%, P<0.01), and aspartate (-20±6%, P<0.001) in the cortex. Hippocampal-dependent spatial memory performance was impaired in GK rats, depicted by the reduced spontaneous alternation relative to controls (-18±5%, P<0.0001). Spontaneous alternation correlated to hippocampal concentrations of ascorbate (r=-0.46, P<0.001), glutamine (r=0.37, P<0.01) and taurine (r=-0.32, P<0.01). Mathematical modelling of the ^{13}C enrichment of glucose, glutamate, glutamine and aspartate upon [1,6-^{13}C]glucose infusion revealed that insulin resistance caused mitochondrial oxidation rate to be reduced in neurons (-16±2%, P<0.001) but increased in astrocytes (+25±3%, P<0.001). Additionally, both glutamatergic neurotransmission (-19±2%, P<0.001) and glutamine synthesis (-16±2%, P<0.001) were reduced in the brain of GK rats compared to controls. Rates of brain glucose transport and consumption were similar in GK and Wistar rats, indicating that diabetic rats are exposed to higher brain glucose levels due to hyperglycaemia.

Conclusions: Insulin-resistance impaired brain energy metabolism and reduced glutamate-glutamine cycle between neurons and astrocytes. This led to neurochemical alterations that were associated with the degree of brain dysfunction, namely impaired memory performance in diabetes.

References: [1] Duarte *et al*. (2012) PLoS ONE 7:e21899. [2] Duarte *et al*. (2009) J Neurochem 111:368. [3] Duarte *et al*. (2011) Front Neuroenergetics 3:3. [4] Henry *et al*. (2003) MRM 50:684.

This work was supported the Swiss National Science Foundation (grant 148250), and the Centre d'Imagerie BioMédicale (CIBM) of the UNIL, UNIGE, HUG, CHUV, EPFL and the Leenaards and Jeantet Foundations.

315
BRAIN-0285
Poster Session

Neurodegeneration

ALTERED THALAMIC GLUCOSE METABOLISM IN PARKINSON'S DISEASE

C. Eggers[1], Y. Nahhas[1], E. Pelzer[1], L. Timmermann[1]
[1]Neurology, University Hopsital, Köln, Germany

Background: The thalamus is the main relay station in the basal ganglia circuitry and the key output pathway for basalganglia-cortex loops. Pathophysiological alterations of thalamic nuclei play a critical role in the development of parkinsonian symptoms like akinesia or rigidity.

Historically, these changes have been conceptualized as a consequence of nigral degeneration; nowadays there is also histopathological evidence that suggests a direct pathology of thalamic nuclei in PD disease. Recent imaging studies could show an increased glucose metabolism in the total thalamus. However, these latest imaging findings did not consider the organization into distinct nuclear regions. Due to the different involvement of thalamic subnuclei we wanted to precise the involved regions by analysis of the glucose metabolism in parkinsonian patients.

Methods: In total 28 akinetic-rigid PD patients and 11 healthy controls were examined with high resolution 18-Fluoro- deoxyglucose PET-imaging. An in-house created VOI-atlas was used to define the local metabolism in the total thalamus and thalamic subnuclei. The VOIs of the atlas were used to calculate the rCMRGlc in the regarding regions. Results for the overall thalamic uptake and the uptake in the thalamic sub nuclei were compared between parkinsonian patients and healthy controls.

Results: Analysis of glucose metabolism revealed a bilaterally increased metabolism in the PD group for the total thalamus in all nuclei except the left dorsal medial nucleus, the left and right nucleus anterior. Statistical analysis showed significantly higher glucose metabolism for the following subnuclei: bilateral ventral lateral nuclei, ventral posterior lateral nuclei and the left nucleus anterior.

Conclusion: The ventrolateral nuclei and the ventral posterior lateral nuclei showed an increased glucose metabolism in PD patients compared to healthy controls. These findings argue for a critical (maybe compensatory) role of the thalamus as a major relay station in the striatothalamocortical network and against a direct disease pathology.

316
BRAIN-0362
Poster Session

Neurodegeneration

REPRODUCIBILITY OF ABNORMAL BRAIN METABOLISM ASSOCIATED WITH PROGRESSIVE SUPRANUCLEAR PALSY: NETWORK AND REGIONAL COMPARISONS BETWEEN A US AND A CHINESE COHORT

J. Ge[1], J. Wu[2], S. Peng[3], P. Wu[1], J. Wang[2], D. Eidelberg[3], C. Zuo[1], Y. Ma[3]
[1]PET center, Huashan Hospital, Shanghai, China
[2]Department of Neurology, Huashan Hospital, Shanghai, China
[3]Center for Neurosciences, Feinstein Institute for Medical Research, Manhasset New York, USA

Objectives

PET with FDG has been used for identification of disease-specific metabolic brain networks associated with parkinsonian disorders (1-3). We have previously shown that brain network and its expression in idiopathic Parkinson's disease were highly reproducible across the patient populations and tomographs (4). In this study, we aimed to evaluate the reproducibility of disease-specific brain network and regional cerebral metabolism associated with progressive supranuclear palsy (PSP) by comparing clinically-confirmed patients with PSP in a US and a Chinese cohort.

Methods

The US cohort consisted of 10 patients with PSP and 10 age-matched healthy controls scanned on a GE Advance PET camera. The sample size was the same in the Chinese cohort scanned on a Siemens Biogragh 64 PET/CT system in China. The study at each site was approved by the respective IRB for which the subjects had signed written informed consent. We first used the network analysis to identify a PSP-related metabolic pattern (PSPRP) in each cohort and computed the corresponding network scores prospectively in the other cohort. We also localized the regions with abnormal metabolic differences in the same sets of FDG PET images by using conjunction and interaction analyses with SPM. The reproducibility of PSP-specific network and metabolic distribution was examined across the study populations, PET instruments and analytical approaches.

Results

Both cohorts revealed similar PSPRPs characterized by metabolic decreases in the medial prefrontal cortex/cingulate, ventrolateral prefrontal cortex, striatum, medial thalamus, and midbrain, along with covarying metabolic increases in the hippocampus and parieto-temporal regions. PSPRP scores were similarly elevated ($P<0.0001$) in the patients relative to the controls in the derivation cohort in the USA and in the validation cohort in China or vice versa. PSPRP scores correlated strongly ($R\geq0.96$; $P<0.001$) in the two corresponding cohorts of patients and healthy controls from the USA and Chinese sites, respectively.

We observed that PSP patients from two cohorts shared a great number of overlapping areas with regional metabolic abnormalities in both cortical and subcortical areas (FWE $P<0.05$). Relative

metabolism decreased in the medial prefrontal cortex/cingulate, ventrolateral prefrontal cortex, striatum, medial thalamus, and midbrain but increased in the hippocampus and parieto-temporal regions. Volume of interest analyses confirmed the significant group differences (P<0.001) in these brain regions.

Conclusion

This study demonstrated the high comparability and reproducibility of PSP-related brain network and regional metabolism across patient populations, tomographs and imaging techniques. Activity of this brain network may serve as a reliable and objective marker of PSP for clinical applications.

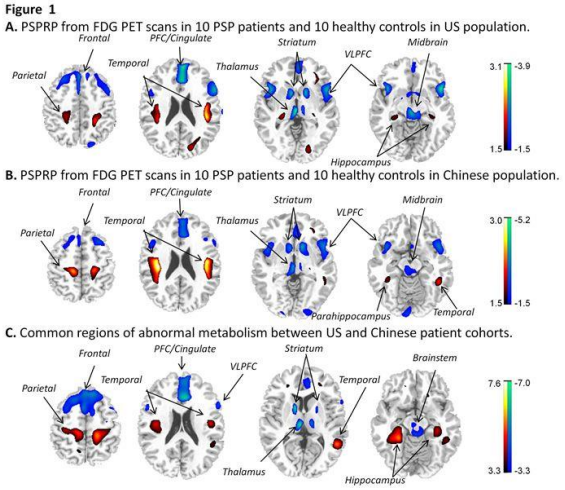

References:

1. Ma Y, Tang C, Spetsieris PG, et al. Abnormal metabolic network activity in Parkinson's disease: test-retest reproducibility. J Cereb Blood Flow Metab. 2007; 27:597-605.

2. Eckert T, Tang C, Ma Y, et al. Abnormal metabolic networks in atypical parkinsonism. Mov Disord 2008; 23: 727-733.

3. Teune LK, Renken RJ, Mudali D, et al. Validation of parkinsonian disease-related metabolic brain patterns. Mov Disord 2013;28:547-551.

4. Wu P, Wang J, Peng S, et al. Metabolic brain network in the Chinese patients with Parkinson's disease based on (18)F-FDG PET imaging. Parkinsonism Relat Disord 2013; 19: 622-627.

317
BRAIN-0495
Poster Session

Neurodegeneration

DIFFERENT RATES OF DOPAMINE TRANSPORTER LOSS IN PARKINSON'S DISEASE AS MEASURED WITH [123I]B-CIT AND [123I]FP-CIT SPECT

J. Hannestad[1], J. Seibyl[2], K. Marek[2], M. Laruelle[3], R. Gunn[4]
[1]Global Exploratory Medicine, UCB Pharma, Braine l'alleud, Belgium
[2]Molecular NeuroImaging, Institute for Neurodegenerative Disorders, New Haven, USA
[3]Neuroscience, Intracellular Therapies Inc, New York, USA
[4]Imanova Ltd, Imperial College London, London, United Kingdom

OBJECTIVES: Progressive loss of dopamine transporter (DAT) density in Parkinson's disease (PD) is well established and considered a biomarker of the underlying dopamine neuron loss. In large, longitudinal studies with [^{123}I]β-CIT SPECT in early PD (CALM-PD[1]; ELLDOPA[2]; PRECEPT[3]), the annualized rate of loss in the striatum was approx. 5%, while in studies using [^{123}I]FP-CIT SPECT in similar patients (PROUD[4], PPMI[5]) the annualized rate of loss was approx. 12%. The explanation for this apparent discrepancy is not known.

METHODS: In the absence of input function data and the possibility to explore kinetics of the two tracers directly, data from Seibyl[6] were used. In that study, control and PD subjects were scanned with both [^{123}Iβ-CITand [^{123}I]FP-CIT to obtain the SUR ratio with the occipital lobe as the reference region. Under the assumption that the SUR is directly proportional to the binding potential (BP_{ND}), one would expect a linear relationship

between the two tracers across subjects and regions intercepting at the origin according to,

$$BP_{ND}^{\text{b-CIT}} = \frac{K_D^{\text{FP-CIT}}}{K_D^{\text{b-CIT}}} \frac{f_{ND}^{\text{b-CIT}}}{f_{ND}^{\text{FP-CIT}}} BP_{ND}^{\text{FP-CIT}}$$

where K_D is the tracer affinity and f_{ND} is the tracer tissue free fraction. The BP_{ND} measures were plotted against each other and their relationship investigated.

RESULTS: Plotting the BP_{ND} measures against each other yielded a linear relationship, but with a positive y-intercept (Figure 1a). Transformation of the derived linear regression enabled the measured reduction in [^{123}I]β-CIT to be expressed in terms of the measured reduction in [^{123}I]FP-CIT (Figure 1b). Linear regression showed that one should expect [^{123}I]β-CIT to underestimate [^{123}I]FP-CIT in the control population by 22.5% and in the PD population by 44.2%. Applying this correction factor to the rates of loss observed in the longitudinal studies in PD shows that the rates of decline of the actual specific binding are equivalent. What is not known is which tracer is biased. Any kinetic effect is unlikely to explain the difference, as the regression line is straight. A difference in selectivity (e.g. vs. the serotonin transporter) or a metabolite that is taken up heterogeneously across regions are more likely explanations for the observed bias.

CONCLUSIONS: In order for DAT imaging to be a useful biomarker of disease progression in disease-modifying trials in PD, ideally the change in DAT imaging over time would closely parallel the underlying change in pathology. At this time, it is unclear which of [^{123}I]β-CIT or [^{123}I]FP-CIT provides the best estimate of the underlying pathology. Longitudinal studies with other DAT tracers (e.g. [^{11}C]PE2I) may be useful to clarify this question.

REFERENCES

1 The Parkinson Study Group. JAMA 2002 287:1653-61(CALM-PD)
2 The Parkinson Study Group. N Engl J Med 2004 351:24 (ELLDOPA)
3 Marek and Parkinson Study Group. Neurology. 2014 82:1791-7 (PRECEPT)
4 Schapira et al. Lancet Neurol 2013 12:747-55 (PROUD)
5 Seibyl and PPMI Investigators. J Nucl Med May 2014 55:304
6 Seibyl et al. J Nucl Med 1998 39:1500-8.

Fig 1

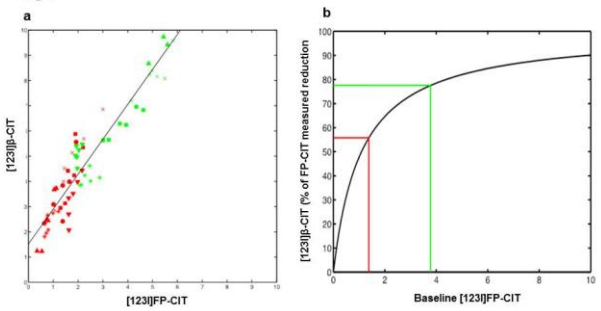

Legend:
(a) Plot of SUR-derived estimates of BPND for [123I]β-CIT against [123I]FPCIT across different regions for healthy control (green) and PD (red) subjects. Different symbols represent individual subjects. Regression line is [123I]β-CIT BP_{ND} = 1.386 [123I]FPCIT BP_{ND} + 1.517
(b) Plot of the predicted [123I]β-CIT measured reduction in signal as a function of the [123I]FPCIT measured reduction. The green line denotes the expected reduction from the mean control population (77.5% lower measure of change for [123I]β-CIT in comparison to [123I]FPCIT) and the mean Parkinson's population (55.8% lower measure of change for [123I]β-CIT in comparison to [123I]FPCIT).

318
BRAIN-0558
Poster Session

Neurodegeneration

LOCALIZATION OF THE SIGMA-2 RECEPTOR/PGRMC1 IN NEURONS AND GLIA

R. Mach[1], *C. Zeng*[1], *N. Garg*[1]
[1]*Radiology, University of Pennsylvania, Philadelphia, USA*

Objectives. A recent report demonstrated that the sigma-2 receptor/PGRMC1 is a potential receptor for amyloid- beta (Abeta) oligomers in rat primary neurons. Sigma-2 antagonists were also shown to block the binding of Abeta in neurons and reduce Abeta-induced neuronal toxicity (1). However, very little is known about the distribution of the sigma-2 receptor/PGRMC1 within the CNS. The goal of this study to compare the relative expression of the sigma-2 receptor /PGRMC1 protein levels by immunohistochemistry and staining using a

sigma-2 fluorescent probe (SW120) in primary cultures of neurons, astrocytes, oligodendrocytes and microglia cells.

Methods. Hippocampal cells were plated onto Poly L-Lysine (PLL)-coated coverslips in 24-well plates at 100,000 cells per well or 6-well plastic plates at 750,000 cells per well and cultured in Neurobasal medium supplemented with B27, penicillin, and streptomycin. Medium was partially replaced every 7 days. Two week old neurons were used for immunocytochemistry studies. Microglia cells were plated onto Poly L-Lysine (PLL)-coated coverslips in 24-well plates at 100,000 cells per well and were fixed 24 hour after plating for immunocytochemistry studies. Astrocytes were separated from microglia via shaking at 280 rpm for 5 hours 37 °C. Cells were trypsinized and plated onto Poly L-Lysine (PLL)-coated coverslips in 24-well plates at 100,000 cells per well and were fixed 24 hour after plating for immunocytochemistry studies. Oligodendrocytes were obtained by growing microglia in oligodendrocyte differentiation media for 7 days. Rat primary brain cells were double immunostained with rabbit or mouse anti-PGRMC1 antibody (Sigma Aldrich, St. Louis, MO) and mouse anti-b3 Tubulin antibody (Cell signaling Technology, Inc. Beverly, MA), goat anti-GFAP antibody (Santa Cruz Biotechnology, Inc. Dallas, TX), goat anti-Iba1 antibody (Novus Biologicals, A-8 Littleton, CO), or rabbit anti-NG2 antibody (Milipore, Temecula, CA). For co-localization studies of PGRMC1 and SW120, rat mixed hippocampal cells were immunostained with PGRMC1 and were then incubated with 500 nM SW120 for 2 hour at room temperature.

Results. The results show that PGRMC1 is prominently expressed in cell bodies and neurites of neurons (A). Similar results were obtained with the sigma-2 fluorescent probe, SW120. There was a lower level of PGRMC1 expression, and SW120 binding, to astrocytes, oligodendrocytes and microglia. The intensity of SW120 appears to depend on the status of cell differentiation or activation of the microglia components. There was also a linear correlation between PGRMC1 expression level and fluorescent intensity of SW120 binding in hippocampal neurons (B).

Conclusions. PGRMC1 expression levels correlates with sigma-2 receptor densities in hippocampal cell culture, which is consistent with our previous finding that PGRMC1 is associated with the sigma-2 receptor binding site (2). A sigma-2 receptor PET radiotracer can be used to noninvasively image sigma-2 receptor/PGRMC1 densities in human brain, a potential target for Abeta oligomers in the CNS.

References. (1) Izzo N et al. PLoS One 9: e111899; 2014; (2) Xu J et al. Nature Communications 2: 380; 2011.

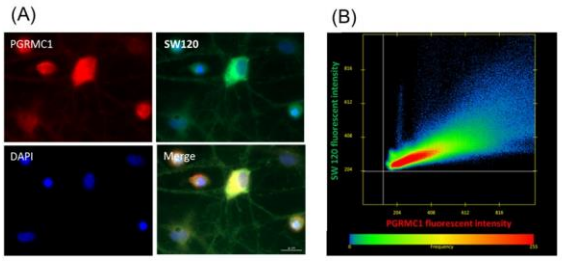

319
BRAIN-0456
Poster Session

Neurodegeneration

EARLY ALTERATIONS OF THE CORTICAL PYRAMIDAL CELLS IN THE 3XTG-AD MOUSE MODEL OF ALZHEIMER'S DISEASE

J. Piquet[1], A. Lacroix[1], X. Toussay[1], E. Faivre[2], J. Le Douce[2], R. Lerchundi[3], R. Hepp[1], G. Bonvento[2], B. Cauli[1]
[1]CNRS UMR 8246, Neuroscience Paris Seine, Paris, France
[2]CNRS UMR 9199, Commissariat à l'Energie Atomique et aux Energies Alternatives (CEA) Département des Sciences du Vivant (DSV) Institut d'Imagerie Biomédicale (I2BM) MIRCen Université Paris-Sud Université Paris-

Saclay, Fontenay-aux-Roses, France
[3]Centro de Estudios Científicos, Arturo Prat 514, Valdivia, Chile

Background and Objectives : Cortical glucose hypometabolism is an early biomarker for Alzheimer's disease (AD) [1] that has been described in AD patients [2] as well as in mouse models of the pathology [3]. Glucose metabolism is essential to maintain brain homeostasis, tissue integrity and synaptic activity [4]. Although early metabolic alteration could contribute to later neuronal dysfunctions and neurodegenerative processes, the mechanisms responsible for such metabolic deficits are still poorly understood. Pyramidal cells play a key role in neuronal processing and regulation of energy supply [5] however it is still unclear whether they contribute to the AD-related hypometabolism. We used 3xTg-AD [6] mice that harbor mutations of APP (Swedish), PS1 (M146V), and tau (P301L) to examine the potential role of cortical pyramidal cells in the AD-related metabolic dysfunction.

Methods : Electrophysiological, molecular and morphological properties of neocortical pyramidal cells were determined in the barrel cortex of 2 week-old wild-type and 3xTg-AD mice by combining patch clamp recording, single cell RT-PCR and biocytin labelling. For each cell, 48 genes related to glucose metabolism and well established molecular markers were analyzed. To further investigate whether these neurons display functional deficits in glucose metabolism, we used Förster Resonance Energy Transfer (FRET) biosensors [7]. Glucose biosensors were transduced in slices with viral vectors, to allow the monitoring of glucose concentration in real-time and at the single cell level.

Results : The molecular analysis revealed a layer-dependent alteration of pyramidal neurons in juvenile 3xTg mice. Layer II-III pyramidal cells of 3xTg mice exhibited a deficit in the expression of the glucose transporter GluT3 (WT n = 27 vs 3xTg-AD n = 28, $p<0.05$). In contrast no significant differences were detected in layer V pyramidal cells (WT n = 26 vs 3xTg-AD n = 22, $p>0.05$). We next investigated glucose dynamics in superficial pyramidal cells. Our preliminary observations showed that under resting conditions, intracellular glucose levels were significantly reduced in pyramidal cells of 3xTg mice (WT n = 22 vs 3xTg-AD n = 26, $p<0.01$).

Conclusions : These observations highlight a very early alteration of glucose metabolism in layer II/III cortical pyramidal cells. Our molecular data suggest an impairment of their glucose uptake ability which is consistent with the lower intracellular glucose level we observed using FRET imaging, but need further investigations to draw a definitive conclusion. This could provide a plausible cellular and molecular origin to the hypometabolism observed in AD.

References :

1. Small et al. (2000) Proc. Natl. Acad. Sci. U. S. A 97, 6037-6042.
2. Vlassenko et al. (2010) Proc. Natl. Acad. Sci. U. S. A.
3. Rachel M. Nicholson et al. (2010) Brain Research 1347, 179-185
4. Allaman et al. (2011) Trends Neurosci. 34, 76-87
5. Lecrux et al. (2011) J. Neurosci. 31, 9836-9847
6. Oddo et la. (2003) Neuron 39, 409-421
7. Bittner et al. (2011) J. Neurosci. 31, 4709-4713

Supported by the Agence Nationale pour la Recherche (ANR 2011, MALZ 003 01, BC) ; the "IHU Institut de Neurosciences Translationelles de Paris"' (ANR-10-IAIHU-06) and the Association France Alzheimer (ASTROinAD).

320
BRAIN-0575
Poster Session

Neurodegeneration

CAN AMIDE PROTON TRANSFER MRI GIVE ADDITIONAL INFORMATION ABOUT HUNTINGTON'S DISEASE?

M. Rega[1], M. Rega[2], J. Fairney[2], F. Torrealdea[2], B. Leavitt[3], R. Scahill[2], R.A.C. Ross[4], B. Landwehrmeyer[5], B. Borowsky[6], S. Tabrizi[2], X. Golay[2]
[1]INSTITUTE OF NEUROLOGY, UCL, London,

United Kingdom
[2]Institute of Neurology, University College London, London, United Kingdom
[3]Department of Medical Genetics, University of British Columbia, Vancouver, Canada
[4]Department of Neurology, University Medical Center, Leiden, Netherlands
[5]Department of Neurology, Ulm University, Ulm, Germany
[6]CHDI, HighQ Foundation Inc, New York, USA

Introduction:

Huntington's disease (HD) is a polyglutamine disease for which no disease-altering treatment currently exists. It is caused by a genetic error on the HTT gene responsible for the formation of polyglutamine tracts (chain of glutamine amino acid) and eventually of the production of Huntingtin protein in the cytoplasm. In healthy individuals the polyglutamine chain consists of no more than 36 repeats. However, in individuals with more than 36 repeats the production of Huntingtin protein takes an altered form, the mutant Htt (mHtt) which is found to be associated with increased neuronal decay[1,2].

While Magnetisation Transfer Imaging (MTI) has been linked to myelin loss[3], Amide Proton transfer (APT) MRI is known to be sensitive to protein size and concentration[4]. In this study we investigate both MTI and APT MRI as potential biomarkers in Huntington's disease patients.

Methods:

Premanifest/ early Huntington's patients (n=21) and healthy controls (sex matched, n=21) were recruited as part of the third visit of the TRACKON-HD study and scanned on a 3T Philips MR scanner in Leiden. The protocol consisted of 3 seconds saturation (50% duty cycle, 50ms duration, FA=540° for the APT and FA= 1620° for MTI) followed by 2 seconds delay and a GRASE (GRadient And Spin Echo) readout (resolution 4mm^3). Frequency offsets included MT (at 10ppm), APT (-4 to -3 & 3 to 4ppm) and a reference scan without saturation. B0 maps were also acquired and used for correction. The APT was calculated as the asymmetry at 3.5ppm while MTI was calculated as a ratio to the reference.

Results/Discussion:

Region of Interest analysis performed over six brain areas (as shown in figure 1) revealed no significant differences in MTI between healthy controls and patients, however APT signal showed significant alterations in both the putamen and globus pallidus regions. Such changes could be indicative of alterations in the total protein structure or concentration in the corresponding regions for HD patients, independently from any measureable atrophy. The lack of changes in MTI would indicate a relative maintenance of the myelin architecture in the same regions.

To our knowledge this work demonstrates for the first time that APT might be used to provide additional information for HD patients which however needs to be included in longitudinal studies as a potential biomarker of disease progression or response to treatment.

References:

1. Tabrizi, S. J. et al, Lancet 2013; 12: 637-649.
2. Tabrizi, S. J. et al, Lancet 2012; 11: 42:52
3. Mallik, S. et al, Neurology 2014; 80
4. Van Zijl, P. C. et a, Magn Reson Med 2011; 65: 927-948

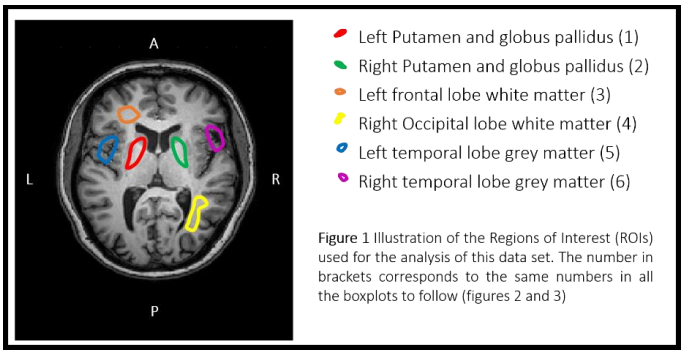

Figure 1 Illustration of the Regions of Interest (ROIs) used for the analysis of this data set. The number in brackets corresponds to the same numbers in all the boxplots to follow (figures 2 and 3)

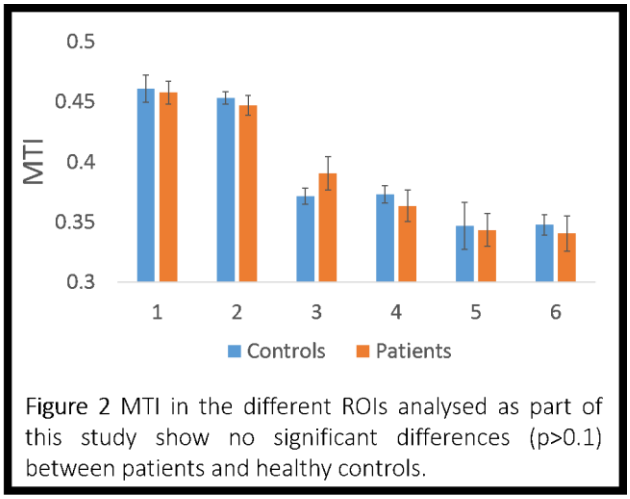

Figure 2 MTI in the different ROIs analysed as part of this study show no significant differences (p>0.1) between patients and healthy controls.

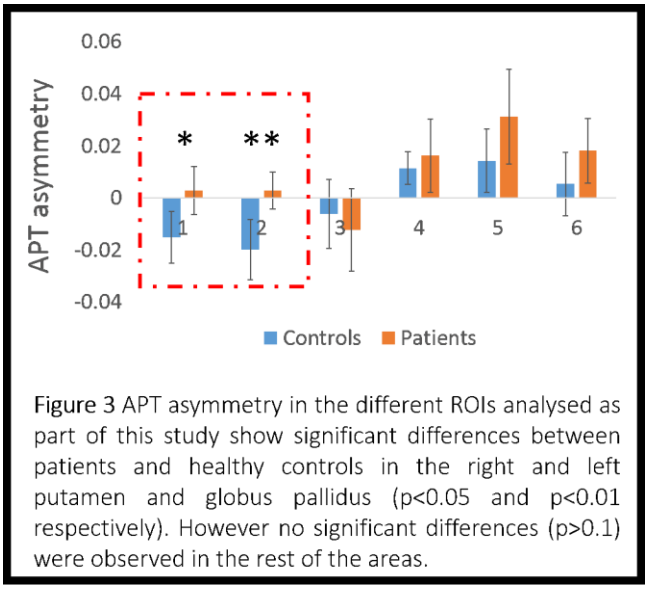

Figure 3 APT asymmetry in the different ROIs analysed as part of this study show significant differences between patients and healthy controls in the right and left putamen and globus pallidus ($p<0.05$ and $p<0.01$ respectively). However no significant differences ($p>0.1$) were observed in the rest of the areas.

321
BRAIN-0178
Poster Session

Neurodegeneration

QUANTITATIVE T2, T2* AND T2'- MR IMAGING IN PATIENTS WITH ISCHEMIC LEUKOARAIOSIS DETECT MICROSTRUCTURAL CHANGES AND CORTICAL HYPOXIA

M. Wagner[1], *M. Helfrich*[1], *S. Volz*[1], *J. Magerkurth*[1], *O.C. Singer*[1], *R. Deichmann*[1], *A. Jurcoane*[1], *E. Hattingen*[1]
[1]*Hospital of Goethe-University, Institute of Neuroradiology, Frankfurt am Main, Germany*

Objectivs: High-resolution, motion-corrected T2, T2* and T2'-mapping has been shown to depict microstructural changes and oxygenation status in men. It should therefore assess the grade of structural damage (T2) and hypoxia (T2') in patients with ischemic leukoaraiosis in white matter (WM) lesions and the normal appearing WM and grey matter (GM) particularly if combined with cortical CBF-mapping and quantification of cortical GM and WM atrophy.

Methods. 15 patients with ischemic leukoaraiosis and 15 age-matched healthy controls were included. High-resolution, motion-corrected T2, T2* and T2'-imaging, CBF-mapping (PASL), and segmentation of GM and WM was used to depict specific changes in both groups. All parameters were compared between patients and healthy controls, using t-testing ($p \leq 0.05$).

Results. Compared with controls, patients showed significantly increased T2 in lesions ($p<0.01$) and unaffected WM ($p=0.05$) as well as increased T2* in lesions ($p=0.01$). A strong trend towards a decrease of T2' could be shown in the patients in unaffected WM ($p=0.09$) and GM ($p=0.06$). Both lesions and unaffected WM and GM showed significantly decreased volume in the patient-group ($p<0.01$). No differences of PASL-based CBF could be shown.

Conclusion. Non-invasive quantitative T2, T2* and T2'-mapping can detect subtle structural und metabolic changes in ischemic leukoaraiosis. While conventional MR imaging only visualizes changes that reflect a broad spectrum of pathologies, quantitative T2, T2* and T2' imaging assess more specifically the pathophysiology of GM and WM damages in patients with IL and might therefore be used as a monitoring and prognostic tool.

322
BRAIN-0290
Poster Session

Neurodegeneration

ISCHEMIC INSULT INDUCES COFILIN ROD FORMATION AND CAUSES SYNAPSE LOSS IN RATS

Y. Wang[1], B. Chen[1], L. Shu[1], H. Xu[1]
[1]Institutes of Brain Science, Fudan University, Shanghai, China

Objectives: Cofilin is the major actin-depolymerizing factor in the CNS. Stress will cause the formation of cofilin rod, a pathological structure that disrupts synapse function and causes neurite lost. Cofilin rod is believed to promote the progress of neurodegenerative diseases such as Alzheimer's and Huntington Disease. However, there is no study on whether cofilin rod forms during ischemic insult.

Methods: Transient focal cerebral ischemia was produced by right middle cerebral artery occlusion (MCAO) for 2 hours and reperfusion for 22 hours. Rat hippocampal neuron culture DIV10 was treated with oxygen and glucose deprivation (OGD) for 90 min. Either brain tissue or cultured neurons were fixed, dehydrated and stained afterwards. Cofilin was immunostained for analysing of cofilin rod formtion. Patch clamp was used for studying the synaptic function.

Results: In this research, we discoveredcofilin rod in the infarct area of MCAO-R rat cortex for the first time. Cofilin rods form during the occlusion period, and area with rods expands withthe spread of infarct area after reperfusion. Cofilin rods mainly accumulate atthe edge of infarct area 24 hours after reperfusion, and fewer at the center.Cultured neurons treated with oxygen and glucose deprivation (OGD) can alsoprove the formation of cofilin rod, and this progress can be suppressed by glutamate receptor antagonists. Rods formed in the neurons after ischemic stimulation disrupted the neurite trafficking and caused synapse loss and synaptic function impairment. Inhibition of the cofilin activity by enhancing its upstream regulator LIMK activity suppressed the cofilin rod formation and rescued the synapses and synaptic function.

Conclusions: This finding shows that cofilin rods are excitotoxic stimulated to form and is likely related to the progressive neuron damage during the ischemic stroke.

323
BRAIN-0266
Poster Session

Neurodegeneration

INHIBITION OF HISTONE DEACETYLASES 3 ALLEVIATES MEMORY DEFICITS IN ALZHEIMER'S DISEASE BY MODULATION OF SYNAPTIC PLASTICITY

L. Yu[1], S. Wang[2], H. Yang[2], X. Zhu[1], Y. Xu[3]
[1]Department of Neurology,
the Affiliated Drum Tower Hospital of Nanjing University Medical School, Nanjing, China
[2]Department of Neurology,
Nanjing Drum Tower Hospital Clinical College of Traditional Chinese and Western Medicine, Nanjing, China
[3]Department of Neurology,
the Affiliated Drum Tower Hospital of Nanjing University Medical School Nanjing Drum Tower Hospital Clinical College of Traditional Chinese and Western Medicine, Nanjing, China

Objectives: The dysfunction of synapse is closely related to the memory deficits in Alzheimer's disease (AD). Preliminary studies demonstrated that H3 and H4 histone acetylation levels in hippocampus of APP/PS1 mice were lower than that of wide-type group, and histone deacetylase

inhibitor could improve cognitive function in APP/PS1 mice. Knocking-down histone deacetylase 3 (HDAC3) could both increase histone acetylation levels and alleviate learning and memory deficits in APP/PS1 mice. However, it is unknown whether HDAC3 could affect cognitive function *in vivo* by regulating the remodeling of the neural memory circuits.

Methods: To knock out or overexpress HDAC3 *in vivo*, lentivirus-mediated short hairpin RNA (shRNA) was injected into the hippocampus of 6-month old C57B/6 or APP/PS1 mice. After 28 days, open-flied test (OF), novel objection recognition test (NOR), Morris water maze (MWM), radial arm maze (RAM), fear condition test (FCT) were undertaken to evaluate the cognitive function. The electrophysiology of treated mice was assessed by long-term depression (LTD) and long term potential (LTP). Spine density was estimated by Golgi staining. Expression of postsynaptic density protein 95 (PSD-95), synaptophysin, GLUR1, GLUR2, NR2A, NR2B, CaMKIIa, Creb and brain derived neurotrophic factor (BDNF) were quantified by real-time polymerase chain reaction (PCR) and western blotting. The levels of Aβ and Tau were determined by immunohistochemical staining.

Results: Inhibition of HDAC3 improved learning and memory function in APP/PS1 mice. However, aggravated cognitive deficits were observed in HDAC3 overexpression mice. Furthermore, HDAC3-deficient mice exhibited an enhanced level of LTP in CA1 and CA3 regions, whereas HDAC3-overexpression mice demonstrated on the contrary. Basal synaptic transmission and LTD were similar in wild-type group and HDAC3 inhibition- or overexpression- mice. HDAC3 inhibition could increase spine density and levels of PSD-95, synaptophysin, GLUR1, GLUR2, NR2A, NR2B, CaMKIIa, Creb and BDNF. Furthermore, the levels of Aβ and Tau decreased when HDAC3 was inhibited.

Conclusions: HDAC3 inhibition could attenuate cognitive deficits in APP/PS1 mice. In HDAC3 inhibited APP/PS1 mice, spine density is increased and LTP is enhanced in CA1 and CA3 regions. The potential mechanism may involve the increasing expression of synapsin and the reducing of Aβ and Tau. Therefore, HDAC3 inhibition promotes synaptic plasticity and attenuates cognitive deficits in AD mice, therefore may provide a new target for early diagnosis and treatment for AD.

324
BRAIN-0271
Poster Session

Neurodegeneration

ORIDONIN ATTENUATES AB1–42-INDUCED SYNAPSE LOSS VIA THE BDNF/TRB/CREB SIGNALING PATHWAY

S. Wang[1], L. Yu[2], H. Yang[1], X. Zhu[2], Y. Xu[3]
[1]Department of Neurology,
Nanjing Drum Tower Hospital Clinical College of Traditional Chinese and Western Medicine, Nanjing, China
[2]Department of Neurology,
the Affiliated Drum Tower Hospital of Nanjing University Medical School, Nanjing, China
[3]Department of Neurology,
the Affiliated Drum Tower Hospital of Nanjing University Medical School Nanjing Drum Tower Hospital Clinical College of Traditional Chinese and Western Medicine, Nanjing, China

Objectives: Increasing studies demonstrate that amyloid beta (Aβ) elicits synapse loss, which contributes to the pathogenesis of Alzheimer's disease (AD). This study aims to investigate whether Oridonin (Ori), a compound of Rabdosia rubescens, could attenuate Aβ-induced synapse loss in $A\beta_{1-42}$-induced AD mice, and to explore the underlying mechanisms.

Methods: Ab_{1-42} was injected to the bilateral hippocampus of adult male C57BL/6 mice by infusion cannulae to make the AD mouse models. The cognitive impairment was measured by Morris water maze. The electron microscopy was used to quantify synaptic numbers in the hippocampus of mouse. The expression of PSD-95 in post-synapses and the expression of synaptophysin in pre-synapses were quantified by immunostaining and western blotting. The

protein levels of BDNF, p-TrkB, TrkB, p-CREB and CREB were determined using western blotting. The mRNA and protein levels of NGF and NT3 were analyzed by real-time PCR and western blotting, respectively.

Results: Ori could attenuate the memory deficits in $A\beta_{1-42}$-induced AD mice, and could inhibit the loss of synapse. In addition, Ori increased PSD-95 and synaptophysin expression in the hippocampus of AD mouse. Furthermore, Ori was able to activate the BDNF/TrkB/CREB signaling pathway. Moreover, Ori also enhanced the expression of NGF and NT3.

Conclusions: Ori attenuated $A\beta_{1-42}$-induced synapse loss through activating BDNF/TrkB/CREB signaling pathway, indicating that Ori might be a potential drug for AD treatment.

325
BRAIN-0761
Poster Session

Neurological Diseases

ALTERATION OF ICTAL AND INTERICTAL PERFUSION IN PATIENTS WITH PAROXYSMAL KINESIGENIC DYSKINESIA

Y.D. Kim[1], I.U. Song[1]
[1]Neurology,
The Catholic University of Korea Incheon St. Mary's Hospital, Incheon, Korea

Although previous cerebral blood fl ow studies have suggested that the basal ganglia or thalamus are involved in the pathogenesis of paroxysmal kinesigenic dyskinesia (PKD), the precise anatomic substrate or pathophysiological networks associated with PKD remain unclear. Here, ictal and interictal single photon emission computed tomography (SPECT) in 2 patients with idiopathic PKD compared to 6 age-matched normal controls and the perfusion fi ndings of subtraction ictal SPECT co-registered to MRI (SISCOM) in 1 patient are reported. The interictal and ictal perfusion changes were diff erent in each of the patients and there were no consistent anatomic substrates observed. 2 patients had signifi cant perfusion changes in the left frontal/temporal cortices compared to controls, whereas the others showed an increased uptake of 99m Tc-ethyl cysteinate dimer (ECD) in the left occipital area on subtraction SPECT imaging. The results of this study suggest that the pathophysiology of PKD cannot be simply explained by lesions of the basal ganglia or thalamus, and that other associated areas of the cortex are likely involved in these movement disorders.

326
BRAIN-0066
Poster Session

Neurological Diseases

STRIATAL DOPAMINE TRANSPORTER INTEGRITY VS. WHOLE-BRAIN DISEASE-RELATED GLUCOSE METABOLIC PATTERNS IN PARKINSONISMS

J. Ko[1], C. Lee[2], D. Eidelberg[3]
[1]Human Anatomy and Cell Science,
University of Manitoba, Winnipeg, Canada
[2]Neurology, Asan Medical Center, Seoul, Korea
[3]Center for Neurosciences,
Feinstein Institute for Medical Research, Manhasset, USA

Objective: To investigate the relationship between striatal dopaminergic cellterminal integrity and glucose metabolic patterns in Parkinson's disease (PD),multiple system atrophy (MSA), progressive supranuclear palsy (PSP) andcortico-basal syndrome (CBS), and their symptom expressions.

Methods: We recruited 18 non-demented PD (PDND), 24 PD with dementia (PDD), 9 dementiawith lewy body (DLB), 32 MSA-parkinsonism (MSA-P), 15 MSA-cerebellum (MSA-C),38 PSP, 42 CBS patients and 16 normal controls (NL). All subjects underwentresting-state metabolic brain imaging with ^{18}F-fluorodeoxyglucosePET. The majority except 14 subjects additionally underwent ^{18}F-FP-CITPET. The disease-related glucose metabolic pattern scores estimatedby scaled subprofile modeling[1, 2] and striatal ^{18}F-FP-CITuptake have been compared across the different patient groups and

theirrelationships with disease duration and symptom severity have been analyzed.

Results: ^{18}F-FP-CIT uptake values and disease-relatedglucose metabolic pattern scores were differently expressed in eachpatient group with potentially more discriminant capacity in the later measurement (Figure 1). In lewy body diseases (LBD, i.e., PDND, PDD and DLB) ^{18}F-FP-CIT uptake in the putamen wassignificantly correlated with PD-related glucose metabolic pattern score[3] ($p<0.001$), but ^{18}F-FP-CIT uptake was not correlated in other atypical parkinsoniansyndrome-related pattern scores.[4, 5] InMSA-P, MSA-related pattern score was significantly correlated disease duration ($p=0.006$)and symptom severity ($p=0.003$), while ^{18}F-FP-CIT uptake was not. In PSP, a trend level of correlation wasalso observed between mini-mental state exam and PSP-related pattern score ($p=0.063$)while^{18}F-FP-CIT uptake wascorrelated with disease duration ($p=0.021$). In CBS, no notable correlationwas observed.

Conclusions: As previously reported, each disease-relatedmetabolic pattern was significantly elevated in the respective patient groups(i.e., LBD, MSA, PSP and CBS), which have enabled differential diagnosis acrossdiseases.[5, 6] In PD,PDD and DLB, the PD-related brain glucose metabolic network abnormality ishighly correlated with dopaminergic degeneration, but similar relationship wasnot found in other atypical parkinsonian syndromes. Especially in MSA-P, thedisease-related pattern (i.e., MSARP) may be directly involved with diseaseduration and symptom severity while dopamine deficiency may not.

References

1. Spetsieris P, Ma Y, Peng S, Ko JH, Dhawan V, Tang CC et al. Identification of Disease-related Spatial Covariance Patterns using Neuroimaging Data. J Vis Exp 2013; (76).
2. Eidelberg D. Metabolic brain networks in neurodegenerative disorders: a functional imaging approach. Trends Neurosci 2009; 32(10): 548-57.
3. Ma Y, Tang C, Spetsieris PG, Dhawan V, Eidelberg D. Abnormal metabolic network activity in Parkinson's disease: test-retest reproducibility. J Cereb Blood Flow Metab 2007; 27(3): 597-605.
4. Eckert T, Tang C, Ma Y, Brown N, Lin T, Frucht S et al. Abnormal metabolic networks in atypical parkinsonism. Mov Disord 2008; 23(5): 727-33.
5. Niethammer M, Tang CC, Feigin A, Allen PJ, Heinen L, Hellwig S et al. A disease-specific metabolic brain network associated with corticobasal degeneration. Brain 2014; 137(Pt 11): 3036-46.
6. Tang CC, Poston KL, Eckert T, Feigin A, Frucht S, Gudesblatt M et al. Differential diagnosis of parkinsonism: a metabolic imaging study using pattern analysis. Lancet Neurol 2010; 9(2): 149-58.

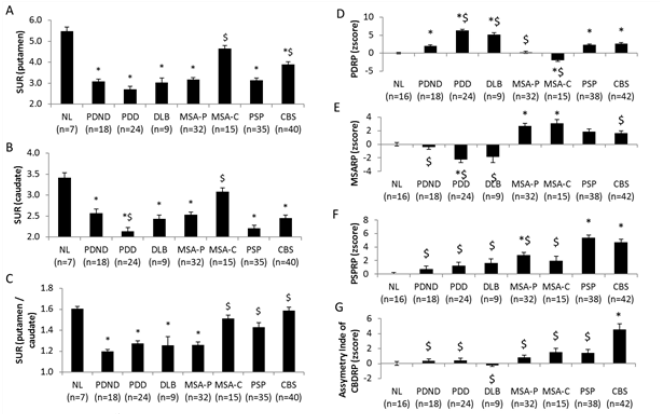

Figure 1. Differences in ^{18}F-FP-CIT standard uptake ratio (SUR) compared to the cerebellum (**A-C**) and disease-related metabolic pattern scores (**D-G**) across diseases. As expected all patient groups showed significantly decreased ^{18}F-FP-CIT uptake in the **A.** putamen and **B.** caudate ($p<0.001$, post-hoc Bonferroni) except MSA-C patients ($p>0.258$, post-hoc Bonferroni). **C.** The ratio of SUR between putamen and caudate was also decreased in PDND, PDD, DLB and MSA-P ($p<0.04$), but it was not altered in MSA-C, PSP and CBS ($p>0.08$, post-hoc Bonferroni). **D.** As expected all Lewy body disease (LBD) patients (PDND, PDD and DLB) showed significantly elevated PD-related pattern scores compared to normal controls (NL) ($p<0.021$, post-hoc Bonferroni). **E.** Both MSA-P and MSA-C patients showed significantly elevated MSA-related pattern scores compared to NL and LBD ($p<0.001$, post-hoc Bonferroni). **F.** PSP-related pattern score was significantly higher in PSP patients compared all other groups ($p<0.001$, post-hoc Bonferroni) except CBS ($p=1.0$, post-hoc Bonferroni). **G.** CBS patients showed significantly increased Asymmetry Index of CBD-related pattern compared to all other groups ($p<0.013$, post-hoc Bonferroni).

327
BRAIN-0061
Poster Session

Neurological Diseases

FREQUENCY-DEPENDENT NEURAL ACTIVITY IN PATIENTS WITH UNILATERAL VASCULAR PULSATILE TINNITUS

H. Lv[1], Z. Wang[1], F.E.I. Yan[2], Z. Liu[2], P. Zhao[1], C. Dong[1], T.I.N.G. Li[2]
[1]Department of Radiology, Beijing Friendship Hospital, Beijing, China
[2]Department of Radiology, Beijing Tongren Hospital, Beijing, China

Objectives: Previous resting-state functional magnetic resonance imaging (RS-fMRI) studies have shown that neurological changes are important findings in vascular pulsatile tinnitus (PT) patients[1].

Methods: Here we utilized R-fMRI to measure the amplitude of low-frequency fluctuations (ALFF) in forty patients with unilateral PT and forty age-, gender-, education-matched normal control subjects. Two different frequency bands (slow-4, 0.027-0.073 Hz; slow-5, 0.010–0.027 Hz) were analyzed to examine the intrinsic brain activity in details[2-3].

Results: Widespread ALFF differences between the two bands were observed, predominantly including the aMPFC (anterior medial prefrontal cortex)/ ACC (anterior cingulate cortex), PCu (precuneus), part of the lateral regions of bilateral superior temporal gyrus etc (Figure 1). Compared to controls, PT patients had increased ALFF values mainly in the PCu, bilateral IPL (inferior parietal lobule), left IFG (inferior frontal gyrus), right IFG/anterior insula, and decreased ALFF values in the multiple occipital areas including bilateral middle-inferior occipital lobe and part of bilateral cerebellum posterior lobe (Figure 2). Intriguingly, the ALFF abnormalities in aMPFC/ACC, PCu, right IPL and some regions of occipital and parietal cortices were greater in the slow-5 band compared to the slow-4 band (Figure 3, A and B). Additionally, the THI score of PT patients was positively correlated with changes in slow-5 (r=0.368, p=0.019) and slow-4 (r=0.342, p=0.031) band in PCu. PT patients enrolled in this study did not show any gray matter volume changes.

Conclusions: This study demonstrated widespread alternation of baseline brain activities in PT patients. The pathophysiological mechanism of these results should be carefully determined to be helpful in the neurological studies of PT patients.

References:
1. Han L, Zhaohui L, Fei Yet al. Abnormal baseline brain activity in patients with pulsatile tinnitus: a resting-state FMRI study. Neural Plast 2014;2014:549162.
2. Xue SW, Li D, Weng XC, Northoff G, Li DW. Different neural manifestations of two slow frequency bands in resting fMRI: A systemic survey at regional, inter-regional, and network levels. Brain Connect 2014.
3. Liu X, Wang S, Zhang X, Wang Z, Tian X, He Y. Abnormal Amplitude of Low-Frequency Fluctuations of Intrinsic Brain Activity in Alzheimer's Disease. J Alzheimers Dis 2014.

Fig. 1 The main effect for frequency band on ALFF. The hot color represents a higher ALFF in the slow-5 band than in the slow-4 band, whereas the cool color represents a lower ALFF.

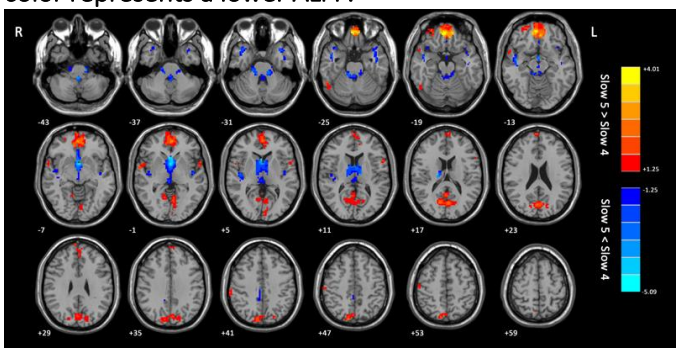

Fig. 2 The main effect for group on ALFF. The hot color represents a higher ALFF in pulsatile tinnitus (PT) patients than in the healthy controls.

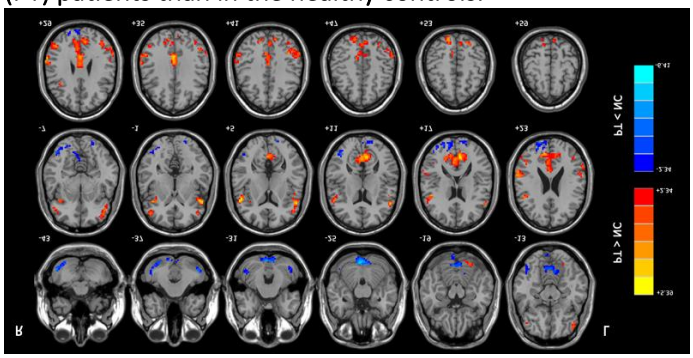

Fig. 3 The interaction between frequency band and group on ALFF. Greater group differences in the aMPFC/ACC, PCu, right IPL and some regions of occipital and parietal cortices and cerebellar showed greater group differences in slow-5 band compared to the slow-4 band.

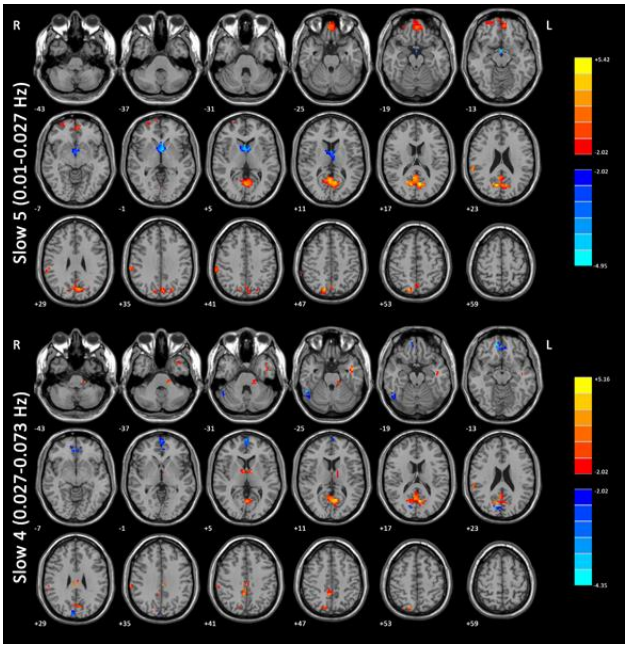

328
BRAIN-0469
Poster Session

Neurological Diseases

AMINO ACID TISSUE LEVELS AND NEURONAL DAMAGE IN CEREBELLUM AFTER STATUS EPILEPTICUS IN THE IMMATURE RAT

J. Ortega Rosado[1], *M. Lopez-Meraz*[2]
[1]*Neurociencias, Neuroetologia, México, Mexico*
[2]*Epilepsia, Centro de Investigaciones Cerebrales, México, Mexico*

Its know that status epileptics (SE) induces neuronal cell damage in the developing rat brain (1,2). However, the consequences of SE on the cerebellum has been less explored.
Objetives: To determinate amino acid tissue levels and neuronal damage in developing rat cerebellum after a episode of SE.
Methods: Fourteen -days-old (P14) rat pups were administered intraperitoneally with lithium chloride (3 mEq/Kg)and, 20 hours later, SE was induced subcutaneous pilocarpine hydrochloride (60 mg/Kg). Control animals was given as equal volume of saline subcutaneously.
Experiment 1: Animals were sacrificed by decapitation 24 hours after induction of SE. Cerebellum was removed and vermis and hemispheres was dissected out on ice. Tissue was homogenized in 0.1 M perchloric acid containing 4 mM sodium bisulfate. Homogenates were centrifugate and supernatant was used to quantify gamma-aminobutyric acid (GABA), glutamate, aspartate,alanine, glycine, glutamine and taurine concentrations by HPLC; pellet was used to determine protein leves by bradford´s methods.
Experiment 2: Animals were transcardially perfused with 4 % paraformaldehyde and 0.9% sodium chloride, 24 hours after induction of SE. Cerebellum was removed, postfixed and embedded in paraffin; 10 um-thickness sagittal section from medial vermis were stained with Fluoro-Jade B (F-JB) or hematoxylin-eosin satining.
Result: SE increased the tissue concentration of inhibitory amino acid taurine (80%) and alanine (91%), as well as glutamine (168%) in cerebellar hemispheres; however, SE did not alter any amino acid level in vermis. No F-JB positive or acidophilic cell were detected in cerebellar vermis after SE.
Conclusion: SE produced region specific change in amino acid concentration in the developing cerebellum, effect that is not associated with neuronal damage.
References :
1. Sankar R, Shin DH, Liu H, Mazarati A, Pereira de Vasconcelos A, Westerlain CG. Patterns of status epilepticus-induced neuronal injury during development and long term consequences. J Neurosci. 1998 Oct 15;18(20): 8382-93
2. Kuvová H, Mares P. Are morphologic and functional consequences of status epileptics in infant rats progressive. Neuroscience. 2013;235:232-49
This studied was supported by CONACyT

329
BRAIN-0388
Poster Session

Neurological Diseases

INFLAMMATION COMBINED WITH ISCHEMIA PRODUCES MYELIN INJURY AND PLAQUE-LIKE AGGREGATES OF MYELIN, AB AND APP IN ADULT RAT BRAIN

X. Zhan[1], B. Ander[1], F. Sharp[1]
[1]Neurology,
MIND University of California at Davis,
Sacramento, USA

Background: Ischemia, white matter injury, and Alzheimer's disease (AD) pathologies often co-exist in aging brain. How one condition predisposes to, interacts with or perhaps causes the others remains unclear.

Objectives: To better understand the link between ischemia, white matter injury and AD, adult rats were administered lipopolysaccharide (LPS) to serve as an inflammatory stimulus, and 24h later subjected to 20-minute focal cerebral ischemia (IS) followed by 30-minute hypoxia (H).

Methods: Myelin and axonal damage, as well as amyloid beta (Aβ) and amyloid precursor protein (APP) deposition were examined by Western blot and immunocytochemistry following LPS/IS/H. Findings were compared to the 5XFAD mouse AD brain.

Results: Myelin/axonal injury was observed bilaterally in cortex following LPS/IS/H, along with an increase in IL-1, granzyme B and LPS. APP deposition was present in ischemic striatum in regions of myelin loss. Aβ1-42 and APP were deposited in small foci in ischemic cortex that co-localized with myelin aggregates. In the 5XFAD mouse AD model cortical amyloid plaques also co-localized with myelin aggregates.

Conclusions: Lipopolysaccharide / ischemia / hypoxia produce myelin injury and plaque-like aggregates of myelin. APP and Aβ deposition co-localize with these myelin

aggregates.

Fig. 1

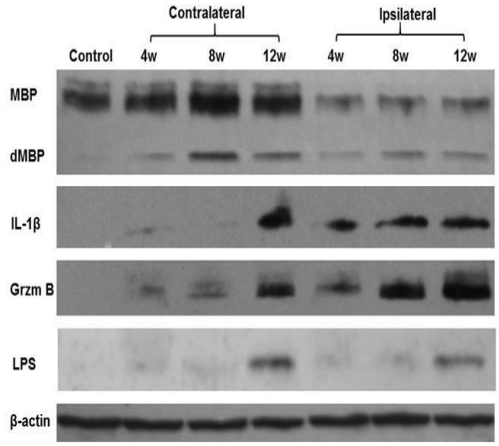

Figure 1. Western blot analysis of brain samples of animals subjected to Lipopolysaccharide /Ischemia /Hypoxia (LPS/IS/H). Animals were subjected to LPS/IS/H and sacrificed 4 weeks, 8 weeks and 12 weeks later. Naïve animals were used as control. The cortex, basal ganglia and hippocampus ipsilateral to the focal ischemia and contralateral to the ischemia were taken for Western blotting. Staining of brain samples was performed using antibodies to Myelin Basic Protein (MBP), Interleukin-1β (IL-1β), Granzyme B (Grzm B) and LPS. Note decreased MBP in the ipsilateral hemisphere compared to control and contralateral hemisphere; appearance of degraded MBP (dMBP) in the ipsilateral and contralateral hemisphere; and the gradual induction of both IL-1β and Grzm B in the ipsilateral and contralateral hemisphere from 4 to 12 weeks after LPS/IS/H. LPS (MW ~ 30kD) was detected on Western blot analysis in cortex ipsilateral and contralateral to the focal cerebral ischemia at 4 weeks, 8 weeks and 12 weeks after the LPS/IS/H. Note increased LPS at 12w compared to that at 4w or 8w. LPS was absent in control brain. β-actin was used as loading control.

Fig. 2

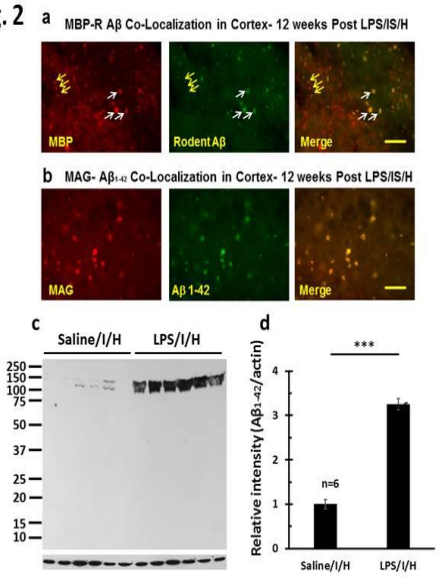

Figure 2. Co-localization of myelin aggregates with rodent Aβ and Aβ1-42 expression in the hemisphere ipsilateral to ischemia at 12 weeks following LPS/IS/H. a. Myelin aggregates stained with Myelin Basic Protein (MBP) co-localized with rodent Aβ (R Aβ) deposits. Most of the MBP stained foci co-localized with rodent Aβ (white arrows, Merge) whereas some did not (yellow arrows). R Aβ likely represents AβPP. **b**. Myelin Associated Glycoprotein (MAG) co-localized with Aβ1-42 deposits. MAG immunostained foci in cortex co-localized with Aβ1-42 (b, Merge). Bars = 50 μm. **c**. Western blot analysis for Aβ1-42 at 12 weeks following saline/IS/H and LPS/IS/H. A Two bands of ~150kD and ~140kD were detected on Western blots using the Aβ1-42 antibody which showed marked induction of both bands following LPS/IS/H compared to saline/IS/H. **d**. Quantification of the expression of Aβ1-42 showed that it markedly increased following LPS/IS/H compared to that following saline/IS/H. ** p<0.01.

Fig. 3

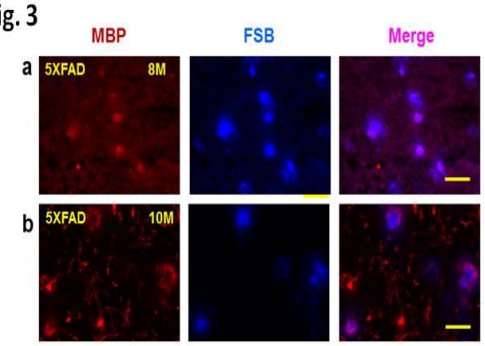

Figure 3. Double staining of MBP and FSB in the amyloid plaques of 5XFAD mice. MBP positive myelin aggregates were detected in cortex of 8 month (8M, left panel) old (a) and 10 month (10M, left panel) old (b) 5XFAD mice. These MBP myelin aggregates co-localized (Merge) with FSB stained amyloid plaques in the cortex of 8 month old (8M, middle upper panel) and 10 month (10M, middle lower panel) old 5XFAD mice. MBP aggregates at 10 months (10M) seemed somewhat fragmented (b). MBP = myelin basic protein. FSB = (E, E)-1-fluoro-2,5-bis (3-hydroxycarbonyl-4-hydroxy) styrylbenzene. Bar = 50μm.

330
BRAIN-0499
Poster Session

Neurological Diseases

THE EFFECT OF EXERCISE ON THE MICROVASCULATURE OF THE SENSORIMOTOR CORTEX IN A MOUSE MODEL OF ALZHEIMER'S DISEASE.

L.A.M. Thomason[1], E. Maliszewska-Cyna[2], A. Dorr[1], J. Steinman[3], J.G. Sled[4], I. Aubert[2], B. Stefanovic[3]
[1]Physical Sciences Platform, Sunnybrook Research Institute, Toronto, Canada
[2]Laboratory Medicine and Pathobiology, University of Toronto, Toronto, Canada
[3]Medical Biophysics, University of Toronto, Toronto, Canada
[4]Medical Biophysics, Mouse Imaging Centre, Toronto, Canada

Objectives: There is growing interest in the role of neurovascular injury in AD etiology and progression. In mouse models of AD, exercise has been shown to reduce amyloid-beta load, improve cognitive function, and increase angiogenesis.[1,2] We thus set out to determine the effects of exercise on the cortical microvascular network in the TgCRND8 model of AD.

Methods: Three-month old TgCRND8 (Tg) and their non-transgenic littermates (nTg) were given ad libitum access to a running wheel until 6-months of age. Twenty-four hours prior to sacrifice mice were injected with Methoxy XO4 to label amyloid-beta. The mice were perfused with a mercox-BABB (Benzyl Alcohol-Benzyl Benzoate) solution containing Nile red to allow visualization of the microvascualture. The brains were fixed in 4% paraformaldehyde, progressively dehydrated with methanol, and cleared by BABB. Two photon fluorescence images were acquired coronally, using 780nm excitation, over 4 partially overlapped regions in the motor and somatosensory cortices, at 0.5x0.5um2 in plane resolution, every 2.5um, spanning 1000 um in the anterior-to-posterior direction. Following deconvolution and stitching of imaged volumes, the microvascular network was tracked using a multi-scale automated segmentation algorithm.[3] Given fixation-induced tissue shrinkage, the capillaries were defined as the vessels 8um or less in diameter.

Results: The primary motor cortex of TgCRND8 mice has ~45% fewer capillaries per mm3 of tissue and exhibits a trend towards shorter total length of capillaries per mm3 of tissue when compared to that of their non-transgenic littermates. Three-month ad libitum access to a running wheel significantly increased the number of capillaries per mm3 and significantly increased the total length of capillaries in the motor cortex of TgCRND8 mice, making their capillary density and capillary length density indistinguishable from those of their nontransgenic littermates. Maximum intensity projections of two-photon florescence microscopy data in sample animals of each of the 4 cohorts is shown in Figure 1A, along with the capillary density histograms across all animals in Figure 1B. In contrast to the capillary plexus, we observed no changes in either number or total length of vessels larger than 8um in diameter.

Conclusions: Our findings offer further insight into the effects of exercise on the brain microvasculature and provide evidence for the potential of exercise in halting capillary degeneration in AD progression.

References:

1. Richter, H., Ambree, O., Lewejohann, L., Herring, A., Keyvani, K., Paulis, W., Palme, R., Touma, C., Schabitz, W-R. And Sachser, N. 2008. Wheel-running in a transgenic mouse model of Alzheimer's disease: Protection or symptom? Behavioural Brain Research. 190: 74-84.
2. Adlard, P.A., Perreau, V.M., Pop, V. And Cotman, C.W. 2005. Voluntary exercsie decreases amyloid load in a transgenic model of Alzheimer's disease. Journal of Neuroscience. 25(17): 4217-4221.
3. Rennie MY, Detmar J, Whiteley KT, Yiang J, Jurisicova A, Adamson SL, and Sled JG. 2011. "Vessel tortuosity and reduced vascularization in the fetoplacental arterial tree after maternal

exposure to polycyclic aromatic hydrocarbons". American Journal of Physiology Heart Circulatory Physiology. 300:H675-H684.

Figure 1A.

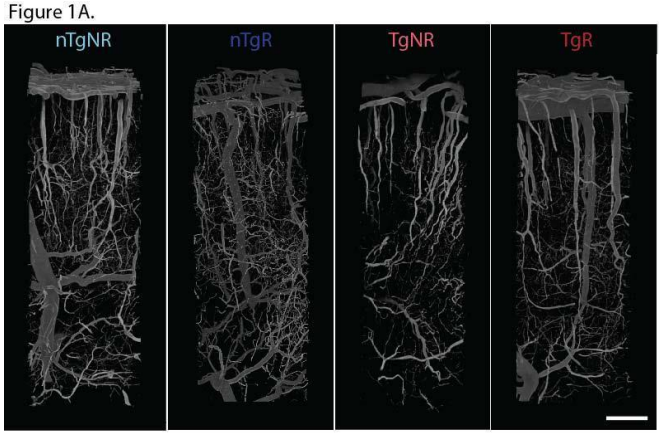

Figure 1B.

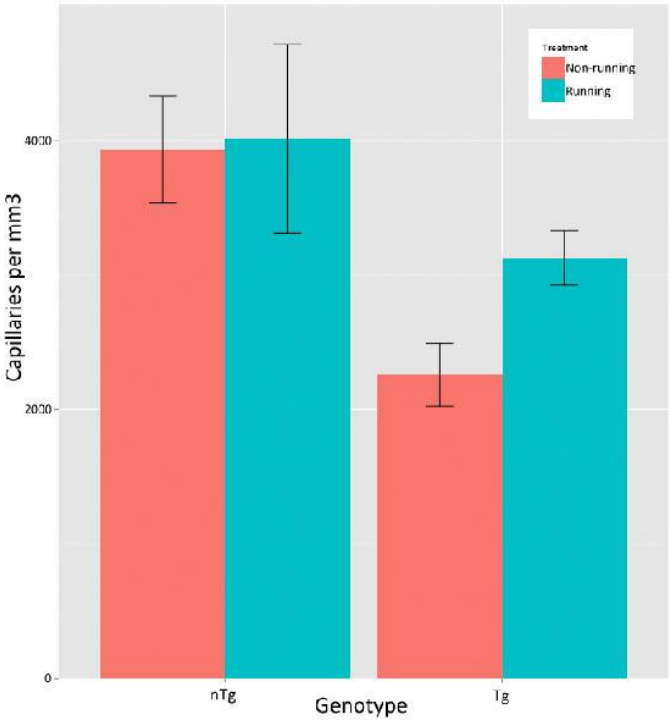

331
BRAIN-0564
Poster Session

Neurological Diseases

ABNORMAL METABOLIC NETWORK ACTIVITY IN IDIOPATHIC RAPID EYE MOVEMENT SLEEP BEHAVIOR DISORDER BASED ON METABOLIC PET AND PERFUSION MRI

P. Wu[1], J. Ge[1], S. Peng[2], H. Yu[3], J. Wang[3], D. Eidelberg[2], Y. Ma[2], C. Zuo[1]
[1]PET Center Department of Nuclear Medicine, Huashan Hospital Fudan University, Shanghai, China
[2]Center for Neurosciences, The Feinstein Institute for Medical Research North Shore-Long Island Jewish Health System, Manhasset, USA
[3]Department of Neurology, Huashan Hospital Fudan University, Shanghai, China

Objectives: Idiopathic rapid eye movement sleep behavior disorder (RBD) is regarded as a prodromal stage of synucleinopathies such as Parkinson's disease (PD), in which abnormal metabolic brain network has been identified for differential diagnosis and evaluating disease progression[1-2]. We have recently reported that RBD is also associated with a disease-related covariance pattern (RBDRP) characterized by increased metabolic activity in pons, thalamus, precentral gyrus, supplementary motor area, medial frontal gyrus, hippocampus, supramarginal gyrus, inferior temporal lobule, and posterior cerebellum, associated with relatively decreased activity in occipital regions, midbrain and superior temporal gyrus[3]. Network expressions in RBD patients were elevated relative to those in healthy controls and produced excellent group discrimination. Network expressions were also elevated in PD patients but decreased with disease progression. In this study we compare the metabolic network activity in RBD obtained using PET and cerebral blood flow images acquired from perfusion MRI.

Methods: A cohort of nine RBD patients (age 66.1 ± 3.5 years) and seven age-matched healthy controls (age 62.9 ± 4.9 years) underwent FDG PET and perfusion MRI with arterial spin labeling (ASL). The study was approved by the IRB with all subjects signed written informed consent. RBDRP expressions were computed for these two imaging modalities and compared in this cohort.

Results: Subject scores of RBDRP obtained from FDG PET were elevated in the patients with RBD relative to the controls (*P*=0.001). Subject scores of RBDRP computed from ASL MRI were also higher in the RBD patients than those in the controls (*P*=0.002). Of note, RBDRP network activities from both imaging modalities correlated significantly (*R* = 0.682, *P*=0.004) in the combined cohort.

Conclusion: Network activity of RBDRP can be quantified using FDG PET and ASL MRI to differentiate patients from normal controls. This is highly similar to the analogous results reported previously in patients with PD using the PD-related pattern[4]. These results suggest that cerebral blood flow and glucose metabolism are comparable in their ability for assessing abnormal metabolic networks [5-6]. Both may provide probable markers to identify those at higher risk for developing neurodegenerative disorders.

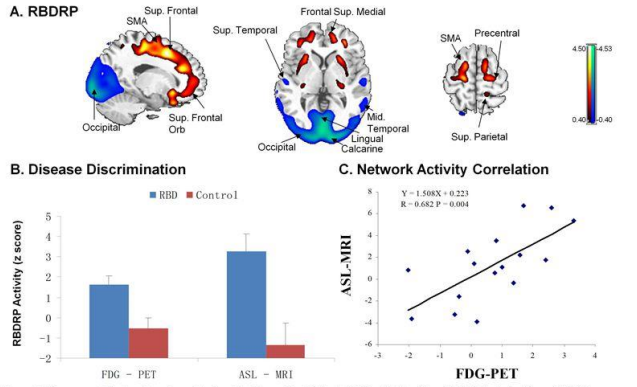

Figure 1. Disease-related pattern in patients with idiopathic RBD. A. RBD-related pattern (RBDRP) derived from 21 RBD patients and 21 age-matched normal controls (Wu et al *Brain* 2014). RBDRP was symmetrical and included positive (*red*) metabolic activity in the sensorimotor cortex, hippocampus, temporal lobe, thalamus, pons and cerebellum, and negative (*blue*) activity in the posterior parieto-occipital cortices. **B.** The expression of RBDRP discriminating the RBD patients from the control subjects ($P < 0.002$) in the derivation cohort was reproducible ($P < 0.01$) in the new smaller sample of control and RBD subjects scanned with FDG PET and ASL MRI. **C.** RBDRP network activity measured using both imaging modalities correlated ($P < 0.005$) with each other . [The covariance map was overlaid on MRI-template images. Error bars represent the standard error of the mean].

References:

1. Ma Y, Tang C, Spetsieris PG, et al. Abnormal metabolic network activity in PD: test-retest reproducibility. J Cereb Blood Flow Metab 2007; 27: 597-605.
2. Wu P, Wang J, Peng S, et al. Metabolic brain network in the Chinese patients with PD based on ^{18}F-FDG PET imaging. Parkinsonism Relat Disord 2013; 19: 622-7.
3. Wu P, Yu H, Peng S et al. Consistent abnormalities in metabolic network activity in idiopathic RBD. Brain 2014; 137:3122-8.
4. Ma Y, Huang C, Dyke JP, et al. Parkinson's disease spatial covariance pattern: noninvasive quantification with perfusion MRI. J Cereb Blood Flow Metab 2010; 30: 505-9
5. Melzer TR, Watts R, MacAskill MR, et al. Arterial spin labelling reveals an abnormal cerebral perfusion pattern in Parkinson's disease. Brain 2011; 134:845-55.
6. Asllani I, Habeck C, Scarmeas N, et al. Multivariate and univariate analysis of continuous ASL perfusion MRI in Alzheimer's disease. J Cereb Blood Flow Metab 2008; 28:725–736.

332
BRAIN-0384
Poster Session

Neurological Diseases

ELLAGIC AICD PREVENTS KAINIC ACID-INDUCED EPILEPTOGENESIS IN MICE

J.M. Yon[1], *C. Lin*[1], *S.Y. Nam*[1]
[1]*College of Veterinary Medicine and Research Institute of Veterinary Medicine, ChungBuk National University, Cheongju-si, Korea*

Objectives: Epilepsy is a neurodegenerative disease with periodic occurrences of spontaneous seizures as the main symptom. The aim of this study was to investigate the neuroprotective effects of ellagic acid (EA), the high levels of berries, in a kainic acid (KA)-induced status epilepticus model. **Methods:** After intraperitoneal injections of KA in 8-week-old male mice, the animals were treated oral administration with EA and then examined for any anti-ictogenic, antioxidative, anti-inflammatory, and anti-apoptotic effects of the EA treatment for 3 days

before KA treatment. All experiments were approved and carried out according to the "Guide for Care and Use of Animals" (Chungbuk National University Animal Care Committee, according to NIH #86–23). **Results:** KA injections significantly enhanced neurodegenerative conditions but EA reduced the detrimental effects of KA in mice. The administered group that received KA and EA showed significantly decreased behavioral seizure activity and also remarkably blocked intense and significantly diminished the levels of nitric concentration and malondialdehyde concentration in the blood of KA-treated mice. In addition, EA significantly ameliorate the KA-induced increase in the NF-kB, TNF-a, IL-6, iNOS, nNOS, bax, and caspase3 mRNA, and decrease in the Bcl-xL, SOD2, and GPx1 mRNA in the brain. Furthermore, co-treatment of KA and EA resulted in considerably decreased apoptotic cell death in the cornu ammonis sections of the hippocampus compared with that seen in the KA-alone group. **Conclusions:** These findings indicate that EA is preventative for the epileptogenesis induced by KA in mice.

References

[1] Ryan *et al.* Temporal and spatial increase of reactive nitrogen species in the kainate model of temporal lobe epilepsy. Neurobiol Dis. 2014;64:8-15

[2] Uzar *et al.* Ellagic acid attenuates oxidative stress on brain and sciatic nerve and improves histopathology of brain in streptozotocin-induced diabetic rats. Neurol Sci. 2012;33:567-74

[3] Vezzani *et al.* The role of inflammation in epileptogenesis. Neuropharmacology. 2013;69:16-24.

333
BRAIN-0363
Poster Session

Vascular Cognitive Impairment

EFFECT OF HYPERFIBRINOGENEMIA-INDUCED CAVEOLAR TRANSCYTOSIS ON SHORT-TERM MEMORY

N. Muradashvili[1], W. Rodriguez[1], C. Maldonado[1], S. Tyagi[1], D. Lominadze[1]

[1]Physiology & Biophysics, University of Louisville, Louisville, USA

Objectives:

Many inflammatory and cognitive disorders are accompanied by elevated blood level of fibrinogen (Fg), called hyperfibrinogenemia (HFg). We showed that acute increase of Fg content to its pathological level (4 mg/ml) enhanced pial venular permeability in mice[1]. Plasma proteins may pass through endothelial barrier via two major, paracellular and/or transcellular, pathways. We hypothesized that HFg increases cerebrovascular permeability through mainly the transcellular transport leading to accumulation of Fg in subendothelial matrix and forming a complex with other proteins such as cellular prion protein (PrP^C)[2]. The latter is involved in memory loss[2,3].

Methods:

Dual-tracer probing method[4] was used to define prevailing role of paracellular or transcellular pathway and assess the changes in pial venular permeability in wild type (WT, C57BL/6J) and transgenic, HFg mice. Fluorescein isothiocyanate (FITC) and bovine serum albumin conjugated with Alexa fluor-647 (BSA-647) were infused to the animals, and leakage of each dye was assessed at 10^{th}, 20^{th}, 40^{th}, 60^{th} and 90^{th} min after infusion. Role of caveolar transcytosis in cerebrovascular protein leakage was studied in HFg mice in the presence or absence of in vivo siRNA against Caveolin-1. Formation of Fg-PrP^C complex was assessed in mouse brain cryo-sections by immunohistochemistry. Short-term memory of mice was evaluated by a novel object recognition test[3].

Results:

Overall, BSA-647 leakage (202±8,% of baseline) was more in HFg than that (136±8,%) in WT mice. Leakage of FITC was greater in HFg animals compared to WT group at 20^{th} and 40^{th} minutes of observation, while BSA-647 leakage was greater than in WT group starting from 20^{th}

minutes. Thus, HFg caused a transient opening of gaps between endothelial cells. After 40th minutes effect of HFg subsided and the difference between FITC leakages in these two animal groups vanished. BSA-647 continued to cross vascular wall even after paracellular pathway was no longer overstimulated by HFg. Thus, BSA-647 moved first through both pathways and later (when gaps were closed) by transcytosis. In HFg mice, overall BSA-647 traversing of vascular wall (193±15,%) was lowered (112±4,%) in the presence of siRNA against Caveolin-1 without affecting the FITC leakage. Fg-PrP^C complex formation in HFg mice was enhanced compared to that in WT mice and this was directly correlated with greater loss in short-term memory.

Conclusion:

HFg increases cerebrovascular permeability via mainly caveolar transcytosis and enhances Fg-PrP^C complex formation, which amplifies short-term memory loss and suggests a functional role of Fg in vasculo-neuronal pathology.

Supported by NIH grant NS-084823

References:

1. Muradashvili N, Qipshidze N, Munjal C, Givvimani S, Benton RL, Roberts AM, Tyagi SC, Lominadze D. Fibrinogen-induced increased pial venular permeability in mice.*J.Cereb.Blood.Flow.Metab.2012;(32):150-163*
2. Gimbel DA, Nygaard HB, Coffey EE, Gunther EC, Laurén J, Gimbel Z, Strittmatter SM. Memory impairment in transgenic Alzheimer mice requires cellular prion protein.*J.Neuroscience.2010;(30):6367-6374*
3. Muradashvili N, Benton RL, Saatman KE, Tyagi SC, Lominadze D. Ablation of matrix metalloproteinase-9 gene decreases cerebrovascular permeability and fibrinogen deposition post traumatic brain injury in mice.*Metab.Brain.Dis.2014(InPress)*
4. Muradashvili N, Tyagi R, Lominadze D. A dual-tracer method for differentiating transendothelial transport from paracellular leakage in vivo and in vitro.*Front.Physiol.2012;(3):166-172*

334
BRAIN-0292
Poster Session

Vascular Cognitive Impairment

BRAIN CONNECTIVITY CHANGES IN A MOUSE MODEL OF VASCULAR COGNITIVE IMPAIRMENT.

P. Boehm-Sturm[1], M. Füchtemeier[2], M. Foddis[1], M. Zille[1], S. Mueller[1], R.C. Trueman[3], I. Amat-Roldan[4], U. Dirnagl[1], T. Farr[3]
[1]Department of Experimental Neurology Center fo r Stroke Research Berlin (CSB), Charité Universitätsmedizin, Berlin, Germany
[2]German Center for Neurodegenerative Diseases (DZNE), German Center for Neurodegenerative Diseases (D ZNE), Berlin, Germany
[3]School of Life Sciences Medical School Queen's M edical Centre, University of Nottingham, Nottingham, United Kingdom
[4]Expert Ymaging SL, Expert Ymaging SL, Barcelona, Spain

Objectives: A mouse model of chronic brain hypoperfusion has been proposed to mimic aspects of small vessel disease, such as white matter damage[1,2,3]. This model has attracted attention on account of its potential, but many groups have failed to observe a distinctive phenotype. This study aimed to increase the severity of hypoperfusion in aged mice in order to obtain a more reliable phenotype that could be detected with multi-modal neuroimaging.

Methods: Aged (9-13 months) male C57/BL6 mice (n=23) were randomized to receive 160µm (n=12) or 500µm (n=10, sham) diameter microcoils around both carotid arteries, and all experiments were performed blind. Cerebral blood flow (CBF) was measured prior to and at 24hrs, 1 and 4wks post-surgery. Spectroscopy, angiography and diffusion tensor imaging (DTI) were performed at 5wks. DTI data was co-registered to a custom template to extract 4 different diffusion indices across 22 different brain regions, and connectomics analysis was applied to a subset of

the DTI data. Spatial learning and reference memory were examined in the Morris water maze at 6wks. Novel object recognition (NOR) (before and at 4wks post-surgery) does not require a hippocampal dependent spatial component, thus it examines working memory impairments that are likely to exist in the patient population. Finally, tissue was processed for immunohistochemistry.

Results: There was a profound decrease in CBF in the hypoperfused group that recovered to near baseline by 4wks. For the first time, we report higher escape latencies in the hypoperfused mice during the 7 day water maze acquisition, indicating reduced spatial learning abilities, though spatial reference memory remained intact. There was reduced exploration of the novel object in the hypoperfused mice after surgery that was not evident at baseline, which suggests some working memory impairments. There were differences in several DTI indices in some of the examined brain regions between sham and hypoperfused mice. Detailed analysis is currently pending for this as well as the spectroscopy. Connectomics revealed decreases in global efficiency (reduced capacity for parallel exchange of information between all connected regions) and modularity (a reflection of the adaptability of the brain network) in the hypoperfused group (Figure 1). A few of the hypoperfused animals also exhibited reactive gliosis (GFAP staining) in the hippocampus.

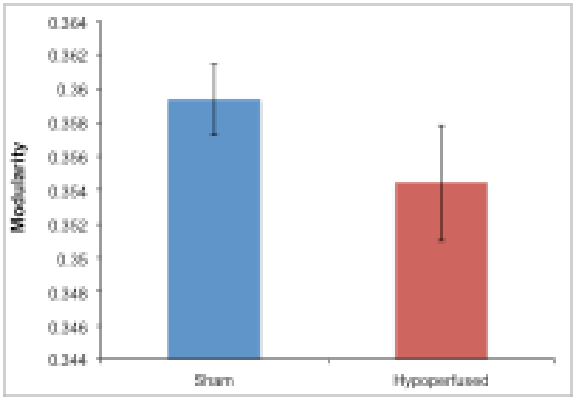

Conclusions: By increasing the degree of hypoperfusion in aged mice subtle impairments in behavioral tests, that were not previously observed, became apparent, though the variability of this model remains an issue. Despite the ability of the mouse brain to eventually compensate and improve CBF, there is still evidence of an overall decline in brain function.

References:

1. Coltman, *et al*, 2011. NeurobiolAge. 2324: 7
2. Shibata, *et al*, 2004. Stroke. 35: 2598
3. Reimer, *et al*, 2011. JNeurosci. 31: 18185

335
BRAIN-0723
Poster Session

Vascular Cognitive Impairment

COGNITIVE FUNCTION AND CEREBROVASCULAR RESERVE IN PATIENTS WITH SEVERE STENO-OCCLUSIVE DISEASE OF AN INTERNAL CAROTID ARTERY OR A MIDDLE CEREBRAL ARTERY

M. Ishikawa[1], H. Saito[1], N. Soma[1], T. Yamaguro[1], M. Ikoda[1], A. Ebihara[1], G. Kusaka[1], Y. Tanaka[1]
[1]Neurosurgery,
Saitama Medical Center Jichi Medical University, Saitama, Japan

Objectives: Patients with severe steno-occlusive disease of a main cerebral artery may demonstrate cognitive impairment without focal neurological deficits and without identification of causative lesions on magnetic resonance imaging (MRI), but the pathophysiology of this condition has not been characterized. We investigated whether cognitive impairment in these patients is associated with cerebral blood flow (CBF), cerebrovascular reserve (CVR), leukoaraiosis, and risk factors of atherosclerosis and whether the CVR decreases widespread-nonselectively on both sides.

Methods: In 65 patients with severe steno-occlusive disease of an internal carotid artery (ICA) or a middle cerebral artery (MCA), we examined cognitive function with COGNISTAT (the Japanese version of the neurobehavioral cognitive status examination), grades of periventricular hyperintensity (PVH) and deep subcortical white

matter hyperintensity (DSWMH) as measured by MRI and cerebral blood flow (CBF) and cerebral vascular reserve (CVR) as calculated by iodine-123-N-isopropyl-p-iodoamphetamine single photon emission computed tomography (^{123}IMP-SPECT) and blood data (hemoglobin A1c [HbA1c], total cholesterol, triglycerides, low-density lipoprotein [LDL] cholesterol, high-density lipoprotein [HDL] cholesterol). In 15 patients who underwent superficial temporal artery (STA)-middle cerebral artery (MCA) anastomosis, the measured values were compared with those collected postoperatively.

Results: Logistic regression analysis revealed that both CVR and DWFMH correlated with cognitive impairment. There was no significant difference in CBF, CVR, or COGNISTAT score when comparing the left side and right side. There were good correlations between CBF or CVR of the ipsilateral MCA area and those of all other areas. For example, in the CBFs of ipsilateral MCA area and contralateral MCA area at the anterior horn level of the lateral ventricle, the regression equation was Y = 0.70x + 14.3, the correlation coefficient was 0.81, and the p value as < 0.0001. In the CVRs between ipsilateral MCA area and contralateral MCA area at the anterior horn level of the lateral ventricle, the regression equation was Y = 0.52x + 33.4, the correlation coefficient was 0.64 and the p value was < 0.0001. In patients who underwent STA-MCA anastomosis, both postoperative CVR and cognitive impairment improved, and the correlations between CBF or CVR of the ipsilateral MCA area and those of all other areas were maintained. However, the COGNISTAT score did not change in the matched control group (without STA-MCA anastomosis)

Conclusions: Cognitive impairment is associated with CVR in the whole brain, and nonselective widespread disconnections may be a reason for cognitive impairment in patients with severe steno-occlusive disease of a main cerebral artery. Cognitive impairment and CVR improved after STA-MCA anastomosis, compared to preoperative values.

336
BRAIN-0842
Poster Session

Vascular Cognitive Impairment

CONNECTOME MODELING TO PREDICT FUNCTIONAL INACTIVATION AFTER ISCHEMIC STROKE

J. Liu[1], O. Schmitt[2], S. Badurek[3], G. Rabiller[3], J. He[3], P. Eipert[2]
[1]Neurological Surgery, UCSF, San Francisco, USA
[2]Anatomy, Uni Rostock, Rostock, Germany
[3]Neurosurgery, UCSF, San Francisco, USA

Introduction: Recent advances in functional connectivity suggest that shared neuronal activation patterns define brain networks linking anatomically separate brain regions. The parietal cortex, the primary lesion site in the distal middle cerebral artery occlusion (dMCAO) model, is functionally interconnected with other brain regions. Because remote brain areas that are not directly affected by ischemia can still undergo functional and plasticity changes, we sought to investigate how ischemic injury in the parietal cortex disrupted multiple brain regions in processing spatial information.

Method: Neuronal activation induced by spatial exploration was mapped in adult rats by the immediate early gene c-Fos, a proxy of neuronal activity of which the expression is induced under conditions of learning and memory. Brain regions with reduced Fos expression following task engagement would reflect stroke induced neuronal hypoactivation. To determine stroke-induced connectome changes, we performed a connectome investigation at the mesoscale level using the neuroVIISAS-framework, which allows to analyze directed and weighted connectivity in bilateral hemispheres of cortical and subcortical brain regions. In addition, the connectivity of regions has been integrated into a digital stereotaxic atlas of the complete rat nervous system. The relationship between brain activation by Fos mapping and the connectome network parameters was also assessed.

Results: Constitutive c-Fos expression was detected in 38 brain regions in awake, sham-operated rats living in their home cages. Spatial exploration induced brain activation in most of the 38 regions. In dMCAO rats compared to sham ones a significant region-specific reduction in neural activation was observed in several hippocampal, parahippocampal and thalamic regions during spatial exploration. We found that the extent of neuronal activation of a particular region of interest is correlated with the spatial distance to the infracted regions in the parietal cortex. Although the correlation coefficients for Eigenvector Centrality and Hubness with c-Fos expressions for the home cage animals are 0.54 and 0.51, respectively; connectome modeling with 43 network parameters failed to predict regions of hypoactivation in stroke rats exploring a novel environment.

Conclusion: The c-Fos mapping study suggests that brain regions are differentially affected by stroke in processing novel spatial information. Although regions of reduced brain activation cannot be predicted by the known connectivity parameters using connectome modeling, the extent of brain activation following spatial exploration is correlated with the spatial distance between the region of interest and the region damaged by stroke, suggesting that the closer the region to the epicenter of stroke, the greater degree it would be impacted during functional activation. Further investigation in the inhibitory versus excitatory neuronal networks and microcircuit connectivity is warranted in order to improve the accuracy of predictability in post stroke functional activation.

337
BRAIN-0514
Poster Session

Vascular Cognitive Impairment

SIMVASTATIN RESCUES COGNITIVE AND CEREBROVASCULAR DEFICITS INDUCED BY HIGH CHOLESTEROL DIET IN A MOUSE MODEL OF CEREBROVASCULAR DISEASE.

X.K. Tong[1], E. Hamel[1]

[1]Laboratory of Cerebrovascular Research Montreal Neurological Institute,
Montreal Neurological Institute McGill University, Montreal, Canada

Introduction: Transgenic mice overexpressing transforming growth factor-ß1 (TGF mice) display a cerebrovascular pathology characterized by vascular fibrosis, cerebrovascular remodeling, and string vessel pathology (1). These alterations result in impaired cerebrovascular reactivity, chronic cerebral hypoperfusion, and neurovascular uncoupling, but TGF mice have normal cognitive function or only minor changes in their performance with increasing age (1, 2).

Objectives: Cardiovascular diseases being a major risk factor for cognitive impairment and, particularly, vascular dementia, we investigated the impact of a high cholesterol diet (HCD) on cerebrovascular and cognitive function in adult and aged TGF mice, and tested whether the anti-cholesterol drug simvastastin (SV) would have any benefits.

Methods: TGF mice and wild-type (WT) littermate controls were fed a HCD (2% cholesterol and 0.5% cholic acid, 3 months), and tested at 6 (adult) or 12 (aged) months. Another cohort of adult mice was concurrently treated with or without SV (40 mg/kg/day) (3). Blood and brain cholesterol levels were measured at endpoint. Spatial learning and memory were assessed in the Morris water maze (MWM) (1, 3). The cerebral blood flow (CBF) response evoked by whisker stimulation (laser Doppler flowmetry), and the vasomotor reactivity of the posterior cerebral artery (online videomicroscopy) were measured. Another group of mice was perfused for immunohistochemical quantification of string vessels and astrogliosis.

Results: HCD significantly increased blood, but not brain cholesterol levels in both WT and TGF mice, and SV treatment exerted no reducing effect. In adult and aged TGF mice, HCD worsened the deficits in the dilatory responses to acetylcholine and calcitonin gene-related peptide in an age-dependent manner. SV normalized these deficits together with dilatations mediated by KATP and

TRPV4 channels that were restored to WT levels. The whisker-evoked increased in CBF was impaired in adult and aged TGF mice. HCD did not worsen this deficit, which was fully normalized by SV. Neither adult nor aged TGF mice displayed any significant deficits in the MWM test. However, cognitive decline developed in TGF mice of both age groups when fed a HCD, and SV rescued this deficit. Except for a small increase (~25%) in the number of string vessels in adult TGF mice, HCD or SV did not affect astrogliosis or had minor effect on string vessel pathology.

Conclusions: The results show that HCD exacerbates cerebrovascular dysfunction and precipitates cognitive decline in TGF, but not in WT mice. These findings suggest that an underlying vascular pathology facilitates the expression of cognitive failure when combined to another risk factor for dementia. SV, independent of its cholesterol lowering effects, countered all deleterious effects of HCD on vascular and neuronal function. These results suggest that SV may bear promise in preventing or delaying cognitive failure related to vascular dementia.

References:

(1) X-K Tong and E Hamel. 2015, JCBFM in press; (2) RF Gaertner, et al. 2005, Neurobiology Dis 19:38; (3) X-K Tong, et al. 2012, J Neuroscience 32:4705.

Acknowledgements: Supported by grants from the Canadian Institute of Health research (CIHR, MOP-126001) and the Heart and Stroke Foundation of Québec.

338
BRAIN-0116
Poster Session

Animal models

AMELIORATING EFFECT OF MINOCYCLINE AGAINST 3-NITROPROPIONIC ACID-INDUCED COGNITIVE DYSFUNCTION AND BRAIN OXIDATIVE STRESS IN MALE RATS

M. AHMAD[1], *M. WADAAN*[2]

[1]*Department of Medical Surgical Nursing, College of Nursing, Riyadh, Saudi Arabia*
[2]*Department of Zoology, College of Science, Riyadh, Saudi Arabia*

Objective:

3-Nitropropionicacid (3-NP) is reported to cause decreased motor performance in animals withlesions primarily in brain regions like hippocampus and striatum. It is aneurotoxin which evokes an experimental model of Huntington's disease.Oxidative stress has also been suggested to play a role in 3-NP toxicity;however, the process behind the oxidative damage is not fully understood.Minocycline, a semi synthetic second-generation tetracycline, has been shown tohave robust neuroprotective effects in rodent models of variousneurodegenerative diseases. Recent studies have clearly demonstrated thatincreased oxidative stress is one of the major deleterious events in3-NPA-induced neurodegenerative process.

Method:

Inthe present study we investigated the effects of minocycline on cognitivebehavioral dysfunction and brain oxidative stress induced by the administrationof 3-NP to adult male rats. 3-NP (20 mg/kg) was given daily *i.p.* toanimals for 7 days. Minocycline (50 and 100 mg/kg) was administered orally, 30min before 3-NP administration for seven days. 24 h after the last 3-NP dose,the animals were subjected to cognitive behavioural assessments(including shuttle-box and water-maze tests). The animals were sacrificedto remove their hippocampus and striatum for biochemical assessments ofoxidative stress indices in these brain regions. Ethical approval was obtainedfrom the Institutional Animal Care and UseCommittee and all care and handling of the animals were humane and inaccordance with the guidelines of EthicsCommittee Review Board of the College of Pharmacy of King Saud University,Riyadh, Saudi Arabia.

Results:

Minocyclinedose-dependently ameliorated 3-NP-induced dysfunction in cognitive behavior. Inaddition, 3-NP produced a marked increase in lipid peroxidation levels measuredas thiobarbituric acid reactive substance (TBARS), and decreased the activitiesof reduced glutathione (GSH), catalase (CAT) and superoxide dismutase (SOD)activities in a dose-dependent manner. Pre-treatment of 3-NP injected rats withminocycline resulted into ameliorating these alterations in all studiedparameters.

Conclusion:

Thepresent finding suggest for the neuroprotective effect of minocyclineagainst 3-NP – induced cognitive dysfunction probably mediated by virtue of itsantioxidant activity. Further studies on these lines may help in foridentifying Minocycline as a possible pharmacological treatment forcognitive impairment and dementia problems in Huntington's patients.

339
BRAIN-0359
Poster Session

Animal models

CREATION OF A NOVEL PRECLINICAL MODEL OF PRIMARY BLAST-INDUCED TRAUMATIC BRAIN INJURY BY USING LITHOTRIPSY SHOCK WAVE

A. Divani[1], H. Sadeghi-Bzargani[2], A. Murphy[1], B. Sweis[1], S. Bachour[1], M. Monga[3]
[1]Neurology, University of Minnesota, Minneapolis, USA
[2]Department of Public Health Sciences, Karolinska Institute, Stockholm, Sweden
[3]Urology, Cleveland Clinic, Cleveland, USA

Objective: We present a novel method to induce blast traumatic brain injury (bTBI) using shockwave (SW) lithotripsy in rats with histological, angiographic, and behavioral outcomes over the course of injury and recovery similar to those observed in clinical settings.

Background: bTBI is the "signature" closed-head injury of the recent Iraq and Afghanistan wars. There are a variety of methods used to study the effects of bTBI including utilizing explosives that can replicate characteristic blast waves; however, such methods are impractical requiring, for example, large open-field space and handling explosives. SW lithotripsy utilizes an electrohydraulic generator that can cause reproducible neurotrauma injury clinically relevant to blast exposure, providing small focused zones of pressure which affords the greatest opportunity for inducing focal brain injury.

Methods: To induce bTBI, anesthetized rats were placed on a lithotripsy machine (shown in Figure 1) to deliver 5 SW pulses of 24kV with 60 Hz frequency to the right frontal cortex of each rat's brain. Animals were assigned to three sacrifice endpoints: 24hrs, 72hrs, and 168hrs. Neurological and behavioral assessments (Garcia's test, beam-walking, Rotarod, and elevated-plus-maze) were performed at 3, 6, 24, 72, and 168hrs post-injury, if applicable. We performed digital subtraction angiography (DSA) to assess presence of cerebral vasospasm. Damage to brain tissue was assessed by an overall histological severity (OHS) score based on injury depth, area of hemorrhage, and extent of axonal injury.

Results: Except for beam-walking, OHS significantly correlated with the other three behavioral outcomes and with at least one measurement during the first 6hrs. OHS correlated most strongly with anxiety at the baseline and 6hrs post-injury ($r_{baseline}$=-0.75, $r_{6\ hrs}$=0.85; P<0.05). Median hemispheric differences for contrast peak values (CPV), obtained from DSA studies, for 24, 72, and 168hrs endpoints were 3.45%, 3.05% and 0.2%, respectively, with significant differences at 24 vs. 168 hours (p<0.05) and 72 vs. 168 hours (P<0.01). According to the nonparametric test results, the differences in CPV were associated with the study endpoints (P<0.01).

Conclusion: We successfully established a preclinical rat model of bTBI with characteristics

similar to those observed in clinical cases. This new method may be useful for future investigations aimed at understanding bTBI pathophysiology.

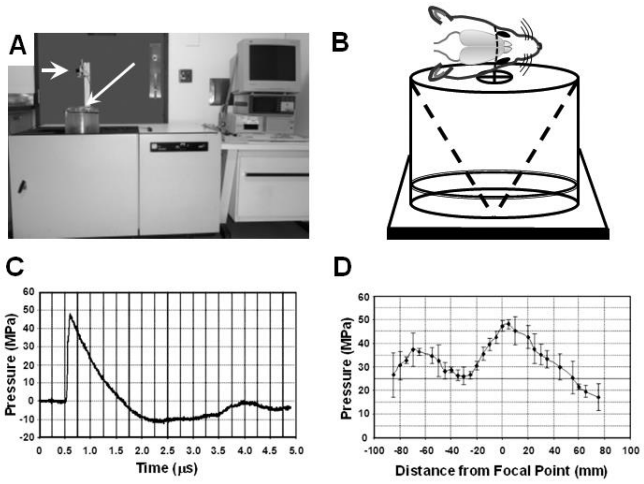

340
BRAIN-0165
Poster Session

Animal models

MECHANISM OF POST-STROKE DEMENTIA: INTERACTION BETWEEN TERRITORIAL INFARCTION AND CHRONIC CEREBRAL HYPOPERFUSION

H.Y. Kim[1], D.B. Back[1], J.H. Seo[1]
[1]Neurology, School of Medicine Konkuk University, Seoul, Korea

Background: Post-stroke dementia (PSD) is one of main consequences after ischemic stroke. Ischemic stroke is accompanied by secondary neurodegenerative with up-regulation of β-amyloid precursor protein (APP) and Aβ deposits localized to the ischemic core and surrounding penumbra. Accordingly, the generation of Aβ and its subsequent deposition under burden of ischemic stress are presumably the pathological link that accounts for the progression of PSD. After territorial infarction, some patients develop PSD and some do not. Nevertheless, the neuropathology of three-fourth of stroke-patients who do not develop clinically new-onset of dementia within their first or recurrent stoke remains unclear. To elucidate this unresolved question, chronic cerebral hypoperfusion (CCH) as a frequent consequence of cerebrovascular dysfunction has considered as the major cause for exacerbating the development of dementia following ischemic stroke.

Methods: The adverse effects of CCH on a neurodegenerative status which deteriorate cognitive functions in the course of post stroke were investigated by designing a novel animal model. Primarily, the right middle cerebral artery was transiently occluded (tMCAo) for 90 min in Wistar rats to mimic focal cerebral ischemia clinically, yielding territorial infarction which triggered the accumulation of Aβ aggregates. After 2-week, tMCAo rat models were subjects to permanent occlusion of bilateral common carotid arteries (BCCAo) for 6 weeks to mimic CCH mechanism. In addition to tMCAo + BCCAo models, three types of models were added to be compared: Sham + sham-operated rats; tMCAo + sham operated rats; Sham + BCCAo operated rats. Spatial memory, motor, perception and cognition functions was assessed in Morris water maze test (MWM), modified neurological severity score test (mNSS), foot fault test, and parallel bar test. To evaluate the degree to which either ischemia or CCH, or both of them affected neurodegeneration, various antibodies for immunoreactivity in the rat brain including the cortex, hippocampus, striatum, thalamus, and penumbra were used as follows: Aβ, APP, tau, ionized calcium binding adaptor molecule 1 (Iba1), glial fibrillary acidic protein (GFAP), NeuN, and microtubule-associated protein 2 (MAP2).

Results: Compared to the other three types of rat models, tMCAo + BCCAo group showed considerable spatial memory impairment. Interestingly, BCCAo group representing the effect of CCH revealed more memory decline than did tMCAo group that clinically corresponded to ischemic disorders. As a result, CCH may be more weighting factor than acute ischemic stress, potentially bringing about the progression of dementia. Immunohistochemical analysis may also suggest that the most increases in aggregated Aβ, tau, inflammatory responses and

neuronal loss in the novel combination model explained PSD mechanism.

Conclusion: tMCAo + BCCAo model provided a novel insight into how CCH has a deleterious effect on the progression of dementia initiated by ischemic stroke. CCH may be the major risk factor that continued to aggravate cognitive dysfunction, leading to post-stroke dementia.

341
BRAIN-0166
Poster Session

Animal models

COGNITIVE IMPAIRMENTS IN A RAT MODEL OF STREPTOZOTOCIN-INTRAVENTRICULAR INJECTION: INTERACTION BETWEEN DIABETES AND ALZHEIMER'S DISEASE

H.Y. Kim[1], J.H. Seo[1], D.B. Back[1]
[1]Neurology, School of Medicine Konkuk University, Seoul, Korea

Background: Diabetes is well known as one of the major risk factors in Alzheimer's disease. However, the mechanism has not been clearly elucidated how diabetes exacerbated cognition in terms of the vascular or Alzheimer pathology. Rat model of streptozotocin-intraventricular injection (STZ-icv) has been recently proposed as an animal model for diabetic dementia or sporadic Alzheimer's disease. We investigated cognitive impairments in STZ-icv rats and vascular and Alzheimer pathology.

Methods: STZ (3mg/kg) was intraventricularly injected bilaterally in 3-month-aged Wistar rats. Morris water maze task and noble object test were performed for the cognitive evaluation. Vascular pathology including cerebral amyloid angiopathy and Alzheimer pathology including amyloid beta and tau were investigated.

Results: Cognitive impairments were prominent in STZ-icv rats. Pathology of cerebral amyloid angiopathy and Alzheimer disease were increased in a time-dependent manner.

Conclusion: STZ-icv rats may be a useful tool to investigate pathomechanism of diabetic dementia. Cerebral amyloid angiopathy and Alzheimer pathology may be one of main culprits for the diabetic dementia.

342
BRAIN-0252
Poster Session

Animal models

DEVELOPMENT OF THE RAT VASCULAR DEPRESSION MODEL

H. Ono[1], H. Imai[1], S. Miyawaki[1], S. Miyata[2], H. Nakatomi[1], M. Mikuni[2], M. Fukuda[2], N. Saito[1]
[1]Department of Neurosurgery, The University of Tokyo, Tokyo, Japan
[2]Department of Psychiatry and Neuroscience, Gunma University, Gunma, Japan

[Objectives]

Vascular depression of the elderly gets familiar with growing aged society in developed countries. The occurrence of white matter hyperintensities on T2-weighted magnetic resonance images is more frequent in patients with vascular depression patients, compared with intrinsic depression patients. This fact indicates that deep white matter injuries (WMIs) may provoke some kind of vulnerability leading to depression with daily stress. In this study, we have developed a selective WMI rat model with restraint stress (RS) to evaluate the correlation between the WMI and depression.

[Methods]

Sprague-Dawley rats (302-380g, n=108) were used in this study. Selective WMI was induced with bilateral endothelin-1 injection under general anesthesia. Animals were randomly assigned to 4 groups: WMI with RS (group 1); sham operation with RS (group 2); WMI no RS (group 3); sham operation, no RS (group 4). Two weeks after surgery, group 1 and 2 animals received 2 hours of RS a day, for 13 days. Some animals in group 1 and 4 received escitalopram

along the protocol. Body weight (BW) was recorded daily and blood samples were collected at three time points for the serum corticosterone level measurment along the protocol. Animals underwent a forced swimming test (FST) on the day following the 13th RS day. Animals were euthanized after the FST, and brain sections analyzed.

[Results]

Conventional histopathology of the operated rat brain revealed the selective damage of the internal capsule. RS significantly suppressed weight gain in groups 1 and 2 compared with non RS groups. Moreover the change in BW over time in group 1 was significantly different from group 2. The body weight reduction in group 1 reversed with the administration of escitalopram. The corticosterone levels were elevated at the seventh stress day and returned to basal levels at the thirteenth day in group 1 and 2. The immobility time on the FST for group 1 was longer than that of other groups.

[Conclusions]

We have investigated whether animals with selective WMI showed evidence of increased stress-induced depressive behavior. Accompanied with WMI, repeated RS induced a reduction in weight gain and prolongation of the immobility time in the FST. These results provide some preliminary evidence that WMI could influence stress vulnerability. Additionally, selective serotonin reuptake inhibitor reversed the weight gain reduction. In order to use this model as rat vascular depression model, further behavioral tests need to be added, but it is considered that this model represents some aspects of the depression related to the WMI, and may have a potential to contribute to the near future aging society.

343
BRAIN-0638
Poster Session

Animal models

THE ALTERATIONS IN BRAIN FUNCTION DUE TO BRAIN TUMOR GROWTH

I. Orukari[1], A. Bauer[1], E. Slat[2], J. Rubin[2], J. Culver[1]
[1]Radiology, Washington University, St. Louis, USA
[2]Pediatrics, Washington University, St. Louis, USA

Objectives: To assess the effects of tumor growth on resting-state functional connectivity in a mouse model of glioma. The resting-state functional connectivity data was obtained using functional connectivity optical intrinsic signal (fcOIS). This technique allowed us to perform functional neuroimaging on the small mouse brain.

Methods: 10^5 U87 gliomas cells were stereotactically injected into the cortical region in between the motor cortex and hindpaw and forepaw somatosensory cortex of adult nude mice. A plastic cover slip was affixed to the exposed skull of the mice for serial OIS imaging. For OIS imaging, illumination of the exposed cortex was provided by four LEDs (wavelengths centered at 478 nm 588 nm 610 nm 625 nm) and reflected light was captured by a CCD camera running at 120 Hz. Each mouse was imaged for at least four trials of five minutes. The modified Beer-Lambert Law was used to interpret the reflected light intensity. Oxy- and deoxy-hemoglobin data were filtered to the functional connectivity band (0.009-0.08 Hz) following previously reported human functional connectivity algorithms [1]. Variance in OIS was a metric used to quantify alterations in the spontaneous hemodynamic response. Seed based functional connectivity analysis was performed on the OIS images to monitor how brain tumor growth affects functional brain networks. Bilateral functional connectivity maps – maps of the correlation value between a pixel and the corresponding pixel in the contralateral hemisphere – were obtained as a metric of functional network disruption.

Results: The amplitude of the spontaneous response within the region of the brain tumor was decreased. A variance map of the OIS images showed a decrease in variance within the region of the brain tumor. Brain tumor growth resulted in a decrease in bilateral functional connectivity within the pixels corresponding to the brain tumor. The region of decreased bilateral functional connectivity increased in size with time.

Conclusions: We have shown that fcOIS is capable of detecting alterations to brain function due to brain tumor growth. Brain tumors have abnormal vasculature and perfusion. This may explain why the amplitude and variance of OIS was decreased within the region of the tumor. Since the hemodynamic response is altered within the borders of the brain tumor, it is no surprise that bilateral functional connectivity metrics were disrupted within the pixels containing the tumor. A better understanding of the role brain tumors play in the development of functional brain deficits may lead to improved outcomes after neurorehabilitation.

References:

1. Fox MD, Snyder AZ, Vincent JL, Corbetta M, Van Essen DC, et al. (2005) The human brain is intrinsically organized into dynamic, anticorrelated functional networks. Proceedings of the National Academy of Sciences of the United States of America 102: 9673-9678.

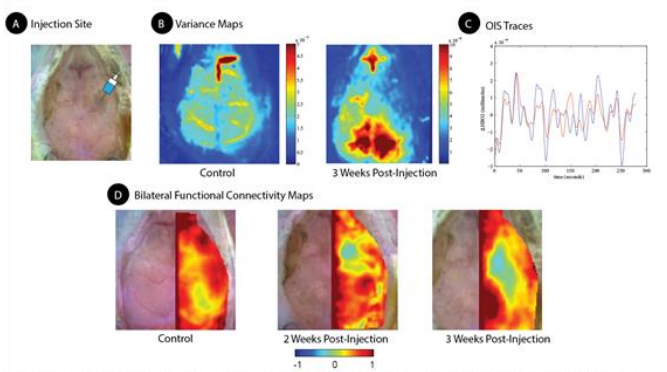

Alterations in brain function due to brain tumor growth. A) Injection site: tumor cells injected into cortical region between the motor cortex and the somatosensory cortices for forepaw and hindpaw. **B)** Variance map for a representative control mouse and a representative mouse with tumor at 3 weeks post-injection **C)** Traces of spontaneous fluctuations in OIS over the course of a 5 minute trial in a representative tumor bearing mouse at 3 weeks post-injection. The red trace represents a pixel in the region of tumor growth and the blue trace represents the corresponding pixel in the contralateral hemisphere. Note the amplitude of the tumor region is decreased compared to the amplitude of the contralateral side. **D)** Bilateral functional connectivity maps of control mice, tumor bearing mice 2 weeks post-injection, and tumor bearing mice 3 weeks post-injection.

344
BRAIN-0341
Poster Session

Animal models

ASSESSMENT OF BRAIN DELIVERY AND METABOLISM OF [18F]FDG IN AN EXPERIMENTAL PARABIOSIS MODEL, FOLLOWING SINGLE PARTNER ADMINISTRATION

M. Palner[1], B. Shen[1], J.C. Castellano[2], J. Luo[2], T. Wyss-Coray[2], F.T. Chin[1]
[1]Molecular Imaging Program at Stanford, Stanford University School of Medicine, Stanford, USA
[2]Department of Neurological Sciences, Stanford University School of Medicine, Stanford, USA

Objectives

Recent discoveries using heterochronic parabiosis—parabiosis of young and old—show that young mice blood rejuvenates cognitive function and neuroplasticity of older mice[1,2]. Parabiosis leads to microvascular anastomosis and a shared circulatory system where circulating factors of one animal affects the other. It has been shown that $Na^{51}CrO_4$ labeled erythrocytes travel from one animal to the other animal, with 50% present after 4 days[3]. However, how this shared circulation develops post surgery has not been studied with short-lived isotopes such as fluorine-18. We hypothesized that brain delivery and metabolism of [^{18}F]FDG would increase in the non-injected partner post parabiotic surgery.

Methods

Eight mice were combined in 4 age-matched isochronic parabiotic pairs by connecting the peritoneal cavity[2]. At day 3, 5, 7,14 and 39 a catheter was placed in the tail vein of one mouse in a pair. The mice pairs were placed in an Inveon microPET/CT (Siemens). And received a 60-min dynamic [^{18}F]FDG PET scan. Tracer activity over time was calculated as a percentage of the injected dose per gram tissue (%ID/g) in each pair and as %uptake in the brain of the non-injected

mouse compared with the injected mouse. [^{18}F]FDG brain metabolism was not corrected to blood glucose levels or body weight due to the difficult interpretation of such a result in the parabiotic mice.

Results

Brain [^{18}F]FDG uptake at 60 minutes in the injected mouse of each parabiotic pair was comparable but slightly lower than in control mice, with an average of 7.1 ± 1.1 %ID/g at Day 3 to 5.5 ± 1.5 %ID/g at Day 39 versus 9.8 ± 2.4 %ID/g in control mice. Simultaneously, the brain [^{18}F]FDG uptake at 60 minutes in the non-injected mouse was 0.09 ± 0.06 %ID/g at day 3, significantly higher than background levels and was increasing up 0.39 ± 0.11 %ID/g at day 14. The rate of [^{18}F]FDG delivery to the brain of the injected mouse was at maximum within 5 minutes, comparable with control mice. However, the delivery to the brain of non-injected mouse was much slower, and still increasing at the 60-minute time point, similarly to what one observes with a slow infusion of a radiotracer.

Conclusions

Our results show that [^{18}F]FDG was delivered to and metabolized in the brain of the injected mouse as early as day 3 in this parabiosis model. However, complex pharmacokinetics of [^{18}F]FDG after microvascular anastomosis formation leads to a slower delivery of [^{18}F]FDG to non-injected mouse. Further PET studies of blood flow (e.g., [^{15}O]water) or angiogenesis (e.g., [^{18}F]FPPRGD2) could offer more insight to the development of this parabiosis model.

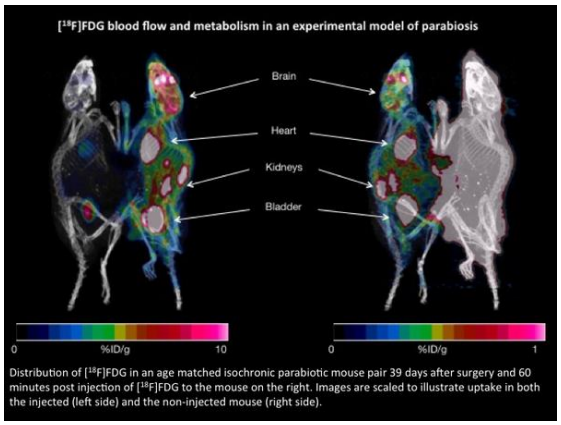

References

1. Katsimpardi L, Litterman NK, Schein PA, et al. Vascular and neurogenic rejuvenation of the aging mouse brain by young systemic factors. *Science*. 2014;344(May):630-634.

2. Villeda S a, Plambeck KE, Middeldorp J, et al. Young blood reverses age-related impairments in cognitive function and synaptic plasticity in mice. *Nat Med*. 2014;20(6):659-663.

3. Sodicoff M, Binhammer RT. The Time of Origin of the Parabiotic Anastomosis. *Anat Rec*. 1964;148:625-629.

345
BRAIN-0451
Poster Session

Animal models

HUMAN NEURAL STEM CELLS ENCODING CHOLINE ACETYLTRANSFERASE GENE RESTORE COGNITIVE FUNCTION AND PHYSICAL ACTIVITY IN ALZHEIMER DISEASE MOUSE MODEL

J.M. Ryu[1], D. Park[2], K. Shin[1], Y. Choi[3], E.K. Choi[3], D.J. Kim[1], S.U. Kim[4], Y.B. Kim[1]
[1]College of Veterinary Medicine, Chungbuk National University, Cheongju, Korea
[2]Department of Physiology, Ajou University School of Medicine, Suwon, Korea
[3]Stem Cell R&D Center, iCellBank, Seoul, Korea
[4]Division of Neurology, University of British Columbia Hospital, Vancouver, Canada

Objectives: Alzheimer disease (AD), one of the most devastating neurological diseases, is characterized by specific memory deficits due to acetylcholine depletion following degeneration of cholinergic system. For AD therapy, administration of acetylcholinesterase (AChE) inhibitors partially recovers cognitive deficits. Since they are only palliative without slowing or reversing disease progress, there is a need for effective therapies for patients with AD, and stem cell-based therapeutic approaches targeting AD should fulfill this requirement.

Methods: We established a human neural stem cell (NSC) line encoding choline acetyltransferase (ChAT) gene, an acetylcholine-synthesizing enzyme. APPswe/PS1dE9 AD model mice transplanted with the F3.ChAT NSCs exhibited improved cognitive function and physical activity. All the animal experiments were conducted according to the Standard Operation Procedures, and approved by the Institutional Animal Care and Use Committee to Chungbuk National University, Korea.

Results: Transplanted F3.ChAT NSCs in the AD mice differentiated into neurons and astrocytes, produced ChAT protein, increased ACh level, and improved the learning and memory function. F3.ChAT cell transplantation reduced Aβ deposits by recovering microglial function; i.e., down-regulation of β-secretase and inflammatory cytokines and up-regulation of Aβ-degrading enzyme neprilysin. F3.ChAT cells restored neurotrophic factors, and induced proliferation of NSCs in the host brain.

Conclusions: These findings indicate that NSCs overexpressing ChAT can ameliorate complex cognitive and physical deficits of AD animals by releasing ACh, reducing Aβ deposit, and promoting neuroregeneration by production of neurotrophic factors. It is suggested that NSCs over-expressing ChAT could be a candidate for cell therapy in advanced AD therapy.

References:

Park D, Joo SS, Kim TK, Lee SH, Kang H, Lee HJ, Lim I, Matsuo A, Tooyama I, Kim YB, Kim SU: Human neural stem cells overexpressing choline acetyltransferase restore cognitive function of kainic acid-induced learning and memory deficit animals. *Cell Transplant.* 2012, 21(1):365-371.

Park D, Lee HJ, Joo SS, Bae DK, Yang G, Yang YH, Lim I, Matsuo A, Tooyama I, Kim YB, Kim SU: Human neural stem cells over-expressing choline acetyltransferase restore cognition in rat model of cognitive dysfunction. *Exp Neurol.* 2012, 234(2):521-526.

Kim SU: Human neural stem cells genetically modified for brain repair in neurological disorders. *Neuropathology* 2004, 24(3):159-171.

346
BRAIN-0119
Poster Session

Animal models

MICROSPHERE EMBOLUS FROM THE COMMON CAROTID ARTERY CAN PRODUCE INFARCTION IN THE WATERSHED AREA IN MICE

N. Tsukada[1], M. Katsumata[1], K. Oki[1], T. Abe[1], S. Takahashi[1], Y. Itoh[2], N. Suzuki[1]
[1]Department of Neurology, Keio University School of Medicine, Tokyo, Japan
[2]Department of Neurology, Osaka City University, Osaka, Japan

Objectives

A watershed infarction often occurs in patients with severe internal carotid artery stenosis. It has long been assumed that a hemodynamic mechanism plays an important role in this event. In recent years, however, clinical evidence indicates that an embolic mechanism is involved in the watershed infarction.[1] In other words, impaired clearance of micro-emboli due to low perfusion pressure is supposed to play a role in cerebral infarction in the watershed area.[2] In the present study, we injected fluorescent microspheres with various diameters into the common carotid artery of mice, characterized their distribution, and evaluated a possible embolic mechanism producing the watershed infarction.

Methods

C57BL/6 mice (6-8 weeks old) were used. After inhalation anesthesia, we injected fluorescent microspheres made of polystyrene divinylbenzene into the left common carotid artery of the mice. Since a previous study indicated that the microsphere size affected the distribution pattern,[3] we used microspheres with four different diameters, i.e., 13, 24, 40, and 69 µm. Microspheres were suspended in saline at a concentration of 1×10^5/ml and a volume of 0.05 ml was injected.[4] After 24 hours, the brains were removed and the distribution pattern of the microsphere located in the brain surface or parenchyma was evaluated using a fluorescence microscope. We specified the watershed areas between the anterior cerebral artery and middle cerebral artery or middle cerebral artery and posterior cerebral artery by staining the brain blood vessels with India ink.

Results

The distribution rates of microspheres in the watershed area were 29.5 ± 14.2% with 13 µm microsphere, 58.7 ± 7.4% with 24 µm, 40.4 ± 12.3% with 40 µm, and 14.2 ± 12.8% with 69 µm (mean ± SD). The distribution rate of 24 µm microsphere in the watershed area was significantly higher than those of other microspheres ($p<0.05$; ANOVA followed by Tukey's test). In addition, the distribution rates in brain parenchyma were 48.6 ± 7.1% with 13 µm, 31.1 ± 5.4% with 24 µm, and 0.7 ± 1.2% with 40 µm. Microspheres with the diameter of 69 µm were not found in the brain parenchyma. The distribution rate of 13 µm microsphere in the brain parenchyma was significantly higher than those of other microspheres ($p<0.05$; ANOVA followed by Tukey's test).

Conclusions

In this study, the mean diameter of the vessels in the watershed area was 26.0 µm (20.1 - 33.1 µm). The vessel diameter in the watershed area was close to that of the 24 µm microspheres, which were distributed in the watershed area. It suggested that microsphere distribution was affected by both microsphere diameter and vessel diameter. Smaller diameter microspheres were not trapped in the watershed area, but in the brain parenchyma. This study suggested an embolic mechanism can produce the typical distribution pattern that resembles a watershed infarction.

References

1. Yamaguchi T, Minematsu K: J Jpn Coll Angiol 1991;31:107-109

2. Caplan LR, Hennerici M: Arch Neurol 1998;55:1475-1482
3. Takagi K, Takeo S: Folia Pharmacol Jpn 2003;121:440-446
4. Pollanen MS, Deck JH: Can J Neurol Sci 1990;17:395-398

347
BRAIN-0269
Poster Session

Animal models

MOUSE MODEL OF LACUNAR INFARCTS WITH LONG-LASTING FUNCTIONAL DISABILITIES

H. Uchida[1], K. Niizuma[1], H. Sakata[1], M. Fujimura[1], M. Dezawa[2], T. Tominaga[1]
[1]Department of Neurosurgery, Tohoku University Graduate School of Medicine, Sendai, Japan
[2]Department of Stem cell Biology and Histology, Tohoku University Graduate School of Medicine, Sendai, Japan

Objectives: Lacunar infarcts account for 25% of all ischemic strokes.[1] Cortico-spinal tract involvement causes severe disabilities in spite of the small lesion size. Recent studies demonstrated that the functional outcome after lacunar infarcts was sometimes unfavorable.[2,3] Thus, preclinical studies using animal models that mimic human lacunar infarcts would be valuable to improve understanding of the disease in humans and develop treatments. However, few pre-clinical animal models that mimic human lacunar infarct have reported.[4] Thus, we attempted to develop a new experimental model of lacunar infarcts using two vasoconstrictive peptides.

Methods: The vasoconstrictor peptide, endothlin-1 (ET-1), in combination with nitric oxide synthase inhibitor, N(G)-nitro-L-arginine methyl ester (L-NAME), was injected in the internal capsule in mice.[5] Behavioral tests (Corner turn test and Cylinder test) were examined from 0 to 8 weeks after injection. Histological assessment and neuronal tracing were performed in 8 weeks after injection.

Results: Behavioral test (Corner tern test) in ET-1 and L-NAME injected group showed significant difference, which continued for up to 8 weeks, compared with phosphate buffered saline (PBS) injected group (Graph). Loss of axons and myelin surrounded by reactive gliosis was identified in the region of ET-1 and L-NAME injection. Moreover, neuronal tracing study revealed the interruption of the axonal flow at the internal capsule.

Conclusions: These results indicate that the present novel model in mice, which exhibits long-lasting neurological deficits, is a simple and reproducible approach for using in further investigation for preclinical studies in lacunar infarcts.

References:

1. Sudlow CL, Warlow CP (1997) Comparable studies of the incidence of stroke and its pathological types: results from an international collaboration. International Stroke Incidence Collaboration. *Stroke* 28: 491-499

2. Jackson C, Sudlow C (2005) Comparing risks of death and recurrent vascular events between lacunar and non-lacunar infarction. *Brain* 128: 2507-2517

3. Norrving B (2003) Long-term prognosis after lacunar infarction. *The Lancet. Neurology* 2: 238-245

4. Sozmen EG, Hinman JD, Carmichael ST (2012) Models that matter: white matter stroke models. *Neurotherapeutics* 9: 349-358

5. Horie N, Maag AL, Hamilton SA, Shichinohe H, Bliss TM, Steinberg GK (2008) Mouse model of focal cerebral ischemia using endothelin-1. *Journal of neuroscience methods* 173: 286-290

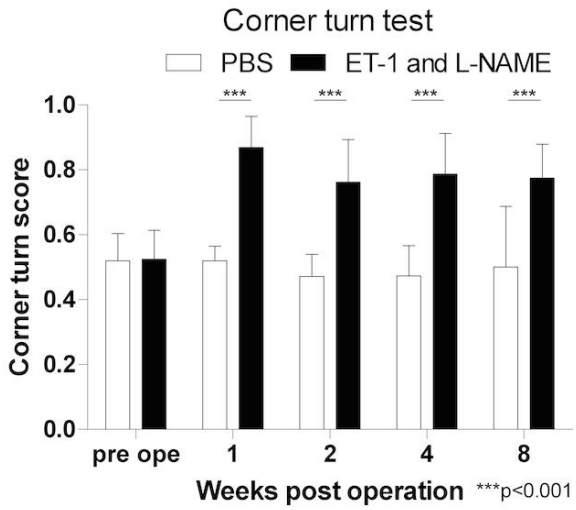

348
BRAIN-0379
Poster Session

Animal models

CHARACTERIZATION OF TWO NON-HUMAN PRIMATE MODELS OF SPORADIC AND INHERITED TAUOPATHIES USING [18F]-FDG AND [18F]-DPA714 PET IMAGING

N. Van Camp[1], M. Guillermier[1], L. Eymin[1], Y. Bramoullé[1], D. Houitte[1], S. Lecourtois[1], C. Jan[1], F. Petit[1], N. Dufour[1], K. Plachytka[1], S. Dujardin[2], A. Bemelmans[1], M. Colin[2], R. Aron Badin[1], N. Deglon[3], L. Buée[2], P. Hantraye[1]
[1]Commissariat à l'Energie Atomique et aux Energies Alternatives (CEA) Département des Sciences du Vivant (DSV), Institut d'Imagerie Biomédicale (I2BM) Molecular Imaging Research Center (MIRCen) Centre National de la Recherche Scientifique (CNRS) Université Paris-Sud Université Paris-Saclay UMR 9199 Neurodegenerative Diseases Laboratory, Fontenay aux Roses, France
[2]Inserm UMR-S 1172 Université Lille 2 Faculté de Médecine, IMPRT JPARC CMRR CHR, Lille, France
[3]Department of Clinical Neurosciences (DNC) Laboratory of Cellular and Molecular Neurotherapies (LNCM), Lausanne University Hospital (CHUV), Lausanne, Switzerland

Introduction: Parallel to the search for specific and selective tau radioligands, there is a need for specific animal models reflecting different aspects of the tau pathology. These models can both be used as a tool to screen new ligands, and as a model of disease to evaluate new therapeutic strategies. In the latter case, non-human primates (NHP) have an obvious translational value due to their brain size and cognitive capacities. Alongside the pathological accumulation of tau, tauopathies are characterized by progressive brain hypometabolism and neuroinflammatory reaction that seem to play a key role in the disease process.

Objectives: Characterization of metabolic and inflammatory dysfunctions in two NHP models of progressive tauopathy by positron emission tomography (PET) imaging.

Methods: 8 NHP bilaterally injected into the CA1 hippocampal region with a viral vector (AAV2/9-CBA) overexpressing either WT h1N4R-Tau (n=4) or mutated h1N4R-Tau-P301L (n=4), and 4 sham controls have been included in this study. All animals underwent ^{18}F-FDG and ^{18}F-DPA714 PET imaging (FOCUS220, Siemens), 10-12 months after viral injection under propofol anaesthesia. Arterial input function was measured and corrected for metabolites for ^{18}F-DPA714. PET images were quantified using Patlak and Logan graphical methods for ^{18}F-FDG and ^{18}F-DPA714, respectively. Parametric images were then coregistered to corresponding MR-images and WT and mutated hTau46 groups were individually compared to healthy controls. Finally, brains were immunostained for AT8, MC1 and AT100 to study the post-translational and conformational modifications of the tau protein.

Results: Segmentation of the hippocampus and its projection areas did not reveal any macroscopical atrophy as compared to the sham controls. The mean CMRglu map of the mutated h1N4R-P301L-Tau group showed evidence of hypometabolism in the parieto-temporal cortical region compared to controls. Cortical hypometabolism was less present in the WT h1N4R-Tau group and was only localized to the parietal cortex. TSPO binding

showed a global increase in parieto-temporal regions in the mutated h1N4R-P301L-Tau group ($p<0.05$), but not in the WT h1N4R-Tau group as compared to controls. The cerebellum remained unchanged in glucose metabolism and TSPO binding in both WT and mutated h1N4R-Tau groups.

Histological analysis demonstrated the presence of tau hyperphosphorylation (AT8) and changes in tau conformation (MC1) in the hippocampus projection areas in both WT h1N4R-Tau and h1N4R-Tau-P301L injected NHPs.

Discussion&Conclusions: Tau pathology was successfully induced in two different NHP models, a sporadic and inherited form of tauopathy. The model for the inherited form demonstrated a tendency towards regional hypometabolism and increased neuroinflammation compared to the sporadic form and sham controls. These models will further be used as a tool to screen *in vivo* new radioligands presumably specific for hyperphosphorylated tau and/or tau aggregates.

349
BRAIN-0820
Poster Session

Animal models

A MULTIPLE MICROINFARCTION BASED ANIMAL MODEL FOR VASCULAR DEMENTIA.

P. Venkat[1], M. Chopp[1], A. Zacharek[1], R. Ning[1], C. Roberts[1], J. Chen[1]
[1]neurology research, Henry Ford Hospital, Detroit, USA

Background and Purpose: Vascular Dementia (VaD) is a progressive disease caused by reduced blood flow to the brain and affects cognition and memory. VaD accounts for about 20% of all dementia patients and is prevalent among the older population. In this study, we investigated a multiple microinfarction (MMI) model using cholesterol crystals in male retired breeder rats as a potential VaD animal model and assessed the consequent progressive cognitive decline and white matter (WM) damage.

Methods: Male young adult (young) rats, retired breeder (RB) rats, and aged (16-18m) rats were subjected to MMI model (500, 70-100 µm cholesterol crystals injected into the internal carotid artery, n=6/group). Neurological deficits and cognitive deficits were evaluated from 2 to 6 weeks after MMI. Additional sets of RB rats were prepared and sacrificed at the end of 2^{nd}, 4^{th} and 6^{th} week after MMI to assess VaD progression and damage.

Results: The MMI rat model induced cognitive decline that worsened with age starting at 2 weeks and persisting to 6 weeks after MMI. In RB rats, significant ($p<0.05$) loss of short term memory (novel object recognition test), over night memory (odor test), anxiety-like behavior (open field evaluation), and impaired spatial learning and memory (Morris water maze test) were observed starting at 2 weeks persisting up to 6 weeks after MMI. In young rats while cognitive loss was seen at 2 weeks, no significant damage in odor test or water maze were detected at 6 weeks. In aged rats, while the cognitive damage was more severe it was accompanied by higher mortality and tumor incidence (combined 40% in n=10/ MMI group) making it unsuitable for establishing a reliable model. Neurological severity score indicated moderate functional deficits that declined over time with scores on a scale of 0-18 (min-max deficit) ranging from 2-4 in young, 4-6 in RB, 5-9 in aged rats. Hence, the RB MMI group was deemed most suitable for further analysis and establishing the VaD model. In RB rats, significant WM rarefaction and infarctions were observed in the corpus callosum (CC), striatum and cortex after MMI. While this WM damage was most severe at 3 weeks and decreased over time, it was still significant compared to control rats even at 6 weeks after MMI. MMI significantly decreased neurite branching and spine density in cortex and hippocampus measured by Golgi staining. Significant loss of Synaptophysin (synaptic protein) was observed in cortex and striatum and loss of myelin and axonal density was seen in CC and striatum. MMI also decreased oligodendrocyte progenitor cells and oligodendrocytes numbers in the CC and striatum.

IBA1 (microglial marker) immunostaining showed MMI induced damaged processes and microglia in activated state in CC.

Conclusion: The MMI model using cholesterol crystals in retired breeder rats is a suitable animal model for VaD. MMI induces significant WM damage mainly in the CC but also in striatum and cortex, loss of axonal density, demyelination, loss of synaptic plasticity, decreased neurite branching and spine density and activated microglia in CC. Further investigation of this model for VaD is warranted.

350
BRAIN-0264
Poster Session

Animal models

A REPRODUCIBLE MODEL OF STRESS-INDUCED NEONATAL HEMORRHAGIC STROKE IN THE RAT

O. Semyachkina-Glushkovskaya[1], O. Sindeeva[1], S. Sindeev[1], E. Zinchenko[1], A. Gekalyuk[1], M. Ulanova[1], I. Agranovich[1]
[1]Biology, Saratov State University, Saratov, Russia

Objectives: Neonatal hemorrhagic stroke (HS) is a major problem of modern neonatal intensive care and produces a significant morbidity, long-term neurologic and cognitive deficits. The advancements in neonatal HS care is hampered by the lack of prognostic criteria for HS and a paucity of prospective data regarding treatment and outcomes. For improvement of prognosis a risk for HS in newborns and existing therapy, an animal model mimicking the mechanisms underlying neonatal HS as closely as possible is absolutely essential. Here we discuss a model of neonatal HS induced by stress with non-invasive interventions.

Methods: To induce HS, conscious newborn rats (1-3 days after birthday) underwent to harmful effect of sound stress (120 dB) in the Plexiglas chamber (2000 sm^3) during 2h with algorithm: 10 sec – the sound, then 60 sec – the pause. The study performed on Group 1 – control included intact newborn rats, Group 2-7 – 4-8-12-16-20-24h after stress, respectively. The pathological changes in the brain tissues/vessels, cerebral blood flow, brain blood barrier (BBB) evaluated by histological methods, laser-speckle imaging, coherent tomography, immunofluorescence, immunoblotting and enzyme immunoassay. For functional assessments, we used standard tests.

Results: The focal infarcts were defined in all regions of cerebral cortex in Group 7. 88% of rats (153 of 173) had moderate infarcts (17.4±1.1 mm^2); 8% (13 of 173) had mild infarcts (1.2±0.5 mm^2); 4% (7 of 173) didn't have visible infarcts. The overall visible infarction rate - 96%. There was no mortality. The cerebral infarcts were accompanied by congestion of excessive blood in cerebral veins/microcirculatory vessels of pia mater and cortex with decrease velocity of blood flow. Additionally, severe perivascular edema and increase in the soma volumes of Betz cells were defined.

The evolution of brain lesions in Groups 2-6 allowed us to classify them in two stages of pre-stroke. Phase one (early) changes (during 8h after stress, Groups 2-3, n=30 in each group) characterized by: accumulation of blood in cerebral veins of pia mater and cortex, the fall of velocity of blood flow, decrease blood outflow from the brain.

The second (transient) phase (12h-20h after stress, Groups 4-6, n=30 in each group) characterized by progression above indicated neurological injuries with appearance of swelling of Betz cells and moderate perivascular edema.

Pre-stroke was associated with upregulation of Sur1, increase B2AR expression and synthesis of beta-arrestin-1.

Stroke is accompanied by decrease permeability of BBB due to higher expression of clauding-5, occluding, ZO-1, collagen IV, laminin and progressively increase in Sur1/B2AR expression and synthesis of beta-arrestin-1 compared with normal stage and pre-stroke.

Using testes adequate age of rats: grid walking, ledged tapered beam, pellet retrieval task, forelimb flexion, forelimb placing, accelerated rotator, adhesive removal test, Morris Water Maze we identify motor, sensory and cognitive deficit in Group 7.

Conclusion: The severe sound stress is non-invasive reproducible method for modeling of HS in newborn rats and is tool for preclinical study of mechanisms preceding HS (pre-stroke) and underlying acute and delayed HS-induced brain injury.

The research supported by grant № 14-15-00128.

351
BRAIN-0256
Poster Session

Angiogenesis

POST-ISCHEMIC EXPRESSION OF AN ANTI-ANGIOGENIC FACTOR VEGF165B AND ITS INHIBITORY EFFECT ON POST-ISCHEMIC ANGIOGENESIS IN RATS.

M. Ishikawa[1], T. Takahashi[1], M. Kanazawa[1], K. Kawamura[1], M. Toriyabe[1], M. Miura[1], M. Koyama[1], M. Nishizawa[1], T. Shimohata[1]
[1]Department of Neurology, Brain Research Institute Niigata University, Niigata, Japan

Objectives

To determine the relationship between $VEGF_{165}b$ expression and angiogenesis by assessing their timing and localization after acute focal cerebral ischemia.

Methods

Male Sprague–Dawley rats were subjected to acute transient focal cerebral ischemia with an intraluminal suture. The suture was removed 90 minutes after ischemia to allow reperfusion. The animals were sacrificed at 1, 3, 7, or 14 days after the ischemia, and the cortex of the ischemic side was examined. Naïve rats were used as controls. $VEGF_{165}b$ expression was evaluated by Western blotting using antibodies against $VEGF_{165}b$. Localization of $VEGF_{165}b$ was evaluated with immunostaining using antibodies against $VEGF_{165}b$, von Willebrand factor (endothelial marker), glial fibrillary acidic protein (astrocyte marker), and microtubule-associated protein 2 (neuronal marker). Proliferating endothelial cells were immunostained with an antibody against Ki-67 (proliferation marker), and endothelial barrier antigen (endothelial marker). Endothelial cells having Ki-67 positive nuclei were considered to be proliferating. The timing and localization of VEGF-associated angiogenesis was evaluated by Western blotting and immunostaining using antibodies against the angiogenesis marker endocan, which is a dermatan sulfate proteoglycan whose expression is upregulated by VEGF signaling.

Results

Western blotting analysis indicated that $VEGF_{165}b$ expression was significantly increased 3 days after ischemia, and immunostaining revealed that it was localized in the endothelial cells of the ischemic core. Proliferating endothelial cells were mainly observed in the ischemic core 3 days after ischemia by immunofluorescence. Endocan expression was observed in peri-ischemic lesions 7 days after ischemia. It was also observed in the ischemic core 3 days after ischemia, but the significant increase in the number of endocan-positive vessels was not observed in ischemic core 3 days after ischemia, compared with control.

Conclusions

We demonstrated that $VEGF_{165}b$ expression was upregulated in the ischemic core 3 days after ischemia. We also demonstrated that endothelial cells proliferated in the ischemic core 3 days after the ischemia, suggesting that angiogenesis can occur in the ischemic core. On the other hand, the significant increase in endocan was not observed in the ischemic core. These findings suggest that angiogenesis in the ischemic core was suppressed by the expression of $VEGF_{165}b$, which inhibits VEGF signaling. $VEGF_{165}b$ may

therefore be a novel target for the treatment of stroke, wherein it enhances angiogenesis after ischemia.

References

Woolard J, et al. $VEGF_{165}b$, an inhibitory vascular endothelial growth factor splice variant: mechanism of action, in vivo effect on angiogenesis and endogenous protein expression. Cancer Res 64: 7822-7835, 2004

Manetti M, et al. Overexpression of $VEGF_{165}b$, an inhibitory splice variant of vascular endothelial growth factor, leads to insufficient angiogenesis in patients with systemic sclerosis. Circ Res 109: e14-26, 2011

Rocha SF, et al. Esm1 modulates endothelial tip cell behavior and vascular permeability by enhancing VEGF bioavailability. Circ Res 29: 581-590, 2014

Kikuchi R, et al. An angiangiogenic isoform of VEGF-A contributes to impaired vascularization in peripheral artery disease. Nature Med 20: 1464-1471, 2014

352
BRAIN-0857
Poster Session

Angiogenesis

INCREASED CEREBRAL CAPILLARY DENSITY FOLLOWING ENVIRONMENTAL ENRICHMENT IN MICE

K. Xu[1], C.P. Tsipis[1], J.C. LaManna[1]
[1]Physiology & Biophysics,
Case Western Reserve University, Cleveland, USA

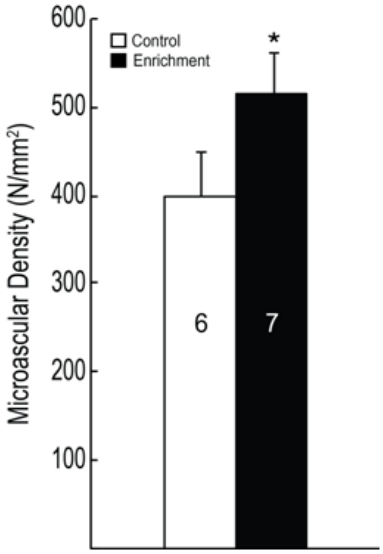

Objectives: Enrichment provides an environment that fosters increased physical activity and sensory stimulation as compared to standard housing. Promoting and sustaining stimulation increases neuronal activity and consequently brain oxygen demand. The mammalian brain modulates its microvascular network to accommodate tissue energy demand in a process referred to as angioplasticity [1]. In this study we investigated the effect of an environmental enrichment on capillary density in mouse brain.

Methods: Male mice (C57BL/6, 2-month old) were randomly placed into the environmental enrichment (n = 7) and non-enriched control (n = 6) groups for the duration of 3 weeks. Enrichment cages were supplied with various toys of different size, shape, and texture to promote visual/sensory stimulation and physical activity through climbing, burrowing, and exploration [2]. Groups of three mice were housed in each enrichment cage to prevent overcrowding/competition. The non-enriched control mice were housed in a standard mouse cage next to the enrichment cage. After 3 weeks of placement, mice were perfused, microvascular density (N/mm^2) was determined by GLUT-1 positive capillary profiles identified in the cerebral cortex [3].

Results: After 3 weeks, environmentally enriched mice exhibited a significant increase (about 30%) in cerebral capillary density (N/mm^2) as compared

to the non-enriched controls (mean ± SD, 514 ± 48, n = 7 vs. 400 ± 48, n = 6, see Figure).

Conclusions: Three weeks of environmental enrichment induced an increase in capillary density in mouse brain, suggesting that change in activity may result in structural change in brain.

References:

1. LaManna, JC. 'Angioplasticity and Cerebrovascular Remodeling" *Adv Exp Med Biol*. 737 (2012): 13-17.
2. Barak B, et al. 'Opposing actions of environmental enrichment and Alzheimer's disease on the expression of hippocampal micro RNAs in mouse models" *Transl Psychiatry* 3 (2013): e304.
3. Tsipis CP, Sun X, Xu K, LaManna JC. 'Hypoxia-induced angiogenesis and capillary density determination" *Methods Mol Biol*. 1135 (2014): 69-80.

353
BRAIN-0409
Poster Session

Angiogenesis

UNDERSTANDING HOW DIFFERENT STROKE RISK FACTORS AFFECT ANGIOGENESIS IN EXPERIMENTAL CEREBRAL ISCHEMIA IN CO-MORBID RATS ANALYZED BY DCE-MRI

J. PRADILLO[1], M. HERNANDEZ-JIMENEZ[1], M.E. FERNANDEZ-VALLE[2], V. MEDINA-ALONSO[1], F. OROZ-GONJAR[1], J.E. ORTUÑO[3], M.J. LEDESMA-CARBAYO[3], A. SANTOS[3], I. LIZASOAIN[1], M.A. MORO[1]
[1]Pharmacology, University Complutense of Madrid, Madrid, Spain
[2]RMN AND RSE CAI, University Complutense of Madrid, Madrid, Spain
[3]Biomedical Imaging Technology Unit, Technical University of Madrid, Madrid, Spain

Introduction

During the last three decades, although there has been a large effort to understand the pathophysiology of cerebral ischemia, none of the drugs and neuroprotective strategies useful in experimental studies have succeeded clinically. To increase the translation to humans, the Stroke Therapy Academic Industry Roundtable (STAIR) has recommended to consider different stroke risk factors and imaging techniques in experimental studies[(1)]. As well as acute treatment, the study of long term post-stroke neurorepair mechanisms, such as angiogenesis, may offer new opportunities of treatment with a broader therapeutic window. Angiogenesis, a process increased after cerebral ischemia around the affected brain area, is reduced by risk factors such as age and obesity[(2,3)]. Dynamic enhanced-contrast imaging (DCE-MRI) is an imaging technique widely used in cancer disease to study angiogenesis, but poorly explored in the stroke field[(4)]. Our purpose was to study the influence of different stroke risk factors on the angiogenic process and its evolution after stroke in an experimental model of cerebral ischemia using DCE-MRI.

Methods

Twenty month-old corpulent (JCR:LA Cp/Cp, a model of atherosclerosis and obesity) and lean rats were used. Experimental stroke was induced by transient MCAO (90 min) by ligature. Post-stroke angiogenesis was analyzed by DCE-MRI made at 3, 7 and 28 days after tMCAO using a Bruker Biospec BMT 47/40 system (Bruker, Ettligen, Germany) operating at 4.7 T and using a 5-cm anatomically shaped homemade surface coil. Using a T1-weighted imaging sequence, 80 serial MR images were acquired before, during, and after intravenous administration of Gd-DTPA (0.2mmol/kg). Then angiogenesis, determined by brain vessel perfusion, permeability and tissue volume fractions, was analyzed by the Kety-Tofts mathematical model. To confirm MRI findings, immunofluorescence techniques were performed on brain sections. Finally, endothelial progenitor cells (EPCs) properties were evaluated using cultures of spleen EPCs from those animals.

Results

At 7 and 28 days after tMCAO, aged lean animals showed higher brain perfusion in the infarcted area than that observed in corpulent rats and, in both, a reduction in the angiogenic parameters was observed at 28d compared with the 7d time point (140% of MRI signal relative to the basal at 7d versus 118% at 28d). Histological examination confirmed that lean rats had a higher number of blood vessels in the affected area than corpulent rats at 28d. Finally, EPCs cultured from aged lean rats showed more adhesion and migration when compared with EPCs from corpulent rats, demonstrating that risk factors affect the angiogenic properties of these cells.

Conclusions

Our results show that co-morbidities impair the angiogenesis process after cerebral ischemia, and confirm that DCE-MRI is a useful technique to evaluate this process in a non-invasive way.

Bibliography

1) Fisher et al. (2009) Stroke, 40: 2244-50. 2) Petcu et al. (2010) J Angiogenes Res, 2:26. 3) Heida et al. (2010) J Am Coll Cardiol, 55(4):357-67. 4) Lin et al. (2008) J Cereb Blood Flow Metab, 28(8):1491-501.

354
BRAIN-0483
Poster Session

Neurogenesis, Angiogenesis, and Gliogenesis

EGF AND B-FGF COMBINED STRONGLY ENHANCED NEUROGENESIS IN THE ISCHEMIC SUBVENTRICULAR ZONE OF THE NEONATAL HYPOXIC ISCHEMIC BRAIN INJURY IN RAT.

M. Iwai[1], K. Momosaki[1], H. Mori[1], J. Kido[1], K. Hirashima[1], H. Yoshimatsu[1], K. Tanaka[1], H. Mitsubichi[1], F. Endo[1]
[1]Neonatology, Kumamoto University Hospital, Kumamoto, Japan

Objectives:We have reported endogenous neural stem cells existed in the ischemic lesion andthe peak of its dividing activity was three days after hypoxia ischemia (HI) inthe neonatal rat brain on XXVI International Symposium on Cerebral Blood Flow,Metabolism and Function. This study was conducted to investigate whether administrationof exogenous EGF and b-FGF combined in the neonatal brain at 3 days after HIcould increase neural stem/progenitor cells as a resource of neuronal repair.

Methods: HI brain injury was induced in 7-days-oldrat pups by the left common carotid artery occlusion followed by 120 minutesexposure to 8% oxygen. Naïve (nonischemic) animals served as controls. Threedays after HI, exogenous EGF (10 mg/kg)and b-FGF (10 mg/kg) wereinjected into the striatum and the cerebral cortex of the ischemic hemisphereusing stereotaxic technique. Bromodeoxyuridine (BrdU, 50 mg/kg) was injectedintraperitoneally twice a day between 4 and 6 days after HI. Seven days afterHI, all brains were removed and coronal sections were cut using a microtome. TheBrain volume loss was determined by calculating the amount of surviving tissueusing cresyl violet staining. Sections for BrdU staining were pretreated with1N HCl followed by 0.1mol/L boric acid (pH 8.5), then incubated with anti-BrdUantibody. Neural progenitor cells were visualized with anti-DCX immunostaining.All sections were observed using an Olympus microscope or Olympus confocalmicroscope. Immunopositive cell numbers in dorsolateral, striatal, and ventralsubventricular zone (SVZ) was calculated by the MCID image analysis system. All values areexpressed as mean ± SD. Statistical comparisons among groups were determinedusing analysis of variance followed by post hoc analysis using Fisher'sprobable least-squares difference tests.

Results: Administration of EGF and b-FGF combined didnot reduce brain volume loss. In the ischemic hemisphere, administration of EGFand b-FGF combined significantly increased the number of BrdU positive cells inthe dorsal SVZ (774 ± 108), striatalSVZ (283 ± 119) compared to

that in vehicle (dorsal; 558 ± 81, striatal; 133 ± 55) and naïve control (dorsal; 449 ± 53, striatal;56± 25), respectively, but not in the ventral SVZ.These effects were not detected in the SVZ of non-ischemic hemisphere. Inthe ischemic hemisphere, with administration of EGF and b-FGF, most BrdUpositive cells were oublepositive for DCX.

Conclusions: In vitro neurosphere method, neuralstem cell proliferation is additive in the presence of EGF and b-FGF combined[1)]. Our results suggest that administration of EGF and b-FGF combined in theischemic hemisphere stimulate neural stem/progenitor cell proliferation and theymay be useful as resources for neuronal repair.

Sources of Funding: This work was supported by JSPS KAKENHI Grant Number 25461649.

Reference: Tropepe V, et al.,Distinct Neural Stem Cells Proliferation in Response to EGF and FGF in theDeveloping Mouse Telencephalon. Dev Biol. 208 (1999): 168-188.

355
BRAIN-0770
Poster Session

Neurogenesis, Angiogenesis, and Gliogenesis

EFFECTS OF CHEMOTHEARAPY AND AN ANTI DEPRESSANT ON THE ASSOCIATION BETWEEN NEURAL STEM CELLS AND ENDOTHELIAL CELLS IN THE NEUROGENIC NICHE

A. MAQBOOL[1], A. chambers[1], M. toledo-rodriguez[1], P. wigmore[1]
[1]SCHOOL OF LIFE SCIENCES, University of Nottingham, Nottingham, United Kingdom

Objectives:

The chemotherapy drug 5-FU has been used for over 40 years to treat various cancers but can have a deleterious effect on cognition. Antidepressant drugs, of the selective serotonin reuptake inhibitor class (e.g., Fluoxetine), increase the generation of new neurons in the dentate gyrus of the adult mammalian brain and increase cognition. SSRIs can also be neuroprotective against damage to the brain (Lyons et al 2012). The present study was designed to investigate the location of dividing cells which are affected by 5-FU and the impact of chronic Fluoxetine on these cells and the microvasculature.

Methods:

4 groups of 8 adult male Lister Hooded rats were used. 1. Saline injection; 2. Saline injection and Fluoxetine (10mg/kg/day) in drinking water for 3 weeks; 3. An injection of 5-FU (30mg/kg), no Fluoxetine; 4. Injection of 5-FU and Fluoxetine in their drinking water. Cell proliferation in the SGZ was quantified by Ki67 immunostaining. Microvasculature density was quantified by immuno staining with an antibody against RECA-1 and stereology (ImageJ).

Results:

A single dose of 5-FU significantly decreased the number of proliferating cells in the sub granular zone of the dentate gyrus one day after treatment. Proliferating cell number returned to normal after one week. The proportion of dividing cells not associated with the micro vasculature was more reduced than those on the surface of blood vessels. Chronic Fluoxetine treatment prior to chemotherapy prevented the decrease in cell proliferation. Neither chemotherapy nor Fluoxetine affected vascular density in SGZ.

Conclusion:

Results of the present study showed that Fluoxetine co treatment with chemotherapy is a viable treatment to prevent the decrease in hippocampal neurogenesis after chemotherapy.

Reference:

Lyons, L., M. Elbeltagy, et al. (2012). "Fluoxetine Counteracts the Cognitive and Cellular Effects of 5-Fluorouracil in the Rat Hippocampus by a Mechanism of Prevention Rather than Recovery." PLoS One 7(1): e30010.

356
BRAIN-0571
Poster Session

Neurogenesis, Angiogenesis, and Gliogenesis

PROLONGED HYPOXIA DEPLETES SVZ NEURAL STEM/PROGENITOR CELL POOLS CRITICAL FOR CORTICAL DEVELOPMENT IN PIGLETS

P.D. Morton[1], L. Korotcova[1], B. Lewis[2], D. Kim[1], V. Kumar[1], F. Shaikh[1], E. Short[1], J.A. Frank[2], V. Gallo[1], R.A. Jonas[1], N. Ishibashi[1]
[1]Center for Neuroscience Research, Children's National Medical Center, Washington DC, USA
[2]Radiology and Imaging Sciences, NIH, Bethesda, USA

Objectives: Many patients suffering from congenital heart disease (CHD) display significant neurological deficits, primarily due to a restricted oxygen supply to the brain during fetal life. The subventricular zone (SVZ) generates neural stem/progenitor cells (NSPCs) that replenish damaged neurons and glia in the brain throughout the human lifespan. The structural and cellular properties of the well-studied rodent SVZ are dissimilar from its human counterpart. The piglet brain is a powerful tool to study human brain development as it displays a highly evolved, gyrencephalic neocortex absent in many other mammals. The aim of this study is to determine the contribution of SVZ NSPCs to cortical development in a human-like, gyrencephalic brain under normal physiological and pathological conditions.

Methods: Female Yorkshire piglets were used in this study. Normal porcine SVZ development was evaluated at 1, 7, and 15 weeks of age with immunohistochemical and anatomical approaches. *In vivo* cell labeling was performed at 1 week of age to analyze migration and differentiation of SVZ-derived cells in the developing brain. We also performed neurosphere assays at postnatal day 2 and 14. Neonatal piglets were housed in a hypoxic environment between postnatal day 3 and 14. To analyze the effects of prolonged hypoxia, immunohistochemical analysis was performed immediately after hypoxia. Cell-tracker green or super-paramagnetic iron oxide nanoparticles were injected into the SVZ 1 day prior to hypoxia and subsequently analyzed by MRI and histology at 14 days of age.

Results: We found that the porcine SVZ shares significant anatomical/structural similarities to the human SVZ; including nearly identical laminar organization with an astrocyte ribbon. The dorsolateral-SVZ contained the largest number of NSPCs and was the predominant proliferative region in early postnatal development. A majority of NSPCs in the SVZ region generated immature neurons that migrated to the frontal cortices and olfactory bulb, indicating that the SVZ contributes to cortical development. Neurospheres isolated from this cell population also displayed multipotency and a tendency for neuronal differentiation. Following hypoxia, our MRI studies demonstrated a reduction in cortical folding of the frontal cortex; a phenomenon commonly seen in CHD patients. A reduction in cell proliferation and neurogenesis was also seen in the SVZ. Additionally, results from *in vivo* cell labeling techniques demonstrated that hypoxia limits the contribution of SVZ-derived neurons to postnatal cortical development. Finally, a decrease in the number of immature neurons was displayed within the frontal cortices with no changes in apoptosis.

Conclusions: Our data suggest that hypoxia reduces the generation of neuronal producing NSPCs in the SVZ, which results in delayed/impaired corticogenesis and gyrencephaly. Future studies aimed at determining the mechanisms coordinating the endogenous response of regenerating SVZ NSPCs will be invaluable in developing novel therapeutic targets and approaches to improve the neurological deficits exhibited in CHD patients

357
BRAIN-0411
Poster Session

Neurogenesis, Angiogenesis, and Gliogenesis

EFFECT OF DELAYED ADMINISTRATION OF INTERLEUKIN-1 RECEPTOR ANTAGONIST ON NEUROGENESIS AFTER EXPERIMENTAL STROKE IN YOUNG/AGED RATS

J. PRADILLO[1], K.N. MURRAY[2], A. MORAGA[1], H. BOUTIN[2], G. COUTTS[2], M.A. MORO[1], I. LIZASOAIN[1], N.J. ROTHWELL[2], S.M. ALLAN[2]
[1]Pharmacology, University Complutense of Madrid, Madrid, Spain
[2]Faculty of Life Sciences, The University of Manchester, Manchester, United Kingdom

Introduction

Stroke is a leading cause of death and disability worldwide with current treatment limited to thrombolysis with tissue plasminogen activator (tPA). Although many drugs have been successful in the acute phase of experimental stroke, there has been a lack of translation to the clinic(1), due possibly to the absence of co-morbidities in experimental studies. Interleukin-1 (IL-1) is a key inflammatory mediator of ischemic brain damage(2), and we have shown that administration of IL-1 receptor antagonist (IL-1Ra) is neuroprotective in aged and co-morbid animals(3). As well as acute treatment study of long term post-stroke neurorepair mechanisms, such as neurogenesis, offers new opportunities of treatment with a broader therapeutic window. In this context, negative actions of IL-1 in neurogenesis have been reported in a broad range of conditions, including stress, depression and Alzheimer's disease(4). Conversely, administration of IL-1Ra has been shown to increase neurogenesis(5). Here we report on effects of delayed IL-1Ra treatment on neurogenesis after stroke in young and aged animals.

Methods

Young (2 month-old; n=10) and aged (13 month-old; n=10) rats were exposed to transient middle cerebral artery occlusion (tMCAO). IL-1Ra or placebo was administered subcutaneously (25mg/kg) at 3 and 6h of reperfusion. Infarct volume was assessed at 24h and 7 days after tMCAO by MRI (T_2W images) and blood brain barrier (BBB) damage by histology at 7d. At 7d effects of IL-1Ra on the proliferation of stem cells in the subventricular zone (SVZ) and the number of migrating neuroblasts to the ischemic area was analysed by immunofluorescence (BrdU and ki67 for proliferation of stem cells and Doublecortin staining for differentiation and migration of neurobrasts).

Results

Administration of IL-1Ra reduced infarct volume at 24h and 7d in both young and aged rats (around 40% of reduction versus placebo), and also reduced BBB damage at 7d (50% of reduction in both young and aged animals). The post-stroke IL-1Ra administration increases in young and aged rats the proliferation of stem cells and the number of neuroblasts in the SVZ. In addition neuroblast migration was enhanced by IL-1Ra treatment. We observed reduced neurogenesis (proliferation of stem cells and neuroblast number) in aged versus young rats, but effects of IL-1Ra in increasing neurogenesis were comparable in each.

Conclusions

Our results demonstrate for the first time that delayed administration of IL-1Ra during reperfusion is neuroprotective and increases the neurogenesis process after experimental stroke in both young and aged animals, lending further support for development of IL-1Ra as a new treatment for stroke.

References

(1). Dirgnal U. (2006) J Cereb Blood Flow Metab. 26:1465-78; (2). Allan S.M. et al. (2005) Nat Rev

Immunol. 5(8):629-40; (3) Pradillo JM. et al. (2012) J Cereb Blood Flow Metab. 32(9):1810-19. (4) Koo JW, Duman RS (2008) PNAS. 105(2):751-6. (5) Menachem-Zidon et al. (2008). Neurospsycopharmacology. 33:2251-62.

358
BRAIN-0505
Poster Session

Neurogenesis, Angiogenesis, and Gliogenesis

SIMVASTATIN IMPROVES ADULT HIPPOCAMPAL NEURONAL MATURATION BY UP-REGULATING THE WNT/ß-CATENIN PATHWAY IN A MOUSE MODEL OF ALZHEIMER'S DISEASE.

X. Tong[1], *E. Hamel*[2]
[1]*Laboratory of Cerebrovascular Research, Montreal Neurological Institute McGill University , Montreal, Canada*
[2]*Laboratory of Cerebrovascular Research, Montreal Neurological Institute McGill University, Montreal, Canada*

Background: Statins are cholesterol-lowing drugs with pleiotropic effects and overall cardioprotective properties. We previously showed that simvastatin (SV) restored memory in adult transgenic mice overexpressing the Swedish and Indiana mutations of the human amyloid precursor protein (APP mice, line J20) (1), a mouse model of Alzheimer's disease (AD, 2). This benefit occurred concomitantly with normalization or upregulation in protein levels of memory-related immediate early genes *c-fos* and *Egr-1* in hippocampal CA1 neurons (1).

Objectives: We interrogated whether the beneficial effects of SV on cognitive improvements could be related to enhanced neurogenesis, and which signaling pathway was involved.

Methods: APP mice and wild-type (WT) littermate controls (120 to 180 days old, 15 days apart) received water or SV (40mg/kg/day, 3 months) (1). Animals were perfused, and their brains processed for immuno- and histochemical stainings. Markers of neurogenesis and neuronal maturation examined in the dentate gyrus (DG) included: Ki67 (cell proliferation), doublecortin (DCX, immature neurons), and calbindin (mature neurons). For Wnt pathway signaling, the ***i)*** canonical Wnt pathway marker b-catenin, ***ii)*** Wnt pathway signaling inhibitor Dickkopf-1 (DKK1) (3), and ***iii)*** Wnt/b-catenin signaling target factor, prospero-related homeobox 1 gene (Prox1) (4) were detected in 180 days old mice. Numbers of neurons, projecting dendrites, and staining intensity were quantified (Image J, Metamorph or semi-quantitatively).
Results: In both SV-treated and untreated APP mice, Ki67 or DCX positive cells were less numerous compared to WT mice. The number of Ki67 nuclei was stable through age, whereas DCX neurons abruptly decreased between 165 and 180 days. SV significantly increased the length (↑34%, $p<0.05$) and branching (↑62.6%, $p<0.01$) of dendrites from DCX positive neurons, reaching values comparable to those in WT mice. Calbindin immunofluorescence was decreased in APP mice, and it was not restored by SV. However, labeling intensity of calbindin-immunostained dendrites was strongly increased (↑ 87.1%, $p<0.001$) following SV. SV treatment significantly increased immunoreactivity to b-catenin (↑42.2%) and its signaling target Prox1 (↑67.7%, $p<0.01$), while decreasing that of the Wnt pathway inhibitor DKK1 (↓61.2%, $p<0.05$).

Conclusion: Our results disclose a possible mechanism underlying the capacity of SV to restore memory in APP mice, related to upregulation of the Wnt-b-catenin pathway and improved neuronal maturation rather than increased neurogenesis. They suggest that downregulation of DKK1, an antagonist of the canonical Wnt-b-catenin signaling pathway, is involved in these beneficial effects. Or findings suggest that SV enhanced DG neuronal maturation and, possibly, synaptogenesis (5), providing a means to re-establish the memory circuit between the entorhinal cortex to the CA1 area of the hippocampus. Our findings may offer a possible novel therapeutic strategy for AD.

References: (1) Tong XK, et al. 2012, J Neuroscience 32:4705; **(2)** Mucke L et al, 2000. J

Neuroscience 20:4050; **(3)** Caricasole A, et al. 2004, J Neurosci 24:6021; **(4)** Stergiopoulos A, et al. 2015, Front Cell Neurosci 8, 454; **(5)** Rosso SB and Inestrosa NC. 2013, Front Cell Neurosci 7, 103.

Acknowledgements: Supported by grants from the Canadian Institutes of Health Research (CIHR MOP-126001 to EH) and the Heart and Stroke Foundation of Québec.

359
BRAIN-0312
Poster Session

Neurogenesis, Angiogenesis, and Gliogenesis

ENHANCING OF NEUROGENIC AND ANTI-ADIPOGENIC EFFECTS BY ORAL ADMINISTRATION OF ARTEMISIA ANNUA IN DIET-INDUCED ANIMAL MODEL

H. Baek[1], H. Shim[1], M. Shim[1], H. Lim[1], C. Kim[2], S. Park[2], Y. Lee[3], K. Song[4], S. Kim[5], S. YI[1]
[1]Department of Biomedical Laboratory Science, Soonchunhyang University, Asan, Korea
[2]Department of Medical Biotechnology, Soonchunhyang University, Asan, Korea
[3]Department of Life Science and Biotechnology, Soonchunhyang University, Asan, Korea
[4]Genomic Informatics Center, Hankyong University, Anseong, Korea
[5]Department of Biotechnology, Hoseo University, Asan, Korea

Recently, people become desperate for a solution of reducing body weight at a group of obesity in the developed countries. A lot of natural compounds and chemical drugs have been introduced for decades, however, many pharmacologic disadvantages, from the agents have found and still academia and industries have been searching for more promising agents. Interestingly, *Artemisia annua* L extract (AA) has been well known for using anti-malarial agent, however, it has been recently proven to reduce adipocyte differentiation *in vitro*. Therefore, the positive effects have been a center of attention for overcoming obesity, currently. Unfortunately, the inhibitory effects of adipocyte differentiation have not validated with animal models and the secondary effects in the other organ and tissues also have not been proved yet. Therefore, we daily injected AA to C57BL/6 mice via oral and provided high fat diet to making diet-induced obesity(DIO) and every factors were compared to its control (normal diet group).
The accumulating body weight, related mRNA expression levels of obtained adipose tissues from the animals showed significance at the AA treated groups, and inhibition of neurogenesis in the hippocampus of obese animals was rescued at the AA treated animals. Therefore, these results showed AA has significant positive effects on inhibition of body weight gain and adipocyte differentiation, and increase brain function related with cognitive, learning and memory by hippocampal neurogenesis at the same time.
This work was carried out with the support of "Cooperative Research Program for Agriculture Science & Technology Development (Project No. PJ01104602)" Rural Development Administration, Republic of Korea.

360
BRAIN-0410
Poster Session

Neurogenesis, Angiogenesis, and Gliogenesis

NOVEL EFFECTS ON INCREASING NEURONAL DIFFERENTIATION BY MINERALOCORTICOID RECEPTOR ANTAGONIST PF3882845 ADMINISTRATION IN TYPE 2 DIABETIC MICE MODEL

H. Beak[1], S. Lee[2], H. Shim[1], E. Lee[3], M. Kwon[3], H. Kim[3], Y. Kim[3], K. Boonloh[3], S. YI[1], E. Lee[2], C. Chung[3]
[1]Department of Biomedical Laboratory Science, Soonchunhyang University, Asan, Korea
[2]Department of Internal Medicine, Soonchunhyang University Cheonan Hospital, Cheonan, Korea
[3]Department of Internal Medicine, Yonsei University Wonju College of Medicine, Wonju, Korea

Aldosterone, a primary steroidal hormone released from adrenal glands, regulates the

sodium and potassium level, binding to mineralocorticoid receptor (MR). However, it was reported that aldosterone has harmful effect to cause inflammatory reaction, accelerating secretion of various cytokines like MCP-1, IL-1 and IL-6, therefore it is directly associated with damaging tissues. In particular, interleukin-6 has a harmful effect on the hippocampus, impairing learning, cognition and memory function and leading to dementia.

Meanwhile, recent clinical testing has demonstrated that MR antagonist reduces accumulation of collagen, TCF-b, IL-6,Icam-1 which impairs glomeruli, and decreases albuminuria, inhibiting aldosterone reaction. However, there are few researches that MR antagonist including PF3882845 has anti-inflammation effect on hippocampus. In this study, we performed oral administration of PF3882845 (PF3882845 was kindly gifted from Pfizer) to db/db mouse model and investigated if this agent reduces the onset of diabetic nephropathies and improves the hippocampus functions.

Food intakes and body weights were measured weekly, GTT, ITT and albuminuria test were performed at week 12 and IPITT was surveyed at week 16. There were no differences in food intakes, body weights, GTT, ITT and IPITT results between ethanol- and PF3882845-administered groups. However, albuminuria examination and related mRNA expressions were different between db/db + Veh and db/db + PF3882845. Immunohistochemistry result shows that neurogenesis was significantly increased in db/db + PF3882845 group than db/db + Veh group. Western blotting resultof hippocampus protein shows same effect. MR expression was reduced in db/db + PF3882845 than db/db + Veh. Cell proliferation was also different between Veh-and PF3882845-administered group.

In conclusion, these results implicate that PF3882845, MR antagonist, has no noticeable effect on inhibiting diabetic nephropathies. However, in hippocampus, there was positive effect that neurogenesis was increased by PF3882845. This study may be applied to research on relation between MR and hippocampus.

361
BRAIN-0732
Poster Session

Developing Brain

LIMB REMOTE ISCHAEMIC POST-CONDITIONING PROTECTS CEREBRAL WHITE MATTER IN A PIGLET MODEL OF PERINATAL ASPHYXIA

D. Alonso-Alconada[1], M. Ezzati[1], A. Bainbridge[2], K.D. Broad[1], G. Kawano[1], A. Oliver-Taylor[1], E. Rocha Ferreira[1], I. Fierens[1], J. Rostami[1], J. Hassell[1], I. Tachtsidis[3], P. Gressens[4], M. Hristova[1], K. Bennett[1], S. Lebon[5], B. Fleiss[4], D. Yellon[6], D.J. Hausenloy[6], X. Golay[7], N.J. Robertson[1]
[1]Neonatology, Institute of Women's Health UCL, London, United Kingdom
[2]Physics and Bioengineering, UCL NHS Trust, London, United Kingdom
[3]Medical Physics and Biomedical Engineering, UCL, London, United Kingdom
[4]Perinatal Imaging and Health, Division of Imaging Sciences and Biomedical Engineering KCL King's Health Partners St. Thomas' Hospital, London, United Kingdom
[5]Inserm, U1141, Paris, France
[6]University College London, The Hatter Cardiovascular Institute, London, United Kingdom
[7]Brain Repair and Rehabilitation, Institute of Neurology, London, United Kingdom

Objectives: The prevention of neurological disabilities following birth asphyxia remains a major public health challenge and the search continues to find new and more effective therapies to ameliorate neonatal brain injury. Remote ischaemic postconditioning refers to the protective effect elicited in one organ from applying several intermittent sub-lethal interruptions to blood flow in another organ, in this case at the onset of reperfusion after severe hypoxia-ischaemia. In rodents, this promising therapy has shown to reduce infarct size and improve long-term motor outcomes after

ischaemia in adult and neonatal brain when it is applied immediately at reperfusion or delayed by up to 24h. The objective of this study was to evaluate the neuroprotective effect of remote ischaemic postconditioning after a global hypoxic-ischaemic insult in a piglet model of neonatal encephalopathy using clinically relevant magnetic resonance biomarkers supported by immunohistochemistry. We also assessed the activity of the mitochondrial respiratory chain and gene expression to examine possible cell survival pathways.
Methods: After a quantified hypoxic-ischaemic insult, 16 Large White female newborn piglets were randomized to: (i) No intervention (n=8); (ii) Remote ischaemic postconditioning - four 10 minute cycles of bilateral lower limb ischaemia/reperfusion started immediately after hypoxia-ischaemia (n=8). White matter and thalamic voxel proton and whole brain phosphorus-31 magnetic resonance spectroscopy were acquired before and during hypoxia-ischaemia and at 24 and 48 h after resuscitation. Animals were terminated at 48h and brains obtained for immunohistochemistry and molecular analyses.
Results: There were no differences in baseline variables or insult severity. Remote ischaemic postconditioning significantly reduced the hypoxic-ischaemic-induced increase in white matter lactate/N acetyl aspartate (p=0.005) and increased the levels of the whole brain phosphorus-31 magnetic resonance spectroscopy nucleotide triphosphate/exchangeable phosphate pool (p=0.039). Immunohistochemistry revealed a correlation with improved white matter energy metabolism, as remote ischaemic postconditioning was able to reduce cell death in the periventricular white matter (p=0.03), internal capsule (p=0.002) and corpus callosum (p=0.021), and effect also linked to the reduction in microglial activation in the corpus callosum (p=0.001) and to the presence of higher numbers of surviving oligodendrocytes in the corpus callosum (0.029) and periventricular white matter (p=0.001). Remote ischaemic postconditioning group also showed a higher activity of mitochondrial cytochrome c oxidase, a significant increase in phosphorylated Erk/Total Erk ratio in the periventricular white matter and changes in the expression of some genes including the KATP channel and the endothelin A receptor.
Conclusions: Immediate remote ischaemic postconditioning was neuroprotective in white matter following hypoxia-ischaemia in a piglet perinatal asphyxia model, becoming a potentially safe and promising therapy for babies with neonatal encephalopathy following perinatal asphyxia.
References: 1) Zhou Y, et al. Remote limb ischemic postconditioning protects against neonatal hypoxic-ischemic brain injury in rat pups by the opioid receptor/Akt pathway. Stroke. 2011;42(2):439-44. 2) Drunalini Perera PN, et al. Delayed remote ischemic postconditioning improves long term sensory motor deficits in a neonatal hypoxic ischemic rat model. PloS one 2014;9(2):e90258.

362
BRAIN-0825
Poster Session

Developing Brain

NEUROPROTECTIVE EFFECT OF ARGON COMBINED WITH THERAPEUTIC HYPOTHERMIA IN A PIGLET MODEL OF PERINATAL ASPHYXIA

D. Alonso-Alconada[1], B. Fleiss[2], K.D. Broad[1], I. Fierens[1], G. Kawano[1], J.K. Hassell[1], M. Ezzati[1], E. Rocha-Ferreira[1], M. Hristova[1], A. Bainbridge[3], D. Price[3], R.D. Sanders[4], X. Golay[5], P. Gressens[2], N.J. Robertson[1]
[1]Neonatology, Institute of Women's Health, London, United Kingdom
[2]Perinatal Imaging and Health, Division of Imaging Sciences and Biomedical Engineering KCL King's Health Partners St Thomas Hospital, London, United Kingdom
[3]Physics and Bioengineering, UCLH NHS Trust, London, United Kingdom
[4]Anesthesiology, University of Wisconsin, Madison, USA
[5]Brain Repair and Rehabilitation, Institute of Neurology, London, United Kingdom

Objective: Therapeutic hypothermia is the only clinical intervention that has proven effectiveness

in reducing brain damage in asphyxiated newborns, being safe and cost effective and becoming standard clinical care for moderate to severe neonatal encephalopathy in high-income settings. However, many infants have an adverse neurodevelopmental outcome despite hypothermic treatment, so the current focus is on adjunct therapies to augment hypothermic neuroprotection. The inert or noble gas argon has shown neuroprotective qualities both in vitro and in vivo in multiple models of brain damage. Further, argon is cheaper and more available than xenon, another noble gas that has shown to be neuroprotectant, making argon an attractive candidate for clinical application. Investigating neuroprotection for perinatal asphyxia, argon treatment provided neuroprotection in a neonatal rat hypoxia-ischemia-induced brain injury model, decreasing infarction volume, maintaining the number of viable neurons to the same value as control animals and improving composite adverse outcome, an effect associated at least in part with the synthesis of pro-survival proteins and inhibition of neuronal apoptosis. The objective of the present work was to determine the safety and efficacy of Argon-augmented hypothermic neuroprotection in a validated piglet model of perinatal asphyxia.
Methods: Following a quantified transient hypoxic-ischemic insult, eighteen newborn piglets piglets were randomized to: (i) Hypothermia alone (n=10); (ii) Hypothermia + 50% Argon (2-26h; n=8). All piglets were cooled to 33.5ºC from 2-26 h after resuscitation. Clinically relevant magnetic resonance biomarkers (proton and whole brain phosphorus-31 magnetic resonance spectroscopy) were acquired before and during hypoxia-ischaemia and at 24 and 48 h after resuscitation. Results were analyzed using random effects regression of n=10 in Hypothermia and n=8 in Hypothermia + Argon groups.
Results: There were no differences in baseline variables or insult severity. Argon-augmented hypothermia group significantly increased the levels of the whole brain nucleotide triphosphate/exchangeable phosphate pool at 48h after hypoxia-ischemia ($p<0.01$) when compared to hypothermia alone group. Argon-augmented hypothermia also reduced the hypoxic-ischaemic-induced increase in white matter lactate/N acetyl aspartate at 48h ($p<0.01$).
Conclusions: Argon-augmented hypothermia was safe and provided significant neuroprotection compared with hypothermia alone in this piglet perinatal asphyxia model.
References: Zhuang L, Yang T, Zhao H, Fidalgo AR, Vizcaychipi MP, Sanders RD, Yu B, Takata M, Johnson MR, Ma D. The protective profile of argon, helium, and xenon in a model of neonatal asphyxia in rats. Crit Care Med. 2012 Jun;40(6):1724-30.

363
BRAIN-0844
Poster Session

Developing Brain

DEXMEDETOMIDINE DOES NOT AUGMENT THE NEUROPROTECTIVE EFFECT OF COOLING FOLLOWING HYPOXIA-ISCHEMIA IN NEONATAL PIGLETS

M. Ezzati[1], D. Alonso-Alconada[1], G. Kawano[1], K.D. Broad[1], I. Fierens[1], E. Rocha-Ferreira[1], B. Fleiss[2], J.K. Hassell[1], A. Bainbridge[3], M. Hristova[1], D. Price[3], X. Golay[4], R.D. Sanders[5], P. Gressens[2], N.J. Robertson[1]
[1]Neonatology, Institute of Women's Health, London, United Kingdom
[2]Perinatal Imaging and Health, Division of Imaging Sciences and Biomedical Engineering KCL King's Health Partners St Thomas Hospital, London, United Kingdom
[3]Physics and Bioengineering, UCLH NHS Trust, London, United Kingdom
[4]Brain Repair and Rehabilitation, Institute of Neurology, London, United Kingdom
[5]Anesthesiology, University of Wisconsin, Madison, USA

Objectives: Despite the continuous effort from the scientific community and the advancements in neonatal intensive care, hypoxic-ischaemic brain injury of the term infant remains a significant problem throughout the world. Neonatal encephalopathy consequent on perinatal hypoxia-ischaemia occurs in 1-3/1000

term births in the developed world and frequently leads to serious and tragic consequences that devastate lives and families. Although the recent introduction of cooling represents a significant advance, despite treatment around 50% survive with adverse neurodevelopmental function. Dexmedetomidine is a highly selective α2-adrenoreceptor agonist that confers sedative, anti-inflammatory, analgesic, sympatholytic and organ-protective properties that may be beneficial for perinatal asphyxia. In vitro, dexmedetomidine dose-dependently attenuated neuronal injury in neuronal-glial co-cultures; in vivo it has shown to be neuroprotective after hypoxia-ischemia in neonatal rats. The objective of the present work was to evaluate the neuroprotectiove effect of the combination therapy of dexmedetomidine and hypothermia in a piglet model of perinatal asphyxia.
Methods: Twenty newborn piglets were surgically prepared and intensively monitored. Following a quantified transient hypoxic-ischemic insult, piglets were randomized to: (i) Hypothermia (n=10); or (ii) Hypothermia + Dexmedetomidine (n=10). Animals receiving dexmedetomidine started with a loading dose of 2 µg/kg followed by 0.028 µg/kg/h infusion for 48 hours. In the Hypothermia + Dexmedetomidine group, fentanyl infusion was stopped following dexmedetomidine bolus and was substituted by dexmedetomidine infusion. All piglets were cooled to 33.5°C from 2-26 h after resuscitation. Magnetic resonance spectra (proton and whole brain phosphorus-31) were acquired before and during hypoxia-ischaemia and at 24 and 48 h after resuscitation. Animals were terminated at 48h and brains obtained for immunohistochemistry assessment.
Results: There were no differences in baseline variables or insult severity. When compared to hypothermia alone group, magnetic resonance spectroscopy showed no differences in the levels of the whole brain nucleotide triphosphate/exchangeable phosphate pool or in lactate/N acetyl aspartate ratio after dexmedetomidine administration. Delayed cell death assessed by TUNEL method showed no difference in the counts of positive cells between both groups. Hypothermia + dexmedetomidine group had more fatal cardiac arrest with blood dexmedetomidine levels within safe sedative range (0.4-0.8microgram/l). No relation was found between dexmedetomidine levels and hemodynamic disturbances.
Conclusions: Dexmedetomidine does not augment the neuroprotective effect of cooling following hypoxia-ischemia in a piglet perinatal asphyxia model.
References: Ma D, Hossain M, Rajakumaraswamy N, Arshad M, Sanders RD, Franks NP, Maze M. Dexmedetomidine produces its neuroprotective effect via the alpha 2A-adrenoceptor subtype. Eur J Pharmacol. 2004 Oct 11;502(1-2):87-97.

364
BRAIN-0273
Poster Session

Developing Brain

PET/MR HYBRID SCANNER IMAGING OF CEREBRAL BLOOD FLOW USING 15O-WATER POSITRON EMISSION TOMOGRAPHY AND ARTERIAL SPIN LABELING MAGNETIC RESONANCE IMAGING IN NEWBORN PIGLETS

J. Andersen[1], W. Henning[1], U. Lindberg[2], C. Ladefoged[1], L. Højgaard[1], G. Greisen[3], I. Law[1]
[1]Department of Clinical Physiology Nuclear Medicine and PET, Rigshospitalet, Copenhagen Ø, Denmark
[2]The Functional Imaging Unit, Glostrup Hospital, Glostrup, Denmark
[3]Department of Neonatology, Rigshospitalet, Copenhagen Ø, Denmark

Objectives:

Abnormality of cerebral blood flow (CBF) distribution can lead to hypoxic-ischemic white matter damage in newborn infants. In this study we measured CBF in seven newborn piglets by comparing simultaneous ^{15}O-water positron emission tomography (PET) and pulsed arterial spin labeling (ASL) MR on a hybrid PET/MR system. The final aim was to develop a clinically useful method for comparison of CBF measurements in white matter in newborn infants.

Methods:

The experimental protocol for the study was approved by the Danish Animal Experiments Inspectorate and conducted in accordance with the Animal Ethics Policy at the University of Copenhagen. Positron emission tomography was performed with repeated IV injections of 20 and 100 MBq ^{15}O-water to test CBF reliability at low tracer dose. On each piglet, four scans at baseline and four scans after acetazolamide stimulus were performed. Cerebral blood flow was quantified using a 1-tissue-compartment model(1) employing two different input functions: either an arterial input function (AIF) or a non-invasive image derived input function (IDIF) generated from the dynamic PET scan using a VOI in the left ventricle of the heart.

Results:

The mean global CBF (95%CL) PET-AIF, PET-IDIF and ASL at baseline were 27 (23;32), 34 (31;37) and 27 (22;32) mL/100g/min, respectively. At acetazolamide stimulus PET-AIF, PET-IDIF and ASL were 64 (55;74), 76 (70;83) and 79 (67;92) mL/100g/min, respectively. At baseline the differences between PET-AIF, PET-IDIF and ASL were 22% ($p<0.0001$) and -0.7% ($p=0.9$). At acetazolamide stimulus the differences between PET-AIF, PET-IDIF and ASL were 19% ($p=0.001$) and 24% ($p=0.0003$). ASL showed the largest variance when accounting for dose and acetazolamide effect ($p=0.01$). There was no significant difference in variation between the 20 MBq CBF PET scans compared to the 100 MBq CBF PET scans ($p=0.06$). Meaningful analysis of white matter CBF was not possible in this piglet model due to insufficient spatial resolution in the 50 g newborn piglet brain. On visual presentation the distribution of regional CBF showed that the variation across voxels was greater in ASL CBF images than in PET CBF images.

Conclusions:

Acceptable concordance between global ASL CBF and PET CBF was found during baseline but not during hyperperfusion. A systematic overestimation of global PET CBF was found when using an IDIF, but the difference was acceptable for a clinical research method. Further evaluation of white matter ASL CBF and PET CBF is needed in newborn infants with low absolute rates of flow and brain weights of 150 to 400 g.

References:

(1) Meyer E. Simultaneous correction for tracer arrival delay and dispersion in CBF measurements by the H215O autoradiographic method and dynamic PET. J Nucl Med 1989 June;30(6):1069-78.

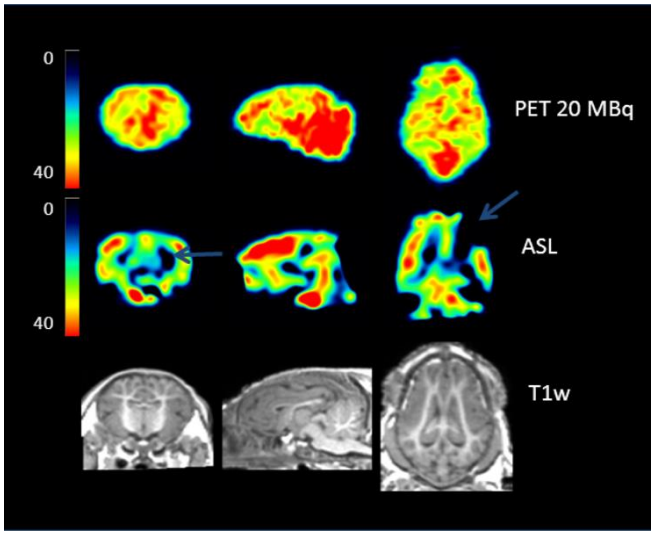

CBF images of a newborn piglet at baseline showing ^{15}O-water PET, ASL and T1-weighted MPRAGE. Low values voxels in ASL images (blue arrows). CBF quantified in mL/100g/min.

365
BRAIN-0823
Poster Session

Developing Brain

DECREASED CELL DEATH IN FEMALE PRIMARY HIPPOCAMPAL NEURONS AFTER IN-VITRO ISCHEMIA: ROLE OF THE ESTROGEN ALPHA AND TYROSINE KINASE B RECEPTOR INTERACTIONS

E. UDHO[1], U. CIKLA[2], V. CHANANA[1], Y. SEYMOUR[1], D. KINTNER[1], W. SUN[1], S. MARQUEZ[1], A. OTLES[1], P. FERRAZZANO[1], J. LEVINE[3], P. CENGIZ[1]
[1]PEDIATRICS, University of Wisconsin-Waisman Center, Madison, USA
[2]NEUROLOGICAL SURGERY, University of Wisconsin-Madison, Madison, USA
[3]NEUROSCIENCE, University of Wisconsin-Madison, Madison, USA

Objective: Hypoxia-ischemia (HI) related brain injury after perinatal asphyxia is a major cause of life-long disability. Female newborns are more resistant to the effects of HI than males, a phenomenon that is poorly understood. We recently studied the role of hippocampal estrogen receptor alpha (ERα) in sexually differentiated phosphorylation of the neurotrophin receptor, tyrosine kinase B (TrkB), in neonatal mice post-HI *in-vivo*. Our preliminary results show that the hippocampal ERα expression, but not ERβ increases significantly in the female hippocampi compared to male hippocampi post-HI. In addition, the sexually differentiated TrkB phosphorylation gets ablated in ERα knockout ($ER\alpha^{-/-}$) mice, indicating a role of ERα in conferring responsiveness to HI and the potent/selective TrkB agonist [7,8 dihydroxyflavone (7,8-DHF)]. We also showed a possible involvement of the cytoplasmic Src Family kinases (SFK) in providing cross talk between the ERα and TrkB in neonatal mice hippocampi post-HI. SFK get significantly phosphorylated in female hippocampus post-HI and after TrkB agonist therapy. This sexually differential response also got ablated in $ER\alpha^{-/-}$ mice. So we hypothesized that rapid membrane ERα signaling is required for SFK phosphorylation which in turn results in TrkB phosphorylation in-vitro in primary hippocampal neuronal cultures. We intend to define the pathway through which this mechanism works in sexed primary hippocampal neuronal cultures *in-vitro* using $ER\alpha^{+/+}$ and $ER\alpha^{-/-}$ mice.

Methods: Sexed hippocampal primary neuronal cultures were prepared from 1-day old C57BL/6J $ER\alpha^{+/+}$ and $ER\alpha^{-/-}$ mouse pups as described previously with some modifications. Neurons were grown on coverslips after being treated with Ara-C to decrease astrocyte growth and then exposed to either normoxia or OGD (1% O_2, 5% CO_2, balance N_2, 37ºC) for four hours on day 7 in vitro. After 24 hours of REOX, cells were stained by either Hoechst, calcein and propidium iodide for cell survival or with ERα, p-src or p-TrkB. Fluorescent signals from culture dish were obtained using confocal microscope by imaging 6-9 random fields (20x). All image file names were coded to blind them to the experimenter. The results from each coverslip were averaged. For multiple comparisons ANOVA was used.

Results: There were increased ERα and p-TrkB expressions in female primary hippocampal neurons compared to males after OGD-REOX. In addition, TrkB agonist therapy (7,8-DHF) increased the p-TrkB expression further and decreased the cell death only in female hippocampal neurons following OGD-REOX. The p-TrkB expression was ablated in both male and female hippocampal neurons obtained from $ER\alpha^{-/-}$ mice. These results support our in-vivo findings of the relative resistance of the female neonatal hippocampus to neurodegeneration mediated by ERα-TrkB interactions post-HI.
Conclusion: There is sexually differential response of the hippocampal neurons to TrkB signaling mediated by the ERα, favoring females after in-vivo and in-vitro ischemia. We will be testing the role of the src in mediating the cross-talk between the ERα and TrkB by using an SFK inhibitor and genetically knocking down the src. Identifying the role of ERα-SFK-TrkB interaction in neuronal survival will provide a new target for preventive and therapeutic interventions and significantly advance the developmental brain injury field.

366
BRAIN-0828
Poster Session

Developing Brain

ROLE OF HYPOTHERMIA IN HIPPOCAMPAL TYROSINE KINASE B RECEPTOR PHOSPHORYLATION AFTER NEONATAL HYPOXIC ISCHEMIC ENCEPHALOPATHY

Y. SEYMOUR[1], U. CIKLA[1], E. UDHO[1], V. CHANANA[1], W. SUN[1], S. MARQUEZ[1], A. OTLES[1], D. KINTNER[1], P. FERRAZZANO[1], P. CENGIZ[1]
[1]Pediatrics, University of Wisconsin-Waisman Center, Madison, USA

Objectives: Cerebral ischemia resulting from hypoxic ischemic encephalopathy (HIE) affects over 20,000 neonates every year in the US. The neurotrophin receptor, tyrosine kinase B (TrkB), plays an important role in neuroprotection and improving the long-term functional recovery following HIE by increasing neuronal survival. We recently published that administration of 7,8 dihydroxyflavone (7,8-DHF; selective TrkB agonist) increases TrkB phosphorylation and hippocampal neuronal survival following HIE in female, but not in male neonatal mice. Currently, in clinical practice therapeutic hypothermia is now considered the standard of care for term neonates with moderate to severe HIE. However, the effects of therapeutic hypothermia on TrkB phosphorylation are unknown. This fact would limit the translatability of the 7,8-DHF therapy to the term human neonates who get treated with hypothermia. In addition, experimental data suggests that hypothermic male neonates have better neuroprotection compared to females post-HIE. Thus, we established the hypothermia model in neonatal mice post-HIE and asked the questions; 1) whether there are sex differences in early neurological damage at different temperatures 2) whether hypothermia induces hippocampal TrkB phosphorylation or not.

Methods: After isoflurane anesthesia P9 mice were undergone Vannucci's neonatal HIE model [left common carotid artery ligation and exposing the mice to hypoxia (10% oxygen, balanced nitrogen) for 50 minutes]. Following hypoxic/ischemic insult, mice were stratified to seven different target temperatures ranging from 31^0C to 38^0C by 1^0C increments for five hours. To monitor core temperatures, rectal temperature of a sentinel mouse was measured. After five hours the mice were returned to dams. Three days after HI, mice were sacrificed and the brains harvested for immunostaining for MAP2 (for neurological injury scoring) and p-TrkB with tyramine amplification. Separate hippocampal slices are individually immunostained for either MAP2 or p-TrkB^{706}. Slides were visualized using either a Zeiss epifluorescent microscope (MAP2) or Nikon A1R-Si confocal microscope (p-TrkB). To semi-quantitate p-TrkB staining, whole brain images were imported into Image J software. The mean pixel values for the CL and IL region of interests were subtracted from background pixel values and expressed as the IL/CL ratio from 3 hippocampal slices per mice. For multiple comparisons ANOVA was used.

Results: Our results show that average MAP2 neurological injury scores increase in both male and female neonate brains as the temperature increases [from 8 ± 2 (31-32^{0}C) up to 25 ± 2 (37-38^{0}C)]. Male brains seem to be more susceptible to hyperthermia as indicated by the MAP2 neurological injury scores. Interestingly, there is a higher % change in IL/CL hippocampal p-TrkB ratio in hypothermic male mice (32-33^{0}C) compared to female mice at 3 days post-HIE (30 ± 5 versus 18 ± 4).

Conclusion: Further studies are needed to characterize the hypothermic neuroprotection and its association with TrkB phosphorylation in neonatal mice post-HIE. TrkB agonist therapy and its long-term effects are yet to be determined in hypothermic neonatal mice post-HIE. Once completed, these studies will help us determine the combined neuroprotective effects of hypothermia and TrkB agonist therapy in both neonatal males and females post-HIE.

367
BRAIN-0085
Poster Session

Developing Brain

PHENOBARBITAL DELAYS SEIZURES BUT DOES NOT IMPROVE DAMAGE IN A NEONATAL STROKE MODEL

C. CHARRIAUT-MARLANGUE[1], *L. MORIN*[1], *P.L. LEGER*[1], *S. AUVIN*[1]
[1]*UMR1141, INSERM, PARIS, France*

Objectives – Neonatal cerebral stroke accounts for 10-15% of the total number of neonates with seizures, and is the main identified cause of congenital hemiplegia (Anderson et al., 2008). We studied the effect of phenobarbital, a well pharmacological drug used in first intention, on 1) the quantity of seizures, and 2) the size of the lesion.

Methods – All animal procedures complied with the ethical guidelines of the Robert Debre´ Hospital Research Council Review Board (A75-19-01), and the INSERM, and the ARRIVE guidelines. P7 (7 day-old) rats were subjected to ischemia-reperfusion (Renolleau et al., 1998), which received either phenobarbital (10, 20, and/or 40 mg/kg) before and/or 3 hours after ischemia or PBS. EEG recordings were acquired and seizures were quantified by using cortical bipolar electrode on the dura, and the animals will be connected to an MP100/EEG100B acquisition system (BIOPAC, Santa Barbara, CA, USA). EEG will be acquired using AcqKnowledge 4.1 software (BIOPAC) along with simultaneous digital video. Two investigators blind to the treatment group determined the number of seizures, the size of the lesion (24 hours after ischemia), and cell death measured with the TUNEL assay.

Results – Very rare epileptic spikes were observed during the ischemic phase. In contrast, all animals exhibited epileptic "bursts" consisting in high voltage spikes and slow waves as early as re-flow occurred, and eighty percent of them displayed seizures beginning at 7.8±8.5 hours of EEG monitoring. Phenobarbital, whatever the dose and timing administration used did not reduce the lesion size (15.1±4.8 *vs* 12.1±2.6, NS), and the number of TUNEL-positive nuclei in the cortex (154.9±30.7 *vs* 148.3±45.9, NS). At a dose of 20 mg/kg given before ischemia, phenobarbital did not significantly reduce the number of seizures but reduced the time of their first occurrence 15.8±8.4 hours ($p<0.05$ *vs* ischemia-PBS). Phenobarbital also significantly reduced the duration of epileptic "bursts" (525±633 vs 1744±864 s, $p=0.0012$).

Conclusions – Our data demonstrate that phenobarbital is not the best pharmacological drug to treat both neonatal seizures and ischemic injury. Our ischemic model in the P7 rat pup, with EEG profiles similar to those observed in most of infants with cerebral infarction, represents a relevant model to further evaluate unsolved questions that cannot be addressed by any clinical research.

This work is supported by a FFRE-FRC grant.

REFERENCES

Andersen GL, Irgens LM, Haagaas I, Skranes JS, Meberg AE, Vik T (2008) Cerebral palsy in Norway: Prevalence, subtypes and severity. European Journal of Paediatric Neurology 12:4-13.

Renolleau S, Aggoun-Zouaoui D, Ben-Ari Y, Charriaut-Marlangue C (1998) A model of transient unilateral focal ischemia with reperfusion in the P7 neonatal rat: morphological changes indicative of apoptosis. Stroke; a journal of cerebral circulation 29:1454-1460; discussion 1461.

368
BRAIN-0109
Poster Session

Developing Brain

PRETREATMENT WITH DEXMEDETOMIDINE OR ERYTHROPOIETIN HAD NO EFFECT ON THE LONG-TERM COGNITIVE FUNCTION AFTER SEVOFLURANE EXPOSURE IN NEONATAL RATS.

T. Goyagi[1], T. Horiguchi[1], T. Nishikawa[1]
[1]Anesthesiology and Intensive Care Medicine, Akita University Graduate School of Medicine, Akita, Japan

Introduction

It is well known that anesthetic exposure induces neural apoptosis and degeneration in neonatal immature brain[1,2]. Previous reports suggested that dexmedetomidine[3-5] and erythropoietin[6] provided neuroprotection against anesthetic-induced neurodegeneration or cognitive impairment in neonatal animal[4,5]. We examined whether dexmedetomidine and erythropoietin attenuate the long-term cognitive dysfunction after 3% sevoflurane exposure in neonatal rats.

Methods

After approval by the animal research committee, 7-day-old rats received intraperitoneal saline (control), dexmedetomidine (6.6, 12.5, 25 μg/kg) and erythropoietin (60, 120, 600U) respectively, 30 min before 3% sevoflurane exposure for 4 hours with 21% oxygen (n=5, each group). Acquisition trials were carried out using Morris water maze 3 weeks after anesthesia exposure, and rats were evaluated for spatial memory 6 weeks after anesthesia exposure. Fear conditioning test was conducted 5 and 6 weeks after anesthesia exposure. Escape latency, swimming path lengths and freezing time were measured. Data (mean ± SD) were analyzed using one-way ANOVA. $P<0.05$ was considered statistically significant.

Results

There were no differences between dexmedetomidine or erythropoietin treated- and control rats in escape latency, swimming path lengths and freezing time at 6 weeks after sevoflurane exposure (Table).

	Escape latency (sec)	Path length (cm)	Freezing time (%)
Dexmedetomidine			
6.6 (μg/kg)	31 ± 37	946 ± 1166	66 ± 12
12.5 (μg/kg)	28 ± 32	625 ± 724	99 ± 1
25 (μg/kg)	7 ± 3	207 ± 161	57 ± 30
Erythropoietin			
60 (U)	25 ± 27	630 ± 733	77 ± 18
120 (U)	20 ± 20	497 ± 507	78 ± 29
600 (U)	21 ± 26	534 ± 693	95 ± 5
Control	19 ± 17	692 ± 637	78 ± 11

Conclusion

Pretreatment with dexmedetomidine or erythropoietin did not affect the long-term cognitive function after 3% sevoflurane exposure for 4 hours in 7-day-old rats

References

1) Jevtovic-Todorovic V, et al. J Neurosci 23: 876–882, 2003
2) Loepke AW, et al. Anesth Analg 106: 1681–1707, 2008
3) Li Y, et al. PLoS One 9: e93639, 2014
4) Sanders RD, et al. Acta Anaesthesiol Scand. 54: 710-716, 2010
5) Sanders RD, et al. Anesthesiology 110: 1077-1085, 2009
6) Dzietko M, et al. Neurobiol Dis 15: 177-187, 2014

369
BRAIN-0864
Poster Session

Developing Brain

DEVELOPMENT OF REGIONAL CEREBRAL HEMODYNAMICS IN NEONATES WITH CRITICAL CONGENITAL HEART DISEASE

T. Ko[1], J.M. Lynch[2], J.J. Newland[3], M. Winters[3], D.R. Busch[2], A.L. McCarthy[3], S.C. Nicolson[4], L.M. Montenegro[4], S. Fuller[5], J.W. Gaynor[5], T.L. Spray[5], M.Y. Naim[6], A.G. Yodh[2], D.J. Licht[3]
[1]Department of Bioengineering, University of Pennsylvania, Philadelphia, USA
[2]Department of Physics, University of Pennsylvania, Philadelphia, USA
[3]Division of Neurology, Children's Hospital of Philadelphia, Philadelphia, USA
[4]Division of Cardiothoracic Anesthesia, Children's Hospital of Philadelphia, Philadelphia, USA
[5]Division of Cardiothoracic Surgery, Children's Hospital of Philadelphia, Philadelphia, USA
[6]Division of Critical Care Medicine, Children's Hospital of Philadelphia, Philadelphia, USA

Introduction— Non-invasive, functional neuroimaging of the primary motor cortex (M1) is needed for assessment of psychomotor function in neonates with critical congenital heart disease (CHD) and other populations at high risk for neurologic morbidity and mortality [1]. At discharge, after a median 25-day length-of-stay, greater than half of newborns with hypoplastic left heart syndrome (HLHS) are unable to independently orally feed [2]. The impact of brain injury and delayed maturation on psychomotor delays (PD) underlying neonatal feeding dysfunction remain difficult to discern. Near-infrared diffuse optical techniques hold the potential to provide portable pediatric functional imaging with real-time sensitivity to changes in both cerebral tissue oxygen saturation (StO_2) and cerebral blood flow index (BFI). Baseline perirolandic cerebral hemodynamics are undetermined in this patient population. This preliminary investigation aims to identifying regional differences as well as elucidate the impact of maturation on baseline values.

Methods— Non-invasive hybrid instrumentation, based on diffuse optical spectroscopy (DOS) for blood oxygen saturation and diffuse correlation spectroscopy (DCS) for blood flow, were used to quantify prefrontal and perirolandic StO_2 and BFI in term neonates (40 + 4 weeks gest.) with critical CHD. Pre-frontal measurements were performed daily from pre-operative recruitment through post-operative MRI. Measurement density was increased to every two hours for twelve hours immediately following surgery. Perirolandic measurements were acquired post-operatively when there was adequate signal-to-noise (SNR). Longitudinal changes and regional differences in cerebral hemodynamics were quantified.

Results— Preliminary measurements do not show a significant difference between left and right or between pre-frontal and perirolandic regional cerebral hemodynamics. In agreement with previous findings, StO_2 decreases as a function of time from birth [3]. Longitudinal regional relationships were not found to be significant.

Conclusions—Feasibility of perirolandic measurement of cerebral tissue oxygen saturation and blood flow index were demonstrated in neonates with CHD. These preliminary measurements will inform the design and interpretation of future functional imaging studies overlying the primary motor cortex. Longitudinal development of StO_2 provides unique insight into the impact of surgical recovery and maturation on cerebral neurovascular response.

References

1. Marino, Bradley S., et al. "Neurodevelopmental Outcomes in Children With Congenital Heart Disease: Evaluation and Management A Scientific Statement From the American Heart Association." Circulation 126.9 (2012): 1143-1172.

2. Medoff-Cooper, Barbara, and Chitra Ravishankar. "Nutrition and growth in congenital heart disease: a challenge in children." Current opinion in cardiology 28.2 (2013): 122-129.

3. Lynch, Jennifer M., et al. "Time-to-Surgery and Pre-operative Cerebral Hemodynamics Predict Post-operative White Matter Injury in Neonates with Hypoplastic Left Heart Syndrome: Lynch: Risks for Post-operative Brain Injury in Neonates with HLHS." The Journal of Thoracic and Cardiovascular Surgery (2014).

370
BRAIN-0579
Poster Session

Developing Brain

NEUROPROTECTION OF IMMATURE BRAIN FROM CONTROLLED CORTICAL IMPACT BY AN INHIBITOR OF 20-HETE SYNTHESIS

S. Shu[1], M. Saraswati[1], D. Spicer[1], S. Kannan[1], C. Robertson[1], R. Koehler[1]
[1]Department of Anesthesiology and Critical Care Medicine, Johns Hopkins University, Baltimore, USA

Background: Previous work has shown that inhibition of 20-hydroxyeicosatetraenoicacid (20-HETE) formation by cytochrome P450 (CYP) omega-hydroxylation of arachidonic acid can protect immature and mature brain from ischemia. Because traumatic brain injury (TBI) can share some common mechanisms ofneurodegeneration, we tested the hypothesis that post-treatment with the 20-HETE synthesis inhibitor N-hydroxy-N-4-butyl-2-methylphenylformamidine (HET0016) can protect the immature brain from traumatic brain injury (TBI). We focused on immature brain because investigation of therapies for pediatric TBI is understudied and infants, in particular, often have poor outcome.

Methods: Male Sprague-Dawley rats (postnatal day 9-10) were subjected to controlled cortical impact (velocity 5.0-5.5 m/s; 3 mmdiameter; depth 1.5 mm). Age-matched rats were randomly divided into three groups:1) sham-operated group, 2) vehicle-treated TBI group, and 3) HET0016-treatedTBI group (1 mg/kg, ip, at 5 min and 3 h post-injury). Lesion volume and microglia morphology (Neurolucida software) were measured on 3, 7 and 30 days post-injury.Gene expression of inflammatory factors (Real-time PCR of TNFalpha, IL-1beta,IL-4, IL-10), microglia activation (CD68/Iba-1), neuron loss (NeuN/DAPI), and astrocyte activation (GFAP) were evaluated on 3 day post-injury. To determine whether HET0016 could exert direct effects on activated microglia, BV2 microglia cells were cultured and divided into control, 0.1-1 uM HET0016, lipopolysaccharide (LPS), and LPS+HET0016 treatments. TNFalpha concentration of the supernatant was determined at 24 h with ELISA. Data were analyzed by unpaired *t*-test or analysis of variance with post-hoc Bonferroni's correction for multiple comparisons.

Results: Lesion volumes in the vehicle-treated TBI group were 12.9±1.9, 15.4±4.9 and 18.2±0.8% of hemisphere on 3, 7 and 30 days post-injury, respectively. The corresponding lesion volumes in the HET0016-treated TBI groups were reduced significantly to 6.2±1.9, 5.5±1.3 and 8.8±0.9%. Microglia with more intersections and greater length of processes were observed in the HET0016-treated group on 3 and 30 days post-injury compared to vehicle. Early HET0016 treatment significantly decreased microglia cell body area on 7 and 30 days post-injury. Peri-lesion gene expression of pro-inflammatory cytokines (TNFalpha, IL-1beta) was lower at 1 day and reparative cytokines (IL-4, IL-10) expression was higher at 3 days in the HET0016-treated TBI group than in the vehicle-treated TBI group. HET0016 decreased the number of CD68-positive microglia in peri-lesion cortex, neuronal loss in ipsilateral thalamus, and GFAP intensity of astrocyte staining around the contralateral hippocampus and cortex. In cultured BV2 microglia, LPS increased expression of CYP 4A, an omega-hydroxylase CYP that generates 20-HETE. The LPS-evoked increase in TNFalpha release was attenuated by HET0016.

Conclusions: In immature ratbrain that developmentally approximates a human infant, the 20-HETE synthesis inhibitor HET0016 reduced lesion volume acutely and attenuated the growth of the lesion normally seen over one month following controlled cortical impact. The potential protective mechanism may be related to 20-HETE-induced pro-inflammatory state of microglia, as evident by HET0016 early attenuation of pro-inflammatory cytokine gene expression at one day of recovery, later augmentation of reparative cytokine gene expression at three days, and an accelerated recovery of microglia to a ramified state.

371
BRAIN-0831
Poster Session

Developing Brain

INTRAOPERATIVE MEASURES OF CEREBRAL PERFUSION AND OXYGEN CONSUMPTION IN ANAESTHETIZED INFANTS USING DIFFUSE CORRELATION SPECTROSCOPY AND NEAR-INFRARED SPECTROSCOPY

P. Lin[1], J. Sutin[1], L. Cornelissen[2], K. Chen[2], P. Grant[3], C. Berde[2], M. Franceschini[1]
[1]Athinoula A. Martinos Center for Biomedical Imaging, Massachusetts General Hospital / Harvard Medical School, Boston, USA
[2]Department of Anesthesiology Perioperative and Pain Medicine, Boston Children Hospital/ Harvard Medical School, Boston, USA
[3]Fetal-Neonatal Neuroimaging and Developmental Science Center, Boston Children Hospital/ Harvard Medical School, Boston, USA

Objectives: More than 1 million children under 4 years of age undergo surgical procedures requiring anesthesia in the United States each year. Exposure to anesthesia before 3 years of age doubles the incidence of deficits in language and abstract reasoning, with risk continuing to increase with each exposure[1]. Animal studies suggest toxicity of anesthetic drugs and disruptions of cerebral perfusion are the principal mechanisms of harm to the developing brain during anesthesia and surgery[2]; however, studies in infants are lacking.

We have developed unique, advanced diffuse correlation spectroscopy (DCS) combined with near-infrared spectroscopy (NIRS), enabling, for the first time, continuous quantification of cerebral blood flow (CBF), oxygen saturation (SO_2) and metabolic rate of oxygen ($CMRO_2$) in the operating room[3]. With this method we continuously measured CBF and $CMRO_2$ in infants under general anesthesia during perioperative periods including induction, maintenance, and emergence phases of anesthesia. These measurements allow us detect changes in $CMRO_2$ due to anesthetic depth and abnormal hypotension, and differentiate them from changes in cerebral SO_2, CBF and $CMRO_2$ due to hypo/hypercapnia and hypoxia.

Methods: Healthy Infants less than 6 month old admitted to Boston Children Hospital for lower-body surgery were eligible for the study. We performed continuous intraoperative cerebral NIRS-DCS measurements correlated with perioperative data from patient monitors, including MAC, end-tidal CO_2 ($ETCO_2$), mean arterial pressure and electrocardiogram. We analyzed the influences of those parameters on our measurements of SO_2, CBF and $CMRO_2$.

Results: Enrollment for these studies is ongoing. To date we have successfully measured 15 infants. From the preliminary analysis we have observed substantial CBF changes corresponding to ventilation-induced changes in $ETCO_2$. We were able to quantify cerebral vascular reactivity (CVR) to CO_2 and found CVR in infants is greater than what reported in adults, but in agreement with values found in young children using transcranial Doppler ultrasound[4]. In a few instances we have recorded hypotensive events. In particular in a 6 month old infant who experienced cardiac arrhythmia due to anesthetic toxicity, we measured a CBF drop of more than 40% in a minute. Interestingly a minute after vasopressor

injection, CBFi was still low and the large oscillations in CBF suggested blood pressure was still low.

Conclusion: With this work we are beginning to demonstrate the clinical relevance of our NIRS-DCS method as a continuous cerebral monitor during general anesthesia in infants. We believe this method will impact the management of patients by providing more quantitative information about the effect of different anesthetic and vasopressor agents and surgical manipulations on cerebral oxygen delivery and utilization, and enabling patient-specific management guided by individual cerebral physiology.

1. Wilder, R. T. *et al. Anesthesiology* 110, 796–804 (2009).
2. Jevtovic-Todorovic, V.. *Anesthesia & Analgesia* 113, 965–968 (2011).
3. Lin, P. Y. *et al. J Vis Exp* e4379 (2013). doi:10.3791/4379
4. Brohi, F. A. *et al.. British Journal of Anaesthesia* 89, 525–author reply 526 (2002).

372
BRAIN-0833
Poster Session

Developing Brain

BEDSIDE MEASURES OF CEREBRAL BLOOD FLOW AND OXYGEN CONSUMPTION CHANGES IN NEWBORNS WITH HYDROCEPHALUS TREATED BY ENDOSCOPIC THIRD VENTRICULOSTOMY COMBINED WITH CHOROID PLEXUS CAUTERIZATION

P. Lin[1], K. Hagan[1], R. Vyas[2], B. Warf[3], P. Grant[2], M. Franceschini[1]
[1]Athinoula A. Martinos Center for Biomedical Imaging, Massachusetts General Hospital Harvard Medical School, Boston, USA
[2]Fetal-Neonatal Neuroimaging and Developmental Science Center, Boston Children Hospital/ Harvard Medical School, Boston, USA
[3]Departments of Neurosurgery and Global Health and Social Medicine, Boston Children Hospital/ Harvard Medical School, Boston, USA

Objectives: Prediction and management of hydrocephalus in newborns are particularly challenging. Existing hydrocephalus treatment assessments rely on radiological estimation of ventricular size, but have low correlation with the incidence of neurodevelopmental delay later in life[1]. Impaired perfusion and oxidative metabolism likely contribute to the development of brain injuries in hydrocephalus. Previous studies using conventional near-infrared spectroscopy (NIRS) found cerebrospinal fluid (CSF) removal is associated with significant improvements of cerebral hemoglobin oxygenation (SO_2) and cerebral blood volume (CBV)[2]. However, these changes are not always reliably correlated with either the volume of CSF removed or the severity of hydrocephalus. Since SO_2 changes only indirectly reflect changes of cerebral blood flow (CBF), measurement of CBF may have stronger correlation with disease trajectory. In this study, we use diffuse correlation spectroscopy (DCS) and frequency-domain NIRS (FDNIRS) to make direct quantitative measurements of CBF and metabolic rate of oxygen ($CMRO_2$) at the patient's bedside and monitor hydrocephalus progression and treatment response. We hypothesized successful hydrocephalus treatment will result in significant increases in both CBF and $CMRO_2$.

Methods: Six newborns (GA: 25.3 -39.1 wks) with progressive hydrocephalus were enrolled in the study. All patients underwent a surgical procedure, endoscopic third ventriculostomy combined with choroid plexus cauterization (ETV/CPC), to treat progressive hydrocephalus. CBF, SO_2, CBV and $CMRO_2$ were measured in the frontal, temporal, and parietal regions by FDNIRS-DCS[3] before and after surgical procedure. Evaluations of treatment response determined by clinical assessments including CUS, MRI and daily head circumference measurements.

Results: After the ETV/CPC procedure we observed large increases in CBF and $CMRO_2$ (22% and 19%, respectively), while SO_2 and CBV increased only 7% and 5% respectively. In all infants, cranial ultrasound also showed reductions of ventricle size after ETV/CPC. The increases in CBF we observed are consistent with results from previous studies after CSF removal[4]. We also found that by estimating CBF from CBV using the Grubb's relationship[5], the approach of prior NIRS studies, significantly underestimates the CBF changes and does not properly reflect intervention-induced changes in cerebral perfusion.

Conclusions: Our preliminary results suggest FDNIRS-DCS bedside measures of CBF and $CMRO_2$ detects hydrocephalus evolution better than CBV and SO_2, measures alone, and thus may have potential to be a better patient-specific management tool.

1. Larysz, P. *et al*. Radiological findings in relation to the neurodevelopmental outcome in hydrocephalic children treated with shunt insertion or endoscopic third ventriculostomy. *Childs Nerv Syst* **30,** 99–104 (2014).

2. Soul, J. S. et al. CSF Removal in Infantile Posthemorrhagic Hydrocephalus Results in Significant Improvement in Cerebral Hemodynamics. *Pediatric Research* **55,** 872–876 (2004).

3. Lin, P. Y. *et al.* Non-invasive optical measurement of cerebral metabolism and hemodynamics in infants. *J Vis Exp* e4379 (2013).

4. Leliefeld, P. H. *et al.* Magnetic resonance imaging for quantitative flow measurement in infants with hydrocephalus: a prospective study. *J Neurosurg Pediatr* **2,** 163–170 (2008).

5. Grubb, R. L. *et al*. The effects of changes in PaCO2 on cerebral blood volume, blood flow, and vascular mean transit time. *Stroke* **5,** 630–639 (1974).

373
BRAIN-0863
Poster Session

Developing Brain

PRE-OPERATIVE CEREBRAL HEMODYNAMICS FROM BIRTH UNTIL SURGERY IN INFANTS WITH CRITICAL CONGENITAL HEART DISEASE

J. Lynch[1], M. Winters[2], D. Busch[2], T. Ko[3], A. McCarthy[2], R. Xiao[4], S. Nicolson[5], L. Montenegro[5], S. Fuller[6], W.J. Gaynor[6], T. Spray[6], A. Yodh[7], D. Licht[2], M. Naim[8]
[1]School of Medicine, New York University School of Medicine, New York City, USA
[2]Neurology, The Children's Hospital of Philadelphia, Philadelphia, USA
[3]Bioengineering, University of Pennsylvania, Philadelphia, USA
[4]Biostatistics and Epidemiology, University of Pennsylvania, Philadelphia, USA
[5]Cardiothoracic Anesthesia, The Children's Hospital of Philadelphia, Philadelphia, USA
[6]Cardiac Surgery, The Children's Hospital of Philadelphia, Philadelphia, USA
[7]Department of Physics and Astronomy, University of Pennsylvania, Philadelphia, USA
[8]Critical Care Medicine, The Children's Hospital of Philadelphia, Philadelphia, USA

Introduction—Infants with critical congenital heart disease (CHD) exhibit a high prevalence of hypoxic-ischemic white matter injury, termed periventricular leukomalacia (PVL). Recent work has shown that the risk for PVL in infants with hypoplastic left heart syndrome and transposition of the great arteries is dependent on the waiting time from birth to surgery. Understanding the changing cerebral physiology during this vulnerable preoperative period may lead to new therapeutic algorithms aimed at prevention.

Methods—Term neonates with critical CHD were recruited for this study. Frequency domain diffuse

optical spectroscopy was employed to noninvasively quantify cerebral tissue oxygen saturation (StO2). Daily StO2 measurements were made from day of recruitment until the day of surgery.

Results—We studied 35 neonates with critical CHD. The subjects were placed in 3 groups depending on their cardiac diagnosis: two ventricle with normal arch (N=17), two ventricle with arch obstruction (N=8), or one ventricle with arch obstruction (N=10). In a linear mixed-effects model, time after birth was significantly predictive of StO2 ($p<0.01$), with StO2 decreasing as a function of time from birth.

Conclusions—We observed decreasing StO2 from birth until surgery in all groups. These results suggest that reported increases in risk for PVL with time-to-surgery could be due to increasing cerebral oxygen extraction. Additionally, these findings suggest that therapeutically increasing cerebral oxygen delivery or decreasing cerebral oxygen demand could mitigate the risk for PVL in cases when earlier surgery is not possible.

374
BRAIN-0827
Poster Session

Developing Brain

USING A HYBRID OPTICAL SYSTEM TO DETECT THE UNCOUPLING OF CEREBRAL BLOOD FLOW AND CEREBRAL OXIDATIVE METABOLISM IN PRETERM INFANTS UNDERGOING TREATMENT FOR PATENT DUCTUS ARTERIOSUS

M. Diop[1], J. Kishimoto[1], V. Toronov[2], D.S.C. Lee[3], K. St Lawrence[1]
[1]Imaging Program, Lawson Health Research Institute, London, Canada
[2]Physics, Ryerson University, Toronto, Canada
[3]Neonatology, London Health Sciences Centre, London, Canada

OBJECTIVE

Preterm neonates are at risk of ischemic brain injury due to a combination of poor cerebral autoregulation and unstable blood pressure. These factors can lead to transient reductions in cerebral blood flow (CBF), resulting in injury if adequate oxygen delivery is not maintained. Optical methods can provide bedside monitoring of CBF (diffuse correlation spectroscopy, DCS), cerebral oxygenation (S_tO_2 by near-infrared spectroscopy, NIRS) and the cerebral metabolic rate of oxygen ($CMRO_2$ by combining the two methods)[1,2]. In addition, quantitative measurements can be determined using dynamic contrast-enhanced (DCE) NIRS to measure absolute CBF[3,4]. The objective of this study was to demonstrate that broadband NIRS combined with DSC could measure the expected uncoupling of CBF and $CMRO_2$ in preterm infants undergoing treatment with the vasoconstrictor, indomethacin[5]. Broadband NIRS was used as the spectral measurements provides the ability to separate absorption changes caused by blood oxygenation from those caused by the contrast agent (indocyanine green, ICG)[6].

METHODS

Experiments involved preterm infants diagnosed with patent ductus arteriosus. NIRS measurements of CBF and S_tO_2 were acquired before and after a 45-min infusion of indomethacin, and DCS data were acquired every 30 s during the infusion to measure relative CBF. DCE NIRS required an intravenous injection of ICG (0.1 mg/kg) and measuring the arterial ICG concentration by dye densitometry[5]. The pre-infusion CBF measurements were used to convert DCS data into units of CBF[3]. S_tO_2 was determined using a spectral derivative method to extract estimates of the concentrations of the main absorbers (water, oxy- and deoxy-hemoglobin)[6]. $CMRO_2$ was determined by combining CBF and S_tO_2[4].

RESULTS

Experiments were performed on 11 preterm infants (birth weight: 950 ± 159, standard error of mean), and complete DCE NIRS and DSC data sets

were obtained from a subset of 8. Mean baseline CBF and $CMRO_2$ measured by NIRS were 18.5 ± 3.3 ml/100g/min and 1.32 ml O_2/100g/min, respectively. The CBF reduction caused by indomethacin was 26.4 ± 4.4% measured by DCE NIRS and 27.8 ± 2.2% measured by DCS. Figure 1 shows the CBF change during treatment, as obtained by combining baseline CBF measured by NIRS with flow changes measured by DCS. Despite the significant change in CBF with treatment, the mean change in $CMRO_2$ (-4.0 ± 6.7%) was not significant.

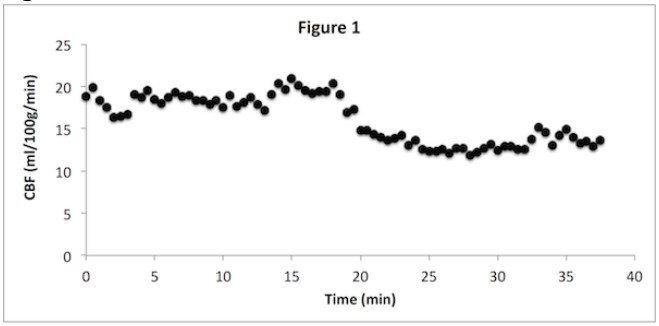

CONCLUSION

The similarity between CBF changes measured by DCS and DCE NIRS is in good agreement with a previous study conducted using a neonatal animal model[3]. As anticipated[5], $CMRO_2$ remained stable despite the drop in CBF due to a compensatory increase in oxygenation extraction. These results demonstrate that broadband NIRS combined with DCS can detect independent changes in perfusion and metabolism. Considering these technologies are safe and portable, they are well suited for neuromonitoring with this fragile patient population.

REFERENCES

1) Roach-Labarbe, J Cereb Blood Flow Metab, 2012;32:481
2) Jain, J Cereb Blood Flow Metab 2014;34:380
3) Diop, Biomed Opt Express 2012;3:1476
4) Verdecchia, J Biomed Opt 2013;18:27007
5) Arora, Pediatr Res 2013;73:713
6) Diop, J Biomed Opt 2014;19:57007

375
BRAIN-0230
Poster Session

Developing Brain

WHITE MATTER APOPTOSIS IS INCREASED BY DELAYED HYPOTHERMIA AND REWARMING IN A NEONATAL PIGLET MODEL OF HYPOXIC ISCHEMIC ENCEPHALOPATHY

B. Wang[1], J. Armstrong[1], E. Kulikowicz[1], M. Reyes[1], D. Spicer[1], U. Bhalala[1], Z.J. Yang[1], R. Koehler[1], L. Martin[1], J. Lee[1]
[1]Anesthesiology and Critical Care Medicine, Johns Hopkins University School of Medicine, Baltimore, USA

Objectives: Therapeutic hypothermia is used to treat neonatal hypoxic ischemic (HI) brain injuries.However, the potentially deleterious effects of delaying the induction of hypothermia and of rewarming remain unclear. We previously found that rewarming from hypothermia increased cortical neuron apoptosis in a neonatal piglet model of HI brain injury (Wang et al., 2015). Because the subcortical white matter is also vulnerable to HI, we assessed the effects of delayed hypothermia and rewarming on forebrain subcortical white matter in a piglet model of HI.

Methods: Male piglets (2-4 days old) underwent HI injury, which was induced by decreasing the inspired oxygen concentration to 10% for 45 minutes followed by 7 minutes of asphyxia. Piglets recovered with normothermia or with 2 hours of normothermia followed by hypothermia. Hypothermic groups were then divided into those with no rewarming, slow rewarming at 0.5°C/hour, or rapid rewarming at 4°C/hour. All piglets were euthanized 29 hours after resuscitation for histologic examination. Apoptotic cells in the subcortical white matter of the motor gyrus were identified morphologically and counted by hematoxylin & eosin (H&E) staining and TUNEL assay at the striatal and hippocampal anatomic levels. White matter neurons were also counted, and apoptotic cells were immunophenotyped with the

oligodendrocyte marker 2',3'-cyclic-nucleotide 3'-phosphodiesterase (CNPase).

Results: After reoxygenation, arterial blood pressure and blood gases were similar among groups throughout the 29-h recovery period. The number of apoptotic profiles by H&E or TUNEL staining were similar between sham-operated (n=8) and naïve unanesthetized (n=7) piglets. This suggests that the anesthetic did not increase subcortical white matter apoptosis above normal developmental levels. In comparison to sham-operated and naïve unanesthetized (n=15) piglets, HI with sustained hypothermia (n=8; $p<0.05$), slow rewarming (n=8; $p<0.05$), and rapid rewarming (n=8; $p<0.05$) increased the number of apoptotic profiles on H&E stained sections and the number of TUNEL-positive cells. The HI normothermic group did not show increased apoptosis above that observed in sham/naïve piglets. There were no statistical differences in apoptotic cell counts between HI piglets that received normothermia, sustained hypothermia, or rewarming (whether slow or rapid). Subcortical white matter neuron numbers were unchanged among all groups, consistent with apoptosis occurring primarily among glial cells. Furthermore, many apoptotic cells were immunophenontyped as myelinating oligodendrocytes, as assessed by CNPase immunohistochemistry.

Conclusions: Oligodendrocyte apoptosis in subcortical white matter is a consequence of delayed induction of hypothermia and rewarming in a piglet model of HI. This study identifies a potentially critical deleterious effect of delayed hypothermia and rewarming on the forebrain subcortical white matter in the HI-injured developing brain.

References: Wang B. et al. J Cereb Blood Flow Metab 2015 Jan 7. doi:10.1038/jcbfm.2014.245 (Epub ahead of print).

376
BRAIN-0675
Poster Session

Biomarkers

COULD VASOMOTION BE AN EMERGENT EARLY BIOMARKER OF CEREBROVASCULAR DISEASE?

J. Berwick[1], P. Patel[1], M. Jones[1], L. Boorman[1], P. Sharp[1], S. Harris[1], C. Martin[1], M. Bruyns-Haylett[2]
[1]Psychology, University of Sheffield, Sheffield, United Kingdom
[2]School of Systems engineering, University of Reading, Reading, United Kingdom

Objectives

Vasomotion is a low frequency (0.1Hz) oscillation in blood flow that emerges when vascular system or delivery of oxygen to any region of the body is perturbed (1). Two recent articles have shown that cerebral vasomotion can occur in patients with brain tumours (*2*) and those undergoing cardiac bypass surgery (*3*). Vasomotion may therefore be a compensatory mechanism to ensure adequate oxygen supply in a compromised circulation and may be a valuable biomarker of cerebrovascular disease. It may also raise a confound in recent fMRI studies investigating changes in spontaneous connectivity networks as possible biomarkers for dementia (*4-6*). These studies are underpinned by the tacit assumption that the BOLD signal equates to neural activity and is unchanging. However, if neurovascular coupling is debilitated in disease this could suggest such connectivity changes to be the product of an emerging vasomotion and not related to neuronal activity. In this study we manipulated the magnitude of cerebral vasomotion in anaesthetised healthy rats by altering blood pressure and respiratory gases.

Methods

Experiments were performed on urethane anaesthetised female Hooded Listar rats. 2D-dimensional imaging spectroscopy (2D-OIS) and multi-channel electrophysiology were used to

measure cortical hemodynamics and neural activity respectively (n=10). 2D-OIS allowed localisation of the whisker sensory and motor cortices following presentation of whisker stimuli. The resultant 'maps' were used to guide electrode placement in both cortical regions. We then performed two experiments in which spontaneous neural and hemodynamic data were collected in the absence of stimuli for a period of 2100s. A known property of urethane anaesthesia is a reduction of mean arterial blood pressure (MABP). Thus in the first period of experiment 1 animals had low blood pressure ('vasomotion' condition) then after 290s a continuous infusion of intravenous phenylephrine began to elevate MABP to physiologically normal levels. In the second experiment the phenylephrine infusion ceased after 290s had elapsed. After 1410s of the data collection period the inspired gases were changed from room air to 100% oxygen. 2D-OIS data was subject to seed based correlation connectivity analysis to assess whether the resultant maps were altered in the different conditions (lowered MABP, normal MABP, lowered MABP with elevated Oxygen).

Results

Low MABP was associated with reliable large cortical vasomotion oscillations in all aspects of hemodynamics. These oscillations qualitatively altered functional connectivity maps across the cerebral cortex. At low MABP increasing oxygen to 100% significantly reduced the magnitude of the vasomotion oscillations.

Conclusions

Data suggest that during perturbations of systemic rodent physiology vasomotion is enhanced and as such may be present at the early stages of cerebrovascular disease as an early defence mechanism to guarantee sufficient transport of oxygen to brain tissue and thus has the potential to be a powerful early biomarker.

References

1. Mayhew, *Neuroimage* **4**, 183 (1996).
2. Rayshubskiy, *Neuroimage* **87C**, 323 (2013).
3. Zanatta, *Neuroimage* **72**, 10 (2013).
4. Hafkemeijer, *Biochimica et biophysica acta* **1822**, 431 (2012).
5. Kenny, *Brain* **135**, 569 (2012).
6. Kenny , *BJP* **203**, 209 (2013).

377
BRAIN-0135
Poster Session

Biomarkers

DECREASED CEREBRAL BLOOD FLOW IS ASSOCIATED WITH WORSE COGNITIVE OUTCOME AFTER REPETITIVE CONCUSSIONS IN MICE

E. Buckley[1], B. Miller[2], J.M. Golinski[3], H. Sadeghian[2], L.M. McAllister[3], C. Ayata[2], W.P. Meehan[4], M.A. Franceschini[2], M.J. Whalen[3]
[1]Biomedical Engineering, Georgia Institute of Technology, Atlanta, USA
[2]Radiology, Massachusetts General Hospital, Boston, USA
[3]Pediatrics, Massachusetts General Hospital, Boston, USA
[4]Sports Medicine, Boston Children's Hospital, Boston, USA

Objectives: Repetitive concussions are associated with long-term cognitive dysfunction that can be attenuated by increasing the time intervals between concussions; however, biomarkers of the safest rest interval between injuries remain undefined. Decreased cerebral blood flow (CBF) has been implicated as one such physiological biomarker, although interpretation of existing human studies is problematic[1-4]. Therefore, we employed a mouse closed head injury (CHI) model that is relevant to human concussion[5] in that it features head impact followed by unrestricted rotational acceleration, resulting in long-term cognitive deficits in the absence of macroscopic and microscopic brain injury[6]. Using a non-invasive optical modality known as diffuse correlation spectroscopy to quantify cortical cerebral blood flow, we explored the effects of

single and repetitive CHI on CBF, and relationships among CBF, CHI, and cognitive outcome.

Methods: A single CHI model and a repetitive CHI model (5 concussions spaced 1 day apart) were employed. Control mice were sham-injured mice that received the same anesthesia exposure but no concussive injury.

For the single CHI model, CBF was measured at baseline, as well as at 4 and 24 h post-CHI or sham injury. For the repetitive CHI model, CBF was measured at the following time points: baseline prior to injury, four hours after the third injury, 4h after the final injury, 72h after the final injury, and 2.5 weeks after the final injury.

Cognitive function was assessed after the final CHI using a version of the Morris water maze (MWM)[7].

Results: After a single CHI, CBF was reduced by 35 ± 4 % at 4 h and returned to pre-injury levels by 24 h. After 5 concussions spaced 1 day apart, CBF was also reduced from pre-injury levels 4 h after each concussion by approximately 20% but returned to pre-injury levels by 72 h after the final concussion and remained at pre-injury levels after 2.5 weeks.

A single CHI did not lead to MWM cognitive deficits as compared to sham). However, repetitive CHI led to significant cognitive deficits in the injured group as compared to sham in both hidden and visible platform trials of MWM tests ($p < 0.001$).

In the repetitive concussion model, lower CBF measured both pre-injury and 4 hours after the third concussion was associated with worse performance in the MWM, as quantified by average performance on hidden trial latencies (Figure 1). Similar relationships were not observed between CBF measured 4h, 72h, or 2.5 weeks after the final CHI and MWM performance.

Conclusions: Closed head injuries sustained by mice result in transient decreases in cortical CBF. Data from this investigation suggest that decreased cortical CBF may be a marker of an acute vulnerable period following concussive brain injury. This result is an important step forward, as current return-to-play/battlefield guidelines incorporate symptom resolution as major criteria[8], despite lack of proof of validity of this approach[4]. Furthermore, baseline CBF in the un-injured may be used to identify those at increased risk for cognitive deficits following CHI.

378
BRAIN-0011
Poster Session

Biomarkers

MATRIX METALLOPROTEINASE-9 AS A MARKER FOR ACUTE ISCHEMIC STROKE AND ITS RELATION TO STROKE SEVERITY.

E. ESMAIL[1], M. Abdulnaseer[1], N. Elfaiomy[1], E.N.G.I. Elsawy[1], M. Kamal[2]
[1]Neurology, Cairo University, Cairo, Egypt
[2]Clinical Pathology, Cairo University, Cairo, Egypt

Introduction: Thrombolytic therapy is currently the only FDA approved treatment for acute ischemic stroke. Hence, early diagnosis and risk stratification is of great importance in management.

Aim of work: to study role of serum level of MMP9 within 24 hours of stroke onset as a marker of acute ischemic stroke and a predictor of clinical severity.

Subjects and Methods: Thirty patients with acute ischemic stroke had measurement of serum MMP9 within 24 hours of stroke onset, and clinical assessment of stroke severity. 30 healthy volunteers were the control subjects.

Results: Fifteen male, and 15 female patients, with a mean age of 61 ±7.11 years were studied. Mean NIHSS stroke scale score on admission was 11.17 ± 4.76. Mean Modified Rankin scale on admission was 4.37 ± 0.76. The serum level of MMP-9 in patients within 24 hours of stroke onset was 998.8 ± 154.72ng/ml, which was

significantly higher than serum level of MMP-9 in control subjects (p value 0.003). The mean NIHSS and mRS on admission of patients with normal serum level of MMP9 was less than the mean NIHSS and mRS on admission of patients with high MMP9 serum levels, (p=0.003 & 0.004 respectively). There was a significant positive correlation between serum level of MMP-9 on admission and NIHSS score and mRS score on admission (p-0.005, p- 0.000 respectively) even after adjustment of other variables (age , Diabetes Mellitus, Hypertension , Intima-media thickness of common carotid artery and size of infarction). There was significant positive correlation between uric acid level and serum MMP-9 level on admission (*p*-0.037), but there was no significant correlation between MMP-9 level on admission and other vascular risk factors. **Conclusion:** MMP9 can be an early serum biomarker of acute ischemic stroke, and a predictor of clinical severity.

379
BRAIN-0480
Poster Session

Biomarkers

CONSISTENT METABOLISM ACROSS RESTING STATE FMRI NETWORKS BUT DIFFERING METABOLISM ACROSS STATES

G.J. Thompson[1], V. Riedl[2], T. Grimmer[3], A. Drzezga[4], P. Herman[1], F. Hyder[5]
[1]Diagnostic Radiology, Yale University, New Haven, USA
[2]Neuroradiology and Nuclear Medicine, Universität München, München, Germany
[3]Psychiatry, Universität München, München, Germany
[4]Nuclear Medicine, Uniklinikum, Koeln, Germany
[5]Diagnostic Radiology and Biomedical Engineering , Yale University, New Haven, USA

Resting state functional magnetic resonance imaging (R-fMRI) is a popular way to measure gray matter networks in the human brain. However, the parameters defined as "resting" for R-fMRI scans remain quite variable. For example, subjects may lie with eyes closed or open. Thus far, no study has examined the rationale for choosing the "rest" condition based on metabolic demand. Here, we compare glucose metabolism (CMR_{glc}) between eyes open and eyes closed and also across R-fMRI networks within each state.
***
Simultaneous R-fMRI (TR=2s, 300 images) and fluorodeoxyglucose PET data were recorded in 11 subjects with eyes open and 11 different subjects with eyes closed. Quantitative calibration of the PET data was used to reflect absolute CMR_{glc} in units of μmol/g/min. R-fMRI data were processed with standard R-fMRI processing techniques, both with and without regression of nuisance signals. Three types of network definition were used. **Definition 1:** Using only the Brodmann regions of 37 previously reported networks. **Definition 2:** The same Brodmann regions, but using them as a seed to generate correlation-based R-fMRI networks. Per-subject and mean networks, at three different thresholds, were examined. **Definition 3:** Independent component analysis (ICA) of R-fMRI data was used with components either within-group (e.g., only eyes closed subjects) or across all subjects. Mean CMR_{glc} was calculated in all of these networks and, for each type of network, 2D ANOVA was used to test for significance, with network as one variable and eyes open vs. eyes closed as the other variable.
***
Figure 1 shows CMR_{glc} at three thresholds using **definition 2**, individual networks and no nuisance signal regression (results were quite similar with nuisance signal regressions). For definitions 1 and 2 there was a significant increase in CMR_{glc} from the eyes closed state to the eyes open state, but no significant difference between R-fMRI networks or interaction between states and between networks. Using definition 3 there was a significant difference between states and between networks, but without significant interactions. However when components representing white matter, CSF, and noise were removed, results were similar to the other network definitions.
***
Globally higher CMR_{glc} was observed in the eyes open state. Although there was a significant CMR_{glc} difference between the two states in both

gray and white matter, there was no significant CMR_{glc} difference across gray matter networks in any given state. Although R-fMRI network analysis does not capture the metabolic state difference, R-fMRI networks were reliably detectable regardless of the state. The results presented here thus suggest that the brain easily transitions between these networks and thus, in terms of metabolic demand, either "rest" condition can be chosen for R-fMRI studies.

***

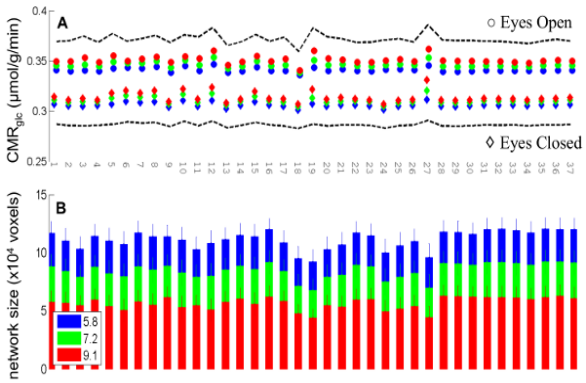

Figure 1. CMR_{glc} across 37 networks created using definition 2. **(A)** Variation of CMRglc across networks with eyes closed (diamond) vs. eyes open (circles) states. **(B)** Sizes of networks. Blue (Z ≥ 5.8), green (Z ≥ 7.2), and red (Z ≥ 9.1) indicate different R-fMRI thresholds. Dashed line/errorbar is maximum SEM.

380
BRAIN-0673
Poster Session

Biomarkers

METABOLIC AND TRANSCRIPTIONAL PROFILING OF ACUTE CEREBRAL ISCHEMIA IN RATS: PART 1. CHANGES OF BRAIN TISSUE

T. Imahori[1], K. Hosoda[1], Y. Irino[2], T. Nakai[1], Y. Yamamoto[1], J. Tanaka[1], E. Kohmura[1]
[1]Department of Neurosurgery, Kobe university graduate school of medicine, Kobe, Japan
[2]Division of Evidenced-based Laboratory Medicine, Kobe university graduate school of medicine, Kobe, Japan

Objectives:

Little is known about biological changes of brain tissue or blood in acute cerebral ischemia. Known as a method for detecting and analyzing endogenously-synthesized metabolites caused by biological activities comprehensively, metabolomics has attracted a lot of attention recently because metabolites are directly linked to the phenotype compared to genes or proteins. We investigated metabolic and transcriptional profiles of brain tissue in middle cerebral artery occlusion model of rats to explore the specific changes associated with acute ischemia.

Methods:

Forty adult male Wister rats weighing between 220 and 260 g were used in this study. Focal cerebral ischemia was induced in rats (n=20) using filament occlusion of the middle cerebral artery for 2 hours under inhalation anesthesia. After 2 hours of occlusion, brains were removed quickly, and tissue samples from cortical areas of the ischemic hemisphere were collected for metabolic profiling (n=15) and for transcriptional profiling (n=5). Sham operated rats (n=20) were treated like ischemic rats except that no suture was inserted into the artery and the samples were also collected as controls for each analysis. For metabolic profiling, water-soluble metabolites were extracted and then analyzed using gas-chromatography/mass-spectrometry (GC/MS). For transcriptional profiling, microarray analysis of the global gene expression was performed using Affymetrix GeneChip® Rat Gene 2.0 ST Array. The obtained data were analyzed by multivariate statistical method.

Results:

1) Metabolomics: Ninety metabolites were detected by GC/MS. As training set, 10 rats from ischemia group and 10 rats from control group were selected at random. Principal component

analysis (PCA) demonstrated clear separation between ischemia and control group on the first component. Heatmap also showed clear differences between the two groups (Figure). Fourteen metabolites including Alanine, GABA, and Citric acid/Isocitric acid had significantly high correlation with the first component of PCA. Using the remaining 10 rats (5 rats from each group) as validation set, PCA with the 14 metabolites showed distinct separation between the two groups. Pathway analyses from these differences in metabolites between the two groups indicated that several pathways including Glutamate metabolism and Glutathione metabolism, with a significant increase of GABA and decrease of Glutamate, were specific to acute cerebral ischemia.

2) Transcriptomics: Of 23,586 genes present on the array chip, ischemia group significantly upregulated 71 genes and downregulated 47 genes compared with control group. Heatmap of genes that had highly significant changes showed clear differences between the two groups (Figure). The significantly changed genes were involved in several pathways including MAPK signaling pathway, TNF signaling pathway, and Oxidative phosphorylation.

Conclusions:

Our study revealed that metabolic and transcriptional profiling in brain tissue of cerebral ischemic rats was associated with acute cerebral ischemia. Although the characteristic changes of metabolites were not fully consistent with the alternation in gene expression, it is considered that the discrepancy may reflect the different time course and pattern between the metabolic changes and transcriptional changes. This combination approach may provide new insights into the mechanism of acute cerebral ischemia and be useful for exploring novel biomarkers in the acute stage.

Figure. Heatmap

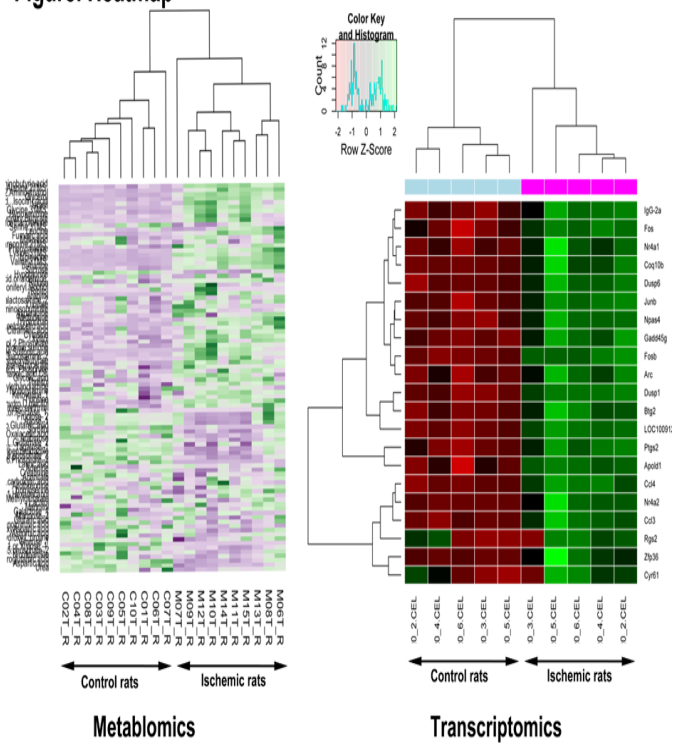

381
BRAIN-0344
Poster Session

Biomarkers

SEARCHING FOR A MOLECULAR SIGNATURE OF ALZHEIMER'S DISEASE IN DOWN SYNDROME PLASMA

M.F. Iulita[1], F. Caraci[2], A.C. Cuello[1]
[1]Pharmacology and Therapeutics, McGill University, Montreal, Canada
[2]Department of Drug Sciences, University of Catania, Catania, Italy

Objectives: A major obstacle to finding an effective therapy for Alzheimer's disease (AD) is its late diagnosis and our -as yet- incomplete understanding of the disease aetiology. AD brains are distinguished by vascular and extracellular aggregates of amyloid-β (Aβ) peptides and intraneuronal neurofibrillary tangles. Although Aβ is an important contributor to neurodegeneration, AD is a multifaceted disorder, where inflammation and cerebrovascular deficits are also early pathological landmarks of the

disease (1,2). Individuals with Down syndrome (DS) are at increased risk of developing AD compared to the normal population. DS brains progressively develop amyloid plaques, tangles, CNS inflammation and deficits in nerve growth factor metabolism (3,4). Diagnosing AD in DS is challenging due to the underlying intellectual disability and cognitive decline associated with aging. Therefore, **the overarching focus of this study was to identify biomarker candidates of an evolving amyloid pathology** in plasma samples from DS individuals, before and after the presentation of dementia. Methods: Fasting venous blood was collected in EDTA-containing tubes, immediately centrifuged and plasma samples were aliquoted and stored at –80° C until analysis. The study cases comprise the following clinical subgroups: healthy controls (age range 20-59 years); asymptomatic DS subjects (age range 22-52 years) and individuals with DS and clinical signs of AD (age range 39-61 years). Karyotyping showed full trisomy in all DS cases included in this study. Aβ peptides ending at amino acids 38, 40 and 42 were quantified using a Multi-Spot quantitative array (MesoScale Discovery, USA). Results: $A\beta_{38}$ was detectable in only ~40% of samples (mostly in the DS group) with no apparent differences between control and DS subjects. In contrast, $A\beta_{40}$ peptides were significantly elevated in asymptomatic individuals with DS ($p<0.01$), compared to age-matched controls, and remained higher in individuals with clinical signs of AD ($p<0.001$). Levels of $A\beta_{42}$ were higher in DS compared to controls but significantly elevated only in DS cases with established dementia ($p<0.05$). Conclusions: Plasma levels of Aβ peptides were elevated early in the disease process, in asymptomatic DS individuals with no signs of AD. These subjects will be longitudinally followed and cognitive function monitored to evaluate possible conversion cases. A second blood draw will be obtained after 12-15 months from the initial sampling. Pro-inflammatory markers will be next evaluated and correlated with amyloid burden. Given that Aβ peptides have potent cerebrovascular effects (2) and that the circulating ones have higher potential to affect cerebral blood flow (CBF), it would be of interest to correlate our results in plasma with CBF data (e.g. MRI) to better understand the pathogenesis of AD. Studies in DS offer the advantage to examine the temporal development of AD pathology in humans.

References: 1. Ferretti and Cuello *Curr Alzh Res* 8: 2011; 2. Iadecola *Nat Rev Neurosci* 5: 2004; 3. Mori et al. *Amyloid* 9: 2002; 4. Iulita et al. *Brain* 137: 2014.

382
BRAIN-0800
Poster Session

Biomarkers

PRECISION OF PHYSIOLOGICAL PARAMETERS FROM DYNAMIC CONTRAST-ENHANCED MRI IN PATIENTS WITH GLIOMA

G. Krokos[1], N. Thacker[2], S. Mills[2], G. Parker[2], M.C. Asselin[1], A. Jackson[1]
[1]The University of Manchester Wolfson Molecular Imaging Centre, Institute of Population Health, Manchester, United Kingdom
[2]The University of Manchester Imaging Sciences, Institute of Population Health, Manchester, United Kingdom

The difficulties in precisely estimating physiological parameters is recognized for complex pharmacokinetic models but often overlooked with the simpler commonly used models[1]. Correlations derived from the minimum variance bound can be used as a surrogate measurement of the precision of the physiological parameters when no ground truth is available like in clinical images.
Objectives: To estimate and compare the parameter correlations from kinetic analysis of dynamic contrast-enhanced (DCE) MR images in patients with glioma where the blood-brain barrier is heterogeneously dysfunctional.
Methods: Five patients with brain tumours underwent a pre-surgical DCE-MRI examination on a 3.0T MR scanner after bolus administration of the contrast agent Omniscan. Dynamic acquisition in oblique sagittal orientation lasted 5.8min at a temporal resolution of 3.46s and spatial resolution of $1.8x1.8x2.1mm^3$[2]. Anatomical post-contrast T_1-weighted images

were used for manual delineation of regions of interest on grey matter (GM), white matter (WM) and tumour. Kinetic analysis was performed at the voxel level using the extended Tofts model (ETM) with the internal carotid artery as the arterial input function. The bolus arrival time was included as an additional fitted parameter. The parameters were estimated by weighted non-linear least squares using a model-independent variance derived from the normally distributed image noise in the pre-bolus volumes and propagating it to the measured concentrations in all post-contrast volumes. The Jacobian matrix was constructed from the numerical derivatives of the cost-function and used to generate the covariance matrix, scaled by the image variance described above, and the correlation matrix. Unlike when estimating the variance from the fit residuals as commonly done, this approach allows quantitative interpretation of the fit statistics since the Chi-square per degree of freedom is calculated, allowing assessment of the goodness of fit.

Results: Contrast transfer coefficient K^{trans} was estimated to be 0.03±0.04min^{-1} (median±standard deviation) and 0.02±0.02min^{-1} in GM and WM, respectively, and higher in tumours (0.05±0.08min^{-1}) for all patients combined. Interstitial volume v_e in tumours (0.07±0.19) was also higher than in GM (0.04±0.03) and WM (0.03±0.05). Blood volume v_b was similar in all tissues but more variable in tumours (0.02±0.04) than in GM (0.02±0.02) and WM (0.01±0.01). K^{trans} and v_p were found to be inversely and highly correlated (figure 1a,b,c) in all tissues (GM -0.79±0.33, WM -0.72±0.15, tumours -0.74±0.31). The correlation between K^{trans} and v_e was weaker overall (**figure 1d,e,f**) but stronger and more variable in tumours (-0.66±1.21) as compared to GM (-0.24±0.39) and WM (-0.46±0.26).

Conclusion: Even for a simple model such as the ETM, high parameter correlations were observed with the highest being between K^{trans} and v_b. The negative correlation (defined by the ETM) contrasts with the biological correlation which was previously reported to be positive in grade IV gliomas[2]. Parameter correlations can potentially be lowered by optimising the methodology. Changes to the acquisition protocol are currently being investigated and different pharmacokinetic models of varying complexity will be evaluated in order to establish the maximal number of parameters that can reliably be estimated from DCE-MR images in glioma patients.

References: [1]Bartoš(2014) Mag.Res.Imag. 32(5):501-513

[2]Mills(2010) AJNR 31(4):726-731

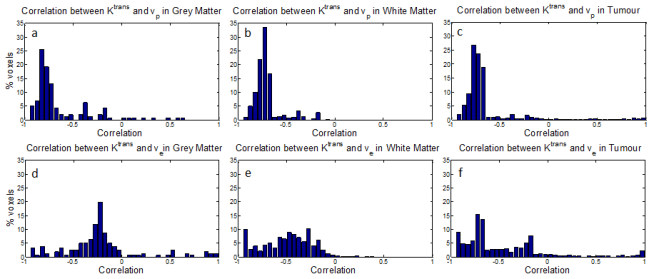

Figure: Correlation for all five patients between K^{trans} and v_p (upper row) and between K^{trans} and v_e (lower row) in grey matter (first column), white matter (second column) and tumour (third column)

383
BRAIN-0221
Poster Session

Biomarkers

EARLY DIAGNOSIS OF BRAIN TUMOURS THROUGH BIOFLUID METABOLOMICS

J.R. Larkin[1], A.M. Dickens[1], T.D.W. Claridge[2], D.C. Anthony[3], N.R. Sibson[1]
[1]CRUK and MRC Oxford Institute for Radiation Oncology Deparment of Oncology, University of Oxford, Oxford, United Kingdom
[2]Department of Chemistry, University of Oxford, Oxford, United Kingdom
[3]Department of Pharmacology, University of Oxford, Oxford, United Kingdom

Objectives: Over 20% of cancer patients develop brain metastases. Current MRI diagnostic techniques only detect late stage metastases, since they rely on blood-brain-barrier permeability to allow contrast enhancement. Thus, new methods enabling earlier diagnosis are urgently needed. We have previously shown that it is possible to discriminate between different inflammatory lesions in the CNS in rats (1), as well as between different stages of multiple sclerosis

in patients (2), through biofluid (blood/urine) metabolomics. We believe that this ability is due, at least in part, to alterations in CNS metabolism, which provoke a specific metabolic signature in the biofluids studied. It is known that tumour metabolism differs markedly from normal brain and that brain metabolism itself will be altered by tumour presence. On the basis of the above, therefore, we hypothesised that the presence of brain metastases could be detected, *in vivo*, through NMR analysis of biofluids.

Methods: Metastatic mammary carcinoma cells (murine 4T1-GFP) were injected into BALB/c mice, via intracerebral, intracardial or intravenous routes to induce differing cerebral and systemic tumour burdens. Urine was collected at days 0 and 10 from all animals, and at days 5, 21 and 35 in animals injected intracerebrally. Samples from naïve, day 0 and vehicle-injected mice served as combined control cohorts. Urine metabolite composition was analysed using ^{1}H-NMR spectroscopy, and statistical pattern recognition and modelling was applied to identify spectral differences and to identify commonalities indicative of brain metastasis burden. A robust method using unknown samples was used to validate model predictions.

Results: Significant metabolic profile separations were found between control cohorts and animals with tumour burdens at all timepoints for the intracerebral 4T1-GFP metastasis model (q^2 = 0.59, 0.70, 0.81 and 0.80 for days 5, 10, 21 and 35, respectively; $q^2 > 0.4$ considered significant). Models became stronger, with higher sensitivity and specificity, as the timecourse progressed indicating a more severe tumour burden. Sensitivity and specificity for predicting a blinded testing set were 0.89 and 0.82, respectively, at day 5, but both rose to 1.00 at day 35. Key metabolites driving the separations were identified and quantified relative to control (Fig. 1).

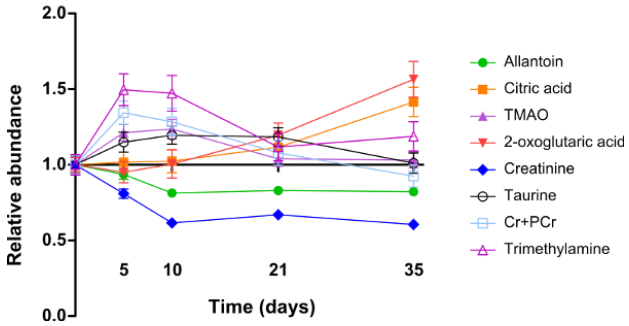

Significant separations were also found between control and day 10 animals for all 4T1-GFP injected mice irrespective of route (q^2 = 0.70, 0.63 and 0.78 for intracerebral, intracardiac and intravenous routes, respectively). The metabolites underpinning separations in each case differed indicating differentiation between systemic and CNS metastatic burden, but with common patterns that suggest a "fingerprint" for brain metastasis.

Conclusions: Our data indicate that animals with brain metastases can be identified using urinary metabolic profiles with NMR metabolomics, and differentiated from animals with a predominantly systemic metastasis burden. This approach may identify a set of biomarkers for the diagnosis of brain metastasis earlier than is currently possible, and may provide insight into metabolic disruption in brain metastasis.

References: (1) Griffin *et al.* (2004) FEBS Letters **568** 49-54; (2) Dickens and Larkin *et al.* (2014) Neurology **83** 1492-99

384
BRAIN-0220
Poster Session

Biomarkers

THE DIAGNOSTIC USEFULNESS OF DETERMINATION OF MATRIX METALLOPROTEINASE 3 (MMP-3) IN PATIENTS WITH MILD COGNITIVE IMPAIRMENT (MCI)

P. Muszynski[1], M. Groblewska[2], B. Mroczko[1], M. Zboch[3], A. Kulczynska-Przybik[1], D. Baranski[1], A. Mor[1], M. Szmitkowski[4], J. Kornhuber[5], P. Lewczuk[5]
[1]Department of Neurodegeneration Diagnostics, Medical University of Bialystok, Bialystok, Poland
[2]Department of Biochemical Diagnostics, University Hospital in Bialystok, Bialystok, Poland
[3]Research-Scientific-Didactic Centre of Dementia-Related Diseases, Medical University of Wroclaw, Wroclaw, Poland
[4]Department of Biochemical Diagnostics, Medical University of Bialystok, Bialystok, Poland
[5]Department of Psychiatry and Psychotherapy, Universitätsklinikum Erlangen and Friedrich-Alexander Universität Erlangen-Nürnberg, Erlangen, Poland

Objectives: Mild cognitive impairment (MCI) is thought to be an intermediate stage between the expected cognitive decline of normal aging and the more severe stage of dementia, eg. Alzheimer's disease (AD). It was shown that activity of matrix metalloproteinases (MMPs) might contribute to various neurodegenerative diseases including AD, which is the most common cause of dementia. The relationship between MMPs with AD were described in the literature, whereas associations of MMPs with MCI were not widely evaluated. The objective of our study was the assessment of the diagnostic usefulness of determination of MMP-3 in the cerebrospinal fluid (CSF) of patients with MCI in comparison with classical AD biomarker amyloid beta 1-42 (Ab_{1-42}).

Methods: The study included 40 subjects: 20 MCI patients and 20 normally aging individuals without cognitive impairment. The levels of MMP-3 and Ab_{1-42} in CSF were determined using ELISA method. The diagnostic criteria, ie. areas under ROC curves (AUC) and diagnostic sensitivity of MMP-3 and Ab_{1-42} were assessed.

Results: The CSF concentrations of MMP-3 were higher in MCI group (Median 305 pg/mL) in comparison (p=0.056) with elderly individuals without cognitive impairment (Median 245 pg/mL). The AUC for determination of MMP-3 was 0.678 but for Ab_{1-42} it was 0.763. However, the percentage of positive results for MMP-3 (80%) was higher than for Ab_{1-42} (60%) and increased up to 90% in combination of both biomarkers analyzed.

Conclusions: Our findings suggest that MMP-3 could serve as the diagnostic biomarker of differentiation between mild cognitive impairment and normally aging subject without cognitive impairment, although further studies are needed.

References:

1. Mroczko B, Groblewska M, Barcikowska M. The role of matrix metalloproteinases (MMPs) and tissue inhibitors of metalloproteinases (TIMPs) in the pathophysiology of neurodegeneration: a literature study. J. Alzheimers. Dis. 2013; 37(2): 273-283

2. Mroczko B, Groblewska M, Zboch M, Kulczyńska A, Koper OM, Szmitkowski M, Kornhuber J, Lewczuk P. Concentrations of matrix metalloproteinases (MMPs) and their tissue inhibitors (TIMPs) in the cerebrospinal fluid of patients with Alzheimer's disease. J Alzheimers Dis. 2014; 40: 351-357

385
BRAIN-0458
Poster Session

Biomarkers

METABOLIC PROFILING TO IDENTIFY DISTINCT CHANGES ASSOCIATED WITH ISCHEMIC CEREBROVASCULAR EVENTS IN CAROTID STENOSIS

T. Nakai[1], K. Hosoda[1], T. Imahori[1], M. Shinohara[2], Y. Irino[3], M. Yoshida[4], E. Kohmura[1]
[1]Department of Neurosurgery, Kobe University Graduate School of Medicine, Kobe, Japan
[2]Integrated Center for Mass Spectrometry, Kobe University Graduate School of Medicine, Kobe, Japan
[3]Integrated Center for Mass Spectrometry& Division of Evidenced-based Laboratory Medicine, Kobe University Graduate School of Medicine, Kobe, Japan
[4]Division of Metabolomics Research & Division of Gastroenterology, Kobe University Graduate School of Medicine, Kobe, Japan

Objectives

The underlying metabolic pathophysiology of ischemic stroke remains poorly understood. To explore the candidate biomarkers associated with cerebral ischemia, we investigated metabolic changes in blood of carotid stenosis patients with or without ischemic cerebrovascular events (ICVE).

Methods

Patients considered for carotid endarterectomy (CEA) were prospectively recruited in our hospital. The inclusion criteria of the current study were patients with carotid stenosis and success of sampling of internal jugular vein (IJV) and/or peripheral blood during CEA. Exclusion criteria were emergency CEA for stroke in evolution, crescendo TIA, or major disabling stroke. The patients were classified into 2 groups: ICVE-positive group was defined as those who had experienced any amaurosis fugax, any TIA, or any stroke within one-year before entry; ICVE-negative group was defined as those who had no history of ICVE and no obvious infarction on MRI.

During CEA, plasma from IJV and peripheral vein was collected before carotid artery clamping. All metabolites data measured using gas-chromatography/mass-spectrometry (GC/MS) were analyzed with multivariate statistical method, such as powered partial least squares-discriminant analysis (PPLS-DA) to discriminate ICVE-negative and -positive group.

Results

During the time of the study, 34 patients fulfilled the criteria described above. Nine patients were women. The mean age was 70.4±7.4 years ranging from 53 to 81. The overall average of the degree of ICA stenosis was 70.0±19%, ranging from 50 to 95% according to the North American Symptomatic Carotid Endarterectomy Trial criteria.

Blood samples from the IJVs of 27 patients were used for the IJV analysis. Thirteen patients were classified into the ICVE-positive group, and 14 were classified into the ICVE-negative group. The clinical characteristics did not differ significantly between two groups with the exception of age. We detected 108 kinds of water-soluble metabolites using GC/MS. PPLS-DA of IJV plasma data demonstrated a significant separation between ICVE-negative and -positive group (Figure left) and led to a construction of prediction model to discriminate the two groups with eight metabolites (ascorbic acid, gluconic acid, glycerol, histidine, lactic acid, methionine, p-hydroxybenzoic acid, and valine). Lactic acid and p-hydroxybenzoic acid were significantly elevated and other six metabolites were reduced in ICVE-positive group (Figure right). The prediction accuracy of the linear discriminant analysis model using the scores of the first and second components from the PPLS-DA model with eight metabolites was 0.96 (p=0.00000052).

Multilevel simultaneous component analysis showed significant metabolic changes between

IJV and peripheral plasma. Then, we also applied the prediction model with the eight metabolites described above to the classification of the peripheral plasma samples from 32 patients including 26 of the same 27 patients used in the IJV analysis and six additional patients. The clinical characteristics did not differ significantly between two groups. Consequently, the model applied to the peripheral plasma demonstrated the prediction accuracy of 0.84 (p=0.000057).

Conclusions

The current data demonstrated metabolic changes in the plasma were associated with cerebral ischemia. The eight specific metabolites were useful biomarkers for detecting ICVE. Finally, the constructed prediction model may be a first-step of a new strategy in screening of stroke.

PPLS-DA of the internal jugular plasma

Box-whisker plots of eight metabolites involved in final PPLS-DA model

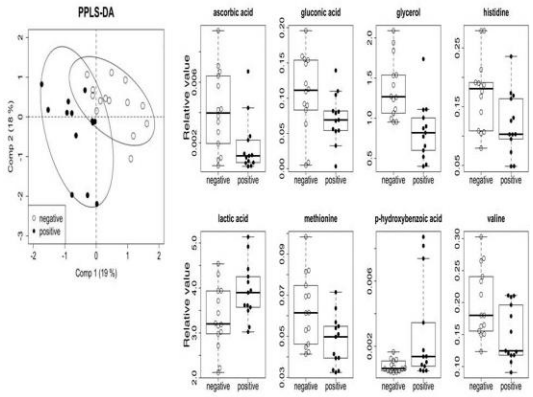

386
BRAIN-0470
Poster Session

Biomarkers

METABOLOMICS PROFILING OF ACUTE ISCHEMIA IN RATS: PART Ⅱ. METABOLIC CHANGES OF BLOOD PLASMA

Y. Yamamoto[1], K. Hosoda[1], T. Imahori[1], Y. Irino[2], J.U.N. Tanaka[1], T. Nakai[1], E.I.J.I. Kohmura[1]
[1]Neurosurgery,
Kobe University Graduate School of Medicine, Kobe, Japan
[2]Evidenced-based Laboratory Medicine, Kobe University Graduate School of Medicine, Kobe, Japan

Objectives:

Inpart I study, we reported that metabolicprofiling in brain tissues of acute cerebral ischemic rats revealed thespecific changes.

Inthis Part 2 study, we investigated the metabolic changes of blood plasma associated with acute cerebral ischemia.

Methods:

Bloodplasma (100 µl) was collected 2 hours after middle cerebral artery occlusion(MCAO) by a nylon monofilament insertion method in Wisterrats (n=14). Plasma samples from sham operated control rats (n=13) were alsocollected. Water-soluble metabolites were extracted and then analyzed usinggas-chromatography/mass-spectrometry (GC/MS). As a training set, 9 rats fromMCAO group and 8 rats from control group were selected at random. As validationset, the remaining 10 rats (5 rats from each group) were used. The obtained data of blood plasma were analyzed bymultivariate statistical method and compared with that of brain tissue.

Results:

Eighty-sixmetabolites were detected by GC/MS. Although principal component analysis (PCA)and Heatmap showed clear separation between the MCAO group and control group in the brain tissue, the same unsupervisedanalysis demonstrated only obscure separation between the two groups in thetraining set of blood samples. However,partial least square discriminant analysis (PLSDA)of the blood sample demonstrated clearer separation between the two groups inthe blood samples. Eight metabolites (alanine, glycerol, lactic acid, lysine,proline, pyroglutamic acid, serine, tyrosine) was selected as biomarkercandidates because they had loading >0.1 on the first component of

the PLSDA.In the validation set, this PLSDA model could discriminate the control and MCAOgroups with 90% of accuracy (p = 0.046).

Only4 (alanine, glycerol, lactic acid, pyroglutamic acid) of the 8 metaboliteswhich were selected as biomarker candidates in blood samples corresponded tothe biomarker candidates (14 metabolites) in the brain tissue.

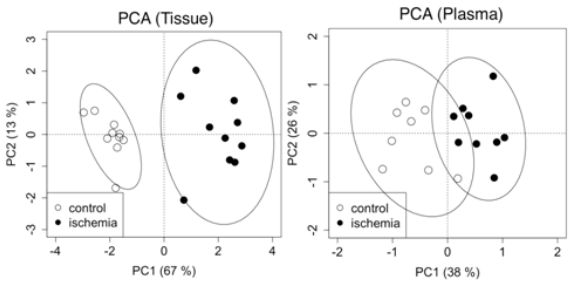

Conclusions:

In the acute cerebralischemia, metabolic changes of blood plasma do not coincide with that of the brain tissues. These discrepancy may be due to theinfluence of metabolic changes of the whole body by anesthesia and surgicalinvasion, or dilution with systemic blood perfusion. Nevertheless, the current results suggested the blood metabolite could be novel biomarkers for acute ischemic stroke.

387
BRAIN-0496
Poster Session

Biomarkers

CD49D EXPRESSION ON T LYMPHOCYTES AND CD8 EFFECTOR PERCENTAGE AS PREDICTORS OF JC VIRUS REACTIVATION IN MULTIPLE SCLEROSIS PATIENTS ON NATALIZUMAB TREATMENT

M. Iannetta[1], M.A. Zingaropoli[2], A. Bellizzi[2], E. Anzivino[2], A. D'Abramo[2], A. Oliva[2], M. Morreale[3], S. Pontecorvo[3], S. Lo Menzo[2], V. Pietropaolo[2], A. Francia[3], C.M. Mastroianni[2], V. Vullo[2], M.R. Ciardi[2]
[1]Infection Immunité Inflammation, INSERM U1016, Paris, France
[2]Public Health and Infectious Diseases Policlinico U mberto I, Sapienza, Roma, Italy
[3]Neurology, Sapienza, Roma, Italy

Objectives

The treatment of relapsing-remitting multiple sclerosis (RRMS) with natalizumab, anti-CD49d monoclonal antibody[1], raises the risk of JC virus (JCV) reactivation and the development of progressive multifocal leukoencephalopathy (PML)[2]. Aim of the study was to identify immunophenotypic markers of viral activation in RRMS patients under natalizumab treatment.

Methods

Blood and urine samples were collected prior to the first administration of natalizumab and after 12 and 24 months (T0, T1, T2, respectively) in 16 RRMS patients and only at T1 and T2 in 10 additional patients. JCV-DNA and peripheral blood T lymphocyte phenotype were detected by real-time PCR and flow cytometry, respectively.

Results

We detected JCV-DNA in both blood and urine (T0: 25% and 19%, T1: 25% and 31%, T2: 31% and 25%, respectively). We observed a reduction of CD49d median fluorescence intensity (MFI) on CD4+ and CD8+ T lymphocytes and their subpopulations, with the exception of naïve cells (CD4 and CD8 central memory [CM] p≤0.0001 and p=0.0087; effector memory [EM] p=0.0388 and p=0.0002; effector [E] p=0.0003 and p=0.0001, respectively) associated with an increased levels of CD8 CM (p=0.0264), EM (p=0.007) and E (p=0.045). CD4 and CD8 immune activation was higher at T2 than T0 (p=0.014 and p=0.016, respectively). Compared with JCV negative subjects, patients with JCV-DNA positive blood and/or urine showed higher levels of CD4 immune activation (p=0.0286, T0 vs T2) and higher percentages of CD4 and CD8 EM and E (p=0.0552 and p=0.0225 at T0 vs T1; p=0.0424 and p=0.0006 T0 vs T2, respectively). Moreover, there was a positive correlation between JCV positivity and CD8 E percentage at T1 and T2

(Spearman r=0.642, p<0.001 and r=0.696, p<0.001, respectively). In multiple linear regression analysis, CD8 E was independently associated with JCV-DNA positivity in blood and/or urine (T1 p<0.001 and T2 p=0.016). The ROC analysis showed that a cut-off of 13.3% for CD8 E at T1 (specificity 83.3%, sensitivity 80%, AUC 0.82, p<0.021) and 11.9% at T2 (specificity 94%, sensitivity 80%, AUC 0.9 p<0.001) was able to predict JCV reactivation.

Conclusions

Natalizumab treatment reduces CD49d expression on T lymphocytes and impairs the migration of T cells from peripheral blood towards the central nervous system (CNS). This could reduce the immune surveillance in CNS with the possibility of JCV reactivation. The percentage of CD8 E could be an useful tool in order to identify patients with an increased risk of JCV reactivation.

References

[1]Yaldizli O, Putzki N. Natalizumab in the treatment of multiple sclerosis. Ther Adv Neurol Disord. 2009 Mar;2(2):115-28. doi: 10.1177/1756285608101861.

[2]Nali LH, Moraes L, Fink MC, Callegaro D, Romano CM, Oliveira AC. Natalizumab treatment for multiple sclerosis: updates and considerations for safer treatment in JCV positive patients. Arq Neuropsiquiatr. 2014 Dec;72(12):960-5. doi: 10.1590/0004-282X20140142. Epub 2014 Dec 2.

388
BRAIN-0377
Poster Session

Blood Brain Barrier

CEREBRAL VASCULATURE AND COGNITIVE IMPAIRMENT IN ACUTE TRYPANOSOMA CRUZI INFECTION

U. Barrie[1], B. Freeman[1], M. Desruisseaux[1], H. Tanowitz[1], F. Chen[1]

[1]Pathology, Albert Einstein College of Medicine, Bronx, USA

The brain is one of the most protected organs in the body, with an intricate blood-brain barrier (BBB) system comprised of endothelial cells, astrocyte end-feet, and pericytes, which tightly regulate the passage of substances. Certain organisms, however, including *Trypanosoma cruzi (T. cruzi)*, are able breach this selectively permeable unit, especially in children and immunocompromised individuals. Damage to the cerebral vasculature is an important feature associated with the neurological impairments in Chagas disease (CD). The vasoactive peptide, endothelin-1 (ET-1), has been shown to mediate BBB permeability, inflammation, and vascular tone, and may be important in the pathogenesis of *T. cruzi*. ET-1 has been shown to reduce the expression of angiopoietin-1 (Ang-1), an angiogenic growth factor that promotes endothelial quiescence and regulates the expression of tight junction proteins responsible for maintaining BBB stability. We postulate that ET-1 contributes to the pathogenesis of impaired neurological function during *T. cruzi* infection by disrupting BBB integrity and potentiating endothelial activation and inflammation. To test this hypothesis, C57BL/6 mice were infected with trypomastigotes of the Tulahuen strain of *T. cruzi* to induce experimental CD. Cognitive function, degree of illness, and levels of inflammatory mediators were assessed in the brains of *T. cruzi* infected mice and compared to uninfected controls. Acute CD caused an increase in parasitemia 12 days post infection, which correlated with the level of illness as determined by the rapid murine coma and behavior scale (RMCBS). Although *T. cruzi* infection resulted in decreased RMCBS scores, infection had no adverse effects on body weight or temperature. Object recognition and placement tests revealed significant impairment in the visual and spatial memory of infected mice. These cognitive deficits were associated with increased levels of the pro-inflammatory cytokine IL-1β and pro-inflammatory cell adhesion molecules, E-selectin, VCAM-1, and ICAM-1. Ang-1 has been shown to suppress the expression of E-selectin, ICAM-1 and

VCAM-1 on endothelial cells, whereas Ang-2 promotes the expression of these adhesion molecules. qRT-PCR performed on whole brain homogenates revealed elevated levels of ET-1 in the brains of *T. cruzi* infected mice as compared to uninfected controls. Increased ET-1 expression correlated with decreased Ang-1 protein, resulting in an increased ratio of Ang-2 to Ang-1. An imbalance in the angiopoietin system illustrates endothelial dysfunction, which may contribute to the neurological impairments and activated endothelium observed in experimental CD. Our data demonstrates that acute *T. cruzi* infection results in an inflamed cerebral vasculature and disruption in the angiopoietin system, which may in part be attributable to the increased levels of ET-1. Further examination of the mechanistic basis of these observations, including the roles of endothelin and angiopoietin are warranted and should provide insight into adjunctive therapy to prevent neurological complications associated with neuro-CD.

389
BRAIN-0397
Poster Session

Blood Brain Barrier

ULTRASTRUCTURAL ANALYSIS OF BLOOD-BRAIN BARRIER PERMEABILITY IN THE PERI-INFARCT CORTEX OF YOUNG ADULT AND AGED MICE

C. Brown[1], P. Reeson[1], P. Nahirney[1]
[1]Medical Science, University of Victoria, Victoria, Canada

Following ischemia and for days afterwards, the blood-brain barrier (BBB) is compromised in the peri-infarct zone, leading to secondary injury and dysfunction that can limit stroke recovery. At present there is considerable uncertainty regarding what structural changes could account for BBB breakdown, particularly in aged animals. Here we employed electron microscopy to analyze early and late changes (3 vs. 72 hours) in the BBB in young and aged mice (3-5 vs. 18 month old) subjected to photothrombotic stroke. At both time points and ages, BBB permeability was reliably accompanied by swollen endothelial cells packed with small trans/endocytotic vesicles (~60 nm in diameter) and vacuoles (>100 nm diameter). In a very small fraction of microvessel tight junctions, we observed a fluid filled space at the junction suggesting that partial, but not complete disruption can occur. Of note, ischemia in young adult mice led to an increase in pericyte area and coverage of endothelial cells, whereas in older mice, pericyte area and coverage was significantly reduced. In both age groups, the basement membrane was expanded, especially at the 3 hour mark. Peri-vascular astrocytes and their mitochondria were severely swollen (~2-3 fold increase in area) at both times points and ages. At 3 days recovery, astrocytes were replete with glycogen deposits suggesting a change in their energy metabolism and storage. Our results indicate that an upregulation of endothelial transcytosis and vacuolation, rather than a loss of endothelial tight junctions, likely mediates BBB permeability in the peri-infarct cortex. Further, our data suggest that pericyte responses to ischemia are affected by aging.

FIGURE 1: Focal ischemia in young adult mice induces endothelial swelling and upregulates transcytotic vesicles and vacuoles in the endothelium of peri-infarct capillaries. A: Electron micrograph of a capillary in the non-ischemic contralateral hemisphere. Endothelium is lightly shaded green. Inset (**A'**) below shows relatively thin endothelial layer and intact tight junction (arrow). **B-C**: Representative capillaries in peri-infarct cortex 3 and 72 h after stroke. **B'-C'':** insets show the swollen endothelium that often contained vacuoles and was packed with vesicles (arrowheads) on the luminal and abluminal sides. However, tight junctions (black arrows) were generally intact at both time points.

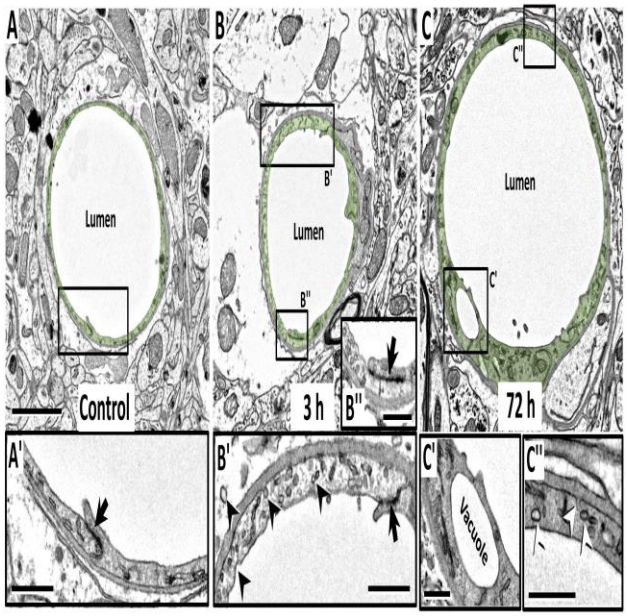

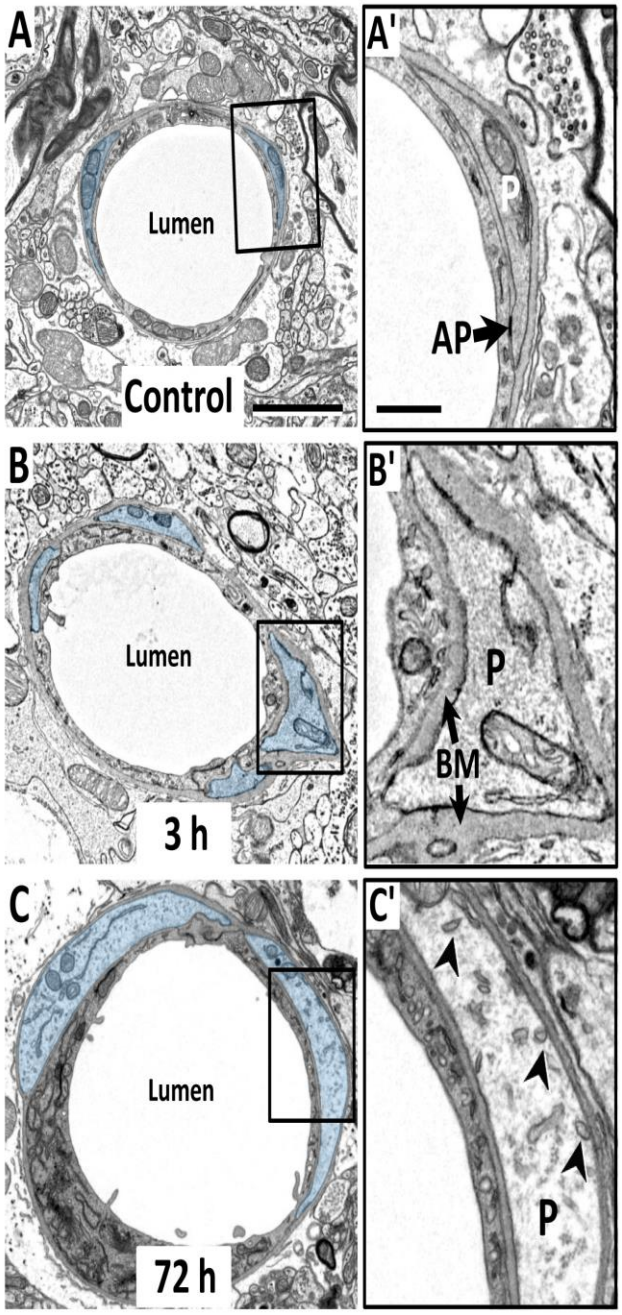

FIGURE 2: Ischemia in young adult mice leads to an increase in pericyte area, basement membrane thickness and pericyte coverage of the vascular endothelium. A: Electron micrograph of a capillary in the contralateral control hemisphere 3 hours after stroke. Pericytes are highlighted in blue. **A'**: Pericytes (P) are encapsulated with basement membrane (BM) and show typical features such as an adhesion plaque (AP). Three (**B**) and 72 (**C**) hours after stroke, the basement membrane thickens (**B'**) and pericytes appear swollen and posses vesicles (**C'**, see arrowheads). Scale bar = 2 µm for A-C. Scale bar = 0.5 µm for A'-C'.

390
BRAIN-0841
Poster Session

Blood Brain Barrier

MONOCARBOXYLIC ACID TRANSPORTER 1: REGULATION IN RAT BRAIN ENDOTHELIAL CELLS BY THE WNT/B-CATENIN PATHWAY AND CROSSTALK WITH NOTCH SIGNALING

L. Drewes[1], *Z. Liu*[2]
[1]*Biomedical Sciences, University of Minnesota Medical School Duluth, Duluth, USA*
[2]*Internal Medicine, Yale School of Medicine, New Haven, USA*

Objectives. The transport of metabolically critical monocarboxylates, such as lactate, pyruvate and β-hydroxybutyrate (BHB), across the brain microvasculature is mediated by monocarboxylic acid transporter 1 (MCT1) [1]. Thus, MCT1 is critical for brain homeostasis and energy metabolism. As a result, MCT1's regulation at blood-brain barrier (BBB) is of great significance under both physiological and pathological conditions [2-3]. Recent findings have indicated an essential role of the canonical Wnt/β-catenin signaling pathway in promoting rodent BBB development [4,5]. Further, this pathway was shown to regulate *Glut1* transcription at BBB [6]. Hence, we hypothesized that brain endothelial MCT1 is also regulated by this potent pathway.

Methods. We used an immortalized rat brain endothelial cell line (RBE4) to study how lithium chloride (LiCl), the Wnt pathway agonist, affects MCT1's expression. qPCR, western blotting, plasmid transfection, biotinylation and GST-pulldown experiments assessed MCT1's expression as well as its ubiquitination status.

Results. LiCl failed to change *Mct1* mRNA levels, but western blotting of whole cellular lysates showed that LiCl increased its protein expression by 50%. This up regulation was confirmed by a GSK-3β inhibitor (SB216763) and was dependent on nuclear β-catenin accumulation. In RBE4 cells, MCT1 protein is regulated by lysosomal but not proteasomal degradation. Accordingly, biotinylation experiment found that LiCl increased MCT1 protein expression on cell surface by 200%. This up regulation was confirmed by transfection of RBE4 cells with mCherry-*Mct1* plasmid, which showed an enhanced fluorescence intensity on the plasma membrane after LiCl treatment. Furthermore in confirmation, LiCl decreased MCT1 ubiquitination by 90%. Notch signaling is critical for vascular development and Notch inhibition by the γ-secretase inhibitor, DAPT, increased MCT1 protein level by 26% in RBE4 cells. Interestingly, the modulatory effect of LiCl on MCT1 was negated upon cotreatment with DAPT, indicating that an intact Notch signaling is indispensably involved.

Conclusions. Our data indicate that the canonical Wnt/β-catenin signaling pathway upregulates brain endothelial MCT1 expression by reducing the endosomal/lysosomal removal of this transporter from the plasma membrane. This regulatory process requires a crosstalk with Notch signaling.

References.

1. Gerhart, D.Z., et al., *Expression of monocarboxylate transporter MCT1 by brain endothelium and glia in adult and suckling rats.* Am J Physiol, 1997. **273**(1 Pt 1): p. E207-13

2. Freeman, J., et al., *The ketogenic diet: from molecular mechanisms to clinical effects.* Epilepsy Res, 2006. **68**(2): p. 145-80.

3. Frykholm, P., et al., *Relationship between cerebral blood flow and oxygen metabolism, and extracellular glucose and lactate concentrations during middle cerebral artery occlusion and reperfusion: a microdialysis and positron emission tomography study in nonhuman primates.* J Neurosurg, 2005. **102**(6): p. 1076-84.

4. Liebner, S., et al., *Wnt/beta-catenin signaling controls development of the blood-brain barrier.* J Cell Biol, 2008. **183**(3): p. 409-17.

5. Stenman, J.M., et al., *Canonical Wnt signaling regulates organ-specific assembly and differentiation of CNS vasculature.* Science, 2008. 322(5905): p. 1247-50.

6. Daneman, R., et al., *Wnt/beta-catenin signaling is required for CNS, but not non-CNS, angiogenesis.* Proc Natl Acad Sci U S A, 2009. 106(2): p. 641-6.

391
BRAIN-0630
Poster Session

Blood Brain Barrier

ASSESSMENT OF CEREBROSPINAL FLUID LEUKOTACTIN-1 (CCL-15) LEVELS AND BLOOD-BRAIN-BARRIER-PERMEABILITY IN THE CLINICAL SETTING.

J. Ivanidze[1], O. Kallas[1], M. Lerario[2], A. Segal[2], A. Gupta[3], M. Jin[1], P. Sanelli[3]
[1]Department of Diagnostic Radiology - Molecular I maging Innovations Institute, NewYork-Presbyterian Hospital - Weill Cornell Medical Colle ge, New York, USA
[2]Department of Neurology, NewYork-Presbyterian Hospital - Weill Cornell Medical Colle ge, New York, USA
[3]Department of Diagnostic Radiology, NewYork-Presbyterian Hospital - Weill Cornell Medical Colle ge, New York, USA

Objectives: Disruption of the Blood-Brain-Barrier (BBB) has been implicated in the pathophysiology of numerous conditions featuring an activated inflammatory milieu such as CNS malignancy, meningitis and autoimmune disorders, however, to date, there is limited clinical data on BBB permeability (BBBP). Recent studies demonstrated correlation of increase in BBBP with poor outcomes in patients with aneurysmal subarachnoid hemorrhage (SAH). CT Perfusion (CTP) allows assessment of quantitative parameters used to describe BBBP, including KEP, PS, Ktrans, and VE. KEP represents the washout rate constant of contrast agent from the EES (extravascular extracellular space) to the IVS (intravascular space), and is inversely related to BBBP. PS, the permeability surface area product, and represents the flow across the blood vessel wall. Ktrans equals plasma flow and VE represents EES volume per unit volume of tissue, respectively. Assessment of these parameters offers a promising technique to evaluate BBBP in the clinical setting.

On the molecular level, increase in BBBP is thought to be mediated by inflammatory chemokines. The matrix metalloproteinase MMP-9 is inducible by chemokines, and plays a key role in the opening of the BBB. Leukotactin-1 (CCL15) is known to modulate MMP-9 release from macrophages in cardiovascular disease, however, the potential role of CCL15 in BBBP modulation has not been examined to date. The objective of this study is to correlate CCL15 protein levels in cerebrospinal fluid (CSF) with BBBP measured by CTP.

Methods: SAH patients underwent CTP in the early phase after aneurysmal rupture. CTP data were post-processed into BBBP quantitative maps of PS, K-trans, KEP, and VE using Olea Sphere software (Olea Medical, La Ciotat, France). Global cortically based ROI mean values were calculated for each patient.

CSF was collected via indwelling ventriculostomy catheter (placed for intracranial pressure management) within 24 hours of CTP.

CCL15 levels were measured in CSF supernatant using multiplex microbead immunoassay technology (Luminex Corp, Austin, TX).

Results: In this preliminary study, BBBP parameters and CSF CCL15 levels were prospectively assessed in 7 patients with SAH admitted to the Neurological Intensive Care Unit at our institution. Spearman correlation analysis was performed to determine correlation between CCL15 and KEP, PS, Ktrans and VE, respectively. In the case of CCL15 and KEP, a statistically highly significant inverse correlation was found ($r = -0.96$, $p = 0.0028$). Correlation results for PS, Ktrans, and VE were not statistically significant,

however, there was a trend for positive correlation as demonstrated in Figure 1.

Conclusions: Elevated BBBP, expressed as low KEP, correlated with elevated CSF levels of CCL15 in the clinical setting in patients with SAH, indicating a pathophysiological correlate for the presumed BBBP disruption via chemokine-induced MMP-9 upregulation. This study is limited due to its proof-of-concept character and small sample size, and future studies evaluating additional chemokines, as well as MMPs, are needed to improve understanding of BBBP disruption and to thereby improve clinical outcomes.

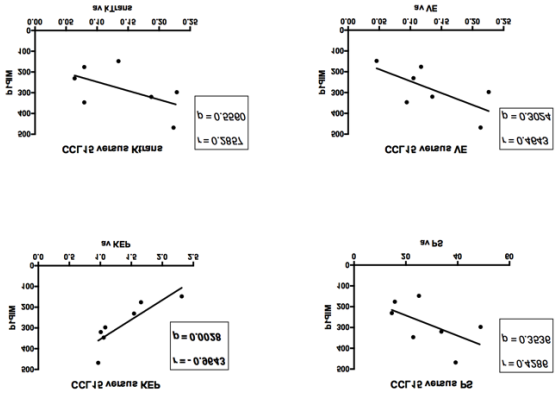

References:
1. AJNR Am J Neuroradiol. 2015 Jan 8.
2. Nutr Res Pract. 2008 Summer; 2(2): 134–137.
3. JCBFM. 1999;19:1020-1028

392
BRAIN-0672
Poster Session

Blood Brain Barrier

REGULATION OF NOD-LIKE RECEPTORS AND INFLAMMASOME ACTIVATION IN CEREBRAL ENDOTHELIAL CELLS

I.A. Krizbai[1], A. Nyúl-Tóth[1], J. Molnár[1], C. Fazakas[1], J. Haskó[1], I. Wilhelm[1], P. Nagyőszi[1]
[1]Institute of Biophysics, Biological Research Centre Szeged, Szeged, Hungary

Objectives. Cerebral endothelial cells forming the BBB (blood-brain barrier) are at the interface of the immune and the central nervous systems and thus may play an important role in the functional integration of the two systems. Here we investigated how CECs recognize and respond to pathogen- and damage-associated molecular patterns in order to regulate the functions of the neurovascular unit.

Methods. In our experiments we used an in vitro BBB model based on the culture of the hCMEC/D3 human cerebral microvascular endothelial cell line. Expression and regulation of NOD-like receptors (NLRs) was studied by endpoint and real-time PCR. Priming (induction of mRNA expression) of inflammasome components was elicited by LPS (lipopolysaccharide), while activation of inflammasomes was induced by muramyl-dipeptide (MDP). Interleukin (IL)-1β secretion was studied by Western-blot and ELISA.

Results. First we detected the expression of several NLRs – including NOD1, NOD2, NLRC4, NLRC5, NLRP1, NLRP3, NLRP5, NLRP9, NLRP10, NLRP12, NLRA and NLRX – in brain endothelial cells. Inflammatory cytokines, such as IFN-γ, TNF-α, and IL-1β had stimulatory effect on the transcription of many of these receptors. Expression of key inflammasome components (NOD2, NLRP3 and caspase-1) along with inflammasome-activated IL-1β could be induced by priming with lipopolysaccharide (LPS) and activation with muramyl dipeptide (MDP). In addition, combined treatment with LPS and MDP resulted in IL-1β secretion in a caspase- and ERK1/2 kinase-dependent manner.

Conclusions. Our findings demonstrate that NLRs and inflammasomes can be activated in cerebral endothelial cells, which may confer a yet unexplored role to the BBB in neuroimmune and neuroinflammatory processes.

Acknowledgements. I.A.K. was supported by the TÁMOP-4.1.1.C-13/1/KONV-2014-0001 project. Grants: OTKA-K-100807, HURO/1101/173/2.2.1.

393
BRAIN-0323
Poster Session

Blood Brain Barrier

METABOLIC DISRUPTION OF THE BLOOD-BRAIN BARRIER BY STRESSFUL AND NON-STRESSFUL ACTIVITIES

T. Lai[1]
[1]*Graduate Institute of Clinical Medical Science, China Medical University, Taichung, Taiwan*

Objectives - The cerebral vasculature maintains homeostasis of the brain by regulating cerebral blood flow (CBF) and maintaining the blood-brain barrier (BBB). Metabolic hyperemia, an increase in CBF to regions of increased neuronal activity, ensures that demands for nutrient supply and metabolite clearance are met. Although one might assume that a transient disruption of the BBB in conjunction with metabolic hyperemia could facilitate the exchange of nutrients and metabolites, no evidence for such a disruption has been reported.

Methods and Results - In this study, we report an activity-driven disruption of the BBB that can facilitate nutrient/metabolite exchange. Stressful activity was particularly effective in disrupting the BBB, and the disruption was only observed in brain regions specific to neuronal activity and ended immediately following termination of the activity. This phenomenon was mimicked by evoked neuronal activity and hypercapnic acidosis and was attenuated by blocking the sodium-hydrogen exchanger (NHE). Non-stressful activity, such as playing with toys, also induced minor BBB disruption that increased the penetration of small molecules but not that of plasma proteins. Consistent with increased pO_2 of cardiac output following BBB-disruptive activities, O_2 markedly potentiated hypercapnic BBB disruption and precipitated disruption of the BBB via hypoventilation.

Conclusions - Our data describe a novel mechanism through which homeostasis is maintained in the brain and show how stress

could convert minor metabolic BBB disruption into a major leakage of plasma proteins. In addition, involvement of gaseous molecules in the control of BBB integrity could provide a basis for the development of new methods to therapeutically disrupt the BBB and facilitate the central delivery of drugs.

394
BRAIN-0745
Poster Session

Blood Brain Barrier

CHARACTERISTICS OF L-CITRULLINE TRANSPORT TO THE BRAIN IN VITRO MODEL OF THE BRAIN CAPILLARY ENDOTHELIAL CELLS

K.E. Lee[1], Y.S. Kang[1]
[1]College of Pharmacy and Research Center for Cell Fate Control, Sookmyung Women's University, Seoul, Korea

Objectives Brain capillary endothelial cells play a main role of the blood-brain barrier (BBB) which restricts to transport the various substances from blood to brain. L-Citrulline is a neutral amino acid and a major precursor of L-arginine in nitric oxide (NO) cycle. As L-arginine can be recycled from L-citrulline in citrulline-NO cycle, L-citrulline plays an important role for controlling NO metabolism disorders. Therefore, we aimed to clarify the mechanism of L-citrulline transport through the blood-brain barrier (BBB).

Methods The uptake study of [^{14}C] L-citrulline was performed in the conditionally immortalized rat brain capillary endothelial cell lines (TR-BBB cells), as an *in vitro* model of the BBB. Inhibition studies in TR-BBB cells were conducted in the presence of L-amino acids and several compounds.

Results The uptake of [^{14}C] L-citrulline was a time-dependent, but sodium and chloride ions-independent in TR-BBB cells. The transport process was two saturable components with Michaelis–Menten constant of 22.0±4.0μM (K_{m1}) and 1.73 ±0.10 mM (K_{m2}) in TR-BBB cells. In functional study, the uptake of [^{14}C]L-citrulline in TR-BBB cells was inhibited significantly by various neutral amino acids and cationic amino acids such as arginine and lysine, but not by several anionic amino acids including L-glutamate and L-aspartate. In addition, [^{14}C]L-citrulline uptake in the cells was inhibited markedly by 2-aminobicyclo-(2,2,1)-heptane-2-carboxylic acid (BCH) which is the inhibitor of system L, B^0, $B^{0,+}$ and harmaline, the inhibitor of system $b^{0,+}$. However, there was no inhibition effect for L-methylmaleimide, homoarginine, and N-(methylamino) isobutyric acid (MeAIB) which are the inhibitors for system y^+L, y^+, and A, respectively. Several drugs such as L-dopa, gabapentin, verpamil, and quinidine inhibited the uptake of L-citrulline, but donepzil, dopamine, riluzole, and tacrine had no effect on [^{14}C] L-citrulline uptake in TR-BBB cells. IC50 values for L-dopa, gabapentin, L-phenylalanine and L-arginine were 501, 223, 68.9 μM and 33.4mM, respectively. In the Lineweaver–Burk plots of L-citrulline uptake for gabapentin and L-dopa as the substrates of system L in TR-BBB cells, gabapentin inhibited the uptake of [^{14}C] L-citrulline competitively, but L-dopa inhibited uncompetitively.

Conclusions Our results suggest that L-citrulline transport to the brain may be mediated by system L and $b^{0,+}$ in TR-BBB cells.

Reference 1. Citrulline: pharmacological perspectives and its role as an emerging biomarker in future, Kaore SN et al., *Fundam Clin Pharmacol,* 2013, 27(1):35-50
2. Transport Characteristics of L-Citrulline in Renal Apical Membrane of Proximal Tubular Cells. Keisuke Mitsuoka et al., *Biopharm. Drug Dispos*, 2009, 30: 126–137

395
BRAIN-0101
Poster Session

Blood Brain Barrier

REGULATORY T CELL TRANSPLANTATION ATTENUATES HEMORRHAGE TRANSFORMATION IN STROKE MICE AFTER THROMBOLYTIC TREATMENT WITH TISSUE RECOMBINANT PLASMINOGEN ACTIVATOR

P. Li[1], L. Mao[2], Y. Gao[1], W. Yu[3], L. Han[2], X. Hu[4], J. Chen[4]
[1]State Key Laboratory of Medical Neurobiology an d Institute of Brain Sciences, Fudan University, Shanghai, China
[2]Department of Neurology and Key Laboratory of Cerebral Microcirculation, University of Shandong Affiliated Hospital of Taish an Medical College, Taian, China
[3]Dept of Anesthesiology, Shanghai Jiaotong University School of Medicine, Shanghai, China
[4]Center of Cerebrovascular Disease Research, University of Pittsburgh School of Medicine, Pittsburgh, USA

OBJECTIVES: Thrombolytic treatment with recombinant tissue plasminogen activator (rtPA) is the only effective treatment for ischemic stroke. However, rtPA associated hemorrhagic transformation (HT) may deteriorate neurological outcomes and lead to lethal consequences. Blood brain barrier (BBB) damage is an important mechanism underlying HT in rtPA-treated stroke. Therefore, therapeutic strategies that fortify the BBB may reduce the incidence of HT and enhance the efficacy and safety of tPA treatment. Based on our recent study which indicated that adoptive transfer of regulatory T cells (Tregs) could afford protection against BBB disruption, we hypothesize that Tregs' transfer could dramatically ameliorate the risk of HT in tPA-treated stroke mice.

METHODS: Cerebral ischemia was induced by 60 min middle cerebral artery occlusion (MCAO). rtPA (10mg/kg) was infused into the femoral vein at 2h after MCAO. Tregs (2×10^6/mouse in 200ml PBS) were isolated from donor animals and transferred to ischemic recipients through femoral vein immediately after rtPA. Control stroke mice received the same volume of PBS after tPA. Cerebral hemorrhage was quantified by spectrophotometric hemoglobin assay of brain homogenates. BBB permeability and structure disruption was quantified at 24h after MCAO. Brain infarction and neurological performance was assessed up to 21 days post-stroke. MMP-9 knockout mice were used to elucidate the underlying mechanism of Tregs' protection.

RESULTS: Administration of Tregs dramatically reduced the rtPA-induced HT in stroke mice as measured by hemoglobin assay. Treg treatment significantly attenuated brain tissue loss at 3d and 21d in tPA-treated stroke mice. These result suggest that Treg-afforded protection against HT happens very early after ischemia and might contribute to later protection against brain tissue loss. Consistent with the reduction in brain damage, the sensorimotor deficits measured by rotarod and corner test were significantly reduced in Treg-treated as compare to PBS-treated stroke mice up to at least 15d after tPA infusion. Electron microscopy demonstrated that Treg treatment attenuated BBB ultra-structure damage. Treg treatment dramatically reduced the otherwise significantly increased Evans blue or fluorescent-labeled tracer (cadaverine) leakage in tPA-infused stroke mice. Similarly, the intracranial leakage of plasma-derived IgG after tPA was lessened in Treg-treated stroke mice as compared to PBS-treated controls. Western blot analysis of tight junction protein ZO-1, occludin and claudin showed that tPA-enhanced BBB breakdown was accompanied by the degradation of TJ proteins. Strikingly, Treg treatment significantly preserved the expression of these junctional proteins in tPA-infused stroke mice. Mechanistic studies using MMP-9 knockout mice suggested that Tregs may inhibit tPA-induced elevation of MMP-9 activity after stroke, which may at least partially contribute to its cerebral protective actions.

CONCLUSIONS: Tregs' adoptive transfer preserves BBB integrity and attenuates rtPA-induced HT in thrombolytic stroke animal model. Therefore,

Tregs adoptive transfer may serve as a novel immune cell-based therapy which has the potential to reduce the catastrophic adverse effect of tPA and extend the therapeutic window of tPA treatment following acute stroke attack.

396
BRAIN-0070
Poster Session

Blood Brain Barrier

ADENOSINE A2B RECEPTOR AGONIST INHIBITS TPA-INDUCED HEMORRHAGIC TRANSFORMATION AFTER CEREBRAL ISCHEMIA

Q. Li[1], C. Chang[2], X. Han[2], X. Lan[2], X. Hong[3], R. Koehler[2], J. Zhou[3], Y. Zhai[1], J. Wang[2]
[1]Shanghai Ninth People's Hospital, Shanghai Jiao Tong University School of Medicine, Shanghai, China
[2]Anesthesiology and Critical Care Medicine, Johns Hpkins University School of Medicine, Baltimore, USA
[3]Division of MR Research Department of Radiology , Johns Hpkins University School of Medicine, Baltimore, USA

Background and Purpose: Tissue plasminogen activator (tPA) is administered after ischemic stroke to dissolve intravascular clots, but its use can lead to hemorrhagic transformation (HT). Therefore, identification of a drug that could be administered with tPA to reduce the risk of hemorrhage would be beneficial. The aim of this study was to explore whether adenosine A2b receptor agonists reduce hemorrhage risk after tPA usage.

Methods: Rats underwent 2 hours of middle cerebral artery occlusion and were administered intravenous tPA with or without BAY 60-6583 before reperfusion. At 24 hours after reperfusion, we measured adenosine receptor (A1, A2a, A2b, and A3) mRNA and protein level; assessed blood-brain barrier (BBB) permeability, brain swelling, brain hemoglobin content, and sensorimotor function; and evaluated the expression of tight junction proteins and matrix metalloproteinase-9 (MMP-9) activity.

Results: The increase in A2bR mRNA and protein was greater than that of the other three receptors after ischemia/reperfusion. tPA administration caused a marked reduction in A2bR expression in the ischemic brain and caused an increase in HT, brain swelling, BBB permeability, MMP-9 activity, and degradation of zonula occludens-1 and claudin-5. Combining BAY 60-6583 administration with tPA significantly attenuated these negative effects of tPA. Furthermore, this combined treatment significantly reduced infarct volume and improved sensorimotor function.

Conclusions: Use of A2b receptor agonists as adjuvants to tPA could be a promising strategy for decreasing the risk of HT during treatment for ischemic stroke.

397
BRAIN-0155
Poster Session

Blood Brain Barrier

IDENTIFICATION OF NEW BLOOD-BRAIN BARRIER TRANSPORTERS AND RECEPTORS BY NEXT GENERATION RNA SEQUENCING

Q. Liu[1], S. Leclerc[1], D. Ly[1], J. Lei[1], E. Baumann[1], H. Haqqani[1], D. Stanimirovic[1]
[1]Human Health and Therapeutics, National Research Council, Ottawa, Canada

Effective treatment of diseases of the central nervous system is often hindered by poor penetration of therapeutic molecules across the blood-brain barrier (BBB). The therapeutic delivery across the BBB is regulated by various classes of transporters including efflux pumps as well as by receptor-mediated transcytosis. However, the full complement (molecular map) of these transporters in the human BBB is still unknown. To facilitate selection of therapeutics with improved BBB-crossing properties, the NRC-HHT has created a map of genes and proteins expressed in BBB endothelial cells and vessels from various species, including human, called 'BBB Carta' [1, 2].

Objective:

The overall objective of this sub-project called 'BBB Selective Carta' was to identify brain vessel-specific/enriched transmembrane proteins that are amenable for targeting to improve delivery of CNS therapeutics.

Methods:

Next Generation RNA-sequencing (RNA-Seq) was performed on RNA derived from rat brain, lung and liver (micro) vessels (approved by Institutional Animal Care and Use Committee), as well as from human brain (micro) vessels. RNA-Seq data was analyzed using Galaxy (useGalaxy.org) and brain vessel enriched transcripts were selected by comparing vessel transcript reads from rat brain with those of lung and liver. Human brain vessel enriched transcripts were obtained by comparing RNA–seq data from post mortem brain vessel, brain cortex total and lung total RNA (approved by Institutional Review Board with signed written informed consent).

Results:

We found 557 transcripts that are 10-fold enriched in the rat brain (micro) vessels compared to those in lung and liver. Among them, there were 28 receptors, 46 transporters and 148 various membrane proteins. Human brain vessel enriched transcripts were obtained by indirect comparison of brain vessel RNA with those of total brain and total lung RNA. This comparison yielded 92 specific transcripts, of which 28 represented membrane transporter proteins and receptors.

Conclusions:

NRC-HHT has developed a comprehensive molecular map of the blood-brain barrier (BBB Carta) that consists of a collection of 'omics' datasets of brain endothelial cells, BBB vessels, and BBB cell-cell interactions. The 'BBB Selective Carta' described here catalogues genes selectively expressed or enriched in brain vessels compared to peripheral vessels and tissues in rat and human. BBB-enriched transmembrane proteins are source of targets for development of drug-delivery carriers, particularly antibodies, with reduced 'off-target' effects and toxicity and better pharmacokinetic profiles, compared to currently used targets such are transferrin receptor [3] and insulin receptor [4].

References:

[1]. Badhwar A, Stanimirovic DB, Hamel E, Haqqani AS. *J Cereb Blood Flow Metab*. 2014, 34(6):1033-46.

[2]. Haqqani AS, Stanimirovic DB. *Cardiovasc Psychiatry Neurol*. 2011;175364.

Soria JC, Massard C, Lazar V et al. *Eur J Cancer. 2013, 49(8):1799-807.*

[3]. Ohshima-Hosoyama S, Simmons HA, Goecks N et al., *PLoS ONE 2012 7(6)*

[4]. Couch JA, Yu YJ, Zhang Y et al. *Sci Transl Med. 2013 1;5(183).*

398
BRAIN-0537
Poster Session

Blood Brain Barrier

IMAGING BLOOD-BRAIN BARRIER DYSFUNCTION AS A BIOMARKER FOR TRAUMATIC BRAIN INJURY

D.Z. Milikovsky[1], D. Rosenbach[1], I. Weissberg[1], N. Elazari[2], S. Lublinsky[1], L. Kamintsky[1], A. Friedman[3]
[1]Department of Physiology and Cell Biology and Zl otowski Center for Neuroscience, Ben Gurion University of the Negev, Beer-Sheva, Israel
[2]Department of Cognitive and Brain Sciences and Zlotowski Center for Neuroscience, Ben Gurion University of the Negev, Beer-Sheva, Israel
[3]Department of Medical Neuroscience Dalhousie University Halifax Nova Scotia Canada and Depart

ment of Physiology and Cell Biology and Departme nt of Cognitive and Brain Sciences and Zlotowski C enter for Neuroscience,
Ben Gurion University of the Negev, Beer-Sheva, Israel

Objectives: 1) To establish imaging protocols for the quantification of blood-brain barrier integrity after repeated mild traumatic brain injury (rmTBI) in rats; 2) To explore short- and long-term sequelae following rmTBI in rats, specifically, inflammation and neurodegeneration and to what extent these are correlated with BBB damage.

Methods: We are using a weight drop model of rmTBI in adolescent rats (method modeified according to the Wayne state model, Kane et al. 2012): Briefly, anesthetized rats undergo mTBI by a custom-built apparatus consisting of a directed weight falling vertically on the head once a day for 7 consecutive days. mTBI was defined such that most animals (>90%) do not demonstrate any neurological (Neurological severity score, Shapira et al. 1994) or radiological (standard magnetic resonance imaging (MRI)) sign of TBI 24 h after the first trauma. BBB permeability is evaluated quantitatively from T1-weighted (T1w) spin echo standard sequence, performed before and after the injection of gadolinium (Gd-DTPA). For each voxel, the percent difference between pre and post images is calculated. Brain voxel is considered as pathologically enhanced if its enhancement value is greater than mean minus 1 standard deviation of the BBB-deprived temporal muscle. Scans were performed before, 24, 48, 72 hrs, 1 week and 1 month after the first impact. Electrocorticographic (ECoG) recordings were performed using cortical electrodes and a wireless transmitter (Data Science International). Animals were recorded 5, 9 and 13 weeks after the first impact.

Results: We demonstrate a gradual increase in BBB breakdown during the week of consecutive impacts, and remarkably, additional increase in the number of disrupted voxels one month later, suggesting a progressive process. Analysis of ECoG recordings detected paroxysmal to long-lasting episodes of abnormal brain activity, characterized by high delta (1-3Hz) band and lower alpha (8-12Hz) compared with control. Importantly, animals with increased BBB pathology after one month demonstrated aggravated abnormality in later ECoG recordings.

Conclusions: Our results point to BBB imaging as a potential approach for the identification of a progressive neural damage and predicting neuroal dysfunction.

399
BRAIN-0157
Poster Session

Blood Brain Barrier

RELEVANCE OF THE LITHIUM-PILOCARPINE RAT MODEL FOR THE STUDY OF P-GLYCOPROTEIN OVEREXPRESSION DURING PHARMACORESISTANT EPILEPSY

S. Marie[1], G. Pottier[1], F. Caillé[1], S. Goutal[1], R. Boisgard[1], F. Dollé[1], S. Stute[1], B. Hosten[1], A. Jacob[1], N. Tournier[1]
[1]IMIV UMR 1023 Inserm/CEA/Université Paris Sud - ERL 9218 CNRS, CEA/DSV/I2BM/SHFJ, Orsay, France

OBJECTIVES: A third of patients with epilepsy do not respond to antiepileptic drugs (AED). One potential mechanism proposed for pharmacoresistance in epilepsy is overactivity of efflux transporters such as the P-glycoprotein (P-gp) at the blood–brain barrier (BBB). This would prevent drugs from reaching therapeutic concentrations at their targets. Several AED are moderate P-gp substrates and it was reported increased P-gp expression and activity at the BBB of patients with pharmacoresistant epilepsy. Therefore, an animal model would be useful to study the regulation of P-gp overexpression at the BBB and its impact on the neuropharmacokinetics of its substrates. The lithium-pilocarpine rat model was described as pharmacoresistant with significant increase of P-gp expression in the brain, using immunohistochemistry analysis[1]. [^{11}C]Metoclopramide is a new PET radiotracer

developed to detect P-gp overexpression, because it is a moderate P-gp substrate with significant baseline brain uptake.

METHODS: Epilepsy was triggered in lithium-pretreated Wistar rats (127 mg/kg IP) by repeated pilocarpine injections (10 mg/kg, IP) until onset of generalized epilepsy. [^{11}C]Metoclopramide microPET imaging was performed (37 MBq IV; 30 min scan, Siemens Inveon) in control (n = 5), P-gp inhibited (n = 4, using tariquidar 8 mg/kg IV, 5 min before tracer injection) and epileptic rats (n = 5, 48 h after epilepsy). Time-activity curves (TAC) obtained in the brain and lungs were compared. Brains of control and epileptic rats were taken out after PET. A validated capillary extraction method from brain cortex samples was performed to isolate brain microvessels forming the BBB. P-gp expression was quantified using Western-Blot analysis (C219 antibody)[2].

RESULTS: PET imaging confirmed [^{11}C]metoclopramide as a P-gp substrate at the BBB. The brain penetration was higher in tariquidar-treated rats ($AUC_{0\text{-}30min}$ = 25.6±4.5 SUV.min) compared to controls ($AUC_{0\text{-}30min}$ = 7.7±0.9 SUV.min). Surprisingly, the brain uptake of [^{11}C]metoclopramide was also higher in epileptic rats ($AUC_{0\text{-}30min}$ = 9.6±1.5 SUV.min). TACs measured in the lungs were similar in control ($AUC_{0\text{-}30min}$ = 23.6±3.4 SUV.min), tariquidar ($AUC_{0\text{-}30min}$ = 22.3±2.2 SUV.min) and epileptic rats ($AUC_{0\text{-}30min}$ = 23.7±3.4 SUV.min), suggesting limited impact of tested conditions on [^{11}C]metoclopramide peripheral kinetics. P-gp expression at the BBB was not significantly different between control (ratio P-gp/actine = 0.13±0.02) and epileptic rats (ratio P-gp/actine = 0.14±0.081).

CONCLUSIONS: [^{11}C]metoclopramide brain kinetics is efficiently influenced by P-gp function at the BBB. We found no significant overexpression of P-gp at the BBB of lithium-pilocarpine rats, suggesting that P-gp is not involved in the pharmacoresistant profile of this model. The brain exposure of [^{11}C]metoclopramide was increased, suggesting enhanced BBB permeation of small molecules, despite P-gp substrate properties.

1. A novel positron emission tomography imaging protocol identifies seizure-induced regional overactivity of P-glycoprotein at the blood-brain barrier, Bankstahl and al, J Neurosci 2011.
2. Induction of P-glycoprotein and Bcrp at the rat blood-brain barrier following a subchronic morphine treatment is mediated through NMDA/COX-2 activation, Yousif and al, J Neurochem 2012.

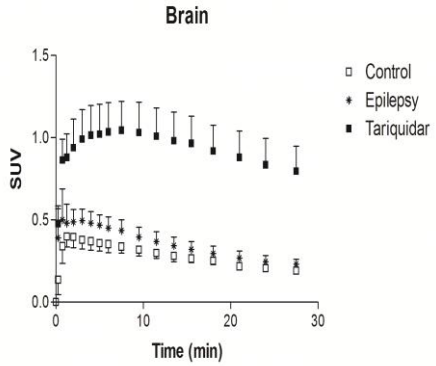

400
BRAIN-0217
Poster Session

Blood Brain Barrier

INTOXICATION OF ENGINEERED NANOPARTICLES IN COLD ENVIRONMENT EXACERBATES ISCHEMIA AND BRAIN PATHOLOGY FOLLOWING TRAUMA

A. Sharma[1], D. Muresanu[2], J. Lafuente[3], R. Patnaik[4], H. Moessler[5], Z. Tian[6], A. Ozkizilcik[6], H. Sharma[7]
[1]Surgical Sciences Anesethesiology & Intensive Car e Medicine, Uppsala University Hospital, Uppsala, Sweden
[2]Clinical Neurosciences, University of Medicine & Pharmacy, Cluj-Napoca, Romania
[3]Neurosciences, University of Basque Country, Bilbao, Spain
[4]Biomedical Engineering, Banaras Hindu University IIT, Varanasi UP, India
[5]drug Development & Discovery, Ever Neuro Pharma, Oberburgau, Austria
[6]Chemistry & Biochemistry, University of Arkansas Faytteville, Faytteville, USA
[7]Surgical Sciences Anesthesiology & Intensive Care

Medicine, University Hospital Uppsala University, Uppsala, Sweden

Military personnel often engaged in peace keeping or combat operation have to work in very cold environment across the Globe. When these soldiers are inflicted with brain or spinal cord injury, their pathological outcome may be more severe in cold environment as compared to room temperature. In addition, these soldiers also are exposed to a variety of nanoparticles (NPs) emanating from the environment or following missile or gunpowder explosions. Thus, a combination of NPs and cold environment may alter the course of brain pathology and affect therapeutic potentials of drugs.

In present investigation we examined the influence of cold environment with or without NPs intoxication on the pathophysiology of blood-brain barrier (BBB), brain edema and cellular injuries in a well-controlled brain trauma model.

Male Wistar rats were (age 10-12 weeks) exposed to cold chamber maintained at 4°C for 2 h daily for 8 weeks. Traumatic brain injury similar to piercing object in the brain was produced by a focal incision of the right parietal cerebral cortex (3 mm deep and 5 mm long) after opening a burr hole into the skull in both cold reared and rats placed at controlled room temperature (21°C). In separate group of rats Ag, or Cu NPs (50-60 nm; 50 mg/kg, i.p.) was administered daily for 1 week and exposed either cold environment or kept at room temperature for 8 weeks. These NPs intoxicated animals were also traumatized in identical manner. In these groups of rats, regional cerebral blood flow (rCBF) was measured using microspheres technique. Also, the BBB, brain edema formation and neuronal injuries were examined. To study the drug effects on neuroprotection identical group of rats were treated with cerebrolysin, a multimodal drug either alone or tagged with TiO2 nanowires after 2 and 4 h of brain injury. The animals were allowed to survive 24 or 48 h after trauma.

Our observations show that identical trauma to the brain resulted in aggravation of regional ischemia, breakdown of the BBB, edema formation and cell injuries in animals exposed to cold environment as compared to the group placed at room temperature. In addition, NPs intoxicated group showed additional deterioration of cerebrla circulation and brain pathology in combination with cold exposure as compared to animals placed normal room temperature. These pathological effects were progressive in nature. Treatment with cerebrolysin (2.5 or 5 ml/kg, i.v.) significantly reduced trauma-induced pathology and enhanced cerebral circulation in normal animals kept at room temperature if given after 4 h of insult. On the other hand higher doses of cerebrolysin (7.5 ml or 10 ml/kg) is needed to induce neuroprotection in rats that were exposed to cold environment before injury. In case of NPs exposure in cold environment TiO2 nanowired delivery of cerebrolysin is needed to achieve comparable neuroprotection. These observations are the first to show that cold environment with NPs exposure exacerbates brain pathology after trauma and in such situations, nanodelivery of neuroprotective drugs e.g., cerebrolysin is needed for effective therapy.

401
BRAIN-0351
Poster Session

Blood Brain Barrier

ASTROCYTE-DERIVED PENTRAXIN 3 SUPPORTS BLOOD-BRAIN BARRIER INTEGRITY

A. Shindo[1], T. Maki[1], E.T. Mandeville[1], K. Itoh[1], A.C. Ling[1], N. Itoh[1], M. Borlongan[1], J.C. Holder[2], T.T. Chuang[2], J.D. McNeish[2], H. Tomimoto[3], J. Lok[4], E.H. Lo[1], K.E.N. Arai[1]
[1]Neuroprotection Research Laboratory Departments of Radiology and Neurology, Massachusetts General Hospital and Harvard Medical School, Charlestown, USA
[2]Department of Vascular Biology, GlaxoSmithKline, Harlow, United Kingdom
[3]Department of Neurology, Mie University Graduate School of Medicine, Tsu, Japan

[4]*Department of Pediatrics,*
Massachusetts General Hospital and Harvard Med ical School, Charlestown, USA

Objectives: Pentraxin 3 (PTX3) is a prototypic long pentraxin and is associated with inflammation. PTX3 can be a biomarker for cardiovascular diseases in the clinic. However, the role of PTX3 in brain is mostly unknown. Since expression level of PTX3 increases after ischemic injury in brain, we asked (i) what cell type(s) increase PTX3 after brain injury, and (ii) whether PTX3 upregulation would be protective for damaged brain.

Methods: In vivo, 2-3 month old male spontaneous hypertensive rats were subjected to focal cerebral ischemia by transient (70 min) middle cerebral artery occlusion. At day 3, rats were sacrificed and brains were analyzed to evaluate PTX3 expression by immunohistochemistry. Blood-brain barrier (BBB) breakdown was assessed by IgG staining. In vitro, rat primary astrocytes and rat brain endothelial RBE.4 cells were cultured separately. Conditioned media from astrocytes (Astro-CM) were prepared, and PTX3 in Astro-CM was removed by filtering with anti-PTX3 antibody. Then, control Astro-CM or PTX3-removed Astro-CM (Astro-CM_{PTX3-}) were added to RBE.4 cells. After 24 hours, RBE.4 cells were used for in vitro cell permeability assay using trans-wells (i.e. in vitro BBB assay) and for immunostaining/western-blots for assessing tight junction protein expression.

Results: PTX3 was expressed under normal conditions, but after ischemic stroke, PTX3 expression dramatically increased in peri-infract area. Double-staining of PTX3 with cell-marker antibodies (endothelium: lectin, astrocyte: GFAP, neuron: NeuN, oligodendrocyte: GST-pi, oligodendrocyte precursor cell: PDGF-R-alpha) showed that the majority of PTX3-positive cells was merged with GFAP-positive astrocytes. Notably, in the peri-infarct area, there was negative correlation between IgG leakage and PTX3 expression, indicating that astrocyte-derived PTX3 may protect the BBB integrity after stroke. Under cell culture conditions, rat astrocytes also expressed and secreted PTX3 into culture media. When brain endothelial RBE.4 cells were treated with Astro-CM, their permeability was significantly decreased. On the other hand, Astro-CM_{PTX3-} did not enhance the in vitro endothelial permeability, suggesting that astrocytic PTX3 support BBB integrity. Correspondingly, Astro-CM increased the expression level of zonula occludens-1, an important accessory protein for tight junction integrity, in RBE.4 cells, but Astro-CM_{PTX3-} did not.

Conclusions: Taken together, astrocytes in the peri-infarct area tend to produce/secrete PTX3 after ischemic stroke, which may support BBB integrity. Astrocytes are located closely to cerebral endothelial cells, and BBB dysfunction is a major clinical problem in stroke. Therefore, this astrocytic response would be a compensatory mechanism, and therefore, astrocytic-PTX3 may be an effective therapeutic target for stroke.

402
BRAIN-0265
Poster Session

Blood Brain Barrier

BLOOD-BRAIN BARRIER DYSFUNCTION CAUSED BY VASCULAR ENDOTHELIAL GROWTH FACTOR UPREGULATION IN RAT MODELS OF SUBACUTE METHYLMERCURY INTOXICATION

T. Takahashi[1], *M. Fujimura*[2], *F. Usuki*[3], *M. Koyama*[1], *M. Kanazawa*[1], *M. Nishizawa*[1], *T. Shimohata*[1]
[1]*Neurology,*
Brain Research Institute Niigata University, Niigata, Japan
[2]*Basic Medical Sciences,*
National Institute for Minamata Disease, Kumamoto, Japan
[3]*Clinical Medicine,*
National Institute for Minamata Disease, Kumamoto, Japan

Objectives:Methylmercury (MeHg) intoxication has been implicated in Hunter-Russell syndrome (Minamata disease), the clinical manifestations of which include cerebellar ataxia, concentric constriction of the visual fields, and sensory and

auditory disturbances. The pathogenesis of MeHg intoxication, especially the mechanism of its selective neuronal degeneration, remains unclear. In human brain autopsy specimens after MeHg exposure, petechial hemorrhage and edema are seen in the cerebellum[1], where intense neuronal cell death occurs, suggesting that blood-brain barrier (BBB) injury may play a role in the neuronal degeneration induced by MeHg. Furthermore, vascular endothelial growth factor (VEGF), which has been shown to decrease the BBB barrier function, is upregulated after MeHg exposure in vitro[2]. Accordingly, the objective of this study was to assess the BBB function and VEGF expression after subacute intoxication of MeHg in vivo.

Methods:Six-week-old male Wister rats were divided into 5 groups: sham and 1/2/3/4-week MeHg exposure groups. The rats were exposed to water or 20 ppm MeHg water, and their brain tissue was harvested after 4 weeks. The brain was separated into the cerebellum and three cerebral portions (frontal, central, and occipital). The BBB function was assessed by endogenous IgG extravasation and RECA1 expression using immunohistochemistry, and the expressions and distributions of VEGF, RECA1, and GFAP were also examined. A VEGF neutralizing antibody was administered to the 4-week MeHg exposure group to assess the effect of blocking the VEGF upregulation after MeHg exposure. The MeHg content in each portion of the brain, body weight changes, and motor functional scale by the hind limb crossing sign were also assessed.

Results: Extravasation of endogenous IgG, characterized by positive immunostaining outside the vessels of the cerebellum, was observed only in the rats exposed to MeHg for 4 weeks. The RECA1 expression was decreased in the MeHg-exposed group compared to that in the control group. In the MeHg-exposed group, increased expression of VEGF was observed, and this VEGF expression was mainly seen in the GFAP-positive cells. There were no differences in MeHg content among the different parts of the brain in all groups. Longer MeHg exposure tended to be associated with lower motor functional scores, and this deterioration was partially recovered by the administration of the VEGF neutralizing antibody.

Conclusions: BBB dysfunction was observed in a rat MeHg intoxication model. Increased expression of VEGF was detected in the cerebellum, which is an area that shows severe neuronal injury. This upregulation was observed mainly in astrocytes, which are one of the BBB components. BBB injury via VEGF upregulation may represent an important mechanism of progression of neuronal degeneration by MeHg, and our data suggest that VEGF blocking therapy may be promising for this condition.

References

1.Eto K, Takizawa Y, Akagi H, et al (1999). Differential diagnosis between organic and inorganic mercury poisoning in human cases--the pathologic point of view. Toxicol Pathol 27:664–71.

2.Hirooka T, Yamamoto C, Yasutake A, et al (2013). Expression of VEGF-related proteins in cultured human brain microvascular endothelial cells and pericytes after exposure to methylmercury. J Toxicol Sci 38:837–45.

403
BRAIN-0189
Poster Session

Blood Brain Barrier

PHOSPHORYLATED HSP27 ATTENUATE BLOOD-BRAIN BARRIER BREAKDOWN IN STROKE RECEIVING INTRAVENOUS TISSUE-PLASMINOGEN ACTIVATOR

R. Tanaka[1], Y. Shimada[1], H. Shimura[2], K. Yamashiro[1], M. Koike[3], Y. Uchiyama[3], T. Urabe[2], N. Hattori[1]
[1]Neurology, Juntendo University School of Medicine, Tokyo, Japan
[2]Neurology, Juntendo University Urayasu Hospital, Chiba, Japan
[3]Cell biology and Neuroscience, Juntendo University School of Medicine, Tokyo, Japan

Objects

Heat shock protein 27 (HSP27), belongs to a subfamily of small HSPs, playan important role in regulating oxidative stress or inhibiting apoptosis that resultin neuroprotection. We have demonstrated that intravenously injected phosphorylated HSP27 (pHSP27), but not non phosphorylated form, resulted insignificant reduction of infarct volume and improved functional recovery in modelsof acute ischemic stroke. We also demonstrated that administration of pHSP27 reduced oxidative stress and apoptotic cell death after focal cerebral ischemia. However, the effects of pHSP27 for blood brain barrier (BBB) breakdown in focal ischemia remains unclear. Thus we investigated the effects of pHSP27 for BBB protection in stroke model receiving intravenous tissue-plasminogen activator.

Methods

Adults,10-week-old, male C57BL/6 mice weighing 20–25g were used in this study. Mice were subjected to transient 1-h middle cerebral artery occlusion (MCAO) followed by reperfusion . D-glucose (6ml/kg at 50% wt/vol) was injected intraperitoneally 15min before MCAO to enhance the hemorrhagic transformation. After 2 hours of reperfusion, the mice were treated by four treatment regimens, 1) tPA treatment (10mg/kg), 2) tPA (10mg/kg) and prHSP27 (50µg/mice), 3) pHSP27 (50µg/mice), and 4) Bovine serum albumin (BSA 50µg/mice). Twenty-four hours after reperfusion, infarct volume, brain swelling, neurological deficit and severity score, IgG leakage,hemorrhagic transformation were evaluated. We also confirmed the expression of matrix metalloproteinase-9 (MMP-9), tight junctionprotein (type 4 collagen), microglial activation (iba-1), and analysis of cytoarchtecture by electron microscopy in each groups. All mice procedures were approved by the Animal Care Committee of the Juntendo University.

Results

Infarct volume of pHSP27 and tPA+pHSP27group were significantly attenuated compared to BSA group. Hemorrhagic transformation was also significantly reduced in tPA+pHSP27 group compared totPA group ($p<0.05$). We found the leakage of immunostained IgG was significantly reduced in tPA+pHSP27 and pHSP27 groups compared to tPA group.Zeratin-zymography demonstrated a significant attenuation of MMP-9 expression in tPA+pHSP27 group than tPA group ($p<0.05$). The expression of type IV collagen was significantly preserved in tPA+pHSP27 group than tPA group ($p=0.016$) and microglial activation (iba-1) was also attenuated in tPA+pHSP27group than tPA group ($p<0.001$). Finally, the analysis by electron microscopy showed the basement membrane was become thin, and obviously degraded by the tPA treatment. In contrast, prHSP27 treatment inhibited both the basement-membrane degradation and the detachment of astrocyte endfeet.

Conclusions

Our data demonstrate tPA treatment enhances the hemorrhagic transformation with BBB breakdown in focal cerebral ischemia.Treatment by intravenous infusion of phosphorylated HSP27 attenuated the hemorrhagic transformation and brain infarct volume accompanied with improvement of neurological deficit. PHSP27 treatment was also associated with reduced MMP-9 expression that resulted in attenuation of BBB breakdown. These data indicate that pHSP27 is useful treatment for thrombolytic therapy to reduce the hemorrhagic complication and may prolong the therapeutic time window in acute ischemic stroke.

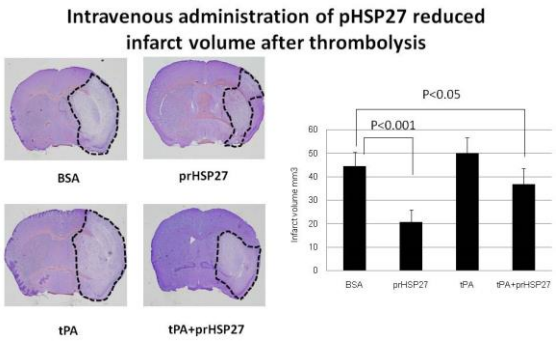

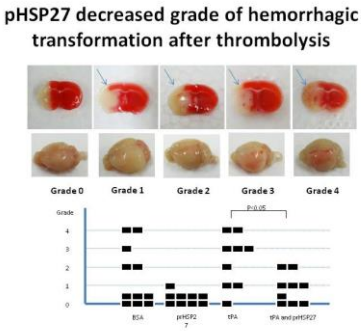

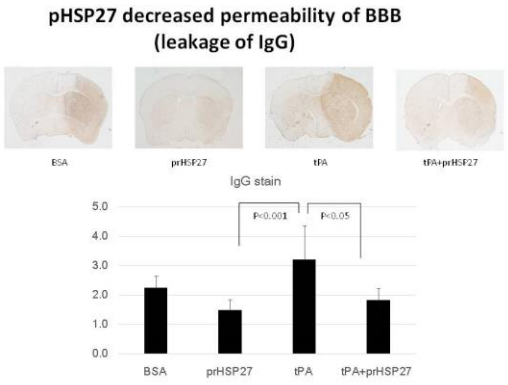

404
BRAIN-0078
Poster Session

Blood Brain Barrier

A PEPTIDE DERIVED FROM TRANSCEND (MTF, P97) IS VERY EFFICIENT IN THE DELIVERY OF BIOLOGICS TO THE CNS USING A PHYSIOLOGIC PATHWAY.

R. GABATHULER[1], L. Ho[1], M.M. Tian[1], R. Hutchison[1], W.A. Jefferies[2]
[1]Research & Development, biOasis Technologies Inc., Richmond, Canada
[2]Michael Smith Laboratories, University of British Columbia, Vancouver, Canada

biOasis Technologies Inc. is a ground-breaking biopharmaceutical company focused on the delivery of therapeutics across the blood-brain barrier and into the brain tissue. The Company is developing proprietary peptide vectors based on Melanotransferrin for the delivery of therapeutics to the CNS, this platform is called 'Transcend".

The delivery of therapeutics across the blood-brain barrier (BBB), represents the single greatest challenge in the treatment of common and rare diseases of the central nervous system. The BBB is formed by brain capillary endothelial cells, which are closely sealed by tight junctions and express high levels of active efflux transport proteins. Specific receptors and transport systems are highly expressed at the BBB to provide essential substances to brain cells. These important characteristics provide a natural defense against toxic circulating in the blood. The development of new technology to cross the BBB for brain parenchyma uptake is of great interest and vital importance for the treatments of neurological disorders and genetic diseases. A family of vectors called Transcend, comprising the full-length protein (Melanotransferrin or MTf) and peptides thereof, have been developed by biOasis Technologies Inc. and are used to facilitate receptor mediated drug delivery into the brain to treat CNS disorders.
Using antibodies and lysosomal enzymes labeled with fluorescent dyes we demonstrated that: antibodies against Her2 (Traztuzumab, TZM);

against ßA$_{1-42}$ peptides (6E10); lysosomal enzymes such as a-L-iduronidase (IDU) or iduronate-2-sulfatase (I2S), are transported at therapeutical concentration across the BBB in brain cells after conjugation to Transcend. Transcend conjugates are rapidly and efficiently transported in the brain parenchyma and in the lysosomal compartment of neurons and astrocytes.
Using laser scanning confocal microscopy, an increase of approximately 10 times of the distribution of BT2111 in the brain parenchyma compared to TZM was observed 2 hr post-IV injection. Therapeutical efficacy was demonstrated in a mice model characterized by the formation of brain metastasis after intracardiac administration of MDA-MB 231BR. It was found that BT2111 reduced the number of human HER2+ breast cancer metastases in the brain by 68% when compared to control animals. The tumours that remained after treatment were 57% smaller than those in controls, equating to an overall 86% reduction in tumour volume. In contrast, TZM alone had no effect.
The family of peptides that we identified from MTf have shown high transcytosis rate across an in-vitro BBB model as well as in vivo. The lead peptide has shown across the BBB and was able to increase significantly the delivery of an antibody to the CNS after its chemical incorporation or expressed in a fusion protein. The application of this new peptide vector to oligonucleotides and on-going studies addressing the brain delivery of enzymes will be discussed. These studies will provide the proof of concept that Transcend both full length MTf and its derived peptides, can be used as carriers capable of shuttling a variety of compounds ranging from small anti-cancer agent to larger biologics across the BBB into the brain parenchyma in therapeutic doses that enable treatment of neurological disorders.

405
BRAIN-0305
Poster Session

Blood Brain Barrier

MESENCHYMAL MIGRATION OF METASTATIC TUMOR CELLS THROUGH THE BRAIN ENDOTHELIUM

I. Wilhelm[1], J. Molnár[1], C. Fazakas[1], J. Haskó[1], A.G. Végh[1], A. Nyúl-Tóth[1], P. Nagyőszi[1], G. Váró[1], I.A. Krizbai[1]
[1]Institute of Biophysics, Biological Research Centre Szeged, Szeged, Hungary

Objectives:

Brain tumors are life threatening pathologies with limited therapeutic options, representing an important cause of death in cancer patients. The majority of the tumors of the central nervous system (CNS) are metastases, among which breast cancer and melanoma metastases are among the most common. Since the CNS lacks a lymphatic system, tumor cells can only reach the brain parenchyma by hematogenous metastasis formation. During this process the first host cell type encountered by circulating melanoma cells are cerebral endothelial cells, which form the morphological basis of the blood-brain barrier (BBB). Despite the undisputable clinical importance, little is known about the mechanisms of extravasation of metastatic tumor cells through the BBB. Here we aimed to compare melanoma and breast cancer cells in respect of mesenchymal vs. amoeboid migration through the brain endothelium. The question whether tumor cells prefer Rho/ROCK or Rac-dependent transendothelial migration is of clinical importance, since inhibitors of both Rho/ROCK (e.g. fasudil) and Rac pathways are emerging as potential therapeutic agents.

Methods:

In order to study the routes and mechanisms of transendothelial migration of melanoma cells, we

have developed a time-lapse video-based transmigration experimental setup.

Results:

Both melanoma and breast cancer cells released large amounts of serine proteases in the presence of brain endothelial cells. Among the expressed proteolytic enzymes, we have identified seprase in melanoma cells and matriptase in breast cancer cells. Increased proteolytic activity and elongated morphology are characteristic to the mesenchymal type of tumor cell movement, which can be induced by Rho/ROCK inhibition and suppressed by Rac inhibition. We have previously shown that ROCK inhibition (using Y27632) strengthened the adhesion force between melanoma and endothelial cells, and increased the number of melanoma cells migrating from the apical to the basolateral side of the brain endothelial monolayer (1). This effect could be reversed by the addition of the EHT1864 Rac inhibitor. In breast cancer cells Y27632 could not increase the adhesion rate; however, EHT1864 significantly reduced the number of breast cancer cells attaching to and migrating through the brain endothelium.

Conclusions:

Melanoma and breast cancer cells preferentially use the mesenchymal type of tumor cell movement during transmigration through the blood-brain barrier.

Acknowledgements:
This work was supported by the following grants: OTKA PD-100958, OTKA K-100807, HURO/1101/173/2.2.1.

References:

(1) Wilhelm I, Fazakas C, Molnár J, Haskó J, Végh AG, Cervenak L, Nagyőszi P, Nyúl-Tóth Á, Farkas AE, Bauer H, Guillemin GJ, Bauer HC, Váró G, Krizbai IA. Role of Rho/ROCK signaling in the interaction of melanoma cells with the blood-brain barrier. Pigm Cell Mel Res. 27:113-23 (2014).

406
BRAIN-0404
Poster Session

Blood Brain Barrier

EFFECT OF ENDOTHELIAL GLYCOCALYX DISRUPTION ON BLOOD-BRAIN BARRIER INTEGRITY IN MICE

J. Yoon[1], E.S. Lee[2], Y. Jeong[1]
[1]Department of Bio and Brain Engineering, Korea Advanced Institute of Science and Technology, Daejeon, Korea
[2]Graduate School of Medical Science and Engineering, Korea Advanced Institute of Science and Technology, Daejeon, Korea

Objective: Endothelial glycocalyx is thought to play an important role as a barrier to move circulating macromolecules toward endothelial surface. However, little is known about its contribution to blood-brain barrier (BBB) function in cerebral vessels. To address this issue, we aimed to see BBB integrity after disrupting cerebral endothelial glycocalyx layer in live mice using two-photon microscopy.

Methods: We observe the cerebral endothelial glycocalyx and vessels using a two-photon microscopy through cranial windows after intravenous injection of FITC-labeled wheat germ agglutinin (FITC-WGA) lectin and tetramethylrhodamine (TMR) dextran 70kD. FITC-WGA lectin and TMR-dextran 70kD were used to label endothelial glycocalyx layer and blood plasma, respectively. For enzymatic disruption of endothelial glycocalyx layer, neuraminidase or heparinase were injected via tail vein. The fluorescent intensity of cerebral endothelial glycocalyx was measured *in vivo* and *ex vivo*. To observe the BBB integrity, we performed *in vivo* time-lapse two-photon imaging of the cerebral blood vessels after intravenous injection of TMR-dextran 40kD. The fluorescent intensity ratio between the extravascular space and the vessel lumen was calculated every 2min for total of 30min.

Results: The cerebral endothelial glycocalyx layer was successfully visualized *in vivo* with the two-photon microscopy. We could observe the FITC-WGA lectin labeled glycocalyx layer lining along the vessels and the vessel lumen filled with TMR-dextran 70kD signal. The fluorescent intensity of cerebral endothelial glycocalyx layer was decreased after treatment of neuraminidase or heparinase indicating the disruption of the glycoclayx layer. However, after intravenous administration of TMR-dextran 40kD, extravasation was not observed indicating BBB was remain intact.

Conclusions: Our results showed that enzymatic disruption of endothelial glycocalyx layer does not alter BBB integrity. This suggests that the cerebral endothelial glycocalyx is not a crucial factor in maintaining BBB integrity but it can be an auxiliary factor.

Reference:

1. J. Vogel et al, J Cereb Blood Flow Metab, 2000, 20:1571-1578
2. Tessa J.M. Wijnhoven et al, J Am Soc Nephrol, 2007, 18:823-832
3. Mark IM Noble et al, Br J Diabetes Vasc Dis, 2010, 10:66-70

407
BRAIN-0295
Poster Session

Neuroinflammation

INFLUENCE OF MORPHINE EXPOSURE AND WITHDRAWAL ON THE BRAIN KINETICS OF THE TSPO RADIOLIGAND [18F]DPA-714: A MICROPET STUDY IN RATS

S. AUVITY[1], S. GOUTAL[1], C. CHAVES[2], B. THEZE[1], B. KUHNAST[1], B. HOSTEN[2], W. SABA[1], R. BOISGARD[1], S. CISTERNINO[2], N. TOURNIER[1]
[1]SHFJ, CEA, Orsay, France
[2]UMR-S 1144, Université Paris Descartes, Paris, France

OBJECTIVES: Many studies have reported that the brain immune response to morphine administration modulates its analgesic effects. This property was also shown to promote tolerance and dependence observed after prolonged use of morphine in the context of chronic pain or opioid abuse*. Positron Emission Tomography (PET) using radioligands of the Translocator Protein 18 kDa (TSPO) is the most advanced strategy for the non-invasive detection of glial activation in the human brain**. This study investigates the relevance of TSPO PET imaging for the detection of potential glial activation after chronic morphine exposure and withdrawal in rats.

METHODS: Sprague-Dawley rats (n=6) were administered escalating doses of morphine (10 mg/kg increasing to 40 mg/kg, *i.p* twice a day during 5 days) to achieve a withdrawal syndrome (behavioral validation) after morphine discontinuation. Control rats were administered NaCl 0.9% instead (n=6). Dynamic microPET imaging (Siemens Inveon) was performed during 68 min, 60h after the last dose of morphine using the TSPO radioligand [^{18}F]DPA-714. Data are expressed as areas under the curve (SUV.min) obtained from the elimination phase of the time activity curves (SUV).The kinetics of glial cell activation biomarkers Iba1, GFAP and CD68 were also assessed using immunohistochemistry (IHC) on brain slices during 14 days after chronic morphine exposure.

RESULTS: The brain distribution of [^{18}F]DPA-714 was similar in the control ($AUC_{30\text{-}68min}$= 9.79E-05 ± 7.31E-06 SUV.min) and morphine treated ($AUC_{30\text{-}68min}$= 1.06E-04 ± 1.40E-05 SUV.min) groups (p = 0.15). IHC revealed the absence of modification in the Iba1, CD68 and GFAP levels of expression after chronic morphine exposure and morphine withdrawal. These glial biomarkers also remained at the same levels during 14 days after morphine discontinuation.

CONCLUSION: [^{18}F]DPA-714 TSPO PET imaging may not be a relevant approach to investigate the brain immune response to morphine exposure and withdrawal. Moreover, conventional invasive biomarkers of glial activation were not measurably impacted either. This study questions

the nature of neuroimmune events that may be related to morphine tolerance and dependence.

REFERENCES:

* *Opioid activation of Toll-Like Receptor 4 contributes to drug reinforcement.* Hutchinson et al, 2012

** *Molecular imaging of microglial activation in amyotrophic lateral sclerosis*. Corcia et al, 2012.

FIGURE:

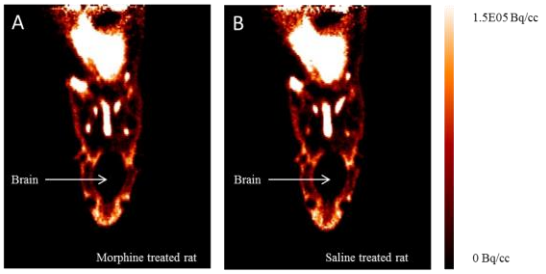

Figure 1. Representative [^{18}F]DPA-714 PET images in coronal section for (A) control group and (B) morphine exposed and withdrawn group.

408
BRAIN-0405
Poster Session

Neuroinflammation

EVIDENCE THAT LY6CHI MONOCYTES ARE PROTECTIVE IN ISCHEMIC STROKE

H. Chu[1], G.R. Drummond[1], C.G. Sobey[1]
[1]Pharmacology, Monash University, Melbourne, Australia

Objective: Ly6C^{hi} monocytes are thought to exert a pro-inflammatory role in acute tissue injury, although their impact following injuries to the central nervous system is poorly defined. CC chemokine receptor 2 (CCR2) is expressed on Ly6C^{hi} monocytes and plays an essential role in their extravasation and transmigration into the brain after cerebral ischemia. We used a selective CCR2 antagonist, INCB3344, to assess the effect of Ly6C^{hi} monocytes recruited into the brain after ischemic stroke.

Methods: Male C57Bl/6J mice (8-12 weeks) underwent transient middle cerebral ischemia for 1 h, followed by 23 h of reperfusion. Mice were administered either vehicle (10% DMSO/0.9% carboxymethylcellulose) or INCB3344 (total dose of 10, 30 or 100 mg/kg) intraperitoneally at 1 h before ischemia, and at 2 h and 6 h after ischemia. At 24 h, we assessed functional outcomes, infarct volume and quantified the number of immune cells in the brain by multicolour flow cytometry. Gene expression of selected inflammatory markers was examined by RT-PCR.

Results: Ly6C^{hi} monocytes were increased 8-fold in the brain after stroke, and this increase was selectively prevented by INCB3344 in a dose-dependent manner. Compared to vehicle treated mice, those treated with INCB3344 exhibited markedly worse functional outcomes and larger infarct volumes at 24 h, in association with reduced expression of genes corresponding to M2 polarised macrophages, Ym-1 and Arg1.

Conclusions: Our data suggests that Ly6C^{hi} monocytes exert an acute protective effect following ischemic stroke to limit brain injury and functional deficit.

409
BRAIN-0526
Poster Session

Neuroinflammation

ACUTE MICROGLIAL ACTIVATION IN TRAUMATIC BRAIN INJURY: A [11C](R)PK11195 POSITRON EMISSION TOMOGRAPHY STUDY

Y. Hong[1], A. Lombardo[2], J. Outtrim[3], R. Canales[1], N. Sudhan[3], T. Huttunen[4], D. Williamson[1], R. Smith[1], A. Helmy[1], F. Aigbirhio[1], P. Hutchinson[1], O. Tenovuo[5], T. Fryer[1], D. Menon[3], J. Coles[3]
[1]Clinical Neurosciences, University of Cambridge, Cambridge, United Kingdom
[2]Physiopathology and Transplant, Milan University, Milan, Italy

[3]*Anaesthesia, University of Cambridge, Cambridge, United Kingdom*
[4]*Neurosurgery, Kuopio University Hospital, Kuopio, Finland*
[5]*Clinical Neurosciences, University of Turku, Turku, Finland*

INTRODUCTION: Neuroinflammation, a key secondary injury mechanism following traumatic brain injury (TBI), involves humoral and cellular components. The cellular component includes recruitment of haematogenous inflammatory cells (polymorphonuclear leukocytes and monocytes) and the activation of resident innate immune cells (microglia). While measurement of inflammatory mediators in jugular venous blood and brain microdialysate can characterise global and focal inflammation in TBI, they do not provide a means of mapping spatial variations in neuroinflammation across the brain. A recent study used [^{11}C](R)PK11195 positron emission tomography (PET) to demonstrate persistent thalamic inflammation years after TBI, which was related to outcome.[1] We have applied [^{11}C](R)PK11195 to map the spatiotemporal patterns of microglial activation in acute moderate/severe TBI.

METHODS: Seven patients (5 male, admission Glasgow Coma Score: 3 – 11) underwent [^{11}C]PK11195 PET and MR imaging twice at a median (range) of 5 (3 – 11) and 15 (13 – 22) days post TBI with a GE Advance, following an i.v. bolus of 485 (296 – 569) MBq of [^{11}C]PK11195; specific activity ~220 GBq/µmol. Fifty-eight frames of emission data were acquired over 90 minutes post-injection. Arterial blood samples were obtained throughout each PET scan to measure whole blood and plasma radioactivity concentrations, together with the plasma parent fraction.[2] Voxel-wise total volume of distribution (V_T) was calculated using Logan graphical analysis with a metabolite-corrected plasma input function. [^{11}C](R)PK11195 binding potentials were calculated in core, perilesional oedema, basal ganglia, white matter and in normal appearing areas of the brain.

RESULTS: There was substantial inter-subject heterogeneity in the spatiotemporal patterns of microglial activation. While some subjects showed early perilesional and lesional [^{11}C]PK11195 binding that increased over time, in other patients, such early binding disappeared at later time points. Given the past demonstration of persistent thalamic microglial activation at late time points after injury,[1] we examined the time course of thalamic [^{11}C]PK11195 binding in our patients. In the thalamus, we observed little or no binding at early time points, and in most patients, no increase over time. While lesion size was not directly related to thalamic tracer binding across the group, the subject with the largest cortical contusions showed a late increase in binding.

CONCLUSIONS: There is marked variability in patterns of microglial activation in early TBI, which may relate to differences in injury type and severity, host response characteristics, and possibly therapy. However, there appears to be a significant increase in lesional (and possibly perilesional) microglial activation over time in large axial and extra-axial lesions, broadly replicating the pattern in stroke. The late thalamic microglial activation reported in past studies does not appear to be a feature of acute TBI, and may represent a late neuroinflammatory response with a long therapeutic window. This variable pattern of microglial activation suggests that neuroinflammation after TBI may be driven by both lesion and host factors. These pilot data suggest hypotheses that can be addressed in larger studies.

References: 1. Ramlackhansingh, A. F. *et al*. *Ann. Neurol.* 70, 374–83 (2011). 2. Folkersma, H. *et al*. *J. Nucl. Med.* 50, 1975–9 (2009).

410
BRAIN-0223
Poster Session

Neuroinflammation

RAPID MICROGLIAL ACTIONS REGULATE EXCITOTOXIC RESPONSES AND BRAIN INJURY AFTER CEREBRAL ISCHEMIA

G. Szalay[1], B. Martinecz[2], N. Lénárt[2], E. Császár[2], B. Rózsa[1], A. Denes[2]
[1]Two-Photon Imaging Center, Institute of Experimental Medicine, Budapest, Hungary
[2]Laboratory of Molecular Neuroendocrinology, Institute of Experimental Medicine, Budapest, Hungary

Inflammation plays a crucial role in the pathogenesis of cerebral ischemia. Inflammatory actions of microglia, the main inflammatory cells in the brain have been widely studied, but their functional contribution to brain injury is controversial. Here we have established a novel, two-photon microscopy-based approach to study early microglial responses in a remote filament model of experimental stroke in mice. In this experimental model, occlusion of the middle cerebral artery and induction of reperfusion are tightly controlled, allowing the assessment of vascular, neuronal and microglial responses in the brain at a millisecond time scale for several hours *in vivo*. By using genetically encoded calcium indicators and transgenic microglia reporter mice, we have assessed changes in neuronal network activity, blood brain barrier injury, Ca^{2+} levels in the tissue and microglia activation simultaneously, in real time. We show that excitotoxic neuronal injury in the ipsilateral cerebral cortex is delayed by several hours after the onset of ischemia. Microglia contact injured neurons in an activity dependent manner. Microglia also react rapidly to early signs of vascular injury, preceding the breakdown of the blood brain barrier and isolate cells showing signs of oxidative stress in the injured brain. Selective depletion of microglia prior to experimental stroke results in altered vascular and excitotoxic responses and lack of spreading depolarisations, leading to markedly increased infarct size. Collectively, our data suggest that microglia could protect the brain from excitotoxic and vascular injury after cerebral ischemia. Understanding the cellular and molecular mechanisms through which microglia contribute to stroke outcome could have important implications to the treatment of stroke and other forms of brain injury.

411
BRAIN-0507
Poster Session

Neuroinflammation

SEVOFLURANE INHIBITS LPS-INDUCED MICROGLIAL ACTIVATION BY MODULATING NFKB SIGNALING PATHWAY

H. WANG[1], H. SHI[2], X. HU[3], J. CHEN[3], Y. GAO[1]
[1]State Key Laboratory of Medical Neurobiology an d Department of Anesthesiology of Huashan Hospi tal, Fudan University, Shanghai, China
[2]Department of Anesthesiology of Shanghai Pulmo nary Hospital, Tongji University, Shanghai, China
[3]Department of Neurology, University of Pittsburgh School of Medicine, Pittsburgh, USA

***Background and Purpose**:* Microglia, the resident immune cells in the central nervous system, produce a variety of neurotoxic factors upon noxious stimulations. Sevoflurane, an inhalational anaesthetic, has been demonstrated to ameliorate Lipopolysaccharides (LPS) or some inflammatory cytokine-induced inflammation in heart, kidney, lung and liver. However, the effect of sevoflurane on microglia-mediated inflammation has not been thoroughly investigated. In the current study, we investigated the effects of sevoflurane on LPS-induced activation of microglia and elucidated the underlying mechanisms.

Methods: The cultured BV2 microglial cells were subjectes to four treatments: 1) PBS+vehicle; 2) LPS(100ng/ml) + vehicle; 3) PBS + sevoflurane; or 4) LPS(100ng/ml) + sevoflurane. For sevoflurane treatment, the microglia received 1 minimum alveolar concentration (MAC) sevoflurane treatment in air for 1hr at 1,6,12 and 23h after LPS challenge. Microglia in the vehicle groups were invented with ambient air. At 24h after LPS exposure, cultured cells and media were collected. Cell death was measured by LDH assay. Cell viability was measured by Alamar blue assay. Inflammatory cytokine production and NFκB activation were assessed by Western blotting tests and immunofluorescent staining.

Results: In comparison with the vehicle, the administration of sevoflurane significantly inhibited the activation of microglia. The cell death of microglia at 1h after LPS-intervention were significantly lower in sevoflurane-treated group (29.17±3.74%) as compare to vehicle-treated group (42.34±4.29%, p<0.01), while the cell survival rate of microglia at 1h after LPS-intervention were much higher in sevoflurane-treated group (53.62±5.45% in vehicle group *v.s.* 71.71±4.85% in sevoflurane group; p<0.01). Importantly, sevoflurane treatment suppressed the elevation of pro-inflammatory mediators (COX-2 and iNOS) at 24h after LPS (p<0.05). Moreover, both Western blots and immunofluorescence staining demonstrated that the LPS-induced NFκB translocation from cytosol to nucleus was robustly inhibited in the sevoflurane group than those in the vehicle group, suggesting that sevoflurane inhibited the activation of NFκB upon inflammatory stimulation.

Conclusion: Sevoflurane suppresses microglial activation upon inflammatory stimulation by inhibiting the activity of NFκB.

412
BRAIN-0604
Poster Session

Neuroinflammation

TLR4 MODULATES NEUTROPHIL INFILTRATION AFTER FOCAL CEREBRAL ISCHEMIA

A. García-Culebras[1], S. Palma-Tortosa[1], A. Moraga[1], M.I. Cuartero[1], I. Ballesteros[1], J.M. Pradillo[1], M.A. Moro[1], I. Lizasoain[1]
[1]Pharmacology, Complutense University, Madrid, Spain

Background. TLR4 has been described to play major roles in the CNS including its participation in inflammation and brain damage caused by stroke. The role that TLR4 plays on inflammation after stroke is well known [1] but it is unknown whether leukocyte infiltration and phenotype is affected by TLR4. Recently our group has reported that, after stroke, the population of infiltrated-neutrophils in the brain is heterogeneous, including a population of neutrophils that express alternative phenotype N2 markers [2].

Objective.The aim of this study is to determine the role of TLR4 in neutrophil mobilization and the polarization of their phenotype on brain damage after stroke.

Methods. Focal cerebral ischemia was induced by permanent occlusion of the middle cerebral artery (pMCAO) in young mice (2-3 months). Experiments were performed on TLR4-deficient mice (C57BL/10ScNJ) and animals that express TLR4 normally (C57BL/10J). Cerebral infarct size was measured by Nissl staining at 24 and 48 hours and by magnetic resonance imaging (MRI) at 24 hours after pMCAO. Leukocyte infiltration was quantified 24 and 48 hours after ischemia onset by double immunofluorescence staining and by flow cytometry.

Results. As previously reported, TLR4-deficient mice presented lesser infarct volumes when compared with wild-type mice. In order to study the role of TLR4 on cell infiltration but avoiding the effect of the different infarct volumes, we included an additional group with a distal MCA occlusion that presented similar infarct volumes (Figure 1A). TLR4-deficient mice also presented an infiltration process of neutrophil and monocyte in the peri-infarct zone 24 hours after stroke when compared with those of wild type mice (flow cytometry). Furthermore, stereological analyses revealed an increase in infiltrated N2 neutrophils ($Ym1^+$, $NIMP\text{-}R14^+$ cells) (Figure 1B) as well as an increase in Ym1 positive cells, in the ischemic core 48 hours after pMCAO, in TLR4-deficient mice ($P<0.05$; n=5-6).

Conclusions. Our data indicate that the absence of TLR4 mediates the polarization of neutrophils into the ischemic core as shown by an increase in the number of N2 neutrophils, indicating that modulation of TLR4 signalling may be useful for resolution of inflammation and subsequent neuroprotection after ischaemic stroke.

References

[1].Caso et al., 2007. Circulation 115:1599-1608.

[2]. Cuartero et al., 2013. Stroke. 44(12):3498-508.

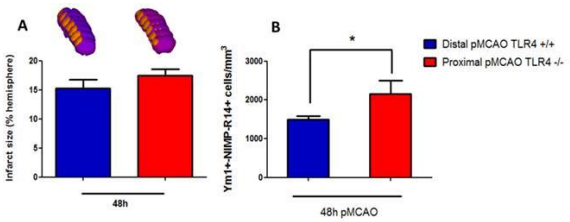

Figure 1. Effect of TLR4 on neutrophil infiltration. **A)** Infarct volume 48 hours after permanent middle cerebral artery occlusion in mice that express TLR4 normally (blue columns; C57BL/10J mice: TLR4+/+, distal occlusion) and in TLR4-deficient mice (red columns; C57BL/10ScNJ mice: TLR4-/-, proximal occlusion). **B)** $Ym1^{+}$-NIMP-$R14^{+}$ cells per cubic millimetre, 48 hours after ischemia in proximal pMCAO TLR4-/- mice (red columns) or distal pMCAO TLR4+/+ mice (blue columns). Ym1+ and NIMP-R14+ cells were sampled in 6 coronal sections by the fractionator technique and normalized by infarct volume (n=5–6; *P<0.05 vs pMCAO TLR4 +/+).

413
BRAIN-0158
Poster Session

Neuroinflammation

DIFFERENTIAL IN VITRO AND IN VIVO SENSITIVITY OF [^{11}C]ER176 TO A SINGLE NUCLEOTIDE POLYMORPHISM IN THE GENE FOR TRANSLOCATOR PROTEIN

M. Ikawa[1], T.G. Lohith[1], K.J. Jenko[1], S.S. Shrestha[1], S. Telu[1], S.S. Zoghbi[1], M. Fujita[1], V.W. Pike[1], R.B. Innis[1]
[1]Molecular Imaging Branch, National Institute of Mental Health, Bethesda, USA

Objectives: For 18 kDa translocator protein (TSPO), the affinities of most second-generation PET ligands, but probably not the prototypical agent PK 11195, are considerably sensitive to the single nucleotide polymorphism rs6971 in the gene for TSPO. We have recently shown that a new quinazoline analog of [^{11}C](*R*)-PK 11195, namely [*methyl*-^{11}C](*R*)-*N*-*sec*-butyl-4-(2-chlorophenyl)-*N*-methylquinazoline-2-carboxamide ([^{11}C]ER176) warrants evaluation in human subjects because it showed little sensitivity to the polymorphism when tested in vitro with tritiated radioligand binding to homogenates of human brain and of white blood cells and performs well as a PET radiotracer for TSPO in monkey brain.[1] Its in vitro ratio of affinities for high (HABs) and low affinity binders (LABs) was 1.3 : 1. The aim of this study is to determine whether the in vivo sensitivity of [^{11}C]ER176 in human subjects is similar to the low sensitivity measured in vitro.

Methods: Nine healthy controls consisting of 2 females and 1 male each for HAB, MAB (mixed affinity binder), and LAB were studied with whole-body PET imaging for 120 min after a bolus injection of [^{11}C]ER176. Area under the time-radioactivity curves (AUCs) from 15 to 120 min post-injection were derived from volumes of interest placed on each organ with visible tracer uptake in the obtained images. The AUCs were compared between binder groups.

Results: [^{11}C]ER176 distributed, as expected, to brain and peripheral organs rich in TSPO. The uptake in TSPO-rich organs, including brain, lungs, heart, spleen, and kidneys, showed a clear and dose-dependent sensitivity to genotype. For example, the ratio of AUC of lungs for HABs (243 ± 31 SUV • min), MABs (173 ± 67), and LABs (97 ± 15) was 2.5 : 1.8 : 1 (Figure 1).

Conclusions: The whole body distribution of [^{11}C]ER176 reflected that for TSPO, but it showed significant sensitivity to the genotype rs6971, which was not expected from in vitro studies. The cause of this discrepancy between in vitro and in vivo is unknown, but may involve in vivo protein-protein interactions that are disrupted by tissue homogenization or other in vitro conditions.

Reference:

1. Zanotti-Fregonara P, et al. Synthesis and evaluation of translocator 18 kDa protein (TSPO) positron emission tomography (PET) radioligands with low binding sensitivity to human single nucleotide polymorphism rs6971. *ACS Chem Neurosci.* 2014;5:963-971.

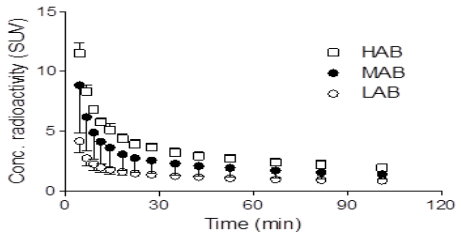

Figure 1. Time-radioactivity curves of lungs show differences between the three genotypes. Data are mean ± SD from n = 3 per group. HAB: high affinity binder, MAB: mixed affinity binder, LAB: low affinity binder.

414
BRAIN-0259
Poster Session

Neuroinflammation

PROTEASE ACTIVATED RECEPTOR-1 ANTAGONIST AMELIORATES THE CLINICAL SYMPTOMS OF EXPERIMENTAL AUTOIMMUNE ENCEPHALOMYELITIS VIA STABILIZATION OF BLOOD BRAIN BARRIER

H.N. Kim[1], Y.R. Kim[1], S.M. Ahn[1], H.K. Shin[1], B.T. Choi[1]
[1]School of Korean Medicine, Pusan National University, Yangsan-si Gyeongnam, Korea

Objectives: The protease-activated receptor-1 (PAR-1) is activated by thrombin in central nervous system and widely recognized their pleiotropic roles. We investigated to evaluatethe question of whether PAR-1 antagonists are a potential therapeutic target in multiple sclerosis.

Methods: The experimental autoimmune encephalomyelitis (EAE) mice were induced by injectionof 50 ug MOG_{35-55} with CFA. EAE mice were treated with newly synthesized non-peptide PAR-1 antagonist KC-0590 (50 ug/kg), and SCH530348 (50ug/kg) was used as a positive control.

Results: Treatment with both antagonists resulted in a significant decrease of clinical characteristics of EAE mice by suppressing demyelination and infiltration of inflammatory cells in the spinal cord and brain. Thrombin and tumor necrosis factor-α were significantly increased in the spinal cord and brain of EAE mice and these expressions were also reduced by treatment with both antagonists. In analysis of vascular breakdown, profound leakage of dextran was observed in the brain of EAE mice. However, treatment with PAR-1 antagonists resulted in stabilization of vascular endothelial cells and reduced blood-brain barrier (BBB) breakdown with suppression of inflammatory response. Treatment with PAR-1 antagonists also resulted in down-regulated expression of matrix metalloproteinase-9 (MMP-9) and preserved expression of occludin and zonula occludens-1 in the brain and confirmed its significant expression in neurons, astrocytes, and vascular endothelial cells. Finally, we treated primary cultured astrocytes with PAR-1 antagonists; both antagonists suppressed thrombin-induced secretion of MMP-9.

Conclusions: Our results suggest that PAR-1 antagonist is effective in attenuation of the clinical symptoms of EAE mice by stabilizing the BBB and may imply a therapeutic potential for treatment of multiple sclerosis.

415
BRAIN-0633
Poster Session

Neuroinflammation

USING MATHEMATICAL MODELING TO TEST THE THERAPEUTIC POTENTIAL OF CD59 TO MITIGATE ASTROCYTIC OEDEMA DUE TO NEUROMYELITIS OPTICA

S. Laranjeira[1], M. Symmonds[2], J. Palace[2], S.J. Payne[1], P. Orlowski[1]
[1]Engineering science, Institute of Biomedical Engineering, Oxford, United Kingdom
[2]Nuffield Department of Clinical Neurology, Division of Clinical Neurology, Oxford, United Kingdom

Objectives

Neuromyelitis Optica (NMO) is a neuro-inflammatory disease with a worldwide incidence of 1/100,000 people [1]. NMO is severe, with a 5-year mortality rate of 32% in patients with a relapsing disease (70% of NMO patients [2]). Although rare, NMO is the only brain inflammatory disease for which the antibody (AQP4-IgG) [2] and antigen - the astrocitic water channels aquaporin-4 (AQP4) - have been identified. Hence, it provides the unique opportunity of being able to simulate it experimentally and with mathematical modeling which might give insight into common mechanisms of neuro-inflammation.
During NMO the antigen-antibody complex has been shown to induce astrocytic oedema [3]. The swelling is due to the activation of the complement system which produces the membrane attack complex (MAC) that perforates the membrane. These pathophysiological mechanisms are summarized in Fig.A. Swelling then leads to activation of the inflammatory response which induces oligodendrocyte damage, demyelination and neuronal death [3].
Currently, there are no disease specific treatments. The work here demonstrates the possibility of using mathematical modelling to test the potential of CD59 - a MAC inhibitory protein expressed at the astrocitic surface [4] – as a therapy to mitigate astrocitic swelling during NMO.

Methods

The complement system model by [5] was implemented to define MAC formation. The rate of hole production (dH/dt) was made proportional to MAC concentration (M) based on [6] which states that each hole comprises of 12 to 16 MAC molecules. Additionally, cells can endure a maximum of 90,000 [7] which is ensured in the model by H_{max}. Equation 1 summarizes the rate implemented.
Cellular oedema due to NMO was modeled by adding the ionic flow I through the holes to the cytotoxic oedema model by [8]. The flow was made dependent on the ionic Nernst potential (v_I), the membrane potential (v) and the hole permeability (k) as in Equation 2. The hole permeability was set to be proportional in terms of radii ratio to that of a respective ion channel from [8] according to Hagen-Poisseuille's equation.
Furthermore, the inhibition of MAC by CD59 was assumed to be a 1st-order reaction for which the stoichiometry rates were derived from *in vitro* data [9] using the least-squares method.

$$\frac{\partial H}{\partial t} = \alpha \frac{\partial M}{\partial t}\left(1 - \frac{H}{H_{max}}\right) \quad (1)$$

$$I = H\, k \sinh(v - v_I) \quad (2)$$

Results

For a given CD59 concentration simulations were performed until the cellular volume reached a steady state. The observed percentage of glial volume increase due to complement lyses for different concentrations of CD59 is presented in Fig.B.

Conclusions

This work is the first where mathematical modeling has been used to test NMO therapies. The simulations show that for CD59 to effectively reduce oedema (<1%) during

NMO its concentration needs to exceed 10^{-1} mM.
In order to further develop this work, experimental measurements would be required on astrocyte swelling due to lysis and on CD59 MAC inhibitory kinetics.

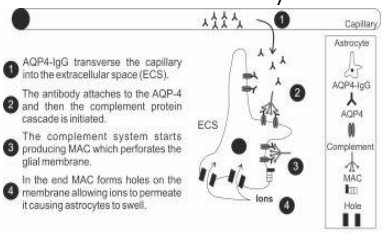

Fig.A. Description of the initial pathophysiological mechanisms of NMO that lead to astrocytic oedema.

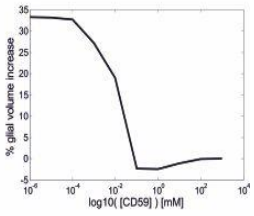

Fig.B.The impact of MAC inhibitor CD59 on glial oedema due to NMO.

References

[1] Matiello,M, *Neurology*.2010.
[2] Wingerchuk,DM, *Neurology*.1999.
[3] Jarius,S, *Brain*.2008.
[4] Papadopoulos, MC. *Nature.*2014.
[5] Korotaevskiy, AA. *Math Biosci*.2009.
[6] Tschopp, J. *Biology Chemistry*.1984.
[7] Taliaferro, WH. Advances in Immylogy, *Academic Press*.1968.
[8] Orlowski, P. *Interface Focus*.2011.
[9] Rollins, SA. *Immunology.*1990.

416
BRAIN-0389
Poster Session

Neuroinflammation

RATIO METHOD FOR 11C-PBR28 IS MORE SENSITIVE FOR DETECTING THE REGIONS WITH INCREASED TRANSLOCATOR PROTEIN BINDING IN ALZHEIMER'S DISEASE

C.H. Lyoo[1], M. Ikawa[2], J.S. Liow[2], S.S. Zoghbi[2], C. Morse[2], V.W. Pike[2], M. Fujita[2], R.B. Innis[2], W.C. Kreisl[3]
[1]Neurology, Gangnam Severance Hospital Yonsei University College of Medicine, Seoul, Korea
[2]Molecular imaging branch, NIMH NIH, Bethesda, USA
[3]Taub Institute for Research on Alzheimer's Disease and the Aging Brain, Columbia University Medical Center, New York, USA

Objectives: Alzheimer's disease (AD) is associated with increased expression of 18 kDa translocator protein (TSPO) in activated microglia and reactive astrocytes. As there is no true reference tissue devoid of TSPO binding in brain, absolute quantitation with arterial blood is required to measure TSPO density with PET. We sought to determine if simple standardized uptake value ratio (SUVR) method is more sensitive for detecting the regions with increased TSPO binding in AD patients than conventional total distribution volume corrected for plasma free fraction (V_T/f_P) for quantitation of ^{11}C-PBR28 PET.

Methods: In 21 healthy controls, 11 mild cognitive impairment, and 25 AD patients, ^{11}C-PBR28 PET was performed. We measured two types of regional binding values. First, regional V_T values were measured by using two-tissue compartmental model and corrected for plasma free fraction of radioligand (V_T/f_P). Second, regional SUVR values were calculated with data between 60 - 90 mins by using cerebellum as a pseudoreference region. We compared both types of binding values between AD and MCI

patients and healthy controls after correcting for TSPO genotype.

Results: The V_T/f_P and SUV values of cerebellar cortex were not different across three diagnostic groups. The AD patients showed greater V_T/f_P values than healthy controls in the inferior parietal, combined middle and inferior temporal, and entorhinal cortices ($P < 0.05$). By using non-invasive SUVR method, the AD patients showed greater binding in the same regions and one additional region (parahippocampal gyrus) with higher significance (e.g. $P < 0.05$ for V_T/f_P *vs.* $P < 0.0005$ for SUVR in the combined middle and inferior temporal cortex). Coefficients of variation of SUVR values were less than one third of those of V_T/f_P. Both binding values of combined middle and inferior temporal cortex correlated with the severity of cognitive impairment ($P < 0.01$).

Conclusion: Simple SUVR method with cerebellum as a pseudoreference tissue is more sensitive for detecting the regions with increased TSPO binding in AD than absolute quantitation. This ratio method also allows non-invasive quantitation with shorter scan time, and thereby increases patients' tolerability. In addition, lower variability of SUVR values allows smaller sample size required for comparable statistical significance.

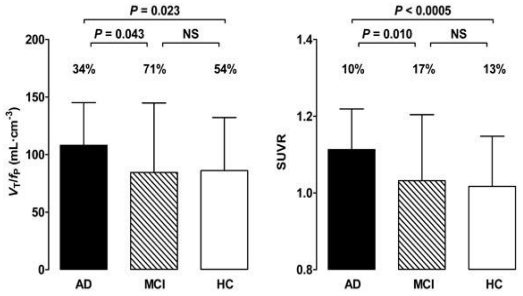

Figure. In the combined middle and inferior temporal cortex, both total distribution volume corrected for free fraction of radioligand (V_T/f_P) and standardized uptake value ratio (SUVR) were greater for Alzheimer's disease (AD) patients than for mild cognitive impairment (MCI) patients or controls. Error bars denote mean ± SD. The coefficient of variation of V_T/f_P was three to four times greater than that for the SUVR, as shown by coefficient of variation (%COV) values above the SD bars.

417
BRAIN-0782
Poster Session

Neuroinflammation

CHARACTERIZING B-CELLS USING MOLDAY ION RHODAMINE B (MIRB) NANOPARTICLES IN A THERAPEUTIC MODALITY OF STROKE

S.B. Ortega[1], N.N. Mithani[1], X. Kong[1], K. Poinsatte[1], G.A. van Tilborg[1], R.M. Dijkhuizen[1], A.M. Stowe[1]
[1]Neurology and Neurotherapeutics, UT Southwestern Medical Center, Dallas, USA

Objectives: Repetitive Hypoxic Preconditioning (RHP) has been shown to ameliorate brain injury in a murine model of stroke.[1] Understanding the mechanism(s) involved in this modality is essential in developing translation therapies for stroke patients. Adoptive transfer of RHP-modulated B-cells significantly reduces infarct volumes in recipient stroke-induced mice *($p<0.05$)*. We hypothesize that therapeutic B-cells extravasate into the central nervous system (CNS) during acute injury and provide protection/repair in areas with neurovascular injury. In order to confirm this spatiotemporal localization, we labeled B-cells with a MRI contrast agent, Molday ION Rhodamine B (MIRB)©, which can be detected *in vivo* by MRI and *in situ* by fluorescence techniques. In this study, optimal labeling was determined using *in vitro* studies that assessed viability and functionality of B-cells, along with stable labeling.

Methods: Highly purified (>95% CD19+) B-cells from adult C57BL/6 mice were labeled with 10, 20, 30, 50 and 100 µg/mL of MIRB overnight at 37°C and 5%CO_2. At days 1, 2 and 9, B-cell viability was determined using trypan blue exclusion. Affirmation of *in vivo* stable labeling was performed by labeling B-cells with MIRB followed by adoptively transferring cells and quantifying the number of MIRB+CD19+ B-cells using flow cytometry, which was validated by flow based

high-resolution microscopy at day 9 post transfer. CNS accessibility was determined by transferring MIRB+ B-cells into mice and inducing blood-brain barrier permeability using pertussis toxin or neurovascular injury by a 45 minute transient middle cerebral artery occlusion. Labeled cells were detected by flow cytometry, which was validated by *in situ* immunofluorescence.

Results: *In vitro* studies revealed the optimal dosage for MIRB labeling was at 20 ug/mL, as this dosage allowed for the highest labeling of purified (>95% CD19+) B-cells (39% MIRB+) while maintaining *in vitro* viability (>95% at day 2 post and >46% at day 7). Activation of B-cells using lipopolysaccharide (LPS) did not increase initial uptake of MIRB (27.5%) but did contribute to long-term stability (25.5±0.5% vs. 17.5±1.5% without LPS). *In vivo* studies revealed maintenance of B-cell labeling at day 9 post transfer (25.7±8.1% of CD19+). MIRB labeled B-cells were able to traffic to the CNS passively as demonstrated by the pertussis toxin-induced CNS permeability (21% of B-cells were MIRB+) and actively using neurovascular injury-induced CNS permeability.

Conclusion: Stroke induces CNS inflammation that may lead to an increase in neuropathology. B-cells however may provide a mechanism for disease amelioration. In order to ascertain if this mechanism involves CNS modulation, we labeled therapeutic B-cells with a non-transfection fluorescent iron-oxide nanoparticle. This labeling was confirmed and was stable for up to 9 days post transfer. In stroke, we have seen that these labeled B-cells are capable of trafficking into the CNS, thereby suggesting an active recruitment of therapeutic immune cells into injured CNS. In conclusion, this novel method of labeling therapeutic B-cells will afford us the ability to monitor brain-immune interactions during disease amelioration *in vivo* by MRI in future studies.

418
BRAIN-0834
Poster Session

Neuroinflammation

DETRAINING AFTER EXERCISE DIMINISHES NEUROPROTECTION AND COUNTERS ADAPTIVE IMMUNE MODULATION FOLLOWING STROKE

K. Poinsatte[1], S. Ortega[1], U. Selvaraj[1], A. Meeuwissen[1], A. Partin[1], I. Noorbhai[1], N. Mithani[1], X. Kong[1], E. Plautz[1], R. Zhang[1], A. Stowe[1]
[1]Neurology and Neurotherapeutics, University of Texas Southwestern Medical Center, Dallas, USA

Objectives:

Exercise decreases stroke severity in both human[1] and animal studies,[2] but it is unknown whether the adaptive immune system contributes directly to exercise-induced neuroprotection. Prior microarray analysis of B cells found that healthy animals that do not sustain exercise intensity over 3 weeks are genotypically closer to sedentary controls, suggesting that changes to the immune system by exercise may rely on the intensity of training. To further elucidate exercise-induced modulation of the immune system, we implemented a detraining protocol of a 2-week sedentary period after exercise training. We hypothesized that the neuroprotective benefits of exercise on infarct volumes and inflammation will be lost following detraining.

Methods:

Adult male Swiss Webster mice (8-12 wks old) were given unrestricted access to computer-monitored running wheels for 3 weeks (n=19). A second detraining cohort had a 2-week sedentary period following 3 weeks of exercise (n=23). All cohorts had sedentary controls housed in similar cages without access to wheels (n=42). Mice underwent a 60-min transient middle cerebral artery occlusion. One experiment sacrificed mice at 24 hrs post-stroke for analysis of infarct volumes via TTC staining. A second experiment

quantified leukocyte populations in the spleen and brain and analyzed them with flow cytometry 72 hrs post-stroke. One-way ANOVA ($p<0.05$) and non-linear second-order polynomial regression ($R^2>0.60$) determined significance with outliers identified by ROUT (Q=1%; Prism).

Results:

Detraining significantly increased infarct volumes compared to exercise-only animals ($p<0.05$). Within the brain, exercise significantly increased $CD45^+$ leukocyte, $TCR\beta^+$ T cell, and regulatory B cell ($CD1d^{hi}CD5^+$; Bregs) diapedesis into the ischemic hemisphere compared to both sedentary and detrained animals. Exercise intensity, determined by average wheel rotations over 3 weeks, induced a non-linear, dose-dependent leukocyte diapedesis into the ischemic brain, with moderate levels of exercise associated with the lowest levels of $CD45^+$ infiltration ($R^2=0.84$). This non-linear relationship was lost with detraining ($R^2=0.04$). Bregs ($R^2=0.78$) and $CD4^+$ T cells ($R^2=0.65$) also exhibited this intensity-modulated effect on diapedesis. This relationship was again lost following detraining. Exercise and detraining did not affect peripheral leukocyte populations in the spleen.

Conclusions:

Exercise reduced infarct volumes concomitant with increased leukocyte populations in the ischemic hemisphere. In particular, exercise increased populations of B and T cell subsets, but only in mice with either low or high levels of exercise. Moderately exercising mice exhibited the lowest levels of leukocyte diapedesis, suggesting that an optimal level of exercise is necessary to limit post-stroke inflammation. The effects of exercise on neuroprotection and the adaptive immune system were lost with a period of detraining. The loss of adaptive immune subsets in the brain after detraining did not affect peripheral leukocyte populations, suggesting that the regulation of post-stroke inflammation after exercise occurs at the blood-brain barrier and is not a systemic effect.

1. Mozaffarian, D. et al. Heart Disease and Stroke Statistics -- 2015 Update. *Circulation* 131 (2015).

2. Zhang F., *et al.* Exercise preconditioning and brain ischemic tolerance. *Neuroscience* 177 (2011).

419
BRAIN-0298
Poster Session

Neuroinflammation

CHARACTERIZATION OF INFLAMMATORY PROCESSES OVER TIME USING [18F]DPA-714 PET AND IMMUNOCHEMISTRY IN TWO ACUTE PRECLINICAL RODENT MODELS

G. POTTIER[1], N. BERNARDS[1], J. SOLET[1], F. DOLLE[1], R. BOISGARD[1]
[1]Inserm / CEA / Université Paris Sud UMR 1023 – E RL 9218 CNRS IMIV, CEA, Orsay, France

Objectives: The continually increasing incidence of neurodegenerative diseases in developed countries has become a major health problem, for which the development of diagnostic and follow-up tools is required. The Translocator protein 18kDa (TSPO) expressed by activated microglial cells has been proposed as a hallmark of neuroinflammation. TSPO is largely used in various animal models and clinical studies to visualize and measure this biological process encountered in many neurological pathologies using Positron Emission Tomography (PET). Today, little information is available regarding the kinetics of expression and cell populations in acute neuroinflammation models. Here we investigated the kinetics of TSPO expression in striatal lesions induced by two different pathways using PET imaging with [^{18}F]DPA-714 and cell populations characterization using immunohistochemistry (IHC).

Methods: PET (Inveon Siemens) dynamic acquisitions (60 min) were performed after intravenous injections of about 37 MBq of [^{18}F]DPA-714 in two rat models (Male ±300 g, Wistar) of acute neuroinflammation obtained by intra striatal injection of AMPA (*R,S*-alpha-amino-

3-hydroxy-5-methyl-4-isoxazolopropioniqueand, 7.5 nmol) or Lipopolysaccharides (LPS 1 µg, from E. Coli 055:B55S). Rats were scanned at different times after induction, ranging from 1 to 14 days for the AMPA model and from 6 h to 7 days for the LPS model. Some animals were euthanized in order to analyze common neuroinflammation markers expression such as *CD68, Iba1* and *TSPO* at these different times using IHC performed on frozen brain tissue sections.

Results: In both neuroinflammatory models, enhanced [^{18}F]DPA-714 uptake was observed in the injected striatum compared to the contralateral side. The intensity of the uptake in the AMPA and LPS models was similar with a ratio between lesions to control of 4.5. The main difference between both models was in the kinetic of this uptake. In the AMPA model, a progressive uptake of the radiotracer reaching a maximum at day 7 was observed (%ID/cc = 0.40±0.07) while in the LPS model, this maximum was reached at day 2 (%ID/cc= 0.38±0.03). In the LPS model, a decrease of the uptake was observed at day 4 and the ratio between lesion and control was lower than 2 at day 7. Immunohistochemistry demonstrated at day 2 in the AMPA model an enhanced expression of neuroinflammation markers (CD68, Iba1) earlier than the maximal [^{18}F]DPA-714 uptake as measured in the PET images At this stage numerous cells are CD68 positive and TSPO negative.

Conclusions: For the two studied neuroinflammation models, TSPO expression as measured in [^{18}F]DPA-714 PET images occurs later than enhancement of other neuroinflammation markers (CD68, Iba1) seen using IHC. [^{18}F]DPA-714 imaging might therefore not be suitable for imaging early phases of neuroinflammation.

This work was supported by the European Union's Seventh Framework Programme [FP7/2007-2013] INMiND (Grant agreement no. 278850)

420
BRAIN-0703
Poster Session

Neuroinflammation

ESTROGEN RECEPTOR BETA REGULATES INFLAMMASOME ACTIVATION IN THE HIPPOCAMPUS OF FEMALE RATS

A. Raval[1], H. Patel[1], F. Brand III[2], H. Bramlett[2], J.P. De Rivero Vaccari[2]
[1]Neurology, University of Miami, Miami, USA
[2]Neurological Surgery, University of Miami, Miami, USA

Objectives: Periodic treatments with an estrogen receptor subtype beta (ER-β) agonist reduce post-ischemic hippocampal injury in ovariectomized rats; however, the underlying mechanism of protection remains unknown [1, 2]. It is known that cerebral ischemia activates the innate immune response and a key component of the innate immune response is the inflammasome. The inflammasome is a multiprotein complex responsible for activation of caspase-1 and processing of the inflammatory cytokines IL-1β and IL-18. The inflammasome is comprised of caspase-1, the adaptor protein apoptosis associated speck-like protein containing a CARD (ASC), and a pattern recognition receptor such as a NOD-like receptor [3] In the present study, we tested the hypothesis that ER-β regulates inflammasome activation in the hippocampus and thus reduces ischemic hippocampal damage in reproductively senescent female rats that received periodic ER-β agonist treatments.

Methods: We determined the effect of ER-β loss on inflammasomes by silencing hippocampal ER-β. Ovariectomized rats were treated with ER-β-antisense (AS) or missense (MS) by bilateral cerebroventricular infusion every 24 h for 4 days to knock down hippocampal ER-β [4]. To stimulate estrogen signaling, rats were injected with a single bolus of 17β-estradiol (E_2; 5 µg) or oil on the 2nd day (48h prior to sacrificing the rats) of AS treatment. Rats were then sacrificed and hippocampal tissue collected for Western blot analysis of inflammasome proteins. Next, we

tested the hypothesis that periodic ER-β agonist treatment reduces inflammasome activation and ischemic damage in reproductively senescent (retired breeder, 9–11 months) Sprague–Dawley female rats. We examined vaginal smears of rats daily to confirm the stages of estrous cycle and rats that remained in constant diestrus stage were considered reproductively senescent. These rats were treated with either ER-β agonist (beta 2,3-bis(4-hydroxyphenyl) propionitrile; DPN; 1 mg/kg; s.c) or vehicle at an interval of every 48h for 10 injections followed by induction of cerebral ischemia at 48h after the last injection. Fourteen days after ischemia, rats were sacrificed and histopathological analysis was performed.

Results: We observed a significant decrease of the inflammasome proteins caspase-1 ($p<0.002$), ASC ($p<0.03$) and IL-1β ($p<0.02$) in the hippocampus of ER-β agonist-treated rats. Silencing of hippocampal ER-β attenuated E_2-mediated decrease in inflammasome proteins, suggesting a role of ER-β in regulation of inflammasome activation. Histopathological analysis of hippocampus revealed that periodic ER-β agonist treatments to reproductively senescent rats increased live neuronal counts to 49% (557 ± 73; n = 6; Mean ± SEM) as compared to 17% (190 ± 23; n = 6; $p<0.05$) in the vehicle-treated group after cerebral ischemia.

Conclusions: ER-β activation regulates inflammasome activation and protects the brain from ischemic damage in reproductively senescent female rats. Further investigation of the role of a periodic ER-β agonist regimen to reduce the innate immune response in the brain could help reduce cerebral ischemia incidence/impact in post-menopausal women.

References:

1 Cue, L.*, et al.* (2014) *Neurochem Res*
2 Raval, A.P.*, et al.* (2013) *PLoS One*
3 de Rivero Vaccari, J.P.*, et al.* (2014) *Journal of cerebral blood flow and metabolism*
4 Raval, A.P.*, et al.* (2012) *Journal of Neurochemistry*

421
BRAIN-0241
Poster Session

Neuroinflammation

INDUCTION AND RESOLUTION OF POST-ISCHEMIC INFLAMMATION BY DAMPS

T. Shichita[1], *M. Ito*[1], *A. Yoshimura*[1]
[1]*Department of Microbiology and Immunology, Keio University School of Medicine, Tokyo, Japan*

(Objectives)

Inflammation is an essential step for the pathology of ischemicstroke. Because brain is a sterile organ, the inflammation is triggered by someendogenous molecules. High mobility group box 1 (HMGB1) is the well-knowndanger associated molecular patterns (DAMPs) which exaggerate the disruption ofblood brain barrier. Here, we have tried to identify another DAMPs whichdirectly activate infiltrating immune cells and regulate the post-ischemicinflammation.

(Methods)

We used 60 minutes transient cerebral ischemia/reperfusion mice. Proteinsincluded in brain homogenates were fractionated, and some specific proteinswhich activate bone marrow derived macrophage were identified by LC/MS.Infiltrating immune cells in ischemic brain were collected by Percoll gradientcentrifugation and were analyzed by realtime PCR or FACS.

(Results)

We could identifyperoxiredoxin (Prx) family proteins as previously unknown DAMPs in the ischemicbrain. Prx activates infiltrating immune cells and induces the inflammatorycytokine production through TLR2 and TLR4 signaling pathway. Both theextracellular release of Prx and the infiltration of immune cells reach thepeak within 1 to 3 days after the onset of ischemic stroke and thereafter theydecrease. This will lead to the resolution of post-ischemic inflammation.Indeed, the gene expression profile

of infiltrating immune cells in the latephase shows the phenotype for anti-inflammation and tissue repair. Our resultsindicate that macrophage and microglia contribute to the resolution ofpost-ischemic inflammation independently.

(Conclusion)

DAMPs regulate not only the induction but alsothe resolution of post-ischemic inflammation. The novel neuroprotective strategyfor ischemic stroke will be developed by promoting the resolution ofpost-ischemic inflammation.

(Reference)

Shichita T, et al. Front Cell Neurosci. 8,319 (2014)

Shichita T, et al. Nat Med. 18, 911-917(2012)

422
BRAIN-0268
Poster Session

Neuroinflammation

ANTI-INFLAMMATORY ACTIVITY OF DALESCONOLS B IN MICE SEPSIS BRAIN INVOLVES ACTIVATION OF NRF2/HO-1 SIGNALING IN MICROGLIAL CELLS

L. Han[1], X. Chen[1], D. Ye[1], Y. Xu[1]
[1]Department of Neurology,
the Affiliated Drum Tower Hospital of Nanjing Uni versity Medical School, Nanjing, China

Objectives- We have demonstrated that Dalesconols B, a polyketide from a mantis-associated fungus, displayed anti-inflammatory effects in BV2 microglial cells. In the present study, we aimed to investigate whether Dalesconols B has anti-inflammatory effects of in lipopolysaccharide (LPS)-treated mice brain, and whether activation of Nrf2/HO-1 signaling in microglial cells is involved in these effects.

Methods- Mice sepsis brain was established by giving LPS (5 mg/kg) intraperitoneally (ip) for 3 h. Dalesconols B (10 mg/kg) dissolved in DMSO and saline was administrated once daily for 2 days prior to injection of LPS . Ibal immunostaining was used to detect microglial activation. Enzyme-linked immunosorbent assay and quatitative PCR was performed to examine protein and mRNA levels of TNF-α and IL-6 in sepsis brain, respectively. Anti-inflammatory and anti-oxidant effects of Dalesconols B were evaluated in LPS-treated BV2 microglial cells. Immunostaining and western blotting was performed to test nuclear translocation of nuclear factor E2-related factor transcription factor (Nrf2) and protein levels of HO-1. Binding activity of antioxidant response element (ARE) in BV2 cells was detected by ARE-luciferase report assay.

Results- Pre-treatment of Dalesconols B significantly inhibited microglial activation and production of TNF-α and IL-6 in sepsis brain, which is accompanied by a strong up-regulation of HO-1 in protein levels. To further investigate the mechanism underlying these anti-inflammatory effects, we employed the LPS-treated BV2 microglial cells *in vitro* model. In BV2 microglial cells, the increased ROS production and decreased GSH/GSSG ratio induced by LPS was reversed by Dalesconols B treatment, providing anti-oxidant protection against LPS stimulus. In addition, treatment of Dalesconols B activated Nrf2/HO-1signaling in BV2 microglial cells, as evidenced by increased nuclear translocation of Nrf2, up-regulation of HO-1 in both protein and mRNA levels and enhancement in ARE binding activity. However, Dalesconols B-stimulated induction of HO-1 was reduced when BV2 microglial cells were transfected with Nrf2-shRNA. In addition, transfection of Nrf2-shRNA or co-treatment with zinc protoporphyrin IX (ZnPP), a HO-1 inhibitor, abolished the inhibitory effects of Dalesconols B on production of TNF-α and IL-6 in LPS-treated BV2 microglial cells.

Conclusions- Dalesconols B treatment inhibits neuroinflammation in mice sepsis brain at least partially via activating Nrf2/HO-1 signaling in microglial cells, indicating that stimulating Nrf2/HO-1 pathway in microglial cells may be a potential therapeutic treatment for neurological disorders associated with neuroinflammation.

423
BRAIN-0733
Poster Session

Neuroinflammation

EARLY COMBINATION DRUG TREATMENT AMELIORATES NEURONAL CELL DEATH AND TISSUE DAMAGE AFTER TRANSIENT GLOBAL AND FOCAL CEREBRAL ISCHEMIA

I. Yu[1], J. Yen[2], P. Kuo[2], B. Hong-Goka[3], R. Sweazey[1], F. Chang[4]
[1]Anatomy and Cell Biology,
Indiana University School of Medicine - Fort Wayne, Fort Wayne, USA
[2]Microbiology and Immunology,
Indiana University School of Medicine - Fort Wayne, Fort Wayne, USA
[3]Alzheimer's & Memory Center,
University of California San Francisco Fresno, Fresno, USA
[4]Medical Education Center,
Indiana University School of Medicine - Fort Wayne, Fort Wayne, USA

Objectives: Cerebral ischemia induced by cardiac arrest or acute stroke results in heterogeneous damages to the brain. The pathogenic mechanisms are complex and can occur after successful restoration of blood flow, leading to reperfusion injury to the brain. Due to heterogeneity of ischemia/reperfusion (I/R) injury, the therapeutic effect of one single agent is limited and many clinical interventions have failed to show beneficial outcomes. The present investigation tests the hypothesis that simultaneously targeting multiple cascades early after cerebral ischemia could significantly improve neuronal survival and suppress brain tissue damage. *Methods*: Two experimental mouse models were employed: the transient cerebral ischemia was induced by bilateral common carotid artery occlusion (BCCAO) or by occlusion of the middle cerebral artery (MCAO). In BCCAO model, mice were subjected to 20 minutes of BCCAO to mimic global cerebral ischemia induced by cardiac arrest. The cocktail drug targeting glutamate excitotoxicity and neuroinflammation was administered intravenously during the reperfusion, mimicking successful cardiopulmonary resuscitation after cardiac arrest. In MCAO model, mice were subjected to 40 minutes of MCAO to mimic focal cerebral ischemia in acute stroke patients. The cocktail drug was administered intravenously at 1 hour after ischemia. *Results*: In BCCAO mice, cocktail drug treatment suppressed production of pro-inflammatory cytokine, tumor necrosis factor alpha (TNFα) mRNA by 9.82 ± 3.57 folds in the forebrain, including the cortex and striatum 6 hours after I/R. Studies suggest that microglia cells trigger delayed neuronal cell death and neuroinflammation by releasing pro-inflammatory cytokines after cerebral ischemia. Using flow cytometry, we observed a 16.81 ± 5.13 % reduction of CD86 activation marker in microglia populations isolated from cocktail drug treated mice as early as 6 hours after I/R. The mRNA expressions of chemokines, Ccl2, Ccl3, and Cxcl2, which attract leukocytes infiltration into the brain further exacerbating tissue damage, were significantly suppressed by 9 to 15 folds in cocktail drug treated mice. The reduced production of brain chemokines suppressed the infiltration of $CD45^{high}/CD11b^{+}$ leukocytes, including macrophages and neutrophils, at later stage. Besides inhibiting different steps in the neuroinflammatory cascade, early cocktail drug treatment down-regulated induction of oxidative stress sensor, Sestrin 2, mRNAs in response to excitotoxic insults at 6 hours after cerebral ischemia. Using histological examinations, we observed that early administration of cocktail drug ameliorated cell death of hippcampal CA1 neurons at 3 days after I/R. In MCAO mice, early administration of cocktail drug was found to significantly reduce the size of cerebral infraction (13.81 ± 1.49% vehicle vs 7.60 ± 1.44% cocktail drug) at 2 days after I/R. *Conclusions*: The cocktail drug treatment was shown to suppress multiple steps in neuroinflammatory cascades when administered early. The delayed neuronal cell death and tissue damage could be ameliorated by early administration of cocktail drug. This is the first report to demonstrate that early neuroprotective intervention simultaneously targeting multiple I/R injury cascades has the potential to benefit patients suffering acute

stroke or post-cardiac arrest brain injury. *References*: Norman et al. 2011, Low et al. 2013, and Wang et al. 2013.

424
BRAIN-0717
Poster Session

Neuroinflammation

N-3 PUFA SUPPLEMENTATION BENEFITS MICROGLIAL RESPONSES TO MYELIN PATHOLOGY

H. Zhang[1], S. Chen[1], H. Pu[1]
[1]Neurology, University of Pittsburgh, Pittsburgh, USA

n-3 PUFAsupplementation benefits microglial responses to myelin pathology

Haiyue Zhang[1,3*],Songela Chen[1*], Hongjian Pu[1,2*], Guohua Wang[1,2],Jun Chen[1,2], Xiaoming Hu[1,2]

[1]Department of Neurology, University of Pittsburgh School of Medicine, Pittsburgh, Pennsylvania15213, USA

[2]State Key Laboratory of Medical Neurobiology and Institute of Brain Science, Fudan University,Shanghai200032, China

[3] Xiangya School of Medicine, Central South University, Changsha, Hunan 410013, China

Background and Purpose: Microglia represent rational but challenging targets for improving white matter integrity because of their dualistic protective and toxic roles. The present study examines the effect of Omega-3 polyunsaturated fatty acids (n-3 PUFAs) on microglial responses to myelin pathology in primary cultures and in the cuprizone mouse model of multiple sclerosis (MS), a devastating demyelination disease.

Methods: The effect of docosahexaenoic acid (DHA) and eicosapentaenoic acid (EPA), the two mainforms of n-3 PUFAs, on inflammatory response of microglia was studied in a MS-related *in vitro* model, which use myelin and IFN-γ as two inflammatory stimulators. We also measured the effect of DHA and EPA on microglia-mediated myelin phagocytosis and microglial polarization. For *invivo* studies, we used cuprizone model of demyelination. 5 week-old C57/BL6 mice were fed for 5 weeks with a diet containing 0.2% cuprizone (CPZ) mixed into a regular laboratory rodent diet with low n-3 PUFAs concentration (0.3%) or into a regular diet supplemented with n-3PUFAs (DHA+EPA, 15g/kg). Sensorimotor and cognitive functions were assessed by Rotarod and Morris water maze test, respectively. Demyelination was quantified by immunohistochemistry staining. Microglial polarization were evaluated by measuring the expression of M1 and M2 phenotypic markers at the end of 5 weeks of cuprizone diet.

Results: DHA and EPA concentration-dependently inhibited the microglial release of inflammatory mediators, including nitric oxide (Figure 1A and 1B) and tumor necrosis factor-α (Figure 1C and 1D), upon IFN-γ and myelin stimulation. DHA and EPA also enhanced phagocytosis of Cy3-labeled myelin (Figure 1E-1G). Further studies demonstrated that DHA and EPA can shift microglial polarization toward the M2 phenotype under physiological *in vitro* condition and inhibit M1 polarization under inflammatory conditions. In *vivo* studies demonstrated that n-3 PUFA supplementation reduced cuprizone-induced demyelination as revealed by enhanced Luxol fast blue staining and MBP staining of myelin. n-3 PUFA supplementation also improved motor and cognitive functions in cuprizone mice as compared tiregular diet control. These beneficial effects of n-3 PUFAs were accompanied by a shift in microglial polarization toward the M2 phenotype.

Conclusions: Our finding suggeststhat n-3 PUFAs may be clinically useful as immunomodulatory agents fordemyelinating diseases through a novel mechanism involving microglial phenotype switching.

Keywords: n-3PUFA, microglia, myelin, inflammation, polarization, cuprizone, multiple

sclerosis

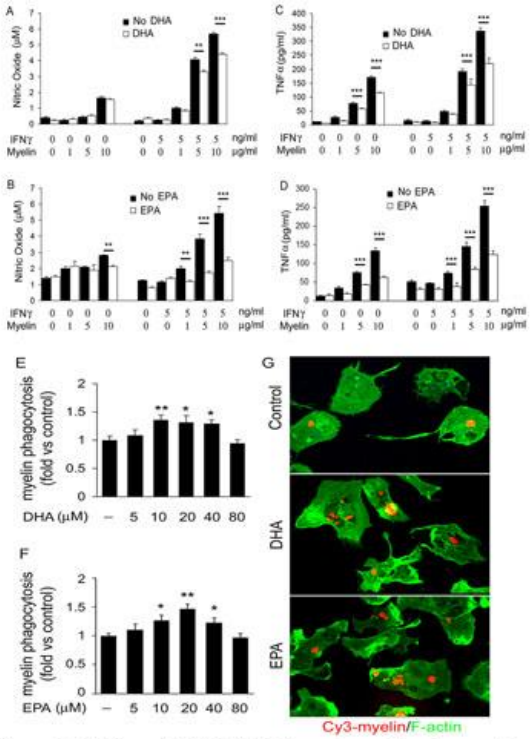

Figure 1. DHA and EPA inhibit the microglial release of inflammatory mediators upon IFN-γ and myelin stimulation, and enhance myelin phagocytosis.

425
BRAIN-0660
Poster Session

Neuroinflammation

A TH2-PROMOTING CYTOKINE LIMITS BRAIN INJURY AFTER CEREBRAL ISCHEMIA IN TH1-DOMINANT MICE

S. Zhang[1], H. Kim[1], G. Drummond[1], C. Sobey[1]
[1]Pharmacology, Monash University, Clayton, Australia

Objective. Brain inflammation is a major contributor to secondary injury and infarction following ischemic stroke, and is thought to be associated with T helper type-1 (Th1) immune reactions within the injured brain tissue. However, it is unknown whether brain injury and functional deficits can be limited by acute therapy to modulate a Th1-type response while promoting a Th2-type immune response.

Aims. We tested if acute administration of interleukin 33 (IL-33), a Th2-promoting cytokine, can reduce brain inflammation and improve functional outcome in Th1-dominant C57BL/6 mice.

Methods. Male mice (total n=175) were treated with vehicle (1% bovine serum albumin) or IL-33 (2 μg, i.p.) 24 h before and 1 h after cerebral ischemia (n=139) or sham surgery (n=36). Mice were anesthetised with ketamine (80 mg/kg) and xylazine (10 mg/kg) i.p. and underwent either sham surgery or filament-induced middle cerebral artery occlusion for 1 h followed by reperfusion for 1 or 3 days when neurological deficit scoring and hanging grip assessments were performed. Antibiotics (ampicillin and gentamycin, 300 mg/kg and 12 mg/kg, respectively, s.c.) were administered to some mice (n=17) in combination with IL-33. Some mice received only post-stroke treatment with IL-33 plus antibiotics (n=13) or vehicle (n=16) daily for 3 days. Brains were frozen and sections (30 μm) were stained with thionin for infarct analysis.

Results. Brain infarct volume was reduced by ~40% following IL-33 treatment, as compared to vehicle (26±3 mm^3 versus 44±5 mm^3, respectively, n=13-16; $P<0.05$). Flow cytometric analysis indicated that IL-33 reduced pro-inflammatory monocytes and macrophages in ischemic brains, as compared to vehicle (n=5-9; $P<0.05$). However, mortality and neurological deficit were exacerbated by IL-33 alone ($n\geq18$; $P<0.01$). Nevertheless, IL-33 combined with antibiotics protected brains from ischemic injury after stroke to a similar degree as did IL-33 alone (n=8-16; $P<0.05$), but also improved functional deficits to be similar to or less than those exhibited by vehicle-treated mice. These effects were sustained for at least 3 days, even when therapy was commenced after cerebral ischemia.

Conclusions. These data indicate that acute administration of a Th2-promoting cytokine together with antibiotics limits brain injury and functional deficits after stroke. The detrimental effect of IL-33 alone on functional status is likely to be due to increased bacterial infection

occurring in association with the promotion of Th2 immunity following stroke. Post-stroke cytokine therapy in combination with antibiotics may therefore be a feasible approach for limiting brain injury in acute ischemic stroke patients.

426
BRAIN-0778
Poster Session

Brain Edema

OFF-TARGET EFFECTS OF AQUAPORIN 4 RNA INTERFERENCE ON CONNEXIN 43 EXPRESSION VIA CHANGES OF MICRORNA EXPRESSION: CONSEQUENCES ON ASTROCYTE GAP-JUNCTIONS AND NEUROIMAGING

A. Jullienne[1], A. Fukuda[1], A. Ikova[2], N. Nishiyama[1], J. Coats[1], C. Ries[2], S.S. Bertrand[2], A. Obenaus[1], J. Badaut[2]
[1]Department of Pediatrics, Loma Linda, Loma Linda, USA
[2]UMR 5287 INCIA, CNRS, Bordeaux, France

Background: Water movement in the brain is critical for cellular function by regulating cell volume, and homeostasis within extracellular and intracellular compartments. We previously showed a 27% decrease in the expression of the water channel, aquaporin 4 (AQP4), after intracortical injection of siRNA targeting AQP4 (siAQP4) in rat wherein water mobility was decreased by 50% within the cortex. It has also been previously reported that siAQP4 also resulted in a decreased expression of the gap junction protein connexin 43 (Cx43) in primary astrocyte cultures. Interestingly, the absence of Cx43 and Cx30 modifies the distribution of AQP4 in astrocytic endfeet.

MicroRNA (miRNA) are small (21-22 nucleotides) noncoding RNA, which have regulatory activities in animals. Several miRNAs target both AQP4 and Cx43 messenger RNA and may regulate simultaneously the level of expression of AQP4 and CX43. We hypothesized that the off-target effects of siAQP4 on Cx43 expression occur via modifications of expression of miRNA targeting both proteins.

Methods: P17 rats were intracortically injected with siAQP4, siCx43 or siGLO (control), on days 0 and 2. On day 3, animals were euthanized after T2WI, DWI and Diffusion Tensor Imaging (DTI) scans. Animals were used for protein assessment (western blot and immunohistochemistry) and for miRNA assessment (PCR). To determine miRNA targeting both AQP4 and Cx43 we used both literature and database searches (targetscan.org and microrna.org). We selected 6 miRNA (miR19a, miR23a, miR130a, miR224, miR381, miR384) that were the most conserved between species.

Primary astrocyte cultures were prepared and transfected with siAQP4 to assess by western blot the effects on Cx43 expression and quantitative RT-PCR for miRNA expression. Astrocytes are connected with gap-jonctions. The effects of CX43 changes on the gap-junctions were tested by intracellular injection of Lucifer yellow (LY) in one astrocyte and measurement of LY fluorescence diffusion through these gap-junctions.

Results: Western blot and immunohistochemistry showed that siAQP4 injection indeed resulted in decreased levels of Cx43 *in vivo* compared to siGLO-injected rats and a 50% decrease in water mobility (DWI). Injection of siAQP4 also induced major changes in DTI parameters with a 12% decrease in radial diffusion and 20% increase in relative anisotropy in the parietal cortex. In contrast, injection of siCx43 did not alter AQP4 levels and no changes in T2WI or DWI were observed. The decreased expression of Cx43 in siAQP4 treated animals relative to controls was associated with a 40% up-regulation of miR224. In contrast, siCX43 induced a decrease of miR224. The consequences of the decrease of Cx43 on astrocyte gap-junctions are now under evaluation using astrocyte cultures, where we observed a decrease of Cx43 following application of siAQP4.

Discussion: The increased miRNA expression could be a molecular mechanism explaining in part the effects of siAQP4 on Cx43 expression. Decreased CX43 is not sufficient to induce changes in brain water mobility; AQP4 decreases are mandatory to drive the reduction in water mobility. Moreover,

AQP4 can actively modulate the directionality of water diffusion in the cortex, suggesting a role of the astrocyte in changes of DTI signals in grey matter.

427
BRAIN-0685
Poster Session

Brain Edema

ROLE OF COTRANSPORTERS IN SPREADING DEPOLARIZATION-INDUCED NEURONAL SWELLING.

S.A. Kirov[1], A.B. Steffensen[2], J. Sword[3], D. Croom[3], N. MacAulay[2]
[1]Neurosurgery,
Medical College of Georgia Georgia Regents University, Augusta, USA
[2]Cellular and Molecular Medicine,
University of Copenhagen, Copenhagen, Denmark
[3]Brain and Behavior Discovery Institute,
Medical College of Georgia Georgia Regents University, Augusta, USA

Objectives:
Spreading depolarizations (SDs) are waves of sustained neuronal and glial depolarization that propagate massive disruptions of ion gradients through the brain. SD is associated with migraine aura and recently recognized as a novel mechanism of injury in stroke and brain trauma patients. During SD, the interstitial space shrinks dramatically reflecting abrupt cytotoxic edema manifested by profound neuronal swelling and dendritic beading with spine loss. The molecular mechanisms generating the focal volume increase underlying SD-induced dendritic beading remain elusive. Simple osmotically-obliged water entry during SD is unlikely to cause beading as membranes of pyramidal neurons display low intrinsic osmotic water permeability due to lack of expression of membrane-bound aquaporins[1]. We hypothesized that dendritic beading, at least in part, occurs secondary to the large SD-induced changes in ion and lactate concentrations. A range of cotransport proteins carry the inherent ability to cotransport water along their translocation mechanism in a manner independent of transmembrane osmotic forces[2]. We propose that SD-induced alterations in transmembrane ion and lactate concentrations activate select cotransporters which then act as the molecular mechanisms responsible for dendritic bead formation. Here, we search for evidence that Cl^--coupled and lactate transporters participate in SD-induced dendritic beading.

Methods:
We used B6.Cg-Tg(Thy1-EGFP)MJrs mice expressing EGFP in sparse subsets of neocortical and hippocampal pyramidal neurons. SD was induced in hippocampal slices and *in vivo* by focal KCl-microinjection. The ensuing dendritic beading was visualized by 2-photon microscopy while simultaneously recording SD.

Results:
We confirmed that dendritic beading failed to arise during large (100 mOsm) hyposmotic challenges, underscoring that neuronal swelling does not occur as a simple osmotic event. SD-induced beading was not prevented by pharmacological interference with the cytoskeleton, supporting the notion that dendritic beading may entirely result from excessive water influx. Dendritic beading was strictly dependent on the presence of Cl^- and accordingly, combined blockade of Cl^--coupled transporters, in addition to lactate transporters, led to a significant reduction in beading without interfering with SD. Furthermore, our *in vivo* data showed a strong inhibition of dendritic beading upon pharmacological blockage of these cotransporters.

Conclusions:
We conclude that SD-induced dendritic beading does not require cytoskeletal rearrangement and is independent of osmotic forces. Extracellular [Cl^-] was not critical for SD generation but essential for the ensuing dendritic beading which, at least in part, took place as a consequence of the altered driving forces, transport direction and activity of a select few neuronal cotransporters. These cotransporters, to some extent, share the ability to cotransport water during their translocation mechanism, in a manner independent of osmotic forces, thereby

contributing to SD-induced beading. We have, by this experimental approach, provided evidence for the SD generation and the dendritic beading occurring by separate molecular mechanisms.

References:

1. Andrew, RD. et al. Physiological evidence that pyramidal neurons lack functional water channels. *Cereb Cortex* **17:**787-802 (2007).
2. MacAulay, N., Zeuthen, T. Water transport between CNS compartments: contributions of aquaporins and cotransporters. *Neuroscience* **168**:941-956 (2010).

Supported by the NIH NS083858 and the American Heart Association 12GRNT16570006 (SAK) and by Thorberg's Foundation (NM).

428
BRAIN-0599
Poster Session

Brain Edema

THE CELLULAR MECHANISMS OF NEURONAL SWELLING UNDERLYING CYTOTOXIC BRAIN EDEMA

R.L. Rungta[1], H.B. Choi[1], J.R. Tyson[1], A. Malik[1], L. Dissing-Olesen[1], P.J.C. Lin[2], S.M. Cain[1], P.R. Cullis[2], T.P. Snutch[1], B.A. MacVicar[1]
[1]Djavad Mowafaghian Centre for Brain Health, University of British Columbia, Vancouver, Canada
[2]Biochemistry and Molecular Biology, University of British Columbia, Vancouver, Canada

Objectives: Cytotoxic brain edema is the principal cause of mortality following brain trauma and cerebral infarct yet the mechanisms underlying neuronal swelling are poorly understood. Neuronal swelling occurs as a result of multiple depolarizing triggers that increase $[Na^+]_i$ including excessive glutamate receptor activation, intense neuronal spiking, activation of non-selective cation channels and inhibition of Na^+, K^+, ATPase. Our experiments were designed to examine the interrelationship between neuronal volume, intracellular Na^+ ($[Na^+]_i$) and intracellular Cl^- ($[Cl^-]_i$) in order to investigate the roles for Cl^- entry pathways that contribute to neuronal swelling leading to cell death.

Methods: Two-photon imaging of cell morphology and fluorescence lifetime measurements (FLIM) of $[Na^+]_i$ and $[Cl^-]_i$ in hippocampal and cortical neurons in acutely prepared brain slices were combined to specifically examine the relationship between increased $[Na^+]_i$, subsequent $[Cl^-]_i$ changes and neuronal swelling. The cytotoxic nature of this swelling was measured by lactate dehydrogenase (LDH) efflux. Pharmacological blockers of known Cl^- channels and exchangers were further examined in order to determine the relative contribution of different Cl^- loading pathways to neuronal swelling. Finally, a lipid nanoparticle (LNP) strategy to introduce siRNA into neurons *in vivo* (Rungta et al., 2013) was employed to determine the exact Cl^- pathway critical and required for the majority of neuronal swelling.

Results: Neuronal swelling and death was triggered by activating either voltage-gated sodium channels or NMDA receptors and was independent of Ca^{2+} entry but required Cl^- entry via an unknown pathway. We quantified the intracellular sodium and chloride concentration of individual cortical neurons as they swelled using fluorescence lifetime imaging. To identify the novel chloride influx pathway that caused neuronal swelling we first took a pharmacological approach to narrow down a list of candidates followed by siRNA knockdown of these targets using LNP delivery systems. Surprisingly, knockdown of a previously unidentified neuronal chloride channel attenuated both neuronal swelling and a Cl^- current that was activated when cortical neurons were depolarized to membrane potentials > -20mV.

Conclusions: We conclude that cytotoxic brain edema occurs when sufficient Na^+ influx depolarizes neurons to activate Cl^- entry, thereby causing subsequent neuronal swelling leading to neuronal death. The identification of a unique Cl^- channel that is activated by depolarization as a significant Cl^- entry pathway during pathological swelling triggered after Na^+ entry suggests that new strategies could be developed towards reducing brain edema. There are numerous

different pathways for Na^+ entry that are activated during conditions such as hypoxia, stroke and TBI. Our observations that cell death is significantly reduced when overall Cl^- entry is prevented suggests that therapeutic strategies to inhibit the distinct and predominant Cl^- entry pathway may have widespread benefit towards treating these different conditions.

References:

Rungta, R.L., Choi, H.B., Lin, P.J., Ko, R.W., Ashby, D., Nair, J., Manoharan, M., Cullis, P.R., and Macvicar, B.A. (2013). Lipid Nanoparticle Delivery of siRNA to Silence Neuronal Gene Expression in the Brain. Molecular therapy Nucleic acids *2*, e136.

429
BRAIN-0233
Poster Session

CNS Trauma

ACUTE STAGES OF CONCUSSION: SUPPRESSION OF BLOOD PRESSURE DURING POSTURAL HEMODYNAMIC DRIVES

S. Bishop[1], R. Dech[1], K. Aravinthan[1], T. Baker[1], T. Burnett[2], M. Butz[1], J.P. Neary[1]
[1]Kinesiology and Health Studies, University of Regina, Regina, Canada
[2]School of Health and Exercise Sciences, University of British Columbia, Kelowna, Canada

This project investigated the potential for altered blood pressure regulation via postural changes in healthy and concussed participants.

Male hockey athletes (n=170; aged 17-24 yrs) were recruited from within the university, the Western Hockey League, and the Junior Hockey League. Concussed participants (n=12) were recruited from within these leagues, and were symptomatic at time of testing (24 - 72 hours post-injury).

All participants had beat-to-beat blood pressure, electrocardiography, and expired gases analyzed. Resting measures (5min), and a cyclical postural challenge consisting of 10s body-weight squatting, followed by 10s of standing, was performed (0.05 Hz, the driven frequency). Systolic, diastolic, and mean arterial pressure (MAP) slopes were measured for the early (0 – 6s), and late (6 - 10s) phases of squatting and standing. The average peak pressure was calculated from 4-7s during squatting and standing; as was the 10s average for both squatting and standing.

During the squat phase, peak average pressure (4-7s average) for systolic (166.21 mmHg vs. 148.26mmHg; $p<.01$), diastolic (89.78 mmHg vs. 84.12 mmHg; $p<.05$), and MAP (115.23 mmHg vs 105.51 mmHg; $p<.01$) were all significantly lower in the concussed group. Overall 10s averages when squatting for systolic (154.16 mmHg vs. 137.30 mmHg; $p < 0.01$), diastolic (84.65 mmHg vs. 79.03 mmHg; $p<0.05$), and MAP (107.80 mmHg vs. 98.44 mmHg; $p< 0.01$), were also significantly supressed in the concussion group. Additionally, the 10s average for systolic pressure during the stand phase (118.80 mmHg vs. 107.79 mmHg; $p<0.05$) was reduced with concussion.

These results indicate that the decreases in pressure during a mild hemodynamic drive are associated with transient perturbations of flow-pressure autoregulation.

430
BRAIN-0845
Poster Session

CNS Trauma

NEUROPATHOLOGY IN APP/PS1 MICE IS EXACERBATED AFTER CHIMERA (CLOSED-HEAD IMPACT MODEL OF ENGINEERED ROTATIONAL ACCELERATION)-INDUCED TRAUMATIC BRAIN INJURY

W.H. Cheng[1], D.R. Namjoshi[1], K.M. Martens[1], A. Wilkinson[1], T. Ward-Able[1], A. Hayat[1], K.A. McInnes[2], P.A. Cripton[2], C.L. Wellington[1]
[1]Pathology and Laboratory Medicine, Djavad Mowafaghian Centre for Brain Health, Vancouver, Canada

[2]*Mechanical Engineering and Orthopaedics, International Collaboration on Repair Discoveries, Vancouver, Canada*

Objectives

Traumatic brain injury (TBI) may increase risk of Alzheimer Disease (AD) up to 10 folds. In particular, mild TBI, which comprises over 75% of all TBI cases, upon repetitive exposure may lead to long-term development of neurodegeneration with Alzheimer-like neuropathologies. This study aims at investigating if mild repetitive TBI exacerbates neuropathologies in an AD mouse model.

Methods

The novel experimental rodent TBI model recently developed by our laboratory - Closed-Head Impact Model of Engineered Rotational Acceleration (CHIMERA) is used to induce impact-acceleration type of closed-head TBI. We subjected 5-mo male APP/PS1 mice to two consecutive mild TBI spaced 24 hours apart. The mice were sacrificed at 2 days after TBI. Behavioral tests were conducted to assess neurological deficits and motor functions. Histological and biochemical assays were performed to assess amyloid, axonal, microglial, and cerebrovascular changes after TBI.

Results

In 5-mo APP/PS1 mice, immediately after TBI they suffered a prolonged loss of righting reflex compared to age-matched sham-operated APP/PS1 controls. By 2 days post-TBI, they showed increased neurological deficits (neurological severity score) and poorer motor coordination (Rotarod), compared to sham-operated APP/PS1 mice. Immunohistochemical staining revealed that 6E10+ve amyloid deposits were increased by 2 days post-TBI. TBI also led to Iba-1 microglial activation, argyrophilic fibre staining (silver staining) and axonal bulb-like structures (phosphorylated neurofilaments) in white matter tracts including optic tract and brachium of superior colliculus. TBI also induced brain A-beta level at 2 days post-TBI. Cerebrovascular changes are being assessed by studying changes in cell adhesion molecules, tight junction proteins and serum protein extravasation.

Conclusions

These findings suggest that mild repetitive TBI acutely exacerbates neuropathology in APP/PS1 mice. The long term consequences of mrTBI in the trajectory of Alzheimer pathology is currently being studied.

431
BRAIN-0647
Poster Session

CNS Trauma

USING FUNCTIONAL NEAR-INFRARED SPECTROSCOPY TO MAP REDUCED INTER-HEMISPHERIC CONNECTIVITY IN PEDIATRIC CONCUSSION PATIENTS

J.F. Dunn[1], K.J. Urban[1], B.G. Goodyear[1], K.M. Barlow[2]
[1]Radiology, University of Calgary, Calgary, Canada
[2]Pediatrics and Clinical Neuroscience, University of Calgary, Calgary, Canada

OBJECTIVES

It is of significant clinical importance to be able to detect changes in the brain after a mild traumatic injury or concussion. It is likely that there is damage to major white matter tracts.[3] This leads to the hypothesis that regional brain communication is impaired. We applied fNIRS to study functional connectivity[6] in brain as a marker of the integrity of inter-regional communication in pediatric mild traumatic brain injury patients.

Fluctuations in brain activity result in fluctuations in microvascular hemoglobin oxygenation, and brain regions in communication exhibit similar hemodynamic frequencies.[1] We showed that, by measuring frequency responses in the motor cortex, we could detect reduced functional connectivity in patients with MS[4] and with chronic

post-concussion symptoms[5]. This is consistent with the concept that both demyelinating disease and structural damage would cause reduced communication in brain.

We describe the method and current results from pediatric mild traumatic brain injury patients.

METHODS

A TechEn CW5 system was used for fNIRS acquisition[2] and HoMER software used to calculate temporal changes in oxy- and deoxhemoglobin. Data were collected from the left and right motor cortex during rest and finger tapping. Coherence analysis was performed at frequencies from 0.02 to 50 Hz. We map regional fluctuations in oxy- and deoxyhemoglobin in the left and right motor cortex. Eight pediatric controls were used to study the sensitivity of coherence to the frequency. Thirteen mTBI patients and 8 controls were studied for coherence during the resting and task activation state.

RESULTS

The largest coherence from inter-hemispheric data were obtained at frequencies of 0.04 to 2 Hz. The lowest coherence was from 4-10Hz. Data from 10-50Hz was analysed as one band and showed similar coherence values to the lower frequencies. During the motor task, interhemispheric coherence was significantly reduced in pediatric patients with chronic post-concussion symptoms.

CONCLUSION

fNIRS data indicate that there can be reduced regional communication in pediatric brain injury patients. fNIRS offers unique capabilities in that it is portable, can measure changes in oxy- and deoxyhemoglobin content and can make these measurements at a higher frequency than can MRI.

REFERENCES

1. Damoiseaux, J. S., S. A. Rombouts, F. Barkhof, P. Scheltens, C. J. Stam, S. M. Smith and C. F. Beckmann (2006) Proc Natl Acad Sci U S A **103**(37): 13848-53.
2. Franceschini, M. A., D. K. Joseph, T. J. Huppert, S. G. Diamond and D. A. Boas (2006) J Biomed Opt **11**(5): 054007.
3. Henry, L. C., J. Tremblay, S. Tremblay, A. Lee, C. Brun, N. Lepore, H. Theoret, D. Ellemberg and M. Lassonde (2011) J Neurotrauma **28**(10): 2049-59.
4. Jimenez, J. J., R. Yang, N. Nathoo, V. Varshney, A.-M. Golestani, B. G. Goodyear, L. M. Metz and J. F. Dunn (2014) J. Biomed. Optics **19**(7): 076008.
5. Urban, K. J., K. Barlow, B. G. Goodyear, J. J. Jimenez and J. F. Dunn (2015) J Neurotrauma.
6. Varshney, V., N. Liaponova and J. F. Dunn (2012) J. Europ. Optical Soc. **7**: 12047.

432
BRAIN-0725
Poster Session

CNS Trauma

EARLY CEREBRAL CIRCULATORY DISTURBANCE IN PATIENTS SUFFERING TRAUMATIC BRAIN INJURY: XENON COMPUTED TOMOGRAPHY AND PERFUSION TOMOGRAPHY STUDY

M. HONDA[1], R. Ichibayashi[1], H. Yokomuro[1], K. Yoshihara[1], H. Masuda[2], J. Nomoto[2], T. Kishi[3], S. Sase[4]
[1]Critica Care Center, Toho University Medical Center Omori Hospital, Tokyo, Japan
[2]Neurosurgery, Toho University Medical Center Omori Hospital, Tokyo, Japan
[3]Education Planning and Development Faculty of Medicine School of medicine, Toho University, Tokyo, Japan
[4]R &D, Anzai medical Co. LTD., Tokyo, Japan

(Objectives) Traumatic brain injury (TBI) is widely known to cause dynamic changes in cerebral blood flow (CBF). Ischemia is a common and deleterious secondary injury following TBI. Detecting early ischemia in TBI patients is important to prevent further advancement and

deterioration of the brain tissue. The purpose of this study was to clarify the cerebral circulatory disturbance during the early phase and verify whether it could be used to predict patient outcome.
(Methods) A total of 90 patients with TBI underwent simultaneous xenon computed tomography (CT) and perfusion CT to evaluate cerebral circulation on Days 1-3. CBF was measured using xenon-CT (Xe-CT) and the MTT using perfusion CT and calculated cerebral blood volume (CBV) using the AZ-7000W98 computer system. The neurological grade at the onset of treatment
was evaluated with Glasgow Coma Scale (GCS) and outcome was evaluated with the Glasgow Outcome Scale (GOS). The relationship of he hemodynamic parameters CBF, MTT, and CBV to GCS, GOS were examined.

(Results) CBF values increased as GCS at the onset of treatment decrease, although there were no significant differences. MTT values increased as GCS at the onset of treatment increase, although there were no significant differences. CBV values also had no relation with GCS at the onset of treatment. Patients with favorable outcome (GR and MD) had significantly higher CBF and lower MTT than those with unfavorable outcome (SD, VS, or D). Discriminant analysis of these parameters could predict patient outcome with a probability of 70.6%. (Conclusions) This study revealed reduced CBF and prolonged MTT in early phase of severe TBI. These changes of parameters were thought to have been caused by elevated intracranial pressure and cerebral microvascular disturbance. Therefore, CBF reduction and MTT prolongation might influence the clinical outcome of TBI. These parameters are helpful for evaluating the severity of cerebral circulatory disturbance and predicting the outcome of TBI patients.

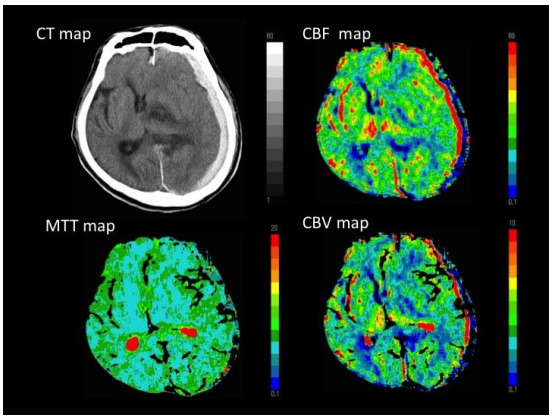

433
BRAIN-0697
Poster Session

CNS Trauma

TIME- AND DOSE-DEPENDENT EFFECTS OF ETHYL PYRUVATE ON HISTOLOGICAL DAMAGE, INFLAMMATORY RESPONSE AND NEUROLOGICAL DEFICITS AFTER CONTROLLED CORTICAL IMPACT (CCI) IN THE RAT

O. Kempski[1], D. Jussen[2], N.I.N.A. Wenda[1], L. Müller[1], M. Mader[1], D. Heimpel[1], B.E.A.T. Alessandri[1]
[1]Inst. Neurosurgical Pathophysiology, University Medical Center, Mainz, Germany
[2]Dept. Neurosurgery, Horst-Schmidt-Clinic, Wiesbaden, Germany

Objective: The inflammatory response after traumatic brain injury (TBI) plays an important role for the development of trauma-associated cerebral damage. The prevention of this inflammatory reaction could therefore show neuroprotective
potential. Ethyl pyruvate (EP), a stable derivative of pyruvate, suppresses the inflammatory reaction after sepsis, hemorrhagic shock, cerebral ischemia and controlled cortical impact. Neuroprotective effects of EP that was injected within the first 24h after CCI could be shown within 3 days after CCI but disappeared after one month of observation (Moro and Sutton, 2010). The aim of this study was to examine the time- and dose-dependent effects of a long-term treatment regimen (14

days) with EP on histological damage, inflammatory response and functional recovery after CCI.

Methods: Male Sprague-Dawley rats were anesthetized with chloral hydrate and mechanically ventilated during surgical preparation, injury induction and pre- and post injury monitoring (mean arterial pressure, MAP; cerebral blood flow, CBF). They were subjected to CCI (4m/s, 200ms, 2mm) or sham operation. They were assigned to one of two experiments. In experiment 1 EP at a dose of 25, 50 or 75 mg/kg (n=28) or vehicle (n=10) were injected 30 minutes after CCI and thereafter daily for 14 days. In experiment 2 vehicle (n=12) or EP (75 mg/kg; n=12) were injected daily until brains were removed 3h, 24h or 72h after CCI. Animals were tested for neurological deficits (beam-walk- and beam-balance-test) on day 13 post-CCI. Injury volume was determined on hematoxylin-eosin stained brain sections. Inflammatory reaction was analyzed with immuno-staining for microglia (IBA), activated astrocytes (GFAP) and interleukine-1b.

Results: EP at all doses studied led to a significant reduction of the neurological deficits after CCI. EP had no influence on CBF. Treatment with EP during 14 days, however, did not reduce cortical damage significantly although the group treated with 75mg/kg EP showed a significantly smaller lesion at day 3 post-CCI ($p<0.05$), and with the smallest lesions on day 14 post-CCI (n.s. vs. vehicle: 9.18 ± 1.17 mm^3; 75 mg/kg: 7.31 ± 0.64 mm^3). 75mg/kg EP reduced significantly the immuno-reactive area of GFAP and Iba-1 at day 3, but not at day 14 post-CCI. IL-1b tended to be smallest after 14 days of treatment with 75 mg/kg EP (n.s.).

Conclusion: Effects of repetitive EP treatment on lesion volume and inflammatory reaction could be observed only during the first days after CCI. Later a tendency to improve histology and inflammation was still seen with the highest EP dose. However, EP reduced significantly behavioral deficits following CCI. These findings are in accordance with results from Moro and Sutton (2010) who treated rats only within the first 24h after CCI. Thus, EP may exerts its effects on pathophysiological mechanisms which are initiated early after injury and repetitive treatment is not necessary after brain injury.

References:

Moro N, Sutton RL: (2010) Beneficial effects of sodium or ethyl pyruvate after traumatic brain injury in the rat. Experimental neurology 225:391-401.

434
BRAIN-0812
Poster Session

CNS Trauma

NOVEL CARBON NANOPARTICLES ARE CATALYTIC ANTIOXIDANTS AND IMPROVE OUTCOME AFTER EXPERIMENTAL TRAUMATIC BRAIN INJURY AT A CLINICALLY RELEVANT TIME POINT

T.A. Kent[1], C.S. Robertson[2], R.L. Garcia[2], R.H. Fabian[1], R. Grill[3], J.M. Tour[4]
[1]Neurology, Baylor College of Medicine, Houston, USA
[2]Neurosurgery, Baylor College of Medicine, Houston, USA
[3]Neuroscience, University of Texas Health Science Center at Houston, Houston, USA
[4]Chemistry, Rice University, Houston, USA

BACKGROUND: Hemorrhagic shock worsens outcome even from mild traumatic brain injury (TBI). We previously demonstrated bursts of superoxide anion following acute TBI, another at the onset of hypotension, and a third during resuscitation (JCBFM 1995). Despite oxidative stress associated with TBI, no antioxidant has improved outcome clinically. We hypothesized (Trends Biotechnology, 2014) that traditional antioxidants possess 1 or more characteristics unfavorable to clinical use, including narrow selectivity, generation of toxic intermediates and requirement for regeneration by molecules consumed by the injury. Carbon nanoparticles have long been known to be antioxidants, but

several issues hindered their development. We developed a new class of carbon nanoparticle, 30-50nm size, the hydrophilic carbon cluster (HCC) from a severe oxidation of parent nanotubes. When pegylated (PEG), have a favorable half-life, and broad action against both superoxide and hydroxyl radical with no activity against nitric oxide. PEG-HCCs were protective against oxidative stress in tissue culture treated *after* mitochondrial toxin or hydrogen peroxide and completely restored cerebrovascular function and normalized oxidative profile in a rat model of experimental TBI accompanied by hypotension and resuscitation administered during blood resuscitation (J. Neurotrauma & ACS Nano 2013). We recently discovered that PEG-HCCs are extremely high capacity, catalytic SOD mimetics equally adept at quenching hyodroxyl radical (PNAS 2015). Here we tested longer term outcomes.

METHODS: Mild TBI was generated with closed cortical impact injury at 30 psi, impact velocity of 3 m/sec as previously described (Mathew/Robertson 2012) in male Long Evans rats (n=57). This model results in loss of autoregulation, impaired motor function and a cortical lesion only if accompanied by hemorrhagic hypotension/resuscitation. Hypotension was produced with blood withdrawal to a mean arterial pressure (MAP) of 40 mmHG. After 50 minutes, saline was administered to 50mmHG followed in 30 minutes by reinfusion of blood. PEG-HCCs or vehicle (PBS or water) were administered at a dose of 4mg/ml at the onset of blood reinfusion (80 minutes) and then repeated 2 hours later (based on a 2-3 hour half-life). Motor recovery was followed daily and histology for lesion size and Fluoro-jade positive staining obtained in a subgroup at 24 hours. Rats were included after blindly assessing the adequacy of hypotension and resuscitation.

RESULTS: PEG-HCCs treatment resulted in 61% reduction in lesion size p=.04; Fig. 1a) and reduced Fluoro-jade positive neurons in the impact zone by 73% (p=.03; data not shown). Treatment also prevented motor impairment (time to cross beam p<.001; Fig. 1b) and improved beam balance (p<.001). PEG-HCCs were generally well tolerated, although a non-significant increase in mortality (p=0.2) was seen when administered in water rather than buffer.

CONCLUSION: PEG-HCCs improved recovery from TBI in this model when administered at a clinically relevant time point, i.e. during definitive resuscitation from hemorrhagic shock, a time when there is access available to administer a potential medication. Our results suggest that oxidative stress continues to be a factor in outcome even at this later time point, perhaps reflecting reperfusion injury from resuscitation consistent with timing of superoxide bursts. Characterization of longer term behavioral outcomes is underway.

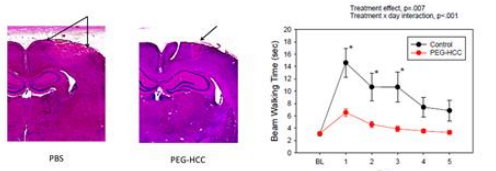

Figure 1. Left panel examples of H&E histology of lesion size 24 hours following mild CCI + Hemorrhagic hypotension. PEG-HCC treatment reduced lesion size by 61% (n=19; p=.04). Right panel: Motor function tested daily, time to cross a 1 meter beam. PEG-HCC treatment prevented significant decrement compared to control (n=38; p=.007).

435
BRAIN-0430
Poster Session

CNS Trauma

DEMONSTRATION OF SUBCLINICAL AUTONOMIC DYSFUNCTION AND EXPLORING THE POTENTIAL OF HEART RATE VARIABILITY AND IL 10 AS BIOMARKERS IN TRAUMATIC BRAIN INJURY: A PILOT STUDY

A. Kumarasamy[1], *D. Shukla*[2], *C. Rita*[3], *T.N. Sathyaprabha*[4], *B. Indira Devi*[2]
[1]*Clinical Neurosciences, National Institute of Mental Health and Neurosciences, Bangalore, India*
[2]*Neurosurgery, National Institute of Mental Health and Neurosciences, Bangalore, India*
[3]*Neurochemistry, National Institute of Mental Health and Neurosciences, Bangalore, India*

[4]*Neurophysiology,*
National Institute of Mental Health and Neuroscie nces, Bangalore, India

Objectives: We explored the subclinical autonomic dysfunction following severe Traumatic Brain Injury (TBI) by serially monitoring the Heart rate Variability (HRV) parameters. We also investigated the longitudinal pattern of serum levels of InterLeukin 10 (IL10) following severe TBI.

Methods: The subjects for the study were recruited from the emergency services of our institute after obtaining informed consent from the patient's nearest kin.The study was approved by the Institute ethics committee. BioHarness™ (Zephyr technologies) a non-invasive telemetry device was used to procure the Lead II ECG. The recordings were done on day 1, day 3 and day 10 after trauma. A 5 minute artifact free segment of the recording was analyzed with the LabChart© software. The serum samples were collected on day 1, day 3 and day 10 after trauma. The serum levels of IL10 were quantitatively analyzed using enzyme-linked immuno assay (ELISA). Appropriate statistical measures were applied to the analysis of the data.

Results: A total of 30 patients with severe TBI (GCS <= 8) were recruited in our study. The mean age of the patients was 32.44 ± 9.26 years. Male to female ratio was 6.5:1. In patients, all the mean values of both time domain and frequency domain parameters were less than the normal expected values. There was significant reduction in the Standard Deviation of NN intervals (SDNN) (p= 0.03), Low Frequency (LF) (p=0.03) and High Frequency power (HF) (p=0.04) on day 1 recording, in patients who died when compared with the patients who survived. Similarly the LF and HF power on day 10 were also significantly reduced in patients with unfavorable outcome. The mean SDNN, RMSSD and all frequency domain parameters showed a serially increasing trend in survivors and a longitudinally decreasing trend in patients who died. Though there was no significant difference in serum levels of IL10 between groups on day 1, the levels significantly decreased in survivors from day 3 (p=0.02). There was significant difference between the serum levels of IL 10 on day 10 between the groups (p=0.04). There was no significant correlation between sympathovagal balance and IL10.

Conclusion: This pilot study reveals the definitive autonomic dysfunction following severe TBI. It also shows that there is significant autonomic dysfunction in subjects with unfavorable outcome as compared to the survivors. Autonomic dysfunction occurs invariably in these patients due to the damage to the central autonomic network, but the degree of dysfunction varies between subjects with favorable and unfavorable outcome. In this study, the IL10 values were found to be increased in patients who died. IL10 being an anti inflammatory cytokine, increased levels of it might lead to a detrimental outcome in these subjects with severe TBI. We suggest that HRV parameters and IL10 can be considered as adjunct predictors of mortality in severe TBI.

436
BRAIN-0123
Poster Session

CNS Trauma

EVALUATION OF MICROTHROMBOSIS IN THE PARENCHYMAL CIRCULATION AFTER EXPERIMENTAL TRAUMATIC BRAIN INJURY BY IN VIVO IMAGING – ROLE OF FACTOR XI

S.M. Schwarzmaier[1], *C. de Chaumont*[2], *M. Balbi*[3], *N.A. Terpolilli*[4], *C. Kleinschnitz*[5], *A. Gruber*[6], *N. Plesnila*[3]
[1]*Department of Anesthesiology and Institute of Str oke and Dementia Research, Ludwig-Maximilians-University, Munich, Germany*
[2]*Department of Neurodegeneration, Royal College of Surgeons in Ireland (RCSI), Dublin, Ireland*
[3]*Institute for Stroke and Dementia Research, Ludwig-Maximilians University, Munich, Germany*
[4]*Department of Neurosorgery and Institute for Str oke and Dementia Research, Ludwig-Maximilians University, Munich, Germany*
[5]*Department of Neurology, Julius-*

Maximilians University, Würzburg, Germany
[6]Knight Cardiovascular Institute,
Oregon Health & Science University, Portland, USA

Objective: Following traumatic brain injury (TBI), reduced cerebral perfusion is associated with poor outcome. Among other factors, the occlusion of cerebral microvessels by microthrombosis is believed to worsen cerebral perfusion after TBI. Since little is known about the dynamics and mechanisms of cerebral thrombogenesis after TBI, the aim of the current study was to investigate the formation of microthrombi after TBI in vivo and to determine the role of the intrinsic coagulation cascade for this process.

Methods: C57BL/6 (n=101) and $FXI^{-/-}$ mice (n=15) were subjected to TBI by controlled cortical impact injury (CCI). Wild type mice received a factor XI (FXI) inhibitory antibody (14E11) or control IgG 24 hours before or 30 minutes or two hours after CCI. The coagulation parameters aPTT and PT were determined in all treatment groups. Brain microvessels and microthrombi were visualized in vivo by 2-photon microscopy 2-3 hours after trauma and histopathological outcome was assessed 24 hours after CCI.

Results: Following TBI the number, volume, and sojourn time of microthrombi in the parenchymal microcirculation significantly increased as compared to sham operated animals ($p<0.001$). Pharmacological or genetic inhibition of FXI significantly prolonged aPTT ($p=0.008$) without affecting PT. This, however, did not reduce thrombogenesis and had no effect on lesion volume, hemispheric swelling, and intracranial hemorrhage.

Conclusion: TBI results in significant microthrombosis of pial and parenchymal microvessels. This process is independent of the intrinsic coagulation cascade since inhibition of FXI did not reduce microthrombosis and had no therapeutic effect after TBI. However, since inhibition of FXI does also not aggravate intracranial hemorrhage, inhibition of the intrinsic coagulation cascade seems to be safe after TBI.

437
BRAIN-0260
Poster Session

White Matter Injuries

SPOTTY AGGREGATION OF THE AMYLOID BODIES CONTRIBUTES TO THE RETENTION OF [11C]-PIB TO THE WHITE MATTER: A POSTMORTEM STUDY OF STROKE PATIENTS WITHOUT ALZHEIMER'S DISEASE

N. Funatsu[1], C. Yokota[1], H. Ishibashi-Ueda[2], T. Hashimoto[1], T. Hino[1], K. Koshino[3], K. Minematsu[1], K. Toyoda[1]
[1]Department of Cerebrovascular Medicine, National Cerebral and Cardiovascular Center, Suita, Japan
[2]Department of Pathology, National Cerebral and Cardiovascular Center, Suita, Japan
[3]Department of Investigative Radiology, National Cerebral and Cardiovascular Center, Suita, Japan

Objective

Pittsburgh Compound B([^{11}C]-PIB) is retained to amyloid-beta (Aβ) plaques in the graymatter of patients with clinically diagnosed Alzheimer's disease (AD). On theother hand, the nature of retention of [^{11}C]-PIB to the whitematter, frequently observed in the healthy individuals, has not been clarified,although [^{11}C]-PIB binding to the white matter was mainlynonspecific in an in-vitro study. The aim of this postmortem study is tocompare the distribution of Aβ deposition between the gray and white matters instroke patients without histopathological AD.

Methods

Five patients died of stroke between October2010 to March 2014 (1 woman, 71-83 years old, 4 hypertensive cerebralhemorrhages, 1 cerebral infarction) were examined histopathologically. Nopatients were diagnosed as having AD. Serial sections (5-7μm thick) fromformalin-fixed paraffin-embedded postmortem brain tissue were obtained fromboth sides of the cerebral cortices and centrum

semiovale in each patient.Hematoxylin-Eosin, Periodic acid-Schiff (PAS) staining and immunohistochemistryusing antibodies to Aβ were performed.

Results

Positive Aβ (10-20µm diameter) deposits withround disks were observed in both sides of the cerebral cortices and centrumsemiovale in all the subjects. No senile plaques were found. The Aβ positiveparticles were always stained with PAS, indicating the amyloid bodies. Amyloidbodies in the cerebral cortices distributed in a linear along the subpial zone,and those in the centrum semiovale aggregated spotty around the area ofdemyelination or perivascular spaces.

Conclusions

Amyloid bodies werenot only located in the subpial but also in the deep white matter of thepostmortem brains without AD. Aggregation of amyloid bodies in the deep whitematter could contribute to the [^{11}C]-PIB retention to the whitematter of healthy individuals.

References

(1)Fodero-Tavoletti,et al. J Nucl Med. 2009;50:198-204

438
BRAIN-0331
Poster Session

White Matter Injuries

BDNF-MEDIATED VECTORIZATION TO THE ISCHEMIC RAT BRAIN BY ULTRASOUND-TARGETED MICROBUBBLES DESTRUCTION IN SUBCORTICAL STROKE

B. Rodriguez-Frutos[1], J. Ramos-Cejudo[1], M. Gutiérrez-Fernández[1], L. Otero-Ortega[1], P. Martínez-Sánchez[1], I. Barahona-Sanz[1], M.T. Vallejo-Cremades[1], T. Navarro-Hernanz[2], E. Díez-Tejedor[1]
[1]Department of Neurology and Stroke Center Neuroscience and Cerebrovascular Research Laboratory,
La Paz University Hospital Neuroscience Area of IdiPAZ Health Research Institute Autónoma University of Madrid, Madrid, Spain
[2]Laboratory for Imaging and Spectroscopy by Magnetic Resonance (LISMAR),
Institute of Biomedical Research Alberto Sols CSIC-UAM, Madrid, Spain

Objectives-Ultrasound-targeted microbubbles destruction (UTMD) is a non-invasive imaging techniqueused in stroke patients routinely that could be use for drug delivery. In previous study of ourgroup, Brain-derivedneurotrophic factor (BDNF) administration has demonstrated efficacy on whitematter repair in subcortical stroke in rats[1]. The purpose ofthis study was to analyze whether the BDNF encapsulated in microbubbleswith focused ultrasound could be more effective than BDNF alone in an experimentalanimal model of subcortical ischemic stroke.

Methods-Ischemia was induced by injection of endothelin-1. MaleSprague-Dawley rats were randomly assigned inthree study groups: 1- BDNF alone (0.4µg/kg IV administered); 2- BDNF+UTMD (0.4µg/kgIV administered plus a single focused UTMD in the brain) and 3- Control (salineIV administered). The treatment was administered at 24h after stroke. Weanalyzed: Functional evaluation (Beam Walking, Rotarod and Rogers'

tests), lesionsize and Apparent Diffusion Coefficient (ADC) on Magnetic Resonance Imaging(MRI) as well as fiber tract integrity on tractography images. Cellular proliferation(KI-67) and white matter repair markers [A2B5; 2',3'-Cyclic-nucleotide3'-phosphodiesterase, CNPase; and myelin oligodendrocyte glycoprotein, MOG] at7d and 28d.

Results-The BDNF-treated animals showed less functionaldeficit than the controls ($p<0.05$). When we compared the animals treatedwith BDNF, BDNF+UTMD group showed significantlyless deficit compared to BDNF alone in Rogers' test at 28d ($p<0.05$).Although T2-MRI did not show differences in lesion size at 7d and 28d betweengroups, ADC maps showed higher diffusion coefficient both treated groups thancontrols at 28d ($p<0.05$). Regarding, Diffusion Tensor Imaging (DTI) tractographyanalysis revealed significantly better tract connectivity at 28d in the BDNF+UTMDin comparison with control and BDNF alone groups ($p<0.05$). Finally, thelevels of white matter repair markers (A2B5, CNPase and MOG at 7d) were higherin the BDNF+UTMD group than in the BDNF alone and control groups ($p<0.05$).

Conclusions-BDNFadministration with focused UTMD increased BDNF brain levels and improved functionaloutcome and white matter process implicated in brain repair (oligodendrogenesis,remyelination and fiber connectivity) compared to BDNF alone administrationafter subcortical ischemic stroke in rats.

References:

[1] *Ramos- Cejudo J,Gutiérrez- Fernández M, Otero-OrtegaL, Rodríguez- Frutos B, Fuentes B,Vallejo-Cremades MT, Navarro-Hernanz T, Cerdán S, Díez -Tejedor E. BDNF-administration mediated Oligodendrocyte Differentiation and Myelin Formation inSubcortical Ischemic Stroke. Stroke 2015; 46(1):221-8.*

This study was supported by research grants PS12/01754, INVICTUS SpanishNeurovascular Network RD12/0014/0006 and Research Institute Carlos III,Ministry of Science and Innovation of Spain.

439
BRAIN-0620
Poster Session

White Matter Injuries

AUGMENTATION OF CAROTID PULSE PRESSURE AND CEREBRAL BLOOD FLOW PULSATILITY IS ASSOCIATED WITH BRAIN WHITE MATTER NEURONAL FIBER INTEGRITY IN OLDER ADULTS

T. Tarumi[1], D. Zhu[2], J. Liu[1], J. Riley[3], M. Turner[3], K. Womack[4], D. Kerwin[5], M. Cullum[4], R. Zhang[6]
[1]Internal medicine, UT Southwestern Medical Center, Dallas, USA
[2]Radiology and Psychology, Michigan State University, East Lansing, USA
[3]Institute for Exercise and Environmental Medicine , Texas Health Presbyterian Hospital Dallas, Dallas, USA
[4]Psychiatry & Neurology and Neurotherapeutics, UT Southwestern Medical Center, Dallas, USA
[5]Texas Alzheimer's and Memory Disorders, Texas Health Presbyterian Hospital Dallas, Dallas, USA
[6]Internal medicine & Psychiatry & Neurology and Neurotherapeutics, UT Southwestern Medical Center, Dallas, USA

Objectives: Advanced age is the single most important risk factor for cognitive decline and dementia. Central arterial stiffness, a hallmark of vascular aging, is associated with brain structural damage and cognitive impairment; however, the underling mechanism(s) remains unclear. The neuronal fiber integrity of brain white matter (WM) is essential for cognitive function and is likely to be sensitive to changes in cerebral hemodynamics. Our recent study[1] demonstrates that age-related central arterial stiffening augments arterial pulse pressure and cerebral blood flow (CBF) pulsatility. The objective of this study was to determine the associations among central and cerebral hemodynamics, brain WM neuronal fiber integrity, and cognitive performance in older adults with normal

cognition (NC) and mild cognitive impairment (MCI). **Methods**: One-hundred forty participants aged 55-80 years (mean age=65±7 years), consisting of 90 NC and 50 MCI diagnosed by Petersen's criteria, were studied. Carotid-femoral pulse wave velocity (cfPWV) and carotid pulse pressure were measured by applanation tonometry. Global CBF and CBF pulsatility were measured by phase-contrast MR imaging and transcranial Doppler. Diffusion tensor imaging (DTI) was acquired to quantify neuronal fiber integrity of brain WM, as assessed by fractional anisotropy (FA) along with radial (RD) and axial (AD) diffusivities. Neurocognitive assessment of memory (California Verbal Learning Test) and executive function (Trail Making Test) were conducted in a subset of 68 subjects. **Results**: MCI patients showed deteriorated cognitive performance on memory and executive function, whereas hemodynamic parameters and DTI metrics of brain WM were not different between the groups. Therefore, data from both groups were combined for subsequent analyses. After adjustments for age and sex, cfPWV was positively correlated with carotid pulse pressure (β=0.34, P<0.001), which in turn was associated with greater CBF pulsatility (β=0.40, P<0.001). As shown in Figure, voxelwise statistics revealed that greater CBF pulsatility is associated with 42.4%, 53.4%, and 8.5% of the WM neuronal fiber tracts with lower FA as well as higher RD and AD, respectively. Specifically, these WM tracts included genu and body of corpus callosum, anterior and posterior limbs of internal capsule, anterior corona radiata, and superior longitudinal fasciculus. Moreover, FA and RD in these neuronal fiber tracts were associated with executive function performance, as assessed by Trail Making Test part B minus A, after adjustments for age, sex, and education (partial correlation coefficients, r = -0.36 and 0.30 respectively). Global CBF was not related to DTI metrics of brain WM fiber integrity. **Conclusions**: Enhanced carotid pulse pressure and CBF pulsatility associated with arterial aging may deteriorate brain WM neuronal fiber integrity in older adults with normal cognitive function and MCI. Thus, lifestyle and/or pharmacological intervention(s) that can ameliorate arterial stiffening may provide protective effects on brain WM fiber integrity.

Reference

1. Tarumi T, Khan MA, Liu J, et al. Cerebral hemodynamics in normal aging: central artery stiffness, wave reflection, and pressure pulsatility. Journal of Cerebral Blood Flow & Metabolism 2014;34:971-978.

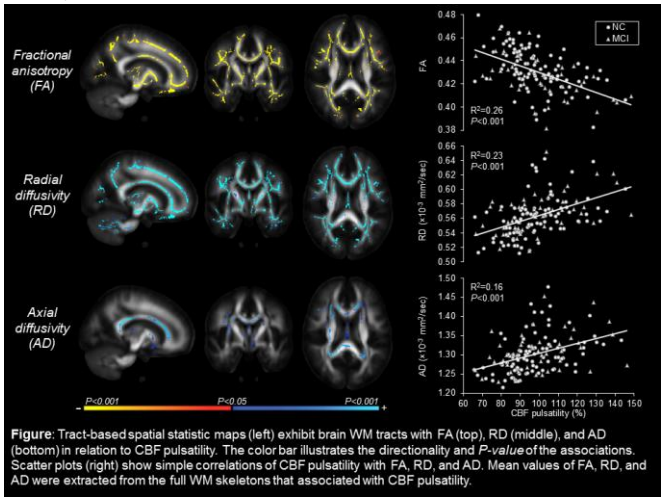

Figure: Tract-based spatial statistic maps (left) exhibit brain WM tracts with FA (top), RD (middle), and AD (bottom) in relation to CBF pulsatility. The color bar illustrates the directionality and *P-value* of the associations. Scatter plots (right) show simple correlations of CBF pulsatility with FA, RD, and AD. Mean values of FA, RD, and AD were extracted from the full WM skeletons that associated with CBF pulsatility.

440
BRAIN-0321
Poster Session

White Matter Injuries

HISTONE DEACETYLASE INHIBITION PREVENTS WHITE MATTER INJURY BY MODULATING MICROGLIA/MACROPHAGE POLARIZATION THROUGH THE GSK3BETA/PTEN/AKT AXIS

G. Wang[1], Y. Shi[2], X. Jiang[1], R. Leak[3], X. Hu[2], Y. Wu[2], H. Pu[2], Y. Wang[1], Y. Gao[1], P. Zheng[1], M. Bennett[4], J. Chen[2]

[1]State Key Laboratory of Medical Neurobiology an d Institute of Brain Science, Fudan University, Shanghai, China

[2]Center of Cerebrovascular Disease Research, University of Pittsburgh, Pittsburgh, USA

[3]Division of Pharmaceutical Sciences Mylan School of Pharmacy, Duquesne University, Pittsburgh, USA

[4]Dominick P. Purpura Department of Neuroscience , Albert Einstein College of Medicine, New York, USA

Objectives: Severe traumatic brain injury (TBI) elicits destruction of both gray and white matter, which is further exacerbated by secondary pro-inflammatory responses. Although white matter injury (WMI) is strongly correlated with poor neurological status, the maintenance of white matter integrity is still poorly understood and there are no current therapies that can protect both gray and white matter. One promising candidate that may fulfill this role is inhibition of class I/II histone deacetylases (HDACs).

Methods: TBI was induced in mice by a controlled cortical impact (CCI). Class I/II HDAC inhibitor Scriptaid was injected at 3.5 mg/kg 2 h after CCI, and repeated daily for the following 2 days. Sensorimoter deficits, WMI, and microglial phenotypic changes were assessed for up to 35 days post-TBI. Functional changes in nerve conduction were examined by measuring compound action potential in the corpus callosum. To reveal the mechanism underlying Scriptaid-afforded white matter protection, primary co-cultures of microglia and oligodendrocytes were used. The role of key signaling molecules was investigated through lenriviral shRNA knockdown in primary microglia cultures.

Results: We demonstrated that inhibition of HDACs by Scriptaid protected white matter up to 35 d after TBI, as shown by reductions in abnormally dephosphorylated neurofilament protein, increases in myelin basic protein, anatomical preservation of myelinated axons, and improved nerve conduction. Interestingly, Scriptaid elicited little direct protection of cultured primary oligodendrocytes against oxygen-glucose deprivation (OGD). Conditioned medium collected from Scriptaid-treated microglia provided significantly greater protection against OGD in oligodendrocyte cultures. More profound protection by Scriptaid was observed using the transwell system of co-cultured microglia and oligodendrocytes. These results suggested that Scriptaid protected oligodendrocytes indirectly through microglia. Further examination revealed that Scriptaid shifted microglia/macrophage polarization toward the protective M2 phenotype and mitigated cerebral inflammation after TBI. Using primary co-cultures of microglia and oligodendrocytes, we showed that Scriptaid increased expression of microglial GSK3β, which phosphorylated and inactivated PTEN, thereby enhancing PI3K/Akt signaling and polarizing microglia toward M2. The increase in GSK3β in microglia and their phenotypic switch to M2 was associated with increased preservation of neighboring oligodendrocytes. In contrast, GSK3β knockdown abolished Scriptaid-mediated Akt activation and protection on white matter.

Conclusions: Our findings illustrated that HDAC inhibition shifted microglia/macrophage phenotype by upregulating GSK3β, which inactivated PTEN through phosphorylation, thereby promoting PI3K/Akt signaling (*graph*). The GSK3β-dependent M2 phenotype exerted potent anti-inflammatory effects that protected myelin-forming oligodendrocytes and diminished WMI. These results reveal a previously unexplored role for GSK3β/PTEN/PI3K signaling in the regulation of microglia/macrophages and show the promise of HDAC inhibition in the treatment of TBI/WMI.

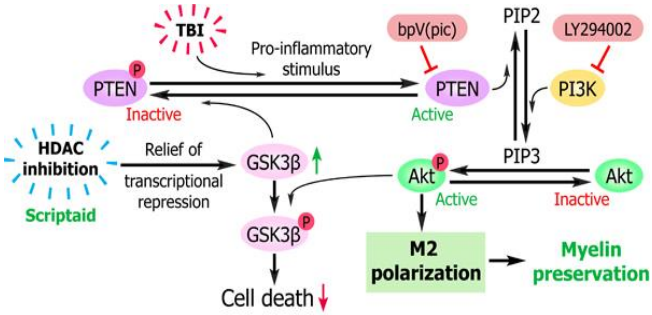

441
BRAIN-0249
Poster Session

Brain Repair

WIDE-NETWORK STIMULATION IS REQUIRED TO IMPROVE MOTOR RECOVERY IN CHRONIC SUBCORTICAL CAPSULAR INFARCT MODEL

D.H. Kwon[1], R.G. Kim[1], H.S. Kim[1], J.W. Cho[1], M.C. Lee[2], H.I. Kim[1]
[1]Department of Medical System Engineering, Gwangju Institute of Science and Technology (GIS

T), Gwangju, Korea
[2]Department of Pathology,
Chonnam National University Medical School,
Gwangju, Korea

Objectives

Subcortical capsular infarct (SCI) is associated with severe long-term motor disability despite conventional rehabilitative training. Cortical stimulation (CS) is known to be an alternative strategy to accelerate the post-stroke recovery, however, the site and mechanism of CS remained inconclusive. We exploited CS of sensory-parietal cortex (SPC) with small or wide-network fashion to determine the better strategy of CS. We also used the longitudinal microPET study to elaborate the underlying change of neural networks involved in the recovery of motor functions.

Methods

Animal experiments were performed according to the institutional guidelines of the Gwangju Institute of Science and Technology (GIST) for experimental research and all procedures were approved by Institutional Animal Care and Use Committee at GIST. Adult male Sprague Dawley rats (n=22) underwent the unilateral photothrombotic subcortical lesioning in the posterior limb of internal capsule [1] and were divided into small-network stimulation group (SSG: n=8), wide-network stimulation group (WSG: n=8) depending on the range of SPC stimulation and sham-operated group (SOG: n=6). Stimulation groups received continuous square wave with half of the movement threshold voltage of 50Hz frequency for 2 weeks concurrently with daily single pellet reaching task [2]. After a [^{18}F]-FDG (0.1mCi/100g) uptake with an electrical stimulation, a static PET acquisition was performed using a Siemens Inveon microPET/CT longitudinally at pre-stimulation, 4th, 7th, and 14th day. The PET images were statistically analyzed using MINC (McConnell Brain Imaging Centre) and AFNI (National Institutes of Health) packages. A linear mixed-effect model was conducted to assess group differences between four follow-up scans for each group [3].

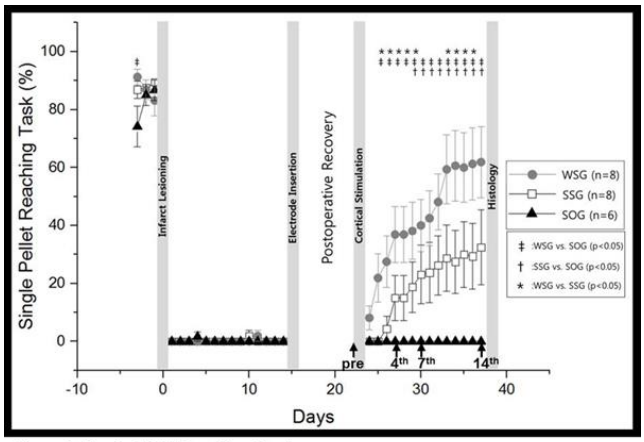

Figure1. Single Pellet Reaching Task

Results

The rats that received wide SPC stimulation showed significant improvement of SPRT scores compared to SOG from 2nd day of stimulation with p^{18}F]-FDG changes in regional glucose metabolism at post-lesion days (4th, 7th, 14th) compared with pre-stimulation scans at the significance level (pSSG), thalamus, and striatum, which are assumed to contribute to motor recovery also. In addition, activations of reward-related areas were observed in hypothalamus, substantia nigra, and septal nucleus in both groups.

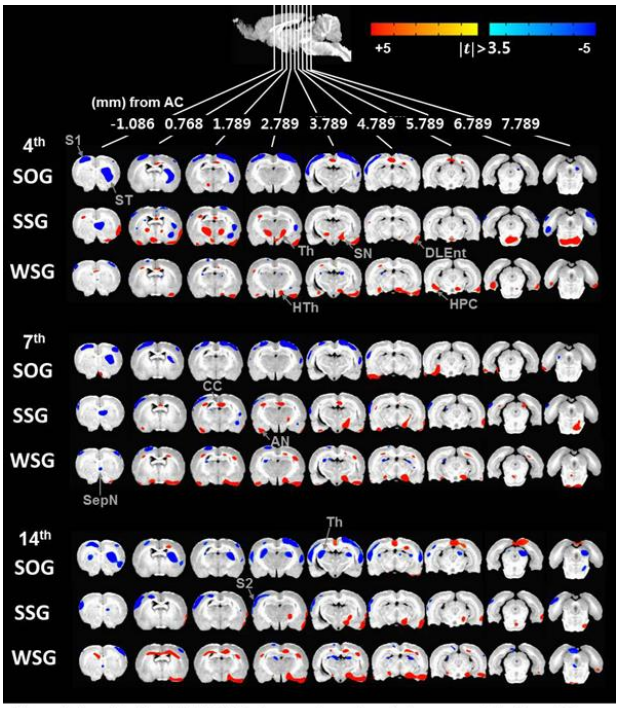

Figure2. Longitudinal [18F]-FDG changes in regional glucose metabolism. AC: anterior commissure, S1: primary somatosensory cortex, ST: striatum (caudate putamen), Th: thalamus, SN: substantia nigra, DLEnt: dorsolateral entorhinal cortex, HTh: hypothalamus, HPC: hippocampus, CC: corpus callosum, AN: amygdaloid nucleus, SepN: septal neucleus, S2: secondary somatosensory cortex

Conclusions

This study suggests that wide SPC stimulation has better prognosis of motor recovery. Abolishment of diaschisis and co-activation of subcortical neural substrates are considered to contribute to the motor recovery in chronic SCI models.

References

1. H.S. Kim, et al., J. Cereb. Blood Flow Metab. 2014;34: 683-689

2. Y. Hau, et al., Stroke 2002; 33: 2478-2484

3. G. Chen, et al., Neuroimage 2013; 73: 176-190

442
BRAIN-0643
Poster Session

Brain Repair

OPTOGENETIC STIMULATION OF CEREBELLAR DENTATE NUCLEUS PROMOTES PERSISTENT FUNCTIONAL RECOVERY AFTER STROKE

I. Shunsuke[1], M.Y. Cheng[1], A.M. Shah[1], E.H. Wang[1], A.R. Bautista[1], G. Sun[1], G.K. Steinberg[1]
[1]Neurosurgery, Stanford University, Stanford, USA

Objective: Functional recovery after stroke has been observed in both human and animal studies (1, 2). Post-stroke brain stimulations are promising neurorestorative techniques as they allow direct manipulation of the target area's excitability (3). Previously we have demonstrated that optogenetic neuronal stimulation of the ipsilesional primary motor cortex promotes functional recovery (4). To determine an optimal brain stimulation target, we test whether optogenetic neuronal stimulation of the contralesional cerebellar dentate nucleus (cDN) can promote recovery. We hypothesize that stimulation of cDN may be more effective, as it sends excitatory outputs to multiple motor and premotor areas (5).

Methods: Thy-1-ChR2-YFP line-18 transgenic male mice were used. Mice underwent stereotaxic surgery to implant a fiber cannula in cDN, followed by an intraluminal middle cerebral artery suture occlusion. Three groups of mice were used: control non-stimulated stroke mice, short-stimulated stroke mice (short-stim: received stimulations from day5-14 post-stroke) and long-stimulated stroke mice (long-stim: received stimulations from day5-28 post-stroke). Sensorimotor behavior tests (rotating beam tests) were used to assess their recovery at day 0, 4, 7, 10, 14, 21 and 28 post-stroke. pCREB and total CREB expression were examined at day15 post-stroke.

Results: Our data showed that both short-stim and long-stim stroke mice exhibited significant

recovery by traveling longer distances ($p<0.05$) and faster speed at day14 post-stroke ($p<0.01$). Interestingly, the short-stim group exhibited persistent recovery after day 14 without further stimulations, and the long-stim group did not further enhance recovery. Analysis of pCREB activation showed that acute cDN stimulation activates the dentatothalamocortical pathway. Interestingly, chronic cDN stimulation-induced recovery is associated with a significant decrease in pCREB and an increase in plasticity marker GAP43.

Conclusion: Our data suggest that chronic cDN stimulations post-stroke can promote persistent recovery, and this recovery is associated with down-regulation of pCREB expression. Current studies examine the mechanisms of cDN stimulation-induced recovery, including CREB signaling pathway and synaptic/plasticity markers.

References:

1. Sharma N, Cohen LG (2010) Recovery of motor function after stroke. *Dev Psychobiol* 54:254–62.

2. Murphy TH, Corbett D (2009) Plasticity during stroke recovery: from synapse to behaviour. *Nat Rev Neurosci* 10:861–72.

3. Liew S-L, Santarnecchi E, Buch ER, Cohen LG (2014) Non-invasive brain stimulation in neurorehabilitation: local and distant effects for motor recovery. *Front Hum Neurosci* 8:378.

4. Cheng MY et al. (2014) Optogenetic neuronal stimulation promotes functional recovery after stroke. *Proc Natl Acad Sci*:1–6.

5. Dum RP, Strick PL (2003) An unfolded map of the cerebellar dentate nucleus and its projections to the cerebral cortex. *J Neurophysiol* 89:634–9.

443
BRAIN-0433
Poster Session

Neuroprotection/Repair

BONE MARROW CELL TRANSPLANTATION TIME-DEPENDENTLY REVERSES G-CSF EFFECTS AFTER STROKE IN HYPERTENSIVE RATS

C. Pösel[1], D.C. Wagner[1], J. Scheibe[1], A. Kranz[1], V. Bothe[2], F. Lange[3], W.R. Schäbitz[4], J. Minnerup[5], J. Boltze[1]
[1]Department of Cell Therapy, Fraunhofer Institute for Cell Therapy and Immunology, Leipzig, Germany
[2]Department for Cell Therapy, Fraunhofer Institute for Cell Therapy and Immunology, Leipzig, Germany
[3]Department of Diagnostics, Fraunhofer Institute for Cell Therapy and Immunology, Leipzig, Germany
[4]Department of Neurology, 3EVK Bielefeld Bethel, Bielefeld, Germany
[5]Department of Neurology, University of Münster, Münster, Germany

Objectives

Granulocyte colony-stimulating factor (G-CSF) is a hematopoietic cytokine and preclinically proven, potent neuroprotectant[1]. A potential reason for the clinical failure of G-CSF may be that relevant G-CSF effects such as the mobilization of mononuclear hematopoietic stem and progenitor cells from the bone-marrow may take too long in humans (up to 9 days[2]) to counter the initial stroke consequences. Systemic transplantation of bone marrow mononuclear cells (BMMNC) is feasible within a relatively short time after stroke onset and may provide an external resource of aforementioned stem and progenitor cells and thereby “bridge the gap” until G-CSF comes to full effect.

Methods

Male spontaneously hypertensive rats (SHR) were randomly assigned into 4 groups after permanent middle cerebral artery occlusion. Groups 1-3 received i.p. G-CSF treatment (50µg/kg) for 5d

starting 1h after stroke onset. Groups 2 and 3 received $1.5x10^7$/kg BMMNC i.v. at 6 or 48h following stroke. Group 4 received placebo treatment. Functional deficits (adhesive removal test), infarct volume, edema (T2 TSE MRI) were repeatedly assessed for one month. Peripheral leukocyte counts and BMMNC biodistribution were analyzed by flow cytometry during the first week after stroke. All experiments were conducted randomized and blinded.

Results

G-CSF mono-treatment reduced functional deficits ($p<0.05$) and partially reversed post-stroke immune depression (overall leuko-/monocyte as well as B-, NK, and T-cell counts; $p<0.01$) and expectedly increased peripheral leukocyte counts massively ($p<0.01$). G-CSF but did not affect infarct volume or edema. BMMNC co-transplantation at 6h did not further improve functional deficits ($p>0.05$ each). Surprisingly, BMMNC transplantation at 48h abolished G-CSF effects. Early biodistribution studies (at 52 hours after stroke onset) revealed splenic accumulation of granulocytes and BMMNC as well as a granulocyte overload in the peripheral circulation and the brain ($p<0.05$).

Conclusions

Although therapeutic effects of G-CSF mono-treatment were observed in SHR, the G-CSF/BMMNC co-treatment did not provide additional functional benefits. Splenic accumulation of transplanted BM MNC may have impaired peripheral granulocyte clearance. Subsequently, increased granulocyte numbers in the circulation and the post-stroke brain prompted a pro-inflammatory bias of the innate immune system's response to stroke, ultimately abolishing G-CSF effects[3]. These surprising findings indicate that systemic effects of experimental stroke therapies need to be carefully considered when assessing the therapeutic potential of such novel approaches.

References

1. Minnerup et al. (2008); Stroke 39(6):1855-1861
2. Hill et al. (2007); Bone Marrow Transplant. 40(10):925-930
3. Pösel et al. (2014); Stroke 45(8):2431-2437

444
BRAIN-0567
Poster Session

Neuroprotection/Repair

POST-STROKE FUNCTIONAL RECOVERY IS IMPROVED BY ALPHA-LINOLENIC ACID SUPPLEMENTATION OF THE DIET.

M. Bourourou[1], O. Le Thuc[1], C. Rovère[1], C. Heurteaux[1], N. Blondeau[1]
[1]Institut de Pharmacologie Moléculaire et Cellulaire,
UMR7275 C.N.R.S / Université de Nice Sophia Antipolis, Valbonne, France

Objectives: Stroke survivors have a high level of disability with more than 50% being left with residual motor or cognitive/mnesic deficits. Meanwhile omega-3 polyunsaturated fatty acids are highlighted as disease modifying factors for cardio or neuro-vascular or diseases. In a mice model of ischemic stroke, nutritional intervention providing omega-3 polyunsaturated fatty acid, alpha-linolenic acid (ALA) reduces mortality and brain lesion. We also demonstrates the capacity of ALA to enhance brain plasticity and increase neurotrophic factor level of the brain, that have been retrospectively shown in numerous studies to be the target of most of the motor and cognitive rehabilitation approaches. Therefore we investigated whether ALA supplementation could improve post-stroke recovery of motor or cognitive function and if it could be correlated with an improvement of the inflammatory, neurotrophic, synaptic plasticity response.

Methods: ALA supplementation was achieved by an experimental diet enriched in ALA by a factor of three compared to regular chows. The ALA enriched diet did not contain any EPA and DHA,

while the regular chow did, in proportions already matching the ‘‘murine’’ recommended intake. After a 6-week diet, stroke was induced by a 30 min MCAo - model acknowledged for characterization of long-term functional in mice. Infarct was assessed on Cresyl violet stained sections 24h-post-stroke. Motor deficits were assessed in the rotarod and pole tests and cognitive deficits in the Morris water maze test. Inflammatory and neurotrophic response and synaptic plasticity were investigated by a combination of immunohistochimistry, real-time Pcr and western blot analysis.

Results: ALA supplementation improved post-stroke motor coordination. The ALA supplemented mice did not display a reduced infarct volume, while, they showed an increased latency to fall off the rotarod from the day 2 to day 4 after stroke and reduced latency to reach the floor at day 3 in the pole test. The improvement of post-stroke motor coordination by the ALA-diet is not correlated to neuronal protection 3 days post-stroke, but to a change in neuroplasticity and neuroinflammatory response of the ipsilateral hemisphere. ALA supplementation improved post-stroke spatial learning and memory. ALA supplemented mice display a shorter time to find the platform during the training days and to enter the platform location on the test day during the second week of recovery post-stroke. We then carefully analyzed the long-term evolution of the lesion, characterizing the loss of cortical, striatal and hippocampal neurons following the 30 min MCAo. Surprisingly, we observed a marked preservation of the hippocampus, a region described as being involved in memory that may explain the post-stroke cognitive improvement.

Conclusions: Our preclinical research highlights the interest of ALA nutritional supplementation to reduce post-stroke mortality, neuronal damage and promote rehabilitation.

This work was supported by ONIDOL, the “Fondation de la Recherche Médicale”, St Hubert and CNRS.

445
BRAIN-0281
Poster Session

Neuroprotection/Repair

BEYOND GLUTAMATE ANTAGONISTS: NEW THERAPEUTIC STRATEGY AGAINST GLUTAMATE EXCITOTOXICITY BASED ON CELLULAR BLOOD GLUTAMATE SCAVENGERS.

F. Campos[1], M. Pérez-Mato[1], E. López[1], A. Silva-Candal[1], H. Fernández-Susavila[1], S. Arias[1], M. Rodríguez-Yáñez[1], J. Castillo[1], T. Sobrino[1]
[1]Neurology, Hospital Clínico Universitario-Clinical Neurosciences Research Laboratory, A Coruña-Santiago de Compostel, Spain

Objectives: Nowadays, the concept of blood glutamate scavenging represents a novel and attractive protecting strategy to reduce the excitotoxic effect of extracellular glutamate in brain. This mechanism is based on the administration of oxaloacetate or recombinant glutamate oxaloacetate transaminase (rGOT) which leads to a metabolization and reduction of glutamate in blood and a subsequently lowering of glutamate in cerebral parenchyma.

The excitatory amino acid transporters systems (known as EAAT) provide the predominant mechanism to uptake of glutamate into the cells and maintain the proper concentration of this potentially excitotoxic amino acid in the brain. Based on the high affinity of EAAT for glutamate, we have artificially induced the expression of this transporter (in particular the subtype EAAT2) in cells, with the aim to generate a cellular therapy able to reduce the blood glutamate after cerebral ischemia.

Methods: A cell line of HEK (Human Em-bryonic Kidney 293 cells) and rat mesenchymal stem cells (MSCs) where transfected with EAAT2 and its expression was determined by means of flow cytometry and immunohistochemistry. Functionality of EAAT2 were determined by means of [3H]glutamate uptake assay. Therapeutic analysis of EAAT2- transfected cells were determined in ischemic model animals

induced through the intraluminal filament occlusion of middle cerebral artery. Six experimental groups were developed: 1) a control group treated with saline (i.v.), 2) a group treated (i.v.) with $3x10^6$ non-transfected MSCs, 3) a group treated (i.v.) with $3x10^6$ EAAT2-transfected MSCs, 4) a group treated (i.v.) with $3x10^6$ non-transfected HEK cells, 5) a group treated (i.v.) with $3x10^6$ EAAT2-transfected HEK cells and finally 6) a group treated (i.v.) with oxaloactete 3.5 mg/Kg used a positive control of blood glutamate reduction. Infarct volume (determined by means of MRI), blood glutamate levels and functional test were determined during 14 days after ischemic onset.

Results: Flow cytometry and immunohistochemistry analysis demonstrated that EAAT2-transfected MSCs and EAAT2-transfected HEK cells express positively the transporter. In vitro [3H]glutamate uptake assay confirmed that protein-induced expression had a functional glutamate uptake, being this effect inhibited for selective EAAT2s blockers, DHK and TBOA. Administration of transfected and non-transfected cells in ischemic model animals showed that artificial expression of EAAT2 in cells induced a significant reduction o blood glutamate levels. Comparative analysis of infarct volume between animals treated with transfected MSCs and transfected HEK showed that a higher beneficial result was observed with transfected MSCs.

Conclusion: Cellular blood glutamate reduction represents a novel strategy to reduce the glutamate excitotoxicity after ischemic damage, which allows to combinate neuroprotection and neurorecovery as an unique cellular therapy.

446
BRAIN-0678
Poster Session

Neuroprotection/Repair

DAIDZEIN AUGMENTS APOE TO PROMOTE RECOVERY OF MOTOR FUNCTION FOLLOWING ISCHEMIC STROKE IN MICE

E. Kim[1], M. Woo[1], L. Qin[1], C. Beltran[1], D. Corbett[2], D. Lahiri[3], R. Ratan[1], S. Cho[1]
[1]Research, Burke-Cornell Medical Research Institute, White Plains, USA
[2]Heart and Stroke Foundation Canadian Partnership for Stroke Recovery, University of Ottawa and University of Toronto, Ottawa, Canada
[3]Psychiatry, Indiana University School of Medicine, Indianapolis, USA

Objectives: Increasing evidence suggests that synaptic plasticity and remodeling occur weeks after stroke. ApoE, the most abundant cholesterol transporter in the CNS, plays an important role in cholesterol homeostasis, neuronal repair, and synaptic plasticity. Through a large-scale chemical screen, we have identified daidzein as a neuroprotective agent *in vitro* and found that it promotes regeneration of axons in an optic nerve crush model *in vivo.* This current study is to investigate whether daidzein increases ApoE and the expression is associated with neuroprotection and functional recovery in chronic stroke.

Methods: C57bl/6 and ApoE KO mice were subjected to 30 min transient middle cerebral artery occlusion and randomly assigned for daily subcutaneous injections of vehicle (Veh) or daidzein (Dz, 10 mg/kg) for 7 days and then continually treated every other day up to one month. Infarct volume was assessed at 3 days and 1month. Longitudinal motor/gait functions by Rotarod and Catwalk gait analyses were performed during acute and recovery phase until 1m post-stroke (n=9-15/group). Gene and protein expression of ApoE, synaptophysin, and Psd-95 was determined in the brain at 1m after stroke.

Results: Infarct size between vehicle and daidzein treated C57 mice were similar at 3d (3d, 43.4+/-14.0 vs 36.1+/-14.6. n=16, ns) and at 1m post-stroke (22.7±3.8 vs 22±3.0, n=13, ns). Compared to vehicle treated mice, chronic daidzein treatments significantly increased stroke-induced *apoe* mRNA (veh vs Dz; 1.16±0.14 vs 1.71±0.70, n=7-11, $p<0.05$) and 30% increase in protein levels. Daidzein also significantly enhanced motor and gait functions displayed by increased walk speed (Fig a). Moreover, daidzein-induced functional recovery was associated with elevated expression of synaptophysin (0.18± 0.03, 0.24±0.04, n=11, p<0.05) in the post-ischemic brain at 1 month. There was no behavior enhancement and synaptophysin increase in ApoE KO mice treated with daidzein (Fig b)

Conclusions: The study showed that the importance of daidzein-induced ApoE up-regulation in fostering stroke recovery. The finding of daidzein-enhanced recovery in the absence of neuroprotection suggests the presence of non-overlapping mechanisms for acute pathology vs recovery process. With its known safety in humans, early and chronic use of daidzein aimed at augmenting ApoE may serve as a novel, translatable strategy to promote recovery in stroke patients.

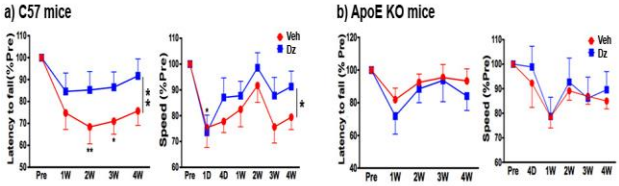

447
BRAIN-0392
Poster Session

Neuroprotection/Repair

THE NOBLE GAS XENON REDUCES SECONDARY INJURY AND IMPROVES LONG-TERM LOCOMOTOR FUNCTION AFTER TRAUMATIC BRAIN INJURY IN RODENTS

R. de Campos Pires Santos e Sousa[1], *S.P. Armstrong*[1], *A. Sebastiani*[2], *K. Radyushkin*[3], *S. Thal*[2], *N.P. Franks*[4], *R. Dickinson*[1]
[1]*Surgery and Cancer, Imperial College London, London, United Kingdom*
[2]*Anaesthesiology, Medical Centre of Johannes Gutenberg University, Mainz, Germany*
[3]*Mouse Behavioural Outcome Unit, Johannes Gutenberg University, Mainz, Germany*
[4]*Life Sciences, Imperial College London, London, United Kingdom*

Objectives

Traumatic brain injury (TBI) represents a major health problem and socioeconomic burden throughout the world [1]. TBI results from external forces applied to the head, causing immediate and irreversible damage that will trigger early, long-lasting cascades of complex inflammatory and neurochemical events known as secondary injury. Secondary injury is often considered the main contributor to the ultimate clinical picture [2]. Despite significant clinical improvements in short term outcomes over the last decades, after moderate and severe TBI, it is still difficult to return these patients to appropriate functioning levels. Clinical treatment is currently mainly supportive and no specific neuroprotective drugs are currently available [1].

Over-activation of N-methyl-D-aspartate (NMDA) receptors is known to play a key role in secondary injury development [1]. The noble anesthetic gas xenon is an NMDA receptor antagonist [3] and has been shown to be neuroprotective in models of ischemic brain injury [4, 5]. Much less is known about xenon effect in the context of brain trauma.

In this study we evaluate xenon's neuroprotective efficacy in a well-established murine controlled cortical impact model of experimental brain injury, mimicking elements found after moderate to severe TBI in humans.

Methods

Adult C57BL/6 male mice (n=196) underwent a right parietal cortical impact under anaesthesia delivered by a custom-made electro-pneumatic impactor as previously described [5]. Animals were then randomly assigned into control (75% nitrogen:25% oxygen) and xenon (30%, 50% or 75% xenon:25% oxygen, balanced with nitrogen) treated groups (duration of treatment 3 hours). Short term and long term outcomes, functional and histological, were measured by researchers blinded to treatment. Statistical significance was assessed with one-way and two-way ANOVA with Bonferroni's *post hoc* test (SigmaPlot software).

Results

Xenon (75%) for 3 hours duration after TBI significantly reduced contusion volume 24 hours post-injury and xenon was effective when treatment start time was delayed up to 3 hours after trauma (Fig. 1). There was a significantly improved neurologic outcome up to 4 days after injury. Improvements were also observed in clinically relevant locomotor deficits (locomotor speed and individual limb swing speed) in the xenon-treated group 1 month after injury. Significant reductions in contusion volume and improvement in neurologic outcome 24 hours after injury were also achieved with 30% and 50% xenon concentrations.

Conclusions

We show for the first time that xenon improves functional outcomes and reduces contusion volume in an animal model of TBI. We demonstrate both a reduction in the development of secondary injury and functional neurological improvement. Our results, including the demonstration of long term neuroprotection and a clinically relevant therapeutic time window, support the hypothesis that xenon may be of benefit as a neuroprotective treatment in TBI patients.

References

[1] Maas A *et al*, J Neurotrauma 2010; **29**:32-46.
[2] Ling G *et al*, Neurologic Clinics 2008; **26**:409-426.
[3] Franks NP *et al*, Nature 1998; **396**:324.
[4] Ma *et al*, Annals of Neurology 2005; **32**:371-75
[5] Sheng SP *et al,* Anesthesiology 2012*;* **117**:1262-75

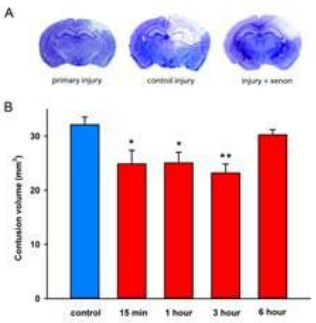

Fig. 1. Delayed xenon treatment following trauma reduces injury 24 hours after trauma. (A) Typical cresyl-violet stained slices, 2.2 mm posterior to Bregma, showing primary injury 15 min after trauma, control injury and xenon-treated injury at 24 hours after trauma. In example shown xenon treatment was delayed until 1 hour after trauma. (B) Xenon-treated animals (red bars) received 75% xenon : 25% oxygen for 3 hours duration starting at 15 minutes, 1 hour, 3 hours or 6 hours after trauma. Control animals (blue bar) received 75% nitrogen:25% oxygen. Contusion volume was measured 24 hours after trauma. Bars represent mean values and error bars are standard errors (*n*=22, control; *n*=9, xenon 15 min; *n*=8, xenon 1 hr; *n*=9, xenon 3 hr; *n*=9, xenon 6 hr). * = $p<0.05$; ** = $p<0.01$ compared to control.

448
BRAIN-0132
Poster Session

Neuroprotection/Repair

CELL-BASED IMMUNOTHERAPY FOR INTRACRANIAL HEMORRHAGE

X. Wang[1], J. Rodriguez[2], T. Thomas[2], L. Zou[2], L. Do[2], H. Dou[2]
[1]Anatomy, Weifang medical university, Weifang, China
[2]Biomedical Sciences, Texas Tech University Health Sciences Center, El Paso, USA

Backgroud: Stroke caused by intracranial hemorrhage (ICH) is an important clinical problem that can leave affected people with permanent neurological deficits for which no treatment is

available. ICH-induced inflammation appears to be a key factor in secondary brain damage, as evidenced by a reduction in brain damage in immune-deficient animal models of central nervous system (CNS) disorders, including stroke. We have found bone marrow derived dendritic cell (DC)-like cells (BMDC) not only to regulate systemic immune responses but also to modulate multiple brain functions following brain injury. **Methods:** For inducing ICH, mice will be anesthetized and secured with ear bars and a mouthpiece on a stereotactic apparatus. Peripheral blood, collected from the facial vein will be injected into the left hemisphere of the brain. Mouse bone marrow cells were treated with IL4+ MCSF for 5-7 days to produce BMDC. In order to study the systemic immune response and neuroprotective activities in BMDC treated to the mouse model of ICH, splenic cells and cytokines of the innate immune activity and neuronal loss were analyzed by flow cytometry, histology, Immunofluorescence staining and RT-PCR. **Results:** BMDC differentiation showed over 94% of CD45+/CD11b+ and CD45+/CD80+ cells following IL4+ MCSF treatment. IL-4 and GM-CSF treatment significantly expanded the activated and matured $CD86^+$, $CD83^+$ and CD163 cells and decreased $CD68^+$ inflammatory populations. $CD11c^+$ cells remained elevated for up to 7 days. ICH-induced *Iba-1*$^+$ microglia activation was correlated with neuron loss. The greatest levels of microglia were parallelled with an increase in degenerated neurons (reflected by pNF aggregation) on day 7 after ICH. Immunohistochemistry was used to examine neuroprotection of BMDC. Quantitation images revealed a significant loss of Map-2^+ density and increase of Iba-1+ staining in ICH group. BMDC treatment prevented neuronal loss and exhibited greater levels of Map-2^+ neuritis. The protective immune responses showed that splenic CD11b+ inflammatory populations and CD8 cytotoxic T cells were decreased in BMDC treated ICH group. With BMDC treatment, ICH mice reduced TNF-α and INF-γ expression and up-regulated IL10 and TGF-β levels in spleen. Importantly, BMDC reversed all tested cytokine levels in the brain. Conclusion: anti-inflammatory activities by exogenous regulators may be too dangerous for injury prevention and repair. BMDC based neuroprotective therapy will lead to an increase in autologous anti-inflammatory activities, a decrease in the inflammatory signaling, and restored neuronal injury.

449
BRAIN-0216
Poster Session

Neuroprotection/Repair

NEUROPROTECTIVE EFFECTS OF MICROGLIAL P2Y1 RECEPTORS AGAINST ISCHEMIC NEURONAL INJURY

Y. Fukumoto[1], S. Koizuimi[2], H. Yoshioka[1], T. Yagi[1], K. Kanemaru[1], H. Kinouchi[1]
[1]Neurosurgery, Yamanashi University, Chuo, Japan
[2]Neuropharmacology, Yamanashi University, Chuo, Japan

Objectives: Microglia are the principal immune cells of the central nervous system (CNS), monitoring and rapidly responding to microenvironment alterations, and exhibit conflicting cytotoxic or protective phenotypes. Although the mechanisms controlling these phenotypes remain to be fully elucidated, adenosine triphosphate (ATP), released or leaked into the extracellular space especially in pathophysiological conditions such as brain ischemia, has been recently regarded as a key molecule. ATP acts on P2 receptors and mediates neuron-to-glia communication. Among these receptors, $P2Y_1$ receptor ($P2Y_1R$) has received a lot of attention, and shows neuroprotective functions in astrocytes. However, the functions or even the presence in microglia is still a matter of debate. In this study, we investigate the presence and pathophysiological consequences of $P2Y_1R$.

Methods: *In vivo* (transient forebrain ischemia) and *in vitro* (oxygen-glucose deprivation (OGD)) ischemia models were used in this study. Male $P2Y_1R$ knockout (KO) mice and their wild-type (WT) littermates were subjected to transient forebrain ischemia by 20-minute bilateral common carotid artery occlusion. Three days after ischemia, the brains were removed after perfusion-fixation, and sectioned into coronal

slices. $P2Y_1R$-positive signal was investigated by immunohistochemical analysis, and histological injury was assessed using terminal deoxynucleotidyl transferase-mediated uridine 5'-triphosphate-biotin nick end labeling (TUNEL) staining in the hippocampal subregions (CA1, CA3, and the dentate gyrus; DG). Organotypic hippocampal cultures obtained from WT, KO and transgenic mice whose $P2Y_1Rs$ are ectopically expressed only in microglia (P2Y1R KO/mOE) were prepared according to the standard interface method. Slice cultures were exposed to OGD using an anaerobic chamber for 40-minute. After 48 hours, cultures were examined propidium iodide (PI) fluorescence in the CA1, CA3, and DG subfields of the hippocampal cultures with a fluorescent microscope as an index of cell death, and the values were normalized by the cell death in the WT mice and were shown as % of WT.

Results: We found that $P2Y_1R$-positive signal was present and colocalized with the microglial marker Iba1 by immunohistochemical analysis of the hippocampus section, and was dramatically increased 3 days after ischemia. The number of apoptotic cells labeled with TUNEL was significantly higher in the hippocampus of the $P2Y_1R$ KO mice (CA1: 33.6 ± 7.5%, CA3: 23.6 ± 6.5%) than that of the WT mice (CA1: 6.2 ± 3.3%, CA3: 3.8 ± 1.5%)(n = 9, p_1R KO slices were significantly higher than those of the WT slices, which was rescued by ectopic expression of the $P2Y_1R$ in microglia (CA1: 87.9 ± 5.1%, DG: 84.3 ± 6.1%, $p < 0.05$).

Conclusion: Microglia express functional $P2Y_1R$, which was accentuated in the pathophysiological condition such as brain ischemia. Furthermore, our data strongly suggest that microglial $P2Y_1R$ could play a neuroprotective role against ischemic injury.

450
BRAIN-0785
Poster Session

Neuroprotection/Repair

INTRANASAL DELIVERY OF PROGESTERONE PROVIDES NEUROPROTECTION AND REDUCES MITOCHONDRIAL DYSFUNCTION AFTER STROKE

R. Guennoun[1], M. Fréchou[1], P. Gaignard[2], S. Zhang[1], P. Liere[1], B. Delespierre[1], P. Thérond[3], M. Schumacher[1], A. Slama[3], C. Mattern[4]
[1]UMR 1195, Inserm and University Paris Sud, Le Kremlin Bicetre, France
[2]UMR 1195 Inserm and University Paris Sud, Biochemistry laboratory Bicêtre Hospital Assistance-Publique Hôpitaux de Paris, Le Kremlin Bicetre, France
[3]Biochemistry laboratory, Bicêtre Hospital Assistance-Publique Hôpitaux de Paris, Le Kremlin Bicetre, France
[4]M et P Pharma AG, M et P Pharma AG, Emmetten, Switzerland

· **Objectives:**Progesterone is a potential neuroprotective agent for stroke treatment(1,2). For a translationaldevelopment, and according to STAIR's recommendations, it is important to testdifferent routes of delivery and to choose an efficient and feasible one inHumans. Intranasaladministration may be an interesting way of delivery because of itsconvenience, quick absorption and avoidance of first pass elimination (3). The objective of this study was to evaluatethe efficiency of intranasal administration of progesterone after experimentaltransient ischemia 1) to reach the brain, 2) to be neuroprotective, and 3) toreduce the brain mitochondrialrespiratory chain (RC)dysunction and oxidative damage.

· **Methods:** Allprocedures concerning animal care and use were carried out in strict accordancewith national guidelines and with French ethical laws (Act 87-848 and Act 2013-11) andEuropean Communities Council Directives (November 24, 1986 86/609/EEC). Male 3-4 monthsold mice were subjected to transient focal cerebral

ischemia (1h) and receivedintranasal administration of progesterone in oleogel (8 mg/kg) or placebo. Experiment1: mice were treated at 1, 6, and 24hpost-MCAO and were killed at 2h or 24h after the last administration ofprogesterone. Levels of steroids were measured by gas chromatography-massspectrometry. Experiment 2: mice were treated at 1, 6, and 24h post-MCAO.Mortality rates, behaviors (Rotarod and neurological score), infarct volume andneuronal density were evaluated at 48h. Experiment 3: Mice were treated at 1hpost MCAO and brain mitochondria were isolated at 6h post-MCAO. Mitochondrialoxygen consumption (NADH and FADH-linked respirations), enzymatic activities ofthe RC complexes, the tricarboxylic acid cycle and the pyruvate dehydrogenasecomplex and mitochondrialoxidative stress were assayed.

· Results:After MCAO and intranasal administration of progesterone, high levels ofprogesterone and its neuroactive metabolites, and low levels of the stress hormone corticosterone were measured in thebrain. Intranasal administration ofprogesterone decreased the mortality rate, improved motor functions, reducedbrain infarct and increased neuronal density. Furthermore, intranasal administration of progesterone, preventedthe decrease of the brain mitochondrial NADH-linked respiration, and reducedthe ischemia-induced oxidative stress as shown by an increase of the aconitase to fumarase activitiesratio and the GSH mitochondrial pool.

· Conclusions: Our data show that the intranasal delivery ofprogesterone offer an efficient, non-stressfuland very easy mode of administration for the treatment of stroke. Our findings demonstrate that progesterone also reduce mitochondrialdysfunction, suggesting that these effects on mitochondria may participate toits neuroprotective effects.

- References

1. Gibson C, Gray LJ, Bath PM, Murphy S. Progesterone for the treatment of experimental brain injury; a systematic review. *Brain*. 2008;131:318–328.

2.Wong R, Renton C, Gibson CL, Murphy SJ, Kendall DA, Bath PMW. Progesterone treatment for experimental stroke: an individual animal meta-analysis. *J. Cereb. Blood Flow Metab.* 2013;33:1362–72.

3. Pires A, Fortuna A, Alves G, Falcão A. Intranasal drug delivery: how, why and what for? *J. Pharm. Pharm. Sci.* 2009;12:288–311.

451
BRAIN-0184
Poster Session

Neuroprotection/Repair

LACTATE NEUROPROTECTION IN CEREBRAL ISCHEMIA: A PROBABLE DUAL MECHANISM OF ACTION.

X. Castillo Tovar[1], K. Rosafio[2], M.T. Wyss[3], A. Buck[4], B. Weber[5], L. Pellerin[6], L. Hirt[7]
[1]Clinical neurosciences, University of Lausanne, Lausanne, Switzerland
[2]Department of Physiology, University of Lausanne, Lausanne, Switzerland
[3]Institute of Pharmacology and Toxicology, University of Zürich, Zürich, Switzerland
[4]University hospital, PET Center Division of Nuclear Medicine, Zürich, Switzerland
[5]University of Zürich, Institute of Pharmacology and Toxicology, Zürich, Switzerland
[6]University of Lausanne, Department of Physiology, Lausanne, Switzerland
[7]Clinical neurosciences, CHUV, Lausanne, Switzerland

Introduction: Stroke is a highly disablingdisease that accounts for one death every four minutes in the United States.Despite enormous efforts worldwide for new treatments, rTPA given within 4.5 hof symptom onset remains the only approved treatment for ischemic stroke, themajor stroke sub-type. We have previously shown that L-lactate administration duringreperfusion exerts

long lasting protection in mice against ischemic damageafter transient middle cerebral artery occlusion (tMCAO). New evidence suggeststhe possible involvement of the Hydroxy-Carboxylic Acid Receptor-1 (HCA1), alactate receptor, in nervous system effects of lactate (Bergersen et al., 2013;Bozzo et al., 2013).

Aim: Elucidate if the neuroprotective effectsof lactate in an animal model of stroke are exerted by lactate acting as ametabolic substrate or signaling through the HCA1 receptor.

Methods: An immunohistochemistry approach wasused to visualize the HCA1 receptor in different brain regions. Ischemia wasmodeled in vivo by *t*ransient MCAO inadult CD1 mice and, in vitro, by 1h oxygen and glucose deprivation (OGD) onorganotypic rat hippocampal slice cultures (OHC). D-lactate, pyruvate, acetateor 3-5 DHBA, a specific agonist of the HCA1 receptor, were added to the culturemedium after OGD. For protein expression analysis, mice were sacrificed 24hafter tMCAO. D-lactate metabolism was assessed by using ^{11}C-D-lactatein Sprague Dawley rats.

Results: HCA1 receptor is expressed mainly inneurons throughout the brain. HCA1 protein expression analysis 24h after tMCAOshowed an increased expression in the ischemic primary motor and somatosensorycortex, in comparison to the contralateral hemisphere. Furthermore, micereceiving a single IV injection of L-lactate at reperfusion showed an increasein the HCA1 protein expression in the ischemic region surrounding the lesionsite (cortex) and in the ischemic striatum, when analyzed 24h after tMCAO. Interestingly,the monocarboxylate transporter MCT2 showed a decreased expression in the sameregions where HCA1 receptor appears to be upregulated. By using the *in vitro* approach, we observed anincrease in the HCA1 protein expression in the OHC subjected to OGD, in comparisonwith the control slices. This upregulation might exert physiological functionssince administration of 3-5 DHBA to the OHC after 1h OGD induced protection bydecreasing the percent of cell death, in comparison with the control slices. Inthe metabolic pathway, administration of D-lactate and pyruvate after OGDimproved cell survival, while the administration of acetate did not. *In vivo,* D- Lactate administrationduring reperfusion significantly reduced lesion size and improved theneurological performance and we provide evidence of D-lactate metabolism usingradiolabeled D-lactate to trace its metabolism and kinetics.

Conclusions: As lactate and its metabolites aswell as the lactate receptor agonist lead to neuroprotection, we suggest a dualmechanism to explain its mode of action. Experiments using HCA1 -/- mice areneeded to confirm the physiological relevance of these findings.

452
BRAIN-0572
Poster Session

Neuroprotection/Repair

ATTENUATION OF POSTISCHEMIC FUNCTIONAL DEFICITS IN RATS WITH ESSENTIAL HYPERTENSION TREATED WITH NPY2R AGONIST.

L. Przykaza[1], H. Domin[2], P. Boguszewski[3], M. Smialowska[2], E. Kozniewska[1]
[1]Laboratory of Experimental Neurosurgery, Mossakowski Medical Research Centre Polish Aca demy of Sciences, Warsaw, Poland
[2]Department of Neurobiology, Institue of Pharmacology Polish Academy of Scien ces, Krakow, Poland
[3]Laboratory of Limbic System, Nencki Institute of Experimental Biology Polish Ac ademy of Sciences, Warsaw, Poland

Objectives: NPY_{13-36} - a specific agonist of type 2 neuropeptide Y receptor is known to inhibit the release of glutamate from presynaptic sites and has been shown to protect neurons against excitotoxicity in vitro and in vivo. Recently we have demonstrated that NPY_{13-36} is capable to diminish brain damage and functional deficits in healthy rats subjected to transient focal brain ischemia/reperfusion. Current study aims to assess neuroprotective potential of NPY_{13-36} in the

same ischemia/reperfusion model in rats with arterial hypertension.

Methods: Twenty one male rats (270-300g) with essential hypertension (SHR) were subjected to 90 min transient focal cerebral ischemia (intraluminal suture occlusion/reperfusion of the right MCA). Severity of ischemia was controlled with a help of a laser-Doppler flowmeter. NPY_{13-36} (10 microg in a volume of 6 microl) or vehicle (6 microl) were administered intracerebroventricularly either 30 min after MCA occlusion (group 1) or 30 min after reperfusion (group 2). Behavioral tests (CatWalk, open field and vibrisse-elicited forelimb placing) were performed before ischemia and 72 hours after reperfusion. The area of infarction was evaluated after the completion of behavioral tests on brain tissue slices stained with 2,3,5-triphenyltetrazolium chloride (TTC) using a computed based image analysis system (GIMP 2).

Results: Seventy two hours after ischemia, volume of infarction was smaller ($p<0.05$) in the groups treated with NPY_{13-36} (group 1 – 27+/- 2 %; group 2 - 31+/-2 %) compared with the vehicle-treated one (40+/-1% of the hemisphere was damaged). Results of the analysis of behavioural tests demonstrated the improvement of selected gait parameters in both groups. There was, however, no improvement of spontaneous locomotor activity. Besides, forelimb placing reflex recovery was observed only in group 1.

Conclusions: Selective stimulation of NPY type 2 receptors is neuroprotective and attenuates some postischemic deficits in rats with arterial hypertension also when applied during reperfusion.

Acknowledgements: The study was supported by Ministry of Science and Higher Education grant No. NN401091037

453
BRAIN-0168
Poster Session

Neuroprotection/Repair

EDARAVONE PROTECTS CEREBRAL WHITE MATTER AGAINST CHRONIC HYPOXIC STRESS THROUGH ENHANCING OLIGODENDROGENESIS

N. Miyamoto[1], T. Maki[2], K. Hayakawa[2], E.H. Lo[2], K. Arai[2], T. Urabe[1]
[1]Neurology, Juntendo University Urayasu Hospital, Urayasu, Japan
[2]Radiology, Massachusetts General Hosp and Harvard Medical School, Charlestown, USA

Background and Purpose: White matter consists of lipid-rich myelin sheathes, and therefore, may be vulnerable to reactive oxygen species (ROS). A free radical scavenger edaravone is clinically used in Japan as an acute phase stroke therapy, but it remains unclear if the drug can be effective for long-lasting white matter-related diseases such as vascular dementia. Here, we use in vivo and in vitro models to show that edaravone may protect white matter against chronic hypoxia by enhancing oligodendrocyte (OLG) regeneration.

Methods: A mouse model of chronic cerebral hypoperfusion was prepared by bilateral common carotid artery stenosis. Mice were randomized into 2 groups; vehicle and edaravone (3 mg/kg ip, twice/week, n=30 each). Matching in vitro studies were performed by subjecting oligodendrocyte precursor cells (OPCs) to sub-lethal 7-day CoCl2 treatment to induce chemical hypoxic stress. ROS production, myelin density, number of OLG, and cognitive function were evaluated in vivo. OPC proliferation/differentiation were assessed both in vivo and in vitro.

Results: Oxy-blot assay confirmed that ROS generation was increased in the white matter at days 14 and 28 in the mouse model of chronic hypoperfusion. White matter dysfunction such as myelin loss and working memory deficits was also

observed, and edaravone treatment ameliorated these changes. In both in vivo and in vitro models, chronic hypoxic stress suppressed OPC differentiation into mature OLG, and edaravone treatment significantly accelerated OPC differentiation, even under hypoxic stress. However, extensive ROS suppression could not increase OPC differentiation under hypoxic condition.

Conclusions: Our data show that under chronic white matter hypoperfusion and hypoxia, ROS attenuates OLG maturation, which leads to white matter dysfunction. The ability of edaravone to ameliorate these deficits suggest that in addition to acute stroke, anti-oxidant therapies may also be a potential therapeutic approach for vascular dementia and other white matter diseases.

454
BRAIN-0130
Poster Session

Neuroprotection/Repair

EXTRA-CELLULAR SIGNAL REGULATED KINASE 1/2 INHIBITION IN THE ACUTE PHASE OF STROKE IMPROVES LONG-TERM NEUROLOGICAL OUTCOME AND PROMOTES NEUROVASCULAR PROTECTION AND ANGIOGENESIS.

M. Mostajeran[1], L. Edvinsson[1], K. Warfvinge[1], R. Singh[1], S. Ansar[1]
[1]Department of Clinical Sciences, Lund University, Lund, Sweden

Objectives

If extracellular signal regulated kinase (ERK) 1/2 activation in stroke is protective or detrimental is controversial [1]. In the acute phase of stroke it mediates neurovascular injury and in the delayed phase of stroke it may support neurovascular remodeling by enhancing angiogenesis and neurogenesis. The aim of this study is to investigate if specific inhibition of ERK1/2 pathway with U0126 in the acute phase following experimental stroke will improve long-term functional outcome, reduce infarct size, and promote angiogenesis and neurovascular protection.

Methods

Transient middle cerebral artery occlusion (tMCAO) was induced in male rats for two hours followed by reperfusion. U0126 treatment or vehicle was given at 0 and 24 h of reperfusion. Neurological functions were assessed by staircase test [2], 6-point [3] and 28-point [4] neuroscore tests. Infarct volume was evaluated by silver infarct staining at day 14. Angiogenesis and neurovascular protection were evaluated by the tyrosine kinase receptor Tie-2 and nestin protein expression at day 14. p-ERK1/2 protein levels were also investigated.

Results

Acute treatment with U0126 significantly improved long-term functional recovery after tMCAO (Figure 1). There was a significant improvement for U0126 treated rats compared to vehicle group in 28- and 6-point neuroscore tests at day 5, 8 and 14. The performance of U0126 treated rats in staircase test was better than vehicle group from day 8 to 13 after tMCAO and this difference reached significant level at day 14. Inhibition of ERK1/2 significantly decreased infarct volume in U0126 treated rats compared to vehicle group at day 14. After U0126 treatment, a significant enhancement of Tie-2 and nestin protein expression were observed in the ischemic border. Furthermore, p-ERK1/2 protein expression was not blocked at day 14 post-stroke.

Conclusions

For the first time it is demonstrated that by blocking the detrimental effect of ERK1/2 in the acute phase of stroke, we do not inhibit the beneficial effect of ERK1/2 activity in the delayed phase. The early prevention of ERK1/2 activity improves long-term functional outcome and promote angiogenesis and neuroprotection. These results provide new insights of using this treatment and are therefore a promising strategy for stroke.

References

1 Sawe N, Steinberg G, Zhao H. Dual roles of the MAPK/ERK1/2 cell signaling pathway after stroke. *J Neurosci Res* 2008; **86**: 1659–1669.

2 Montoya CP, Campbell-Hope LJ, Pemberton KD, Dunnett SB. The 'staircase test": a measure of independent forelimb reaching and grasping abilities in rats. *J Neurosci Methods* 1991; **36**: 219–28.

3 Engelhorn T, Goerike S, Doerfler A, Okorn C, Forsting M, Heusch G *et al.* The Angiotensin II Type 1 – Receptor Blocker Candesartan Increases Cerebral Blood Flow , Reduces Infarct Size , and Improves Neurologic Outcome After Transient Cerebral Ischemia in Rats. 2004; : 467–474.

4 Encarnacion A, Horie N, Keren-Gill H, Bliss TM, Steinberg GK, Shamloo M. Long-term behavioral assessment of function in an experimental model for ischemic stroke. *J Neurosci Methods* 2013; **196**: 247–257.

Figure 1

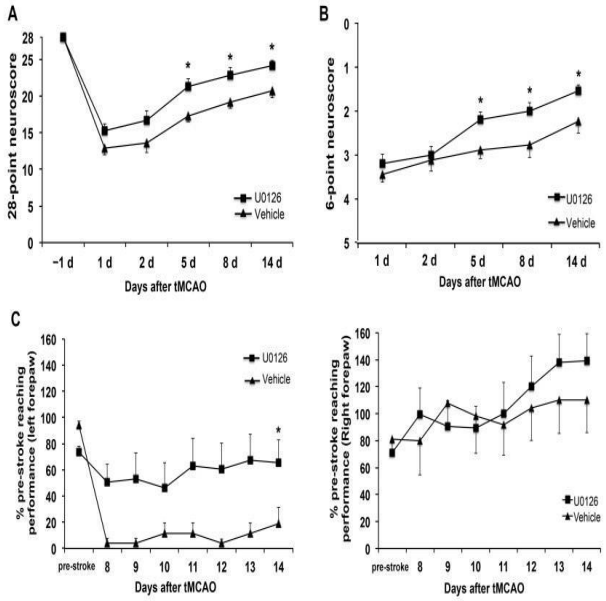

Figure 1. ERK1/2 inhibition resulted in improved neurological function after tMCAO. (A) Recovery of sensorimotor function up to 14 days after tMCAO with the 28-point neuroscore. (B) Gross neurological function graded in six levels from 0 – no visible defects, to 5 – death. Vehicle; n=9 and U0126; n=15. (C) Success rate of the rats in staircase test compared to their pre-stroke reaching performance. Calculation was performed for both left and right forepaw. Vehicle; n=4 and U0126; n=8. Data are expressed as mean ± SEM, * p<0.05

455
BRAIN-0443
Poster Session

Neuroprotection/Repair

MOLECULAR HYDROGEN AFFORDS NEUROPROTECTION IN A NEW PERINATAL ASPHYXIA PIGLET MODEL

J. Nemeth[1], V. Varga[1], V. Toth-Szuki[1], F. Domoki[1]
[1]Department of Physiology,
University of Szeged School of Medicine, Szeged, Hungary

Objectives: According to WHO estimates, perinatal asphyxia (PA) affects 4 out of 1000 live births often leading to the so-called hypoxic-ischemic encephalopathy (HIE) in the survivors. The exact pathophysiology of HIE is not fully understood, thus animal models with different asphyxia protocols are in use to mimic human pathology. The evaluation of neuroprotective applications such as ventilation with molecular hydrogen requires a large animal HIE model offering clinical translation. We aimed to develop a new HIE model in newborn pigs that reproduce all major features of PA/HIE and result in more severe brain damage compared to our previous results obtained with 8 min PA induced by halting ventilation. We then tested hydrogen-induced neuroprotection in our new model.

Methods: Approval was obtained from the Institutional Animal Care and Use Committee, care and handling of the animals were in accord with National Institutes of Health guidelines. Anesthetized and mechanically ventilated newborn pigs were aseptically instrumented and divided into 3 experimental groups: time control (C), asphyxia group (A) and asphyxia + hydrogen ventilated (AH) group. PA was induced in groups A and AH by ventilation with a gas mixture containing 6% O_2 and 20% CO_2 for 20 min while respiratory rate was decreased from 30 to 15 1/min, and iv glucose administration was stopped. Reventilation was commenced either with air (group A) or a gas mixture containing 2.1% H_2 21% O_2 and balance N_2 (group AH) for 4 hours. Then all animals were ventilated with air until 24

hours of survival. Throughout the experiments, core body temperature was tightly controlled (38.5±0.2°C), MABP, O_2 saturation, and EEG was continuously monitored, arterial pH and blood gases were checked regularly. At the end of the survival period, the brains were perfused, fixed and harvested for neuropathology analysis. EEG activity and neuronal damage were quantified with a scoring system, scores from 1-7 and 1-9, respectively. Data were analyzed with rank ANOVA, SNK post hoc test ($p<0.05$).

Results: Asphyxia resulted in severe hypercapnia, hypoxia and mixed acidosis (pCO_2=114±11 mmHg, pO_2=27±4 mmHg, pH=6.76±0.04, lactate=9.1±2.6 mmol/L mean±SE). The EEG became isoelectric during asphyxia, recovery of EEG activity was significantly better in the AH compared to the A group: data were: 1 (1;3) vs. 7 (4.5;7) at 20 hours (median (25^{th}; 75^{th} percentile)). Neuronal damage was more severe in our new HIE model, for instance parietal cortex scores were 2 (0;2) vs. 8 (5.5;9) vs. 5.5 (2.5;7), control vs. present vs. previous HIE model, respectively.

Conclusion: Our new PA/HIE model is suitable to reproduce severe PA mimicking metabolic and hemodynamic changes during the insult. The severity of PA was found to be sufficient to produce considerable neuronal damage often leading to even confluent necrosis in cortical areas enabling the model to assess the efficacy of neuroprotective techniques. Our present findings suggest that molecular hydrogen can be effective in protecting neurons after severe PA ameliorating the severity of subsequent HIE.

Reference:

Olah et al. Delayed neurovascular dysfunction is alleviated by hydrogen in asphyxiated newborn pigs. Neonatology. 2013;104(2):79-86.

Financial support: OTKA K100851, KTIA_13_NAP-A-I/13

456
BRAIN-0795
Poster Session

Neuroprotection/Repair

POST-STROKE DOCOSAHEXAENOIC ACID TREATMENT WITH COMBINED OMEGA-3 POLYUNSATURATED FATTY ACID DIET SUPPLEMENTATION IMPROVES LONG-TERM NEUROLOGIC RECOVERY AFTER CEREBRAL ISCHEMIA

H. Pu[1], L. Mao[1], J. Xia[1], G. Wang[1], H. Zhang[1], Y. Wu[1], Y. Shi[1], X. Hu[1], Y. Gao[2], J. Chen[1]
[1]Neurology,
Center of Cerebrovascular Disease Research Unive rsity of Pittsburgh School of Medicine, pittsburgh, USA
[2]Neurobiology,
State Key Laboratory of Medical Neurobiology and Institute of Brain Sciences, shanghai, China

Objectives: Stroke is a leading cause of serious long-term disability in adults in the US. Previous studies have demonstrated that food supplement of omega-3 polyunsaturated fatty acids (n-3 PUFAs) could prevent brain damage after stroke attack. However, the therapeutic effect of post-stroke n-3 PUFAs supplementation has not been well characterized. In this study, we investigated whether n-3 PUFAs food supplement, alone or in combination with post-stroke docosahexaenoic acid (DHA) injection, could provide long-tern protection against ischemic brain injury in a mouse model of stroke.

Methods: Transient focal cerebral ischemia was induced in C57/BL6 mice by unilateral middle cerebral artery occlusion (MCAO) for 60 minutes. The animals were randomly assigned to 5 groups: 1) sham, 2) vehicle, 3) DHA, 4) n-3 PUFAs and 5) DHA+n-3 PUFAs groups. DHA (10mg/kg) was given intraperitoneally immediately after MCAO and then once daily until 10 day after MCAO. Diet n-3 PUFAs (50 mg in every gram of regular diet) supplementation started from 5 days after MCAO until animal sacrifice. 5-bromo-2'-deoxyuridine (BrdU, 50mg/kg) was given intraperitoneally to label newly generated cells. Functional deficits

were determined up to 28 days after MCAO. Post-stroke neurogenesis, angiogenesis and white matter integrity were assessed by immunohistochemistry stainings at 28 days after MCAO.

Results: Both DHA administration alone or diet supplementation of n-3 PUFAs alone improved long-term sensorimotor and cognitive functions after MCAO, as revealed by improved performance in cylinder and rotarod test (sensorimotor function) and in morris water maze test (cognitive function) for at least 28 days after MCAO. DHA or n-3 PUFAs treatment alone also significantly reduced the tissue loss at 28 day after MCAO. Intriguingly, the animals that were subjected to n-3 PUFAs food supplement in combination with post-stroke DHA treatment exhibited further improvement in neurological behavior and further reduction in tissue loss as compared to animals with either intervention alone. Further studies demonstrated the beneficial effects of post-stroke DHA treatment or n-3 PUFA food supplementation in the following aspects: 1) enhancing post-stroke neurogenesis and neuronal replacement as indicated by increased number of Brdu+NeuN+ cells in the peri-infarct cortex and striatum; 2) promoting angiogenesis after MCAO as demonstrated by increased number of Brdu+CD31+ vessels in the infarct areas; 3) improving white matter integrity as shown by reduced loss of NF200 staining of axons and enhanced staining of MBP+ and CNPase+ myelin sheath. Remarkably, all these beneficial effects were significantly boosted by combined treatment with both post-stroke DHA injection and n-3 PUFAs food supplement.

Conclusions: Our results suggest that post-stroke DHA treatment with combined n-3 PUFA diet supplementation promotes long-term neurologic recovery after cerebral ischemia through multiple restorative mechanisms involving enhanced neurogenesis, angiogenesis and improved white matter integrity.

457
BRAIN-0236
Poster Session

Neuroprotection/Repair

NANOWIRED CEREBROLYSIN POTENTIATES MESENCHYMAL STEM CELLS INDUCED NEUROPROTECTION AND NEUROREPAIR FOLLOWING HEAT STROKE

D. Muresanu[1], A. Sharma[2], J. Lafuente[3], R. Patnaik[4], Z. Tian[5], A.S.Y.A. Ozkizilcik[5], H. Moessler[6], H. Sharma[7]
[1]Clinical Neurosciences, University of Medicine & Pharmacy, Cluj-Napoca, Romania
[2]Surgical Sciences Anesethesiology & Intensive Car e Medicine, Uppsala University Hospital, Uppsala, Sweden
[3]Neurosciences, University of Basque Country, Bilbao, Spain
[4]Biomedical Engineering, Banaras Hindu University IIT, Varanasi UP, India
[5]Chemistry & Biochemistry, University of Arkansas Faytteville, Faytteville AR, USA
[6]Drug Development & Discovery, Ever Neuro Pharma, Oberburgau, Austria
[7]Surgical Sciences Anesthesiology & Intensive Care Medicine, Uppsala University Hospital Uppsala University, Uppsala, Sweden

Our military personnel are often exposed to high heat in summer in desert areas where they are more susceptible to heat stroke that leads to either instant death or lifetime disabilities. Since stem cell therapy enhances neurorepair in brain or spinal cord injuries, this is quite likely that this may be effective in heat stroke as well. In this investigation we used nanowired delivery of mesenchymal stem cells (MSCs) intravenously following heat stroke and also added a known neuroprotective multimodal drug Cerebrolsyin to see whether this combination can result in good neurorepair following heat stroke in our rat model.
Heat stroke was inflicted in rats in a Biological oxygen demand (BOD) incubator at 38°C for 4 h

(relative humidity 45-47%; wind velocity 20-25 cm/sec). This model induces summer weather in desert areas and simulates heat stroke conditions in clinical situations. Heat stressed animals developed profound brain edema and volume swelling along with breakdown of the blood-brain barrier (BBB) and neuronal injuries as compared to controls (21±1°C). Commercially available MSCs (1 million cells, i.v.) given after1 h after heat stroke resulted in a mild but significant reduction in volume swelling and brain edema formation. However, when TiO2 nanowired MSCs are given under identical conditions the rats did not develop brain edema or volume swelling after heat stroke. Interestingly when TiO2 nanowired Cerebrolsyin (2.5 ml/kg) was co-administered with nanowired MSCs either 1 or 2 h after heat stroke significant reduction in brain pathology and brain edema formation was seen in these rats. These observations are the first to demonstrate that a combination of nanowired Cerebrolsyin and MSCs synergistically induced efficient neurorepair in heat stroke, not reported earlier.

458
BRAIN-0248
Poster Session

Neuroprotection/Repair

LOW-LEVEL LIGHT THERAPY PROTECTS BLOOD-BRAIN BARRIER INTEGRITY AND REDUCES INFLAMMATORY RESPONSE AFTER FOCAL CEREBRAL ISCHEMIA

H. Lee[1], J. Park[2], N. Kim[3], K. Park[3], B. Choi[2], Y. Shin[1], H. Shin[2]
[1]School of Medicine, Pusan National University, Busan, Korea
[2]School of Korean Medicine, Pusan National University, Busan, Korea
[3]Medical Research Center, Color Seven, Seoul, Korea

Objectives: Low-level light therapy (LLLT) modulates various biological processes such as increasing mitochondrial respiration and ATP synthesis, facilitating wound healing and promoting the process of skeletal muscle regeneration and angiogenesis. In the last few years, this therapy has been extended for the improvement of more severe conditions such as stroke, myocardial infarctions and traumatic brain injury. This study was designed to examine the effects of LLLT on the blood-brain barrier (BBB) dysfunction and brain damage induced by focal cerebral ischemic brain injury.

Methods: LLLT was used transcranially on the exposed skull by placing the tip of the fiber optic onto the skin at two locations on the head (the right midpoint of the parietal bone and the posterior midline of the seventh cervical vertebra). The mice received LLLT (20 min) twice a day for 2 days prior to the ischemic event. Focal cerebral ischemia was induced in C57BL/6J mice by middle cerebral artery occlusion (MCAO) and photothrombotic cortical ischemia model. We evaluated the infarct volume and neurological and motor function 24 h after ischemic brain injury.

Results: In both models of stroke, LLLT significantly decreased infarct size, edema and improved neurological and motor function. In molecular studies, the proportion of apoptotic cells, astrocyte and microglia in the cortex were markedly decreased in LLLT groups. LLLT also attenuated iNOS, COX-2, TLR-2, proinflammatory cytokines and chemokines expression. Brain edema-induced change of Evans blue extravasation, water content, occludin and claudin-5 expression in ipsilateral hemisphere were alleviated by LLLT.

Conclusions: Our data suggest that a noninvasive intervention of LLLT in focal cerebral ischemic injury may provide a significant functional benefit with an underlying mechanism possibly being suppression of inflammatory response and reduction of BBB disruption.

459
BRAIN-0852
Poster Session

Neuroprotection/Repair

EVIDENCE OF NEUROPLASTICITY IN CORONARY ARTERY DISEASE PATIENTS AFTER CARDIAC REHABILITATION.

U. Anazodo[1], J.K. Shoemaker[2], N. Suskin[3], D.J. Wang[4], K.S. St Lawrence[1]
[1]Medical Biophysics Western University, Lawson Health Research Institute, London, Canada
[2]School of Kinesiology Western University, Laboratory for Brain and Heart Health, London, Canada
[3]LHSC, London Health Sciences Cardiology Rehabilitation Program, London, Canada
[4]University of California, Department of Neurology, Los Angeles, USA

Introduction: Regional brain atrophy[1] and hypoperfusion[2] have been demonstrated in cardiovascular disease patients in regions associated with cognition and perception such as in the insula, medial frontal, cingulate and postcentral gyrus. These regional abnormalities in brain structure can be reversed with aerobic exercise even after a few weeks of fitness training[3]. In this study we examined if moderate aerobic exercise, as part of a cardiac rehabilitation program, would improve cortical brain thickness and cerebral blood flow (CBF) in coronary artery disease (CAD) patients in brain regions vulnerable to vascular disease. Regional CBF and brain volume were measured with pseudocontinous ASL (pCASL) and cortical thickness analysis, respectively.

Materials and Methods: Data from 18 CAD patients (age 59 ± 6 years) were acquired before and after 6 months of moderate exercise training on a Siemens 3.0T Verio system using a 32-channel array coil. 2D-pCASL[4]imaging parameters include 1.5s label duration,1.0s post-label delay, TR/TE =3500ms/12ms, FOV=24cm, matrix=64x64, and 12 axial slices. 1.0mm^3 isotropic T1-weighted MPRAGE data was acquired for cortical thickness analysis (CTA).

CTA was performed with Brainvoyager (Brain Innovation, NL) and pCASL EPI images were processed using SPM8 (UCL, London, UK) and in-house MATLAB scripts. Average perfusion-weighted images were generated by surround subtraction of pCASL pairs and smoothed with an 8mm FWHM Gaussian filter. A gray matter (GM) mask was applied to the CBF images and only voxels containing 80% GM were selected for region of interest analysis (ROI). Student t-test was conducted across the whole brain in CTA images to determine regions of increased brain volume with exercise. ROI analysis was performed in CBF images inregions revealed from CTA and paired t-test was performed between images acquired at baseline and after exercise. Fitness was measured by a graded exercise test and breath-by-breath measurements of maximal O_2 consumption (VO_2max) was recorded.

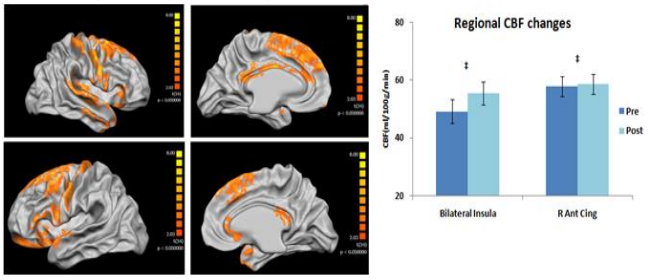

Fig1: *left*: areas (orange) of increase cortical thickness post exercise; *right*: CBF change in *two regions(‡ p<0.05).*

Results: A ~10% increase in mean CTA and 7% increase in mean GM CBF were observed in patients after exercise training. Regions with increased cortical thickness following exercise include right (R) inferior frontal, R precentral, bilateral middle frontal and bilateral superior frontal gyri (*Fig. 1*). Increases in regional CBF were observed in R anterior cingulate and bilateral insula (*Fig. 1*). A trend (5%) towards increased VO_2max was observed after exercise training.

Discussion and Conclusion: This study demonstrates evidence of brain plasticity with exercise training in regions of the brains of

coronary artery disease patients including regions associated with vascular disease[1-2] and regions involved in cognitive control.

Reference: [1] Anazodo et al,*NeuroImaging Clinical* 2013. [2] Anazodo et al, *Proc. ISMRM*, 2015 [3] Colcombe et al, *J Greonotol* 2006. [4] Wang, *Proc. ISMRM*, 2007

460
BRAIN-0646
Poster Session

Neuroprotection/Repair

ASSESSMENT AT THE SINGLE-CELL LEVEL IDENTIFIES NEURONAL GLUTATHIONE DEPLETION AS A TREATABLE CAUSE OF REPERFUSION INJURY

R.A. Swanson[1], S. Won[1], J. Kim[1]
[1]Neurology, UCSF, San Francisco, USA

Objectives: Oxidative stress contributes to neuronal death in brain ischemia-reperfusion. Brain levels of the endogenous anti-oxidant glutathione (GSH) are depleted during ischemia-reperfusion, but it is not known whether this depletion is a cause or an effect of oxidative stress, or whether it occurs in neurons or other cell types. It is also uncertain whether neurons even contain appreciable amounts of GSH, relative to astrocytes. Here we aimed to resolve these issues by simultaneously evaluating GSH, superoxide, and oxidative stress in mouse hippocampal neurons after ischemia-reperfusion.

Methods: Adult male mice were subjected to transient forebrain ischemia by 12-minute occlusions of the bilateral carotid arteries. Immunohistochemical methods were used to evaluate GSH, superoxide, oxidative stress, and neuronal survival in mouse hippocampal neurons. For some studies, post-ischemic superoxide production was increased by rendering the mice hyperglycemic, and suppressed by using the NADPH oxidase inhibitor apocynin or mice genetically deficient in NADPH oxidase. Neuronal glutathione synthesis was supported by administration of N-acetyl cysteine, 7.5 - 15 mg/kg, at the time of reperfusion.

Results: Baseline GSH levels were higher in hippocampal pyramidal neuron cell bodies and processes than in the surrounding neuropil, and underwent a time-dependent decrease during the first few hours of reperfusion. Co-labeling for GSH and superoxide during reperfusion revealed a striking inverse correlation, with the highest superoxide signal present in the neurons with lowest GSH content. (See figure: left panel shows hippocampal neurons labeled with markers for glutathione or superoxide formation, and right panel shows data from 430 hippocampal neurons each plotted according to their glutathione and superoxide signals.) Mice in which superoxide production was increased during reperfusion showed accelerated loss of GSH, whereas mice in which superoxide production was inhibited showed preserved GSH, thus demonstrating that the post-ischemic neuronal GSH depletion is a result of oxidative stress. Conversely, mice treated with in N-acetyl cysteine to promote GSH synthesis showed reduced levels of neuronal superoxide, oxidative stress, and neuronal death

Conclusions: Hippocampal pyramidal neurons *in situ* contain high levels of GSH relative to non-neuronal cells. Neuronal GSH depletion is both a cause and a result of neuronal oxidative stress after ischemia-reperfusion. Post-ischemic treatment with N-acetyl-cysteine maintains neuronal GSH levels and reduces neuronal death.

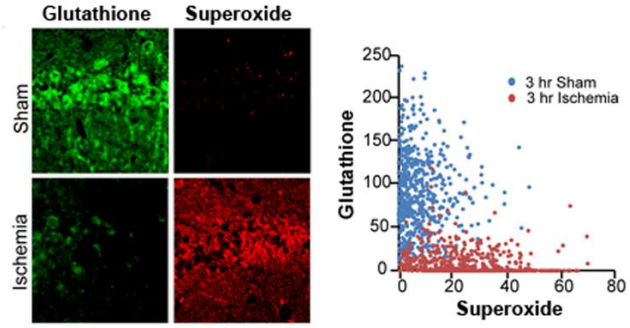

461
BRAIN-0156
Poster Session

Neuroprotection/Repair

OVEREXPRESSED LOTUS IMPROVES FUNCTIONAL RECOVERY AFTER BRAIN FOCAL ISCHEMIA IN MICE.

H. Takase[1], *T. Yokoyama*[1], *Y. Kurihara*[2], *K. Takei*[2], *N. Kawahara*[1]
[1]*Department of Neurosurgery, Yokohama City University Graduate School of Medicine, Yokohama, Japan*
[2]*Molecular Medical Bioscience Laboratory Department of Medical Life Science, Yokohama City University Graduate School of Medical Life Science, Yokohama, Japan*

Abstract Text:

Objectives: Axon growth inhibitors such as Nogo proteins, myelin-associated glycoprotein (MAG), oligodendrocyte myelin glycoprotein (OMgp), and B lymphocyte stimulator (BLyS) commonly bind to Nogo receptor-1 (NgR1), leading to restriction of functional recovery after damage in the adult central nervous system [1] [5] [4] [2]. It is recently reported that lateral olfactory tract usher substance (LOTUS) antagonizes NgR1-mediated signaling [3]. However, effect of global blockade of NgR1 signaling by LOTUS *in vivo* is unknown. To examine the role of LOTUS overexpression *in vivo*, we generated lines of transgenic mice in which neurons overexpress LOTUS protein, and examined whether overexpressed LOTUS would improve the functional recovery after stroke.

Methods: Adult wild-type mice (9-11 weeks of age, body weight 28-34g) underwent transient middle cerebral artery occlusion (MCAO) for 45 minutes using the intraluminal filament technique resulting in a focal ischemic stroke. Animals were sacrificed at 8 time-points after stroke. Brains were removed and separated into hemisphere and cortex/white matter. Protein expression levels of LOTUS were analyzed by Western blotting. Functional improvement after ischemic stroke was analyzed by Bederson score in the adult homozygous transgenic mice of strain C57BL/6J carrying mice LOTUS gene, and wild-type animals. Measurement of infarct volume was also performed.

Results: Western blotting analysis revealed that LOTUS expression in the brain of MCAO wild-type mice was obviously increased in the white matter of contralateral hemisphere at 42 days after stroke. Both the wild type and LOTUS transgenic (LOTUS-Tg) mice showed similar neurological score in early stages after stroke. Both animals showed a gradual improvement in several weeks after stroke, such improvement in LOTUS-Tg mice, however, was significantly earlier and better than the wild-type.

Conclusions: These findings suggest that expression of LOTUS may increase in late stages after stroke and overexpression of LOTUS may give rise to early and better functional recovery. The data in this study would highlight a promoting effect of LOTUS in functional recovery following ischemia and administration of LOTUS may be useful for a future therapeutic strategy.

References:
1. Domeniconi M, et al. Neuron 2002; 35: 283-90.
2. Fournier AE, et al. Nature 2001; 409: 341-6.
3. Sato Y, et al. Science 2011; 333: 769-73.
4. Wang KC, et al. Nature 2002; 417: 941-4.
5. Zhang L, et al. J Neurosci 2009; 29: 6348-52.

Graph:

The graph showing Bederson's neurological score. ¶; There were statistical difference between groups. ($p<0.05$, Mann-Whitney's U test)
§, *; There were statistical difference ($p<0.05$,

versus day7, Wilcoxon signed-rank test)

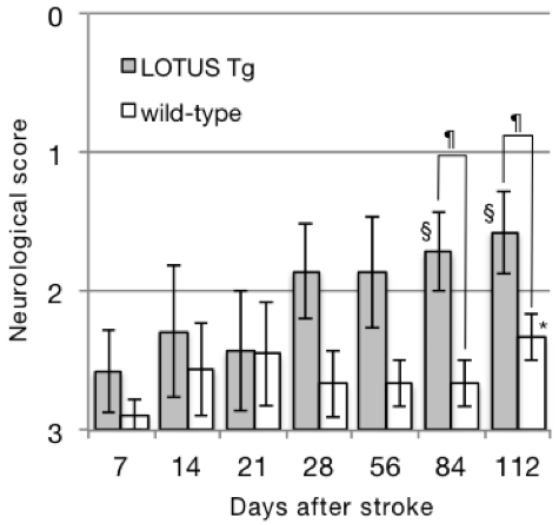

462
BRAIN-0173
Poster Session

Neuroprotection/Repair

OPTOGENETIC STIMULATION OF THALAMOCORTICAL PROJECTIONS TO PROMOTE STRUCTURAL PLASTICITY AND RECOVERY OF FUNCTION AFTER SOMATOSENSORY CORTEX STROKE

K.A. Tennant[1], *C.E. Brown*[1]
[1]*Division of Medical Sciences, University of Victoria, Victoria, Canada*

The large majority of stroke survivors must cope with some level of chronic disability, often affecting the upper limbs, and improved use of the stroke-affected limb is generally accompanied by neuroplasticity in intact brain areas surrounding the stroke. Thus, modulating this innate plasticity should promote further gains in recovery. Potential key areas for neuroplastic modulation include sub-cortical brain areas, which are affected by cortical stroke by diaschisis, but remain intact and thus may ultimately contribute to recovery of function. One relatively unknown issue in stroke research involves the role of the thalamus, the brain's relay center for sensory information en route to the cortex, in recovery from stroke in the forelimb area of the somatosensory cortex (FLS1). Unpublished data from our lab has shown that while peri-infarct thalamocortical axons are relatively resilient to the effects of ischemia (i.e. they survive long-term), they lose a significant number of terminaux and en passant boutons in the first few weeks after stroke. We now expand on this by asking whether optogenetic stimulation of peri-infarct thalamocortical projections promotes the re-wiring of axonal boutons and improves behavioural recovery after FLS1 stroke. Thalamocortical axons extending from the ventroposterior lateral (VPL) nucleus of the thalamus to primary somatosensory cortex were transfected with a fluorescently tagged adeno-associated virus that expressed channelrhodopsin-2, AAV2.CamKII.hChR2(E123A), and a chronic cranial window was implanted over the sensorimotor cortex to allow for longitudinal *in vivo* two-photon imaging of axon terminals before and at various times after photothrombotic stroke. Optogenetic stimulation was driven by a blue LED (475 nm, 8-10mW/mm^2) magnetically attached to the cranial window and was initiated 3 days after stroke. The entire infarct and peri-infarct cortex visible through the window were subject to light, but only those cells that express ChR2 were stimulated. Optical stimulation (5 ms pulses at 5 Hz every 5 seconds) or control procedures (head cap on but light turned off) were administered in awake mice for 1 hour per day, 5 days per week for 6 weeks after stroke. Behavioural performance on the Tape Removal Test and Ladder Walking Test were assessed once weekly throughout the entire imaging period. Changes in axonal branching patterns, length, and the number of axonal varicosities were analysed. Preliminary data suggest that post-stroke optogenetic stimulation of thalamocortical projections improves stroke-related deficits in tactile perception.

463
BRAIN-0247
Poster Session

Neuroprotection/Repair

ERYTHROPOIETIN PROTECTS NEURAL CELL AND BLOOD BARRIER FROM ISCHEMIA-REPERFUSION INJURY BY INTERFERING IN ENDOPLASMIC RETICULUM STRESS

R. Wang[1], H. Zhao[1], X. Wu[2], X. Liu[1], L. Min[2], X. Ji[3], Y. Luo[1]
[1]Cerebrovascular Diseases Research Laboratory, Xuanwu Hospital of Capital Medical, Beijing, China
[2]Neurology,
The First Affiliated Hospital of Liaoning Medical U niversity, Jinzhou, China
[3]Neurology, Xuanwu Hospital of Capital Medical, Beijing, China

Abstract

Objectives—Erythropoietin (EPO) in combination with tissue plasminogen activator (tPA) causes serious side effects in acute ischemic stroke preclinical and clinical trials for some possible reasons, including high-dose EPO associated with red cell aplasia, and increased risk of thrombosis. To improve the outcome of this combination therapy in experimental ischemic stroke, the present study intended to establish a new strategy by optimizing the dosage of EPO and its route of administration, and examine the effects of this strategy on cerebral ischemia and reperfusion injury as well as its underlying mechanisms associated with endoplasmic reticulum (ER) stress.

Methods—Male Sprague–Dawley rats subjected to middle cerebral artery occlusion (MCAO) following 2 h ischemia/24 h reperfusion. Rats were randomly divided into 6 groups (N=6): sham, vehicle, EPO (800 IU/kg), tPA (10 mg/kg), EPO+tPA, and salubrinal (an ER stress inhibitor) group. After MCAO, rats were treated with EPO or tPA through MCA infusion at the beginning of reperfusion. In another set of experiments, FITC-labeled EPO was given via middle cerebral artery injection (MCAI) or subcutaneous injection (SI) for comparison of the 2 modes of administrations. Neurological deficits were assessed using Ludmila Belayev and forelimb foot-fault tests, the brain infarct volume and swelling volume were evaluated by TTC staining, the expression of tight junction proteins (Claudin-5 and Occludin), matrix metallopeptidase-9, caspase-3, AQP4 and ER stress-associated proteins (GRP78, CHOP, and ATF6α) were detected by immunofluorescence staining and western blotting.

Results—FITC-labeled EPO test demonstrated that a higher EPO level in cerebrospinal fluid and brain tissue was reached by low dosage of EPO (800 IU/kg) through MCA injection than usual dosage of EPO (5000 IU/kg) through subcutaneous injection. The infarct volume, brain edema, neurobehavioral deficits, and downregulation of Claudin-5 and Occludin were alleviated significantly by monotherapy of EPO or combination therapy of EPO and tPA, compared with the vehicle and tPA alone group following 2 h ischemia/24 h reperfusion. The monotherapy of EPO and combination therapy of EPO with tPA both markedly reduced the expression of Caspase-3 and AQP4 in brain tissue, and MMP-9 levels in isolated microvessels, respectively, while decreased ER stress markers GRP78, CHOP, and ATF6α.

Conclusions—Administration of low-dose EPO in combination with tPA through MCA infusion at the onset of reperfusion enhanced its neuroprotective effects following 2 h acute ischemic stroke in rats, which prevents apoptosis, cell swelling as well as BBB disruption, that may be correlated with the potential of EPO to antagonize ER stress. This result suggests that tPA did not abolished the beneficial effects of EPO, the mode of EPO administration reported in this study as a new therapeutic strategy for patients with acute ischemic stroke.

464
BRAIN-0019
Poster Session

Neuroprotection/Repair

EFFECTS OF LIPOCALIN-2 IN THE REGULATION OF GLIAL ACTIVATION AND ANGIOGENESIS

C. Xing[1], L. Wu[1], W. Leung[1], J. Lok[1], E.H. Lo[1]
[1]Radiology and Neurology, Massachusetts General Hospital, Charlestown, USA

Objectives - Inflammation is a key part of central nervous system pathophysiology. Recently, it is thought that inflammatory factors may have both beneficial and deleterious actions. Here, we examine the hypothesis that lipocalin-2, an inflammatory molecule that can be upregulated in the distressed central nervous system, may regulate glial activation and enhance angiogenesis in brain cells. ***Methods*** – In vitro, microglia, astrocytes, or brain endothelial cells were exposed to lipocalin-2 and various markers and assays of glial activation and angiogenesis including tube formation and migration were quantified. ***Results*** - In primary glial cell cultures, exposing microglia and astrocytes to lipocalin-2 resulted in glial activation. In microglia, lipocalin-2 converted resting ramified shapes into a long-rod morphology with reduced branching, increased interleukin-10 release, and enhanced phagocytosis. In astrocytes, lipocalin-2 upregulated GFAP, BDNF and thrombospondin-1. Adding lipocalin-2 (0.5-2.0μg/ml) to RBE.4 rat brain endothelial cells significantly increased matrigel tube formation and scratch migration, and also elevated levels of iron and reactive oxygen species (ROS). Co-treatment with a radical scavenger (UE83836E), a Nox inhibitor (apocynin) and an iron chelating agent (deferiprone) significantly dampened the ability of lipocalin-2 to enhance tube formation and scratch migration in brain endothelial cells. ***Conclusions*** - These findings provide in vitro proof-of-concept that lipocalin-2 may contribute to gliovascular recovery aspects of inflammation by activating microglia and astrocytes into potentially pro-recovery phenotypes and promoting angiogenesis via iron and ROS-related pathways.

465
BRAIN-0067
Poster Session

Neuroprotection/Repair

SEVOFLURANE PRECONDITIONING REVITALIZES ENDOGENOUS BRAIN SELF-REPAIRING ABILITY IN RATS FOLLOWING CEREBRAL ISCHEMIC INJURY

Q. Yu[1], L.I. Li[1], H. Saiyin[2], W. Liang[1]
[1]Anesthesia Department, Huashan Hospital, Shanghai, China
[2]Key Laboratory of Genetic Engineering School of L ife Sciences, Fudan University, Shanghai, China

Purpose: Ischemic stroke causes irreversible neuronal death within the infarction region. Although an ideal therapy doesn't currently exist, it would target the affected region, ultimately restoring its function. Sevoflurane preconditioning has been demonstrated to play a neuroprotective role in penumbra region, whether it could promote neural regeneration and accelerate brain repair in infarct region remains unclear.

Methods: Transient middle cerebral artery occlusion (MCAO) model was established in rats. Rats were randomly divided into sham group, MCAO group, Sevo + MCAO group and killed at 1, 3, 7, 14, 28d after surgery. TTC staining, immunofluorescent staining and confocal three dimensional reconstruction were used to observe brain repair process of different groups at different time.

Results: Sevoflurane preconditioning not only enhanced proliferation of neural stem cells in SVZ at 3days, but also guaranteed those newborn neurons to survive in the infarct area. These benefits were achieved by accelerating BDNF secreted by microglia, and enhancing microglia phagocytic activity to swiftly clear the dead debris of infarct area. Early clearance of dead debris promoted astrocytes migration to infarct area, and provided a fine scaffold for neuroprogenitor

cells migration into the cleared infarct area. Then neuroprogenitor cells quickly differentiated into mature neurons and different type of glial cells at 14days. The newborn neurons connected with each other by synapses, and built up a circuit with axons from the undamaged parts.

Conclusions: These results demonstrated that sevoflurane preconditioning facilitated brain self-repair process by enhancing the systemic neurogenesis and synaptogenesis in the infarct region of cerebral ischemic injury model, which may provide a new strategy to the ischemic stroke patients.

466
BRAIN-0532
Poster Session

Neuroprotection/Repair

THE NEUROPROTECTIVE ROLE OF MITOCHONDRIAL LOCATED PKC BETA II IN ISCHEMIA-REPERFUSION INJURY

O. Poleszak[1], M. Beresewicz[1], E. Sitkiewicz[2], M. Dadlez[2], A. Misicka-Kesik[3], B. Fedorczyk[3], B. Zablocka[1]
[1]Molecular Biology Unit, Mossakowski Medical Research Centre, Warsaw, Poland
[2]Mass Spectrometry Lab, Institute of Biochemistry and Biophysics, Warsaw, Poland
[3]Department of Chemistry, University of Warsaw, Warsaw, Poland

Objectives: Isoforms of Protein Kinase C (PKCs) are ubiquitously expressed in all cell types and implicated in multiple cellular functions. By phosphorylation of serine/threonine residues in target proteins, these kinases act as regulators of growth, differentiation, cell survival, carcinogenesis and learning and memory (1). Strong emphasis is also placed on the participation of PKC in ischemia/reperfusion-induced signal transduction (I/R). Activation of multiple PKC isozymes has been shown to occur after I/R injury in multiple organs including heart, liver, kidney and brain, suggesting its role in ischemic response pathways (2). Protein Kinase C β (PKCβ) is a kinase whose role in neurons survival/regeneration/protection needs further investigation. Our previous studies revealed that transient ischemic injury induces a rapid and long lasting increase of PKCβ in mitochondria fraction but mainly in ischemia-resistant part of hippocampus, what may bespeak neuroprotection (3). Hence, we set out to determine the role of PKCβ isozymes βI and βII in two models of brain ischemia i) *in vitro* in rat organotypic hippocampal cultures subjected to excitotoxic injury which mimic ischemic injury and (ii) *in vivo* – transient brain ischemia in gerbils.

Methods: All animal procedures were conducted in accordance with the Local Commission for Ethics of Experiments on Animals and the care and handling of the animals were in accord with NIH guidelines . We tested: (i) the effect of I/R on PKCβ isozymes localisation and activityin mitochondria isolated from ischemia-vulnerable and -resistant hippocampal regions (ii) the effect of isozyme-selective inhibitors of PKCβI and βII *in vivo* and *in vitro* models of I/R injury and (iii) by pull down followed by mass spectrometry the potential PKCβII mitochondrial partners to elucidate PKCβII-mediated neuroprotective mechanisms.

Results: Here we have observed that transient ischemic episode induces a significant elevation of PKCβII protein level and activity in ischemia-resistantpart of hippocampus in mitochondrial fraction. Moreover, exclusive inhibitionof PKCβII is sufficient to increase by 29% the damage area in hippocampal organotypic slices. Thus resultssuggest that it is rather PKCβII than PKCβI which may be akey element responsible for neuroprotection. To elucidate the mechanisms of PKCβII-mediated neuroprotection its mitochondrial partners were identified. The analysis recognised a number ofproteins belonging to mitochondrialinner and outer membrane as well as mitochondrial matrix. They are involved inregulation of different metabolic pathways such as fatty acid oxidation,glucose metabolism, electron transport chain and others. Using phophosite we verified that most of

identified PKCβII-protein partners have putative PKC phosphorylation sites indicating that regulation of these metabolic pathways by PKCβII phosphorylation may lead to PKCβII - mediated neuroprotection. The functional significance of the PKCβ mitochondrial localization is being studied.

Conclusions: Postischemic translocation of PKCβ to mitochondria may be involved in endogenous mechanisms of postischemic neuroregeneration.

References:

1.Gould,C.M., Newton,A.C. The life and death of protein kinase C. Curr. Drug Targets. 2008, 9: 614-625.

2.Bright,R., Mochly-Rosen,D. The role of protein kinase C in cerebral ischemic and reperfusion injury. Stroke 36,2781-2790.

3.Kowalczyk,J.E., Kawalec,M., Beresewicz,M., Debski,J., Dadlez,M., Zablocka,B. Protein kinase C beta in postischemic brain mitochondria. Mitochondrion. 2012; 12(1):138-43.

The study is supported by NSC grant2012/05/B/NZ/00415 and KNOW-MMRC project.

467
BRAIN-0229
Poster Session

Neuroprotection/Repair

ENHANCED NEUROPROTECTIVE EFFECTS AGAINST ISCHEMIA OF G-CSF DELIVERED BY INTRANASAL APPROACH

B. Sun[1], S. Zhang[1], L. Mao[1], C. Fan[1], H. Yuan[1], R. Stetler[2], J. Chen[2], F. Zhang[2]
[1]Neurology Key Laboratory of Cerebral Microcirculation, Taishan Medical University, Taian, China
[2]Department of Neurology and Center of Cerebrovascular Disease Research, University of Pittsburgh, Pittsburgh, USA

Objectives: Stroke remains the third leading cause of death and top cause of long-term disability worldwide with a limited treatment approaches. Granulocyte-colony stimulating factor (G-CSF) is a hematopoietic growth factor with strong neuroprotective properties. However, it has limited capacity to cross blood-brain barrier. Recent studies demonstrated that intranasal drug administration is a promising way in delivering neuroprotective agents to the central nervous system. This study therefore aimed at determining if intranasal administration of G-CSF increases its delivery to brain and its neuroprotective effect against ischemic brain injury. Methods: Transient focal cerebral ischemia in rats was induced with middle cerebral artery occlusion and intranasal application of G-CSF or vehicle was carried out at two hours after ischemia. Neurological outcomes were evaluated by neurological function, infarct volume, intracellular calcium concentration, immunohistochemical stain and Western blot. Neurogenesis and angiogenesis were also analyzed. Results: Our resulted showed than intranasal administration is 8-12 times more effective that subcutaneous injection in delivering G-CSF to cerebrospinal fluid and brain parenchyma. Intranasal delivery enhanced the protective effects of G-CSF against ischemic injury in rats, indicated by decreased infarct volume and increased recovery of neurological function. The neuroprotective mechanisms of G-CSF involved

enhanced upregulation of HO-1 and reduced calcium overload following ischemia. Intranasal G-CSF application also promoted angiogenesis and neurogenesis following brain ischemia.
Conclusions: Taken together, our results confirm that G-CSF is a legitimate neuroprotective agent, and further reveal that intranasal administration of G-CSF is more effective in delivery and neuroprotection and could be a practical approach in clinic.

470
BRAIN-0497
Poster Session

Cardiac Arrest/Global Cerebral Ischemia

THERAPEUTIC HYPOTHERMIA REVERSES ISCHEMIA-INDUCED IMPAIRMENT OF SYNAPTIC PLASTICITY FOLLOWING PEDIATRIC CARDIAC ARREST IN A GENDER-SPECIFIC MANNER.

R.M. Dietz[1], X. Hui[1], J.E. Orfila[2], G. Deng[3], R.J. Traystman[3], P.S. Herson[2]
[1]Pediatrics,
University of Colorado School of Medicine, Aurora, USA
[2]Anesthesiology,
University of Colorado School of Medicine, Aurora, USA
[3]Pharmacology,
University of Colorado School of Medicine, Aurora, USA

Objectives: Pediatric cardiac arrest (PCA) can be a devastating condition, often leading to poor neurologic outcomes in children, including deficits in learning and memory. An increase in synaptic efficiency, termed long-term potentiation (LTP), is a well-accepted cellular model for learning and memory. Therapeutic hypothermia (TH) is still in the experimental stages in the pediatric population, despite its use in neonates and adults. Our group recently showed persistent impairment on synaptic function following CA in adult mice. However, little is known about the affect of PCA on synaptic plasticity or the effects of hypothermia on synaptic function. Further, few studies have examined the influence of hypothermia between genders and none have done so on pediatric subjects. Thus, the goal of the current study was to measure the effects of PCA on synaptic function in pediatric mice and assess the therapeutic potential of TH.
Methods: Male and female pediatric mice (postnatal day 20-25) were subjected to 8 min cardiac arrest and cardiopulmonary resuscitation (CA/CPR) and were recovered in normothermia (37^{o}C) or hypothermia (32^{o}C). Hippocampal CA1 function and synaptic plasticity were evaluated using acute brain slices 7 or 30 days after CA/CPR or sham controls. Synaptic plasticity was measured by long term potentiation of synaptic signals following theta-burst stimulation (TBS). Increase in field excitatory post-synaptic potential (fEPSP) slope 60 min after TBS was analyzed as a measure of synaptic plasticity (LTP).
Results: In control male mice, TBS resulted in LTP that increased fEPSP slope to 153% (n=8) of baseline and female control mice increased to 155% (n=6) of baseline. In contrast, 7 days after CA/CPR, there was significant impairment in both sexes, with LTP increasing to 114% and 113% of baseline (n=6 each) respectively ($p<0.05$ compared to control mice). By 30 days, synaptic plasticity had recovered in both sexes to control levels (155% in males and 149% in females). Mice exposed to 30 min hypothermia (32^{o}C) following PCA showed recovery of synaptic plasticity 7 days after CA/CPR in which males had 135% synaptic plasticity (n=8) and females had 155% synaptic plasticity (n=7, $p<0.05$ from 7 day mice and between genders). Deeper hypothermia in the males to 30^{o}C retained significantly higher LTP (156%) than at 32^{o}C but was not different from females at 32^{o}C.
Conclusions: The mouse PCA model provides important insights into the long-term recovery of synaptic function following CA/CPR. We have found that PCA causes impairment in synaptic plasticity in the sub-acute time after CA/CPR (7 days) that recovers by 30 days. This remarkable recovery of plasticity in the pediatric brain is in contrast to several recent reports using adult mice, where the impairment persists beyond 30 days. Further, we found that hypothermia provides significant protection against the loss of synaptic plasticity but males may recover better at deeper levels of hypothermia. This data adds to

the literature describing differences in gender susceptibility to ischemia as well as adding support for hypothermia following CA in pediatric patients.

471
BRAIN-0865
Poster Session

Cardiac Arrest/Global Cerebral Ischemia

THE SUBBAND-BASED EEG MARKER AND NEUROLOGICAL OUTCOME WITH TEMPERATURE MANIPULATION AFTER CARDIAC ARREST

R. Deng[1], L. Young[1], X. Jia[1,2]
[1]Biomedical Engineering,
Johns Hopkins University, Baltimore, USA
[2]Neurosurgery,
University of Maryland School of Medicine, Baltimore, USA

Objective: The ischemic brain afterasphyxia-cardiac arrest is sensitive to trivial temperature fluctuation.However, the differences in neurologic outcomesamong different rhythms in EEG waves, which are associated with functionalbehaviors and underlying temperature manipulation, has not been elucidated. We investigatedthe cortical recovery with temperature manipulation by using a novelquantitative EEG, subband-based information quantity (SIQ) in this study. SIQis a quantitative measure of the entropy of information embedded in each EEGband.

Methods: Total 24 rats under 7-min asphyxia-cardiac arrestwere randomly divided into three immediate temperature intervention groups:hypothermia (32°C-34°C),normothermia (36.5–37.5°C) and hyperthermia (38.5°C-39.5°C) (n=8 per group).For each rat, EEG was recorded for the first 8 hours and then for contineous 30minutes per day until 72 hours. Neurologic Deficit Score was applied toevaluate the functional outcomes.

Results: Greater recovery of conventionalSIQ (the mean of SIQs in five EEG rhythms) was found in the hypothermia group (Mean±S.E.M, 0.80±0.021) thanin the normothermia group (0.69±0.024)($p<0.01$) and in the normothermia group than the hyperthermia group (0.66±0.023) ($p<0.05$), consistent with their result of NDSscore. There were notable changes in five sub-band SIQs among the three temperaturegroups as early as 30 minutes after resuscitation. Nevertheless, the leastsignificant recovery in hypothermia was found in delta rhythm; whereas gammaband under hypothermia indicated the best recovery throughout 72-hourexperiment. Moreover, the gamma-band SIQ showed the strongest correlation with72-hour NDS and accurately predicted neurologic condition, whereas thedelta-band SIQ had no association.

Conclusion: The improvement of recovery by hypothermia and the further damageto ischemic brain can be precisely indicated by our SIQ-qEEG markers. TheSIQ-qEEG markers can provide more details on predicting cerebral functionaloutcome during the first 4 hours after cardiac arrest even in a coma state. Temperatureintervention may affect neuronal oscillations primarily on gamma rather than delta rhythm.

References:

1. Shin HC,Jia X, Nickl R, et al. A subband-based information measure of EEG during braininjury and recovery after cardiac arrest. IEEE transactions on bio-medicalengineering 2008;55(8):1985-1990.
2. Jia X, Koenig MA, Nickl R, et al. Early electrophysiologicmarkers predict functional outcome associated with temperature manipulationafter cardiac arrest in rats. Critical care medicine 2008;36(6):1909-1916.
3. Jia X, Koenig MA, Shin HC, et al. Quantitative EEG andneurological recovery with therapeutic hypothermia after asphyxial cardiacarrest in rats. Brain research 2006;1111(1):166-175.

The work was supported by R01HL118084 from NIH(to XJ) and 09SDG2110140 from American Heart Association (to XJ).

472
BRAIN-0804
Poster Session

Cardiac Arrest/Global Cerebral Ischemia

IMPAIRED AUTOPHAGOSOME CLEARANCE CONTRIBUTES TO NEURONAL DEATH AFTER ISCHEMIA/REPERFUSION INJURY TRIGGERED BY CARDIAC ARREST IN NEONATAL PIGLETS

D. CUI[1], Z. Yang[1], E. Kulikowicz[1], J. Armstrong[1], M. Reyes[1], J. Lee[1], W. Jiang[1], R. Koehler[1]
[1]Department of Anesthesiology and Critical Care Medicine, Johns Hopkins University, Baltimore, USA

Objectives-Dysregulation of autophagy contributesto neuronal cell death in several neurodegenerative diseases and traumatic brain injury [1]. Markers of autophagy are also increased after cerebral ischemia-reperfusion induced by cardiac arrest(CA), but autophagic mechanisms and function are not known. Recent studies suggest that autophagy played protective roles in the cerebral ischemia[2]and reperfusion[3] phases, whereas reperfusion after cardiac arrest stimulates neuronal autophagy activation with BECLIN-1 upregulation and is implicated in causing neuronal cell death. We examined autophagic flux through the macroautophagy pathway as a determinant of the neurodegeneration induced by cardiac arrest.

Methods-Asphyxic cardiac arrest was produced with 45 min hypoxia and 7 min asphyxia. To impair autophagy flux, mouse neonatal cortical neurons were subjected to rapamycin (Rapa; 100 nmol/L) and chloroquine (CQ; 5µmol/L) pretreatment. CyclosporineA (CSA; 10µmol/L) was used to stabilize mitochondrial transition pore.

Results-We observed accumulation of LC3-positive autophagosomes in vulnerable sensorimotor cortical neurons at 24 h after return of spontaneous circulation. This accumulation was not due to increased initiation of autophagy but rather to a decrease in clearance of autophagosomes, as reflected by accumulation of the autophagic substrate SQSTM1/p62, LC3, BECLIN-1.The early impairment of autophagy is at least in part caused by lysosomal dysfunction, as evidenced by lower protein levels of Lysosome-associated membrane protein-2 (LAMP2). Furthermore, immediately after ischemia both autophagosomes and SQSTM1 accumulated predominantly in neurons. This was accompanied by appearance of SQSTM1/p62-positive puncta in the affected cells, suggesting that, similar to the situation observed in neurodegenerative diseases, impaired autophagy may contribute to neuronal injury. Mouse neonatal cortical neurons that were subjected to rapamycin (Rapa; 100 nmol/L) together with chloroquine (CQ; 5µmol/L) pretreatment increased cell death in neonatal mouse cultured cortical neurons compared with controls, markedly increased autophagosomes but not autolysosomes, indicating impaired autophagic flux. The resultant autophagosome accumulation was associated with increased cell death, which was attenuated by Cyclosporine A pretreatment.

Conclusion-Cerebral ischemia-reperfusion injury induced by CA impairs autophagosome clearance mediated, in part, by decline in LAMP2 and upregulation of BECLIN-1 contributing to increased neuronal death.

References-

1. Sarkar et al. Autophagy.2014 Nov 11:0.
2. Zhang et al. Autophagy.2014 Oct 1;10:1801-1
3. Zhang et al.Autophagy. 2013 Sep;9:1321-33.

473
BRAIN-0824
Poster Session

Cardiac Arrest/Global Cerebral Ischemia

ALTERATIONS OF THE CEREBRAL MICROVASCULAR CIRCULATION AFTER ASPHYXIAL CARDIAC ARREST IN DEVELOPING RATS

L. Li[1], S.M. Poloyac[1], A.L. Vazquez[2], C.M. St Croix[3], H. Alexander[4], G. Gibson[3], S.C. Watkins[3], R.S.B. Clark[5], P.M. Kochanek[5], M.D. Manole[6]
[1]School of Pharmacy, University of Pittsburgh,

Pittsburgh, USA
[2]McGowan Institute of Regenerative Medicine, University of Pittsburgh, Pittsburgh, USA
[3]Center for Biologic Imaging, University of Pittsburgh, Pittsburgh, USA
[4]Safar Center for Resuscitation Research, University of Pittsburgh, Pittsburgh, USA
[5]Children's Hospital of Pittsburgh Safar Center for Resuscitation Research Department of Critical Car e Medicine, University of Pittsburgh, Pittsburgh, USA
[6]Children's Hospital of Pittsburgh Safar Center for Resuscitation Research, University of Pittsburgh, Pittsburgh, USA

Background: Approximately 16,000 pediatric patients suffer cardiac arrest (CA) each year in the US, with asphyxia as the major cause. Most patients who survived the initial insult had impaired autoregulation and poor neurological outcome. In our previous study, decreased cortical blood flow was observed from 15-180 min post-CA in a clinically relevant pediatric rat asphyxial CA model using arterial spin labeled MRI (ASL-MRI). In order to further elucidate the mechanism underlying the decreased cortical blood flow post-CA, we propose to characterize the microvascular blood flow in our pediatric CA model, with the goal of enhancing the understanding of vascular dysfunction post-CA and establishing a scaffold to evaluate potential vasoactive therapeutic agents.

Hypothesis: After pediatric asphyxial CA there are alterations of the cortical microvascular circulation at the level of the arterioles, capillaries, and venules.

Methods: Postnatal 17 day old rats underwent tracheal intubation, arterial and venous cannulation, and were equipped with a cranial window for in-vivo two photon laser scanning microscopy. Asphyxial CA of 9 min was induced by cessation of mechanical ventilation after neuromuscular blockade. Rats were resuscitated with chest compressions, epinephrine and sodium bicarbonate. Using in vivo multiphoton microscopy, we measured the diameter of cortical arterioles, capillaries, and venules and red blood cell (RBC) velocity and flux at baseline and post-CA at 5, 30, and 60 minutes post-resuscitation.

Results: The diameter of arterioles (n=33) was similar to baseline at 5 min and 30min post-CA , but decreased significantly at 60 min post-CA (16.92±2.86 µm vs 19.60±2.45 µm at baseline, p=0.01). The diameter of venules (n=120) post-CA was increased significantly at 5min post-CA (23.37±1.89 vs 21.46±1.64µm at baseline, p<0.001) but showed a trend of decreasing at 60min post-CA (20.74±1.66 vs 21.46±1.64µm at baseline, p=0.085). The diameter of the capillaries (n=126) was significantly increased at 5 and 30min post-CA (8.31±0.36 and 7.78±0.40 vs 7.01±0.27 µm at baseline, p<0.001 and p=0.034, respectively).

The capillary flow of RBC was homogenous at baseline, with most capillaries exhibiting continuous RBC flow. However, capillary RBC flow was markedly heterogenous post-CA. Post-CA, we observed a high variability of RBC flow at the level of the capillary bed, with ~40% capillaries having no or very low RBC flow, the remaining 60% capillaries having either baseline RBC flow, or few capillaries having higher than baseline RBC flow.

Conclusions: There are important alterations of the microvascular tone and RBC flow in the cortical area post-CA. There appears to be arteriolar constriction, venules and capillaries dilation. At the capillary level we observed a highly variable RBC flow, suggesting a redistribution of RBC flow in the capillary bed secondary to no or low RBC flow in multiple capillaries. These data suggest that two pronged interventions would be of benefit, targeting both arterial vasodilatation and mitigation of capillary no-reflow and decreased flow.

474
BRAIN-0622
Poster Session

Cardiac Arrest/Global Cerebral Ischemia

CHARACTERIZATION OF PALMITIC ACID METHYL ESTER: A NOVEL VASODILATOR

H.C. Lee[1], C.S. Wilkins[2], A. Couto e Silva[1], S.E. Valido[1], D.D. Klein[1], J.J. Goyanes[1], J.A. Chen[1], H.W. Lin[1]
[1]Neurology, University of Miami Miller School of Medicine, Miami, USA
[2]Medicine, Florida International University Herbert Wertheim College of Medicine, Miami, USA

Objectives: We previously identified palmitic acid methyl ester (PAME) as a new vasodilator and neuroprotectant under ischemic conditions, from preganglionic neurons derived from the superior cervical ganglion (SCG) innervating major cerebral arteries[1]. Direct application of PAME (EC_{50}=0.19nM), but not palmitic acid (PA), onto the rat/rabbit thoracic aorta denuded of endothelium caused vasodilation more potent than NO donors and other vasoactive peptides[1]. These results suggest that methylation of PA is crucial for vasodilation further perpetuated by arginine analogs. The goals of this study are to 1) characterize PAME under normal conditions [effects on systemic circulation and cerebral blood flow, (CBF)], 2) to investigate the potential CBF and neuroprotective effects of PAME administered post-ischemia, and 3) to investigate the importance of (PA) methylation of PAME rendering its activity.

Methods: *Laser-Doppler Flowmetry (LDF):* LDF measurements of blood perfusion were performed at the start of the experiment and continuously recorded until the end of the final drug injections. A 2mm^2 burr hole was made over the left frontoparietal cortex ~1mm lateral to the bregma. A fiber optic probe (1mm^2) was placed thereupon measuring CBF in a 1mm^3 tissue region[2].

Two-photon Laser Scanning Microscopy (TPLSM): Fluorescent images were captured at 910nm with the introduction of fluorescein isothiocyanate (FITC)-dextran (0.2mg/kg), IV. Linescans for red blood cell (RBC) velocities were analyzed with Image J analysis software[2].

Asphyxial Cardiac Arrest (ACA): To induce ACA, apnea was induced by disconnecting the ventilator from the endotracheal tube. 6mins after asphyxia, resuscitation was initiated by administering a bolus injection of epinephrine and sodium bicarbonate followed by mechanical ventilation.

SCG extraction: Ganglionectomy was performed by making a midline incision on the skin longitudinally on top of the larynx. Both SCG were excised under normal conditions and hung on the superfusion bioassay cascade for perfusion/drug treatments[1].

Reverse transcriptase-polymerase chain reaction: We used Life Technologies' *SuperScript® III First-Strand Synthesis System (cat#18080-051) and Platinum® PCR SuperMix High Fidelity (cat#12532-016) for RT-PCR as accordance to the manufacturer's recommendations.*

Results: Our results suggest that PAME inhibited ethanol-induced vasoconstriction over 60min (vehicle/drug was applied every 10min). In addition, CBF was enhanced in the presence of PAME as compared to ethanol (vehicle) control. PAME (post-ischemia) also inhibited ACA-induced hypoperfusion 24hrs after ACA as compared to ethanol. Protein arginine methyltransferases (PRMTs) 2,3,4,5,8 mRNA are enhanced in the presence of the electrically-stimulated SCG in the presence of N^w-Nitro-L-Arginine (NLA).

Conclusions: Administration of PAME (IV) decreases systemic blood pressure, enhances cortical CBF, and attenuates post-ischemic hypoperfusion. Additionally, the presence of PRMTs 2,3,4,5,8 in the SCG may be responsible for the functional role of PA methylation released from the sympathetic nervous system modulating brain cerebral blood flow and metabolism.

1. Lin HW *et al.* Endogenous methyl palmitate modulates nicotinic receptor-mediated transmission in the superior cervical ganglion. *PNAS* 2008; 105:19526-31.

2. Lin HW *et al.* Derangements of post-ischemic cerebral blood flow by protein kinase C delta. *Neuroscience* 2010; 171:566-76.

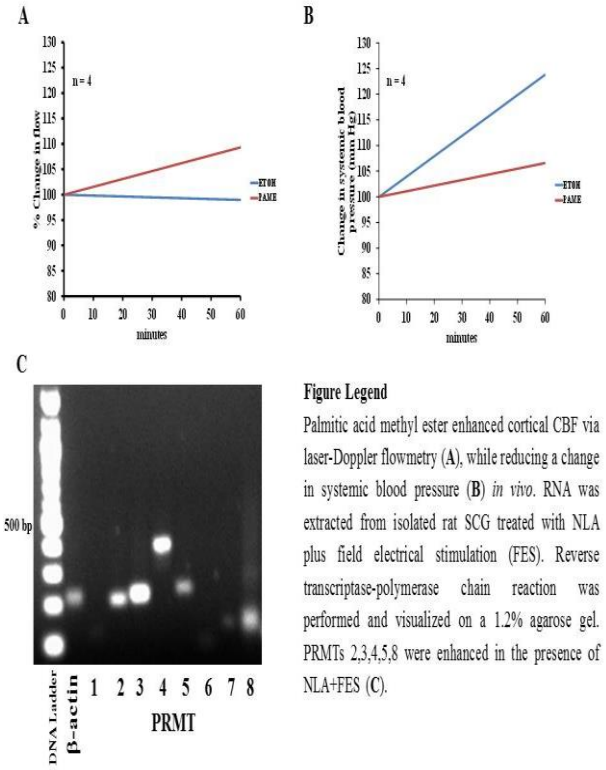

Figure Legend

Palmitic acid methyl ester enhanced cortical CBF via laser-Doppler flowmetry (**A**), while reducing a change in systemic blood pressure (**B**) *in vivo*. RNA was extracted from isolated rat SCG treated with NLA plus field electrical stimulation (FES). Reverse transcriptase-polymerase chain reaction was performed and visualized on a 1.2% agarose gel. PRMTs 2,3,4,5,8 were enhanced in the presence of NLA+FES (**C**).

475
BRAIN-0342
Poster Session

Cardiac Arrest/Global Cerebral Ischemia

ACTIVATION OF DELTA PKC REDUCES LONG-TERM POTENTIATION AND PAIRED-PULSE FACILITATION

J. Neumann[1], *M. Perez-Pinzon*[1]
[1]*Neurology,*
University of Miami Miller School of Medicine, Miami, USA

Objective: Cerebral ischemia (i.e., stroke or cardiopulmonary arrest [CA]) is a leading cause of death and disability in the USA. While survival rates following cerebral ischemia have remained low, a commonality among survivors is a diminished quality of life (i.e., decreased motor and/or cognitive function) from the ensuing ischemic neurological damage. Previous studies from our laboratory have demonstrated that 6min of asphyxia CA (ACA) induces significant damage in the highly susceptible cornu ammonis 1 (CA1) region of the hippocampus and inhibition of long-term potentiation (LTP) in the Schaffer collateral-CA1 synaptic pathway 24hr following ACA[1]. In addition, ACA induced the activation/translocation of delta protein kinase C (δPKC) to the particulate fraction 24hr post-ACA[2]. Direct inhibition of δPKC prior to ACA provided neuroprotection to the CA1 region of the hippocampus and cortical neurons[2]. Interestingly, the degradation of δPKC improved spatial learning[3]; therefore, we hypothesized that the activation of δPKC alters memory formation (i.e., LTP) following ACA.

Methods: To test this hypothesis, we used hippocampal slices from 3-month-old naïve rats to investigate the specific effects of δPKC activation or inhibition on LTP. Hippocampal slices were treated with ΨδRACK (specific agonist of δPKC), δV1-1 (specific antagonist of δPKC), or Tat peptide for 1hr at 33°C before recordings were initiated. LTP was induced through theta-burst stimulation after 30min of baseline population spike recordings.

Results: Specific activation of δPKC resulted in a significant reduction of LTP (Figure 1A, $p<0.05$). In addition, paired-pulse facilitation (PPF) was investigate at numerous intervals, where activation of δPKC resulted in a significant reduction in PPF (Figure 1B, $p<0.001$). In contrast, inhibition of δPKC (δV1-1) did not alter LTP or PPF (Figure 1C&D).

Conclusions: These studies indicate that activation of δPKC may contribute to the synaptic dysfunction following CA and suggest δPKC as a potential therapeutic target for improving cognitive function. Future studies will investigate the signaling pathways by which δPKC depresses LTP in order to ameliorate LTP suppression following ACA. This work was supported by AHA

Greater Southeast Affiliate grant 13POST16720001 and NIH grants NS45676 and NS34773.

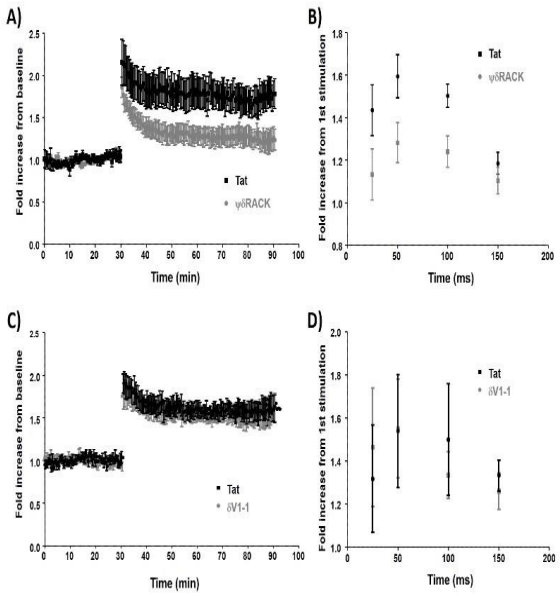

Figure 1. δPKC activation reduces LTP and PPF in hippocampal slices. **A)** Normalized fold increase of population spike amplitude from Tat- or ΨδRACK-treated slices. There was a significant reduction in LTP in ΨδRACK-treated compared to Tat-treated slices ($p<0.05$, n=6-8). **B)** PPF ratio at various intervals for slices treated with Tat or ΨδRACK. There was a significant reduction in the PPF ratio of ΨδRACK-treated compared to Tat-treated slices ($p<0.001$, n=11-13). **C)** Normalized fold increase of from Tat- or δV1-1-treated slices ($p>0.05$, n=4-5). **D)** PPF ratio at various intervals for slices treated with Tat or δV1-1 ($p>0.05$, n=4-5).

References

1. Dave KR *et al.* Mild cardiopulmonary arrest promotes synaptic dysfunction in rat hippocampus. *Brain Res* 2004; 1024(1-2):89-96.

2. Lin HW *et al.* Derangements of post-ischemic cerebral blood flow by protein kinase C delta. *Neuroscience* 2010; 171(2):566-76.

3. Conboy L *et al.* Curcumin-induced degradation of PKC delta is associated with enhanced dentate NCAM PSA expression and spatial learning in adult and aged Wistar rats. *Biochemical pharmacology* 2009; 77(7):1254-65.

476
BRAIN-0196
Poster Session

Cardiac Arrest/Global Cerebral Ischemia

NANOPARTICLES FROM METALS EXACERBATE CARDIAC ARREST INDUCED BRAIN PATHOLOGY. NEUROPROTECTIVE EFFECTS OF CEREBROLYSIN

H. Sharma[1], *A. Nozari*[2], *D. Muresanu*[3], *H. Moessler*[4], *J. Lafuente*[5], *A. Sharma*[6]
[1]*Surgical Sciences Anesthesiology & Intensive Care Medicine, Uppsala University hsopital, Uppsala, Sweden*
[2]*Anesthesiology & Intensive Care Medicine, Massachusetts General Hospital, Boston, USA*
[3]*Clinical Neurosciences, University of Medicine & Pharmacy, Cluj-Napoca, Romania*
[4]*Drug Development & Discovery, Ever Neuro Pharma, Oberburgau, Austria*
[5]*Neurosciences, University of Basque Country, Bilbao, Spain*
[6]*Surgical Sciences Anesthesiology & Intensive Care Medicine, University Hospital Uppsala University, Uppsala, Sweden*

Background: Military personnel engaged in combat operations in the desert areas are often exposed to SiO2 nanoparticles (NPs) from the sand, as well as Carbon, Cu or Ag NPs from gunfire, missile explosion or blast injuries. NP intoxication can worsen neurological injury after cardiac arrest (CA) via an aggravated blood-brain barrier (BBB) disruption, edema formation, and oxidative injury. Therapeutic interventions aimed at mitigating the oxidative and the NP-induced post-resuscitation injuries can, therefore, improve the neurological outcome.

Methods: CA was induced in rats using apneic asphyxia for 3-4 min. Return of spontaneous circulation (ROSC) was obtained after 4-5 min of no-flow CA by standard CPR (Katz et al., 1995. JCBFM 15: 1032-1039). The NP-group was

pretreated with SiO2, Cu or Ag NPs (50-60 nm, 50 mg/kg, i.p. /day) for 7 days prior to the experiment. Animals were allowed to survive 4 h or 8 h after ROSC. Cerebrolysin (Ever NeuroPharma, Austria) was administered (2.5 or 5 ml/kg, i.v.) 30 to 60 min after ROSC.

Results: CA resulted in a 10- to 14-fold increase in the BBB breakdown, 3-4x increase in brain edema, and 4-6x increase in astrocytic activation and myelin damage in the NP- treated animals. Treatment with Cerebrolysin (2.5 or 5 ml) significantly reduced CA induced brain pathology in non-NP animals, but repeated administration of Cerebrolysin in high doses (5 ml, 30, 60 and 90 min after ROSC) was required for comparable neuroprotection in NP-treated rats.

Conclusions: These observations are the first to suggest that NP- intoxication exacerbates CA induced brain pathology. An almost 2- 3 times increase in the dose of the neuroprotective drug Cerebrolysin is needed to achieve comparable neuroprotection in NP-treated animals after CA.

477
BRAIN-0143
Poster Session

Cardiac Arrest/Global Cerebral Ischemia

PHYSICAL EXERCISE FACILITATES RECOVERY OF SPATIAL MEMORY AND SYNAPTIC FUNCTION AFTER CARDIAC ARREST

H.M. Stradecki[1], C.H. Cohan[1], M. Youbi[2], D. Perez[1], K.R. Dave[2], J.T. Neumann[2], M. Perez-Pinzon[2]
[1]Neuroscience Program,
University of Miami Miller School of Medicine, Miami, USA
[2]Neurology Department,
University of Miami Miller School of Medicine, Miami, USA

Objectives: Cardiac arrest affects over half a million people in the US annually. Currently, no treatment exists to eradicate the cognitive impairments afflicting survivors[1]. Physical exercise can reduce cognitive deficits after cerebral ischemia by augmenting brain plasticity[2]. This study sought to examine if forced treadmill exercise improved performance of Sprague Dawley rats on spatial memory tests (e.g. Barnes Maze and contextual fear conditioning) and restored induction of long-term potentiation (LTP) after moderate global cerebral ischemia.

Methods: Three month old Sprague Dawley rats were acclimated to human touch and treadmill walking. Rats underwent asphyxial cardiac arrest (ACA) or sham surgery (sham) as previously described[3] with moderate duration (8 minutes) of ischemia. Rats were allowed 3 days of recovery then treadmill exercised (or not) for 5 days. After the last day exercise, animals were used for electrophysiological studies or subject to spatial memory task (Barnes Circular Platform Maze and fear conditioning, see below). For electrophysiological studies, acute slices were obtained from rats 3 days after ACA or the day after exercise completion. CA1 population spikes were induced in response to Schaffer collateral stimulation and used to determine slice health. LTP was induced after theta burst stimulation (TBS). Barnes Maze testing consisted of 3 trials/day for 8 days with probe trials occurring before first trial on odd days and 24 hours after last trial. Animals were subjected to contextual fear conditioning following completion of Barnes Maze; rats were placed in the fear conditioning chamber for 8 minutes with a 2 second 1.5 mA shock delivered at minute 7.5 then returned to the chamber 24 hours later. Percent time freezing was quantified with FreezeFrame software. Data are analyzed with two-way ANOVA or student's t-test where appropriate with significance set at $\alpha = 0.05$.

Results: Preliminary data suggests that 3 days after cardiac arrest (ACA), there is a reduced ability to induce LTP as compared to naïve animals (Figure A). When ACA animals are exercised for 5 days (beginning 3 days after ACA), LTP induction is similar to naïve controls. ACA induces cognitive deficits after global cerebral ischemia as measured by reduced percentage of time in target quadrant during probe trials on the Barnes Maze (Figure B, 2-way ANOVA, $p<0.0075$ for surgery). Exercise after ACA enhances

duration of freezing in fear conditioning chamber (Figure C; Baseline: p = 0.64; Contextual p = 0.104; with n=2-3; Student's t-test).

Conclusions: Global cerebral ischemia impairs cognitive functioning. Early induction of exercise restores synaptic functioning and may also improve performance on spatial memory tasks.

References:

1. Treger, I., Shames, J., Giaquinto, S. & Ring, H. Return to work in stroke patients. Disability and rehabilitation 29, 1397-1403, doi:10.1080/09638280701314923 (2007).
2. Mang, C. S., Campbell, K. L., Ross, C. J. & Boyd, L. A. Promoting neuroplasticity for motor rehabilitation after stroke: considering the effects of aerobic exercise and genetic variation on brain-derived neurotrophic factor. Physical therapy 93, 1707-1716, doi:10.2522/ptj.20130053 (2013).
3. Dave, K. R. et al. Mild cardiopulmonary arrest promotes synaptic dysfunction in rat hippocampus. Brain research 1024, 89-96, doi:10.1016/j.brainres.2004.07.050 (2004).

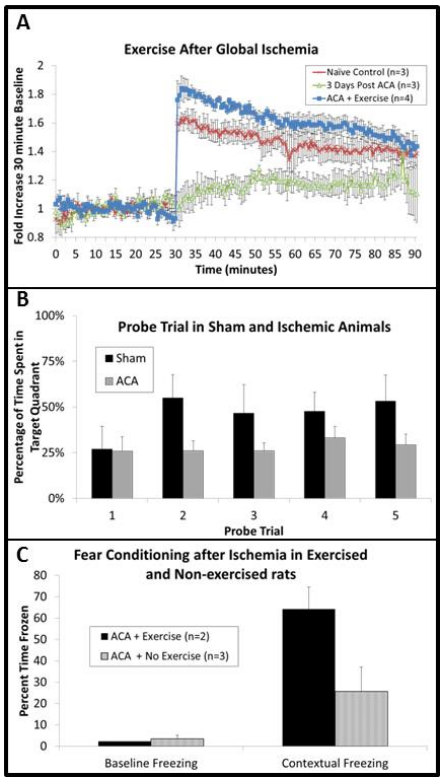

478
BRAIN-0464
Poster Session

Cardiac Arrest/Global Cerebral Ischemia

BRAIN-HEART AXIS MODULATION THROUGH VASCULAR OXIDATIVE STRESS DURING MILD HYPOTHERMIA INDUCES DECREASED GLOBAL ISCHEMIA IN THERAPEUTIC HYPOTHERMIA AFTER CARDIAC ARREST

A. Jantanukul[1], S. Muengtaweepongsa[2], K. Suwanprasert[3]
[1]Division of cardiothoracic surgery, Ramathibodi hospital, Bangkok, Thailand
[2]Division of Neurology, Faculty of Medicine Thammasat University, Patumthani, Thailand
[3]Division of Physiology, Faculty of Medicine Thammasat University, Patumthani, Thailand

Background: Brain-Heart axis is recently proposed as control axis indicating synaptic function of neuromodulator, namely nitric oxide. Therapeutic hypothermia(TH) is an ideal protocol to reduce brain injury and systemic hypoxia. We hypothesize that nitric oxide(NO), is synthesized from 3 isoforms of nitric oxide synthase(NOS), plays a crucial role as neuromodulator of autonomic control and being oxidative stress(OS) marker derived from reactive oxygen species(ROS) during therapeutic hypothermia.

Objective : To verify changes of NO, H_2O_2 and symphatho-vagal balance determined by LF/HF ratio of heart rate variability(HRV) in global ischemic model of cardiac arrest(CA) patients.

Method : 14 CA patients who treated with TH were classified by 28 days survival outcome(7:7) and their protocols were approved by local ethical committee(MTU-EC-PH-2-062/55). Plasma NO and H_2O_2 concentrations were measured by electrochemistry technique. LF/HF ratio of 15 minutes -HRV were analyzed by Kubios-HRV software. All signals and blood samples were collected through out four phases of treatment:

induction, sustainment, rewarm and recover to normothermia.

Results: In survivors, NO concentrations were gradually increased as seen in sustainment vs. recover phase($p< 0.05$) and LF/HF ratios were significant changed in rewarm vs recover phase ($p< 0.05$). *Inverse relationship* between NO concentrations and LF/HF ratios have shown in non-survivors ($r= -0.33$) that contrasted to those in survivors ($r= 0.33$). Although the H_2O_2 concentrations were not changed significantly in both groups but their profiles tended to decline corresponding to gradually increased NO in survivors ($r = -0.54$, $p = 0.002$).Contrast to non-survivors, NO levels and LF/HF ratios were positive *correlation ($r = 0.41$, $p=0.04$)*.

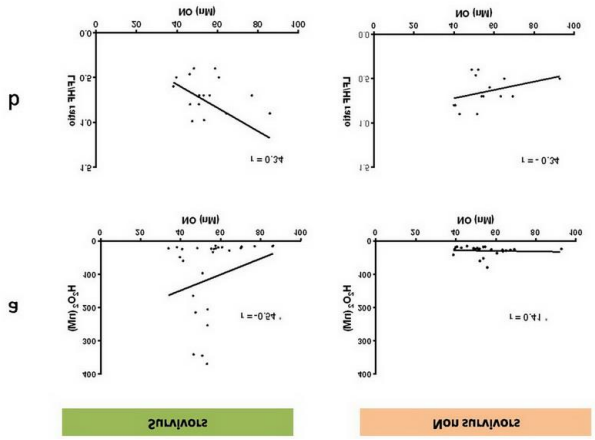

Conclusion: Reduced OS are mainly involved in down regulation of TH effect. NO plays a paradox function of NOS/ROS activities and neuromodulator. Ratio of NO/ H_2O_2 and NO associated with LF/HF ratio are proposed to be effective index of survival.

Acknowledgement: This work supported by National Research University Project of Thailand Office of Higher Education Commission and faculty of medicine, Thammasat University.

References:

1. Herring N, Danson EJ, Paterson DJ. Cholinergic control of heart rate by nitric oxide is site specific. News Physiol Sci. 2002 Oct;17:202-6.
2. Oštádal P, Krüger A, Vondráková D, Janotka M, Herget J, Nitrotyrosine and nitrate/nitrite levels in cardiac arrest survivors treated with endovascular hypothermia. Physiol Res. 2012 Sep 17,61(4):425-30.
3. Pfeifer R, Hopfe J, Ehrhardt C, Goernig M, Figulla HR, Voss A. Autonomic regulation during mild therapeutic hypothermia in cardiopulmonary resuscitated patients. Clin Res Cardiol. 2011 Sep,100(9):797-805.
4. Task force of the European society of cardiology and the North American society of pacing and electrophysiology. Heart rate variability: Standards of measurement, physiological interpretation, and clinical use. Circulation.1996,93: 1043-1065.

479
BRAIN-0613
Poster Session

Cell Death/Survival

EARLY PERI-INFARCT NEURONAL LOSS AS INDICATOR OF CHRONIC POST-STROKE NEURODEGENERATION? A COMBINED HIGH-RESOLUTION PET AND CORTICAL THICKNESS STUDY.

M.H. Alkuwaiti[1], T. Funck[2], P. Zepper[3], C. Lepage[2], A. Thiel[4]
[1]Neurology, Montreal Neurological Institute McGill University, Montreal, Canada
[2]McConnell Brain Imaging Centre, Montreal Neurological Institute McGill University, Montreal, Canada
[3]Neurology, Klinikum rechts der Isar Technical University Munich, Munich, Germany
[4]Department of Neurology & Neurosurgery, Lady Davis Institute for Medical Research McGill University, Montreal, Canada

Objective: A reduction of peri-infarct GABA-A receptors has been shown to indicate acute (necrotic)(1) and delayed (apoptic) cell death (2). It has recently been suggested that ischemia may also trigger long term degenerative changes in structurally normal cortex which e.g. may contribute to more chronic progressive disease processes like post-stroke cognitive decline(3). In this study, we investigated the fate of normal

peri-infarct cortex in a longitudinal study using high-resolution 18F-FMZ-PET and MRI to measure neuronal density and surface cortical thickness (SCT) (4) to track gray matter changes in patients with acute supra-tentorial ischemic stroke. It is hypothesized that an initial reduction in GABA-A receptor density that decreases over time, together with an reduction of SCT may be indicative of ischemia triggered ongoing neurodegeneration.

Method: A total of 11 patients with first supra-tentorial cortical ischemic stroke (7 male, median age of 63 years, range (50 – 87 years) were recruited within 4 weeks after symptom onset (mean first clinical assessment 14.36 days), repeat assessments were performed at 6 months. At both time points patients were assessed using a clinical test battery (NIHSS, mRS, Fugl-Meyer test and MoCA) and underwent MR imaging on a 3T Siemens Trio and PET imaging with 18F-FMZ on an Siemens HRRT scanner. Surface Cortical Thickness was measured on T1-weighted images using an automated processing pipeline "CIVET; version 2.0.0" (5) and infarct volumes were segmented on FLAIR images. Parametric images of non-displaceable binding potential (BPnd) were calculated from dynamic [^{18}F]Flumazenil (FMZ) images using the Logan Plot method with the white matter of the oval center as reference region.

Concentric regions of interest (ROI) were automatically generated from the intersection of the infarct ROIs with the cortical surface gray matter, respecting sulcal anatomy and vascular territories. These concentric surface ROIs were also mirrored to the non-affected hemisphere for comparison and ROI differences in BPnd and SCT between affected and unaffected hemisphere were analyzed at both timepoints for all ROIs by repeated measures ANOVA.

Results: BPnd differences were significantly reduced in ROIs in the proximity of the infarct up to 6 mm from the infarct border in both initial (dBPnd = 1.23 +/- 1.17, P< 0.001) and follow-up scans (dBPnd = 2.05, P< 0.01), while dSCT was significantly reduced only at follow-up ($p < 0.001$) but not initially (p=0.77).

Conclusion: The GABA-$_A$ receptor density is reduced in structurally normal peri-infarct cortex in the sub-acute as well as in the chronic phase after stroke. This reduction in receptor density is followed by cortical atrophy over the observation period of 6 months indicating ongoing neuronal loss. The fact that the loss of neurons leads to measurable atrophy may suggest that secondary degenerative processes in addition to delayed cell death maybe involved.

References:

1. Heiss WD. Stroke; 1992;23(11):1668-72.
2. Baron JC et al, Journal of cerebral blood flow and metabolism. 2014;34(1):2-18.
3. Thiel A et al. Stroke; 2014;45(9):2825-9.
4. la Fougere C et al. NeuroImage. 2011;56(3):951-60.
5. MacDonald D et al. NeuroImage. 2000;12(3):340-56.

480
BRAIN-0127
Poster Session

Cell Death/Survival

DSEPA ANTAGONIZES HIGH GLUCOSE-INDUCED NEUROTOXICITY: EVIDENCES FOR ROS-MEDIATED OXIDATIVE DAMAGE AND AKT PATHWAY

K. Wang[1], M. Yang[2], S. Zhang[2], Y. Hou[2], Z. Zhang[2], D. Li[2], L. Mao[2], C. Fan[2], B. Sun[2]
[1]Neurobiology,
Taishan Vocational College of Nursing, Taian, China
[2]Key Lab of Cerebral Microcirculation in Universitie s of Shandong, Taishan Medical University, Taian, China

Objectives: Hyperglycemia as the major hallmark of diabetic neuropathy severely limited its therapeutic efficiency. Selenium (Se) an essential trace element is of fundamental importance to humans due to its multiple pharmacological properties. Increasing evidences also indicate that

Se supplement can effectively reduce the risk of neurological diseases. In the present study, 3, 3′-diselenodipropionic acid (DSePA), a derivative of selenocystine, was employed to investigate its protective effective against high glucose-induced neurotoxicity in PC12 cells and evaluate the underlying mechanism.

Methods: Several methods of cell biology and molecular biology *in vitro* were employed.

Results: The results suggested that high glucose (100 mM) treatment for 48 h induced mitochondria-mediated apoptosis in PC12 cells, accompanied by poly (ADP-ribose) polymerase (PARP) cleavage, caspase activation, depletion of mitochondrial membrane potential ($\Delta\psi m$). Moreover, high glucose treatment also resulted in DNA damage and dysregulation of MAPKs and AKT pathways through triggering intracellular reactive oxygen species (ROS) overproduction. p53 RNA interference partially suppressed high glucose-induced cytotoxicity and apoptosis. Addition of four chemical inhibitors of MAPKs and AKT pathways further confirmed that MAPKs and AKT pathways both contributed to high glucose-induced neurotoxicity. However, DSePA pre-treatment for 6 h effectively attenuated high glucose-induced cytotoxicity, inhibited the loss of $\Delta\psi m$ through regulation of Bcl-2 family expression, and ultimately reversed high glucose-induced apoptotic cell death in PC12 cells. Attenuation of caspase activation, PARP cleavage, DNA damage, and accumulation of ROS all confirmed its protective effects. Moreover, DSePA markedly alleviated the dysregulation of the MAPK and AKT pathways induced by high glucose.

Conclusions: Our findings revealed that the strategy of using DSePA could be a highly effective way in prevention or therapy of diabetic neuropathy.

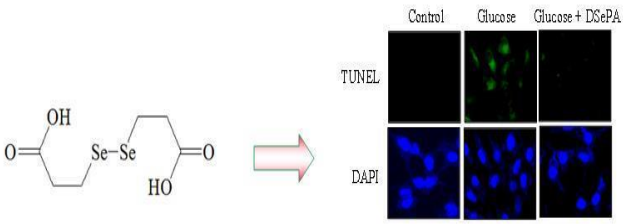

References:
1. Edwards JL, Vincent AM, Cheng HT et al., "Diabetic neuropathy: mechanisms to management," *Pharmacol Ther* 120:1–34; 2008.
2. Amit Kunwar, P. Bansal, S. Jaya Kumar et al., "*In vivo* radioprotection studies of 3,3′-diselenodipropionic acid, a selenocystine derivative" *Free Radical Biology & Medicine* 48:399-410; 2010.
The study was supported by the National Natural Science Foundation of China No.81471212, 81271275, 81070947, 30770759 to B.-L. Sun; Natural Science Foundation of Shandong No. ZR2012HZ006 to B.-L. Sun.
***Corresponding author**: Cun-dong Fan, Bao-liang Sun, Tel: +86-538-6230027, E-mail: tsmc_nks@tsmc.edu.cn; blsun@tsmc.edu.cn

481
BRAIN-0149
Poster Session

Cell Death/Survival

ATTENUATION OF CISPLATIN-INDUCED NEUROTOXICITY BY CYANIDIN, A NATURAL INHIBITOR OF ROS-MEDIATED APOPTOSIS IN PC12 CELLS

D. Li[1], J. Sun[2], K. Wang[3], S. Zhang[1], Y. Hou[1], M. Yang[1], C. Fan[1], B. Sun[1]
[1]Key Lab of Cerebral Microcirculation in Universities of Shandong, Taishan Medical University, Taian, China
[2]School of Basic Medicine, Taishan Medical University, Taian, China
[3]Nursing Department, Taishan Vocational College of Nursing, Taian, China

Objectives: Cisplatin-based chemotherapy in clinic is severly limited by its adverse effect, including neurotoxicity. Oxidative damage contributes to cisplatin-induced neurotoxicity, but the mechanism remains unclearly. Cyanidin a natural flavonoid compound exhibits powerful antioxidant activity. Hence, we investigated the

protective effects of cyanidin on PC-12 cells against cisplatin-induced neurotoxicity and explored the underlying mechanisms.

Methods: MTT assay, flow cytometry analysis, TUNEL-DAPI co-staining, caspase activity, detection of ROS accumulation and western blotting assay were all employed to detect the protective mechanism.

Results: The results showed that cisplatin-induced cytotoxicity was completely reversed by cyanidin through inhibition of PC-12 cell apoptosis, as proved by the attenuation of Sub-G1 peak, PARP cleavage and caspases-3 activation. Mechanistically, cyanidin significantly inhibited reactive oxygen species (ROS)-induced DNA damage in cisplatin-treated PC-12 cells.

Conclusions: Our findings revealed that cyanidin as an apoptotic inhibitor effectively blocked cisplatin-induced neurotoxicity through inhibition of ROS-mediated DNA damage and apoptosis, predicating its therapeutic potential in prevention of chemotherapy-induced neurotoxicity.

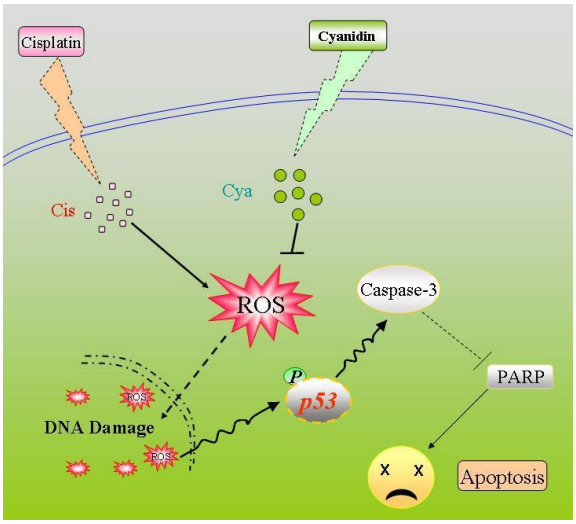

References:

1. Gulec, M., Oral, E., Dursun, O.B., Yucel, A., Hacimuftuoglu, A., Akcay, F., Suleyman, H. 2013. Mirtazapine protects against cisplatin-induced oxidative stress and DNA damage in the rat brain. *Psychiatry Clin Neurosci*, 67, 50-8.

2. Acquaviva, R., Russo, A., Galvano, F., Galvano, G., Barcellona, M.L., Li Volti, G., Vanella, A. 2003. Cyanidin and cyanidin 3-O-beta-D -glucoside as DNA cleavage protectors and antioxidants. *Cell Biol Toxicol*, 19, 243-52.

The study was supported by the National Natural Science Foundation of China No.81471212, 81271275, 81070947, 30770759 to B.-L. Sun; Natural Science Foundation of Shandong No. ZR2012HZ006 to B.-L. Sun.

482
BRAIN-0062
Poster Session

Cell Death/Survival

PYROPTOTIC CELL DEATH OF MICROGLIA AFTER OXYGEN-GLUCOSE DEPRIVATION

D.W. Kang[1], H.G. Jeong[1], I.Y. Choi[1], J.Y. Kim[1], C.K. Kim[1], S.H. Lee[1]
[1]Neurology, Seoul National University Hospital, Seoul, Korea

Objectives: Pyroptosis, a cell death mechanism distinct from apoptosis and necrosis, is triggered by caspase-1 after its activation by various inflammasomes[1]. Both pyroptosis and apoptosis are dependent on different caspases, unlike necrosis. But unlike apoptosis, pyroptosis makes pores in plasma membrane and results in cell swelling and lysis which is similar to necrosis. NLRP1 and NLRP3 inflammasomes are activated in ischemic stroke and results in post-stroke inflammation[2]. The aim of this study was to investigate the presence of pyroptotic cell death in microglia and its association with inflammasome after oxygen-glucose deprivation (OGD).

Methods: BV-2 cells, a murine microglial cell line, were cultured in a humidified incubator at 37 ºC with 5 % CO_2. OGD was induced by washing and incubating the cultures in a preequilibrated glucose-free balanced salt solution in the Billups-Rothenberg anaerobic chamber containing 95 % nitrogen and 5 % CO_2 for 2 hours. At the end of the procedure, cultures were removed from the

chamber and replaced with serum containing DMEM prior to returning the microglia cultures to normoxia (95 % oxygen and 5 % CO_2). Western blot were performed to determine the protein expression of NLRP3, caspase-1, interleukin 1-beta. One group was pretreated with 50 μmol/L Ac-YVAD-cmk (an irreversible caspase-1 inhibitor). Both large (YOYO-1, 1 μmol/L) and small (Propidium Iodide (PI), 5 μmol/L) impermeable dye were treated for 15 minutes to examine small pore formation. Active caspase-1 stain was done with FAM-YVAD-fmk (Fluorescent active caspase-1 inhibitor).

Results: NLRP3, caspase-1, and interleukin 1-beta were highly expressed after 2 hours of OGD. OGD induced formation of pores in the plasma membrane was showed by the uptake of PI (a small dye) with exclusion of YOYO-1 (a larger dye). Pretreatment with YVAD (caspase-1 inhibitor) significantly decreased uptake of PI and YOYO-1 [Fig.1]. Active caspase-1 was stained with FAM-YVAD-fmk in the same cell with PI [Fig.2].

Conclusions: These results revealed OGD induced pyroptotic cell death of microglia via NLRP3 inflammasome pathway. Further studies are necessary to confirm the presence of pyroptotic microglial death and its association with post-stroke inflammation in animal stroke models.

References:1. T. Bergsbaken, S. L. Fink, B. T. Cookson, Pyroptosis: host cell death and inflammation. Nat. Rev. Microbiol. 7, 99–109 (2009).2. D. Y.-W. Fann et al., Intravenous immunoglobulin suppresses NLRP1 and NLRP3 inflammasome-mediated neuronal death in ischemic stroke. Cell Death Dis. 4, e790 (2013). [Fig.1]

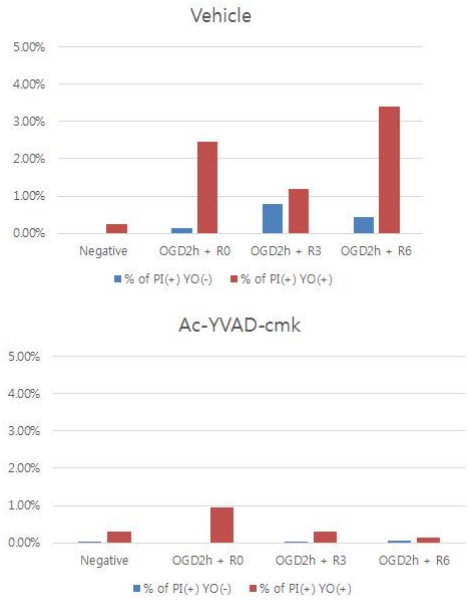

[Fig.2] PI (red), active caspase-1 (green), and nuclei (blue)

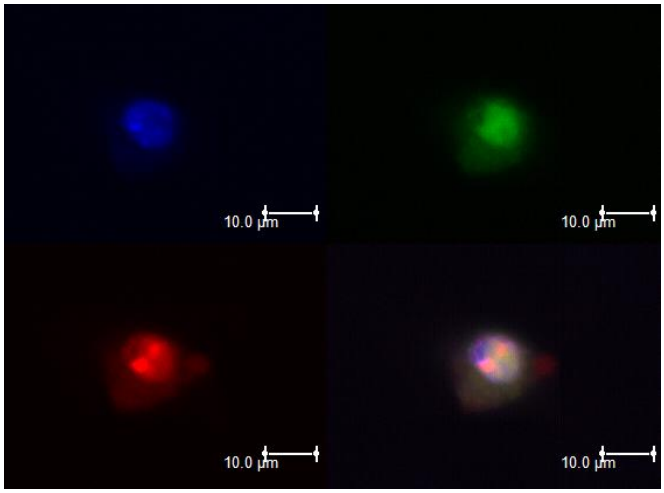

483
BRAIN-0762
Poster Session

Cell Death/Survival

A NOVEL MOLECULAR METHOD, IMAGING MASS SPECTROMETRY, ENABLES ANALYSIS OF SPATIO-TEMPORAL MOLECULAR CHANGES IN HIPPOCAMPUS CA1 AFTER TRANSIENT GLOBAL ISCHEMIA

S. Miyawaki[1], H. Imai[1], T. Hayasaka[2], H. Ono[1], T. Ochi[1], H. Nakatomi[1], M. Setou[2], N. Saito[1]
[1]Department of Neurosurgery, The University of Tokyo, Tokyo, Japan
[2]Department of Molecular Anatomy, Hamamatsu University, Hamamatsu, Japan

(Back ground) The mechanisms of vulnerability to ischemia of certain neuronal populations remain unclear due to the limitations of current methods. We evaluated dynamic molecular changes in rat hippocampus after transient globalischemia(TGI) for 6 min using a novel molecular imaging method, imaging mass spectrometry (IMS).

(Methods) A transient global cerebral ischemia (6 min) model was created using Sprague-Dawley rats (300–360g males). Fresh frozensections were obtained after euthanizing the rats on Days 1,2,4,7,10,14, and 21. Histopathology and IMS on adjacent sections compared morphological andmolecular changes, respectively, focused on phosphatidylcholine (PC) species.

(Results) At Days 2 to 7 after TGI (subacute phase), histopathology revealed neuronaldeath associated with gliosis, inflammation and accumulation of activatedmicroglia in CA1. Inthis phase, by IMS analysis, PC (diacyl-16:0/18:1) increases in the CA1 domain. Sothis molecular change was supposed to correspond to the inflammatory change. On the other hand, histopathological changes were absent on Day 1(superacute phase). However, IMS detected significant molecular changes in thesame CA1 domain: an increase in polyunsaturated fatty acids, such asarachidonic acid (20:4) and docosahexaenoic acid (22:6).

(Conclusion) Histopathology and IMS can provide comprehensive and complementing informationon cell death mechanisms in the hippocampal CA1 after global ischemia. IMS provided novel data on molecular changes in phospholipids in the superacutephase after TGI. Increased level of PC (diacyl-16:0/22:6) in cell organellesand membranes prior to the histopathological change may represent an early stepin delayed neuronal death mechanisms.

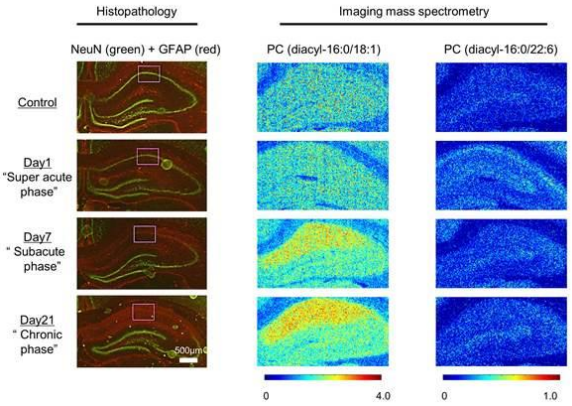

484
BRAIN-0122
Poster Session

Cell Death/Survival

INDUCTION OF BCL2 IN MOTOR NEURON AFTER TRANSIENT SPINAL CORD ISCHEMIA IN HYPOTHERMIC RABBIT MODEL

S. Fujita[1], M. Sakurai[2], H. Baba[3], K. Abe[4], R. Tominaga[1]
[1]Cardiovascular Surgery, Kyushu University, Fukuoka, Japan
[2]Cardiovascular Surgery, Sendai Medical Center, Sendai, Japan
[3]Cardiovascular Surgery, Kyushu University, fukuoka, Japan
[4]Neurology, Okayama University, Okayama, Japan

The mechanism of spinal cord injury has been thought to be related to the vulnerability of spinal motor neuron cells against ischemia. However, the mechanisms of such vulnerability are not

fully understood. Because we previously reported that spinal motor neurons were lost probably by programmed cell death, we investigated the role of autophagy by immunohistochemical analysis for Beclin 1 (BCLN1, Bcl-2 interacting protein), B cell leukemia 2 protein (Bcl-2) and γ-aminobutyric-acid type-A-receptor-assosiated protein (GABARAP). We used a rabbit normothermic spinal cord ischemia model and hypothermic spinal cord ischemia model with use of a balloon catheter. The spinal cord was removed at 8 hours, 1, 2, or 7 days after 15 min of transient ischemia in each model, and histological changes were studied with hematoxylin-eosin staining. Western blot analysis for BCLN1, Bcl-2 and GABARAP, temporal profiles of BCLN1, Bcl-2 and GABARAP immunoreactivity, and double-label fluorescence immunocytochemical studies were performed. In the normothermic model, the majority of motor neurons were preserved until 2 days, but were selectively lost at 7 days of reperfusion. On the other hand, in the hypothermic model, the majority of motor neuron were preserved at 7 days. Western blot analysis revealed scarce immunoreactivity for BCLN1, Bcl-2 and GABARAP in the sham-operated spinal cords. In the normothermic model, BCLN1, Bcl-2 and GABARAP immunoreactivity became apparent at 8 hours after reperfusion, BCLN1 and GABARAP expression were preserved unti 2days. On the other hand, in hypothermic model, BCLN1, Bcl-2 and GABARAP became apparent at 8 hours after reperfusion, BCLN1 and GABARAP returned to the baseline level at 1 day. In Double-label fluorescence immunocytochemical study revealed that both BCLN1 and Bcl-2, and BCLN1 and GABARAP were positive at 8 hours of reperfusion in the same motor neurons, which eventually die. This study demonstrated that immunoreactivities for both BCLN1, Bcl-2 and GABARAP were induced in the same motor neuron, which eventually die. The induction of BCLN1 and GABARAP proteins at the early stage of reperfusion might be one factors responsible for the delay in neuronal death, and the induction of Bcl-2 may be inhibiting factor in the programmed cell death change after transient spinal cord ischemia.

485
BRAIN-0463
Poster Session

Cell Death/Survival

NEUROPROTECTIVE EFFECTS OF PEPTIDES ANALOGOUS TO TETHERED LIGANDS RELEASED BY ACTIVATED PROTEIN ON NEURONS AND ASTROCYTES.

I. Savinkova[1], L. Gorbacheva[1], S. Strukova[2], V. Pinelis[3]
[1]Physiology, Pirogov Russian National Research Medical Univer sity, Moscow, Russia
[2]Physiology, Lomonosov Moscow State University, Moscow, Russia
[3]Cell Technologies, Scientific Centre for Children`s Health RAMS, Moscow, Russia

Background. The search and creation of novel protective agents preventing neuronal death are the important challenges of modern physiology. It has been shown that haemostatic serine proteinases (thrombin and activated protein C (APC)), interacting with the same PAR1 receptor, exert multidirectional effects during excitotoxicity and inflammation. Thrombin increases the expression of proinflammatory and proapoptotic factors together with the procoagulant effect (Riewald et al, 2005) while APC is a neuroprotector in stressed neurons and in hypoxic brain endothelium (Mosnier et al, 2007; Zlokovic et al, 2011). It has been shown recently that the multidirectional effects of thrombin and APC may be due to biased agonism under the action of thrombin and APC proteinases on endothelial cell PAR1 (Mosnier et al, 2011; Mosnier et al, 2012). Under conditions of biased agonism, APC-specific noncanonic cleavage at Arg46 has been identified in the PAR1 exodomain instead of the canonic cleavage by thrombin at Arg41 (Mosnier et al, 2012). The new tethered ligand (the Tp-47 peptide) simulated APC-induced but not thrombin-induced signaling on cultured endothelial cells (Mosnier et al, 2012).

Objectives. We have supposed that the peptide analogs of the PAR1 tethered ligand liberated by APC (Peptide 9) may also have protective effects on neurons and astrocytes similar to APC.

Methods. We have used the model of glutamate excitotoxicity to simulate ischemic brain damage on the hippocampal neurons and the model of neuroinflammation (the thrombin-induced activation of glia) on the cortical astrocytes. The cell survival and proliferation were estimated on primary culture of hippocampal neurons and cortical astrocytes by morphological and biochemical methods (with fluorescent probes Hoechst 33342, Syto-13, EthD and MTT method).

Results. We found that thrombin at a concentration of 50 nM (the highest concentration within the physiological range) increased astrocyte proliferation about 2.5-fold in comparison with the control. Preincubation of astrocytes with APC (1 nM) reduced the proliferation till 10% compared to the individual effect of thrombin. We detected that peptide 9 (20 μM) effectively decreased the thrombin-induced activation of astrocytes also. Pretreatment of neurons with APC or peptide-9 (20 μM) under glutamate toxicity reduced cell apoptosis 2- 3.6-fold, respectively for 1nM and 10 nM of APC. The results of this research demonstrate for the first time the protective effects of peptide 9 under excitotoxicity on neurons and at thrombin-induced activation of astrogliosis similar to the effects of APC.

Conclusion. The peptides analogs of the PAR1 tethered ligand liberated by APC have neuroprotective effects and can prevent the activation of astrocytes during pathological condition similar to APC. Our results demonstrate new properties of synthetic peptides-agonists of PAR1 as a protective agent for brain at trauma and neuropathology.

References.

1) Riewald M., Ruf W. 2005. *J. Biol. Chem*. 280, 19808–19814;
2) Mosnier L.O., Zlokovic B.V., Griffin J.H. 2007. *Blood*. 109 (8), 3161–3172.

3) Zlokovic B.V., Griffin J.H. 2011. *Trends Neurosci.* 34 (4), 198 –209.
4) Mosnier L.O., Griffin J.H. 2011. 118 (21), 247–248.
5) Mosnier L.O., Sinha R.K., Burnier L., Bouwens E.A., Griffin J.H. 2012. *Blood*. 120 (26), 5237–5246.

486
BRAIN-0167
Poster Session

Cerebral Hemorrhage/Subarahcnoid Hemorrhage (SAH)/Vasospasm

INFLUENCE OF PERICAPILLARY NITRIC OXIDE LEVELS AND EDEMA ON CAPILLARY FLOW PATTERNS IN MOUSE MODELS OF SUBARACHNOID HEMORRHAGE

M. Anzabi[1], L. Østergaard[1], N. Kerting Iversen[1], R. Aamand Olesen[1], B. Hansen[1]
[1]CFIN&MIND Lab, Aarhus University, Århus C, Denmark

Background:

Subarachnoid hemorrhage (SAH) is a devastating disease associated with high mortality and morbidity. Despite decades of intense research, delayed cerebral ischemia (DCI) remains the most important cause of poor outcome after SAH. The key role of angiographic cerebral vasospasm as the main cause of DCI has been questioned recently and cerebrovasculature widespread constriction is identified as a potential contributing mechanism. This is suggested, brain oxygen availability is limited not only by cerebral blood flow (CBF), but also by the microscopic distribution of blood, the so-called capillary transit time heterogeneity (CTH)[1], meaning any constriction or compression of cerebral capillaries can change capillary flow pattern and increase CTH, causing severe hypoxia and poor outcome, even without any dramatic reductions in CBF [2].

Nitrite administration has been shown to prevent vasospasm and might be neuroprotective by preventing capillary constrictions. Hypertonic saline (HS) would also be expected to improve outcome by reducing edema and thus CTH.

Objectives:

1. To assess capillary flow pattern changes and CTH in SAH mouse models in comparison with sham operated animals.
2. To investigate the effect of pericapillary nitric oxide levels restoration by nitrite administration, and edema reduction by HS on capillary flow patterns, CTH, and DCI development in SAH mouse models.

Methods:

· SAH induction: (Circle of Willis perforation method)

A filament is inserted into external carotid artery and advanced to the skull base via internal carotid artery. At the branching point of middle cerebral artery, the filament perforates vessel and induces bleeding into subarachnoid space at the skull base. Bleeding results in a sharp increase of the ICP up to 120 mmHg. ICP values then stabilize within 5 min at approximately 20 mmHg.

· Treatment studies:

Treatment study 1: Sodium nitrite administration

Treatment study 2: Hypertonic saline administration

· Capillary flow pattern evaluation:

Capillary diameter and red blood cell velocity are evaluated by two-photon microscopy[3] after 4 days of SAH induction.

· DCI and Cerebral Edema assessment:

DCI will be defined as an infarct zone on Diffusion Weighted Magnetic Resonance Imaging (DW-MRI) at the mentioned time point, and cerebral edema will be assessed by DW-MRI (ADC and Kurtosis).

Results:

Using a thinned-skull cortical window, we employed two-photon microscopy as a tool to investigate cerebral capillary flow pattern. Preliminary results showed SAH animals have lower capillary diameter and red blood cell velocity after 4 days of SAH induction compared to sham operated animals. However for further investigation of CTH, optical coherence tomography (OCT) will be recruited.

Conclusion:

Capillary flow pattern are disturbed after SAH, which may precede hypoxia and poor outcome, emphasizing on cerebral microcirculation potential role in SAH sequels and DCI development. The results may improve our understanding of capillary flow pattern and unveil new treatment strategies.

References:

1. Jespersen SN, Østergaard L. J Cereb Blood Flow Metab 2012; 32: 264–277.
2. Leif Østergaard. J Cereb Blood Flow Metab 2013; 33:1825–1837.
3. Sava Sakadžić. Nat Methods. 2010; 7(9): 755–759.

487
BRAIN-0036
Poster Session

Cerebral Hemorrhage/Subarahcnoid Hemorrhage (SAH)/Vasospasm

NEUROVASCULAR COUPLING AFTER SUBARACHNOID HEMORRHAGE (SAH) IN VIVO

M. Balbi[1], *N. Plesnila*[1]
[1]*Institute for stroke and dementia (ISD), LMU, Munich, Germany*

Objective: Cerebral blood flow (CBF) needs to be adjusted to neuronal activity, a process called neurovascular coupling (NVC) [1]. Subarachnoid hemorrhage (SAH), a subtype of stroke responsible for more than 20% of all cerebrovascular-related deaths[2], is associated with severe reduction in cerebral blood flow[3]. If, however, also CBF regulation is impaired following SAH has not been investigated in vivo yet.

Methods: Male 6 weeks old C57Bl6 mice were subjected to sham surgery or SAH by the filament perforation model. The diameter of pial and parenchymal arteries in the barrel cortex was investigated by 2-photon microscopy, CBF by laser Doppler fluxmetry 3 hours after SAH. NOS-dependent vasodilatation was elicited by inhalation of 10% carbon dioxide (CO_2), NVC by sensory stimulation of the forepaw.

Results: NVC was not impaired after SAH as compared to the sham group. In contrast, neither pial nor parenchymal arterioles reacted to CO_2 while vessels in sham operated mice showed a normal response.

Conclusion: Our study shows impaired CO_2 reactivity in the cerebral microcirculation after SAH while NVC was normal. This suggests that neuron-vessel communication is not affected, while NOS signaling is completely lost after SAH. Accordingly, targeting NO-signaling may represent a novel therapeutic target following SAH.

References:

[1]Girouard H, Iadecola C. Neurovascular couplingin the normal brain and in hypertension, stroke, and Alzheimer disease. J ApplPhysiol (1985) 2006; 100(1): 328-35.

[2]Weaver JP, Fisher M. Subarachnoid hemorrhage: anupdate of pathogenesis,diagnosis and management. J Neurol Sci 1994; 125:119–131.

[3]G. A. Schubert, M. Seiz, A. A. Hegewald, J. Manville, and C.Thom´e,“Acute hypoperfusion immediately after subarachnoid hemorrhage: a xenoncontrast-enhanced CT study,” Journal of Neurotrauma, vol. 26, no. 12, pp.2225–2231, 2009.

488
BRAIN-0616
Poster Session

Cerebral Hemorrhage/Subarahcnoid Hemorrhage (SAH)/Vasospasm

THE POTENTIAL INTERACTION OF FACTOR XIII WITH THE NEUROVASCULAR UNIT PARTICULARLY AFTER SUBARACHNOID HEMORRHAGE

B. Bosche[1], J. Ai[1], B.M. Alharby[1], M.K. Tso[1], H. Wan[1], M. Molcanyi[2], T. Noll[3], R.L. Macdonald[1]
[1]Neurosurgery, St. Michael's Hospital, Toronto, Canada
[2]Institute of Neurophysiology, Center of Physiology and Pathophysiology University of Cologne, Cologne, Germany
[3]Institute of Physiology, Medical Faculty Carl Gustav Carus Technical University of Dresden, Dresden, Germany

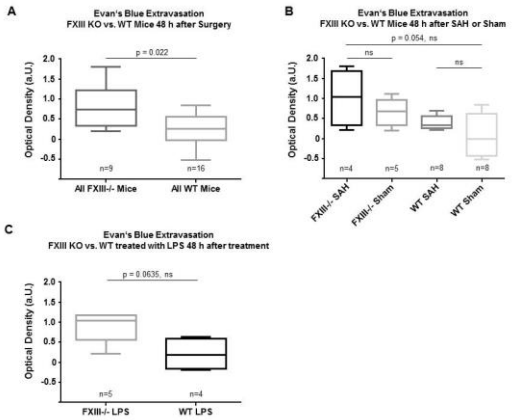

Objectives–The neurovascular unit (NVU) is the regulated interface between the cerebral blood flow and the brain tissue; it includes the blood-brain barrier (BBB) and is a key structure in the pathophysiology of various cerebrovascular diseases [1]. The pathophysiology of the NVU in stroke is still insufficiently understood. However, it is known that a dysfunction of the NVU like in ischemic stroke (IS) or subarachnoid hemorrhage (SAH) may lead to harmful vascular leakage with vasogenic edema or to impaired autoregulation with impending cerebral vasospasm [2-4]. Therefore, protecting the NVU could be a promising target in these diseases including their typical complications. Since the enzymatic action of the *coagulating factor XIII (*FXIII) has multiple functions in vascular biology beyond the coagulation, e.g. stabilizing endothelium [5], it may represent a potential candidate for a novel strategy to protect the NVU.

Methods–We used different *in-vivo* mouse models, i.e. a SAH injection model and a model of BBB disruption using two lipopolysaccharide (LPS, 5mg/kg) I.P. injections, to study the impact of FXIII on the NVU but also on barrier function of other vascular territories. FXIII knock-out (FXIII-/-) and wild type (WT) mice were randomized into a SAH or sham group (4 groups with n=8, respectively) or into LPS groups (2 groups with n=5 and 4). Survival of the mice was evaluated for 48 hours. Evans blue (2%, 1.67ml/kg) were injected into the tail vein at 46 hours after SAH/sham or first LPS injection. Two hours later, mice were sacrificed after transcardial perfusion with saline solution. Thereafter brains were extracted. For assessing BBB disruption and edema, we evaluated brain water content by wet and dry brain weights and Evans blue extravasation by spectrophotometry. Mann-Whitney-U-test or Fisher's exact test were performed for non-parametric independent group comparisons.

Results–After surgery, the mortality of FXIII-/- mice were significantly higher than in WT mice (FXIII: n=7/16 vs. WT: n=0/16, p=0.0068; detailed mortality rates: FXIII-/-: SAH 50%, Sham 37.5% vs WT: 0% and 0% respectively). Comparing SAH to sham treatment, no significant difference in the mortality of the mice were found (SAH: 25% vs Sham: 18.75%, p>0.05, ns). Evans blue extravasation of surgically treated FXIII-/- mice was significantly higher compared to WT mice (Figure 1A). As a result of the high mortality of FXIII-/- mice, the other group comparisons showed trends only (1B). Similar observations were found by comparing the LPS-treated FXIII-/- mice with the WT ones (1C). Brain water content of the mice showed no significant differences between the individual groups.

Conclusions–Despite the high mortality rate of FXIII-/- mice after surgery these results improve our knowledge of the interactions between FXIII and the NVU including the BBB, thereby casting

light on novel strategies potentially protecting the NVU in cerebrovascular diseases such as SAH. However, further research is needed in this field.

References

1. Stanimirovic and Friedman, JCBFM 2012
2. Wijdicks et al., Stroke 2014
3. Bosche et al., Ann Neurol 2010
4. Macdonald, Nat Rev Neurol 2013
5. Schroeder and Kohler, J Thromb Haemost 2013

489
BRAIN-0238
Poster Session

Cerebral Hemorrhage/Subarahcnoid Hemorrhage (SAH)/Vasospasm

DECOMPRESSIVE CRANIECTOMY AFTER SUBARACHNOID HEMORRHAGE - EXPERIMENTAL RESULTS IN MICE

D. Bühler[1], S. Azghandi[1], K. Schüller[1], N. Plesnila[1]
[1]Institute for Stroke and Dementia Research, University of Munich Medical Center, Munich, Germany

Objectives:
Subarachnoid hemorrhage (SAH) is accompanied by high mortality and morbidity. Major pathophysiological features of SAH are elevated intracranial pressure (ICP) and subsequently reduced cerebral blood flow (CBF). In this study, we wanted to evaluate whether decompressive craniectomy is able to reduce post-hemorrhagic intracranial hypertension and thereby improving outcome following experimental SAH.
Methods:
SAH was induced in male C57BL/6 mice by endovascular Circle of Willis perforation. Four groups were investigated: Sham, SAH, SAH and bilateral decompressive craniectomy (DC) before hemorrhage, and bilateral DC after SAH. ICP and CBF were monitored until 45 min after SAH. Neurological function was evaluated daily for 7 days. Finally, brains were harvested and white matter damage, hydrocephalus formation, and survival of hippocampal neurons were quantified on paraffin-embedded coronal brain sections.
Results:
DC relieved intracranial hypertension, but it did not improve cerebral hypoperfusion after SAH. Additionally, it led to more rebleedings, to a higher mortality rate and surviving animals had a worse long-term functional outcome. At the histopathological level, no significant differences could be identified between surviving mice after SAH with or without DC.
Conclusions:
In contrast to ischemic stroke and traumatic brain injury, DC had no beneficial effect after experimental SAH, although it markedly reduced post-hemorrhagic intracranial hypertension. Moreover, decompressed animals had a higher incidence of rebleeding and worse functional outcome. These results suggest that elevated ICP shortly after SAH is important for cessation of the bleeding. Therefore DC in SAH patients needs to be considered carefully with special emphasis on timing and degree of bleeding.
Reference:

Bühler D, Azghandi S, Schüller K, Plesnila N. Effect of Decompressive Craniectomy on Outcome Following Subarachnoid Hemorrhage in Mice. Stroke. 2015 (epub ahead of print)

490
BRAIN-0081
Poster Session

Cerebral Hemorrhage/Subarahcnoid Hemorrhage (SAH)/Vasospasm

CYCLOPHILIN A/CD147 INTERACTIONS PARTICIPATE IN EARLY BRAIN INJURY AFTER SUBARACHNOID HEMORRHAGE IN RATS

B. Dang[1], H. Li[1], C. Meng[1], H. Shen[1], Y. Wang[1], A. Gao[1], X. Duan[1], Z. Wang[1], G. Chen[1]
[1]Neurosurgery,
1st Affiliated Hospital Soochow University, Suzhou, China

Objective: Apoptotic pathway and inflammatory response play important roles in the pathogenesis of early brain injury (EBI) following subarachnoid hemorrhage (SAH). As the most abundant member of cyclophilins, cyclophilin A (CyPA) can

be secreted from cells in response to inflammatory stimuli. In addition, CyPA has been found to be involved in many inflammatory diseases via its receptor, CD147 [1]. This study was designed to estimate the potential role of CyPA/CD147 in SAH-induced EBI.

Methods: A prechiasmatic cistern single-injection model was used to produce experimental SAH in Sprague–Dawley rats. The expressions of CyPA and CD147, the interaction between CyPA and CD147, and the secretion of CyPA were assessed using immunofluorescence staining, western blot analysis, and co-immunoprecipitation analysis. Down-regulation of CyPA expression by siRNA was performed and recombinant human CyPA (rh CyPA) and monoclonal antibody of CD147 (anti-CD147) was exploited to study the role of CyPA/CD147 in SAH-induced EBI.

Results: The expressions of CyPA and CD147 in neurons were higher than that of the sham group, and peaked at 24 h after SAH (Figure.1A-C). Compared with sham group, SAH was found to increase the interaction between CyPA and CD147 and the secretion of CyPA (Figure.1D and E). CyPA siRNA alleviated SAH-induced CyPA secretion, while rh CyPA promoted CyPA secretion (Figure.1E). In addition, CyPA siRNA and anti-CD147 treatments decreased SAH-indued the phosphorylation of ERK 1/2, the increaesd protein level of p53 and active-caspase-3, and the activation of NF-κB (Figure.1F and G). Finally, CyPA siRNA and anti-CD147 treatments were found to ameliorate SAH-induced EBI, including damage to the blood-brain barrier, brain edema, cortical apoptosis and necrosis, and neurobehavioral deficits (Figure.2). Remarkably, compared with CyPA siRNA and anti-CD147 treatments, rh CyPA treatment resulted in an opposite effect, which was inhibited by anti-CD147 treatment (Figure.1 and 2).

Conclusions: Intracellular CyPA in neurons secreted to the extracellular space under the stimulation of SAH. Then, extracellular CyPA binds to its receptor CD147 and may activate ERK 1/2 and NF-κB, then upregulate p53 and caspase-3 expression to induce neuron apoptosis. The whole pathological process aggravates EBI after SAH. CyPA/CD147 may be a suitable therapeutic target for SAH (Figure.3).

References：

1. Seizer P, Gawaz M, May AE. Cyclophilin A and EMMPRIN (CD147) in cardiovascular diseases. Cardiovasc Res. 2014;102(1):17-23.

Figure legends：

Figure.1: Subarachnoid hemorrhage (SAH) activated the ERK1/2-NF-κB pathway and cell apoptosis (F and G) via increasing the expressions of cyclophilin A (CyPA) and CD147 (A-C), the interaction between CyPA and CD147 (D), and the secretion of CyPA (E).

Figure.2: Cyclophilin A (CyPA)/CD147 participate in subarachnoid hemorrhage (SAH)-induced the blood-brain barrier damage (A), brain edema (B), cortical apoptosis (C), and necrosis (D), which is increased by rh CyPA and alleviated by siCyPA and anti-CD147 treatments. Arrows point to TUNEL-positive cells in the brain in C.

Figure.3: Mode pattern illustrating the role of cyclophilin A (CyPA)/CD147 interaction in induced brain cell apoptosis and possible mechanisms underlying CyPA/CD147 interaction in brain injury after subarachnoid hemorrhage (SAH).

Figure 1:

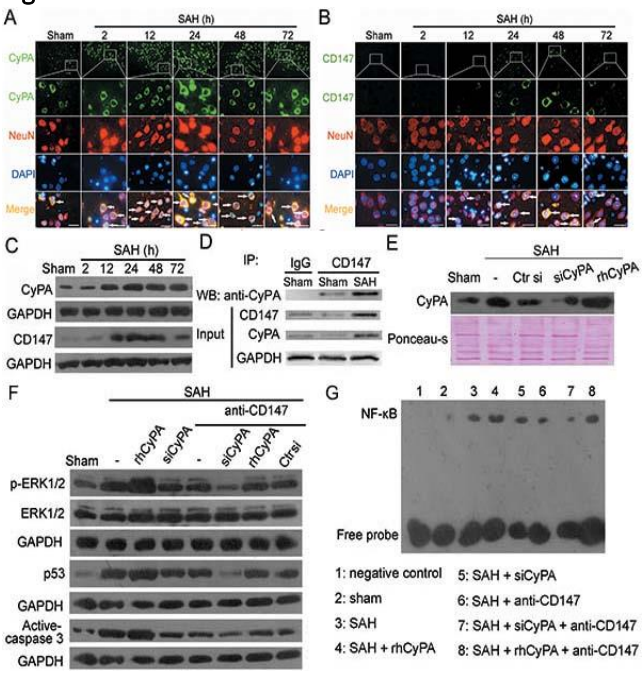

Figure 2:

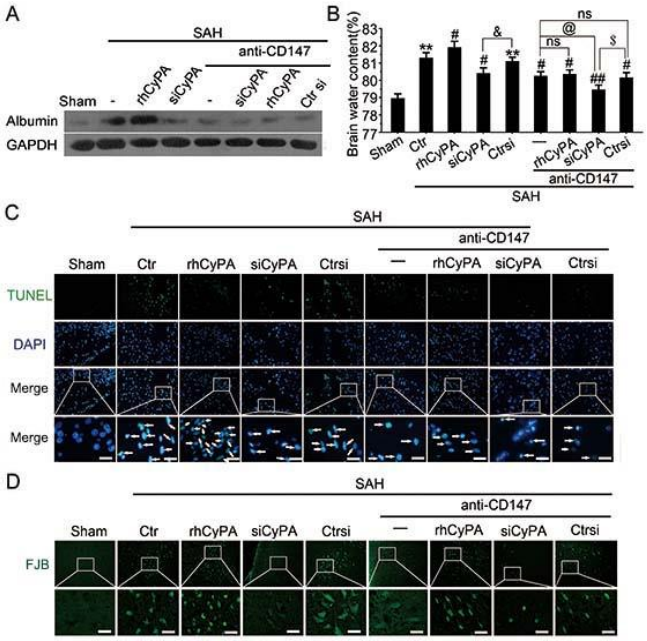

Figure 3:

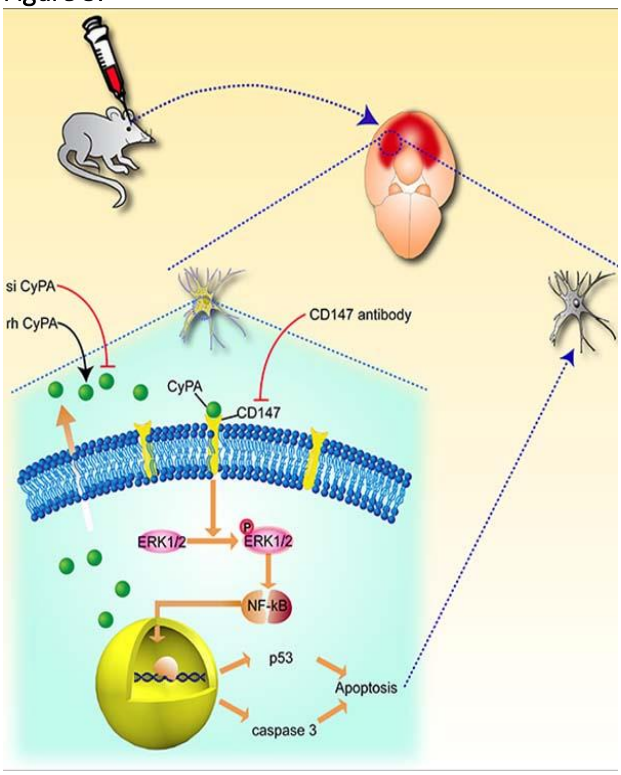

491
BRAIN-0082
Poster Session

Cerebral Hemorrhage/Subarahcnoid Hemorrhage (SAH)/Vasospasm

HYDROGEN SULFIDE AMELIORATES EARLY BRAIN INJURY IN SUBARACHNOID HEMORRHAGE IN RATS : POSSIBLE INVOLVEMENT OF REDOX REACTION AND ANTI-INFLAMMATORY SIGNALING

Y. Cui[1], H. Li[1], X. Duan[1], Y. Wang[1], A. Gao[1], H. Shen[1], Z. Yu[1], G. Chen[1]
[1]Neurosurgery,
1st Affiliated Hospital Soochow University, Suzhou, China

Objective: Increasing studies have demonstrated the neuroprotective effect of hydrogen sulfide (H2S) in central nervous system (CNS) diseases. However, the potential application value of H2S in the therapy of subarachnoid hemorrhage (SAH) is still not well known [1]. This study was to investigate the potential effect of H2S on early brain injury (EBI) induced by SAH and explore the underlying mechanisms.

Methods: The role of sodium hydrosulfide (NaHS), a donor of H2S, in SAH-induced EBI was investigated in both in vivo and in vitro. A prechiasmatic cistern single injection model was used to produce experimental SAH in vivo. In vitro, cultured primary rat cortical neurons and human umbilical vein endothelial cells (HUVECs) were exposed to OxyHb at concentration of 10 μM to mimic SAH.
Results: Endogenous production of H2S in the brain was significantly inhibited by SAH . The protein levels of the predominant H2S-generating enzymes in the brain, including cystathionineb-synthase (CBS) and 3-mercaptopyruvate sulfur transferase (3MST), were also correspondingly reduced by SAH, while treatment with NaHS restored H2S production and the expressions of CBS and 3MST (Figure.1A). Remarkably, NaHS treatment abolished the elevation of the levels of inflammatory cytokines and oxidative stress following SAH (Figure.1B). Consistently, NaSH inhibited OxyHb-induced oxidative stress and

apoptosis in cultured neurons and HUVECs (Figure.2C and D). More importantly, NaHS treatment also could inhibit SAH-induced cortical apoptosis and VEC apoptosis in anterior cerebral artery and middle cerebral artery (Figure.2E). Finally, NaHS treatment could significantly attenuate EBI (including cerebral vasospasm, brain edema, blood-brain barrier disruption, and neurobehavioral deficits) after SAH (Figure.2).

Conclusions: After induction of SAH, NaSH treatment not only restored H2S production, but also up-regulated the protein levels of CBS and 3MST. There may be a positive feedback between circulating H2S level and CBS/3MST gene expression. H2S significantly reduces EBI induced by SAH at least partially mediated by its anti-inflammatory and anti-oxidative stress activities. Our results suggest that NaSH as an exogenous H2S donor could significantly reduce EBI induced by SAH (Figure.3).

References :

1. Yu YP, Chi XL, Liu LJ. A hypothesis: hydrogen sulfide might be neuroprotective against subarachnoid hemorrhage induced brain injury. ScientificWorldJournal 2014; 2014: 432318.

Figure legends:

Figure.1 NaSH inhibited subarachnoid hemorrhage (SAH)-induced deregulation of the expressions of cystathionineb-synthase (CBS) and 3-mercaptopyruvate sulfur transferase (3MST) (A), oxidative stress (B-D), and cell apoptosis (C-E). Data are means ± SEM. *p < 0.05, **p < 0.01 vs. sham group; # p < 0.05, ## p < 0.01 vs. SAH group; & p < 0.05, n = 6. Arrows point to TUNEL-positive cells in E.

Figure.2 NaSH alleviated subarachnoid hemorrhage (SAH)-induced cerebral vasospasm (A), brain edema (B), and blood-brain barrier damage (C). Data are means ± SEM. **p < 0.01 vs. sham group; # p < 0.05, ## p < 0.01 vs. SAH group; & p < 0.05, n = 6.

Figure.3 A potential process illustrating the effects of NaHS on early brain injury following SAH and the underlying mechanisms.

Fig.1

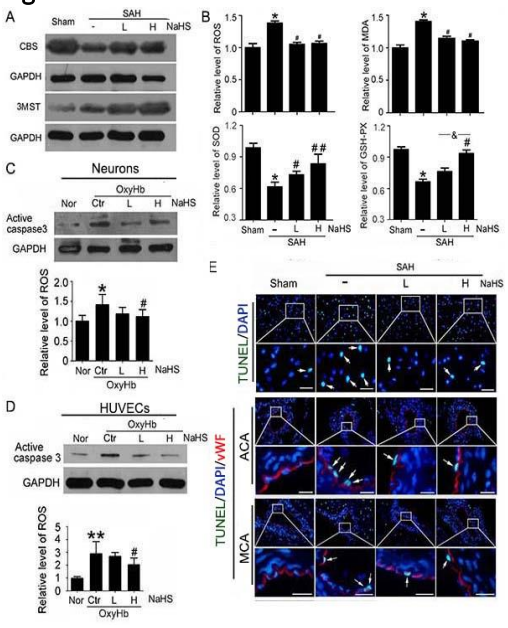

Fig.2

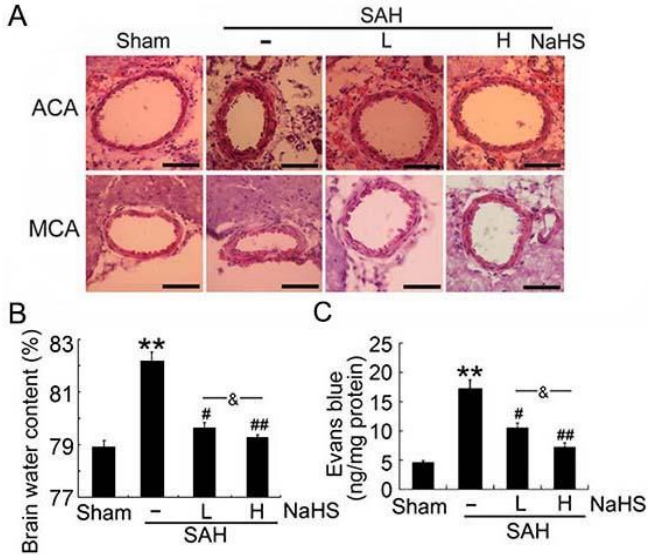

Fig.3

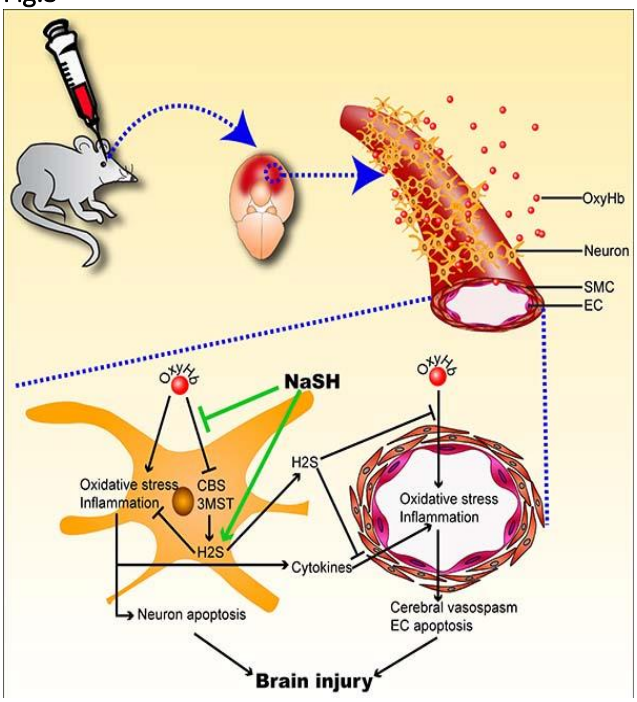

492
BRAIN-0560
Poster Session

Cerebral Hemorrhage/Subarahcnoid Hemorrhage (SAH)/Vasospasm

ACUTE EFFECT OF INTRAVENOUS SILDENAFIL ON CEREBRAL BLOOD FLOW IN PATIENTS WITH VASOSPASM AFTER SUBARACHNOID HEMORRHAGE

R. Dhar[1], C. Washington[2], M. Diringer[1], C. Derdeyn[3], G. Zipfel[2]
[1]Neurology, Washington University, St. Louis, USA
[2]Neurosurgery, Washington University, St. Louis, USA
[3]Radiology, Washington University, St. Louis, USA

Objectives: Vasospasm is a common complication of aneurysmal subarachnoid hemorrhage (SAH) and has been implicated in the pathogenesis of delayed cerebral ischemia (DCI). We recently demonstrated that intravenous administration of the phosphodiesterase-5 inhibitor sildenafil can improve angiographic vasospasm in SAH patients. Whether such a vasodilator can directly improve cerebral blood flow (CBF) and minimize brain at risk for cerebral ischemia is unknown. Here we evaluated the acute effect of high-dose intravenous sildenafil on cerebral blood flow (CBF), specifically assessing whether it could improve CBF to regions with low baseline flow in patients with vasospasm after SAH.
Methods: Six subjects with vasospasm after aneurysmal SAH (confirmed on digital-subtraction angiography, DSA) were enrolled in this physiologic study. Each underwent ^{15}O-PET imaging twice to measure pre-infusion CBF and then received a 30-minute infusion of 30-mg sildenafil. PET was repeated 15-mins after infusion was completed. We measured global CBF and regions with CBF < 25 ml/100g/min as a proportion of brain volume as well as plotting pixel-wise histograms of regional CBF distribution (compared pre- vs. post-infusion).
Results: The study was performed a mean of 9±2 days after SAH. 5 of 6 subjects had moderate-severe vasospasm on DSA (performed a median of 1.5 days prior to PET); the other had only mild vasospasm. Two subjects had symptoms consistent with DCI at time of PET. The only physiologic variable that changed after sildenafil infusion was mean arterial pressure (135±17 mm Hg at baseline vs. 125±14 mm Hg after infusion, p=0.01). ICP and P_aCO_2 remained stable. Mean global CBF was 34.5±6.6 ml/100g/min at baseline and did not change after sildenafil (33.9±8.0, p=0.59). We did not find a positive correlation between change in MAP and CBF in this cohort. The proportion of brain pixels with low CBF varied from 11-35% of total brain volume at baseline and we did not observe any reduction in hypoperfused brain after sildenafil. We did observe two patients (see Figure 1) who had a left-shift in regional CBF histograms after sildenafil infusion (associated with a small reduction in MAP). The other four patients had stable CBF despite lower MAP.
Conclusions: Despite evidence that it can be effective as a cerebral vasodilator in the setting of vasospasm, we did not find any improvement in global or regional CBF after intravenous infusion of sildenafil in patients with SAH. A subset of patients exhibited a small reduction in CBF, perhaps due to impaired cerebrovascular

autoregulation and a drop in MAP.

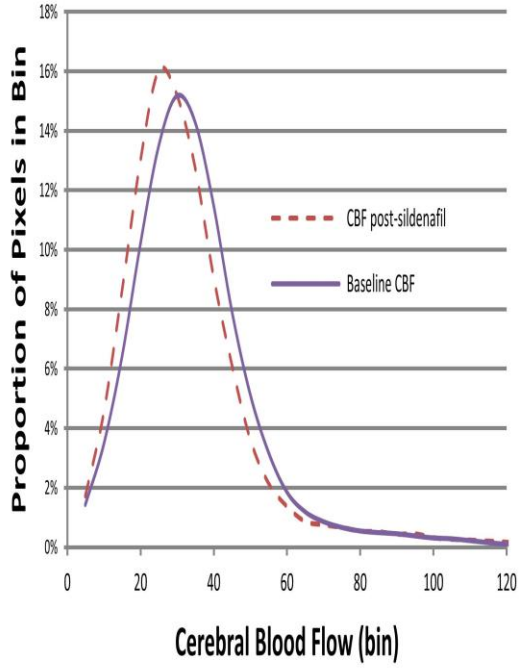

493
BRAIN-0713
Poster Session

Cerebral Hemorrhage/Subarahcnoid Hemorrhage (SAH)/Vasospasm

VALPROATE REDUCES BRAIN INJURY IN A RAT MODEL OF SUBARACHNOID HEMORRHAGE WITH SPREADING DEPOLARIZATIONS

A.M. Hamming[1], A. Van der Toorn[2], U.S. Rudrapatna[2], L. Ma[3], H.J. Van Os[1], M.D. Ferrari[1], A.M.J.M. Van den Maagdenberg[4], A.M. Stowe[3], R.M. Dijkhuizen[2], M.J.H. Wermer[1]
[1]Neurology, Leiden University Medical Center, Leiden, Netherlands
[2]Biomedical MR Imaging and Spectroscopy Group Image Sciences Institute, University Medical Center Utrecht, Utrecht, Netherlands
[3]Department of Neurology and Neurotherapeutics, University of Texas Southwestern Medical Center, Dallas Texas, USA
[4]Neurology and Human Genetics, Leiden University Medical Center, Leiden, Netherlands

Objectives

Spreading depolarization (SD) is a proposed mechanism involved in the development of delayed cerebral ischemia after aneurysmal subarachnoid hemorrhage (SAH).[1] However, it is unknown if inhibition of SD results in less ischemic damage and better outcome. We tested our hypothesis that SD inhibitor valproate[2] reduces brain injury in a rat model of SAH with and without artificial SD induction.

Methods

Rats were randomized in a 2x2 design. Groups A (n=15) and C (n=17) were treated with placebo, and groups B (n=15) and D (n=17) with valproate (200 mg/kg). After four weeks of daily i.p. pretreatment, we performed endovascular SAH induction by puncturing the internal carotid artery.[3] On day 1 after SAH, brain tissue damage was measured with T_2-weighted MRI, followed by cortical application of 1M KCl for SD induction (groups C and D) or saline (groups A and B), ipsilateral to the SAH. Cortical Laser-Doppler Flowmetry (LDF) was performed to record SDs. MRI was repeated on day 3 after SAH. Primary outcome measure was lesion growth between day 1 and 3. Other outcome measures included mortality.

Results

Comparing the groups without SD induction (groups A and B), there were no statistically significant differences in lesion growth (figure). Mortality between days 1 and 3 was 7% in placebo group A versus 33% in valproate group B (p=0.09).

Comparing the groups with SD induction (groups C and D), lesion growth was 243±233 mm^3 in placebo group C versus 61±76 mm^3 in valproate group D (p=0.01, figure). Between days 1 and 3, 25% of the rats in placebo group C died versus 0% in valproate group D (p=0.08).

Conclusions

In our rat model of SAH with artificial SD induction, valproate treatment significantly reduced brain lesion growth between days 1 and 3. Inhibition of SDs may thus contribute to reducing delayed cerebral ischemia after SAH.

References

1. Dreier JP. The role of spreading depression, spreading depolarization and spreading ischemia in neurological disease. *Nature medicine* 2011; 17(4): 439-47.

2. Ayata C. Spreading depression: from serendipity to targeted therapy in migraine prophylaxis. *Cephalalgia* 2009; 29(10): 1095-114.

3. Kooijman E, Nijboer CH, van Velthoven CT, Kavelaars A, Kesecioglu J, Heijnen CJ. The rodent endovascular puncture model of subarachnoid hemorrhage: mechanisms of brain damage and therapeutic strategies. *Journal of neuroinflammation* 2014; 11: 2.

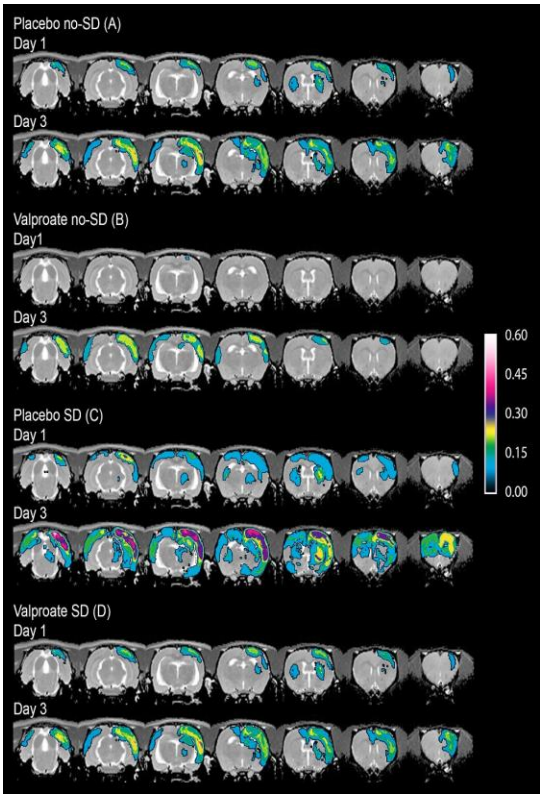

Figure 1. Lesion incidence maps. Voxel-based representations of fraction of rats with lesioned tissue identified on multislice T_2 maps at days 1 and 3 after SAH with or without artificial SD induction, projected over a rat brain T_2 template. In animals with SAH and SD, there was significantly less lesion growth in the valproate group (D) than in the placebo group (C).

494
BRAIN-0721
Poster Session

Cerebral Hemorrhage/Subarahcnoid Hemorrhage (SAH)/Vasospasm

VASOSPASM AFTER ANEURYSMAL RUPTURE: AN ANALYSIS OF MODALITY, PATIENT CHARACTERISTICS AND CLINICAL CONDITIONS AND ITS CORRELATION TO VASOSPASM

J. Garcia[1]
[1]*Neurosurgery, University of Santo Tomas, Manila, Philippines*

INTRODUCTION: Cerebral vasospasm is an acknowledged complication of subarachnoid hemorrhage secondary to a ruptured aneurysm. This carries a clinically significant increase in mortality and morbidity. Various studies have shown vasospasm to be correlated to by clot volume, age, location, and density of the SAH seen on the initial computed tomography scans.

OBJECTIVES: This retrospective cohort study was designed to correlate the prevalence of vasospasm in our local setting to treatment modality, age, gender, presence of intracranial hemorrhage and smoking history. The results of which may lead to better prediction of patients who are at higher risk to develop vasospasm due to subarachnoid haemorrhage from a ruptured aneurysm

METHODS: We included 43 patients from our institution who were diagnosed with subarachnoid hemorrhage due to a ruptured intracranial artery aneursym as demonstrated by 4 vessel angiogram or CT angiogram. Baseline Transcranial Doppler monitoring was done on day

1 post clipping or coiling. Values used for transcranial Doppler were a Lindegaard ratio of less than 3 which was recorded as absence of vasospasm and a Lindegaard ratio of greater than or equal to 3 recorded as presence of vasospasm.

RESULTS: There was no statistically significant difference in the prevalence of vasospasm in relation to modality used to treat the aneurysm (post-clipping and post coiling: p value=.088). Based on the univariate analysis of patients with vasospasm, we noted those with Fischer grade 2 were 99% less likely to have vasospasm (Odds Ratio=0.01;Confidence Interval 0-0.27), while those with grade 3 were 50.61 times more likely to have vasospasm(Odds Ratio=50.61; Confidence Interval 4.99-2688.05). Those with Fischer grade 4 were 33.35 times more likely to have vasospasm (Odds Ratio=33.35; Confidence Interval 1.6-682.4) Hunt and Hess grade III were 33.35 times (Odds Ratio=33.35; Confidence Interval:1.6 – 682.4) more likely to have vasospasm. The presence of ICH and other factors such as age, gender, smoking, had no significant association with vasospasm.

CONCLUSION: Our current study finds that a higher Fischer grades and those with a higher volume of subarachnoid blood were associated with a higher prevalence of vasospasm. It however finds no difference in the prevalence of vasospasm in relation to modality used, age gender, presence of ICH and smoking history.

REFERENCES:

1. Hoh BL et al: Effect of Clipping, Craniotomy or Intravascular Coiling on Cerebral Vasospasm and Patient Outcome after Aneurysmal Subarachnoid Hemorrhage. Neurosurgery Vol. 55: 779-789 2004.
2. Harod CG et al: Prediction of Cerebral Vasospasm in Patients presenting with Anrueysmal Subarachnoid Hemorrhage: Review. Neurosurgery Vol. 56: 633-654 2005.
3. Marshal SA et al:The Role of Transcranial Doppler Ultrasonography in the Diagnosis and Management of Vasospasm After Aneurysmal Subarachnoid Hemorrhage. Neurosurgery Clinics: 291–303 2010.
4. Ibrahim GM et al :Method of Aneurysm Treatment Does Not Affect Clot Clearance After Aneurysmal Subarachnoid Hemorrhage. Neurosurgery Vol.70:102–109 2012.
5. Fisher et al: Relation of cerebral vasospasm to subarachnoid hemorrhage visualized by computerized tomographic scanning. Neurosurgery Vol 6:1–9, 1980.

495
BRAIN-0574
Poster Session

Cerebral Hemorrhage/Subarahcnoid Hemorrhage (SAH)/Vasospasm

ACUTE SUBARACHNOID HEMORRHAGE TRIGGERS SEVERE RESPITRATORY SUPPRESSION AND ARREST OF CEREBROSPINAL FLOW CIRCULATION

E. Golanov[1], R. Federley[1], E. Bovshik[1], S. Wong[2], G. Britz[1]
[1]Neurosurgery,
The Houston Methodist Research Institute, Houston, USA
[2]Systems Medicine and Bioengineering,
The Houston Methodist Research Institute, Houston, USA

Objectives

SAH, blood accumulation in subarachnoid space (SS), is caused by rupture of intracranial aneurisms or by traumatic brain injury. CSF circulating throughout SS and brain parenchyma forms glymphatic paravascular pathways for waste removal (1). We explored changes in CSF circulation and basic physiological parameters following acute SAH

Methods

In isoflurane anesthetized spontaneously breathing C57BL mice, using the perforation model of subarachnoid hemorrhage we explored effects of a hemorrhage on arterial (AP) and intracranial pressure (ICP), local cerebral blood

flow (CBF), respiration and heart rate (for up to one hour) and alterations of CSF circulation at various time (1 hour to 30 days). To monitor CSF circulation fluorescent microspheres (μS, 0.02 μm) were injected into the cisterna magna (CM) or brain parenchyma. The spread of μS across the brain was monitored using *in vivo* multiphoton or *ex vivo* fluorescence microscopy.

Results

Our model of SAH was highly reproducible (n=123), and can be classified as 'moderate" (2) with the lethality not exceeding 15%. Immediately following the perforation ICP sharply increased by 65%, CBF dropped by 68% in the ipsilateral hemisphere, cerebrovascular resistance increased by 78%. At the moment of perforation acute apnea took place in 97% of cases. The degree of apnea did not correlate with the volume of hemorrhage, suggesting reflexive nature of the response. In naive mice μS administered into CM were observed at the surface of the brain stem and paraarterially along Willis circle and middle cerebral artery. Caudally μS spread down the spinal cord. Intraparenchymally injected μS were associated with paravascular space. One hour after SAH, μS were confined to the CM and brain stem region. No μS were observed along the Willis circle indicating drastic impairment of CSF flow. The distribution of μS along the spinal cord was abolished. CSF flow showed recovery signs only 30 days after SAH. Intraparenchymally μS were no longer associated with paravascular space. Intravital examination of the vasculature in the same cortical area before and after SAH showed vasoconstriction in 15 minutes post-SAH, and suppression of the slow high amplitude vasomotion.

Conclusions

Our study provides two important observations. First, acute SAH at the base of the brain triggers apneic reaction, which, most probably has neurogenic origin and may be a part of the trigeminocardiac reflex (3). This important observation being in line with the earlier clinical reports (4), may be an important reason of early death following SAH in patients. Second, acute and long lasting arrest of CSF observed here in perforation model of SAH may be an important factor participating in the long-lasting ailments affecting SAH survivors.

References

1 .Iliff J., Wang, M., et al., Sci. Transl. Med. 2012, 4, 147ra111.
2. Sugawara T., Ayer R., et al., J. Neurosci.Method, 2008, 167 (2), 327-334
3. Chowdhury, T., Mendelowittz, D., et al., J Neurosurg. Anesthesiol., 2015
4. Hijdra, A., Braakman R., et al., Stroke, 1987, 18 (6), 1061-1067

Research supported by The Ting Tsung and Wei Fong Chao Center for BRAIN, John Dunn Research Foundation, The Oden Brain Aneurysm Research Foundation.

496
BRAIN-0227
Poster Session

Cerebral Hemorrhage/Subarahcnoid Hemorrhage (SAH)/Vasospasm

INHIBITION OF PROSTAGLANDIN E2 RECEPTOR EP3 PROTECTS AFTER INTRACEREBRAL HEMORRHAGE

X. han[1], X. Lan[1], Q. Li[1], Y. Gao[1], T. Cheng[1], J. Wang[1]
[1]Anesthesiology and Critical Care Medicine, Johns Hopkins School of Medicine, Baltimore, USA

Objective: Prostaglandin (PG) E_2 plays a critical role in inflammation and secondary brain injury after intracerebral hemorrhage (ICH). EP3 is the only PGE_2 receptor that couples to multiple G-proteins, but its role in ICH has not been examined. In the present study, we investigated the role of EP3 receptor (EP3R) after thrombin or blood-induced ICH in mice and explored its underlying cellular and molecular mechanisms of action.

Methods: Using in vitro hippocampal slice cultures and in vivo injection of thrombin or autologous

arterial blood, we tested the effects of EP3R antagonist AE240, EP3 agonist AE248, rho kinase inhibitor HA1077, and thrombin inhibitor hirudin. We assessed outcomes with neurologic function tests, brain lesion and edema measurement, immunohistology, and Western blotting.

Results: In vitro, EP3R inhibition reduced thrombin-induced hippocampal CA1 cell death. In the in vivo thrombin-induced ICH model, EP3R was expressed mostly in astrocytes and to a lesser extent in microglia in the perilesional region. EP3R inhibition reduced lesion volume, neurologic deficit, cell death, matrix metalloproteinase-9 activity, neutrophil infiltration, and the number of $CD68^+$ microglia, but increased the number of $Ym\text{-}1^+$ M2 microglia. RhoA-Rho kinase levels were increased after thrombin injection and were decreased by EP3R inhibition. Thrombin inhibition did not block the EP3R agonist-induced RhoA increase after blood-induced ICH.

Conclusions: PGE_2 receptor EP3 contributes to thrombin-induced brain damage via Rho-Rho kinase–mediated cytotoxicity and proinflammatory responses. Modulating EP3R may promote alternative activation of microglia and provide a viable means to mitigate ICH impairment.

497
BRAIN-0074
Poster Session

Cerebral Hemorrhage/Subarahcnoid Hemorrhage (SAH)/Vasospasm

ROLE OF LIPOCALIN-2 IN BRAIN INJURY AFTER INTRACEREBRAL HEMORRHAGE

Y. Hua[1], W. Ni[1], M. Zheng[1], G. Xi[1], R. Keep[1]
[1]Neurosurgery, University of Michigan, Ann Arbor, USA

Objective: Lipocalin2 (LCN2) is a siderophore-binding protein involved in cellular iron transport and neuroinflammation [1]. Iron and inflammation are two factors affecting brain injury after intracerebral hemorrhage (ICH) [2]. This study investigates the effect LCN2 deficiency on the expression of ferritin (an iron storage protein), microglia activation, neuronal death and neurological deficits in a mouse model of ICH. In addition, the role of LCN2 in iron-induced brain injury was also examined.

Methods: Male adult C57BL/6 wild type (WT) or LCN2 deficient ($LCN2^{-/-}$) mice had an intracerebral injection of autologous blood or iron. Control animals had a sham operation or saline injection. T2 weighted magnetic resonance imaging and behavioral tests were performed at days 1, 3, 7, 14 and 28 after injection. Brains were used for histology, immunohistochemistry and Western blot analysis.

Results: In WT mice, brain LCN2 levels were increased in the ipsilateral basal ganglia after ICH (LCN2/β-actin: 1.34 ± 0.33 vs. 0.85 ± 0.25 in the sham, $p<0.05$) or iron injection (7522 ± 2951 vs. 1843 ± 394 pixels in saline, $p<0.05$). LCN2 positive cells were astrocytes and microglia but not neurons. ICH resulted in a significant increase in ferritin expression in the ipsilateral basal ganglia ($p<0.05$). Compared to WT mice, ICH caused less ferritin upregulation (FTH/β-actin: 0.77 ± 0.06 vs. 1.51 ± 0.38 in WT, $p<0.01$; FTL/β-actin: 0.71 ± 0.25 vs. 2.16 ± 0.65 in WT, $p<0.01$), microglia activation (Iba-1/β-actin: 0.51 ± 0.17 vs. 0.95 ± 0.22 in WT, $p<0.01$) and brain swelling (3.17 ± 3.32 vs. 6.75 ± 3.55% in WT group, $p<0.01$) in $LCN2^{-/-}$ mice at 24 hours after ICH. ICH also resulted in less neuronal death (DARPP-32/β-actin: 0.9 ± 0.11 vs. 0.68 ± 0.07%, $p<0.05$ at day-3) and neurological deficits ($p<0.05$) in $LCN2^{-/-}$ mice. In addition, iron induced less T2 lesion (16.0 ± 4.7 vs. 26.6 ± 13.6 mm^3 in WT mice, $p<0.05$), brain swelling ($p<0.05$) and BBB disruption ($p<0.05$) in $LCN2^{-/-}$ mice at 24 hours.

Conclusion: ICH induced LCN2 upregulation in brain and knockout of LCN2 resulted in less brain swelling, microglia activation, neuronal death and neurological deficits after ICH. Iron induces less brain swelling and BBB disruption in $LCN2^{-/-}$ mice. These results suggest a role of LCN2 in brain injury and iron toxicity following ICH.

Reference:

1. Dong M, Xi G, Keep RF, Hua Y. Role of iron in brain lipocalin 2 upregulation after intracerebral hemorrhage in rats. *Brain Res* 2013;1505:86-92.
2. Keep RF, Hua Y, Xi G. Intracerebral hemorrhage: mechanisms of injury and therapeutic targets. *Lancet Neurol* 2012;11:720-731.

498
BRAIN-0651
Poster Session

Cerebral Hemorrhage/Subarahcnoid Hemorrhage (SAH)/Vasospasm

THE VASCULAR RESPONSES AND THE VELOCITIES OF BLOOD CELLS IN CEREBRAL ARTERIOLES AND CAPILLARIES IMMEDIATELY AFTER SUBARACHNOID HEMORRHAGE

M. Ishikawa[1], M. Kajimura[2], T. Morikawa[2], Y. Tanaka[1], E. Watanabe[3], M. Suematsu[2]
[1]Neurosurgery,
Saitama Medical Center Jichi Medical University, Saitama, Japan
[2]Biochemistry, Keio University, Tokyo, Japan
[3]Neurosurgery, Jichi Medical University, Tochigi, Japan

Objectives: Immediately after subarachnoid hemorrhage (SAH), brain injury begins and determines the acute phase mortality and the long-term prognosis, but its mechanism is not well understood. When SAH from the skull base induces platelet-leukocyte-endothelial cell interactions in venules, the cerebral blood flow is kept well at the cerebral surface [1]. We investigated cerebral microcirculation through a mouse cranial window using two-photon laser scanning microscopy at a depth of about 100μm [2,3], after SAH was induced at the skull base with a mouse thread model.

Methods: Tracheotomy was performed and femoral artery and vein were cannulated in mice. Q-dot 655 nanocrystal (Q21021MP; Invitrogen) or rhodamine-6G was injected from the cannulated femoral vein, after a craniotomy at the parietal bone without cutting dura matter. SAH was induced at a prone position by using the endovascular perforation model [4]. Immediately and 45min. after SAH, blood cell velocities were measured with a line scan method in precapillaries and capillaries using two-photon laser scanning microscopy.

Results: A penetrating arteriole branched into a precapillary arteriole at the depth of 85.9 +/- 21.0μm (n=7). Arterioles dilated immediately after SAH and then gradually constricted (n=5/7) and the blood flow disappeared immediately after SAH in the others (n=2/7). The blood cell velocity of the precapillary arteriole decreased from 10.7 +/- 3.0 mm/s before SAH to 0.9 +/- 0.4 mm/s after SAH. The blood cell velocities were able to be measured with a line scan method. The thick fluorescence line was considered as a leukocyte. The thin fluorescence line was considered as a platelet. The black line was a red blood cell, following continuous injection of rhodamine-6G. The capillary-velocities of all blood cells (red blood cells, platelets and leukocytes) decreased and rolling and adherent leukocytes prevented blood flow in capillaries.

Conclusion: The cerebral blood flow decreases in arterioles and capillaries immediately after the SAH. Rolling and adhesion of leukocytes may aggravated cerebral microcirculation.

References

1) Ishikawa M et al. Neurosurgery 64:546-554, 2009.
2) Nakamura T et al. Acta Physiol 203:187-196, 2010.
3) Morikawa T et al. Proc Natl Acad Sci USA 109:1293-1298, 2012.
4) Ishikawa M et al. Stroke 30:1679-1686,1999.

499
BRAIN-0593
Poster Session

Cerebral Hemorrhage/Subarahcnoid Hemorrhage (SAH)/Vasospasm

HYPOTHERMIA TREATMENT OF RAISED INTRACRANIAL PRESSURE IN A RAT MODEL OF INTRACEREBAL HEMORRHAGE

R. John[1], *F. Colbourne*[2]
[1]*Neuroscience, University of Alberta, Edmonton, Canada*
[2]*Psychology, University of Alberta, Edmonton, Canada*

Objective

Elevated intracranial pressure (ICP) is a potentially life-threatening complication after an intracerebral hemorrhagic stroke (ICH). Animal and clinical studies suggest that mild (~33ºC) hypothermia reduces ICP after ischemic stroke and traumatic brain injury[1]. In this study, we tested whether brain-selective cooling reduces the rise in ICP found in adult rats subjected to a large collagenase-induced ICH[2]. Localized cooling methods are expected to have fewer deleterious cardiovascular effects than whole body hypothermia (e.g. altered blood pressure). However, both cooling approaches can aggravate intraparenchymal bleeding even when administered many hours after collagenase infusion[3]. We avoided this complication by delaying treatment onset for 24 hours, and tested whether brain cooling reduced ICP after ICH, or the re-warming rate mattered. Finally, we assessed cerebral edema, as it is a key contributor to ICP.

Methods

All protocols followed Canadian Council of Animal Care Guidelines and were approved by the Biosciences Animal Care and Use Committee at the University of Alberta. In Experiment 1, telemetry blood pressure transmitters monitored ICP in the epidural space of 12 animals immediately after surgery until euthanasia on day 3 when edema was measured using the wet/dry weight method[2]. In Experiment 2, 24 animals were randomly assigned to either post-ICH: normothermia, hypothermia and instantaneous re-warming, or hypothermia and gradual re-warming (i.e. over 6 hours). Mild localized cooling (31-34°C) of the injured hemisphere was achieved as previously described by implanting a metal cooling device under the temporalis muscle[2]. ICP was monitored continuously after ICH until euthanasia on day 4 to assess edema.

Results

As we previously observed[2], severe ICH significantly elevated ICP for 3 days after ICH (~6 mmHg in sham animals versus ~17 mmHg in ICH-treated animals, p[FC1] (p>0.70). However, cooling reduced peak ICP after gradual re-warming (p=0.03; Figure 1B) on day 4. Large elevations in water content were observed after instantaneous re-warming (p=0.01), but this did not predict ICP.

Conclusions

In summary, 24-hour delayed cooling reduced ICP but it did not appear to reduce edema. On the contrary, fast re-warming increased edema on day 4, but this did not noticeable affect ICP responses. Furthermore, these findings and earlier work suggest that cooling loses its ability to mitigate edema as intervention delays increase (and edema sets in)[4]. If so, a therapeutic goal is to intervene as quickly as possible, as with ischemia, but not so quickly as to aggravate bleeding and thereby worsen outcome after ICH. Further pre-clinical work is needed to provide better insight into cerebral pressure management, and optimize the effectiveness of therapeutic temperature management strategies.

References

1. Kollmar et al. *Crit Care*. 2012;16:A2.
2. Hiployee and Colbourne. *Exp Neurol*. 2014;255:49-55.
3. John et al. *THTM*. 2014;In Press.

4. Yenari and Hemmen. *Stroke*. 2010;41:S72–S74.

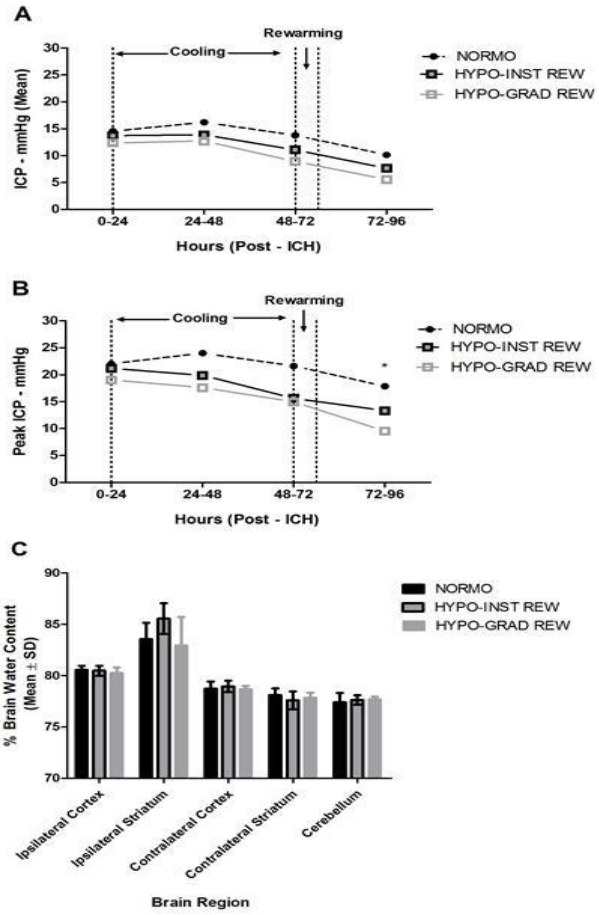

Figure 1.

500

BRAIN-0763

Poster Session

Cerebral Hemorrhage/Subarahcnoid Hemorrhage (SAH)/Vasospasm

POST-HEMORRHAGIC HYDROCEPHALUS AFTER GERMINAL MATRIX INTRAVENTRICULAR HEMORRHAGE: FIRST RESULTS FROM A NEW IVH-MODEL IN ONE DAY RAT PUPS

O. Kempski[1], A. Hashemi[2], B. Alessandri[1], M. Terekov[3], A. Unterberg[2]

[1]Inst. Neurosurgical Pathophysiology, University Medical Center, Mainz, Germany

[2]Dept. Neurosurgery, University Heidelberg, Heidelberg, Germany

[3]Dept. Radiology, University Medical Center, Mainz, Germany

Objective: 50 percent of pre-term infants which are born before 31st gestation week are prone to a germinal matrix intraventricular hemorrhage (GM-IVH). As a consequence pathologies such as post-hemorrhagic hydrocephalus (PHH), ventriculomegaly, leukomalacia and peri-ventricular infarcts may develop leading to functional and cognitive disabilities. The pathophysiological mechanisms for these secondary injuries, however, are poorly understood. In contrast to other published PHH models we tried to establish a model using P1/P2 old rat pups in order to be as close to pre-term infants in respect to brain development.

Methods: 30 Newborn Sprague-Dawley rats at the age of P1-P2 (5-7 g body weight) were used to induce an IVH. Under deep isoflurane anesthesia (max. duration 25 min) pups were fixed in a stereotaxic frame. The skull was disinfected and a small burr hole was prepared at AP= 1 mm and ML= 1 mm. Homologous, venous blood was withdrawn from an adult, female rat. A 26G needle was connected to a micropump, filled with blood and lowered to a depth of 3 mm. A volume of 15, 25 or 50 µl blood was infused at an infusion rate of 25 µl/min. Thereafter, the intraventricular needle was left in place for additional minutes and carefully removed. The burr hole was sealed off using tissue glue. All pups were transferred to their appropriate cage. To examine the position of the blood volume MRT and histology were performed on the day of IVH. To analyze PHH development additional MRTs and histology followed between day 7-21 after IVH. Some of these animals (n=20) were also tested for behavioral deficits (Rotarod, forelimb strength on a beam, exit from a circle).

Results: MRT and histology analysis on the day of IVH showed correct placement of infused blood. All animals receiving 50 µl blood developed a PHH, whereas only 30% of animals receiving 25 µl showed a PHH. Animals injected with 25 µl (n=5) and 50 µl blood (n=6) remained significantly shorter on the Rotarod (48.6 s, 55.5 s) when compared to NaCl-injected animals (n=4; 115.6 s). Forelimb strength was also reduced by 25 µl (61.0 s) and 50 µl (31.0 s) in comparison to the control

group (189 s). Time to exit a circle was not affected significantly.

Conclusion: Our results show that an IVH could be induced reliably in P1/P2 young rat pups and that a PHH always developed using 50 µl blood. The IVH also induced behavioral deficits. Thus, this model of pre-term infants will be useful to study pathophysiological mechanisms which correlate to behavioral and histological deficits.

501
BRAIN-0240
Poster Session

Cerebral Hemorrhage/Subarahcnoid Hemorrhage (SAH)/Vasospasm

THERAPEUTIC HYPOTHERMIA REDUCES SEIZURE ACTIVITY AFTER INTRACEREBRAL HEMORRHAGE IN RATS

A.C. Klahr[1], C.T. Dickson[2], F. Colbourne[2]
[1]Centre for Neuroscience, University of Alberta, Edmonton, Canada
[2]Centre for Neuroscience and Department of Psychology, University of Alberta, Edmonton, Canada

Objectives: Seizures are a common complication after intracerebral hemorrhage (ICH)[1]. While they are undesirable, it is not known whether they contribute to brain injury. Recently, we found that the collagenase model of striatal ICH causes seizures in 66% of rats[2], making it an appropriate model to study the impact of anti-epileptic drugs as well as neuroprotective treatments on seizure activity after ICH. Therapeutic hypothermia (TH), reducing brain temperature to ~ 33°C, has been studied for decades to treat various brain insults[3]. In ICH patients, cooling appears to reduce edema and improve neurological outcome[4], results that were predicted from animal models[3]. In the current study, we hypothesized that TH reduces seizure activity after ICH in rats.

Methods: All procedures were in accordance with the Canadian Council on Animal Care and were approved by the Biosciences Animal Care and Use Committee at the University of Alberta. Rats were implanted with a telemetry probe that records electroencephalographic (EEG) activity, and were given an intra-striatal injection of bacterial collagenase, which subsequently causes bleeding[2]. As well, a cooling device was attached to the affected side of the skull. Rats were then randomized to receive unilateral TH (HYPO; N=12) or normothermia (NORMO; N= 11) for 48 hours beginning 6 hours after collagenase-induced ICH. Rats' EEG activity from both the ipsi- and contralesional sides was recorded for 14 days after the stroke, and visualized for analysis[2]. Rats were euthanized at 14 days.

Results: Confirming our recent report[2], we observed that 63% (7/11) of NORMO rats experienced seizures (see figure for seizure example). Cooling reduced the number of rats undergoing seizure activity to 33% (4/12) although this did not reach significance (p=0.220). Seizure activity started between 5 and 27 hours post-ICH, and could be detected up to 5 days after the stroke. The number of seizures, which varied considerably from 3 to 60 episodes, was reduced by 66% in the HYPO group but it was not statistically significant (NORMO: M= 16.3; HYPO: M= 7.16, p=0.224; Figure 3). Duration of time spent in seizure activity, power, and coherence analyses are being performed. The present findings suggest that cooling will have a large impact on seizure activity in the days following an ICH. At present, however, additional animals (total = 24 / group) are being added to reach 80% power to detect a 50% reduction in seizure incidence, our primary endpoint.

Conclusions: Our preliminary results suggest that hypothermia has the potential to reduce seizure activity after ICH, which agrees with data in models of ischemic and traumatic brain damage. Further study is needed to evaluate how this ultimately affects cell death and functional recovery, but it suggests that this is a new means by which hypothermia would confer neuroprotection.

References:

1. Balami and Buchan. Lancet Neurol. 2011;11:101-118

2. Klahr et al. Transl Stroke Res. 2015;6:29-38
3. MacLellan et al. J Neurotrauma. 2009;26:313-323
4. Kollmar et al., Stroke. 2010;41:1684-1689

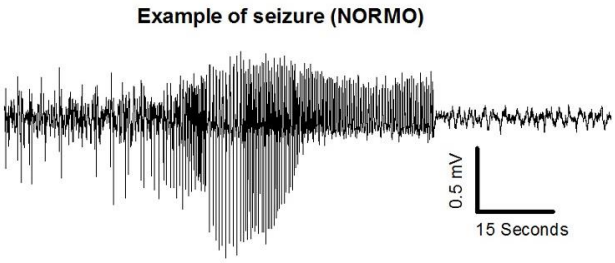

502
BRAIN-0536
Poster Session

Cerebral Hemorrhage/Subarahcnoid Hemorrhage (SAH)/Vasospasm

CHANGES OF CORTICAL PERFUSION IN EARLY PHASE OF SUBARACHNOID BLEEDING IN A RAT MODEL AND THE EFFECT OF DECOMPRESSIVE CRANIECTOMY – DOES SIZE MATTER? (PRELIMINARY RESULTS)

M. Kolar[1], K. Nohejlova[2], J. Polach[2], J. Mares[2], J. Pachl[1]
[1]Dept. of Anesthesiology and Critical Care, Charles University 3rd Faculty of Medicine, Prague 10, Czech Republic
[2]Dept. of Normal Pathological and Clinical Physiol ogy, Charles University 3rd Faculty of Medicine, Prague 10, Czech Republic

Objectives: To describe immediate perfusion changes after subarachnoid hemorrhage (SAH) and assess the effect of decompressive craniectomy (DC) in a rat model.

Material and Methods:

SAH induction: Male Wistar rats (180–220 g) were used in the experiment. Study animals were assigned into 3 groups: SAH animals (n = 10), animals with SAH + bi-parietal craniectomy (bi-P group, n = 8), animals with SAH + bi-fronto-temporo-parietal craniectomy plus durotomy (bi-FTP group, n = 4). SAH was modeled by injection of arterial blood into the prechiasmatic cistern. All animals received 200 microL of fresh allogenic non-heparinized blood. In groups receiving DC, the craniectomy was performed prior to SAH induction. The bi-parietal craniectomy was done by circular trepanation (diameter 3,3 mm), bi-fronto-temporo-parietal craniectomy was done by removal of skull bones in the area approximately 5 x 10 mm.

Brain perfusion measurement: Laser Speckle Contrast Analysis (PeriCam PSI HR, Perimed, Sweden) was used to measure perfusion. Changes of perfusion were recorded for 30 min/animal during and immediately after induction of SAH. The data were analysed by original software (PIMsoft, Perimed, Sweden). The baseline perfusion before SAH induction was used as reference value. The relative change of perfusion (in % of baseline values) was recorded. Results were accepted as significantly different when $p < 0.05$.

Results: In SAH group the intracisternal injection of blood led to significant decrease in cortex perfusion comparing to resting values (p

Conclusions: In SAH animals without craniectomy, administration of arterial blood into perchiasmatic cistern leads to prolonged reduction of blood flow in the brain cortex. These changes show a biphasic pattern – after a recovery towards baseline between approx. 10 – 15 min, another period of hypoperfusion follows. Neither bi-parietal nor large bi-fronto-temporo-parietal decompressive craniectomy improved the hypoperfusion after SAH. This finding suggest that vasoconstrictive effect of arterial blood plays more important role in early brain injury than increased intracranial pressure. Preliminary results also suggest that the large bi-fronto-temporo-parietal decompression can have even deleterious effect on the perfusion in the early phase.Support: IGA NT 14426-3/2013, 260045/SVV/2014, CSM7/CRP/2014

503
BRAIN-0206
Poster Session

Cerebral Hemorrhage/Subarahcnoid Hemorrhage (SAH)/Vasospasm

EDARAVONE (MCI-186) ALLEVIATES ACUTE BRAIN INJURY AFTER SUBARACHNOID HEMORRHAGE IN RATS

K. Niizuma[1], A. Ito[1], T. Sasaki[1], M. Fujimura[1], P.H. Chan[2], T. Tominaga[1]
[1]Department of Neurosurgery, Tohoku University Graduate School of Medicine, Sendai, Japan
[2]Department of Neurosurgery Department of Neurology and Neurological Sciences and Program in Neurosciences, Stanford University School of Medicine, Stanford, USA

Objectives: subarachnoid hemorrhage (SAH) results in a high mortality rate, despite sophisticated medical management and neurosurgical techniques. Although few studies had targeted on acute brain injury after SAH, recent studies have emphasized the importance of acute brain injury after SAH, in which apoptosis plays major roles.[1] Our group demonstrated that a reduction in oxidative stress by copper/zinc-superoxide dismutase (SOD-1) overexpression attenuates acute brain injury after SAH through phospho-Akt (pAkt) and phospho-glycogen synthase kinase-3β (pGSK-3β) upregulation, which are survival signals in apoptotic cell death.[2,3] We hypothesize that oxidative stress play a major role in Akt/GSK-3β signaling that may control neuronal death/survival after SAH. The purpose of this study is to determine whether a drug approach is effective in alleviating acute brain injury after SAH.

Methods: Edaravone (MCI-186), which is a free radical scavenger used clinically for human cerebral infarction, was used as an anti-oxidant. SAH was induced by endovascular perforation[4,5] in edaravone-treated and vehicle-treated rats. One, 6 and 24 h after SAH, samples were taken and used for apoptotic cell death assay, hydroethidine for superoxide radical study, western blot or immunohistochemistry.

Results: Apoptotic cell death at 24 h, detected by a cell death assay, significantly decreased in the cerebral cortex of the edaravone-treated rats compared with the vehicle-treated rats (Graph). A hydroethidine study revealed that superoxide anion production after SAH was reduced in the cerebral cortex of the edaravone-treated rats. Moreover, Western blot analysis and immunohistochemistry showed that pAkt and pGSK-3β, was upregulated in the cerebral cortex of the edaravone-treated rats. In contrast, cytochrome *c* release decreased in the cerebral cortex of the edaravone-treated rats.

Conclusions: Edaravone alleviated acute brain injury after SAH through uplegulation of pAkt and pGSK-3β. We propose that edaravone can be used as a treatment against acute brain injury after SAH.

References:

1. Matz PG, Fujimura M, Chan PH (2000) Subarachnoid hemolysate produces DNA fragmentation in a pattern similar to apoptosis in mouse brain. *Brain Res* 858:312-319.

2. Endo H, Nito C, Kamada H, Yu F, Chan PH (2006) Akt/GSK3b survival signaling is involved in acute brain injury after subarachnoid hemorrhage in rats. *Stroke* 37:2140-2146.

3. Endo H, Nito C, Kamada H, Yu F, Chan PH (2007) Reduction in oxidative stress by superoxide dismutase overexpression attenuates acute brain injury after subarachnoid hemorrhage via activation of Akt/glycogen synthase kinase-3b survival signaling. *J Cereb Blood Flow Metab* 27:975-982.

4. Bederson JB, Germano IM, Guarino L (1995) Cortical blood flow and cerebral perfusion pressure in a new noncraniotomy model of subarachnoid hemorrhage in the rat. *Stroke* 26:1086-1091.

5. Kamii H, Kato I, Kinouchi H, Chan PH, Epstein CJ, Akabane A, Okamoto H, Yoshimoto T (1999) Amelioration of vasospasm after subarachnoid hemorrhage in transgenic mice overexpressing CuZn-superoxide dismutase. *Stroke* 30:867-871.

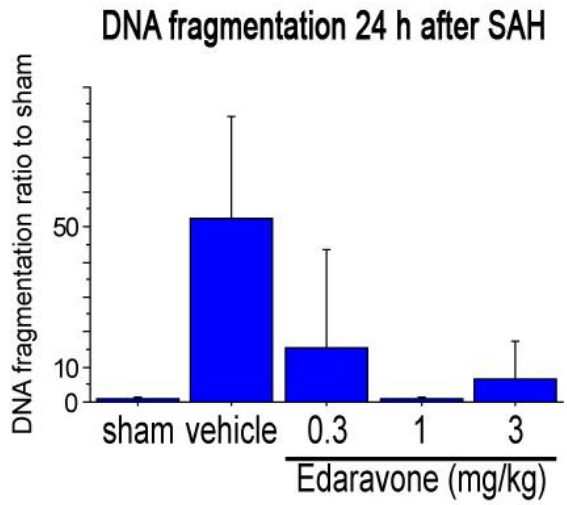

504
BRAIN-0301
Poster Session

Cerebral Hemorrhage/Subarahcnoid Hemorrhage (SAH)/Vasospasm

SPREADING INJURY DEPOLARIZATIONS AND THE INTERFACE BETWEEN SUBARACHNOID HEMORRHAGE AND CEREBRAL ISCHEMIA

F. Oka[1], S.P. Chen[1], U. Hoffmann[1], J.H. Lee[1], K.P. Hopson[1], I. Yuzawa[1], T. Qin[1], C. Ayata[2]
[1]Radiology, Massachusetts General Hospital, Charlestown, USA
[2]Radiology and Neurology, Massachusetts General Hospital, Charlestown, USA

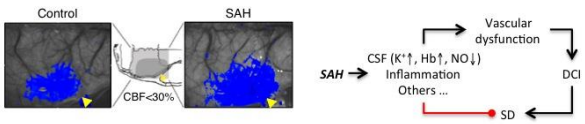

Objectives:

Delayed focal cerebral ischemia (DCI) is a devastating complication of aneurysmal subarachnoid hemorrhage (SAH). Cortical spreading depolarizations (CSDs) occur after SAH, and are thought to cause DCI. We, therefore, aimed to characterize CSDs in animal models of SAH, and establish the direction of causality.

Methods:

Mice (C57BL/6, male) and rats (Sprague-Dawley, male) were used. SAH was achieved by injecting non-heparinized arterial blood (vs. saline) into the pre-chiasmatic cistern or the cisterna magna. Cortical electrophysiology, laser Doppler (LDF) or speckle flowmetry (LSF), myogenic tone measurements in isolated cerebral arteries, and transient focal ischemic (middle cerebral artery occlusion; MCAO) outcome assessments were performed after SAH.

Results:

Unlike human SAH, spontaneous CSD was never detected in mice when monitored for up to 6h starting 3h, 12h or 72h after SAH in mice (n=15) or rats (n=3). Indeed, susceptibility to KCl- or electrical stimulation-induced CSDs was significantly reduced 12h or 72h after SAH in mice (n=27), and 5d after SAH in rats (n=12). Similarly, spontaneous peri-infarct CSD frequency strongly tended to be reduced after filament MCAO when induced 12h after SAH in mice (n=13). Nevertheless, filament MCAO still caused more severe neurological deficits and 60% larger infarcts when induced 12h after SAH in mice (n=27). Worse outcomes were linked to two-fold larger perfusion defects as shown by LSF during distal MCAO in mice (n=29) suggesting severe vascular dysfunction compromising collateral flow. Consistent with this, increased myogenic tone was found in posterior cerebral arteries isolated from mice 12h after SAH (n=13). However, blood flow response to individual CSDs in non-ischemic brain was not significantly altered when measured by LSF 12h, 72h or 10d after SAH in mice (n=20), or when measured by LDF 5d after SAH in rats (n=12), when corrected for reduced resting (i.e., baseline) CBF levels after SAH. All

results were irrespective of SAH model (i.e., pre-chiasmatic vs. cisterna magna injection) when compared side by side.

Conclusions:

Our data suggest that SAH reduces intrinsic susceptibility of brain tissue to CSD, but renders cerebral vasculature dysfunctional, thereby increasing the severity of ischemia upon focal arterial occlusion. We propose that the origin of CSDs frequently detected in human brain after SAH is ischemia caused by focal perfusion defects secondary to large, medium or microvascular dysfunction. Therefore, DCI may be the cause of CSDs in SAH, rather than their consequence. In other words, ischemia may be required for CSDs to occur after SAH. Once triggered, CSDs can still impact the outcome by worsening DCI and supply-demand mismatch.

505
BRAIN-0491
Poster Session

Cerebral Hemorrhage/Subarahcnoid Hemorrhage (SAH)/Vasospasm

COGNITIVE DYSFUNCTION IN A PRE-CHIASMATIC CISTERN BLOOD INJECTION MODEL OF ANEURYSMAL SUBARACHNOID HEMORRHAGE IN MICE

F. Oka[1], Y.B. Atalay[1], T. Qin[1], C. Ayata[2]
[1]Radiology, Massachusetts General Hospital, Charlestown, USA
[2]Radiology and Neurology, Massachusetts General Hospital, Charlestown, USA

Objectives:

Majority of aneurysmal subarachnoid hemorrhage (SAH) survivors develop cognitive dysfunction. To better understand the underlying mechanisms and develop treatments, predictive animal models are required. We carried out a detailed physiological and cognitive characterization of pre-chiasmatic cistern (PC) and cisterna magna (CM) SAH models in mice.

Methods:

SAH was induced by arterial blood injection into the PC (40 µl) or CM (60 µl) in C57BL6/J mice (male, 25g). Controls received normal saline. Cerebral blood flow (CBF) was imaged using laser speckle flowmetry during and for 60 min after SAH. Intracranial pressure (ICP) and blood pressure (BP) were monitored to calculate cerebral perfusion pressure (CPP). Neurological and cognitive function was assessed 3 weeks after the injection, using pole, novel object recognition, Y maze and Morris water maze tests.

Results:

In both groups, CPP decreased from about 65 mmHg to less than 10 mmHg immediately after the injection, and recovered to 40 mmHg within 10 min after PC (n=8) and 7 min after CM (n=8) SAH (Fig A). In both groups, CBF was severely reduced to ~20% of baseline in both hemispheres immediately after SAH. CBF recovered to >40% within 5 min after PC and 2 min after CM SAH (Fig A). In saline controls (n=5 in PC and CM each), CPP and CBF changes were much milder and shorter-lasting. Compared with controls (n=12), PC SAH mice (n=12) performed significantly worse in a subset of sensorimotor and cognitive tests for up to 3 weeks (Fig B). CM SAH did not significantly impact neurological function.

Conclusions:

Pre-chiasmatic cistern but not cisterna magna SAH model reproduces cognitive dysfunction observed in patients with low mortality and high

reproducibility in mice.

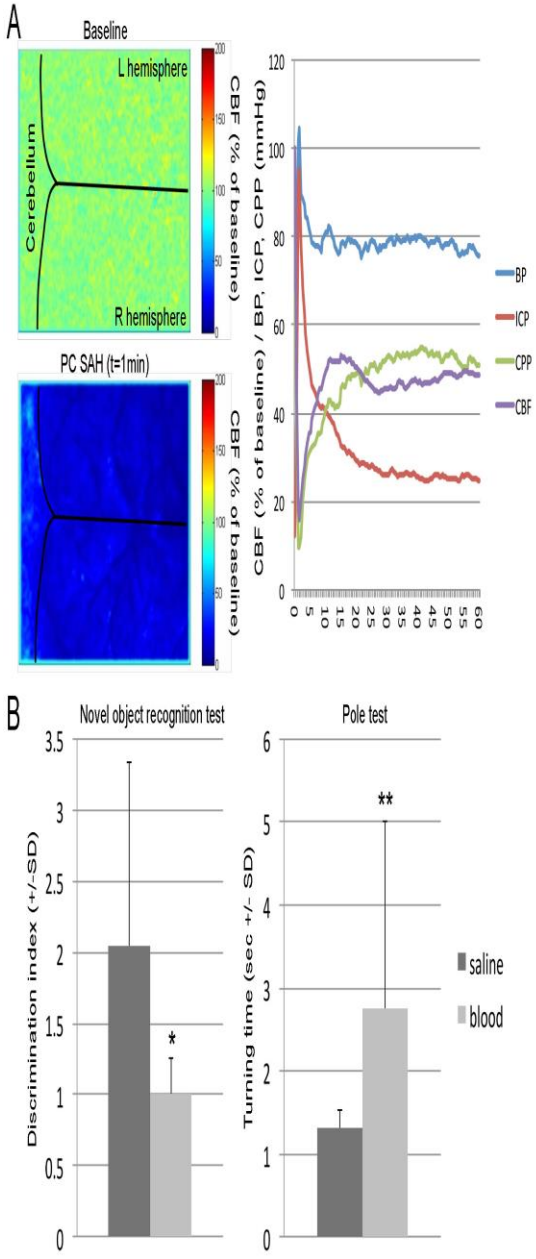

506
BRAIN-0612
Poster Session

Cerebral Hemorrhage/Subarahcnoid Hemorrhage (SAH)/Vasospasm

PATHOLOGICAL CHANGES IN THE REGULATION OF CEREBRAL BLOOD FLOW IN ADULT AND NEWBORN RATS UNDER STRESS-INDUCING HEMORRHAGIC STROKE

O. Sindeeva[1]
[1]*Biology, Saratov State University, Saratov, Russia*

Objectives: Neonatal stroke is very relevant problem in medicine now, because of the stroke after-effects: morbidity, neurological and cognitive deficits [1]. In adults most frequent form of the stroke is ischemic, while in newborns - hemorrhagic stroke (HS). Development mechanisms of these diseases are different. The lack of information in this area makes diagnostic criteria of HS appearance in newborns and treatment methods development impossible.

Methods: To induce HS, conscious adult (n=36) and newborn (n=36) rats were underwent to harmful effect of sound stress. Before 7 weeks of stressing silver clips were implanted on the left renal artery of adult rats to create hypertension, since they are more resistant to the damaging effect of sound. The control group included intact adult (n=36) and newborn (n=36) rats. The mechanisms of pathological changes in the brain were studied on the next day after stressing, using laser-speckle imaging, coherent tomography, immunohistochemical analysis, biochemical and pharmacologic tests.

Results: HS was accompanied by progressive sagittal vein dilatation in adult and newborn animals. Vascular tone is predominantly controlled by adrenergic and NO-dependent systems. In normal case phenylephrine (2,5 mkg/kg, iv) - stimulator of α1-adpenoreceptors, caused blood velocity increasing in adult rats, which was higher than in newborns. But after injection, blood velocity of adult rats with HS was lower than basal level. In newborns reaction was

not observed. In the next step, we used isoproterenol (0,05 mkg/kg, iv) – stimulant of β2-adpenoreceptors. In healthy rats, regardless of age, injection caused blood velocity decrease in sagittal vein, dilatation was more expressed in newborn rats. In newborns with HS after injection blood velocity decreased more, than in healthy. In adult rats reaction was not observed.

There was no significant differs in NO production within healthy groups of adults and newborn rats. Development of HS is connected with NO production and iNOS activity increase in such tissues as brain cortex, hypothalamus, cerebellum, brainstem, blood only in adult rats. Injection of non-specific NO-synthase blocker - L-NAME (10 mg/kg, iv) was accompanied by falling blood velocity in cerebral arteries of adult animals; after HS velocity decrease was higher. Newborn rats showed no reaction on L-NAME in both cases (healthy and with HS).

Conclusion: HS in adults and newborns characterizes by progressing sagittal vein dilatation, that leads to vein insufficiency and decrease of venous outflow in brain. Pathological changes in cerebral venous blood flow after stress-induced HS are largely provided by adrenergic vasoconstriction mechanisms in adult rats and high activity of adrenergic vasodilation mechanisms in newborn rats. HS development is accompanied by NO hyperproduction with elevation of iNOS expression in adult rats, but not in newborns. Insensivity to NO-synthase blocker in newborn rats also indicates immaturity of NO-dependent endothelial mechanisms.

The research supported by grants № 14-15-00128, МД-2216.2014.4, 14-02-00526-а.

References:

1. Beslow L.A. at all. Predictors of outcome in childhood intracerebral hemorrhage: A prospective consecutive cohort study // Stroke. – 2010. – Vol. 41. – P. 313–318.

507
BRAIN-0545
Poster Session

Cerebral Hemorrhage/Subarahcnoid Hemorrhage (SAH)/Vasospasm

EARLY BRAIN INJURY IN SUBARACHNOID HEMORRHAGE: AN MRI STUDY ON HEMODYNAMIC CHARACTERIZATION

Y. Sun[1], Q. Shen[2], L. Watts[2], E. Muir[2], S. Huang[2], G.Y. Yang[3], T. Duong[2]
[1]Department of Neurosurgery, Ruijin Hospital Shanghai Jiao Tong University School of Medicine, Shanghai, China
[2]Research Imaging Institute, The University of Texas Health Science Center at San Antonio, San Antonio, USA
[3]Neuroscience and Neuroengineering Research Center, Med-X Research Institute Shanghai Jiao Tong University School of Medicine, Shanghai, China

Objectives

Subarachnoid hemorrhage (SAH) is a medical emergency and occurs in 5% of all stroke cases [1]. Much has been learned about the delayed vasospasm and cerebral ischemia of SAH, but two-thirds of deaths occur within 48 hrs [2], and less is known about the mechanisms of brain injury during this early period. Magnetic resonance imaging has the unique ability for noninvasive, longitudinal assessment of early brain injury but has not been widely utilized in subarachnoid hemorrhage (SAH). Additionally, the hemodynamic changes underlying SAH remain uncertain.

Methods

To address these issues, we used a multimodal approach by measuring cerebral blood flow, blood oxygenation-level-dependent (BOLD) responses, magnetic resonance angiography (MRA), and magnetic resonance venography (MRV) changes using an 11.7-T MRI scanner. Blood or artificial cerebral-spinal fluid (ACSF) was injected into the cisterna magna to induce SAH or

mimic SAH associated intracranial hypertension. Hemodynamic changes were evaluated before and after SAH establishment.

Results

1) Transient CBF decreases were observed after blood or ACSF injection. Autoregulation was intact in control animals with ACSF injection. In contrast, hypercapnic challenge CBF response in the SAH group decreased significantly and showed transient significant differences from the control (p<0.05). It reveals that SAH impairs both basal CBF and autoregulation during the acute phase. 2) No changes in the arteries were observed after 3h (p>0.05). While basal CBF and autoregulation remained lower level at the period of 2 - 3 hrs following SAH, the cerebral artery constriction has already recovered. This implies that SAH induced transient cerebral vasospasm is not essential for hypoperfusion 3) At 3 hrs and 2 days, vein dilation could be detected in the cortex compared to control animals (p<0.05), indicative of additional effects of blood-induced vein dilation.

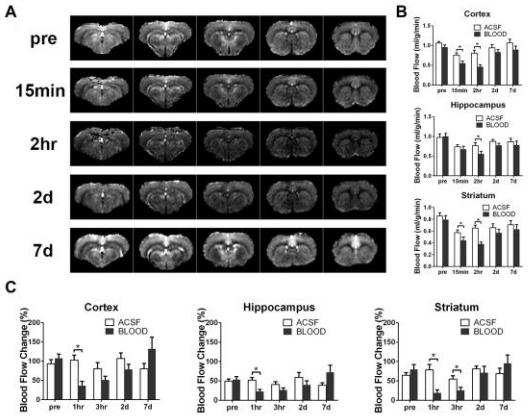

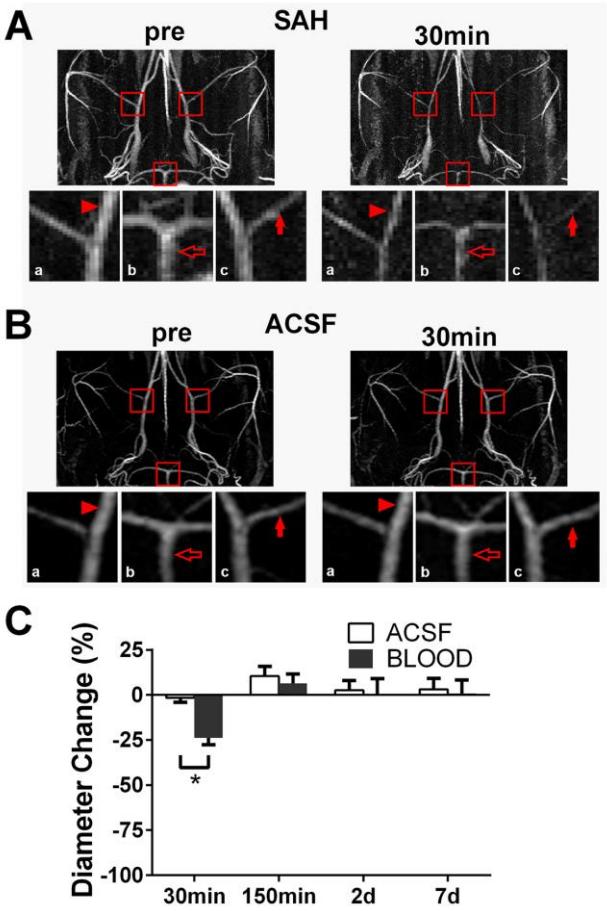

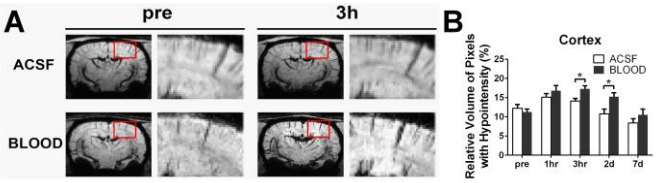

Conclusions

The multimodal functional imaging findings support the hypothesis that hemodynamic responses are dominated by neurovascular coupling and phlebectasia, rather than blood irritated artery constriction. MRI offers a means to probe the attributes of the cerebral vein when being insulted, provide novel insights into the autoregulation and neurovascular coupling in SAH, and the exploration of therapeutic targets aimed at early brain injury.

References

1. Suarez, J.I., R.W. Tarr, and W.R. Selman, *Aneurysmal subarachnoid hemorrhage.* N Engl J Med, 2006. **354**(4): p. 387-96.

2. Schievink, W.I., et al., *Sudden death from aneurysmal subarachnoid hemorrhage.* Neurology, 1995. **45**(5): p. 871-4.

508
BRAIN-0079
Poster Session

Cerebral Hemorrhage/Subarahcnoid Hemorrhage (SAH)/Vasospasm

INHIBITION OF ENDOTHELIN-1-RECEPTORS (ET-A-RECEPTOR) DOES NOT INFLUENCE MICROVASOSPASM AND NEUROLOGICAL OUTCOME AFTER EXPERIMENTAL SUBARACHNOID HEMORRHAGE

N. Terpolilli[1], A. Dienel[1], N. Heumos[2], K. Schöller[1], N. Plesnila[2]
[1]Neurosurgery, Ludwigs-Maximilians-Universität, München, Germany
[2]Institute for Stroke and Dementia Research, Ludwigs-Maximilians-Universität, München, Germany

Objective

Subarachnoid hemorrhage (SAH) is a devastating subtype of stroke with high mortality and morbidity. For decades spasms of large cerebral vessels occurring later than five days after SAH were believed to be the main factor ischemic deficits and, thus, for bad outcome of SAH patients. Recently, however, clinical and experimental data suggest that long-lasting spasms of the cerebral microcirculation developing within the first few hours after SAH may be an important factor contributing to post-hemorrhagic brain injury and delayed ischemia. So far, however, the etiology of this microcirculatory dysfunction is largely unknown. Among others, overabundance of vasoconstrictors like Endothelin-1 (ET-1) is a putative mechanism of cerebrovascular microvasospasm. The aim of the current study was to assess the impact of an ET-1 receptor antagonist on microcirculatory dysfunction and outcome after experimental SAH.

Methods

We performed a dose finding study using the ET-A-receptor antagonist Clazosentan at different i.v. doses and evaluated possible side effects of the drug. SAH was induced by the MCA filament perforation model in C57BL/6 mice. 3 hours after SAH the cerebral microcirculation was studied before, during, and after i.v. Clazosentan application (10mg/kg/min) using epifluorescence intravital microscopy (with FITC dextran). In a second part of the study neurological outcome (measured by multivariate neurological score) and brain edema formation (brain water content) were evaluated up to 3 days after SAH with or without Clazosentan treatment.

Results

Clazosentan did not influence MAP, ICP, and CBF when given at 1, 3, or 10 mg/kg bodyweight, MAP tended to be lower at 20 mg/kg b.w. All further experiments were therefore conducted using 10 mg/kg b.w. Clazosentan did not reduce number and intensity of cerebral microvasospasms in the pial microcirculation. While ET-1 receptor inhibition showed a trend towards dilating larger arterioles (< 35 µm diameter), the diameter of smaller arterioles (10-35 µm) remained unchanged. Furthermore, the number of microvasospasms was not affected by ET-1 receptor blockade. Three days after SAH brain water content was significantly lower in Clazosentan-treated mice. However, functional outcome was not different to the control group.

Conclusion

ET-1 receptors do not seem to play a role in the formation of microarterial spasms early after SAH and their inhibition does not improve neurological outcome. The previously reported effect of Clazosentan on larger vessels was confirmed and may contribute to the reduction in brain edema

formation observed in this study. Further studies are needed in order to improve our understanding of the pathophysiology of microvasospasm formation.

509
BRAIN-0629
Poster Session

Cerebral Hemorrhage/Subarahcnoid Hemorrhage (SAH)/Vasospasm

CEREBRAL ARTERY VASOSPASM IN THE CANINE DOUBLE-HEMORRHAGE MODEL IS REVERSED BY ENDOVASCULAR RING BEAM IRRADIATION WITH AN ULTRAVIOLET LASER

B. Watson[1], C. Sadasivan[2], J.A. Solomon[3], R.W. Hurst[4]
[1]Neurology, University of Miami Miller School of Medicine, Miami, USA
[2]Department of Neurological Surgery, Stony Brook University, Stony Brook, USA
[3]Veterinary Interventional Radiology, Infiniti Medical, Menlo Park, USA
[4]Department of Radiology - Neuroradiology, Hospital of the University of Pennsylvania, Philadelphia, USA

Objective: To reverse basilar artery spasm in canines subjected to hemorrhagic stroke.

Methods: A standard double-hemorrhage model (1) was used in in 3 mongrel dogs (22-29 kg) to induce vasospasm of the basilar artery (BA) documented angiographically (Siemens Angiostar). On Day 4, endovascular treatment was begun by emplacement of a 36° conical-tip optical fiber ensheathed in a microcatheter (Opus-14 system; OpusGen LLC, Doral, FL) in the vicinity of the BA origin, and the inner arterial wall was then irradiated with a ring-shaped beam of 355 nm ultraviolet laser irradiation (12-20 W/cm^2) pulsed at 7 KHz for 30 sec, while the optical path was cleared by saline flush. A new formula for ring beam intensity as a function of geometrical parameters and beam power was derived and utilized. BA diameters were calculated as full width at half-maximum of the angiographic grayscale intensity distribution plotted perpendicularly to the arterial wall, with BA edges determined by a semi-automated method (Matlab, Mathworks). Diameters were measured over three BA segments: proximal, medial, and distal. Statistical comparisons by ANOVA (Graphpad, Instat). The table shows BA segment diameters (mean±SD) as percentage of average baseline diameter. **Bold** font indicates statistical significance (ANOVA multiple comparison, $p<0.05$) compared to previous stage.

Results: By treatment day (Day 4), the proximal, medial and distal basilar artery segment diameters had significantly ($p<0.001$) constricted by 22±10% of the baseline. The UV irradiation dilated the segments essentially to their respective baseline values (94±14%) within 2-3 minutes. The dilation was still present at 24 hr follow-up (93±10%) (Dog 1 died later on Day 4 from uncontrollable femoral artery hemorrhage at the arteriogram puncture site); the diameters at 24 hr follow-up were not statistically different from baseline ($p>0.05$). The dilation extended up to 6 cm from the fiber-optic tip; the difference between the pre-treatment and post-treatment diameters was inversely correlated with distance from the fiber-tip (r =-0.77, p=0.027).

Animal/Segment	Pre-UV Treatment	Post-UV Treatment	24 hr Follow-up
Dog1/Medial	**92.4% (6.0%)**	**113.8% (3.6%)**	–
Dog1/Distal	**88.3% (4.9%)**	**116.2% (5.1%)**	–
Dog2/Proximal	**79.9% (8.4%)**	**102.0% (3.7%)**	101.3% (6.9%)
Dog2/Medial	**68.6% (7.8%)**	85.1% (6.6%)	93.9% (9.7%)
Dog2/Distal	**75.3% (3.5%)**	**81.6% (3.8%)**	85.1% (6.6%)
Dog3/Proximal	**75.8% (3.4%)**	**93.6% (5.3%)**	98.2% (4.5%)
Dog3/Medial	**76.1% (5.5%)**	84.6% (8.5%)	**97.3% (7.5%)**
Dog3/Distal	**71.3% (5.0%)**	78.8% (5.0%)	89.0% (5.5%)

Conclusions: Basilar artery vasospasm was mitigated by non-thermal endovascular irradiation with an ultraviolet laser. A possible mechanism is the release of nitric oxide via UV-mediated photophysical scission of nitrites in the arterial wall at electronic (non-thermal) state energies (2,3). We suggest this process restores that portion of smooth muscle cell nitric oxide scavenged by Hb infiltration (from lysed erythrocytes (4) into the arterial wall, and stimulates regeneration and propagation of dilation (5), which can reverse cerebral vasospasm locally while avoiding possible deleterious effects of systemic treatment.

References: (1) Varsos et al., J. Neurosurg. 58:11-17, 1983; (2) Rodriguez et al., PNAS 2003;100:336-341; (3) Watson et al., Stroke 33: 428-434, 2002.; (4) Zemke et al., Vasc. Med. 12: 243-249, 2007; (5) Nedospasov et al., PNAS 97:13543-13548, 2000.

510
BRAIN-0258
Poster Session

Cerebral Hemorrhage/Subarahcnoid Hemorrhage (SAH)/Vasospasm

PROGNOSTIC SIGNIFICANCE OF EXTENT OF EARLY CEREBRAL INFARCTION AFTER ANEURYSMAL SUBARACHNOID HEMORRHAGE

G.K. Wong[1]
[1]*Surgery, The Chinese University of Hong Kong, Hong Kong, Hong Kong China*

Background: Aneurysmal subarachnoid hemorrhage (SAH) is a serious disease with high case fatality and morbidity. Recently, early cerebral infarction was suggested as a risk factor for poor outcome.

Objectives: We aimed to assess the impact of extent of early cerebral infarction on outcomes of aneurysmal subarachnoid hemorrhage at three months.

Methods: We prospectively enrolled consecutive aneurysmal subarachnoid hemorrhage (SAH) patients presenting to an academic neurosurgical referral center (Prince of Wales Hospital, the Chinese University of Hong Kong) in Hong Kong. The study was approved by Joint CUHK-NTEC Clinical Research Ethics Committee. All images are reviewed by 2 blinded radiologists. Extent of cerebral infarction was the sum scores of the bilateral modified ASPECTS (Alberta Stroke Programme Early CT Score) and posterior circulation Acute Stroke Prognosis Early CT Score (pc-ASPECTS). A third radiologist adjudicator independently assessed the infarct extent when discrepancy arose among the 2 reviewers. Clinical outcome assessments were carried out 3 months after ictus by trained research assistants (psychology graduates) blinded to other clinical data.

Results: Cerebral infarction occurred in 24(48%) patients, in which 14(27%) patients had early cerebral infarction and 14(28%) patients had delayed cerebral infarction. In multivariable analyses, extent of early cerebral infarction correlated with CT Hijdra SAH Score (OR -0.06, 95%CI: -0.13 to 0.00, P=0.050) and predicted outcome at three months [modified Rankin Scale (OR 0.42, 95%CI: 0.19 to 0.65, P=0.001), Lawton Instrumental Activity of Daily Living (OR -1.61, 95%CI: -2.66 to -0.57, P=0.003), Mini-Mental State Examination (OR -2.29, 95%CI: -4.04 to -0.54, P=0.012), and Montreal Cognitive Assessment (OR -2.61, 95%CI: -4.31 to -0.91, P=0.004)].

Conclusions: Our data supported that early cerebral infarction was related to the severity of subarachnoid hemorrhage and had prognostic significance.

511
BRAIN-0386
Poster Session

Cerebral Hemorrhage/Subarahcnoid Hemorrhage (SAH)/Vasospasm

THE EFFECTS OF THERAPEUTIC HYPOTHERMIA ON HEMATOMA RESOLUTION AND IRON-INDUCED TOXICITY AFTER INTRACEREBRAL HEMORRHAGE

S. Wowk[1], Y. Ma[2], H. Nichol[3], F. Colbourne[2]
[1]Neuroscience, University of Alberta, Edmonton, Canada
[2]Psychology, University of Alberta, Edmonton, Canada
[3]Anatomy and Cell Biology, University of Saskatchewan, Saskatoon, Canada

Objectives: Therapeutic hypothermia (TH) is a promising treatment for large intracerebral hemorrhages (ICH) as clinical data show that it mitigates edema[1] and several mechanisms of secondary damage including blood brain barrier dysfunction and inflammation.[2] However, animal studies have not consistently found TH to reduce damage and improve behavioural deficits.[2] We suggest that negative side effects of TH may negate beneficial effects or TH may inadequately target key mechanisms of secondary injury. Specifically, we were concerned that the anti-inflammatory properties of TH may alter the spread of iron, hematoma resolution, and/or otherwise negatively affect iron-mediated injury.

Methods: Experimental procedures are in accordance with the Canadian Council of Animal Care and were approved by the Biological Science's Animal Care and Use committee. In all experiments, rats were randomized to either normothermia or whole-body TH (33°C), which was induced with a servo-regulated system (water mister, fan, and heat lamp). In experiments involving collagenase-induced ICH, TH was initiated after a 12 hour delay while in the $FeCl_2$ experiments TH was initiated after a 1 hour delay. In experiment 1, the spread of iron was evaluated 72 hours after ICH using synchrotron x-ray fluorescence imaging, which has the advantage of both spatially mapping and quantifying iron in tissue sections.[3] In experiment 2, the effect of TH on hematoma resolution was evaluated using a hemoglobin assay where rats were given an ICH and blood volume was assessed at 24 and 72 hours. For experiment 3, rats were euthanized 72 hours after ICH and levels of ferritin and heme oxygenase-1, proteins important in iron metabolism and hematoma resolution, were quantified. Finally in experiments 4 and 5, a striatal injection of $FeCl_2$ was used to isolate the effect of TH on iron-induced injury and behavioural deficits out to 7 and 28 days, respectively.

Results: By 3 days post-ICH iron had leached from the hematoma into peri-hematoma tissue declining as a function of distance ($r=0.333$, $p=0.007$), but TH does not influence this process ($p=0.825$). TH also does not affect the amount of blood at 24 or 72 hours compared to normothermia ($p\geq0.340$). After a $FeCl_2$ injection, TH did not mitigate behavioural deficits at either time ($p\geq0.1159$) nor was it neuroprotective at 7 days ($p=0.110$). We are currently evaluating levels of ferritin and heme oxygenase-1 and tissue loss at 28 days after $FeCl_2$ injection.

Conclusions: Presently, TH does not appear to influence hematoma resolution. Although TH reduces inflammation, this did not affect the spread of iron beyond the peri-hematoma or impair the degradation of blood (i.e., hemoglobin) by 3 days post-ICH. By assessing ferritin and heme oxygenase-1 levels, we will better understand whether TH impacts other mechanisms of iron metabolism and hematoma resolution. Finally, TH does not appear to target iron-induced damage. Thus, a combination of TH with an iron chelator may lead to a more effective neuroprotective therapy for ICH.

References:

1. Staykov et al. 2013 Neurocrit Care. 18:178.
2. MacLellan et al. 2006 Stroke. 37:1266.
3. Auriat et al. 2012. Exp Neurol. 234:136.

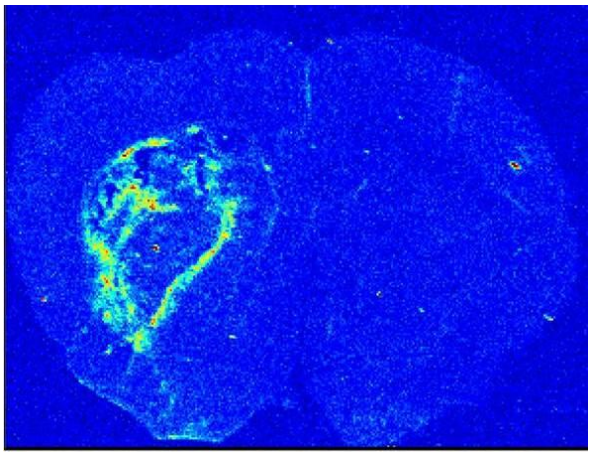

512
BRAIN-0552
Poster Session

Imaging Pre-Clinical

SHIFT AGENT ENHANCED 23NA-IMAGING IN THE LIVING BRAIN

A.A. Bajwa[1], A. Neubauer[2], L. Schilling[1]
[1]Division of Neurosurgical Research, University Medical Center Mannheim, Mannheim, Germany
[2]Computerassisted Clinical Medicine, University Medical Center Mannheim, Mannheim, Germany

Objective: Sodium (^{23}Na) plays a crucial role in cellular function. Recently, MRI-based methods have become available to measure the ^{23}Na signal *in vivo*. Unfortunately, conventional sequences yield the total tissue ^{23}Na content only. Currently the most reliable way to distinguish between the intra- and extracellular components of ^{23}Na is the use of shift reagents such as $Tm[DOTP]^{5-}$. This experimental approach has successfully been used in peripheral organs including the heart, the liver, and the kidney [1-3]. However, studies in the brain were not successful yet because $Tm[DOTP]^{5-}$ does not cross the intact BBB [4]. Here, we present a method to transiently open the blood-brain barrier (BBB) followed by loading the brain with $Tm[DOTP]^{5-}$.

Methods: Male Sprague Dawley rats were anesthetized with thiobutabarbital (15 mg/100 g body weight) and equipped with a tracheal cannula and catheters in the femoral artery (blood pressure monitoring, withdrawal of blood samples) and the left carotid artery for bolus injection of mannitol (25% solution, 1.5 ml over 45 sec) and infusion of $Tm[DOTP]^{5-}$ (80 mM solution, 6 ml over 60 min). At the end the observation period the blood was flushed from the vascular system and the Tm concentration measured in brain tissue samples using total reflection X-ray fluorescence analysis (T-XRF) methodology. MRI measurements were performed on a 94/20 Biospec scanner (Bruker) using a Hanning-weighted CSI sequence (parameters: TR, 50 ms; acquisition delay, 0.38 ms; number of scans, 14,340; FID sampling time, 400 ms). Each scan took 10 min. The spatial resolution was 1.7x1.7x1.6 mm3. A ^{1}H surface coil was employed to allow coregistration of the ^{1}H/^{23}Na signal for subsequent analyses in coronal sections of the brain selectively. A Fourier transform was applied to the FIDs and the resonance frequency determined. The chemical shift was determined in both hemispheres spectroscopically 30 and 60 min after start of $Tm[DOTP]^{5-}$ infusion (see figure).

Results: After bolus infusion of normotonic mannitol no $Tm[DOTP]^{5-}$ was detectable and the ^{23}Na signal did not change. Following opening of the BBB loading with $Tm[DOTP]^{5-}$ resulted in the ipsilateral hemisphere in an estimated extracellular concentration of 2.3±1.8 mM (mean±SD) and in a marked chemical shift in the spectroscopic analysis. The shifted peak was attributed to the extracellular ^{23}Na.

Conclusions: Despite high repellent properties of the BBB for $Tm[DOTP]^{5-}$ we successfully accumulated $Tm[DOTP]^{5-}$ in brain tissue high enough to induce a chemical shift. This approach for the first time allows distinction of the intra- and extracellular compartment of the ^{23}Na signal

in the living brain.

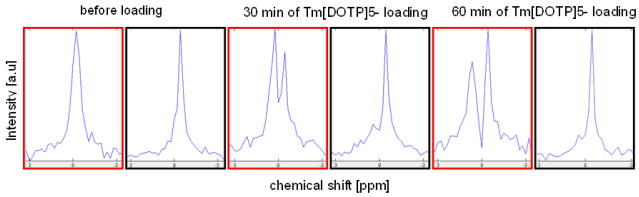

In vivo spectroscopic analysis in the perfused (red) and non-perfused (black) hemisphere

References

[1] Weidensteiner et al, Magn Reson Med. (2002) *48*, 89-96.
[2] Bansal et al, Biochemistry, (1993) *32*, 5638-5643.
[3] Seshan et al, Magn Reson Med. (1995) *34*, 25-31.
[4] Bansal et al, JMRI (1992) *2*, 385-391.

513
BRAIN-0100
Poster Session

Imaging Pre-Clinical

CEREBRAL BLOOD-FLOW IN NON-ANESTHETIZED RODENTS AS MEASURED BY ARTERIAL SPIN-LABELING MAGNETIC-RESONANCE IMAGING FOLLOWING ADMINISTRATION OF SEROTONINERGIC (5-HT2C) AGONISTS

S. Baker[1], K.U. Drescher[2], J. Lynch[1], P. Banfor[1], S. Mittelstadt[1], G. Fox[1], J. Beaver[1], A. Basso[1]
[1]ZR13, AbbVie, Chicago, USA
[2]0000262501, AbbVie, Chicago, USA

Changes in cerebral blood flow (CBF) have been associated with a number of diseases and conditions including aging, depression, Alzheimer's disease, and the maintenance of neuronal network integrity (1, 2, 3).

Objectives: The current study used arterial spin labelling (ASL) MRI to measure CBF in rodents following administration of 5-HT_{2C}selective agonists, vabicaserin and meta-chlorophenylpiperazine (mCPP), in non-anesthetized rodents. ASL measures a biological correlate for neuronal activity by quantitatively estimating CBF with comparable sensitivity to [^{15}O]H_2O positron emission tomography (PET), but uses no ionizing radiation, is non-invasive and not restricted by the necessity of an on-site cyclotron (4).

Methods: Male Sprague Dawley rats (300-350g; n=6-10/group) were used in the present experiment. MRI data was collected using a Bruker 70/30 Biospec magnet. The ASL protocol included a T1-weighted globally pulsed 3' flow-sensitive alternating inversion recovery-echo planar imaging (FAIR-EPI) pulse sequence and a 2mm selective-inversion pulse with coronal orientation in the middle of the brain parenchyma. A baseline acquisition was followed by additional acquisitions at 10 and 30 minutes post dose (i.p.) with vehicle (0.9% saline 1ml/kg); vabicaserin (30mg/ml/kg) or mCPP (3mg/ml/kg). Heart and respiration rates were continuously monitored during the scans. ASL data was processed with the Bruker-ParaVision ASL analysis software. Statistical significance was calculated with GraphPad Prism using a one-way ANOVA and Tukey's multiple comparison post-test. Telemetry data was collected using Dataquest A.R.T. acquisition and analysis system that allows monitoring physiologic data from conscious, freely moving animals.

Results: Compared to baseline, both vabicaserin and mCPP caused a significant CBF increase in specific brain regions at 10 minutes following the administration of 5HT2c compounds. At 30 minutes, a CBF increase still trended with both compounds although it was no longer significant. Neither vehicle, vabicaserin, nor mCPP caused a significant change in either heart or respiration rates for the duration of the ASL MRI scan, suggesting that CBF changes could be independent of systemic ones. Further, previous in-house BOLD fMRI following vabicaserin and mCPP administration showed a statistically significant increase in BOLD signal in cortical brain areas, implicit of increased neuronal activity. Previous in-house data with telemeterized rats showed vabicaserin (30mg/kg i.p.) to induce a significant decrease in heart-rate, and a

significant increase in mean arterial pressure (MAP), hemodynamic changes that lasted for about 6 h.

Conclusions: Pre-clinically, ASL-MRI data has translational potential to inform on how various factors such as age, disease or therapeutic intervention can affect CBF. The present study was able to measure CBF with ASL without the use of anesthesia. Administration of 5-HT_{2C} agonists increased CBF/ brain perfusion and are likely associated with changes neuronal activity. The lack of simultaneous changes on systemic measures, heart and respiration rates, suggest this could be a localized 5-HT_{2C} mediated effect. Motion is a major confound in ASL-MRI animal experiments. However, motion reducing anesthetics could have an independent effect on CBF (5), confounding interpretation of the data and reducing their translational potential. Future studies with 5-HT_{2C} selective antagonist blockade could be used to gauge the magnitude and selectivity of this effect.

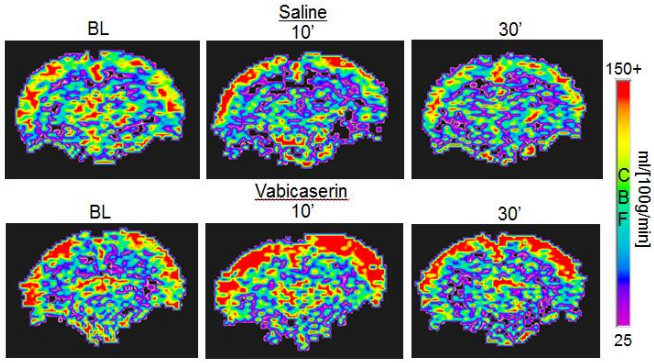

514
BRAIN-0034
Poster Session

Imaging Pre-Clinical

CLEARANCE OF THE BRAIN BY INTERSTITIAL DRAINAGE INTO THE VENTRICLES

B. Bedussi[1], M. van Lier[1], J. Bartstra[1], J. de Vos[1], M. Siebes[1], E. VanBavel[1], E. Bakker[1]
[1]Biomedical Engineering and Physics, Academic Medical Center University of Amsterdam, Netherlands

Objectives: Neurodegenerative pathologies, such as Alzheimer's disease and cerebral amyloid angiopathy, are associated with failure of amyloid-β removal that leads to its deposition along the brain vasculature. The aim of this study is to visualize the removal of tracers from the rodent brain, focusing on ventricular, subarachnoid and perivascular space (PVS) as possible transport pathways [1; 2].

Methods: We performed confocal fluorescence imaging of horizontal mouse brain sections after 30 min of controlled infusion of a mix of FITC-dextran (MW 500 kD) and Texas Red-dextran (MW 3 kD) into the cisterna magna (5 µL) or striatum (2 µL). Distribution of the dyes was analyzed for each injection site. In addition, we obtained 3D reconstructions of the mouse brain and vasculature, using an imaging cryomicrotome [3]..

Results: After infusion into the striatum, dyes spread in the parenchyma and found their way to the closest lateral ventricle. From there, they reached the ventricular system, cisterns and subarachnoid space (SAS). The 500 kD dye moved along intercellular spaces from the injection site to the ventricle. The 3 kD dextran followed the same direction, but was also taken up by parenchymal cells and the choroid plexus. Following cisterna magna infusion, dyes dispersed throughout the SAS, the cisterns and along the PVS. The high molecular weight dye remained confined to the SAS and PVS of cortical vessels, whereas the small dye also crossed the pia mater into the adjacent parenchyma. However, dyes could not be detected in the ventricular system, irrespective of molecular weight. In both groups, the signal in the SAS was stronger on the ventral side as compared to the dorsal side of the brain. Despite earlier reports [1; 2], there was no association of dyes with capillaries or veins in the parenchyma in either group. .

Conclusion: These data reveal a flow of interstitial fluid from the parenchyma to the ventricular system, from where dyes reach the SAS via the cerebrospinal fluid (CSF). Dyes disperse from the SAS along perivascular space, and partly reenter

the parenchyma. We speculate that this is a consequence of the strong mixing action of pulsations that are known to occur in the CSF. Failure in this transport pathway could hinder the physiological drainage of amyloid-β and play a role in the pathophysiology of Alzheimer's disease and cerebral amyloid angiopathy. .

References: .

1) Carare RO et al, Neuropathology and applied neurobiology. 2008;34(2):131-44.

2) Iliff JJ et al, Science translational medicine. 2012;4(147):147ra11. .

3) Spaan JA et al, Med Biol Eng Comput. 2005 Jul;43(4):431-5..

This project has received funding from the European Union's Seventh Framework Programme for research, technological development and demonstration under grant agreement no 606998.

515
BRAIN-0459
Poster Session

Imaging Pre-Clinical

MICRO-INFRACTS AS POTENTIAL WATERWAYS FOR BRAIN METASTASES

A. Benbenishty[1], *A. Lubart*[1], *P. Blinder*[1]
[1]*Neurobiology, Tel Aviv University, Tel-Aviv, Israel*

Brain metastases are prevalent in various types of cancer and are associated with poor prognosis, mostly due to the lack of efficient treatment. Thus, it is important to elucidate possible risk factors in an effort to decrease the frequency of brain metastases occurrence. Since malignant cells reach the brain via the blood stream, any changes in cerebral blood flow dynamics, vascular structure, and BBB permeability may affect the metastatic process in the brain. Therefore, micro-infracts, which alter these factors and are now reported to be predominant in the aging brain, represent a potential risk factor. To test this hypothesis, we set out to study whether, and how, micro-occlusions affect the capacity of brain metastasis occurrence.

We combine targeted photo-thrombotic occlusion of cortical vessel and injection of malignant cells. Using two-photon microscopy through a thinned-skull craniotomy, we longitudinally image blood flow dynamics and the metastatic process. We inject malignant cells to the internal carotid artery of mice following vessel occlusion using a novel method that avoids transient and permanent disruption of cerebral blood flow, and image and quantify the dynamics of the different steps of the metastatic process in the brain, including arrest, extravasation, and proliferation. Using histological methods we study metastasis-promoting changes in the microenvironment that result from the micro-infracts.

Occlusion of a single penetrating artery resulted in a transiently impaired blood-brain barrier and the formation of a permanent micro-infract, characterized by a necrotic lesion and astrogliosis. The lesion displayed a robust enhancement in infiltration and proliferation of malignant cells. Moreover, this phenomenon repeated itself in different time points of cancer cell injection.

Our results indicate that micro-infracts are a significant risk factor for brain metastasis in cancer patients. Recently introduced high resonance imaging (7T MRI) allows detecting micro-infracts and perhaps should be routinely used to monitor brains of cancer patients.

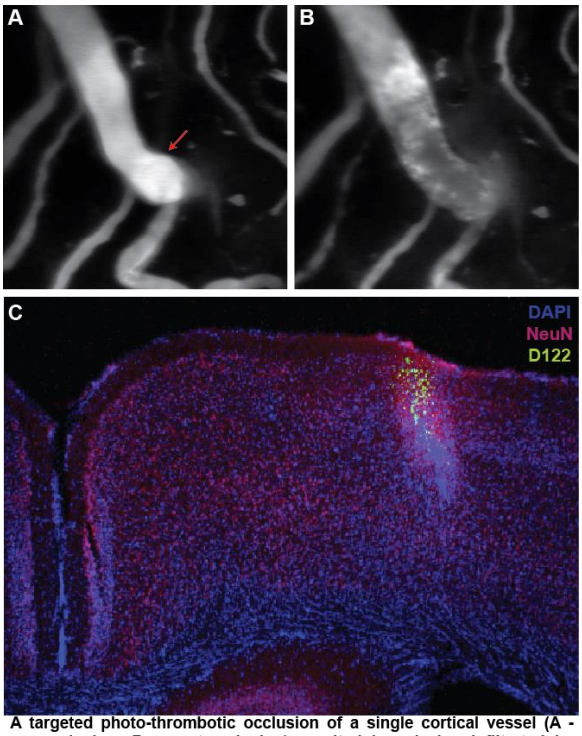

A targeted photo-thrombotic occlusion of a single cortical vessel (A - pre-occlusion; B - post-occlusion) resulted in a lesion infiltrated by malignant cells (C). C57BL/J6 mice were injected with FITC (5%;25µl;IV) for blood vessels two-photon imaging. Thereafter, they were injected with Rose Bengal (5%;50µl;IV) which was immediately photo activated with a 530nm laser (arrow in panel A). 72 hours post-occlusion mice were injected with D122-GFP cells to the internal carotid artery (10^5;100µl). 7 days post-injection, brains were perfused and fixed (4% PFA and 30% sucrose). 40µm slices were stained for DAPI and NeuN.

516
BRAIN-0815
Poster Session

Imaging Pre-Clinical

INFLUENCE OF LOW-FREQUENCY RTMS ON CORTICAL FUNCTIONAL CONNECTIVITY AND PERFUSION IN RATS

J. Boonzaier[1], G.A. van Tilborg[1], W.M. Otte[1], A.D. de Weijer[2], G. van Vliet[1], P. Petrov[3], S.F. Neggers[3], A. van der Toorn[1], R.M. Dijkhuizen[1]
[1]Biomedical MR Imaging and Spectroscopy Group, University Medical Center Utrecht, Utrecht, Netherlands
[2]Oxford Centre for Functional MRI of the Brain (F MRIB), University of Oxford, Oxford, United Kingdom
[3]Department of Psychiatry, University Medical Center Utrecht, Utrecht, Netherlands

Introduction: Repetitive transcranial magnetic stimulation (rTMS) is a promising, non-invasive neurostimulation technique that has the ability to inhibit or facilitate cortical excitability[1]. This makes rTMS a favorable therapeutic approach to modulate brain activity in neurological disorders associated with alterations in cortical excitability. For example after stroke, modulation of the interhemispheric imbalance of cortical excitability may promote functional and sensory motor recovery[2]. Despite the therapeutic potential of rTMS, the precise modes of action and optimal stimulation protocols remain unknown. To explore the mechanism of action of rTMS, the aim of our study was to assess the early effects of a single session of low-frequency (inhibitory) rTMS on cortical functional connectivity and perfusion in the stimulated hemisphere.

Methods: Animal procedures were conducted according to the guidelines of the European Communities Council Directive and approved by our institution's Ethical Committee on Animal Experiments. Four naive adult male Sprague Dawley rats were subjected to 20 minutes of low-frequency (1Hz, 1200 pulses) rTMS while under propofol anesthesia (700 µg/kg/min i.v.). Animals were stimulated with a 100mm figure-of-eight coil (SFEC-02-50, Neuro-MS/D stimulator, Neurosoft Ltd.) that was positioned lateral to the midline, with the center of the coil over the right sensorimotor cortex. Shortly after rTMS, animals were placed into a 4.7 T MRI system (Varian Instruments), and structural, functional and perfusion imaging were performed within 2h after stimulation. CBF, calculated from arterial spin labeling[3], was measured in the sensorimotor cortex. Low-frequency BOLD fluctuations ($0.01<f<0.1$ Hz) were measured from resting state-fMRI[4]. Functional connectivity (Fisher-transformed correlation (z') of signal time-courses) was calculated between the primary- (M1) and secondary (M2) motor cortices, the forelimb region of the somatosensory cortex (S1FL), and the secondary somatosensory cortex (S2).

Results: CBF in the sensorimotor cortex of the stimulated hemisphere (90±13% of contralateral)

was not significantly different from values in the non-stimulated hemisphere 2h after rTMS. There was a trend for reduced functional connectivity between cortical sensorimotor regions in the stimulated hemisphere (z' (stimulated vs. non-stimulated): M1-M2, 0.06±0.57 vs. 0.50±0.41; M1-S1FL, 0.14±0.52 vs. 0.29±0.39; S1FL-S2, 0.34±0.15 vs. 0.42±0.50), but this was not statistically significant.

Conclusion: Low-frequency rTMS may induce decreases in functional connectivity due to its inhibitory effect on cortical excitability. Our preliminary data reveal a trend towards lowered cortical functional connectivity, while CBF remained relatively unaffected, after a single rTMS session. However, the observed changes were not statistically significant. Larger and longer lasting effects may be achieved by multiple sessions of rTMS, which has been shown to induce robust changes in various aspects of brain functioning[5], as well as functional improvement in stroke patients[6]. Prospective studies will further investigate how multiple rTMS sessions affect physiological and functional brain parameters in healthy and diseased brain.

References:

1. Nowak et al. (2009). Neurorehabil Neural Repair 23:641-56
2. Fregni and Pascual-Leone (2007). Nat Clin Pract Neurol 3:838-93
3. Leithner et al. (2008). Exp Neurol 201:118-27
4. Van Meer et al. (2012). J Neurosci 32:4495-507
5. Van der Werf et al. (2010). BMC Neuroscience 11:145
6. Chang et al. (2010). J Rehabil Med 42:758-764

517
BRAIN-0577
Poster Session

Imaging Pre-Clinical

IN VIVO, MESOSCALE VOLTAGE IMAGING OF CORTICAL DYNAMICS AS A PLATFORM FOR INVESTIGATING MOUSE MODELS OF NEURODEGENERATIVE AND PSYCHIATRIC DISEASE

A.W. Chan[1], M.H. Mohajerani[2], J.M. LeDue[3], Y.T. Wang[3], T.H. Murphy[3]
[1]Psychiatry, Djavad Mowafaghian Centre for Brain Health, Vancouver, Canada
[2]Neuroscience, University of Lethbridge, Lethbridge, Canada
[3]Djavad Mowafaghian Centre for Brain Health, Djavad, Vancouver, Canada

Objectives: Increasingly, functional neuroimaging, principally using fMRI, is being applied to the investigation of psychiatric and neurodegenerative disease to reveal underlying pathologies in brain function and the potential discovery of novel biomarkers(1). We propose that parallel neuroimaging approaches, using modalities that more directly reflect neuronal activity, in mouse models of psychiatric and neurodegenerative disease presents a complimentary approach that can reveal much about disease pathology not possible in human imaging paradigms alone and may provide a platform for testing therapeutic interventions.

Methods: We used high-speed (150 Hz), wide-field (8.5x8.5 mm), voltage-sensitive dye (RH1692) imaging to examine spontaneous and sensory-evoked (somatosensory, visual, and auditory) networks of cortical activity in head-fixed awake and isoflurane-anesthetized C57Bl6 mice(2). Animal protocols were approved by the University of British Columbia Animal Care Committee and were in accordance with guidelines set forth by the Canadian Council for Animal Care.

Results: We demonstrate that infraslow (<0.1 Hz) and slow (0.5-6.0 Hz) spontaneous activity can

recapitulate analogs of human resting-state networks. In particular, we describe a mouse analog of the Default Mode Network, involving medial cortical structures centered on retrosplenial cortices, alterations to which, are linked with abnormal brain function. More significantly, our approach also allows for analyses of cortical dynamics such as altered sensory processing, impaired plasticity, and excitation/inhibition imbalance that are common features of disturbed brain function.

Conclusions: Mesoscale voltage imaging of resting-state connectivity and cortical dynamics may present a neuroimaging strategy with great potential utility. These approaches along with chronic imaging and the advent of genetically-encoded reporters of neuronal activity hold great promise in furthering our understanding of these complex pathologies.

References:
1. Zhang D & Raichle ME (2010) Disease and the brain's dark energy. *Nature reviews. Neurology* 6(1):15-28.

2. Mohajerani MH*, et al.* (2013) Spontaneous cortical activity alternates between motifs defined by regional axonal projections. *Nature neuroscience* 16(10):1426-1435.

518
BRAIN-0209
Poster Session

Imaging Pre-Clinical

EVALUATING THE EFFECTS OF TRADITIONAL CHINESE MEDICINE ON DOPAMINE D2 RECEPTOR AND GLUCOSE METABOLISM WITH F-18-FDG AND I-123-EPIDEPRIDE

M.C. Lin[1], K.W. Chang[2], L.W. Lin[3], H.Y. Chen[1]
[1]Department of Nuclear Medicine, E-DA Hospital, Kaohsiung, Taiwan
[2]Division of Isotope Application, Institute of Nuclear Energy Research (INER), Taoyuan, Taiwan
[3]The School of Chinese Medicines for Post-Baccalaureate, I-Shou University, Kaohsiung, Taiwan

Objective: Traditional Chinese medicine (TCM) is commonly used to nourish the blood, activate the circulation and so on. In this study, we treated mice with TCM and assessed the effects on dopamine D2 receptor and glucose metabolism in brain.

Methods: TCM was extract from the plant is used as for human health. All mice were allocated to one of three groups (0.25 g/ml or 0.125 g/ml in sterile water was fed to the mice twice daily for two weeks). Than acquired with a small-animal F-18-FDG/PET/CT camera (nanoPET/CT) and I-123-Epidepride/SPECT/CT camera (nanoSPECT/CT) for dynamic study image. The region of interest (ROI) was manually placed over the brain regions.

Results: High quality of F-18-FDG and I-123-Epidepride (Radiochemical purity >95%, by radio-HPLC) were synthesized by auto-synthesizer in INER. In vivo imaging, dynamic nanoPET/CT and nanoSPECT/CT showed that TCM treatment mice brain section/reference (cerebellum) ratio lager than control mice.

Conclusions: In the report, we modified the synthesize protocol (I-123-Epidrpride) on auto-synthesizer instrument and estimate in vivo assay. Now, superiority result show the TCM will increase dopamine D2 receptor and glucose metabolism between experiment and control groups. In future study, we will monitor in different monoamine with TCM treatment on mice. Our plan was using PET, SPECT and radiopharmaceuticals in vivo imaging, wish to exploitative the platform for diagnosis TCM on brain function.

519
BRAIN-0727
Poster Session

Imaging Pre-Clinical

MONITORING TISSUE PERFUSION DURING CEREBRAL ISCHEMIA CAUSED BY SINGLE VESSEL PHOTOTHROMBOSIS USING LASER SPECKLE CONTRAST IMAGING

A. Cho[1], C.M. Yeon[2], E. Chung[2]
[1]School of Mechatronics,
Gwangju Institute of Science and Technology,
Gwangju, Korea
[2]Medical System Engineering,
Gwangju Institute of Science and Technology,
Gwangju, Korea

Objectives: Surrounding tissue perfusion and reperfusion during photochemically induced occlusion of a single blood vessel, was analyzed using spatial and temporal domain laser speckle contrast (LSC) imaging.

Methods: Animal experiments were performed according to the institutional guidelines of the Gwangju Institute of Science and Technology, which are compliant with ARRIVE guidelines. C57BL/6 mice with cranial window were used for experiments. Mice with 25-30 g body weight and ages of 8-10 weeks were anesthetized with Zoletil™/Xylazine solution (Zoletil™ 60 mg + Xylazine 10 mg/kg body weight). Body temperature was kept 37 degree throughout the experiments with heat plate [1].

The laser speckle imaging instrumentation consists of a Helium-neon laser, a scientific-CMOS camera, and a microscope. Images were captured with 5 msec exposure time at 20 fps.

To analyze the speckle data, speckle contrast K is calculated as, $K = \sigma/I_{mean}$, where σ and I_{mean} represent standard deviation and mean intensity, respectively. The value of speckle contrast lies between 0 and 1: The value of one means static while the value close to zero signifies fast motion [1]. For the spatial domain, the contrast was determined with 7 by 7 window pixels, whereas temporal domain contrast was determined with single pixel over 18 temporal sequences of raw images.

For photothrombosis model, Rose Bengal dye (0.03 mg/g body weight, diluted to 10 mg/ml in PBS) was injected into the tail vein. A focused 532 nm laser has been used to illuminate the targeted single vessel, during approximately 5 min [2].

Results: Compared with white light images, LSC images provide clear blood flow maps where blood vessels contain fast moving scatterers. After photothrombosis, the noticeable reperfusion may be caused by collateral flows from deeper cortex [3].

Throughout the duration of photothrombosis, the targeted vessel perfusion was fluctuating and the penumbral tissue perfusion was also dynamically changing over time.

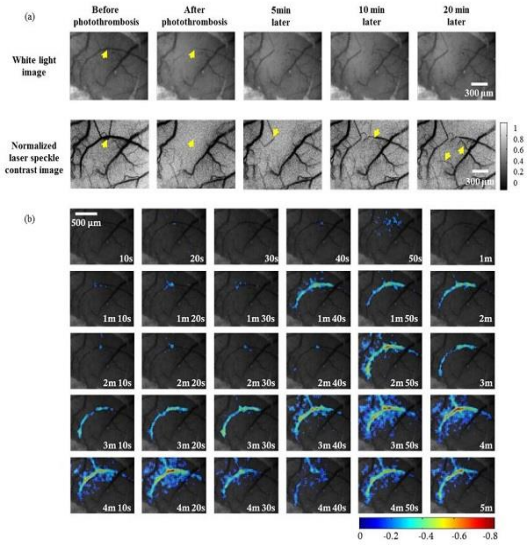

Figure. Progression of photothrombotic occlusion of single vessel. (a) White light and temporal domain LSC images before and after photothrombosis, and during reperfusion, (b) changes in speckle contrast during photothrombosis using spatial domain LSC images.

Conclusions: LSC imaging provides relatively high spatio-temporal resolution of cerebral blood flow using simple optical instrumentation. LSC images before and after photothrombotic event was obtained as a model of ischemic stroke. We monitored changes in tissue perfusion as well as vascular structures in response to photothrombotic occlusion of single vessel. The LSC imaging setup with photothrombosis preclinical model may provide insight into the mechanistic understanding of thrombotic dynamics.

References

[1] Boas, D.A. and A.K. Dunn, *Laser speckle contrast imaging in biomedical optics*. J Biomed Opt, 2010. 15(1): p. 011109.

[2] Sigler, A., A. Goroshkov, and T.H. Murphy, *Hardware and methodology for targeting single brain arterioles for photothrombotic stroke on an upright microscope*. Journal of neuroscience methods, 2008. 170(1): p. 35-44.

[3] Paul, J.S., et al., *Imaging the development of an ischemic core following photochemically induced cortical infarction in rats using laser speckle contrast analysis (LASCA)*. Neuroimage, 2006. 29(1): p. 38-45.

520
BRAIN-0224
Poster Session

Imaging Pre-Clinical

SPECT IMAGING REVEALS EARLY EFFECTS OF SYSTEMIC INFLAMMATION ON BRAIN INJURY AND CHANGES IN PERIPHERAL ORGANS AFTER CEREBRAL ISCHEMIA

K. Szigeti[1], I. Horváth[1], S.D. Veres[1], B. Martinecz[2], N. Lénárt[2], N. Kovács[3], E. Bakcsa[1], M. Semjéni[3], D. Máthé[3], A. Denes[2]
[1]Department of Biophysics and Radiation Biology, Semmelweis University, Budapest, Hungary
[2]Laboratory of Molecular Neuroendocrinology, Institute of Experimental Medicine, Budapest, Hungary
[3]Translational Research Centers, CROmed, Budapest, Hungary

Inflammation that develops in the brain and peripheral organs after stroke contributes profoudly to the outcome of patients. Clinical decision making would higly benefit from rapid assessment of central and peripheral inflammatory changes after acute brain injury, but appropriate medical imaging tools are not available yet. Here we show that single-photon emission computed tomography (NanoSPECT/CT Plus) allows early visualization of blood brain barrier injury and inflammation in the brain after experimental stroke, well before signs of brain injury can be detected with magnetic resonance imaging (MRI). Penetration of 99mTc-DTPA into the brain parenchyma overlaps with areas of brain injury and perfusion deficits after cerebral ischemia. In addition, this approach allows for the detection of increased blood brain barrier injury induced by systemic inflammation after experimental stroke. Acute brain injury also leads to infectious complications in peripheral organs such as the lung, the urinary tract or the gut and early visualization of these changes would enable appropriate therapies to be initiated. Using specific radioligands such as 99mTc-DTPA, 99mTc-HMPAO or 125I-HSA, SPECT imaging revealed early changes in perfusion, barrier function and / or inflammation in the lungs and the gut after experimental stroke with good predictive value for outcome. Collectively, our results suggest that early inflammatory changes as detected by SPECT imaging precede injury in the brain and peripheral organs and these imaging tools could be developed further to support decision making in the clinic.

521
BRAIN-0631
Poster Session

Imaging Pre-Clinical

MEASURING OXYGEN UPTAKE IN CORTICAL GRAY MATTER USING MRI AND NIRS-EVIDENCE FOR INCREASED METABOLIC RATE IN THE EAE MODEL OF MULTIPLE SCLEROSIS

J.F. Dunn[1], T.W. Johnson[1], L. Li[2], K. Murari[2]
[1]Radiology, University of Calgary, Calgary, Canada
[2]Electrical and Computer Engineering, University of Calgary, Calgary, Canada

OBJECTIVES: The goal was to develop a combined near-infrared spectroscopy/MRI system (NIMRI) to estimate cerebral metabolic rate for oxygen ($CMRO_2$) in the gray matter of a mouse model. We then applied the method to study the mouse experimental autoimmune encephalography pre-clinical model of multiple sclerosis.

The EAE model is largely used for studying demyelination. There is increasing evidence for gray matter involvement in MS and in the EAE model. We also have evidence for hypoxia, which suggests abnormalities in the oxygen delivery/utilization pathway. Oxygen uptake may increase as there is demyelination in gray matter and there is increased inflammation. Conversely oxygen uptake may decline as there is axonal loss. To understand how oxidative metabolism and hypoxia are involved in the disease pathophysiology, we combined MRI and quantitative near-infrared spectroscopy to compare the relative $CMRO_2$ in control and EAE mice.

METHODS: Control (n=8) and long term EAE (day 35; n=3) C57BL/6 mice were spontaneously ventilated with 2% isofluorane, 30% O_2, and 68% N_2. Breathing, heart rate and temperature were monitored. $CMRO_2$ was calculated using the Fick principle. Cerebral blood flow was obtained with ASL-MRI; Sa is arterial blood saturation and is obtained through pulse oximetry; Sv is venous blood saturation and is obtained with NIRS assuming that Sv can be calculated using a weighted difference of Sa and the microvascular saturation measured with NIRS. Arterial spin labelling data was collected with a 9.4T Bruker system with a CASL-HASTE sequence (matrix 128 x 128, FOV=3cm, TE=2.66ms, TR=3000ms). Broadband NIRS data were obtained using an Andor camera, Shamrock spectrograph and a custom designed NIRS probe. Data were processed based on a second-differential spectrum least-squares fitting algorithm and a hypoxia calibration.[2; 3]

RESULTS: $CMRO_2$ for the control group (n=8) was 2.69 ± 0.84 mL µmol O_2/g per min and for EAE mice (n=3) was 6.09 ± 1.14 µmol O_2/g per min (mean ± S.D).

CONCLUSION: We developed a new combined NIRS/MRI system to calculate $CMRO_2$ in GM of mouse models of neurological disease. Limitations include 1) a potential partial volume issue with the NIRS, in that some absorption arises from regions outside of the brain, and 2) we have to estimate the fraction of blood in arterial, microvascular and venous to calculate venous hemoglobin saturation. Even so, the control value of 2.7 is very similar to that of 2.6±0.4 µmol O_2/g per min (mean±SD, n=28) obtained using ^{17}O-NMR.[1] Finally, these data indicate that the EAE model of MS has an increased $CMRO_2$ relative to controls—perhaps caused by demyelination and inflammation.

REFERENCES: 1. Cui, W., X. H. Zhu, M. L. Vollmers, E. T. Colonna, G. Adriany, B. Tramm, J. M. Dubinsky and G. Oz (2013) J Cereb Blood Flow Metab **33**(12): 1846-9.
2. Dunn, J. F., Q. Zhang, Y. Wu, S. Srinivasan, M. R. Smith and R. A. Shaw (2008) J Biomed Opt **13**(6): 064043.
3. Matcher, S. J. and C. E. Cooper (1994) Phys Med Biol **39**: 1295.

522
BRAIN-0250
Poster Session

Imaging Pre-Clinical

VISUALIZING CEREBRAL ANEURYSMS IN MICE BY A CONVENTIONAL THREE TESLA MRI

K. Hokamura[1], H. Makino[2], T. Natsume[3], T. Kimura[2], Y. Kamio[4], Y. Magata[5], H. Namba[4], T. Katoh[2], S. Sato[2], T. Hashimoto[6], K. Umemura[1]
[1]Pharmacology, Hamamatsu University School of Medicine, Hamamatsu, Japan
[2]Anesthesiology and Intensive Care, Hamamatsu University School of Medicine, Hamamatsu, Japan
[3]Radiological Technology, Fujita Health University School of Health Sciences, Toyoake, Japan
[4]Neurosurgery, Hamamatsu University School of Medicine, Hamamatsu, Japan
[5]Medical Photonics Research Center, Hamamatsu University School of Medicine, Hamamatsu, Japan
[6]Anesthesia and Perioperative Care, University of California San Francisco, Hamamatsu, USA

[Objectives]

We report the feasibility of using readily available, conventional 3-T magnetic resonance imaging (MRI) to serially image cerebrovascular remodeling in mice. We used a mouse model of intracranial aneurysm as a mouse model of dynamic, pathological remodeling of cerebral arteries to demonstrate the feasibility of detecting aneurysm formation, growth, and rupture.

[Methods]

Intracranial aneurysms were induced in 7-week-old male mice. We combined induced systemic hypertension with a single injection of elastase into the cerebrospinal fluid in the right basal cistern. For mouse cerebral vessel imaging, it was used conventional 3-T MRI. We used nonenhanced magnetic resonance angiography (MRA) to detect intracranial aneurysm formation and T2-weighted imaging to detect subarachnoid hemorrhage. In all mice with aneurysms, it was able to detect aneurysm formation, and location of the low-intensity area matched that of aneurysmal subarachnoid hemorrhage after euthanasia.

[Results]

We induced intracranial aneurysms in 10 mice. Subsequently, five developed neurological symptoms associated with aneurysmal rupture. When the brains of these mice were inspected, all exhibited intracranial aneurysms with subarachnoid hemorrhage. MRA showed clear enlargement of the aneurysm.

All five symptomatic mice presented a low-intensity area on T2-weighted imaging. However, in two mice, the low-intensity area was detected before the mice became symptomatic. In these mice, growth of the low-intensity area coincided with the onset of symptoms. The location of the low-intensity area matched that of aneurysmal subarachnoid hemorrhage revealed by the inspection of the brain after euthanasia.

[Conclusions]

We showed the feasibility of using conventional 3-T MRI for the serial imaging of mouse cerebral arteries with aneurysms and subarachnoid hemorrhages. These imaging methods without using highly specialized imager will be a useful tool for researchers in the field of stroke.

523
BRAIN-0635
Poster Session

Imaging Pre-Clinical

LONGITUDINAL IN SITU TWO PHOTON FLUORESCENCE MICROSCOPY IN RATS

M.M. Koletar[1], L.A.M. Thomason[1], A. Dorr[1], B. Stefanovic[2]
[1]Medical Imaging Research, Sunnybrook Research Institute, Toronto, Canada
[2]Physical Sciences Medical Biophysics, University of Toronto, Toronto, Canada

Objectives: There is mounting evidence for the role of cerebral micro-vessels in the etiology and progression of both cerebrovascular disease and neurodegeneration. In addition, behavioural assessment has become the norm in defining response/outcome in these studies. Given the much wider array of behavioural tests available in rats than in mice, establishing an imaging platform for longitudinal, high resolution in vivo imaging of cortical cerebral microvasculature in the rats is of wide interest, yet has proven difficult hitherto (Shih et al., 2012).

Methods: Aseptic surgery was undertaken to implant a 6mm by 5mm cranial window over forelimb representation in the primary somatosensory cortex of 2-month old Sprague-Dawley rats. Rats were anesthetized with isoflurane (5% induction, 2% maintenance) and placed on a heated blanket. Rectal temperature monitoring and pulse oximetry were conducted throughout the surgical procedures to ensure stable systemic state of the animal. The brain surface was continuously irrigated with cooled sterile saline to minimize inflammation. The skull was removed via a dental drill, and the dura resected using Dumont forceps and micro-scissors. The exposed brain was covered with sterile saline and an 8mm glass coverslip secured using cyanoacrylate glue. Dental cement was employed to form a well for later imaging sessions. The rats were administered Dexamethasone and Buprenorphine following surgery, and returned to the colony. Each animal was imaged on two photon fluorescence microscope (2PFM; FV1000MPE from Olympus Corp.) at bi-weekly intervals up to 10 weeks following the craniotomy. During each imaging session, two photon fluorescence images were acquired parallel to the cortical surface, using 25x, 1.05NA 2-mm working distance objective (Olympus) and 900nm excitation, following tail vein injection of 70uL of 70-kDa Texas Red fluorescent dextran (Invitrogen), at 0.5x0.5um^2 in plane resolution, every 1.5um.

Results: The microvasculature was imageable down to 400um below the cortical surface weekly for 2.5 months following the cranial window implantation. Figure 1A shows a photograph of the cranial window along with the maximum intensity projection of the 2PFM data 10 weeks following the craniotomy (1B). Over this imaging depth, sufficient intra- to extra-vascular contrast was present to allow semi-automated segmentation of the microvasculature. No significant time-dependent deterioration of the signal-to-background ratio was observed over the 10 week experimental period. In contrast, up to 25% variation in imaging depth was seen across different animals.

Conclusions: Our findings provide initial evidence for longitudinal at-depth imaging of cortical microvasculature in situ in rats equipped with carefully implanted cranial windows. This imaging platform affords study of the remodelling of rat cerebral microvascular networks over weeks to months following cranial window implantation and can thus be employed to both track vascular degeneration and response to treatments in various rat models of CNS pathologies.

References: Shih AY, Driscoll JD, Drew PJ, Nishimura N, Schaffer CB and Kleinfeld D (2012). Two-photon microscopy as a tool to study blood flow and neurovascular coupling in the rodent brain. Journal of Cerebral Blood Flow & Metabolism. 32:1277-1309.

524
BRAIN-0669
Poster Session

Imaging Pre-Clinical

OPTICAL CLEARING OF BRAIN TISSUE FOR THREE-DIMENSIONAL ULTRAMICROSCOPIC IMAGING OF THE CEREBRAL VASCULATURE

N. Lachkar[1], J. de Vos[1], E. Bakker[1], E. VanBavel[1]
[1]Biomedical Engineering & Physics
Academic Medical Center University of Amsterdam, Netherlands

Objectives: Whole brain imaging without time-consuming tissue sectioning, imaging and 3D reconstruction can be performed by light-sheet ultramicroscopy. For this 3D imaging technique, optical clearing of biological tissue is required. Several techniques have become available to make mouse brains optically transparent. Here we report on clearing rat brain tissue to recover the 3D architecture of the vascular bed.

Methods: Endothelial cells were labeled in vivo by intravenous injection of lectin (DyLight 488 Labeled tomato). The cerebral vasculature was visualized by light-sheet laser-scanning ultramicroscopy. We tested two methods for optical clearing of whole rat brains; passive CLARITY [1], which involves tissue clearing by the transformation of lipids to a hydrogel network, and 3DISCO [2], which uses organic solvents (tetrahydrofuran and dibenzylether) to match the refractory indexes of the different brain tissue layers.

Results: Clearing of adult rat brains using 3DISCO resulted in optically transparent tissue. The entire protocol took 8 days and consisted of sequential 24-hour-incubation steps with an increased concentration of tetrahydrafuran (i.e. 50-100%) followed by incubation in dibenzylether for 2 days. As a result, we obtained a hard glass-like tissue sample. Although the ultramicroscope imaging of the brain contained background noise, the images showed the vasculature with penetrating arteries. Passive clearing of adult rat brains with CLARITY took 3 months, which

1A

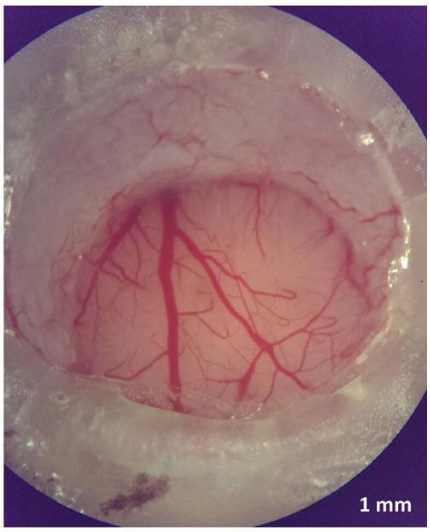

Chronic cranial window at 10 weeks post-surgery.

1B

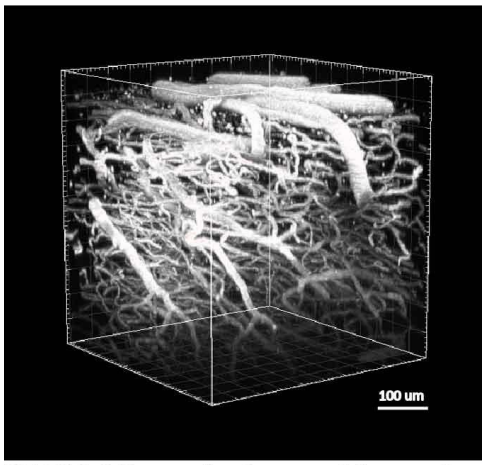

2PFM 3D rendering at 10 weeks.

included hydrogel embedding, lipid removal and glycerol incubation. From this protocol we retrieved an expanded brain as a gel-like structure, which was optically clear. The cerebral arteries were clearly imaged by the ultramicroscope. However, smaller arteries could not be distinguished from the brain tissue due to background noise.

Conclusion: Rat brains could be cleared by 3DISCO and CLARITY and subsequently imaged by ultramicroscopy. The obtained images contained background noise, likely due to the scattering of light in the large brain tissue sample. Based on these preliminary data, in optical clearing of rat brain samples for the purpose of imaging the vascular architecture, 3DISCO might be superior to the CLARITY protocol.

References:

1. Chung, K. and K. Deisseroth, CLARITY for mapping the nervous system. Nat Methods, 2013. 10(6): p. 508-13.

2. Erturk, A., et al., Three-dimensional imaging of solvent-cleared organs using 3DISCO. Nature Protocols, 2012. 7(11): p. 1983-1995.

525
BRAIN-0654
Poster Session

Imaging Pre-Clinical

IMPAIRED COLLATERAL STATUS DURING ACUTE AND CHRONIC ISCHEMIA IN TYPE 2 DIABETES

J. Liu[1], Y. Akamatsu[1], Y. Nishijima[1], R.K. Wang[2]
[1]Neurological Surgery, UCSF, San Francisco, USA
[2]Bioengineering and Ophthalmology, U Washington, Seattle, USA

Introduction: Cerebral collateral circulation has long been reported to alter the risk of stroke. Collateral status is also an independent predictor of stroke outcome. As a major vascular risk factor, type 2 diabetes mellitus (T2DM) worsens the outcome of stroke. However, the mechanisms that are responsible for the worse stroke outcome in this population are incompletely understood. The current study sought to determine the effect of T2DM on collateral flow dynamics after MCA stroke and chronic hypoperfusion.

Method: Adult male db/db and db/+ mice (16-20 weeks of age) were subjected to temporary distal middle cerebral artery occlusion (MCAO) or permanent unilateral common carotid artery occlusion (CCAO). In vivo imaging of blood flow and flow velocity was performed with Doppler optical coherence tomography (DOCT). The numbers of connecting collateral vessels and vessel diameter were quantified after DiI-labeling. Motor function and infarct volume were assessed at one week after stroke.

Results: db/db mice displayed impaired leptomeningeal collateral flow during acute MCAO, which coincided with a worse stroke outcome compared to db/+ mice, regardless of their equally well-collateralized anastomoses. Despite the improvement in collateral flow over the course of one week, db/db mice still exhibited significantly reduced retrograde flow into the MCA territory compared to db/+ mice. Acutely induced hyperglycemia in the db/+ mice did not impair collateral flow after stroke, suggesting that the state of hyperglycemia alone was not sufficient to impact collateral flow. Human albumin significantly improved leptomeningeal collateral flow in the db/db mice. An impairment of leptomeningeal collateral recruitment was also observed in db/db mice compared to db/+ following unilateral CCAO, which coincided with a delay in outward collateral vessel growth in the circle of Willis.

Conclusion: Our results demonstrate that T2DM is associated with impaired collateral status not only between the MCA and ACA vascular networks, but also in the primary collateral circulation. The impaired collateral status might underlie the increased risk of ischemic injury in T2DM with carotid disease or stroke.

526
BRAIN-0428
Poster Session

Imaging Pre-Clinical

OPTICAL IMAGING OF INTRACELLULAR PH CHANGES WITH SPREADING DEPOLARIZATION IN THE INTACT AND ISCHEMIC RAT BRAIN

A. Menyhart[1], D. Zölei-Szénási[1], T. Puskás[1], O. M. Tóth[1], B. Szepes[1], P. Hertelendy[1], F. Bari[1], E. Farkas[1]
[1]Department of Medical Physics and Informatics, University of Szeged Faculty of Medicine Faculty of Science and Informatics, Szeged, Hungary

Objectives

Ischemia-related spreading depolarizations (SDs) are part of the pathophysiology of cerebrovascular diseases and predict worse outcome. SDs may exacerbate ischemic injury via related atypical hemodynamic responses, but their consequences on tissue pH changes are not yet understood. The regulation of pH changes of neurons is crucial in both physiological and ischemic conditions, because acid loading makes them susceptible for injury. Therefore we set out to compare intracellular pH changes associated with SDs propagating across the intact and the ischemic cortex of rats, visualized by live optical brain imaging.

Methods

Animal procedures were approved by the Ethical Committee for Animal Care of the University of Szeged adhering to national regulation. A closed cranial window was mounted over the right parietal bone of isoflurane anesthetized adult male Sprague-Dawley rats. The cranial window incorporated a glass capillary through which 1 µl 1M KCl was applied topically for the distinct elicitation of SD. Neutral red (NR), a pH sensitive vital fluorescent dye was injected i.p. (35mM, 2 x 1 ml,) 30 min before the start of image acquisition. Following a baseline period of 50 min, transient incomplete global forebrain ischemia was achieved by 60 min of bilateral common carotid artery occlusion (2VO). SDs were elicited at 15 min intervals prior ischemia induction and during ischemia. Two separate CCD cameras, synchronized to suitable illumination, were used for the dual imaging of changes in cerebral blood flow (CBF, laser speckle contrast imaging) and intracellular pH (NR fluorescence intensity). CBF was expressed relative to baseline (%), while pH changes were extracted as fluorescence intensity changes with baseline considered (ΔF/F).

Results

CBF was reduced to 77±7.7% after the passage of 3 SDs initiated during the baseline period. 2VO onset caused a further reduction to 34±4.3% followed by a mild recovery to 38±4.8% after the passage of additional 3 SD waves prior 2VO release. All SDs were coupled with hyperemic CBF responses, with lower amplitude (48±10 vs. 155±23%) and longer duration (279±55 vs. 163±21 s) during ischemia with respect to baseline. SD-associated pH changes were biphasic (initial acidosis followed by transient alkalosis) during baseline, and monophasic (dominant acidosis) during ischemia. The amplitude of acidosis was almost 3 times higher for ischemic as compared with baseline SDs (ΔF/F 0.37±0.04 vs. 0.13±0.02), the ischemic value considerably exceeding the peak of the 2VO induced acidosis (ΔF/F 0.25±0.05). The duration of acidosis tripled for ischemic as compared with baseline SDs (155±33 vs. 45±3.5 s).

Conclusions

Marked tissue acidosis correlates with the extent of brain injury, and has been traditionally considered as a damaging component of cerebral ischemia. On the other hand, mild acidosis appears to be neuroprotective by delaying SDs and limiting ischemic injury. We propose that the SD-associated, prominent, transient acidosis superimposed on ischemic acidosis worsens tissue survival, thereby rendering SDs malignant in cerebral ischemia. In contrast, the less pronounced pH changes with SDs in the non-ischemic cortex are suggested not to be harmful.

Support: Hungarian Scientific Research Fund (K111923), János Bolyai Research Scholarship of the Hungarian Academy of Sciences.

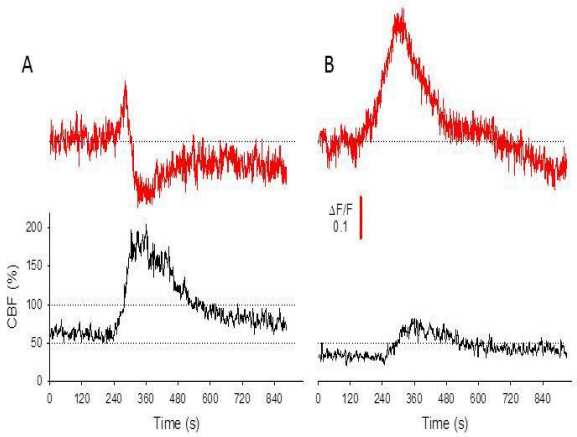

Figure 1. Synchronous changes in cerebral blood flow (lower traces) and intracellular pH (upper traces) with waves of spreading depolarizations (SDs) in the intact (A) and ischemic (B) cortex of the rat. Traces are averages of 8 SD signatures. CBF is expressed relative to baseline (%), while pH changes are given as fluorescence intensity changes with baseline considered (ΔF/F).

527
BRAIN-0707
Poster Session

Imaging Pre-Clinical

NON-INVASIVE FUNCTIONAL NEUROIMAGING IN THE MOUSE USING DIFFUSE OPTICAL TOMOGRAPHY

M. Reisman[1], A. Bauer[2], Z. Markow[3], G. Baxter[2], J. Culver[2]
[1]Physics, Washington University, St. Louis, USA
[2]Radiology, Washington University, St. Louis, USA
[3]Biomedical Engineering, Washington University, St. Louis, USA

I. Objective. The study of correlated spontaneous activity in functionally related brain regions using functional connectivity magnetic resonance imaging (fcMRI) has recently allowed comprehensive mapping of distributed brain networks in humans.[1] Extending analogous fcMRI studies to the mouse has been challenging due to technical limitations that preclude high resolution and high signal-to-noise measurements in the small volume of the mouse brain. Instead, optical intrinsic signal (OIS) techniques, which use a simple planar imaging geometry, have provided most of the observations of fc in the mouse brain.[2] While effective and efficient, fcOIS methods require retraction of the scalp and are limited to superficial cortical tissues. Diffuse Optical Tomography (DOT) is a non-invasive optical imaging modality, but current systems are either too sparse of a spatial sampling[3] or are too slow for capturing functional response in the mouse brain.[4] Here we develop a DOT system that combines the sensitivity and spatial sampling of camera-based systems with the rapid-imaging capabilities of structured light illumination[5] to map brain activity in the mouse.

II. Methods. The DOT system is comprised of a single sCMOS camera and a digital micromirror device (Fig 1A) that produce ~10^6 source-detector pair measurements with 0.15mm spacing at a speed of ~10Hz. This system increases the spatial sampling by >10x compared to existing human functional neuroimaging DOT systems,[3] and increases the speed by >10x over previous CCD-based mouse DOT.[4] System performance was tested in 5 mice by imaging cortical responses to electrical forepaw stimulation and measuring resting state functional connectivity patterns with the scalp intact.

III. Results. Activations in the somatosensory region of the cortex upon electrical stimulation of the forepaw are seen non-invasively, through the intact scalp (Fig 1B). Extending the technique to imaging spontaneous activity reveals expected resting state functional connectivity within the cortex as previously observed using OIS, but extends with deeper depth sensitivity (Fig 1C).

IV. Conclusions. Establishing analogous functional imaging in both mouse and man is one of the most promising strategies for providing clinical translation. We have developed a method for optical imaging of the mouse brain using DOT with structured light source patterns. This method extends our previous mouse neuroimaging techniques to imaging through the scalp and with increased sensitivity to deeper regions of the mouse cortex.

V. References

[1] Biswal, B, et al. *Magnetic resonance in medicine,* **34.4**, 537-541 (1995).

[2] White, B.R. et al., *PLoS ONE*, **6(1)**, e16322 (2011).

[3] Zeff, B.W. et al., *Proc. Natl. Acad. Sci. U.S.A.*, **104(29)**, 12169 (2007).

[4] Patwardhan, S.V. and Culver, J.P., *Journal of Biomedical Optics,* **13(1)**, 011009 (2008).

[5] Cuccia DJ, et al., *J. Biomed. Opt.* **14(2),** 024012

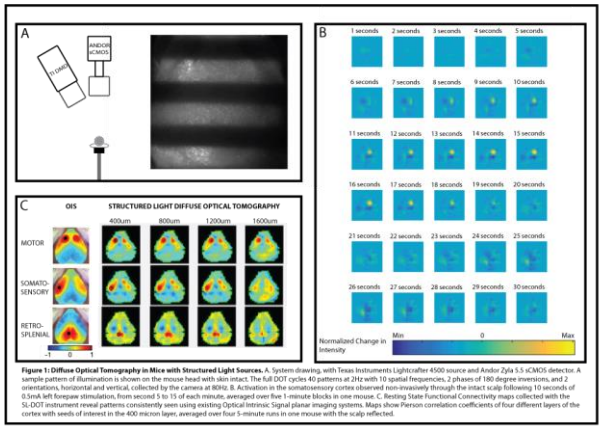

Figure 1: Diffuse Optical Tomography in Mice with Structured Light Sources. A. System drawing, with Texas Instruments Lightcrafter 4500 source and Andor Zyla 5.5 sCMOS detector. A sample pattern of illumination is shown on the mouse head with skin intact. The full DOT cycles 40 patterns at 2Hz with 10 spatial frequencies, 2 phases of 180 degree inversions, and 2 orientations, horizontal and vertical, collected by the camera at 80Hz. B. Activation in the somatosensory cortex observed non-invasively through the intact scalp following 10 seconds of 0.5mA left forepaw stimulation, from second 5 to 15 of each minute, averaged over five 1-minute blocks in one mouse. C. Resting State Functional Connectivity maps collected with the SL-DOT instrument reveal patterns consistently seen using existing Optical Intrinsic Signal planar imaging systems. Maps show Pierson correlation coefficients of four different layers of the cortex with seeds of interest in the 400 micron layer, averaged over four 5-minute runs in one mouse with the scalp reflected.

528
BRAIN-0794
Poster Session

Imaging Pre-Clinical

TWO-PHOTON EXCITATION FLUORESCENCE MICROSCOPY FOR FAST SCANNING, REAL TIME VOLUMETRIC IMAGING OF NANOPARTICLES TRANSPORT IN RAT CORTEX

J. Rosch[1], *P. Gadamsetty*[2], *C.B. Schaffer*[2], *W. Olbricht*[1]
[1]*Chemical and Biomolecular Engineering, Cornell University, Ithaca, USA*
[2]*Biomedical Engineering, Cornell University, Ithaca, USA*

Objective: Convection-enhanced delivery (CED) is a novel drug delivery method that circumvents the blood-brain barrier by infusing therapeutics directly into brain parenchyma through a needle. CED has been used to deliver a variety of therapeutics ranging in size from small molecules to drug-laden nanoparticles [1,2]. The outcome of CED therapy is often determined by the rate of transport of the infused material. This study focuses on nanoparticle transport in the brain interstitium and the perivascular space (PVS), which refers to thin annular regions surrounding cortical blood vessels. Transport in the interstitium is strongly hindered, especially for nanoparticles, but the structure of the PVS may enhance fluid flow and nanoparticle transport, leading to the possibility of preferential transport of infused material through the PVS. Furthermore, the motion of fluid and nanoparticles in the PVS may be affected by the pulsations of the blood vessel walls due to the heartbeat. Together, these effects may influence the spatial distribution of infused compounds and the concentration of drug molecules that reach a target destination. We use real time two-photon excitation microscopy to investigate transport mechanisms of nanoparticles in the PVS and in the interstitium during CED infusions.

Methods: We developed an imaging platform to study transport of nanoparticles in the rat cortex *in vivo* with high temporal and spatial resolution. A fluorescent tracer is injected into the bloodstream to identify vasculature, and a suspension of fluorescently labeled polystyrene beads is infused directly into the cortex of an anesthetized rat through a glass micropipette. The exposed brain is placed under a two-photon microscope. Nanoparticles are tracked in the brain interstitium and the PVS surrounding cortical blood vessels. The spatial distribution of infused particles is then imaged by fast scanning, real time volumetric imaging. (Approved by Cornell IACUC.)

Results: The infusion cloud is anisotropic, and the anisotropy is directly correlated with high conductivity paths provided by the PVS near the needle [Figure 1]. Measurements of nanoparticle speeds show that the resistance to motion in the PVS is roughly a factor of 10 less than resistance to motion through the interstitium.

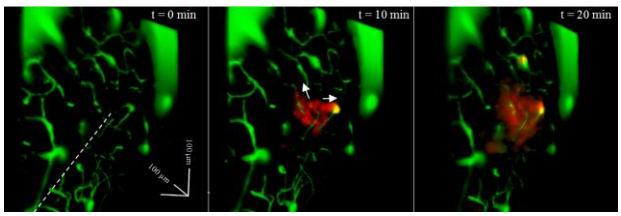

Figure 1: Time lapse visualization of infusion of

nanoparticles in the cortex of rats.
Imaging infusion of 40 nm nanoparticles (red) injected at 0.2 µL/min. Vasculature labeled with FITC-dextran (green). PVS near needle outlet leads to anisotropy of infusion cloud. Dotted line indicates needle shaft location. Arrows indicate direction of PVS flow.

Conclusions: To improve CED for delivering therapeutics in brain disorder, it is essential to understand and optimize nanoparticle transport. Real time imaging of nanoparticle motion in the interstitium and the PVS provides information that can be used to design and optimize CED therapy.

References:
1. M. S. Fiandaca, M. S. Berger, K. S. Bankiewicz, *Toxins* 3, 369-397 (2011).
2. M. T. Krauze, J. Forsayeth, J. W. Park, K. S. Bankiewicz, *Pharmaceutical Research* 23, 2493-2504 (2006).

529
BRAIN-0460
Poster Session

Imaging Pre-Clinical

CELLULAR INJURY ASSOCIATES WITH PERI-ISCHEMIC BLOOD-BRAIN BARRIER DYSFUNCTION IN THE RAT PHOTOTHROMBOSIS MODEL: AN IN-VIVO IMAGING APPROACH

K. Schoknecht[1], O. Prager[2], U. Vazana[2], L. Kamintsky[2], R. Kovács[3], J.P. Dreier[4], U. Heinemann[3], A. Friedman[5]
[1]Institute for Neurophysiology, Charité Universitätmedizin-Berlin, Berlin, Germany
[2]Department of Physiology & Cell Biology Cognitive & Brain Sciences the Zlotowski Center for Neuroscience, Ben-Gurion University of the Negev, Beer-Sheva, Israel
[3]Institute for Neurophysiology, Charité - Universitätsmedizin Berlin, Berlin, Germany
[4]Center for Stroke Research Berlin Department of Experimental Neurology, Charité- Universitätsmedizin Berlin, Berlin, Germany
[5]Medical Neuroscience, Dalhousie University, Halifax, Canada

Objective: Stroke is one of the leading causes of death and morbidity[1]. An ischemic core and a surrounding dysfunctional region characterize the ischemic brain[2]. The peri-ischemic tissue, which often displays blood-brain barrier compromise[3], may either recover or undergo secondary damage; however, assessing the propensity of the peri-ischemic brain to undergo secondary damage, understanding the underlying mechanisms, and adjusting treatment accordingly remain clinically unmet challenges.

Methods: Cerebral ischemia was induced by photothrombosis using Rose bengal in male Sprague Dawley rats. BBB permeability, vascular diameters and cell damage were assessed through longitudinal intravial microscopy following the peripheral injection of fluorescein sodium salt (for perfusion and BBB permeability assessment) and propidium iodide (a membrane integrity marker to assess cell death). Topically applied 4-Amino-5-methylamino-2',7'-difluorofluorescein diacetate and ROSstar 650 served to detect nitric oxide (NO) and superoxide respectively. Free radical signaling was inhibited by topical perfusion of 2-(4-carboxyphenyl)-4,4,5,5-tetramethyl-imidazoline-l-oxyl-3-oxide (NO scavenger), L-NG-Nitroarginine methyl ester (nitric oxide synthase inhibitor) and phenyl-N-t-butylnitrone (free radical spin trap and inhibitor of induction of NO synthase).

Results: The hypoperfused core gradually expanded during the first hours after photothrombosis. BBB dysfunction propagated as well, and was found in both hypo- and normally perfused regions. Importantly, the increase in the number of injured cells within the peri-ischemic region correlated to BBB dysfunction and was also observed in normally perfused brain regions. Superoxide gave a diffuse peri-ischemic vascular as well as parenchymal signal, whereas NO levels increased most prominently in arterioles. Inhibiting free radical signaling significantly reduced progressive cellular damage only in

adequately perfused areas, and had no significant effect on cerebral perfusion and BBB permeability.

Conclusions: Our novel approach to assess different patho-physiological parameters in parallel in vivo allows in-depth studies into the sequence of events leading to brain damage and the efficacy of therapeutic agents. While perfusion measurement alone was insufficient to predict progressive cell damage, increased vessels' permeability may become an important biomarker to delineate tissue at risk.

References:

1. Corbyn Z. Statistics: A growing global burden. Nature. Nature Publishing Group; 2014 Jun 25;510(7506):S2–3.
2. Astrup J, Siesjo BK, Symon L. Thresholds in cerebral ischemia - the ischemic penumbra. Stroke. 1981 Nov 1;12(6):723–5.
3. Latour LL, Kang D-W, Ezzeddine MA, Chalela JA, Warach S. Early blood-brain barrier disruption in human focal brain ischemia. Ann Neurol. 2004 Oct;56(4):468–77.

530
BRAIN-0439
Poster Session

Imaging Pre-Clinical

DETECTION OF PRIMARY AND SECONDARY BRAIN TUMOURS USING MOLECULARLY-TARGETED MAGNETIC RESONANCE IMAGING

S. Serres[1], M. Kirkman[1], N. de Pennington[1], C. Bristow[1], N.R. Sibson[1]
[1]CRUK and MRC Oxford Institute for Radiation Onc ology Department of Oncology, University of Oxford, Oxford, United Kingdom

Objectives: Currently, both primary and secondary brain tumours are diagnosed and monitored clinically using passive contrast-enhanced magnetic resonance imaging (MRI). Although these methods provide reasonable information on tumour size and spatial extent, they often fail to accurately delineate tumour margins; an essential criterion for effective surgical resection and/or radiotherapy. Recent advances in molecularly-targeted MRI offer a number of advantages over conventional methodologies, including identification of specific molecular processes, such as upregulation of endothelial cell adhesion molecules (e.g. vascular cell adhesion molecule 1 [VCAM-1]), that may be particularly active in the invasive margins of the tumour. The aim of this study, therefore, was to determine whether VCAM-1-targeted MRI could facilitate improved spatial delineation of tumour margins and more accurate assessment of tumour activity.
Methods: Three cohorts of nude rats were injected intracerebrally. Cohorts 1 and 2 were injected in the left striatum with either a metastatic human breast carcinoma cell line (MDA231BR-GFP; 10,000 cells in 1µl) or a multiform glioblastoma cell line (U87-MG; 10,000 cells in 1µl), and used 4 weeks after injection. For the third cohort, animals were injected in the cerebellum with a desmoplastic medulloblastoma cell line (DAOY; 10,000 cells in 1µl) and used 8 weeks after injection. All animals underwent T1- and T2-weighted MRI to follow macroscopic structural changes, and post-gadolinium T1-weighted gradient echo 3D MRI to assess blood-brain barrier (BBB) integrity. For VCAM-1-targeted MRI, animals underwent T2* gradient echo 3D MRI after injection of microparticles of iron oxide (MPIO) functionalised with either an anti-VCAM-1 antibody (VCAM-MPIO) or a control IgG antibody (IgG-MPIO). Immunohistochemical assessment was performed post-mortem to detect tumour cells (GFP or human Vimentin), blood vessels (CD31), vascular cell adhesion molecule-1 (VCAM-1) and a proliferative marker (Ki67).
Results: In all cases, brain tumours were detected using T1- and T2-weighted imaging and exhibited a compromised BBB using post-gadolinium T1-weighted imaging. In all cases, marked hypointensities were evident on T2*-weighted MRI following intravenous injection of VCAM-MPIO, but not IgG-MPIO, and this was particularly evident at the margins of the tumours. VCAM-1 upregulation detected immunohistochemically was significantly greater on blood vessels associated with the tumour margins than the tumour core, and co-localised with proliferative

regions of the tumour, as confirmed by Ki67 immunohistochemistry. Spatial comparison of VCAM-MPIO binding and gadolinium-enhanced signal, using a 3D composite analysis method, indicated clearer delineation of tumour margins with the molecularly-targeted approach. Conclusion: The results of this study indicate that upregulation of VCAM-1 is closely associated with the proliferative tumour margin, and that this can be detected with high sensitivity using molecularly-targeted MRI. These findings suggest that VCAM-1-targeted MRI may enable improved detection of tumour margins, as compared to the current clinical gold standard of gadolinium-enhanced MRI, for both primary and secondary tumours in the brain. Clinical application of this approach may, thus, provide a sensitive biomarker for effective surgical resection and/or radiotherapy and improved outcomes in brain tumour patients.

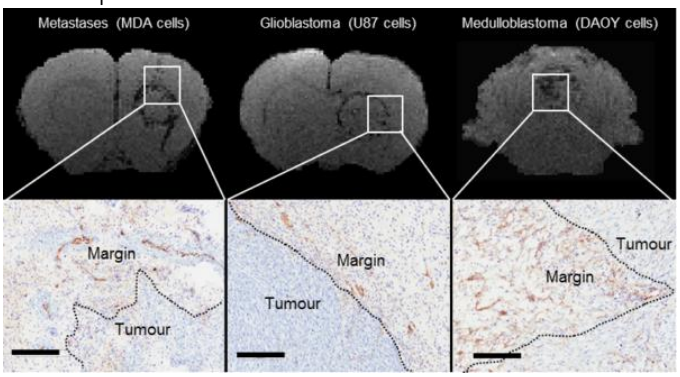

Figure 1- T_2*-weighted MRI following intravenous injection of VCAM-MPIO reveals VCAM-MPIO binding at the margins of the tumours and correlates with immunohistochemical detection of VCAM-1 (brown).

531
BRAIN-0204
Poster Session

Imaging Pre-Clinical

GENDER DIFFERENCE OF THE CORPUS CALLOSUM-SUBREGIONAL INSPECTION

A. Shiino[1], K. Tanigaki[2], Y. Chen[3], A. Yamada[4], I. Tooyama[1]
[1]Molecular Neuroscience Research Center, Shiga University of Medical Science, Otsu, Japan
[2]Research Institute, Shiga Medical Center, Moriyama, Japan
[3]College of Information Science and Engineering, Ritsumei University, Kusatsu, Japan
[4]Biomedical Innovation Center, Shiga University of Medical Science, Otsu, Japan

It has been contended that any observed differencebetween groups is not gender specific but is due to differences in brain size. A current report (Ardekani, et al.),however, showed that the cross-sectional area of the corpus callosum (CC) wassignificantly larger in females when analyzed on a subset of 37 pairs of youngadults (18–29 years) matched closely to brain size. Since this study wasperformed using the OASIS (Open Access Series of Imaging Studies) database, wetried to clear this assignment by using a method of voxel-based morphometry(VBM), and further investigated subregional sex difference of CC including theother white matter (WM) regions using the same subset.

We obtained MR images from OASIScross-sectional dataset composed of 138 normal brains including 61 male and 77female under 30 years old. All subjects were right-handed dominance. VBM analysis was performed using SPM 8 software. Resultingstatistics were transformed to z-scores and displayed as parametric maps usingBAAD software that was developed in our laboratory (http://www.shiga-med.ac.jp/~hqbioph/saito/BAAD(English)). BAAD alsocalculates regional z-scores by using MarsBar software (http://marsbar.sourceforge.net) of which results are independent frommasking threshold. ROI of the CC area and the CC volume

were made by usingITK-SNAP (http://www.itksnap.org/pmwiki/pmwiki.php)and WFU PickAtlas software (http://fmri.wfubmc.edu/software/pickatlas),and were equipped with MarsBar software.

First we made two sets of region of interest, CC area and CC volume, tostudy whether we could get the similar results using VBM technique. As aresult, both the CC area and volume were significantly larger in females ($p < 0.0018$ and 0.0006 respectively),and this was not conflicting the previous report. VBM indicated that genu of CCwas the subregion of the most significant sex difference (FWE rate < 0.05).There were no apparent significant differences in another WM regions, but thedeep frontal WM was larger in female whereas the cerebellar WM was larger inmales (uncorrected $p < 0.001$).Females also have larger WM in the left prefrontal WM close to Broca's area. Weconcerned the regional white matter difference related to TIV, we analyzed therelation in 138 young normal subjects. Here, we set TIV as contrast, and ageand sex were set as nuisance variable, and used proportional scaling for globalnormalization. As a result, white matter of the frontal lobe was highly relatedto the brain size whereas pyramidal tract was less. The degreed of the TIVeffect on the corpus callosum was slightly larger than average except itssubregion of the posterior middle part that was slightly smaller than average.

Since the subjects of the study were the pairs of matched brain size, theresults of our VBM study must be a strong evidence indicating existence of sexdimorphism of the brain.

Ardekani BA, Figarsky K, Sidtis JJ.2013. Sexual dimorphism in the human corpus callosum: an MRI study using theOASIS brain database. Cerebral cortex 23:2514-2520.

532
BRAIN-0792
Poster Session

Imaging Pre-Clinical

IN VIVO MONITORING OF BRAIN-ACTIVATION PATTERNS INDUCED BY OPTOGENETIC VTA-STIMULATION IN RATS: SPECT-IMAGING OF REGIONAL CEREBRAL BLOOD FLOW VERSUS BOLD FMRI

D. Vincenz[1], M.J. Brocka[1], F. Angenstein[2], F.W. Ohl[1], M.T. Lippert[1], J. Goldschmidt[1]
[1]Systems Physiology of Learning, Leibniz Institute for Neurobiology, Magdeburg, Germany
[2]Special Lab for Noninvasive Brain Imaging, Leibniz Institute for Neurobiology, Magdeburg, Germany

Objectives:

Optogenetic stimulation of neuronal circuits is increasingly used for manipulating behavior and analyzing functional connectivities in the brains of laboratory animals. Mapping the brain-wide effects of these stimulations is crucial for understanding the link between behavioral output and activated circuits. The effects of stimulations can be imaged in vivo using BOLD-fMRI but this technique requires the animals to be restrained inside the scanner and is commonly performed in anesthetized animals.
We have recently introduced a novel approach for imaging brain-wide effects of stimulations in awake behaving rodents (Kolodziej et al., 2014). We intravenously injected rodents with the blood-flow tracer 99mTc-HMPAO during ongoing behavior and mapped the distribution of the trapped tracer after stimulation using single-photon emission computed tomography (SPECT). We here compared brain-activation patterns as revealed by 99mTc-HMPAO SPECT versus BOLD-fMRI in rats upon optogenetic stimulation of the VTA. We used wild-type rats expressing channelrhodopsin-2 in principal neurons of the VTA and TH-Cre-rats expressing ChR2 in dopaminergic neurons. We studied anesthetized animals with both methods and awake animals with SPECT.

Methods:

Wild type and TH-Cre Long Evans rats were infused with viral solutions (AAV2/5-CamKIIa-C1V1-p2a-eYFP or AAV2/5-EF1a-DIO-ChR2(H134R)-eYFP resp.) into the left VTA and implanted with a custom made optical fiber assembly. The effectiveness of the optogenetic stimulation was tested by training the animals for self-stimulation. In the imaging studies rats were passively stimulated. Optical stimulation consisted of 8 light-bursts spaced one second apart and followed by 52 s of rest. This sequence was repeated ten times for each animal.
fMRI measurements were performed using an EPI sequence on a 4.7 T animal scanner. Animals were initially anesthetized with isoflurane. Anesthesia was maintained with domitor.
For SPECT-imaging rats were implanted with jugular vein catheters. Animals were injected with ^{99m}Tc-HMPAO and scanned in four subsequent sessions (counterbalanced design): stimulation awake, stimulation under the same anesthesia conditions as in the fMRI experiments, no stimulation awake and no stimulation anesthetized. After tracer injection animals were anesthetized and co-registered SPECT/CT scans were made. SPECT-images were fused with MR-images using CT landmarks, normalized and statistically analyzed in a voxelwise manner.

Results:

Both methods, BOLD-fMRI and 99mTc-HMPAO SPECT, showed stronger signal changes upon stimulation of principal neurons in the VTA of wild-type rats versus stimulation of dopaminergic neurons in TH-Cre-rats. The most widespread network of activated brain areas, including the stimulated VTA, accumbens nucleus and prefrontal cortex was visualized with SPECT-imaging in awake wild-type rats. Anesthesia markedly suppressed stimulus-induced signal changes as revealed by comparison with SPECT-imaging and BOLD-fMRI under anesthetized conditions.

Conclusion:

Our study supports the view that anesthesia reduces stimulus-induced signal changes in metabolic imaging methods and BOLD-fMRI. Larger networks of activations are present and / or can be detected in the awake state. 99mTc-HMPAO SPECT imaging can provide images from brain activation patterns in awake behaving rodents in a similar manner as 18F-FDG-PET, but with higher spatial and temporal resolution. The technique is well suited for in vivo imaging of brain-wide effects of optogenetic stimulations.

References:

Kolodziej A et al. (2014) NeuroImage 103:171-80.

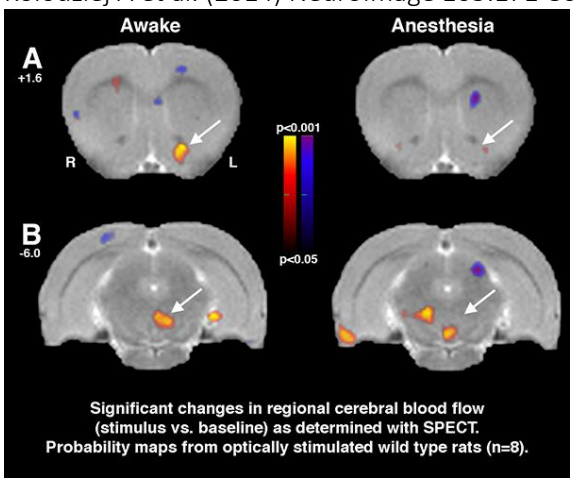

533
BRAIN-0694
Poster Session

Imaging Pre-Clinical

RECONSTRUCTION OF DEPTH-RESOLVED FIBER ORIENTATIONS IN THE BRAIN WITH POLARIZATION SENSITIVE OPTICAL COHERENCE TOMOGRAPHY

H. Wang[1], *D. Boas*[1], *T. Akkin*[2]
[1]*Radiology,*
Massachusetts General Hospital/ Harvard Medical School, Charlestown, USA
[2]*Biomedical Engineering, University of Minnesota, Minneapolis, USA*

Objectives

Neuroanatomical pathways form the structural basis of complex brain functions. Our previous polarization sensitivity optical coherence tomography (PS-OCT) studies have shown that neuronal fibers can be visualized and their orientations quantified with microscopic

resolution [1, 2]. One caveat with PS-OCT is that while it provides a clear measure of neuronal fiber tract orientation in the transverse imaging plane in superficial layers of the tissue, the measured orientation in deeper layers is confounded by differing orientations in superficial layers. The objective of our present effort is to resolve this problem and obtain depth-resolved fiber orientation maps with PS-OCT.

Methods

With our PS-OCT setup, circularly polarized light is incident on the sample. Light back scattered from the tissue is detected in orthogonal polarization channels. Birefringent tissue can be modeled with a Jones matrix of a linear retarder (δ) and a rotation matrix ($R(\vartheta)$),

$$J = R(\theta)\begin{pmatrix} e^{ik\delta} & 0 \\ 0 & e^{-ik\delta} \end{pmatrix} R(-\theta)$$

where δ is the retardance and ϑ is the fast optic axis. For samples with fixed axis in depth, $\delta(z)$ and $\vartheta(z)$ are obtained from the complex depth profiles ($A_{1,2}(z)exp\{i\Phi_{1,2}(z)\}$) on the two channels [1].

$$\delta(z)=arctan(A_1(z)/A_2(z))$$

$$\vartheta(z)=(\Phi_1(z)-\Phi_2(z))/2-\vartheta_0$$

ϑ_0 is an offset induced in the polarization maintain fiber (PMF) of our setup, which is constant in depth and can be removed with a reference calibration [3].

For samples having two layers with different axes, the Jones matrix after double-passing the sample is

$$J_{s2}=J_1^T J_2^T J_2 J_1 = J_1^T (J_2^T J_2) J_1$$

where J_1 and J_2 represent Jones matrices for the first and second layers, respectively. As J_1 and J_{s2} can be reconstructed from the measurements in depth, the Jones matrix for layer 2 is derived by

$$J_2^T J_2=(J_1^T)^{-1} J_{s2} (J_1)^{-1}$$

The retardance and optic axis orientation for the second layer are computed from the eigenvalues and the eigenvectors of the matrix $J_2^T J_2$. Therefore, the depth-resolved optic axis for an n-layer tissue with varied axis can be derived iteratively.

$$J_n^T J_n=(J_{c\_n-1}^T)^{-1} J_{sn} (J_{c\_n-1})^{-1}$$

where

$J_{sn}=J_1^T J_2^T \ldots J_{n-1}^T J_n^T J_n J_{n-1} \ldots J_2 J_1$ and $J_{c\_n-1}=J_{n-1}\ldots J_2 J_1$.

Results

We validate the algorithm by imaging two retarder films (retardance: 38.8° at 1300 nm wavelength) stacked together. The axis of the second retarder was fixed at 0° (along the horizontal axis), and the axis of the first retarder was rotated from -90° to 90° with an interval of 10°. The direct measures of retardance and the optic axis orientation for the second retarder change with the rotation angle of the first retarder, while after correction the result matches the prediction (Fig. 1).

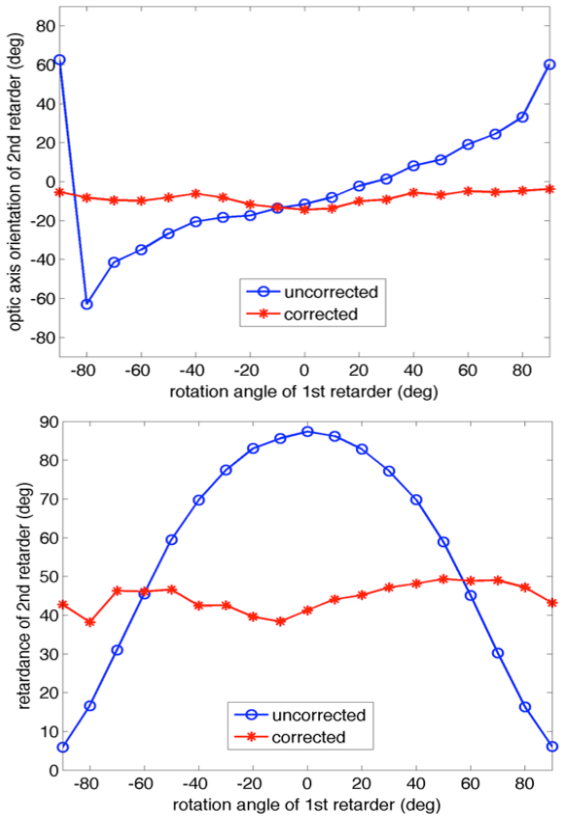

Fig. 1 The optic axis orientation (left) and retardance (right) of the second retarder film before and after correcting the effect of the first retarder.

We will conduct experiments in brain tissue and show the depth-resolved fiber orientation maps.

Conclusions

We have previously demonstrated neuronal fiber orientation maps with a PS-OCT. Here, a Jones matrix based algorithm is shown to resolve the depth-varying axis problem and attain the correct depth-resolved optic axis orientation. The study is important in creating high-resolution maps of neuronal pathways in the brain.

References

1. Wang et al, *Opt. Lett.* **35**, 154–156 (2010).

2. Wang et al, *Neuroimage* **58**, 984–992 (2011).

3. Wang et al, *Neuroimage* **84**, 1007–1017 (2014).

534
BRAIN-0851
Poster Session

Imaging Pre-Clinical

ASSESSING THE SIGNIFICANCE OF MULTIPLE ENZYME-BOUND FORMULATIONS OF CEREBRAL NADH RESOLVED BY IN VIVO 2-PHOTON LIFETIME MICROSCOPY

M.A. Yaseen[1], *S. Sakadžić*[1], *W. Wu*[1], *B. Fu*[1], *D.A. Boas*[1]
[1]*Martinos Center for Biomedical Imaging, Massachusetts General Hospital, Charlestown, USA*

Objectives

Understanding cerebral energy metabolism and its pathological alterations requires nondestructive measurement techniques with high spatial and temporal resolution. Here, we utilize 2-photon fluorescence lifetime imaging (2P FLIM) to collect minimally-invasive, *in vivo* measurements of various enzyme-bound formulations of reduced nicotinamide adenine dinucleotide (NADH), the electron carrier that plays a prominent role in both anaerobic glycolysis and aerobic oxidative metabolism. Previous reports suggest that the enzymatic formulations, or species, of NADH constitute more specific indicators of glycolysis or oxidative metabolism[1]. In an effort to more thoroughly explore their significance, we observed the effects of well-characterized metabolic inhibitors on the fluorescence lifetime signatures of these multiple NADH species *in vivo* using a cranial window model.

Methods

2P imaging was performed through sealed cranial windows in male Sprague Dawley rats over the somatosensory cortex. A gravity-feed perfusion system was developed to topically administer solutions to the exposed cortex through the sealed cranial window. Animals were mechanically ventilated, anesthetized, and

cannulated. Blood pressure, body temperature, and blood gases were monitored continuously during surgical preparation and the experiment. Time-Correlated Single Photon Counting (TCSPC) hardware was used to control the 2P portion of our custom-designed, multimodal imaging system. FLIM measurements of NADH autofluorescence were performed before and after administering chemical reagents to modulate either glycolysis, the citric acid cycle, the electron transport chain, or oxidative phosphorylation, or to induce seizure activity.

Results

Four distinct NADH species, with fluorescence lifetimes ranging from picoseconds to nanoseconds, were identified using custom-designed multi-exponential fitting software. Chemically-induced seizures or manipulations of the Kreb's cycle and oxidative phosphorylation induce notable, distinct changes in the NADH intensity and the relative proportions of these NADH species.

Conclusions

2P fluorescence lifetime imaging allows for resolution between different enzyme-bound states of NADH, extending its utility to indicate metabolic activity with greater specificity. Analyzing the relative proportions of NADH species shows promise to provide more comprehensive information than NADH intensity measurements, potentially indicating inhibition of different metabolic pathways. NADH FLIM measurements could ultimately lead to a deeper understanding of cerebral energetics and its pathology-related alterations. Such knowledge will aid development of therapeutic strategies for neurodegenerative diseases such as Alzheimer's Disease, Parkinson's disease, and stroke.

References

1. H. D. Vishwasrao, A.A. Heikal, K.A. Kasischke, W.W. Webb "Conformational Dependence of Intracellular NADH on Metabolic State Revealed by Associated Fluorescence Anisotropy," Journal of Biological Chemistry 280, 25119-25126 (2005).

535
BRAIN-0787
Poster Session

Imaging Clinical

MAPPING BRAIN RESPONSE TO AN ADENOSINE A2A ANTAGONIST USING [11C]SCH442416 PET AND ARTERIAL SPIN LABELING (ASL) CEREBRAL BLOOD FLOW (CBF) PERFUSION MAGNETIC RESONANCE IMAGING

R.D. Newbould[1], C. Bishop[1], G. Searle[1], A.P. Brown[1], R.N. Gunn[1], E.A. Rabiner[1]
[1]Applications,
Imanova Centre for Imaging Sciences, London, United Kingdom

Objective:

A_{2A} (adenosine) antagonists are being developed for the treatment of Parkinson's disease. A_{2A} receptors are located in the vasculature, as well as neurons, with the highest density in the striatum but significant levels in several areas including the thalamus, hippocampus, and cerebellum [1]. This study quantified A_{2A} receptor occupancy of V81444 [2] using [^{11}C]SCH442416 PET [3] and ASL MRI CBF in the same subjects.

Methods:

Six healthy males (28-51y) underwent PET immediately followed by MRI at baseline and ~3 hours after 50, 100, or 250 mg of V81444. A third PET scan was performed ~23 hours post-dose. MRI ASL was performed at 3T using PICORE [4] with Q2TIPS to cutoff the 10cm labelling region 22mm proximal to the imaging slices and inflow time (1800ms) to reduce residual arterial signal [5], bolus cutoff time (TI_{1s}) 1600ms, and bolus durations (TI_1) 700, 1000, and 1300ms. Seventeen 5mm slices were acquired (240x240 FOV, 64x64 matrix, TE=11ms, TR=2500ms) from each of 30 tag/control pairs for each of 3 series of 2m:40s.

Bolus width (τ) and CBF were determined using nonlinear fitting to the single compartment model of the tag/control signal difference: $\Delta S = 2\alpha \cdot CBF \cdot (M_0/\lambda) \cdot \tau \cdot exp(-TI_2(\text{slc})/T1_a)$. To differentiate vascular A_{2A} effects from local neuronal effects the local CBF values were scaled to the global CBF value for grey matter (GM) ROI analysis. PET-derived receptor occupancy (RO) was determined from the binding potential relative to the non-displaceable component (BP_{ND}) in the putamen using the simplified reference tissue model. ROIs for both PET and ASL were derived from an isotropic MPRAGE acquired at each MRI session.

Results

PET data were consistent with a direct kinetic model between plasma and receptors. RO was determined to be 64-100% during the ASL acquisitions, dependent on dose. Global GM CBF was seen to decline an average of 11.4% from baseline across all doses. After normalizing to the global CBF, local CBF increases were detected in the globus pallidus and the thalamus. CBF in the thalamus could be related to the dose, with a trend towards a relationship to RO.

Conclusions

Administration of V81444 significantly reduced global GM CBF as determined by ASL data acquired ~3 hours after administration, which had near-complete receptor occupancy in most doses. A dose-ASL CBF response was noted in the pre-selected ROI of the thalamus, with a trend to a RO-CBF relationship. A study of another A_{2A} antagonist, SYN115, [6] detected a 7% CBF decrease globally and 12% in the thalamus. Caffeine, a less selective A_{2A} antagonist, is associated with vasoconstriction and reduced cerebral blood flow of up to 35% [7]. This study was limited due to the small numbers studied, but also cannot rule out order effects and diurnal variations as the baseline and post-dose scans were acquired in a fixed order.

References:

[1] Moreau, Brain Research Reviews 31:65-82,1999.
[2] Brown, J Neurological Sciences 333:e125,2013.
[3] Moresco, Eur J Nucl Med Mol Imaging 32:405-413,2005.
[4] Luh, MRM 41:1246-1254,1999.
[5] Donahue, NMR Biomed 19:1043-1054,2006.
[6] Black, JNeuroscience 30:16284-16292,2010.
[7] Perthen, NeuroImage 40:237-247,2008.

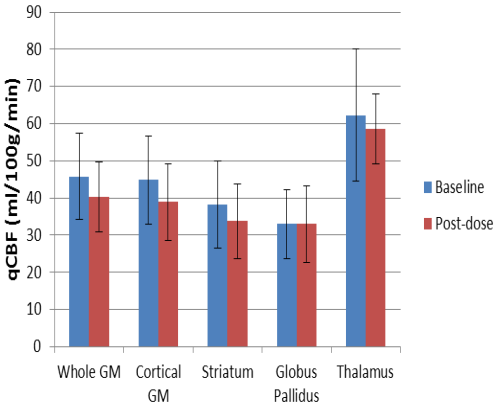

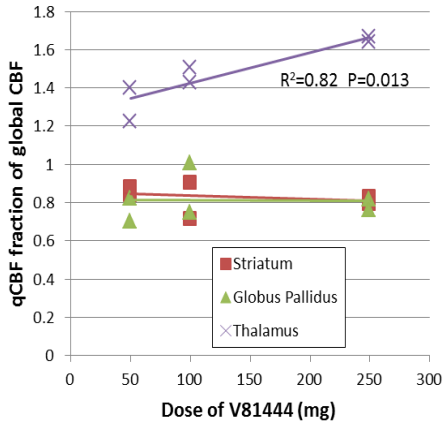

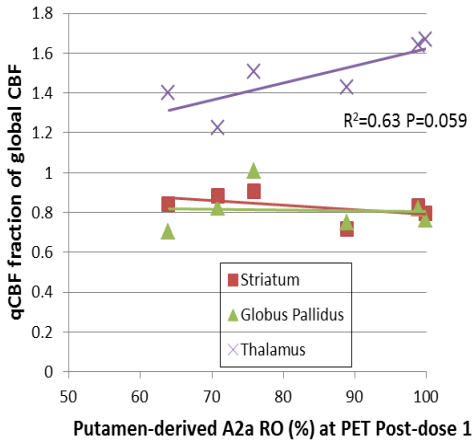

536
BRAIN-0873
Poster Session

Imaging Clinical

IMPROVED ACCURACY OF DIFFUSE CORRELATION SPECTROSCOPY BRAIN PERFUSION MEASUREMENTS USING MULTI-DISTANCE MEASUREMENTS IN CONJUNCTION WITH A MONTE CARLO LIGHT TRANSPORT MODEL

OBJECTIVES: The emerging technique of Diffuse Correlation Spectroscopy (DCS [1,2]) offers an alternative way to directly estimate cerebral blood flow (CBF), and the combination of DCS and near-infrared spectroscopy (NIRS) measurements can offer robust quantification of the cerebral metabolic rate of oxygen (CMRO2). However, both techniques employ diffusely reflected light that has traveled mostly through extracerebral tissues. Recent studies indicate that depth sensitivity profiles are different for NIRS vs DCS measurements, with DCS appearing to be more sensitive to the brain than NIRS methods for a given source-detector separation [3,4]. This mismatch can lead to erroneous conclusions not only with respect to the amount but also to the direction of change in CMRO2. Previously, theoretical two or multi-layer theoretical models based on the correlation diffusion equation have been developed for improving the accuracy of DCS-based perfusion measurements in layered media [5,6]. However these models are limited by their assumption of a flat, infinite slab geometry. Recently, our group has demonstrated the use of Monte Carlo (MC) based multi-layer, multi-distance fitting [7], which offers increased accuracy for complex tissue structures such as the adult brain. In this paper we present a method to employ a realistic head geometry that can be derived from MRI scans (if available) or approximated from head shape measurements.

METHODS: We combine DCS measurements taken at two or more distances with a MC based forward model (based on a version of the tMCimg Monte Carlo software package [8] modified to store momentum transfer at each scattering event). The MC head geometry is a variable thickness 2-layer model derived from the external head surface by sequentially eroding 22 1-mm thick tissue layers (Fig. 1a, colorbar indicates layer index). Photon history from the superficial and deep layer groups, respectively, was concatenated to achieve an effective 2-layer representation.

RESULTS: A key element in multi-layer modeling is determining the layer thickness. Fig. 1b shows the fitting residual variation vs the thickness of the superficial layer for an adult human subject. The residual has a clear minimum at a value close to the actual scalp+skull thickness measured on the subject's MRI scan. Figs. 1c and 1d demonstrate that the MC based model results in more realistic estimates of the increase in cerebral blood flow (CBF) due to a 4/8 mmHg etCO2 hypercapnic challenged as well as increased CBF timecourse signal to noise ratio vs. the analytical model fit.

CONCLUSIONS: Monte Carlo based analysis of multi-distance DCS measurements of cerebral perfusion variation offers improved quantitation vs. the commonly employed semi-infinite correlation diffusion equation model and can be performed even in the absence of detailed structural information as long as measurements of the external head geometry are available.

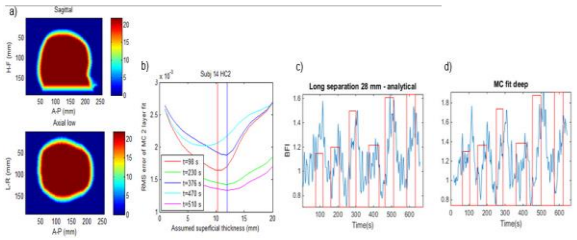

Figure 1 a) Multi-layer MC geometry definition; b) Fitting residual vs. assumed superficial thickness at several timepoints (the red vertical line represents the MRI estimate, while the blue line is the median thickness derived from fitting DCS data); c) Long separation analytical fit of CBF changes during hypercapnia; d) brain perfusion changes estimated through the multi-distance MC based fit of the same data

References: 1. Boas D.A, et al., PRL, 75(9), p1855 (1995). 2. Buckley E.M. et al., Neurophoton., 1(1), 011009 (2014) 3. Buckley E.M. et al., JBO, 17(3), Art. 037007 (2012). 4. Selb J. et al., Neurophoton., 015005 (2014) 5. Li J. et al., JBO, 10(4), Art. 44002 (2005). 6. Gagnon, L. et al. Opt. Expr, 16(20), p.15514 (2008). 7. Carp S.A. et al. OSA BIOMED 2014 BM3A.20. 8. Boas D.A. et al., Opt. Expr. 62(3), p.1999 (2002).

537
BRAIN-0773
Poster Session

Imaging Clinical

CEREBRAL METABOLIC RATE OF GLUCOSE (CMRG) IN COGNITIVELY-NORMAL OLDER PERSONS: IS LOWER CMRG IN THE FRONTAL CORTEX A FEATURE OF NORMAL AGING?

S.C. Cunnane[1], *S. Nugent*[1], *C.A. Castellano*[1], *T. Fulop*[2]
[1]*Clinical Axis, Research Centre on Aging, Sherbrooke, Canada*
[2]*Medicine, Université de Sherbrooke, Sherbrooke, Canada*

Introduction: Lower cerebral metabolic rate of glucose (CMRg) is present pre-symptomatically, i.e. before the onset of cognitive decline, in the temporal and parietal cortex in those at genetic or familial risk of Alzheimer's disease (AD). Old age is a risk factor for AD, but it is unclear whether regional CMRg differs in cognitively-healthy older people or whether regional CMRg should be age-normalized when cognitive tests are normal in older people.

Objective: The primary aim of the present study was to quantify whole brain and regional CMRg in young and older adults with normal cognitive scores.

Methods: Participants were 25±4 years old (Young adults; n=34), or 72±5 years old (Older adults; n=41). All participants completed an extensive cognitive battery. Exclusion criteria included a Mini-Mental State Examination (MMSE score <26/30), smoking, diabetes or glucose intolerance. T_1-weighted MR images were acquired on a 1.5 Tesla scanner. Dynamic brain FDG-PET scans were acquired and automatically co-registered to each participant's respective MR image (PMOD 3.3). Co-registered PET images were corrected for partial volume effect (PVE) (Nugent et al, 2014). CMRg was then quantified and expressed as µmol/100 g/min using the graphical Patlak method within each ROI defined by FreeSurfer Suite 5.0 (Nugent et al, 2014). Percent differences in regional CMRg underwent a $p \leq 0.01$ false discover rate (FDR) correction.

Results: There was no statistical difference in the scaled cognitive scores between the two age groups in either the speed processing or executive function domains ($p>0.20$). Older participants scored 9–10% higher than the young group in immediate and delay recall tasks from the Rey complex figure test ($p \leq 0.001$). Compared to the Young adults, PVE-corrected CMRg in the Older group was 7% lower in whole brain (31±4 vs. 33±5 µmol/100 g/min; p=0.028), 7% lower in cortical gray matter (33±4 vs. 35±5 µmol/100 g/min; p=0.030), 8% lower in sub-cortical regions (24±3 vs. 26±3 µmol/100 g/min; p=0.005), but not different in white matter (21±3 vs. 23±3 µmol/100 g/min; p=0.075). In the Older group, FDR- and PVE-corrected regional CMRg was 11%

lower in the inferior parietal cortex ($p \leq 0.002$), 18% lower in the caudate ($p \leq 0.001$) and lower in seven frontal cortical regions: superior frontal (-14%, $p \leq 0.001$), rostral middle frontal (-11%, $p = 0.003$), caudal middle frontal (-14%, $p \leq 0.001$), pars opercularis (-10%, $p \leq 0.003$), pars triangularis (-10%, $p \leq 0.003$).

Conclusions: Lower CMRg in the inferior parietal cortex is seen in AD so it's presence in cognitively-normal older persons may be indicative of an increased risk of cognitive decline associated with AD. However, lower CMRg in frontal cortical regions and in the caudate are not commonly not reported in AD so their presence in our Older group appears to be a normal feature of brain metabolism in older people with normal age-corrected cognitive scores.

References: Nugent S et al, Neurobiol Aging 35, 1386-1395, 2014

Acknowledgements: Supported by the FRQS, CIHR, CFI, CRC, Université de Sherbrooke Research Chair (SCC), CFQCU program of the FQRNT and INAF.

538
BRAIN-0839
Poster Session

Imaging Clinical

THE ROLE OF METHIONINE POSITRON EMISSION TOMOGRAPHY IN THE EVALUATION OF CENTRAL NERVOUS SYSTEM TUMORS IN CHILDREN

T. Danfors[1], V. Velickaite[2], N. Canto Moreira[2]
[1]Surgical Sciences,
Section for Nuclear medicine and PET, Uppsala, Sweden
[2]Surgical Sciences Uppsala University,
Section for Radiology, Uppsala, Sweden

Objectives

Tumors of the central nervous system rank amongst the most common in pediatric age. They constitute a heterogeneous group, ranging from low-grade astrocytomas and glioneuronal tumors to highly aggressive medulloblastomas and ependymomas.

The diagnostic workup for pediatric tumors is CT, MRI, but other special modalities such as PET may be used to evaluate the degree of malignancy and cell proliferation [1] , surgical planning [2] or response to therapy [3].

Positron emission tomography with [11C]Methionin (MET PET) reflects areas of high cellular proliferation and microvascular density [4], that may help to identify tumors and even differentiate radiation necrosis from tumor recurrence [5].

PET studies of the brain have been performed clinically in children at the Uppsala University hospital since the mid- 80's and the total number of examinations is more than 200, making this center one of the most experienced in Europe

In this study the results from the last ten years use of MET PET in children (below 18 at their first examination). We aimed to answer the following questions:

1) What was the reason for the PET examination?

2) If the question was tumor-not tumor, how many were correctly answered by PET ?

3) What tumor types have been investigated?

4) How did the uptake ratio vary between the different tumor types?

Methods

The uptake ratio (i.e. maximum intensity of MET uptake compared to the average uptake at the contralateral cortex) was measured in all PET MET scans

Information about surgery, diagnosis, treatment and if the patient is alive or was collected from the hospital files.

Results

81 scans were performed on 61 patients (14 patients had two scans, 2 had three and 1 had four scans.

	Reason for PET:	Number of scans	Number of patients
A	Tumor- not tumor on a new untreated lesion	24	23
B	Malignancy grade where biopsy is not possible - Brainstem	6	6
C	Malignancy grade where biopsy is not possible – Brain	6	4
D	Tumor recurrence after surgery, radiation and/or chemo therapy	21	12
E	Tumor recurrence after surgery only	13	10
F	Metastases - medulloblastoma	2	1
G	Pituitary tumor	9	5
	Total	**81**	**61**

21 patients never went through surgery. Of the remaining 40 were 16 astrocytomas, 1 oligoastrocytoma, 3 oligodendroglioma, 9 ependymoma, 1 craniopharyngeoma, 1 gliomatosis cerebri, 2 DNET, 1 PNET, 1 ganglioglioma, 1 germinoma, 1 hemangiotelioma, 2 medulloblastoma, and a Arnold Chiarii malformation.

Twenty-three patients with new untreated lesions (group A) were investigated. Of these 23 were 12 operated at and MET PET could preoperative correctly identify a tumor on all but one of them (Arnold Chiarii malformation and cerebellar oedema were mistaken for a low-grade tumor). Tumors with elevated MET uptake in this group were astrocytomas, oligodendrogliomas, oligoastrocytomas, ependymomas, craneopharyngeomas and gliomatosis cerebri.

Tumors with normal or decreased uptake were DNET and PNET.

Conclusions

Methionine PET has the possibility to provide important information in the management of children and young adults with brain tumors. In particular it is valuable to differentiate between tumors and non-tumorous lesions.

539
BRAIN-0147
Poster Session

Imaging Clinical

KETAMINE-INDUCED CHANGES IN [11C]ABP688 BINDING IN HEALTHY AND DEPRESSED HUMAN SUBJECTS

I. Esterlis[1], N. DellaGioia[2], D. Matuskey[1], G. Sanacora[2], N. Nabulsi[3], C. Abdallah[2], J. Yang[4], J. Krystal[2], R. Parsey[5], R. Carson[6], C. DeLorenzo[7]
[1]Psychiatry and Diagnostic Radiology, Yale School of Medicine, New Haven, USA
[2]Psychiatry, Yale School of Medicine, New Haven, USA
[3]Diagnostic Radiology, Yale School of Medicine, New Haven, USA
[4]Preventive Medicine, Stony Brook University, Stony Brook, USA
[5]Psychiatry Radiology, Stony Brook University, Stony Brook, USA
[6]Diagnostic Radiology Biomedical Engineering, Yale School of Medicine, New Haven, USA
[7]Psychiatry Biomedical Engineering, Stony Brook University, Stony Brook, USA

Background: Ketamine, an uncompetitive NMDA receptor antagonist, rapidly improves depressive symptomatology; however, its mechanisms of action have not been fully elucidated. We previously showed that ketamine administration leads to a reduction in [^{11}C]ABP688 (negative allosteric modulator of metabotropic glutamate receptors, subtype 5) binding in healthy controls (HC), likely due to ketamine-induced surge in glutamate [1]. The present study examined whether

1) this ketamine-induced change is different in individuals with major depressive disorder (MDD); 2) the changes in binding are related to changes in mood in MDD; and 3) the observed changes in [^{11}C]ABP688 are prolonged.

Methods: Thirteen healthy (33.1±13.1 years) and 8 MDD (32.4±12.6 years) nonsmokers participated in two 60-min bolus [^{11}C]ABP688 PET scans on the same day – before (baseline) and during i.v. ketamine administration (0.23mg/kg over 1min, then 0.58mg/kg over 1h; ketamine began 1 min after tracer injection) and a third 60 min bolus [^{11}C]ABP688 PET scan 1 day after ketamine administration. Distribution volume, V_T, was estimated using metabolite-corrected arterial input functions. Mood assessments were administered before, immediately after, and 1 day post ketamine.

Results: We did not observe a significant difference in baseline V_T between control and MDD groups (p>0.1). We observed a significant reduction from baseline V_T during administration of ketamine in both MDD and control subjects (average of 14.5±7.2% and 20.1±22.9%, respectively, in the grey matter regions). A significant reduction (11.7±13.7% and 15.8±27.0% in MDD and HC, respectively) in V_T remained 24-hours after ketamine administration. Ketamine-induced V_T differences were not significantly different between diagnostic groups at either time point. There was a significant reduction in depressive symptoms following ketamine administration (57% following ketamine administration and 70% day after ketamine) in the MDD group. Importantly, we observed a trend positive association between change in binding and change in mood symptoms immediately after ketamine administration in the MDD group (p=0.07), but not at the 1-day assessment.

Conclusion: We found ketamine-induced decreases in radioligand binding, likely driven by glutamate release, in both MDD and control subjects. Interestingly, 1 day after ketamine administration, there appears to remain a decrease in radioligand binding in both HC and MDD groups. This may be explained by residual glutamate increases, receptor internalization due to the rapid increase in glutamate, or other effects of ketamine that may cause downstream effects at mGluR5. Importantly, in the MDD sample, greater changes in ligand binding were associated with greater decrease in depressive symptomatology after ketamine administration. Although the variability in response is large, especially 1-day post ketamine, this study may provide insight into ketamine's mechanism of action and potentially imaging-based prediction of response.

REFERENCES

1. DeLorenzo C, DellaGioia N, Bloch M, Sanacora G, Nabulsi N, Abdallah C, Yang J, Wen R, Mann J, Krystal J, Parsey R, Carson R, Esterlis I. In Vivo Ketamine-Induced Changes in [11C]ABP688 Binding to Metabotropic Glutamate Receptor Subtype 5. *Biol Psychiatry.* 2014;77:266-275.

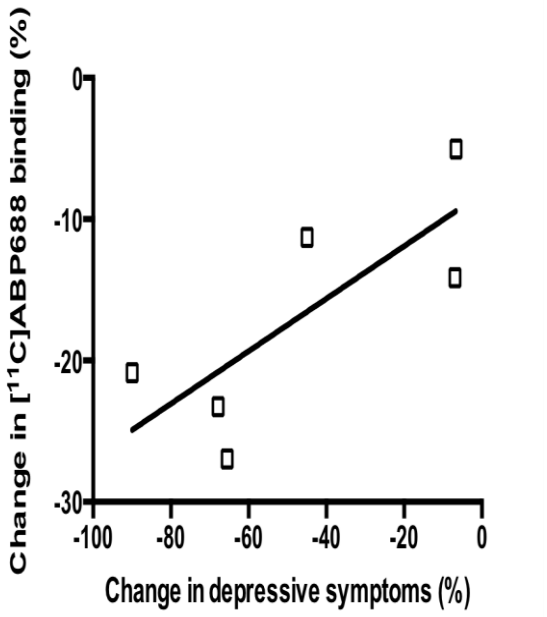

540
BRAIN-0758
Poster Session

Imaging Clinical

MOLECULAR AND STRUCTURAL AGE-RELATED CHANGES IN THE BASAL GANGLIA. A HIGH RESOLUTION PET STUDY WITH 11C-RACLOPRIDE AND 18F-MNI-659 .

P. Fazio[1], M. Schain[1], L. Mrzljak[2], N. Amini[1], N. Al-Tawil[3], C. Fitzer-Attas[2], J. Bronzova[2], B. Landwehrmeyer[2], C. Sampaio[2], C. Halldin[1], A. Varrone[1]
[1]Department of Clinical Neuroscience Centre for P sychiatry Research, Karolinska Institutet, Stockholm, Sweden
[2]CHDI, Foundation, Princeton, USA
[3]Karolinska Trial Alliance, Karolinska University Hospital, Stockholm, Sweden

Objectives

Dopamine D2 receptors (D2R) and phosphodiesterase 10A enzyme(PDE10A) are two striatal molecular targets that might be useful for the evaluation ofpatients affected by neurodegenerative disorders (e.g Huntington disease). In the basal ganglia, the two targets might beinfluenced by age and age-related structuralchanges. These changes along with the limited resolution of PET might lead to underestimation of the outcome measures. The aim of thisstudy was to examine the relative distribution of PDE10A and D2 receptors in the differentsubdivisions of the basal ganglia and toexamine the availabilitiesof PDE10A and D2 receptors in relation with age.

Methods

Fifteen control subjects (10M/5F, age: 46±11y, age range29-65) were examined with the High-Resolution Research Tomograph (HRRT) with the D2R radioligand^{11}C-raclopride and the PDE10A radioligand ^{18}F-MNI-659. Arterialinput functions were obtained for ^{18}F-MNI-659.

Definition of regionsof interest and morphometric assessment in the Striatum (STR) and globus pallidus (GP) was evaluated using FreeSurfer processing of 3T-MR images. PVE correction (PVEc) based onthe geometric transfer matrix approach was applied to PET data. Binding potential (BP_{ND}) for ^{11}Craclopride was estimated using the simplified reference tissue model with cerebellum as a reference region. $BP_{ND}$for ^{18}F-MNI659 was estimated indirectly, from distribution volumes (V_T) in striatum andcerebellum using Logan plot. The estimated cerebellar V_T (V_{ND})was corrected for blood volume. Differences between the two targets wereassessed with unpaired,two- tailed t-test (p<0.05). Linear regressionanalysis was used to assess correlations between D2R and PDE10A availability. The effect of age on the outcome measures and structuralvolumes was examined with a multiple linear regression analysis.

Results

^{18}F-MNI-659 BP_{ND} in the GP was significantly higher than D2R BP_{ND} (p<0.05). ^{18}F-MNI-659BP_{ND} and ^{11}C-racloprideBP_{ND} did not show eithersignificant differences (p=0.11) nor correlation (r=0.388, p=0.15) in the STR.A significant inverse correlation with age was found in the STR for ^{18}F-MNI-659BP_{ND} (beta= -0.499, p=0.013) and for thestructural volumes (beta = -0.459, p =0.013). D2R did not show significantcorrelations in this age range in either STR or GP. The PDE10A age-relateddecline per decade was 14.9% in the STR and 11.7% in GP. ^{11}C-raclopride BP_N decline rates were less evident in the STR (-4.2%per decade) and in the opposite direction for GP (+5.7 % each decade). Volume lossin STR (-4.7% per decade) was greater than in GP (0.38 %) (**Fig 1**).

Conclusions

The PDE10A enzyme shows a different distribution comparedwith the D2 receptor, with higher density in the GP. Striatal and pallidal PDE10A availability showedan age-related decline that was larger compared to the age-related

volume loss. Striataland pallidal D2R availability and volumes showed similar decline rates. These results indicate that aging is associated with aconsiderablephysiological reduction of the availability of PDE10A enzyme.Clinical PET studies examining the two targets in patients affected by basal ganglia neurodegenerationwill require adequate age-matchingand correction for PVE.

This study has been supported by CHDI Foundation Inc.

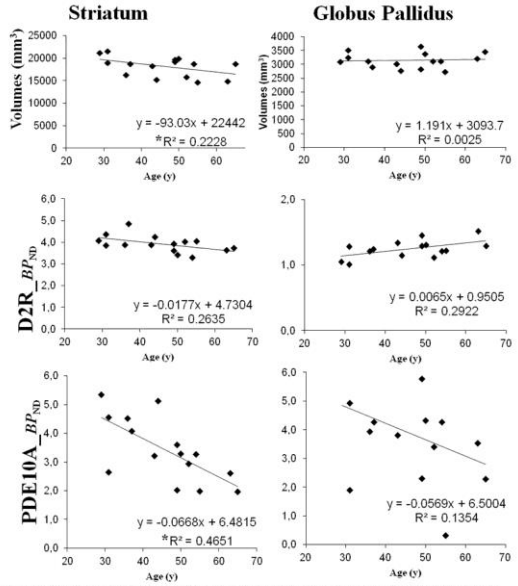

Fig 1. Relations between Volumes, D2R and PDE10A availability and Age. Freesurfer Volumes (mm^3), Binding potentials (BP_{ND}) of ^{11}C- raclopride and ^{18}F-MNI-659 were plotted against age (years) in the Striatum (left panels) and Globus Pallidus (right panels). * = $p<0.05$ (obtained with the multilinear regression analysis).

541
BRAIN-0343
Poster Session

Imaging Clinical

CHRONIC INFLAMMATION IN BRAIN PARENCHYMA DETECTED BY PET IMAGING OF TRANSLOCATOR PROTEIN FOLLOWING A SUBDURAL HEMATOMA, ABSENT OF MRI FINDINGS OF BRAIN INJURY

M. Fujita[1], C. Turtzo[2], C. Shenouda[3], E. Fennell[1], D. Rallis-Frutos[1], S. Zoghbi[1], S. Telu[1], J. Hong[1], J. Dsurney[3], V. Pike[1], R. Innis[1], R. Diaz-Arrastia[4], L. Latour[5]
[1]Molecular Imaging Branch, National Institute of Mental Health, Bethesda, USA
[2]Diagnostic Radiology, National Institutes of Health, Bethesda, USA
[3]Rehabilitation Medicine, National Institutes of Health, Bethesda, USA
[4]Center for Neuroscience and Regenerative Medicine, National Institute of Mental Health, Rockville, USA
[5]Acute Stroke Research Section, National Institute of Neurological Disorders and Stroke, Bethesda, USA

Objectives:
Neuroinflammation is presumed to impact the clinical course after traumatic brain injury (TBI). MRI is clinically used but in many patients, cannot detect injury to the brain despite prolonged clinical symptoms. The purpose of this study was to investigate whether PET imaging of translocator protein (TSPO) detects neuroinflammation in regions of parenchyma that appears normal on MRI.

Methods:
Two male subjects in their 60's were studied. Both had a significant unilateral subdural hematoma that required surgical drainage. The subjects had MRI and CT scans within two days of injury and around the time of the ^{11}C-PBR28 PET scans to image TSPO. A ^{11}C-PBR28 PET scan with metabolite-corrected arterial input function was performed for each subject 12 – 15 months after the brain injury, and total distribution volume, V_T, was calculated.

Results:
Other than the subdural hematoma, on MRI and CT within two days, neither of these subjects showed evidence of damage in brain parenchyma. MRI scans around the time of PET were absent of evidence of injury to the brain. However, subject #2 showed widespread MRI contrast enhancement of the meninges in the injured hemisphere, from frontal to parietal areas, suggesting persistent extra-axial inflammation. Subject #1 showed MRI contrast enhancement only in a limited parietal area.

The PET scans showed a marked ~20% increase of V_T, only in subject #2 but not in #1. The increase

in ^{11}C-PBR28 was widespread and matched the area that was compressed by the hematoma. Time stability of V_T was similar between affected and contralateral sides indicating that the increased binding was not an artifact by accumulating radiometabolites.

Conclusions:
Subjects with only a remote indication of meningeal inflammation in MRI may also have concomitant inflammation in the brain detectable by PET TSPO imaging. More subjects with similar MRI findings need to be studied.

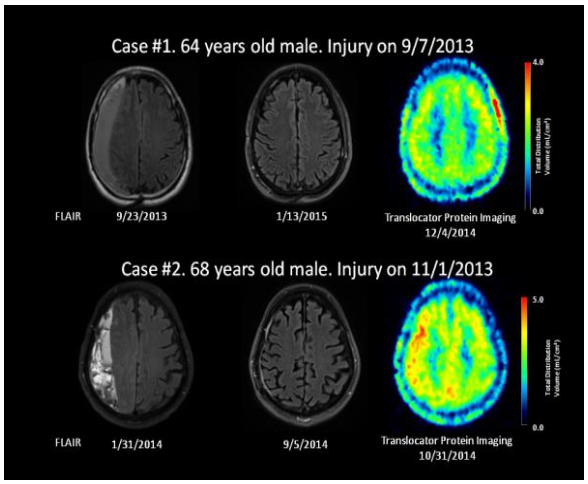

542
BRAIN-0700
Poster Session

Imaging Clinical

A BAYESIAN FRAMEWORK FOR THE ESTIMATION OF OEF BY CALIBRATED MRI

M. Germuska[1], A. Merola[1], A. Stone[2], K. Murphy[1], R. Wise[1]
[1]School of Psychology, Cardiff University, Cardiff, United Kingdom
[2]fMRIB, Oxford University, Oxford, United Kingdom

Introduction

The calculation of OEF from calibrated MR requires the analysis of ASL and BOLD data, which are typically analysed independently to determine changes in blood flow and BOLD signal (due to hypercapnic and hyperoxic stimuli) [1,2]. Sequential analysis of the data in this way has the potential to cascade errors along the analysis pipeline, producing large instabilities in the results. Here we present an analysis method that uses a forward signal model to simultaneously estimate all physiological parameters. Re-posing the problem as a forward model makes it amenable to numerical analysis and regularization. We use Bayesian fitting framework to stabilise the results with prior information.

Methods

The analysis framework incorporates a detailed model of the MRI perfusion signal (as acquired by ASL) [3] and a general BOLD signal model (equation 1) that can be applied to both hypercapnic and hyperoxic stimuli.

$$\text{Eq. 1.}\quad \frac{\Delta S}{S_0} = K\cdot([Hb]\cdot OEF_0)^{\beta}\cdot\left\{1-\left(\frac{f}{f_0}\right)^{\alpha}\cdot\left(\frac{f_0}{f}-\frac{1}{[Hb]\cdot OEF_0}\left[\frac{1}{\varphi}\left(CaO_2-\frac{f_0}{f}\cdot CaO_{2|0}\right)\right]+[Hb]\left(\frac{f_0}{f}-1\right)\right)^{\beta}\right\}$$

where the subscript '0' represents the baseline condition, S is the BOLD signal, f is cerebral blood flow, [Hb] is the haemoglobin concentration, ϕ is the oxygen carrying capacity of haemoglobin, CaO_2 is the arterial oxygen content, and K is a BOLD calibration parameter (proportional to the cerebral blood volume).

By combining the ASL and BOLD signal models a forward signal model, g(θ), is created to describe the acquired MR data, where the unobserved variables in this model are: OEF_0, f_0, f/f_0, K, M_0, ΔM_0, ΔT_1, $R_{2|0}{}^*$, and transit delay. The MR data (y) is then described by this forward signal model and additive noise (e), equation 2. Estimates of the unobserved variables (θ) and the noise variance are made using a variational Bayes approach [4], where the hyperparameters are optimised to produces a robust solution without significant bias of the physiological parameters.

$$\text{Eq. 2.}\quad y = g(\theta) + e$$

Results

The proposed method has been applied to dual-echo ASL data from 6 healthy volunteers. The acquired time series were each 18 minutes in duration and contained two periods of hypercapnia and four periods of hyperoxia interleaved with normocapnic/normoxic baseline periods. The resulting estimates of OEF are in the expected range, with a group mean grey matter OEF of 0.36 ± 0.08. Figure 1 shows an individual OEF map masked to show only grey matter voxels. The map appears smooth throughout the slice, although there is a region of high OEF in the anterior of the brain (possibly caused by the susceptibility effects of molecular oxygen in the anterior sinuses).

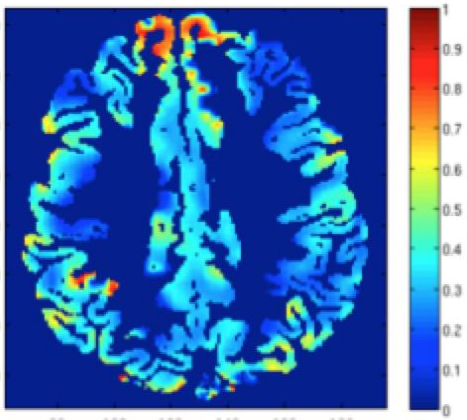

Figure 1. Grey matter OEF map for a single subject

Conclusions

The presented framework takes advantage of a detailed signal model and Bayesian analysis to produce stable estimates of OEF. Initial results are promising and the method is expected to improve the accuracy and reliability of in-vivo estimates.

References

[1] Bulte et al. Neuroimage (2012) 60(1):582-91 [2] Wise et al. Neuroimage (2013) 83:135-47
[3] Woolrich M et al. MRM (2006) 56:891-906 [4] Daunizeau J. et al. Physica D. (2009) 238: 1089-2118

543
BRAIN-0202
Poster Session

Imaging Clinical

TITLE: ASSESSMENT OF INTERNAL CAROTID ARTERY TERRITORY BEFORE AND AFTER CAROTID ENDARTERECTOMY BY REGIONAL PERFUSION IMAGING OF ARTERIAL SPIN LABELING

K. Hosoda[1], *D. Yamamoto*[1], *Y. Uchihashi*[1], *E.I.J.I. Kohmura*[1]
[1]*Neurosurgery,*
Kobe University School of Medicine, Kobe, Japan

[Purpose and background] An MR imaging technique known as arterial spin labeling (ASL) is useful because it allows noninvasive measurement of brain perfusion by using magnetically labeled blood as an endogenous tracer. Regional perfusion imaging (RPI) visualizes cerebral perfusion territories by selective ASL. We investigated change of internal carotid artery (ICA) territory before and after carotid endarterectomy in carotid stenosis by RPI.
[Methods] We prospectively recruited patients who were being considered for carotid endarterectomy because of carotid stenosis. Exclusion criteria were the followings: hypoplastic A1, contralateral carotid stenosis, intracranial artery stenosis. All subjects underwent RPI with 3 tesla MRI. MRI sequence with the following parameters were used: the field of view (FOV) = 240mm, matrix = 64x64, number of slices=7slices (thickness = 6mm, gap = 2mm), TR/TE/ = 4000/22.0 ms, flip angle = 35°, TI1/ΔTI = 43/300 ms (13 time points), SENSE factor = 2.5, averages = 24 (for label or control), acquisition time = 3 minutes 20 seconds. Seven axial slices of RPI covered upper part of the cerebrum, basal ganglia, and cerebral lobes. Perfused volume of each ICA was calculated from perfused area and thickness of slices. Asymmetry Index (AI) was also calculated from perfused volume of ICA on each side. Ipsilateral ICA flow was measured by electromagnetic flowmeter before and after CEA. Healthy volunteers also underwent RPI as normal control group.
[Results] (1) This study includes 11 controls (7 men, mean age 43.5 years) and 31 patients with carotid stenosis (28 men, mean age 73.4 years, CEA 26, CAS 5). The carotid stenosis group was significantly older than control group.

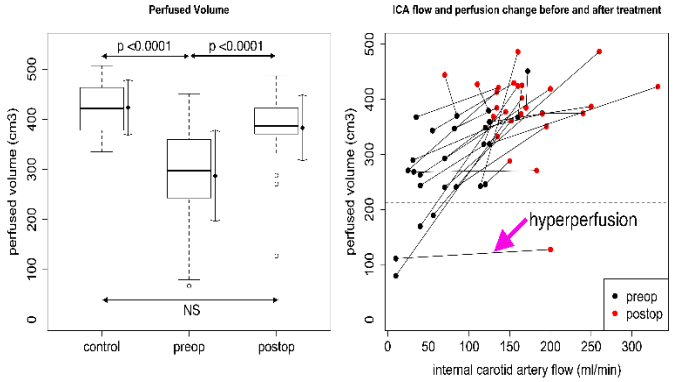

(2) Preoperative PV of carotid stenosis (287cm3) was significantly smaller than controls (424cm3), and postoperative PV significantly increased to the normal level (383cm3) (Figure left). (3) Preoperative AI of carotid stenosis (0.66) was significantly lower than controls (0.98), and postoperative AI significantly increased (0.98). (4) In 5 carotid stenosis patients with PV<50% of controls (212 cm3), PV of the 4 patients increased to >212 cm3 after surgery. However, 1 patient showed no increase of PV (111 to 127 cm3) and ICA flow dramatically increased from 10 to 200 ml/min, resulting in postoperative hyperperfusion (Figure right).
[Conclusions] (1) CEA equalize ICA territory bilaterally in most patients with carotid stenosis. (2) Dysfunction of this equalization might be associated with pathophysiology of hyperperfusion after CEA.

544
BRAIN-0655
Poster Session

Imaging Clinical

VALIDATION OF CT PERFUSION-DERIVED CBF MAPS IN PATIENTS WITH CEREBROVASCULAR STENO-OCCLUSIVE DISEASE: A COMPARATIVE STUDY WITH ^{15}O PET

M. Ibaraki[1], T. Ohmura[1], K. Matsubara[1], T. Kinoshita[1]
[1]Department of Radiology and Nuclear Medicine, Akita Research Institute of Brain and Blood Vessels , Akita, Japan

Objectives
In the bolus tracking technique with computed tomography (CT) or magnetic resonance imaging, CBF is computed from deconvolution analysis, but its accuracy is still elusive. This study evaluated the reliability of CT perfusion (CTP)-derived CBF for patients with cerebrovascular steno-occlusive disease, by comparing with ^{15}O PET as a reference standard. We focused deconvolution-induced CBF errors in relation to hemodynamic compromise, characterized by prolongation of arterial-tissue delay (ATD) and mean transit time (MTT) in the lesion hemisphere.

Methods
A total of 27 patients with unilateral cerebrovascular steno-occlusive disease who underwent both CTP and ^{15}O PET were included. In PET, CBF, CBV, MTT (= CBV/CBF), and oxygen metabolism parameters were obtained [1]. In CTP, dynamic brain scanning with 1-sec temporal resolution was performed with a bolus injection of contrast media. CBF maps were calculated from three deconvolution algorithms, standard singular value decomposition (sSVD) and two types of delay-insensitive algorithms: delay-corrected SVD (dSVD) [2] and block-circulant SVD (cSVD) [3]. ATD maps, required for dSVD, were calculated from the CTP data independently of the deconvolution analysis. Hemispheric regions of interest (ROIs) were bilaterally defined on cortical MCA regions, and the lesion-to-normal ratio of CBF was calculated ("CBF ratio"). To investigate CBF errors in relation to hemodynamic compromise, we correlated CTP-PET differences in CBF ratios with prolongation of ATD and MTT in the lesion hemisphere. A simulation study was also performed.

Results
CTP-derived lesion-to-normal CBF ratios significantly differed from PET CBF ratios. Compared with PET CBF ratios (0.90 ± 0.08), sSVD yielded lower (0.81 ± 0.09), and dSVD (0.94 ± 0.09) and cSVD (1.01 ± 0.06) higher, CBF ratios, all with statistical significance ($P < 0.05$). For sSVD, the difference in CBF ratio between CTP and PET was negatively correlated with the ATD difference ($r = -0.44$, $P = 0.02$). For cSVD, the difference in

CBF ratio was positively correlated both with ATD difference (r = 0.42, P = 0.03) and MTT difference (r = 0.54, P = 0.01). There was no significant correlation for dSVD (P = 0.37 with ATD, P = 0.17 with MTT). Computer simulations showed ATD-dependent underestimation of CBF ratios for sSVD and MTT-dependent overestimation of CBF ratios for cSVD, supporting the patient data. For a representative patient case with significant CBF reduction and extremely elevated OEF and CBV in PET, that is misery perfusion, cSVD yielded the CBF map with no left-right asymmetry because of the MTT-dependent errors.

Conclusions

CTP results strongly depended on the deconvolution algorithms used. MTT dependence is critical factor for interpreting CBF maps. cSVD showed overestimation of the CBF ratio when MTT was severely prolonged in the lesions. Deconvolution by dSVD can provide lesion-to-normal CBF ratios less dependent on ATD and MTT, but requires accurate ATD maps in advance. A practical and accurate method for CTP is required to assess CBF in patients with MTT-prolonged regions.

References

[1] Ibaraki M. *JCBFM* 2010; 30: 1296. [2] Ibaraki M. *JCBFM* 2005; 25: 378. [3] Wu O. *MRM* 2003; 50: 164.

545
BRAIN-0030
Poster Session

Imaging Clinical

QUANTITATIVE MEASUREMENT OF CEREBRAL BLOOD FLOW USING SINGLE PHOTON EMISSION COMPUTED TOMOGRAPHY WITH VENOUS BLOOD SAMPLING

T. Inoue[1], H. Shimizu[2], M. Fujimura[2], K. Sato[3], H. Endo[3], K. Niizuma[2], H. Sakata[3], T. Tominaga[2]
[1]Neurosurgery, Sendai Medical Center, Sendai, Japan
[2]Neurosurgery, Tohoku University Graduate School of Medicine, Sendai, Japan
[3]Neurosurgery, Kohnan Hospital, Sendai, Japan

Object. Quantitative cerebralblood flow (CBF) measured by single photon emission computed tomography (SPECT)with arterial blood sampling is one of the most reliable methods to assess thehemodynamics in individual patients. Although venous blood sampling is lessinvasive, few reports estimate the accuracy of quantitative CBF with venousblood sampling. The present study compared the measurement of CBF using N-isopropyl-p-(iodine-123)-iodoamphetamineSPECT with venous blood sampling and with arterial blood sampling in patientswith major cerebral artery occlusive disease.

Methods. Twelve normalsubjects and 14 patients with major cerebral artery occlusive disease underwentSPECT with arterial and venous blood sampling. The microsphere method was usedfor quantitative SPECT imaging. Whole brain radioactivity was corrected when thedetectors rotated in the forward direction (F_1-F_7).Venous sampling was performed 30 minutes after radiotracer injection. Arterial blood radioactivity was estimatedby multiple regression analysis from these parameters. The cerebrovascularreactivity to acetazolamide was also measured.

Results. Multiple regression analysis established the following formula:

Ca_{10}= –1.099F_1 + 1.629F_2 – 2.143F_3 – 2.766 F_4– 1.208F_5 + 2.113F_6 + 3.259F_7 + 1.241Cv_{30}+ 94.958 (Where Ca_{10}: arterial blood radioactivity at 10 minutes, F_1–F_7:whole brain radioactivity in the forward direction, Cv_{30}: venousblood radioactivity at 30 minutes)

MeanCBF values were 32.2 ± 6.6 ml/100 g/min for measured arterial radioactivity and42.2 ± 7.8 ml/100 g/min for calculated arterial radioactivity based on venousradioactivity.

Conclusions.The present modified method of calculating quantitative CBF from whole brainand venous blood radioactivities correlated well with

values determined witharterial blood radioactivity.

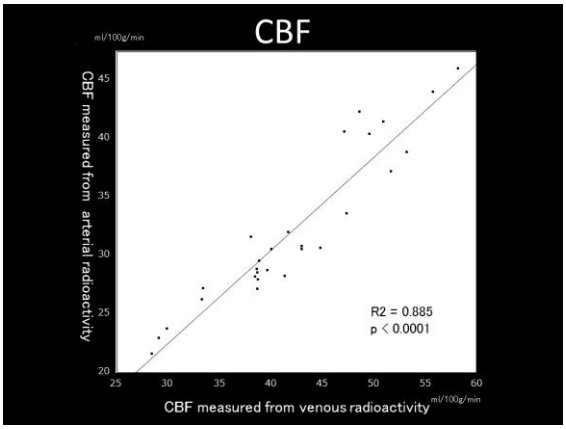

546
BRAIN-0195
Poster Session

Imaging Clinical

GLOBAL BLOOD BRAIN BARRIER PERMEABILITY IN PATIENTS WITH ANEURYSMAL SUBARACHNOID HEMORRHAGE: CORRELATION WITH CLINICAL OUTCOMES.

J. Ivanidze[1], O. Kallas[1], D. Mir[1], A. Giambrone[2], A. Segal[3], A. Gupta[4], J. Claassen[5], P. Sanelli[6]
[1]Department of Diagnostic Radiology - Molecular I maging Innovations Institute, NewYork-Presbyterian Hospital - Weill Cornell Medical Colle ge, New York, USA
[2]Department of Healthcare Policy and Research, NewYork-Presbyterian Hospital - Weill Cornell Medical Colle ge, New York, USA
[3]Department of Neurology, NewYork-Presbyterian Hospital - Weill Cornell Medical Colle ge, New York, USA
[4]Department of Diagnostic Radiology, NewYork-Presbyterian Hospital - Weill Cornell Medical Colle ge, New York, USA
[5]Department of Neurology, NewYork-Presbyterian Hospital - Columbia University Medic al Center, New York, USA
[6]Department of Diagnostic Radiology, NewYork-Presbyterian Hospital - Columbia University Medic al Center, New York, USA

Abstract:

Objectives: Aneurysmal subarachnoid hemorrhage (SAH) is a devastating condition with high morbidity and mortality. CT Perfusion (CTP) with extended pass technique allows measurement of blood brain barrier permeability (BBBP), however, there is currently limited understanding regarding the utility of BBBP evaluation. Multiple variables representing BBBP have been described, including PS, KEP, and Ktrans. We assessed whether BBBP parameters correlate with poor clinical outcomes in SAH patients.

Methods: A retrospective analysis was performed on 22 patients who underwent CTP on days 0-3 after aneurysmal rupture. CTP data were post-processed into BBBP quantitative maps of PS, VE, KEP and Ktrans using Olea Sphere software (Olea Medical, France). Clinical outcomes data on permanent neurologic deficit and modified Rankin scores (mRS) were collected at discharge. Univariate and multivariate analyses utilizing unpaired t tests and receiver operating characteristic (ROC) analysis were performed to determine statistical significance.

Results: The 22 patients were stratified based on their clinical outcomes of permanent neurological deficit and mRS score. PS and VE were significantly increased in patients with poor clinical outcomes (permanent neurologic deficit and mRS 3-6), while KEP and Ktrans were significantly decreased. When the four parameters were combined in a multivariate ROC analysis, AUC was 0.80 for permanent neurologic deficit, and 0.89 for mRS 3-6.

Conclusions: We found significantly elevated PS in SAH patients with poor outcomes indicating increased BBBP. Furthermore, patients with poor outcomes had significantly increased VE and decreased KEP suggesting persistent interstitial edema, which has been implied in the underlying mechanism of early brain injury. Evaluation of BBBP parameters allows for the prognostication of poor outcomes in SAH patients and may help guide management.

References:

1. Claassen J, et al. Global cerebral edema after subarachnoid hemorrhage: Frequency, predictors, and impact on outcome. Stroke. 2002;33:1225-1232

2. Sanelli PC, et al. Using quantitative ct perfusion for evaluation of delayed cerebral ischemia following aneurysmal subarachnoid hemorrhage. AJNR. 2011;32:2047-2053

3. Bennink E, et al. A fast nonlinear regression method for estimating permeability in ct perfusion imaging. JCBFM. 2013;33:1743-1751.

		Poor Outcome: Permanent Deficit (n = 9)	Favorable Outcome: No Permanent Deficit (n = 13)	p-value	Poor Outcome: mRS 3-6 (n = 5)	Favorable Outcome: mRS 0-2 (n = 17)	p-value
Mean Age (years)		52	48	0.44	51	47	0.47
Gender	Female	67% (6/9)	77% (10/13)	0.60	60% (3/5)	76% (13/17)	0.47
	Male	33% (3/9)	23% (3/13)		40% (2/5)	24% (4/17)	
Focal Deficit at presentation		33% (3/9)	23% (3/13)	0.60	80% (4/5)	71% (12/17)	0.68
Loss of Consciousness		33% (3/9)	38% (5/13)	0.81	40% (2/5)	35% (6/17)	0.85
Mean Hunt & Hess Score		2.80	2.60	0.49	3.20	2.50	0.05
Ventriculostomy Catheter		89% (8/9)	69% (9/13)	0.28	100% (5/5)	29% (5/17)	0.01
Aneurysm Location	Anterior circulation	78% (7/9)	54% (7/13)	0.25	60% (3/5)	65% (11/17)	0.84
	Posterior circulation	22% (2/9)	46% (6/13)		40% (2/5)	35% (6/17)	
Treatment	Coiled	33% (3/9)	46% (6/13)	0.55	0% (0/5)	53% (9/17)	0.03
	Clipped	66% (6/9)	54% (7/13)		100% (5/5)	47% (8/17)	

Table 1. Clinical Characteristics of the Study Population. Patients were stratified by presence of a permanent deficit (poor outcome) versus absence of permanent deficit (favorable outcome), and mRS 3-6 (poor outcome) versus mRS 0-2 (favorable outcome). P-values were calculated using Chi-square test for frequency distributions and Student t-test for mean values.

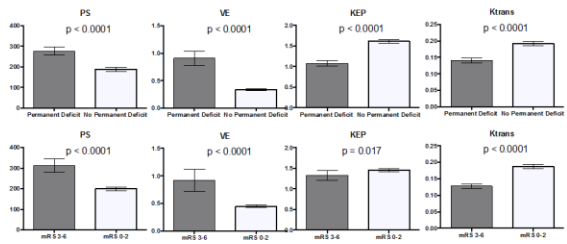

Figure 1. BBBP Parameters in SAH Patients stratified by clinical outcomes. Patients were stratified as described in the legend for Table 1.

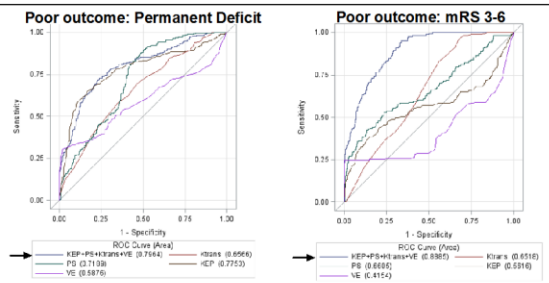

Figure 2. Univariate and Multivariate ROC Analysis of PS, VE, KEP and Ktrans in SAH Patients with Poor Clinical Outcomes compared to Patients with Favorable Cinical Outcomes.

547
BRAIN-0194
Poster Session

Imaging Clinical

ASSESSMENT OF BLOOD-BRAIN-BARRIER PERMEABILITY IN GLOBAL CEREBRAL EDEMA.

J. Ivanidze[1], O. Kallas[2], D. Mir[2], A. Giambrone[3], A. Segal[4], A. Gupta[2], J. Claassen[5], P. Sanelli[2]
[1]Department of Diagnostic Radiology - Molecular I maging Innovations Institute, NewYork-Presbyterian Hospital - Weill Cornell Medical Colle ge, New York, USA
[2]Department of Diagnostic Radiology, NewYork-Presbyterian Hospital - Weill Cornell Medical Colle ge, New York, USA
[3]Department of Healthcare Policy and Research, NewYork-
Presbyterian Hospital - Weill Cornell Medical Colle ge, New York, USA
[4]Department of Neurology, NewYork-Presbyterian Hospital - Weill Cornell Medical Colle ge, New York, USA
[5]Department of Neurology, NewYork-Presbyterian Hospital - Columbia University Medic al Center, New York, USA

Objectives: Global cerebral edema (GCE) occurs after SAH and is associated with disruption of the BBB. GCE is an important predictor of morbidity and mortality. Detection of GCE remains challenging using current imaging standards with NCCT. The etiology of GCE is thought to reflect early diffuse ischemic injury due to transient cerebral circulatory arrest, diffuse inflammatory or neurotoxic effects of blood, or abnormal autoregulation due to microvascular damage or dysfunction of vasomotor centers. Currently, there are no established methods to assess microvascular dysfunction in the clinical setting. The rationale that underlies this project is that quantitative imaging of microvascular parameters, such as blood brain barrier permeability (BBBP), will provide methods for earlier and more accurate detection as well as monitoring of GCE compared to the current noncontrast CT-based criteria used to guide management and treatment decisions.

Our objective was to evaluate BBBP alterations in patients with CGE after SAH using extended pass CT Perfusion (CTP).

Methods: SAH patients underwent CTP in the early phase after aneurysmal rupture (days 0-3) and were classified as GCE or non-GCE using established NCCT criteria. CTP data were post-processed into BBBP quantitative maps of PS (permeability surface area product), K-trans (volume transfer constant from blood plasma to extravascular extracellular space, EES), KEP (washout rate constant of the contrast agent from EES to intravascular space, IVS), VE (EES volume per unit of volume of tissue), VP (plasmatic volume per unit of volume of tissue) and F (plasma flow) using Olea Sphere software. Mean values were calculated and compared using t-Tests to determine statistical significance.

Results: 22 patients were included in the analysis. KEP (1.32 versus 1.52, $p < 0.0001$), K-trans (0.15 versus 0.19, $p < 0.0001$), VP (0.51 versus 0.57, $p = 0.0007$) and F (1176 versus 1329, $p = 0.0001$) were decreased in GCE compared to non-GCE while VE (0.81 versus 0.39, $p < 0.0001$) was increased. There was a trend for PS elevation in GCE compared to non-GCE, however this result was not statistically significant. Figure 1 demonstrates BBBP quantitative maps of KEP, Ktrans and PS in a representative GCE patient (top panel) and a representative non-GCE patient, respectively.

Conclusions: Altered BBBP function can be detected in GCE using CTP. KEP may be the most useful parameter given that its derivation is not dependent on blood flow. Decreased KEP suggests the presence of interstitial edema, which plays a role in early brain injury. These findings support further work in studying BBBP using CTP for improved diagnosis and monitoring of GCE.

References:

1. Claassen J, et al. Global cerebral edema after subarachnoid hemorrhage: Frequency, predictors, and impact on outcome. Stroke. 2002;33:1225-1232

2. Sanelli PC, et al. Using quantitative ct perfusion for evaluation of delayed cerebral ischemia following aneurysmal subarachnoid hemorrhage. AJNR. 2011;32:2047-2053

3. Bennink E, et al. A fast nonlinear regression method for estimating permeability in ct perfusion imaging. JCBFM. 2013;33:1743-1751.

		GCE (n = 11)	No GCE (n = 11)	p-value
Mean Age (years)		51	49	0.67
Gender	Female	82% (9/11)	64% (7/11)	0.92
	Male	18% (2/11)	36% (4/11)	
Focal Deficit at presentation		46% (5/11)	36% (4/11)	0.66
Loss of Consciousness		18% (2/11)	27% (3/11)	0.61
Mean Hunt & Hess Score		3.0	2.5	0.15
Ventriculostomy Catheter		82% (9/11)	82% (9/11)	1.00
Aneurysm Location	Anterior circulation	64% (7/11)	54% (6/11)	0.66
	Posterior circulation	36% (4/11)	46% (5/11)	
Treatment	Coiled	27% (3/11)	54% (6/11)	0.19
	Clipped	73% (8/11)	46% (5/11)	

Table 1. Clinical Characteristics of the Study Population.

	GCE	Non-GCE	p-value
KEP	1.32 (1.272 - 1.368)	1.52 (1.451 - 1.589)	< 0.0001
Ktrans	0.1516 (0.1421 - 0.1612)	0.1932 (0.1825 - 0.2038)	< 0.0001
PS	221.7 (209.1 - 234.3)	208.4 (189.7 - 227.2)	0.23
F	1176 (1133 - 1219)	1329 (1259 - 1398)	0.0001
E	0.1302 (0.1261 - 0.1343)	0.1343 (0.1269 - 0.1418)	0.31
VE	0.5663 (0.5006 - 0.632)	0.5023 (0.4631 - 0.5415)	< 0.0001
VP	0.5064 (0.4873 - 0.5254)	0.5655 (0.5353 - 0.5957)	0.0007

Table 2. Quantitative BBBP Results. Mean values are provided, with 95% confidence intervals in parentheses. KEP, Ktrans, VP, and F were statistically significantly decreased in the GCE group compared to the Non-GCE group, while VE was statistically significantly increased. Differences in PS and E did not reach statistical significance.

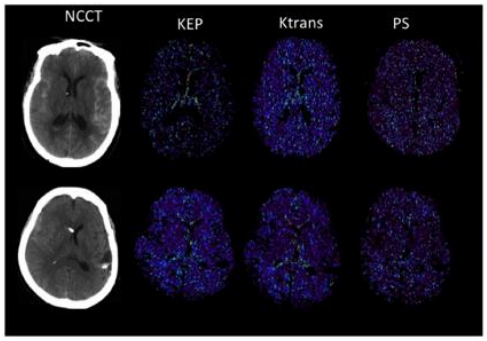

Figure 1. BBBP quantitative maps of KEP, Ktrans and PS in a representative GCE patient (top panel) and a representative non-GCE patient (bottom panel), respectively. NCCT images demonstrate loss of grey-white matter differentiation and presence of sulcal effacement in the GCE patient. Corresponding BBBP maps reveal markedly decreased KEP, increased Ktrans, and slightly increased PS in the same patient.

548
BRAIN-0797
Poster Session

Imaging Clinical

INTRAOPERATIVE INFRARED IMAGING OF CEREBRAL CORTEX SURFACE IN PATIENTS DIAGNOSED WITH BRAIN TUMOURS

K. Kaczmarska[1], M. Zębala[2], Z. Czernicki[1], M. Kastek[3], T. Piątkowski[3], H. Polakowski[3]
[1]Department of Neurosurgery, Mossakowski Medical Research Centre, Warsaw, Poland
[2]Department of Neurosurgery, Medical University of Warsaw, Warsaw, Poland
[3]Institute of Optoelectronics, Military University of Technology, Warsaw, Poland

Objectives

Intracranial tumours are one of the most common pathological changes in central nervous system, caused by uncontrolled cell growth of any tissue type [1]. Imaging plays a crucial role in the diagnosis of brain tumours [2, 3]. The primary aim of our study was intraoperative analysis of cortex surface temperature and vascularity and determination of brain tumours location and borders.

Methods

Temperature changes of cortex surface were analysed intraoperatively before and during tumour resection. Thirteen patients diagnosed by CT or MRI with brain tumours were studied. Examined tumours can be classified according to their origin and histology as gliomas, meningiomas and metastatic tumours. The following report concerns the temperature changes in 4 cases of metastatic tumours.

The analysis of the temperature distribution of observed surface was performed continuously and in real time. Temperature measurements were recorded using infrared camera (SilverSC5600, FLIR) with 54 mm lens (field of view 10° x 8°). This camera was fitted with cooled InSb detector array with temperature resolution of 25 mK and operates in MWIR band of infrared spectrum (wavelength from 3 µm to 5 µm).

Results

Initial analysis shows that during resection temperature of normal tissue is significantly higher ($p = 0.028943$) than temperature of metastatic tumour. Similar results were obtained for temperature of normal and pathological tissues before resection. Temperature of metastatic tumour during devascularization is 30.80 ± 1.64 °C and temperature of normal tissue is 33.49 ± 1.14 °C (median ± QR, $\alpha = 0.05$). We can observe that difference between temperature of normal and pathological tissues increases during resection. It is caused mainly by decreased metabolism in the tumour caused by devascularization, as the blood supply to cancerous tissue gets gradually reduced.

Conclusions

Results of intraoperative measurement confirmed the usability non-invasive thermal imaging to record cerebral cortex temperature changes. Thermal camera can be effectively used to assess the blood supply of both healthy and pathological tissues. Thermal images recorded during neurosurgery allow to locate and determine the brain tumour borders, which is extremely important in order to precisely resect tumour and minimize the neurological deficits occurring after the surgical procedure.

References

[1] Kleihues P, Burger PC, Scheithauer BW, The new WHO classification of brain tumours, Brain Pathol., 3, 255 – 268, 1993
[2] Watson JC, Gorbach AM, Pluta RM, Rak R, Heiss JD, Oldfield EH, Real-time detection of vascular occlusion and reperfusion of the brain during surgery by using infrared imaging, J Neurosurg, 96, 918 – 923, 2002
[3] Frangioni, JV, New technologies for human cancer imaging. J Clin Oncol, 26, 4012 – 4021, 2008

549
BRAIN-0120
Poster Session

Imaging Clinical

VULNERABLE PLAQUES AND DELINEATION OF THE VASA VASORUM : EVALUATION WITH CAROTID FLUORESCEIN VIDEOANGIOGRAPHY

H. Katano[1], K. Yamada[1]
[1]Neurosurgery,
Nagoya City University Graduate School of Medica l Sciences, Nagoya, Japan

Objectives: The aim of the study was to investigate the depiction of the carotid artery by fluorescein sodium (FS) videoangiography compared with indocyanine green (ICG) videoangiography, focusing on how the vasa vasorum of the carotid artery is depicted.

Methods: Thirty-five patients (19 FS patients, 16 ICG patients, mean age 69.4 ± 5.1 y/o, mean degree of stenosis 78.7% ± 11.7%) who underwent a carotid endarterectomy (CEA) were enrolled. FS (5–6 mg/kg) or ICG (0.2–0.3 mg/kg) was injected intravenously as a bolus before the arterectomy during the CEA. The intravascular fluorescence signal was recorded with a digital video camera integrated on a microscope. MRI black-blood (BB) T1-weighted imaging (WI) was preoperatively performed using a 1.5-tesla whole-body imager, and the signal intensity ratio (SIR) relative to the ipsilateral sternocleidomastoid muscle on BB-T1WI (BB-SIR) was calculated. We also performed an immunohistochemistry study using CD31 and CD68 antibodies for plaque specimens.

Results: In the FS videoangiography series, the vasa vasorum of carotid adventitia was depicted first, followed by augmentation of FS of the wall and partially the inner lumen (pattern A) in six cases. Augmentation of FS of the wall and inner lumen prior or simultaneous to the depiction of the vasa vasorum of the carotid adventitia (pattern B) were observed in 13 cases. The average BB-SIR value of the pattern B cases was significantly higher than that in the pattern A group (p

Conclusions: The early depiction of adventitial vasa vasorum in FS videoangiography was inversely associated with the BB-SIR values of the plaques, along with many microvessels and macrophages that have been reported to have a tendency of intraplaque hemorrhage or symptoms. The present results may support the idea of an intimal origin of the neovascularization in vulnerable carotid plaques, and they demonstrated the potential of intraoperative plaque imaging by FS videoangiography

550
BRAIN-0200
Poster Session

Imaging Clinical

EVALUATION OF STRIATAL OXIDATIVE STRESS IN PARKINSON'S DISEASE USING [CU-62]ATSM PET

H. Okazawa[1], M. Ikawa[2], T. Tsujikawa[1], T. Mori[1], Y. Kiyono[1], M. Yoneda[3]
[1]Biomedical Imaging Research Institute, University of Fukui, Fukui, Japan
[2]Department of Neurology, University of Fukui, Fukui, Japan
[3]Faculty of Nursing and Social Welfare Sciences, Fukui Prefectural University, Eiheiji, Japan

Objectives: Our previous preliminary study showed the effects of oxidative stress and mitochondrial dysfunction in neuronal degeneration in the living human brains of Parkinson's disease (PD). To confirm the relationship between oxidative stress caused mainly by mitochondrial dysfunction and the degree of dopaminergic neurodegeneration, PET imaging with ^{62}Cu-ATSM, which is known as a PET probe for delineation of hypoxia and excessive reduction, was performed in greater number of patients with PD and the images were compared with those of healthy controls.

Methods: Thirty PD patients (mean age 73 ± 7 yr) and 10 healthy controls (mean age 61 ± 8 yr)

were involved in this study. The severity of symptoms was evaluated with the Unified Parkinoson's Disease Rating Scale (UPDRS). They underwent a 20-min dynamic ^{62}Cu-ATSM PET scan after the tracer injection, and early- and delayed-phase images were calculated by averaging the dynamic PET data for the first 3 min and the last 10 min of frames, respectively. Each image was converted to standardized uptake value (SUV) scale, and anatomical standardization parameters were obtained by Statistical Parametric Mapping 2 (SPM2) using the early-phase image. The delayed-phase SUV image was used for evaluation after anatomical normalization and global normalization with whole brain mean of 1. The regional SUV values were compared between patients and controls using region of interest (ROI) analysis in which the ROIs were set in the bilateral striata and cerebellar hemispheres. The striatum-to-cerebellar SUV ratio (S/C ratio) was also calculated from these SUV values for each patient and control.

Results: Average images of ^{62}Cu-ATSM PET showed a significant increase in striatal accumulation in PD patients compared with healthy controls, suggesting an increase in oxidative stress associated with neuronal degenerative changes. The mean SUVs in bilateral striatum of patients were significantly greater than those of controls (1.16 ± 0.05 vs. 1.09 ± 0.04, $P < 0.05$). The mean S/C ratio of the patients was also significantly greater than that of the controls (1.13 ± 0.10 vs. 1.08 ± 0.02, $P < 0.01$). The S/C ratio and UPDRS scores showed a parabolic correlation ($r = 0.65$, $P < 0.05$), suggesting that the symptomatic severity of PD and oxidative stress in the striatum correlated well positively until moderate clinical phases, and then neurons in the striatum were significantly damaged in advanced phases.

Conclusions: The present results from ^{62}Cu-ATSM PET imaging suggest that PD patients showed greater oxidative stress in the striatum compared with controls. The degree of oxidative stress correlated well with clinical severity, indicating possibility of associated neurodegenerative change in these patients.

References:

Ikawa M, Okazawa H, et al. Nucl Med Biol. 2011; 38: 945 - 951.
Okazawa H, Ikawa M, et al. Q J Nucl Med Mol Imaging 2014; 58: 387 - 397.
Ikawa M, Okazawa H, et al. Neurology 2015 (in press).

551
BRAIN-0075
Poster Session

Imaging Clinical

EVALUATION OF BRAIN TEMPERATURE BY MAGNETIC RESONANCE SPECTROSCOPY IN EARLY-ONSET PARKINSON DISEASE: A 1-H MRS STUDY.

M. Piatti[1], M. Rango[1], A. Di Fonzo[2], V. Barbieri[1], L. Airaghi[3], N. Bresolin[1]
[1]Excellence Centre for Advanced MR Studies Depar tment of Neurological Science, IRCCS Cà Granda-Ospedale Maggiore Policlinico Foundation Univers ity of Milan, Milano, Italy
[2]Department of Neurological Science, IRCCS Cà Granda-Ospedale Maggiore Policlinico Foundation Univers ity of Milan, Milano, Italy
[3]Department of Internal Medicine, IRCCS Cà Granda-Ospedale Maggiore Policlinico Foundation Univers ity of Milan, Milano, Italy

Objectives: Since the 90s, magnetic resonance spectroscopy has been used to study the brain temperature in vivo, allowing to get the temperature of a specific area of the brain non-invasively. Brain temperature is regulated most of all by vascular and metabolic factors, like mitochondrial energetic metabolism, even if the correct mechanism of this regulation has not been fully understood yet. In the present study we focused on patients with Early Onset Parkinson Disease (EAPD) as often mutations involved in mitochondrial machinery are associated to this pathology.

Methods: Five patients with EAPD, 3 men and 2 women, were first genotyped and four of them

presented mutations (2 regarding PARK2, one PARK9 and one PINK1). In all subjects, cerebral temperatures were assessed by magnetic resonance spectroscopy in visual cortex, posterior cingulate, hypothalamus, centrum semiovale and basal ganglia and they were compared to 10 healthy subjects matched for age and gender. Metabolic profiles were also obtained.

Results: Patients with EAPD always had brain temperatures higher than the corresponding brain temperatures obtained in healthy subjects in all areas, most of all in the centrum semiovale and basal ganglia. The values of the metabolites were significantly lower, and the centrum semiovale and basal ganglia were still the most interested areas. This result appears also related to the duration of illness.

Conclusion: This innovative work has shown that the control mechanisms of brain temperature are significantly impaired in patients with EAPD. This suggests a specific connection between genes involved in EAPD and the mitochondrial complex V (ATP Synthase), whose dysfunction causes brain temperature raise. More detailed studies will certainly be useful in the future to clarify the points of interest raised by this work.

References:

Rango M et al. Brain temperature: What do we know? Neuroreport (2012) 23,483-487.
Rango M.et al. Increased brain temperature in Parkinson disease. Neuroreport (2012) 23,129-133.
Schrag A. et al. Young-onset Parkinson's disease revised-clinical features, natural history and mortality. Movement Disorders (1998) 13,885-894.
Baron N. et al. Mitochondrial dysfunction in neurodegenerative disorders. Biochemical Society Transaction (2007) 35,1228-1231.
Rango M. et al. Magnetic Resonance Spectroscopy in Parkinson's disease and parkinsonian syndromes. Functional Neurology (2007) 22,75-79.
Ghione I. et al. Parkin polymorphisms and environmental exposure: decrease in age at onset of Parkinson's disease. Neurotoxicology. (2007) 28,698-701.
Powers W.J. et al. Cerebral mitochondrial metabolism in early Parkinson's disease. Journal of Cerebral Blood Flow Metabolism (2008) 28,1754–1760.
Whitworth A.J. et al. The PINK1/Parkin pathway: a mitochondrial quality control system? Journal of Bioenergetic Biomembranes (2009) 41,499–503.
Morais V. et al. Parkinson's disease mutations in PINK1 result in decreased Complex I activity and deficient synaptic function. EMBO Molecular Medicine (2009) 1,99–111.
Greene A.W. et al. Mitochondrial processing peptidase regulates PINK1 processing, import and Parkin recruitment. EMBO Report (2012) 13,378-385.
Lefevre V. et al. Genome-wide RNAi screen identifies ATPase inhibitory factor 1 (ATPIF1) as essential for PARK2 recruitment and mitophagy. Autophagy (2013) 9, 1770–1779.
Schapira A.H., Targeting mitochondria for neuroprotection in Parkinson's disease. Antioxidants Redox Signaling (2012) 16,965-973.

Table: Demographic, clinical and genetic characteristics of patients with early-onset Parkinson disease

Subjects	Age (yrs)	Gender	Family History	Age of Onset	Duration of disease (yrs)	Hoen & Yahr Score	Gene Mutations	Most involved side	Therapy
1	31	M	Yes	27	4	1	PARK2	DX	LevoDopa 100 mg Rasagiline 1 mg
2	40	M	No	25	15	4	PARK9	No	Biperidene 4 mg Baclofen 10 mg Clonazepam 10 gtt
3	44	F	No	41	3	1	PARK2	SX	LevoDopa 100 mg Rasagiline 1 mg Pramipexole 2 mg
4	48	M	Yes	45	3	1	No mutations	SX	NO
5	44	F	Yes	32	12	1.5	PINK1	DX	LevoDopa 300 mg Rasagiline 1mg

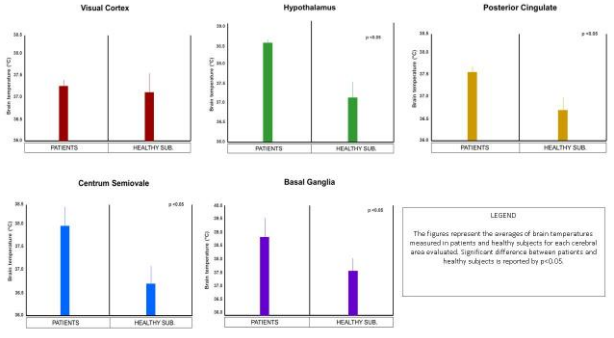

552
BRAIN-0137

Poster Session

Imaging Clinical

ESTABLISHMENT OF A METHOD FOR CREATING QUANTITATIVE CBF IMAGES OF OUTER AND INNER LAYERS OF THE BRAIN BY XENON-ENHANCED COMPUTED TOMOGRAPHY: APPLICATION TO DEMENTIA

S. Sase[1], H. Yamamoto[2], E. Ito[2], S. Tan[2], Y. Sawa[3]
[1]R&D Division, Anzai Medical Co. Ltd., Tokyo, Japan
[2]Psychiatry, Sawa Hospital, Osaka, Japan
[3]The Director, Sawa Hospital, Osaka, Japan

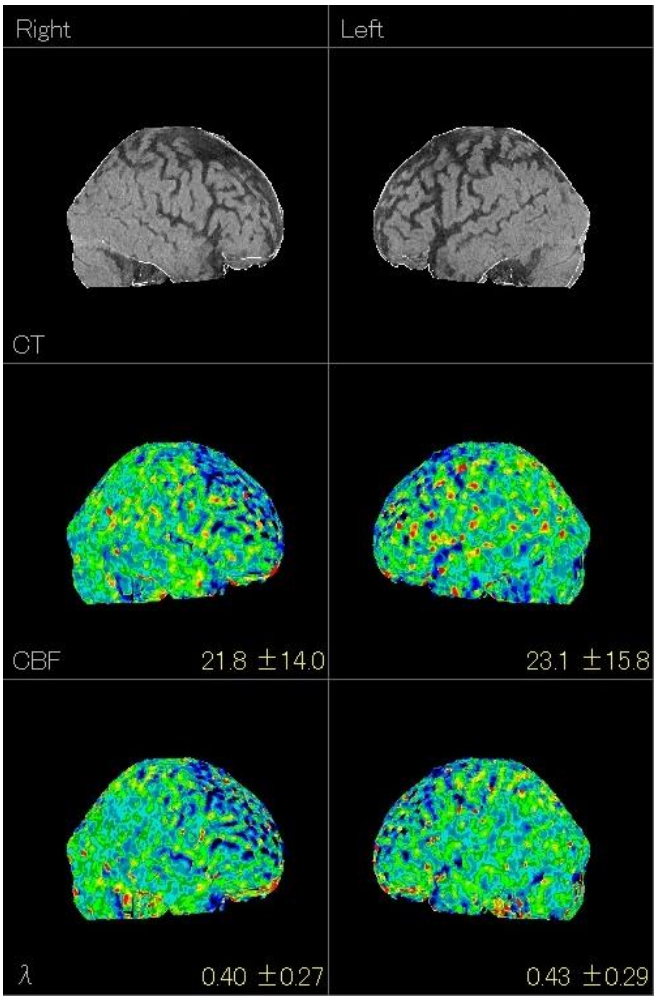

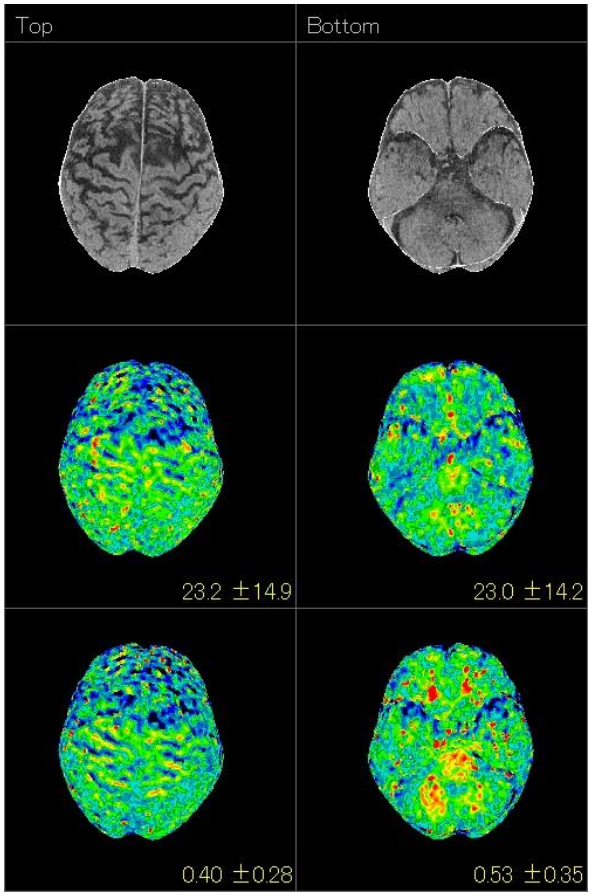

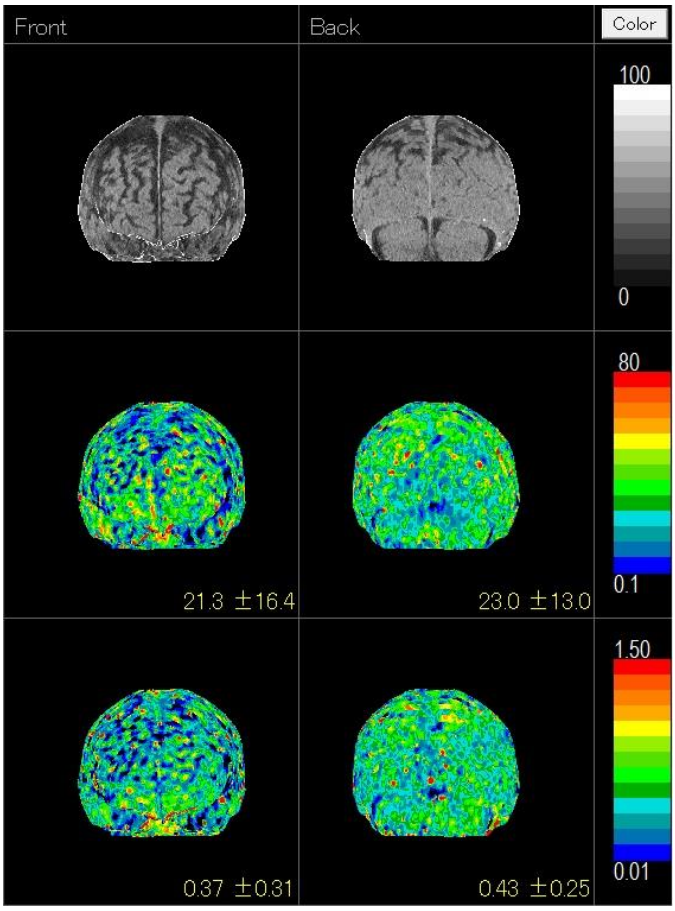

Objectives: To our knowledge, there has been no report on quantitative blood flow of the surface of the human brain. The purpose of this work was to establish a method for creating quantitative cerebral blood flow (CBF) images of the outer and inner layers along the surface of the brain by means of xenon-enhanced computed tomography (Xe-CT) and to assess the usefulness of this method in diagnosing dementia.

Methods: Using newly developed flat-panel volume CT (Aquilion ONE, Toshiba, Tokyo), the whole-brain CT image was obtained with one rotation (one scan). The whole-brain CT image consisted of thin tomographic images. In Xe-CT, 30% non-radioactive xenon gas was inhaled for 4 minute, followed by 4-min breathing of air; meanwhile, CT scanning was conducted at 1 minute intervals. Corresponding to each individual CT image composing the whole-brain CT image, CBF and partition coefficient (lambda) images were obtained. CT, CBF and lambda images provide information on morphology, neuronal activity, and foreign substance accumulation, respectively. We invented a method of creating brain surface images of CT, CBF and lambda by stacking their respective thin tomographic images with 5 mm thickness. With removing thin layers one by one from the surface, we could observe the changes from the outer to inner layers of the brain for CT, CBF and lambda images.

Seven patients with Alzheimer's disease (AD) (77.7±9.8 years), ten patients with dementia with Lewy body (DLB) (79.4±5.0 years) and twenty healthy volunteers (73.7±6.7 years) underwent Xe-CT studies. We created the first (0-5 mm from the surface) to tenth (45-50 mm from the surface) layer images with right lateral, left lateral, superior, inferior, anterior and posterior views.

Results: There were significant differences in CBF for the seventh layer with superior view between the healthy volunteers and the AD patients (P=0.0019) and between the healthy volunteers and the DLB patients (P=0.0447). The average CBF values were 30.2±5.0, 22.8±4.4 and 26.3±4.4 mL/100g/min for the healthy volunteers, AD patients and DLB patients, respectively. The seventh layer (30-35 mm from the surface) with superior view approximately corresponded to the layer just outside of lateral ventricles. There were significant differences in CBF for the second layer with superior (P=0.0060) and inferior (P=0.0289) views between the AD and DLB patients. The average CBF values for the AD and DLB patients were 27.6±3.0 and 33.5±4.3 mL/100g/min respectively for the superior view, and 22.7±3.9 and 29.7±6.9 mL/100g/min respectively for the inferior view.

Conclusions: AD and DLB patients could be distinguished from age-matched control subjects using inner layer CBF images with superior view, and AD and DLB patients could be distinguished from each other using outer layer CBF images using superior and inferior views. Each of the four major forms of dementia (AD, DLB, vascular dementia, and fronto-temporal lobe degeneration) has been reported to have different pattern of CBF. There would be a strong possibility of specifying the form of dementia and

detecting the dementia in its early stage through evaluation of the outer and inner layer images of CT, CBF and lambda.

553
BRAIN-0300
Poster Session

Imaging Clinical

CT PERFUSION AS AN INDEX TO ANTICIPATE INCREASE OF BLOOD SAMPLING OEF

K. YOSHIOKA[1], T. MORI[1], T. IWATA[1], Y. TANNO[1], S. KASAKURA[1]
[1]Stroke Treatment,
Shonan Kamakura General Hospital Stroke Center, Kamakura, Japan

Objectives

It is important to anticipate the risk of cerebral hyperperfusion syndrome (CHS) before carotid artery stenting (CAS). CHS is likely to occur in patients with stage 2 hemodynamic failure, where oxygen extraction fraction (OEF) increases. However, OEF can not be measured in all institutions, because OEF is usually measured with PET. If some parameters of CT perfusion (CTP) widely used in many institutions have close relation to increase of OEF, it is beneficial for many institutions. In addition, OEF can be measured by blood sampling. The aim of our study was to investigate whether or not parameters of CTP had some relation to blood sampling global cerebral OEF (gcOEF) before or after CAS.

Methods

Included in our retrospective study were patients 1) who underwent elective CAS from January 2013 to December 2014, 2) who underwent CTP and blood sampling gcOEF before and after CAS. Excluded from the study were patients who underwent CAS within 30 days after last ischemic stroke. Evaluated were the relationship between gcOEF before or after CAS, usual parameters of CTP (CBF, CBV, MTT, TTP) measured in the territories of the bilateral middle cerebral artery (MCA) and peak value (PV) derived from time-density curve. Comparing the affected side parameter with the contralateral one, CBF ratio was defined as CBFa divided by CBFc, CBV ratio as CBVa divided by CBVc, MTT delay as MTTa minus MTTc, TTP delay as TTPa minus TTPc, PV ratio as PVa divided by PVc, and PV/TTP ratio as PV/TTPa divided by PV/TTPc.

Results

Twenty-three patients were analyzed. Mean age was 74.5 (SD: 8.5) years old. Twenty were male. Median pre-CAS gcOEF, post-CAS gcOEF, CBF ratio, CBV ratio, MTT delay, TTP delay, PV ratio, and PV/TTP ratio was 0.40 (quartile: 0.46), 0.42 (quartile: 0.45), 0.96 (quartile: 0.87 - 1.03), 1.05 (quartile: 1.00 - 1.12), 0.24 (-0.06 - 0.43), 0.41 (0.18 - 1.07), 1.00 (0.92 - 1.11), and 0.96 (0.89 - 1.05), respectively. There is no significant linear correlation between any CTP parameters and pre-CAS gcOEF. However, PV/TTP ratio of less 0.8 seemed to have relation to increased pre-CAS gcOEF of 0.46 or more ($p = 0.05$, OR: 7.5). There is a significant inverse correlation between CBF ratio and post-CAS gcOEF ($p < 0.05$). Among 4 patients with CBF of less than 0.83, 3 patients had increased post-CAS gcOEF of 0.45 or more($p = 0.06$, OR: 8.4).

Conclusions

Pre-CAS PV/TTP ratio of less than 0.80 had probable relation to increased pre-CAS gcOEF of 0.46 or more, and pre-CAS CBF ratio of less than 0.83 had relation to increased post-CAS gcOEF of 0.45 or more.

554
BRAIN-0829
Poster Session

Translational Studies

A MULTI-CENTRE PRECLINICAL STUDY ON THE EFFECTIVENESS OF INTERLEUKIN-1 RECEPTOR ANTAGONIST IN STROKE

S.M. Allan[1], S. Maysami[1], R. Wong[1], J. Pradillo[2], A. Denes[3], H. Dhungana[4], J. Koistinaho[4], T. Malm[4], C. Orset[5], M. Rahman[6], M. Rubio[5], M. Schwaninger[6], D. Vivien[5], P. Bath[7], N.J. Rothwell[1]
[1]Faculty of Life Sciences, University of Manchester, Manchester, United Kingdom
[2]Department of Pharmacology, University of Complutense, Madrid, Spain
[3]Laboratory of Molecular Neuroendocrinology, Institute of Experimental Medicine, Budapest, Hungary
[4]A. I. Virtanen Institute for Molecular Sciences, University of Eastern Finland, Kuopio, Finland
[5]GIP Cyceron, University Caen Lower-Normandy, Caen, France
[6]Institute of Experimental and Clinical Pharmacology and Toxicology, University of Lubeck, Lubeck, Germany
[7]Division of Clinical Neuroscience, University of Nottingham, Nottingham, United Kingdom

Objectives

To date translation of findings from preclinical research to new treatments for stroke has proved largely unsuccessful. Amongst several things, more rigorous testing of new drug candidates in different experimental models of stroke and initiation of preclinical cross-laboratory studies have been suggested as ways to improve translation. However, to our knowledge, no drugs currently in clinical stroke trials have been investigated in preclinical cross-laboratory studies. We have identified the cytokine interleukin 1 (IL-1) as a key mediator of neuronal injury and shown that the naturally occurring IL-1 receptor antagonist (IL-1Ra) markedly reduces brain injury in a number of different experimental models and our aim here was to further investigate the efficacy of IL-1Ra in different research laboratories across Europe.

Methods

All studies used male mice (three studies with BALB/C and three using C57BL/6) with four studies using transient models of occlusion (confirmed by blood-flow measurements by laser Doppler) and four using permanent models (confirmed visually). Studies used animals of either 2.5 months (six studies) or 10 months (two studies) of age. All studies used the same dosing regimen of 100mg/kg IL-1Ra at both 30 and 180 min post-occlusion or corresponding vehicle treatment. Treatment was administered via subcutaneous injection bar one study, which administered treatment intravenously. Lesion volumes and oedema were measured by histological staining (three studies) or MRI (three studies). All lesion volumes and oedema measured by staining methods were assessed 7 days-post occlusion while MRI measurements ranged from 1 to 28 days post-stroke. Functional outcome was assessed using the corner (four studies) test (one study), assessed up to 28 days posts-stroke. Data from a total of 241 experimental animals were retrieved. Data were transferred to the project's coordinating centre in Manchester merged into a single Microsoft Excel sheet using common field names with one row per animal for analysis. Cochrane Review Manager (version 5.2) was used to analyse the effect of IL-1Ra treatment compared to vehicle on post-stroke outcomes.

Results

IL-1Ra reduced lesion volume, assessed using histological staining and MRI: standardised mean difference -1.84 (95% CI -2.55 to -1.12, p=<0.0001) and -1.04 (95% CI -1.96 to -0.11, p=0.03). Neurological scores showed IL-1Ra treatment to reduce neurological deficit compared to vehicle overall (-1.79, 95% CI -2.44 to -1.13, p=<0.001). Subgroup analysis found IL-1Ra treatment to be beneficial at days 1 to 28 (p=<0.001), but not shortly after surgery (p=0.11).

In the corner test overall analysis found IL-1Ra treatment to be beneficial (-0.92, 95% CI -1.25 to -0.59, p=<0.001). Analysis of subgroups found IL-1Ra at days 1 (p=0.001), 2 (p=<0.001) and 7 (p=0.01) to be beneficial after stroke but not at day 28 (p=0.34).

\Conclusions

IL-1Ra treatment was beneficial overall in terms of reducing lesion damage, neurological deficit and improve functional outcomes after experimentally induced stroke in a specific sub-population of young to middle aged male mice. Furthermore we show that multi-centre preclinical studies are feasible, but require careful planning and a clearly defined experimental design.

555
BRAIN-0357
Poster Session

Translational Studies

DEFICIENCY OF THE STROKE-RELEVANT HDAC9 GENE IS ATHEROPROTECTIVE

S. Azghandi[1], C. Prell[1], M. Schneider[1], R. Malik[1], K. Berer[2], C. Haffner[1], M. Dichgans[1]
[1]Institute for Stroke and Dementia Research (ISD), Klinikum der Universität München, Munich, Germany
[2]Department of Neuroimmunology, Max Planck Institute of Neurobiology, Martinsried, Germany

Objectives: By conducting a genome-wide association study for ischemic stroke we recently identified the 7p21.1 region as the strongest risk locus for large vessel stroke. Variants at this locus were also found to be associated with coronary artery disease, suggesting atherosclerosis as the underlying mechanism. The 7p21.1 locus overlaps with the tail end of the histone deacetylase 9 (HDAC9) gene. In this study we investigated the candidacy of HDAC9 and the biological relevance of HDAC9 in atherosclerosis.

Methods: We analyzed allele-dependent expression of HDAC9 and of the two other genes in the 7p21.1 region, TWIST1 and FERD3L, in peripheral blood mononuclear cells of healthy donors. Carrier status at rs2107595, the lead SNP of METASTROKE, was determined by direct sequencing.
Effects of HDAC9 on atherogenesis were analyzed in ApoE deficient mice ($ApoE^{-/-}$), an established model for atherosclerosis. We investigated atherosclerotic plaque size and immune cell infiltration in 18- and 28-week-old $ApoE^{-/-}$ mice by histology and immunohistochemistry. In addition, leukocyte distribution was measured by flow cytometry of the blood and the spleen.

Results: HDAC9 mRNA levels were found to be increased in peripheral blood mononuclear cells of healthy risk allele carriers suggesting that increased HDAC9 expression enhances the risk for large vessel stroke. Compared to $HDAC9^{+/+}$ $ApoE^{-/-}$ mice, $HDAC9^{-/-}$ $ApoE^{-/-}$ mice showed reduced atherosclerotic lesion sizes at the level of the aortic valves and in the aortic arch. In addition, $HDAC9^{-/-}$ $ApoE^{-/-}$ mice had significantly less advanced lesions throughout aortas.[1] Histological analysis of CD45, CD3 and Mac3 positive cells showed no differences in immune cell infiltration between $HDAC9^{+/+}$ $ApoE^{-/-}$ and $HDAC9^{-/-}$ $ApoE^{-/-}$ mice. But immunological analyses of blood and spleen from $HDAC9^{-/-}$ $ApoE^{-/-}$ mice showed altered proportions of different leukocyte subsets indicating an immune-cell mediated mechanism.

Conclusion: Our results suggest that HDAC9 represents the relevant gene at the 7p21.1 locus. We could show that HDAC9 inhibition is atheroprotective and provide initial evidence for an immune-mediated mechanism. Specific pharmacological inhibition of HDAC9 might be a promising strategy to prevent atherosclerosis and large vessel stroke.

References:

[1] S. Azghandi, C. Prell, S. W. van der Laan, M. Schneider, R. Malik, K. Berer, N. Gerdes, G. Pasterkamp, C. Weber, C. Haffner, and M. Dichgans. Deficiency of the Stroke Relevant Hdac9

Gene Attenuates Atherosclerosis in Accord with Allele-Specific Effects at 7p21.1. *Stroke.* 2015;46:197-202

556
BRAIN-0283
Poster Session

Translational Studies

REPOSITIONING OF THE DRUG CBG000592 FOR TREATMENT OF ISCHEMIC STROKE.

F. Campos[1], A. Silva-Candal[1], B. Argibay[1], A. Vieites-Prado[1], C. Correa[1], T. Sobrino[1], M. Blanco[1], M. Loza[2], J. Castillo[2]
[1]Neurology, Hospital Clínico Universitario-Clinical Neurosciences Research Laboratory, A Coruña-Santiago de Compostel, Spain
[2]Pharmacy, Centro de Investigación en Medicina Molecular y E nfermedades Crónicas (CIMUS), A Coruña-Santiago de Compostel, Spain

Objectives: After ischemic stroke, there is a rapid elevation of glutamate into the extracellular space which leads to a neuronal death of the cerebral tissue. Consequently, glutamate antagonists have been widely studied as protective agents; unfortunately, they failed or displayed severe adverse effects when they were tested in clinical trials. Blood glutamate scavenging has becoming in a novel and attractive protecting strategy to reduce the excitotoxic effect of extracellular glutamate released in brain during acute phase of stroke.

We have discovered that compounds like oxaloacetate are able to acts as an effective blood scavengers of glutamate; however, its administration in humans has potential serious limitations as the required effective dosage to induce significant effect corresponding to that used in rats might be toxic. With the aim to solve this limitation, we have performed a screening analysis of repositioning drugs with blood glutamate scavenging activity with the aim to find a human approved drug which can be test immediately in stroke patients.

Methods: Prestwick Chemical Library composed of 1120 hits was used to detect drugs with blood glutamate scavenging activity. In vitro screening of blood glutamate scavenging activity was determinate based on the capacity of the hits to activate the enzyme glutamate oxaloacetate transaminase (GOT). The drug selected in the in vitro test with higher activity on GOT was proved in healthy animals to confirm its blood glutamate scavenging activity. Subspecialty the protective effect was tested in ischemic model animals induced through the intraluminal filament occlusion of middle cerebral artery occlusion (MCAO). Infarct volume (determined by means of MRI), blood glutamate levels and functional test were determined during 7 days after ischemic onset.

Results: We have discovered a new drug defined as CBG000592 with high blood scavenging activity determined either in vitro and in vivo analysis. Administration of CBG000592 (1 mg/Kg) in ischemic animal model 1 hour after artery occlusion induced a significant (p

Conclusions: In this study we have described the use the drug CBG000592 as new a potential treatment for ischemic stroke. Due to CBG000592 has been used previously in humans for other pathologies, human toxicity and pharmacokinetic analysis are not needed before to test its effects in stroke patients. Repositioning drugs represent an interesting alternative to reduce the risk in the study of new drugs in the field of ischemic pathology.

557
BRAIN-0197
Poster Session

Translational Studies

TRANSCRANIAL CHARACTERIZATION OF CEREBRAL BLOOD FLOW DYNAMICS DURING INDIVIDUAL OBSTRUCTIVE SLEEP APNEA EVENTS BY DIFFUSE OPTICS

P. Zirak[1], I. Blanco[1], C. Gregori[1], P. Bramon[1], A. Fortuna[2], G. Cotta[2], A. Mola[2], M. Mayos[2], T. Durduran[1]
[1]Medical Optics Group, ICFO-Institut de Ciències Fotòniques, Castelldefels, Spain
[2]Department of Pneumology, Hospital de la Santa Creu i Sant Pau, BARCELONA, Spain

Objectives: An obstructive apnea event (OAE) is the complete cessation of airflow for longer than 10 seconds with simultaneous respiratory movements [1], and is associated with increased risk of cerebrovascular and cardiovascular diseases [2]. Microvascular cerebral blood flow (CBF) dynamics during OAE may reveal the mechanisms of tissue damage. CBF measurement during sleep requires non-invasive, bed-side and continuous techniques, which is challenging for traditional methods. We demonstrate the feasibility of utilizing a diffuse optical technique, diffuse correlation spectroscopy (DCS) [3], for direct measurement of microvascular CBF changes during individual apneas of night sleep. We have characterized the dynamics of these changes and studied their relation to sleep parameters such as apnea duration, changes in arterial saturation and sleep stage.

Methods: Concurrent and continuous optical and polysomnography (PSG) data were obtained for sixteen severe OAE patients during the whole night sleep. DCS probe pads were placed and secured on the forehead. The PSG data were used to identify apnea events. The percent relative CBF change, ΔrCBF, relative to the average of twenty seconds before every individual apnea start was calculated. The maximum and minimum CBF during each OAE and their relative time from apnea start were extracted and used to study the effect of sleep parameters on CBF dynamics.

Results: 972 individual OAE were measured, and averaged based on their duration in four groups, as shown in Figure 1. Similar CBF dynamics is observed for OAE independent of their duration with a significant effect from previous nearby OAEs. We confirmed this effect of previous apneas by isolating apneas that were separated by a 20 seconds from a previous apnea. Statistical analysis have shown significant relationships between both the temporal characteristics and the amplitudes of CBF changes with apnea duration, sleep stage, and arterial desaturation at per apnea basis but not on average sleep parameters during the whole night.

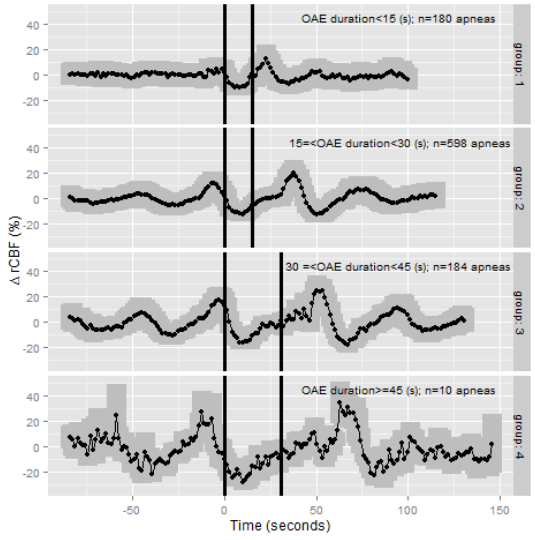

Figure 1: Average CBF changes during OAE for different apnea durations. Vertical lines show the start and the end of the apneas.

Conclusion: Microvascular CBF was measured during nocturnal sleep with sufficient signal-to-noise ratio to characterize individual apnea episodes. These microvascular CBF changes measured by DCS are similar, yet local, than those of CBF velocity measured by transcranial Doppler ultra-sound [4]. These repetitive cerebral hypo- and hyper-perfusion periods which occur simultaneously with cerebral hypoxia and hyperoxia may explain the reported association between disease risk and sleep apnea. We will

present detailed results and statistics and discuss potential of diffuse optics for sleep studies.

References

[1] Karl A Franklin. Cerebral haemodynamics in obstructive sleep apnoea and cheyne-stokes respiration. Sleep medicine reviews, 6(6):429-441, 2002.

[2] Douglas M Wallace, Alberto R Ramos, and Tatjana Rundek. Sleep disorders and stroke. International Journal of Stroke, 7(3):231{242, 2012.

[3] Turgut Durduran and Arjun G Yodh. Diffuse correlation spectroscopy for non-invasive, micro-vascular cerebral blood flow measurement. NeuroImage, 85:51-63, 2014.

[4] EM Balfors and Karl A Franklin. Impairment of cerebral perfusion during obstructive sleep apneas. American journal of respiratory and critical care medicine, 150(6):1587-1591, 1994.

558
BRAIN-0756
Poster Session

Translational Studies

CEREBRAL 5-HT RELEASE CORRELATES WITH PET MEASURES OF THE 5-HT2A RECEPTOR OCCUPANCY IN THE PIG BRAIN.

L.M. Jørgensen[1], P. Weikop[2], J. Villadsen[1], T. Visnapuu[3], A. Ettrup[1], H.D. Hansen[1], A.O. Baandrup[4], F.L. Andersen[5], C.R. Bjarkam[6], C. Thomsen[7], B. Jespersen[8], G.M. Knudsen[1]
[1]Neurobiology Research Unit, Copenhagen University Hospital Rigshospitalet, Copenhagen, Denmark
[2]The Laboratory of Psychiatry, Copenhagen University Hospital Rigshospitalet, Copenhagen, Denmark
[3]Center for Excellence in Translational Medicine, University of Tartu, Tartu, Estonia
[4]Research Center for Advanced Imaging, Hospital of Køge and Roskilde, Roskilde, Denmark
[5]Department of Clinical Physiology Nuclear Medicine and PET, Copenhagen University Hospital Rigshospitalet, Copenhagen, Denmark
[6]Department of Neurosurgery, Aarhus University Hospital, Aarhus, Denmark
[7]Department of Radiology, Copenhagen University Hospital Rigshospitalet, Copenhagen, Denmark
[8]Department of Neurosurgery, Copenhagen University Hospital Rigshospitalet, Copenhagen, Denmark

Objectives

Several studies have investigated PET radioligands for their ability to be displaced by endogenously released 5-HT, but the outcomes in humans have been somewhat contradictory and have not supported findings in animal experiments[1]. Two recent studies in humans suggested that the PET radioligands [11C]CUMI-101[2] and [11C]AZ10419369[3] may be sensitive to endogenous changes in 5-HT levels, but this is not supported by others[4]. Moreover, these two studies show an *increase* in binding rather than the expected decrease[2,3]. However, the apparently conflicting outcomes may be due to differences in how the pharmacological challenges affect synaptic 5-HT levels. The aim of the present study was to measure the pharmacological challenges' effect on 5-HT by cerebral microdialysis and to correlate this to the occupancy of the 5-HT2A receptor agonist radioligand [11C]Cimbi-36. We measured pharmacologically induced changes in 5-HT levels in the medial prefrontal cortex (mPFC) in vivo in pigs and assessed simultaneously changes in [11C]Cimbi-36[5] binding.

Methods

Thirteen pigs were scanned for 90 minutes in a HRRT scanner with [11C]Cimbi-36 at baseline and after serotonergic challenges aimed to increase extracellular 5-HT levels. The pharmacological interventions were 2 mg/kg escitalopram (serotonin reuptake inhibitor), escitalopram + 1

mg/kg pindolol (5-HT_{1A} autoreceptor agonist), 0.5 mg/kg fenfluramine (serotonin releaser) or saline.

The pigs had implanted microdialysis probes bilaterally in the mPFC (MRI verified) from which extracellular fluid were collected during PET scanning and analyzed off-line for 5-HT with HPLC. We made a correlation analysis between the peak 5-HT level relative to baseline and the 5-HT_{2A} receptor occupancy.

In two pigs, pharmacological depletion of 5-HT was done by pre-treatment with para-chlorophenylalanine (pCPA) (5-HT synthesis inhibitor) that substantially reduces 5-HT in the brain. This served to confirm that the decreased [11C]Cimbi-36 binding was not caused by direct interaction between fenfluramine and the 5-HT_{2A}-receptor.

Results

The extracellular 5-HT level increased to 725% following 0.5 mg/kg fenfluramine, to 337% following 2 mg/kg escitalopram + 1 mg/kg pindolol and to 171% following escitalopram alone. In pCPA pre-treated pigs, the 5-HT level was significantly reduced ($p<0.01$, $n=2$). The 5-HT_{2A} receptor occupancy as measured with [11C]Cimbi36 correlates significantly ($p=0.002$, $n=13$) with the changes in extracellular 5-HT levels in mPFC, as measured by microdialysis (figure 1).

Conclusions

We here show that 2 mg/kg escitalopram iv is associated with a smaller increase in 5-HT as compared to the other challenges and without any associated change in radioligand binding. The observed correlation between changes in the extracellular 5-HT level in the pig brain and the 5-HT_{2A} receptor occupancy indicates that [11C]Cimbi-36 is sensitive to changes in endogenous 5-HT levels, but that is only detectable on a global brain level when the 5-HT release is sufficiently high. Differences in earlier studies may thus be ascribed to the efficacy of the pharmacological interventions to change interstitial brain 5-HT levels.

References

1. Paterson. *J Cereb Blood Flow Metab*. 2010;30(10):1682-1706.

2. Selvaraj. *Mol Psychiatry*. 2012;17(12):1254-1260.

3. Nord. *Int J Neuropsychopharmacol*. 2013;16(07):1577-1586.

4. Pinborg. *Synapse*. 2012;66(10):880-884.

5. Ettrup. *J Cereb Blood Flow Metab*. 2014.

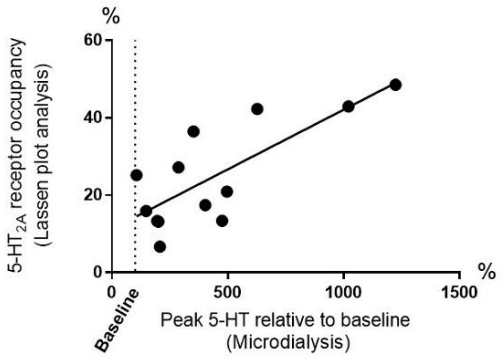

Figure 1. Correlation between pharmacologically induced changes in 5-HT pig brain (n =13) relative to baseline (100%) and 5-HT2A receptor occupancy quantified with kinetic modeling with Logan plot and Lassen plot analysis. The correlation is statistical significant (p=0.002).

559
BRAIN-0652
Poster Session

Translational Studies

MODIFICATION OF FUNCTIONAL CONNECTIVITY BY ACUPUNCTURE IN THE MOUSE BRAIN

H. Park[1], J. Park[1], S. Lee[1], A. Lee[1], J. Jang[1]
[1]Acupuncture and Meridian Science Research Center, Kyung Hee University, Seoul, Korea

Purpose: To identify the scientific mechanism of acupuncture therapy fromperipheral to central,

the molecular event at the acupuncture point in the skinlayer and the neural activity of the brain regions for the functionalconnectivity after acupuncture needling were investigated.

Methods: Acupuncturestimulation was performed on GB34 acupuncture point of C57BL/6 mice. Afteracupuncture stimulation, changes of proteins related to tissue deformation(Rho-kinase, ERM), neurotrophins (NT-3, BDNF, NGF), cell signaling (HSP27) and initiateimmune (PRDX1, transketolase) were assessed. To investigate the correlationbetween the molecular signaling, inhibitors of ERK, ROCK, TRPV1 and A1R weretreated before acupuncture needling, then the activation of p-ERK, p-ERM,p-HSP27, PRDX1 and transketolase in the skin layer was investigated. Next, toinvestigate the whole brain neural activity after acupuncture needling, c-Fosexpression in thirty brain regions of Cortex, Cerebral nuclei, Thalamus,Hypothalamus, Hippocampus, Midbrain and Medulla was investigated and partialleast squares (PLS) analysis and network generation was performed.

Results: After acupuncture stimulation, Rho-kinase, ERM, NT-3 and HSP27 wereup-regulated and BDNF, NGF, PRDX1 and transketolase were down-regulated in skintissues at acupuncture needling point. Then we found that ERK activation workedas a trigger molecule to produce local molecular signaling. After acupunctureneedling, c-Fos positive cells were significantly increased in the brainregions of cingulate cortex area 1 (Cg1), cingulate cortex area 2 (Cg2), primarysomatosensory cortex (S1), secondary motor cortex (M2), insular cortex (Insul),piriform cortex (Pir), nucleus of solitary tract (NTS), dorsomedialperiaqueductal gray (DMPAG) and lateral periaqueductal gray (LPAG) anddecreased in the brain region of paraventricular thalamic nucleus posterior(PV) and the field CA1 of hippocampus (CA1). And these changes were inhibitedby U0126 administration. Inter-regional correlations were significantly increasedafter acupuncture needling, and inhibited by U0126 administration. Among thebrain regions, RMg, ST-DM, CA1 and NTS were determined as hub regions.

Conclusion: In conclusion, acupuncture-induced ERK expression at acupunctureneedling point plays a trigger role to acupuncture-induced cell signalingpathway, and it seem to play an important role in initiating central functionalconnectivity of acupuncture needling.

This research was supported by a grant of the Korean HealthTechnology R&D Project, Ministry of Health and Welfare, Republic of Korea(No. HI13C0540).

560
BRAIN-0698
Poster Session

Translational Studies

MULTI-PART SURVEY: THE RISK OF BIAS IN IN VIVO STROKE RESEARCH

E.S. Sena[1], S.M. Allan[2], P.M. Bath[3], U. Dirnagl[4], D.W. Howells[5], M.R. Macleod[1], I.M. Macrae[6], J. Montaner[7], N. Percie du Sert[8], A.M. Planas[9], A. Rosell[7], H.B. van der Worp[10], D. Vivien[11], H. Würbel [12]
[1]Centre for Clinical Brain Sciences, Univeristy of Edinburgh, Edinburgh, United Kingdom
[2]Faculty of Life Sciences, University of Manchester, Manchester, United Kingdom
[3]Division of Stroke Medicine, University of Nottingham, Nottingham, United Kingdom
[4]Department of Experimental Neurology, Charité Universitätsmedizin, Berlin, Germany
[5]Stroke Division, The Florey Institute of Neuroscience and Mental H ealth, Melborune, Australia
[6]Wellcome Surgical Institute, University of Glasgow, Glasgow, United Kingdom
[7]Neurovascular Research Laboratory, Vall d'Hebron Research Institute, Barcelona, Spain
[8]Experimental Design Analysis and Reporting, National Centre for the Replacement Refinement and Reduction of Animals in Research, London, United Kingdom
[9]Cerebrovascular Research team, Spanish National Research Council, Barcelona,

Spain
[10]Department of Neurology Rudolf Magnus Institute of Neuroscience,
University Medical Center Utrecht, Utrecht, Netherlands
[11]INSERM U919 unit,
University Caen Lower Normandy, Caen, France
[12]Animal Welfare Division, University of Bern, Bern, Switzerland

Objectives: The Multi-PART (Multicentre Preclinical Animal Research Team; www.multi-part.org) consortium seeks to contribute to improvements in the validity and generalisability of preclinical stroke research by developing a capacity for international multicentre animal studies. This approach has been driven by systematic analyses of preclinical stroke data showing: (i) a failure to report measures to reduce the risk of bias is associated with substantial overstatements of treatment effects; and (ii) declining efficacy in cumulative meta-analysis, with stable estimates of efficacy occurring with datasets for 1000 animals or more.

As part of developing a framework for multicentre animal studies we performed a survey of *in vivo* stroke scientists. Our aim was to ascertain current practice, including measures to reduce the risk of bias, to inform the central coordination of multicentre animal studies.

Methods: We conducted an online survey in July 2014 of *in vivo* ischaemic stroke scientists identified through membership of the Multi-PART consortium or those that have expressed interest in the consortium. We asked respondents to state whether they randomly allocate animals to treatment groups and if applicable, the method used to perform randomisation. We also asked respondents if they blinded the conduct of surgery, animal handling, and assessment of infarct volume and behavioural deficits. Separately, we assessed the reporting of randomisation, allocation concealment and blinded assessment of outcome in *in vivo stroke* studies identified in systematic reviews, published after 2010 and curated in the CAMARADES database (www.camarades.info).

Results: We invited 59 laboratories to participate in the survey of which 32 (54%) responded; 23 were European-based laboratories and nine from the rest of the world. Of these, 29 (91%) stated that they randomly allocate animals to treatment groups. However, 6 of these 'picked animals randomly from the cage' or used 'alternate allocation', not considered true randomisation. Most (25) respondents induced focal ischaemia blinded to treatment allocation and of these 90% maintained blinding for the duration of the experiment. All respondents blinded the assessment of infarct volume and behavioural deficits.

Of 80 experiments in the CAMARADES database published after 2010, 23% reported allocation concealment, 36% reported randomisation and 44% reported blinded assessment of outcome.

Conclusions: Self-reporting of measures to reduce the risk of bias in leading stroke laboratories was substantially higher than in published reports. We purport that either (i) those responding to our survey may not be typical of the *in vivo* stroke scientist population, (ii) published reports do not adequately reflect experimental conduct and may actually underestimate the measures taken to reduce the risk of bias or (iii) reporting guidelines and increased awareness of the impact of bias has improved the quality of preclinical stroke research. In addition, our survey raised concerns of different interpretations of what is meant by randomisation. Protocols for multicentre animal studies must therefore take care to ensure that all aspects of experimental design are clearly defined and, where appropriate, provide training to address this.

The authors acknowledge support from the European Commission Seventh Framework Programme Coordination and Support Action, Grant Agreement number: 603043

561
BRAIN-0619
Poster Session

Translational Studies

MULTI-PART BETA-TEST: TESTING THE FEASIBILITY AND FUNCTIONALITY OF MULTICENTRE PRECLINICAL ANIMAL STUDIES

R.C. Trueman[1], S.M. Allan[2], P.M. Bath[3], U. Dirnagl[4], D.W. Howells[5], M.R. Macleod[6], I.M. Macrae[7], J. Montaner[8], N. Percie du Sert[9], A.M. Planas[10], H.B. van der Worp[11], D. Vivien[12], H. Würbel[13], E.S. Sena[6]
[1]Life Sciences, University of Nottingham, Nottingham, United Kingdom
[2]Faculty of Life Sciences, University of Manchester, Manchester, United Kingdom
[3]Division of Clinical Neuroscience, University of Nottingham, Nottingham, United Kingdom
[4]Center for Stroke Research, Charité Universitätsmedizin, Berlin, Germany
[5]The Florey Institute of Neuroscience and Mental Health, University of Melbourne, Melbourne, Australia
[6]Department of Clinical Neurosciences, University of Edinburgh, Edinburgh, United Kingdom
[7]Centre for Stroke and Brain Imaging Research, University of Glasgow, Glasgow, United Kingdom
[8]Neurovascular Research Group, Vall d'Hebron Research Institute, Barcelona, Spain
[9]NC3Rs, Gibbs Building, London, United Kingdom
[10]IIBB Department of Brain Ischemia and Neurode generation, Consejo Superior de Investigaciones Científicas (CS IC), Barcelona, Spain
[11]Department of Neurology and Neurosurgery, University Medical Center Utrecht, Utrecht, Netherlands
[12]INSERM UMR-S 919, Serine Proteases and Pathophysiology of the Neur ovascular Unit, Caen, France
[13]Division of Animal Welfare, University of Bern, Bern, Switzerland

Objectives

Multi-PART (**Multi**centre **P**reclinical **A**nimal **R**esearch **T**eam; www.multi-part.org) has developed a framework for the design and conduct of adequately powered multicentre 'phase III'-type preclinical trials with improved internal and external validity, using ischaemic stroke as an exemplar.

We are now undertaking a beta-test of this platform. We will use glyceryl trinitrate (GTN), a nitric oxide donor, in rodent models of ischaemic stroke. GTN has shown promise in patients with acute ischaemic stroke and will be further tested in the RIGHT 2 clinical trial.[1,2]

The aim of this beta-test is to establish the functionality, feasibility and effectiveness of this multicentre approach for preclinical testing.

Methods

We have designed an international multicentre preclinical trial to test GTN to treat stroke, across 10 participant sites from the UK, Spain, France, Germany, Australia and the USA. We will include two models of stroke: transient middle cerebral artery occlusion (MCAO) using an intraluminal filament and permanent distal (diathermy) MCAO, both in male C57BL/6 mice. A neuroscore and sensorimotor test will be used to assess functional recovery and 2,3,5-triphenyltetrazolium chloride (TTC) staining to quantify infarct volume at 48hrs post-MCAO.

Results

We will present the successes and hurdles of implementing a multicentre preclinical trial, Specifically, we will present the functionality and feasibility of the following components of the Multi-PART platform: (1) The ability to seek ethical approval from multiple regulatory authorities, (2) experimental design and sample size calculations, (3) centralised randomisation and blinding, (4) standard operating procedures, (5) centralised data collection and scoring, (6) a

web-based data management system, and (7) statistical analysis and data monitoring systems.

Conclusions

Performing this beta-test will establish the functionality, feasibility and effectiveness of this multicentre approach for preclinical testing.

The authors acknowledge support from the European Commission Seventh Framework Programme Coordination and Support Action, Grant Agreement number: 603043.

References

1. Ankolekar, S. *et al.* Feasibility of an ambulance-based stroke trial, and safety of glyceryl trinitrate in ultra-acute stroke: the rapid intervention with glyceryl trinitrate in Hypertensive Stroke Trial (RIGHT, ISRCTN66434824). *Stroke; a journal of cerebral circulation* **44**, 3120–8 (2013).

2. The ENOS Trial Investigators. Efficacy of nitric oxide, with or without continuing antihypertensive treatment, for management of high blood pressure in acute stroke (ENOS): a partial-factorial randomised controlled trial. *The Lancet* (2014).doi:10.1016/S0140-6736(14)61121-1

562
BRAIN-0406
Poster Session

Translational Studies

LOWERING ICP FOLLOWING STROKE: NK1 ANTAGONIST AS EFFECTIVE AS DECOMPRESSIVE SURGERY

R. Turner[1], *A.V. Leonard*[1], *R. Vink*[2]
[1]*Anatomy and Pathology, University of Adelaide, Adelaide, Australia*
[2]*Division of Health Sciences, University of South Australia, Adelaide, Australia*

OBJECTIVES: Brain swelling and elevated intracranial pressure (ICP) are life-threatening complications of stroke, associated with poor outcomes and a mortality rate in excess of 60-80%. Currently, therapy is limited to osmotic agents that aim to dehydrate the swollen brain or decompressive surgery to remove bone overlying the swollen brain to relieve pressure. Although this is a lifesaving procedure it is highly invasive and not without risk. Clearly, each of these approaches does not address the cause of the swelling, rather treating the symptoms of swelling. As such, alternate non-surgical treatments targeting the mechanisms associated with elevated ICP are urgently required. We have previously documented the efficacy of NK1 receptor antagonists in reducing brain swelling and barrier permeability whilst also improving functional outcome following stroke in a rodent model. The aim of this study was to compare the effect of NK1 receptor antagonist treatment to the gold-standard treatment of decompressive craniectomy in their capacity to lower ICP following middle cerebral artery (MCA) occlusion in a clinically relevant ovine model.

METHODS: Female Merino sheep (n=25) were subject to either sham surgery or proximal MCA occlusion achieved by diathermy under Isoflurane and ketamine anaesthesia. Animals were randomized to vehicle (saline) NK1 antagonist or decompressive craniectomy treatment groups. Vehicle or NK1 antagonist (1 dose = 4h; 2 dose = 4h and 9h; 3 dose = 4h, 9h, and 14h following stroke) treatment was given as a slow intravenous bolus. Animals in the decompressive surgery group underwent bone removal (3cm x 6cm)overlying the ischaemic tissue at 4hrs following stroke onset with synthetic dura (Durepair) used to maintain ICP dynamics. Blood pressure, blood gases and ICP were recorded for 24hrs after the induction of stroke. At 24hrs animals underwent magnetic resonance imaging (MRA, T1, T2, DWI).

RESULTS: Blood pressure and blood gases remained stable in all groups. There was a 30% mortality rate in the vehicle-treated group, whereas all animals in the NK1 antagonist and decompressive craniectomy groups survived the 24hr-monitoring period. Permanent MCA

occlusion resulted in significant increases in ICP over the 24hr-monitoring period in vehicle animals. Either 2 or 3 doses of NK1 antagonist significantly reduced ICP, with no significant difference when compared to the decompressive craniectomy group. Vehicle-treated animals demonstrated marked midline shift and tonsillar herniation associated with in significant cerebral oedema on MRI. NK1 antagonist treatment or decompressive surgery completely prevented tonsillar herniation and a reduced degree of midline shift. NK1 antagonist treated animals showed evidence of reduced cerebral oedema. A subset of decompressive animals demonstrated marked transcalvarial herniation out of the craniotomy site.

CONCLUSIONS: NK1 receptor antagonist treatment is as effective as decompressive craniectomy in lowering intracranial pressure following ovine stroke. As such, NK1 antagonist treatment provides a potential alternative to invasive surgery when managing cerebral oedema and elevated ICP following stroke. This study using a clinically relevant animal model provides good evidence for progression to clinical assessment, an approach that may assist in improving the clinical translation of novel therapeutics in stroke.

563
BRAIN-0272
Poster Session

Clinical Studies

MULTIPLE PATHOLOGICAL CONDITION OF HYPERPERFUSION AFTER STA-MCA BYPASS FOR MOYAMOYA DISEASE

E. Hamano[1], H. Kataoka[1], Y. Abekura[1], D. Maruyama[1], J. Nakagawara[1], J. Takahashi[1]
[1]Neurosurgery,
National Cerebral and Cardiovascular Center, Osaka-Suita, Japan

Objectives

Hyperperfusion was presumed to be a leading cause of postoperative transient neurological symptom after STA-MCA bypass for Moyamoya disease. We examined cerebral blood flow and metabolism of hyperperfusion by perioperative O^{15}-gas PET retrospectively.

Method

Among 35 patients (41 hemispheres) underwent STA-MCA bypass between April 2013 and April 2014, 13 patients (15 hemispheres) who underwent O^{15}-gas PET prior to and after surgery were enrolled in this study. Preoperative PET was performed for all patients. Postoperative PET was indicated when transient neurological deficit appeared and/or postoperative SPECT showed hyperperfusion. For quantitative assessment of CBF, CMRO2, OEF and CBV, 1cm diameter of regions-of-interest delineated the area of increased CBF using Qview software. Postoperative quantitative values of each parameter were compared with those before operation.

Result

CBF increased from 29.7 ml/100g/min before surgery to 52.67±18.1ml/100g/min after surgery except 1 case with hypoperfusion due to graft spasm. CMRO2 was unchanged from 2.9±0.9 ml/100g/min to 2.9±4.0 ml/100g/min. Change ratios of each parameter were categorized into 4 groups. Group1: increased CBF, unchanged CMRO2 (n=9, 60.0%). Group2: increased CBF, increased CMRO2 (n=2, 13.3%). Of these, 1 case revealed abnormal EEG. Group3: increased CBF, decreased CMRO2 (n=3, 20.0%). In the Group3, postoperative cerebral infarction occurred in 2 (66.7%) cases, showing vasogenic edema on MRI. Group4: decreased CBF, decreased CMRO2 (n=1, 6.6%). Repetitive MRA showed transient graft spasm at the time of PET scan.

Conclusion

Although the common cause of postoperative neurological symptom after STA-MCA bypass in patient with Moyamoya disease, hyperperfusion was categorized into 3 groups. Group1 was the most common type of hyperperfusion. It was

suggested that multiple factors such as nonconvulsive status epilepticus and vasogenic edema may be involved in. Postoperative infarction occurred despite of increased CBF, suggesting that hypoperfusion was not the only factor of postoperative infarction.

References

Kaku, Y. (2012). Cerebral blood flow and metabolism of hyperperfusion after cerebral revascularization in patients with moyamoya disease. J Cereb Blood Flow Metab32 2066-75

564
BRAIN-0083
Poster Session

Clinical Studies

ISCHEMIC STROKE DURING TREATMENT WITH DABIGATRAN IS ASSOCIATED WITH DECREASED SEVERITY AND FAVORABLE PROGNOSIS

T. Hayashi[1], Y. Kato[1], T. Fukuoka[1], I. Deguchi[1], H. Maruyama[1], Y. Horiuchi[1], H. Sano[1], Y. Nagamine[1], S. Mizuno[1], M. Takao[1], N. Tanahashi[1]
[1]Neurology and Cerebrovascular Medicine, International Medical Center Saitama Medical University, Hidaka, Japan

Objectives: Anticoagulation therapy with warfarin is associated with a favorable prognosis in ischemic stroke (1). Dabigatran, a new oral anticoagulant, is widely used to prevent ischemic stroke in non-valvular atrial fibrillation (NVAF) patients (2). However, its association with decreased severity and favorable prognosis once ischemic stroke has occurred remain unknown. We therefore investigated whether dabigatran has a protective effect against ischemic stroke even if it occurs.
Methods: We retrospectively reviewed all patients with NVAF-associated ischemic stroke admitted to our hospital from April 2011 to December 2014, and included those who took dabigatran. We assessed whether patients were under regular use of the drug or tentative discontinuance, and classified them into 2 groups, treatment and discontinuation groups. Data on age, sex, ASCOD stroke phenotype, NVAF type (i.e., paroxysmal or persistent), comorbidities, CHADS2 score, National Institute of Health Stroke Scale (NIHSS) score on admission, modified Rankin scale (mRS) score at discharge, D-dimer, and BNP were investigated and compared between the groups.
Results: There were 15 patients with NVAF-associated ischemic stroke, to whom dabigatran had been prescribed. Nine patients were under regular dabigatran therapy, and 6 were under discontinuance of the drug. As shown in Table, age, sex, ASCOD stroke phenotype, NVAF type, comorbidities, and CHADS2 scores were similar between the 2 groups; however, NIHSS scores were significantly lower in the treatment group (P = 0.019). mRS scores at discharge were also lower in the treatment group (P = 0.027). Moreover, D-dimer levels were lower in the treatment group (P = 0.010), suggesting a possible role in decreased stroke severity.

Table. Comparison of demographics, risk factors, laboratory data, CHADS2 score, NIHSS score, and mRS in stroke patients with and without regular dabigatran use

	Treatment group (n = 9)	Discontinuation group (n = 6)	P value
Age (mean ± SD)	73.9 ± 9.6	75.5 ± 8.5	0.739
Male sex	9 (100%)	4 (66.7%)	0.063
Heart failure	0 (0%)	2 (33.3%)	0.063
Hypertension	5 (55.5%)	4 (66.7%)	0.667
Diabetes mellitus	2 (22.2%)	2 (33.3%)	0.634

Past history of stroke	5 (55.5 %)	2 (33.3%)	0.398
D-dimer	0.56 ± 0.08	3.07 ± 1.25	0.010
BNP	227.0 ± 206.1	762.6 ± 1381.1	0.388
CHADS2 before admission (median, range)	3 (0–4)	2.5 (1–4)	0.563
NIHSS on admission (median, range)	1 (1–5)	12.5 (1–19)	0.019
mRS at discharge (median, range)	1 (0–3)	4 (1–5)	0.027
Abbreviations: BNP, brain natriuretic peptide; mRS, modified Rankin Scale; NIHSS, National Institute of Health Stroke Scale			

Conclusions: Dabigatran is associated with decreased severity and a favorable prognosis even when ischemic stroke occurs. It was indicated that thrombi tended to be smaller in the treatment group.

References: (1) Nakamura A, Ago T, Kamouchi M, et al. Intensity of anticoagulation and clinical outcomes in acute cardioembolic stroke: the Fukuoka Stroke Registry. Stroke 44: 3239–3242, 2013. (2) Connolly SJ, Ezekowitz MD, Yusuf S, et al. Dabigatran versus warfarin in patients with atrial fibrillation. N Engl J Med 361: 1139–1151, 2009.

565
BRAIN-0746
Poster Session

Clinical Studies

USE OF DYNAMIC SUSCEPTIBILITY CONTRAST MAGNETIC RESONANCE IMAGING TO PREDICT THE TYPE OF STROKE AND EXTENT OF INFARCTION IN ACUTE ISCHEMIC STROKE

Y. Ishii[1], T. Nariai[2], Y. Tanaka[2], Y. Suyama[1], H. Aihara[1], T. Ohshita[3], H. Kajikawa[1], S. Wakabayashi[1], T. Maehara[2]
[1]neurosurgery, Suiseikai Kajikawa Hospital, Hiroshima, Japan
[2]neurosurgery, Tokyo Medical and Dental University, Tokyo, Japan
[3]neurology, Suiseikai Kajikawa Hospital, Hiroshima, Japan

Background: Dynamic susceptibility contrast (DSC) MRI is the powerful tool to measure cerebral hemodynamics non-invasively and is widely used in the management of cerebrovascular disease. It has not been defined yet, however, whether DSC-MRI measured parameters can predict the tissue fate of ischemic brain in acute phase stroke. It also has not been well clarified whether the subtype of stroke can been distinguish by DSC-MRI measured parameters. As such information is inevitable to chose an appropriate treatment plan for acute stroke patients, we performed clinical study to clarify the role of DSC-MRI in acute stroke management.

Subjects and Methods: Thirty patients with cerebral infarction due to major vessel occlusion were included in this study. Patients were divided into 3 groups according to the subtype of stroke (atherothrombosis group, cardioembolism group, others group). All of the patients showed no recanalization for at least 3 days from onset confirmed by MRA. DSC-MRI was conducted within 24 hours of stroke onset and following parameters were calculated, referred to the counter region of the contralateral hemisphere as a control; time to peak (TTP), cerebral blood flow (CBF), cerebral blood volume (CBV), mean transit time (MTT), and time to maximum residue

function (Tmax). DWI was also obtained at the same time with DSC-MRI and 3 days after onset, to identify the tissue fate of diffusion-perfusion mismatch area. The DSC parameters were compared among groups of stroke subtype, and between the areas with or without irreversible change. Parameters with a significant difference were assessed by receiver-operator characteristic (ROC) analysis to identify the optimal parameters and parameter thresholds for predicting the type of stroke and extent of infarction.
Results: There were 18, 10, and 2 patients included in atherothrombosis group, cardioembolism group, others group, respectively. Relationship between the subtype of stroke and DSC-MRI parameters were examined first. Atherothrombosis group showed significantly higher CBV ratio (CBV%) and CBF ratio (CBF%) than in cardioembolism group. When CBV% of 110% was used to distinguish between the two groups, the sensitivity was 0.966, the specificity was 0.724, and the area under the curve (AUC) was 0.904 (95%CI: 0.850-0.941)(Fig.1). Secondly we examined the fate of tissue in relation to DSC-MRI parameters in acute phase. In atheroscrelotic patients, on the other hand CBF% was the most useful parameters to predict the extent of infarction compared to other parameters [threshold 82.3%, sensitivity 0.800, specificity 0.941, and AUC 0.918 (0.749-0.977)](Fig.2). In cardioembolic stroke, a low CBV% [threshold of 87.8%, sensitivity of 0.963, specificity of 0.938, and AUC 0.968 (0.893-0.991)](Fig.3) was the most useful parameter.
Conclusions: CBV% was the most useful parameter to determine the subtype of stroke in acute ischemic stroke. CBF% was a useful parameter to predict the extent of infarction in atheroscrelotic patients. In cardioembolic stroke, CBV% was also useful to predict the fate of ischemic tissue. We concluded that DSC-MRI is a reliable method to distinguish the type of stroke and to predict the fate of ischemic tissue. Such information must be useful for the management of patients suffering from acute stroke.

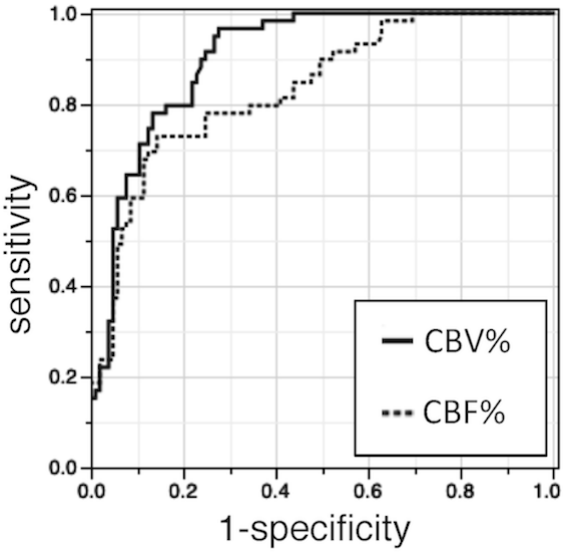

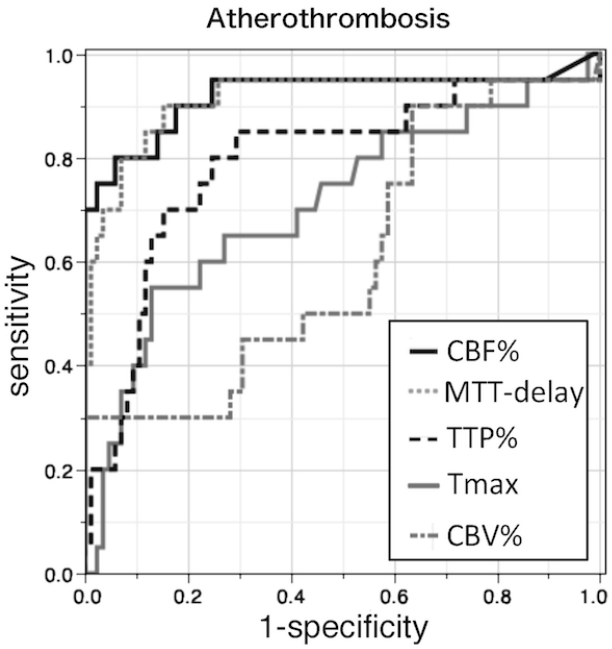

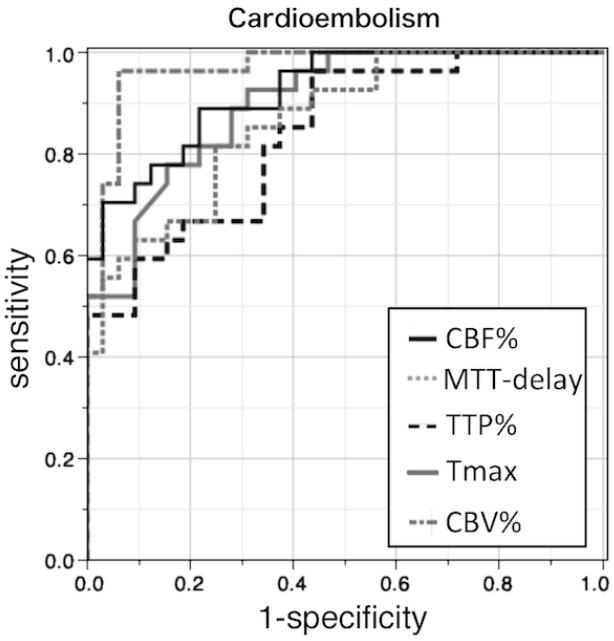

566
BRAIN-0369
Poster Session

Clinical Studies

DIFFUSION TRACTOGRAPHY OF FACIAL NERVE IN CEREBELLO-PONTINE ANGLE TUMOURS

M. Krakowiak[1], P. Słoniewski[1], T. Szmuda[1]
[1]Neurosurgery, Medical University of Gdansk, Gdansk, Poland

Introduction. Preoperative imaging of the facial nerve (FN) in relation to cerebello-pontine angle (CPA) tumour would allow the surgeon to increase the safety of tumour resection. Tractography based on diffusion tensor imaging (DTI) is a novel method for visualisation of the white matter fibres and the cranial nerves.

Aim. To evaluate the correspondence of preoperative DTI with real FN position and assess the impact of FN imaging on reduction of facial paresis rate.

Material and methods. In 2013-2014, DTI with 3D modelling of CPA tumor was performed in 7 patients in the Neurosurgery Department of the Medical University of Gdańsk. Various factors were analysed, including age, gender, tumour size, its histopathology, and FN real and DTI location.

Results. Postoperative facial paresis was diagnosed in 3 patients (42.9%). In one patient, an eigenvector error of DTI occurred. The real position of FN corresponded with DTI only in 57% of patients. The sensitivity of 80% (95%CI:28.8-96.7%) was achieved. None of examined factors was significantly related to the agreement of the DTI with the real FN position. The correct prediction of FN location by means of DTI did not influence the reduction of postoperative facial paresis.

Conclusions. Contrary to some previous reports, sensitivity of DTI in CPA tumours has been found to be low in our study. Further prospective studies involving a greater number of subjects are required to establish a firm position of DTI in FN visualisation.

567
BRAIN-0371
Poster Session

Clinical Studies

QUANTIFICATION OF WHITE MATTER FIBRE PATHWAYS DISRUPTION IN FRONTAL TRANSCORTICAL APPROACH TO THE LATERAL VENTRICLE OR THE INTERVENTRICULAR FORAMEN IN DIFFUSION TENSOR TRACTOGRAPHY.

M. Krakowiak[1], P. Słoniewski[1], T. Szmuda[1]
[1]Neurosurgery, Medical University of Gdansk, Gdansk, Poland

Introduction: Pathologies occupying the interventricular foramen (foramen of Monro — FM) or the anterior part of lateral ventricle (LV) are accessed by the transcortical or transcallosal route. As severing of rostral corpus callosum has been deemed inferior to cortical incision, the approaches through various points of frontal lobe have been developed. Superior (F1), middle (F2) frontal gyrus or occasionally superior frontal sulcus are used as an entry of neurosurgical

corridor. In spite of the fact that every approach to LV or FM causes its characteristic irreversible damage to white matter, to date all of transcortical routes are regarded as equivalent.

Methods: The current study compared the damage of main neural bundles between virtual trans-F1 and trans-F2 corridors by means of diffusion tensor tractography method (DTT) in 11 magnetic resonance imaging (MRI) exams from clinical series (22 hemispheres, regardless of dominance).

Results: Corpus callosum, cingulum, subdivisions I and II of superior longitudinal fasciculus (SLF I and SLF II), corticoreticular as well as pyramidal tracts crossing both approaches were subjected to surgical violation. Both approaches served a similar total number of fibres (0.94 to 1.78 [× 103]). Trans-F1 route caused significantly greater damage of total white matter volume (F1: 8.26 vs. F2: 7.16 mL), percentage of SLF I fibres (F1: 78.6% vs. F2: 28.6%) and cingulum (F1: 49.4% vs. F2: 10.6%), whereas trans-F2 route interrupted more corticoreticular fibres (F1: 4.5% vs. F2: 30.7%). Pyramidal tract (F1: 0.6% vs. F2: 1.3%) and SLF II (F1: 15.9% vs. F2: 26.2%) were marginally more vulnerable in case of the access via middle frontal gyrus. Both approaches destroyed 7% of callosal fibres. Conclusions: trans-F2 route disrupted a greater number of fibres from eloquent neural bundles (SLF II, pyramidal and corticoreticular tracts), therefore is regarded as inferior to trans-F1 one. Due to lack of up-to-date guidelines with recommendations of the approaches to LV or FM, an individual preoperative planning based on DTT should precede a surgery.

568
BRAIN-0830
Poster Session

Clinical Studies

EFFECT OF SILDENAFIL ON CEREBROVASCULAR REACTIVITY IN PATIENTS WITH BECKER MUSCULAR DYSTROPHY

U. Lindberg[1], N. Witting[2], S. Joergensen[3], J. Vissing[2], E. Rostrup[1], H.B.W. Larsson[1], C. Kruuse[4]

[1]Functional Imaging Unit Department of Diagnostics, Glostrup Hospital, Glostrup, Denmark
[2]Neuromuscular Research Unit and Department of Neurology, Rigshospitalet, Copenhagen, Denmark
[3]Dept Neurology Lundbeck Foundation Centre Neurovascular Signalling, Glostrup Hospital, Glostrup, Denmark
[4]Neurovascular Research Unit Dept Neurology, Herlev Hospital and University of Copenhagen, Herlev, Denmark

Objectives: Patients suffering from Becker Muscular Dystrophy(BMD) may be deficient in neuronal nitric oxide synthase (nNOS) in muscle and brain[1] because ofdysfunctional dystrophin. A functional ischemia during activity may apply [2]. nNOS is thoughtto play an important role in the regulation of microvascular circulation, whichcan be measured in brain using the blood oxygen level dependent (BOLD) response.BMD patients are known to show cognitive deficits. In a mouse model of Duchennemuscular dystrophy, sildenafil, which augment NO effects, has been shown toreduce associated skeletal muscle and cardiac dysfunction [3].We hypothesized that treatmentwith a phosphodiesterase 5 (PDE5) inhibitor (sildenafil), which potentiates nitricoxide responses, will augment both the BOLD-response and CBF in patients withBMD.

Methods: Seventeen patients (38.5 ± 10.8 years) with BMD were included in a randomised,double-blinded, placebo-controlled crossover design. Magnetic Resonance Imaging (MRI) was performed on a3.0 T Philips Achieva scanner using a 32-channel head coil. The cerebral effects of sildenafil were assessed by sensory evokedpotentials, somatosensory task-induced BOLD-fMRI, regional and global perfusion,angiography, and resting-state network. Threescans were done, before and after 4 weeks daily treatment with sildenafil20 mg or placebo, using BOLDcontrast imaging. For the electrical stimulation, all patients underwent two identical somatosensory electrical stimulationtasks; one outside the scanner with recording of EEG and one inside the scannerduring BOLD-recording.

Results: Twelve patients completed all scans. Treatment with sildenafil compared to placebo in BMDpatients showed a significant increase in the somatosensory BOLD response ($p<0.01$) thoughwithout corresponding changes in sensory evoked potentials. Minor changes inresting state networks were detected in the posterior cingulate/cerebellarconnectivity. No significant changes were detected in the remainingparameters of CBF and arterial diameter.

Conclusions: In conclusion, nNOS could play a role in both event-related andresting state neurovascular response. The results indicate a specific change in the neurovascular reactivityof BMD patients, perhaps due to altered dystrophin or nNOS function. Further studies in BMD patients may help to understand the role ofdystrophin and nNOS in neurovascular coupling in general, and in BMD patientsin particular.

References

1. Waite A, Tinsley CL, Locke M,Blake DJ. The neurobiology of the dystrophin-associated glycoprotein complex. *Annals of medicine* 2009; **41**(5): 344-59.

2. RandoTA. Role of nitric oxide in the pathogenesis of muscular dystrophies: a"two hit" hypothesis of the cause of muscle necrosis. *Microsc Res Tech* 2001; **55**(4): 223-35.

3. AdamoCM, Dai DF, Percival JM, et al. Sildenafil reverses cardiac dysfunction in themdx mouse model of Duchenne muscular dystrophy. *Proc Natl Acad Sci U S A* 2010; **107**(44):19079-83.

569
BRAIN-0159
Poster Session

Clinical Studies

CLINICAL CHARACTERISTICS OF CEREBRAL VENOUS THROMBOSIS IN A SINGLE CENTER IN KOREA

C. Moon[1], *D.S. Park*[1]
[1]*Neurosurgery, Konkuk University Medical Center, Seoul, Korea*

Objective: The purpose of this study is to investigate the clinical characteristics of cerebral venous thrombosis (CVT) in a single center in Korea.

Methods: A total of 36 patients were diagnosed with CVT from August 2005 to May 2013. The patient data regarding age, sex, disease stage, pathogenesis, location, laboratory findings, radiological findings, and treatment modalities were retrospectively collected. The results were compared with those of previous studies in other countries.

Results: The patient group comprised 21 men and 15 women with a mean age of 46.9 years (ranging from three months to 77 years). The most common cause was a prothrombotic condition (8 patients, 22.2%). Within the patient group, 13 patients (36.1%) had a hemorrhagic infarction, whereas 23 (63.9%) had a venous infarction without hemorrhage. By location, the incidence of hemorrhagic infarction was the highest in the group with a transverse and/or sigmoid sinus thrombosis (n=9); however, the proportion of hemorrhagic infarction was higher in the cortical venous thrombosis group (75%) and the deep venous thrombosis group (100%). By pathogenesis, the incidence of hemorrhagic infarction was the highest in the prothrombotic group (n=6), which was statistically significant ($p=0.016$).

Conclusion: According to this study, CVT was more prevalent in men, and the peak age group comprised patients in the sixth decade. The most common cause was a prothrombotic condition.

This finding was comparable with reports from Europe or America, in which CVT was more common in younger women. Hemorrhagic infarction was more common in the prothrombotic group (p=0.016) than in the non-prothrombotic group in this study.

570
BRAIN-0045
Poster Session

Clinical Studies

PREVENTIVE DETECTION OF AROU OF ACUTE STROKE PATIENTS

P.M. Ng[1]
[1]*ASU Medical & Geriatric, Princess Margaret Hospital, Hong Kong, Hong Kong China*

Background/Objectives: Bladder dysfunction following stroke is common. The importance of acute retention of urine (AROU)[(9)(28)]has been underestimated among complications of acute stroke[(9)(14)(15)(18)(21)(23)(26)(27)(30)(33)(36)]. The purpose of this study is to study the prevalence and risk factors of AROU in acute major stroke [(2)(6)(21)(23)(30)(33)], and the feasibility of an AROU assessment protocol with the use of ultrasonic bladder scan [(3)]for early detection of AROU.

Methods: A retrospective observation study on 100 acute major stroke patients admitted to the Acute Stroke Unit of Princess Margaret Hospital, Hong Kong from July 2012 to October 2012. Data collected include age, sex, etiology of stroke (Figure1), medical comorbidities related to AROU (diabetes mellitus (DM), benign prostatic hyperplasia (BPH), urinary tract infection (UTI)) or urinary system, Glasgow Coma Scales (GCS) [(4)], National Institutes Heath Stroke Scales (NIHSS)[(5)] and Modify Barthel Index (MBI)[(6)]. Following an in-house AROU assessment flowchart (Flowchart1), ultrasonic bladder scanning with BVI9400 bladder scanner [(3)] was used to document the presence of urinary retention.

Result: 27 patients had been detected to develop AROU after acute major stroke, a prevalence of 30%. Brainstem infarction appeared to be associated with AROU, while age, sex and severity of stroke were not. Patients have been had past history of urinary retention was more prone to develop AROU (Table1).

Conclusion: Prevalence of AROU after acute major stroke was high. An AROU assessment protocol with the use of ultrasonic bladder scan was a useful tool for early detection of AROU.

Flowchart 1: Assess AROU in ASU patients

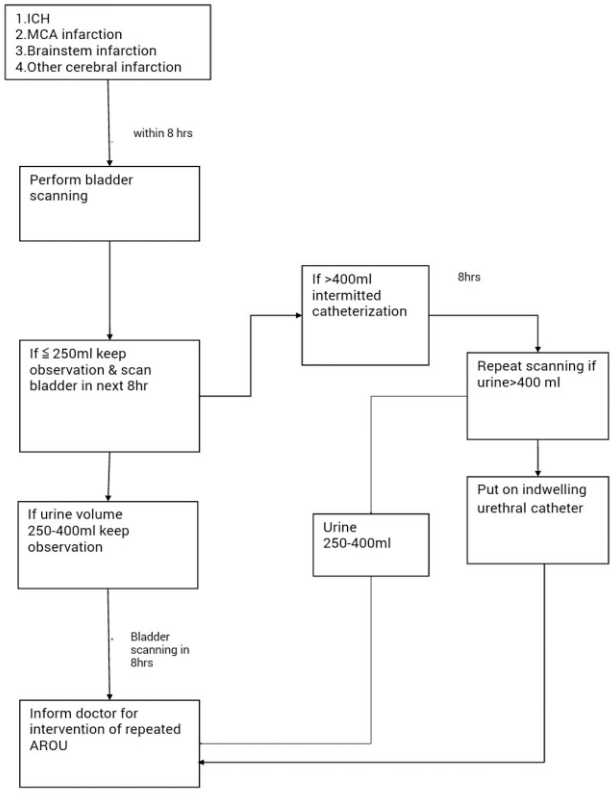

Figure 1: Etiology of acute stroke patients

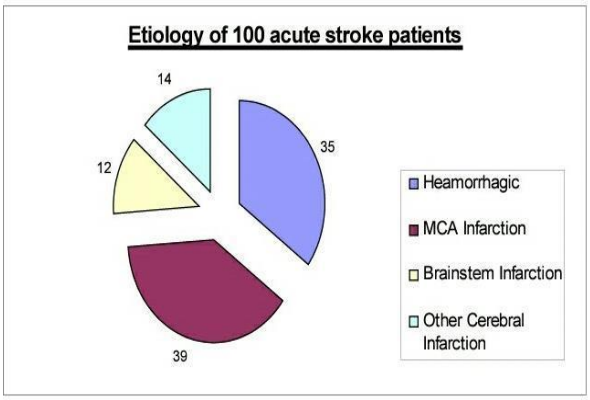

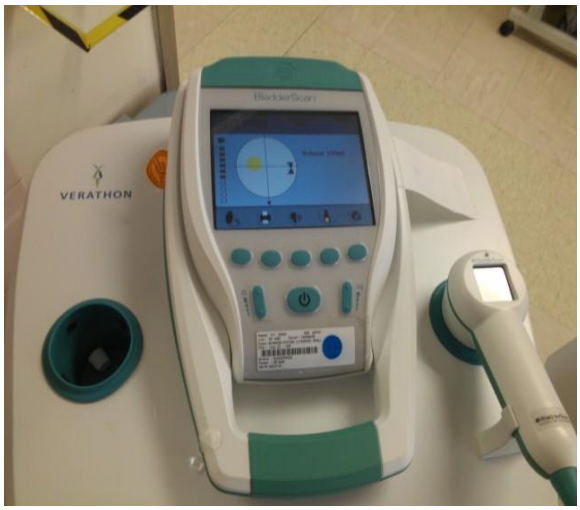

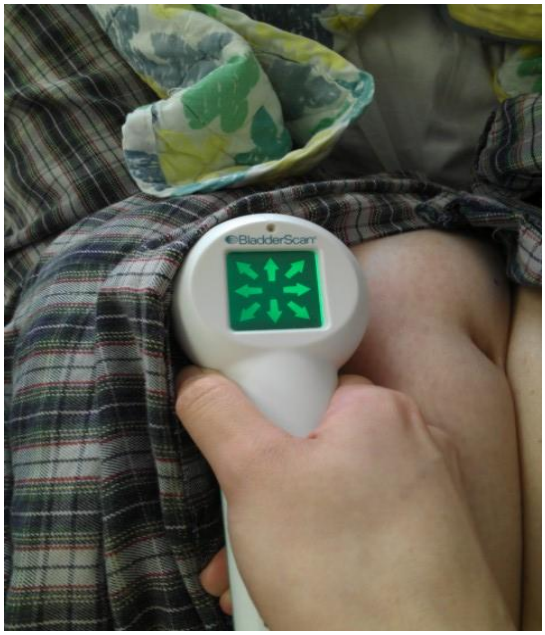

Table 1: Characteristic of AROU and non-AROU patients

	AROU (n=27)	No AROU (N=64)	
Age (mean)	73	69	NS
Men	66.7%	70.3%	NS
Stroke etiology			NS
ICH	10	20	
MCA infarction	9	28	
Brainstem infarction	4	4	
Other cerebral infarction	4	12	
Side of lesion			NS
Left	14	26	
Right	12	31	
Bilateral	1	5	
Severity of stroke			
GCS (median)	14	14	NS
NIHSS (median)	19	17.5	NS
MBI (median)	15	18	NS
Co-morbidities			
DM	25.9%	20.3%	NS
History of ROU	18.5%	7.8%	NS
Urinary tract infection	40.7%	29.7%	NS
Hospital mortality	18.5%	20.3%	NS

NS= not significant

Reference:

1:Hospital Authority Statistic Report (2002-2003) Hong Kong Hospital Authority

2:World Health Organization: International Classification of Functioning, Disability and Health: ICF, Geneva, World Health Organization.2001

3:Urinary Retention Diagnosis, bladder scanBVI9400, Verathon Medical Devices: http://verathon.com/products/bladderscan/bvi-9400 【website】

4: Glasgow-Coma-Scale:

http://zh.scribd.com/doc/57804330/Glasgow-Coma-Scale【website】

5:National Institutes of Health Stroke Scale: http://www.nihstrokescale.org/【website】

6: Modify Barthal Index:
http://www.dundee.ac.uk/medther/Stroke/Scales/barthel.htm【website】

7: Barnes M.P. Continence and stroke. *Recovery after stroke*. Cambridge University Press.2005; 15:415-435

8: Becker H.D. Neurogenic Urinary Incontinence. *Urinary and Fecal incontinence*. Springer 2005; 7:95-102

9: Brooker C. *Nursing Adults-The Practice of Caring*. Mosby 2003;12:231-35; 14:288-292

10: Brown M.M. Diagnosis of stroke with advanced CT and MRI imaging. *Stroke*. vol 56. British Medical Bulletin 2000, 318-322

11: Chan H. Bladder management in acute care of stroke patients: a quality improvement project. *J Neurosci Nurs*. 1997 Jun; 29 (3):187-90

12: Daviet J.C., Borie M.J., Salle J.Y., et al. Epidemiology and prognostic significance of bladder sphincter disorders after an initial cerebral hemisphere vascular accident *Ann Readapt Med Phys* 2004 Oct;47(8):531-6.

13: Douugherty L. Observations: neurological. *The Royal Marsden Hospital Manual of Clinical Nursing Procedures (6 edition)* Blackwell Publishing 2004; 26:492-5

14: Ersoz M, Tunc H, Akyuz M, Ozel S. Bladder storage and emptying disorder frequencies in hemorrhagic and ischemic stroke patients with bladder dysfunction. *Cerebrovasc Dis* 2005; 20 (5):395-9. *Epub* 2005 Oct 3.

15: H Yaguchi, H Soma, Y Miyazaki. A case of acute urinary retention caused by periaqueductal grey lesion. *J Neurol Neurosurg Psychiatry* 2004; 75:1202-1203.

16: Felipe De Los Ríos La Rosa, Khoury J., Brett M Kissela, Matthew L. Eligibility for Intravenous Recombinant Tissue-Type Plasminogen Activator Within a Population. The Effect of the European Cooperative Acute Stroke Study (ECASS) III Trial. Stroke: *A Journal of Cerebral Circulation* 2012 Jun; 43(6):1591-5

17: Fisher M. Critical Care of Cerebrovascular Disease. *Stroke Therapy*. Butterworth Heinemann 2001; 13:240-245

18: Funakoshi K., Fukutake T., Nishino H. Urinary retention caused by a small cortical infarction. *J Neurol Neurosurg Psychiatry* 2005;76: 457-458.

19: **Gelber DA**, **Good DC**, **Laven LJ**, **Verhulst SJ**. Causes of urinary incontinence after acute hemispheric stroke. *Stroke* 1993 Mar; 24 (3):378-82.

20: Ghandehari K., Saffarian-Toosi G., Masoudinezhad S. Comparative interrater reliability of Asian Stroke Disability Scale, modified Rankin Scale and Barthel Index in patients with brain inarction. *ARYA Atheroscler* 2012 fall; 8(3):153-157.

21: Golerstein L.B., Samsa G.P. Relibility of the National Institutes of Health Stroke Scale: extension to non-neurologists on the context of a clinical trail. *Stroke* 1997; 28:307-310

22: Hasgim H., Reynard J. & Cowan N.C. Lower Urinary Tract Emergencies. *Urological Emergencies in Clinical Practice*. Springer 2001; 2:9-16

23: Hennerici M.G. Clinical signs & Diagnostics. *Stroke*. Mosby.2004; 49-67

24: Juha T Korpelainen, Kyosti A. Sotaniemi, Vilho V. Myllyla. Autonomic nervous system disorders in stroke. *Clinical Autonomic Research* 1999,9:325-333.

25: Lyden P, Brott T. Tilley B, Welch K.M., Mascha E.J. et al. Improved reliability of the NIH Storke Scale using video training. *Stroke* 1994; 25:2220-2226

26: Lee KB, Jang IM, Roh H, Ahn MY, Woo HY. Transient urinary retention in acute right lateral medullary infarction. *Neurologist* 2008 Sep;14 (5):312-5.

27: Mike Bennett, Using the modified Barthel index to estimate survival in cancer patients in hospice: observational study. *BMJ* 2000 December 2; 321(7273): 1381–1382.

28: Mumtaz F. Urinary retention and obstruction uropathy. *Management of Urology Emergencie*s. Taylor & Francis Group, London and New York. A martin dunitz book 2004; 5:77-90

29: Norman R.W. & Currow D.C. The patients presenting with urinary retention. *Supportive care for the urology patients*. Oxford University Press 2005; 9:123-145

30: Pfluger H., Maier U. & Hubner W. (co. eds.) Impact of central bervous system alterations to bladder dysfunction in elderly people. *The Aging Bladder*. Springer Wien New York 2004; 97-110.

31: **Pettersen R**, **Wyller TB**. Prognostic significance of micturition disturbances after acute stroke. *J Am Geriatr Soc* 2006 Dec; 54 (12):1878-84.

32: Rodrigo-Gil J, Suñer-Soler R, Cruz-Díaz V *et al*. Care for patients with acute stroke: effectiveness of portable vesical ultrasound imaging in the stroke unit. *Rev Neurol* 2012 Feb 1; 54 (3):151-8.

33: Sakakibara R, Hattori T, Yasuda K, Yamanishi T.J Micturitional disturbance after acute hemispheric stroke: analysis of the lesion site by CT and MRI.*J Neurol Sci* 1996 Apr; 137 (1):47-56.

34: Sakakibara R, Hattori T, Yasuda K, Yamanishi T.Micturitional disturbance and the pontine tegmental lesion: urodynamic and MRI analyses of vascular cases. *J Neurol Sci* 1996 Sep 15;141(1-2):105-10.

35: Wessells H & Mcaninch J.W. Urgent and Emergent Management of Acute Urinary Retention. *Urological Emergencies*. Humana Press, Totowa, New Jersey 2005; 18:281-294

36: Wu M.N., Guo YC, Lai CL, Shen JT, Lior LM. Department detrusor hyporeflexia in a patient with left medial pontine infarction. *Neurologist* 2012 Mar;18 (2):73-5

571
BRAIN-0748
Poster Session

Clinical Studies

MITOCHONDRIAL DNA POLYMERASEΓMUTATIONS IN CHINESE PATIENTS WITH MITOCHONDRIAL ENCEPHALOMYOPATHY

F. Niu[1], J. Chen[1], F. Meng[1], Y. Xu[2]
[1]Pathology Department,
Affiliated Drum Tower Hospital of Nanjing Universi ty Medical School, Nanjing, China
[2]Neurology Department,
Affiliated Drum Tower Hospital of Nanjing Universi ty Medical School, Nanjing, China

Objectives: The nuclear POLG (DNA polymeraseγ) gene is the solo DNA polymerase essential for replication and repair of mitochondrial DNA (mtDNA). Thus mutations in the POLG gene have emerged as one of the most common causes of nuclear inherited mitochondrial diseases[1]. This study aims to determine the prevalence of POLG mutations in Chinese patients with mitochondrial diseases, displaying clinical presentations suggestive of POLG deficiency.

Methods: 1. Patients selection: From January 2008 to December 2013, 83 patients with suspected mitochondrial dysfunction were recruited. Patients were chosen for POLG screening if they had three or more of the following clincial manifestations commonly suggestive of POLG related disease[2]: such as CPEO, seizures or an abnormal electroencephalogram, peripheral neuropathy, ataxia, liver funciton abnormalities, migraine, or dysphagia/dysarthria. Eighteen patients in our groups were selected for POLG detection. 2. Molecular Analysis: we chose the most five common POLG mutations: p.A467T, p.W748S, p.G848S, p.T251I + p.P587L and p.T914P (giving the mucleotide change c.1399 G>A, c.2542 G>A, c.2243 G>A, c.752 C>T, c.1760 C>T and c.2740 A>C, respectively). DNA sequences were analyzed using POLG reference sequence on the NCBI website (GenBank: NM_002693.2).

Results: Out of the 83 patients with mitochondrial diseases, we detected 18 patients with suggestive POLG related disease, and found 3 patients had identified POLG mutations: 1 cases (#1) were homozygous for p.A467T alteration, 1 case (#2) were heterozygous for p.A467T in trans p.W748S, 1 case (#3) were heterozygous for G848S (supplementary table). The abnormal mitochondrial changes were the appearance of ragged-red fibers (RRFs) on muscle biopsies, which represented an abundance of pathological proliferated mitochondrial. However, there was no significant RRFs in the first two patients with p.A467T homozygous and p.A467T in trans p.W748S heterozygous. The third patients with heterozygous for G848S was associated with an mtDNA 3242 A>G point mutation (but not the common 3243 mutation). There were significant RRFs and increased activity of cytochrome c oxidase (COX), the fourth complex of respiratory chain, which similarly reflect the compensatory mitochondrial proliferation[3].

Conclusions: Our study showed that: 1) the prevalence of pathogenic POLG mutations in our selected Chinese cohort with suggestive clinical manifestation was 16.6%, 2) POLG mutations may not associated with morphological anomalies of muscle biopsy, although mtDNA alteration often links to muscle pathology. In conclusion, POLG gene analysis should be considered as a part of routine screening for mitochondrial disorders, even in the absence of apparent mitochondrial DNA abnormalities and/or muscle biopsy abnormalities.

Keywords: mitochondrial encephalomyopathy, POLG, DNA polymerase γ, mtDNA, muscle biopsy

Reference:

1. Tang, S., et al., *Mitochondrial DNA polymerase gamma mutations: an ever expanding molecular and clinical spectrum.* J Med Genet, 2011. **48**(10): p. 669-81.

2. Tchikviladze, M., et al., *A diagnostic flow chart for POLG-related diseases based on signs*

sensitivity and specificity. J Neurol Neurosurg Psychiatry, 2014.

3. Liu, A.H., et al., *High cytochrome c oxidase expression links to severe skeletal energy failure by (31)P-MRS spectroscopy in mitochondrial encephalomyopathy, lactic acidosis, and stroke-like episodes.* CNS Neurosci Ther, 2014. **20**(6): p. 509-14.

Supplementary Table: Identified POLG mutations

Patients	Gender	Age	Nucleotide Change		Amino Acid Change			diagnosis	mtDNA mutation
			Allele 1	Allele 2	Allele 1	Allele 2			
1*	F	15	c.1399 G>A	c.1399 G>A	p.A467T	p.A467T	Homozygous	CPEO	mtDNA depletion
2*	M	19	c.1399 G>A	c.2243 G>C	p.A467T	W748S	Heterozygous	MELAS-like syndrome	—
3*	M	34	c.2542 G>A	—	G848S	—	Heterozygous	MELAS	mt.3242 G>A

572
BRAIN-0287
Poster Session

Clinical Studies

LOCAL RESISTANCE EXERCISE IMPROVES COGNITIVE EXECUTIVE FUNCTION IN A DOSE-DEPENDENT MANNER

H. Tsukamoto[1], *T. Suga*[1], *S. Takenaka*[1], *T. Takeuchi*[1], *D. Tanaka*[1], *T. Hamaoka*[1], *T. Isaka*[1], *T. Hashimoto*[1]
[1]*Graduate school of sport and health science, Ritsumeikan university, shiga, Japan*

Objectives: Cognitive executive function (CEF) is especially concerned with working memory, reasoning, task flexibility and problem solving [1]. Therefore, CEF is now becoming the target for experimental and therapeutic investigations in the basic and clinical sciences. CEF is acutely improved by aerobic exercise [2]. On the other hand, a few studies have demonstrated that multiple bouts of whole-body resistance exercise can acutely improve CEF [3]. However, the effect of a single bout of local resistance exercise on CEF remains unknown. Thus, the present study examined whether simple resistance exercise could improve CEF, and if so, whether this improvement was dependent on exercise intensity.

Methods: Twelve healthy male subjects (mean ± SEM, age: 22.9 ± 0.4 yr, height: 171.3 ± 1.5 cm, weight: 67.3 ± 2.9 kg) performed a color-words Stroop task (CWST) before and after the experimental conditions, which consisted of 2 resistance exercises and a resting control (CON). Local bilateral knee extension was used to create 2 resistance exercise conditions; light-intensity resistance exercise (LRE) and high-intensity resistance exercise (HRE) conditions were 40% and 80% of one-repetition maximum, respectively. The resistance exercise session was programed for 6 sets (10 repetitions per set) with 3-min rest intervals. The CON condition consisted of being at rest in a sitting position on an exercise machine. During the experimental sessions, cardiovascular, skeletal muscle, and psychological parameters were recorded. The CEF was assessed on the basis of both reaction time and response accuracy in CWST. We used 2 types CWST (neutral task and incongruent task). To evaluate executive function, a reverse-Stroop interference score was calculated from reaction time of 2 types CWST difference.

Results: The reaction time of 2 types CWST in the post-intervention data was significantly shortened by LRE and HRE, but not by CON. The CEF as evaluated using a reverse-Stroop interference score in CWST was significantly improved following LRE and HRE, but it did not improve following CON.The improved CEF was significantly greater in HRE than in LRE, which corresponds to some of the cardiovascular, skeletal muscle, and psychological parameters.

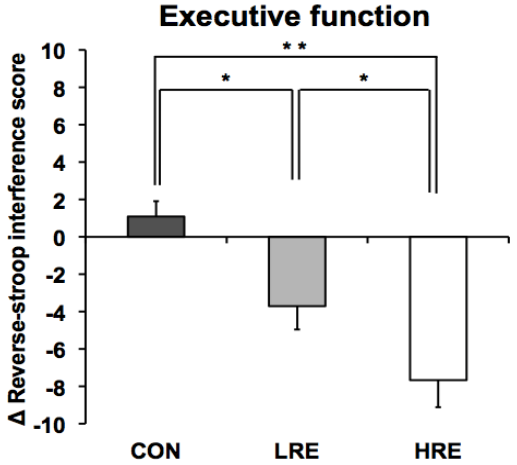

Conclusion: Our findings suggest that a single bout of local resistance exercise, especially with a high-intensity load, was effective in improving CEF

in healthy young individuals. The present findings may provide an impetus to develop an optimum resistance exercise method for the clinical treatment of CEF in older people and patients with chronic disease.

References: [1] Monsell S, Trends Cogn Sci, 2003. [2] Ogoh S et al., Physiol Rep, 2014 [3] Tsai CL et al., Front Behav Neurosci, 2014.

573
BRAIN-0821
Poster Session

Clinical Stroke

COGNITION AND RESTING STATE CONNECTIVITY IN CHRONIC STROKE.

A. Auriat[1], J. Ferris[1], L. Boyd[1]
[1]Physical Therapy, University of British Columbia, Vancouver, Canada

Objectives

Although rehabilitation research tends to focus on motor function it is clear that cognition has a critical role in determining quality of life after stroke. Unlike motor deficits, which are often predicted from size and location of injury, cognitive deficits are more difficult to relate to specific lesions. Resting state functional MRI (rfMRI) allows the study of brain networks in the absence of task performance and can identify connectivity abnormalities. The current study assesses cognition and resting network activity, as identified by independent component analysis (ICA), in chronic stroke participants and healthy controls.

Methods

Neuropsychological assessment and magnetic resonance imaging, including several structural scans and 8 minutes of rfMRI, was obtained from controls (n = 7) and participants with chronic stroke (n = 7). The Montreal Cognitive Assessment was used to screen potential participants for cognitive impairment. Composite memory (California Verbal Learning Test, and Visual Reproduction Test) and non-memory (Blocks, Symbol Search, Word Association, Digit Span, and Trails) scores were compared between participants with stroke and controls; results are reported as a percentage of the max test score (mean ± SD). Standard preprocessing of rfMRI was completed in SPM 8. ICA was completed using SPM 8 based Group ICA toolbox (GIFT). Previously identified network templates were used to classify activation in the mean composite activity maps. Networks of interest were selected for further comparison between stroke and healthy control groups, specifically the default mode network (DMN), executive control network (ECN), middle frontal network (MFN), and sensory motor network (SMN).

Results

Stroke and healthy control groups were not significantly different in age (stroke, control: 67.0 ± 7.0, 62.1 ± 5.7; $p = 0.179$). Stroke participants were assessed at least 6 months after stroke (75.1 ± 44.3 months). The stroke and healthy groups were significantly different on the MoCA (stroke, control: 25.1 ± 1.9, 28.4 ± 1.3; $p = 0.002$). Stroke participants had significantly impaired memory (stroke, control: 64.6 ± 6.9, 75.4 ± 11.0; $p = 0.048$). However, non-memory cognition did not differ significantly between stroke and healthy controls (stroke, control: 62.1 ± 17.2, 73.7 ± 6.6; $p = 0.123$). Several differences existed between stroke and control participants within the resting state networks identified using ICA. Within the ECN healthy controls had greater frontal medial cortex connectivity than stroke participants ($T = 6.26$, $p < 0.001$). In the DMN healthy controls had more connectivity in the central opercular cortex than stroke participants ($T = 6.83$, $p < 0.001$). In the SMN healthy controls had greater connectivity than stroke participants in the middle temporal gyrus ($T = 5.37$, $p < 0.001$), left VI cerebellum ($T = 5.33$, $p < 0.001$), and the anterior cingulate ($T = 4.77$, $p < 0.001$).

Conclusions

In a relatively high functioning group of chronic stroke participants (i.e. independent community

dwelling) memory is significantly impaired. Decreased connectivity in DMN and ECN may contribute to the cognitive deficits. Future analyses will examine the relationship between resting network activity, cognitive outcome and lesion size/location.

574
BRAIN-0788
Poster Session

Clinical Stroke

THE RHEOLOGICAL PROPERTIES OF BLOOD IN ACUTE STAGE OF ISCHEMIC STROKE AND THEIR RELATION TO THE SEVERITY OF THE NEUROLOGICAL IMPAIRMENT

M.N. Azhermacheva[1], D.M. Plotnikov[1], O.I. Aliev[2], M.B. Plotnikov[2], V.M. Alifirova[1], S. Agaev[1]
[1]Neurology and neurosurgery, Siberian state medical university, Tomsk, Russia
[2]Laboratory of circulation and pharmacology, Institute of Pharmacology Russian Academy of Medical Sciences, Tomsk, Russia

Introduction. Numerous studies have demonstrated valid hemorheological disturbances in acute ischemic stroke. Hemorheological parameters influence the development of the zone of ischemia, local stasis, plugging of capillaries, causing hypoxia.

Aim. To evaluate hemorheological parameters at ischemic stroke in patients with different severity of disease.

Methods. The study included 94 patients with acute ischemic stroke (age 62 [53;69] years). According to the criteria TOAST the subtypes of stroke were identified as large-artery atherosclerosis 36,2% , cardioembolism 27,7%, small-artery occlusion 14,8%, other determined cause 4,3%, undetermined cause 17,0%. The hemorheological indices assessed were: blood viscosity, plasma viscosity, plasma fibrinogen concentration, hematocrit, red blood cell aggregation and deformability. Hemorheological indexes were assessed three times – in the first 12 hours of stroke, in 3-5 day and in 18-20 day. The severity of stroke was assessed by clinical scales: Glasgow coma scale, the scale NIHSS, Barthel index.

Results. Impairment of consciousness at admission were observed in 25% of patients, clouding of consciousness to 3-5 days observed in 11% of patients, to 18-20 days - in 2% of patients. In the most acute stage of ischemic stroke died 11% of patients. Depending on the severity of neurological deficit patients were divided into three groups: severe impairment (NIHSS 15-24), moderately severe impairment (NIHSS 5-14), mild impairment (NIHSS <5) [Adams, HP, et al. (1999)]. Patients have positive clinical dynamics on neurological scales due to treatment in the hospital. The severity of neurological deficit in the dynamics of acute ischemic stroke represented in the figure.

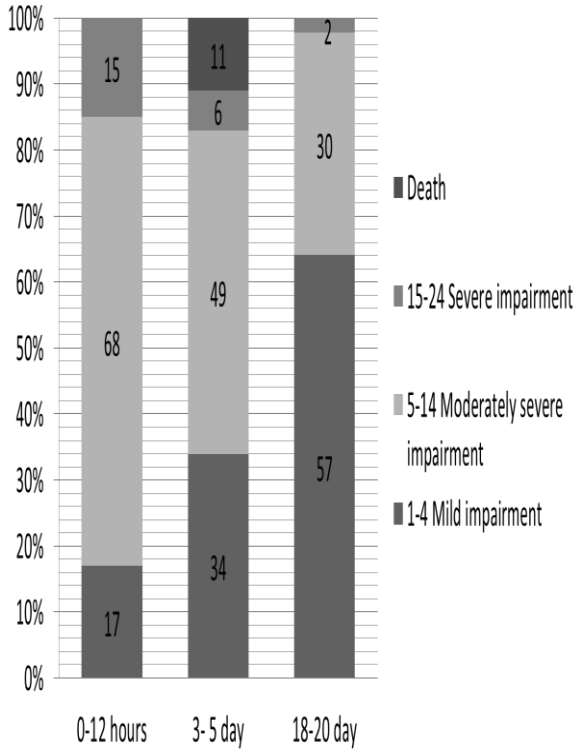

The study analyzed hemorheological parameters in the first hours after the onset of stroke in patients with different severity of disease. Patients in most acute phase of ischemic stroke had significant changes in hemorheological parameters (increased blood and plasma viscosity, plasma fibrinogen concentration,

aggregation of erythrocytes) which can be described as hyperviscosity syndrome. The results showed that blood viscosity significantly different in groups with mild 5.3 [4.9; 5.8], moderate 6.1 [5.5, 6.6] and severe 6.8 [5, 7; 7.0] stroke at a shear rate of 50 s^{-1}. Fibrinogen level was significantly different in the groups studied: mild 2.5 [2.2, 3.3], moderate 3.5 [3.1, 4.1] and severe 3.9 [3.7; 4.0] impairment. Patients with severe stroke was increased erythrocyte aggregation activity as evidenced by significantly shorter half-life of erythrocyte aggregation ($T_{1/2}$ = 2.5 [1.8, 3.2] c) compared with patients with mild stroke ($T_{1/2}$ = 5.8 [3.3, 7.7] c).

Conclusion. The study showed heterogenicity hemorheological disturbances in patients with different severity of ischemic strokes. Patients with mild stroke were not significant changes hemorheological parameters. In patients with moderate and severe ischemic stroke syndrome was observed hyperviscosity blood syndrome. There was a direct correlation between increased levels of plasma fibrinogen, increasing red blood cell aggregation and increase the severity of the stroke. Out results show that to assess the effectiveness of the treatment should be considered recovery of neurological deficit and dynamics of rheological parameters, specifically the concentration of fibrinogen, hematocrit, red blood cell aggregation and deformability.

575
BRAIN-0274
Poster Session

Clinical Stroke

STRESS AT WORK AND 16-TH YEARS RISK OF HYPERTENSION AND STROKE IN FEMALE POPULATION 25-64 YEARS IN RUSSIA: MONICA-PSYCHOSOCIAL EPIDEMIOLOGICAL STUDY

V. Gafarov[1], D. Panov[1], E. Gromova[1], I. Gagulin[1], A. Gafarova[1]
[1]Collaborative laboratory of cardiovascular diseas es epidemiology SB RAMS,
FSBI Institute of Interna and Preventivel Medicine SB RAMS, Novosibirsk, Russia

Objective: To study the job stress effect on relative risk of hypertension (AH), stroke in female population of 25-64y in Russia over 16 years of follow-up.

Methods: Under the third screening of the WHO program "MONICA-psychosocial" random representative sample of women aged 25-64y (n=870) were surveyed in Novosibirsk. Questionnaire based on Karasek's job demands-control model was used to estimate levels of job stress. From 1995 to 2010 women were followed for the incidence of AH and stroke. Cox regression model was used for risk assessment (HR).

Results: The prevalence of high job stress level in women aged 25-64y was 31.6%.

HR of stroke was 1.96-fold higher (95.0%CI:1.01-3.79, p<0.05) in women with job stress compared to those without stress. HR of AH over 16 years of follow-up in women with job stresswas 1.39-fold higher (95.0%CI:1.08-1.78, p=0.01) compared to those without it. There were tendencies of increasing AH and stroke in married women experienced stress at work compared to unmarried, divorced and widowed with the same stress level. AH significantly higher developed in women with university ($\chi2$=8.23 df=1 p<0.01), college ($\chi2$=3.98 df=1 p<0.05) and high school education ($\chi2$=5.29 df=1 p<0.05) having job stress compared to those with elementary school education and stress at work. As the tendency there was a decline in stroke development in those with university education having job stress. With regard to occupational class higher AH rates was found for physical workers with job stress compared to pensioners without it ($\chi2$=5.47df=1 p<0.05) and AH rates were tend to be higher in managers experienced stress at work ($\chi2$=3.24 df=1 p=0.07). Stroke more likely developed in “physical workers” with stress at work.

Conclusions: There is high prevalence of stress at work in female population aged 25-64y and high job stress level is 31.6% in Russia. Women with job stress have significantly higher risk of AH and stroke over 16-th years of follow-up. Rates of AH, stroke development were more likely in married

women with high job stress, in professional classes of physical workers and managers.

576
BRAIN-0277
Poster Session

Clinical Stroke

FAMILY STRESS AS PSYCHOSOCIAL PREDICTOR OF LONG-TERM RISK OF ARTERIAL HYPERTENSION AND STROKE IN FEMALE POPULATION 25-64 YEARS IN RUSSIA: MONICA-PSYCHOSOCIAL EPIDEMIOLOGICAL STUDY

V. Gafarov[1], D. Panov[1], E. Gromova[1], I. Gagulin[1], A. Gafarova[1]
[1]Collaborative laboratory of cardiovascular diseases epidemiology SB RAMS,
FSBI Institute of Internal and Preventive Medicine SB RAMS, Novosibirsk, Russia

Purpose: We studied the influence of family stress on risk of an arterial hypertension (AH) and stroke in female population aged of 25-64 years in Russia.

Methods: Under the third screening of the WHO"MONICA-psychosocial" program (MOPSY) random representative sample ofwomen aged 25-64 years (n=870) were surveyed in Novosibirsk in 1994. Family stress levels were measured by questionnaire MOPSY. From 1995 to 2010 womenwere followed for the incidence of AH and stroke. Cox regression model was usedfor relative risk assessment (HR).

Results: The prevalence of high family stress in women25-64 years was 20.9%. HR of AH over 16 years of follow-up in women with family stress was 1.39-fold higher (95.0%CI:1.99-15.70, p=0.001) compared to thosewithout stress. HR of stroke over 16 years was 3.53-fold higher (95.0%CI:1.82-6.84, p<0.001) for those with stress.

There were tendencies of increasing AH and stroke rates in married women experienced stress in family. AH developed significantly higher in women with university and specialized secondary education compared to those having elementary school with (χ^2=5.63 df=1 p<0.05; χ^2=4.01 df=1 p<0.05, for university and specializedsecondary, respectively) or without stress at home (χ^2=5.45 df=1 p<0.05; χ^2=4.39 df=1 p<0.05, respectively). In relation to occupational class AH rates were higher in groups first-line manager (χ^2=5.94 df=1 p<0.05) and physical worker (χ^2=8.14 df=1p<0.01) experienced stress in family. Higher stroke rates were more likely in physical workers with family stress compared to those without it (p=0.055).

Conclusions: There is high prevalence of family stress in female population aged 25-64 in Russia. Women with high family stress had significantly higher risk of AH/stroke over 16-th years of follow-up,especially in married women with higher educational level, in professional class managers and physical workers.

577
BRAIN-0319
Poster Session

Clinical Stroke

TRANSCRANIAL OPTICAL MONITORING OF CEREBRAL HEMODYNAMICS DURING EARLY HOURS AFTER ISCHEMIC STROKE AND ITS RELATIONSHIP TO THREE MONTH OUTCOME

I. Blanco[1], P. Zirak[1], C. Gregori[1], R. Marín-Bueno[2], M. Sestelo[3], I. Mochales[4], J. Martí-Fàbregas[2], T. Durduran[1], R. Delgado-Mederos[2]
[1]Medical Optics, ICFO-
Institut de Ciències Fotòniques, Castelldefels, Spain
[2]Stroke Unit, Hospital Santa Creu i Sant Pau, BARCELONA, Spain
[3]Centre of Mathematics and Department of Mathematics and Applications, University of Minho, Braga, Portugal
[4]Department of Mathematics,
Centre for Mathematical Research (CRM), Cendanyola, Spain

Background: Diffuse correlation spectroscopy (DCS) allows to non-invasively monitor microvascular cerebral blood flow (CBF) [1] and has been used to study the CBF response to an

orthostatic challenge in acute ischemic stroke (AIS) patients [2-3]. Previous studies showed variability between hemispheres in the CBF response obtained 24-72 hours after stroke onset without any correlations with patient status and outcome [2-3]. In this study, we extend a similar protocol to early (<12 hours) after the stroke onset to explore whether, during this critical period where the injury is rapidly evolving with the bulk of clinical interventions there is a relationship with the outcome. We have hypothesized that CBF response to raising the head-of-the-bed (HOB) from 0º to 30º during the early hours after stroke (<12h after stroke onset) will correlate with the National Institutes of Health Stroke Scale (NIHSS) and might predict long term outcome (modified Rankin Scale (mRS) at 3 months).

Methods: AIS patients with middle cerebral artery occlusion and involvement of the frontal lobes were recruited. Two DCS probes were placed on each frontal lobe to measure ipsi- and contra-lateral hemispheres. Patients remained on each HOB position (0º and 30º) for ten minutes. Changes in CBF as a function of the NIHSS or mRS were explored through linear mixed effects models. mRS relationship was further explored as dichotomized variable grouping patients with mRS ≤2 (minimal morbidity) and mRS>2 (medium to severe morbidity).

Results: Eleven AIS patients (median age 85±20) were measured. The average CBF responses were similar to previous studies [2-3]. Most interestingly, a significant difference between (p=0.002) ipsi-lateral CBF changes (-14.3%,IQR:5.6%) for mRS ≤2 group and CBF changes (2.8%, IQR:11.1%) for mRS >2 groups was observed (Figure 1). On the other hand, the contra-lateral CBF changes (-6.2%,IQR:12.6 vs 10.0%, IQR:8.4%) between two groups were not significantly different. There also was no significant correlation between either the absolute NIHSS or its changes (relative to admission) on admission, at the measurement time, at 24 or 48 hours or at the discharge.

Conclusions: This significant difference between the two mRS based groups suggest that DCS in combination with a HOB challenge could be used to assess long term patient outcome at early hours of AIS evolution. In the long run, this could potentially allow individualized AIS management strategies. ADCS is a promising modality for clinical stroke research.

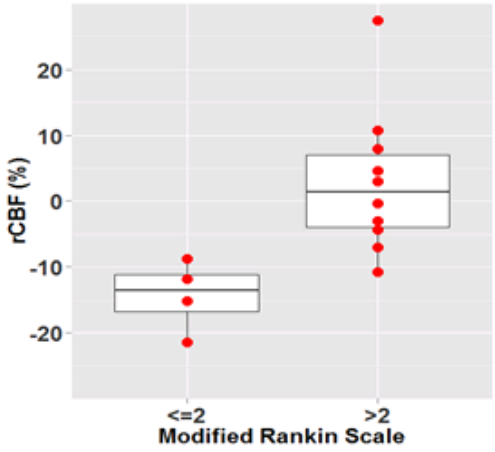

The project was funded by Fundació Cellex Barcelona, LlumMedBCN (La Caixa), Ministerio de Economía y Competitividad (PHOTOSTROKE) and LASERLAB-EUROPE.

References:

[1] Durduran, T. *et al.* (2014). Diffuse correlation spectroscopy for non-invasive, micro-vascular cerebral blood flow measurement. Neuroimage, 85, 51-63.

[2] Durduran, T. *et al.* (2009). Transcranial optical monitoring of cerebrovascular hemodynamics in acute stroke patients. Optics express, 17(5), 3884-3902.

[3] Favilla, C. G. *et al* (2014). Optical bedside monitoring of cerebral blood flow in acute ischemic stroke patients during head-of-bed manipulation. Stroke, 45(5), 1269-1274.

578
BRAIN-0846
Poster Session

Clinical Stroke

CLINICAL RESULTS AND ANALYSIS OF OUTCOME REVASCULARIZATION PATTERN OF EXTENSIVE REVASCULARIZATION SURGERY (TODAI PROTOCOL) FOR MOYAMOYA DISEASE

H. Imai[1], S. Miyawaki[1], H. Ono[1], H. Nakatomi[1], Y. Yoshimoto[2], N. Saito[1]
[1]Neurosurgery, The University of Tokyo, Tokyo, Japan
[2]Neurosurgery, Gunma University, Maebashi, Japan

Objectives: Moyamoya disease (MMD) has specific patter of alteration of the cerebral circulation, leading to "misery" perfusion of some areas of the brain, called "penumbra". Several surgical procedures are applied for treatment: direct anastomosis of superficial temporal artery (STA) to middle cerebral artery (MCA), indirect revascularization (anastomosis): encephalo-duro-arterio-synangiosis (EDAS) and/or encephalo-myo-synangiosis (EMS), and combinations of direct and indirect methods. The optimal revascularization strategy is still a matter of debate. For the last 10 years we have applied a surgical procedure (TODAI protocol) of combined EMS with STA-MCA anastomosis for the adults and EMS with EDAS for children. We evaluated the overall clinical outcome of surgically treated moyamoya patients under the protocol and next we examined the relative contribution of direct and indirect anastomosis in the revascularization pattern. We analyzed the results in view of our previous research (1), explaining the findings with the concept of angiogenesis and arteriogenesis

Methods: Sixty-five patients with moyamoya disease (91 hemispheres, including 48 in 29 childhood cases) were treated by the TODAI protocol. Clinical outcome was evaluated retrospectively. Digital subtraction angiography (DSA) was used for post-operative evaluation of revascularization in 47 patients (62 hemispheres: adults/children=27/35). We have categorized our observations into 4 patterns of revascularization depending on the dominancy of the donor artery scored by two independent observers as follows: pattern 1 was defined as a STA with higher score than EMS (STA > EMS), pattern 2 - as a STA with similar score to EMS (STA ≈ EMS) and pattern 3 – an EMS with higher score than STA (STA < EMS). Pattern 4 was complete absence of revascularization.

Results: The mean follow-up period was 90 months in children and 72 months in adults. Perioperative complications were seen in 4/48 operations in children and 1/43 operations in adults. Except for one child with recurrent transient ischemic attacks and one adult with intracerebral hemorrhage, the patients showed excellent clinical outcomes. Post-operative DSA evaluation showed that in STA-MCA anastomosis + EMS cases (34 hemispheres: adults/children=25/9) STA provided greater revascularization than EMS (pattern 1) in 7 hemispheres, the opposite was seen (pattern 3) in 14, equal contribution to revascularization (pattern 2) was present in 12, and 1 had no functioning anastomoses. In cases of EDAS + EMS (28 hemispheres: adults/children=2/26) all hemispheres showed revascularization: in one, EDAS was dominant to EMS (pattern 1), 14 showed the opposite (pattern 3) and in 13 EDAS was equivalent to EMS (pattern 2). EMS + direct or indirect anastomosis was an effective surgical procedure both in adults and children.

Conclusions: The surgical procedures applied under the TODAI protocol showed clear efficacy of revascularization for moyamoya patients (2). Revascularization patterns indicated that EMS play a pivotal role for the successful revascularization in both combined direct with indirect anastomosis in adults and combined indirect with indirect anastomosis in children because an adaptable revascularization is developed adequately to the demand of blood supply in the misery perfusion area.

References

(1)Nakamura M et al., J Neurosurg Pediatr (2009)
(2)Imai H et al., World Neurosurg: (in press)

579
BRAIN-0104
Poster Session

Clinical Stroke

A CASE OF SERPENTINE ICA ANEURYSM PRESENTED WITH VISUAL SYMPTOMS

B. Kim[1], D. Shin[1]
[1]Neurosurgery, Soonchunhyang University, Bucheon, Korea

Object: To present an interesting clinical manifestation by serpentine internal carotid artery aneurysm.

Material and methods: 44 year-old female was visited with the decreased right visual acuity for one month. She complained the dry eye two weeks ago. Ophthalmologist diagnosed as a optic neuritis and transferred her to our hospital. Right visual acuity decreased to 0.04 (left is 1.0) and right visual filed showed defect 3/4 except right lateral upper quadrant in the neurologic examination. Brain MRI showed large aneurysm on right cavernous sinus and brain CT angiography showed fusiform dilatation of right cavernous ICA. Fundus photography showed right optic atrophy with pale neural rim on right optic disc. Similar finding was shown on transfemoral catheter angiography with brain MRI/brain CT angiography and the size was about 11.7mm*22.5mm. She passed Matas test and the collateral flow was tolerable. Vascular reserve was well maintained after Matas test on SPECT study.

Result: Coil embolization with parent artery occlusion was performed on the serpentine aneurysm. Patients didn't show any neurologic deficit after coil embolization and visual acuity and flied defect were much improved at three month later.

Conclusion: Occlusion of aneurysm may effective for the improvement of clinical symptoms of the optic pathway compression.

580
BRAIN-0203
Poster Session

Clinical Stroke

TREATMENT OF INTRACRANIAL ANEURYSMS, INCOMPLETELY-CLIPPED OR RECURRED AFTER CLIPPING

D. Lim[1], S. Ha[1], J. Choi[1], S. Kim[1], S. Kim[1], S. Jin[1], S. Lee[1]
[1]Neurosurgery, Korea University Ansan Hospital, Ansan-si, Korea

Treatments to exclude aneurysm remnants of significant size identified following clipping or recurred aneurysms after clipping are often challenging to neurosurgeon. We report our experience of treatment residual or recurred aneurysms in a small series of surgically treated patients at a single institution.
Between July 2008 and June 2014, 10 patients with remnant or recurred aneurysms are surgically treated. Four aneurysms were recurred and six were remnant after clipping. Four patients were treated with repeated microsurgery and other six patients underwent endovascular coil embolizations.
Surgical morbidity happened in one patient with repeated microsurgical clipping. The endovascular coiling surgeries were successful for all six patients and the latest follow-up angiograms demonstrated no recurrence. There was no incidence for hemorrhage after treatment.
Repeated open surgery to recurred or remnant aneurysms after clipping are often technically difficult and may carry an increased risk of complications. Endovascular treatment of remnant or recurred cerebral aneurysm following prior surgical clipping can be accomplished with acceptable morbidity and mortality rates.

581
BRAIN-0401
Poster Session

Clinical Stroke

THE EMBOLIC SOURCE BY DETECTING TRANSESOPHAGEAL ECHOCARDIOGRAPHY IN CRYPTOGENIC STROKE

M. Osaki[1], S. Fujimoto[1], M. Kumamoto[1], M. Kanazawa[1], N. Tagawa[1], A. Nakamizo[2], S. Yamaguchi[2], R. Tsuchimochi[2], T. Isitsuka[1]
[1]Cerebrovascular Medicine, Steel Yawata Memorial Hospital, Kitakyushu, Japan
[2]Neurosurgery, Steel Yawata Memorial Hospital, Kitakyushu, Japan

Objectives: Cryptogenic stroke (CS) diagnosed by using common examinations without the transesophageal echocardiography (TEE) has some underlying etiologies. TEE can be detected various embolic sources, such as aortic arch plaque, patent foramen ovale, left atrial spontaneous echo contrast, and atrial septal aneurysm [1-2]. Clinical features of CS are also different in accordance with the etiology. We aimed to examine the clinical features of CS.
Method: From 2008 to 2013, 834 stroke patients within 7 days after the onset with ischemic lesions in the initial diffusion-weighted images were studied. Using MRI, MR angiography, electrocardiography, including long-term monitoring, and transthoracic echocardiography, all patients were classified according to the modified Trial of Org 10172 in Acute Stroke Treatment (TOAST) criteria and CS was defined as stroke without an identified cause. Aortogenic embolic (AE) source was defined as an aortic arch atheroma of >4 mm in thickness evaluated by using TEE. Patent foramen ovale, left atrial spontaneous echo contrast, and atrial septal aneurysm on TEE were diagnosed as cardioembolic (CE) sources.
Results: CS was diagnosed in 215 cases (123 men, 74 ± 11 years old). TEE was performed in 167 (78% of CS) cases. Among them, any embolic source was observed in 137 (82%) cases; 134 (80%) had AE source and 47 (28%) had CE source. As compared with non-AE source group, AE source group patients were older (74±l vs. 66±vs, P<0.001) and hypertension (84% vs. 46%, P<0.001), chronic kidney disease (46% vs. 21%, P=0.010) and secondary prevention by antiplatelet therapy (87% vs. 58%, P<0.001) were more frequent in AE source group. As compared with non-CE source group, hypertension (62 vs. 82%, P<0.001) was less frequent, and chronic heart failure (9% vs. 2%, P=0.030), left atrial enlargement (left atrial diameter ≧42mm) and secondary prevention by anticoagulant therapy (43% vs. 18%, P<0.001) were more frequent in CE source group. On multivariate analysis, older age (OR 1.122, 95%CI 1.060–1.199 per 1 year-old; P<0.001) and hypertension (OR 9.291, 95%CI 3.102–31.739; P<0.001) were associated with AE source. Hypertension (OR 0.305, 95%CI 0.120-0.754; P=0.010) and chronic heart failure (OR 8.873, 95%CI 1.235-91.927; P=0.030) and Left atrial enlargement (OR 2.145, 95%CI 1.224-7.616; P=0.009) were associated with CE source.
Conclusion: Any embolic source was observed in 78% of CS patients who underwent TEE. Older age and hypertension were positively associated with AE source. Hypertension was negatively and chronic heart failure and left atrial enlargement were positively associated with CE source. TEE should be performed for evaluating the stroke etiology especially in CS patients with such predictive factors.

References:
1. Amarenco P, Duyckaerts C, Tzourio C, Henin D, Bousser MG, Hauw JJ. The prevalence of ulcerated plaques in the aortic arch in patients with stroke. *N Engl J Med*. 1992;326:221–225.
2. McGrath ER, Paikin JS, Motlagh B, Salehian O, Kapral MK, O'Donnell MJ. Transesophageal echocardiography in patients with cryptogenic ischemic stroke: a systematic review. *Am Heart J.* 2014;168(5):706-712.

582
BRAIN-0722
Poster Session

Clinical Stroke

LOCATION OF THE CLOT, COLLATERAL SCORE AND CT ANGIOGRAPHY SOURCE IMAGES IN THE PREDICTION OF OUTCOME OF INTRAVENOUS THROMBOLYSIS

N. Sillanpaa[1], H. Rusanen[2], J.T. Saarinen[3]
[1]Medical Imaging Center,
Tampere University Hospital, Tampere, Finland
[2]Department of Neurology,
Oulu University Hospital, Oulu, Finland
[3]Department of Neurology,
Vaasa Central Hospital, Vaasa, Finland

Objectives: Collateral circulation, the location of the occluding clot and the infarct volume are important determinants of stroke outcome. We studied the impact of leptomeningeal collateral circulation with regard to the location of the thrombus, and the interplay between collateral circulation, the location of the thrombus and infarct extent based on evaluation of CT angiography source images (CTA-SI) in predicting the clinical outcome of patients treated with intravenous thrombolytic therapy (<3h) in a retrospective cohort.

Methods: Anterior circulation thrombus was detected with computed tomography angiography in 105 patients. Baseline clinical and imaging information was collected, the site of the occlusion recorded, collaterals were assessed using a five-grade Collateral Score (CS) and Alberta Stroke Program Early CT score (ASPECTS) was evaluated from CTA-SI. This data was analyzed using logistic regression modeling to predict favorable clinical outcome (three-month modified Rankin Scale 0-2).

Results: Two thirds of the patients with a proximal occlusion displayed poor collateral filling (CS 0-1) whereas in more distal clot locations about one third had poor collaterals. Only 36% of patients with a proximal occlusion and good collaterals experienced favorable clinical outcome. CTA-SI ASPECTS was highly correlated with CS (Spearman's rho = 0.63, p=0.01). The mean CTA-SI ASPECTS score became progressively lower when the status of the collateral circulation deteriorated (ANOVA p<0.001). In univariate analysis a good CTA-SI scan at the admission predicted favorable three-month outcome (p<0.001). In a multivariate model containing CTA-SI ASPECTS, CS and the site of the occlusion along with significant clinical parameters, CTA-SI ASPECTS was rendered non-significant (p=0.43) in the presence of CS, and was dropped from the model. Both clot location and CS were highly significant (p=0.003 and p=0.001) and independent predictors of favorable clinical outcome. Good collateral status increased the odds of favorable clinical outcome about nine fold (OR=9.3, 95% CI 2.4-35.8). After dichotomization, a distal clot location had larger odds ratio (OR=13.3, 95% CI 3.0-60.0) compared to that of good collaterals (OR=5.9, 95% CI 1.8-19.0).

Conclusions: A proximal occlusion in the anterior circulation is associated with poorer collateral status when compared to a more distal occlusion. Both the clot location and CS are important and independent predictors of favorable clinical outcome of hyperacute stroke treated with intravenous thrombolysis. The location of the clot is a stronger determinant of the outcome than CS. CTA-SI and CS convey overlapping information. CTA-SI is not a significant predictor of the 3-month clinical outcome when CS and the clot location are considered simultaneously. However, CTA-SI may have a role in the assessment of the extent of irreversible ischemic changes at admission.

References:

1. Saarinen JT, Rusanen H, Sillanpää N: Collateral score complements clot location in predicting the outcome of intravenous thrombolysis. AJNR Am J Neuroradiol. 2014 Oct;35(10):1892-6. doi: 10.3174/ajnr.A3983.
2. Sillanpää N, Saarinen JT, Rusanen H: Computed tomography angiography source images closely reflect the integrity of collateral circulation. J Neuroradiol. 2014 Nov 6. doi: 10.1016/j.neurad.2014.06.001.

583
BRAIN-0468
Poster Session

Clinical Stroke

A HYBRID SIGNAL PROCESSING OF RR INTERVAL FROM QTC VARIATION OF EKG AND HEART RATE VARIABILITY ASSESSMENT IN ATRIAL FIBRILLATION DURING ACUTE STROKE

S. Rangsungnoen[1], T. Rungrot[1], N. Mathuradavong[2], K. Suwanprasert[2]
[1]Medical Engineering Program, Thammasat University, Pathumthani, Thailand
[2]Faculty of Medicine, Thammasat University, Pathumthani, Thailand

Objectives : Abnormal QTc , tachycardia and arrhythmia with high risks for sudden cardiac death have been reported in stroke patients. Brain-heart axis is shifted affecting autonomic modulation in AF patient with stroke (1). An effective improvement of HRV analysis is needed to verify the complexity of autonomic modulation during acute stroke. Moreover, missing beats in silent AF, prolonged or shorten QTc or even ventricular tachycardia during acute stroke is still unknown mechanism . In this study, we develop a hybrid signal processing of Pan Tompkins QRS detection and Kalman Filter estimator for correction of missing beat during RR interval and then quantitate HRV by Kubios Program. We investigate autonomic changes whether QTc variation in AF stroke and non AF stroke patients.

Methods: 15 acute stroke patients with AF and those of 15 in non AF stroke (7 men, 8 women, age 65 $\pm$ 4 years old, matching control) were recruited. All subjects gave informed consent according to the Declaration of Medicine Ethic Committee (MTU-EC-IM-4-018/54). The Lead II ECG recordings (sampling rate of 1000 Hz, 5-minute long) were performed during 24 hours acute stroke, thereafter, RR intervals were analyzed by our software algorithms. AF and non AF with QTc variation in stroke patients were determined by physician. Two groups of acute stroke were assessed by HRV Kubios Program. All data in linear and nonlinear functions of HRV were analyzed.

Results: All values show significant difference between AF stroke and non AF stroke .
Mean RR in AF stroke is less than those in non AF stroke. Greater parasympathetic activity is evident showing as pNN50, HF, and SD1. Decreasing sympatho-vagal balance is seen in lower level of LF/HF ratio in AF stroke. An irregularity of signals (SamEn and ApEn) in AF stroke is greater than in non AF stroke .

Conclusions: This finding suggests that a hybrid signal processing that we have developed for better RR detection is needed in QTc variation AF stroke and non AF stroke. Decreased HRV is shown in AF stroke clearly. Greater parasympathetic activity in AF stroke plays a vital role in variation of QTc.

References:
1. Sungnoon R, Suwanprasert K, Muengta weepongsa S. Atrial electrophysiological property analysis by sample entropy and atrial fibrillatory rate with cardiac autonomic derangements in acute ischemic stroke with atrial fibrillation Neurology Asia 2014; 19(1): 11-8
2. Korpelainen JT, et al. Dynamic behavior of heart rate in ischemic stroke. Stroke.1999;30:1008-1013
3. Montazeri N, et al. Paroxysmal atrial fibrillation prediction using Kalman Filter in Proceeding of the 4th International Symposium on Applied Sciences in Biomedical and Communication Technologies No 89, ACM, 2011

584
BRAIN-0429
Poster Session

Clinical Stroke

RISK FACTORS AND OUTCOME IN STROKE PATIENTS WITH AORTIC COMPLICATED LESIONS

N. Tagawa[1], S. Fujimoto[1], M. Osaki[1], M. Kumamoto[1], M. Kanazawa[1], A. Nakamizo[1], S. Yamaguchi[1], R. Tsuchimochi[1], T. Ishitsuka[1]
[1]Stroke Center, Steel Memorial Yawata Hospital, Kitakyushu, Japan

Objectives: Aortic complicated lesions (ACLs) is well known as an important embolic source for ischemic stroke [1]. It has been reported that age, hypertension, diabetes mellitus, dyslipidemia and smoking were associated with ACLs [2]. Whereas, clinical outcome in stroke patients with ACLs has not yet been clarified. We retrospectively investigated the relationships between background risk factors and ACLs in stroke patients and outcome in stroke patients with ACLs.
Methods: We studied 552 consecutive stroke or transient ischemic attack (TIA) patients within 7 days after the symptom onset were diagnosed as having a brain embolism and underwent transesophageal echocardiograph (TEE) for embolic sources from February 2008 to December 2013. Sources of cardioembolism, right-to-left shunt, and aortic atheroma were evaluated in all patients. In addition, electrocardiography, including long-term monitoring, and transthoracic echocardiography were performed in order to evaluate the heart disease and chronic or intermittent arrhythmia for possible embolic sources. ACLs was defined as an atheroma of >4 mm in thickness. We investigated the relationships between background risk factors and ACLs, and also observed stroke recurrence during one year from discharge.
Results: Of the total 553 patients (328men, 72.8±11.1 years old), ACLs were identified in 364 patients (65.8%, 215 men), atrial fibrillation in 144 (26.1%), left atrial thrombus in 15 (2.7%), spontaneous echo contrast in 120 (21.7%), patent foramen ovale in 54 (9.8%), pulmonary arteriovenous fistula in 28 (5.1%), atrial septal aneurysm in 36 (6.5%). Patients with ACLs were older (75.6±9.2 vs. 67.5±12.6 years old, P<0.0001) and more likely to have significant stenosis (50% or more in diameter) in the cerebral arteries in their ischemic lesion territory (23.9% vs. 17.0%, P=0.063), history of hypertension (78.2% vs. 68.6%, P=0.016), high pulse pressure (73.6±24.9 vs. 65.9±23.3 mmHg, P=0.0005), ischemic heart disease (25% vs. 14.4%, P=0.004), arteriosclerosis obliterans (6.3% vs. 1.1%, P=0.005), and reduced eGFR [<60ml/min/1.73m^2] (42.0% vs. 30.3%, P=0.007) than those without ACLs. On multivariate analysis, age (OR 1.07, 95%CI 1.05-1.10, P<0.0001), higher pulse pressure (OR 1.01, 95%CI 1.00-1.02, P=0.0161), history of ischemic heart disease (OR 1.69, 95%CI 1.23-2.85, P=0.0403), and history of arteriosclerosis obliterans (OR 4.72, 95%CI 1.29-30.6, P=0.0165) were associated with ACLs. The rate of stroke recurrence during one year from discharge was more frequent in patients with than without ACLs (79.6% vs. 65.1%, P=0.041). ACLs was an independent predictor for stroke recurrence (OR 2.04, 95%CI 1.03-4.44, P=0.0408).
Conclusions: Aortic complicated lesions was associated with age, pulse pressure history of ischemic heart disease and history of arteriosclerosis obliterans. Patients with ACLs were more likely to have stroke recurrence.
References:
[1] Amarenco P, et al: N Eng J Med. 1994; 331: 1474-9
[2]Zavala JA, et al: Int J Stroke. 2006; 1: 74-80

585
BRAIN-0187
Poster Session

Clinical Stroke

STROKE COMPLICATION ANALYSIS IN LEFT VENTRICULAR ASSIST DEVICE APPLICATION FOR DILATED CARDIOMYOPATHY PATIENTS

Y. ONDA[1], H. IMAI[1], O. KINOSHITA[2], M. KIMURA[2], M. ONO[2], N. SAITO[1]
[1]Neurosurgery, Tokyo Univesity, Tokyo, Japan
[2]Cardiac surgery, Tokyo Univesity, Tokyo, Japan

Introduction:Stroke complications are common in patients with left ventricular assist devices (LVADs) and the complication affect the prognosis of them.
Methods:In this single center, retrospective study, LVAD surgeries were performed at our institution between March 2001 and March 2013. We enrolled 59 dilated cardiomyopathy cases (54 patients) without biventricular assist devices in our study. Clinical characteristics and laboratory data were analyzed. Stroke was including transient ischemic attack (TIA), and brain infarction or brain hemorrhage an imaging study.
Results:
Patients were followed-up for 472 ± 372 days. Stroke complications developed in 18 cases (TIA 1; ischemic cerebrovascular accidents 8, hemorrhagic cerebrovascular accidents 9) after LVAD implantation. Kaplan-Meier analysis revealed 1- and 2-year stroke complication rate was 31.3 and 37.6%. Multivariate analysis revealed preoperative statin administration (hazard ratio [HR] = 0.10; 95% confidence interval [CI] = 0.004-0.66; p = 0.01), preoperative albumin profile (HR = 0.35; CI = 0.13-0.92; p = 0.03) and postoperative sepsis (HR = 0.30; CI = 0.09-0.91; p = 0.03) were associated with stroke complications after LVAD surgery.
Conclusions:
We suggested preoperative statin, control of postoperative infection and improvement of nutritional status as the most important factors to reduce the risk of stroke after LVAD surgery.

586
BRAIN-0581
Poster Session

Cerebral Ischemia: Animal Models

TARGETING RECOMBINANT THROMBOMODULIN FUSION PROTEIN TO RED BLOOD CELLS PROTECTS AGAINST STROKE

D. Atochin[1], S. Zaitsev[2], R. Carnemolla[2], V. Muzykantov[2], P.L. Huang[1]
[1]Department of Medicine Cardiology Cardiovascular Research Center, Massachusetts General Hospital, Charlestown, USA
[2]Department of Pharmacology Center for Targeted Therapeutics & Translational Nanomedicine ITMAT/CTSA Translational Research Center, University of Pennsylvania, Philadelphia, USA

Objectives

Thrombomodulin (TM) is an endothelial glycoprotein that protects against thrombosis and inflammation in a domain-specific manner[1]. TM neutralizes cytokines via its N-terminal lectin-like domain, binds thrombin via its EGF-like domain, inhibiting its thrombotic and inflammatory effects, while facilitating thrombin's cleavage of plasma protein C into activated protein C, a protease with anti-thrombotic and anti-inflammatory activities. We fused TM with a single chain fragment (scFv) of a monoclonal antibody to mouse red blood cells[2]. We hypothesized that red blood cells (RBC)-targeted scFv/TM will protects against ischemic stroke via anti-thrombotic and anti-inflammatory pathways.

Methods

The surgical procedure for the middle cerebral artery (MCA) occlusion (MCAO) was performed on adult male C57BL/6 mice under anesthesia (30% oxygen, 70% nitrous oxide, and 1.5% isoflurane). Body temperature was maintained at 36-37°C. The left common and internal carotid arteries were exposed through a neck incision and ligated. The external carotid artery was isolated and incised. Vehicle or scFv/TM solution (bolus,

200 microliters, 1mg/kg) was injected in right jugular vein 20 minutes before carotid arteries ligation. Silicon-covered nylon filament (Doccol) was advanced via the proximal external carotid artery into the internal carotid artery, occluding the MCA for 30 minutes with subsequent reperfusion for 48 hours as described[3] with Laser Doppler cortical blood flow monitoring. Mice were examined for neurologic deficits by 5 point scale 48 hours after stroke. The brain was cut into 2-mm-thick coronal blocks, and stained in dark with 2,3,5-triphenyltetrazolium chloride for 1 h at 37^0C. The volume of infarct was calculated by indirect method as described[4].

Results

30 minutes of MCAO with 48 hours of reperfusion produced decreased cerebral infarct volume in mice injected with scFv/TM (28±20 mm^3, Mean±SD, n=5) as compared with control (58±15, n=6, $p< 0.05$) mice. This was associated with a functional impairment in the neurologic deficit, as quantities by neurologic scoring (1.3 for mice injected with scFv/TM and 2.3 for control mice).

Conclusion

Stroke injury was less pronounced in mice pretreated with scFv/TM. Targeting recombinant thrombomodulin fusion protein to RBC resulted in decreased infarct volume and neurological deficit.

References

1. Esmon CT: Thrombomodulin as a model of molecular mechanisms that modulate protease specificity and function at the vessel surface, Faseb J 1995, 9:946-955

2. Zaitsev S, Kowalska MA, Neyman M, Carnemolla R, Tliba S, Ding BS, Stonestrom A, Spitzer D, Atkinson JP, Poncz M, Cines DB, Esmon CT, Muzykantov VR: Targeting recombinant thrombomodulin fusion protein to red blood cells provides multifaceted thromboprophylaxis, Blood 2012, 119:4779-478

3. Shuvaev VV, Han J, Tliba S, Arguiri E, Christofidou-Solomidou M, Ramirez SH, Dykstra H, Persidsky Y, Atochin DN, Huang PL, Muzykantov VR. Anti-inflammatory effect of targeted delivery of SOD to endothelium: mechanism, synergism with NO donors and protective effects in vitro and in vivo. PLoS One. 2013 Oct 11;8(10):

4. Li Q, Atochin D, Kashiwagi S, Earle J, Wang A, Mandeville E, Hayakawa K, d'Uscio LV, Lo EH, Katusic Z, Sessa W, Huang PL. Deficient eNOS phosphorylation is a mechanism for diabetic vascular dysfunction contributing to increased stroke size. Stroke. 2013 Nov;44(11):3183-8.

587
BRAIN-0387
Poster Session

Cerebral Ischemia: Animal Models

MR-BASED T2' MAPPING AS A SURROGATE FOR TISSUE HYPOXIA IN ACUTE ISCHEMIC STROKE: A VALIDATION STUDY AGAINST 18F-FLUOROMISONIDAZOLE (FMISO) PET IN RODENTS.

U. Jensen-Kondering[1], M. Roie[2], S. Ejaz[1], S.J. Steve[2], T.D. Fryer[2], F.I. Aigbirhio[2], T.A. Carpenter[2], D.J. Williamson[1], J.C. Baron[1]
[1]Department of Clinical Neurosciences, Stroke Research Group, Cambridge, United Kingdom
[2]Department of Clinical Neurosciences, Wolfson Brain Imaging Centre, Cambridge, United Kingdom

Introduction

BOLD imaging using T2' may detect increased oxygen extraction fraction and as such is a potential candidate to map the penumbra in acute stroke [1]. T2' has already yielded promising results in the clinical setting [2,3]; however, validation is still missing. Here we sought to validate T2' imaging against FMISO, a PET tracer that provides maps of hypoxic tissue including the penumbra [4]. Specifically, we determined whether high FMISO uptake was present within T2' lesions.

Methods

Five male Wistar rats were subjected to permanent thread MCAo, immediately followed by FMISO injection and MR (4.7 T Bruker) scanning. These sequences were repeated twice (time-points 1 and 2), interleaved with DWI. Additionally, DSC-MRI was performed in three rats. Following MR acquisition, the animal was transferred to a microPET P4 scanner (Concorde Microsystems). List-mode data were acquired from 120-150 min post-injection and measured attenuation correction was performed. Voxel data were converted to standardized uptake value (SUV) using the injected activity and animal weight. TTC staining was used at end of the protocol to map the final infarct.

T2' was calculated voxel-wise from a multi-echo T2 and a multi-echo T2* according to:

$SI(t) = SI_0\, e^{-t/qT2 \text{ or } qT2^*}$

$1/T2' = 1/T2^* - 1/T2$ (with $1/T2' = R2'$)

T2' and R2' lesion ROIs were independently delineated by two observers on a slice-by-slice basis for both time points. Any disagreement was resolved in a consensus session. ADC lesion ROIs were automatically generated utilizing a threshold of 530^*10^{-6} mm^2/s.

Results

There were no statistically significant differences in T2' lesion volumes between observers 1 and 2. However mean ROI overlap between observers was 37% only. FMISO SUV was almost two-fold higher within the consensus T2' lesion ROI compared to mirror ROI at both time-points (2-tailed p= 0.08 and 0.009, respectively). Overlap of the T2' ROI with the ADC lesion ROI was small (≤ 10%). CBF and CBV were consistently lower and MTT and TTP higher within the T2' ROI relative to mirror ROI at both time-points (p range: 0.27-0.01). Similar findings were obtained using the R2' ROI. TTC staining showed an MCA infarct in each rat.

Discussion

Poor inter-observer reproducibility indicates that T2' and R2' lesions are difficult to delineate, consistent with previous clinical data [2]. However, consensus ROIs do show the expected hypoxia and hypoperfusion characteristic of ischemic brain tissue. The small overlap with the ADC lesion is not inconsistent with T2' reflecting mainly the penumbra given the former is expected to mainly show the 'core'. These data suggest that the issue with T2' imaging stems from voxel-based data processing to generate the images, which inherently creates noise due to non-linear equations. Whether this could be improved by optimizing image acquisition, image processing and/or experience of the observers should be addressed in further studies given the intrinsic validity of T2' imaging.

References

1. Jensen-Kondering U, Baron JC. Stroke. 2012; 43:2264-9.
2. Siemonsen S et al. Radiology. 2008; 248:979-86.
3. Bauer S et al. Stroke. 2014; 45:3280-6.
4. Takasawa M et al, Exp. Neurol., 2011; 229:251–8.

588
BRAIN-0757
Poster Session

Cerebral Ischemia: Animal Models

MIDDLE CEREBRAL ARTERY OCCLUSION WITH GOOD COLLATERALS CAUSES EARLY INTRACRANIAL PRESSURE ELEVATION POST STROKE

D.J. Beard[1], *C.L. Logan*[1], *D.D. McLeod*[1], *R.J. Hood*[1], *D. Pepperall*[1], *L.A. Murtha*[1], *N.J. Spratt*[1]
[1]*School of Biomedical Sciences and Pharmacy, University of Newcastle, Newcastle, Australia*

Objectives: We recently showed that intracranial pressure (ICP) increases markedly 24 h after temporary middle cerebral artery occlusion (MCAo) in Wistar rats, although infarct volumes

were small[1]. This suggests that reperfusion of the penumbra may be necessary for the ICP elevation at 24 hours. Collateral perfusion may also help salvage the penumbra. We have recently demonstrated that inadvertent occlusion of the Anterior Choroidal Artery (AChA) (a branch of the internal carotid artery providing collateral supply to the MCA territory) during intraluminal MCAo results in larger strokes[2]. Here our aim was to monitor ICP following MCAo with good (patent AChA) and poor (occluded AChA) collaterals and assess stroke severity using both behavioural and histological techniques in order determine whether the presence of penumbra is needed for ICP elevation at 24 h after stroke.

Methods: Permanent intraluminal thread occlusion of the MCA (pMCAo) was induced in male Wistar rats (n=12) using either intraluminal threads with short (1.5mm; 'good collaterals') or long (4mm; 'poor collaterals') silicon coated tips. ICP was monitored at baseline, 24 h and 72 h post stroke. Neurological deficit was assessed by measuring time-to-touch in the adhesive removal test at baseline and 12 h post stroke. Infarct volume was measured histologically at 72 h post stroke.

Results: Twenty-four hour ICP increased by 10.5 ± 6.2 mmHg from baseline (ΔICP; $p < 0.001$) in the 'good collateral' group, with a slight decrease in the 'poor collateral' group (ΔICP = 1.8 ± 2.2 mmHg; $p > 0.05$). There was no significant difference in ICP from baseline or between good- and poor-collateral groups at 72 h. There was signicantly less neurological deficit at 12 h in animals with good collateral supply (time-to-touch = 37 ± 19 s in the 'good collateral' group vs. 58 ± 6 s in the 'poor collateral' group, $p < 0.05$). There was no significant difference in infarct volumes between good- and poor-collateral groups at 72 h (93 ± 89 mm^3 vs. 87 ± 43 mm^3; respectively; $p > 0.05$).

Conclusions: Good collaterals are associated with ICP elevation at 24 h after pMCAo. Behavioural deficit was less at 12 h, in keeping with our previous data showing smaller 24 h infarct volumes in animals with a patent AChA. However, 72 h infarct volume (after ICP rise) was not significantly different. We suggest that the ICP elevation may reduce collateral flow in the 'good collateral' group resulting in infarct expansion and ultimately similar final infarct volumes in both groups. We conclude that a process occurring in areas of submaximal ischemia (penumbra) causes ICP elevation 24 h post-stroke.

References:

1 Murtha, L. A. *et al.* Short-duration hypothermia after ischemic stroke prevents delayed intracranial pressure rise. *Int J Stroke* **9**, 553-559, doi:10.1111/ijs.12181 (2014).

2 McLeod, D. D. *et al.* Inadvertent occlusion of the anterior choroidal artery explains infarct variability in the middle cerebral artery thread occlusion stroke model. *PloS one* **8**, e75779, doi:10.1371/journal.pone.0075779 (2013).

589
BRAIN-0861
Poster Session

Cerebral Ischemia: Animal Models

TREATMENT OF BRAIN ISCHEMIA BY RHEOLOGIC MODULATION OF BLOOD CIRCULATION USING DRAG REDUCING POLYMERS

D. Bragin[1], S. Thomson[1], O. Bragina[1], Z. Peng[2], G. Staton[1], M.V. Kameneva[3], E.M. Nemoto[1]
[1]Department of Neurosurgery, University of New Mexico School of Medicine, Albuquerque, NM, USA
[2]Department of Neurosurgery, Central South University, Changsha, China
[3]McGowan Institute for Regenerative Medicine Un iversity of Pittsburgh, Pittsburgh, PA, USA

Objectives: Our objective was to study a previously unexplored approach for the treatment of cerebral ischemia after severe brain insults by the modulation of the rheology of blood flow by drag-reducing polymers (DRP). Nanomolar intravenous concentrations of linear, blood-soluble DRP have been shown to improve circulation and survival in animal models of the

ischemic myocardium and limbs, but not yet in the brain. Using traumatic and ischemic brain injury models in rats, we examined the acute effects of DRP on the cerebral circulation and long-term recovery.

Methods: The suture permanent middle cerebral artery occlusion (pMCAO) was used as a model of ischemic injury and fluid percussion with a gas-driven device (1.5 ATA, 50 ms pulse) as a model of traumatic brain injury (TBI) in rat. Using in vivo 2-photon laser scanning microscopy we studied the acute effects of DRP (high MW polyethylene glycol) on microvascular blood flow velocity, tissue oxygenation (NADH) and blood brain barrier permeability (BBB) in the rat parietal cortex. Cortical Doppler flux, temperature, arterial pressure and blood gases and electrolytes were monitored. DRP (2 μg/ml in blood) was injected i.v. after baseline and post-sham/injury recordings. Controls were injected with saline. Neurodegeneration was evaluated by Fluoro-Jade at 24 hours and neurological motor deficit by Rotarod at 1 week after the injury.

Results: TBI/pMCAO progressively decreased microvascular flow in peri-injury/penumbra zones, induced hypoxia and BBB damage leading to neurodegeneration and neurological deficit. DRP significantly increased arteriolar blood flow volume and re-recruited collapsed capillaries (24±6.7 and 31±7.1%, $p<0.05$, n=10), reducing ischemia (by 16±4.6 vs 17±6.5%) and BBB damage (by 18±3.9 vs 15±5.5%), respectively ($p<0.05$), all data presented as Mean±SEM. Arteriolar blood flow velocity profiles, obtained by line scans at different distances from the vessel midline, revealed that DRP drastically changed blood flow velocity profile increasing near-wall velocity which resulted in a significant increase in blood flow volume. The improved microvascular flow decreased neurodegeneration at 24 hours after insults by 44.2±12.6% (pMCAO) and 37.6±11.2% (TBI), $p<0.05$. Rotarod tests showed that one week after insults, DRP treated rats performed better than controls with times of 75.6±16.0% vs. 47.3±15.2% (TBI) and 78.2±19.0%vs. 51.4±17.3% (pMCAO), respectively, as percent of baseline.

Conclusions: DRP improved cerebral microvascular perfusion and tissue oxygenation in both models of acute ischemia and traumatic injury resulting in improved long-term neurologic recovery. DRP increased blood flow velocity and concentration of erythrocytes near the wall of arterioles along with the previously demonstrated increase in the precapillary pressure, thereby increasing blood volume flow and the number of erythrocytes entering capillaries thus countering the effects of capillary stasis. Improved microvascular perfusion by DRP may be effectively used in the treatment ischemic stroke and traumatic brain injury.

590
BRAIN-0136
Poster Session

Cerebral Ischemia: Animal Models

IN VIVO MONITORING OF CEREBRAL HEMODYNAMICS IN THE IMMATURE RAT: EFFECTS OF HYPOXIA-ISCHEMIA AND HYPOTHERMIA

E. Buckley[1], S.D. Patel[2], B.F. Miller[3], M.A. Franceschini[3], S.J. Vannucci[2]
[1]Biomedical Engineering, Georgia Institute of Technology, Atlanta, USA
[2]Pediatrics/Newborn Medicine, Weill Cornell Medical School, New York, USA
[3]Radiology, Massachusetts General Hospital, Boston, USA

Objectives: Neonatal hypoxic-ischemic encephalopathy (HIE) occurs in 1-4/1000 live term births and can cause devastating neurodevelopmental disabilities[1, 2]. Currently, therapeutic hypothermia (TH) is the only treatment with proven efficacy[3, 4]. Since TH is associated with decreased cerebral blood flow (CBF), it is important to assess CBF at the bedside; however, CBF measurements in human neonates with HIE can be fraught with logistical difficulties. In this initial study, we employ a well-established neonatal rat model of HIE to describe the evolution of CBF following hypoxia-ischemia (HI) with or without TH, and we investigate potential relationships between acute CBF changes and subsequent brain damage.

Methods: HI was induced in postnatal day 10 or 11 rat pups by right common carotid artery ligation followed by 60-70 minutes hypoxia (8% oxygen). After HI, pups recovered for 4 hours under hypothermia (HI-TH group, target rectal temperature of 30-32°C, N=23) or normothermia (HI-N group, N=23) before being returned to the dam. Animals were sacrificed at either 1 or 4 weeks, and brain injury was scored on an ordinal scale of 0-5 (0 = no injury).

Diffuse correlation spectroscopy was employed to quantify an average hemispheric index of cerebral blood flow (CBF_i) in awake, un-anesthetized animals at baseline, pre-HI, and 0, 1, 2, 3, 4, 5, and 24 hours post-HI.

Results: Carotid ligation alone led to average decreases in ipsilateral CBF_i of 19 (3) % when measured 2 hours after occlusion. CBF_i was also minimally reduced in the contralateral hemisphere by 6 (3) %.

Following HI, an initial hyperemia was observed that was more prominent in the contralateral than ipsilateral hemisphere. This effect subsided within 5-10 minutes. After initiation of TH, CBF_i in the HI-TH group dropped significantly below baseline levels to approximately 30% of baseline and remained depressed for the duration of TH. In contrast, during this same period, CBF_i in the HI-N group was not significantly decreased from baseline levels (**Figure 1**). By 24 hours post-HI, ipsilateral CBF_i was significantly elevated in the HI-N group compared to HI-TH animals, and CBF_i in both hemispheres in the HI-N group was increased more than HI-TH and age-matched controls.

Animals in the HI-TH group demonstrated significant neuroprotection relative to the HI-N group at both the 1- and 4-week post-HI study end points ($p = 0.001$). Reductions in CBF_i after 4 hours of TH were not associated with reduced damage at 1 or 4 weeks. However, elevated ipsilateral CBF_i and ipsilateral-to-contralateral CBF_i ratios at 24 hours were associated with worse outcome at 1-week post-HI.

Conclusions: TH causes significant reductions in CBF in a rat HIE model. Although TH improves brain injury following HI, we did not observe a relationship between CBF_i during treatment and subsequent brain damage. However, elevated ipsilateral CBF_i and ipsilateral-to-contralateral CBF_i ratios at 24 hours were positively associated with injury at 1 week.

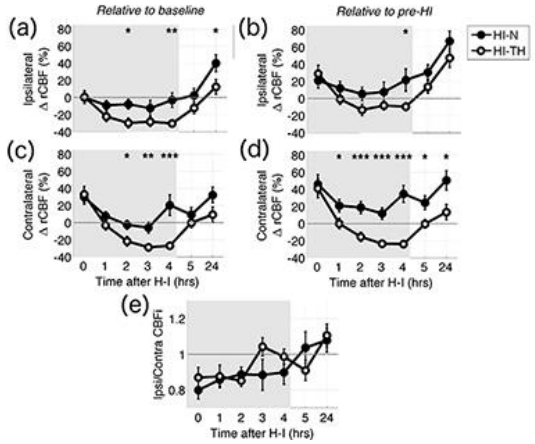

Figure 1, Relative change in CBF (ΔrCBF) from baseline (a, c) and from post-ligation levels (b, d) for HI-N (solid circles) and HI-TH (open circles) animals.

591
BRAIN-0602
Poster Session

Cerebral Ischemia: Animal Models

HIGH THROUGHPUT IDENTIFICATION AND QUANTIFICATION OF PERI-INFARCT DEPOLARIZATION IN MOUSE CORTEX WITH OPTICAL INTRINSIC SIGNAL IMAGING

J.R. Bumstead[1], A.W. Kraft[2], J. Lu[2], X. Yang[2], A.Q. Bauer[3], J.P. Culver[3], J.M. Lee[2]
[1]Biomedical Engineering, Washington University in Saint Louis, Saint Louis, USA
[2]Neurology, Washington University in Saint Louis, Saint Louis, USA
[3]Radiology, Washington University in Saint Louis, Saint Louis, USA

Objectives

Focal brain ischemia results in repetitive waves of electrophysiological hyperactivity followed by silence in surrounding cortex, a phenomenon known as peri-infarct depolarization (PID). Propagating at a rate of 2 – 6 mm/min [1], PIDs are hypothesized to exacerbate ischemia in the penumbra [2]. Despite the potential role that PIDs play in ischemic injury, their spatiotemporal propagation over the entire mouse cortex has not been well studied. We have developed an optical intrinsic signal (OIS) imaging system and image processing algorithms that enable high throughout identification of PIDs over majority of the mouse cortex. The automated and robust algorithm that has been developed is essential for analyzing the large datasets required to compare PIDs between different groups of mice.

Method

Ten mice (male C57Bl6/J, 12-14 weeks old) were anesthetized with 0.75% isoflurane and imaged up to 6 hours during middle cerebral artery occlusion (MCAO). Light emitting diodes (LEDs) operating at four wavelengths (478 nm, 588 nm, 610 nm, and 625 nm) illuminated the skull, and diffuse reflected light was detected by an EMCCD camera. Images collected from light reflected at 478nm were most suitable for detecting and quantifying PIDs (Fig 1A). After mean-subtraction, PIDs were detected by applying several criteria to create an image mask over the trial: (1) an image intensity threshold, (2) a minimum image area threshold, and (3) a minimum distance of propagation threshold (Fig 1B). In addition to detecting PIDs, the algorithm also calculated the duration, source and sink, average velocity, and spatial trace of the PID. After the automated identification of PIDs, the user can inspect the intensity trace (Fig 1C), the spatial location of the mask over the trial (Fig 1D), and the trace of the PID (Fig 1D) to identify potential false positives and false negatives. The efficiency of the algorithm was determined by identifying PIDs manually and comparing these findings to the PIDs detected by the algorithm.

Results

Our algorithm automatically detected PIDs that occurred after MCAO in mice. During the 50 hours of data analyzed, there was a total of 208 PIDs (4.16 PIDs/hour). The sensitivity and specificity of the algorithm was 0.93 and 0.97 respectively, and there was a false positive and false negative rate of 0.11 and 0.07. Using our data visualization output, a trained user can identify these false positives and negatives at around five times faster than manually watching all trials.

Conclusion

Our imaging system and processing algorithm efficiently identifies PIDs over mouse cortex, and provides quantitative information about the propagation of PIDs that cannot be calculated by manual inspection. This high-throughput approach to analyzing PIDs significantly reduces the need for manual user input. An exciting application of this system and detection algorithm is to identify differences in duration, number, or propagation of PIDs in mouse models of stroke. Drugs or genetic manipulations that reduce PIDs after MCAO could be tested for attenuation of ischemic brain injury.

References

1. Somjen, G.G., Physiol Rev, 2001. 81:1065-96.

2. Dreier, J.P., Nat Med, 2011. 17: 439-47.

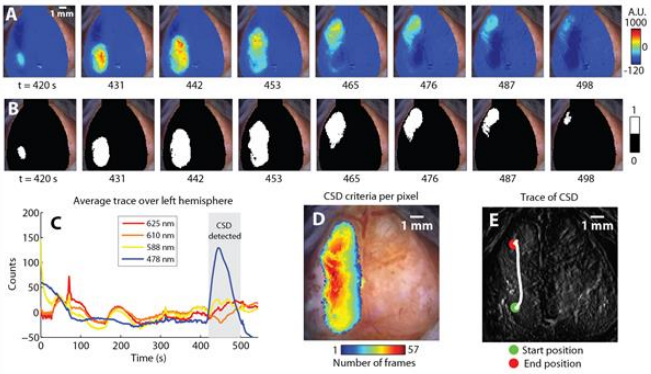

Figure 1. PID detection in mouse cortex after MCAO. **A.** Image sequence of PID in mouse after MCAO. The PID propagates at an average velocity of 3.5 mm/min from posterior to anterior. **B.** Image sequence of mask generated after passing all criteria of the detection algorithm. **C.** Average light intensity over the left hemisphere over time. Time traces of four different color LEDs are shown. In gray is the time epoch in which the algorithm detected the PID shown in A & B. **D.** The number of frames that each pixel satisfied the PID detection criteria. **E.** Trace of the PID over the mouse cortex. The start position is in green and the end position is in red.

592
BRAIN-0398
Poster Session

Cerebral Ischemia: Animal Models

DIFFUSION MR ASSESSMENT OF SPATIOTEMPORAL EVOLUTION OF FOCAL CEREBRAL ISCHEMIA IN RATS: A NOVEL ROBUST METHOD VERSUS THRESHOLD METHOD

S.H. Cha[1], C.H. Choi[2], K.S. Yi[1], H.J. Lee[3], S.R. Lee[4], Y.J. Lee[4], J.W. Hwang[5], C.H. Lee[6]
[1]Radiology, Chungbuk National University Hospital, Cheongju-si, Korea
[2]Radiology, National Medical Center, Seoul, Korea
[3]Medical Research Institute, Chung-Ang University College of Medicine, Seoul, Korea
[4]National Primate Research Center, Korea Research Institute of Bioscience and Biotechnology, Cheongju-si, Korea
[5]Clinical Science, Philips Healthcare, Seoul, Korea
[6]Division of Magnetic Resonance Research, Korea Basic Science Institute, Cheongju-si, Korea

PURPOSE
There are limitations which prevent accurate MR evaluation of spatiotemporal evolution of ADC-derived brain lesions after middle cerebral artery occlusion (MCAO) in rats. ADC values of a specific brain location differ from time to time even in a subject. Background noise, ischemic lesion, normal brain parenchyma and CSF have overlapping ADC values. This is to present our novel method for the spatiotemporal diffusion MR assessment of focal cerebral ischemia in rats after MCAO applying registration, noise/CSF removal, standardization and lesion segmentation in series.

MATERIALS AND METHODS
Immediately after right MCAO, 3T Diffusion MR scans were repeated every 10 minutes up to post-occlusion 50 minutes in 33 rats. Successful MCAO was confirmed in nine (9/33) and they were analyzed using both well-known threshold method and our robust method. Threshold method was made by removal of background noise (cut–off voxels below 150 x 10-6 mm2/sec) and CSF (above 1200 x 10-6 mm2/sec) signals. Modified method was made by following 3 steps (Fig 1): 1. Registration (registration of images with different time points and animals by 3dvolreg in AFNI) 2. Removal of background noise and CSF signals (Removal of background noise with brain mask and removal of CSF with CSF mask on minimal intensity map (Tmin map) by fslmaths within FSL) 3. ADC value standardization for relative ADC value (rADC) map (histogram standardization in contralateral normal left hemispheres by 3dROIstats of AFNI). To compare two methods, coefficients of variance (=standard deviation/mean) in normal left hemispheres were calculated. Lesion segmentation was performed with modified method (voxels below 90% of rADC) and then hemispheric lesion volumes (%HLV) and relative ADC values were calculated.

RESULTS
In every time points (Fig 2A) and in each animal (Fig 2B), coefficients of variation in normal contralateral left hemispheres were much lower with our robust method than those with threshold method respectively ($p<0.001$, respectively). ADC-derived abnormal lesions were developed on the first MR scan at 10 minutes (mean %HLVs = 40.5±1.4%) and ADC values of the ischemic lesions were stable from the 1st MR during the time course for 50 minutes (mean= 69.9±1.7%) (Fig 3).

CONCLUSION
Using our novel robust method, we were able to

assess spatiotemporal characteristics of focal cerebral ischemia in rats more reliably.

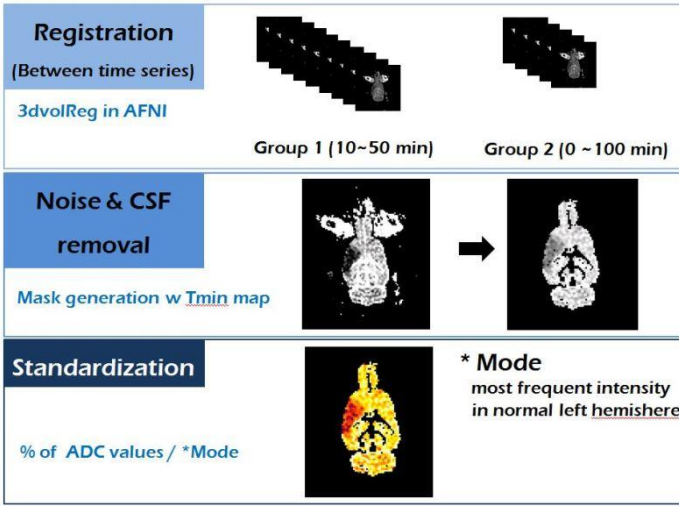

Figure 1. Steps of image processing in a robust method.

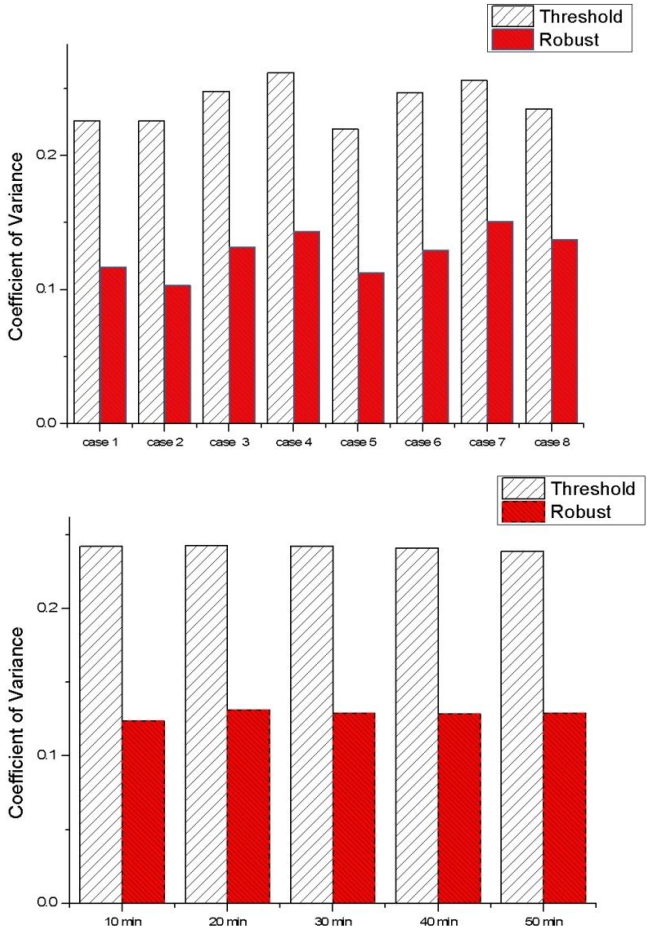

Figure 2. Coefficient of variation (CV) in normal left hemispheres. A) CVs at different time points and B) CVs in different animals.

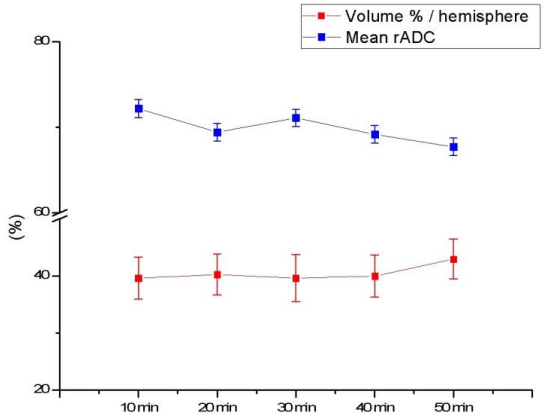

Figure 3. Spatiotemporal evolution of ADC-derived hemispheric lesions volumes (%HLVs) and relative ADC values (rADCs).

593
BRAIN-0399
Poster Session

Cerebral Ischemia: Animal Models

DIFFUSION LESION REVERSAL AFTER TRANSIENT MCAO IN NONHUMAN PRIMATE STROKE MODELS

S.H. Cha[1], S.R. Lee[2], H.J. Lee[3], C.H. Choi[4], J.W. Hwang[5], K.S. Yi[1], Y.J. Lee[2], Y.B. Jin[2]
[1]Radiology, Chungbuk National University Hospital, Cheongju-si, Korea
[2]National Primate Research Center, Korea Research Institute of Bioscience and Biotechnology, Cheongju-si, Korea
[3]Medical Research Institute, Chung-Ang University College of Medicine, Seoul, Korea
[4]Radiology, National Medical Center, Seoul, Korea
[5]Clinical Science, Philips Healthcare, Seoul, Korea

PURPOSEThough early diffusion lesion reversal (DLR) after recanalization treatment of acute ischemic stroke has been observed in clinical settings, still controversial is diffusion weighted imaging (DWI) lesions are truly reversible. This is to present our observation of sustained DLR after

transient middle cerebral artery occlusion (MCAO) / reperfusion in nonhuman primate (NHP) models.

MATERIALS AND METHODSSeven rhesus monkeys were subjected to transient MCAO using endovascular technique to achieve focal cerebral ischemia and had been followed for 4 weeks after MCAO. Immediately after occlusion, prospective MRI scans were repeated every 10 ~ 20 minutes. Occlusion was maintained until diffusion MRI showed plateau of lesion volume (peak volume) which was calculated by real time measurement technique using ImageJ (v1.46, NIH). Early DLR was defined as the ADC-derived lesion volume difference between peak volume and volume at 3 hours after reperfusion. We defined sustained DLR as voxels of acute ADC-derived lesion at the peak that corresponded to normal-looking brain on follow-up FLAIR MRI at 4 weeks. 3D volume analysis was used for quantitative analysis of ADC-derived lesion characteristics with AFNI software package (http://afni.nimh.nih.gov/afni/), FSL software (http://www.fmrib.ox.ac.uk/fsl) and ITKsnap (http://www.itksnap.org/pmwiki/pmwiki.php).

RESULTSPeak volume percentages of ADC-derived hemispheric lesions (%HLVs) were ranged 4.0 ~ 21.7% (mean=10.3%). Hemispheric early DLRs were ranged 1.1 ~ 10.5% and percentages of early DLR/Peak volume 9.9 ~ 68.9% (mean=36.3±19.3%). Final %HLVs on FLAIR images at 4 weeks were between 0.9 and 11.0% (mean=4.8%). Sustained DLR was detected in all animals (9/9), and percentages of sustained DLR/Peak volume were 15.7 to 84.9% (mean=58.6±25.8%).

CONCLUSIONWe confirmed that sustained DLR as well as early reversal is persistent in all transient focal cerebral ischemia monkey models.

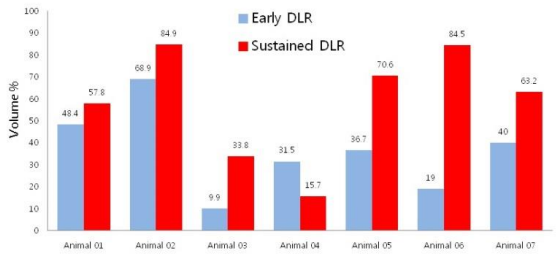

Figure 1. Percentages of early and sustained diffusion lesion reversal/peak volume in each animal.

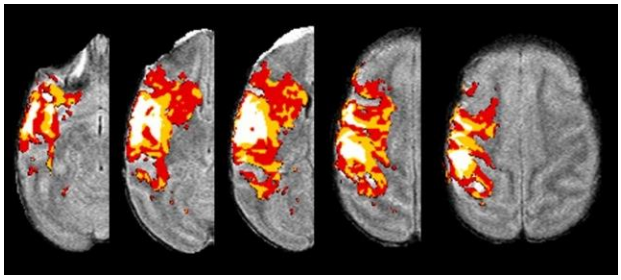

Figure 2. Representative images of diffusion lesion reversal (DLR) in animal 1. (Red, early DLR; Red+Orange, sustained DLR; White, final infarction)

594
BRAIN-0641
Poster Session

Cerebral Ischemia: Animal Models

THE IMPACT OF PIAL COLLATERALS ON INFARCT GROWTH RATE IN EXPERIMENTAL ACUTE ISCHEMIC STROKE

G. Christoforidis[1], *P. Vakil*[2], *T. Carroll*[2]
[1]*Radiology, University of Chicago, Chicago, USA*
[2]*Radiology, Northwestern University, Chicago, USA*

Objective: Understanding infarct volume growth rate and its relationship to pial collateral recruitment in acute ischemic stroke has the potential to influence decision making during reperfusion treatment. This work sought to develop a predictive model which links infarct growth rate to pial collateral recruitment in a setting of acute middle cerebral artery occlusion (MCAO) in a canine model.

Methods: Using a previously published endovascular MCAO method, 6 mongrel canines underwent permanent MCAO. Pial collaterals were quantified using digital substraction angiography (DSA) acquired 15 minutes following permanent MCAO based on previously published methodologies (a scoring system which takes into account arterial arrival tine (AAT) and spatial extent of collateralization as well as AAT alone). Infarct volumes were calculated using a previously published threshold technique by two observers using mean diffusivity (MD) maps acquired 1, 1.5, 2, 3, 4 and 24 hours using Magnetic Resonance Imaging (MRI) (3T Achieva, Philips). Infarct growth was modeled and fitted in order to derive an index of infarct growth rate for each animal (figure 1). Linear bivariate analysis was then used to assess the correlation between infarct growth rate index and pial collateral scores and AAT.

Results: Changes in infarct size can be parameterizesd as, $V(t) = Vf\ (1\text{-}e^{(-Gt)})$ (figure 1). The calculated growth index, G, has a linear relationship to both pial collateral score and 24-hour infarct volume (Vf). R-square (r^2) linear fit between pial collateral score was 0.908 ($p=0.0033$) whereas r^2 linear fit between AAT and growth rate index was 0.685 ($p=0.0419$) (figure 2). Bland-Altman statistic indicates that reproducibility using the MD maps (15.9%) and FLAIR images (13.3%) is not substantially different. None of the animals demonstrated significant hemorrhagic conversion by 24 hours. Because of a linear association between Vf and pial collateral score one may be able to replace Vf with A*p and derive $V(t)= A*p*(1\text{-}e^{(-Gt)})$ where A represents a constant.

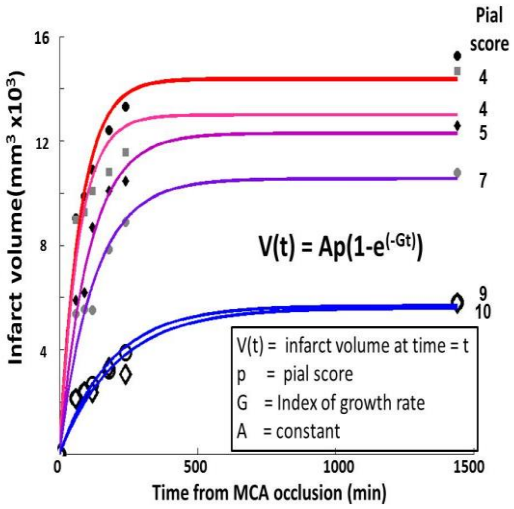

Figure 1: Infarct volume growth over time. Each asymptotic funciton corresponds to one canine to derive the index of growth rate. The pial scores for each curve are listed on the left.

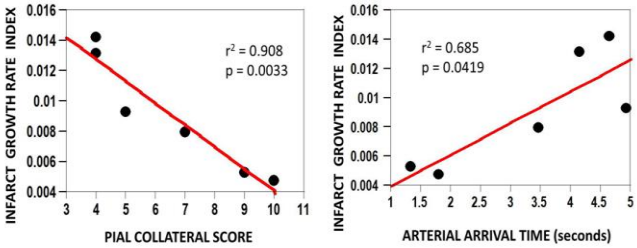

Figure 2: Infarct growth rate index derived from fitted asymptotic functions has a linear relationship with pial collateral score and arterial arrival time.

Conclusion: An assessment of pial collaterals during MCAO correlates with an index for infarct growth using an asymptotic infarct growth function in canines undergoing permanent MCAO. It may thus be feasible to use an assessment of pial collaterals to predict the asymptotic growth of acute cerebral infarction.

Reference:

Christoforidis GA, Rink C, Kontzialis MS, Mohammad Y, Koch RM, Abduljalil AM, Bergdall VK, Roy S, Khanna S, Slivka AP, Knopp MV, Sen CK. 2011. An endovascular canine middle cerebral artery occlusion model for the study of leptomeningeal collateral recruitment. Investigative Radiology. 46(1):34-40.

595
BRAIN-0400
Poster Session

Cerebral Ischemia: Animal Models

PREFRONTAL CORTEX STROKE INDUCES DELAYED IMPAIRMENT IN SPATIAL MEMORY.

L. Zhou[1], T. Wright[1], A. Clarkson[1]
[1]Anatomy, Otago Medical School, Dunedin, New Zealand

Objectives: Stroke is the leading cause of long-term disability with the focus of research primarily on improving motor deficits. Research into motor impairments is well established, however little is known about the effects on cognitive deficits after stroke. The prefrontal cortex is a brain region, which is central to these cognitive control processes. The subtle nature of cognition and the division of cognitive domains into areas such as working memory and attention can make this difficult to diagnose and treat.

Methods: All procedures were carried out as per the guidelines specified by the University of Otago Animal Ethics Committee. Here we have established a photothrombotic model of focal stroke that targets the medial prefrontal cortex (mPFC). Stroke and sham mice were assessed at one and four weeks post-insult on the open-field task to assess activity; on the grid-walk and cylinder task to assess motor impairments; on the elevated plus maze to assess anxiety; and on the novel-object and object-location recognition tasks to assess memory impairments. All assessments were carried-out by observers blind as to the treatment group.

Results: Assessment of stroke mice in the open-field showed a small increase in activity with no effects on gross motor tasks at 1 and 4-weeks post stroke. Similarly, stroke to the mPFC had no effects on anxiety ($P \geq 0.05$). Assessment of stroke mice on the novel object task showed no differences at either 1 or 4-weeks compared to sham mice ($P \geq 0.05$). However, assessment of stroke mice on the object-location recognition task revealed a significant ($P \leq 0.05$) impairment in spatial memory by 4-weeks compared to sham controls.

Conclusions: This is the first experimental evidence that stroke to the mPFC result in a delayed onset impairment in spatial memory, a finding that is similar to human epidemiological data. We suggest that this model may therefore be a useful tool in assessing potential rehabilitative/cognitive therapies after stroke.

596
BRAIN-0309
Poster Session

Cerebral Ischemia: Animal Models

EFFECTS OF HYPERGLYCEMIA ON SEVERITY OF INITIAL CEREBRAL BLOOD FLOW DEFICIT, LESION GROWTH AND INFARCT SIZE INDUCED BY MIDDLE CEREBRAL ARTERY OCCLUSION IN RATS

D. Dewar[1], L. Roy[1], W. Holmes[1], I.M. Macrae[1], K.W. Muir[1]
[1]Institute of Neuroscience & Psychology, University of Glasgow, Glasgow, United Kingdom

Objectives. Hyperglycemia is associated with worse outcome after ischemic stroke but pathophysiological mechanisms are poorly understood. In a rat model of permanent middle cerebral artery occlusion (MCAO), hyperglycemia, at clinically-relevant blood levels, exacerbated lesion growth determined by diffusion-weighted imaging (DWI), and increased infarct volume[1]. A potential mechanism is a hyperglycemic influence on perfusion. In this study we tested the hypothesis that the cerebral flood flow (CBF) deficit following MCAO is greater in hyperglycemic compared to normoglycemic rats.

Methods. Adult male Wistar rats were randomly allocated to vehicle (water)- or 15% glucose-treated groups; the experimenter was blind to rat identity and group allocation. Rats were injected (10ml/kg i.p.) 10 minutes prior to MCAO by diathermy under isoflurane anaesthesia. Study 1 (n=10 vehicle; n=11 glucose): CBF assessed semi-quantitatively using ^{99m}Tc-HMPAO blood flow autoradiography 1 hour after MCAO.

Autoradiograms were analysed by thresholding and region of interest (ROI) approaches. Study 2 (n=10 vehicle; n=10 glucose): immediately following MCAO, rats were serially imaged for 4 hours in a 7T MRI scanner for CBF using pseudo-continuous arterial spin labelling and for ischemic injury using DWI with lesion volume calculated from apparent diffusion coefficient (ADC) maps. Infarct volume was measured at 24h using T2-weighted imaging.

Results. Study 1: the proportion of the ischemic hemisphere exhibiting severely (0-43%), moderately (43-75%) or mildly (75-100%) reduced ^{99m}Tc-HMPAO uptake, compared to the contralateral non-ischemic hemisphere, was not different between vehicle and glucose groups. There were no significant differences between groups by ROI analysis. Study 2: the perfusion deficit volume (PDV), calculated by applying an abnormal perfusion threshold (30 ml/100g/min), was not different between vehicle and glucose groups over the first 4 hours after MCAO. ADC-derived lesion volumes were larger in the glucose compared to vehicle group. 24h infarct volume was larger in the glucose than the vehicle group.

	Blood glucose	PDV 1h	PDV 2h	PDV 3h	PDV 4h
Vehicle	6 ± 2	140 ± 37	130 ± 39	147 ± 47	151 ± 42
Glucose	11 ± 3*	164 ± 40	167 ± 41	173 ± 48	191 ± 54

	ADC 1h	ADC 2h	ADC 3h	ADC 4h	Infarct volume
Vehicle	50 ± 11	50 ± 9	55 ± 10	56 ± 12	56 ± 22
Glucose	60 ± 13	72 ± 25†	77 ± 24†	81 ± 28†	90 ± 19*

Mean ± SD. Blood glucose: 1h after MCAO (mmol/L). PDV, infarct volume, ADC lesion (mm^3). *P<0.05 vs vehicle, unpaired t test; † P<0.05 vs vehicle, 2-way ANOVA with Bonferroni post-test.

Conclusions. Hyperglycemia did not exacerbate the perfusion deficit induced by MCAO as measured by either in vivo autoradiography or MRI. It therefore appears that the detrimental effects of hyperglycemia predominantly occur in brain parenchyma rather than in the cerebrovasculature. However, consideration should also be given to the potential for hyperglycaemia-induced capillary dysfunction which could compromise tissue oxygen and glucose extraction in the absence of changes in blood flow.

Reference. 1. Tarr et al. J Cereb Blood Flow Metab. 2013 33:1556

597
BRAIN-0148
Poster Session

Cerebral Ischemia: Animal Models

INTRANASAL DELIVERY OF GRANULOCYTE COLONY-STIMULATING FACTOR ENHANCES ITS NEUROPROTECTIVE EFFECTS AGAINST ISCHEMIC BRAIN INJURY IN RATS

M. Yang[1], K. Wang[2], S. Zhang[1], Y. Hou[1], Z. Zhang[1], D. Li[1], L. Mao[1], C. Fan[1], B. Sun[1]
[1]Key Lab of Cerebral Microcirculation in Universities of Shandong, Taishan Medical University, Taian, China
[2]Taishan Vocational College of Nursing, Taian Shandong Province 271000 China, Taian, China

Objectives: Granulocyte colony-stimulating factor (G-CSF) is a hematopoietic growth factor with strong neuroprotective properties. However, it has limited capacity to cross the blood-brain barrier and thus potentially limiting its protective capacity. Recent studies demonstrated that intranasal drug administration is a promising way in delivering neuroprotective agents to the central nervous system. The current study therefore aimed at determining whether intranasal administration of G-CSF increases its delivery to the brain and its neuroprotective effect against ischemic brain injury.
Methods: Transient focal cerebral ischemia in rat was induced with middle cerebral artery occlusion.

Results: Our resulted showed that intranasal administration is 8-12 times more effective than subcutaneous injection in delivering G-CSF to cerebrospinal fluid and brain parenchyma. Intranasal delivery enhanced the protective effects of G-CSF against ischemic injury in rats, indicated by decreased infarct volume and increased recovery of neurological function. The neuroprotective mechanisms of G-CSF involved enhanced upregulation of HO-1 and reduced calcium overload following ischemia. Intranasal G-CSF application also promoted angiogenesis and neurogenesis following brain ischemia.

Conclusions: G-CSF is a legitimate neuroprotective agent and intranasal administration of G-CSF is more effective in delivery and neuroprotection and could be a practical approach in clinic.

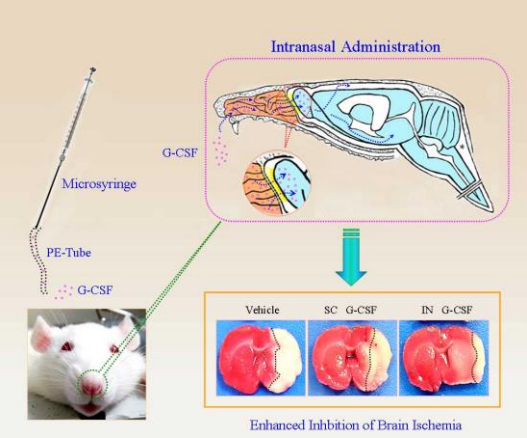

References:

1. Rother J (2008) Neuroprotection does not work. Stroke 39(2):523-524.
2. Ginsberg MD (2009) Current status of neuroprotection for cerebral ischemia: synoptic overview. Stroke 40(3 Suppl):S111–S114.
3. Hasselblatt M et al (2007) Granulocyte-colony stimulating factor (GCSF) and G-CSF receptor expression in human ischemic stroke. Acta Neuropathol 113(1):45–51.

The study was supported by the National Natural Science Foundation of China No.81471212, 81271275, 81070947, 30770759 to B.-L. Sun; Natural Science Foundation of Shandong No. ZR2012HZ006 to B.-L. Sun.

***Corresponding author**: Cun-dong Fan, Bao-liang Sun, Tel: +86-538-6230027, E-mail: tsmc_nks@tsmc.edu.cn; blsun@tsmc.edu.cn

598
BRAIN-0040
Poster Session

Cerebral Ischemia: Animal Models

EFFECT OF GABAB RECEPTOR ANTAGONISTS (CGP FAMILY) ON LEARNING AND MEMORY FORMATION IN ALBINO MICE FOLLOWING NEONATAL HYPOXIA ISCHEMIA INSULT.

Q. Gillani[1], *M. Ali*[2], *F. Iqbal*[2]
[1]*Institute of Pure and applied biology, Bahauddin Zakariya University Multan Pakistan, Multan, Pakistan*
[2]*Institute of Molecular Biology and Biotechnology, Bahauddin Zakariya University Multan Pakistan, Multan, Pakistan*

Objective: $GABA_B$ receptor antagonist are experimentally proved to act as spatial memory enhancers in mouse models but has not been studied under Hypoxic Ischemic insult.

Method: 10 days old albino mice were subjected to murine model of hypoxia and ischemia. During short term experiments various reflexes were studied in pups. During long term experiments, following hypoxia ischemic insult at postnatal day 10, mice were divided into three groups. All mice fed on normal rodent diet till they were 13 week old. At this time point, group 1 received saline, group 2 CGP 35348 and group 3 received CGP 55845 intraperitonaly for 12 days at the rate of 1mg/kg body weight/day. A battery of tests used to assess long term neurofunction.

Result: During short term experiments albino mice pups exhibited poor sensorimotor reflexes 1 and 24 hour after brain damage but effect was more pronounced in female than in male pups. During long term experiment $GABA_B$ receptor antagonists improved the motor function in male and female albino mice. In open field, both $GABA_B$ receptor antagonists in female albino mice they worsen their exploratory and locomotry behavior. During MWM study, gender specific effects were observed as CGP 35348 improved spatial learning and memory and swimming speed in male albino mice but had no effect in female albino mice

following hypoxia ischemia encephalopathy. CGP 35348 helped in reducing the inflammatory IL-6 and 18 concentrations in male albino mice but CGP 55845 caused increased in IL-6 and IL-18 concentrations in female albino mice following HIE.

Conclusion: Overall CGP 35348 improved the neuromuscular coordination in female albino mice, improved spatial learning and memory and reduced IL-6 and IL-18 concentration level in male albino mice.

599
BRAIN-0753
Poster Session

Cerebral Ischemia: Animal Models

ROLE OF RENEXIN, A MIXED COMPOUND OF GINKGO BILOBA EXTRACT AND CILOSTAZOL, FOR SYNAPTIC PLASTICITY IN HIPPOCAMPUS OF RAT MODEL OF CHRONIC CEREBRAL HYPOPERFUSION

Y. HA[1], S. Han[2], J. Cheong[1], H. Lee[1], H. Park[1], K. Cho[1], M. Kim[2]
[1]Neurology,
Wonkwang University Hospital and Jeonbuk Regio nal Cardio Cerebrovascular Center, Iksan, Korea
[2]Physiology,
Wonkwang University School of Medicine and Brai n Research Institute at Wonkwang University, Iksan, Korea

The impairment of cognitive function such as memory and attention has been recognized in patients with chronic mild cerebral ischemia. The hippocampal memory and long-term potentiation (LTP), a cellular correlate of learning and memory, were impaired by chronic cerebral hypoperfusion induced by permanent, bilateral occlusion of the common carotidartery (2VO). Recent animal study reported that renexin, a mixed compound of ginkgo biloba extract and cilostazol improved the deficit of spatial memory andthe lesion of the white matter in the rat 2 VO model.

Objectives: The purpose of present study wasto evaluate the effects of renexin on the impaired LTP and expression of mRNA genes involving neuronal plasticity in the rat 2 VO model.

Methods: Adult male Sprague-Dawley rats were randomly divide three experimental groups into:1) Sham without 2VO, 2) 2VO+vehicle, 3) 2VO+renexin. The permanent ligation of bilateral common carotid arteries was performed to elicit chronically lower blood flow to the brain. Animals were treated with oral administration of renexin(gingko biloba 20 mg/kg/day + cilostazol 25 mg/kg/day) or vehicle every day from 1 day after surgery for 3 weeks. We recorded LTP induced by brief high frequency stimulation to the Schaffer collateral–CA1 pathway of the hippocampus under anesthesia *in vivo*. Two hours after induction of LTP, the animal was sacrificed and the hippocampus was isolated for quantitative detection of mRNA for BDNF, Arc, Egr-1 and CREB using quantitative real-time RT-PCR technique.

Results: In sham-operated control group, high frequency stimulation was sufficient to induce robust LTP (110 ± 15% of control field excitatory postsynaptic potential (fEPSP) slope; n =7). Animals of 2VO+vehicle group showed a highly significant deficit in LTP induction (15 ± 3%of control fEPSP slope; n= 7; $P< 0.01$) 3 weeks after 2VO. On the other hand, daily oral administration of renexin showed the marked preservation of LTP induction (98 ± 17% of control fEPSP slope; n =7; $P<0.01$). Other parameters of synaptic excitability such as baseline fEPSP slope and input-output relation showed no significant difference between the 2VO+vehicle and the 2VO+renexin group. On the real-time RT-PCR analysis, a significant reduction of CREB, Arc and BDNF mRNA expression was observed inthe hippocampus of 2VO+vehicle group compared with that of sham group ($P< 0.01$). In contrast, renexin treatment increased significantly the expression of these mRNAs in the hippocampus compared with that of 2VO+vehicle group ($P< 0.05$).

Conclusion: These results suggest that daily oral administration of renexin can ameliorate cognitive deficit through the preservation of

synaptic plasticity on the level of neural circuit in rodent model of chronic cerebral hypoperfusion.

600
BRAIN-0128
Poster Session

Cerebral Ischemia: Animal Models

SPREADING DEPOLARIZATIONS MEDIATE EXCITOTOXICITY IN THE DEVELOPMENT OF ACUTE CORTICAL LESIONS

J. Hinzman[1], V. DiNapoli[1], E. Mahoney[1], G. Gerhardt[2], J. Hartings[1]
[1]Neurosurgery, University of Cincinnati, Cincinnati, USA
[2]Anatomy and Neurobiology, University of Kentucky, Lexington, USA

Spreading depolarizations (SD) are mass depolarizations of neurons and astrocytes that occur spontaneously in acute brain injury and mediate time-dependent lesion growth. Glutamate excitotoxicity has also been extensively studied as a mechanism of neuronal injury, although its relevance to *in vivo* pathology remains unclear. Here we hypothesized that excitotoxicity in acute lesion development occurs only as a consequence of SD. Using glutamate-sensitive microelectrodes, we found that SD induced by KCl in normal rat cortex elicits increases in extracellular glutamate (11.6 ± 1.3 µM) that are synchronous with the onset, sustainment, and resolution of the extracellular direct-current shift of SD (Fig 1A,B). Inhibition of glutamate uptake with $_{D,L}$-threo-β-benzyloxyaspartate (TBOA, 0.5 and 1 mM) significantly prolonged the duration of the direct-current shift (148% and 426%, respectively) and the glutamate increase (167% and 374%, respectively) in a dose-dependent manner ($P<0.05$) (Fig 1C). These prolonged events produced significant cortical lesions as indicated by Fluoro-Jade staining ($P<0.05$), while no lesions were observed after SD in control conditions or after cortical injection of 1 mM glutamate (extracellular increase: 243 ± 50.8 µM) or 0.5 mM TBOA (glutamate increase: 8.5 ± 1.6 µM) without SD.

Increases in extracellular glutamate mirror changes in the DC potential during SD.

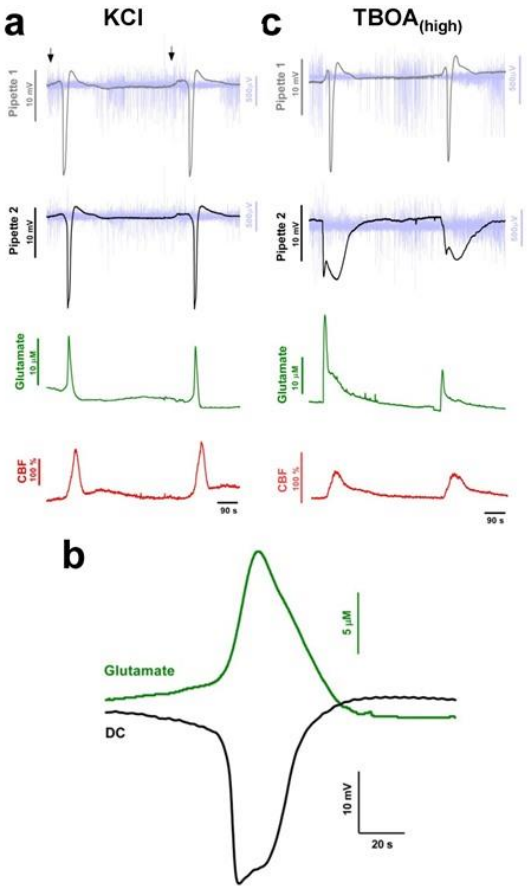

We then used an embolic focal ischemia model to determine whether glutamate elevations occur independent of SD in the natural evolution of a cortical lesion. In both the ischemic core and penumbra, glutamate increased only in synchrony with anoxic terminal SD (6.1± 1.1 µM) and transient SDs (11.8 ± 2.4 µM), and not otherwise (Fig 2). Delayed terminal SDs were also observed in two animals at 98 and 150 min after ischemic onset and induced similar glutamate elevations. Durations of SDs and glutamate increases were significantly correlated in both normal and ischemic animals ($P<0.05$).

Delayed Terminal Depolarization After Embolic Focal Ischemia

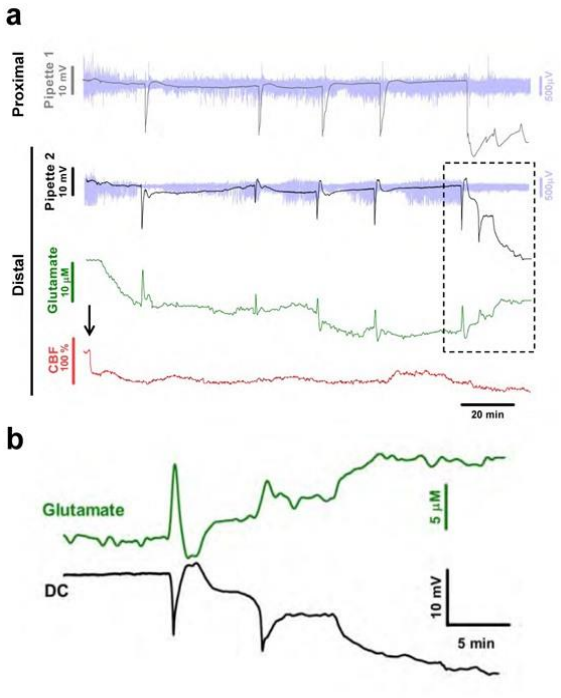

These data suggest that pathologically prolonged SDs are a required mechanism of acute cortical lesion development and that glutamate elevations and the mass electrochemical changes of SD and are merely different facets of the same pathophysiologic process.

601
BRAIN-0679
Poster Session

Cerebral Ischemia: Animal Models

GENDER AND AGE DIFFERENCES IN HISTOLOGICAL INJURY FOLLOWING THE CONTROLLED CORTICAL IMPACT MODEL OF TRAUMATIC BRAIN INJURY IN MICE

H. Kim[1], K.M. Rodgers[1], R.J. Traystman[1], P.S. Herson[1]
[1]Anesthesiology, University of Colorado School of Medicine, Aurora, USA

Purpose: Although the mechanism is unknown, there is a growing body of clinical evidence supporting the influential role of gender on the acute and chronic outcome of traumatic brain injury (TBI). However, there are limited published studies regarding gender-related effects in experimental animal models of TBI. It is not clear if gender could have an equal influence on the outcome of TBI in pediatric and adult males and females. Our study aims to compare the injury in pediatric and adult females with those of males after controlled cortical impact (CCI) injury to assess the gender difference of short and long-term outcome using histologic characterization.

Methods: This experiment used a CCI model of experimental TBI to examine the gender and age effects. Male and female C57Bl/6 pediatric (21-25 day old) & adult (8–12 week old) mice underwent CCI at varying depths of deflection (1.0-2.0 mm) and histological injury was compared amongst groups and to sham mice. Cresyl violet staining was performed 7 or 30 days after recovery from TBI and volume of injury was analyzed.

Results: In the subacute (7 days after TBI) and the chronic group (30 days after TBI), we observed significant injury in all mice tested (male and female adult and pediatric mice), at all deflection depths tested, 1.0, 1.5 and 2.0-mm deflections (diameter (d) = 3 mm; velocity = 3 m/s; and duration = 500 ms) compared to sham controls. Importantly, a graded injury was observed, corresponding to depth of deflection. Adult female mice exhibited significantly smaller injury at both 7 and 30 days after TBI following severe TBI (2 mm deflection) compared to adult male mice ($p < 0.05$). In contrast, no difference was observed in magnitude of injury in male and female pediatric mice. Iterestingly, pediatric mice were less vulnerable to cortical damage after CCI compared to adult mice ($p < 0.05$).

Conclusions: Our findings demonstrate that histologically, a graded injury response was seen in both ages at injury and the gender difference in cortical contusion damages was observed only in adult mice. In addition, an aging difference of tissue loss after CCI was observed, with pediatric mice being significantly less vulnerable to injury compared to young adults.

602
BRAIN-0559
Poster Session

Cerebral Ischemia: Animal Models

NEUROPHYSIOLOGICAL RESPONSES OF RECOVERY IN PEDIATRIC MICE COMPARED TO ADULT MICE WITH TRANSIENT FOCAL CEREBRAL ISCHEMIA.

J.E. Orfila[1], H. Grewal[1], T. Shimizu[1], R.M. Dietz[2], R.J. Traystman[3], P.S. Herson[3]
[1]Anesthesiology,
University of Colorado School of Medicine, Denver, USA
[2]Pediatrics,
University of Colorado School of Medicine, Denver, USA
[3]Pharmacology / Anesthesiology,
University of Colorado School of Medicine, Denver, USA

Introduction: Ischemic stroke is the fourth leading cause of death in the United States and is increasingly being recognized as a disease that occurs in people of all ages, not just the elderly. Studies suggest that the immature developing brain may have a greater degree of plasticity compared to the adult, thereby enhancing functional recovery to a greater extent during development.

Hypothesis: Pediatric mice exhibit greater recovery from hippocampal synaptic function following experimental stroke than adults.

Methods: Extracellular field recordings of CA1 neurons were performed in acute hippocampal slices prepared at 24 hrs, 7 or 30 days after recovery from middle cerebral artery occlusion (MCAO) and compared to sham control mice.

Results: In adult mice, hippocampal long-term potentiation (LTP) is impaired as early as 24 hrs after experimental stroke and remains impaired for at least 30 days in both the ipsilateral and contralateral, non-injured hemisphere. However, in pediatric mice, LTP is impaired as early as 24 hrs after MCAO and remained impaired in the ipsilateral side 7 days after MCAO, but recovered in the contralateral side at 7 days after MCAO. At day 30 post-stroke, pediatric mice display a full recovery of synaptic function in both hemispheres. Furthermore, significant experimental data is emerging demonstrating an imbalance between inhibitory and excitatory cortical pathways after ischemic stroke, suggesting that reducing GABAergic inhibitory transmission enhances recovery. To test this, hippocampal slices were incubated in L655,708 (100nM), an inverse agonist selective for α5 subunit-containing $GABA_A$ receptors. Our data shows that synaptic plasticity was rescued in both pediatric and adult mice in the presence of

Conclusion: The present study demonstrates that transient focal ischemia causes functional impairment in the hippocampus at various time points after MCAO and that recovery of synaptic function is more robust in the young brain. In addition, we observed that excessive GABA activity may contribute to impaired synaptic function following ischemic injury, thus inhibition of specific GABA activity may provide a new therapeutic approach to improve functional recovery after stroke.

603
BRAIN-0605
Poster Session

Cerebral Ischemia: Animal Models

INHIBITED CAMKII ACTIVITY DECREASES HIPPOCAMPAL NEURONAL DAMAGE IN BOTH NORMOTHERMIC AND MILD THERAPEUTIC HYPOTHERMIC CA/CPR MOUSE MODEL

G. Deng[1], K. Bayer[1], R. Traystman[1], P. Herson[1]
[1]Pharmacology, University of Colorado, Denver, USA

Objective: Glutamate excitotoxicity is an important mechanism of ischemic neuronal damage, however inhibition of glutamate receptors has proven an unsuccessful strategy. Ca^{2+}/calmodulin-dependent protein kinase II (CaMKII) is a major downstream target of glutamate signaling. There are two major forms of CaMKII activity: stimulated by Ca2+/CaM and

Ca2+-independent autonomous that outlasts the initial stimulation. Studies shows that inhibition of autonomous CaMKII activity post-insult in culture reduces glutamate-induced neuronal cell death. The aim of this study is to examine the neuroprotective potential of inhibition of autonomous CaMKII activity using novel peptide inhibitors (tatCN21,19o) and transgenic mice.

Methods: C57BL/6 male wild-type (WT) and T286A mutant mice were subjected to 6 min of cardiac arrest and CPR. Mice were randomized to tatCN21 (1 mg/kg), tatCN19o (0.01,0.1,1 mg/kg) or control (tatSCR; 1 mg/kg), administered 30 min after CPR (iv). Separate experiments were performed to assess mild post-arrest hypothermia (rectal T = 34 ±0.2 ℃ for 1 hr after CPR). Hippocampal neuronal damage was analyzed 3 days after CA/CPR by H&E staining. Total CaMKII and Thr-286 phosphorylation levels were measured by western blot. Statistical analyses were performed using ANOVA and t tests, with $P<0.05$ considered significant.

Results: Analysis of histological damage 72 hrs after CA/CPR showed that tatCN21 significantly reduced neuronal injury; 28.9±5.6% (n=11) compared to 55.4±4.0% (n=8, $P<0.05$) in tatSCR-treated mice. Mild hypothermia decreased damage from 55.4±4.0% (n=8) to 31.9±10.5% (n=6, $P<0.05$), which could be further reduced by tatCN21, reducing to 7.2±4.0% (n=4, $P<0.05$). Interestingly, the more potent tatCN19o decreased neuronal damage at all doses tested, reducing damage to 23.6±10.8% (n=7, $P<0.05$) for 1 mg/kg, 25.8±8.8% (n=8, $P<0.05$) for 0.1 mg/kg and 10.9±3.7% (n=8, $P<0.05$) for 0.01 mg/kg. Western blot analysis showed that CA/CPR significantly increases p-T286 CaMKII 3 (4.5±0.31, n=4,) compared to sham controls (0.91±0.14, n=4, $P<0.05$). Finally, T286A mutant mice had less neuronal damage after CA/CPR (4.0 ± 0.9%, n=8) compared to WT mice (28.9 ± 10.9%, n=8; $P<0.05$), indicating a role for autonomous CaMKII activity in CA/CPR-induced neuronal injury.

Conclusions: The novel CaMKII inhibitors decrease neuronal damage under both normothermic and hypothermic condition following CA/CPR, indicating that inhibition of autonomous CaMKII activity is a promising new therapeutic approach.

References:

1. Vest, RS, O'Leary, H, Coultrap, SJ, Kindy, MS, Bayer, KU. 2010. Effective post-insult neuroprotection by a novel Ca2+/calmodulin-dependent protein kinase II (CaMKII) inhibitor. The Journal of biological chemistry 285: 20675–82.
2. Coultrap, SJ, Vest, RS, Ashpole, NM, Hudmon, A, Bayer, KU. 2011. CaMKII in cerebral ischemia. Acta pharmacologica Sinica 32: 861–72.

604
BRAIN-0198
Poster Session

Cerebral Ischemia: Animal Models

THE EARLY ELEVATION OF HIPPOCAMPAL BDNF BY EXERCISE AFTER CEREBRAL MICROEMBOLI REDUCES THE APOPTOSIS OF NEURON.

N. Himi[1], H. Takahashi[2], N. Okabe[1], F. Lu[1], E. Nakamura[1], T. Shiromoto[1], K. Narita[1], T. Koga[2], O. Miyamoto[1]
[1]Physiology 2, Kawasaki Medical School, Kurashiki, Japan
[2]Rehabilitation, Kawasaki Univ Med Welfare, Kurashiki, Japan

Objective: Exercise in the early stage ofpoststroke has been shown to facilitate the recovery from cognitive dysfunction.We have showed that the recovery of spatial memory function was depend on the hippocampallevel of brain-derived neurotrophic factor (BDNF). However, time dependentchanges of BDNF and its protective effects from apoptosis of neuron wereunknown. In the present study, we investigated chronological changes of BDNF byexercise and apoptotic cell damage after brain ischemia using cerebral microembolimodel rats.
Methods: To induce the multifocalmicroemboli in the brain, 3,000 perticles of microspheres (MS, ϕ45μm) were injected via rightinternal carotid artery of rats. Mild exercise was started at the 24 hoursafter MS injection by a treadmill (15 m/min,

30 min/day for 7 days) in theearlier stage exercise group (Early). A later stage exercise group (Late)started at 8 days after MS injection, and non-exercise group (NE) and shamoperated group were also examined as control groups. The spatial memoryfunction was evaluated by Morris water maze test that was performed at 15-19days after MS injection. BDNF concentration in transected hippocampus weremeasured at 6hrs., 8, 15 and 22 days after MS injection by ELISA. Toinvestigate the relationship between the elevation of BDNF in hippocampus andrecovery of memory function, rats were infused BDNF into their hippocampuscontinuously by osmotic pump during 1-7 days (the Early-BDNF group), or 8-14days (the Late-BDNF group) after MS injection. Furthermore, rats were infused K252a, TrkB receptorantagonist, and forced to exercise during 1-7 days (the KE group) to test the effectsof BDNF. The apoptotic damage of neuronwas detected by immunostaining of activated caspase-3 at 2 days after MS injectionboth the Early and NE groups.

Results:The Memory functions in the Early group was significantly improved comparedwith the Late and NE groups. BDNF concentration was gradually elevated byexercise (Early group: 6 hrs: 2.9 ± 0.21, 8 days: 4.8 ± 0.97; Late group: 8days: 2.6 ± 0.67, 15 days: 4.9 ± 0.72 pg/mg-protein) and decreased after the completionof exercise in both groups. Moreover, the Early-BDNF group showed significantrecovery in memory function, however, the Late-BDNF and KE group did not. In addition,activated caspase-3 positive neurons were observed in the hippocampus, especiallyin CA1, and tended to decrease in Early group at 2 days after MS injection.

Conclusion: These results suggest thatthe transient elevation of hippocampal BDNF by exercise in early stage might playa major role in protection from neuronal apoptosis, resulting in recovery of memorydysfunction after cerebral ischemia.

605
BRAIN-0780
Poster Session

Cerebral Ischemia: Animal Models

BRUTON'S TYROSINE KINASE (BTK) IS AN ESSENTIAL COMPONENT FOR NLRP3 INFLAMMASOME ACTIVATION AND A POTENTIAL THERAPEUTIC TARGET FOR INFLAMMATION AFTER ISCHEMIC BRAIN INJURY

M. Ito[1], T. Shichita[1], A. Yoshimura[1], R. Morita[1]
[1]Microbiology and Immunology,
Keio University School of Medicine, Tokyo, Japan

Objectives

Among inflammatory cytokines, IL-1b has beenimplicated in post-ischemic inflammation after stroke. The multiple proteincomplex, inflammasome, is indispensable for converting pro-IL-1b to an activeform IL-1b p17. Thus, inhibition of inflammasome activation may remedy the stroke-inducedneurological dysfunction. In this study, we tried to find an inflammasomeinhibitor to reduce post-ischemic inflammation in the brain.

Methods

First, to select a pharmacological inhibitorthat suppresses NLRP3 inflammasome activation, we treated LPS-primed human andmurine macrophages with several candidate inhibitors, stimulated them with alumor ATP, and then determined caspase-1 activation and IL-1b secretion inmacrophages. Next, to evaluate the effects of the selected inhibitor on post-ischemicinflammation, we induced focal brain ischemia in mice by occluding the rightmiddle cerebral artery for 60 min and then intravenously administered theinhibitor.

Results

We found that Bruton's tyrosine kinase (BTK)inhibitors suppressed NLRP3 inflammasome activation *in vitro*. Importantly, BTK consisted of NLRP3 inflammasome by physicallyinteracting

with both NLRP3 and apoptosis-associated speck-like proteincontaining a caspase-recruitments domain (ASC). The FDA-approved BTK inhibitor ibrutinib(PCI-32765) significantly suppressed infarct volume growth and neurologicaldamage in the brain ischemia model. Ibrutinib suppressed caspase-1 activation,thereby inhibiting IL-1b secretion of macrophages infiltrated in theinfarct lesion. These results revealed that BTK is essential for NLRP3inflammasome activation and could be a potent therapeutic target in stroke.

606
BRAIN-0609
Poster Session

Cerebral Ischemia: Animal Models

THE ELECTRICAL THRESHOLD OF SPREADING DEPOLARIZATION IS REDUCED AND SPREADING ISCHEMIA IS PROLONGED IN SPONTANEOUSLY HYPERTENSIVE STROKE-PRONE RATS UNDER JAPANESE DIET

E. Kang[1], O. Prager[2], A. Friedman[3], J.P. Dreier[4]
[1]Dept. of Experimental Neurology, Charite University Medicine Berlin, Berlin, Germany
[2]Dept. of Physiology & Neurobiology, Ben-Gurion University of the Negav, Beer-Sheva, Israel
[3]Dept. of Medical Neuroscience, Dalhousie University, Halifax, Canada
[4]Center for Stroke Research Berlin (CSB), Charite University Medicin Berlin, Berlin, Germany

Objectives: Spreading depolarization (SD) induces tone alterations in resistance vessels, causing either transient hyperperfusion (physiological hemodynamic response) in healthy tissue; or hypoperfusion [inverse hemodynamic response = cortical spreading ischemia (SI)] in tissue at risk for progressive damage.[1] Here, we investigated the susceptibility to SD and SI in spontaneously hypertensive stroke-prone rats (SHRSP) in comparison to Wistar Kyoto (WKY) control rats. SHRSP rats represent an animal model for human cerebral small vessel disease (SVD).[2]

Methods: Animals were anesthetized with thiopental-sodium, tracheotomised, and artificially ventilated. In series 1, one group of each strain (G1: SHRSP, n=7; G3: WKY, n=6) was fed a Japanese diet with 1% NaCl in drinking water from the 9th week to the 14th week, whereas the other groups (G2: SHRSP, n=6; G4: WKY, n=8) received normal rat chow. A closed cranial window was implanted. Direct current (DC) changes were measured by two Ag/AgCl electrodes and regional cerebral blood flow (rCBF) with laser speckle contrast analysis (LASCA) imaging. SD/SI was induced by topical application of artificial cerebrospinal fluid (ACSF) containing the NO-synthase inhibitor nitro-L-arginine (L-NNA) and elevated potassium. In series 2, the electrical threshold of SD was determined using a bipolar stimulation electrode over frontal cortex (G5: SHRSP, n=16; G6: WKY, n=14).

Results: In series 1, topical application of L-NNA and high potassium led to spontaneous SD/SI in all groups. However, the initial hypoemic phase was significantly longer in G1 [(first SD): 907 (356, 1187)s; median (first, third quartile)] compared to control group G4 [143 (97, 231)s; *P*=0.013; Kruskal-Wallis ANOVA on Ranks with Dunn's post hoc tests], whereas G2 [303 (183, 589)s] and G3 [116 (89, 131)s] were not significantly different from the control group. Consistently, the duration of the negative DC shift of SD was significantly longer in G1 [1639 (1271, 1725)s] compared to control group G4 [305 (268, 495)s; *P*=0.019], whereas G2 [538 (128, 2008)s] and G3 [289 (267, 296)s] were not significantly different from control. In series 2, the threshold for electrically triggered SD was significantly lower in SHRSP rats [G5 (SHRSP): 1300 (625, 2300)µA; G6 (WKY): 3500 (1300, 7000)µA; *P*=0.049; Mann-Whitney rank sum test].

Conclusions: These findings may partially explain the greater susceptibility to ischemic damage of SHRSP rats under Japanese diet. The reasons may lie in anomalies of both microvasculature and neuronal/astrocytic network.

References:

1. Dreier JP. (2011) Nat Med. 17(4):439-47
2. Hainsworth AH, Markus HS. (2008) J Cereb Blood Flow Metab. 28(12):1877-91

607
BRAIN-0129
Poster Session

Cerebral Ischemia: Animal Models

RESVERATROL PRECONDITIONING INDUCES A NEW EXTENDED WINDOW OF ISCHEMIC TOLERANCE IN THE MOUSE BRAIN.

K.B. Koronowski[1], K.R. Dave[1], I. Saul[1], J.W. Thompson[1], J.T. Neumann[1], V. Camarena[2], J.I. Young[2], M.A. Perez-Pinzon[1]
[1]Neurology and Neurosurgery, University of Miami Miller School of Medicine, Miami, USA
[2]Human Genetics and Genomics, University of Miami Miller School of Medicine, Miami, USA

Objectives: Prophylactic treatment is an alternative means for significant neuroprotection against stroke with potential agents emerging from the field of ischemic preconditioning[1]. Resveratrol preconditioning (RPC) mimics ischemic preconditioning and reduces ischemic injury when administered two days prior to cardiac arrest in rats[2]. This protection is postulated to occur at least in part through signaling pathways involving silent information regulator two 1 (Sirt1) and mitochondrial function[3]. We hypothesized that RPC confers neuroprotection against focal ischemia in mice, possibly through a Sirt1-mediated mechanism. Additionally, we wanted to determine whether chronic RPC treatment could enhance this protection.

Methods: We tested two different RPC (10 mg/kg resveratrol i.p.) treatment paradigms in a middle cerebral artery occlusion model of stroke. Functional outcome was assessed by neurological scoring and infarct volume was quantified via tetrazolium chloride staining 24 hours post-stroke. Sirt1-chromatin binding was evaluated by ChIP-qPCR. A percoll gradient fractionation protocol was used to obtain synaptic fractions for protein analysis. Protein was probed for via western blot. Brain-derived neurotrophic factor (BDNF) concentration was measured by way of an ELISA assay. Data are represented in the graphs as mean ± SEM.

Results: Both RPC treatment paradigms reduced infarct volume (Fig. 1). Strikingly, a single application of RPC 14 days prior to stroke afforded the most robust protection, reducing infarct volume by 33.2% (student's t-test, $p<0.01$, veh n=9, RPC n=10) and improving neurological score by 27.9% (student's t-test, $p<0.05$) compared to vehicle (Fig. 1). 14 days following RPC, cortical Sirt1 protein levels were increased 1.5 fold of vehicle (student's t-test, $p<0.01$, n=10) and Sirt1 binding to the BDNF and mitochondrial uncoupling protein 2 (UCP2) promoter regions was observed (n=3) (Fig. 2). At the same time point, synaptic UCP2 protein decreased by 22.6% (student's T-test, $p<0.05$, n=6) and cortical BDNF concentration increased 26.6% of vehicle (student's T-test, $p<0.05$, n=7) (Fig. 3).

Conclusions: RPC induces a new extended window of chronic ischemic tolerance in the brain that lasts for at least 14 days. One possible explanation for this tolerance is potentially mediated by Sirt1 and two of its potential targets that are involved in modification of mitochondrial function and the synapse. These results demonstrate a novel time frame of ischemic tolerance induced by resveratrol preconditioning; the current studies are ongoing and the results of which will provide substantial evidence for resveratrol as a prophylactic agent in the treatment of cerebral ischemia.

References:

1. Gidday JM. Cerebral preconditioning and ischaemic tolerance. *Nature reviews. Neuroscience*. 2006;7:437-448

2. Della-Morte D, Dave KR, DeFazio RA, Bao YC, Raval AP, Perez-Pinzon MA. Resveratrol pretreatment protects rat brain from cerebral ischemic damage via a sirtuin 1-uncoupling protein 2 pathway. *Neuroscience*. 2009;159:993-1002

3. Yang Y, Duan W, Li Y, Yan J, Yi W, Liang Z, et al. New role of silent information regulator 1 in cerebral ischemia. *Neurobiology of aging*. 2013;34:2879-2888

Funding: NIH Grants NS45676, NS054147, NS34773

Fig. 1

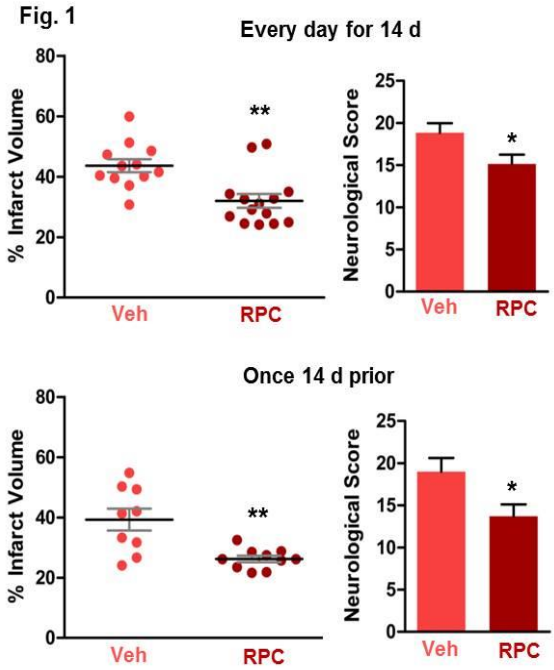

Fig. 2

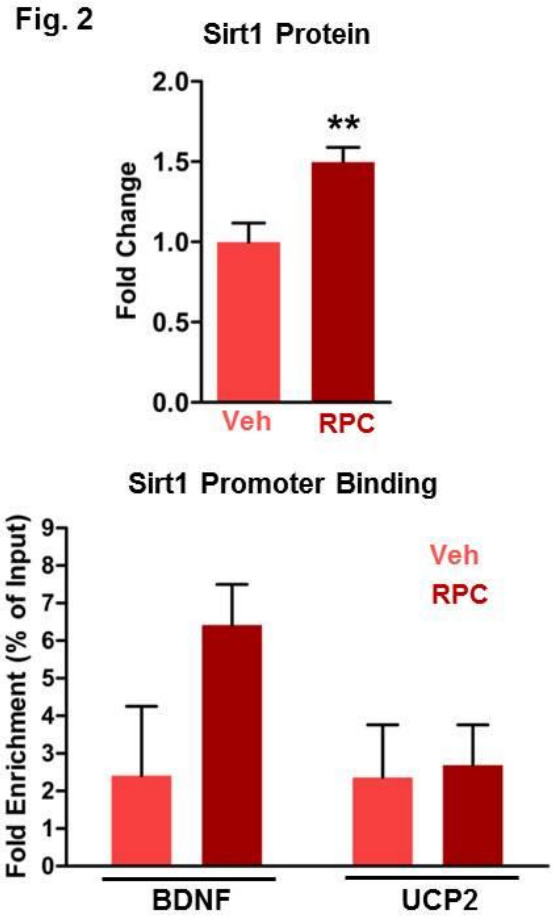

Fig. 3

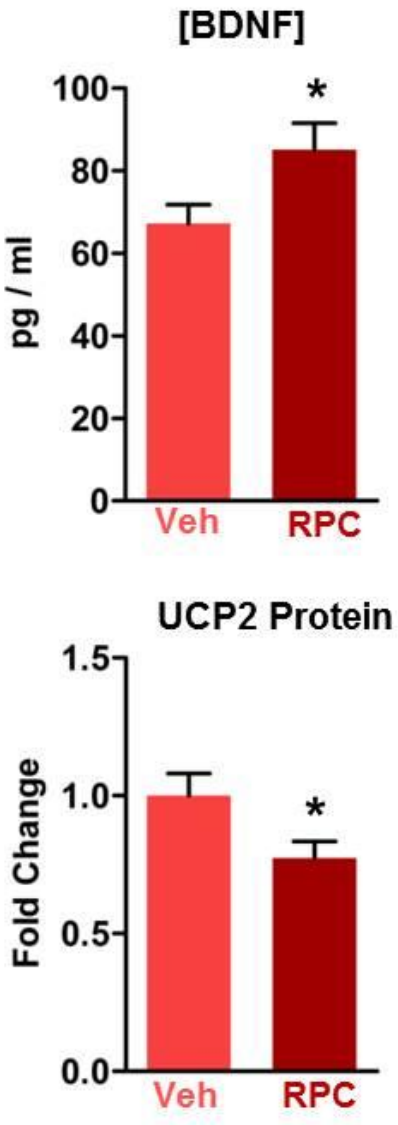

608
BRAIN-0729
Poster Session

Cerebral Ischemia: Animal Models

KIR6.1 LIMITS PERI-INFARCT DEPOLARIZATION FREQUENCY DURING FOCAL CEREBRAL ISCHEMIA

A.W. Kraft[1], J. Lu[2], H. Zhang[3], J. Bumstead[4], A.Q. Bauer[5], M.S. Remedi[3], C.G. Nichols[3], J.P. Culver[6], J.M. Lee[7]
[1]Neurology, Washington University, St. Louis, USA
[2]Neurosurgery, Guangzhou First People's Hospital, Guangzhou, China
[3]Cell Biology and Physiology, Washington University, St. Louis, USA
[4]Biomedical Engineering, Washington University, St. Louis, USA
[5]Radiology, Washington University, St. Louis, USA
[6]Radiology Physics Biomedical Engineering, Washington University, St. Louis, USA
[7]Neurology Radiology Biomedical Engineering, Washington University, St. Louis, USA

Objective:

Focal cerebral ischemia results in recurring spreading depression-like events initiated within the ischemic core, leading to peri-infarct depolarizations (PIDs) in the surrounding tissue [1]. PIDs are thought to exacerbate ischemia, expanding the core and further contributing to neuronal death [2]. Pathologic increases in extracellular potassium concentration due to anoxic K^+ release play a critical role in PID initiation and propagation, but the molecular mechanisms driving PID phenomena are poorly understood. ATP-sensitive channels (K_{ATP}), composed of pore-forming ($K_{ir}6.1$ or $K_{ir}6.2$) and regulatory sulfonylurea receptor (SUR1 or SUR2) subunits, open under low ATP conditions (e.g. ischemia) and facilitate transmembrane K^+ fluxes [3]. Both $K_{ir}6.1$ and $K_{ir}6.2$ are expressed in neural tissue, including neurons, astrocytes, and endothelial cells [3,4], and thus these channels may be critical for maintenance of extracellular K^+ homeostasis during ischemia. We sought to determine the role of these channels in PID occurrence during ischemic injury.

Methods:

Male mice (wild-type, $K_{ir}6.1^{-/-}$, or $K_{ir}6.2^{-/-}$, on a C57Bl6/J background) aged 12-14 weeks were anesthetized with isoflurane (2.5% induction, 1% maintenance) and middle cerebral artery occlusion (MCAO) was achieved by intra-arterial filament. The scalp was retracted and wide-field OIS imaging was performed through the intact skull for 4 hours. Light emitting diodes (LEDs) operating at four wavelengths (478 nm, 588 nm, 610 nm, and 625 nm) illuminated the skull, and

diffuse reflected light was detected by an EMCCD camera running at 120Hz. PIDs were scored by manual viewing of data. PID frequency was compared between groups using ANOVA with repeated measures and Newman-Keuls multiple comparisons test.

Results:

MCAO in wild-type mice resulted in the initiation of PIDs 39±9 minutes into ischemia. PIDs continued to occur throughout the 4-hour imaging window at a consistent frequency of 2.8±1.0 PIDs/hr. In $K_{ir}6.1^{-/-}$ mice, PID initiation was earlier (21±6 min vs. 39±9 min, $p<0.05$), and occurred with increased frequency compared to control mice (5.0±1.8 PIDs/hr vs. 2.8±1.0 PIDs/hr, $p<0.05$). In $K_{ir}6.2^{-/-}$ mice, PID initiation time and frequency were unchanged compared to controls (34±14 min vs. 39±9 min, N.S.; 2.6±1.7 PIDs/hr vs. 2.8±1.0 PIDs/hr, N.S.).

Conclusion:

These results demonstrate a critical role for $K_{ir}6.1$ in limiting PIDs during ischemia. Given relevant activation of this channel during ischemia, it may play a role in removing excess extracellular K^+. Previous studies have shown that $K_{ir}6.1$ gene deletion results in increased infarct volumes [5], consistent with the idea that PIDs contribute to infarction. Kir6.1 and Kir6.2 exhibit different cell-type distributions [4], suggesting K_{ATP} channel activation in a specific cell type may be necessary for limiting PIDs. We are currently working to identify that cell type in order to better understand how K_{ATP} channels limit ischemic depolarization and neuronal death.

References:

1. Shin et al., *JCBFM*. 26(8):1018-30 (2006)
2. Eikermann-Haerter et al., *Circulation*. 125(2):335-45 (2012)
3. Seino. *Annu Rev Physiol*. 61:337-62 (1999)
4. Thomzig et al., *Mol Cell Neurosci*. 18(6):671-90 (2001)
5. Dong et al., *CNS Neurosci Ther*. 19(8)617-24 (2013)

609
BRAIN-0425
Poster Session

Cerebral Ischemia: Animal Models

NO EFFECT OF CHRONIC PHOTOPERIOD DISRUPTION ON VULNERABILITY TO FOCAL CEREBRAL ISCHEMIA IN RATS

K. Ku Mohd. Noor[1], L. Roy[1], C. Wyse[2], C. McCabe[1], D. Dewar[1]
[1]Institute of Neuroscience and Psychology, University of Glasgow, Glasgow, United Kingdom
[2]Institute of Biodiversity Animal Heath and Compa rative Medicine, University of Glasgow, Glasgow, United Kingdom

Objectives. Epidemiological data associates shift work with increased risk of cardiovascular and cerebrovascular disease [1]. Shift work involves photoperiod disruption (PD) such that exposure to light dark cycles are regularly altered compared to normal day/night schedules. Previous studies have reported that PD induced changes in metabolism or physiology, (e.g. hypertension, hyperglycemia) that have the potential to adversely affect stroke outcome. The objective of this study was to investigate if PD affects vulnerability to stroke, by determining the impact of PD on infarct size following permanent middle cerebral artery occlusion (MCAO).
Methods. Adult male Wistar rats (200-250g) were housed singly under two different dark light cycle conditions (n=10 each). Controls were maintained on a standard 12:12 light dark cycle for 9 weeks. For rats exposed to PD: every 3 days for 9 weeks the lights were switched on 6h earlier than in the previous photoperiod. Locomotor activity was monitored continuously by cage-top infrared movement sensors to examine temporal associations between light dark periods and activity only in rats exposed to PD. In all rats body weight (BW) and food intake (FI) was measured weekly; systolic blood pressure (BP) was recorded by tail cuff plethysmography at baseline and at the end of the 9 week protocol; blood glucose was measured immediately following induction of isoflurane anaesthesia for permanent MCAO by diathermy. Infarct volume was assessed by T_2-

weighted MRI 48h following MCAO by an experimenter blinded to rat identity.

Results. Control and PD rats displayed comparable body weight gain and food intake. BP was not significantly different at the end of the 9 week period compared to baseline in either control or PD rats. Immediately prior to MCAO there was a small increase in blood glucose in PD rats compared to control. Infarct volume at 48h after MCAO was not significantly different between control and PD rats.

	% BW increase	Food intake	BP baseline	BP 9 weeks	Blood glucose	Infarct volume
Control	64±16	1481	97.7 ±9.8	96.1±12.8	9.8 ± 1.9	77.8±34.7
PD	56±11	1384	108.9±12	101.8±9.2	11.4±1.5*	94.8±22.8

% BW increase: % change between baseline and end of the 9 week experimental period. Food intake (g): total food provided less that recovered over the 9 week period. BP (mmHg); Blood glucose (mmol/L); infarct volume (mm^3). *P=0.049, control vs PD, unpaired t test.

Conclusions. Disruption of the photoperiod in young healthy rats for a duration of 9 weeks did not alter key physiological variables that can impact on ischaemic damage, e.g. BP and blood glucose. There was no effect of photoperiod disruption on infarct size after MCAO. We conclude that the potentially adverse impact of shift work on stroke outcome may require additional factors such as high fat/high sugar diet or pre-existing co-morbidities.

Reference:

[1] M. V Vyas, et al 2012 *BMJ* 345: e4800

610
BRAIN-0318
Poster Session

Cerebral Ischemia: Animal Models

THE TRIALS AND TRIBULATIONS OF MODELLING STROKE IN AGED OBESE ANIMALS

A.E. Learoyd[1], T. England[2], K.C.F. Fone[1], D.A. Kendall[1], S.E. O'Sullivan[2], R. Trueman[1]
[1]School of Life Sciences, University of Nottingham, Nottingham, United Kingdom
[2]Division of Medical Sciences and Graduate Entry Medicine, University of Nottingham, Nottingham, United Kingdom

Objectives: Nearly 75% of all strokes occur in people over the age of 65. Despite this, animals used to model the condition are predominantly young and healthy (1). Common co-morbidities for stroke include hypertension (2) and diabetes (3), but these are rarely included in animal stroke models which currently possess little or no predictive validity. Some of these co-morbidities can be induced in aged animals by feeding a high fat diet (4, 5) and this study examines the feasibility of modelling stroke in aged, obese rats to develop a model that would better reflect the clinical situation.

Methods: 12 month old Wistar-Han rats (500-650g, n=15) were maintained on a diet containing 60% fat for 8 months to induce obesity and an associated metabolic syndrome. A subset of these animals was used to determine the optimal duration of occlusion in the middle cerebral artery occlusion (MCAO) model of stroke. Remaining rats underwent this optimised procedure alongside 6-month old controls to determine effects of age and metabolic syndrome on post-stroke survival and functional deficits. Histology and blood vessel myography were performed at termination and infarct volume assessed. The development of a metabolic syndrome was analysed by serial blood samples, using multiplex ELISAs. This study was performed in accordance to the UK Animals (Scientific Procedure) Act 1986 under a project license from the UK Home Office.

Results: In the 8 months prior to surgery rats gained a large amount of weight (750–1050g). Animals on the high fat diet did not become significantly hypertensive (106±6.2 vs. 96±5.7). However, blood samples indicated the presence of pre-diabetes and an altered inflammatory response. 30 minutes was determined to be the

optimal occlusion length in this model. But full analysis of infarct volumes and vessel myography is still ongoing.

Conclusions: While modifications were required to provide the optimal care for these rats (including restraint, housing density and during surgery heating), this more translational, aged obese model can feasibly be used in stroke research.

References:

1. Ankolekar S, Rewell S, Howells DW, Bath PMW. The influence of stroke risk factors and comorbidities on assessment of stroke therapies in humans and animals. International Journal of Stroke. 2012;7(5):386-97.
2. Johansson BB. Hypertension mechanisms causing stroke. Clinical and experimental pharmacology & physiology. 1999;26(7):563-5. Epub 1999/07/16.
3. Jorgensen HS, Nakayama H, Raaschou HO, Olsen TS. Stroke in Patients with Diabetes - the Copenhagen-Stroke-Study. Stroke; a journal of cerebral circulation. 1994;25(10):1977-84.
4. Chuffa LGD, Seiva FRF. Combined effects of age and diet-induced obesity on biochemical parameters and cardiac energy metabolism in rats. Indian J Biochem Bio. 2013;50(1):40-7.
5. Tomada I, Fernandes D, Guimaraes JT, Almeida H, Neves D. Energy restriction ameliorates metabolic syndrome-induced cavernous tissue structural modifications in aged rats. Age. 2013;35(5):1721-39.

611
BRAIN-0107
Poster Session

Cerebral Ischemia: Animal Models

RIVAROXABAN AND APIXABAN REDUCE HEMORRHAGIC COMPLICATION BY PROTECTION OF NEUROVASCULAR UNIT AFTER RECANALIZATION WITH TISSUE PLASMINOGEN ACTIVATOR IN ISCHEMIC STROKE OF RAT

R. Morihara[1], S. Kono[1], T.O.R.U. Yamashita[1], K. Deguchi[1], Y. Omote[1], T. Yunoki[1], K.O.T.A. Sato[1], T. Kurata[1], N. Hishikawa[1], K.O.J.I. Abe[1]
[1]Neurology, Okayama University, Okayama, Japan

Objectives

This study aimed to assess the risk and benefit of tissue-type plasminogen activator treatment after oral anticoagulation with rivaroxaban or apixaban compared with warfarin or placebo.

Methods

Pretreatment with warfarin (0.2 mg/kg per day), rivaroxaban (2 mg/kg per day), apixaban (10 mg/kg per day), or vehicle (0.5% carboxymethyl cellulose sodium salt) was performed for 7 days. Transient middle cerebral artery occlusion was then induced for 120 minutes, followed by reperfusion with tissue-type plasminogen activator (10 mg/ kg per 10 mL). Clinical parameters, including cerebral infarction volume, hemorrhagic volume, and blood coagulation, were examined. Twenty-four hours after reperfusion, markers for the neurovascular unit at the peri-ischemic lesion were immunohistochemically examined in brain sections, and matrix metalloproteinase-9 activity was measured by zymography.

Results

The paraparesis score was significantly improved in the rivaroxaban-pretreated group compared with the warfarinpretreated group. Intracerebral hemorrhage was observed in the warfarin-pretreated group, and this was reduced in the rivaroxaban and apixaban-pretreated groups compared with the vehicle group. Marked dissociation of astrocyte foot processes and the basal lamina or pericytes was observed in the warfarin-pretreated group, and this was improved in the rivaroxaban and apixaban-pretreated groups. Furthermore, activation of matrix metalloproteinase-9 in the ipsilateral warfarin-pretreated brain was greatly reduced in rivaroxaban- and apixaban-pretreated rats.

Conclusions

This study shows a lower risk of intracerebral hemorrhage after tissue-type plasminogen activator treatment in rats with ischemic stroke that are pretreated with rivaroxaban and

apixaban compared with pretreatment with warfarin. Reducing neurovascular dissociation by rivaroxaban and apixaban compared with warfarin could partly explain a reduction in hemorrhagic complications reported in clinical studies.

612
BRAIN-0110
Poster Session

Cerebral Ischemia: Animal Models

PERICYTE PROTECTION BY EDARAVONE AFTER TPA TREATMENT IN RAT CEREBRAL ISCHEMIA

Y. Nakano[1], K. Deguchi[1], S. Kono[1], R. Morihara[1], T. Yamashita[1], K. Abe[1]
[1]neurology,
Okayama University Graduate School of Medicine Dentistry and Pharmaceutical Sciences, Okayama, Japan

i) Background & Objectives: Pericytes play a pivotal role in contraction, mediating inflammation, and regulation of blood flow in the brain. In the present study, changes of pericytes in the neurovascular unit (NVU) were examined in relation to the effects of exogenous tissue plasminogen activator (tPA) and a free radical scavenger, edaravone.

ii) Methods: Immunohistochemistry and Western blot analyses showed that the overlap between PDGFRβ-positive pericytes and N-acetylglucosamine oligomers (NAGO)-positive endothelial cells increased significantly at 4 days after 90 min of transient middle cerebral artery occlusion (tMCAO).

iii) Results: The number of pericytes and the overlap with NAGO decreased with tPA, but recovered with edaravone 4 days after tMCAO with proliferation. Thus, tPA treatment damaged pericytes resulting in the detachment from astrocytes and a decrease in GDNF secretion. However, treatment with edaravone greatly improved tPA-induced damage to pericytes.

iv) Conclusion: The present study demonstrates that exogenous tPA strongly damages pericytes and destroys the integrity of the NVU, but edaravone treatment can extremely ameliorate such damage after acute cerebral ischemia in rats.

613
BRAIN-0257
Poster Session

Cerebral Ischemia: Animal Models

MONONUCLEAR CELLS (MNCS) INCLUDING ENDOTHELIAL PROGENITOR CELLS (EPCS) PROTECT CEREBRAL ISCHEMIC DAMAGE ON MICE.

T. Nakayama[1], E. Nagata[1], H. Masuda[2], S. Kohara[1], H. Yuzawa[1], Y. Takahari[3], T. Asahara[2], S. Takizawa[1]
[1]Neurology, Tokai University School of Medicine, Isehara, Japan
[2]Regenerative Medicine Science, Tokai University School of Medicine, Isehara, Japan
[3]Support Center for Medical Research and Educati on, Tokai University, Isehara, Japan

【Objectives】

EPCs were reported to enhance repairing andregenerating neurovascular units.[1, 2] So far many papers have reported repairing and regenerating experiments using EPCsderived from bone marrow, spleen, or peripheral blood. However, the results were not always satisfied. Recently, we succeeded to get MNCs including higher grade quality EPCs using a novel colony assay system which we have developed. [3] In the present study, we used this novel colony assay system, and evaluated effects with MNCs including EPC on ischemic stroke model in mice.

【Methods】

We made 41 ischemic stroke model mice (10 weeks male C57BL/6 mice) with permanent middle cerebralartery occlusion (MCAO). From peripheral blood, we collected mononuclear cells, which was called peripheral blood MNCs (PB-

MNCs) including primitiveEPCs, lymphocytes, and monocytes. For 5 days, we had cultured PB-MNCs, which were called quality and quantity MNCs (QQ-MNCs) including definitive EPCs, M2 macrophages and so on. We injected PBS as control, PB-MNCs,or QQ-MNCs into external carotid artery at 24 hours after MCAO. At 3 weeks after MCAO, we took the brains and investigated time-lapse physiological parameters including cerebral blood flow and immunohistochemistry against some antibodies related to vasculogenesis and inflammatory.

【Results】

The stroke volume decreased with QQ-MNCs injected mice comparing to the control. The blood flows were no different between the control and other cell-injected mice. Positive cells with the antibodies related to vasculogenesis and inflammatory in cell-injected mice tended to increase comparing with the control.

【Conclusions】

Those results indicate QQ-MNCs possibly protected the brains from ischemic damage through thier immunity. Those QQ-MNCs could enhance repairing and regenerating neurovascular units after ischemic stroke.

【References】

1. Decano, J.L., et al. PLoS One, 2013. **8**(1): p. e55222.

2. Kaneko,Y., et al., Curr Pharm Des, 2012. **18**(25):p. 3731-4.

3. Masuda,H., et al., Circ Res, 2011. **109**(1):p. 20-37.

614
BRAIN-0366
Poster Session

Cerebral Ischemia: Animal Models

AWAKE RECORDING OF PERI-INFARCT DEPOLARIZATIONS IN THE SPONTANEOUSLY HYPERTENSIVE RAT

K. Kudo[1], *T. Nowak*[2]
[1]*Neurosurgery, Juntendo University, Tokyo, Japan*
[2]*Neurology,*
University of Tennessee Health Science Center, Memphis, USA

Objectives -- Peri-infarct depolarizations (PIDs) have pathophysiological significance in both experimental and clinical stroke. Anesthesia profoundly impacts PID incidence and propagation, yet awake animals have been monitored in only one prior study (1), which involved intraluminal filament occlusion in Sprague-Dawley rats, a strain with robust collateral perfusion. For comparison, the present study investigated PID number and time course after surgical middle cerebral artery occlusion (MCAO) in the more vulnerable Spontaneously Hypertensive Rat (SHR).

Methods -- Male SHR were fitted with epidural electrode arrays under isoflurane anesthesia. After recovery intervals of 1 day to 5 weeks they were subjected to permanent or transient (2-hour) focal ischemia by tandem occlusion of the MCA and ipsilateral common carotid arteries (2), and PIDs were monitored for up to 3 days. An additional experiment examined the impact of maintaining anesthesia during the initial hours after MCAO. Brains were removed after recording and sectioned to determine infarct volume.

Results -- Total PID number was minimally impacted by the time between electrode placement and occlusion surgery. Awake SHR exhibited 28 ± 9 PIDs (mean ± SD, n=27) during permanent occlusions, all within 4 hours following MCAO. Maintaining isoflurane anesthesia during this initial 4-hour interval significantly reduced total PID number (10 ± 4, n=6), and extended the

time course for several more hours after recovery from anesthesia. A much more prolonged time course was observed through 36 hours after transient occlusions, but PID number during recirculation was highly variable (10 ± 9, n=8). PID number generally correlated with infarct size, but this relationship was dissociated by prolonged anesthesia, which reduced PID number without significantly impacting infarct size.

Conclusions -- The short window of PID incidence after permanent MCAO in the SHR differs markedly from that previously described after filament occlusions in Sprague-Dawley rats (1). That study showed a biphasic time course through 24 hours after both permanent and transient occlusions, and total PID number was several-fold higher than in the SHR. Nevertheless, the present results appear to agree with a conclusion of the prior study that PID incidence correlates with the timing of infarct expansion, which progresses rapidly after permanent occlusions in the SHR. In addition, attenuated collateral perfusion and smaller penumbra volume in the SHR may reduce the probability of triggering PIDs, reducing their total number in this model. Maintained isoflurane anesthesia appears to delay recruitment of penumbra and prolong PID time course. Although without impact in the SHR, it might be predicted that such a mechanism could contribute to persistent protective effects of volatile anesthetics in strains with more robust collateral circulation.

1) Hartings J, Rolli ML, Lu X-CM, Tortella FC (2003) J. Neurosci. 23:11602-11610

2) Brint S, Jacewicz M, Kiessling M, Tanabe J, Pulsinelli W (1988) J. Cereb. Blood Flow Metab. 8:474-485

Supported by USPHS grant R21-NS077039

615
BRAIN-0498
Poster Session

Cerebral Ischemia: Animal Models

CADASIL MUTATIONS INCREASE STROKE VULNERABILITY

F. Oka[1], J.H. Lee[1], I. Yuzawa[1], D.V. Bornstädt[1], T. Qin[1], K. Eikermann-Haerter[1], A. Joutel[2], C. Ayata[3]
[1]Radiology, Massachusetts General Hospital, Charlestown, USA
[2]Medicine, INSERM and Univ Paris Diderot, Paris, France
[3]Radiology and Neurology, Massachusetts General Hospital, Charlestown, USA

Objectives:
Cerebral autosomal dominant arteriopathy with subcortical infarcts and leukoencephalopathy (CADASIL), linked to mutations in *NOTCH3* expressed predominantly in vascular smooth muscle cells in adult brain, is characterized by progressive leukoaraiosis, and recurrent ischemic strokes in young or middle aged adults. Mechanisms underlying vascular dysfunction and stroke are unclear. We aimed to characterize the focal cerebral ischemia phenotype in transgenic mice expressing naturally occurring CADASIL mutations, to elucidate the mechanisms rendering the CADASIL brain vulnerable to stroke.

Methods:
We transiently (45min or 1h) occluded the middle cerebral artery by either an intraluminal filament proximally (fMCAO) or a microvascular clip distally (dMCAO) in two different CADASIL mutant mice (*NOTCH3* R90C or R169C). We recorded cerebral blood flow (CBF) using laser Doppler (LDF) or speckle flowmetry (LSF), in each stroke model, respectively. We also studied cortical electrophysiology during acute stroke, tissue and neurological outcomes 24 hours after reperfusion, and gross cerebrovascular anatomy, including the diameter of major cerebral arteries, patency of posterior communicating artery and number of pial artery anastomoses. Mutants were

compared with their age-matched wild-type (WT) littermates. Group sizes indicated below include WT controls of each strain.

Results:
Both R90C and R169C mutants developed significant larger infarcts (40% and 25% larger than WT, n=65 and 34, respectively, $p<0.05$) after filament MCAO. Outcome was not age-dependent, but appeared to be slightly worse in females. Surprisingly, neither LDF during filament MCAO nor LSF during distal MCAO showed worse CBF deficits (n=26 in R90C and n=20 in R169C), in either mutant. Cerebrovascular anatomy also did not differ between R90C mutant and WT (n=17). Interestingly, peri-infarct depolarization frequency was increased (1.5 fold) in the mutants during filament MCAO ($p=0.07$, n=13), a finding consistent with previous demonstration of increased susceptibility to spreading depression in non-ischemic CADASIL mutants (Eikermann-Haerter et al, Ann Neurol 2011). Presumably as a consequence of this, CBF threshold for tissue viability (figure) was significantly higher in R90C mutants compared with wild type (40±1% versus 33±2% of baseline CBF, respectively, $p=0.032$, n=14), suggesting increased sensitivity to ischemic injury.

Conclusions:
Our results show that outcome of focal cerebral ischemia is worse in CADASIL mutants independent of cerebral hemodynamic factors or collateral function, suggesting higher parenchymal sensitivity to ischemia possibly linked to frequent peri-infarct spreading depolarization events. The latter may be a reflection of increased susceptibility to spreading depression as a hyperexcitability phenotype in CADASIL.

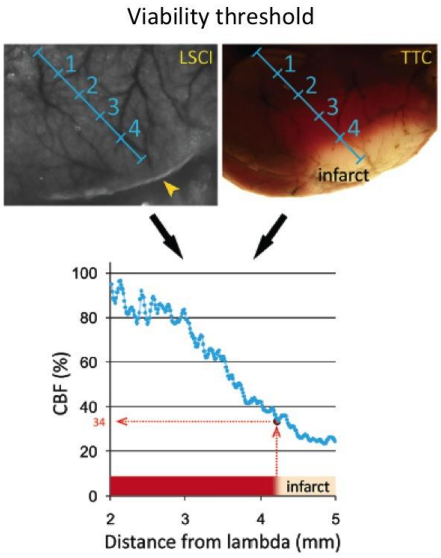

616
BRAIN-0380
Poster Session

Cerebral Ischemia: Animal Models

MOUSE CEREBELLAR PHOTOTHROMBOTIC STROKE MODEL

J. Parmar[1], A.J. Craig[1], G.D. Housley[1]
[1]Translational Neuroscience Facility & Department of Physiology, UNSW Australia, Sydney, Australia

Objective: Cerebellar strokes represent 2-3% of acute strokes worldwide, with a mortality rate 23% greater than strokes in other brain regions (Macdonell, Kalnins, & Donnan, 1987). The widely used small animal stroke models of middle cerebral artery occlusion, or global ischemia, have limited application for analysis of therapeutics directed at hindbrain strokes. Presently, hindbrain strokes in small animals involve microsphere-induced embolism via the internal carotid artery (Sekiguchi et al., 2005), or injection of autologous blood clots in the vertebral artery (Henninger et al., 2006), both of which are highly invasive and not temporally or spatially confined. Here we present a photothrombotic mouse model of cerebellar ischaemia to study neuroprotection for hindbrain strokes. We aim to determine the validity of the photothrombotic stroke model to

produce a site-specific ischaemic brain injury in the cerebellum, by examining the progression of the cerebellar infarct via magnetic resonance imaging (MRI), histology and immunohistochemistry.

Methods: All experiments were approved by the UNSW animal care and ethics committee. Photothrombosis in the cerebellum was achieved by intravenous administration of rose bengal dye (40 mg/kg) followed by illumination at 561nm of the vermis region of the cerebellum in the anaesthetised mouse (129SvEv). Infarcts were examined by T2 weighted MRI (Bruker 9.4T) at days 1, 4, and 7 post-ischaemia. Following MRI, the tissue was paraffin embedded, sectioned, stained with haematoxylin and eosin (H&E), and immunostained with anti-glial fibriliary acidic protein (GFAP) antibody and anti-calbindin antibody to detect astrocytes and assess damage to Purkinje neurons respectively.

Results: The thrombus formation was determined in real-time using intravital multiphoton LSM to detect aggregation of fluorophore-conjugated anti-CD42 immunolabelled platelets. MRI scans in the days following the infarct showed development of oedema within the area delineated by the platelet labelling. This was well correlated with histological assessment of the infarct. H&E staining, and immunohistochemistry for GFAP and calbindin, delineated astrocyte infiltration, loss of Bergmann astrocyte processes, and a loss of Purkinje neurons.

Conclusion: The photothrombotic stroke model in the cerebellum is a robust model of focal ischaemia, which delivers thrombi to a specific and contained area; compared to the previous existing models of hindbrain strokes which are not spatially or temporally restrained. Hence, this model can aid investigations into novel therapeutic options targeting the hindbrain.

References:
Henninger, N., Eberius, K. H., Sicard, K. M., Kollmar, R., Sommer, C., Schwab, S., & Schabitz, W. R. (2006). A new model of thromboembolic stroke in the posterior circulation of the rat. *J Neurosci Methods, 156*(1-2), 1-9. doi: 10.1016/j.jneumeth.2006.01.028
Macdonell, R. A., Kalnins, R. M., & Donnan, G. A. (1987). Cerebellar infarction: natural history, prognosis, and pathology. *Stroke, 18*(5), 849-855.
Sekiguchi, M., Takagi, K., Takagi, N., Date, I., Takeo, S., Tanaka, O., . . . Nowakowski, R. S. (2005). Time course and sequence of pathological changes in the cerebellum of microsphere-embolized rats. *Exp Neurol, 191*(2), 266-275. doi: 10.1016/j.expneurol.2004.09.012

617
BRAIN-0352
Poster Session

Cerebral Ischemia: Animal Models

DELAYED INHIBITION OF VEGF SIGNALING AFTER STROKE ATTENUATES BLOOD BRAIN BARRIER BREAKDOWN AND IMPROVES FUNCTIONAL RECOVERY IN A CO-MORBIDITY DEPENDENT MANNER

P. Reeson[1], K. Tennant[1], K. Gerrow[1], S. Novak[1], P.C. Nahirney[1], C.E. Brown[1]
[1]Division of Medical Sciences, University of Victoria, Victoria, Canada

Diabetes is a common comorbidity in stroke patients and a strong predictor of poor functional outcome. To provide a more mechanistic understanding of this clinically relevant problem, we focused on how diabetes affects blood brain barrier (BBB) function after stroke. Since the BBB can be compromised for days after stroke and thus further exacerbate ischemic injury, manipulating its function presents a unique opportunity for enhancing stroke recovery long after the window for thrombolytics has passed. Using a mouse model of type 1 diabetes, we discovered that ischemic stroke leads to an abnormal and persistent increase in vascular endothelial growth factor receptor 2 (VEGF-R2) expression in peri-infarct vascular networks. Correlating with this, BBB permeability was markedly increased in diabetic mice which could not be prevented with insulin treatment after stroke. Imaging of capillary ultrastructure

revealed that BBB permeability was associated with an increase in endothelial transcytosis rather than a loss of tight junctions. Pharmacological inhibition (initiated 2.5 days post-stroke) or vascular-specific knockdown of VEGF-R2 after stroke attenuated BBB permeability, loss of synaptic structure in peri-infarct regions, and improved recovery of forepaw function. However, the beneficial effects of VEGF-R2 inhibition on stroke recovery were restricted to diabetic mice, and appeared to worsen BBB permeability in non-diabetic mice. Collectively, these results suggest that aberrant VEGF signaling and BBB dysfunction after stroke plays a crucial role in limiting functional recovery in an experimental model of diabetes. Furthermore, our data highlight the need to develop more personalized stroke treatments for a heterogeneous clinical population.

618
BRAIN-0570
Poster Session

Cerebral Ischemia: Animal Models

VALIDATION OF AMIDE PROTON TRANSFER (APT) AS A MEASURE OF PH BY 31P MRS IN A PIGLET MODEL OF HYPOXIA ISCHEMIA ENCEPHALOPATHY (HIE)

M. Rega[1], F. Torrealdea[1], A. Bainbridge[2], M. Sokolska[1], K. Broad[3], I. Fierens[3], M. Ezzati[3], N. Robertson[3], S. Walker-Samuel[4], D.L. Thomas[1], X. Golay[1]
[1]Institute of Neurology, University College London, London, United Kingdom
[2]Medical Physics, University College London Hospitals, London, United Kingdom
[3]Institute for Woman Health, University College London, London, United Kingdom
[4]Center for Advance Biomedical Imaging, University College London, London, United Kingdom

Introduction: Hypoxia-ischemia (HI) in the newborn infant causes dramatic metabolic disturbances in the brain leading to alterations in tissue pH[1,2]. ^{31}P MRS allows quantitative pH measurements; however this technique provides at best limited spatial information. Amide proton transfer (APT) has been shown to be sensitive to pH via the exchange rate between amide protons and water, thought to be base-catalysed[3]. Here, we aim at mapping regional pH changes in the piglet brain undergoing neonatal HI insult using APT.

Methods: Newborn piglets (n=16) were surgically prepared[1,4] and HI was induced. ^{31}P MRS was acquired at baseline, during, at 1 hour and at 24 hours post HI (pulse-acquire sequence, TR=10S). APT scans were also acquired pre-, 1 hour and 24 hours post HI (80 Gaussian pulses dur=50ms, FA=400°, 91% duty cycle, Turbo-Flash readout of TR=4.14ms, TE=2.09ms FA=10°, FOV=100x100mm^2, matrix=128x128, thickness=4mm). Saturation frequencies: linearly spaced (77 points), range ±6ppm. The pH_i values were quantified from ^{31}P MRS[2].The APT was calculated pixel by pixel as the difference between the Z-Spectrum and a linear interpolation from 3 to 4ppm. The sensitive volume of the ^{31}P coil corresponded to the cortical watershed area of the brain. The APTp signal was averaged in this area, to match the source tissue of the pH_i measurements for calibration purposes.

Results/Discussion: In animals with severe insult (n=7), the mean height of the APT peak was reduced at 1 hour post HI. Figure 1 shows the typical appearance of the Z-spectra pre and post HI. Figure 2 is a demonstration of pH-calibrated brain images where variations are clearly observed. This work demonstrates how regional brain pH can be mapped in the piglet brain undergoing HI. The disappearance of the amide peak following HI is most likely due to the amide exchange rate reduction caused by brain acidification. pH_i confirms the trend seen with APT. This work highlights the advantage of spatial information of pH variations across the brain. APT has the potential to be used in the clinic for pH change mapping and assessment of treatment in newborn suffering from asphyxiation at birth.

References:
1. Kurinczuk JJ,et al."Epidemiology of neonatal encephalopathy and hypoxia-ischemia encephalopathy".Early Human Development 2010;86:329-38
2. Robertson CM, et al."Follow-up of the term infant after hypoxic-ischemic encephalopathy". Paediatric Child Health 2006; 11: 278-82.
3. Sun PZ, et al."Association between pH-weighted endogenous APT CEST MRI and tissue lactic acidosis during ischemic stroke". Journal of Cerebral Blood Flow and Metabolism 2011; 31: 1743-50.
4. Lorek A, et al."Delayed (secondary) cerebral energy failure after acute hypoxia-ischemia in the newborn piglet: continuous 48-hour studies by phosphorus MRS". Paediatric Research 1994; 36: 699-706.

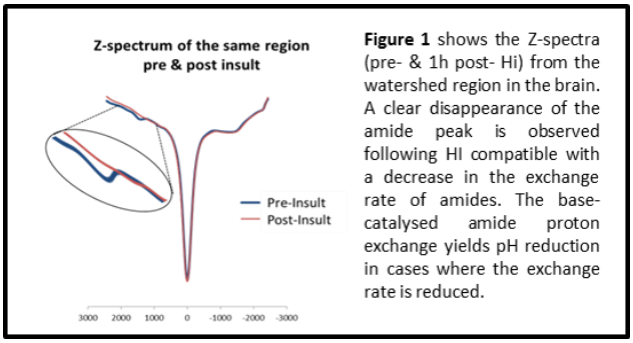

Figure 1 shows the Z-spectra (pre- & 1h post- Hi) from the watershed region in the brain. A clear disappearance of the amide peak is observed following HI compatible with a decrease in the exchange rate of amides. The base-catalysed amide proton exchange yields pH reduction in cases where the exchange rate is reduced.

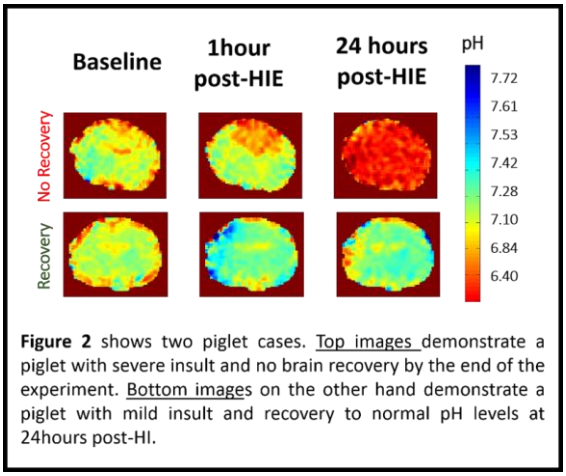

Figure 2 shows two piglet cases. Top images demonstrate a piglet with severe insult and no brain recovery by the end of the experiment. Bottom images on the other hand demonstrate a piglet with mild insult and recovery to normal pH levels at 24hours post-HI.

619
BRAIN-0849
Poster Session

Cerebral Ischemia: Animal Models

CHARACTERIZATION OF A MODIFIED LONG TERM SURVIVAL MOUSE MODEL OF CEREBRAL ISCHEMIA

H. Sheng[1], L. Zhang[2], X. Chen[3], S. Lin[4], D. Warner[1]
[1]Anesthesiology, Duke University Medical Center, Durham, USA
[2]Neurosurgery, Tianjin 5th hospital, Tianjin, China
[3]Neurosurgery, 1st Hospital of Qinhuangdao City, Qinhuangdao City, China
[4]Anesthesiology, China-Japan Friendship hospital, Beijing, China

Objectives: Current mouse models of focal cerebral ischemia present limitations for assessing long-term outcome due to a high mortality rate in the filament middle cerebral artery (MCA) occlusion (MCAO) model and insufficient behavioral deficit in the distal MCAO model. To meet the needs of preclinical stroke research, we modified a mouse cerebral ischemia model to enable long-term survival with persistent neurologic deficit.

Methods: 8-10 week old C57Bl/6J mice were anesthetized with isoflurane, intubated and ventilated. Rectal temperature was controlled at 37±0.2°C. An observer, blinded to group assignment, measured neurological deficit and infarct volume.[1] **Experiment 1:** Pilot studies. The right MCA was exposed through a temporal craniectomy.[2,3] Proximal to the olfactory tract, the MCA was randomly occluded for 0, 1, 2, or 3 hr or was left permanently occluded. In another group, the MCA and ipsilateral common carotid artery (CCA) were occluded in tandem for 2 hr. Neurologic deficit and infarct volume were measured at 24 hr post-ischemia (n=5 per group). **Experiment 2:** Compare tandem occlusion with filament MCAO in long-term recover. Mice were randomly assigned to sham surgery (n=5), 2 hr tandem MCA and CCA occlusion (n=7), or 1 hr

filament MCAO (n=7) followed by 4 weeks recovery. Survival rate, neurological deficit, and infarct volume were then measured.

Results: **Experiment 1:** Overall, longer transient MCAO durations produced worsened neurological scores ($p < 0.01$), although infarct volume was similar for 2 and 3 hr MCAO, with both being greater than 1 hr or permanent MCAO. 2 hr tandem MCA and CCA occlusion caused worse neurologic scores than 2 hr MCAO only (16±2 vs. 9±1, respectively, $p < 0.01$). The tandem group also had more severe deficit than permanent MCAO (11±2, $P < 0.01$). **Experiment 2:** After 4-weeks recovery, the 2 hr tandem MCA and CCA occlusion group had a low mortality rate compared to 1 hr filament MCAO (14.3% vs. 85.7%, respectively, $P < 0.01$), but neurological deficit persisted 8±3 vs. Sham surgery group = 0, , $P < 0.01$).

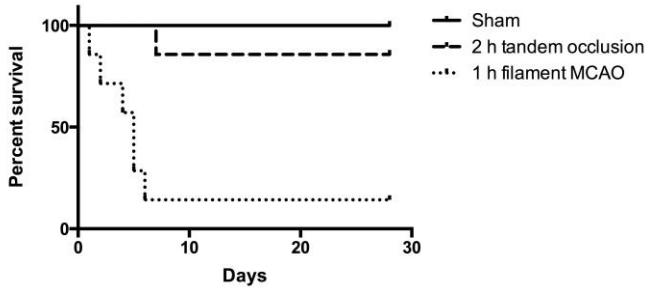

Conclusion: The tandem MCA+CCA occlusion mouse focal cerebral ischemia model allows long-term survival, tissue damage in both cortex and striatum, and persistent neurologic deficit. This model may be of use to investigators examining sustained efficacy of therapeutic intervention or delayed mechanistic responses to focal cerebral ischemia.

References:
1. Sheng et al. Neuroprotective efficacy from a lipophilic redox-modulating MnPorphyrin, MnTnHex-2-PyP: Rodent models of ischemic stroke and subarachnoid hemorrhage: J Pharmacol Exp Ther 338: 906-16, 2011
2. Tamura et al. Focal cerebral ischemia in the rat: 1. Description of technique and early neuropathological consequences following middle cerebral artery occlusion. J Cereb Blood Flow Metab 1:53-60, 1981
3. Benderson et al. Rat middle cerebral artery occlusion: evaluation of the model and development of a neurologic examination. Stroke 17: 472-476, 1986

620
BRAIN-0071
Poster Session

Cerebral Ischemia: Animal Models

NEUROPROTECTIVE EFFECTS OF HUMAN NEURAL STEM CELLS OVER-EXPRESSING CHOLINE ACETYLTRANSFERASE IN A MIDDLE CEREBRAL ARTERY OCCLUSION MODEL

K. Shin[1], J. Kim[1], Y. Choi[2], E.K. Choi[2], J. Yon[1], Y.B. Kim[1]
[1]Veterinary medicine, Chungbuk National University, Cheongju, Korea
[2]Stem Cell R&D Center, iCellBank, Seoul, Korea

Objectives. Ischemic stroke is one of the most-devastating brain diseases causing acute death or permanent disability. Although tissue-type plasminogen activator was approved by Food and Drug Administration for early reperfusion of the occluded vessels, oxidative injury may cause an extensive brain infarction. Accordingly, there is a need for effective neuroprotection during reperfusion, and stem cell-based therapeutic approaches should fulfill this requirement.
Methods. In the present study, we established human neural stem cells (NSCs) encoding gene of choline acetyltransferase (F3.ChAT), an acetylcholine-synthesizing enzyme, and investigated whether infusion of the F3.ChAT cells attenuate the ischemia-reperfusion brain damage in a middle cerebral artery occlusion (MCAO) model. After 2-hour occlusion with a silicone-coated thread, the middle cerebral artery of male Sprague-Dawley rats was reperfused, along with intravenous

infusion of the stem cells (1 **x** 10^6 cells/100 µl/rat). All the animal experiments were conducted according to the Standard Operation Procedures, and approved by the Institutional Animal Care and Use Committee of Chungbuk National University, Korea.

Results. In western blot analysis, F3.ChAT cells were found to produce much higher amounts of ChAT as well as neuroprotective and anti-inflammatory growth/neurotrophic factors including vascular endothelial growth factor, glial cell-derived neurotrophic factor, nerve growth factor, and ciliary neurotrophic factor than their parental F3 NSCs. Treatment with F3.ChAT cells markedly reduced the infarction volume and improved both the cognitive dysfunction (in water-maze trials) and behavioral deficits (in locomotor activity and rota-rod performance) of MCAO animals, in which F3.ChAT cells were superior to F3 cells. F3.ChAT cells not only restored microtubule-associated protein 2, a neuronal cytoskeletal protein, but also decreased pro-inflammatory interleukin-1β, glial fibrillary acidic protein, and intercellular adhesion molecule 1 in the brain tissue.

Conclusions. The results demonstrate that early intravenous infusion of NSCs expressing ChAT and growth/neurotrophic factors attenuate brain injury and restore neurobehavioral functions via neuroprotective and anti-inflammatory activities, and that F3.ChAT cells could be a candidate for the neuroprotection and functional recovery of acute stroke patients.

References.

Abe K: Therapeutic potential of neurotrophic factors and neural stem cells against ischemic brain injury. J Cereb Blood Flow Metab. 2000, 20(10):1393-1408.

Choi BI, Park D, Lee SH, Bae DK, Yang G, Yang YH, Kim TK, Choi EK, Lee HJ, Choi KC, Nahm SS, Kim YB: Neurobehavioural deficits correlate with the cerebral infarction volume of stroke animals: a comparative study on ischaemia-reperfusion and photothrombosis models. Environ toxicol Pharmacol. 2012, 33(1):60-69.

621
BRAIN-0239
Poster Session

Cerebral Ischemia: Animal Models

ISCHEMIA-INDUCED SPREADING DEPRESSION IN THE IN VIVO RETINA

A.I. Srienc[1], *K.R. Biesecker*[1], *A. Shimoda*[1], *E.A. Newman*[1]
[1]*Neuroscience, University of Minnesota, Minneapolis, USA*

Objective: To characterize retinal spreading depression (RSD) in acute branch retinal vessel occlusion and assess the contribution of RSD to tissue injury following ischemia.

Methods: Using a focal photothrombosis model of ischemia in the in vivo rat, a primary retinal vessel was occluded and the intrinsic optical signal from the retinal surface was imaged by confocal microscopy to detect RSD events. Blood flow, vessel diameter, tissue oxygen tension, or DC potential was monitored concurrently.

Results: RSD waves were generated following occlusion of a single primary arteriole or venule. Waves were typically initiated near the optic disc and spread peripherally, but waves were also initiated peripherally and spread centrally. Wave velocities range from 1.4 – 3.3 mm/min. The wave front was associated with a drop in tissue oxygen tension, constriction of primary arterioles, and a negative shift in DC potential.

Conclusions: We demonstrate, for the first time, that RSD waves are generated following occlusion of retinal vessels. The properties of in vivo RSD waves are similar to those of cortical spreading depression (CSD) waves. CSD is associated with delayed cell death following ischemic stroke and a similar RSD-mediated delayed cell death may occur in the retina following vessel occlusion.

References:
Lauritzen M, et al. *J Cereb Blood Flow Metab*. 2011;31:17-35.
Netto M, et al. *Brain Res.* 1999;827:221-4.

622
BRAIN-0502
Poster Session

Cerebral Ischemia: Animal Models

NEUROPROTECTIVE EFFECTS OF THE INSULIN-LIKE GROWTH FACTOR IGF-I AND 17B-ESTRADIOL AFTER TRANSIENT FOCAL CEREBRAL ISCHEMIA IN THE ENDOTHELIN-1 RAT MODEL.

W. Stoop[1], *D. De Geyter*[2], *J. De Keyser*[3], *R. Kooijman*[1]
[1]*Experimental Pharmacology Center for Neurosciences, Vrije Universiteit Brussel, Brussels, Belgium*
[2]*Laboratory of Clinical Biology, UZ Brussel, Brussels, Belgium*
[3]*Department of Neurology Center for Neurosciences, UZ Brussel, Brussels, Belgium*

Introduction: Stroke is the second cause of death and the leading cause of adult disability worldwide (*1-2*). To date, thrombolytic therapy using recombinant tissue plasminogen activator (tPA) is the only approved therapy for acute ischemic stroke. However, only 5-10% of all patients benefit from this treatment because of the inclusion criteria (*2*). Targeting different processes involved in the ischemic cascade, which include excitotoxicity, oxidative stress, inflammation and cell death, could be promising for the future of stroke treatment. IGF-I is an anti-apoptotic pleiotropic factor exerting effects on different levels of the ischemic cascade (*3*). It has been shown in both in vitro and vivo models that the neuroprotective effects of the IGF-IR and ER are interdependent (*4*). This interdependency creates the possibility to increase the efficacy of IGF-I by co-treatment with estradiol.

Aim: Possible synergistic or additive effects of IGF-I and 17β-estradiol (E2) will be studied in the endothelin (Et)-1 rat model for stroke. Effects on infarct size motor/sensory deficits and glial activation will be investigated.

Material and methods: Via a guide cannula, implanted using stereotactic surgery, 200 pmol Et-1 was administered in the vicinity of the middle cerebral artery of male albino Wistar Kyoto (WKY)

rats. Rats were treated with E2 (1mg/kg, s.c.) 30 min and/or IGF-I (1 or 3 mg/kg, s.c.) at 30 min or 2 h after the induction of stroke. Motor/sensory functions were determined 24 h after the insult using the neurological deficit score (NDS). Infarct size was assessed using a cresylviolet staining. To assess effects on microglial activation and astrogliosis immunohistochemistry was performed using antibodies directed against Iba-1 and GFAP.

Results: Rats treated with E2 (1 mg/kg) or IGF-I (1 and 3 mg/kg) alone showed smaller infarct sizes when compared to vehicle treated animals. Treatment with a combination of E2 and IGF-I lead to a more pronounced reduction in infarct size, only when a high dose of IGF-I (3 mg/kg) was used 30 min after stroke induction. This combination also increased the number of round shaped microglia in striatum. In contrast, the effects of 1 mg/kg IGF- I administered 2 h after stroke induction and E2 at t = 30 min were additive. Furthermore, stroke induction significantly reduced the NDS in vehicle-treated animals but not in rats treated with E2 and/or IGF-I

Conclusion: The neuroprotective effects of E2 and IGF-I are additive and a combination of these factors markedly reduces infarct size after a transient focal cerebral ischemia and increases the number of amoeboid shaped microglial cells in striatum. It remains to be established whether stimulation of microglial activation is instrumental to neuroprotection in our model.

References:

1. G.A. Donnan, M. Fisher, M. Macleod, S. M. Davis, *Lancet* 371, 1612 (May10, 2008).
2. A.R. Young, C. Ali, A. Duretete, D. Vivien, *JNeurochem* 103, 1302 (Nov, 2007).
3. R.Kooijman, S. Sarre, Y. Michotte, J. De Keyser, *Stroke* 40, e83 (Apr,2009).
4. L.M. Garcia-Segura, M. A. Arevalo, I. Azcoitia, *Prog Brain Res* 181, 251(2010).

623
BRAIN-0339
Poster Session

Cerebral Ischemia: Animal Models

A COMMON EXPERIMENTAL STROKE MODEL PRODUCES A BIMODAL PATTERN OF INJURY

M.E. Trotman[1], M. Kelly[2], R. Fern[3], C.L. Gibson[1]
[1]School of Psychology, University of Leicester, Leicester, United Kingdom
[2]Centre for Core Biotechnology Services, University of Leicester, Leicester, United Kingdom
[3]Peninsula School of Medicine and Dentistry, University of Plymouth, Plymouth, United Kingdom

Objectives: Efficacy of potential stroke interventions are frequently tested using rodent focal ischemia models, however these have a poor record of detecting clinically useful drugs. Variability in lesion volume produced by transient middle cerebral artery occlusion (tMCAO) is high, whilst cost and ethical concerns result in small sample sizes. Generally, significance is tested using parametric analysis of mean lesion volume, an approach that requires a Gaussian distribution within each group. However, the small sample sizes used limit the statistical power of formal normality tests. The use of parametric analyses, if incorrect, may contribute to the poor discrimination of effective treatments affecting the progress of determining clinically viable treatments. To test the application of this approach the current study retrospectively evaluates lesion volume data distribution within 8 separate studies conducted over 10 years under identical protocols (by CL Gibson). In addition, we have begun to explore possible explanations for such a bimodal pattern of injury by focusing initially on whether such differences are attributed to variations in cerebrovascular anatomy.

Methods: 60min tMCAO was induced in male C57Bl/6j mice followed by post-mortem lesion volume analysis as detailed previously[1]. Osmotic mini-pumps filled with vehicle/drug were implanted 24hrs prior to MCAO, remaining in

place for 2 days post-MCAO. Data was collated with lesion volume data from 8 control studies performed under identical surgical protocol over the last 10yrs. A further cohort of mice are undergoing pre-MCAO angiography MRI scans to assess vasculature patency, followed by post-MCAO T2 diffusion weighted MRI scans for lesion volume assessment in addition to post-mortem TTC staining.

Results: Analysis of total lesion volume data within a recent study showed lesions centered on the striatum, encroachment into the cortex was only present in larger lesions. Correlation of striatal and cortical lesion volume per lesion showed no cortical component in lesions <40mm^3. A single distribution of collated data from 8 identical control series spanning 10 years fitted two overlapping Gaussian curves (r^2=0.95). Modified Shapiro-Wilk (Ryan-Joiner) analysis produced $p<0.01$ for these data, rejecting the hypothesis of normal distribution accepting the hypothesis of bimodal distribution of small (<40mm^3) striatal and large (>40mm^3) striato-cortical lesions.

Conclusions: The observation that lesion volume within a single 60min tMCAO data set can be either small/striatal or large/striato-cortical is consistent with the presence of two normally distributed peaks in a larger data set collated over 10 years using an identical protocol. A similar bimodal lesion volume distribution is apparent in published data from several prior studies in various species and reversible ischemia models. Much of the variability within MCAO studies may be caused by anatomical variation within the Circle of Willis and the patency of the ipsilateral posterior communicating artery. Anatomical studies do not show correlations between cerebrovascular anatomy and lesion volume as anatomical investigation if often undertaken using non-MCAO mice. Using non-invasive MRI imaging techniques we can better determine the influence of cerebrovascular anatomy on lesion volume variation following MCAO.

References:

1 Gibson CL, Murphy SP. Progesterone enhances functional recovery after MCAO in male mice. JCBFM. 2004;24:805-13.

624
BRAIN-0642
Poster Session

Cerebral Ischemia: Animal Models

ISCHEMIC INJURY PRODUCED BY PHOTOTHROMBOSIS DIFFERS IN NEONATAL AND ADULT BRAIN

U.I. Tuor[1], M. Qiao[2], M. Sule[2], Q. Deng[2], M. Morgunov[2], D. Rushforth[3], T. Foniok[3]
[1]Physiology and Pharmacology Clinical Neurosciences and Radiology, University of Calgary, Calgary, Canada
[2]Physiology and Pharmacology, University of Calgary, Calgary, Canada
[3]Experimental Imaging Centre, University of Calgary, Calgary, Canada

Introduction: Neonatal and adult brain differ in their susceptibility to ischemic injury, particularly in periventricular white matter with differences in gray matter being less established. Photothrombosis produces direct cortical ischemia via thrombotic occlusion of vessels; and, we established methods to produce mild and moderate ischemic insults. In adult rats, a mild lesion was associated with reperfusion, modest magnetic resonance (MR) imaging (T_2) changes and scattered cell death. We hypothesized mild changes could also be produced in immature brain but might differ compared to adults in ischemic injury progression as detected with MR.

Objective: To investigate whether ischemic injury produced by a mild or moderate photothrombotic insult differs in neonatal compared to adult brain.

Methods: Photothrombotic ischemic lesions were produced in anesthetized neonatal (P5) or adult rats. The skull was exposed and in adults was thinned. Rose Bengal was administered IV (10mg/kg) or IP (60mg/kg) in adults and neonates,

respectively. The cortex was illuminated with white light for 5 min in adults and commonly from 5-15 min in neonates. MR scans were acquired the next day using a 9.4T Bruker MR system to acquire T_2 maps and Apparent Diffusion Coefficient (ADC) maps. Regions of interest included: normal cortex, perilesion area of altered image intensity, and, core lesion of marked image intensity change.

Results: Irrespective of age, photothrombosis produced small lesions that varied according to slice and were separated into mild (<1mm^2) and moderate severity (1-3mm^2) (5-6/group). Lesions were hyperintense regions of increased T2 (Fig A,B) and decreased ADC (Fig E,F) (arrows). In adults there were substantial areas of modestly increased T2 and ADC (Fig B,F, arrow heads; C,G). In neonates, peri-lesion regions had minimal to nil regions of increased T2 or ADC. The T_2 increases and ADC decreases in the core lesion areas were similar between groups (Fig D,H). Although smaller in neonates than adults, T2 in peri-lesion regions were similarly elevated whereas only adults had substantial increased ADC adjacent to the lesion (Fig H).

Discussion: The results demonstrate that there are differences detectable with MRI regarding the ischemic injury produced by photothrombosis in the peri-infarct region depending on the maturity of the subject. The reason is unclear but may reflect and include: 1. that immature animals have a much lower resting cerebral blood flow and blood pressure than adults limiting the extent of penumbra, 2. that there is more spontaneous lysis of the thrombotic clots in adults resulting in peri-infarct reperfusion injury 3. there are different age-dependent endothelial effects of Rose Bengal on the formation of thrombus. Irrespective, this model provides a promising approach to study ontogenic differences in mechanisms of gray matter injury associated with ischemia and potential reperfusion - of relevance to the increasing efforts to treat more patients with thrombolytics or endovascular therapy not only in the elderly but also in pediatric stroke patients.

Conclusion: Neonatal and adult cortex have differential sensitivity to photothrombosis injury with adult brain having greater signs of injury in peri-infarct regions than mature brain. (Supported by Canadian Institutes of Health Research).

).

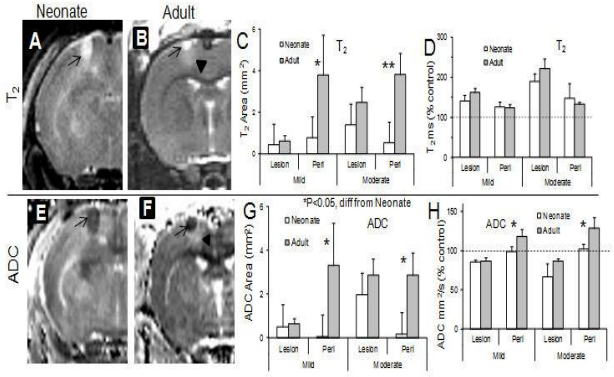

625
BRAIN-0177
Poster Session

Cerebral Ischemia: Animal Models

THE ROLE OF ENDOTHELIN RECEPTORS IN NEUROCHEMICAL CHANGES DURING FOCAL CEREBRAL ISCHEMIA INDUCED BY INTRAHIPPOCAMPAL INJECTION OF THE ENDOTHELIN-1 IN IMMATURE RATS

K. Vondrakova[1], *K. Syslova*[2], *M. Mikoska*[2], *P. Kacer*[2], *J. Burchfiel*[3], *H. Kubova*[1], *K. Vales*[4], *G. Tsenov*[1]

[1]*Department of Developmental Epileptology, Institute of Physiology v.v.i. Academy of Sciences of the Czech Republic, Prague, Czech Republic*

[2]*Department of Organic Technology, Institute of Chemical Technology, Prague, Czech Republic*

[3]*Department of Neurology University of Rochester Medical Center, Strong Epilepsy Center, Rochester, USA*

[4]*Department of Neurophysiology of Memory, Institute of Physiology v.v.i. Academy of Sciences of the Czech Republic, Prague, Czech Republic*

Objectives: The age group with the highest risk of ischemic stroke is elderly population but it affects

also children and newborns. As we reported earlier, there is a disassociation between seizures generation, development of ischemia and neurodegeneration. The activation of ET_A receptors is crucial for ischemia development, however either ET_A or ET_B receptors mediate the development of seizures following the application of ET-1 in immature rats. The dissociation between the ischemic-producing and seizure-producing processes suggests that damage is not necessary to induce seizures, although it may exacerbate them. To determine metabolic changes that are associated with mentioned detachment in these processes a microdialysis study had been performed.

Methods: The model of focal cerebral ischemia induced by the intrahippocampal infusion of the endothelin-1 (ET-1) in 12-day-old rat was used (P12). ET-1 (40 pmol/µl) was infused either alone or co-administered with selective antagonist of ET_A receptors (BQ123; 70nmol/µl). An effect of activation of ET_B receptors was studied using selective agonist 4-Ala-ET-1 (40pmol/µl). Controls received corresponding volume of 10mM phosphate buffer solution (PBS).

Cannula for drug infusion was stereotaxically implanted into the right dorsal hippocampus under isoflurane anesthesia. Microdialysis probe was implanted caudally in the close proximity of the infusion cannula and perfused with an artificial cerebrospinal fluid (1.5µl/min). Samples were taken sequentially during 2 hours after drug infusion, stored in -80°C and then analyzed by UHPLC-MS. During all experiments animals were maintained at 34.5 ± 0.5°C.

Results: Intrahippocampal infusion of ET-1 led to significant decrease of glutamic acid about 48 % in P12 animals, while in adult (60-days-old rats) a significant increase by 50 % induced by the same concentration of the ET-1 was observed. Moreover, in immature rats we found a significant decrease of aspartic acid (by 25 %), GABA (by 98 %) and pyruvate (by 39 %) during first hour after ET-1 infusion. On the other hand, at the same time a significant increase of dopamine (by 176 %) and lactate (by 570%) had been observed. Among others, there was a 250% increase in concentration of leukotriene B4 (LTB4), prostaglandin E2 (increase by 50%) and 1000% increase of ET-1 concentration in brain dialysate. Similar changes in metabolite concentrations were observed when ET_A receptors were blocked by selective antagonist (BQ123) or ET_B receptors agonist (4-Ala-ET-1) was used in P12 rats. However, in both latter cases, changes of measured metabolites were smaller in comparison with ET-1 group.

Conclusions: Our results indicate crucial role of the inflammatory reaction in the development of seizures followed intrahippocampal infusion of the ET-1 in immature brain. Likewise, lactate induced acidosis can contribute to seizure development in immature brain. Other fact that can contribute to postischemic damage is an increase of endogenous endothelin-1, which can be involvement in severe damage or seizure development and as well as a disbalance between glutamate and GABA concentration. These findings should be confirmed by additional research.

Support: This study was supported by Grant Agency of the Czech Republic through research grants GACR 104/09/1497, P106/12/1276, P304/11/P383, P304/12/G069 and P304/14/20613S

626
BRAIN-0529
Poster Session

Cerebral Ischemia: Animal Models

SPONTANEOUS CHANGES IN SENSORIMOTOR FUNCTION AND BOLD FMRI MAPS IN ADULT RATS AFTER CORTICAL STROKE

C. Wayman[1], D.A. Duricki[2], M. Mesquita[1], T. Wood[1], D. Cash[1], L.D.F. Moon[2]
[1]Department of Neuroimaging, King's College London, London, United Kingdom
[2]Wolfson Centre for Age Related Diseases, King's College London, London,

United Kingdom

Most ischemic strokes occur in the middle cerebral artery (MCA), inducing infarcts affecting the sensorimotor cortex, causing persistent hemi-plegia or -paresis. Neurotrophin-3 (NT3) is a growth factor shown to increase sprouting of neurons after axonal injury. We have used diathermy of the middle cerebral artery (MCA) and occlusion of the common carotid arteries (CCA) to model stroke in young rats over 12 weeks. Motor (horizontal ladder, cylinder), sensory (bilateral tactile stimulation) and fine movement (staircase) behavioral tests were conducted at baseline then performed weekly after stroke surgery. Stroke rats (n=25) were anaesthetised and a craniotomy performed to expose, then occlude the MCA using coagulating bipolar forceps. The ipsilesional CCA was ligated, and the CCA on the distal side was occluded for 60 minutes. Treatment using AAV-NT3 or AAV-GFP was given into disabled bicep and tricep brachii 4 weeks after stroke to determine if there would be a beneficial effect. Lesion volume was measured 24 hours after stroke using T2-weighted MRI under isoflurane anesthesia. Functional MRI (fMRI) was then performed using an EPI sequence during stimulation of the left, right or both paws simultaneously *via* platinum electrodes placed in the forepaw at baseline then 1, 4, 8 and 12 weeks after stroke. Resulting images were analysed in SPM8 to obtain group mean probabilities of activation and region-of-interest analyses. Results from all behavioural tests show no difference between stroke animals treated with AAV-NT3 compared to AAV-GFP, possibly due to the treatment being given too late to take effect. AAV treatment was delivered at 4 weeks, and NT3 was still present in the blood serum 8 weeks later in the group given AAV-NT3 (56.8±5.0pg/mg) compared with 7.13±1.7pg/mg in the AAV-GFP group (mean±SEM, Kruskal-Wallis $p<0.001$). fMRI shows a decreased BOLD activation in the somatosensory cortex of the affected hemisphere 1 week after stroke, shown in group maps by the loss of significance in the red areas of the heat map (Figure 1). Negative BOLD in blue on these maps is of particular interest to us as they may suggest a role of inhibitory mechanisms after lesion.

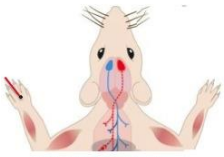

Red areas denote positive BOLD activation, whilst areas in blue correspond to negative BOLD signal.

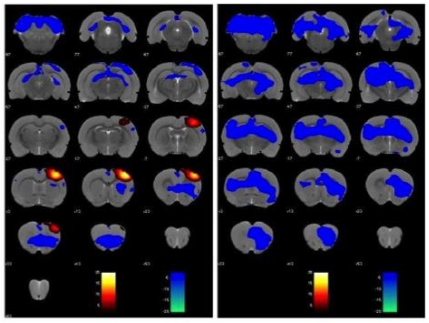

Baseline n=30 1 week Stroke n=10

Group analysis is being conducted at 8 and 12 weeks to determine whether there is a difference between treatment groups. Region-of-interest analysis to date indicates a decline in activity in the lesioned sensory cortex forelimb area one week after stroke (Figure 2), and analysis of other regions and timepoints is ongoing.

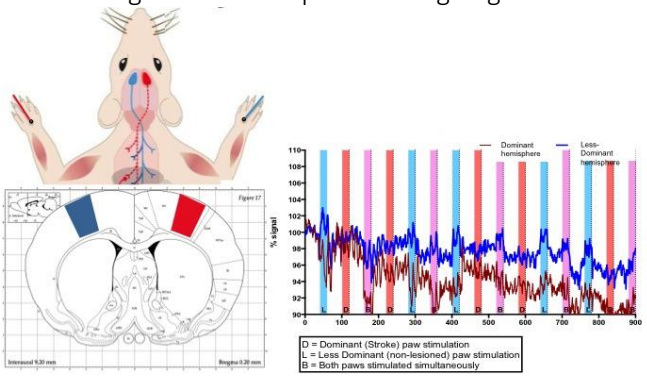

The behavioral results, after showing the expected initial deficit from stroke, indicate a recovery of both treatment groups back towards baseline. This spontaneous recovery of young animals has been previously observed in other young animal stroke models. Whilst treatment of these stroke animals with AAV-NT3 has not shown a functional improvement, we need to further elucidate time points at which this treatment can be effective, as previous work in our lab has shown a functional

recovery when AAV-NT3 is delivered at 24 hours. We hope that the fMRI data acquired will enable us to understand more about mechanisms of spontaneous recovery seen in this study.

627
BRAIN-0479
Poster Session

Cerebral Ischemia: Animal Models

A SPECIFIC MULTI-NUTRIENT INTERVENTION AS THERAPEUTIC APPROACH FOR STROKE

M. Wiesmann[1], B. Zinnhardt[2], M. Hellwich[3], S. Eligehausen[2], D. Reinhardt[2], L.M. Broersen[4], A. Heerschap[5], J.A.H.R. Claassen[6], A.J. Kiliaan[3]
[1]Anatomy & Geriatric Medicine, RadboudUMC, Nijmegen, Netherlands
[2]European Institute for Molecular Imaging, (EIMI), Münster, Germany
[3]Anatomy, RadboudUMC, Nijmegen, Netherlands
[4]Nutricia Research,
Nutricia Advanced Medical Nutrition, Utrecht, Netherlands
[5]Radiology and Nuclear Medicine, RadboudUMC, Nijmegen, Netherlands
[6]Geriatric Medicine, RadboudUMC, Nijmegen, Netherlands

Objectives

Occlusion of the middle cerebral artery (MCAo) is among the most common causes of ischemic stroke in human. Cerebral ischemia leads to brain lesions existing of an irreversibly injured core and ischemic boundary zone, the penumbra, containing damaged but potentially salvageable tissue. Using a transient MCAo mouse model we investigated the effect of a specific multi-nutrient intervention as a therapeutic approach to counteract impairments of cerebral (structural+functional) connectivity, cerebral blood flow (CBF), cognition, motor function and neurodegeneration.

Methods

Male C57BL/6j mice (3 months) were subjected to transient (30 min) right MCAo using the intraluminal filament model. Success of surgery was verified intraoperatively via Laser Doppler. Before tMCAo, baseline measurements of motor parameters (open field test, rotarod, grip test, pole test) and spatial learning and memory

(Morris Water Maze) were performed and repeated after tMCAo. Starting directly after tMCAo, animals were fed either a control diet or the specific experimental diet. At 14 and 35 days after tMCAo, MRI scanning was conducted to identify stroke location and size (RARE+DWI), and functional and neuronal connectivity and CBF measures (rsfMRI, DTI, MRS, FAIR-ASL) on the 11.7T magnet (Bruker BioSpec). Directly following the MR measurements, brains were collected and immunohistochemical analyses were performed.

Results

Data processing is ongoing and the final results will be presented. First results show that at 7 days after tMCAo, all mice showed a decreased CBF in the occluded cerebral hemisphere compared to the left control hemisphere. Mice fed experimental diet had a higher cortical CBF in the ischemic hemisphere than control fed mice. 35 days post tMCAo, experimental diet fed animals had a restored cortical and hippocampal CBF in the ischemic hemisphere. On control diet, cortical and hippocampal CBF remained decreased in the right occluded cerebral hemisphere compared to the left control hemisphere. The first functional benefits of the experimental diet were noted in the open field, where locomotor activity was improved at 16 days after tMCAo as compared to animals on the control diet.

Conclusions

No therapeutic intervention is available for stroke yet. Our present data show that a specific dietary intervention has beneficial effects on the cerebral hemodynamics after tMCAo. In addition, the diet may reduce some of the functional consequences of tMCAo. Together our data indicate that specific multi-nutrient interventions may be able to counteract harmful effects of ischemic stroke, protecting against neuronal and connectivity loss and accompanying functional deficits.

628
BRAIN-0356
Poster Session

Cerebral Ischemia: Animal Models

MIR-181 ANTAGOMIR REDUCES FOCAL CEREBRAL ISCHEMIA INJURY IN OVARIECTOMIZED FEMALE MICE

L. Xu[1], J. Zhao[1], X. Xiong[1], Y.B. Ouyang[1], R.G. Giffard[1]
[1]Anesthesia, Stanford University, Stanford, USA

Objectives: Our previous study reported that miR-181 antagomir treatment protected from acute ischemic stroke in male mice (1). Women are protected relative to men when younger, but when older have more severe strokes, stroke deaths, and worse functional outcome than men (2). 17β-estradiol (E2) has been shown to be neuroprotective *in vivo* using models of focal cerebral ischemia (3). Ovariectomized female animals with and without E2 replacement are the most widely-used rodent model of post-menopausal woman. We tested miR-181 antagomir in ovariectomized female mice.

Methods: Adult female C57B6 mice (10 weeks) were ovariectomized after being anesthetized to eliminate endogenous ovarian steroids. E2 replacement via subcutaneous placement of a Silastic capsule with 30µl of sesame oil (control) or 17β-estradiol (100 µg/ml in sesame oil through the ovariectomy incision) (3). The blood was sampled from the jugular vein before and 14 days after ovariectomy. The E2 level in serum was assayed with a mouse/rat Estradiol ELISA. Day 13 after ovariectomy the mice were infused with either miR-181a antagomir or a control (mismatch, MM) mixed with the cationic lipid DOTAP by left intracerebroventricular (ICV) as previously described (1). After ICV treatment, focal cerebral ischemia was produced 24 hours later by 1 hour of middle cerebral artery occlusion (MCAO) with a silicone-coated 6-0 monofilament followed by reperfusion for 24 hours. The mice were assessed for neurological deficits using a deficit score (1). The mouse brains were removed after overdose of anesthesia and were stained by

Triphenyltetrazolium chloride (TTC) or fixed to assess infarction volume by cresyl violet.

Results: E2 levels were significantly reduced with ovariectomy (25.9±12.9 ng/ml) compared to the E2 replacement group (90.2±2.6 ng/ml) at 14 days. The E2 replacement group showed a significantly reduced infarction size (about 25% reduction) and improved neurological outcome compared to the oil only control group. When ovariectomized females were treated with miR-181a antagomir prior to MCAO the infarction size was smaller (28.5±10.6%) compared to the control group (43.4±8.9%). The neurological deficit score was worse in control mice (2.8 ±0.6) compared with antagomir treated mice (1.9±0.5).

Conclusions: These findings indicate that miR-181a antagomir has neuroprotective effects against acute ischemic neuronal damage and neurological impairment in female ovariectomized mice without E2 replacement, a model for post-menopausal women. miR-181a antagomir may be an innovative new target for stroke therapy in older women.

References:

1) Ouyang YB, Lu Y, Yue S, Xu L, Xiong X, White RE, Sun X, Giffard RG. miR-181 regulates GRP78 and influences outcome from cerebral ischemia in vitro and in vivo. *Neurobiology of Disease* 45: 555–563, 2012.
2) Appelros P, Stegmayr B, Terént A. Sex Differences in Stroke Epidemiology A Systematic Review. Stroke. 2009;40(4):1082–1090
3) Rusa R, Alkayed NJ, Crain BJ, Traystman RJ, Kimes AS, London ED, Klaus JA, Hurn PD (1999). 17β-Estradiol Reduces Stroke Injury in Estrogen-Deficient Female Animals. Stroke, 30(8):1665–1670.

629
BRAIN-0213
Poster Session

Cerebral Ischemia: Animal Models

SYSTEMIC INFLAMMATION AND EXACERBATED BRAIN DAMAGE TO TRANSIENT FOCAL ISCHEMIA IN TYPE 2 DIABETIC MICE

K. Yamashiro[1], T. Kuroki[1], R. Tanaka[1], Y. Ueno[1], T. Urabe[2], N. Hattori[1]
[1]Department of Neurology, Juntendo University, Tokyo, Japan
[2]Department of Neurology, Juntendo Urayasu Hospital, Chiba, Japan

Objectives: Type 2 diabetes is associated with the increased incidence of stroke and poor functional outcome in stroke patients [1]. It has been recently reported that gut dysbiosis is associated with an increased intestinal lipopolysaccharide (LPS) permeability that causes systemic inflammation in type 2 diabetes mice [2]. Considerable research shows a relationship between systemic inflammation and exacerbation of ischemic brain injury in stroke patients and experimental models [3]. Our aim was to investigate the effect of LPS and systemic inflammation on ischemic brain injury in type 2 diabetes.

Methods: Infarct volume, blood-brain barrier permeability, and neurological scores were measured in type 2 diabetic mice (*bd/bd*), and normoglycemic genetic control mice (*db/+*) subjected to transient middle cerebral artery occlusion. The plasma levels of cytokine and LPS were determined by ELISA.
Results: Compared with *db/+* mice, *db/db* mice exhibited larger increases in infarct volume, blood-brain permeability, microglia counts and worse outcomes in neurological tests. *Db/db* mice exhibited higher plasma levels of interleukin-1β, interleukin-6, and LPS than *db/+* mice.

Conclusions: Our study showed the exacerbated ischemic brain injury and elevated levels of inflammatory cytokine and LPS in type 2 diabetic mice. These results suggest that systemic

inflammation and LPS contributes to exacerbation of ischemic brain injury.

References

1. Tanaka R, Ueno Y, Miyamoto N, Yamashiro K, Tanaka Y, Shimura H, Hattori N, Urabe T. Impact of diabetes and prediabetes on the short-term prognosis in patients with acute ischemic stroke. J Neurol Sci 2013;332:45-50
2. Cani PD, Bibiloni R, Knauf C, Waget A, Neyrinck AM, Delzenne NM, Burcelin R. Changes in gut microbiota control metabolic endotoxemia-induced inflammation in high-fat diet-induced obesity and diabetes in mice. Diabetes 2008;57:1470-1481.
3. McColl BW, Allan SM, Rothwell NJ. Systemic infection, inflammation and acute ischemic stroke. Neuroscience 2009;158:1049-1061.

630
BRAIN-0262
Poster Session

Cerebral Ischemia: Animal Models

Z-AJOENE AMELIORATES NEURONAL DAMAGE INDUCED BY CEREBRAL TRANSIENT ISCHEMIA IN THE GERBIL HIPPOCAMPUS.

D. Yoo[1], H. Jung[1], S. Nam[1], J. Kim[1], I. Park[2], Y. Yoon[1], J. Choi[3], I. Hwang[1]
[1]Department of Anatomy and Cell Biology, College of Veterinary Medicine and Research Institute for Veterinary Science Seoul National University, Seoul, Korea
[2]Department of Anatomy and BK21 Center for Advanced Medical Education, College of Medicine Inha University, Incheon, Korea
[3]Department of Anatomy, College of Veterinary Medicine Kangwon National University, Chuncheon, Korea

Objective

Z- and E- ajoene isomers are found in oil-macerated garlicproducts[1]. We investigated their neuroprotective effects againstischemic damage in the gerbil hippocampus.

Methods

Male Mongolian gerbils were divided into 2 groups: sham-operated(control) and ischemia-operated groups. The latter group was further dividedinto 3 subgroups, treated with vehicle (corn oil), E-ajoene, or Z-ajoene. Vehicle(corn oil), or *Z*- or *E*-ajoene (25mg/kg)[2] was orallyadministered 30 min prior to the induction of transient forebrain ischemiaby occlusion of the common carotid arteries for 5 min.

Results

One day after ischemia/reperfusion (I/R), I/R-inducedhyperactivity significantly reduced in the E- and Z-ajoene-treated groups,compared to that in the vehicle-treated group. Five days after I/R, the numberof cresyl violet-positive neurons in the E- and Z-ajoene-treated groupsincreased, compared to that in the vehicle-treated group. Reactive gliosis inthe CA1 region of E- and Z-ajoene-treated groups reduced, compared to that inthe vehicle-treated group. These neuroprotective effects were more prominent inanimals treated with Z-ajoene, than in those treated with E-ajoene. Inaddition, Z-ajoene significantly decreased lipid peroxidation, as indicated by4-hydroxy-2-nonenal levels in hippocampal homogenates, compared to thatobserved in the vehicle-treated group at a range of time points after I/R.

Conclusions

These results suggest that *Z*-ajoene protects I/R-induced delayed neuronal death and gliosis byreducing lipid peroxidation in the gerbil hippocampal CA1 region.

References

1. Naznin MT, Akagawa M, Okukawa K, Maeda T, Morita N.2008. Characterization of E- and Z-ajoene obtained from different varieties ofgarlics. Food Chem 106, 1113-1119.

2. Yamada N, Hattori A, Hayashi T, Nishikawa T, FukudaH, Fujino T. 2004. Improvement of

scopolamine-induced memory impairment byZ-ajoene in the water maze in mice. Pharmacol. Biochem Behav 78, 787-791.

631
BRAIN-0263
Poster Session

Cerebral Ischemia: Animal Models

NEUROPROTECTIVE EFFECTS OF VALERIANA OFFICINALIS IN THE GERBIL HIPPOCAMPAL CA1 REGION AFTER TRANSIENT FOREBRAIN ISCHEMIA

D. Yoo[1], H. Jung[1], S. Nam[1], J. Kim[1], I. Park[2], S. Yi[3], Y. Yoon[1], I. Hwang[1]
[1]Department of Anatomy and Cell Biology, College of Veterinary Medicine and Research Institute for Veterinary Science Seoul National University, Seoul, Korea
[2]Department of Anatomy and BK21 Center for Advanced Medical Education, College of Medicine Inha University, Incheon, Korea
[3]Department of Biomedical Laboratory Science, College of Biomedical Sciences Soonchunhyang University, Asan, Korea

Objective

As a medicinal plant, the roots of Valeriana officinalis havebeen used as a sedative and tranquilizer[1,2]. In the present study,we evaluated the neuroprotective effects of valerian root extracts (VE) on thehippocampal CA1 region of gerbils after 5 min of transient cerebral ischemia.

Methods

The male gerbils were divided into four groups as follows; 1)sham-operated (Control group), 2) vehicle-treated ischemia (Vehicle group), 3)25 mg/kg VE-treated ischemia (VE25 group), and 4) 100 mg/kg VE-treated ischemiagroup (VE100 group). Vehicle or VE was orally administered to gerbils once aday for 3 weeks before the ischemic surgery.

Results

The administration of 100 mg/kg VE (VE100 group) significantlyreduced the ischemia-induced hyperactivity in spontaneous motor activity 1 dayafter ischemia/reperfusion. Four days after ischemia/reperfusion, animalstreated with VE showed abundant cresyl violet-positive neurons in thehippocampal CA1 region when compared to the vehicle or 25 mg/kg VE-treatedgroups. In addition, VE treatment markedly decreased microglial activation inthe hippocampal CA1 region 4 days after ischemia. Compared to the other groups,the VE100 group showed the lowest level of lipid peroxidation during the first24 h after ischemia/reperfusion.

Conclusions

Pre-treatment with VE has protective effects againstischemic injury in the hippocampal pyramidalneurons by decreasing microglialactivation and lipid peroxidation.

References

1. Leuschner J, Müller J, Rudmann M. 1993.Characterisation of the central nervous depressant activity of a commerciallyavailable valerian root extract. Arzneimittel-Forschung 43, 638-641.

2. Hadley S, Petry JJ. 2003. Valerian. Am FamPhysician 67, 1755-1758.

632
BRAIN-0413
Poster Session

Cerebral Ischemia: Animal Models

THE ROLES OF HAX-1 AFTER TRANSIENT FOREBRAIN ISCHEMIA IN MICE

H. Yoshioka[1], T. Yagi[1], T. Wakai[1], Y. Fukumoto[1], K. Kanemaru[1], P.H. Chan[2], H. Kinouchi[1]
[1]Neurosurgery, Yamanashi University, Chuo, Japan
[2]Neurosurgery, Stanford University, Stanford, USA

Objectives- HS-1 associated protein X-1 (Hax-1) was originally identified as a 35-kDa mitochondria protein that interacts with HS1, a Src kinase substrate, and was suggested to be involved in B cell signal transduction. Subsequent studies have revealed that Hax-1 is expressed in various tissues and is involved in the regulation of apoptosis. However, its role in ischemic neuronal injury remains obscure. In this study, we analyzed the expression change of Hax-1 after transient forebrain ischemia to elucidate its role. In addition, we examined the effect of reactive oxygen species (ROS) on the expression change of Hax-1 after ischemia, using knockout (KO) mice of NADPH oxidase (NOX), a major source of ROS.

Methods – Male gp91^{phox}-/- (NOX KO) mice with a C57BL/6 background and their respective wild-type (WT) littermates were subjected to transient forebrain ischemia by bilateral common carotid artery occlusion for 22 minutes, and neuronal injury was assessed in the striatum. The brains were removed 3, 6, 24, and 72 hours after ischemia, and sectioned into coronal slices. Terminal deoxynucleotidyl transferase-mediated uridine 5'-triphosphate-biotin nick end labeling (TUNEL) staining was used to detect apoptosis after ischemia. Expression and localization of Hax-1 was examined by immunohistochemical analysis. Both sides of the striatum were removed 3, 6, 24, and 72 hours after ischemia, then the tissue was homogenized and protein was extracted. The protein samples were subjected to Western blot analysis to investigate the Hax-1 expression.

Results- Apoptotic change appeared in the striatal neurons of the WT mice 24 hours after ischemia. On the contrast, apoptosis in the NOX KO mice was suppressed, and the number of TUNEL-positive cells in the striatum 24 hours after ischemia was significantly reduced in the NOX KO mice compared with the WT mice ($n = 6$, $P<0.05$). Hax-1 was localized to the mitochondria of neurons under physiological conditions in both the WT and NOX KO mice. Western blot analysis revealed that the Hax-1 expression in the WT mice was gradually reduced 3 hours after ischemia, and significantly decreased 6-72 hours after ischemia ($n = 4$, $P<0.05$). In the NOX KO mice, the down-regulation of Hax-1 after ischemia was significantly suppressed ($n = 4$, $P<0.05$).

Conclusion-Since the down-regulation of Hax-1 after ischemia preceded appearance of apoptosis, there is a possibility that the decrease of Hax-1 would induce apoptosis after ischemia. Furthermore, ROS produced in NOX should be involved in the down-regulation of this anti-apoptotic protein.

633
BRAIN-0802
Poster Session

Cerebral Ischemia: Animal Models

OPTICAL IMAGING OF NEURAL ACTIVITY, OXYGENATION AND BLOOD FLOW DYNAMICS DURING THE PROGRESSION OF ACUTE STROKE

H.T. Zhao[1], D. Chow[2], M.G. Kozberg[3], M.A. Shaik[1], S.H. Kim[1], E.M.C. Hillman[1]
[1]Biomedical Engineering, Columbia University, New York City, USA
[2]Radiology, Columbia University, New York City, USA
[3]Neuroscience, Columbia University, New York City, USA

Objectives: Determining the risks and benefits of thrombolytic therapy in individual stroke patients poses a major challenge. Diffusion- and perfusion-

weighted magnetic resonance imaging (DWI and PWI) have been proposed as a clinical method to identify the stroke core and salvageable penumbra, with mismatch thought to correlate with hemorrhagic risk. However, this metric has failed to be advantageous in clinical trials.[1] More information is needed about the early progression of acute stroke and the true nature of the regions presenting DWI and PWI contrast at each stage.

In this study, we use high-speed optical imaging of the bilaterally-exposed cortex of Thy1-GCaMP mice during localized, optically-induced unilateral acute stroke. We chart the progression of spatiotemporal changes in blood flow, hemoglobin oxygenation, and spontaneous neural activity over 1-3 hours. We additionally presented somatosensory stimulation on both the affected and unaffected sides. Our goal is to characterize the minute-by-minute progression of acute stroke in terms of metabolic support, vascular reactivity and the downstream effects on neural function and recoverability. Our results also allow us to probe the properties of neurovascular coupling during stroke progression to assess the potential of functional MRI and resting state fMRI techniques as tools for clinical evaluation.

Methods: Our studies used multispectral optical intrinsic signal imaging (MS-OISI)[2] to simultaneously capture hemodynamics, fluorescence and speckle-flow imaging in Thy1 GCaMP 3 mice following bilateral thinned-skull craniotomy. Stroke was induced via IV injection of Rose Bengal, a photosensitizer, followed by 532 nm focused illumination with a green laser of a branch of the middle cerebral artery feeding the somatosensory cortex (within the window, and during real-time imaging). Hemodynamic recordings were obtained via strobed 625 and 595 nm LED illumination, with a notch filter to remove interference from the laser. GCaMP fluorescence was captured with a 500 long pass filter during 490 nm LED illumination, while speckle data was acquired during illumination with an 800 nm laser diode. TTC staining was performed postmortem to confirm the infarct. All methods were approved by the Institutional Animal Care and Use Committee of Columbia University and the care and handling of the animals were in accord with National Institutes of Health guidelines.

Results and conclusions: The gradual progression of acute stroke can be observed, with expected changes in blood flow, levels of oxy-, deoxy- and total hemoglobin. Spreading depressions beyond the stroke region were also observed. Bilateral spontaneous neural activity observed prior to stroke onset continued during early ischemia, with bilaterally symmetric waves of activity traversing the affected region. Prolonged ischemia was found to attenuate these neural events, with some evidence of a gradual phase lag prior to abolition of observable activity. Hemodynamic responses to stimulation were altered in the affected region, although ongoing analysis will determine whether these changes reflect deterioration of purely neural, or combined neurovascular effects.

References

[1] Kim, B.J., et al, J Stroke, 2014. **16**(3): p. 131-145.
[2] Bouchard, M.B., et al, Opt Express, 2009. **17**(18): 15670-8.

634
BRAIN-0475
Poster Session

Cerebral Ischemia: Cellular and Molecular

COMBINATION TREATMENT WITH U0126 AND RT-PA PREVENTS THE DETRIMENTAL EFFECTS INDUCED BY DELAYED RT-PA TREATMENT AND PROVIDES POTENT NEUROPROTECTION AFTER STROKE

C. Orset[1], A. Anfray[1], K. Warfvinge[2], D. Vivien[1], S. Ansar[2]
[1]Serine Proteases and Pathophysiology of the Neu rovascular Unit, INSERM UMR-S 919, Caen, France
[2]Clinical Sciences, Lund University, Lund, Sweden

Objectives

Only one approved treatment for ischemic stroke is available, i.e. the thrombolytic agent

recombinant tissue type plasminogenactivator (rt-PA). The rt-PA approach has many limitations, recanalization efficacy is far from optimal and it can only be administered within 4.5 hours after stroke onset in order to reduce risk of hemorrhagic transformation and neurotoxicity. Elevated metalloproteinase (MMP) plasma levels have been reported to correlate with the frequency of hemorrhagic transformation following stroke[1]. We have shown that inhibitors of the Mitogen–activated protein kinasekinase extracellular signal–regulated kinase kinase (MEK) 1/2 pathways have a beneficial effect on stroke outcome[2]. Besides reducing infarct size and improving neurological outcome, they also reduce the MMPs following experimental stroke. By adding a MEK1/2 inhibitor we hypothesize that we can improve the safety of delayed rt-PA treatment. The aim of this study was to investigate if the combination therapy of a MEK/1/2 inhibitor and rt-PA can prevent the detrimental effects of delayed rt-PA treatment in stroke.

Methods

Thromboembolic stroke was induced by local injection of thrombin directly into the right MCA of C57 black/6J mice. Combination treatment with a specific MEK1/2 inhibitor U0126 and rt-PA was administrated at 4 h post stroke-onset. The efficiency of rt-PA to induce thrombolysis was measured by laser Doppler. After 24 h, all animals were euthanized and matrixmetalloproteinase (MMP)-9 and phosphorylated extracellular signal regulated kinase (ERK) 1/2 protein levels were investigated by immunofluorescence. Presence of hemorrhage was verified by histology and infarct volume was measured using MRI.

Results

Delayed administration of rt-PA (4 h post-stroke onset) had deleterious effect versus control group. An increased infarct volume, presence of hemorrhage and enhanced MMP-9 protein levels was observed in the MCAO group treated with rt-PA alone compared to control animals. Combination treatment with U0126 and rt-PA prevented hemorrhagic transformation and significantly decreased infarct volume, and MMP-9 protein levels compared to rt-PA alone and control group. Furthermore, p-ERK1/2 protein expression was blocked after combination treatment compared to control animals.

Conclusions

Combination therapy with rt-PA and U0126 decreases cerebral infarct volume, MMP-9 protein levels and prevents rt-PA induced hemorrhagic transformation. These results suggest that a MEK1/2 inhibitor is a promising adjuvant strategy to alleviate the detrimental side effects of delayed rt-PA treatment. These results provide new insights into how we may improve the only FDA approved treatment for ischemic stroke.

References

1. InzitariD, Giusti B, Nencini P, Gori AM, Nesi M, Palumbo V, et al. Mmp9 variation afterthrombolysis is associated with hemorrhagic transformation of lesion and death.Stroke; a journal of cerebral circulation. 2013;44:2901-2903

2. Edvinsson LI, PovlsenGK. Vascular plasticity in cerebrovascular disorders. Journal of cerebral bloodflow and metabolism : official journal of the International Society of CerebralBlood Flow and Metabolism. 2011;31:1554-1571

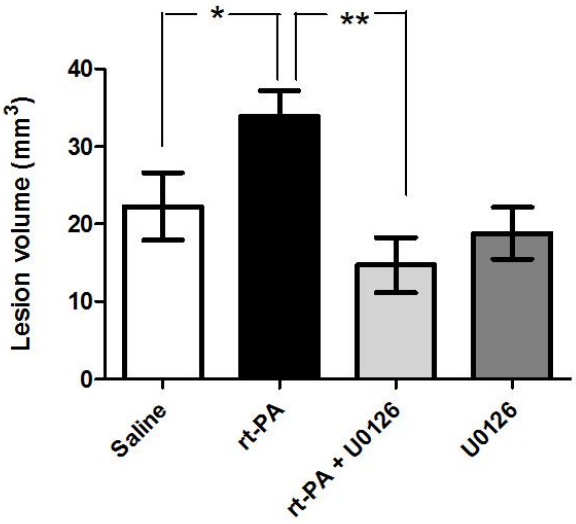

Figure: We observe a significantly increase in the infarct volume after delayed rt-PA treatment (4 h post-stroke onset). Combination treatment with U0126 and rt-PA at 4 h post stroke onset significantly decreased infarct volume compared to vehicle treated animals and rt-PA alone. Data are presented as mean ± SEM. ***** p<0.05 ****** p<0.01

635
BRAIN-0358
Poster Session

Cerebral Ischemia: Cellular and Molecular

EFFECT OF HDAC9 DEFICIENCY ON ISCHEMIC STROKE OUTCOME

S. Azghandi[1], D. Bühler[1], U. Mamrak[1], M. Schneider[1], M. Dichgans[1], N. Plesnila[1]
[1]Institute for Stroke and Dementia Research (ISD), Klinikum der Universität München, Munich, Germany

Objectives: In a genome-wide association study for ischemic stroke the so far strongest risk locus for large vessel stroke was identified in the 7p21.1 region. This locus contains the tail end of the histone deacetylase 9 (HDAC9) gene. HDAC9 mRNA levels were found to be increased in peripheral blood mononuclear cells of healthy risk allele carriers, suggesting that increased HDAC9 expression enhances the risk for large vessel stroke. These findings make HDAC9 a promising candidate gene for atherosclerosis and stroke. We recently showed that HDAC9 deficiency attenuates atherosclerosis in ApoE deficient mice, an established model for atherosclerosis.[1] The aim of the current study was to investigate the consequences of HDAC9 deficiency on ischemic stroke outcome.

Methods: We used a transient focal ischemia model based on middle cerebral artery (tMCAo) occlusion for one hour using a filament inserted via the internal carotid artery. Experiments were done in 6-week-old male HDAC9 knockout mice and wildtype littermates. Infarct volumes were analyzed after 24 hours and 7 days on cresyl violet stained cryosections. Cell death was assessed by quantification of TUNEL positive cells in peri-ischemic regions 24h post MCAo. Neurological status was determined daily during the 7 days after MCAo using a general MCAo score sheet. In addition, we monitored cerebral blood flow by Laser-Doppler-measurement in the reperfusion phase and edema formation by assessing the wet and dry weight of both hemispheres.

Results: HDAC9$^{-/-}$ mice exhibited increased infarct volumes and worse neurological scores 24 hours after stroke. TUNEL staining revealed increased numbers of dying cells in peri-ischemic areas of HDAC9$^{-/-}$ mice, whereas HDAC9 deficiency had no effect on reperfusion and edema formation. During the observation period of 7 days, HDAC9 deficient mice displayed higher neurological scores and more pronounced weight loss, but no difference in mortality as compared to wildtype littermates. Larger infarct volumes in HDAC9 deficient mice were still present 7 days after MCAo.

Conclusion: Our results suggest a protective role of HDAC9 in experimental stroke and hence opposing effects on atherosclerotic plaque progression and stroke outcome. Pharmacological inhibition of HDAC9 might be a promising strategy to prevent atherosclerosis, but might have opposite effects on stroke outcome. Strategies to target HDAC9 will have to consider potential off-target effects.

References:

[1] S. Azghandi, C. Prell, S. W. van der Laan, M. Schneider, R. Malik, K. Berer, N. Gerdes, G. Pasterkamp, C. Weber, C. Haffner, and M. Dichgans. Deficiency of the Stroke Relevant Hdac9 Gene Attenuates Atherosclerosis in Accord with Allele-Specific Effects at 7p21.1. *Stroke.* 2015;46:197-202

636
BRAIN-0442
Poster Session

Cerebral Ischemia: Cellular and Molecular

PHOSPHOINOSITIDE 3-KINASE GAMMA DEFICIT ENHANCES NEUROTOXIC EFFECTS OF MICROGLIA AFTER TRANSITORY FOCAL CEREBRAL ISCHEMIA

R. Bauer[1], C. Schmidt[1], N. Schneble[1], C. Frahm[2], M. Brodhun[3], I. Franco[4], O.W. Witte[2], E. Hirsch[4], R. Wetzker[1]
[1]Institute of Molecular Cell Biology, Jena University Hospital, Jena, Germany
[2]Department of Neurology, Jena University Hospital, Jena, Germany
[3]Institute of Pathology, HELIOS Klinikum, Erfurt, Germany
[4]Department of Genetics Biology Biochemistry, University of Torino, Torino, Italy

Objectives: Phosphoinositide 3-kinase γ (PI3Kγ) is linked to neuroinflammation and phagocytosis. This study was conducted to investigate the specific role of lipid kinase-dependent and -independent function of PI3Kγ in evolvement of brain damage induced by focal cerebral ischemia/reperfusion.
Methods: PI3Kγ wild-type, knockout ($PI3K\gamma^{-/-}$), and kinase-dead ($PI3K\gamma^{KD/KD}$) mice as well as wildtype chimeras containing $PI3K\gamma^{-/-}$-bone marrow and $PI3K\gamma^{-/-}$ chimeras containing wildtype-bone marrow were subjected to middle cerebral artery occlusion (45 minutes) followed by 6h, 12h and 48h as well as 7d of reperfusion and immunohistochmical (IHC) investigations were performed. Additionally, primary microglial cells derived from respective mouse genotypes were used for mechanistic analysis of PI3Kγ effects on matrix metalloproteinase-9 (MMP-9) release, phagocytic activity and cAMP content and signaling after oxygen/glucose deficit (OGD) challenge.
Results: Enlargement of brain infarction was more pronounced in $PI3K\gamma^{-/-}$ mice compared to wild-type and $PI3K\gamma^{KD/KD}$ mice as well as chimeras 48 h after reperfusion, whereas early infarct demarcation (6 and 12 h after reperfusion) was similar. IHC analysis revealed a reduced amount of PMN invasion within infarct core of brains derived from $PI3K\gamma^{-/-}$ mice, compared to wild-type mice, and a distinct immunoreactivity for MMP-9 in Iba-1 positive cells. Furthermore, number of Galectin-3/MAC-2-positive microglial cells indicating activated phagocytosis[1] was reduced in brain slices of $PI3Kg^{-/-}$ mice. Cell culture studies revealed enhanced MMP-9 secretion in supernatants derived from microglia of PI3Kγ-deficient mice after 2h OGD and 48h recovery. Furthermore, PI3Kγ-deficient microglial cells showed a markedly diminished phagocytic activity already under normal conditions and a failed phagocytic activation throughout the observed recovery period of 48h following OGD. Lastly, PI3Kγ-deficient microglia exhibited strongly increased cAMP levels and an activated cAMP signaling verified by CREB phosphorylation in comparison with wild-type microglia or cells expressing $PI3K\gamma^{KD/KD}$. This effect was enhanced after OGD/Reox challenge.
Conclusions: Our data suggest kinase-independent control of cAMP phosphodiesterase activity by PI3Kγ as a crucial mediator of microglial cAMP control, MMP expression, activation of phagocytic activity and subsequent attenuation of infarct enlargement following focal brain ischemia/recirculation. The results identify the suppressive effect of PI3Kγ on cAMP as a critical mediator of ischemia-induced immune cell functions.
References: [1]Rotshenker S. The role of Galectin-3/MAC-2 in the activation of the innate-immune function of phagocytosis in microglia in injury and disease. J Mol Neurosci 2009;39:99-103.

637
BRAIN-0766
Poster Session

Cerebral Ischemia: Cellular and Molecular

G PROTEIN-COUPLED ESTROGEN RECEPTOR SIGNALLING PROVIDES NEUROPROTECTION IN FEMALE MICE POST-STROKE

B. Broughton[1], G. Jansen[1], C. Sobey[1]
[1]Dept. of Pharmacology, Monash University, Clayton, Australia

Objectives. Estrogen has been assumed to provide neuroprotection following stroke entirely via classical estrogen receptors. Recent evidence from our group and others shows that activation of the non-classical G protein-coupled estrogen receptor (GPER) using the selective ligand, G-1, can improve stroke outcome in ovariectomised mice. However, it remains to be determined if estrogen-mediated neuroprotection occurs via GPER signalling. Thus, the aim of this study was to test if the selective GPER antagonist, G-15, might worsen stroke outcome in intact females whereas tamoxifen, a clinically approved GPER agonist, might provide neuroprotection following stroke in ovariectomised mice.

Methods. To address the first aim, intact female C57Bl6 mice (8-12 wks old) were treated i.p. with vehicle (dimethyl sulfoxide, n=8) or G-15 (300 µg/kg, n=7) 1 h prior to 0.5 h middle cerebral artery occlusion (MCAO). To address the second aim, mice were ovariectomised and 14 days later were treated i.p. with vehicle (dimethyl sulfoxide, n=9), tamoxifen (10 µg/kg, n=8) or a combination of G-15 and tamoxifen (n=9) 1 h prior to MCAO. Neurological scoring, hanging grip and adhesive removal tests were performed to assess functional outcomes at 24 h post-stroke and infarct volume was measured using thionin staining of brain sections. In addition, numbers of infiltrating T lymphocytes and neutrophils were assessed in the ischemic hemisphere using CD3 and myeloperoxidase immunohistochemistry, respectively.

Results. Intact female mice treated with G-15 exhibited a shorter hanging grip time (G-15: 38±5 s vs vehicle: 16±5 s; $P < 0.05$) and more severe neurological deficit (G-15 median score: 3 vs. vehicle: 1; $P < 0.05$) than vehicle-treated mice. Consistent with functional outcomes, cerebral infarct volume was larger in mice treated with G-15 (G-15: 24±6 mm^3 vs vehicle: 7±2 mm^3; $P < 0.05$). In addition, immunohistochemistry revealed a greater number of neutrophils (G-15: 16±2 cells vs. vehicle: 8±2 cells; $P < 0.05$), but not T lymphocytes (G-15: 8±1 cells vs. vehicle 6±2 cells) in the ischemic hemisphere of G-15-treated mice. In ovariectomised mice, tamoxifen treatment reduced the neurological deficit score (tamoxifen: 1 vs. vehicle: 3; $P < 0.05$), adhesive removal time (tamoxifen: 95±21 s vs. vehicle: 173±7 s; $P < 0.01$) and infarct volume (tamoxifen: 8±2 mm^3 vs. vehicle: 31±11 mm^3, $P < 0.05$). Tamoxifen limited the infiltration of T lymphocytes (G-15: 6±0 cells vs. vehicle 14±3 cells; $P < 0.05$) and neutrophils (G-15: 14±4 cells vs vehicle 41±5 cells; $P < 0.05$) into the ischemic hemisphere. The protective effects of tamoxifen were blocked by G-15.

Conclusions. In females, GPER activation contributes to endogenous estrogen-mediated neuroprotection following stroke. Tamoxifen can improve stroke outcome following surgical menopause in a GPER-dependent manner.

638
BRAIN-0639
Poster Session

Cerebral Ischemia: Cellular and Molecular

STAT3 IS A POSITIVE REGULATOR OF ENDOTHELIAL FUNCTION IN THE BRAIN

C.M. Davis[1], E. Varlamov[2], W. Zhang[3], N.J. Alkayed[1]
[1]Anesthesiology and Perioperative Medicine & Knight Cardiovascular Institute, OHSU, Portland, USA
[2]Department of Medicine, Norwalk Hospital affiliated with Yale University School of Medicine, Norwalk, USA
[3]Anesthesiology and Perioperative Medicine, OHSU, Portland, USA

Objectives

Signal Transducer and Activator of Transcription 3 (STAT3) is protective to the brain following ischemic injury[1,2,3]. Ablation of STAT3 specifically in neurons does not alter infarct size. We therefore hypothesized that endothelial STAT3 is responsible for protection from ischemic brain injury.

Methods

Endothelial- specific STAT3 knock-out mice (STAT3 floxed; Tie2Cre) were subjected to 1 hour middle cerebral artery occlusion (MCAO) and infarct volume determined by 2,3,5-triphenyltetrazolium chloride (TTC) staining. Primary mouse brain microvascular ECs were isolated and cultured from 2 month old male C57BL6 mice. ECs were subjected to varying durations of OGD and p-STAT3 levels determined by Western blot. STAT3 was pharmacologically inhibited by AG490 and Stattic; cell death was determined by Calcein/ PI labeling, barrier integrity by transendothelial electrical resistance (TEER) measurement and FITC-Ficoll 70 flux across the cell monolayer and nitric oxide response to acetylcholine by nitrate/ nitrite fluorometric assay.

Results

Our in vivo studies show that cerebral infarct volume is increased following MCAO in mice with conditionally attenuated STAT3 specifically in endothelial cells compared to control littermates. We found that STAT3 protein levels and phosphorylation are regulated by OGD; decreasing immediately following OGD and increasing again during reoxygenation. Pharmacological attenuation of STAT3 signaling induces EC death, while sub-lethal inhibition of STAT3 results in endothelial dysfunction, assessed by increased permeability and decreased resistance of the endothelial monolayer as well as a reduced nitric oxide response to acetylcholine.

Conclusions

STAT3 is a positive regulator of endothelial function and integrity in the brain, playing an important role in determining susceptibility to ischemic damage. Since endothelial dysfunction is a contributing factor, as well as an outcome of pathological states, regulation of endothelial STAT3 may have important consequences in cerebrovascular disease.

Acknowledgements

We thank Dr X-Y Fu at Indiana University–Purdue University Indianapolis for the STAT3 floxed mice and Dr W Fleming at OHSU for the Tie2-Cre mice.

This work was supported by a Pacific Mountain Affiliate Postdoctoral Fellowship from the American Heart Association to CMD.

References

1. Dziennis S, Alkayed NJ. Role of signal transducer and activator of transcription 3 in neuronal survival and regeneration. Rev Neurosci. 2008;19(4-5):341-61
2. Dziennis S, Jia T, Rønnekleiv OK, Hurn PD, Alkayed NJ. Role of signal transducer and activator of transcription-3 in estradiol-mediated neuroprotection. J Neurosci. 2007;27(27):7268-74.
3. Jung JE, Kim GS, Narasimhan P, Song YS, Chan PH. Regulation of Mn-superoxide dismutase

activity and neuroprotection by STAT3 in mice after cerebral ischemia. J Neurosci. 2009;29(21):7003-14.

639
BRAIN-0139
Poster Session

Cerebral Ischemia: Cellular and Molecular

FIRST ESTIMATION OF NONLINEAR DYNAMICS OF GLOBAL CEREBRAL ISCHEMIA

D. DeGracia[1], F.T. Anggraini[1], D. Taha[2], Z.F. Huang[2]
[1]Physioloy, Wayne State University, Detroit, USA
[2]Physics and Astronomy, Wayne State University, Detroit, USA

Objectives: Acute cell injuries such as cerebral ischemia can be mathematically modeled by a nonlinear dynamical competition between total damage, *D*, and total induced stress responses, *S* [1]. Conceptual breakthroughs of this approach include explaining cell death in terms of *D* and *S* attractor states, and using bistable solutions to explain, predict, and control neuroprotection. To apply the theory in a practical manner requires physically measuring *D* and *S*. We hypothesized that temporal changes in polysomal mRNAs, and protein aggregation would estimate *S* and *D*, respectively.

Methods: Male Long Evans rats were subjected to 10 min normothermic global cerebral ischemia by two-vessel occlusion plus hypotension and reperfused for 1, 8, 16, 24, 48, & 72 hours (n = 30/group). Hippocampal CA1 and CA3 were dissected. Five animals were pooled per region per replicate; half were used to estimate *D*, half for *S*. To estimate *S*, polysomes were pelleted from post-mitochondrial supernatants, RNA extracted, and analyzed on Rat Gene 2.0 ST Arrays (Affymetrix). Gene expression differentials, relative to controls, for ~30,000 probe sets were expressed as multi-dimensional distances and plotted vs. time. To estimate *D*, protein aggregates were isolated, detected by anti-ubiquitin Western blot, and total density of high molecular weight smears plotted vs time.

Results: Time plots of protein aggregate levels and polysome mRNA levels, used to estimate *D* and *S*, respectively (Figure 1A), were fit to solutions (Figure 1B) of the nonlinear dynamic model (Figure 1C). The measured time courses allowed refinement of the theory by indicating that the velocity parameter in the theory, *v*, was a function of time, *t*, and the decay parameter, *k*, depended on $|D\text{-}S|$. The refined model allowed the first-ever estimation of the injury dynamics of CA1 and CA3. In CA1 the rate parameter c_1 increased 5X and the decay parameter c_3 decreased 10X compared to CA3. Thus, injury in CA1 occurs 5 times faster, but decays 10X slower than in CA3, providing novel insight into CA1 injury dynamics. A strong secondary genetic response occurred in CA3 after 48 hr reperfusion, constituting a second injury dynamic, that also occurred more weakly in CA1.

Conclusions: These studies examined the feasibility of measuring the two variables of the nonlinear theory of cell injury: *D* and *S*. Temporal quantification of polysomal mRNAs and protein aggregation reasonably estimated *S* and *D*, respectively. This data allowed refinement of the theory. The modified theory will allow modeling multiple injuries over time to generate realistic simulations of time-dependent spatial evolution of injured tissue, such as occurs in stroke. The reported results are proof of principle of feasibility of our approach, allowing us to envision its application to solving the as-yet-intractable problem of neuroprotection following brain ischemia and reperfusion.

References: [1] DeGracia, D. J., Huang, Z.-F., and Huang S. (2012). JCBFM (32):1000–1013.

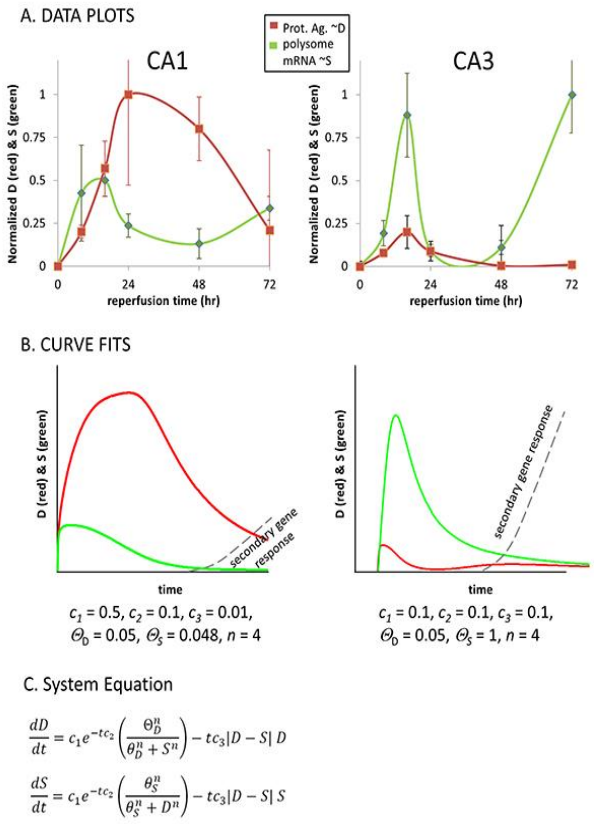

640
BRAIN-0311
Poster Session

Cerebral Ischemia: Cellular and Molecular

HYPOXIC PRECONDITIONING PROTECTS AGAINST WHITE MATTER INJURY AFTER NEONATAL HYPOXIA-ISCHEMIA THROUGH AMELIORATING MICROGLIAL-MEDIATED INFLAMMATION

M. XU[1], X. HU[2], Y. SHI[2], W. ZHANG[1], J. CHEN[2], Y. GAO[1]
[1]State Key Laboratory of Medical Neurobiology an d Institute of Brain Sciences, Fudan University, Shanghai, China
[2]Center of Cerebrovascular Disease Research, University of Pittsburgh Medical Center, Pittsburgh, USA

OBJECTIVES: Neonatal hypoxic-ischemic (H/I) brain injury can cause white matter injury, which is characterized by the disruption of myelin and the loss of the oligodendrocyte lineage cells. The oxidative stress, inflammation and excitotoxicity are all contribute to the white matter injury after H/I. Many previous studies showed that hypoxic preconditioning (HPC) can protect against H/I injury in the developing brain. However, limited data is available concerning the effects of HPC on white matter integrity. In this study, we investigated whether HPC could ameliorate the white matter injury after neonatal H/I by inhibiting the activation of microglia.

METHODS: Rats (Sprague-Dawley, P6 days) were subjected to normoxia (21% O_2) or HPC (7.8% O_2) for 3 h followed by 24 h of reoxygenation. Rats were then subjected to permanent right carotid artery ligated followed by 2.5h of hypoxia (7.8% O_2). Sham pups underwent the same procedure without occlusion and were maintained in room air. 5-bromo-2'-deoxyuridine (Brdu) was administered intraperitoneally to lable newly generated cells. Brains were removed 7days after H/I for evaluation of tissue loss. Neurological impairment after H/I was assessed up to 5 weeks by gait, righting reflex, foot fault, and Morris water maze test. White matter integrity and the differentiation of oligodendrocyte precursor cells were detected by immunofluorescence staining at 7d and 14d after H/I. Microglial polarization were evaluated by measuring mRNA expression of M1 and M2 phenotypic markers at 7 days after H/I using real-time PCR.

RESULTS: HPC significantly reduced brain tissue loss and improved short–term and long-term neurological outcomes up to 5 weeks after neonatal H/I injury. Immunofluorescence staining showed an increase in myelin basic protein (MBP, a marker of myelin integrity) staining and a decrease in beta-amyloid precursor protein (APP, a sensitive marker for axonal damage) staining in HPC-treated H/I mice, indicating that HPC could prevent myelin damage and preserving the axon Integrity. HPC significantly increased oligodendrogenesis and maturation of oligodendrocytes, as manifested by increased number of $Brdu^+APC^+$ cells at 7d and14d after H/I. These white matter protective effects of HPC were associated with a decrease in microglial activation, as revealed by reduced number of Iba-1+ cells in the lesioned hemisphere. Moreover,

HPC-treated mice exhibited a decreased expression of M1 markers an increased expression of M2 markers at 1d, 3d and 7d after H/I.

CONCLUSIONS: Our results suggest that HPC can provide both gray matter and white matter protection to the brain and promote functional recovery after H/I. These protective effects might be partially attributed to the effect of HPC in alleviating microglial activation and shifting microglial polarization towards beneficial M2 phenotype.

641
BRAIN-0485
Poster Session

Cerebral Ischemia: Cellular and Molecular

CEREBROVASCULAR RESPONSES IN SPONTANEOUSLY HYPERTENSIVE RATS AFTER ISCHEMIC STROKE

A. Grell[1], M. Mostajeran[2], L. Edvinsson[1], S. Ansar[2]
[1]Clinical Experimental Research, Glostrup Research Institute, Glostrup, Denmark
[2]Experimental Vascular Research, Clinical Sciences, Lund, Sweden

Objectives:
Stroke is the third most common cause of death in Europe why it is global and socio-economic important. Furthermore, hypertension is known to be an important controllable risk factor of stroke (1). Despite numerous animal models, new drugs that appear effective in ischemic stroke models have not worked in clinical trials. A main reason proposed for this is that the majority of pre-clinical studies are performed in healthy rodents. It is previously shown that cerebrovascular endothelin type B receptors are upregulated after ischemic stroke mediating a significant contraction of the occluded blood vessel. In addition, increased expression of endothelin type B receptors in lethal stroke patients has been observed (2). We hypothesize that hypertension enhances the cerebrovascular damages that are associated with reduced cerebral blood flow after ischemic stroke. In this project, vascular changes in the cerebral blood vessels after ischemic stroke were investigated in spontaneously hypertensive rats (SHR).

Methods:
Middle cerebral artery occlusion (MCAO) was induced in 12-week-old male SHR (Permit number: 2014-15-0201-00042). After occlusion of the right middle cerebral artery (MCA) for 2 hrs the filament was withdrawn to allow reperfusion. The contractile response to different agonists were investigated in the MCAs after 48 h of reperfusion in the wire-myograph. The endothelin type B receptor agonist Sarafotoxin 6c (S6c) was added with and without the endothelium inhibitors L-NAME and Indomethacin, and the endothelin type A receptor agonist Endothelin-1 (ET1) was added with and without the endothelin type B receptor antagonist BQ788. In addition, potassium and endothelium responses were examined.

Results:
The contractile response to ET1 was increased in the occluded MCA compared to the non-occluded MCA. The response was mediated by endothelin type A (ETA) receptors confirmed by an endothelin type B receptor antagonist BQ788. There was no contractile response to S6c in any groups with or without the endothelium inhibitors L-NAME and Indomethacin. The potassium and endothelium responses were significant increased in the occluded MCA compared to the non-occluded MCA.

Conclusion:
MCAO in SHR increased the contractile response to ET1 in the occluded MCA mediated by ETA receptors. There was no difference in the contractile response to S6c. Interestingly, an enhanced endothelium response was demonstrated in the occluded MCA perhaps indicating a protective mechanism. The role of the endothelium in SHR after ischemic stroke will be further investigated.

References:
1. Garcia et al. Comparison of infarct volume and behavioral deficit in Wistar Kyoto and

Spontaneously hypertensive rat after transient occlusion of the middle cerebral artery. SpringerPlus 2013 2:2014
2. Edvinsson et al. Vascular plasticity in cerebrovascular disorders. Journal of Cerebral Blood Flow and Metabolism 2011 31;1554-1571

642
BRAIN-0769
Poster Session

Cerebral Ischemia: Cellular and Molecular

A NEW THERAPEUTIC STRATEGY AGAINST TOXIC NASCENT PEPTIDE CHAIN AGGREGATION AFTER BRAIN ISCHEMIA

B.R. Hu[1], C.H. Liu[1], Y.J. Park[1], T.F. Luo[1]
[1]Shock Trauma and Anesthesiology Research Center, University of Maryland School of Medicine, Baltimore, USA

Objectives: To study toxic aggregation of newly synthesized polypeptides, known as nascent peptide chains (NPCs) after transient cerebral ischemia. NPCs are the major source of unfolded proteins in normal cells. Without protection from molecular chaperones, NPCs expose their hydrophobic segments, are prone to protein aggregation, and thus highly toxic to cells.

Methods: The rat 2VO + hypotension transient cerebral ischemia model was used in this study. Detergent/salt-insoluble protein aggregates were isolated with subcellular fractionations. Co-translational complex components and their associated protein aggregates were separated with sucrose gradient centrifugation and Western blotting. Confocal and electron microscopy were utilized to examine toxic protein aggregation and organelle damage in brain sections after brain ischemia. Protein synthesis initiation was monitored using SUnSET confocal and immunoblot analysis. Delayed neuronal death was quantified using the computer StereoInvestigator program.

Results: Transient cerebral ischemia damages several molecular chaperones, resulting in toxic aggregation of NPCs, together with NPC-associated eukaryotic initiation factors, co-translational chaperones, as well as ribosomes after transient cerebral ischemia. The NPC protein aggregates are associated with multiple subcellular lipid membranes and damage multiple subcellular organelles. Inhibition of protein synthesis initiation with newly developed drugs depletes NPCs and protects hippocampal CA1 neurons from delayed neuronal death after brain ischemia.

Conclusions: Toxic NPC aggregation contributes significantly to delayed neuronal death after brain ischemia. Transient depletion of NPCs may be a new therapeutic strategy that can offer strong neuroprotection after transient cerebral ischemia.

643
BRAIN-0774
Poster Session

Cerebral Ischemia: Cellular and Molecular

THE BETA/PIX – RAC1 - COFILIN PATHWAY AFTER BRAIN ISCHEMIA

C.H. Liu[1], T.F. Luo[1], Y.J. Park[1], I. Sabirzhanova[1], B.R. Hu[1]
[1]Shock Trauma and Anesthesiology Research Center, University of Maryland School of Medicine, Baltimore, USA

Objectives: To study the role of the beta-PIX - Rac1 - cofilin pathway in delayed neuronal death after transient cerebral ischemia. The beta-PIX - Rac1 - cofilin pathway plays a key role in synaptic transmission, synaptic connection and cell movement. Understanding this pathway is essential for developing neuroprotective therapeutics to facilitate functional recovery after brain ischemia. However, how this pathway is regulated following brain ischemia remains largely unknown.

Methods: The following methods were used in this study: the rat 2VO + hypotension transient cerebral ischemia model, subcellular fractionation, Western blotting, confocal microscopy, pull-down assay, the

StereoInvestigator quantification of the numbers of dead and normal neurons, and Rac1 inhibitory drug treatment studies.

Results: The Rac1 GTPase is significantly upregulated and translocated to the synaptic and nuclear fractions after transient cerebral ischemia. Cool1/beta-PIX (beta-PIX hereafter), a Rac1 guanine nucleotide exchange factor, is also significantly translocated to the synaptic membrane and nuclear structure initially, and then depleted after transient cerebral ischemia. Correspondingly, an episode of brain ischemia leads to transient activation of cofilin, a Rac1 downstream effector, by dephosphorylation. Inhibition of this pathway with NSC23766 protects hippocampal CA1 neurons from delayed neuronal death after brain ischemia.

Conclusions: Activation of the beta-PIX – Rac1 – cofilin pathway contributes significantly to delayed neuronal death after transient cerebral ischemia. Transient inhibition or preservation of this pathway may be a new therapeutic strategy to protect neurons from transient cerebral ischemia-induced injury.

644
BRAIN-0461
Poster Session

Cerebral Ischemia: Cellular and Molecular

CEREBROVASCULAR ENDOTHELIN-1 HYPERREACTIVITY IS ASSOCIATED WITH TRANSIENT RECEPTOR POTENTIAL CANONICAL CHANNELS 1 AND 6 ACTIVATION AND DELAYED CEREBRAL HYPOPERFUSION AFTER FOREBRAIN ISCHEMIA IN RATS

S.E. Johansson[1], X.E. de Ridder Andersen1[1], R.H. Hansen[2], G.K. Povlsen[1], L. Edvinsson[1]
[1]Dept. of clinical experimental research, Glostrup research Institute, Glostrup, Denmark
[2]Dept. of Radiology, Copenhagen University Hospital, Herlev, Denmark

Objectives: Delayed post-ischemic hypoperfusion is a secondary recirculation disturbance after global cerebral ischemia, contributing to the development of delayed ischemic brain damage. The delayed post-ischemic hypoperfusion phase is characterized by increased cerebrovascular tone but the underlying pathophysiological mechanisms are still not clear. Endothelin-1 (ET-1) has shown to mediate increased contraction in cerebral arteries after experimental forebrain ischemia. Furthermore, upregulation of contractile smooth muscle Endothelin type B (ET_B) receptors has been suggested to underlie this enhanced ET-1-mediated vasoconstriction. The major determinant of vascular smooth muscle cell (VSMC) contractility is a rise in intracellular Ca^{2+} levels. However, the relative contribution of these calcium sources in ET-1-mediated vasoconstriction after forebrain ischemia is unknown.

Here, we aimed to investigate the association between enhanced ET-1-mediated vasoconstriction in cerebral arteries and calcium channel plasticity in the post-ischemic hypoperfusion phase after induced forebrain ischemia in rats.

Methods: Experimental forebrain ischemia was induced in Wistar male rats (permit number: 2012-0726) by a two vessel occlusion model and the cerebral blood flow was measured by MRI two days after reperfusion. In-vitro vasoreactivity studies, immunofluorescence and qPCR were performed on cerebral arteries from ischemic or sham-operated rats to evaluate changes in vascular voltage-dependent calcium channels (VDCC), transient receptor potential canonical channels (TRPC) as well as ET-1 receptor function and expression.

Results: The expression of TRPC1 and TRPC6 in the VSMC was enhanced and correlated with decreased cerebral blood flow in cerebral arteries 2 days after forebrain ischemia. Furthermore, VDCC-independent ET-1-induced cerebrovascular contraction was enhanced 2 days after forebrain ischemia and this enhancement was mediated, at least partly, by calcium influx via upregulated TRPC6/1 channels.

Conclusion: Our data demonstrates that increased ET-1-mediated influx of extracellular calcium via upregulated TRPC6/1 channels in VSMC is involved in enhanced ET-1-mediated cerebral vasoconstriction in the delayed post-ischemic hypoperfusion phase after experimental forebrain ischemia.

645
BRAIN-0069
Poster Session

Cerebral Ischemia: Cellular and Molecular

EFFECT OF TH2 IMMUNITY ON STROKE OUTCOME

H. Kim[1], S. Whittle[1], S.R. Zhang[1], S. Lee[1], H.X. Chu[1], Z. Wei[1], T.V. Arumugam[2], A. Vinh[1], G.R. Drummond[1], C.G. Sobey[1]
[1]Department of Pharmacology, Monash University, Clayton, Australia
[2]Department of Physiology, National University of Singapore, Singapore, Singapore

Stroke is the world's second leading cause of mortality and over a third of survivors are left with major neurological injury making it the sixth leading burden of disease worldwide. Following an ischemic stroke, immune cells including macrophages, lymphocytes, neutrophils and dendritic cells infiltrate the ischemic brain hemisphere and contribute to secondary brain damage. Growing evidence shows the importance of T lymphocytes, in particular T regulatory cells, in the brain following stroke where they appear to modulate tissue injury. This is likely to involve the direction of non-T regulatory $CD4^+$ T cells (T helper (Th) cells) towards a Th2-type anti-inflammatory response and away from a Th1 pro-inflammatory response. Commonly, the C57Bl/6 mouse strain is known to exhibit a Th1-prone, pro-inflammatory type response to injury, whereas the FVB strain is relatively Th2-prone, or anti-inflammatory, in its immune response. We tested the hypothesis that stroke outcome is more severe in C57Bl/6 than FVB mice. We compared functional outcomes and quantitated immune cell numbers in brains of the two strains of mice following stroke. C57Bl/6 and FVB mice (n=127) were subjected to sham surgery or 1 h occlusion of the right middle cerebral artery followed by 23 h of reperfusion. C57Bl/6 mice displayed greater functional deficits than FVB mice after stroke, as assessed by neurological scoring and hanging grip test (n=28-34, $P<0.01$). Total numbers of $CD45^+$ leukocytes tended ~2-fold greater in the brains of C575Bl/6 than FVB mice despite a similar infarct size. Moreover, there were marked differences in the composition of leukocyte types in the ischemic hemispheres of the two mouse strains after stroke. Compared with sham-operated mice, fold-increases in cell numbers after stroke in C57Bl/6 vs FVB mice (n=5-8) included: neutrophils, 6.7 vs 96.9; $CD3^+$ cells, 3.1 vs 1.6; $CD4^+$ cells, 4.7 vs 1.9; $CD8^+$ cells, 0.8 vs 2.8; macrophages, 2.2 vs 7.9; dendritic cells, 3.5 vs 4.8. We then further tested whether acutely inducing a Th2 immune response in C57Bl/6 mice might improve functional outcome following stroke. These differing immune cell compositions may have contributed to the differential functional outcomes of C57Bl/6 and FVB mice following stroke. Finally, we used the Th2 cytokine, interleukin-4 (IL-4), to induce a Th2 immune profile, with mice receiving either mouse recombinant IL-4 (5 µg i.p.) or vehicle (1% bovine serum albumin) 24 h before stroke. This treatment resulted in ~35% smaller infarct volumes than in vehicle-treated mice ($P<0.05$, n=17-24). Thus, a Th2 immune profile leads to milder brain injury after stroke, and acute administration of a Th2-promoting cytokine can provide neuroprotection.

646
BRAIN-0674
Poster Session

Cerebral Ischemia: Cellular and Molecular

EXPRESSION, DISTRIBUTION AND CELLULAR LOCALIZATION OF SIRTUINS IN THE NORMAL AND ISCHEMIC BRAIN OF RAT

J. Kim[1], O.H. Lee[1], H.J. Choi[1], I. Kwon[1], J.H. Heo[1]
[1]neurology, Yonsei University. Medical Center, Seoul, Korea

Objectives: Sirtuins (SIRTs) are nicotinamide adenine dinucleotide-dependent histone deacetylases. To date, seven sirtuins (SIRT1-SIRT7) have been identified in mammals. While basic knowledge on the cellular expression and anatomical localization of sirtuins in the brain is essential to understand the role of sirtuins in brain diseases, only limited information is available on this issue.[1, 2] We investigated the distributions and cellular localization of sirtuins in the normal brain as well as ischemic brain of the rat.

Methods: Male Sprague-Dawley rats were used. Normal whole brain samples of rats were obtained through transcardiac perfusion under inhalation anesthesia. Cerebral ischemia was induced by 2 h of middle cerebral artery occlusion and 22 h of reperfusion using nylon thread. In paraffin or frozen sections, immunohistochemistry was performed and whole brain was examined into regions: olfactory bulb, cerebrum and cerebellum. To examine the cell types that express sirtuins, double immunofluorescence staining was performed using antibodies for each sirtuin and those for specific cell markers such as NeuN or β-III tubulin (neuron), myelin basic protein (MBP, myelin), CNPase (oligodendrocyte), glial fibrillary acidic protein (astrocyte), and collagen type IV or RECA-1 (vessels).

Results: SIRT1, SIRT3 and SIRT5-7 were colocalized with neuronal markers and SIRT2 was colocalized with myelin markers. SIRT6 and SIRT7 were also partially colocalized with oligodendrocyte markers. SIRT4 was expressed in vessels. As a result, SIRT1 and SIRT5-7 were widely distributed and highly expressed in the olfactory bulb, cerebrum, and cerebellum. SIRT1-3 and SIRT5 were not detected in the corpus callosum and internal capsule, while SIRT6 and SIRT7 showed signals in them. SIRT2 was highly expressed in the glomerular layer and anterior olfactory nucleus of olfactory bulb, the cerebral cortex, hippocampus, and the granular layer of cerebellum. SIRT3 showed extensive distribution in the olfactory bulb and cerebellum except for the molecular layer of cerebellum. SIRT3 was also expressed in the cerebral cortex, hippocampus and thalamus. SIRT4 showed wide distribution through whole brain except for the molecular layer and purkinje layer of cerebellum. After induction of cerebral ischemia, SIRT2, SIRT4 and SIRT7 showed increased expression in the ischemic and peri-infarct region. However, expression of SIRT1 and SIRT6 was decreased in the ischemic regions. Expression of SIRT3 and SIRT5 was not changed after cerebral ischemia.

Conclusions: Distribution and cellular localization in the rat brain were different among sirtuins. Expression in the ischemic brain was also different. Findings of this study might provide with basic information for studying pathophysiologic role of sirtuins in the brain.

References:

1 G. Donmez, 'The Neurobiology of Sirtuins and Their Role in Neurodegeneration', *Trends Pharmacol Sci,* 33 (2012), 494-501.
2 K. C. Morris, H. W. Lin, J. W. Thompson, and M. A. Perez-Pinzon, 'Pathways for Ischemic Cytoprotection: Role of Sirtuins in Caloric Restriction, Resveratrol, and Ischemic Preconditioning', *J Cereb Blood Flow Metab,* 31 (2011), 1003-19.

647
BRAIN-0412
Poster Session

Cerebral Ischemia: Cellular and Molecular

HSP70 PROTECTS THE BRAIN FROM STROKE BY INTERFERING WITH DYNAMIN-FAS MEDIATED SIGNALING IN NEURONS

N. Kim[1], J.Y. Kim[1], Z. Zheng[1], J.E. Lee[2], M.A. Yenari[1]
[1]Neurology, San Francisco Veterans Affairs UCSF, San Francisco, USA
[2]Anatomy, Yonsei University College of Medicine, Seoul, Korea

Objective: The 70 kDa heat shock protein (Hsp70) is known to protect brain cells in animal and cell culture models of cerebral ischemia. We carried out proteomic screening of mice subjected to middle cerebral artery occlusion (MCAO), which identified dynamin as a major downregulated gene in Hsp70-overexpressing transgenic mice (Tg) compared to wildtype (Wt). Dynamin is a protein involved in endocytosis, and is expressed in neurons. Dynamin has been found to transport the death receptor Fas to the cell surface where it can be bound by its ligand (FasL) and lead to apoptosis.
Methods: We subjected groups of wildtype, Hsp70 transgenic, and Hsp70 knockout (Ko) mice to cerebral ischemia using distal MCAO (dMCAO). Brains were assessed for dynamin and Fas expression 3d following dMCAO as well as for infarct size and neurological behavior 14d post dMCAO. To explore the significance of dynamin in brain ischemia, we then injected mice with a dynamin inhibitor (dynasore).
Results: We found that dynamin is upregulated by ischemia and colocalizes primarily to neurons. Further, Hsp70 overexpression protects the brain following dMCAO as evidenced by decreased infarct volume (n=6/group, P<0.05), improved neurobehavioral outcomes (P<0.05), and decreased brain dynamin and Fas expression relative to wildtype and KO groups. Dynasore also protects against ischemic brain damage and improves neurological outcome out to 14 days post dMCAO (n=7~9/group; **P<0.05). Dynasore (Dyna) treatment alsoattenuated surface expression of Fas in experimental stroke (P<0.01).
Condclusion: Our results showed that Hsp70 disrupts apoptotic pathways after experimental stroke in mice by downregulating dynamin, which may be involved in Fas trafficking to the cell surface, thus triggering apoptosis . These findings suggest a new molecular target for treating stroke.

648
BRAIN-0859
Poster Session

Cerebral Ischemia: Cellular and Molecular

THE ROLE OF A-SYNUCLEIN IN ISCHEMIC BRAIN DAMAGE

T. Kim[1], B. Kaimal[1], R. Vemuganti[1]
[1]Neurological Surgery,
University of Wisconsin School of Medicine and Public Health, Madison, USA

Objectives: α-synuclein (α-syn) is one of the most abundant proteins in mammalian brain that is known to be a major player in the neurodegeneration observed in chronic conditions like Parkinson's disease and Alzheimer's disease[1]. Several mechanisms were proposed for α-syn-induced neuronal death in PD including inflammation, oxidative stress, mitochondrial fission, and autophagy[2,3]. Interestingly, all these pathophysiologic mechanisms also mediate neuronal death after acute CNS insults like stroke[4-8]. Therefore, we examined whether α-syn contributes to post-stroke neuronal death and neurological dysfunction.

Methods: Rats were subjected to 60 min transient middle cerebral artery occlusion and α-syn induction was silenced with either miRNA-7 or Silencer Select α-syn siRNA. The levels of α-syn were estimated with qPCR and Western Blots. Post-ischemic motor deficit was evaluated with rotarod, beam walk and adhesive removal test 1 to 7 days after ischemia, and brain damage was measured on cresyl violet stained brain sections.

Cellular changes after ischemia were examined using immunofluorescence staining.

Results: We found that silencing α-syn by a specific siRNA cocktail significantly decreased the infarction and improved the motor function. We identified that α-syn is a target of microRNA miR-7a. When challenged with a miR-7a mimic, the α-syn 3'UTR vector expression was significantly curtailed confirming that the miR-target relationship. Following transient MCAO, miR-7a levels were significantly down-regulated. When miR-7a levels were replenished by treating with a miR-7a mimic, post-ischemic neuronal death and motor deficits were significantly decreased. Furthermore, α-syn suppression significantly mitigated the post-ischemic oxidative stress (OX-42, 8-OHdG and 3-NT), apoptosis (Caspase-3) and mitochondrial dysfunction (phospho-Drp1).

Conclusions: Therefore we show that α-syn also plays a critical role in neuronal death following acute insults to brain like stroke and preventing α-syn expression is neuroprotective indicating α-syn as a potential therapeutic target.

References

1. Takeda, A, Hasegawa, T, Matsuzaki-Kobayashi, M, *et al*. Mechanisms of neuronal death in synucleinopathy. *J Biomed Biotechnol.* 2006;19365.
2. Dias V, Junn E, Mouradian MM. The role of oxidative stress in Parkinson's disease. *J Parkinsons Dis*. 2013;3:461-491
3. Pacheco C, Aguayo LG, Opazo C. An extracellular mechanism that can explain the neurotoxic effects of alpha-synuclein aggregates in the brain. *Front Physiol*. 2012;3:297
4. Baek SH, Noh AR, Kim KA, *et al*. Modulation of mitochondrial function and autophagy mediates carnosine neuroprotection against ischemic brain damage. *Stroke*. 2014
5. Garcia-Bonilla L, Benakis C, Moore J, Iadecola C, Anrather J. Immune mechanisms in cerebral ischemic tolerance. *Front Neurosci*. 2014;8:44
6. Mehta SL, Li PA. Neuroprotective role of mitochondrial uncoupling protein 2 in cerebral stroke. *J Cereb Blood Flow Metab* 2009;29:1069-1078
7. Nakka VP, Gusain A, Mehta SL, Raghubir R. Molecular mechanisms of apoptosis in cerebral ischemia: Multiple neuroprotective opportunities. *Molecular neurobiology*. 2008;37:7-38
8. Rodrigo R, Fernandez-Gajardo R, Gutierrez R, *et al.* Oxidative stress and pathophysiology of ischemic stroke: Novel therapeutic opportunities. *CNS & Neurol Disord Drug Targets*. 2013;12:698-714

649
BRAIN-0462
Poster Session

Cerebral Ischemia: Cellular and Molecular

EXPRESSIONAL CHANGES IN AN ENRICHED FRACTION OF THE CEREBRAL MICROVASCULATURE AFTER TRANSIENT GLOBAL CEREBRAL ISCHEMIA – A PROTEOMIC SCREEN

S.S. Larsen[1], S.E. Johansson[1], A.V.G. Edwards[2], M.R. Larsen[2], J. Nielsen[1], G.K. Povlsen[1], L. Edvinsson[1]
[1]Clinical Experimental Research, Glostrup Research Institute, Glostrup, Denmark
[2]Biochemistry and Molecular Biology, University of Southern Denmark, Odense, Denmark

Objectives: Global cerebral ischemia (GCI) is most often seen as a pathological complication following cardiac arrest. Little is known about the expressional changes of the cerebral microvasculature in the days after GCI and the contribution of these changes to GCI. The aim of this study was to obtain an overview of the expressional changes after GCI by performing a mass spectrometry-based screen of the isolated intracortical vasculature. Furthermore, the effect of treatment with a MEK1/2 inhibitor U0126 on GCI-induced expressional changes of the microvasculature was investigated.

Methods: GCI was induced in rats by occlusion of the common carotid arteries combined with systemic hypotension. All animal experiments were carried out in accordance with national guidelines and approved by the Danish

Experimental Animal Inspectorate (protocol no. 2012-15-2934-00726). Subsequently, rats were treated with either vehicle or the MEK1/2 inhibitor U0126 at 0, 12, 36, 48 and 60 hours post-ischemia. Sham-operated animals served as a control group. 72 hours after GCI-induction, cerebral cortical microvasculature (microvessels in the brain parenchyma) was isolated and the protein content analysed with state-of-the-art mass spectrometry.

Results: The proteomic profile of the enriched fraction of cerebral microvasculature 72 hours after GCI compared to sham indicates changes mainly within the following 9 categories: 1) cellular respiration, 2) ribosomal activity, 3) expression of chromatin structure-related proteins, 4) clathrin-mediated endocytosis, 5) remodelling of the extracellular environment, 6) contractile phenotype, 7) synaptic activity, 8) G-protein signalling, 9) sodium-potassium ATPase activity. Treatment with U0126 partly reversed the protein changes related to category 1, 2, 4, 5, 7 and 8. Validation of these findings is still in progress.

Conclusion: Collectively, these results point to several pathological expressional changes 72 hours after GCI which are partly rescued by early U0126 treatment. We believe that these results will aid the understanding of the pathophysiological mechanisms in the microvasculature after GCI and enlighten the effect of U0126 treatment upon these changes.

650
BRAIN-0799
Poster Session

Cerebral Ischemia: Cellular and Molecular

SUMO2/3 CONJUGATION AS AN ENDOGENOUS NEUROPROTECTIVE MECHANISM

G. Lättig-Tünnemann[1], B. Brommer[1], J. Schwab[2], C.J. Hoffmann[1], F. Yildirim[3], P. Euskirchen[2], C. Harms[1]
[1]Department of Experimental Neurology, Center for Stroke Research Berlin (CSB) Charité-Universitätsmedizin, Berlin, Germany
[2]Department of Experimental Neurology, Clinic for Neurology Charité-Universitätsmedizin, Berlin, Germany
[3]Department of Psychiatry, Cluster of Excellence NeuroCure Charité-Universitätsmedizin, Berlin, Germany

Objectives

Small ubiquitin-like modifier (SUMO) conjugation to a broad range of target proteins was identified in animal models of hibernation and ischemia as an endogenous brain protective mechanism.[1,2]

SUMOylation predominantly targets chromatin-associated transcription factors and epigenetic modifiers and thereby modifies transcriptional profiles.[3] The maintenance of SUMO-conjugation levels in post-mitotic neurons during the course of multiple and multicellular damaging cascades following an ischemic insult may therefore increase the survival rate of neurons and improve the outcome after stroke.

Methods

We investigated the loss of SUMO2/3[4] and the SUMO-deconjugating enzyme sentrin-specific isopeptidase (SENP) 7 in primary cultures of cortical neurons following a combined oxygen- and glucose deprivation (OGD) damaging protocol. The impact of SENP7 mutations on SUMO-modified proteins was studied by fluorescence microscopy localization and kinetics assays. Further, we assessed neurite outgrowth after SENP7 depletion in retina explants to evaluate its influence on regeneration.

Results

The loss of free SUMO2/3 in cortical neurons reduced cell viability and survival already in case of sub-threshold OGD where almost all control neurons maintained healthy morphology. While SENP7 depletion in cortical neurons improved their survival during OGD, the number of neurites and the length of neurite outgrowth was reduced in retina explants.

Conclusions

SUMO2/3 conjugation to nuclear proteins is an important mechanism to modify cellular transcriptional activities. Insufficient amounts of SUMO2/3 limit the cellular stress tolerance of cortical neurons to OGD. However, maintenance of the pool of SENP7-cleavable SUMO2/3 conjugation levels enhances survival after OGD. Loss of SENP7 had a detrimental effect in a neurite outgrowth assay in retina explants. This illustrates the complex and intricate interplay between endogenous neuroprotection and endogenous regeneration and recovery after stroke.

References

1. Lee YJ, Miyake S, Wakita H, McMullen DC, Azuma Y, Auh S, Hallenbeck JM (2007). Protein SUMOylation is massively increased in hibernation torpor and is critical for the cytoprotection provided by ischemic preconditioning and hypothermia in SHSY5Y cells. J Cereb Blood Flow Metab. 27(5):950-62.

2. Yang W, Sheng H, Warner DS, Paschen W (2008). Transient focal cerebral ischemia induces a dramatic activation of small ubiquitin-like modifier conjugation. J Cereb Blood Flow Metab. 28(5):892-6.

3. Nayak A, Müller S (2014). SUMO-specific proteases/isopeptidases: SENPs and beyond. Genome Biol. 15(7):422.

4. Datwyler AL, Lättig-Tünnemann G, Yang W, Paschen W, Lee SL, Dirnagl U, Endres M, Harms C (2011). SUMO2/3 conjugation is an endogenous neuroprotective mechanism. J Cereb Blood Flow Metab. 31(11):2152-9.

651
BRAIN-0286
Poster Session

Cerebral Ischemia: Cellular and Molecular

THE CHOROID PLEXUS IN BRAIN LYMPHOCYTE INVASION AFTER STROKE

G. Llovera[1], *F. Hellal*[1], *T. Arzberger*[2], *B. Engelhardt*[3], *A. Liesz*[1]
[1]*Institute for Stroke and Dementia Research (ISD), Klinikum der Universität München, Munich, Germany*
[2]*Center for Neuropathology and Prion Research, Ludwig-Maximilians-Universität, Munich, Germany*
[3]*Theodor Kocher Institute, Universität Bern, Bern, Switzerland*

Objectives: Acute brain ischemia triggers an inflammatory response, which activates detrimental cascades contributing to secondary brain damage. Brain leukocyte invasion is the key mechanism of post-stroke neuroinflammation. Previous studies investigating post-stroke leukocyte brain invasion have focused on transendothelial migration across the blood-brain-barrier. However, the choroid plexus (CP) is an alternative route of leukocyte entry to the brain, which has been well described in autoimmune brain disorders but has previously not been analyzed after stroke.

Methods: Adult C57BL/6J mice were subjected to permanent middle cerebral artery (MCA) occlusion (pMCAo) or transient filament MCA occlusion (tMCAo) and brains were analyzed at several timepoints after stroke. Cerebral leukocyte accumulation was studied by immunohistology and flow cytometry. Leukocyte localization in respect to the infarct core was further assessed by 3D-imaging of solvent-cleared whole brains. Chemokine levels were determined in the peri-infarct cortex and CP by RT-PCR of laser-microdissected tissue samples. Apoptosis of CP epithelium was characterized by TUNEL staining in both stroke models. Leukocyte migration from the CP epithelium to the peri-infarct region was investigated using a novel

transgenic animal model with photoactivatable-GFP expression in leukocytes. Four days after stroke, a laser probe was inserted into the ipsilateral ventricle and leukocytes present into the CP were irradiated at 405nm, inducing GFP-photoactivation. Consecutively, 24h after photoactivation presence of GFP+ cells was histologically examined. Finally, we immunohistologically analyzed autoptic human choroid plexus samples of 6 stroke patients and 5 control patients for leukocyte subpopulations.

Results: Lymphocytes as well as monocytes invaded the ipsilateral hemisphere as early as 6h after stroke and increased in number until 5 days after pMCAo. Whole brain 3D-imaging showed monocytes surrounding the cortical infarct core in the pMCAo model, while lymphocytes specifically accumulated in the dorsal peri-infarct cortex in projection of the corpus callosum (CC). This localization indicated a potential invasion of lymphocytes from the CP and migration along the CC to the lesion. This hypothesis was confirmed by tracking lymphocyte migration originating from the CP after stroke in a lymphocyte-specific photoactivation paradigm. GFP+ lymphocytes were detected in the peri-infarct cluster 24h after photoactivation in the ipsilateral CP. In contrast, we detected significantly less lymphocytes after tMCAo with extensive brain lesions compared to the pMCAo model and also did not observe the specific localization pattern as described above. Analysis of CP epithelial apoptosis revealed substantial CP damage, indicating a possible CP dysfunction after tMCAo as the cause of inter-model difference in lymphocyte invasion. A range of lymphocyte-attractant chemokines analyzed in ipsi- and contralateral cortex and CP after pMCAo revealed a chemokine gradient between cortex and CP in the ipsilateral hemisphere, indicative for directed lymphocyte migration to the lesion site. In accordance with results from the animal studies, we detected an increased leukocyte number in the ipsilateral CP of stroke patients compared to matched controls.

Conclusions: Our study demonstrates for the first time a key role for the choroid plexus in post-stroke lymphocyte brain invasion. This invasion route has to be considered in future studies analyzing neuroinflammatory mechanisms and developing immunotherapeutics for stroke.

652
BRAIN-0755
Poster Session

Cerebral Ischemia: Cellular and Molecular

IS THE ISCHEMIC PENUMBRA AT THE CORE OF EARLY INTRACRANIAL PRESSURE ELEVATION FOLLOWING EXPERIMENTAL STROKE?

C.L. Logan[1]
[1]*School of Biomedical Sciences and Pharmacy, University of Newcastle, Newcastle, Australia*

Objectives: Intracranial pressure (ICP) elevation after ischemic stroke may cause secondary damage. It has historically been accepted that ICP elevation following stroke is primarily caused by edema and therefore ICP only increases significantly after large strokes. Little is known about ICP in patients who have small infarcts. We have shown that ICP increases dramatically 24 hours after temporary intraluminal middle cerebral artery occlusion (MCAo) in animals with small infarcts and little edema. Preliminary data from our lab suggests that a change in CSF volume may contribute to the ICP elevation. This may be explained by choroid plexus ischemia, a known complication of the thread occlusion model. However, we have recently discovered that 24 hour ICP elevation can also occur in a cortical photothrombotic (PT) stroke model that induces submaximal infarction without choroid plexus damage. Animals with completed infarction had no ICP rise. Our aims were to use a cortical PT stroke model to: 1. Test whether the ICP elevation 24 hours post stroke occurs in the absence of choroid plexus ischemia. 2. Determine whether ICP elevation is associated with submaximal infarction (ischemic penumbra).

Methods: PT stroke was induced in male Wistar rats (n= 16) by intravenous infusion of 10 mg/kg Rose Bengal followed by illumination of the right parietal bone using either low light exposure (2 min at 0.13 W/cm^2) or the standard light

exposure (20 min at 0.3 W/cm^2), to produce submaximal or maximal infarct, respectively. Epidural intracranial pressure was measured at baseline and 19 – 25 hours following stroke. Infarct and edema volumes were measured histologically.

Results: Animals subjected to low light exposure had smaller infarcts than the standard light exposure group (9.3 ± 8.3 mm^3 *v.* 43 ± 18.8 mm^3, respectively, p<0.01). Smaller infarcts associated with low light exposure were restricted to the upper layers of the cortex, without damage to the choroid plexus or ventricles. Oedema volumes were 0.2 ± 0.4 mm^3 *v.* 2.82 ± 3.8 mm^3, p>0.05. ICP increased by 12.8 ± 2.5 mmHg from baseline only in animals exposed to low light (p<0.01), with no significant rise in the standard light group (1.9 ± 0.9 mmHg).

Conclusions: ICP elevation occurred approximately 24 hours after small cortical PT stroke. This indicates that early ICP elevation observed in previous studies is not simply a product of choroid plexus ischemia that may occur in the thread occlusion MCAo model. Significant ICP elevation was only observed in animals subjected to low light exposure, which has been shown to induce submaximal infarcts with a penumbra-like region at risk. PT strokes induced with standard light exposure were larger and clearly demarcated, consistent with reported absence of penumbra in this model. This group was not associated with ICP elevation. It is well known that that many molecular processes occur within the penumbra. We propose that the ICP elevation seen at 24 hours following stroke is triggered by an as yet unidentified active molecular mechanism in the ischemic penumbra.

653
BRAIN-0492
Poster Session

Cerebral Ischemia: Cellular and Molecular

LONG NON-CODING RNA FOSDT PROMOTES ISCHEMIC BRAIN DAMAGE BY INTERACTING WITH CHROMATIN MODIFYING PROTEINS

S.L. Mehta[1], T. Kim[1], J. Balog[1], R. Vemuganti[1]
[1]Neurological Surgery,
University of Wisconsin School of Medicine and Public Health, Madison, USA

Objectives: Ischemia induces extensive temporal changes in cerebral transcriptome that influences the neurologic outcome after stroke. In addition to protein-coding RNAs, many classes of noncoding (nc) RNAs like microRNAs (miRNAs) and long non-coding RNAs (LncRNAs; lincRNAs) also undergo changes in the post-stroke brain. We currently evaluated the functional significance of an lncRNA called Fos downstream transcript (FosDT) that was induced in rat brain after focal ischemia. We also evaluated if the association with chromatin modifying proteins (CMPs) Sin3A and coREST (corepressors of the transcription factor REST) and the resulting modulation of REST-downstream genes GRIA2 and NFKB2 is the mechanism of action of FosDT after stroke.

Methods: Focal ischemia was induced in adult rats by transient middle cerebral artery occlusion (MCAO). FosDT was silenced with a siRNA cocktail. Post-ischemic motor deficits were evaluated with rotarod, beam walk and adhesive removal tests between 1 to 7 days after ischemia. Infarct volume was estimated using Cresyl violet stained brain sections. Expression of Fos, FosDT and the down-stream genes was evaluated with real-time PCR. Binding of FosDT to CMPs was evaluated with RNA immunoprecipitation.

Results: Expression of FosDT, Fos and REST were induced significantly during the acute period (3h to 24h) of reperfusion following focal ischemia. FosDT knockdown resulted in significantly ameliorated post-ischemic motor deficits and resulted in smaller infarcts. FosDT binding to REST corepressor Sin3A and coREST was also significantly enhanced after focal ischemia. FosDT knockdown resulted in attenuation of REST downstream genes GRIA2 and NFKB2 without altering the levels of REST.

Conclusions: These studies indicate that induction of FosDT, its interactions with REST-associated CMPs and thereby regulation of REST-

downstream genes modulates ischemic brain damage and neurologic outcome. Thus, lncRNAs such as FosDT can be targeted therapeutically to minimize post-ischemic outcome in future.

654
BRAIN-0517
Poster Session

Cerebral Ischemia: Cellular and Molecular

REVERSAL OF IN VIVO ISCHEMIC LONG-TERM POTENTIATION CAUSED BY CARDIAC ARREST AND CARDIOPULMONARY RESUSCITATION IMPROVES SYNAPTIC FUNCTION

N. Quillinan[1], J.E. Orfila[1], G. Deng[2], P.S. Herson[2]
[1]Anesthesiology, University of Colorado, Denver, USA
[2]Pharmacology, University of Colorado, Denver, USA

Objective: Experience-dependent memory acquisition, *in vitro* tetanic stimulation and simulated ischemia results in long-term potentiation (LTP) of hippocampal CA1 synapses. The goal of this study was to determine whether *in vivo* cerebral ischemia results in iLTP of CA1 synapses. We hypothesized that iLTP resulting from CA/CPR prevents physiological LTP.

Methods: Cardiac arrest (8 minutes) followed by cardiopulmonary resuscitation (CA/CPR) or sham surgery was performed on adult (8-12 week) male mice. Electrophysiology was performed in hippocampal slices from sham and 7 and 30 days after CA/CPR. Field excitatory postsynaptic potentials (fEPSP) resulting from Schaffer collateral stimulation were recorded and rising slope was analyzed. Theta burst stimulation (TBS) was used for LTP induction and low frequency stimulation for reversal of LTP (depotentiation). Western blot analysis of synaptic isolations were performed from hippocampi collected from shams and 7 and 30 days after CA/CPR.

Results: TBS resulted in LTP of fEPSP to 164±9.8% (n=7, $P<0.05$) of baseline in sham controls, however no increase was observed at 7 (106±15.9% n=4) and 30 days (109±13.9% n=7) after CA/CPR. A depotentiation stimulus had no effect in sham controls (110±5.1%, n=6), but caused a 55% reduction in fEPSP in control slices that received LTP induction and 23% reduction in slices from CA/CPR mice. Importantly, in slices form CA/CPR mice, LTP induction protocol applied subsequent to depotentiation stimulus resulted in physiological LTP to 126.9±11.8% (n=3) of the original baseline, an effective increase of approximately 40%. Glutamate receptor subunit GluR1 phosphorylation and expression in synaptic fractions were increased at 7 and 30 days after CA/CPR.

Conclusions: Depotentiation in slices from CA/CPR mice suggests CA1 synapses are in a chronically potentiated state. Increased GluR1 phosphorylation and expression after CA/CPR also suggest *in vivo* ischemia causes iLTP. Our ability to induce physiological LTP after depotentiation in slices from CA/CPR suggests that reversing iLTP allows for normal synaptic plasticity. The results of this study are significant as they demonstrate *in vivo* iLTP and suggest a physiological stimulus has the potential to reverse synaptic impairments in the chronic phase after cerebral ischemia and reset synaptic function.

655
BRAIN-0378
Poster Session

Cerebral Ischemia: Cellular and Molecular

ABERRANT ACTIVATION OF APOPTOSIS SIGNAL-REGULATING KINASE 1 MEDIATES PRO-INFLAMMATORY AND NEUROTOXIC MICROGLIAL RESPONSES AFTER ISCHEMIC/REPERFUSION BRAIN INJURY

Y. Shi[1], H. Pu[1], X. Hu[1], R. Stetler[1], R. Leak[2], P. Zheng[3], Y. Gao[3], J. Chen[1]
[1]Neurology, University of Pittsburgh, Pittsburgh, USA
[2]Division of Pharmaceutical Sciences, Duquesne University, Pittsburgh, USA
[3]State Key Laboratory of Medical Neurobiology an d Institute of Brain Sciences, Fudan University, Shanghai, China

Objectives: Neuronal cell death and pro-inflammatory microglial reactions both contribute to the pathogenesis of ischemic/reperfusion (I/R) brain injury. However, the molecular interplay of these two events is still poorly understood. Apoptosis Signal-regulating Kinase 1 (ASK1) is a key mitogen-activated protein kinase kinase kinase (MAPKKK) that activates the JNK and p38 MAPK signaling cascades under conditions of ischemia or oxidative stress. In this study, we investigated the role of ASK1 in neuronal cell death and microglial neurotoxicity after I/R injury and identified the underlying mechanism. In addition, we tested whether targeting ASK1-dependent signaling pathways could improve long-term functional outcomes after I/R *in vivo*.

Methods: We created ASK1 kinase-dead (containing the catalytically inactive K716R mutation) knock-in mice (ASK1-ki) with universal loss of ASK1 kinase activity. Transient focal cerebral ischemia (tFCI) was induced by 60-min middle cerebral artery occlusion and reperfusion. Mice were randomly assigned to groups. Outcome measurements, including brain injury and sensorimotor and cognitive assessments, were performed up to 28 days after tFCI with strict adherence to STAIR guidelines. Cell-cell interactions were studied using transwell-based primary neuron and microglia co-cultures and lentiviral shRNA-mediated gene knockdown. Cell-permeable small peptides mimicking the docking sites on ASK1 for MKK3/6 (TAT-M3i) or MKK4/7 (TAT-M4i) were delivered into cultured cells or administered intranasally into mice after tFCI to inhibit ASK1-mediated p38 MAPK and JNK signaling pathways, respectively.

Results: tFCI induced robust activation of the ASK1/JNK/p38 signaling cascade in wild-type mice but not in ASK1-ki mice. The infarct size in ASK1-ki mice was significantly reduced by 41.8% at 28d ($p \leq 0.01$, n=8/group). ASK1-ki mice also showed improved long-term sensorimotor and cognitive performance after tFCI compared to wild-type littermates. In primary cultures, 60 min of oxygen-glucose deprivation (OGD) caused neuronal death (45-55% of total neurons) at 24h, which was attenuated by ~30% in neurons derived from ASK1-ki mice or in wild-type neurons treated with TAT-M4i. Conditioned medium from post-OGD neurons robustly activated microglia toward the cytotoxic M1 phenotype in co-cultures, resulting in increased release of neurotoxic cytokines and NO. These pro-inflammatory responses and neurotoxic effects were suppressed in microglia derived from ASK1-ki mice or wild-type microglia treated with TAT-M3i or shRNA targeting p38α MAPK. Consistent with the role of ASK1 in regulating microglial polarization, ASK1-ki mice exhibited markedly reduced expression of microglial M1 (but not M2) markers and decreased levels of pro-inflammatory cytokines 3d after tFCI compared to wild type littermates, as determined with quantitative PCR and cytokine-array assays, respectively. Finally, intranasal administration of TAT-M4i and TAT-M3i peptides (2, 24, and 48h after tFCI), but not either peptide alone, conferred long-term protection and improved sensorimotor and cognitive performance of wild type mice up to 35d after tFCI.

Conclusions: This study identifies a previously unexplored role for the ASK1 signaling cascade as an essential mediator of pro-inflammatory and pro-death neuron-microglia interactions in I/R

brain injury. Thus, inhibiting the ASK1 signaling cascade is a promising and clinically feasible therapeutic strategy with the potential to achieve sustained histological protection and long-term improvements of neurological function after stroke.

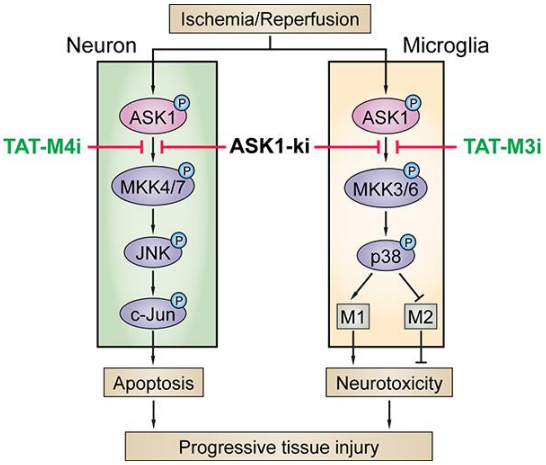

656
BRAIN-0325
Poster Session

Cerebral Ischemia: Cellular and Molecular

CASPASE-1 ACTIVATION LINKS DAMP-MEDIATED PERIPHERAL MONOCYTE ACTIVATION AND PYROPTOTIC LYMPHOCYTE CELL DEATH AFTER STROKE.

V. Singh[1], *S. Roth*[1], *A. Liesz*[1]
[1]*Institut für Schlaganfall- und Demenzforschung (I SD), Klinikum der Universität München, München, Germany*

Objectives: Ischemic brain injuries induces substantial peripheral immune alterations with a multiphasic pattern: While significant peripheral immune cell (over-)activation can be observed in the acute phase after stroke, the subacute phase after brain injuries is denoted by severe immune dysfunction and lymphocyte cell death. The mechanisms underlying these divergent immune alterations after stroke are largely unknown. Notably, the association between early innate immune cell activation and later lymphocytic immunosuppression is still unclear. In this study we evaluated the role of caspase-1, a proteolytic enzyme cleaved by inflammasomes, for immune activation and inflammatory cell death (pyroptosis) after acute brain ischemia.

Methods: Acute brain lesions were induced by transient focal brain ischemia (MCAO) in WT, caspase-$1^{-/-}$, $RAGE^{-/-}$ and $HMGB1^{-/-}$ mice. A different group of mice was treated with the specific caspase-1 inhibitor z-YVAD-FMK or control. We analyzed differential cell percentages of lymphocyte and monocyte subpopulations by flow cytometry. Pyroptosis as a cause of immune cell death was measured by intracellular caspase-1 labelling and membrane disruption by 7-AAD. Serum cytokine levels were analyzed by ELISA and cellular activation after stroke detected by intracellular cytokine assays. Results from experimental studies were validated by analyses of stroke patient samples and matched controls.

Results: We detected an early activation of monocytes and delayed lymphocyte death after murine MCAO. Monocyte activation was associated with enhanced expression of pro-inflammatory cytokines after stroke. In addition, we found a reduction in the percentages of splenic T cells and expansion of monocytes in the subacute phase after stroke. Genetic as well as pharmacological disruption of caspase-1 signaling abrogated on one side the early inflammatory reaction as well as subsequent lymphocyte pyroptosis. Attenuation of stroke-induced immune alterations in $RAGE^{-/-}$ and $HMGB1^{-/-}$ mice indicated a possible involvement of DAMP signaling underlying these effects. Furthermore, we observed increased plasma levels of caspase-1 and interleukin-1β in ischemic stroke and intracerebral hemorrhage patients. Notably, these inflammatory responses were positively correlated with the brain lesion volumes and immune dysfunction in stroke patients.

Conclusions: We detected caspase-1 as a key molecule in the regulation of post-stroke peripheral immunomodulation. It induces early monocyte activation as well as delayed pyroptotic lymphocyte death, thereby, suggesting a novel and comprehensive molecular target to treat the complex immune dysregulation after acute brain injuries.

657
BRAIN-0653
Poster Session

Cerebral Ischemia: Cellular and Molecular

PINEAL HORMONE MELATONIN WORKS VIA NEUROPROTECTIVE NOVEL MECHANISM; INTERLEUKIN-4 (IL-4) DEPENDENT M2 MICROGLIAL POLARIZATION, AFTER FOCAL CEREBRAL ISCHEMIA/REPERFUSION (FI/R)

J. Suenaga[1], L. Mao[1], X. Hu[1], H. Pu[1], J. Chen[1]
[1]Neurology,
Department of Neurology University of Pittsburgh, Pittsburgh, USA

Objectives;

Microgliarepresent rational but difficult therapeutic targets for stroke due totheir diverse phenotypes that playdual-faced protective (M2 phenotype) and toxic (M1 phenotype) effects. Previousstudy has shown that subcutaneous melatonin injection increased the level ofIL-4, the best known M2 inducing cytokine, in the blood. In this study, weinvestigated the role of melatonin in microglia M2 polarization and its effecton long-term recovery after stroke.

Methods;

Focal cerebralischemia was induced for 60 min FI/R. Animals were randomly assigned to receiveeither melatonin or vehicle treatmentat 2h after stroke. Brains were assessed for cerebral tissue loss at 3 and 14days of reperfusion. Neurological performance was analyzed up to 14 days afterischemia. Markers for microglia polarization were assessed usingimmunofluorescent staining and RT-PCR. Invitro experiments using primary microglia and in-transwell microglia-neuroncoculture were done to confirm the effect of melatonin on microglialinflammatory responses and its effect on microglia-potentiated neuronal injuryupon OGD.

Results;

Melatoninsignificantly reduced infarct volume and attenuated sensorimotor deficits 3-14day after FI/R. IL-4 deficiency, abolished melatonin-afforded long termprotection. Melatonin-treated mice showed significantly reduced expression ofinflammatory cytokine and chemokines, which is accompanied by significantlyincreased expression of M2 markers and decreased expression of M1 markers inmicroglia. In primary microglial cultures, melatonin inhibited LPS (a M1inducer)-induced production of NO and TNFα, confirming that melatonin hasdirect anti-inflammatory effect on microglia. Furthermore, melatoninameliorated the neurotoxic effect of M1 microglia on OGD neurons, and thiseffect was absent in IL-4 deficient microglia.

Conclusions;

Melatoninmay represent an innovative therapeutic strategy that shifts microgliapolarization toward a protective M2 phenotype in an IL-4-dependent manner andthus enhance long-term recovery after stroke.

658
BRAIN-0112
Poster Session

Cerebral Ischemia: Cellular and Molecular

SERIAL CHANGE FOR PHOSPHODIESTERASE 3A AND 3B EXPRESSION AFTER TRANSIENT FOCAL ISCHEMIA IN MICE BRAIN

T. Urabe[1], Y. Mitome-Mishima[2], N. Miyamoto[1], R. Tanaka[3], H. Oishi[4], H. Arai[2], N. Hattori[3]
[1]Department of Neurology, Juntendo University Urayasu Hospital, Urayasu, Japan
[2]Department of Neurosurgery, Juntendo University School of Medicine, Tokyo, Japan
[3]Department of Neurology, Juntendo University School of Medicine, Tokyo, Japan
[4]Department of Neuroendovascular Therapy, Juntendo University School of Medicine, Tokyo, Japan

Objectives: Phosphodiesterasetype 3 (PDE3) is a superfamily of enzymes involved in the degradation of cyclicadenosine monophosphate (cAMP) and cyclic guanosinemonophosphate (cGMP). PDE3A and PDE3B of two different gene products have beenidentified as part of the PDE3 family. However, the distribution of PDE3A andPDE3B in mammalian forebrain has not been elucidated. Inhibition of PDE3increases the intracellular levels of cAMP by suppressing its conversion intoAMP, which could increase cAMP-responsive element binding protein (CREB)phosphorylation and induce subsequent activation of various target genesrelated to neuronal survival, learning and memory, and neurotrophic factors. In the presentstudy, we used a mouse model of transient focal ischemia to examine the expressionof PDE3A and PDE3B in the forebrain by immunohistochemistry. In the next step,we evaluated the expression profiles of PDE3A and PDE3B in the ischemicboundary zone (IBZ) after focal ischemia, and analyzed the relationship betweentheir expression and CREB phosphorylation.

Methods: Allanimal procedures were approved by the Animal Care Committee of Juntendo University.Adult male C57BL/6 mice weighing 20–25 g underwent transient focal ischemia,which was induced by intraluminal middle cerebral artery occlusion using an 8-0nylon monofilament coated with silicone resin and a hardener. Immunohistochemistry,double immunofluorescence histochemistry, and Western blotting for PDE3A andPDE3B, several neuronal and glial markers, phosphorylated CREB (p-CREB), B-cellleukemia/lymphoma 2 protein (Bcl-2), and brain derived neurotrophic factor (BDNF)were analyzed at baseline and at days 1, 3, and 7 after ischemia.

Results: Thenumber of PDE3A-positive cells (neurons and endothelial cells) remainedunchanged, while PDE3B-positive cells gradually increased afterischemia/reperfusion ($P<0.001$). In the corpus callosum, PDE3B was expressedin oligodendrocytes, oligodendrocyte progenitor cells, and astrocytes.PDE3B-expressing astrocytes showed gradual increase after ischemia/reperfusion($P<0.001$). In the cortex, the majority of PDE3B-expressing cells beforeischemia were neurons, though few were astrocytes. Ischemic insult resulted ingradual and time dependent increase in the number of PDE3-positive cells in theIBZ area of the cortex and corpus callosum at days 1, 3, and 7 after reperfusion($P<0.05$). Expression of BDNF and Bcl-2 was detected in pCREB-positive cells,not in PDE3B-positive cells.

Conclusions: Thepresent results identified the expression of PDE3A/B in neurons, astrocyte andoligodendrocyte lineage cells in the normal brain, and increased number of PDE3B-expressingcells after focal transient brain ischemia. Our findings suggest that thepattern of PDE3B brain localization could play a crucial pathophysiological rolein ischemic brain damage, and that regulation of PDE3B production could protectagainst the progression of ischemic brain damage.

References:Mitome-Mishima Y, Miyamoto N, Tanaka R,Oishi H, Arai H, Hattori N, Urabe T:

Differences in phosphodiesterase3A and 3B expression after ischemic insult. Neurosci Res 75: 340-348,2013.

659
BRAIN-0450
Poster Session

Cerebral Ischemia: Cellular and Molecular

DETERMINATION OF MICRO-RNA PROFILES IN EXTRACELLULAR VESICLES ISOLATED FROM SERUM OF HUMAN STROKE PATIENTS.

J.C. van Kralingen[1], C.R. Breen[1], C. Groome[2], C. McCabe[3], I.M. Macrae[3], J. Dawson[1], L. Work[1]
[1]Institute of Cardiovascular and Medical Sciences, University of Glasgow, Glasgow, United Kingdom
[2]School of Medicine, University of Glasgow, Glasgow, United Kingdom
[3]Institute of Neuroscience and Psychology, University of Glasgow, Glasgow, United Kingdom

Stroke is the 3rd leading cause of death in the UK and the leading cause of long-term adult disability. There is only one licensed pharmacological intervention, intravenous delivery of thrombolytic recombinant tissue plasminogen activator within 4.5 hours of stroke, beyond which time there are significant haemorrhagic risks. An alternative intervention is needed and through their ability to alter the expression of multiple genes involved in stroke pathophysiology miRNAs offer a novel therapeutic intervention. miRNA expression is altered in experimental stroke and in patients with stroke. Recently, active transport of miRNA in extracellular vesicles (EV), such as exosomes, has been demonstrated pre-clinically between cells in atherosclerosis. We hypothesised that miRNAs packaged in EV would differ between patients with stroke and patients without stroke, raising the potential for novel miRNAs to be used as biomarkers or therapeutic agents for modulation.

We recruited 169 patients with suspected stroke and a blood sample was taken at 48h post-stroke. All participants gave full informed consent and the study was approved by the Scotland A Research Ethics Committee. A miRNA microarray was performed (Openarray™ platform) on samples from 39 patients (n=10 non-stroke, n=29 with stroke – further subdivided by TOAST classification into large artery (n=9), cardioembolic (n=10) or small vessel disease (n=10) stroke). Validation of results was performed using samples from 169 patients. EVs were isolated from 200 µL serum before RNA was extracted and the concentration determined using nanodrop spectrophotometry. Taqman™ real-time quantitative polymerase chain reaction was used to determine the expression levels of specific miRNA(s).

The microarray identified 26 miRNAs that were significantly dysregulated between stroke vs non-stroke patients or between specific TOAST subtypes and non-stroke control. Of these, changes in 17 miRNA were validated in the larger cohort: levels of miRNAs -17 (relative quantification, RQ vs non-stroke=1.74*), -20b (RQ, vs non-stroke=1.95*), -27 (RQ, vs non-stroke=1.83*), -30a-5p (RQ, vs non-stroke=1.67*), -93 (RQ, vs non-stroke=1.80*), -199a-3p (RQ, vs non-stroke=1.91*) and hsa-let-7e (RQ, vs non-stroke=1.61*) were significantly increased in stroke vs non-stroke patients (*$p<0.05$ by unpaired Student's t-test). Furthermore, differences between TOAST subtypes were shown with small vessel disease consistently having the highest levels of miRNA. There was no significant difference observed in the expression of 10 miRNAs including miRNAs-520b (RQ, vs non-stroke=1.09), -660 (RQ, vs non-stroke=1.21) and -218 (RQ, vs non-stroke=1.57) between non-stroke and stroke patients. Bioinformatic analysis highlighted a number of important target genes implicated in stroke pathophysiology for each miRNA including genes involved in the regulation of apoptosis, angiogenesis and cell migration.

We have identified and validated changes in EV packaged miRNA expression in patients with stroke across differing stroke subtypes. This will direct future studies looking into paracrine signalling in the setting of stroke and the modulation of specific miRNAs as a novel therapy in the setting of experimental stroke.

660
BRAIN-0275
Poster Session

Cerebral Ischemia: Cellular and Molecular

NEURONAL SOLUBLE FAS LIGAND DRIVES M1-MICROGLIA POLARIZATION AFTER ISCHEMIA

H. Meng[1], X. Li[1], D. Ye[1], L. Weng[1], Y. Chen[1], Y. Xu[1]
[1]Department of Neurology,
the Affiliated Drum Tower Hospital of Nanjing University Medical School, Nanjing, China

Objectives: Post-stroke immune and inflammatory responses play important roles in the pathogenesis of ischemic stroke. Microglia act as sensors of disturbance in CNS and can polarize to pro-inflammatory (M1) and anti-inflammatory (M2) phenotype responding to different stimuli. The Fas ligand (FasL)-Fas system has been implicated in a number of pathogenic states including inflammatory cascades. However, the FasL expression in neuron and the potential role of neuronal soluble Fas ligand (sFasL) in modulating microglial phenotype are not well understood.

Methods: *In vivo*, middle cerebral artery occlusion (MCAO) was induced for 1 h followed by 6h, 24h and 72h of reperfusion in both FasL mutant *gld* mice and wild-type control C57BL/6J mice. Expression of FasL in the ischemic brain was detected by western blot. Microglial morphology and function were determined by immunohistochemical staining, flow cytometry and real-time polymerase chain reaction (PCR). *In vitro*, primary cortical neuronal culture and microglial culture were prepared separately, and neuron-microglia coculture was also used to assess the molecular crosstalk between neuron and microglia. Cortical neuronal culture and coculture were subjected to oxygen glucose deprivation (OGD) for 30 min following by 6h of reperfusion. sFasL level in the culture supernatant was evaluated by ELISA assay. Meanwhile the neuronal-conditioned medium was applied to primary microglia. PCR, CBA assay and flow cytometry were used to evaluate M1/M2 microglial phenotypes. Furthermore, exogenous sFasL stimulation was used to confirm effects of sFasL on microglia polarization, and FasL neutralizing antibody and neuronal culturs prepared from *gld* mice were employed to block FasL actions. STAT3 activity in microglia was inhibited by the specific inhibitor AG490. Expression of total STAT3, phosphorylated STAT3 (Y705 and S727), CCL5 were examined by western blot.

Results: *In vivo*, the expression of FasL protein and M1-microglial phenotype markers (iNOS and CD86) were increased in wild-type mice after MCAO, which were attenuated in *gld* mice. *In vitro*, the expression of sFasL was increased after OGD-induced neuronal injury. Both neuron OGD conditioned medium and exogenous sFasL treatment could induce the microglial polarization toward M1 phenotype. However, this M1 phenotype shift was blocked with the utilization of neutralizing antibody or *gld* neuronal culture. Consistently, phosphorylated STAT3 (Y705 and S727) and CCL5 levels were increased in microglia after neuronal-conditioned medium or exogenous sFasL treatment, and accordingly decreased when FasL was inhibited.

Conclusions: Ischemic neuronal injury triggers the release of sFasL, which contributes to M1-microglial polarization. The underlying mechanisms may involve the phosphorylation of STAT3.

661
BRAIN-0288
Poster Session

Cerebral Ischemia: Cellular and Molecular

DOUBLE NEGATIVE T LYMPHOCYTES FROM GLD MICE UP-REGULRATE M2 MICROGLIA IN ISCHEMIC STROKE THROUGH FAS/FASL

L. Weng[1], D. Ye[1], H. Meng[1], X. Li[1], Y. Chen[1], Y. Xu[1]
[1]Department of Neurology,
the Affiliated Drum Tower Hospital of Nanjing University Medical School, Nanjing, China

Objectives: The crosstalk between T lymphocyte and microglia plays an important role in ischemia

reperfusion injury. The FasL mutation *gld* mice demonstrated attenuated ischemic brain damage after experimental stroke, with double negative (DN) T lymphocytes accumulating in peripheral blood and spleen. However the biological actions of DN T lymphocytes are no clear. This study aims to explore the effects of DN T lymphocytes in experimental stroke.

Methods: *In vivo*, the subtypes of T lymphocytes and microglia in brain tissue after cerebral ischemia were measured by flow cytometry and immunofluorescence. *In vitro*, different subtypes T lymphocytes isolated from C57BL/6 or *gld* mice were co-cultured with primary microglia, which were subjected to different treatments. Flow cytometry and Real-time PCR were used to measure the phenotype of primary microglia. CBA and ELISA assay were used to quantify the levels of cytokines and chemokines.

Results: DN T lymphocytes were accumulated in ischemic cerebral hemisphere in *gld* mice 3 days after MCAO, the percentage of CD4+ or CD 8+ T lymphocyte were slightly decreased in *gld* mice, compared with wild type C57BL/6 mice. Meanwhile, the activation of microglia in ischemic tissue was alleviated in *gld* mice. Compared to wild type C57BL/6 mice, A shift to alternative-activated microglia rather than classical-activated microglia was observed in *gld* mice. *In vitro*, primary microglia underwent a shift to alternative-activated microglia when co-cultured with different subtypes of T lymphocytes isolated from spleen in *gld* mice, whereas emerged a shift to classical-activated microglia when co-cultured with T splenic lymphocytes isolated from C57BL/6 mice. In addition, pro-inflammatory cytokines like IL-1β, TNF-α and MCP-1 secreted by microglia and T lymphocytes were decreased, anti-inflammatory cytokines such as IL-4, IL-10 and TGF-βwere increased when primary microglia co-cultured with CD4+ T lymphocytes and DN T lymphocytes separated from *gld* mice.

Conclusions: The neuroprotective effects in *gld* mice may be related to the immune regulation of DN T lymphocytes on microglial polarization in stroke. The new understanding on DN T lymphocytes may provide additional views on post-stroke immune regulation.

662
BRAIN-0105
Poster Session

Cerebral Ischemia: Cellular and Molecular

HYPERGLYCEMIA AND POST-STROKE SEIZURES

Z. Lei[1], L. Xia[1], Z. Shi[1], Z. Xu[1]
[1]Anatomy & Cell Biology,
Indiana University School of Medicine,
Indianapolis, USA

Seizures are the most common neurological sequelae of stroke and are considered as a major cause of epilepsy. Diabetes mellitus has been identified as an independent predictor of acute seizures in stroke patients. However, the pathogenesis of post-stroke seizures in diabetes is not fully understood. It is well known that abrupt increase of neuronal excitability causes seizures/epilepsy. Potassium currents are important to maintain the baseline membrane potential and regulate neuronal excitability. Accumulating evidence indicates that down regulation of A-type potassium current (I_A) is associated with seizures after stroke by increasing neuronal excitability. The present study tested the hypothesis that down-regulation of I_A contributes to seizure generation after ischemia in diabetes and explored its underlying mechanisms.

Transient forebrain ischemia was produced in adult Wistar rats using the 4-vessel occlusion (4-VO) method. Hyperglycemia (>300 mg/dL) was induced by injection of glucose solution (i.p.) 15 min prior to ischemia. The seizure activity was defined using the Racine scale of III - V. The expression of potassium channels was analyzed by immunohistochemical staining and Western blotting. The alteration of I_A and excitability of hippocampal neurons was examined using patch-clamp techniques in brain slices.

The incidence of seizures after ischemia significantly increased in hyperglycemic rats

(100%) as compared to the normoglycemic ones (0%). The neuronal damage in the cortex and hippocampus after ischemia was about the same in these two groups of animals, suggesting that neuronal injury is not the major contributor to seizure generation in hyperglycemia. The brain water content after ischemia in hyperglycemic rats was significantly higher than the control ones, indicating the severe edema in hyperglycemic brains. However, administration of Mannitol (1.5 g/Kg, i.v.) reduced the brain edema but the seizure rate remained the same after ischemia (100%), suggesting that brain edema is not the major cause of post-stroke seizure in hyperglycemia. On the other hand, immunohistochemistry and protein analysis showed a significant reduction of I_A channel subunit Kv4.2 expression in hyperglycemic rats with seizures. Electrophysiological data also showed that the current density of I_A in hippocampal neurons was reduced in hyperglycemic rats after ischemia and the neuronal excitability was increased.

There results demonstrate that hyperglycemia facilitates seizures generation after ischemia. The down-regulation of I_A in hippocampal neurons might contribute to the post-ischemic seizure generation in hyperglycemia.

663
BRAIN-0144
Poster Session

Cerebral Ischemia: Cellular and Molecular

20-HETE IS DIRECTLY INVOLVED IN NEURONAL INJURY IN AN IN VITRO MODEL OF ISCHEMIA

Z. Yang[1], H. Zhang[1], J. Falck[2], R. Koehler[1]
[1]ACCM, Johns Hopkins School of Medicine, Baltimore, USA
[2]Biochemistry, University of Texas Southwestern Medical Center, Dallas, USA

Objectives: 20-Hydroxyeicosatetraenoic acid (20-HETE), an arachidonic acid metabolite from cytochrome P450 (CYP) families with w-hydroxylase activity, such as CYP4A and 4F, is involved in the pathophysiological process of adult focal cerebral ischemia and neonatal hypoxia-ischemia. Although it had been postulated that 20-HETE may act as a potent vasoconstrictor of cerebral microvessels after brain ischemia, our work showed that neuroprotection of 20-HETE synthesis inhibitors in immature brains appears to be independent of cerebral blood flow (CBF) and relates to changes of key proteins involved in excitotoxicity. Results from oxygen-glucose deprivation (OGD) in hippocampal slices also indicate a toxic effect of 20-HETE independent of CBF. Moreover, we found CYP4A immunopositive neurons in ischemic brains, thereby suggesting that neuronal 20-HETE induction after brain ischemia may exacerbate neuronal injury. Here, we tested the hypothesis that CYP 4A and 4F isoforms can be induced in primary cultured neurons and that 20-HETE can directly lead to neuronal cell death after OGD.

Methods: Primary cortical neurons were isolated from embryonic day 16-17 mice or rats and cultured for 7-9 days before OGD. OGD was initiated by replacing medium with deoxygenated and glucose-free solution and exposing cells to humidified 95%N_2/5% CO_2 at 37 °C for different time periods using a modular incubator chamber. After OGD, cells were replaced with medium with glucose under normoxia condition in humidified 95% air/5% CO_2 at 37 °C for different additional periods. Control cells were replaced with medium with glucose and exposed to hypoxia and reoxygenation for the same duration.

Results: Double-immunostaining results indicated that CYP4A signals were widely distributed in cortical neurons of P7 mice and cultured neurons. Results from CellTiter Blue cell viability assay and propidium iodide staining both indicated that around 40% neurons were dead at 24h after 1h OGD. Quantitative real-time PCR analysis showed significant induction of CYP4F1 and 4F4 mRNA at 1h after OGD and significant induction of CYP4A8 and 4F1, 4F5, and 4F6 at 3h after OGD. At the same time, media 20-HETE levels were significantly increased at 3h after OGD. HET0016 administration reduced 20-HETE production and protected neurons from OGD insult (75 ± 5%,

mean ± SD). That protection could be diminished by co-administration of 20-HETE stable mimic 20-5,14-HEDGE (52 ± 10%). In addition, treatment with 50 μM of the 20-HETE antagonist 20-6,15-HEDGE protected neurons from OGD insult. Pan-caspase inhibitor z-VAD-fmk, PARP inhibitor DR2313, and RIP1 inhibitor necrostatin-1 all attenuated OGD-induced neurotoxicity and kept 73%, 82%, and 88% neurons viable, respectively.

Conclusions: We conclude that 20-HETE can be directly induced in neurons after reoxygenation from *in vitro* ischemia and that 20-HETE augments neuronal cell death through caspase-dependent apoptosis, PARP-dependent parthanatos, and RIP1-dependent necroptosis.

664
BRAIN-0208
Poster Session

Cerebral Ischemia: Cellular and Molecular

INVOLVEMENT OF MIR-181C IN CLINICAL ACUTE ISCHEMIC STROKE AND EXPERIMENTAL STROKE

H. Zhao[1], Z. Tao[1], R. Wang[1], F. Yan[1], X. Ji[1], Y. Luo[1]
[1]Cerebrovascular Diseases Research Institute, Xuanwu hospital of Capital Medical University, Beijing, China

Objectives Though the investigation of microRNA-181 family in acute stroke is available, the role of miR-181c in clinical stroke and experimental stroke has not been characterized. In present study we profiled the miRs in the peripheral lymphocyte of acute stroke patients and healthy persons, and analyzed the clinical relevance of miR-181c in ischemic stroke, and then researched the effect and mechanism of miR-181c in experimental stroke.

Methods The peripheral lymphocyte from blood sample of acute stroke patients and healthy persons was collected, and analysed with miRNA array and Real time PCR. In *in vitro* experiment, neuro2a cells were exposed to H_2O_2 and treated with miR-181c agomir. Cell viability was evaluated using CCK-8 Kit and lactate dehydrogenase (LDH) release assay. The expression of activated caspase-3 in neuro2a cells was determined by western blotting. For in vivo study, focal ischemia was induced in mouse by transient middle cerebral artery occlusion (tMCAO), and the mice were administered with miR-181 agomir immediately after ischemia by intracerebroventricular injection. The infarct volume was detected using TTC after 45 minute ischemia and 24 hour reperfusion. The expression of activated caspase-3 and Bax in ipsilateral brain tissue was analyzed by western blotting.

Results We identified 70 down-regulated and 35 up-regulated miRs (>2-fold change) by differential analysis in the miRNAs expression profile of peripheral lymphocyte of acute stroke patients. The 7 randomly selected deregulated miRs (miR-99b, -181c, -181d, -212, -424, and -532-5p) were verified in patients' plasma by qRT-PCR. Levels of hsa-miR-99b, -181c, and -424 was significantly decreased in the plasma of stroke patients compared with normal persons, consistent with the result of miRNA array of lymphocytes, though the relative fold change was not as significant as that in lymphocytes. Levels of hsa-miR-181d and -532-3p decreased as well in the plasma of stroke patients, and has-miR-212 level in the plasma of stroke patients increased with no statistical significance, inconsistent with the result of miRNA array of lymphocytes. Levels of miR-181c in the plasma was positive correlated with neutrophils percentage, blood platelet count and ApoB levels, while was negative correlated with lymphocyte percentage. In neuro-2a cells exposed to H_2O_2, miR-181c reduced cell viability and increased LDH release, as well as increased the expression of activated caspase-3. In tMCAO mouse model, miR-181c increased the level of caspase-3 and Bax in ipsilateral brain tissue, while had no act on cerebral infarction volume.

Conclusions In summary, we screen out and verified a significantly decreased miR-181c from a miRNAs expression profile in lymphocytes of acute stroke patients. Correlation analysis of clinical parameters showed that miR-181c is a potential risk factor of acute stroke. MiR-181c agomir aggravates the neural cell apoptosis in vitro and in vivo, while had no significant function

on cerebral infarction volume.

665
BRAIN-0226
Poster Session

Cerebral Ischemia: Reperfusion

COMBINED LATE TISSUE PLASMINOGEN ACTIVATOR AND ISCHEMIC POSTCONDITIONING: POSSIBLE ROLE OF REPERFUSION REDUCTION IN NEUROPROTECTION FOLLOWING EMBOLIC STROKE

M. Allahtavakoli[1], J. Mashayekhimazar[1]
[1]Physiology,
Rafsanjan University of Medical sciences,
Rafsanjan, Iran

Objective: It has been reported that ischemic postconditioning (iPC) changes the reperfusion pattern in permanent or transient models of stroke and confers neuroprotection. However, the effects of iPC on reperfusion induced by tissue plasminogen activator (tPA) in the embolic model of stroke have not been yet investigated.

Materials and Methods: Rats were subjected to embolic stroke by injection of a preformed clot into the middle cerebral artery and randomly assigned to vehicle (saline 0.1 ml/100 g; i.v.), tPA (3 mg/kg; i.v.), iPC or iPC+ tPA (3 mg/kg; i.v.). Saline or tPA was injected at 6 h after embolic stroke and iPC was conducted at 6.5 h after ischemia, by a total of five cycles of 10 sec occluding and 30 sec of reopening of bilateral CCAs. Cerebral blood flow was monitored by Laser-doppler flowmetry (LDF) from the time of tPA injection up to 60 min. Infarct size, blood brain barrier disruption, brain edema, neurological deficits, reactive oxygen species (ROS) level and apoptosis were measured 2 days later.

Results: Compared to the control or tPA groups, iPC and iPC+tPA decreased infarct volume, but iPC+tPA was more neuroprotective than iPC alone. While tPA alone dramatically increased CBF, conducting iPC caused a slow and gradual increase in CBF. Combination of iPC+tPA reduced BBB leakage, brain edema, TUNEL-positive cells and ROS levels. Conducting iPC alone also decreased BBB disruption, brain edema, apoptosis or ROS levels. Furthermore, Combination of iPC+tPA increased grasping ability or sensory-motor function and decreased neurological deficits at 48 h following stroke.

Conclusion: Based on our data, iPC allowed a gradual reperfusion pattern after delayed thrombolysis with tPA and hampered malignant hyperemia or reperfusion injury.

666
BRAIN-0623
Poster Session

Cerebral Ischemia: Reperfusion

ANGIOTENSIN-(1-7) INCREASES TISSUE SALVAGE FOLLOWING FOCAL CEREBRAL ISCHAEMIA WITH REPERFUSION.

M. Arroja[1], E. Reid[1], W. Holmes[1], S. Nicklin[2], L. Work[2], C. McCabe[1]
[1]Glasgow Experimental MRI Centre (GEMRIC) Institute of Neuroscience & Psychology College of Medical Veterinary & Life Sciences,
University of Glasgow, Glasgow, United Kingdom
[2]BHF Glasgow Cardiovascular Research Centre Institute of Cardiovascular & Medical Sciences College of Medical Veterinary & Life Sciences,
University of Glasgow, Glasgow, United Kingdom

Objective: Recent studies have demonstrated that pre-treatment with centrally administered Ang-(1-7) has beneficial effects in ischaemic stroke models[1]. However, its actions during cerebral ischaemia/reperfusion injury and impact on tissue salvage, neurological score (NS) and blood pressure (BP) as a post-stroke treatment have not yet been fully investigated. In this study we determined the effect of post-stroke central administration of Ang-(1-7) on the extent of tissue salvage following transient middle cerebral artery occlusion (tMCAO).

Methods: All procedures were performed under license from the UK Home Office and approved by the University Ethical Review Panel. tMCAO was

performed in male Wistar rats (300-382g; n=13) via the intraluminal filament model. An 18 point NS was carried out prior to tMCAO, at 3 and 7 days post tMCAO. Conscious systolic BP was measured prior to and at 7 days post tMCAO. Rats were randomised and surgeon was blinded to either artificial cerebrospinal fluid (aCSF; 1µl/h; n=8) or Ang-(1-7) (1.1nM; 1µL/h; n=5) treatment delivered intracerebroventricularly (i.c.v) as a continuous infusion at reperfusion for 7 days. Magnetic resonance angiography (MRA) was undertaken in a Bruker 7T Pharmascan MRI scanner to confirm MCA occlusion and at day 7 to confirm reperfusion. Ventricle cannulation was confirmed with T_2 weighted MRI. Diffusion weighted imaging (DWI) was performed at 30 and 60min post MCAO to calculate lesion volume during ischaemia. Rats were reperfused 90min following tMCAO and final infarct volume determined at day 7 by T_2 weighted MRI. Thresholded apparent diffusion coefficient (ADC) maps, generated from DWI were used to define ischaemic lesion volumes. Final infarct size was calculated by manually delineating hyperintense regions on T_2-weighted images using ImageJ. The lesion volume at 60min post MCAO was used to calculate the effect of treatment on infarct evolution. Data are presented as Mean±SD.

Results: ADC lesion volumes at 30 & 60min post MCAO were not significantly different between aCSF and Ang-(1-7) groups (30min: 159.9±57.3mm^3 & 137.3±32.0mm^3, 60min: 184±49mm^3 & 169.7±60.3mm^3, respectively). Following 7 days of treatment, final infarct volume was not significantly different between aCSF and Ang-(1-7) treatment groups (150.5±59.4mm^3 vs 106.4±60.9mm^3, respectively). When normalising data to lesion size at 60min ischaemia, Ang-(1-7) infusion with reperfusion decreased lesion volume to a greater extent than aCSF alone (40.9±13.4% vs 20.1±14.4% lesion volume reduction from 60min post MCAO to 7 days post reperfusion, $P<0.05$; Figure 1). There were no significant differences in NS between aCSF and Ang-(1-7) groups prior to MCAO, at 3 and 7 days post reperfusion. Systolic BP was comparable between treatment groups prior to MCAO (103±20mmHg vs 107±13mmHg for aCSF & Ang-(1-7) groups, respectively) and treatment had no significant effect on BP at day 7 post tMCAO (122±19mmHg vs 124±22mmHg).

Conclusion: This study demonstrated that central infusion of Ang-(1-7) following reperfusion increased tissue salvage when compared to vehicle treatment, with no effect on systemic BP. This highlights the therapeutic potential of Ang-(1-7) post-stroke.

References:

1. Mecca AP., Regenhardt RW., O'Connor TE., Joseph JP., Raizada MK., Katovich MJ & Sumners C (2011). Cerebroprotection by Angiotensin (1-7) in Endothelin-1 induced Ischemic Stroke. *ExpPhysiol* 96: 1084-96.

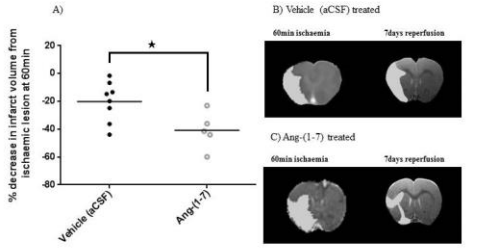

Figure 1 Effects of Ang-(1-7) treatment in infarct volume following tMCAO. **A)** Percentage decrease in infarct volume from ischaemia lesion at 60min to 7 days reperfusion in vehicle (aCSF; 1µl/h; n=8) and Ang-(1-7) (1.1nM; 1µl/h; n=5) treated animals. *P<0.05 versus aCSF (unpaired students *t* test). **B) & C)** Median rat from vehicle and Ang-(1-7) treated groups showing ADC lesion at 60min post MCAO and T_2 weighted infarct at 7 days post reperfusion (highlighted in whiter regions).

667
BRAIN-0361
Poster Session

Cerebral Ischemia: Reperfusion

ISCHEMIC INJURY MONITORED WITH A NOVEL MICROPERFUSION DEVICE UNVEILS THE ROLE OF PH IN I/R INJURY

S. Bhowmick[1], J. Moore[2], K. Drew[2]
[1]Department of Chemistry and Biochemistry Institute of Arctic Biology,
University of Alaska Fairbanks, Fairbanks, USA
[2]Institute of Arctic Biology,
University of Alaska Fairbanks, Fairbanks, USA

Objective: Ischemia and reperfusion (I/R) causes neuronal injury due to disruption in ion homeostasis including acidosis. Acidosis is a common feature of ischemia and assumed to play a critical role in brain injury. Previous study shows that low pH modulates NMDAR, AMPAR and acid sensing ion channels (ASIC); however, the mechanism is not clear. This study tests the hypothesis that mild acidosis protects against I/R injury via modulation of NMDAR, but produces injury via activation of AMPAR and acid sensing ion channels (ASIC1a). To test this hypothesis we monitored the time course of cerebral I/R injury using a novel microperfusion system to define the role of pH in neuronal injury and protection.

Methods: Hippocampal brain slices (400 micron) from rat (3- 4 months) were subjected to conditions that mimicked I/R in vivo. Perfusates were collected every 15min and analyzed for glutamate efflux and neuronal injury (LDH release). Role of pH was deciphered by treating the slices with mild acidosis (artificial cerebrospinal fluid, pH=6.4) with and without ASIC, NMDAR antagonists or AMPAR agonists.

Results: With this preparation, our results show that injury due to OGD insult or low pH is ischemic based and low pH delays OGD induced neuronal injury. In addition, our result support that injury mediated by low pH or low pH OGD is caused in part by ASIC1a and is independent of NMDAR or AMPAR.

Conclusions: Previous studies decipher the role of ASIC mediated injury caused by low pH during OGD in cortical and hippocampal cultures. Another study shows a role for ASIC in an in vivo rodent model of stroke; however, a clear understanding of the acute phase of injury in adult tissue is still elusive. Our microperfusion technique monitors the acute phase injury associated with OGD or reperfusion, the time course of injury and the effects of low pH in acute hippocampal adult slices. Our results supports that low pH has both protective and damaging effects; the injury being caused in part by ASIC but does not involve NMDAR suggesting that injury during low pH OGD inhibits NMDAR but produces an ASIC-mediated injury that is as deleterious as NMDAR mediated injury. These findings may help the design of novel therapeutic neuroprotective strategies for brain ischemia by targeting ASIC as one of the candidate for treatment of I/R caused by stroke and cardiac arrest.

668
BRAIN-0368
Poster Session

Cerebral Ischemia: Reperfusion

TOLERANCE TO ISCHEMIA IS MODULATED IN PART VIA TARGETING NITRIC OXIDE SIGNALING PATHWAY BY AN ENDOGENOUS FACTOR, NEUROGLOBIN

S. Bhowmick[1], K. Drew[1]
[1]Department of Chemistry and Biochemistry/ Institute of Arctic Biology,
University of Alaska Fairbanks, Fairbanks, USA

Objective: Cerebral ischemia/ reperfusion (I/R) injury is due to the initiation of a cascade of events that produces toxic levels of nitric oxide (NO) and superoxide ($O_2^{\cdot-}$) that combines to produce a more potent oxidant, peroxynitrite ($ONOO^-$). Neuroglobin (Ngb), a globin family of protein expressed in brain neurons exhibit high binding affinity for NO, $O_2^{\cdot-}$ and $ONOO^-$. Ngb overexpression in cultures of fetal neurons and transgenic models provide protection against cerebral I/R injury [2,3,4,5,6], however, the

mechanism by which Ngb increases resistance to I/R injury or if Ngb protects against injury in a natural model of high Ngb expression are not well understood. Previous studies have revealed that the Arctic Ground Squirrel (AGS) is a natural model of high Ngb expression that tolerates I/R better than rats [1]. This study tests the hypothesis that Ngb attenuates neuronal injury by detoxifying $ONOO^-$ generated during cerebral I/R.

Methods: The approach is designed specifically for in vitro study of cerebral I/R in hippocampal slices [7]. Hippocampal slices (400 micron) from rat and AGS were subjected to oxygen glucose deprivation (OGD) to mimic I/R in vivo using a novel microperfusion technique. Injury consisted of exposing the brain slices to: 1) NO, $O_2^{\cdot-}$, $ONOO^-$ donors with and without OGD; 2) pretreatment of slices with inhibitors of NO, $O_2^{\cdot-}$ and $ONOO^-$ followed by manipulation 1. In control slices, treatment was administered by switching to standard aCSF. Perfusates were collected every 15 min and analyzed for LDH release, an indicator of cell death and nitrosylation of protein, a marker for $ONOO^-$ mediated injury..

Results: Results show the effect of NO, $O_2^{\cdot-}$ and $ONOO^-$ mediated injury in ischemic tolerant AGS and ischemic susceptible rat species. 1) Effect of NO mediated Injury: NO donor alone is not sufficient to aggravate injury but with OGD enhances the neuronal injury higher in rat than AGS; an inhibitor of nNOS attenuates injury in rat but no effect in AGS. 2) Effect of $O_2^{\cdot-}$ mediated injury: $O_2^{\cdot-}$ donor alone caused injury to a greater extent in rat than AGS and the injury aggravates along with OGD; an SOD mimetic attenuates injury in rat but no effect in AGS. 3) Effect of $ONOO^-$ mediated injury: $ONOO^-$ inhibitor attenuates OGD injury in rat but had no effect in AGS. Rat also shows higher level of nitrotyrosine formation with OGD insult than AGS suggesting that greater level of injury is via formation of $ONOO^-$ during cerebral I/R injury.

Conclusions: Based on the results, we conclude that the possible phase of endogenous neuroprotection in AGS might reside downstream of NO synthesis and involves $ONOO^-$ detoxification. The increase in injury in combination with NO or $O_2^{\cdot-}$ with OGD suggest that the injury is in part contributed via generation of $ONOO^-$. AGS reflects a much lesser insult as compared to rat suggesting that high Ngb expression in AGS acts a detoxifier for $ONOO^-$ thus attenuates injury.

Reference:

[1] Dave,K.R.,etal.Stroke,2006.37(5):p.1261-5.
[2] Burmester,T.,etal.Nature,2000.407(6803):p.520-3.
[3] Fordel,E.,etal.NeurosciLett,2006.410(2):p.146-51.
[4] Khan., etal.ProcNatlAcadSciUSA, 2006.103(47):p.17944-8.
[5] Li,R.C.,etal.JCerebBloodFlowMetab,2010.30(11):p.1874-82.
[6] Sun,Y.,etal.ProcNatlAcadSciUSA,2001.98(26):p.15306-11.
[7] Kirschneretal.JNeurosci, 2009,87:p.2812-2820

669
BRAIN-0810
Poster Session

Cerebral Ischemia: Reperfusion

PERICYTES ON MICROVESSELS PREVENT COMPLETE REPERFUSION AFTER RETINAL ISCHEMIA

L. Alarcon-Martinez[1], M. Yemisci[1], J. Schallek[2], K. Kiliç[1], T. Dalkara[1]
[1]Institute of Neurological Sciences and Psychiatry, Hacettepe University Faculty of Medicine, ANKARA, Turkey
[2]Center for Visual Science, University of Rochester, Rochester NY, USA

Background: During cerebral ischemia, pericytes constrict microvessels, which do not relax after recanalization, causing an incomplete reperfusion. Since the retina contains the highest density of microvascular pericytes of any organ, retinal reperfusion after ischemia may also be impaired by

pericyte-induced microvascular constrictions.
Aim: To analyze whether pericytes constrict retinal microvessels during in vivo ischemia and hinder reperfusion.
Methods: We used wild type (n=35) and NG2-DsRed (n=9) mice. We induced clot formation in the central retinal artery by topical 20%-FeCl3 application over the artery for 3 minutes. After 60 minutes of ischemia, we infused tissue plasminogen activator (tPA) through tail vein to induce recanalization. We monitored the retinal blood flow by laser speckle contrast imaging. We also imaged retinal pericytes in vivo under conditions of normal perfusion, ischemia, and reperfusion animals by using a two channel adaptive optics scanning laser ophthalmoscopy (AOSLO). In one channel, fluorescent NG2-DsRed pericytes were imaged while in a second channel imaged, simultaneously, blood cell movement was recorded in the near infrared regime. After, we labeled whole mount retinas ex vivo with markers for pericytes (NG2, alpha-SMA) and vessels (Claudin-5, lectin) and, stereologically counted the constrictions and labeled cells.
Results: We found a significantly higher number of microvessel constrictions and a decreased microvessel diameter in ischemic (n=5) retinae compared to the sham group (n=6). Constrictions were not restored after recanalization of the retinal artery (n=3). We confirmed these ex vivo observations with in vivo retinal imaging (n=9). Intravitreal injections of a Ca2+-channel antagonist, amlopidine (1mg/ml) 60 minutes before ischemia prevented ischemia-induced microvascular constrictions (n=3, $P<0.05$), suggesting a role for Ca2+ overload during ischemia. There was a significant co-localization between pericytes and microvascular constrictions ($P<0.05$). We did not observe any diameter changes in upstream retinal macrovessels between cohorts ($P>0.05$).
Conclusions: Incomplete microcirculatory reperfusion caused by ischemia-induced persistent contractions of pericytes causing microvascular constrictions are one of the problems facing recanalization therapies.

670
BRAIN-0553
Poster Session

Cerebral Ischemia: Reperfusion

IRON OVERLOAD ANTICIPATES THE SIDE EFFECT OF HEMORRHAGIC TRANSFORMATION AFTER EXPERIMENTAL ISCHEMIA.

I. García-Yébenes[1], P. Negredo[2], C. Avendaño[2], P. López-G[1], D. Fernández-López[1], M.C. Godino[1], J.M. Pradillo[1], M. Castellanos[3], A. Dávalos[4], M.A. Moro[1], I. Lizasoain[1]
[1]Farmacology, Universidad Complutense de Madrid School of Medicine, Madrid, Spain
[2]Anatomy, Universidad Autónoma de Madrid School of Medicine, Madrid, Spain
[3]Neurology, Hospital Dr. Josep Trueta, Girona, Spain
[4]Neurology, Hospital Germans Trias i Pujol, Barcelona, Spain

Background: Recanalization of the artery remains as the main treatment for acute stroke patients, but the complication of hemorrhagic transformation (HT) limits it. Identification of those patients that more likely suffer this phenomenon and the underlying mechanisms implicated could help to improve this therapy. Since the decade of 1990, iron has been known as one of the early mediators of the ischemic damage. Several publications have demonstrated that iron overload could be also reducing the benefits from tissue-type plasminogen activator (tPA) in patients (Millán et al., 2007). The aim of this study was to evaluate the effect of iron overload in HT as well as the mechanisms implicated using an experimental model.

Methods: For the experiments, control or iron overload mice (diet-supplemented) were used. Cerebral ischemia was performed by the *in situ* thromboembolic model (Orset et al., 2007) by injecting thrombin in the middle cerebral artery

(MCA) to produce a clot that can be dissolved administering tPA (10 mg/kg). 10 experimental groups, 5 for each diet, n=8, were completed: Sham (animals subjected to surgery but not to the artery occlusion), MCAO (permanent MCA occlusion, saline treated), tPA 20min, tPA 1h and tPA 3h (occluded and reperfused with tPA at indicated time points). 24 hours after the surgery infarct volume was measured by Nissl staining and hemorrhage was evaluated macroscopically and measuring the area after red cell staining. Besides, some mediators of HT such as matrix metalloproteinase 9 (MMP-9) and infiltrated neutrophils (NIMP-R14$^+$ cells) were measured by immunohistochemistry.

Results: Control group with early reperfusion (tPA 20 and 1h) had a decreased infarct volume compared to permanent and late reperfusion groups ($p<0.05$), while only tPA 20min succeeded in rescuing part of the compromised tissue in animals with iron overload. Besides, in the groups tPA 20min and 1h, animals with high level of iron experienced larger lesions ($p<0.05$ vs control animals). Hemorrhage evaluation proved that late recanalization increased the most severe bleeding type and the total hemorrhage area compared to permanent ischemia ($p<0.05$ vs MCAO). Iron overload only exacerbated HT in tPA 1h ($p<0.05$ vs control animals), showing that iron could be accelerating the process. The number of infiltrated neutrophils was increased in groups with iron overload compared to control animals, especially in the tPA 3h group. MMP-9 expression in the infarcted tissue was also elevated in the late reperfusion group, an effect that was potentiated by iron overload.

Conclusions: These results strongly support the idea that iron overload participates in the ischemic damage, and particularly in HT, reducing the tissue rescued by early recanalization and anticipating the side effect of HT through several elevated mediators such as neutrophils and proteases.

Bibliography:
Millán M. et al., 2007, Stroke.
Orset C. et al., 2007, Stroke.

671
BRAIN-0465
Poster Session

Cerebral Ischemia: Reperfusion

REAL-TIME TRANSCRANIAL OPTICAL MONITORING OF MICROVASCULAR CEREBRAL BLOOD FLOW AND OXYGENATION IN ACUTE ISCHEMIC STROKE AFTER RECOMBINANT TISSUE PLASMINOGEN ACTIVATOR TREATMENT

C. Gregori[1], P. Zirak[1], I. Blanco[1], L. Dinia[2], R. Marín-Bueno[2], J. Martí-Fàbregas[2], T. Durduran[1], R. Delgado-Mederos[2]
[1]Medical Optics, ICFO-Institut de Ciències Fotòniques, Castelldefels, Spain
[2]Stroke unit, Hospital de Sant Pau i de la Santa Creu, Barcelona, Spain

Background: Diffuse correlation spectroscopy (DCS) and near-infrared diffuse optical spectroscopy (NIRS) measure local microvascular cerebral blood flow (CBF) and oxygenation, respectively, at the bedside [1]. Recombinant tissue plasminogen activator (rt-PA, alteplase) is used as a treatment for acute ischemic stroke (AIS) patients within 4.5 hours of onset but with variable outcomes [2]. Studies suggest that local tissue reperfusion predicts better the outcome after rtPA thrombolysis than recanalization [3]. Therefore, we hypothesize that outcomes will be improved with individualized treatments based on local tissue microvascular perfusion and metabolism. Unfortunately, these variables are difficult to monitor in the stroke unit. We have, for the first time, introduced a hybrid NIRS/DCS device to the emergency room and tested whether the effect of rtPA on cerebral perfusion can be assessed by NIRS/DCS at the bedside in patients with AIS.

Methods: AIS patients with middle cerebral artery occlusion were recruited. After rtPA injection, continuous DCS and continuous-wave near-infrared spectroscopy data in both frontal lobes

were obtained for the first two hours. We have evaluated the hemodynamic temporal profile in both hemispheres by averaging a 6-minute window every 15 minutes, beginning 15 minutes after treatment initiation. The results were evaluated in relation to the presence of recanalization on follow-up transcranial Doppler and clinical status.

Results: To date, five patients (median NIHSS - National Institute of Health Stroke Scale- 19) were measured with complete arterial recanalization. At 24 hours of the stroke onset, all patients improved significantly (median NIHSS 3). Good signal-to-noise ratio was obtained for all optical variables. Significant increases in CBF, oxy- and total hemoglobin concentrations were observed 90 minutes following rtPA treatment in the ipsilateral, but not in the contralateral hemisphere (Fig.1).

Conclusions : Bedside NIRS/DCS showed the capability for monitoring continuously the effect of reperfusion therapy on AIS in the emergency room. More patients are being recruited and non-treated subjects are being included as a control group. We will explore the feasibility of the method, the specifics of the individual responses and their relationship to the outcome. We will discuss our findings and speculate on the advantages and disadvantages of the method.

The project was funded by Fundació Cellex Barcelona, LlumMedBCN (La Caixa), Ministerio de Economía y Competitividad (PHOTOSTROKE), LASERLAB-EUROPE and Fondo de Investigaciones Sanitarias (Spanish Ministry of Health).

References:

[1] Durduran and Yodh. Diffuse correlation spectroscopy for non-invasive, micro-vascular cerebral blood flow measurement. NeuroImage, 85:51-63, 2014.
[2] Emberson **et al.**. Effect of treatment delay, age, and stroke severity on the effects of intravenous thrombolysis with alteplase for acute ischaemic stroke: a meta-analysis of individual patient data from randomised trials. **Lancet, 384(9958): 1929–1935, 2014.**
[3] An et al.. Early changes of tissue perfusion after tissue plasminogen activator in hyperacute ischemic stroke. Stroke, 42(1):65-72, 2011.

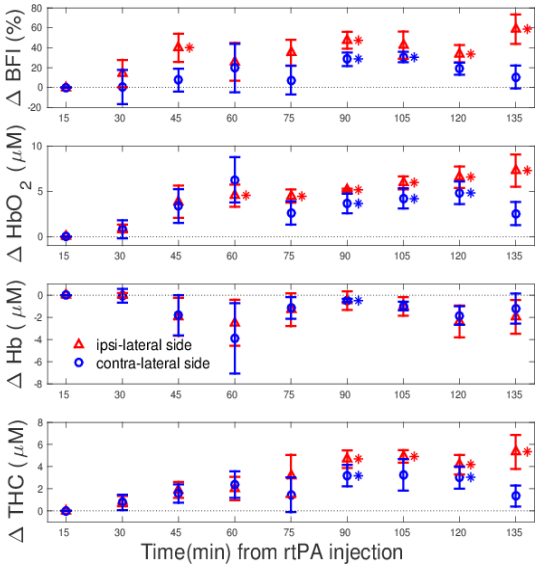

Figure 1: Microvascular, bilateral cerebral blood flow (CBF), oxy- (HbO_2) and deoxy-hemoglobin (Hb) and total hemoglobin concentration (THC) changes are shown from the frontal lobes. The time axis shows the time elapsed from the rtPA treatment onset. (*) indicates significant ($p<0.05$) change from the baseline (time=15 minutes after rtPA injection).

672
BRAIN-0734
Poster Session

Cerebral Ischemia: Reperfusion

THE EFFECT AND SAFETY OF EARLY STA-MCA BYPASS IN ACUTE ISCHEMIC STROKE

P.W. Huh[1], T.Y. Won[1], S.B. Lee[1], D.S. Yoo[1], T.G. Lee[1], K.S. Cho[1]
[1]Neurosurgery, Uijeong-Bu St. Mary's Hospital, Uijeongbu, Korea

Purpose and background: We should focuses on small group of patients withsteno-occlusive cerebral arteries (SOCA) that could not be treated with IV tPAor endovascular management. It has been reported to bevery high subsequent stroke recurrence(SSR) within 2wks of acute ischemic stroke. This ischemic stroke mainly occursby the

hemodynamic insufficiency. In order to prevent SSR, we performed STA-MCAbypass in the early stage after stroke, and demonstrate their effects andsafety.

Materialsand methods: From 2006-2014, 55 patients (47 malesand 8 females) with atherosclerotic ICA (24) or MCA (31) stenosis or occlusionwere performed STA-MCA bypass by the reason of hemodynamic insufficiencyfollowing own surgery indication guideline. STA-MCA bypass were completedwithin 2 weeks from symptom onset.

Results: The male to female ratio was 47:8, mean age 55.3 years (range 24 to76) and FU period (mean. 26months). The mean time interval between symptomonset and bypass surgery was 5.1 days. The NIHSS (mean NIHSS ± SD) score wassignificantly improved after bypass surgery (preoperative NIHSS score, 4.30 ± 3.53;at discharge, 2.96 ± 1.96, P = 0.000; 90 days follow up, 2.52 ± 3.51, P = 0.000;at last follow up, 2.45 ± 3.48, P = 0.000). Four patients (2 STA occlusion, 1ICH, 1 silent embolic infarct) had experienced perioperative neurological deficits.

Conclusion: Only 3/55 (5.4%) bypass patients took place SSR during follow upperiod. The SOCA of 6 patients were even restored to normal after bypasssurgery. Therefore, early STA-MCA bypass surgery for the acute ischemicpatients who are cause of hemodynamic insufficiencywith SOCA and not qualify ornot respond for IV tPA seems to be very effective andsafe.

673
BRAIN-0448
Poster Session

Cerebral Ischemia: Reperfusion

MILD HYPOTHERMIA PROTECTS THE BRAIN FROM ISCHEMIA/REPERFUSION BY ATTENUATING P63/P73-INDUCED APOPTOSIS THROUGH IASPP

X. Liu[1], S. Zhao[2], F. Yan[3], J. Kang[2], C. Zhang[1], H. Zhao[1], Y. Luo[1], X. Ji[4]
[1]Cerebrovascular Diseases Research Institute, Xuanwu Hospital of Capital Medical University, Beijing, China
[2]Department of Neurosurgury, Beijing Tongren Hospital Capital Medical Universit y, Beijing, China
[3]Cerebrovascular Diseases Research Institute, Xuanwu hospital of Capital Medical University, Beijing, China
[4]Department of Neurosurgury, Xuanwu Hospital of Capital Medical University, Beijing, China

Objectives—Mild hypothermia, as a robust neuroprotectant, reduces neuronal apoptosis, but the precise mechanism is not well understood. Inhibition of the function of p53 family (p53, p63 and p73) can reduce apoptosis and induce endogenous nerve regeneration in ischemic brain injury. iASPP, a member of Apoptosis Stimulating Proteins of p53 (ASPP) family, recently discovered as an inhibitor of apoptosis. In the present study, we tested the hypothesis that mild hypothermia applied after experimental stroke provides neuroprotection by mechanisms involving attenuating p63/p73-induced apoptosis through iASPP.

Methods—The MCA occlusion was induced for 1 hour using a filament model in mice. Body temperature was measured by means of a thermocouple probe placed in the rectum and was maintained at normothermia (37° C) throughout the experiment by a circulating heating pad and a warming lamp. Hypothermia (33° C) applied from the beginning of ischemia and lasted 2 hours in animal model. Infarct volume and neurological outcomes at 24 hours

after ischemia were evaluated. Expression of p63, p73, iASPP, ASPP1, ASPP2 and p21 was determined by Western blotting and immunofluorence. To evaluate the role of iASPP, siRNA were transfected into C57 mice by intracerebroventricular injection.
Primary cortical neurons at days in vitro (DIV) 10 were subjected to 1 hour of oxygen glucose deprivation (OGD), an in vitro model of ischemic stroke.

Results—Increased iASPP expression and decreased p63, p73, ASPP1 and ASPP2 expression was observed under hypothermia treatment in experimental stroke. Furthermore, mild hypothermia given immediately after ischemia also increased infarct volume. Mild hypothermia significantly reduced infarct volume and improved functional outcomes at 24 hours after ischemia. iASPP siRNA (iASPPi) or control siRNA (Coni) were injected into the right lateral ventricle of mice treated with normothermia or hypothermia at 10 min after the beginning of reperfusion. iASPPi or hypothermia+iASPPi application increased infarct volume and aggravated the neurological function in MCAO mice. Furthermore, the protein level of iASPP was decreased and the expression of its target p21 was increased in these two groups. Moreover, hypothermia increased iASPP expression in primary cultures of cortical neurons under oxygen glucose deprivation (OGD) and promoted neuronal survival.

Conclusions—Mild hypothermia protects against ischemia/reperfusion brain injury in rats by attenuating p63/p73-induced apoptosis through inducing iASPP expression.

References

1. Yenari MA, Han HS. Neuroprotective mechanisms of hypothermia in brain ischaemia. Nat Rev Neurosci. 2012; 13(4):267-278.
2. Sullivan A, Lu X. ASPP: a new family of oncogenes and tumour suppressor genes. Br J Cancer. 2007;96:196–200.
3. Bergamaschi D, Samuels Y, O'Neil NJ, Trigiante G, Crook T, Hsieh JK, et al. iASPP oncoprotein is a key inhibitor of p53 conserved from worm to human. *Nat Genet*. 2003;33:162–167.
4. Liu X, Li F, Zhao S, Luo Y, Kang J, Zhao H, Yan F, Li S, Ji X. MicroRNA-124-mediated regulation of inhibitory member of apoptosis-stimulating protein of p53 family in experimental stroke. *Stroke*. 2013;44(7):1973–1980.

674
BRAIN-0444
Poster Session

Cerebral Ischemia: Reperfusion

EFFECTS OF GHRELIN ON NITRIC OXIDE PRODUCTION, HYDROXYL RADICAL METABOLISM DURING CEREBRAL ISCHEMIA AND REPERFUSION IN MICE

R. Nishioka[1], Y. Ito[1], M. Yamazato[1], M. Hirayama[1], A. Tanaka[1], A. Miyake[1], T. Sasaki[1], K. Takahashi[1], T. Yamamoto[1], N. Araki[1]
[1]Department of Neurology, Saitama Medical University, Moroyama Saitama, Japan

Objectives: It is suggested that ghrelin may protect brain tissue during cerebral ischemia. The purpose of this study is to investigate the nitric oxide (NO) production, hydroxyl radical metabolism during cerebral ischemia and reperfusion in mice treated with ghrelin.

Methods: C57BL/6 mice were used. Ghrelin group; ghrelin (14 µmol/kg/day) was given orally in 6 mice for 14 days and others (n=10) were used for control group. Both NO production and hydroxyl radical metabolism were continuously monitored by *in vivo* microdialysis. Microdialysis probes were inserted into the bilateral striatum. The *in vivo* salicylate trapping method was applied for monitoring hydroxyl radical formation via 2,3 dihydroxybenzoic acid (2,3-DHBA), and 2,5 dihydroxybenzoic acid (2,5-DHBA). A Laser Doppler probe was placed on the skull surface. Blood pressure, pulse rate and body temperature were monitored and maintained within normal ranges throughout the procedure. Blood gases were also maintained whitin normal range. Forebrain cerebral ischemia was produced by transient occlusion of both common carotid

arteries (BCAO) for 10 minutes using micro plastic clips for surgical aneurysma clipping. Levels of nitric oxide metabolites, nitrite (NO_2^-) and nitrate (NO_3^-), in the dialysate were determined using the Griess reaction.

Results: (1) Blood Pressure: There were no significant differences between the groups. (2) Cerebral Blood Flow (CBF): No significant differences were obtained between the groups. (3) Nitric oxide metabolites (NO_2^- and NO_3^-): There were no significant differences between the groups. (4) Hydroxyl radical metabolites: 1) 2,3-DHBA; Ghrelin group showed significantly lower than that of control group in 100 minutes after the start of reperfusion ($p<0.05$).(Fig.1) 2)2,5-DHBA; There were no significant differences between the groups.

Conclusion: These *in vivo* data suggest that ghrelin influences on the hydroxyl radical production in mice, and may protect against cerebral ischemic injury following ischemia and reperfusion.

References:

1) Nagaya N, Kanagawa K: Ghrelin, a novel growth hormone-releasing peptide, in the treatment of chronic heart failure. Regulatory Peptides 114: 71-7, 2003
2) Ito Y, Ohkubo T, Asano Y, Hattori K, Yamazato M, Nagoya H, Kato Y, Araki N: Nitric oxide production during ischemia and reperfusion in eNOS-knockout mice. Curr Neurovasc Res 7(1): 23-31, 2010

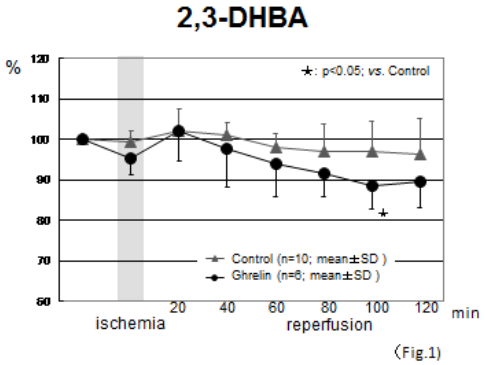

(Fig.1)

675

BRAIN-0636
Poster Session

Cerebral Ischemia: Reperfusion

BRAIN INJURY FOLLOWING RECURRENT CEREBRAL ISCHEMIA: EFFECT OF RECOVERY TIME BETWEEN ISCHEMIC INSULTS

U. Tuor[1], M. Qiao[2], Z. Zhao[3], P. Barber[3], T. Foniok[4], D. Rushforth[4]
[1]Physiology and Pharmacology Clinical Neurosciences and Radiology, University of Calgary, Calgary, Canada
[2]Physiology and Pharmacology, University of Calgary, Calgary, Canada
[3]Clinical Neurosciences, University of Calgary, Calgary, Canada
[4]Experimental Imaging Centre, University of Calgary, Calgary, Canada

Introduction: A transient ischemic attack (TIA) can produce mild ischemic brain damage that includes selective necrosis (1,2); however, knowledge is limited regarding the combined effects of recurrent mild ischemic insults. We hypothesized that depending on the time between insults, cumulative damage from such multiple mild transient ischemic events would vary.

Objectives: 1. to determine whether the brain injury produced following multiple episodes of relatively short transient cerebral ischemia differs with acute or chronic recovery times between insults. 2. To determine whether the extent of damage is related to the initial injury (e.g. measures of progression of cerebral inflammation, blood-brain barrier dysfunction or systemic inflammation).

Methods: Mild ttransient cerebral ischemia was produced in 56 anesthetized rats by microclip placement on the middle cerebral artery (MCA) for 30 min. Then a variable recovery time (1d, 3d or 1mo) ensued prior to a second transient cerebral ischemia of 30 min. Brains from 31 additional animals (i.e. sham controls or animals with single MCA occlusion with various recoveries post insult) were also investigated. Paraffin sections were assessed for injury using standard

hematoxylin and eosin or immunohistochemical stains (e.g. IgG for BBB dysfunction, TNF for increased cytokines or GFAP and ED1 for glial activation). Staining was assessed using methods similar to those described previously (1). Blood samples from additional groups of animals were used for complete analysis, including leukocyte and granulocyte counts.

Results: A mild transient episode of middle cerebral artery occlusion, eliciting mild ischemic changes alone, produced greater brain damage when multiple insults were separated by 1d compared to 3d or 1mo (Fig. A). The enhanced damage did not correspond to increased injurious factors following the first insult such as BBB disruption, increased cytokines (TNF) or inflammatory glial changes; these had differing profiles. Investigation of systemic inflammatory changes demonstrated an acute transitory increase in granulocytes (Fig B), suggesting a potential interaction of systemic inflammation with initial ischemic injury to enhance damage.

Discussion: These results provide new insights into the pathophysiology of transient cerebral ischemia of a severity sufficient to cause mild ischemic injury and can help explain some of the increased severity observed with early stroke recurrence in the first days following stroke or TIA. The results suggest that management and potential treatment of TIA should consider an early greater susceptibility of the brain to damage from a second insult.

Conclusions: Following a mild ischemic insult, there are distinct progressive parenchymal and systemic injury responses. Damage with mild stroke recurrence is greatest if the interval between two mild ischemic insults is acute (i.e. 1d) compared to subacute (3d) or chronic (1 mo).

(Supported by the Canadian Institute for Health Research)

References: 1: Clark D, Tuor UI, et al. Protection against recurrent stroke with resveratrol: endothelial protection. PLoS One. 2012;7(10):e47792. 2: Baron JC et al. Endres M. Selective neuronal loss in ischemic stroke and cerebrovascular disease. J Cereb Blood Flow Metab. 2014; 34:2-18.

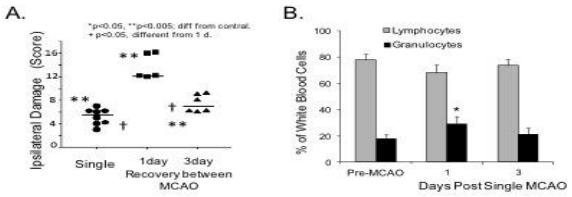

676
BRAIN-0087
Poster Session

Cerebral Ischemia: Reperfusion

EFFECTS OF RAPAMYCIN ON CEREBRAL OXYGEN SUPPLY AND CONSUMPTION DURING REPERFUSION AFTER CEREBRAL ISCHEMIA

H. Weiss[1], *O.Z. Chi*[2], *X. Liu*[2]
[1]*Neuroscience & Cell Biology, Rutgers Robert Wood Johnson Medical School, Piscataway, USA*
[2]*Anesthesiology, Rutgers Robert Wood Johnson Medical School, Piscataway, USA*

Activation of the mammalian target of rapamycin (mTOR) leads to cell growth and survival. We tested the hypothesis that inhibition of mTOR with rapamycin would increase infarct size and decrease microregional O_2 supply/consumption balance after cerebral ischemia-reperfusion. This was tested in isoflurane anesthetized rats after middle cerebral artery blockade for 1 hour and reperfusion for 2 hours with and without rapamycin (20 mg/kg once daily for two days). Regional cerebral blood flow was determined using a C^{14}-iodoantipyrine autoradiographic technique. Regional small vessel arterial and venous oxygen saturations were determined microspectrophotometrically. The control group ischemic-reperfused cortex has a similar blood flow and O_2 consumption to the contralateral cortex. However, microregional O_2 supply/consumption balance was significantly reduced in the ischemic-reperfused

cortex. Rapamycin significantly increased cerebral O_2 consumption and reduced O_2 supply/consumption balance. This was associated with an increased cortical infarct size (13.5 ± 0.8% control vs 21.5 ± 0.9% rapamycin). This suggests that mTOR is important for not only cell survival, but also for the control of oxygen balance after cerebral ischemia-reperfusion.

677
BRAIN-0735
Poster Session

Preconditioning and Post-Conditioning

COMBINED PROTECTIVE EFFECTS OF HYPOTHERMIA AND HYPOXIC POSTCONDITIONING IN RAT ORGANOTYPIC HIPPOCAMPAL SLICE CULTURES

N. Jones[1], L.J. Thai[1]
[1]Pharmacology School of Medical Sciences, University of New South Wales, Sydney, Australia

Objectives: Hypoxic-ischemic (HI) brain injury in newborns is associated with high morbidity and mortality rates, with many survivors suffering neurological impairments. Hypothermia is currently the standard of care used for newborns that suffer from mild to moderate HI and can reduce the mortality and disability in these infants [1]. Recent studies have demonstrated the neuroprotective potential of combining hypothermia with other treatments such as erythropoietin and melatonin in animal models of HI [2, 3]. Hypoxic postconditioning or exposure to mild hypoxia following an injury has been shown to result in neuroprotection against brain damage through a variety of mechanisms [4, 5]. Here, we aimed to examine the effects of hypothermia and hypoxia as monotherapies, as well as in combination, against glutamate-induced injury in organotypic hippocampal slices obtained from neonatal rats.

Methods: Organotypic hippocampal slices were obtained from Sprague Dawley rat pups (postnatal day 7), cultured for 12-14 days and exposed to glutamate (10mM for 24h) to induce injury. Hypothermia (33°C, with a delay of 30min, 3h or 24h for 6, 24 or 72h) or hypoxia (8, 10 and 12% oxygen, 1h/day for 5 days or 2h/day for 3 days) were applied post-injury as monotherapies to determine which conditions were protective. The degree of cell death was determined using propidium iodide staining in the CA1 and dentate gyrus in the hippocampal slices. Once protective conditions were established, a combination treatment strategy was applied. All experiments were performed in duplicate with slices obtained from n=3 different animals.

Results: There was no protection observed with 6 or 24h exposure to hypothermia. However, 72 hours of hypothermia was shown to be neuroprotective when applied to slices post-injury. In addition, all of the hypoxic treatments (8, 10 and 12% oxygen) were able to protect the hippocampal slices against injury. Combination treatment, using hypothermia (33°C for 72h, with a delay of 30min after injury and hypoxia (8% and 10% oxygen for 1h/day for 5 days) was able to reduce cell death levels following glutamate-induced injury in both the CA1 and dentate gyrus regions of hippocampal slices.

Conclusions: Here, we have demonstrated that there is the potential for neuroprotection resulting from combination treatment with hypothermia and hypoxic postconditioning in hippocampal slices. While we did not observe a synergistic neuroprotective effect with our combined treatments, our results suggest that that the strategy of mild hypoxia with hypothermia may extend the therapeutic time window for hypoxia and is worthy of further investigation. Our future studies will examine protective mechanisms involved in this combination treatment strategy.

References:
1. Azzopardi et al, (2009) New Eng J Med. 361, 1349-1358.
2. Traudt CM, et al, (2013) Dev Neurosci. 35: 491-503.
3. Robertson NJ et al (2013) Brain 136: 90-105.
4. Galle AA and Jones NM (2013) Brain Res. 1498: 1-8.

5. Leconte C et al (2009) Stroke 40: 3349-3355.

678
BRAIN-0364
Poster Session

Preconditioning and Post-Conditioning

PERI-INFARCT DEPOLARIZATIONS IN THE SPONTANEOUSLY HYPERTENSIVE RAT. EFFECT OF PRECONDITIONING BY ANESTHESIA AND CORTICAL LESIONS

L. Zhao[1], K. Kudo[2], T. Nowak[1]
[1]Neurology,
University of Tennessee Health Science Center, Memphis, USA
[2]Neurosurgery, Juntendo University, Tokyo, Japan

Objectives -- Ischemic preconditioning appears to include distinct components contributed by prior anesthesia exposure and cortical injury (1). Recent results showed that these have differing effects on peri-infarct depolarizations (PIDs) during subsequent stroke (Zhao and Nowak, submitted manuscript). Isoflurane preconditioning reduced PID incidence when monitored by perfusion imaging under the same isoflurane anesthesia, without affecting PID number recorded under alpha-chloralose, whereas the latter was additionally impacted in animals with prior cortical lesions. The current studies were designed to evaluate the persistence of anesthetic preconditioning effects on PIDs, and to assess the impact of lesion preconditioning on PID incidence in awake animals.

Methods -- Spontaneously Hypertensive Rats (SHR) were preconditioned by producing small 2-5 mm^3 cryogenic cortical lesions (CL), or by the corresponding sham surgery under isoflurane anesthesia. Focal ischemia was produced the next day by tandem occlusion of the middle cerebral artery (MCA) and ipsilateral common carotid artery. PIDs were detected by speckle contrast perfusion imaging during 4 hours under isoflurane anesthesia, or were recorded for 24 hours in the awake state via electrode arrays implanted at varied intervals prior to occlusion.

Results -- PID-associated hyperemic flow transients recorded under isoflurane anesthesia were significantly reduced from 8.5 ± 2.4 (mean ± SD, n=12) in naïve rats to 3.3 ± 1.3 (n=9) after isoflurane exposure the previous day ($P < 0.05$, one-way ANOVA). Recovery was variable at 1 week (6.6 ± 4.1, n=10), but the control range was regained after 2 weeks or longer (7.2 ± 2.6, n=16). Electrophysiologically recorded PIDs were more numerous in awake rats, but occurred within the same 4-hour window after occlusion. PIDs numbered 25 ± 4, 21 ± 6, 32 ± 9 and 29 ± 11 at 1 day and 1, 3, and 5 weeks, respectively. There was no effect of the interval between electrode placement and occlusion surgery for individual time points, although pooled results for ≤ 1 week (23 ± 5, n= 10) vs. ≥ 3 weeks (31 ± 10) achieved significance ($P < 0.03$, unpaired t-test). With chronic electrode placement, PID incidence was reduced from 28 ± 4 (n=8) in sham-operated rats to 21 ± 8 (n=7) after CL preconditioning ($P < 0.05$).

Conclusions -- Prior isoflurane exposure reduces PID incidence through a 1-week interval, as typically described for infarct reduction by anesthetic preconditioning. This effect is only observed when PIDs are monitored under the same isoflurane anesthesia, indicating that some aspect of the response to this agent is altered by repeated exposure and mediates the preconditioning effect. Previous results suggest that this involves increased penumbral CBF (1). Minimal impact of prior isoflurane exposure is detected in rats allowed to recover from anesthesia immediately after occlusion surgery. In contrast, lesion-preconditioning effects on PID incidence continue to be observed during awake recordings.

1) Zhao L, Nowak Jr TS (2006) J. Cereb. Blood Flow Metab. 26:1128-1140
Supported by the Ganey Fund, Department of Neurology, University of Tennessee Health Science Center, and by USPHS grant R21-NS077039
679

BRAIN-0589
Poster Session

Preconditioning and Post-Conditioning

POST-STROKE LIMB CONDITIONING INDUCED BENEFITS OCCUR THROUGH MODULATING PERIPHERAL IMMUNITY

J. Yang[1], *C. Beltran*[1], *S. Cho*[1]
[1]*Research, Burke-Cornell Medical Research Institute, White Plains, USA*

Objectives; Neuroprotective strategies that were effective in animal models have not been successfully translated into clinical settings. Remote ischemic limb conditioning is a currently used therapeutic strategy in clinical trials, which shows benefits on stroke or myocardial infarct patients. However, mechanisms underlying the benefits have not been defined. This study investigated whether benefits of post-stroke limb conditioning (PSLC) induces changes in the peripheral immune system by modulating pro- and anti-inflammatory monocytes/macrophages (MMs) subsets.

Methods; C57BL/6 male mice (10 to 12-week-old) were subjected to a 30 min middle cerebral artery occlusion (MCAO) by an intraluminal thread method. PSLC was induced 2 h after MCAO by applying 5 cycles (200 mmHg, 5 min x 5 min interval between cycles) of inflation and deflation with a cuff on the left hind limb. Infarct volume and swelling were measured 3D after stroke. Mononuclear cells were isolated from the blood, spleen and brain at 3D post-stroke and analyzed by a flow cytometer. MM subsets in the blood and spleen were identified by Lin-/CD11b+ population and in the brain were identified by CD45+/CD11b+ population. The selected populations were further analyzed by Ly6C expression: Ly6C^{Hi} [pro-inflammatory, CCR2+] and Ly6C^{Low} [anti-inflammatory, CCR2-] subset. Motor and gait functions were assessed by Rotarod and Catwalk Gait Analysis at 4W post-stroke and compared to pre-ischemic baseline.

Results; Acute stroke outcome (infarct size and swelling) was similar between sham and PSLC mice. There was no significant changes in %MMs by PSLC in the blood at 3D post-ischemia. MM subset analysis showed a significant decrease in Ly6C^{Low} subset in the blood and ipsilateral region of the brain without significant changes in Ly6C^{Hi} subset (Figure). PSLC did not induced changes of MM subsets in the spleen. Mice with PSLC showed tendency of better motor function assessed by Rotarod performance at 4W post-stroke (p=0.0688, n=5). Similarly, PSLC also improved mean intensity and maximum contact area of the impaired limb by Catwalk Gait Analysis at 4W after stroke ($p<0.05$, n=5).

Conclusions; PSLC-induced stroke recovery is associated with changes in peripheral immunity. Selective reduction of Ly6C^{Low} in the blood and brain indicates PSLC induces a potential conversion of anti-inflammatory Ly6C^{Low} to pro-inflammatory Ly6C^{Hi} subset in the blood. The conversion may provide more immunocompetent Ly6C^{Hi} MMs for post-stroke survival and enhanced long-term recovery. This study provides a potential application of PSLC as a neuroimmune-based strategy for patients with ischemic stroke.

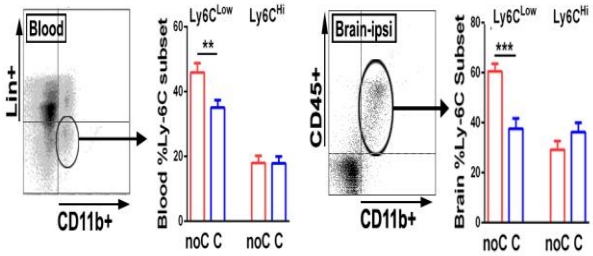

680
BRAIN-0154
Poster Session

Cerebral Metabolic Regulation

THE EFFECTS OF CAPILLARY TRANSIT TIME HETEROGENEITY (CTH) ON BRAIN OXYGENATION

H. Angleys[1], L. Østergaard[1], S.N. Jespersen[1]
[1]Center of Functionally Integrative Neuroscience & MINDLab, Aarhus University Hospital, Århus C, Denmark

Background: We recently extended the classical flow-diffusion equation, which is traditionally used to infer brain tissue oxygenation from cerebral blood flow, to take capillary transit time heterogeneity (*CTH*) into account[1]. This modelling has generated new hypotheses for understanding Alzheimer's disease[2] and stroke[3]. However, it is based on several simplifying assumptions which we seek to relax here.

Objectives: We present a new model[4] where we explicitly incorporate the effects of oxygen metabolism on tissue oxygen tension and extraction efficacy, and compare the predictions obtained with the new and the original model.

Additionally, we evaluate the dependence on the specific form of the capillary transit time distribution (CTD).

Methods: Based on a three compartments (hemoglobin, plasma, tissue) model, and assuming that the metabolism in tissue is governed by Michaelis-Menten kinetics, the mean oxygen extraction fraction and tissue oxygen tension over the capillary network are computed by summing the contribution of each capillary weighted by the assumed CTD.

To assess the extent to which the type of CTD affects the overall influence of *CTH* on flow-metabolism, we analyzed the model with four different transit time distributions.

We tested the model assuming that the maximum metabolic rate of oxygen v_{max} is kept constant, and in a second step that it slightly increases during cerebral activation, proportionally to stimulation intensity.

Results: Figure 1 compares contour plots of $CMRO_2$ maps obtained with the new and original models.

Our model predicts that for large *CTH* values, a blood flow increase fails to cause significant improvements in oxygen delivery, and can even lower it; a condition of malignant *CTH*.

During activation, increases in $CMRO_2$ are found to be smaller in the new model[4] than in the original model[1], due to the high degree of saturation in oxygen consumption already in the resting state.

A small (10%) increase in v_{max} during activation leads to an increase in $CMRO_2$ about twice as large as with v_{max} kept constant.

These results are found to be largely insensitive to the choice of CTD, in particular when considering physiological values.

Conclusion: Explicitly modelling oxygen metabolism to alleviate the assumption of a constant extravascular oxygen tension assumed in Ref.[1] did not qualitatively change the conclusions of the original model. Furthermore, increases in $CMRO_2$ were smaller in the new model than in the original model, resulting in neurovascular coupling in better agreement with experimental data, especially when v_{max} increases slightly during activation. Both micro- and macro-heterogeneity of oxygen tension may lead to an apparent increase in v_{max}, but the potential mechanism and extent to which it increases has yet to be determined.

The relation between *MTT*, *CTH* and $CMRO_2$ was robust across CTDs: the malignant *CTH* phenomenon is hence an inherent property of oxygen extraction.

References:
1. S.N. Jespersen & L. Østergaard, J. Cereb. Blood Flow Metab. **32**, 264 (2012).
2. L. Østergaard et al., Neurobiol. Aging **34**, 1018 (2013).
3. L. Østergaard et al., J. Cereb. Blood Flow Metab. **33**, 635 (2013).
4. H. Angleys et al., J. Cereb. Blood Flow Metab., *in press.*

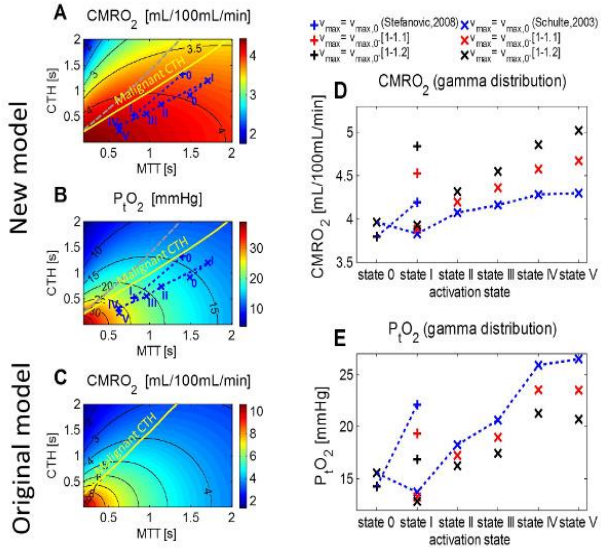

Fig. 1: Model of the effects of *MTT* and *CTH* on oxygenation. Comparison between the expected $CMRO_2$ with the new (A) and the original model (C). P_tO_2 (B) is also shown for the new model. Expected $CMRO_2$ (D) and P_tO_2 (E) for different physiological conditions when v_{max} increases (blue: no increase; red: 10%; black: 20%) during activation. *MTT*, mean transit time; *CTH*, capillary transit time heterogeneity; $CMRO_2$, oxygen consumption; P_tO_2, mean tissue oxygen tension; v_{max}, maximum metabolic rate of oxygen.

681
BRAIN-0705
Poster Session

Cerebral Metabolic Regulation

BRAIN GLUCOSE AND KETONE METABOLISM IN ADULTS DURING MODERATE DIET-INDUCED KETOSIS: A DUAL TRACER QUANTITATIVE PET-MRI STUDY

A. Courchesne-Loyer[1], C.A. Castellano[2], V. St-Pierre[1], M. Hennebelle[1], S. Tremblay[3], M. Lepage[4], T. Fülöp[2], E. Turcotte[4], S.C. Cunnane[2]
[1]Physiology, Université de Sherbrooke, Sherbrooke Qc, Canada
[2]Research Center on Aging, University Institute of Geriatrics of Sherbrooke, Sherbrooke Qc, Canada
[3]Sherbrooke Molecular Imaging Center, Université de Sherbrooke, Sherbrooke Qc, Canada
[4]Nuclear Medicine and Radiobiology, Université de Sherbrooke, Sherbrooke Qc, Canada

Introduction: Regional brain glucose hypometabolism occurs during aging and may contribute to the onset of aging-related cognitive impairment in humans (1). Ketones are the main alternative energy substrate to glucose for the brain. Several studies show that brain ketone uptake and metabolism are unaltered in cognitively-normal older persons and in Alzheimer's disease (AD; 2). Nutritional ketosis is reported to have a positive impact on cognitive performances in mild cognitive impairment and AD (3). Nevertheless, changes in regional brain glucose and ketone uptake in adults are poorly understood during diet-induced experimental ketosis. Our hypothesis was that during diet-induced ketosis, brain ketone uptake would be directly correlated with the elevation of blood ketone levels and inversely correlated to brain glucose uptake.

Objective: To use quantitative dual tracer brain PET to measure brain uptake of both ketones and glucose in adults in moderate diet-induced ketosis and their relationship to plasma ketones.

Methods: To induce moderate ketosis, ten healthy adults (28 ± 3 y) received a ketogenic diet (4.5:1; lipid:protein plus carbohydrates) for four days. Brain ketone (^{11}C-acetoacetate [^{11}C-AcAc]) and glucose (^{18}F-FDG) uptake were quantified using a PET/MRI protocol (PET Philips Gemini-TF – MRI Siemens 1.5T) both before and on the last day of the ketogenic diet. Blood clinical chemistry parameters were also obtained for each participant.

Results: While on the ketogenic diet, plasma ketones (acetoacetate and β-hydroxybutyrate) increased 16 fold (0.31 ± 0.18 to 5.21 ± 0.34 mM) and plasma glucose decreased by 18% from 5.0 ±

0.3 to 4.1 ± 0.5 mM. While on the ketogenic diet, whole brain ^{11}C-AcAc uptake increased 14 fold (0.52 to 7.43 µmol/100 g/min) but whole brain ^{18}F-FDG uptake did not change significantly (25.9 to 25.7 µmol/100 g/min). Increases in ^{11}C-AcAc uptake in AD-related regions while on the ketogenic diet were similar to those in the whole brain, i.e. 16 fold in temporal cortex (0.4 ± 0.1 to 6.2 ± 1.7 µmol/100 g/min) and 17 fold in hippocampus (0.3 ± 0.1 to 5.1 ± 1.5 µmol/100 g/min). ^{18}F-FDG uptake in these same regions did not differ after compared to before the ketogenic diet. Plasma ketones where positively correlated with whole brain ^{11}C-AcAc uptake (r=0.829; p = 0.05).

Discussion: These results show a rapid positive response (both regionally and in the whole brain) of higher brain ^{11}C-AcAc uptake to higher plasma AcAc while on the ketogenic diet. Unexpectedly, brain ^{18}F-FDG intake did not differ pre- to post-ketogenic diet despite significantly lower plasma glucose while on the ketogenic diet. It will be interesting to evaluate if brain metabolic response to a ketogenic diet is affected by normal aging or AD.

Funding: CRC, CFI, CIHR, FRQS, Université de Sherbrooke research chair (SCC)

References: (1) Cunnane SC et al. Nutrition 2011; 27: 3-20.
(2) Castellano CA et al. J Alzheimer Dis 2015; .43(4): 1343-1353.
(3) Krikorian R et al. Neurobiol Aging 2012; 33(2): 425.

682
BRAIN-0691
Poster Session

Cerebral Metabolic Regulation

MAGNETIC RESONANCE IMAGING FINDINGS IN HYPOGLYCEMIC ENCEPHALOPATHY

T. Ikeda[1], T. Takahashi[1], M. Kanazawa[1], M. Nishizawa[1], T. Shimohata[1]
[1]Department of Neurology, Brain Research Institute Niigata University, Niigata, Japan

Objective:
To clarify the relationship between prognosis and magnetic resonance imaging (MRI) findings in hypoglycemic encephalopathy.

Background:
Hypoglycemia causes neurological symptoms due to a decrease in blood glucose levels and generally refers to blood glucose levels of ≤ 60 mg/dL. In most cases, hypoglycemia rapidly improves with glucose administration; however, severe cases in which neurological symptoms do not improve with glucose administration are referred to as 'hypoglycemic encephalopathy". Features of brain MRI findings in hypoglycemic encephalopathy reportedly include, (1) lesion distribution unrelated to vascular territories, (2) the possibility of various lesion distributions, (3) no cerebellum/brain stem impairment. However, the relationship between these findings and prognosis is unclear.

Methods:
Subjects comprised patients who underwent brain MRI at least once after being diagnosed with hypoglycemic encephalopathy between 2005 and 2011. Medical records were obtained from retrospectively investigate age, sex, cause of hypoglycemia, neurological findings on admission, body temperature, minimum blood glucose, duration of hypoglycemia, corrected blood glucose levels, lactic acid levels, brain MRI findings and prognosis (Glasgow outcome scale; GOS).

Results:
Of the 165 patients diagnosed with hypoglycemic encephalopathy, 44 (27.6%) underwent brain MRI. High signal intensity lesions were observed on diffusion weighted imaging (DWI) in 26 (59.6%) patients and 25 (56.8%) patients had a poor prognosis (GOS 1–4). Prognosis tended to be poorer in cases with high signal intensity lesions on DWI than those without (P=0.084). Lesion sites included the cerebral cortex (18 patients), cerebral white matter (15 patients), the internal capsule (10 patients), the basal ganglia (5 patients), the hippocampus (8 patients) and the splenium of corpus callosum (2 patients). Lesions

were observed in multiple these sites in 16 patients. High signal intensity lesions on DWI were unilateral in 8 (30.8%) patients and no significant difference in prognosis was observed between patients with unilateral and bilateral lesions (P=0.272). With regards to the relationship between lesion site and prognosis, prognosis was poor in 1 subject where a lesion was noted in the internal capsule (10%), whereas prognosis was poor in all patients where lesions were noted in the basal ganglia and hippocampus. Although prognosis was poor in 1 (25%) of the 4 patients where a lesion was noted in the white matter only, prognosis was poor in 9 (90%) of the 10 patients where lesions were noted in the white matter and the cortex. Results also suggested that a high body temperature contributes to the appearance of high signal intensity lesions on DWI (P=0.066).

Conclusions:
A relationship was observed between lesion site and prognosis as the appearance of high signal intensity lesions on DWI was suggestive of a poor prognosis. Moreover, high body temperature may be related to the appearance of high signal intensity lesions on DWI.

683
BRAIN-0808
Poster Session

Cerebral Metabolic Regulation

FITTING 13C MRS DATA TO EVALUATE ALTERNATIVE METABOLIC PATHWAY MODELS FOR SYNAPTIC TRAFFICKING OF NEUROTRANSMITTER GLUTAMATE

P. Maciejewski[1]
[1]*Radiology, Weill Cornell Medical College, New York City, USA*

Objectives: The glutamate-glutamine (Glu-Gln) cycle is the principal model for understanding synaptic trafficking of neurotransmitter glutamate. However, observing conceptual difficulties with the Glu-Gln cycle model, including the imbalance of nitrogen in the intercellular exchange of glutamate for glutamine between presynaptic neurons and astrocytes, Maciejewski and Rothman (2008) proposed alternative models for glutamatergic neurotransmission. Presently, there is no method for evaluating the likelihood that any of these alternative metabolic pathway models provides a better explanation of neurotransmitter glutamate trafficking than the conventional Glu-Gln cycle model. The present work aims to introduce methods for comparing how well alternative metabolic pathway models for synaptic trafficking of neurotransmitter glutamate fit data from 13C magnetic resonance spectroscopy (MRS) isotopic label-transfer studies of brain metabolism and glutamatergic neurotransmission, and to apply these new methods in model-fit comparisons between the Glu-Gln cycle model and alternative metabolic pathway models for glutamatergic neurotransmission.

Methods: Metabolic pathways models representing the Glu-Gln cycle and alternative cycles for glutamatergic neurotransmission in which presynaptic neurons exchange glutamate for glutamine plus a tricarboxylic acid cycle metabolite, i.e., citrate (Cit), oxoglutarate (OG), or malate (Mal), with astrocytes in a ratio of 2:1:1 to maintain intercellular nitrogen balance were constructed based on stoichiometric principles as described previously (Maciejewski and Rothman, 2008). These models were then used to fit 13C MRS isotopic label-transfer data associated with brain metabolism and synaptic neurotransmission reported in Oz et al. (2004). An information-theoretic procedure, tailored to the fitting of metabolic pathway models to 13C MRS isotopic labeling data, was developed and used to compare model-fits among competing models. A pathway representing *de novo* glutamine synthesis in astrocytes was included in each model to account for observed asymmetric 13C labeling of glutamate and glutamine in the C2 and C3 positions.

Results: Based on Akaike's Information Criterion, a (2 Glu)-(Gln-Mal) cycle model represents the most likely pathway for synaptic trafficking of neurotransmitter glutamate given the Oz et al. (2004) data among the metabolic pathway

models considered, followed in order of likelihood by (2 Glu)-(Gln-OG), Glu-Gln, and (2 Glu)-(Gln-Cit) cycle models. Figure 1 compares the Oz et al. (2004) data to estimates for the Glu-Gln and (2 Glu)-(Gln-Mal) cycle models, illustrating that the latter model fits the 13C MRS glutamate C4 and aspartate (Asp) C3 position data better than does the Glu-Gln cycle model.

Conclusions: An information-theoretic procedure allows alternative models for synaptic trafficking of neurotransmitter glutamate to be compared directly to each other on a probabilistic basis based on how well each model fits data from 13C MRS isotopic label-transfer studies. Preliminary results employing this information-theoretic model-fit approach indicate that a glutamate-(glutamine-malate) cycle model fits the 13C MRS data of Oz et al. (2004) better than the conventional glutamate-glutamine cycle model.

References: Maciejewski PK, Rothman DL. Proposed cycles for functional glutamate trafficking in synaptic neurotransmission. Neurochem Int 2008;52:809

Oz G, Berkich DA, Henry P-G, Xu Y, LaNoue K, Hutson SM, Gruetter R. Neuroglial Metabolism in the Awake Rat Brain: CO2 Fixation Increases with Brain Activity. J Neurosci 2004;24(50):11273

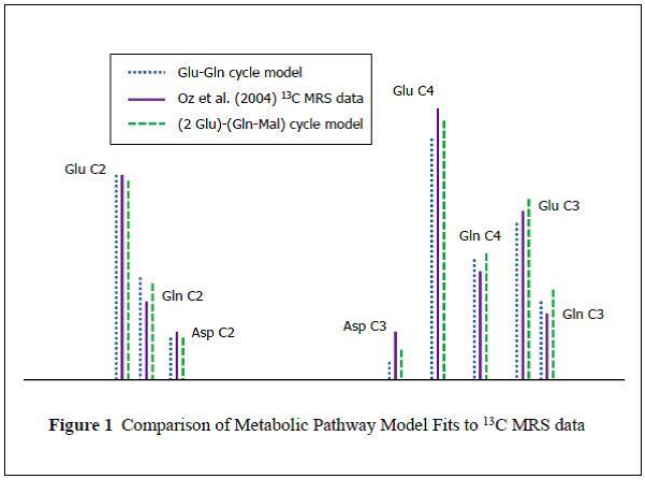

Figure 1 Comparison of Metabolic Pathway Model Fits to ^{13}C MRS data

684
BRAIN-0291
Poster Session

Cerebrovascular Regulation

HYPEROXIC GAS-INDUCED CHANGES IN TWO MODELS OF GLIOMA: AN MRI STUDY TO ASSESS BLOOD VOLUME AND OXYGEN SATURATION IN RATS.

A. Chakhoyan[1], A. Corroyer-Dulmont[1], E. Petit[1], L. Chazalviel[1], J. Toutain[1], D. Divoux[1], M. Bernaudin[1], E.T. MacKenzie[1], O. Touzani[1], S. Valable[1]
[1]1 CNRS UMR 6301 ISTCT 2 Université de Caen Bas se-Normandie 3 CEA DSV/I2BM 4 Normandie Univ, CERVOxy Group, Caen, France

Objectives: Tumor hypoxia, feature of high grade glioma (GBM), is a well-established cause of resistance to radiotherapy. Although administration of a mixture of O_2 with 5% CO_2 (Carbogen) is thought to alleviate tumor hypoxia, the overall results are unsatisfactory in terms of increased radiotherapeutic efficacy (1). These results could be attributed to the morphologically and functionally disturbed vessels in glioma. The objective of this study was to assess, with multiparametric MRI, the ability of Carbogen to oxygenate the tissue based on two GBM models with different patterns of blood volume and hypoxia.

Methods: U87 and U251 human glioma cells were stereotactically injected into a caudatoputamen of athymic rats (n=3/group). MRI was performed in a 7T magnet. The animals were anesthetized with 2% isoflurane in air and mechanically ventilated; body temperature was maintained at 37.5±0.5°C. Brain tumors were visualized on a T2w image. Fractional Cerebral Blood Volume (*f*CBV) was measured after injection of P904 (200µmol/kg) (2). Blood oxygen saturation ($S_{MRI}O_2$) maps were computed by a quantitative BOLD approach (3). *f*CBV maps and $S_{MRI}O_2$ maps were generated for each rat under two conditions: baseline (air) or during Carbogen ventilation. *f*CBV and $S_{MRI}O_2$ maps were then used

to calculate the Carbogen-induced change (expressed as Δ*f*CBV & $\Delta S_{MRI}O_2$). Data processing was performed with ImageJ® and two region of interest (tumor and contralateral) were used for signal analyses. All data are presented as mean±SD.

Results: In the U87 model, resting *f*CBV was greater in the tumor compared to the contralateral hemisphere. In contrast, U251 exhibited a *f*CBV similar to healthy tissue. The mean Δ*f*CBV induced by Carbogen inhalation was markedly increased in the contralateral side (16.7±7.8% and 18.3±8.2%, in rats of the U87 and U251 models, respectively). Carbogen resulted in an increase in Δ*f*CBV only in the U87 tumor (8.9±3.4%). The U251 tumor displayed insignificant changes to Carbogen inhalation (1.5±3.9%) (Figure 1A).

Carbogen increased mean $\Delta S_{MRI}O_2$ values by 1.8±5.0% and 4.3±4.2% in the contralateral brain of rats implanted with U87 and U251 cells, respectively. Interestingly, the U87 tumor was responsive to the hyperoxic gas with 1.5±4.0% of difference. In contrast, the U251 tumor seems unresponsive to Carbogen (0.0±3.0%) in the animals so far studied (Figure 1B).

Conclusion: In all instances, ventilation with Carbogen increased *f*CBV, associated with a minor increase in $\Delta S_{MRI}O_2$ in the healthy contralateral tissue. However, the response was tumor-dependent. In the mildly hypoxic U87 model, Δ*f*CBV was modestly increased and $\Delta S_{MRI}O_2$ was similar to, or greater than, that of normal brain. Nonetheless, in the severely hypoxic U251 model, neither $\Delta S_{MRI}O_2$ nor Δ*f*CBV were modified by Carbogen. Our study underlines the heterogeneity of the flow/metabolism interactions in various models of GBM. This variability should be taken into account in order to palliate intratumoral hypoxia for radiotherapy in GBM patients.

References: 1. Miralbell R *et al.,* J Clin Oncol **17**:3143-9 (1999); 2. Valable S *et al.,* NMR Biomed. **21**:1043-56 (2008); 3. Christen T *et al.,* NMR Biomed. **24**:393-403 (2011).

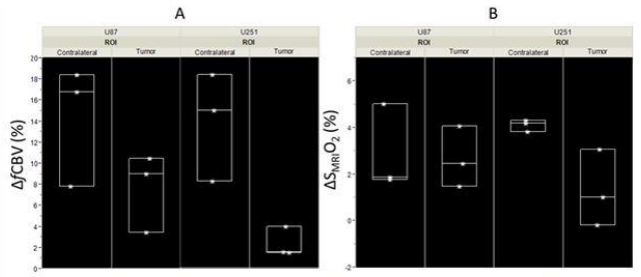

Figure 1 : Quantification of the change (Δ%) in *f*CBV and $S_{MRI}O_2$ during inhalation of Carbogen. Data are plotted as boxes, showing median values, 25% and 75% percentiles.

685
BRAIN-0390
Poster Session

Cerebrovascular Regulation

INVESTIGATING THE PHYSIOLOGICAL ORIGIN OF SPONTANEOUS CHANGES IN CEREBRAL HAEMODYNAMICS FOLLOWING BRAIN INJURY.

A. Edwards-Bailey[1], *D. Highton*[2], *I. Tachtsidis*[3], *M. Smith*[2]
[1]*Institute of Neurology, University College London, London, United Kingdom*
[2]*Neurocritical Care, University College Hospitals Queen Square, London, United Kingdom*
[3]*Medical Physics and Bioengineering, University College London, London, United Kingdom*

Objectives: Cerebral haemodynamic regulation is frequently impaired following acute brain injury; this is associated with cerebral hypoxia-ischaemia and worse patient outcome. Strategies that optimise cerebral perfusion by manipulation of systemic physiology are associated with improved outcome[1]. Various cerebral autoregulation (CA) indices have been used to guide such treatment – most notably Mx and PRx, which are correlations between arterial blood pressure (ABP) and transcranial Doppler monitored cerebral blood flow velocity (FV) and intracranial pressure (ICP) respectively [2]. Non-invasive near infrared spectroscopy derived CA indices have also been reported - TOx and THx are derived as correlations between ABP and tissue oxygenation index (TOI), a measure of cerebral haemoglobin oxygen saturation, and tissue haemoglobin index

(THI), a measure of cerebral total haemoglobin, respectively [2]. In addition to ABP, cerebral haemodynamic regulation is influenced by arterial carbon dioxide (CO2), arterial oxygen saturation (SaO2) and neuronal metabolic activity. These are not assessed by standard indices of CA, which consider only ABP.

The aim of this study is to measure the influence of systemic variables (ABP, CO2 and SaO2) on changes in cerebral variables (TOI, THI, ICP and FV). We hypothesise that all the systemic variables, not only ABP, will have significant influence on monitored cerebral physiology, and describe additional dimensions of the physiological state.

Methods: Data were collected on 20 mechanically ventilated brain injured patients over 60 minutes following ethics approval and representative consent. TOI and THI (NIRO 100, Hamamatsu Photonics KK), FV and ICP, and ABP, end tidal CO2 and SaO2 were monitored continuously. The influence of the systemic variables on the cerebral variables was examined using multivariate analysis (canoncial correlation analysis), generating a linear model to explain variation in the cerebral physiology by variance in ABP, CO2 and SaO2. For robustness, subsequent analysis was performed only in patients in whom canonical analysis explained more than 10% of the variance (R^2 >10%)

Results:: The multivariate models were significant in all 20 patients (chi-squared $p<0.0001$). The mean R^2 and squared structure coefficient of variables in the 14 patients identified for further analysis are shown in Table 1. The structure coefficient represents each variable's relative importance in describing the observed effect. Thus, while ABP has the strongest influence on measured cerebral physiology, CO2 and SaO2 also have important effects.

Variable	Mean squared structure coefficients	Standard Deviation
TOI	0.27	0.24
THI	0.46	0.24
ICP	0.33	0.28
FV	0.29	0.27
ABP	0.44	0.3
CO2	0.33	0.33
SpO2	0.2	0.27
Mean R^2	26%	

Conclusion: In addition to changes in ABP, cerebral haemodynamic changes are also associated with changes in CO2 and SaO2. This suggests that systemic physiological changes will confound interpretation of CA defined by indices such as PRx that are based on ABP alone. Some unaccounted variability could be explained by the effect of neuronal activity on cerebral haemodynamics, and further work is required to assess its contribution. Multimodal monitoring of cerebral haemodynamics holds considerable potential for monitoring all aspects of haemodynamic regulation, but requires advanced multivariate analysis strategies to derive robust predictions of all aspects of the complex underlying physiology.

References:

1. Dias C, et al. *Neurocrit Care* 2015: Jan 8, (Epub ahead of print)
2. Zweifel C, et al. *Med Eng Phys* 2014; 36: 638-45

686
BRAIN-0551
Poster Session

Cerebrovascular Regulation

ASSESSING BRAIN DAMAGE AFTER PERINATAL HYPOXIC-ISCHAEMIA USING AN AUTOMATED PROTOCOL FOR COMBINED REGIONAL ANALYSIS OF THE CEREBRAL BLOOD FLOW AND MR SPECTROSCOPY

M. Sokolska[1], C. Uria-Avellanal[2], M.J. Cardoso[3], M. Proisy[2], A. Bainbridge[4], S. Ourselin[3], D. Thomas[1], N. Robertson[2], X. Golay[1]
[1]Brain Repair & Rehabilitation, UCL Institute of Neurology, London, United Kingdom
[2]Neonataology, UCL Institute for Women's Health, London, United Kingdom
[3]Medical Physics & Bioengineering, UCL Centre for Medical Image Computing, London, United Kingdom
[4]Medical Physics & Bioengineering, UCLH NHS Foundation Trust, London, United Kingdom

MOTIVATION: Perinatal hypoxia-ischemia (HI) can cause catastrophic alteration of brain metabolism and physiology[1], resulting in neonatal encephalopathy. Metabolic changes detected using magnetic resonance spectroscopy (MRS) have been used as a reliable predictor of clinical outcome[2]. Similarly, abnormalities in cerebral blood flow (CBF), reflecting cerebral physiology, have been linked to HI[3,4]. Therefore this study aims to investigate the added value of combining thalamic MRS with automatic regional CBF analysis as a potential biomarker of outcome in HIE.

METHODS: Fourteen term neonates (GA 38-41 weeks) with neonatal encephalopathy were included. All neonates underwent therapeutic hypothermia and were scanned between the 3rd and 7th day of life. The protocol included: T1, T2 and diffusion-weighted imaging, MRS (TR/TE=2288/288ms) and pseudo-continuous arterial spin labeling (pCASL[5] label duration=1.7s,PLD=1.5-2s). Thalamic lactate to N-acetylaspartate (Lac/NAA) peak area ratio was calculated. Subjects were divided into two groups based on Lac/NAA: below 0.29[2] (likely favorable outcome; n=9) and above 0.29 (high risk of poor outcome; n=5). Raw ASL images were corrected for motion before averaging and CBF quantification[6,7]. CBF was calculated in automatically defined regions, based on both atlas based probabilistic tissue segmentation of 5 tissue classes[8] and joint multi-atlas label propagation with fusion of 50 neonatal brain regions[9]. T-tests and F-tests were computed to investigate the statistical differences in mean and variance of CBF values between low- and high-risk groups.

RESULTS: Examples of CBF maps and analysis of regional CBF are shown in Figure 1 and 2 respectively. Boxplots show the range, median and interquartile range. In the low risk group, all CBF values are within a tight range for all brain regions (8-47ml/100g/min), whereas in the high-risk group, the range is much broader: (7-128ml/100g/min). In this group, CBF in the lentiform nuclei and parasagittal cortex is especially high. There were statistical differences for CBF in the lentiform nuclei between the high- and low-risk groups (t-test, F-test<0.05) but not in the parasagittal cortex (t-test=0.07,F-test<0.05).

DISCUSSION & CONCLUSION: This study presents a detailed analysis of regional CBF from ASL in conjunction with Lac/NAA peak area ratio. ASL was used here as it provides physiological information complementing structural scans noninvasively. Generally, an increase in CBF accompanies an increase in Lac/NAA, most notably within the deep grey matter nuclei and parasagittal cortex. This may relate to the loss of autoregulation in severely affected neonates, and this information has the possibility to further separate this high risk group of patients from the moderately affected, which is difficult using current imaging and clinical criteria. It is expected that long-term follow-up data of these neonates will enable correlation between CBF findings and final clinical outcome.

The proposed automated method of segmentation and parcellation increases the

objectivity of ROI placement, making it user-independent. It is less labour-intensive and time-consuming, and therefore more amenable to implementation in clinical practice.

REFERENCES: [1]Pryds Annals of Neurology(1991), [2]Thayyil et al. Pediatr Res(2010), [3]Pryds O et al. J Pediatr(1990), [4]De Vis et al. Eur Radiol(2014), [5]Dai et al. MRM(2008), [6]Buxton et al. MRM(1998), [7]Varela et all. NMR Biomed(2011), [8]http://biomedic.doc.ic.ac.uk/brain-development/index.php?n=Main.Neonatal,[9]http://biomedic.doc.ic.ac.uk/brain-development/index.php?n=Main.Neonatal3

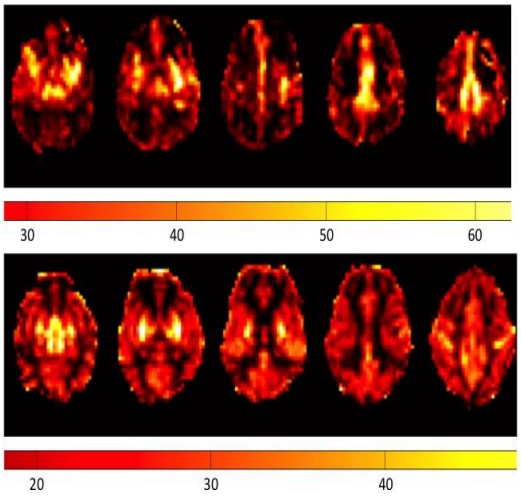

Figure 1. CBF maps of 2 neonates from the high risk group (thalamic Lac/NAA > 0.29)

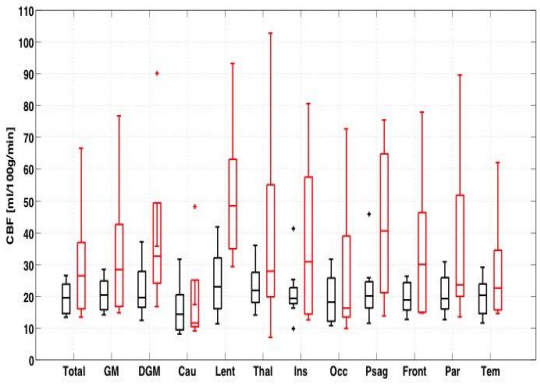

Figure 2. Results of detailed regional CBF analysis; neonates with thalamic Lac/NAA peak ratio below (black) and above (red) predictive value of 0.29

687
BRAIN-0381
Poster Session

Cerebrovascular Regulation

ASTROCYTES CONTRIBUTE TO THE CEREBRAL BLOOD FLOW RESPONSE TO HYPERCAPNIA

C. Howarth[1], B.A. Sutherland[2], H.B. Choi[3], C. Martin[1], B.L. Lind[4], L. Khennouf[4], J.M.P. Pakan[3], G.C.R. Ellis-Davies[5], M.J. Lauritzen[4], N.R. Sibson[6], A.M. Buchan[2], B.A. MacVicar[3]
[1]Department of Psychology, University of Sheffield, Sheffield, United Kingdom
[2]Radcliffe Dept. of Medicine, University of Oxford, Oxford, United Kingdom
[3]Djavad Mowafaghian Centre for Brain Health, University of British Columbia, Vancouver, Canada
[4]Department of Neuroscience and Pharmacology and Center for Healthy Aging, University of Copenhagen, Copenhagen, Denmark
[5]Department of Neuroscience, Mount. Sinai School of Medicine, New York, USA
[6]Cancer Research UK and Medical Research Council Oxford Institute for Radiation Oncology Dept. of Oncology, University of Oxford, Oxford, United Kingdom

Objectives: Although astrocyte $[Ca^{2+}]_i$ transients can evoke cerebral blood flow (CBF) changes[1], their role in CBF regulation has been questioned[2,3]. Based on the signalling pathways which occur within astrocytes, we investigated whether astrocytes contribute to hypercapnia-evoked CBF responses.

Methods: All procedures were approved by the relevant Institutional Animal Care and Use Committees and treatment of animals complied with the Animals (Scientific Procedures) Act, 1986. $[Ca^{2+}]_i$ responses to hypercapnia (10% CO_2) *in vivo* in C57/BL6 mice and astrocyte $[Ca^{2+}]_i$-evoked vasodilation in hippocampal slices from Sprague-Dawley rats were measured using 2-photon laser scanning microscopy. Evoked CBF responses were measured *in vivo* using laser Doppler flowmetry or laser speckle

contrast imaging in Wistar rats. Intracerebral injection of buthionine sulfoximine lowered glutathione (GSH) levels *in vivo*. GSH levels and PgE_2 release were measured by biochemical assay.

Results: *In vivo*, hypercapnia selectively increased astrocyte $[Ca^{2+}]_i$ and evoked COX-1-dependent CBF increases. *In vitro*, astrocyte $[Ca^{2+}]_i$ transients resulted in PgE_2 formation (via a COX-1 and GSH-dependent pathway) and evoked GSH- and COX-1-sensitive vasodilations. *In vivo*, hypercapnia-evoked CBF responses were attenuated when GSH levels were lowered.

Conclusions: These data indicate a novel role for astrocytes in regulating CBF responses to hypercapnia *in vivo*. Hypercapnia evokes an increase in astrocyte $[Ca^{2+}]_i$ transients, activating COX-1 and resulting in PgE_2 release. Lowering GSH levels reduces astrocyte release of PgE_2 and, therefore, vasodilations *in vitro* and hypercapnia-evoked CBF increases *in vivo*. Hence, regulation of CBF may be impaired in CNS pathologies in which GSH levels are depleted.

References

1 Attwell, D. *et al.,* (2010) Nature 468: 232-243
2 Nizar, K. *et al.,* (2013) J Neurosci 33: 8411-8422
3 Bonder, D.E. & McCarthy, K.D. (2014) J Neurosci 34: 13139-13150

688
BRAIN-0199
Poster Session

Cerebrovascular Regulation

CHANGES IN EFFECTIVE DIFFUSIVITY FOR OXYGEN DURING NEURAL ACTIVATION AND DEACTIVATION ESTIMATED FROM CHANGES IN CAPILLARY DIAMETER MEASURED BY TWO-PHOTON LASER MICROSCOPE

H. Ito[1], H. Takuwa[2], Y. Tajima[2], H. Kawaguchi[2], Y. Ikoma[2], C. Seki[2], M. Ibaraki[2], K. Masamoto[2], I. Kanno[2]
[1]Advanced Clinical Research Center, Fukushima Medical University, Fukushima, Japan
[2]Molecular Imaging Center, National Institute of Radiological Sciences, Chiba, Japan

Objectives: The relation between cerebral blood flow (CBF) and cerebral oxygenextraction fraction (OEF) can be expressed using the effective diffusivity foroxygen in the capillary bed (D) as OEF=1-exp(-D/CBF) [1]. The D value isproportional to capillary blood volume. In the present study, changes in Dduring neural activation and deactivation were estimated from changes incapillary diameter measured by in vivo two-photon laser microscopic imaging inawake mice, and compared with those calculated from measures by PET in humansreported previously [2,3].

Methods: The cortical vasculature was imaged with two-photon lasermicroscope through a chronic cranial window at the somatosensory cortex andcerebellum in awake mice (C57BL/6J mice, N=6) after intraperitonealadministration of sulforhodamine 101 for labelling blood plasma. Capillaryvessels diameter in the somatosensory cortex was measured at baseline anddduring whisker stimulation. Capillary vessels diameter in the cerebellum wasmeasured at baseline and one day after permanent occlusion of contralateralmiddle cerebral artery which could cause crossed cerebellar diaschisis (CCD), amodel of neural deactivation. Changes in capillary diameter during neuralactivation and deactivation were calculated, and then changes in D wereestimated.

Results: Percentage changes in capillary diameter during whisker stimulationwere 5.0 ± 3.5%, 11.4 ± 6.3%, and 15.2 ± 4.9% for capillary diameter of lessthan 6 μm, 6–10 μm, and 10–15 μm, respectively. Percentage changes in capillarydiameter during CCD were -9.2 ± 2.9%, -12.0 ± 6.1%, and -12.7 ± 7.3% forcapillary diameter of less than 6 μm, 6–10 μm, and 10–15 μm, respectively. Percentagechanges in D during whisker stimulation and CCD are 10.3 ± 7.3% and -17.5 ±5.3% for capillary diameter of less than 6

µm, respectively. When the capillarydiameter was smaller, absolute values of percentage changes in D during bothwhisker stimulation and CCD were smaller. Using mean values of CBF and OEF inthe primary motor cortex at baseline and during motor task previously reportedwith PET [2], calculated percentage change in D during neural activation was6.8%. Using mean values of CBF and OEF in both CCD and unaffected sides ofcerebellar cortex previously reported with PET [3], calculated percentagechange in D during neural deactivation with consideration of unaffected side asbaseline was -11.4%.

Conclusions: For capillary diameter of less than 6 µm, percentage changes in Dduring both neural activation and deactivation were most closed to percentagechanges in D calculated from human PET data previously reported. This canindicate that more thin capillary may manly play a role in oxygen transportfrom blood to brain tissue.

References:

1. Hyder F et al., J Appl Physiol 1998; 85:554-564.
2. Ito H et al., J Cereb Blood Flow Metab2005; 25: 371-377.
3. Ito H et al., Ann Nucl Med. 2002; 16: 249-254.

689
BRAIN-0626
Poster Session

Cerebrovascular Regulation

CHARACTERIZATION OF CHANGE IN CEREBRAL MICROVASCULAR NETWORK IN RESPONSE TO HYPERCAPNIA THROUGH CAROTID ARTERY INJECTION OF FLUORESCENT DEXTRAN

L. Joo[1], M. Koletar[2], L. Thomason[2], A. Dorr[2], B. Stefanovic[1]
[1]Medical Biophysics, University of Toronto, Toronto, Canada
[2]Physical Sciences, Sunnybrook Research Institute, Toronto, Canada

Objectives: The CBF elevation with hypercapnia has been well-characterized at the millimeter scale by hemodynamically weighted neuroimaging. However, little is known about the changes in the brain microvascular network geometry that underlie the global increase in CBF to hypercapnia (1), yet this knowledge is necessary for understanding the coupling between flow and volume in the brain (2). Earlier work from our lab demonstrated reproducible, but unexpectedly high spatial heterogeneity of changes in caliber of individual microvessels in response to functional stimulation (3). We here set out to examine the spatiotemporal pattern of changes in the cerebral microvascular network in response to hypercapnia.

Methods: Two-photon fluorescence microscopy was employed to image the microvessels of the rat's primary somatosensory cortex in vivo while eliciting global vasodilation through periodic, graded hypercapnia. In addition to the 3-by-3-mm diameter cranial window implantation, the animals were tracheostomized and mechanically ventilated, with inspired CO2 concentration profiles prescribed via a digitally programmable gas mixer. The microvascular transit times were quantified by bolus tracking analysis of the 2D data acquired during periodic injections of boluses of 70-kDa Texas Red dextran into the carotid artery. The bolus injection was triggered by the microscope to allow estimation of absolute microvascular transit times as a function of the inspired CO2 concentration. To allow steady-state to be reached, boluses were injected at least 60s following the change in the CO2 concentration, with the 10s inter-bolus interval.

Results: Attached figure shows representative maps of transit time changes, upon CO2 elevation from 0 to 5%, from vessels found at 150µm (B), 200µm (C), and 250µm (D) deep from the surface of the brain. Three boluses were administered at each level of inspired CO2. The transit time changes, encoded by the colormap, correspond to the average difference in the time of the peak fluorescence signal intensity in each vessel. Both elongations (red) and shortening (blue) of vessel-

wise transit times were observed in response to hypercapnia.

Conclusion: Compared to the tail vein injection of the fluorescent dextran, injection into the carotid artery greatly expedites the arrival of fluorophore into the cerebral microvasculature and reduces, by at least half an order of magnitude, the volume of fluorescent dextran required for bolus tracking through the cerebral circulation. These methodological developments which enable imaging of large number of boluses through the microvascular bed, allowing the interrogation of the spatial heterogeneity and temporal repeatability of the changes in the microvascular hemodynamics elicited by hypercapnic challenges, lies at the heart of understanding the flow-volume coupling in the cerebral microcirculation.

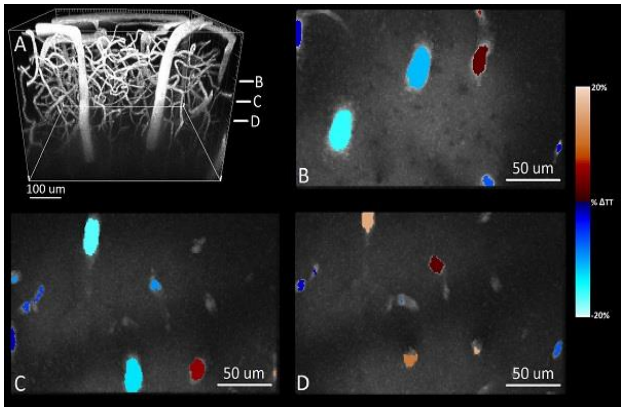

References

1. Villringer et al. Capillary perfusion of the rat brain cortex. An in vivo confocal microscopy study. Circ Res, 75(1):55-62, 1994.

2. Piechnik et al. Modelling vascular reactivity to investigate the basis of the relationship between cerebral blood volume and flow under CO2 manipulation. NeuroImage, 39:107-118, 2008.

3. Lindvere et al. Cerebral microvascular network geometry changes in response to functional stimulation. NeuroImage, 71:248-259, 2013.

690
BRAIN-0557
Poster Session

Cerebrovascular Regulation

BRAIN MICROVASCULAR ENDOTHELIAL CELLS EXPRESS CONSTITUTIVELY ACTIVE NEURONAL NITRIC OXIDE SYNTHASE DISTINCT FROM THE ISOFORM EXPRESSED IN NEURONS

N.R. Peterson[1], V.N. Sure[1], A.O. Gordon[1], G. Rajaprabhakaran[1], S. Dutta[1], D. Liu[1], I. Rutkai[1], D.W. Busija[1], P.V.G. Katakam[1]
[1]Pharmacology,
Tulane University School of Medicine,
New Orleans, USA

Objectives. Experimental stroke in animals with gene deletions of endothelial (eNOS) and neuronal (nNOS) nitric oxide synthase isoforms have shown opposite effects on infarct injury. nNOS has been identified recently in endothelial cells, however, its functional significance is unclear. Our objective was to localize nNOS in brain microvascular endothelial cells (MECs) and characterize its functional role.

Methods and Results. Both male and female pups were utilized for cell culture studies. Primary MECs from humans (hMECs), rats (rMECs), and mouse (mMECs) along with cultured primary rat cortical neurons were used in the studies. Immunohistochemistry identified von Willebrand factor, eNOS, and nNOS but stained negative for GFAP and Neu1 in rMECs. Western blot analysis using antibodies targeting N-terminal domain of nNOS revealed immunoband of a potential nNOS splice variant at ~130 kD in the homogenates of rMECs as opposed to 160 kD in rat cerebral cortex and cultured neurons. In contrast, antibodies targeting C-terminal domain of nNOS did not show any specific immunoband that matched with the size of known nNOS splice variant previously reported. Furthermore, western blot analysis of the homogenates of rat cerebral arteries using antibodies targeting N-terminal domain identified two immunobands that corresponded to 160 kD and 130 kD nNOS peptides and the intensity of the immunobands

diminished with endothelial denudation. PCR experiments identified the mRNA of nNOS in MECs and siRNA targeting rat nNOS in rMECs was able to knockdown nNOS mRNA. Oxygen consumption rate measurements by Seahorse Analyzer in hMECs treated with selective inhibitors of nNOS (50 nmol/L or 1 µmol/L N-ω-Propyl-L-arginine; NPA) and eNOS (1 µmol/L L-N^5-(1-Iminoethyl)ornithine;NIO) revealed that maximal mitochondrial respiration was enhanced by NPA but diminished by NIO or L-NAME. Measurements of superoxide in MECs by electronspin resonance spectroscopy showed that NPA reduced but NIO increased superoxide generation.

Conclusions. Thus, we identified a constitutively active nNOS splice variant in brain MECs that is distinct from the isoform expressed in neurons. nNOS appears to tonically produce superoxide and negatively regulate mitochondrial respiratory capacity whereas eNOS elicited opposite responses. We conclude that brain MECs express a unique nNOS isoform exhibiting effects which are distinctly opposite of eNOS.

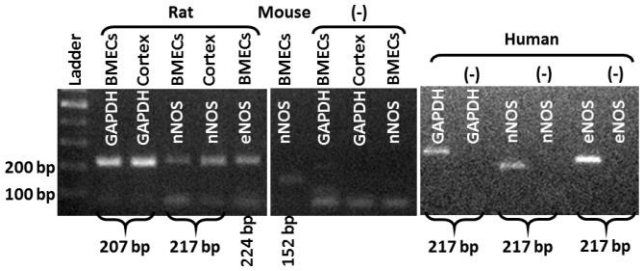

691
BRAIN-0816
Poster Session

Cerebrovascular Regulation

ACUTE HYPONATREMIA IMPAIRES FUNCTION OF LARGE CONDUCTANCE CALCIUM-ACTIVATED POTASSUIM CHANNELS (BKCA) IN THE MIDDLE CEREBRAL ARTERY OF THE RAT.

M. Aleksandrowicz[1], B. Dworakowska[2], E. Kozniewska[3], E. Kozniewska[1]
[1]Laboratory of Experimental Neurosurgery, Mossakowski Medical Research Centre Polish Academy of Sciences, Warsaw, Poland
[2]Department of Biophysics, Warsaw University of Life Sciences SGGW, Warsaw, Poland
[3]Department of Experimental and Clinical Physiology, Medical University of Warsaw, Warsaw, Poland

Objectives: Moderate to severe hyponatremia (decrease of extracellular concentration of sodium ions from 144 to 121 mM) affects the regulation of the isolated middle cerebral artery (MCA).[1] In hyponatremia, MCA does not dilate in response to acidosis, hyperkalemia and nitric oxide/endothelium-dependent acetylcholine. It does also not respond to nitric oxide (NO) donor (S-nitroso-N-acetyl-DL-penicylamine). Based on these results we hypothesize that in smooth muscle cells cGMP-related signal transduction and/or large conductance calcium-activated potassium channels (BK_{Ca}) function is impaired during acute hyponatremia. Present experiments aimed to test this hypothesis by studying the reactivity of the isolated MCA to 8Br-cGMP (membrane permeable analog of cGMP, 10^{-5}M) and to an activator (NS1619, 10^{-5}M) or inhibitor (paxilline, 10^{-5}M) of BK_{Ca} channels in normo- and hyponatremia. Moreover, the effect of hyponatremia on the characteristics of BK_{Ca} currents in smooth muscle cells isolated from MCAs was studied using patch-clamp method.

Material and Methods: Forty MCAs harvested from the brains of the adult male Wistar rats were used. Thirty one of them were mounted in an organ chamber filled with 3-(N- morpholino) propanesulfonic acid (MOPS) – buffered saline solution and pressurized. The chamber was placed on the stage of inverted microscope equipped with video camera for the recording of changes in the internal diameter of the vessels. Hyponatremia was induced by decreasing intra – and extraluminal concentration of Na^+ from 144 to 121 mM one hour prior to the reactivity tests. MCAs placed in normonatremic buffer (Na^+=144 mM) served as a reference group.

Middle cerebral artery myocytes were isolated from 9 MCAs according to the method described by Holland et al.[2] Conventional patch-clamp electrophysiology was used to measure whole cell BK_{Ca} currents using an Axopatch 200B amplifier (Axon Instruments).

Results: MCA dilated in response to 8Br-cGMP similarly in normo- (21±7% of baseline, $p<0.01$) and hyponatremia (15±3% of baseline, $p<0.05$). Activation of BK_{Ca} by NS1619 which resulted in the dilation of MCA by 16±1% ($p<0.001$) in normonatremia did not produce dilation of this vessel during hyponatremia. Slight, albeit not statistically significant constriction of MCAs by 4±2% of baseline was observed instead. In contrast, the was no difference in the response of MCA to the inhibitor of BK_{Ca} - paxilline which resulted in the constriction of MCA both in normo- (by 14±5% of baseline, $p<0.05$) and hyponatremia (by 13±5% of baseline, $p<0.05$). Hyponatremia did not affect BK_{Ca} current intensity in isolated MCA myocytes. It resulted, however, in a decrease of the sensitivity of BK_{Ca} channel to its opener – NS1619.

Conclusion: Our results demonstrate that a decreased sensitivity of BK_{Ca} channels in the middle cerebral artery smooth muscle cells to agonists might be responsible for the impaired regulation of this artery during acute moderate to severe hyponatremia.

Refrerences:

1. Aleksandrowicz M, Kozniewska E. Disturbed regulation of the isolated middle cerebral artery in acute hyponatremia. Folia Neuropathol 2013; 51: 227-234.

2. Holland M, Langton PD, Standen NB, Boyle JP. Efect of the activator, NS1619, on rat cerebral artery smooth muscle. Br J Pharmacol 1996; 17(1): 119-129.

692
BRAIN-0190
Poster Session

Cerebrovascular Regulation

EFFECTS OF PHYSICAL EXERTION AND HEAT ON CEREBROVASCULAR RESPONSE IN PROFESSIONAL FIREFIGHTERS

J.P. Neary[1], M. Butz[2], B.G. Dahlstrom[1], J. Smirl[3], S. Bishop[1]
[1]Kinesiology & Health Studies, University of Regina, Regina, Canada
[2]Medicine, University of Saskatchewan, Regina, Canada
[3]Health & Exercise Sciences, University of British Columbia Okanagan, Kelowna, Canada

Firefighting is a physically demanding occupation and a number of factors can compromise the firefighter's health during duty, including inadequate cerebral blood flow (CBF) regulation. We hypothesized that dynamic cerebral pressure–flow relationships will be altered in Professional Firefighters in response to acute physical exertion in the heat. Seven firefighters (age=30.8 ± 10.3 yrs) performed 30 minutes of treadmill walking at 65% of heart rate maximum in full turn-out gear in an environmental chamber at 39°C. Testing involved: 5 minutes squat-stand maneuvers at a point estimate at 0.05 Hz (the driven frequency) performed before and after the 30 minute treadmill test. CBF velocity was monitored in the middle cerebral artery (MCAv) using transcranial Doppler, non-invasive continuous blood pressure (BP) was recorded continuously using finger plethysmography, and 3-lead electrocardiography recorded heart rate. Transfer function analysis (TFA) was used to determine the autoregulatory metrics. The results showed that the driven TFA metrics were not significantly different ($p<0.05$) pre- to post-exercise for coherence (0.991 ± 0.007 vs 0.966 ± 0.037), gain (0.62 ± 0.15 vs 0.582 ± 0.199 cm/s/mmHg) and phase (0.634 ± 0.20 vs 0.612 ± 0.32 Rad), and power spectral density for both MCAv (22954.1 ± 11271.2 vs 24958.1 ± 13909.4 cm/s^2) and BP (56121.0 ± 16177.9 vs 62612.6 ±

23002.4 mmHg^2). In conclusion, the cerebral pressure – flow relationship in FF was unaltered pre- to post- moderate intensity exercise in the heat.

693
BRAIN-0658
Poster Session

Cerebrovascular Regulation

INTERACTION OF INTRACRANIAL PRESSURE AND CEREBRAL PERFUSION PRESSURE IN ISCHEMIC INJURY OF THE HEALTHY RAT BRAIN.

X. Dai[1], O. Bragina[2], T. Zhang[3], Y. Yang[4], G. Rao[5], D. Bragin[6], G. Statom[6], E. Nemoto[6]
[1]Department of Traditional Chinese and Western Medicine,
Xiangya Hospital Central South University, Changsha Hunan, China
[2]Neurosurgery, University of New Mexico, Albuquerque, USA
[3]Neurology, University of New Mexico, Albuquerque, USA
[4]College of Pharmacy, University of New Mexico, Albuquerque, USA
[5]Pathology and Laboratory Medicine,
VA University Health Care System, Pittsburgh, USA
[6]Neurosurgery, University of New Mexico, Pittsburgh, USA

Introduction: The commonly accepted clinical threshold, triggering implementation of ICP lowering maneuvers, is ICP of 20 to 25 mmHg persisting for longer than five to ten minutes. This threshold is based upon observations in patients suffering traumatic brain injury (TBI) or cerebrovascular accidents (CVA) with poor outcome at ICP >20-25 mmHg. However, the relationship between ICP and outcome depends upon many variables including arterial hypotension and hypoxia. While suggesting that ICP >20 is a predictor of poor outcome, they do not address the question of whether ICP>20 to 25 mmHg is injurious to healthy brain tissue. High ICP of up to 44 mmHg have been reported in idiopathic intracranial hypertension; hydrocephalus often associated with cognitive deficits.

In previous studies in healthy rats, we showed that a progressive increase in ICP from 10 to 30 and 50 mmHg induces microvascular shunting (MVS), characterized by tissue hypoxia, edema and increased blood brain barrier permeability even at normal to high CPP. Thus, high ICP may cause ischemic injury by MVS in the healthy brain. Our aim was to determine whether high ICP as a function of CPP causes ischemic injury in the healthy brain

Methods: A total of 38 male Sprague Dawley rats used to study the interaction between ICP and CPP on ischemic brain injury at ICP of 10 (normal), 30 and 50 mmHg for up to two hours duration at CPP of 70, 50 and 30 mmHg. Measurements of cerebral arterial-venous difference for oxygen (CAVDO2), magnetic resonance imaging (MRI) of CBF by arterial spin labeling (ASL), apparent diffusion coefficient (ADC) by diffusion tensor imaging (DTI) and neuronal ischemic injury by Fluorojade staining (FJS) were made. FJS neurons were counted by an observer blinded to treatment at 10X on three sections obtained on the dorsal, lateral cortex and striatum of both hemispheres.

Results: In the healthy rat brain, ICP at 50 mmHg at a CPP of 50 mmHg increased the average number of ischemic neurons and the sum of the total number of ischemic neurons (Fig). Changes in CBF showed evidence of hyperemia suggestive of microvascular shunting at an ICP of 30 mmHg and CPP of 70 mmHg with a broadening of the frequency histogram generated by voxel analysis. Increased ICP at 30 mmHg at low CPP resulted in a global decrease in CBF.

Conclusions: Our results suggest that high ICP to 30 and 50 mmHg for up to two hours at CPP of 50 mmHg results in ischemic neuronal injury in the healthy brain. The flattening of the CBF frequency histogram to higher flow values at high ICP even at normal CPP suggests microvascular shunting.

Fig. Legend: Sum and average Fluorojade stained neurons in 18 sections taken from one section of the rat brains at the level of the

striatum. Cerebral perfusion pressures at intracranial pressures of 10, 30 and 50 mmHg were 80, 55 and 50 mmHg, respectively.

* = P <0.05 compared to ICP 10 and 30 mmHg.

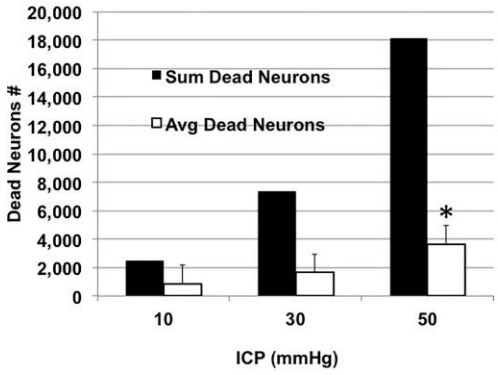

694
BRAIN-0847
Poster Session

Cerebrovascular Regulation

ACUTE INCREASES IN SYMPATHETIC TONE DURING COLD PRESSOR TEST RESULTS IN INCREASED GLOBAL BRAIN BLOOD FLOW

J.M. Serrador[1], *L.A. Reyes*[2], *M. Blatt*[3], *B. Ghobreal*[1], *M. Falvo*[1]
[1]*Pharmacology and Physiology, Rutgers Biomedical Health Sciences, Newark, USA*
[2]*War Related Illness and Injury Study Center, New Jeresy VA Hospital, East Orange, USA*
[3]*War Related Illness and Injury Study Center, New Jersey VA Hospital, East Orange, USA*

Objectives: The role of sympatheticregulation of cerebral vascular tone is under debate. The goal of this work sought to clarify sympathetic regulation of cerebral blood flow in the acute setting of a cold pressor test. Previous work has found increased velocity in the middle cerebral artery which could be indicative of either increased flow, or vasoconstriction at the site of insonation. We measured both cerebral blood velocity and carotid blood flow during sympathetic activation to determine if changes in velocity represented increases in brain blood flow or cerebral vasoconstriction.

Methods: To assess the role of sympathetic activity, 16 healthy individuals participated in a cold pressor test in which they immersed their dominant hand in ice cold water for 84±60 seconds. We continuously monitored beat-by-beat blood pressure; cerebral flow velocity in the middle (MCA), anterior cerebral (ACA) and internal common carotid artery (ICA) and end tidal CO_2.

Results: As expected the cold pressor test produced a significant increase in sympathetic tone as evident in the increased mean arterial blood pressure (MAP) from 107±4 to 122±6 mmHg (P=0.005). In addition to the rise in MAP the cold pressor resulted in increased bloodflow to the MCA (+11.4±3.7%); ACA (+8.6±3.2%), and internal carotid arteries. This increase in flow could not be attributed to CO_2 levels, as these values did not change from baseline measurements to end of cold pressor (40.1±0.7 vs 40.1±0.8 mmHg).

Discussion: Results from these data demonstrate that increases in middle and anterior cerebral velocities match closely with increases in carotid artery blood flow. This would suggest that acute increases in sympathetic activation from the cold pressor test results in global increases in cerebral blood flow but not cerebral vasoconstriction. Had sympathetic activity caused vasoconstriction at either the arteriolar or MCA level, we would expect to see reductions in carotid flow, rather than increases. Thus changes in velocity in the MCA and ACA appear to represent a global increase in brain blood flow most likely associated with the pain and other sensory activity that occurs during a coldpressor. These findings do not support a role for a sympathetic vasoconstrictionin the brain.

Support: This work was funded by the Dept of Veteran Affairs, NIH and the War Related Illness and Injury Study Center. Dr. Serrador was a recipient of the SFI Walton Visiting Fellowship at the National University of Ireland Galway.

695
BRAIN-0625
Poster Session

Cerebrovascular Regulation

CEREBRAL AUTOREGULATION IN PATIENTS WITH SEVERE BRAIN INJURY

C.G. Riberholt[1], N.D. Olesen[2], M. Thing[3], T.H. Petersen[1], J. Mehlsen[4]
[1]Department of Neurorehabilitation TBI Unit, Glostrup University Hospital, Glostrup, Denmark
[2]Department of Anaesthesia, Rigshospitalet University of Copenhagen, Copenhagen, Denmark
[3]Department of Paediatrics, Copenhagen University Hospital Hvidovre, Hvidovre, Denmark
[4]Coordinating Research Centre, Frederiksberg Hospital, Copenhagen, Denmark

Objectives: Early mobilisation is of great importance for the functional outcome in patients with severe acquired brain injury. However, these patients show orthostatic intolerance and signs of autonomic nervous dysfunction complicating mobilisation. Changes in autoregulation of cerebral blood flow (CBF) may contribute to the impediments and therefore we examined CBF autoregulation in patients with severe brain injury and impaired consciousness using a tilt table and compared the results to those of healthy volunteers.

Methods: Fourteen patients *(7 men, mean age 56.6 ±17.5 years)* with severe brain injury and 15 healthy volunteers *(7 men, mean age 36.1±12.5 years)* were included. The CBF was measured by Transcranial Doppler (TCD) in the middle cerebral artery and expressed as the flow velocity. Continuous blood pressure (BP) was recorded from the index finger using photoplethysmography. CBF autoregulation was determined by the beat to beat correlation between CBF and BP. After 30 min of resting, baseline values were obtained as the mean of 5 min. The subjects were then tilted head-up to 30, 60, and 80 degrees with 1 min's interval and remained at 80 degrees for 20 minutes or until the occurrence of significant hemodynamic changes ie. fall in BP > 20 mmHg, systolic or > 10 mmHg, diastolic or an increase in heart rate > 30 bpm. Measurements were continued in the subsequent supine position to ensure a total recording period of 30 min. Simultaneous measures of BP and TCD were obtained at 2 min's interval deriving the correlation between these parameters in the supine and tilted position.

Results: In the supine position, mean BP and heart rates were higher in the patients compared to the controls (96.3±11.6 mmHg versus 79.2±11.0 mmHg (p=0.001) and 95.1±16.1 bpm versus 62.2±9.1 bpm (p<0.001), respectively). TCD was lower in the patients (42.7±10.2 cm/s versus 63.8±10.4 cm/s, p<0.001). MeanBP was reduced more by tilt in the patients compared to controls (-14.4±5.4 mmHg and -6.4±4.9 mmHg (p=0.001), respectively), whereas heart rate increased to the same degree in the two groups (11.5±8.5 bpm and 13.8±5.2 bpm, respectively). The correlation analysis showed higher values in the patients at baseline and a significant increase in the correlation in patients during tilt (p=0.002), whereas the correlation remained unchanged in the controls.

Conclusions: Patients with severe brain injury differ from normal controls with respect to blood pressure, heart rate and middle cerebral blood flow velocity in the supine position. The postural blood pressure reduction is greater in the patients without compensatory increase in heart rate pointing to a state of baroreflex dysfunction. The increase in correlation between cerebral flow velocity and blood pressure in the tilted position suggests that the patients were operating at the lower limit of their cerebral autoregulation being unable to maintain an adequate flow in the upright position.

696
BRAIN-0764
Poster Session

Cerebrovascular Regulation

CEREBRAL OXYGENATION DURING TILT IN SEVERE BRAIN INJURY

C.G. Riberholt[1], N.D. Olesen[2], M. Thing[3], T.H. Petersen[1], J. Mehlsen[4]
[1]Department of Neurorehabilitation TBI Unit, Glostrup University Hospital, Glostrup, Denmark
[2]Department of Anaesthesia, Rigshospitalet University of Copenhagen, Copenhagen, Denmark
[3]Department of Pediatrics, Copenhagen University Hospital Hvidovre, Hvidovre, Denmark
[4]Coordinating Research Centre, Frederiksberg Hospital, Copenhagen, Denmark

Objectives: Early mobilisation is of great importance for the functional outcome in patients with severe acquired brain injury. However, these patients show orthostatic intolerance and signs of autonomic nervous dysfunction complicating mobilisation. Changes in cerebral oxygenation may contribute to the impediments and therefore we studied this by use of near infrared spectroscopy in patients with severe brain injury and impaired consciousness using a tilt table test and compared the results to those of healthy volunteers.

Methods: Fourteen patients (7 men, mean age 56.6 ±17.5 years) with severe brain injury and 15 healthy volunteers (7 men, mean age 36.1±12.5 years) were included. Regional cerebral tissue oxygen saturation (rSt_{O2}) of the frontal lobe was measured by near-infrared spectroscopy (NIRS) using the INVOS 5100c Cerebral Oximeter® (COVIDIEN, Mansfield, Massachusetts, USA) with the INVOS™ cerebral/somatic oximetry adult sensor. The sensor was placed on the forehead of the participants, above margo orbitales superior and lateral to the midline of the forehead. Changes in light absorption are considered to relate to haemoglobin oxygenation in blood vessels under the optode with some contribution from skin and skull. Oxygenation was expressed as the saturation (rSt_{O2}). Continuous blood pressure (BP) was recorded from the index finger using photoplethysmography. Measurements were continued in the subsequent supine position to ensure a total recording period of 30 min.

Results: In the supine position, meanBP was higher in the patients compared to the controls (96.3±11.6 mmHg versus 79.2±11.0 mmHg (p=0.001). Supine rSt_{O2} did not differ between groups (64.9±9.2% versus 68.2±8.5%). MeanBP was reduced more by tilt in the patients compared to controls (-14.4±5.4 mmHg and -6.4±4.9 mmHg (p=0.001), respectively). rSt_{O2} was significantly reduced in the patients to 60.5±9.8% (p=0.001), but unchanged in the controls at 67.1±8.4% (p=0.125). rSt_{O2} was higher in the controls in the supine position following tilt compared to baseline (73.8±7.6%, p=0.001), but unchanged in the patients (63.6±9.9%, p=0,096).

Conclusions: Patients with severe brain injury differ from normal controls with respect to blood pressure, and cerebral oxygenation during head up tilt. The postural blood pressure reduction is greater in the patients who were not able to maintain oxygenation at supine levels in the upright position. As shown by others, normal subjects exhibited an in cerebral oxygen saturation following tilt whereas this was not the case in the patients. Patients with severe head injury seem to have reduced cerebral oxygenation most likely as a result of reduced cerebral blood flow caused by postural hypotension.

697
BRAIN-0520
Poster Session

Cerebrovascular Regulation

CHRONIC ANGIOTENSIN IV ADMINISTRATION RESCUES CEREBROVASCULAR DEFICITS IN A MOUSE MODEL OF ALZHEIMER'S DISEASE

J. Royea[1], P. Martinot[1], X.K. Tong[1], E. Hamel[1]
[1]Laboratory of Cerebrovascular Research, Montreal Neurological Institute McGill University, Montreal, Canada

Background: Hypertension is the main risk factor of Alzheimer's disease (AD). Interestingly, anti-hypertensive medications acting on the renin-angiotensin system have lead to preserved cognitive function and reduced AD onset and disease progression[1]. When antagonizing the angiotensin II (AngII) type 1 receptor (AT1R) with losartan, an angiotensin receptor blocker, both cerebrovascular and cognitive deficits were restored in an AD mouse model[2]. The underlying mechanism of action initiating these beneficial effects remains unknown; however, the blockade of the AT1R is believed to favor the conversion of AngII to AngIV[3]. Insulin regulated aminopeptidase (IRAP), the AngIV receptor, has been implicated in cognitive performance and cerebrovascular dilatory function[4,5]. Recently, we demonstrated that divalinal, an IRAP antagonist, can counter losartan's ability to rescue cerebrovascular reactivity, neurovascular coupling to sensory stimulation, and spatial learning and memory in the Morris Water Maze (MWM) independent of changes in arterial blood pressure[6].

Objective: We sought to investigate whether chronic intracerebroventricular administration of AngIV could restore vasodilatory function, neurovascular coupling, and memory function in transgenic mice overexpressing the Swedish and Indiana mutations of the human amyloid precursor protein (APP mice, line 20).

Methods: APP mice and wild-type littermates (4-5 months old) were separated into two equally representative groups matched for spatial learning and memory deficits. Administration (intracerebroventricular
, 1 month) of artificial CSF (control) or AngIV (~1.3 nmol/day), an IRAP agonist, was delivered using osmotic minipumps. At the end of treatment, a MWM[7] was performed to assess spatial learning and memory. Neurovascular coupling response to whisker stimulation was measured using laser Doppler flowmetry. Subsequently, cerebrovascular vasodilatory function was measured in segments of isolated and pressurized posterior cerebral artery. Blood pressure was monitored by non-invasive tail-cuff plethysmography.

Results: Chronic AngIV administration rescued neurovascular coupling to whisker stimulation. AngIV also rescued dilatations of cerebral arteries to acetylcholine, calcitonin gene-related peptide, ATP-sensitive potassium (KATP) channel opener levcromakalim and transient receptor potential vanilloid 4 (TRPV4) channel opener GSK1016790A, as well as baseline production of nitric oxide measured by incubating vessel segments with N^{ω}-nitro-$_{L}$-arginine. Neither spatial learning and memory retention nor arterial blood pressures were altered following one month of AngIV delivery.

Conclusions: We conclude that the AngIV/IRAP cascade can rescue impairments in neurovascular coupling and cerebrovascular dilatory function in APP mice. However, the treatment regimen used did not result in improved cognitive function in APP mice. These findings potentially identify the AngIV/IRAP cascade as a promising target of restoring cerebrovascular deficits in AD. Moreover, they may provide insight on the reported decreased incidence of AD in hypertensive patients treated by AT1R blockers[1].

References: 1. Wolozin B et al., Alzheimers.Dement, 2008, 4: T118; 2. Ongali B et al., Neurobiol.Dis, 2014, 68: 126-136; 3. Braszko JJ et al., JRAAS, 2006, 7(3): 168-174; 4. Braszko JJ et al., J.Neurosci, 1988, 27(3): 777-783; 5. Albiston AL et al., Neurobiol.Learn.Mem, 2010, 93(1): 19-30; 6. Royea J et al., CANAD Abstract, 2014; 7.

Deipolyi AR et al., Neurobiol.of.Aging, 2008, 29: 253-66

Acknowledgements: Supported by grants from the Canadian Institutes of Health Research (MOP-126001) and the Heart and Stroke Foundation of Canada.

698
BRAIN-0360
Poster Session

Cerebrovascular Regulation

INTRACRANIAL PRESSURE IS A PHYSIOLGICAL STRESSOR THAT DETERMINES SYMPATHETIC NERVOUS SYSTEM ACTIVITY

E. Schmidt[1], F. Despas[2], A. Pavy- Le Traon[3], M. Czosnyka[4], J.D. Pickard[4], K. Rahmouni[5], A. Pathak[2], J.M. Senard[2]
[1]Neurosurgery, University Hospital, Toulouse, France
[2]I2MC, INSERM UMR-1048, Toulouse, France
[3]Neurology, University Hospital, Toulouse, France
[4]Neurosurgery, University Hospital, Cambridge, United Kingdom
[5]Pharmacology, University Hospital, Iowa City Iowa, USA

Objectives:

Intracranial pressure (ICP) is a determinant of cerebral perfusion pressure (CPP) that is the difference between arterial blood pressure (ABP) and ICP. Raised ICP reduces CPP and blood delivery to the brain. Massive ICP rise is also known to produce an increase in ABP, bradycardia and respiratory irregularities termed the Cushing response[1]. This mechanism is a terminal event occurring in extreme pathological conditions of brainstem ischaemia leading to a sympatho-adrenal response[2]. However, it is still debated whether the Cushing response is an acute pathological response to brain ischemia or part of an important physiological reflex mechanism for ABP regulation[3]. Indeed clinical and experimental studies suggest that modest ICP increase modulates systemic hemodynamics probably via the sympathetic nervous system (SNS)[4-7]. We hypothesize that modest ICP changes drive sympathetic activity. Using state-of-the-art technique to measure SNS, we performed two different sets of experiments in human subjects and mice. In both species during controlled hydrostatic modest ICP increase and decrease, SNS was measured directly by microneurography and indirectly by heart rate variability analysis (HRVA).

Methods:

In 10 patients, ICP was measured and increased during lumbar infusion study. Signed consent was always obtained. Heart rate and ABP were non-invasively monitored. Muscle sympathetic nerve activity (MSNA) was recorded by a microelectrode in the right fibular nerve.

In 15 anesthetized mice, ICP was measured and intraventricular infusion was performed. Heart rate and ABP were invasively monitored. Renal sympathetic nerve activity (RSNA) was recorded by a microelectrode at the level the left kidney's nerves.

In human and mice, HRVA allows calculating high frequency (HF) and low frequency (LF) bands. LF and LF/HF ratio represent sympathetic indices, whereas HF is an index of parasympathetic activity [8]

Results:

Table 1 gives the human and animal results. Strikingly, modest increase in ICP was associated with a parallel increase in MSNA in humans; blood pressure was stable. Similarly, modest rise in ICP increased RSNA in mice. In both species ICP drop significantly reduced MSNA and RSNA. Spectral analysis of heart rate variability confirmed that raising ICP augments sympathetic indices in humans and mice.

Conclusions:

Using gold-standard measurement of SNS, we demonstrate that ICP drives efferent SNS outflow. ICP is not only a determinant of CPP but also a

physiological stressor that influences and reversibly modulates SNS activity. We demonstrate a new physiological link between ICP and SNS activity which may represent an important highly regulated circuit. Our findings strongly suggest the presence of a novel intracranial baroreflex that might participate to the physiology of the heart-brain cross-talk, but also to the pathophysiology of various sympathetically-driven diseases.

References:

1. Cushing H. Bulletin of the Johns Hopkins Hospital 1901;12:290-2.
2. McGillicuddy JE *et al.* J Neurosurg 1978;48(5):730-40.
3. Paton JF *et al.* Exp Physiol 2009;94(1):11-7.
4. Dickinson CJ. Clin Sci 1981;60(5):471-7.
5. Schmidt EA *et al* Acta Neurochir Suppl 2005;95:253-6.
6. Hu X *et al.* IEEE Trans Biomed Eng 2007;54(8):1407-17.
7. Osborn JW. Physiol 2005;32(5-6):384-93.
8. Task Force of the North American Society of Electrophysiology. Circulation. 1996;93(5):1043-65.

Table 1a: Human results: (n=10 patients) * p<0.05, ** p<0.01 *vs* baseline ; † p<0.05, †† p<0.01 *vs* 25mmHg

Parameters	Baseline	10 mmHg	15 mmHg	20 mmHg	25 mmHg	3 min after end of infusion
ICP (mmHg)	8.28 ± 1.05	10.72 ± 0.40	15.64 ± 0.22	20.43 ± 0.31**	25.05 ± 0.33**	14.83 ± 0.91†
MSNA (Bursts min^{-1})	51.24 ± 2.52	53.85 ± 2.54	59.95 ± 2.96**	66.50 ± 4.17**	66.70 ± 2.88**	58.85 ± 2.62*†
Systolic ABP (mmHg)	145.89 ± 9.56	148.04 ± 9.96	149.64 ± 9.42	150.43 ± 9.97	153.28 ± 10.04	152.67 ± 10.67
Diastolic ABP (mmHg)	74.57 ± 3.83	75.36 ± 3.84	74.41 ± 3.84	74.41 ± 3.78	77.10 ± 3.18	77.79 ± 4.08
HR (beats min^{-1})	62.39 ± 3.54	62.44 ± 3.75	61.63 ± 3.30	62.37 ± 3.52	63.04 ± 3.66	63.44 ± 3.17
LF (nu)	33.68 ± 3.29				40.87 ± 4.55*	
HF (nu)	23.59 ± 4.53				17.19 ± 3.81*	
LF/HF (%)	2.01 ± 0.30				3.48 ± 0.79*	

Table 1b: Animal results (n=15 mice) * p<0.05, ** p<0.01 *vs* baseline ; † p<0.05, †† p<0.01 vs 40 mmHg

Parameters	Baseline	10 mmHg	20 mmHg	30 mmHg	40 mmHg	3 min after end of infusion
ICP (mmHg)	6.65 ± 0.67	11.72 ± 0.46	21.51 ± 0.43**	30.96 ± 0.23**	38.57 ± 1.02**	9.14 ± 0.83††
RSNA (spikes s^{-1})	29.87 ± 4.00	32.29 ± 4.10	37.17 ± 4.69	43.36 ± 6.25**	45.73 ± 6.42**	34.82 ± 5.65†
Syst ABP (mmHg)	94.21 ± 7.25	90.22 ± 7.35	92.06 ± 6.26	94.90 ± 6.24	97.52 ± 6.34	90.35 ± 6.54
Diast ABP (mmHg)	68.67 ± 6.19	65.72 ± 6.35	67.06 ± 5.39	69.17 ± 4.98	71.36 ± 4.76	67.84 ± 5.41
HR (beats min^{-1})	307.14 ± 17.59	311.51 ± 18.20	308.76 ± 17.00	321.47 ± 17.64	329.74 ± 16.43	356.57 ± 17.80**
LF (nu)	5.54 ± 1.82				9.03 ± 2.58**	
HF (nu)	25.17 ± 5.64				16.46 ± 5.40*	
LF/HF	1.41 ± 0.82				3.02 ± 1.46**	

699
BRAIN-0850
Poster Session

Cerebrovascular Regulation

RUGBY PLAYERS WITH CONCUSSIONS DEMONSTRATE INCREASED BLOOD PRESSURE AND ESTIMATES OF INTRACRANIAL PRESSURE IMMEDIATELY POST CONCUSSION WHILE CEREBRAL AUTOREGULATION REMAINS INTACT

J. Serrador[1], *J. Tosto*[2], *L. Reyes*[2], *M. Blatt*[2], *J. Klein*[2], *B. Ghobreal*[2], *M. Falvo*[2]
[1]*Pharmacology & Physiology, Rutgers - New Jersey Medical School, Newark, USA*
[2]*War Related Illness & Injury Study Center, Dept of Veteran Affairs, East Orange, USA*

Objectives: Increasing evidence suggests that even mild concussions in athletes may result in long term cognitive and health problems. Despite this, there is a lack of data on the physiological changes immediately following a concussion, including cerebral blood flow measures. The goal of this work was to determine if concussion causes impairment of cerebral blood flow regulation in the first few hours after injury.

Methods: 54 subjects (25 with concussions) were recruited during recreational rugby tournaments and tested at the field to assess cerebral blood flow using Doppler, beat-by-beat blood pressure, and end-tidal CO_2. Subjects performed three sit to stand and a supine to 60^o upright recumbent sitting. The majority of data was collected within 2 hours of the head trauma. Only players classified as having a mild concussion that did not require further medical treatment were participated.

Results: Concussed players demonstrated significantly greater mean arterial pressure (Concussed: 95±1; Controls: 89±1 mmHg, P=0.005) and increased cerebrovascular resistance (Concussed: 0.95±0.01; Controls: 0.88±0.01 mmHg/%, P=0.001). However cerebral blood flow changes from sitting to standing or supine to head up tilt were unaffected. Similarly

examination of autoregulatory index or transfer function measures of cerebral autoregulation demonstrated no difference from controls. Using a non-invasive estimate of intracranial pressure (ICP) derived from the cerebral flow velocity indices, we found that concussed players had significantly greater ICP (Concussed: 14±3; Controls: 7±1 mmHg, P=0.032).

Discussion: These data suggest that players with mild concussions demonstrate increased ICP immediately following the head injury that is associated with increased cerebrovascular resistance. However, cerebral blood flow to changes in posture and cerebral autoregulation do not appear to be impaired. Thus, increased blood pressure following concussion may be compensating for the increased ICP to maintain cerebral perfusion pressure. Supported by the Dept of Veteran Affairs, NIH and the War Related Illness and Injury Study Center.

700
BRAIN-0854
Poster Session

Cerebrovascular Regulation

EFFECT OF MENSTRUAL CYCLE ON CEREBRAL BLOOD FLOW REGULATION IN YOUNG WOMEN

A. Fox[1], M. Favre[2], J. Serrador[3]
[1]War Related Illness & Injury Study Center, Dept of Veteran Affairs, East Orange, USA
[2]Pharmacology & Physiology, Rutgers New Jersey Medical School, Newark, USA
[3]Pharmacology & Physiology, Rutgers - New Jersey Medical School, Newark, USA

Objectives: The aim of our study was to determine if cerebral blood flow regulation in women is affected by the phases of the menstrual cycle, which could lend insight into whether hormone levels in women may affect their susceptibility to cerebrovascular injury.

Methods: Four young (mean age 22 ±1.4 years) healthy women were tested at three time points; during menstruation (M), late follicular (F), and the luteal phase (L) of the menstrual cycle. Each visit consisted of a cerebrovascular reactivity test to assess cerebral endothelial function and a sit-to-stand test to assess cerebral autoregulation. Beat-by-beat blood pressure, ECG, $P_{ET}CO_2$, and transcranial Doppler sonography of the middle and anterior cerebral artery were taken for each subject.

Results: During the late follicular phase compared to the other phases, average heart rate was significantly lower (M: 76±1; F: 69±1; L: 73±2 bpm, P=0.026), mean cerebral flow velocity while standing was significantly lower (M: 100±2; F: 94±1; L: 99±1 %, P=0.003), and cerebrovascular resistance increased while standing to a greater degree (M: +0.03±0.01; F: +0.06±0.02; L: +0.01±0.06 mmHg/%, P=0.049). In contrast, blood pressure changes during standing were unaffected by cycle phase. Examining cerebral autoregulation, autoregulatory index values were higher during the menstrual phase with a tendency for decreasing scores during late follicular and the luteal phase in the MCA (M: 4.4±0.6; F: 3.4±0.4; L: 2.0±0.6, P=0.032) but not the ACA (M: 4.2±0.6; F: 3.4±0.4; L: 3.4±0.5, P=NS). $P_{ET}CO_2$ values might account for some of these changes but this needs more exploration.

Discussion: While more data is necessary to fully interpret the findings, our preliminary results indicate that phase of the cycle may affect cerebrovascular tone and the ability to maintain cerebral blood flow when upright. The impairment in autoregulatory response during the luteal phase may be related to increasing progesterone levels. The lower cerebral blood flow values while standing during the follicular phase is consistent with previous data finding increased incidence of orthostatic intolerance during this phase. Supported by the Dept of Veteran Affairs, NIH and the War Related Illness and Injury Study Center. Dr. Serrador was a recipient of the SFI Walton Visiting Fellowship at the National University of Ireland Galway.

701
BRAIN-0437
Poster Session

Cerebrovascular Regulation

MECHANISTIC PATHWAYS UNDERLYING ALTERED NEUROVASCULAR COUPLING IN BRAIN METASTASIS

M. Sarmiento Soto[1], S. Serres[1], C. Bristow[1], V. Economopoulos[1], J.R. Larkin[1], C. Escartin[2], G. Bonvento[2], N.R. Sibson[1]
[1]CRUK and MRC Oxford Institute for Radiation Onc ology Department of Oncology, University of Oxford, Oxford, United Kingdom
[2]MIRcen UMR9199 CEA CNRS, University of Paris Sud, Fontenay-aux-Roses, France

Objectives: It is recognised that astrocytes form a physical bridge between neurons and the cerebrovasculature. Astrocytic end-feet help maintain endothelial tight junctions to support the blood–brain barrier (BBB) and release vasoactive molecules that regulate vascular tone. In secondary cancer (metastasis) to the brain, astrocytes are displaced from the vasculature and become activated, and we have shown that neurovascular coupling is compromised in rat model of brain metastasis (Serres et al., abstract submitted). The aim of this study, therefore, was to characterise the effects of astrocyte activation on astrocyte-vascular structure, vascularity and production of vasoactive molecules, using in vivo magnetic resonance imaging (MRI) and immunofluorescent microscopy.
Methods: Two cohorts of BD-IX rats were injected intracortically in one node of the whisker barrel cortex pathway (the barrel field somatosensory cortex) with either (i) a lentivirus expressing ciliary neurotrophic factor (Lv-CNTF) known to switch astrocytic phenotype to an activated state, or (ii) a metastatic N-ethyl-N-nitrosourea-induced mammary adenocarcinoma cell line (ENU1546). Lv-CNTF injected animals were studied 6 weeks after intracortical injection, and ENU1546 injected animals were studied 1 week after injection. All animals underwent T1- and T2-weighted MRI to follow macroscopic structural changes, and post-gadolinium T1-weighted MRI to assess BBB integrity. Immunofluorescent microscopy was performed post-mortem to identify activated astrocytes (GFAP), neurons (NeuN), blood vessels (CD31), cyclooxygenase-1 and 2 (COX-1/2), inducible isoform of nitric oxide synthase (iNOS), glutathione (GSH), cytochrome p450 a precursor of 20-hydroxyeicosatetraenoic acid (20-HETE), alpha-smooth muscle actin (α-SMA) and proteoglycans of the basement membrane (β-dystroglycan).
Results: In both cohorts, persistent activation of astrocytes, revealed by strong upregulation of GFAP, was observed in the injected cortex, which was not associated with BBB disruption as assessed by MRI. Disruption of the dystroglycan-laminin interaction was observed in the area of astrocyte activation causing dissociation of astrocytes from blood vessels, as shown by a lower immuno-colocalisation of blood vessel, astrocyte and β-dystroglycan, for both Lv-CNTF and ENU1546 injected animals (Fig1).
Enlargement of blood vessels was also observed in both models. Together with structural changes in the astrocyte-vessel complex, upregulation of iNOS, COX-1, COX-2 and GSH were observed in activated astrocytes. Whilst upregulation of cytochrome p450 was observed in α-SMA-positive arterioles found in the area of astrocyte activation.
Conclusion: Our findings suggest that astrocyte-vessel dissociation, leading to enlargement of blood vessels, together with dysregulation of signalling pathways controling vessel diameter likely underlie disruption of neurovascular coupling in brain metastasis. Upregulation of vasoconstrictory molecules (p450/20-HETE) at the arteriole end of the vascular bed may lead to reduced basal blood flow as observed ***in vivo*** (see Serres et al., submitted abstract) and suppression of response to stimulation, whilst upregulation of vasodilatory mediators (iNOS, COX, GSH) downstream of the arterioles may reduce vascular reserve and, hence, vascular responses to stimulation.

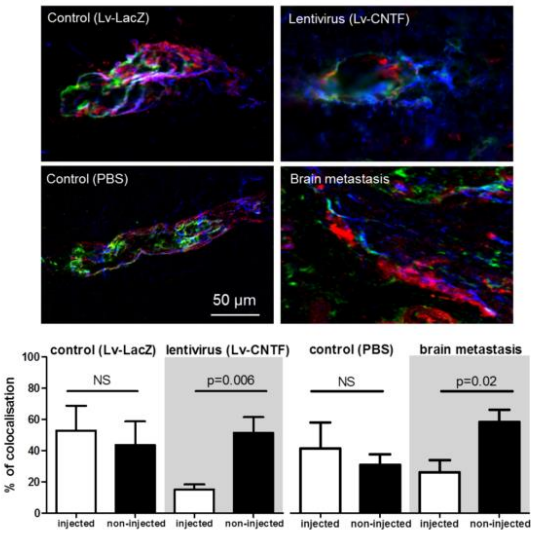

Figure 1- Co-localization of β-dystroglycan (green), astrocyte (blue) and blood vessel (red) is reduced in the area of either Lv-CNTF or brain metastasis induced astrocyte activation.

702
BRAIN-0868
Poster Session

Cerebrovascular Regulation

EFFECTS OF INTERNAL JUGULAR VEIN STENOSIS ON VENOUS COLLATERAL FLOW USING MAGNETIC RESONANCE IMAGING

S. Sethi[1], G. Gadda[2], D. Utriainen[1], E.M. Haacke[1]
[1]The MRI Institute of Biomedical Research, Detroit, MI, USA
[2]University of Ferrara, Ferrara, Italy

Objectives: Jugular venous structure and flow anomalies have been noted in a subset of multiple sclerosis (MS) patients using MRI[1, 2]. This study was to investigate effects of internal jugular vein stenosis on venous collateral outflow in a large cohort of MS and healthy controls (HC) using MRI. All analyses are retrospective from an imaging database.

Methods: A group of 569 MS subjects and 95 HC subjects were imaged with 3T scanners. Magnetic resonance (MR) venographic imaging and phase contrast flow quantification at two different neck levels (C5/C6 and C2/C3) were exclusively to image anatomy and flow of the extracranial vessels. MR venography was used to classify venous vessels into three categories: Type I: Primary (jugular vein), Type II: Paraspinal, and Type III: Superficial veins. Presence, type, and location of jugular anomalies were also evaluated based on criteria previously established[1,2]. Venous flow normalized to arterial brain inflow was calculated for individual and bilateral totals. The effects of stenosis type on venous collateral flow subtotals were assessed. Student t-tests were performed to compare means between groups. Chi-square tests were used to check differences in prevalence of jugular anomaly between the HC and MS groups.

Results: Forty-six of the 95 HC did not have venography data for anatomic evaluation. Vertebral artery inflow showed good consistency from the upper neck level to the lower neck level for the entire data set (Figure 1). Thirty-eight of the 49 HC classified as non-stenotic, while 11/49 HC classified as stenotic; of the MS cohort, 213/569 classified as non-stenotic while 346/569 showed stenosis. For normalized IJV flow, differences were seen in stenotic (M=0.51, SD=0.21) and non-stenotic (M=0.77, SD=0.12) HC groups ($p<0.05$), as well as stenotic (M=0.52, SD=0.21) and non-stenotic (M=0.72, SD=0.12) groups ($p<0.05$). When grouping both MS and HC groups, differences in Type I, II, and III flows were seen between non-stenotic and stenotic groups, with the stenotic group showing elevated Type II, and III flow compared to the non-stenotic groups ($p<0.05$).

Conclusions: Consistency in scanning and conservation of arterial inflow between neck levels was established based on the vertebral artery flow. Anatomical jugular stenosis was more prevalent in the MS cohort compared to HC ($X^2=28.9$, $p<0.05$). For cases with anatomical jugular stenosis in both MS and HC, flow is redirected to Type II and III venous collaterals while maintaining similar total normalized venous flow to the non-stenotic group.

References:
1. Haacke EM, Feng W, Utriainen D, et al.

Patients with multiple sclerosis with structural venous abnormalities on MR imaging exhibit an abnormal flow distribution of the internal jugular veins. J Vasc Interv Radiol 2012;23:60-68 e61-63
2. Sethi SK, Utriainen DT, Daugherty AM, et al. Jugular Venous Flow Abnormalities in Multiple Sclerosis Patients Compared to Normal Controls. J Neuroimaging 2014.

703
BRAIN-0523
Poster Session

Cerebrovascular Regulation

IMPACT OF AUTONOMIC MODULATION DURING CEREBROVASCULAR REACTIVITY IN SMALL ARTERY STROKE

K. Intharakham[1], K. Suwanprasert[2]
[1]Stroke Unit, Thammasat University Hospital, Pathumthani, Thailand
[2]Faculty of Medicine, Thammasat University, Pathumthani, Thailand

Abstract—Autonomic modulation involves in brain-heart axis havereported in AF stroke and hypothermia treated patients. Predominant activity ofparasympathetic nerve and significant increase in mean cerebral blood flowvelocity during cerebrovascular reactivity (CVR) in healthy was evident. Cerebrovascularreactivity by breath holding induces vasodilation. Recently, many reports suggest that endothelialdysfunction may be involved in the pathogenesis of small artery stroke. In this study, weexamine the impact of ANS modulation by heartrate variability (HRV) to cerebral reserve function in small artery stroke.

Method: 15 small arterystroke patients were recruited (7 men, 8 female, age 65.6+ 13.61 years old), gave informed consent according to the local ethic committee and were monitored during CVR for arterial blood pressure (ABP), electrocardiography (EKG) and mean cerebral blood flow velocity(mCBFV) of middle cerebral arteries (MCA) with transcranial Doppler. Shortterm-one minute HRV was analyzed for LF/HF ratio, nonlinear of SD2/SD1 andSampEn.

Result: An increase in LF/HF ratio from 0.92± 0.70 to 2.28± 2.03 ($p<0.05$) was evident. Significant increaseof SD2/SD1 and decreasing SampEn during the experiment phase indicatespredominant of parasympathetic activity associated with less irregularity. Lessscatter signals of SD1 and SD2 with low value was illustrated from Poincaréplot. Significant increase in mCBFV during breath holding and recovery comparedwith baseline suggests hypercapnia induced-vasodilatation. Moreover,significant positive correlation between systolic blood pressure vs mCBFVsuggests impact of autonomic control to cerebral blood flow. This is firstreport that nonlinear HRV is applied to patho-physiological mechanism ofvasodilatation triggered by hypercapnia from CVR in patient.

In conclusion, nonlinear HRV with frequencydomain is proposed in CVR assessment which it needed tocompromise the lower cerebral blood volume velocity in small artery stroke.

Reference :
1.Sungnoon R, Suwanprasert K, Muengtawee pongsa S. Atrial electrophysiological property analysisby sample entropy and atrial fibrillatory rate with cardiac autonomic derangementsin acute ischemic stroke with atrial fibrillation Neurology Asia 2014; 19(1):11-8
2. Intharakham K, Suwanprasert K. Complexity of autonomic control during cerebrovascular reactivity. Proceeding in the 2013 biomedical engineering international conference, Krabi,Thailand, 2013

704
BRAIN-0080
Poster Session

Cerebrovascular Regulation

HYPERCAPNIA-INDUCED CEREBRAL VASODILATION IS MEDIATED PREDOMINANTLY BY ENOS

N. Terpolilli[1], A. Dienel[1], S. Schwarzmaier[2], N. Plesnila[3]
[1]Neurosurgery, Ludwigs-Maximilians-Universität, München, Germany
[2]Anesthesiology, Ludwigs-Maximilians-Universität, München, Germany
[3]Institute for Stroke and Dementia Research, Ludwigs-Maximilians-Universität, München, Germany

Objective: CO_2-reactivity is an important feature of cerebral autoregulation. Increase of CO_2 partial pressure (pCO_2) induces a CPP independent increase of cerebral perfusion. Lack of CO_2-mediated vasoreactivity is an important feature of the pathophysiology of several cerebral insults, especially subarachnoid hemorrhage; after SAH, impaired CO2-reactivity is associated with worse neurological outcome. The mechanism of CO_2-elicited hyperemia has not been completely elucidated. There is consensus that nitric oxide (NO) is heavily implicated, however, the role of the individual NOS-isoforms in inducing arterial dilation is not completely clear. The present study was initiated in order to evaluate the CO_2-elicited CBF-responses of the cerebral microcirculation in mice deficient for eNOS, nNOS, and iNOS.

Methods: $eNOS^{-/-}$, $iNOS^{-/-}$, $nNOS^{-/-}$ mice, and wildtype C57BL/6 littermates were anesthetized, intubated, and mechanically ventilated with 30% oxygen in room air. Temperature, endtidal pCO_2, and respiration parameters were continuously monitored and kept within physiological range. MAP measured via femoral artery catheter and CBF measured via bitemporal Laser-Doppler-Flowmetry over MCA territory were continuously monitored. The cerebral microcirculation was studied using in-vivo-epifluorescence microscopy under baseline conditions, during, and after a 30-minute hyperkapnic stimulus (addition of 10% CO_2). At the end of the experiments, ex vivo blood gas analysis was performed.

Results: As previously described, eNOS-deficient mice had an elevated arterial blood pressure under baseline conditions. All other parameters obtained were comparable in the 4 groups examined. As expected, increasing the CO_2-concentration to 10% led to an immediate and significant increase in CBF in control animals; MAP remained stable during CO_2 inhalation (iCO_2). The CBF-increase was mainly mediated by dilation of small cerebral arterioles (10-20µm) since these vessels had the biggest change in diameter compared to baseline. After cessation of iCO_2 CBF returned quickly to baseline. iNOS-transgenic animals showed a CO_2 vessel reactivity similar to wildtype controls while this response was significantly blunted in nNOS-transgenic mice and completely absent in eNOS-deficient animals. Interestingly, iCO_2 tented to reduce CBF in eNOS KO mice.

Conclusion: The vasodilation elicited by hypercapnia is mediated by precapillary arterioles (diameter 10-20µm) and predominantly by eNOS and, to a lesser degree, by nNOS while iNOS is not involved in this process. The current study clarifies the role of the individual NOS isoforms for hypercapnia-induced vasodilatation and further deepens our understanding on this fundamental process in the cerebral microcirculation.

705
BRAIN-0775
Poster Session

Cerebrovascular Regulation

BEHAVIOR OF RED BLOOD CELLS IN INTRAPARENCHYMAL CAPILLARIES DURING CORTICAL SPREADING DEPRESSION OBSERVED WITH HIGH-SPEED CAMERA CONFOCAL FLUORESCENCE MICROSCOPE IN ANESTHETIZED MICE

Y. Tomita[1], M. Unekawa[1], H. Toriumi[1], T. Osada[1], K. Masamoto[2], H. Kawaguchi[3], Y. Itoh[4], I. Kanno[3], N. Suzuki[1]
[1]Neurology, Keio University School of Medicine, Tokyo, Japan
[2]Brain Science Inspired Life Support Research Center, University of Electro-Communications, Chofu, Japan
[3]Molecular Imaging Center, National Institute of Radiological Sciences, Chiba, Japan
[4]Neurology, Osaka City University Graduate School of Medicine, Osaka, Japan

[Objective] Cortical spreading depression (CSD) involves mass depolarization of neurons and glial cells, followed by sustained suppression of spontaneous neuronal activity. CSD induces marked increases in glucose utilization and metabolism, resulting in severe tissue hypoxia (1), accompanied with marked constriction, followed by dilation and subsequent mild constriction of pial arteries (2), and suppression of red blood cell (RBC) velocity (3). Since changes of capillary diameter are limited, control of RBC velocity in capillaries is essential to meet local neuronal requirements. To further understand the microcirculatory response during CSD, we observed and analyzed the temporal changes of RBC velocity and its distribution in individual capillaries by two-dimensional spatial analysis.

[Methods] Male Tie 2-green fluorescent protein transgenic mice, in which fluorescent vascular endothelial cells can be specifically identified, were used (N=13). Under urethane anesthesia and artificial ventilation, intraparenchymal images (approximately 50 μm from the surface) were obtained using a high-speed camera laser-scanning confocal fluorescence microscope at 125 fps for 60 sec through a cranial window (4) made on the parieto-temporal cortex, with simultaneous recording of DC potential and regional cerebral blood flow (rCBF) by laser-Doppler flowmetry. A fluorescein isothiocyanate (FITC)-labeled RBC suspension was intravenously injected, and the velocity of RBCs was automatically measured with our original Matlab domain software (KEIO-IS2) (5). CSD was induced by application of KCl to the cortical surface through an additional hole.

[Results] RBC velocity in individual capillaries at rest fluctuated irregularly, but we confirmed that the average was stable for at least 10 to 12 sec before KCl application. We took the averaged RBC velocity for 30 sec before KCl application as baseline and calculated % change from the baseline in each capillary during and after passage of CSD (in total; n=122). Application of KCl elicited repeated transient depolarization, seen as DC potential deflection and delayed hyperperfusion (Figure A-C; middle and lower panels). During the first CSD passage, RBC velocity was significantly decreased approximately in concurrence with the trough of DC potential and a transient drop of rCBF (FigureA). Subsequent CSD did not induce temporal changes in RBC velocity, which were rather high during CSD passage, whereas rCBF was increasing without a transient drop (Figure B and C). RBC velocity remained high (+6 to +22%) after passage of CSD, whereas rCBF significantly decreased by 13 to 19% (post-CSD oligemia). The changes in RBC velocity were heterogeneous in space, though the average velocity was well maintained.

[Conclusion] We demonstrated temporal change of RBC velocity in intraparenchymal capillaries and its spatial heterogeneity during CSD. This model is useful to investigate regulatory mechanisms of cerebral capillary flow and coupling between neurons and nearby capillaries.

[References] (1) Takano T, *et al.*, Nat Neurosci 10: 754-62: 2007. (2) Unekawa M, *et al.*, J Cereb Blood Flow Metab, *in press* (doi:10.1038/ jcbfm.2014.250). (3) Unekawa M, *et al.*, Microcirculation 19: 166-74: 2012. (4) Tomita Y, *et al.*, J Cereb Blood Flow Metab, 25: 858-67: 2005. (5) Tomita M, *et al.*,Microcirculation 15: 163-174: 2008.

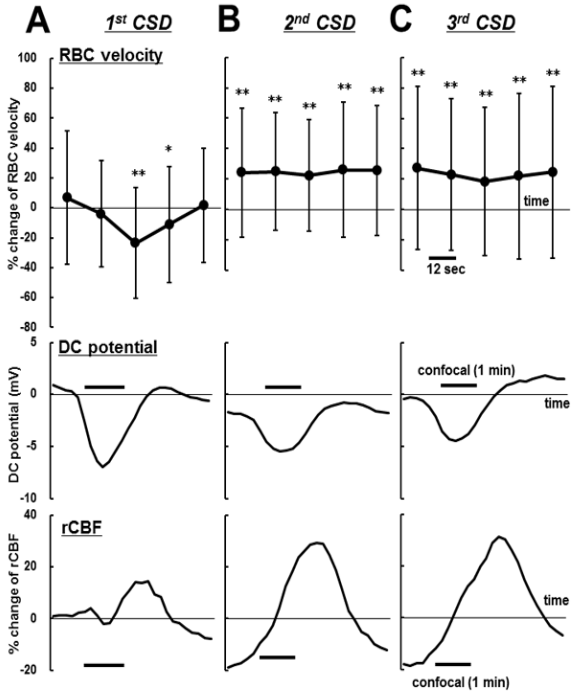

Figure. Temporal changes of RBC velocity (upper panels; mean ± SD) in intraparenchymal capillaries associated with first (A), second (B) and third (C) passage of CSD (66~108 capillaries at each time point). Measurement times (confocal imaging) for temporal averaging of DC potential (middle panels) and rCBF (lower panels) are shown . * p<0.05, **p<0.01 vs pre-KCl.

706
BRAIN-0375
Poster Session

Cerebrovascular Regulation

SUPPLY-DEMAND MISMATCH TRANSIENTS TRIGGER PERI-INFARCT DEPOLARIZATIONS IN ISCHEMIC PENUMBRA

D. von Bornstädt[1], M. Houben[2], J. Seidel[3], Y. Zheng[3], E. Dilekoz[4], T. Qin[3], N. Sandow[5], K. Sreekanth[6], K. Eikermann-Haerter[3], M. Endres[7], D. Boas[6], M.A. Moskowitz[3], E.H. Lo[3], J.P. Dreier[7], J. Woitzik[5], S. Sakadžić[6], C. Ayata[8]

[1]Neurology and Radiology, Massachusetts General Hospital Harvard Medical School and Charité-Universitätsmedizin Berlin, Berlin, Germany
[2]Neurology and Radiology, Massachusetts General Hospital Harvard Medical School and Leiden University Medical Center, Leiden, Netherlands
[3]Radiology, Massachusetts General Hospital Harvard Medical School, Boston, USA
[4]Radiology and Pharmacology, Massachusetts General Hospital Harvard Medical School and Gazi University Faculty of Medicine, Ankara, Turkey
[5]Neurosurgery, Charité-Universitätsmedizin Berlin, Berlin, Germany
[6]Athinoula A Martinos Center for Biomedical Imaging, Massachusetts General Hospital Harvard Medical School, Boston, USA
[7]Neurology, Charité-Universitätsmedizin Berlin, Berlin, Germany
[8]Radiology and Neurology, Massachusetts General Hospital Harvard Medical School, Boston, USA

Background: Peri-infarct depolarizations (PIDs) worsen the outcome of ischemic stroke (1, 2, 3). Unlike their impact on metabolism and perfusion, triggering factors are virtually unknown (1, 2, 3). We hypothesized that transient worsening of O2 supply-demand mismatch precipitates a PID in critically hypoperfused penumbra.

Methods: We optically imaged cortical blood flow and oxygenation during distal middle cerebral artery occlusion in mice under full systemic physiological monitoring, and tested whether a transient (5 min) drop in O2 supply (hypotension or hypoxia) or increase in O2 demand (somatosensory cortical activation) can trigger PIDs during acute focal cerebral ischemia.

Results: Transient hypotension (<70 mmHg) or hypoxia (<90 mmHg) triggered a PID 90% of the time (p<0.01). Increasing the O2 demand by

functional activation (tactile stimulation) of moderately ischemic cortex (contralesional forepaw or shoulder S1) increased the 5-min incidence of PIDs by approximately five-fold (p=0.001). Electrophysiological mapping of the somatosensory cortex revealed that triggered PIDs actually started in the cortical representation of the stimulated forelimb. Cortical oxyhemoglobin levels dropped by 35-40% in the activated S1 immediately before a PID (p=0.004) confirming increased O2 demand. Cortical foci from which PIDs originated during tactile stimulation had 27-32% residual CBF, indicating the presence of a critical range of ischemia vulnerable to PID initiation upon increased demand. Consistently, activation of non-ischemic cortex (hindpaw S1) or severely ischemic cortex (whisker S1) did not significantly increase the PID rate. We confirmed the range of critical ischemia for the initiation of PIDs by lowering the blood pressure (~60 mmHg) to reduce the residual blood flow in the hind paw region to within the critical range (~30%). In this group, tactile stimulation of the hindpaw triggered PIDs at a high rate (60%). Conversely, activation of the shoulder cortex did not increase the PID frequency in this group because residual CBF was now reduced below the critical range. Both tetrodotoxin (1 µM topical) and normobaric hyperoxia prevented somatosensory triggering of PIDs. Lastly, we showed that tactile stimulation-induced increased PID rate was associated with larger infarcts by TTC staining at 24h and HE staining at 72h.

Conclusion: PIDs are triggered upon O2 supply-demand mismatch transients in metastable peri-infarct hot zones due to increased demand or reduced supply. We propose that minimizing sensory stimulation and hypoxic or hypotensive transients in the early stages of stroke and brain injury might reduce PID incidence and their adverse impact on outcome.

References:

(1) Dohmen, C., Sakowitz, O.W., Fabricius, M., Bosche, B., Reithmeier, T., Ernestus, R.I., Brinker, G., Dreier, J.P., Woitzik, J., Strong, A.J., and Graf, R. (2008). Spreading depolarizations occur in human ischemic stroke with high incidence. Ann Neurol 63, 720-728.
(2) Eikermann-Haerter, K., Lee, J.H., Yuzawa, I.*, et al.* (2012). Migraine mutations increase stroke vulnerability by facilitating ischemic depolarizations. Circulation 125, 335-345.
(3) Dreier, J.P., Woitzik, J., Fabricius, M.*, et al.* (2006). Delayed ischaemic neurological deficits after subarachnoid haemorrhage are associated with clusters of spreading depolarizations. Brain 129, 3224-3237.

707
BRAIN-0396
Poster Session

Cerebrovascular Regulation

THE EFFECT OF RAPAMYCIN ON COLLATERALS IN RODENT CEREBRAL ISCHEMIA USING NOVEL MULTI-SCALE DYNAMIC IMAGING MODALITIES

J. Wang[1], X. Lin[1], Z. Mu[1], Z. Zhang[1], K. Jin[2], Y. Wang[1], G.Y. Yang[1]
[1]Neuroscience and Neuroengineering Research Ce nter, Med-X Research Institute and School of Biomedical Engi neering, Shanghai, China
[2]Pharmacology and Neuroscience, University of North Texas Health Science Center, Fort Worth, USA

Objectives: Increased cerebral collateral circulation could prevent or delay neural damage through compensating blood flow in the ischemic region after stroke.[1] Therefore, long-term collateral opening is important for the blood restoration and brain tissue repairing after cerebral ischemia. However, methods of dynamic observation of collateral situation are not well established yet. Using novel synchrotron radiation angiography (SRA), laser speckle contrast imaging (LSCI) and two-photon laser scanning microscopy (TPLSM) techniques, we investigated the dynamic changes of collateral circulation in rodent models after middle cerebral artery occlusion (MCAO) following rapamycin treatment, along with outcome assessment.

Methods: SRA was performed to examine the effect of rapamycin on collaterals between the inter-cranial and extra-cranial circulations as well as the collaterals between the posterior cerebral artery and the middle cerebral artery after MCAO. In addition, LSCI was used to examine the cortical collaterals between the anterior cerebral artery and the middle cerebral artery, and TPLSM was performed to investigate changes of cortical microcirculation in the normal and ischemic animals. The collateral opening, collateral blood flow, and the diameter of collateral vessels following MCAO in rodents were analyzed. Rapamycin was used as a pharmacological regulator to study the function of collaterals during cerebral ischemia.

Results: SRA results showed that the collaterals between internal carotid artery and ophthalmic artery and the collaterals between the internal carotid artery and pterygopalatine artery opened after MCAO. The diameter of collateral vessels consistently increased for up to 28 days after MCAO. LSCI results showed that the cortical collaterals between anterior cerebral artery and middle cerebral artery immediately appeared after MCAO in C57/B6 mouse. Rapamycin treatment consistently improved collateral opening between anterior cerebral artery and middle cerebral artery compared to the control (p<0.05), and increased focal blood flow in the ischemic mouse brain (p<0.05). SRA results revealed that the probability of collateral opening between posterior cerebral artery and middle cerebral artery was about 75% after MCAO in rats. Rapamycin treated rats developed enlarged collaterals **(Fig 1.)** and increased vessel density around the ischemic region. TPLSM results showed that rapamycin treatment induced arteriole dilation in both normal **(Fig 2.)** and ischemic mice. Our results also showed that rapamycin treated mice presented decreased infarct volume and improved neurological outcomes compared to the control group (p<0.05).

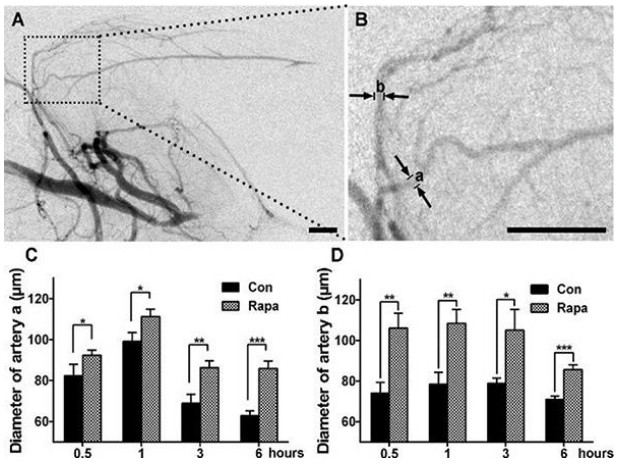

Figure 1. SRA image of collateral circulation (A) and (B) between posterior cerebral artery and middle cerebral artery after MCAO in rats.The statistical bar graphs (C, D) showed the diameter of collateral a and b 0.5, 1, 3 and 6 hours after MCAO in control and rapamycin treated rats. Bar: 1 mm.

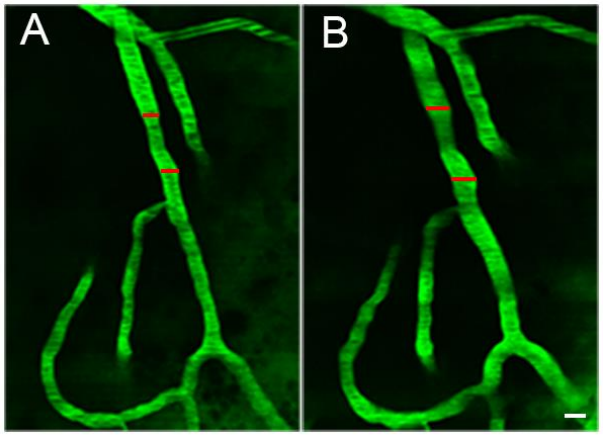

Figure 2. TPLSM image of arterioles before (A) and (B) after rapamycin treatment in living normal mice. Bar:10μm.

Conclusions: Our results suggest that a combination of SRA, LSCI, and TPLSM provides unique tools to dynamically study the collaterals in rodents. Rapamycin could improve neurological outcomes through promoting collateral opening, which is crucial for the ischemic stroke therapy.

References: Shuaib A, etal. Collateral blood vessels in acute ischaemic stroke: A potential therapeutic target. *Lancet Neurol*.2011;10:909-921

708
BRAIN-0169
Poster Session

Cerebrovascular Regulation

EFFECT OF MAXIMAL BREATH HOLD APNEA ON PIAL ARTERY PULSATION AND SUBARACHNOID WIDTH IN HUMAN

P.J. Winklewski[1], J. Wolf[2], E. Swierblewska[2], K. Kunicka[2], M. Gruszecki[3], W. Guminski[4], M. Wszedybyl-Winklewska[1], A.F. Frydrychowski[1], L. Bieniaszewski[2], K. Narkiewicz[2]
[1]Institute of Human Physiology, Medical University of Gdansk, Gdansk, Poland
[2]Department of Hypertension and Diabetology, Medical University of Gdansk, Gdansk, Poland
[3]Department of Radiology Informatics and Statistics, Medical University of Gdansk, Gdansk, Poland
[4]Department of Computer Communications Faculty of Electronics Telecommunications and Informatics, Gdansk University of Technology, Gdansk, Poland

Objectives: Little is known about intracranial pressure (ICP)-cerebral hemodynamic interplay during maximal breath-hold apnea. A recently developed method based on near-infrared transillumination/backscattering sounding (NIR-T/BSS) non-invasively measures changes in pial artery pulsation (cc-TQ) as well as subarachnoid width (sas-TQ) in humans [1,2,3,4]. Changes in sas-TQ correlate with ICP to a considerable extent [1], whereas cc-TQ reflects the functional status of the pial artery [1,3,4]. We tested the complex response of the pial artery and subarachnoid width to apnea using this method.

Methods: The pial artery and subarachnoid width response to maximal breath-hold (91.1±23.1 s) was studied in 20 healthy volunteers. The cc-TQ and sas-TQ were measured using NIR-T/BSS; cerebral blood flow velocity (CBFV), pulsatility index (PI) and resistive index (RI) were measured using Doppler ultrasound of the left internal carotid artery; heart rate (HR) and beat-to-beat systolic (SBP) and diastolic (DBP) blood pressure were recorded using a Finometer; end-tidal CO2 (EtCO2) was measured using a medical gas analyzer. The relationship between spontaneous oscillations in BP and cc-TQ at frequencies between 0.5 Hz and 5 Hz was assessed using wavelet transform analysis.

Results: With reference to baseline recordings apnea evoked a multiphasic response in BP, cc-TQ and sas-TQ (Figure 1, 2). First, SBP declined (-15.2%, P<0.01), which was accompanied by an increase in cc-TQ (17.1%, P<0.01) and sas-TQ (47.6%, P<0.001). Directly after these changes, SBP exceeded baseline values (14.4%, P<0.001), which was associated with a decline in cc-TQ (-12.3%, P<0.001) and the return of sas-TQ to baseline. During these initial changes CBFV first borderline increased (P<0.01) which was followed by its normalization (P=NS). However, toward the end of the apnea, BP, cc-TQ and CBFV increased (29.2%, P<0.001; 46.7%, P<0.01 and 73.3%, P<0.001, respectively) while PI, RI and sas-TQ declined (-42.5%, P<0.01; -21.2%, P<0.001 and -26.7%, P<0.01, respectively). A multivariate analysis showed that changes in sas-TQ were linked to variations in EtCO2, HR and SBP. Increase in wavelet coherence between augmented BP and cc-TQ oscillations was observed by the end of apnea (P<0.05; Figure 3).

Conclusions: Apnea is associated with ICP swings, closely reflecting changes in EtCO2, HR and peripheral BP. The baroreflex influences the pial artery response. Apnea increases the contribution of cardiac activity to BP and cc-TQ oscillations. Baroreflex and ICP changes are involved in a complex and intricate mechanism aiming at the stabilization of CBF.

References

1. Frydrychowski AF, Gumiński W, Rojewski M, Kaczmarek J, Juzwa W. Technical foundations for noninvasive assessment of changes in the width of the subarachnoid space with near-infrared transillumination-backscattering sounding (NIR-TBSS). IEEE Trans Biomed Eng. 2002;49:887-904.
2. Frydrychowski AF, Szarmach A, Czaplewski B, Winklewski PJ. Subarachnoid space: new tricks by an old dog. PLoS One. 2012;7:e37529.
3. Frydrychowski AF, Wszedybyl-Winklewska M, Bandurski T, Winklewski PJ. Flow-induced changes

in pial artery compliance registered with a non-invasive method in rabbits. Microvasc Res. 2011;82:156-62.
4. Wszedybyl-Winklewska M, Frydrychowski AF, Winklewski PJ. Assessing changes in pial artery resistance and subarachnoid space width using a non-invasive method in healthy humans during the handgrip test. Acta Neurobiol Exp. 2012;72:80-8.

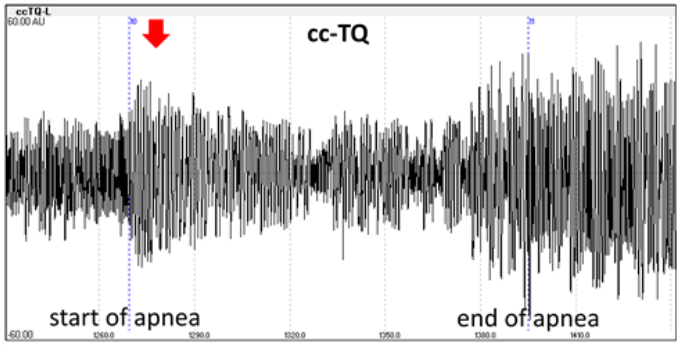

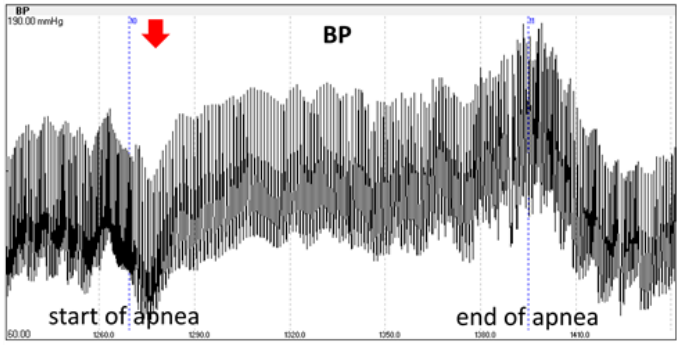

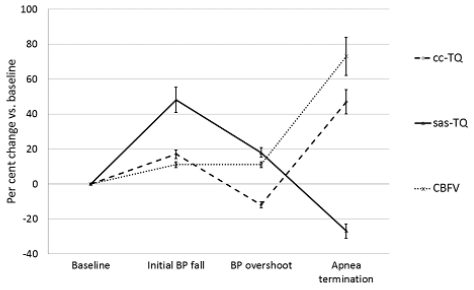

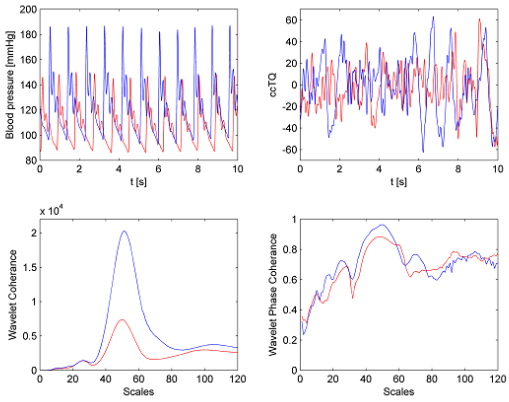

709
BRAIN-0585
Poster Session

Cerebrovascular Regulation

ELECTRICAL COMMUNICATION IN THE CEREBRAL ARTERIES: IMPORTANCE TO GLOBAL BLOOD FLOW REGULATION AND STROKE INJURY

A. Zechariah[1], *U.I. Tuor*[1], *C.H. Tran*[1], *D.G. Welsh*[1]
[1]*Physiology and Pharmacology, University of Calgary, Calgary, Canada*

Introduction: An integrated network of cerebral arteries actively controls brain perfusion in response to metabolic demand. Precise harmonization is made possible by: 1) global control, where multiple vessel segments dilate and constrict in a coordinated manner; and by 2) local control where a vascular segment responds independently of the network. To coordinate responses among multiple vessels, calcium concentration/myosin light chain phosphorylation must be synchronized among thousands of smooth muscle cells. This regulated process is thought to be facilitated by gap junctions,

intercellular pores that allow vascular cells to electrically communicate with each other.

Objectives: We sought to examine electrical communication in cerebral arteries and to determine whether compromising this process predisposes brain to stroke injury.

Methods and Results: Animal procedures were approved by the Animal Care and Use Committee at the University of Calgary in accordance with the Canadian Council on Animal Care guidelines. Using isolated cerebral arteries from mouse, hamster and resected human tissue, we show that electrical stimuli can effectively spread along vascular cells in an endothelium dependant manner. Genetic deletion of Connexin40 ($Cx40^{-/-}$) compromised charge spread in cerebral arteries, a finding consistent with a key role for this gap junctional subunit in electrical communication, across species. Subjecting $Cx40^{-/-}$ mice to focal cerebral ischemia (60 min) induced greater reduction in cerebral blood flow (during stroke and reperfusion phases) than wild type controls. The attenuation of blood flow enhanced stroke injury in $Cx40^{-/-}$ mice.

Conclusions: Overall, these findings demonstrate the presence of robust intercellular communication in the cerebral vasculature; this biological process plays a crucial role in collateral blood flow responses during stroke.
Funding: This study was supported by CIHR and A Zechariah is supported by AIHS and Eyes high postdoctoral scholarship.

710
BRAIN-0530
Poster Session

Cerebrovascular Regulation

PERICYTE CONTROL OF THE MICROCIRCULATION IN ISCHEMIC BRAIN

D. Zeppenfeld[1], W. Zhu[1], D. Hong[1], M. Grafe[2], J. Iliff[1], N. Alkayed[1]
[1]Anesthesiology and Perioperative Medicine, Oregon Health & Science University, Portland, USA
[2]Pathology, Oregon Health & Science University, Portland, USA

Objective: Despite successful recanalization of the occluded cerebral artery using tissue plasminogen activator or endovascular devices, more than half of stroke patients still end up with a poor clinical outcome[1]. This may be due to prolonged changes within the microvasculature contributing to microvascular perfusion deficits. We investigated whether pericyte constriction is associated with impaired microvascular blood flow in a mouse model of ischemic stroke with reperfusion. We then evaluated the role of epoxyeicosatrienoic acids (EETs), previously shown to regulate microvascular perfusion in brain[2], in the regulation of pericyte tone in the cerebral microcirculation.

Methods: The cortical microvasculature in the penumbra of Tie2-GFP/NG2-DsRed mice was imaged with two-photon microscopy through a chronic thin skull window before, 6 and 24 hours after 1-hour middle cerebral artery occlusion (MCAO). The resultant z-stacks were analyzed with Imaris FilamentTracer to detect capillary diameter changes, and red blood cell (RBC) velocity and flux were assessed by capillary line scans. At 24 hours of reperfusion, animals were fixed and stained with Hoescht dye to detect evidence pericyte death in the ischemic penumbra. In a separate set of animals, the following agents were microinjected into the cortex through a craniotomy to investigate their roles in pericyte contractility: ATP, the EETs antagonist 14,15-Epoxyeicosa-5(Z)-enoic acid (14-15-EEZE) or vehicle.

Results: After MCAO, the majority of capillaries in the ischemic penumbra underwent a bidirectional response with the majority of capillaries experiencing a loss of tone, while others experienced constriction. BBB integrity was compromised surrounding pericytes that lost tone after stroke. Application of 14-15 EEZE resulted in robust pericyte contraction, suggesting that endogenous EETs tonically promote pericyte relaxation, whereas ATP elicited more subtle and inconsistent pericyte contraction. Regardless of

diameter change, the majority of capillaries scanned exhibited markedly reduced RBC velocity and flux after MCAO. Pericyte cell death was evident in the ischemic core but not in the ischemic penumbra.

Conclusion: Capillaries in the ischemic penumbra undergo either dilation or constriction, which seem to reflect different responses to ischemic injury. RBC velocity and flux are compromised in the penumbra regardless of dilation or constriction while BBB permeability is associated with loss of pericyte tone and capillary dilation. Based on the constrictor activity of the EETs antagonist 14,15-EEZE, we propose that endogenous EETs mediate pericyte relaxation at baseline, which is lost after ischemia.

References:
1. Saver, J. L., Jovin, T. G., Smith, W. S., Albers, G. W., Baron, J.-C., Boltze, J., … Yoo, A. J. (2013). Stroke treatment academic industry roundtable: research priorities in the assessment of neurothrombectomy devices. *Stroke; a Journal of Cerebral Circulation*, *44*(12), 3596–601. doi:10.1161/STROKEAHA.113.002769
2. Alkayed, N. J., Birks, E. K., Hudetz, A. G., Roman, R. J., Henderson, L., & Harder, D. R. (1996). Inhibition of brain P-450 arachidonic acid epoxygenase decreases baseline cerebral blood flow. *The American Journal of Physiology*, *271*(4 Pt 2), H1541–6.

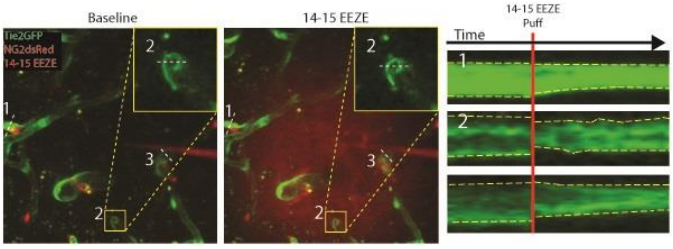

711
BRAIN-0163
Poster Session

Cerebrovascular Regulation

SKULL OPTICAL CLEARING FOR IMPROVING CEREBROVASCULAR IMAGING

D. Zhu[1]
[1]*Wuhan National Lab for Electronics, Huazhong University of Science & Technology, Wuhan, China*

Various optical imaging methods for visualization of both structural and functional architecture with high temporal-spatial resolution have shown tremendous advantages in investigation of cortical neurons and microvasculature. However, the applications usually depend on cranial window by craniotomy because the turbid skull reduces the imaging contrast and resolution. Fortunately, we developed an innovative skull optical clearing solution (SOCS), which could make the skull transparent within 20-30 minutes. With the optical clearing cranial window, it is easy to monitor the blood flow with the laser speckle contrast imaging and blood oxygenation with the multispectral imaging. Not only the resolution, but the signal to noise ratio and sensitivity were significantly improved. The transparent cranial window was introduced in an acoustic resolution photoacoustic microscopy (AR-PAM) or optical resolution photoacoustic microscopy (OR-PAM) for mapping the cerebral vasculature. The results demonstrated that the former's signal level can be effectively elevated under the case of retaining the resolution. For the latter, the resolution can be increased by more 2 times. For the both modes PAMs, the signal from deeper can be obtained. The skull optical clearing technique is hopeful to provide a simple and effective method for visualizing cerebral microvascular structure and function.

712
BRAIN-0482
Poster Session

Cerebrovascular Regulation

EFFECT OF ADRENALINE ON CEREBRAL BLOOD FLOW IN HEALTHY RATS AND RATS WITH INTRACRANIAL HEMORRHAGE

E. Zinchenko[1], *O. Semyachkina-Glushkovskaya*[1], *O. Sindeeva*[1], *M. Kassim*[1]
[1]*Biology, Saratov State University, Saratov, Russia*

Objectives: The cerebral circulation is one of the main precursors of cerebral hemorrhage. Issue of

methods of brain haemorrhage in the neonatal period diagnosis and correction is particularly acute [1]. Leading role in the regulation of cerebral vascular tone plays adrenergic system. Thus, the study of adrenergic mechanisms of regulation of cerebral blood flow and molecular factors underlying them, can shed light on the nature of cerebral vessels breaks under different precipitating factors [2].

Methods: The study was carried out on 69 newborn female rats. Cerebral blood flow in the cerebral vessels was studied at rest and after the stress exposure. Rats were exposed to loud noise (70 dB, frequency 110 Hz) without interruption for 60 minutes. After the completion of the sound exposure studies of cerebral hemodynamics with the use of optical coherence tomography (OCT) in animals were conducted.

In the next stage the role of adrenergic effects in the regulation of cerebral blood flow in neonatal rats under normal conditions and during the development of stress-induced cerebral hemorrhage with the use of OCT was examined. The results were recorded in 4 hours and 24 hours after stress.

Results: In 4 hours after sagittal vein of stressed rats diameterincreased in comparison with basal values and dilatation was accompanied by a decrease in blood flow and perfusion in it. 24 hours later, intracranial hemorrhage, which was accompanied by the progression of pathological changes in the venous blood flow, occurs in all newborn rats. Blood flow velocity and perfusion in all the arteries of the cerebral cortex decreased in stressed rats in comparison with control animals.

The diameter of arteries increased, large-diameter arteries were insensitive to the effects of the drug under the influence of adrenaline. Blood flow velocity in the cerebral arteries was significantly reduced. Sagittal vienna decreased in response to the injection of adrenaline. However, the velocity of blood flow and perfusion in it did not significantly change. Loss of reactivity to epinephrine was observed either 4 hours after the stress or a day later in stressed rats.

Conclusion: Reduction of venous outflow from the cranial cavity is one of the important causes of intracranial hemorrhage in newborns. In the experiments with adrenaline, we have shown that adrenaline relaxes cerebral vessels in normal conditions. On the background cerebral hemorrhage unresponsiveness to the drug is observed in neonatal rats.

The research supported by grants № 14-02-00526-a, MD-2216.2014.4

Reference:

1. Oxana V. Semyachkina-Glushkovskaya , Sergey S. Sindeev , Ekaterina M. Zinchenko, Mohhanad M. Kassim , Valery V. Tuchin. The assessment of pathological changes in cerebral blood flow in hypertensive rats with stress induced intracranial hemorrhage using Doppler OCT: Particularities of arterial and venous alterations // Photonics & Lasers in Medicine.- 2013. – ISSN 2193-0635. –Vol. 2, No. 2. – P. 109-116.

2. Semyachkina-Glushkovskaya O., Sindeev S., Zinchenko E., Kassim M., Tuchin V. The experimental study of stress-realted pathological changes in cerebral venous blood flow in newborn rats assessed by DOCT // Jornal of Innovative Optical Health Science. 2013. – Vol. 3. –No. 12. –P. 1-9.

713
BRAIN-0582
Poster Session

Neurovascular Coupling

TUMOR EFFECTS ON BOLD FMRI SIGNAL IN BROCA'S AREA

B. Hou[1], J. Bao[2], X.L. Zhang[3], B. Sanjay[4], J. Zhang[3], C. Jeffrey[1], Q. Wu[5]
[1]Radiology, WVU, Morgantown, USA
[2]Bio-Enginnering, University of Washington, Seattle, USA
[3]Neurosurgery, Huashan Hospita, Shanghai, China
[4]Neuoral surgery, WVU, Morgantown, USA
[5]Neural Surgery, Huashan Hospita, Shanghai, China

Objectives: We investigated patients with left GBMs on or next to the Broca's areas for exploring the tumor effects on the BOLD signal in the motion speech area.

Subjects/ Methods: 8 patients (50.2± 10.6 years) who performed an object-naming task were included in this abstract. An anatomical and a task fMRI scans on each subject were performed using a 3.0 Tesla scanner with a 12-channel head matrix coil. The subjects were asked to perform the object- naming task in the "on" acquisitions and doing nothing and keeping mind wandering in the "off" (i.e., rest) acquisitions. The task fMRI data were analyzed offline by AFNI (1). The functional cortices including the Broca's area for each patient were determined from the fMRI data by a correlation coefficient (CC) analysis, and the location of the area was recorded by the voxel inside the area with the highest CC value. The average signal with 5 maximum values in the area was calculated. The position of the GBM for the case was determined by the voxel with the highest signal intensity in the contrast enhanced T1-weighted anatomical images. The distance between the GBM and the Broca's area was calculated from the coordinates of the two voxels. A plot of the distance vs. the average signal was drawn and fitted.

Results: The coordinates for two voxels (one representing the location of the Broca's area and another representing the location of the GBM) were listed in the Table 1 in which the distance between the GBM to the Broca's area and the average BOLD fMRI signal in the area were also included. With the data of the distance and the average signal, we plotted and fitted the 8 data points in a figure. A linear fitting were found, and the r value for the linear fitting is 0.71.

Discussions: The high r value in the fitting suggests that with the distance increasing the BOLD signal increases. The good exponential curve fitting exhibits that with the distance increasing to approximate 50 mm the increasing signal seems to be saturated. Considering a GBM having high densities of tumor blood vessels and cells and the BOLD signal mechanisms, the results seem to support that the linear and saturated efforts result from both the tumor vasculature-neuron's decoupling (2) and tumor cell's replacing of NAA cells (i.e., the neuron cells) (3).

References: [1] Cox, RW., 1996. [2] Hou, BL. et. al., 2006,.[3] Hou, BL, et. al., **a** talk in the 15th Annual Meeting of the ISMRM, 2007.

Patient	Left Broca's Coord (x, y, z) mm	GBM's Coord (x,y, z) mm	Distance(mm) (GBM to Broca')	Average BOLD sig. in the left Broca's (%)
1	14.772/-30.795/56.918	21.608/-19.077/62.778	50.678	0.912
2	42.508/-27.446/27.126	28.840/-9.663/12.916	26.525	0.763
3	37.598/-24.902/3,906	29.785/-7.324/9.277	33.592	0.850
4	46.501/-44.304/35.937	11.345/-21.843/80.370	60.949	0.875
5	41.815/-27.020/68.727	54.510/-14.813/71.657	17.854	0.599
6	21.659/-39,373/58.778	41.190/-4.220/22.160	60.189	0.897
7	40.527/0.602/51.827	51.758/-16.716/27.413	31.970	0.848
8	27.927/-7.578/71.458	49.900/-22.950/81.710	28.710	0.884

714
BRAIN-0680
Poster Session

Neurovascular Coupling

MAPPING LARGE-SCALE FUNCTIONAL CONNECTIONS WITH CHR2-EVOKED HEMODYNAMIC SIGNALS

A.Q. Bauer[1], G. Baxter[1], A.W. Kraft[2], M.R. Bruchas[3], J.M. Lee[2], J.P. Culver[1]
[1]Radiology, Washington University in Saint Louis, Saint Louis, USA
[2]Neuroscience, Washington University in Saint Louis, Saint Louis, USA
[3]Anesthesiology, Washington University in Saint Louis, Saint Louis, USA

Objectives: A major goal of neuroscience is the development of a connectome for understanding structural and functional connections of the mammalian brain[1]. Optogenetic methods, which use activation of light-gated, opsin-expressing neurons, are a natural approach for probing local and global brain circuitry[2]. While fMRI is an attractive method for investigating the distribution of neural activity at the mesoscale, optogenetic-fMRI mapping of the entire cortex is challenging due to space constraints[3]. To satisfy this need, we combined optogenetic mapping with wide-field optical intrinsic signal (OIS) imaging in awake mice. Functional mapping was performed after determining which optical stimulus parameters elicit linear hemodynamic responses within these functional circuits.

Methods: A cranial window is secured to the intact mouse skull with dental cement. Once recovered, mice are trained to become behaviorally-acclimated to the imaging system (**Fig. 1A**) over a period of 5 days. Imaging was performed in 4 awake mice (Thy1-ChR2, line 18 Jackson Labs) in order to measure how the hemodynamic response relates to titrated doses of optical power, stimulus frequency and pulse duration. Stimuli found to evoke hemodynamic

responses within a linear regime were scanned over the cortex for functional mapping.

Results: Increasing optical stimuli generally resulted in greater peak hemodynamic response (**Fig. 1B**). However, an analysis of the ChR2-induced hemodynamic response function (HRF) resulted in a different picture. For fixed optical power and stimuli shorter than 3 seconds, we observe canonical HRFs that increase in magnitude as a function of increasing stimulus frequency up to 10 Hz and plateau at 20Hz (**Fig. 1C top row**). This response was not observed in experiments titrating stimulus duration with fixed power and frequency (**Fig. 1C, bottom row**). For shorter stimuli, a similar HRF to the first experiment is observed, but for stimuli lasting 10s or longer, we see the emergence and separation of two distinct HRFs (**Fig. 1C**). ChR2 stimulation of left barrel cortex (S1BC) produces hemodynamic responses in S1BC as well as highly correlated (Pearson r=0.8) activity in primary motor cortex (M1, **Fig. 1D**) Interestingly, while stimulation of M1 evokes a reciprocal connection with S1BC, the time course of S1BC activity to M1 stimulation is less coherent (Pearson r=0.6). Future work will examine asymmetries in connection strengths between functional regions, which could be indicative of a connection bias regarding information flow within networks[4].

Conclusions: Incorporating optogenetics and wide-field OIS imaging is one method for investigating cortical ensemble activity and functional networks on the meso-scale. Understanding how neurons integrate multiple inputs, and the function of coordinated population activity within the larger scope of a circuit are important components to developing a fully-realized functional connectome, and may help deduce impaired functional relationships between cortical areas in disease models.

References

[1]. Lichtman, J. W, et al., *Science* 334, 618–623 (2011)
[2]. Boyden, E. S., et al, *Nat. Neurosci*. 8, 1263–1268 (2005)
[3]. Desai, M., et al., *J. Neurophysiol*. 105, 1393–1405 (2010)
[4]. Lim, D. H. et al., *Front. Neural Circuits* 6:11. (2012)

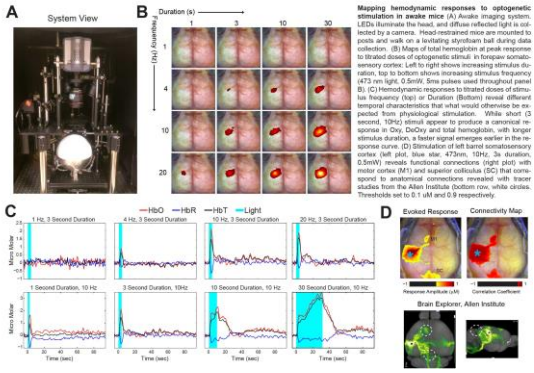

715
BRAIN-0058
Poster Session

Neurovascular Coupling

IN VIVO OPTOGENETIC MANIPULATION OF CELLS WITHIN THE NEUROVASCULAR UNIT LEADS TO LOCAL CHANGES IN NEURAL ACTIVITY

T. Brown[1], *C. Moore*[1]
[1]*Neuroscience, Brown University, Providence, USA*

Changes in neural activity can drive vasodilations in local blood vessels, a process measured by functional magnetic resonance imaging. Despite substantial investigation of the relationship between neural and vascular dynamics, the potential impact of vascular responses on local neural activity is unknown. Here, using *in vivo* two-photon imaging of neural calcium responses in sensory cortex, we found that sensory-evoked changes in neural activity lead and follow vasodilations. To determine if vasodilations drive changes in local neural activity, we developed optogenetic control of cerebral vascular responses (vasOpto) to shape vascular dynamics similar to the vasodilations that occur during sensory processing. VasOpto-evoked dilations led to rapid changes in neural activity and these changes predicted the dynamics observed with

natural sensory-driven vasodilations in a significant portion of neurons. Our results capture a previously inaccessible dimension of sensory processing and may reveal new strategies to treat neurological and vascular disease.

716
BRAIN-0219
Poster Session

Neurovascular Coupling

DYNAMIC MAGNETISATION TRANSFER MRI: THE EFFECT OF CARDIAC PULSATION ON CELLULAR WATER EXCHANGE

D. López[1], *C.M. Kerskens*[1]
[1]*Institute of Neuroscience, Trinity College Dublin, Dublin, Ireland*

Objectives : MRI methods can measure dislocation of water molecules [1]. They can differentiate between flow and diffusion but not between flow and movement. This is the reason why signal changes in diffusion-weighted imaging which coexist with the cardiac pulse are considered generally related to movement [2]. Here, we show a method to measure the intra-extracellular water exchange with a low sensitivity for movement. Because of insensitivity to movements, signal changes in the tissue related to the cardiac pressure wave are detectable.

Methods: The MRI sequence consists of a magnetisation transfer (MT) preparation phase followed by single-slice echo-planar imaging sequence. MT effect was introduced by a negative (-5236.8 ± 894.18Hz) and a positive off frequency (6982.5 ± 894.18Hz Hz) RF pulse. Imaging parameters were voxel size of 3.5 x 3.5 x 3 mm, TR = 60 ms, TE = 11 ms, FA = 35 degrees and 2000 repetitions. For comparison, a control sequence with the same read out parameter but without the MT preparation was used.

12 subjects were scanned with the protocols approved by the Trinity College ethics committee and the Irish Department of Health.

Results: A comparison between the time series acquired, both with and without MT preparation, is shown in the figure. For both cases, a voxel was extracted to showcase the difference between each time series. Only for the MT preparation, strong cardiac peaks are resolved while for the control sequence physiological noise is dominant. Peaks can be observed in all regions except the periventricular area whereby white matter, in general, shows higher peaks than grey matter. These results are consistent over all subjects.

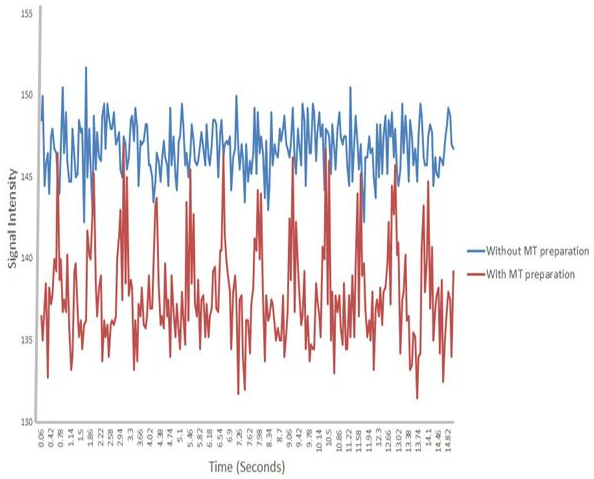

[Figure] Time series extracted from a voxel with MT preparation (red) and without MT preparation (blue).

Conclusions: To our knowledge, the observation of a cardiac related MT change has not yet been reported, therefore the mechanism behind this contrast is extremely interesting. Most likely, the pool of free water that exchanges with the macromolecules [3], is removed or separated by the pressure wave with the effect that the proton exchange between the pools is interrupted. Our explanation is that the pulse wave compresses cells with the result that water is pumped out of the cells. Hypothetically, this could then help to facilitate the lymphatic clearance of extracellular solutes and fluid from the brain parenchyma.

This would be consistent with new findings that astroglial AQP4 water channel play an important role in the interstitial solute clearance [4].

References
[1] Le Bihan, D., et al. *Acad. Sci.* 1985, 301(15): 1109–1112.
[2] Skare, S., et al. *Magnetic Resonance Imaging* 2001; 19: 1125–1128.
[3] Henkelman, R.M., et al. *NMR biomed.* 2001; 14:57-64.
[4] Iliff, J.J., et al. *Stroke* 2013, 44(suppl 1): S93–S95.

717
BRAIN-0186
Poster Session

Neurovascular Coupling

SIMULTANEOUS VISUALIZATION AND ANALYSIS OF CELLS AND BLOOD VESSELS IN A WHOLE MOUSE BRAIN

B. Xiong[1], J. Wu[1], Q. Luo[1], H. Gong[1]
[1]Wuhan National Laboratory for Optoelectronics, Huazhong University of Science & Technology, Wuhan, China

Abstract

Objectives: The brain consists of neurons, glia cells, and blood vessels that form a complex interconnected neurovascular network. The blood vessels provide neurons and glia cells with energy and nutrition and clear away waste. Acquiring data on the detailed vascular networks and other types of neural cells data simultaneously is a significant task of brain research. To understand the correlation between vascular density and neuronal activity, a whole brain co-localized vascular supplying pattern and detailed cellular and vascular density need to be acquired.

Methods: Our approach is to developed an automatic micro-optical sectioning tomography (MOST) instrument to determine the details of both individual cells and capillaries with 1 micron voxel resolution. We modified Nissl staining method that can be quickly labeled the cells and blood vessels simultaneously in an entire mouse brain. Combining the MOST technique and a novel whole-brain Nissl staining method, the cytoarchitecture and vascular networks information data were acquired simultaneously. The results showed that the morphology of both the cells and the blood vessels was well maintained. Unprecedented details of both individual cells and blood vessels, including capillaries were acquired. We developed an automatic image-processing pipeline to perform brainwide vectorization and analysis of cells and blood vessels. And a semi-automatic method was proposed to distinguish arties and veins, meanwhile to get the brainwide vascular supplying pattern.

Results: The main brain regions that were used to localize were labeled through the cytoarchitecture. The density of cells and blood vessels in many regions of brain, including FrA, M1, PMBSF, V1 of the cortex and amygdala, striatum, hippocampus, cerebellum, thalamus, hypothalamus, have been quantitatively analyzed and contrasted. The detailed arterious and venous networks were distinguished meanwhile the vascular supplying patterns were aquired in the whole mouse brain.

Conclusions: We found the proximity of cells to blood vessels was linearly correlated with vascular length density, rather than the cell number density. The results of co-localized vascular supplying patterns and the detailed cellular and vascular density in the whole mouse brain provide an anatomical resource and could be beneficial for the state comparison of the developing and diseased brain.

References:

1. Li A, Gong H, Zhang B, et al. Micro-optical sectioning tomography to obtain a high-resolution atlas of the mouse brain. Science, 2010, 330(6009): 1404-1408.

2. Wu J, He Y, Yang Z, et al. 3D BrainCV: Simultaneous visualization and analysis of cells and capillaries in a whole mouse brain with one-micron voxel resolution. Neuroimage, 2014, 87: 199-208.

718
BRAIN-0566
Poster Session

Neurovascular Coupling

FUNCTIONAL ACTIVATION OF VISUAL CORTEX AND THE EFFECT ON CYTOCHROME C OXIDASE OXIDATION STATUS

D. Highton[1], P. Phan[2], I. Tachtsidis[2], C.E. Elwell[2], M. Smith[1]
[1]Neurocritical Care,
National Hospital for Neurology and Neurosurgery
University College London Hospitals, London,
United Kingdom
[2]Medical Physics and Bioengineering,
University College London, London,
United Kingdom

Objectives: Neurovascular coupling results in typical task evoked functional hyperaemia. This is exploited in functional imaging because direct measurement of metabolic activity is problematic[1]. Cytochrome c oxidase (CCO), the terminal electron acceptor in the mitochondrial respiratory chain, exhibits task evoked changes in oxidation status, and its measurement likely reflects metabolic changes at the mitochondrial level. Using in-house broadband functional near-infrared spectroscopy optimised for detection of CCO in adults we have previously demonstrated different patterns of CCO change during frontal cortex activation[2], which may reflect differences in neurovascular coupling or metabolism. The V1 visual cortex is defined histologically into two areas (blob, interblob) by their CCO concentration – and it is thought that this is an adaption to deliver a greater capacity for oxidative metabolism in the blob region. However the nature of flow-metabolism coupling in this region remains disputed. The aim of this work is to examine the CCO response to functional activation in blob/interblob regions.

Methods: Optodes of an in-house broadband spectrometer[2] were placed over left frontal (control) and left visual cortex. The visual stimulation paradigm consisted of an isoluminant chromatic challenge (red-green 4Hz flicker - blob stimulation) and luminance challenge (black and white checkerboard - interblob stimulation). Each epoch consisted 20sec periods of chromatic, black, luminance and black, repeated 20 times. Concentration changes in oxy-[HbO2] deoxy-haemoglobin [HHb] and the oxidation status of CCO [oxCCO] were derived by fitting the broadband spectra between 780-900nm at a 3.5cm source detector spacing. Results were averaged across the repeated blocks and the [oxCCO] change at time 20 and 40sec compared using Students t-test. Because the partial pathlength of light is likely to vary between the two brain regions, derived concentration changes may not reflect actual differences. Therefore we compared the gradient of [Hbdiff] ([HbO2]-[HHb], marker of oxygen delivery) to [oxCCO] using linear regression, for each challenge.

Results: 8 healthy volunteers were recruited following ethics approval and written consent. Figure 1 demonstrates the changes in [HbO2], [HHb] and [oxCCO] observed across the group. The chromatic and luminance challenge generated significant elevations in [oxCCO] 0.06 micromol/L ($p<0.001$, 95%CI 0.04-0.08) and 0.11 micromol/L ($p<0.001$, 95%CI 0.08-0.15) respectively in the visual cortex. No such changes were seen in the frontal brain region. There was a difference in the ([oxCCO]/[Hbdiff] gradient between the two challenges in the visual cortex - chromatic 0.17 (99%CI 0.15 – 0.19) and luminance 0.10 (99%CI 0.08-0.12).

Conclusions : We have demonstrated differences in [oxCCO] dynamics between two different visual stimulation paradigms in different regions of visual cortex. This might reflect differences in metabolism or oxygen delivery between blob and interblob regions proposed by other investigators, and is also consistent with our previous observations and mathematical modeling of [oxCCO] dynamics[2]. Further work is required to elucidate the physiological significance of these data, but our findings suggest that [oxCCO] may have unique potential to provide a window on cellular energetics in the investigation of neurovascular coupling.

References

1. Hillman EMC. 2014, Annu Rev Neurisci *37*, 161–181.
2. Kolyva, C. et al 2012, *Biomedical Optics Express*, *3*(10), 2550–2566.

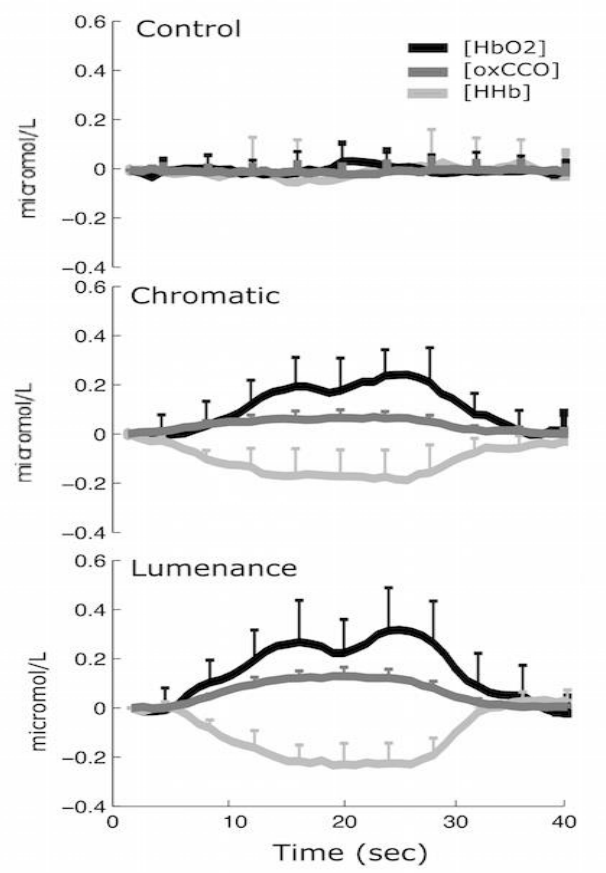

719
BRAIN-0218
Poster Session

Neurovascular Coupling

ROLE OF NEUROTRANSMITTERS ON THALAMOCORTICAL REGULATION OF THE ACTIVATED BARREL CORTEX: A FUNCTIONAL MR SPECTROSCOPY STUDY.

N. Just[1], *R. Gruetter*[1]
[1]*CIBM, Ecole polytechnique fédérale de Lausanne, Lausanne, Switzerland*

Objectives: Our aims were to explore the role of neurotransmitters on the neuro-metabolic and vascular regulation of the barrel cortex (S1BF) by the thalamus.

Methods: Male Sprague-Dawley rats (n=24) were anesthetized with α-chloralose. Body temperature and blood parameters were maintained at physiological levels. Each rat underwent trigeminal nerve stimulation[1]. fMRS experiments were performed on an actively shielded 9.4T/31cm bore magnet (Agilent, USA) with a surface coil. After shim adjustements[2], localized Proton spectroscopy was performed using SPECIAL[3]. The voxels of interest for the thalamus (3x3x4mm^3) and S1BF (1.5x3x5mm^3) were chosen by reference to the Paxinos and Watson atlas. ^{1}H spectra were acquired during 32-minutes of rest followed by 32 minutes of TGN stimulation corresponding to 480scans (30x16) per period. The raw ^{1}HMRS spectra corrected for frequency drift and summed were used for LCModel analysis with a basis set of 21 simulated metabolites. The neurochemical profiles in the thalamus and S1BF were measured serially for 11 rats starting with the thalamic nuclei at rest followed by a 32-min TGN stimulation period. BOLD responses in S1BF were measured post-fMRS measurements using single shot gradient echo EPI and assessment of BOLD effect was performed. A one-way Anova test with Bonferroni correction was used to compare metabolite concentrations at rest and during stimulation. The significance level was set at 0.05. All the results are presented as Mean±SEM.

Results: In S1BF, Lac, Glu, GABA levels were significantly higher during stimulation (p=0.0015, p=0.015 and p=0.021 respectively). Glc and Asp demonstrated a tendency to decrease (p>0.05). Within S1BF, the group difference spectrum between rest and stimulation using data from 18 rats confirmed these findings. A 0.3Hz line broadening factor was applied to the NAA linewidth of the stimulation spectrum to match the NAA linewidth of the rest spectrum. The BOLD free difference spectrum shows positive peaks at 1.33ppm for Lac and at 2.13 and 2.35 ppm for Glu. This BOLD free difference spectrum was fit with LCmodel and a simulated basis set yielding positive quantitative changes for Glu and Lac

(+0.34±0.05µmol/g and +0.23±0.05µmol/g) but not for Asp and Glc although negative peaks (at 2.72 and 2.84 ppm for Asp and 3.5ppm for Glc) were observed. In the thalamus, Gln was significantly higher during TGN stimulation ($p<0.009$) while Glu only showed a strong tendency to decrease.

A strong trend towards a negative correlation of BOLD percent changes between S1BF and the thalamus was found. At Rest, BOLD changes in S1BF were strongly and negatively correlated to GABA levels (Pearson's coefficient=-0.75, $p=0.013$). In S1BF, Glu levels were correlated at rest with BOLD changes but not during stimulation. ΔGlu were strongly and negatively correlated to ΔBOLD (Pearson's coefficient=-0.70. $p=0.024$).

Conclusions: The neurochemical consequences of TGN stimulation were measured in two structures pertaining to the whisker to barrel cortex pathway. The influence of GABA and Glu thalamic levels during S1BF activation were highlighted.

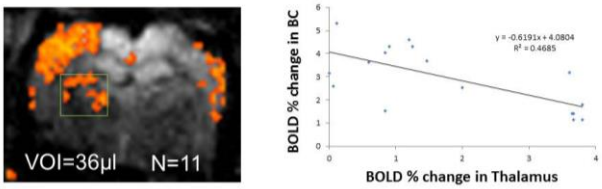

References: 1. Just N et al. Neuroimage. 2013;74:343-51. 2. Gruetter R et al. Magn. Reson. Med. 2000;43:319-323.3.Mlynarik V et al. Magn Reson Med 2006; 56:965-70.

720
BRAIN-0426
Poster Session

Neurovascular Coupling

CORTICAL SPREADING DEPRESSION AND IN VIVO CALCIUM IMAGING IN TRANSGENIC MICE WITH FAMILIAL HEMIPLEGIC MIGRAINE TYPE 1

L. Khennouf[1], B. Gesslein[1], A.M. Van Der Maagdenberd[2], M. Lauritzen[1]
[1]TransNeuro, Institute of Neuropharmacology, Copenhagen, Denmark
[2]Department of Human Genetics, Leiden University Medical Centre, Leiden, Netherlands

Familial hemiplegic migraine type 1 (FHM1) is a rare autosomal dominantly inherited subtype of migraine with prolonged aura of visual and sensory symptoms. The disease is caused by a mutation of the CACNA1A gene that encodes the α1A-subunit of voltage-gated Ca^{2+} channel in presynaptic terminals. The migraine aura is most likely caused by cortical spreading depression (CSD), a transient slowly propagating depolarization wave, which is strongly dependent on the interaction between glutamate and pre- and postsynaptic glutamate NMDA receptors. Due to increased action-potential-evoked Ca^{2+} influx in presynaptic terminals there is an increased probability of glutamate release at pyramidal cell synapses in FHM1; in comparison inhibitory neurotransmission at fast-spiking interneuron synapses remained unchanged. However, it is incompletely understood to what extent this expected enhancement of excitatory neurotransmission is reflected in Ca^{2+} activities in cortical pyramidal cells and glia under physiological conditions and CSD in vivo. It is also unclear how the basal facilitation is reflected in the mechanisms that couple rises in synaptic activity to changes in the cerebral blood flow (CBF) and the cerebral metabolic rate of oxygen ($CMRO_2$).

We here explored the effect of somatosensory stimulation and CSD on neuronal and glial Ca^{2+} activities and the corresponding changes in CBF and $CMRO_2$ in FHM1 with the R192Q mutation as compared to wild type mice in vivo. We report that in the mouse somatosensory cortex of FHM1 mice, afferent stimulation produced smaller, not larger, rises in neuronal and glial Ca^{2+} activities than in WT mice. In comparison, Ca^{2+} rises and the DC potential changes induced by CSD were similar for FHM1 and WT mice. CSD produced a larger increase in $CMRO_2$ in FHM1 than in WT

mice, but a similar rise in CBF. This indicated a mismatch between O_2 use and supply that was reflected in protracted tissue anoxia in FHM1 mice, while WT animals only displayed a reduced level of tissue O_2. FHM1 mice showed a slower recovery of cerebral blood flow to pre-CSD baseline values than wild-type after a CSD, and following the CSD, evoked CBF and Ca^{2+} responses were moderately decreased in WT mice and severely affected in FHM1 mice.

This study shows that the R192Q mutation leads to impairment in control of activity-.dependent rises in neuronal and glial Ca^{2+} activities in vivo. This impairment is not reflected on the overall EPSP amplitudes, but in impaired neurovascular coupling in FHM1 mice. Collectively, the data support the notion that affection of selective Ca^{2+} -dependent regulation of neurovascular coupling may underlie several key features of FHM1 such as the prolonged aura in the human phenotype. Specifically, the protracted anoxia and the abolished neurovascular coupling response during and following CSD provide a potential mechanism for the severe and prolonged neurological deficits in FHM patients. This underscores that genetic factors affecting the supply of substrates for brain energy metabolism and in turn brain ion homeostasis contribute to the phenotypic diversity of human migraine syndromes.

721
BRAIN-0322
Poster Session

Neurovascular Coupling

NEW MODEL FOR THE BOLD HEMODYNAMIC RESPONSE EVOKED BY BRIEF NEURAL ACTIVATION IN HUMAN CEREBRAL CORTEX

J.H. Kim[1], *D. Ress*[1]
[1]*Neuroscience, Baylor College of Medicine, Houston, USA*

Objective

The BOLD signal evoked by short stimulation, the hemodynamic response function (HRF), is the basis for linear analysis of most functional magnetic resonance imaging (fMRI) experiments. We propose a new model that includes only CBF and CMRO2 responses as drivers of the BOLD HRF, excluding venous cerebral blood volume (CBV) changes based on many recent experimental findings [1-4]. The CBF response is modeled using a linear network as a biomechanical model of the pial vasculature [5]. A stereotypical parametric temporal form is assumed for the CMRO2 response. We test this model against measurements of the BOLD HRF in human visual cortex evoked by brief stimulation using high-resolution fMRI to avoid contamination from large pial blood vessels.

Methods

The BOLD signal depends on changes in oxygen saturation (SO2) in capillaries and veins. To model longitudinal oxygen transport, we assume a uniform cylindrical geometry for the capillary and finely grid its length. We then use differential mass balance, including the processes of blood flow, hemoglobin dissociation, and oxygen diffusion into extravascular tissue, to obtain a continuous SO2 spatial profile, Fig 1A. Venous oxygen saturation is assumed spatially constant from the value at the distal end of the capillary.

The CBF response was modeled using a linear network model to describe the upstream arterial impulse response produced by prompt arterial dilation. We simulated CMRO2 response using a gamma-variate-function kernel.

In experiments, stimulus was a 2-s pulse of 4-Hz flickering dots followed by a 26-s blank period to let the HRF evolve and subside. High-resolution fMRI data (0.9-mm voxels) was obtained in 7 subjects (3-shot spiral acquisition, 8 slices, 1.5-s/volume). Each session produced ~85 HRF responses that were averaged together throughout the activated gray matter in prescribed portions of areas V1—3.

Results

The BOLD model successfully fit the experimental data, Fig. 1B. The model explains the early latency as competition between CBF and CMRO2, Fig 1C. After the CMRO2 demand peaks, the CBF continues to increase for a few seconds while the CMRO2 decreases. The late-time behavior of the HRF is explained by the

underdamped oscillatory CBF response, and there is significant variability of the undershoot between subjects.

The model predicts the largest contribution (68%) on the BOLD signal is from the intravascular venous compartment, followed by intravascular capillary (22%), then extravascular venous (10%). There is minimal contribution (< 1%) from the extravascular capillary compartment.

Conclusion

We developed a new BOLD model based on prompt arterial dilation evoked by brief neural stimulation in human cortex. The model provides a simple, self-consistent biomechanical mechanism for an underdamped CBF response, and integrates it with oxygen transport. Our theory successfully fits measurements of the HRF evoked in early visual cortex, and explains the HRF time course as competition between CBF and CMRO2, a much simpler picture that appropriately neglects blood volume effects for brief stimulation periods.

Reference

1. Drew, P.J. (2011), PNAS
2. Fernandez-Klett, F. (2010), PNAS
3. Hillman, E. (2007), NeuroImage
4. Vazquez, A (2010), JCBFM
5. Kim, J.H (2013), JCBFM

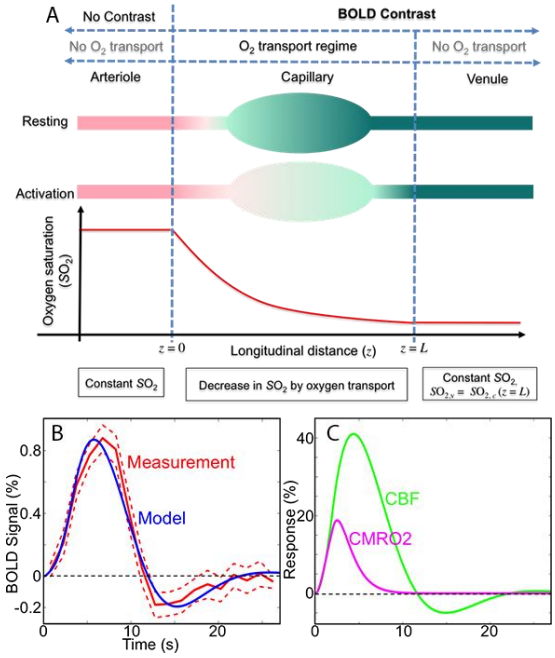

722
BRAIN-0801
Poster Session

Neurovascular Coupling

HEMODYNAMIC AND NEURONAL RESTING STATE FUNCTIONAL CONNECTIVITY MAPPING IN THE AWAKE MOUSE BRAIN

S. Kim[1], M.A. Shaik[1], Y. Ma[1], H.T. Zhao[1], M.G. Kozberg[2], V. Voleti[1], E.M.C. Hillman[1]
[1]Biomedical Engineering, Columbia University, New York City, USA
[2]Neurobiology and Behavior, Columbia University, New York City, USA

Objectives: In the field of human brain research, functional connectivity mapping via analysis of low-frequency correlations in functional magnetic resonance imaging (fMRI) blood oxygen level dependent (BOLD) signals has become an important tool. However, the BOLD signal is sensitive to local changes in deoxy-hemoglobin, widely assumed to be tightly coupled to preceding local neuronal events, though the coupling between these is not well characterized. This study aims to characterize the coupling of hemodynamic and neuronal activity in the awake mouse cortex by simultaneously imaging both signals in the same mice longitudinally using widefield optical techniques. Up until now, many studies in the optical imaging field have focused on collecting either neuronal or hemodynamic data, or have collected both but in a limited area of cortex [1, 2, 3].

Methods: Our study used adult restraint-habituated Thy1-GCaMP3 mice (genetically encoded with calcium indicator of neuronal activity in cortical layers II/III and V) with thinned-skull craniotomies and acrylic head plate implants for restraint during awake imaging [4]. A high-speed multispectral optical intrinsic signal imaging (MS-OISI) system was used to concurrently collect spontaneous hemodynamic and GCaMP3 fluorescence change signals in the awake and anesthetized states longitudinally for up to 3 months.

Results and Conclusions: Preliminary data indicate that even in the awake state where optimal correlation would be expected, the coupling between hemodynamic and GCaMP3 activity can vary and is not always one-to-one. We will present the results of our continued analysis comparing awake resting state functional connectivity maps for hemodynamic and neuronal activity.

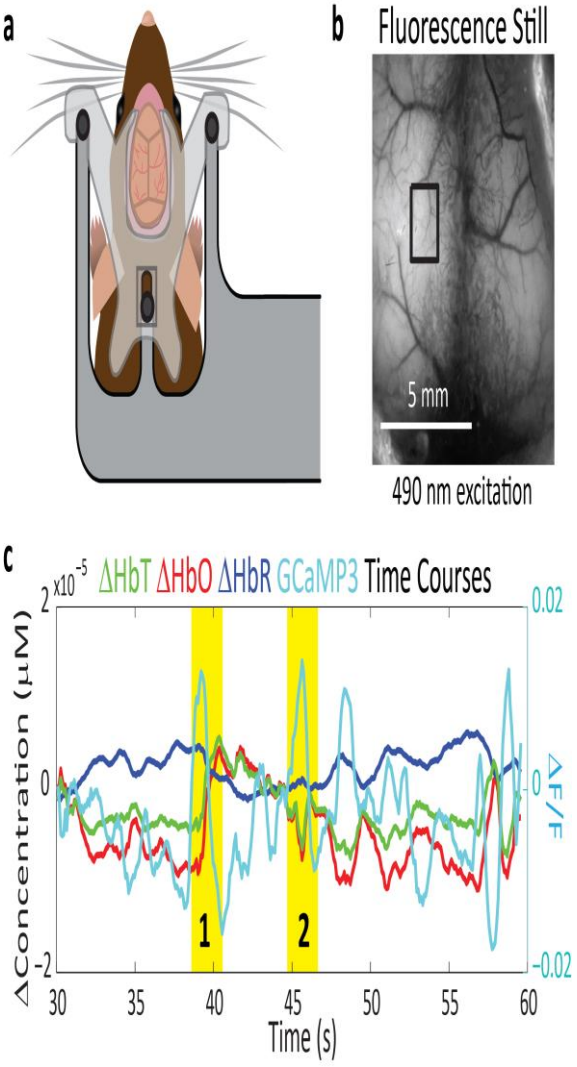

Figure 1. **(a)** Acrylic head plate implant and thinned skull preparation allows for maximized cortical visibility and minimized motion artifact during imaging. **(b)** Single frame MS-OISI image of GCaMP3 fluorescence. **(c)** Timecourses spatially averaged from pixels of cortical region denoted by the black box in (b) contain two epochs of interest highlighted in yellow, the first (epoch 1) an instance of a neuronal event followed by hyperemia, and the second (epoch 2) an instance where a neural event is unaccompanied by a hemodynamic event.

References:

[1] White B.R., et al. PloS one, 2011.
[2] Vanni M.P., Murphy T.H., J. Neurosci, 2014.
[3] Ferezou I, et al., Neuron, 2007.
[4] Chen Q, et al. Neuron, 2012.

723
BRAIN-0494
Poster Session

Neurovascular Coupling

SIMVASTATIN RESCUES IMPAIRED HIPPOCAMPAL NEUROVASCULAR COUPLING BY NORMALIZING VASCULAR REACTIVITY TO NEURONAL AND ASTROCYTIC STIMULATIONS IN APP TRANSGENIC MICE

H. Girouard[1], L. Li[1], E. Hamel[2]
[1]Department of Pharmacology, Université de Montréal, Montreal, Canada
[2]Montreal Neurological Institute, McGill University, Montreal, Canada

Objectives: Simvastatin, a drug used in the treatment of hypercholesterolemia, has been found to rescue both cerebrovascular and memory deficits in a dose- and time-dependent manner in a mouse model of Alzheimer's disease (AD) (APP transgenic mice) (1,2). Simvastatin exerts beneficial effects on the tight coupling between neuronal activity and cerebral blood flow termed neurovascular coupling (NVC) in APP transgenic mice. However, the underlying mechanisms remain unclear. Since simvastatin can preserve both vascular and astrocytic functions in experimental models of AD (1,3), the focus of this study was to determine the effect of simvastatin on the communication between astrocytes and cerebral arteries in APP transgenic mice. Methods: Heterozygous transgenic C57BL/6 mice that overexpress an amyloid precursor protein (APP) carrying the human Swedish

(K670N, M671L; APPSwe) and Indiana (V717F; APPInd) familial AD mutations (APP mice, J20 line) and their wild-type (WT) littermate controls were used. 3-month-old mice were treated or not with simvastatin (40 mg/kg/d, added in drinking water) for 3 months. Astrocyte endfoot Ca^{2+} signaling and vascular diameter were monitored simultaneously in mouse brain slices by fluorescence (fluo4-AM) and infrared-differential interference contrast using two-photon microscopy. Astrocytic Ca^{2+} increases were controlled using two paradigms: electric field stimulation (EFS) and two photon photolysis of caged Ca^{2+} (4). The vascular reactivity was also studied in isolated and pressurized hippocampal arteries. Results: 1) EFS induced arteriole dilation was impaired in APP mice. Simvastatin normalized arteriole response to EFS in these mice. Those effects were not accompanied by changes in astrocyte endfoot Ca^{2+} levels. 2) Even after bypassing neuronal activity with astrocytic endfoot Ca^{2+} uncaging, APP mice arteriole did not dilate normally compared with WT mice. Simvastatin rescued arteriole response to both EFS and Ca^{2+} uncaging in APP mice. 3) The metabotropic glutamate receptor (mGluR) agonist, *t*-ACPD, induced arteriole constriction in both APP and WT mice without changing astrocytic endfoot Ca^{2+}. Surprisingly, simvastatin reversed the contractile response to mGluR-agonist to a vasodilation in both WT and APP mice. Conclusions: Simvastatin prevents the impaired vascular responses to EFS and Ca^{2+} uncaging in the hippocampus of APP transgenic mice and did not modify astrocytic Ca^{2+} levels. Simvastatin reverses the polarity of the vascular response to mGluR activation in both WT and APP mice. These results suggest that simvastatin rescues impaired hippocampal neurovascular coupling in APP mice mostly by imroving vascular functions. References: 1. Tong et al. *J Neurosci*. 2012; 2. Tong et al. *Neurobiol Dis.* 2009; 3. Tramontina et al. *J Neural Transm.* 2011; 4. Girouard et al. *Proc Natl Acad Sci.* 2010.

724
BRAIN-0659
Poster Session

Neurovascular Coupling

SPONTANEOUS OPTICAL NEURAL, HEMODYNAMIC AND METABOLIC SIGNALS TO ACCESS RESTING-STATE FUNCTIONAL CONNECTIVITY IN NORMAL AND DISEASED BRAIN

J. Lu[1], B.I.N. Li[1], Q.I.N. Huang[1], D.O.N.G. Wen[1], S.H.E.N. Gui[1], P. Li[1]
[1]Wuhan National Laboratory for Optoelectronics, Huazhong University of Science and Technology, Wuhan, China

Resting-state functional connectivity (RSFC) of spontaneous hemodynamic fluctuations is widely used to investigate large-scale functional brain networks. However, there is still a lack of the direct comparison between the functional connectivity based on high-resolution neural activity signal and that based on hemodynamic signals to understand the neural mechanisms underlying RSFC. Moreover, it is necessary to investigate whether the RSFC based on hemodynamic signal can reflect the functional brain networks during those conditions that neurovascular uncoupling may occur. Here we investigated the RSRC of cortical networks based on spontaneous optical neural and hemodynamic signals accessed by optical imaging of voltage-sensitive dyes and optical spectral imaging in normal and diseased brain of mice.

725
BRAIN-0628
Poster Session

Neurovascular Coupling

LOCAL UP-REGULATION OF TISSUE PO2 BY CAPILLARY DILATIONS - A SIMULATION STUDY

A. Lücker[1], *B. Weber*[2], *P. Jenny*[1]
[1]*Institute of Fluid Dynamics, ETH Zurich, Zurich, Switzerland*
[2]*Institute of Pharmacology and Toxicology, University of Zurich, Zurich, Switzerland*

Objectives. Neurovascular coupling is essential in healthy brain function and has fundamental implications in medical imaging. Recently, it has been shown that pericytes play an active role in neurovascular coupling at the capillary level [1]. However, the influence of changes in capillary diameter on oxygen transport is still unknown. We aim at quantifying the impact of capillary dilations on tissue oxygenation using a new oxygen transport model.

Methods. The hemodynamics were modeled using a red blood cell (RBC) transport model, which is able to track individual RBCs [2]. The resulting RBC trajectories were used in the oxygen transport model by Lücker et al. [3] with resolved, moving RBCs. The unsteady advection-diffusion-reaction equations for oxygen partial pressure (PO_2) and hemoglobin saturation were solved using a finite-volume method. This new framework enables us to capture the influence of erythrocyte-based flow phenomena on tissue oxygenation with unprecedented detail.

Results. We ran simulations in a simple capillary network (d = 4µm) contained in a rectangular tissue domain (150µm x 80µm x 40µm, Fig. 1A) with an average inflow tube hematocrit of 0.3. The active capillary was dilated by a factor of 1.2 (d = 4.8 µm) and results were compared to the baseline case (Fig. 1B). $CMRO_2$ was set to the same value in both simulations. Oxygen tension was averaged for 3 seconds after a steady state had been reached. At 20µm above the dilated capillary, the time-averaged tissue PO_2 increased by >2.9mmHg compared to baseline. Oxygen tension below the passive capillary stays almost constant. The oxygen extraction fraction decreases by 2.5% due to the higher tissue PO_2. We also discuss transient dilations and the interplay between arteriolar and capillary dilations.

Conclusions. Capillary dilations are an effective potential mechanism for local up-regulation of tissue PO_2. This is due to the higher number of RBCs in the dilated capillaries [2], which increases the oxygen availability in that vessel. Therefore, we hypothesize that dilations induced by pericytes have the ability to partly compensate local $CMRO_2$ increases. Although the simulated tissue PO_2 increase was moderate, it was caused by the dilation of a single capillary segment. Future work will focus on multiple capillary dilations in larger networks and on the conjugate effects of transient capillary and arteriole dilations.

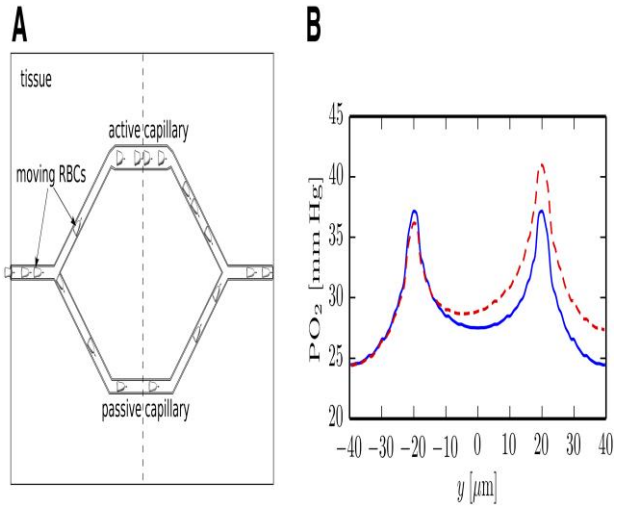

Fig. 1: A: Schematic of the computational domain with dilation of the active capillary. B: Time-averaged PO_2 profiles along the dashed line shown in A. Solid line: baseline case with d = 4µm; dashed line: dilated active capillary with d = 4.8µm.

References.
[1] Hall et al., *Nature*, 508:55-60 (2014)

[2] Schmid et al., *AJP Heart Circ Phys*, in press (2015), DOI:10.1152/ajpheart.00335.2014
[3] Lücker et al., *AJP Heart Circ Phys*, 308:H206-H216 (2015)

726
BRAIN-0503
Poster Session

Neurovascular Coupling

COMPARING STIMULUS-EVOKED AND RESTING-STATE NEUROVASCULAR COUPLING WITH SIMULTANEOUS ELECTROPHYSIOLOGY, WIDE-FIELD NEURONAL GCAMP AND HEMODYNAMIC IMAGING

Y. Ma[1], M. Kozberg[2], S. Kim[1], E. Hillman[1]
[1]Biomedical Engineering, Columbia University, New York City, USA
[2]Department of Neuroscience, Columbia University, New York City, USA

Objectives: Functional magnetic resonance imaging (fMRI) measures local changes in hemodynamics as a surrogate for neuronal activity. Resting state functional connectivity captures spontaneous fluctuations in the fMRI blood oxygen level dependent (BOLD) signal, and infers neuronal network connectivity from regional hemodynamic synchronization [1]. These methods assume that hemodynamics faithfully reflect neuronal activity, and that neurovascular coupling is static and predictable in both stimulus-evoked and resting state conditions.
Here, we test these assumptions by imaging both neural activity and hemodynamics simultaneously in the mouse brain both during somatosensory stimulation and resting state conditions.

Methods: All experiment procedures were approved by the Columbia University Institutional Animal Care and Use Committee.
Wide-field multi-spectral optical intrinsic signal imaging (MS-OISI) was used to image the exposed cortex of mice expressing genetically encoded fluorescence calcium sensor GCaMP under the Thy1 promoter targeting pyramidal neurons located at cortical layers II/III and V [2]. By using this method, we can simultaneously acquire cortical neuronal and hemodynamic activity with high temporal and spatial resolution. Local electrophysiology was simultaneously acquired from the hindpaw region of the somatosensory cortex in urethane anesthetized mice (n=9), with and without hindpaw stimulation.
Because both the excitation and emission light for GCaMP fluorescence are contaminated by the changing hemodynamics, detected fluorescence was corrected by linear regression of its log.
To test whether stimulus-evoked and resting state neurovascular coupling is equivalent, a hemodynamic response function (HRF) based model was developed that predicted stimulus-evoked hemodynamics from GCaMP fluorescence. This model was then used to predict expected resting state hemodynamics from spontaneous GCaMP activity.

Results: After eliminating hemodynamic cross-talk, GCaMP fluorescence was found to agree well with multi-unit activity (MUA) measured by electrophysiology, both with and without stimuli. The hemodynamic response evoked by stimulation was found to consist of two parts: (1) A linear component that can be predicted by length of stimulation or neuronal activity and (2) a constant component which is present at the beginning of the response, whose waveform is independent of stimulus duration.
Our HRF model-based comparison revealed epochs of neurovascular uncoupling during resting-state recordings, whereas other periods were well-predicted. Objectively generating a best-fit HRF function from resting state data revealed that compared to the HRF driven by stimulation, the HRF at resting-state has a significantly smaller amplitude and faster decay, although time to peak was similar between the two.

Conclusions: Wide-field GCaMP recordings can provide accurate representations of MUA after correction for hemoglobin absorption. Stimulus-evoked and resting state neurovascular coupling have similar, but different HRF properties. Additionally, resting state recordings revealed epochs of apparent neurovascular de-coupling.

Understanding factors leading to these mismatches between neural activity and hemodynamics could provide improved methods for analysis of resting state fMRI data, and could provide clues to the basis of altered resting state functional connectivity in pathological states.

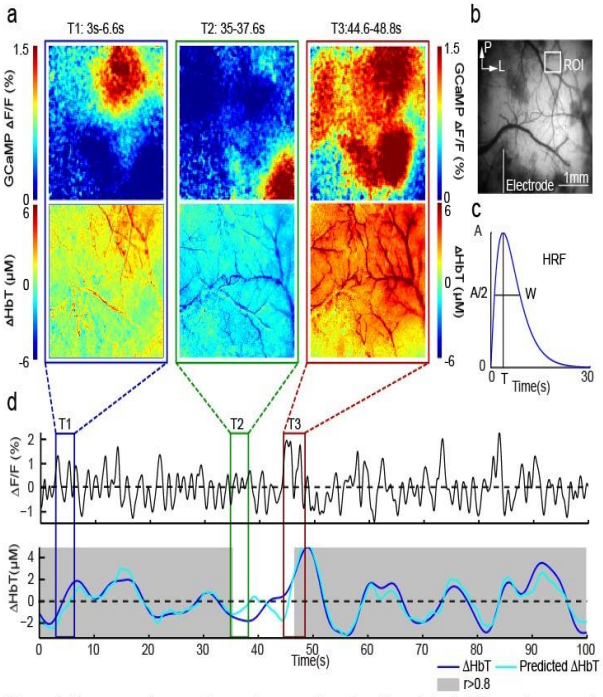

Figure 1. Neurovascular coupling and uncoupling at resting state. (a) Maps of neuronal activity (top) and total hemoglobin (ΔHbT) hemodynamics (bottom) for three neuronal events. The first and the third events are seen to evoke corresponding increases HbT. However, the second event fails to evoke localized hyperemia. (b) Gray scale image showing the exposed cortex of a representative Thy1-GCaMP3 mouse. (c) The HRF used to predict ΔHbT based on GCaMP fluorescence. A is the amplitude, T is the time of the peak and W is the width at half maximum. (d) The time courses of GCaMP fluorescence (top) and ΔHbT (bottom) from the region of interest (ROI) marked in (b). The coupling and uncoupling event in (a) was also marked across the time courses. Gray regions show epochs where the correlation coefficient (r) between measured ΔHbT (blue) and predicted ΔHbT (cyan) is above 0.8.

References

1. Raichle, M.E., *Behind the scenes of functional brain imaging: a historical and physiological perspective.* PNAS, 1998. **95**(3): p. 765-72.
2. Chen, Q., et al., *Imaging neural activity using Thy1-GCaMP transgenic mice.* Neuron, 2012. **76**(2): p. 297-308.

727
BRAIN-0561
Poster Session

Neurovascular Coupling

NEUROVASCULAR COUPLING IN PRETERM NEONATES WITH INTRA-VENTRICULAR HEMORRHAGE: COMBINED HIGH DENSITY EEG-NIRS STUDY

M. Mahmoudzadeh[1], G. Dehaene-Lambertz[2], M. Fournier[1], G. Kongolo[3], S. Goudjil[3], F. Wallois[1]
[1]Neuropediatrics, Centre Hospitalier Universitaire, Amiens, France
[2]brain development, Neurospin, Gif/Yvette, France
[3]NICU, Centre Hospitalier Universitaire, Amiens, France

Can we detect auditory neurovascular impairment during the early phase of infancy? Continuous measurements during sleep were performed in healthy (n=12) and Intra Ventricular Hemorrhage (IVH grade III & IV, n=7) preterm neonates (28-32 weeks GA) using functional Near-Infrared Spectroscopy (fNIRS) in conjunction with EEG. We have shown that the preterm brain is able to discriminate a change of phonemes (ba vs ga) and a change of voices (male vs female) (Mahmoudzadeh, 2013). The dynamic of the responses reveals a structured network evolving differently in time and space (temporal/frontal lobes areas, left/right hemispheres). The study described here aims also to investigate the impact of the IVH on auditory hemodynamic responses. While EEG disclosed active language neural network, fNIRS revealed much weaker auditory hemodynamic responses, showing neurovascular coupling impairment. The present data confirm the existence of neurovascular coupling in healthy premature brain. It also shows that IVH premature neonates have lack of local mechanisms that allocate blood oxygen and to the active neurons. These results demonstrate that particular regions of the cortex, critical for language acquisition and processing, contain innate language specific representations in early infancy. In addition, the approaches we developed provide early diagnosis of auditory neurovascular coupling impairment in IVH

preterms which is known to induce learning disabilities.

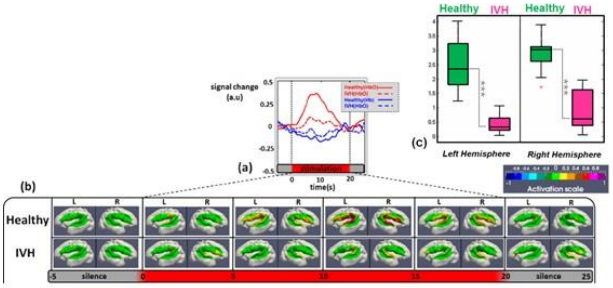

Figure (1): (a) Shows an example of grand-average NIRS channel HBO (red lines), Hb (blue lines) for healthy newborns (solid lines) and IVH (dashed lines) for auditory stimulation. The thick horizontal red bar indicates the period of stimulation (20 seconds). This response is more pronounced for healthy newborns, with a significant increase in the HBO signal. (b) Mapping of activations HBO signal in time. (c) comparison between healthy subjects and IVH, mean changes (AUC) of oxy-hemoglobin induced by auditory stimulation. For each hemisphere, activations in IVH group were significantly lower than those on healthy subjects.

728
BRAIN-0563
Poster Session

Neurovascular Coupling

MULTIMODAL IMAGING OF NEUROVASCULAR COUPLING RELATIONSHIP BETWEEN SPONTANEOUS EEG, CMRO2 AND HEMODYNAMIC RESPONSES IN PRETERM INFANTS

M. Nourhashemi[1], M. Mahmoudzadeh[1], G. Kongolo[2], S. Goudjil[2], F. Wallois[3]
[1]medicine, University of Picardie Jules Verne, Amiens, France
[2]NICU, centre hospitalier Universitaire, Amiens, France
[3]Neuropediatrics, centre hospitalier Universitaire, Amiens, France

Objectives: We previously demonstrated [Roche, 2007] that spontaneous hemodynamic response and electroencephalography (EEG) simultaneously recorded from human preterm infant are coupled with the burst of activity, characteristic of the discontinuity EEG pattern observed at this period of the development. On the other hand, our studies [Mahdmoudzadeh et al., 2013; 2014 submitted] have reported that the preterm brain can exhibit distinct hemodynamic responses to external stimulation under auditory task, which may indicate a neurovascular coupling relationship. One relevant and interesting question would be the neurovascular coupling relationship between spontaneous EEG and CMRO2/hemodynamic responses in

the resting premature brain.

Methods: We used the simultaneous acquisition of electroencephalography (EEG, 8 channels) and functional optical imaging (Near infrared spectroscopy-Diffuse correlation spectroscopy) as only potentially executable- noninvasive multimodal imaging technique for measuring the functional activity of the preterm brain. Continuous measurements during sleep were performed in healthy and Intra Ventricular Hemorrhage (IVH grade II), preterm neonates (28-35 weeks GA). The Global Mean field Power (GMFP) were first calculated from the continuously recorded EEG signals. Then an HRF, which was modeled as a gamma probability density function, was convoluted with the power of EEG (extracted by GMFP); then correlation between convolved EEG power signal and CMRO2 was calculated.

Results: To answer the neurovascular coupling relationship question, we analyzed the correlation between CMRO2 and EEG signal linking spontaneous CBV/CBF and EEG signals measured on preterm infants. The results indicate that an EEG power change is fairly correlated (~0.3) with CMRO2 in healthy preterm while in pathological case it is considerably less correlated (~0.07).

Conclusions: Given that EEG measures the electrical activity of neural populations while NIRS and DCS measures their relative hemodynamics via change in blood oxygenation and in blood flow signal respectively. Simultaneous EEG/NIRS/DCS offers multi-modality imaging to investigate the

neurovascular relationship. There is still substantial debate regarding the relationship between local neuronal activity and hemodynamic changes (Logothetis and Wandell, 2004; Sirotin and Das, 2009). That is, our results shed light on a more comprehensive understanding of the specific mechanisms underlying neurovascular coupling. Perhaps the most compelling reason for EEG/NIRS/DCS is that temporally specific variations in the EEG fluctuations can be captured and correlated with the functional optical hemodynamic signal. Many aspects of neurovascular coupling and brain maturation are essentially characterized by EEG signals fluctuations, however there is a potential that many of the associated neural-vascular correlates can be measured via multimodal neurovascular imaging noninvasively (scalp EEG/NIRS/DCS).

729
BRAIN-0524
Poster Session

Neurovascular Coupling

FUNCTIONAL ULTRASOUND IMAGING OF INTRINSIC CONNECTIVITY IN THE LIVING RAT BRAIN WITH HIGH SPATIOTEMPORAL RESOLUTION

B. osmanski[1], S. Pezet[2], A. Ricobaraza[2], Z. Lenkei[2], M. Tanter[1]
[1]Wave Physics for Medicine, Institute Langevin ESPCI CNRS UMR7587 INSERM U979, PARIS, France
[2]Brain Plasticity Unit, ESPCI-ParisTech UMR8249, PARIS, France

Objectives

The brain dynamically integrates and coordinates responses to internal and external stimuli across multiple spatiotemporal scales through large-scale functional networks. Assessment of its functional connectivity (FC), through the measurement of regionally correlated, spontaneous, low frequency (0.01–0.1 Hz) fluctuations in blood oxygen level dependent (BOLD) signals with functional magnetic resonance imaging (fMRI), particularly during resting-state/task-free periods (resting-state fMRI), has greatly advanced our understanding of the functional organization of the human brain[1]. Here we propose a novel, highly resolved connectivity mapping approach using ultrafast functional ultrasound (fUS)[2]. This technique enables imaging of cerebral microvascular haemodynamics deep in the anaesthetized rodent brain, through a large thinned-skull cranial window, with pixel dimensions of 100µm x 100µm in-plane and a millisecond time resolution allowing unambiguous cancellation of low-frequency cardio-respiratory noise. Both seed-based and singular value decomposition analysis of spatial coherences in the low-frequency (<0.1 Hz) spontaneous fUS signal fluctuations reproducibly report, at different coronal planes, overlapping high-contrast, intrinsic functional connectivity patterns[3].

Methods

The experiment was carried out using a 15MHz ultrasound probe on 20 anesthetized rats (metomidine/ketamine) with a thinned skull. The concept of functional ultrasound relies on ultrafast Doppler based on acoustic plane-wave transmission. The brain was insonified with a succession of ultrasound plane waves at 500Hz. Their backscattered echoes were recorded and beamformed to produce an echographic image every 2ms. Ten-minute duration acquisitions were performed at three anterior/posterior coordinates: Bregma +0.84, -0.6 and -2.16 mm.

Results

Functionally correlated contralateral cortical areas activated by electrical stimulation of the right or left sciatic nerve were identified using fUS (see figure 1a) then the spontaneous fUS signal of this coronal slice was measured without stimulation. We found that these functionally similar regions were highly correlated at rest (correlation coefficient>0.8) (figure 1b).

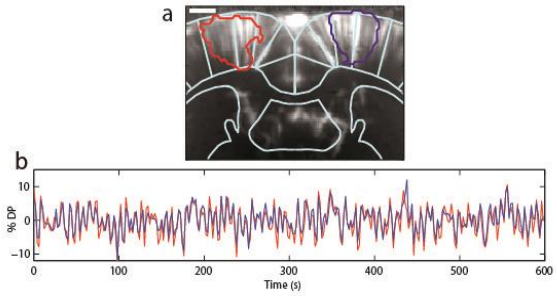

Figure 1 : a) Functionally correlated contralateral cortical areas activated by electrical stimulation of the right (red curve) and left sciatic nerve (blue curve) superimposed on the vascularization map. b) Spontaneous variations in the power Doppler signal (%PD) in the seed regions marked by the evoked response of the right (blue curve) and left (red curve) S1HL show high temporal correlations. Scale bar, 1 mm

In addition, different regions of interest can be defined using the spatial referential frame of the Paxinos (figure 2a) and a functional connectivity (FC) matrix can be computed (figure 2b). This FC matrix was found highly reproducible (r=0.85+/-0.03, p<0.001, N=6), all the coefficient >0.2 were reproducible (p<0.05).This matrix showed strong bilateral correlations in cortical brain areas. By contrast, cerebral structures such as the CPu and septum showed no correlation with the 'sensory-motor resting-state network' as found by Schwarz *et al*[3].

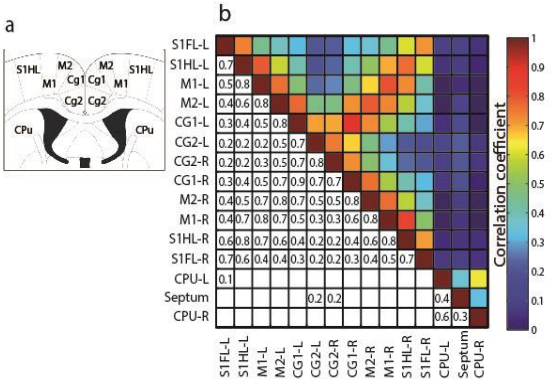

Figure 2 : a) Anatomical organization of the rat brain at Bregma = -0.6. b) FC matrix at Bregma = -0.6mm. It indicates a high correlation observed principally between the contralateral cortical areas and somatosensory and motor areas.

We also used singular value decomposition based data treatment to retrieve anticorrelated FC patterns revealing distinct functional networks (figure 3).

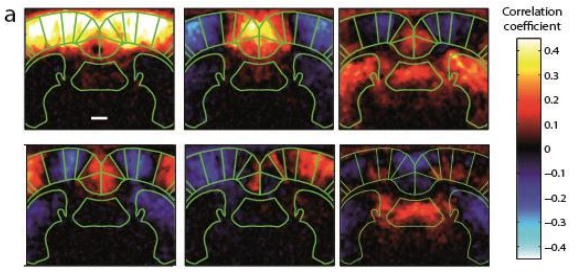

Figure 3 : Anticorrelated fUS connectivity patterns revealed by 6 different spatial modes using singular value decomposition. Scale bar, 1 mm

The same type of results can be extracted from the anterior/posterior coordinate (bregma=+0.84, -2.16mm).

Conclusions

fUS imaging was able to detect FC patterns of distinct neuro-anatomical systems with 100µm spatial resolution. These patterns are similar to major functional networks described in humans by resting-state fMRI, such as the lateral task-dependent network putatively anticorrelated with the midline default-mode net-work. These results introduce fUS as a powerful novel neuroimaging method, which could be extended to portable systems for three-dimensional functional connectivity imaging in awake and freely moving rodents.

References

1 Hutchison. *Neuroimage* 80,360–378 (2013)

2 Mace. *Nat. Methods* 8, 662–664 (2011).

3 Osmanski. *Nat. Commun*.5:5023 (2014)

4 Schwarz.. *Brain Connect*. 3,503–511 (2013).

730
BRAIN-0284
Poster Session

Neurovascular Coupling

THE EFFECT OF GLUCOSE SUPPLY ON NEUROVASCULAR COUPLING IN ANESTHETIZED RATS

S. Pinkernell[1], M. Beier[2], U. Lindauer[1]
[1]Department of Neurosurgery Universitätskliniku m Aachen RWTH University, Translational Neurosurgery and Neurobiology, Aachen, Germany
[2]Department of Neurosurgery Technical University Munich, Experimental Neurosurgery, Munich, Germany

Objectives:
Physiological stimulation leads to increased neuronal activity in the brain, accompanied by increases in local cerebral blood flow (CBF) to ensure supply of oxygen and glucose. In resting state the vast majority of ATP is metabolized via oxidative phosphorylation, but during activation the ratio changes towards a larger contribution of non-oxidative aerobic glycolysis (Fox et al., 1988). We tested the hypothesis whether the level of glucose supply changes the balance between oxidative and non-oxidative metabolism during activation. It may be suggested that during reduced glucose supply, a change in favor of oxidative phosphorylation, which uses glucose more effectively than aerobic glycolysis, occurs.
Methods:
Electrical forepaw stimulation (1.8 mA, 3 Hz, 16s) was used in ALPHA-chloralose-urethane anesthetized male Wistar rats to induce changes in neuronal activity in the brain. Changes in CBF and regional blood oxygenation (CBO) were recorded by a combined microfiber optical hemoglobin spectroscopy and laser-Doppler flowmetry probe under different glucose levels over a time period of 3h. Cerebral metabolic rate of oxygen ($CMRO_2$) was calculated (Leithner et al., 2010) and somatosensory evoked potentials (SEPs) were recorded. CBF and $CMRO_2$ at rest as well as SEPs, averaged CBF and CBO responses during stimulation and the time required to return to resting values after end of stimulation under highest (>22.2mmol) resp. lowest glucose levels (<0.8mmol) were expressed as % changes from prior values under euglycemia (= baseline values, normalized to 100%, data expressed as mean +/- SD) and compared to baseline values by paired Students t-test.
To exclude time related effects, a time-control group under euglycemia was tested (n=6), which showed a slight decrease in resting CBF and an attenuation of SEP amplitudes after 3h by 32+/- 12%.
Results:
During hyperglycemia (n=10), resting CBF and $CMRO_2$ remain unaltered, whereas CBF (154 +/- 60%, p=0.02) and $CMRO_2$ responses (132 +/- 47%, p=0.06) were increased during unchanged SEPs. Under hypoglycemia (n=8) resting CBF (120%, +/- 22) was increased. Similar to control group, during stimulation CBF and $CMRO_2$ responses remained unaltered, whereas SEPs were slightly attenuated. After end of stimulation the time to return to resting values for CBF was significantly prolonged (134%, +/- 38), whereas time to return for $CMRO_2$ remained unchanged (119+/- 27%, p=0.09).
Conclusions:
During hyperglycemia the absence of SEP attenuation shown in time control might be responsible for the hyperglycemia induced increase in $CMRO_2$ and CBF. Under severe hypoglycemia our results give no evidence of increased oxidative phosphorylation during neuronal activation. However, we found a prolonged increase of blood flow after the end of stimulation, which may suggest that during low glucose supply more time is required to get adequate amount of glucose from the blood to meet activation induced demand.

References:
Fox, P.T., Raichle, M.E., Mintun, M.A., Dence, C., 1988. Nonoxidative glucose consumption during focal physiologic neural activity. Science. 241, 462-4.

Leithner, C., Royl, G., Offenhauser, N., Fuchtemeier, M., Kohl-Bareis, M., Villringer, A., Dirnagl, U., Lindauer, U., 2010. Pharmacological

uncoupling of activation induced increases in CBF and CMRO2. J Cereb Blood Flow Metab. 30, 311-22.

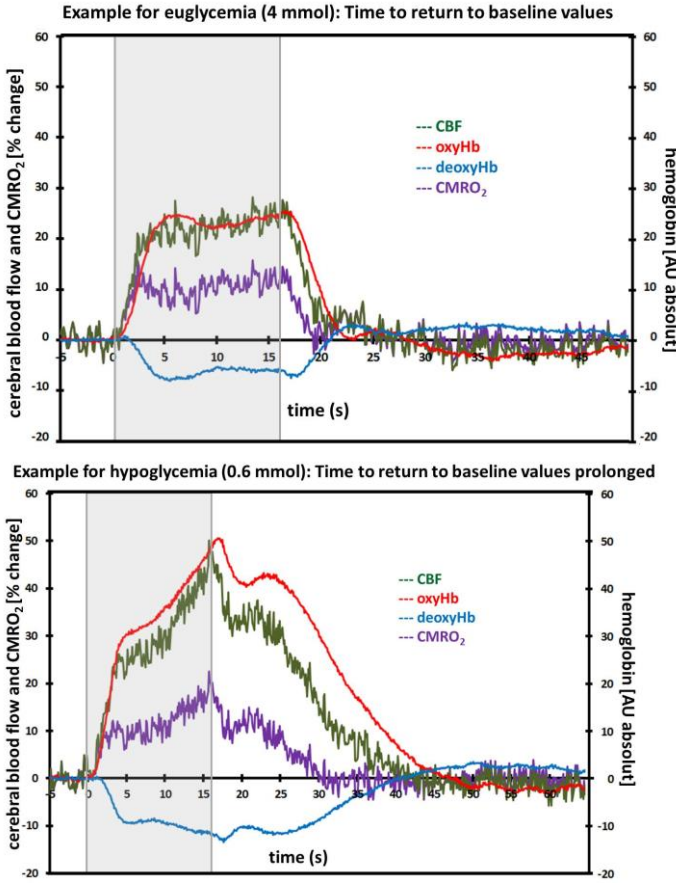

731
BRAIN-0595
Poster Session

Neurovascular Coupling

TONIC BLOOD FLOW CONTROL BY ASTROCYTES

D. Rosenegger[1], *C.H. Tran*[1], *G.R. Gordon*[1]
[1]*Physiology and Pharmacology, Hotchkiss Brain Institute, Calgary, Canada*

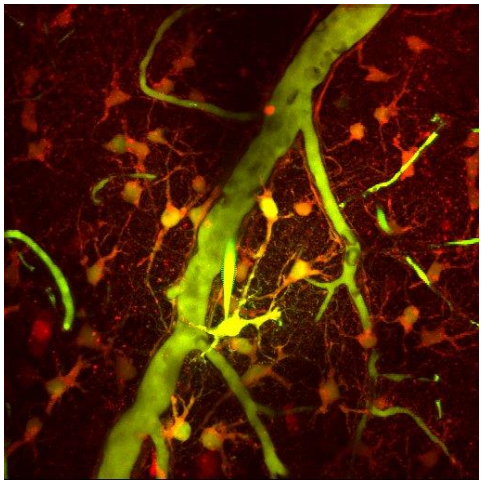

Objectives: Local brain blood flow control requires intricate communication by neurons and astrocytes to vascular contractile cells that make fine adjustments to arteriole diameter to control blood perfusion. Neurovascular coupling accounts for phasic, activity-dependent blood flow control but it remains unclear whether local brain cells can control blood flow tonically to provide steady-state arteriole diameter regulation. We propose a novel role of astrocytes in helping to set the basal arteriole diameter of cerebral vessels, thereby helping to set the perfusion rate to meet the ongoing metabolic demands of the brain.

Methods: Two-photon imaging and patch clamp electrophysiology was performed in acute slices of rat sensory-motor cortex. Animals were IV injected with an FITC dextran to label the vasculature, and brain slices were incubated in the Ca2+ indicator Rhod-2/AM for imaging. In-vivo experiments were performed on mice

expressing the genetic Ca2+ indicator GCaMP3 in astrocytes using the GLAST promoter.

Results: Using intracellular delivery of the Ca2+ chelator BAPTA into astrocytes, we observed a vasoconstriction upon the arrival of BAPTA to the endfeet. This result suggests that astrocytes are providing tonic vasodilation which is determined by the astrocyte resting Ca2+ concentration. Further experiments indicate that astrocytes are tonically releasing prostaglandins, mediated by the constitutive action of COX-1. Application of the COX-1 specific inhibitor SC560 will itself cause vasoconstriction and will also occlude the astrocyte BAPTA induced constriction, suggesting the two are part of the same pathway.

Conclusions: We propose that astrocytes help regulate the steady-state diameter of cerebral arterioles, thus ensuring that the supply of blood to the brain is sufficient to meet its ongoing metabolic demands.

732
BRAIN-0809
Poster Session

Neurovascular Coupling

THE INFLUENCE OF ENDOTHELIAL DYSFUNCTION ON NEUROVASCULAR COUPLING

M. Shaik[1], S. Kim[1], H. Zhao[1], E. Hillman[1]
[1]Biomedical Engineering, Columbia University, New York City, USA

Objectives:

Several cell-types have been implicated in mediating the hyperemic response to neuronal activity, including neurons[1], astrocytes[2] and pericytes[3]. Recent studies have added endothelial cells to this list by demonstrating the presence of conducted vasodilation along arterioles in brain[4] during functional hyperemia. Light-induced reactive-oxygen species (ROS) mediated transection of the vascular endothelium was shown to interrupt conducted vasodilation in the brain[4], altering both the amplitude and timing of the hemodynamic response to stimulus. These results demonstrate that normal neurovascular coupling is reliant on endothelial mechanisms of vasodilation.

In addition to extrinsic ROS damage, disease states that cause intrinsic ROS up-regulation are known to cause impaired endothelial vasoactivity. These conditions include systemic cardiovascular diseases like diabetes and hypertension, but also neurodegenerative diseases including Alzheimer's[5], all of which are associated with long-term cognitive decline. In addition to other mechanisms for neuronal damage, we hypothesize that these conditions would cause alterations in dynamic coupling between neural activity and functional hemodynamics, which may have a direct effect on neuronal health. Here, we explore the effect of pharmacological modulation of endothelial function on neurovascular coupling.

Methods:

Sprague-Dawley rats were anesthetized with 3% isoflurane, ventilated via tracheostomy and the right femoral artery and vein were cannulated for blood pressure monitoring and drug delivery respectively. A craniotomy was performed over the right somatosensory cortex and the dura was reflected. The pial surface was resealed with ACSF in agar under a glass coverslip. Anesthesia was switched to IV alpha-chloralose for stimulus-evoked imaging using multispectral optical intrinsic signal imaging (MS-OISI[6]). Square-wave hindpaw electrical stimuli at 3 Hz and 0.3 ms pulse-width of varying durations were used. Data was converted to show changes in total hemoglobin concentration (Δ[HbT]), averaged from 1 hour before and after intravenous bolus injection of either Ketorolac, a non-blood brain barrier (BBB)-permeable non-selective COX inhibitor, and Enalaprilat, a non-BBB permeable ACE inhibitor.

Results and Conclusions:

Both Ketorolac and Enalaprilat potentiated hemodynamic response at the central region of activation (Figure 1). Towards the periphery of the responding region, Enalaprilat had a large effect on the Δ[HbT] response, while Ketorolac had little effect. The spatial differences between the effects of these drugs can be explained by their properties. Ketorolac inhibits slowly conducted endothelial vasodilation, which stays

restricted to the region of neuronal activation. Enalaprilat has a large effect on the mean arterial pressure, and changes basal tone of the pial arteries, which may potentiate the hemodynamic response in a spatially uniform manner. Further experiments targeted at slow and fast components of conducted vasodilation are in progress. The current data suggests that selective modulation of endothelial function has significant effects on the hyperemic response to stimulus implying that endothelial disease models could similarly affect neurovascular coupling and brain health.

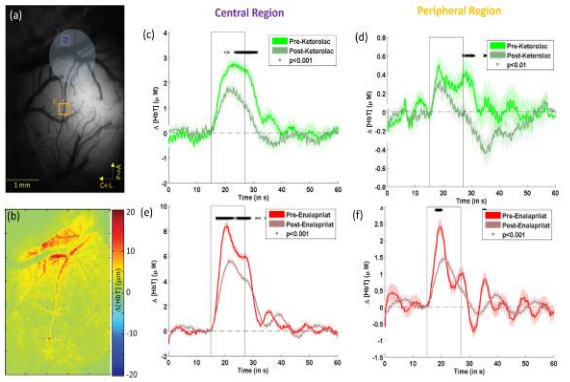

Figure 1. (a) Exposed cortex showing hindlimb region in blue with central and peripheral regions indicated in purple and orange. (d) Averaged Δ[HbT] (total hemoglobin) showing hyperemia on the cortical surface. (c), (d) Time-courses for hemodynamic changes pre- and post-ketorolac in central and peripheral regions respectively. (e), (f) Time-courses pre- and post-enalaprilat in central and peripheral regions.

References:

1. Lecrux C, et. al., JNeurosci. 2011;31(27), 9836-9847.
2. Lind BL, et. al., PNAS. 2013;110(48), E4678-4687.
3. Hall CN, et. al., Nature. 2014;508(7494), 55-60.
4. Chen BR, et. al., JAMA. 2014;3(3), e000787.
5. Zhang L, et. al., BJP. 2013;170(3), 661-670.
6. Bouchard MB et. al., Optics Express;17(18), 15670-15678.

733
BRAIN-0730
Poster Session

Neurovascular Coupling

NEUROVASCULAR COUPLING DURING CEREBROVASCULAR REACTIVITY IN SMALL ARTERY STROKE BY NITRIC OXIDE, HYDROGEN PEROXIDE AND HEART RATE VARIABILITY

K. Suwanprasert[1], *K. Intharakham*[2]
[1]*physiology, Faculty of Medicine Thammasat University, Pathumthani, Thailand*
[2]*Medical Engineering Program, Faculty of Engineering Thammasat University, Pathumthani, Thailand*

Objectives: It has beenreported recently that nitric oxide (NO) and hydrogen peroxide (H_2O_2)play a vital role as neurovascular coupling in normal subjects duringcerebrovascular reactivity (CVR). Both of them are also free radicals andoxidant if they are accumulated reaching pathological level. H_2O_2 acts as vasodilator and vasoconstrictorin mesenteric artery. Moreover, NO is also neurotransmitter and released fromautonomic synapse. In small artery stroke, vascular inflammation due toendothelial dysfunction is pathogenesis. In this study, we examine the role ofNO, H_2O_2 and autonomic regulation related to cerebralblood flow in term of neurovascular coupling during cerebral vasodilationactivated by CVR.

Methods: fifteen small arterystroke patients (7 men, 8 women, age 65.6±13.61) were recruited afterthey gave informed consent according to local ethiccommittee (MTU-EC-PH-6-076/55). 30 second breath holding induced-hypercapniaexperiment was carried out for cerebrovascular reactivity (CVR) and performedas basal, experiment and recovery phases. Mean cerebral blood flow velocity (mCBFV) bytranscranial Doppler and short term-one minute heart rate variability (HRV)analysis by lead II ECG recording were monitored. Plasma NO and H_2O_2were measured by electrochemistry technique. Sympatho-vagal balance andpotential modulation of autonomic control were examined as LF/HF ratio offrequency domain, SD2/SD1 and Sample Entropy (SampEn) of nonlinear model.

Results: Values of meanarterial pressure between basal and experiment phases are closely. mCBFV and LF/HFratio were increased significantly during breath holding when compared to basalphase ($p< 0.05$). There are significant increase in SD2/SD1 and decreasing SampEn during experiment phase. H_2O_2levels were lower significantly in experiment and recovery phases compared

withbasal phase but no significant difference of NO was evident. Graphical plotof NO and H_2O_2 with mCBFV changes is showed (figure). NO andH_2O_2 meet the samepoint at 35 cm/s of mCBFV in small artery stroke.

*Conclusions:*DuringCVR test, vasodilation is mediated by NO and H_2O_2 from neurovascular unit and autonomic synapse.Parasympathetic drive by increasing LF/HF ratio and SD2/SD1 associated with decreasing SampEnis dominated. Cerebral reserve functionis limited in small artery stroke.

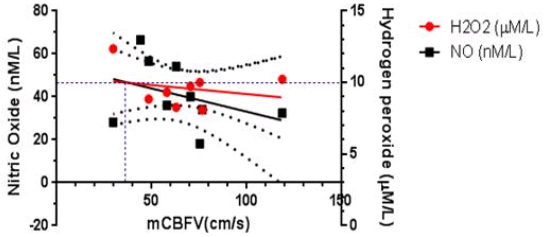

References:

1. Intharakham K, Suwanprasert, K. Neurovascular Coupling assessed by Heart Rate Variability (HRV), Circulating Nitric Oxide and Hydrogen Peroxide during Cerebrovascular Reactivity. In: IBRO-APRC Associated School of Neuroscience 2013 and Proceeding of 17 Thai Neuroscience Society Conference; 2013 July 29 - August 3; Bangkok, Thailand, 2013: 66.
2. P. A. Lucchesi*, et al.*, "Hydrogen peroxide acts as both vasodilator and vasoconstrictor in the control of perfused mouse mesenteric resistance arteries," *J Hypertens,* vol. 23, pp. 571-9, Mar 2005.
3. Lavi S, Egbarya R, Lavi R, Jacob G. Role of nitric oxide in the regulation of cerebral blood flow in humans: chemoregulation versus mechanoregulation. Circulation 2003;107:1901-1905.

734
BRAIN-0299
Poster Session

Neurovascular Coupling

DIAMETER CHANGES TO CEREBRAL BLOOD VESSELS DURING NEURAL ACTIVATION AND DEACTIVATION MEASURED BY TWO-PHOTON MICROSCOPY IN AWAKE MICE

H. Takuwa[1], Y. Tajima[1], H. Kawaguchi[1], Y. Ikoma[1], C. Seki[1], K. Masamoto[1], I. Kanno[1], H. Ito[2]
[1]Molecular Imaging Center, National Institute of Radiological Sciences, Chiba, Japan
[2]Advanced Clinical Research Center, Fukushima Medical University, Fukushima, Japan

Objectives: Neural activation monitored with positron emission tomography (PET) has been reported to a cause larger increase in cerebral blood flow (CBF) than cerebral blood volume (CBV) in humans [1]. It has also been reported that neural activation evokes larger increases in red blood cell (RBC) velocity than RBC concentration in mice when measured with Laser-Doppler flowmetry (LDF) [2]. Crossed cerebellar diaschisis (CCD) caused by contralateral supratentorial lesions can be considered to be a model of neural deactivation, and hemodynamic changes in CCD measured with PET in humans have been reported to show similar percentage decreases in CBF and CBV [3]. Recently, we developed a mouse model of CCD induced by middle cerebral artery occlusion (MCAO) that also showed similar percentage decreases in CBF and RBC concentration [4]. On the other hand, changes to the diameter of microvessels during neural activation and deactivation are still unclear. Using two-photon microscopy, we investigate microvessels diameter changes in these mouse models of neural activation and deactivation.

Methods: Two-photon microscopic imaging was performed on mouse models of neural activation and deactivation (C57BL/6Jmice, 7-9weeks, N=5). Neural activation was induced by air-puff stimulation and a permanent occlusion of the

MCAO was used to mimic deactivation. Microvessels were fluorescently labeled with sulforhodamine 101 and changes to the diameter of arterioles, capillaries and venula were measured in cerebral cortex (activation) and cerebellar cortex (deactivation). Baseline diameters of arterioles, capillaries and venula in cerebral cortex were 17 ± 20µm, 6 ± 7µm and 17 ± 17µm, respectively (mean ± SD). Baseline diameters of the same vessels in cerebellar cortex were 16 ± 12µm, 6 ± 6µm and 14 ± 13µm, respectively. The two-photon imaging was performed on awake animals immobilized using a hand-made fixation apparatus [5].

Results : Using two-photon imaging of mouse brain in the awake state, vasodilation and vasoconstriction were observed during neural activation and deactivation, respectively. Percentage changes in diameter during whisker stimulation were +19 ± 3%, +8 ± 4%, and +3 ± 1% for arterioles, capillaries and venula, respectively. Percentage changes in diameter during CCD were -23 ± 3%, -11 ± 3%, and -2 ± 7% for arterioles, capillaries and venula, respectively.

Conclusions: In the case of microvessels, the degree of vasoconstriction under neural deactivation was similar to the degree of vasodilation under neural activation. These results only partially agree with our previous results obtained PET and LDF [1], [2], [3], [4]. PET and LDF measure hemodynamic changes in a broad brain region that includes large arteis and veins which deffers from situation measured with two-photon imaging in this study. Therefore, changes in microvessels may different from changes in large vessels during the neural activation and deactivation.

References

[1] Ito H, et al. J Cereb Blood Flow Metab 2005; 25: 371-377.
[2] Takuwa H, et al. Brain Res. 2012; 1472: 107-112
[3] Ito H, et al. Ann Nucl Med 2002; 16: 249-254.
[4] Takuwa H, et al. Brain Res. 2013; 1537: 350-355
[5] Takuwa H, et al. Brain Res. 2011; 1369: 103-111

735
BRAIN-0340
Poster Session

Neurovascular Coupling

EXPERIMENTAL NEUROVASCULAR UNCOUPLING PROMOTES COGNITIVE IMPAIRMENT IN MICE: IMPLICATIONS FOR BRAIN AND CEREBROMICROVASCULAR AGING

S. Tarantini[1], T. Zsuzsanna[1], M. Valcarcel-Ares[1], S. Nataliya[2], E. Farkas[3], E. Hodges[1], R. Towner[2], F. Deak[1], W. Sonntag[1], A. Csiszar[1], P. Toth[1], Z. Ungvari[1]
[1]Reynolds Oklahoma Center on Aging, University of Oklahoma Health Sciences Center, Oklahoma City, USA
[2]Advanced Medical Resonance Center, Oklahoma Medical Research Foundation, Oklahoma City, USA
[3]Department of Medical Physics and Informatics, University of Szeged, Szeged, Hungary

Objectives
Increasing evidence shows that vascular risk factors such as aging, hypertension, diabetes mellitus, and obesity promote cognitive impairment, however, the underlying mechanisms are not well understood. Cerebral blood flow (CBF) is adjusted to neuronal activity via neurovascular coupling (NVC) and this mechanism is known to be impaired in the aforementioned pathophysiological conditions. To establish a direct, causal relationship between impaired NVC and cognitive decline, we induced neurovascular uncoupling pharmacologically in mice by inhibiting the synthesis of vasodilator mediators involved in NVC.
Methods
Male C57BL/6J mice (n=20 in each group) were assigned into two groups: 1) the pharmacological treatment was carried on for 7 days and included the administration of MS-PPOH (20 mg/kg/day, s.c.), a specific inhibitor of EET-producing epoxidases. Indomethacin (7.5 mg/kg/day, p.o.) and L-NAME (100 mg/kg/day, p.o.) were

administered in drinking water to inhibit cyclooxygenase-derived vasodilator metabolites and NO synthase activity respectively; 2) vehicle control. A battery of behavioral test was performed to characterize the effect of pharmacologically-induced neurovascular uncoupling on learning and memory, sensory-motor function, gait and locomotion. NVC was assessed by measuring changes in CBF (laser Doppler flowmetry), extracellular glucose (amperometry) and evoked filed potentials in the whisker barrel in response to contralateral whisker stimulation. Arterial spin labeling magnetic resonance imaging was used to measure changes in basal CBF. To determine whether pharmacological treatments result in primary neuronal dysfunction, extracellular recordings were performed from acute hippocampal slices to assess synaptic function and long-term potentiation (LTP).
Results
Mice treated with MS-PPOH+L-NAME+Indomethacin exhibited a ~75% decline in functional hyperemia in response to neuronal activation and impaired performance on the Y maze, the elevated plus maze and the novel object recognition tests, indicating impaired spatial working memory and novelty-seeking behavior. Neurovascular uncoupling in mice was associated with impaired motor coordination (rotarod) and static force production (grip strength), whereas olfactory ability and gustatory motivation (buried food retrieval) and gait function (CatWalk) were unaffected. The pharmacological treatments did not alter basal CBF, evoked field potentials and LTPs.
Conclusions
Selective experimental disruption of NVC per se leads to impairment of cortical function, including cognitive decline, recapitulating some of the neurological symptoms and signs observed in brain aging and pathophysiological conditions associated with accelerated cerebromicrovascular aging.

736
BRAIN-0244
Poster Session

Neurovascular Coupling

CORTICAL ARTERIOLES MODULATE ASTROCYTES CA2+ DYNAMICS

C. Tran[1], *G. Gordon*[1]
[1]*Physiology and Pharmacology, Hotchkiss Brain Institute, Calgary, Canada*

Objective

Recent *in vivo* evidence conducted in anesthetized or slightly sedated animals questions the direct role of astrocyte intracellular Ca^{2+} in mediating functional hyperemia as spatial and temporal profile of astrocyte Ca^{2+} transients are poorly associated with the onset of functional hyperemia (*1*). Our objective was to uncover the spatiotemporal basis of the communication between astrocytes and the vasculature in fully awake, behaving mice.

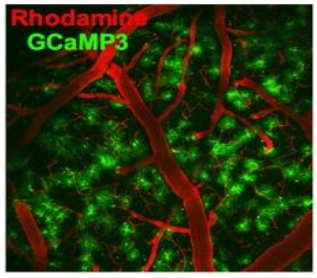

Methods

A craniotomy over the barrel cortex with the dura removed was performed. A custom build two-photon microscopy was used to image the vasculature and astrocytes Ca^{2+} from either C56Bl/6 mice or GLAST-cre-LSL-GCaMP3 mice or TEK-cre-LSL-ArchT3 mice. A cannula was inserted into the tail artery for dye and drug injections.

Results

We found that 5-second whiskers' stimulation induced fast vasodilatory responses in penetrating arterioles while generated a delayed onset of endfoot and cell-wide Ca^{2+} transients.

Interestingly, the onset of these Ca^{2+} transients was typically observed at the peak of the sensory induced vasodilation and toward the end of the vibrissae stimulation. Thus, we tested if the vasculature was communicating back to the astrocytes and consequently modulating astrocytes Ca^{2+}. We showed that intraluminal perfusion of acetylcholine, but not the mGluR5 agonist DHPG, caused vasodilation that was followed by an increase in astrocytes Ca^{2+} fluctuations. Activation of endothelial expressed archaerhodopsins with brief yellow laser induced fast vasodilation followed by an initiation of endfoot Ca^{2+} transient.

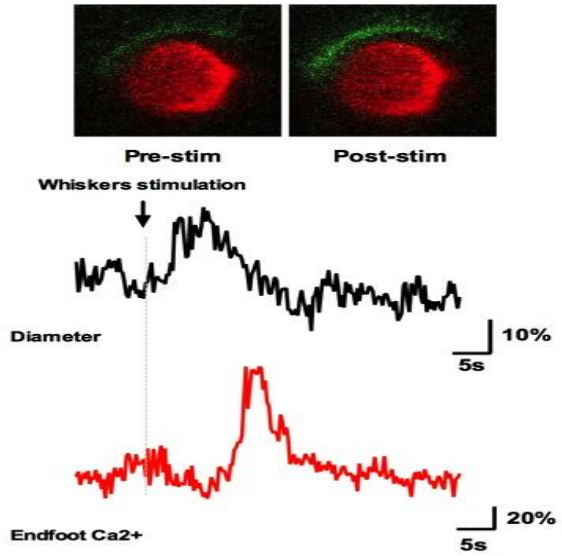

Conclusions

Our data redefine the uni-directional communication between astrocytes and the vasculature. We introduce a potential role of the vasculature as the modulator of astrocytes Ca^{2+} transients and propose that astrocytes act as responders to changes in blood flow.

Reference

1. K. Nizar *et al.*, *J. Neurosci.* **33**, 8411–8422 (2013).

737
BRAIN-0427
Poster Session

Neurovascular Coupling

DOPAMINE AND ALPHA2-ADRENOCEPTORS INTERACT TO MODULATE THE VASCULAR RESPONSE IN THE DORSAL HIPPOCAMPUS AFTER MESOLIMBIC DOPAMINE ACTIVITY

A. Weitemier[1], *T.J. McHugh*[1]
[1]*Laboratory for Circuit and Behavioral Physiology, RIKEN BSI, Wako-shi, Japan*

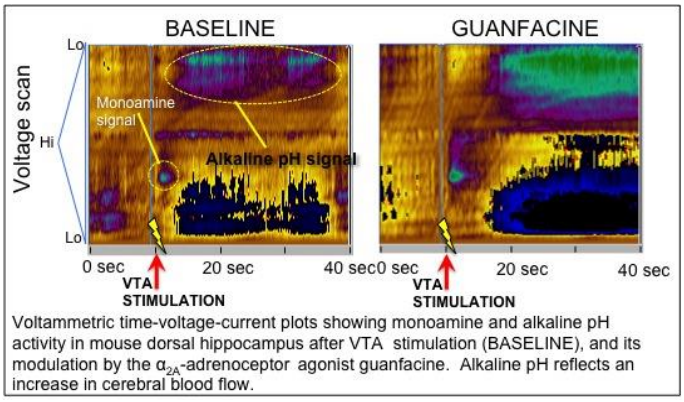

Voltammetric time-voltage-current plots showing monoamine and alkaline pH activity in mouse dorsal hippocampus after VTA stimulation (BASELINE), and its modulation by the α_{2A}-adrenoceptor agonist guanfacine. Alkaline pH reflects an increase in cerebral blood flow.

Objectives: Fast-scan cyclic voltammetry (FSCV) can detect rapid changes in brain monoamine concentrations and pH. Although dopamine can modulate hippocampal neuronal circuit function[1], endogenous dopamine input to the dorsal hippocampus is not well characterized. Transient alkaline pH shifts often observed during FSCV in vivo reflect increases in cerebral blood flow via CO_2 clearance[2]. The objective of the present experiments was to pharmacologically characterize the monoamine input and accompanying neurochemical events (i.e. pH shift) in the dorsal hippocampus upon activity in the dopaminergic ventral tegmental area (VTA).

Methods: Nontreated mice, or mice pretreated with the norepinephrine-depleting agent N-(2-chloroethyl)-N-ethyl-2-bromobenzylamine (DSP-4) were anesthetized for stereotactic recording, and voltammetric monoamine signals were elicited in the dorsal hippocampus upon electrical stimulation of the VTA (0.1 mA, 60 Hz, 50 pulses, 4 ms/pulse). For pharmacological

characterization, we administered (i.p.) compounds selective for the different α_2-adrenoceptor subtypes thought to be differentially expressed between the VTA and the other midbrain nuclei[3] (guanfacine, α_{2A} agonist, 5 mg/kg; clonidine, non-selective α_2 agonist, 1 mg/kg; idazoxan, non-selective α_2 antagonist, 0.3 mg/kg). In subsequent experiments, the non-selective dopamine receptor antagonist cis-flupenthixol (0.5 mg/kg) was administered before or after guanfacine to test for the interaction of the adrenoceptor and dopamine systems. All experimental protocols were approved by the RIKEN Institutional Animal Care and Use Committee.

Results: VTA stimulation elicited small monoamine signals but robust alkaline pH signals in the dorsal hippocampus. DSP-4 did not abolish the monoamine signal, but reduced the pH signal. In all mice, the monoamine signal was only slightly modified by α_2 agonists, albeit in the predicted direction according to regional α_2 subtype expression. In contrast, the alkaline pH signal was reliably and significantly increased by guanfacine, including in DSP-4 treated animals, but was paradoxically reduced below pre-drug levels upon subsequent administration of clonidine. Idazoxan reliably increased the monoamine signal, and returned the pH signal to near-predrug levels in non-treated mice. Idazoxan had no effect in DSP-4 treated mice. In all mice, dopamine antagonism by cis-flupenthixol prevented or reduced the enhancement of the pH signal by guanfacine.

Conclusions: Our experiments suggest that while functional dopamine input to the dorsal hippocampus may be small, a unique and possibly robust way dopamine may influence hippocampal activity is through modulating vascular activity. The outcomes of the pharmacological experiments support the unique hypotheses that dopamine and adrenoceptors interact to generate the pH/vascular response upon VTA stimulation, and that different α_2 adrenoceptor subtypes play different (and opposing) roles in regulating cerebral vascular activity. Future experiments will investigate the significance of these outcomes in behaving animals.

References:

1. Hansen, Manahan-Vaughan (2014) Dopamine D1/D5 receptors mediate informational saliency that promotes persistent hippocampal long-term plasticity. Cereb Cortex 24(4);845-58

2. Venton et al., (2003) Correlation of local changes in extracellular oxygen and pH that accompany dopaminergic terminal activity in the rat caudate–putamen. J. Neurochem., 84: 373-381

3. Rosin et al., (1996) Distribution of α_{2C}-adrenergic receptor-like immunoreactivity in the rat central nervous system. J. Comp. Neurol. 372:135-165

738
BRAIN-0490
Poster Session

Neurovascular Coupling

COUPLING OF SPONTANEOUS AND SENSORY EVOKED HEMODYNAMIC SIGNALS TO NEURAL ACTIVITY IN THE BARREL CORTEX OF AWAKE MICE

A. Winder[1], P.J. Drew[1]
[1]Engineering Science and Mechanics, Penn State University, University Park, USA

Objectives:

Spontaneous hemodynamic signals, measured in the absence of overt sensory stimulation, are used as indicators of neural activity in resting-state MRI experiments. However, it is not clear whether spontaneous hemodynamic signals reflect ongoing neural activity in the same way that sensory evoked hemodynamic signals do. To determine if coupling of neural activity and hemodynamic signals is the same for both sensory-evoked and spontaneous activity, we examined neurovascular coupling in the barrel cortex of awake, head-fixed mice during several

behaviors (passive sensation, volitional whisking, and rest).

Methods:

We simultaneously measured local neural activity, cerebral blood volume (CBV), and behavior in awake, head-fixed mice. Blood volume changes were quantified by illuminating the vibrissa cortex with 530 nm light through a reinforced thinned-skull window. The local field potential (LFP) and multi-unit activity (MUA) were measured via a tungsten stereotrode implanted in the imaged area of the vibrissa cortex. Whisker position was tracked to detect volitional movements. The vibrissae were also stimulated with brief puffs of air during data acquisition. The data were then categorized into three behaviors: sensory evoked, volitional whisking, and rest. We calculated a hemodynamic response function (HRF), which quantitatively relates the measured CBV to the local neural activity for each behavior. We then used these HRFs to determine what fraction of the spontaneous and sensory evoked changes in CBV could be explained by neural activity.

Results:

Whisker stimulation and volitional whisking were accompanied by increases in the MUA, CBV, and gamma band power of the LFP, though responses to whisker stimulation were substantially stronger. During resting behavior, neural activity and CBV were weakly correlated. These correlations were not disrupted by transection of the facial nerve, indicating that they could not be attributed to undetected whisker movements. HRFs calculated from each of the three behaviors were similar, indicating that neurovascular coupling was conserved across behavioral state. However, there were substantial differences in the variance of the hemodynamic signal captured by the HRFs across behaviors. Sensory evoked hemodynamics, both on average and for individual trials, were better predicted by local neural activity than hemodynamic changes measured during volitional whisking or resting behaviors. The prediction error, for all behaviors, could be attributed to the presence of additive, ongoing CBV fluctuations that were not associated with any measured neural activity. This uncorrelated signal obscures neurally-evoked hemodynamics to a greater degree during volitional whisking and resting behaviors since they are accompanied by smaller neural increases than sensory-evoked activity.

Conclusions:

Neurovascular coupling was similar across all three behavior types that we monitored. However, the measured hemodynamics were not equally representative of local neural activity across behaviors. This discrepancy can be attributed to the presence of a separate component of the hemodynamic signal which was uncorrelated to the measured neural activity. Thus, spontaneous fluctuations in CBV cannot be directly related back to local neural activity.

739
BRAIN-0556
Poster Session

Neurovascular Unit

HUMAN UMBILICAL CORD PERIVASCULAR CELL (HUCPVC) THERAPY FOR TRAUMATIC BRAIN INJURY: TARGETING THE NEUROVASCULAR UNIT.

T. Barretto[1], E. Park[2], E. Liu[2], L. Maghen[1], S. Kenigsberg[1], A. Gauthier-Fisher[1], K. Park[1], A. Baker[2], C. Librach[3]
[1]Research, Create Fertility Centre, Toronto, Canada
[2]Critical Care, St. Michael's Hospital, Toronto, Canada
[3]Obstetrics & Gynaecology, University of Toronto, Toronto, Canada

White matter sparing after traumatic brain injury (TBI) is an important predictor of survival and outcome. Mesenchymal stem cells derived from the bone marrow (BMSCs) are currently being used in clinical trials for treatment of neurodegenerative diseases including stroke[1]. MSCs demonstrate great potential to provide therapeutic benefit, and have thus far proven to be safe in early trials[2]. Accordingly, we were interested in evaluating the potential of human umbilical cord-derived perivascular cells (HUCPVCs), a less differentiated type of MSC, on

their therapeutic potential in TBI. HUCPVCs have several advantages over BMSC therapies including ease of procurement and greater rates of expansion. HUCPVCs are a rich source of pericyte-like cells, and are positive for the pericyte markers CD146, NG2, and PDGFRβ[3].

Objective: We hypothesize that HUCPVCs have the potential to contribute to recovery of white matter through paracrine means, and through structural stabilization of the injured blood-brain barrier (BBB).

Methods: A gene array analysis was performed on HUCPVCs to relevant modulators of inflammation, angiogenesis and neurogenesis. An *in vitro* and an *in vivo* injury model were used to evaluate HUCPVC treatment on outcome after injury. *In vitro:* Cortical neurons were derived from E17 rat pups and cultured for 7 days, then subjected to sublethal oxygen-glucose deprivation for 90 minutes resulting in axonal degeneration[4]. This was followed by co-culturing with HUCPVCs for 3 days to assess outcome in degenerating axons. *In vivo*: Adult male Sprague-Dawley rats underwent a lateral fluid percussion injury, and injected with $2.5x10^6$ HUCPVCs via the tail vein 24 hours after injury. Animal studies were approved by the Animal Care Committees at UHN and St. Michael's Hospital according to CCAC guidelines.

Results: Gene expression analysis indicates expression of key neurotrophic (BDNF, NGF, NT3, GDNF), angiogenic (VEGF-A, FGF5, BMP1) and inflammation-modulating factors (CSF, IL members, CXCL members) in HUCPVCs. Preliminary *in vitro* data indicates that HUCPVCs rescue OGD-induced axon degeneration. *In vivo* results indicate no adverse effects related to HUCPVC treatment. Labeled HUCPVCs were found in the injured cerebral cortex at 24 hrs post-injection. This observation was consistent with CXCR4 immunohistochemistry labeling on HUCPVCs *in vitro*, suggesting that HUCPVCs possess chemotactic ability and are responsive to SDF1-α, known to be expressed by injured neuronal tissue.

Conclusions: Neuroinflammation and neurovascular injury are components of TBI that have potential to be simultaneously addressed with HUCPVC therapy. Our data suggests that HUCPVCs may protect white matter after TBI, and are a potential therapeutic strategy warranting further investigation.

References:

1. Joyce, N., et al., *Mesenchymal stem cells for the treatment of neurodegenerative disease.* Regen Med. 5(6): p. 933-46.
2. Lee, J.S., et al., *A long-term follow-up study of intravenous autologous mesenchymal stem cell transplantation in patients with ischemic stroke.* Stem Cells. 28(6): p. 1099-106.
3. Hong, S.H., et al., *Ontogeny of human umbilical cord perivascular cells: molecular and fate potential changes during gestation.* Stem Cells Dev. 22(17): p. 2425-39.
4. Park, K.J., et al., *Bone marrow-derived endothelial progenitor cells protect postischemic axons after traumatic brain injury.* J Cereb Blood Flow Metab. 34(2): p. 357-66.

740
BRAIN-0228
Poster Session

Neurovascular Unit

AMYLOID BETA INTERFERES WITH ENDOTHELIAL PROGENITOR CELL ADHERENCE VIA MMP UPREGULATION

K. Hayakawa[1], E. Lo[1]
[1]Radiology, Massachusetts General Hospital, Charlestown, USA

Objectives – Cerebral amyloid angiopathy (CAA) is associated with hemorrhagic stroke. But how the vascular deposition of beta-amyloid (Aβ) damages vessels is not fully understood. Here, we ask whether Aβ1-40 can interfere with interactions between EPCs and brain endothelium.

Methods – EPC adhesion assay was performed after 24 hours incubation with or without IL-1β to assess interactions between EPCs and RBE.4 rat

brain endothelial eclls. Ac-LDL labeled EPCs (1 × 10^4 cells/well) were incubated in RBE.4 monolayer cultured onto collagen I-coated 24 well plates at 37°C. The numbers of adhered cells were quantified by directly counting the number of ac-LDL positive cells.

Results – IL-1β -stimulated EPCs were significantly more adherent to the RBE.4 endothelial monolayer. An integrin mechanism may be involved since IL-1β upregulated β2 integrin levels on EPCs, and CD18 neutralizing antibodies significantly decreased the adherence between stimulated EPCs and the RBE.4 monolayer. Next, we asked which corresponding receptor on endothelial cells was involved. Blockade of RAGE but not TLR2 or TLR4 significantly reduced the adherence between stimulated EPCs and the endothelial monolayer. Exposure of RBE.4 to Aβ1-40 for 24 hours reduced RAGE expression on its membrane in accompanied with upregulations of MMP2 and MMP9. Consequently, Aβ1-40 inhibited the adherence between IL-1β -stimulated EPCs and RBE.4. Finally, MMPs inhibitor, GM6001 improved EPC adhesion to RBE.4 along with restoration of RAGE expression.

Conclusions – Targeted adhesion between EPCs and brain endothelial cells may be mediated by an interaction between endothelial RAGE and β2 integrins on EPCs. Aβ1-40 interfered with this interaction between EPCs and brain endothelium. These initial findings suggest that rescuing cell-cell interactions between circulating EPCs and brain endothelium may be a therapeutic strategy to improve endogenous neurovascular repair after CAA associated stroke.

741
BRAIN-0231
Poster Session

Neurovascular Unit

ASTROCYTIC HMGB1 INDUCES AN ANGIOGENIC RESPONSE IN ENDOTHELIAL PROGENITOR CELLS

K. Hayakawa[1], K. Arai[1], E. Lo[1]
[1]Radiology, Massachusetts General Hospital, Charlestown, USA

Objective - Reactive astrocytes are traditionally thought to be detrimental after stroke. However, accumulating evidence suggest that reactive astrocytes derived soluble factors may also be supportive of remodeling cells after stroke. Here, we examine whether astrocytic HMGB1 can induce angiogenic responses in endothelial progenitor cells (EPCs) that play a major role in the endogenous repair of vascular injury after stroke or brain injury.

Methods – To test the angiogenic effect of astrocytic HMGB1 on EPCs, we performed cell culture medium-transfer experiments. Stimulated-astrocyte-conditioned media or no cells conditioned media was collected 24 hours with or without interleukin-1beta (0.1 ng/ml). Conditioned media was filtered using 0.20 µm filter before use. The astrocyte-conditioned medium was used without dilution in all experiments. Assays for proliferation and endothelial-trans-migration were performed in early phase of EPCs day 5 after seeding.

Results – Stimulated astrocytes increased reactive astrocyte markers. Conditioned media from stimulated astrocytes (sACM) induced EPCs proliferation more dramatically compared with that of non-stimulated astrocytes (ACM). This effect was significantly attenuated in the conditioned media from HMGB1-knocked down astrocytes and inhibited by blocking the receptor for advanced glycation endproducts (RAGE) of EPC. Blockade of ERK signaling with U0126 cancelled the EPCs proliferation induced by sACM. To assess whether reactive astrocytes also enhanced endothelial-trans-migration in the EPCs, co-culture experiments were performed using transwell systems. The RBE.4 monolayer was prepared onto collagen-coated membrane in the upper chamber. Interestingly, HMGB1 released from IL-1β-stimulated astrocytes or HMGB1 itself in lower chamber enhanced the migration of EPCs through β2 integrin-RAGE signaling.

Conclusion - Reactive astrocytes release HMGB1 that may promote vascular repair through EPC proliferation or migration. This suggests that

astrocytic HMGB1 could be targeted for enhancing stroke recovery via EPC-mediated revascularization.

742
BRAIN-0086
Poster Session

Neurovascular Unit

PROGRANULIN MEDIATES NEUROVASCULAR PROTECTION VIA MULTIPLE THERAPEUTIC EFFECTS IN EXPERIMENTAL ACUTE ISCHEMIC STROKE

M. Kanazawa[1], K. Kawamura[1], T. Takahashi[1], M. Miura[1], Y. Tanaka[2], M. Koyama[1], M. Toriyabe[1], H. Igarashi[3], T. Nakada[3], M. Nishizawa[1], M. Nishihara[2], T. Shimohata[1]
[1]Neurology,
Brain Research Institute Niigata University, Niigata, Japan
[2]Veterinary Physiology,
Graduate School of Agricultural and Life Sciences The University of Tokyo, Tokyo, Japan
[3]Center for Integrated Human Brain Science, Brain Research Institute Niigata University, Niigata, Japan

Objectives; In central nervous system, progranulin (PGRN), a glycoprotein growth factor, is considered to play crucial roles in maintaining physiological functions, and mutations in *PGRN* gene cause TAR DNA-binding protein-43 (TDP-43)-positive frontotemporal lobar degeneration.[1] In addition, PGRN is known for its role in biological processes such as anti-inflammation and wound healing.[2] Although several studies reported that PGRN plays protective roles against ischemic brain injury,[3,4] it remains unknown the precise mechanisms by which PGRN exerts protective effects on the ischemic brain injury.

Methods; We determined the temporal changes of expression and localization of PGRN after ischemia as well as therapeutic effects of PGRN on ischemic brain injury using *in vitro* and *in vivo* models.

Results; First, we demonstrated a dynamic change of PGRN expression in ischemic Sprague-Dawley rats, including increased levels of PGRN expression in microglia within the ischemic core, and increased level of PGRN expression in survived neurons as well as induction of PGRN expression in endothelial cells within the ischemic penumbra. Second, we demonstrated that PGRN could protect against acute focal cerebral ischemia by variety of mechanisms including via attenuation of blood-brain barrier disruption, suppression of neuroinflammation, and neuroprotection: we found that PGRN may regulate vascular permeability via vascular endothelial growth factor (VEGF), that PGRN may suppress neuroinflammation after ischemia via anti-inflammatory interleukin-10 (IL-10) in microglia, and that neuroprotective effect of PGRN may be explained in part by inhibition of cytoplasmic redistribution of TDP-43 using PGRN knock-out mice (C57Bl/6 background). Finally, we demonstrated the therapeutic potential of PGRN against acute focal cerebral ischemia using a rat autologous thromboembolic model with delayed tissue plasminogen activator (tPA) treatment. Intravenously administered recombinant PGRN reduced volumes of cerebral infarct and edema, suppressed hemorrhagic transformation, and improved motor outcome ($P = 0.007$, 0.038, 0.007, and 0.004, respectively).

Conclusions; PGRN may be a novel therapeutic target that provides neurovascular protection, anti-neuroinflammation, and neuroprotection related in part to VEGF, IL-10, and TDP-43, respectively. We demonstrated for the first time that intravenous administration of recombinant PGRN with tPA treatment showed therapeutic effects on the volumes of cerebral infarct and edema, hemorrhagic transformation, and prognosis.

References;
1. Baker M, et al. Mutations in progranulin cause tau-negative frontotemporal dementia linked to chromosome 17. Nature 2006; 442: 916-919.
2. He Z, et al. Progranulin is a mediator of the wound response. Nat Med 2003; 9: 225–9.
3. Egashira Y, et al. The growth factor progranulin attenuates neuronal injury induced by cerebral ischemia-reperfusion through the suppression of

neutrophil recruitment. J Neuroinflammation 2013; 10: 105.
4. Jackman K, et al. Progranulin Deficiency Promotes Post-Ischemic Blood–Brain Barrier Disruption. J Neurosci 2013; 33: 19579-89.

743
BRAIN-0573
Poster Session

Neurovascular Unit

HUMAN UMBILICAL CORD PERIVASCULAR CELLS (HUCPVCS) EXPRESS AND SECRETE NEUROTROPHIC FACTORS AND PROTECT SYMPATHETIC AXONS FROM DEGENERATION

K. Park[1], T. Barretto[1], L. Maghen[1], S. Kenigsberg[1], A. Gauthier-Fisher[1], C. Librach[2]
[1]Research, Create Fertility Centre, Toronto, Canada
[2]Obstetrics and Gynecology, University of Toronto, Toronto, Canada

The vascular system and the nervous system are mutually dependent during development[1, 2]. Vascular remodeling takes place after the establishment of peripheral nerves, and in turn, requires neural input for proper patterning. Axons provide vascular endothelial growth factor (VEGF) which is necessary for arteriole development and vascular remodelling in the skin [2]. Blood vessels also provide molecular cues to guide the development of neurons. **Objectives:** Given the role of vascular cells in guiding axon development, we wanted to examine the effects of perivascular cells on sympathetic axon survival, and specifically to determine if these cells provide axonal survival cues. Because of the intimate relationship that exists between pericytes and axons, we hypothesized that perivascular cells (PVCs) can prevent axonal degeneration. In the human umbilical cord, there is a discrete collection of cells expressing the pericyte markers NG2 and CD146 [3]. These cells surround the endothelial cell layer of the umbilical vessel walls. Perivascular cells that are isolated and cultured over several passages have a large population that are positive for the perictye markers CD146, NG2 and PDGFRβ[3]. **Methods:** In the present study we examined the growth factor gene expression of HUCPVCs using QPCR analysis from SABioscineces. Protein expression of important neural growth factors was also examined using ELISA assays, and we validated the role of HUCPVCs in rescuing axon degeneration using an in vitro model of axonal injury. Sympathetic neurons were grown in Campenot chamber cultures[4] and at 7 DIV the axons were subjected to an NGF withdrawal injury. Following the NGF withdrawal, HUCPVCs were added to the axon compartments for 3 additional days, after which the cells were either lysed for Western blot analysis, or immunostained for tubulin integrity to count axon degeneration. Animal use was in compliance with the Animal Care Committee regulations at UHN in accordance with CCAC guidelines. **Results:** Our data indicate that HUCPVCs express neurotrophic and neural survival factors in gene array analysis. They also express relevant growth and survival proteins in the secretome of HUCPVCs cultured alone, or in the presence of injured axons. Also, we found that HUCPVCs interact preferentially with axons when co-cultured with sympathetic neurons. Moreover, co-culturing with HUCPVCs in the axon compartment rescued the injury induced axon degeneration and resulted in increased Akt phosphorylation. **Conclusions:** The data presented here indicate an important role for perivascular cells in protecting sympathetic axons from injury, and point to a potential cell-based therapy option for neurodegenerative diseases.

References:

1. Kuruvilla, R., et al., *A neurotrophin signaling cascade coordinates sympathetic neuron development through differential control of TrkA trafficking and retrograde signaling.* Cell, 2004. **118**(2): p. 243-55.

2. Mukouyama, Y.S., et al., *Sensory nerves determine the pattern of arterial differentiation and blood vessel branching in the skin.* Cell, 2002. **109**(6): p. 693-705.

3. Hong, S.H., et al., *Ontogeny of Human Umbilical Cord Perivascular Cells: Molecular and Fate*

Potential Changes During Gestation. Stem Cells Dev.

4. Park, K.J., et al., *p75NTR-dependent, myelin-mediated axonal degeneration regulates neural connectivity in the adult brain.* Nat Neurosci. **13**(5): p. 559-66.

744
BRAIN-0718
Poster Session

Neurovascular Unit

DIFFERENTIAL NEUROVASCULAR SUSCEPTIBILITY TO OXYGEN-GLUCOSE DEPRIVATION AND RESPONSE TO CYTOPROTECTION

P. Rajput[1], J. Bai[1], P.D. Lyden[1]
[1]Neurology, Cedars-Sinai Medical Center, Los Angeles, USA

Objectives- The Neurovascular Unit (NVU) contains multiple cell types that exhibit differential vulnerability during ischemia: neurons, astrocytes and endothelial cells. Traditionally, vulnerability of neurons was greater than astrocytes, which was greater than endothelial cells. To elucidate the mechanisms of differential vulnerability will require a reproducible model system. Therefore, we sought to determine whether different NVU elements exhibit different vulnerability using a model system of oxygen glucose deprivation (OGD) and protection by hypothermia. **Methods-** Primary neuronal and endothelial cells were isolated from E16 –E17 embryos and survived for 8-10 days for further experiments. Astrocytes were isolated from P1 pups. Primary cultured cells at confluence were exposed to OGD for various durations to determine the optimum time point for 80% cell death or cell viability measured using lactate dehydrogenase (LDH) release assay and 3-(4,5-dimethylthiazol-2-yl)-2,5-diphenyltetrazolium bromide (MTT) assay. Then neurons, astrocytes and endothelial cells were exposed to OGD with subsequent hypothermia for various durations, temperatures and delay combinations. Results were compared with ANOVA followed by Dunnett's test for multiple post-hoc comparisons. **Results-**Cell viability was reduced by 80% of control (MTT and confirmed with LDH) for neurons after 2 hours OGD, endothelial cells after 4 hours and astrocytes after 10 hours, confirming the presence of differential vulnerability in this model. Surprisingly, in these primary cultures astroctyes exhibited much greater resistance to injury than endothelial cells. After neurons were subjected to 2 hours OGD, immediate hypothermia (no delay) protected neurons regardless of hypothermia duration 2, 6 or 24 hours; target-depth 33°C was superior to 35°C hypothermia ($p<0.001$ with MTT assay and $p<0.01$ for 2h and $p<0.05$ for 6 and 24 h with LDH assay). When hypothermia was initiated 90min after 2h OGD, 6 and 24 h but not 2 h treatment duration showed protection ($p<0.001$ with MTT and LDH) and again 33°C hypothermia provided significant neuroprotection when compared to 35°C hypothermia ($p< 0.001$, with MTT and LDH assays for 6h and 24 h duration whereas, $p<0.001$ with MTT and $p<0.05$ with LDH for 2 h duration). Endothelial cells and astrocytes were subjected to 4 h or 10 hours of OGD respectively, followed by hypothermia for 2h, 6h and 24h treatment duration with no delay or 90min delay to onset of hypothermia. As with the neurons, hypothermia for various durations in endothelial cells or astroctyes after OGD showed significant protection ($p<0.001$, MTT assay). Immediate hypothermia for 2, 6 or 24 hours duration protected endothelial cells and astrocytes ($p<0.001$). However, after 90 min. delay, only 33°C hypothermia only continued for 24 h duration showed significant effect ($p<0.001$). In fact, target-depth 33°C was superior to 35°C ($p<0.001$) when hypothermia was initiated 30 min, 60 min or 90 min after OGD in astrocytes and endothelial cells. In contrast, 35°C hypothermia, showed no significant changes in cell viability in comparison to normothermia (37°C). **Conclusion.** Three elements of the NVU exhibit differential susceptibility to OGD and response to cytoprotection with hypothermia. This model will provide a highly reproducible model system for studying the mechanisms of

differential vulnerability in the NVU.

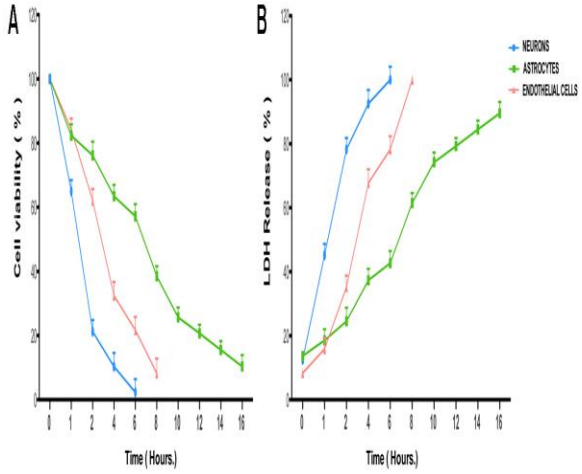

745
BRAIN-0317
Poster Session

Neurovascular Unit

PERICYTES INTERACT WITH OLIGODENDROCYTE PRECURSOR CELLS IN PERIVASCULAR REGION IN CEREBRAL WHITE MATTER

T. Maki[1], M. Maeda[2], M. Uemura[3], E. Lo[1], Y. Terasaki[1], A. Liang[1], A. Shindo[1], R. Takahashi[3], M. Ihara[4], K. Arai[1]
[1]Neurology and Radiology, Massachusetts General Hospital, Charlestown, USA
[2]Regenerative Medicine, Institute of Biomedical Research and Innovation, Kobe, Japan
[3]Neurology, Kyoto University, Kyoto, Japan
[4]Stroke and Cerebrovascular Diseases, National Cerebral and Cardiovascular Center, Osaka, Japan

Objectives: Pericytes are embedded within basal lamina and play multiple roles in the perivascular niche in brain. Although oligodendrocyte precursor cells (OPCs) are recently reported to be adjacent to cerebral endothelial cells, the spatial and functional relationship between pericytes and OPCs are mostly unknown. In this study, we examined whether pericytes attach to OPCs and support OPC function in the perivascular region in cerebral white matter.

Methods: Brains from C57BL/6 mice (postnatal days 0, 60, 240) were used for immunostaining. Pericytes were stained with anti-PDGF-R-β antibody, and OPCs were observed with anti-PDGF-R-α and anti-NG2 antibodies. Genetically fluorescent-labeled (PDGFR-α-creER^{T2}/ROSA26-GFP) mice were also used to assess the pericyte-OPC interaction. Autopsied human brains, which were obtained from Kyoto University Hospital, were analyzed with anti-PDGF-R-β and anti-PDGF-R-α antibodies to observe the OPC-pericyte interaction in human. For electron microscopic investigation, brains from Sprague-Dawley rats were stained with anti-PDGF-R-α and anti-NG2 antibodies. For in vitro experiments, cultured primary OPCs and pericytes were maintained separately. Then conditioned media from pericytes (Pericyte-CM) were prepared and added to OPC cultures. OPC proliferation was assessed with WST assay and direct-cell-counting 48 hours after Pericyte-CM treatments. OPC maturation was assessed with western blot using anti-myelin-basic-protein antibody 5 days after Pericyte-CM treatments.

Results: Immunostaining showed that OPC number in mouse white matter decreased from postnatal day 0 to day 60. By contrast, pericyte numbers were relatively stable between postnatal day 0 and day 240. However, at all the stages (i.e. postnatal days 0, 60 and 240), pericytes and OPCs were localized in close contact with each other in mouse white matter. PDGFR-α-creER^{T2}/ROSA26-GFP transgenic mice showed that some GFP-labeled OPCs were located in close apposition to pericytes immediately adjacent to cerebral endothelium in corpus callosum. Electron microscopic analysis confirmed that pericytes attached to OPCs via basal lamina in the perivascular region. The close proximity between these two cell types was also observed in postmortem human brains. Functional support from pericytes to OPCs was assessed by in vitro media transfer experiments. When OPC cultures were treated with pericyte-conditioned media, OPC number increased accompanied with enhanced myelin-basic-protein expression, which indicate that pericyte-derived factors promoted OPC proliferation and differentiation.

Conclusions: Taken together, our data suggest that OPCs may receive functional support by pericyte in the perivascular region. Given that both pericytes and OPCs exchange signals in the perivascular niche, the triangular communication among pericytes, OPCs, cerebral endothelium would play pivotal roles in brain homeostasis.

746
BRAIN-0175
Poster Session

Oxidative Mechanisms

EFFECTS OF NMDA RECEPTOR ANTAGONIST MEMANTINE ON NO PRODUCTION, HYDROXYL RADICAL METABOLISM AND ISCHEMIC CHANGE OF HIPPOCAMPAL CA1 DURING CEREBRAL ISCHEMIA AND REPERFUSION IN MICE

N. Araki[1], Y. Ito[1], T. Sasaki[1], M. Yamazato[1], R. Nishioka[1], M. Hirayama[1]
[1]Department of Neurology, Saitama Medical University, Saitama, Japan

Introduction: It is suggested that NMDA receptor antagonist memantine may protect brain tissue during cerebral ischemia. The purpose of this study is to investigate the nitric oxide production, hydroxyl radical metabolism and ischemic change of hippocampal CA1 during cerebral ischemia and reperfusion in mice.

Methods: (1) C57BL/6 mice [n=15] were used. Memantine 25 µmol/ kg was given in 5 mice 30 minutes before ischemia, and others were contol group. Both NO production and hydroxyl radical metabolism were continuously monitored by *in vivo* microdialysis. Microdialysis probes were inserted into the bilateral striatum. The *in vivo* salicylate trapping method was applied for monitoring hydroxyl radical formation via 2,3 dihydroxybenzoic acid (DHBA), and 2,5-DHBA. A Laser doppler probe was placed on the skull surface. Forebrain cerebral ischemia was produced by occlusion of both common carotid arteries for 10 minutes. Levels of NO metabolites, nitrite (NO_2^-) and nitrate (NO_3^-), in the dialysate were determined using the Griess reaction. (2) Survival rate in hippocampal CA1 neurons: Hippocampal CA1 neurons were analyzed into three phases (severe ischemia, moderate ischemia, survive), and the ratio of the number of surviving neurons was calculated as survival rate 7 days after the start of reperfusion.

Results: (1) Blood pressure: There were no significant differences between the groups. (2) Cerebral blood flow (CBF): There were no significant differences between the groups. (3) NO_2^-; Memantine group (120.9±5.00%; mean±SD) showed significantly higher than that of the control group (88.5±18.0) after repurfusion 60 minutes ($p<0.05$). (4) NO_3^-; Memantine group (97.2±10.1%; mean±SD) showed significantly higher than that of the control group (65.3±21.0) at ischemia ($p<0.05$). (5) 2,3-DHBA; Memantine group (90.7±2.90%; mean±SD) showed significantly lower than that of the control group (99.5±2.66) at ischemia, after repurfusion 20, 80-120 minutes ($p<0.05$). (6) Survival rate in CA1 area: There were no significant differences between the groups.

Conclusion: These *in vivo* data suggest that memantine effects on NO and hydroxyl radical metabolites in mice, and may have neuroprotective effect against cerebral ischemic injury.

747
BRAIN-0862
Poster Session

Oxidative Mechanisms

FRET PROBES VISUALIZE ERK AND JNK PHOSPHORYLATION AND CONSEQUENTLY CELL DIVISION OR CELL DEATH IN HT22 CELLS.

Y. Karasawa[1], H. Imai[2], K. Kunida[3], T. Tsuchiya[3], T. Wada[3], S. Kuroda[3], N. Saito[1]
[1]Neurosurgery, Graduate School of Medicine The University of Tok yo, Bunkyo City, Japan
[2]Neurosurgery, The University of Tokyo Hospital, Bunkyo City, Japan
[3]Biological Sciences, The University of Tokyo HospitalGraduate School o

f Science The University of Tokyo, Bunkyo City, Japan

【Backgraound】
Sufficient data exist that Oxidative stress plays critical role in neuronal cell death under ischemic conditions. The immortalized mouse hippocampal HT22 cell in vitro model is widely used for evaluating the mechanisms of oxidative stress-associated neuronal cell death. The HT22 cells do not possess glutamate receptors, and treatment with high levels of glutamate can inhibit the synthesis of intracellular glutathione (Li et al., 1997). Typically, cystine is rapidly reduced to cysteine, which is necessary for the formation of glutathione (GSH) and then, reactive oxygen species (ROS) levels become increased .
It has been clearly demonstrated that the activation of Mitogen-activated protein Kinase (MAPK): while phosphorilation of ERK or JNK is detected during the death of HT22 cells by Western blotting assay, MAPK activity apparently decides the fate of cell (survival or death) under stress. Western blotting reflects the average status of a specific cell population and we cannot understand the spatiotemporal dynamics of signaling molecules within a single cell. To overcome these limitations, the Förster resonance energy transfer (FRET) biosensors, which quantifies molecular interactions in biology and chemistry, can be used. We applied the FRET probe that is able reflect the interaction between proteins, and by using ERK-FRET probes, we made possible measurement of intensity as real-time visualization of ERK or JNK phosphorylation in a single cell nucleus.
【Materials and methods】
Plasmids of ERK-FRET probes and JNK-FRET utilizing a PiggyBac transposon system to generate HT22 cell lines with stable expression of FRET biosensors (Aoki et al., 2012) were used. Cells were seeded onto 35 mm glass-based dishes. At 24-36 hr after seeding, we exchanged medium to CO2-independent medium and time-lapse FRET images were obtained by epifluorescence microscope (Olympus IX83) We induced oxidative stress in the HT22 cell line with glutamate of varied concentration (0~10mM)

【Result】
In the cells whith JNK-FRET probe transfer, FRET efficiency were elevated according to level of phosphorylation of JNK. All cells with JNK activation died and opposite, those without JNK activation survived. We confirmed cell death by Propidium Iodide staining.On the other hand, in cells with ERK-FRET probe induction, phosphorylation of ERK was observed just before cell division.

【Discussion】
We developed a new model for real-time visualization of MAPK activity under oxidative stress in HT22 cells and confirmed that phosphorylation of ERK can be seen in cell proliferation, to differ from phosphorylation of JNK, which is seen in cell death.

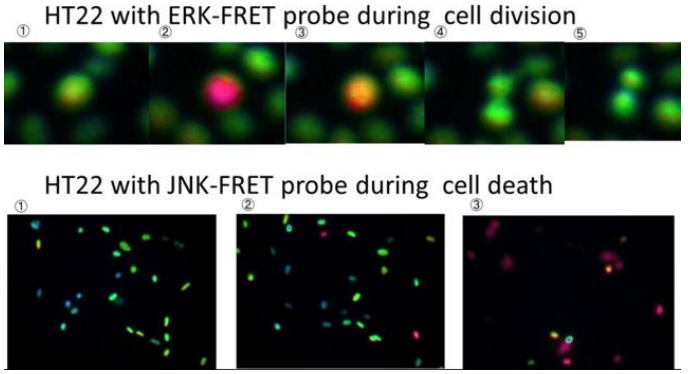

748
BRAIN-0278
Poster Session

Oxidative Mechanisms

NATURAL BIOACTIVE COMPOUNDS FROM RESOURCE ANIMALS : ANTIOXDATIVE AND CURATIVE EFFECT IN DISEASE MODEL CELLS

S.Y. KANG[1], M.H. HONG[1], M.J. YOU[1], S. YI[2], K.D. SONG[3], H.K. LEE[3], S. KIM[1]
[1]Department of Biotechnology, Hoseo University, Asan, Korea
[2]Department of Biomedical Laboratory Science, Soonchunhyang University, Asan, Korea
[3]The Animal Genomics and Breeding Center, Han-Kyong National University, Anseong, Korea

Neuronal cell death is the suggested cause of neurodegeneration in many disease, the molecular mechanism remains uncertain. We recently suggested that the cell cycle profile and its regulatory factors in lysosomal storage disease cells. We found G1/G0 cell cycle arrest, with overexpression of p21, sphingosine, glucosylceramide, and sulfatide. We also observed enhanced levels of α-synuclein oligomers and gangliosides GM1, GM2, and GM3 and reduced levels of sphingomyelin and autophagy. We report here that one of the pathogenic mechanism of neuronal cell death in lysosomal storage disease (Batten disease and Gaucher disease) is mediated by cellular stress, also upregulate the production of reactive oxygen species (ROS), destabilize mitochondrial membrane potential (MMP). Furthermore, we demonstrate that the levels of cell death indicators (ROS, MMP etc) in disease model cells are markedly decreased by bioactive compounds from resource animal. Our results provide that the availability of suitable bioactive compounds for testing and validation. This work was carried out with the support of 'Cooperative Research Program for Agriculture Science & Technology Development (Project No. PJ01104601)" Rural Development Administration, Republic of Korea.

749
BRAIN-0540
Poster Session

Oxidative Mechanisms

COBALT CHLORIDE-INDUCED-CHEMICAL HYPOXIA PROVOKES CHANGES IN SUBCELLULAR LOCALIZATION OF HEMEOXYGENASE ISOFORMS.

J. Muñoz-Sanchez[1], M. Orozco-Ibarra[2], P. Maldonado[1], M. Chanez[1]
[1]Patologia Vascular Cerebral, Instituto Nacional de Neurologia y Neurocirugia, Mexico City, Mexico
[2]Laboratorio de Neurobiologia Celular y Molecular , Instituto Nacional de Neurologia y Neurocirugia, Mexico City, Mexico

Objectives: The hemeoxygenases (HO)-1 and-2 are microsomal oxidoreductase enzymes that remove oxidant heme to biliverdin, carbon monoxide and Fe^{2+}. Non-enzymatic roles have been proposed for both enzymes. HO-1 is an inducible isoform; under hypoxic and hyperoxic stress migrates to the nucleus. HO-1 also increases in mitochondrial fractions by different stimuli. HO-2 is not an inducible enzyme, however its expression is differentially regulated by hypoxia. C-terminal HO-2-deleted mutants have been observed in the nucleus suggesting its translocation. The objective of this work was to determine the behavior of HO isoforms in hipoxia mimicking conditions at transcript and protein levels as well as in the subcellular localization (nucleus, mitochondria and cytoplasm) using the $CoCl_2$ induced-chemical hypoxia model in PC12 cells.

Methods: Cell death and viability with increasing $CoCl_2$ concentrations (0.1-1.0 mM) for 24 or 48h were determined by $SubG_0$ and MTT reduction assays. Stabilization, nuclear translocation and binding activity of HIF-1α were quantified by ELISA in nuclear fractions. ROS production was meeasured by DCF-DA fluorescence. HO-1 and HO-2 transcript levels were determined by real-time PCR and protein levels were measured by western blot and ELISA in cytoplasm, nucleus and mitochondria purified fractions.

Results: $CoCl_2$ affected cell viability and cell death in a concentration- and time-dependent manner. A significant reduction in cell viability was observed. At 0.5 mM $CoCl_2$ at 24 and 48h the percentage was 65 and 50% respectively, while at 1.0 mM $CoCl_2$ a considerable reduction was observed (30% at 24h and 10% with 48h). However, cell death determination by $SubG_0$ shows that at 24h there is only a 5 and 15 % of dead cells at 0.5 and 1.0 mM $CoCl_2$; while at 48h 22 and 40 % dead cells were observed. Cells incubated 24h at 0.5 and 1.0 mM $CoCl_2$ showed stabilization, nuclear translocation and binding activity of HIF-1α about 6- and 4-fold at 0.5; while 48h incubation induced an increase of 19- and 35-fold at 0.5 and 1.0 mM $CoCl_2$ respectively. In addition to HIF-1α protein stabilization, $CoCl_2$ mimics other hypoxia responses, including ROS generation. HO-1 transcript increased 210–fold

with 0.5 mM $CoCl_2$ and 80-fold at 1.0 mM (24h). Transcript levels were maintained until 48h. In contrast, HO-2 transcript only decreased in both $CoCl_2$ concentrations at 24h. Subcellular fractionation evidenced that HO-1 was localized in nucleus and mitochondria and had dependent increase on $CoCl_2$ concentration and incubation time. HO-2 was detected in cytoplasm, showing a decrease with $CoCl_2$ 0.5 and 1.0 mM at 24 and 48h by WB and ELISA. Surprisingly HO-2 was detected in nucleus decreasing with $CoCl_2$ treatment. In addition, the presence of mitochondrial HO-2 increased with $CoCl_2$ at 48h.

Conclusions: HO system responds differentially in a $CoCl_2$-induced chemical hypoxic stress in PC12 cells. HO-1 and HO-2 proteins are translocated to nucleus and mitochondria as result of chemical hypoxia stress. Understanding these roles and finding therapeutic tools to specifically alter them could lead to clinical interventions that prevent hipoxic oxidative injury, tumor progression, and cell proliferation.

750
BRAIN-0779
Poster Session

Oxidative Mechanisms

EVALUATION OF SCAVENGING ACTIVITY AGAINST MULTIPLE SPECIES OF FREE RADICALS BY ELECTRON SPIN RESONANCE SPECTROSCOPY

O. Tokumaru[1], K. Ogata[1], T. Kitano[2], I. Yokoi[1]
[1]Neurophysiology,
Oita University Faculty of Medicine, Yufu, Japan
[2]Anesthesiology,
Oita University Faculty of Medicine, Yufu, Japan

Objectives: Evaluation ofantioxidative activity of antioxidants is important to understand theirmechanism of neuroprotective activity. Although measurement of lipid peroxideis often employed for the evaluation, their direct free radical scavengingactivity is not necessarily always measured, and, especially, data concerningtheir concentration-response relationship against multiple free radical species remain sparse. The authors haveevaluated direct scavenging activity of antioxidants against multiple speciesof free radicals by electron spin resonance (ESR) spectroscopy. Here theauthors illustrate an example of evaluation of multiple free radical scavengingactivity by presenting the data of edaravone, a powerful free radical scavengerand the only drug currently available in clinical use for the treatment ofcerebral infarction.

Methods: Free radicalscavenging activity of edaravone was evaluated by ESR spectroscopy using spintrapping method. The spectrum of its dose-response relationships to multiplefree radical species was estimated.

Results: Edaravone scavengedthe following six kinds of free radicals with the IC_{50} as indicated:hydroxyl radical (IC_{50} = 0.4 mM), superoxide anion (4 mM), ascorbylfree radical (8 mM), *tert*-butyl peroxyl radical (0.3 mM), DPPH (5 μM),nitrous oxide (0.04 mM). No radical scavenging activity was observed againstthe methyl radical.

Conclusions: The estimated dose-response relationship of radicalscavenging activity by edaravone varied among free radical species examined.Since the IC_{50} varied among different species of free radicals, itis suggested that it is not sufficient to demonstrate antioxidative activity orscavenging activity against a single species of free radical to understand itstherapeutic mechanism. When evaluating antioxidative activity of antioxidants,it is necessary to evaluate scavenging activity against multiple species offree radicals to fully understand their neuroprotective mechanism againstoxidants

751
BRAIN-0115
Poster Session

Oxidative Mechanisms

FOCAL ISCHEMIC INJURY WITH COMPLEX MIDDLE CEREBRAL ARTERY IN STROKE-PRONE SPONTANEOUSLY HYPERTENSIVE RATS WITH LOSS-OF-FUNCTION IN NADPH OXIDASES

H. Yao[1], M.Z. Ferdaus[2], H.M. Zahid[2], H. Ohara[2], T. Nakahara[1], K. Matsumoto[3], T. Nabika[2]
[1]Laboratory for Neurochemistry, National Hospital Organization Hizen Psychiatric Center, Saga, Japan
[2]Department of Functional Pathology, Shimane University School of Medicine, Izumo, Japan
[3]Division of Laboratory Animal Research, Shinshu University, Matsumoto, Japan

Introduction: The nicotinamide adenine dinucleotide phosphate (NADPH) oxidases (Nox), only enzymes in terms of its primary function of generating superoxide, are the predominant source of reactive oxygen species. Nox-knockout mice generally showed protection against focal ischemia or experimental stroke (i.e., the evidence for detrimental effects of Nox on stroke outcome). As measurements of physiological variables and cerebral blood flow (CBF) in mice are difficult due to their small body size, we attempted to construct a new rat model lacking Nox activities.

Method: The National Hospital Organization Hizen Psychiatric Center Institutional Review Board (the Animal Care and Use Committee) approved all animal experimental and maintenance procedures (approval number: 26-6). By means of introgressing a loss-of-function mutation in the p22phox gene from the Matsumoto Eosinophilia Shinshu (MES) rat [1] to stroke-prone spontaneously hypertensive rats (SHRSP), we constructed the SHRSP-based congenic strain lacking the P22PHOX expression (i.e., lacking NOX activities) (SHRSP.MES-Cyba^{mes}/Izm; hereafter referred to as SP.MES). The distal middle cerebral artery (MCA) was occluded by 561-nm laser-driven photothrombosis.

Results: Resting mean arterial blood pressure (MABP) was 150±11 mmHg in SP.MES, which was significantly lower than 165±13 mmHg in PM0/SHRSP ($p=0.006$). After MCA occlusion, blood pressure increased in both groups, but the intra-ischemic MABP levels were still lower in SP.MES than in PM0/SHRSP (2-way ANOVA, $p<0.001$). CBF decreased to 37±13% in SP.MES and 35±17% in PM0/SHRSP at 10 min after MCA occlusion (2-way ANOVA, not significant). The changes in CBF from 10 min to 60 min after MCA occlusion were 7±8% and -4±8% in SP.MES and PM0/SHRSP, respectively ($p=0.006$). Infarct volume in the SP.MES group was 89±39 mm^3, which was not significantly different from 83±35 mm^3 in the PM0/SHRSP group. The distal MCA pattern was more complex in SP.MES (median 3, IQR 3-5) than PM0/SHRSP (median 2, IQR 1-3) (Mann-Whitney u-test, $p=0.001$). Because more complex distal MCA is known to produce larger infarction after distal MCA occlusion in SHR [2], we adjusted for the branching pattern in an ANCOVA. The adjusted mean of infarct volume was significantly smaller in SP.MES compared with that in PM0/SHRSP (67 [95% CI 46 to 87] mm^3 vs. 100 [95% CI 82 to 118] mm^3, $p=0.032$).

Conclusions: Elimination of the P22PHOX expression induced complex distal MCA, which would suggest the presence of 'loss of complexity' induced by enhanced oxidative stress in SHRSP. Infarct size in SP.MES was significantly attenuated compared with that in PM0/SHRSP when adjusted for distal MCA complexity. In a future study, the effect of P22PHOX deprivation on infarction under transient focal ischemia (i.e., reperfusion injury) should be addressed in SP.MES.

References

1. Mori M, Li G, et al. Pivotal Advance: Eosinophilia in the MES rat strain is caused by a loss-of-function mutation in the gene for cytochrome b(-245), alpha polypeptide (Cyba). J Leukoc Biol 2009;86:473-478.

2. Cai H, Yao H, Ibayashi S, et al. Photothrombotic middle cerebral artery occlusion in spontaneously hypertensive rats: influence of substrain, gender, and distal middle cerebral artery patterns on infarct size. Stroke 1998;29:1982-1986.

752
BRAIN-0313
Poster Session

Oxidative Mechanisms

CHRONOLOGICAL CHANGES OF GLUCOCORTICOID RECEPTORS IN THE HIPPOCAMPUS OF STREPTOZOTOCIN-TREATED TYPE 1 DIABETIC RATS

H. Shim[1], H. Baek[1], M. Shim[1], I. Hwang[2], J. Seong[3], Y. Yoon[2], S. Yi[1]
[1]Department of Biomedical Laboratory Science, Soonchunhyang University, Asan, Korea
[2]Department of Anatomy and Cell Biology College of Veterinary Medicine, Seoul National University, Seoul, Korea
[3]Laboratory of Developmental Biology and Genomics, Seoul National University, Seoul, Korea

Type 1 diabetes is a common metabolic disorder accompanied by increased blood glucose levels along with glucocorticoid and cognitive deficits. The disease is also thought to be associated with environmental changes in brain and constantly induces oxidative stress in patients. Therefore, glucocorticoid-mediated negative feedback mechanisms involving the glucocorticoid receptor (GR) binding site are very important to understand the development of this disease. Many researchers have used streptozotocin (STZ)-treated diabetic animals to study changes in GR expression in the brain. However, few scientists have evaluated the hyperglycemic period following STZ exposure. In the present study, we found GR expression in the hippocampus varied based on the period after STZ administration for up to 4 weeks. We performed immunohistochemistry and Western blotting to validate the sequential alterations of GR expression in the hippocampus of STZ-treated type 1 diabetic rats. GR protein expression increased significantly until week 3 but decreased at week 4 following STZ administration. GR expression after 70 mg/kg STZ administration was highest at 3 weeks post-treatment and decreased thereafter. Although STZ-induced increase in GR expression in diabetic animals has been described, our data indicate that researchers should consider the sequential GR expression changes during the hyperglycemic period following STZ exposure.
This work supported by a grant (20120261) funded by Soonchunhyang University

753
BRAIN-0314
Poster Session

Oxidative Mechanisms

TIME-DEPENDENT CHANGES OF CALBINDIN D-28K AND PARVALBUMIN IMMUNOREACTIVITY IN THE HIPPOCAMPUS OF STREPTOZOTOCIN-TREATED TYPE I DIABETES

Y. Lee[1], H. Baek[2], H. Shim[2], S. YI[2]
[1]Department of Life Science and Biotechnology, Soonchunhyang University, Asan, Korea
[2]Department of Biomedical Laboratory Science, Soonchunhyang University, Asan, Korea

The hippocampus is affected by various stimuli that include hyperglycemia, depression, and ischemia. Calcium-binding proteins (CaBPs) have protective roles in the response to such stimuli. However, little is known about the expression of CaBPs under diabetic conditions. This study was conducted to examine alterations in the physiological parameters with type 1 diabetes induced with streptozotocin (STZ) as well as time-dependent changes in the expression of two CaBPs changes of were being evaluated. Rats treated with STZ (70mg/kg) had high blood glucose levels (>21.4 mmol/L) along with increased food intake and water consumption volumes compared to the sham controls. In contrast, body weight of the animals treated with STZ was significantly reduced compared to the sham group. CB-specific immunoreactivity was generally increased in the hippocampal CA1 region and granule cell layer of the dentate gyrus (DG) 2 weeks after STZ treatment, but decreased

thereafter in these regions. In contrast, the number of PV-immunoreactive neurons and fibers was unchanged in the hippocampus and DG 2 weeks after STZ treatment. However, this number subsequently decreased over time. These results suggest that CB and PV expression is lowest 3 weeks after STZ administration, and these deficits lead to disturbances in calcium homeostasis.

This research supported by the Soonchunhyang University Research Fund

754
BRAIN-0440
Poster Session

Molecular Mechanisms

LACTATE REGULATES PLASTICITY-RELATED GENE EXPRESSION IN NEURONS THROUGH A MECHANISM INVOLVING POTENTIATION OF THE NMDA RECEPTOR.

I. Allaman[1], E. Ruchti[1], P. Jourdain[1], J. Yang[1], G. Grenningloh[1], J.M. Petit[1], P.J. Magistretti[2]
[1]Brain Mind Institute, Ecole Polytechnique Fédérale de Lausanne, Lausanne, Switzerland
[2]Division of Biological and Environmental Sciences and Engineering, KAUST, Thuwal, Saudi Arabia

Objectives: Glycogen-derived L-lactate release by astrocytes and its uptake by neurons is required for long-term memory formation (Suzuki et al, 2011; Newman et al, 2011). In this study, we aimed to determine whether L-lactate directly contributes to neuronal plasticity by activating the expression of synaptic plasticity-related genes in neurons and to address the underlying mechanism.

Methods: Primary cultures of mouse cortical neurons were incubated with L-lactate, or different energy substrates, and different biological indexes were quantified.

Results: In cultured neurons L-lactate significantly stimulates mRNA expression of key immediate early genes (IEGs) involved in plasticity-related processes, in a time- and concentration-dependent manner. For instance, following one hour of treatment with 20 mM L-lactate, Arc, Zif268 and c-Fos mRNA levels are increased between 4-8 fold. The increased IEGs mRNA expression levels induced by L-lactate are correlated at the protein level with respectively 5.5, 4.0 and 3.2 fold increase compared to control values. In addition to IEGs, an increase of BDNF mRNA levels is also demonstrated after 4 hours of treatment. Remarkably, these effects are specific for L-lactate, since D-lactate, L-pyruvate and D-glucose have no effect on gene expression (Yang et al, 2014).
The effects of L-lactate involve potentiation of NMDA receptor activity, as they are prevented in the presence of specific inhibitors of NMDA receptors (MK801, APV and the glycine site blocker L-689.560). Consistent with this observation, L-lactate potentiates NMDA receptor-mediated currents (induced by co-application of glutamate and glycine) and the ensuing increase in intracellular calcium. The NMDA receptor downstream signaling cascade Erk1/2 is critically involved in L-lactate effects since induction of IEGs expression by L-lactate is prevented in the presence U0126, an Erk1/2 kinases inhibitor.

All effects of L-lactate are mimicked by NADH, suggesting that changes in redox state of neurons following conversion of L-lactate to L-pyruvate are crucial in the effect of L-lactate.

Conclusions: Taken together these findings demonstrate that L-lactate acts as a direct signaling molecule which regulates neuronal plasticity-related IEGs expression. Interestingly, the underlying mechanism of action of L-lactate involves potentiation of NMDA receptors and changes in the redox state. These results provide insights for the understanding of the molecular mechanisms underlying the critical role of astrocyte-derived L-lactate in long-term memory formation. This set of data reveals a previously unidentified action of L-lactate as a signaling molecule for neuronal plasticity in addition to its role as an energy substrate.

References:

1) Suzuki A, Stern SA, Bozdagi O, Huntley GW, Walker RH, Magistretti PJ, Alberini CM. Astrocyte-neuron lactate transport is required for long-term memory formation. Cell. 2011;144(5):810-23.

2) Newman LA, Korol DL, Gold PE. Lactate produced by glycogenolysis in astrocytes regulates memory processing. PLoS One. 2011;6(12):e28427.

3) Yang J, Ruchti E, Petit JM, Jourdain P, Grenningloh G, Allaman I, Magistretti PJ. Lactate promotes plasticity gene expression by potentiating NMDA signaling in neurons. Proc Natl Acad Sci U S A. 2014;111(33):12228-33.

755
BRAIN-0170
Poster Session

Molecular Mechanisms

ELAV/HU PROTEINS ARE DEFICIENT IN CONTROL HIPPOCAMPAL CA1: CONSEQUENCES FOR ISCHEMIC INJURY.

H. Wang[1], F. Anggraini[1], X. Chen[1], D.J. DeGracia[1]
[1]Department of Physiology,
Wayne State University, Detroit, USA

Objectives: Translation arrest (TA) after global cerebral ischemia and reperfusion (I/R) persists in vulnerable CA1 but reverses in resistant CA3. TA correlated with the absence of ELAV/Hu granules in CA1 [1]. ELAV/Hu proteins bind and regulate adenine and uridine rich (ARE) mRNAs. We tested the hypothesis that ELAV proteins facilitate ARE-mRNA binding to polysomes during reperfusion by assessing: (1) ELAV-polysome interactions, (2) ELAV binding partners, and (3) binding of ARE-mRNAs on polysomes. We expected levels of polysome-bound ELAV proteins to correspond to levels of ARE-mRNAs on polysomes.

Methods: Male Long Evans rats were subjected either to sham surgery (non-ischemic control, NIC) or to 10 min normothermic global cerebral ischemia by two-vessel occlusion plus hypotension and 8 hr reperfusion (8R). Hippocampal CA1 and CA3 were dissected. Five animals were pooled per region per replicate. Polysome pellets were isolated by sucrose pad, followed by LC-MS proteomics to determine polysome-RNA binding protein (RBP) profiles. To determine ELAV binding partners, homogenates of CA1 and CA3 were immunoprecipitated (IP) with anti-ELAV antisera and bound proteins subject to LC-MS proteomics, and IP-Western validation. To determine polysome-bound ARE-mRNAs, RNA was extracted from polysome pellets and then analyzed on Rat Gene 2.0 ST Arrays (Affymetrix). ARE-mRNAs were determined by searching the ARE Database.

Results: Proteomics validated that polysome pellets consisted of ~25% ribosomal subunit protein. A complex pattern of polysome-RBP association was found between NIC and 8R CA1 and CA3. The main finding was lack of ELAV proteins associated with NIC CA1 polysomes. Following ELAV IP, LC-MS detected different RBPs associated with each group. Again, the main finding was, surprisingly, ELAV proteins were not detected in NIC CA1. This result was validated by IP-Western where the ELAV proteins HuD, HuC and HuB were undetectable in NIC CA1. However, ARE-containing mRNAs accounted for 9% and 4% of all differentially expressed mRNAs at 8R CA1 and CA3 polysomes, respectively. The largest differentially expressed ARE-mRNA, *hsp70*, was detected on polysomes of both CA1 and CA3. Significantly, ELAV proteins were detected in 8R CA1, and the mRNAs for these proteins increased in 8R CA1 compared to 8R CA3, suggesting ELAV proteins are translated during reperfusion in CA1 but not CA3.

Conclusions: ELAV proteins were undetectable in control CA1 and our data suggests they are translated in CA1 during reperfusion. Lack of ELAV proteins would put CA1 neurons at a disadvantage compared to CA3 neurons who already express them at the onset of ischemia. These results suggest that a differential in the control state contributes to outcome following brain I/R. Therefore, in addition to inhibition of damage, and bolstering injury-

induced stress responses, accounting for intrinsic differences in the control state of neurons may contribute to developing successful neuroprotection.

References: Jamison et al (2008). Neuroscience (154):504–520.

756
BRAIN-0781
Poster Session

Molecular Mechanisms

INDICATIONS OF INCREASED BRAIN GLYCOLYSIS AND CITRIC ACID CYCLE ACTIVITY IN RATS ON A HIGH FAT KETOGENIC DIET: AN NMR STUDY WITH [1-13C]-GLUCOSE AND [2,4-13C2]-BETA-HYDROXYBUTYRATE.

S.C. Cunnane[1], M. Roy[2], M.C. Beauvieux[3], J. Naulin[3], D. El Hamrani[3], C.A. Castellano[1], J.L. Gallis[3], A.K. Bouzier-Sore[3]
[1]Clinical Axis, Research Centre on Aging, Sherbrooke, Canada
[2]Physiology and Biophysics, Université de Sherbrooke, Sherbrooke, Canada
[3]UMR5536 CNRS, Université de Bordeaux, Bordeaux, France

Introduction: The neuroprotective effect of mild ketosis induced by a very high fat ketogenic diet (KD) remains enigmatic. Few studies have directly compared brain metabolism of carbon-13 (^{13}C)-enriched forms of glucose and ketones in rats on a KD.

Objective: The primary aim of the present study was to investigate how the KD affects ^{13}C enrichment in brain metabolites following infusion of [1-^{13}C]-glucose (^{13}C-Glc) or [2,4-$^{13}C_2$]-β-hydroxybutyrate (^{13}C-β-HB).

Methods: Four week old male Sprague-Dawley rats consumed a control diet (CTL; low fat) or underwent 48 h fasting followed by the KD for 7 days. All rats were then anesthetized with chloral hydrate i.p. and infused via the tail vein with ~2 mmol of ^{13}C-Glc or ^{13}C-β-HB for one hour (n=6/diet group and labeled substrate; n=24 in total). After the infusions, rats were euthanized with focused brain microwaves and the brain and the liver surgically removed and put immediately in liquid nitrogen. Brain metabolites were extracted into perchloric acid and ^{13}C and ^{1}H-NMR spectra were obtained.

Results: Specific enrichments (SEnr) of brain amino acids were similar between CTL and KD rats after ^{13}C-Glc infusion. 32% higher SEnr of brain lactate in the KD group after ^{13}C-Glc infusion suggested higher brain glycolysis on the KD. After ^{13}C-β-HB infusion, SEnr was higher in brain lactate-C3 (+31%), alanine-C3 (+26%), glutamate-C4 (+52%), glutamine-C4 (+54%), gamma-aminobutyric acid (GABA)-C2 (+57%) and aspartate-C3 (+30%) in the KD group only. Homonuclear couplings on C4, C2 and C3 of glutamate were higher after ^{13}C-β-HB infusion in the KD group, suggesting greater citric acid cycle efficiency on the KD. Regardless of the infused substrate, brain GABA/glutamate was 11% higher in KD group. The branched-chain amino acids, leucine and isoleucine, accumulated in the liver and brain in the KD group but were not detected in the CTL group.

Conclusions: Under the present conditions, the KD appears to have increased both glycolysis and citric acid cycle activity in the brain. The increase in liver leucine and isoleucine on the KD could in part be the result of metabolic competition between hepatic metabolism of branched chain amino acids and free fatty acids, because both are ketone precursors. Higher brain GABA/glutamate could contribute to the mechanism by which the KD is neuroprotective and reduces seizures in epilepsy.

Acknowledgements: Supported by the FRQS, NSERC, CFI, CRC and Université de Sherbrooke Research Chair (SCC), CFQCU program of the FQRNT and INAF. AKBS was supported by a public grant from the French “Agence Nationale de la Recherche” within the context of the Investments for the Future Program, referenced ANR-10-LABX-57 and named TRAIL.

757
BRAIN-0583
Poster Session

Molecular Mechanisms

AGONISTS OF PROTEASE-ACTIVATED RECEPTOR-1 MODULATE CELL DEGENERATION FROM RAT BRAIN.

L. Gorbacheva[1], I. Savinkova[1], S. Strukova[2], G. Reiser[3]
[1]Physiology, Pirogov Russian National Research Medical University, Moscow, Russia
[2]Human and animals physiology, Lomonosov Moscow State University, Moscow, Russia
[3]Institut Inflammation und Neurodegeneration, Otto-von-Guericke-Universität Medizinische Fakultät, Magdeburg, Germany

Ischemic and hemorrhagic stroke, traumatic brain injury accompanied by glutamate (Glu)-induced toxicity, as well as the appearance in the brain tissue of thrombin and activated protein C (APC) as a result of damage to the vessel wall and the blood-brain barrier permeability disorders.
Objectives. The aim of this study was to investigate the effect of thrombin, APC as endogenous agonists of PAR-1 and new synthetic peptide-agonist of PAR-1 on the function of cultured neurons and astrocytes of rat brain in toxic conditions.
Methods. In this study neuronal and astrosytic cultures from rat brain were used. Western blot, immunocytochemistry and immunoassay were used for detection of protein levels in cells. Cell survival was estimated by morphological and biochemical methods.
Results. We have shown that thrombin in high (50 nM) concentrations causes the death of more than 30% of neurons (compared with control), comparable to the Glu-excitotoxicity. Pre-incubation of cells with APC (1-10 nM) abolished the neuronal death induced by thrombin as well as toxic effects of Glu. Moreover, the thrombin concentration of 1-10 nM prevented apoptosis induced by Glu. Analysis of the proliferation of cultured astrocytes revealed that increasing concentrations of thrombin activates cell proliferation dose-dependent manner. The pretreatment cell cultures with APC blocked this effect of thrombin. It is known that pro-inflammatory effect on endothelial cells is realized through translocation to the nucleus of the transcription factor NF-kB. We have shown that both Glu and thrombin at high toxic concentrations caused translocation of NF-kBp65 into the nucleus of neurons. APC protects neurons and reduces the level of NF-kBp65 in the nucleus. The receptor mechanism of action of these proteases was investigated using specific blocking antibody to the protease-activated receptor-1 and 3 (PAR-1 and PAR-3) and endothelial protein C receptor (EPCR). We have shown that the action of both thrombin and APC realizes via PAR-1. The protective effect of APC requires the participation of its own receptor - EPCR. It is known that activation of PAR-1 occurs through proteolytic cleavage of its N terminus, revealing a tethered ligand sequence that binds intramolecularly to the receptor to trigger transmembrane signaling PAR-1. Because the APC protective effect requires the both PAR1 and EPCR receptors, and not one as in the case of thrombin and direction of the effect of these proteases is different, we believe that, despite the involvement of PAR-1 in action both proteinases, the result of activation this receptor is probably due to the activation of various intracellular signaling pathways. "Biased agonism" for PARs (Mosnier et al., 2012) was described on endothelial cells. We supposed that this mechanism is present in neurons and astrocytes of rat brain. New synthetic peptide, analogous to tethered ligand of PAR-1 released by APC, was tested on these cell cultures. We found that effect of peptide-agonist of PAR-1 has effects similar to APC action.
Conclusions. Thus, the activation of PAR-1 by thrombin and APC led to different results on brain cells, which were depended from concentrations of protease and type of tethered ligand of PAR-1 released by protease.

758
BRAIN-0744
Poster Session

Molecular Mechanisms

FACTOR(S) WITHIN CEREBROSPINAL FLUID POST-STROKE CAUSE INTRACRANIAL PRESSURE TO RISE IN HUMANS AND ANIMALS

R.J. Hood[1], D.D. McLeod[1], C.L. Logan[1], D.J. Beard[1], R. Li[2], N.J. Spratt[1]
[1]School of Biomedical Sciences and Pharmacy, University of Newcastle, Newcastle, Australia
[2]Department of Neurology, Second University Hospital of Harbin Medical University, Harbin, China

Objectives: Intracranial pressure (ICP) elevation after ischemic stroke causes secondary damage. Recent data from our laboratory show a previously unrecognised, consistent, dramatic (>300%) but transient increase in ICP 24 hours after minor stroke. It also showed that edematous swelling, the previously assumed mechanism for ICP elevation in all disorders of acute neurological injury, was not the primary cause for this ICP rise. A potential alternative mechanism could involve cerebrospinal fluid (CSF) volume (a known contributor in many ICP disorders). It is known that, in response to elevated ICP, factors within CSF are produced to reduce CSF production and thus lower ICP. From this, we hypothesised that CSF factors may be altered as a result of stroke that contribute to ICP elevation. Our aim was to investigate whether post-stroke factors in CSF from our animal model influence ICP and whether there was a similar effect in clinical stroke.

Methods - Study 1: CSF was removed from stroke (3 hour middle cerebral artery occlusion/ 3 hours of reperfusion) or control (6 hours anesthesia) donor rats (n=6/group). **Study 2:** CSF was removed from stroke or hydrocephalic (control) patients (n=2/group). CSF was infused into the left lateral ventricle of naïve recipient male Wistar rats (n=16); ICP was monitored in recipients from 0-1 hours and 16-24 hours post-infusion using an epidural fibreoptic pressure sensor.

Results - Study 1: ICP increased significantly in stroke-CSF recipient rats, by 12.8 ± 16.9 mmHg (ΔICP; $p<0.05$) peaking at 17 ± 1 hours post-infusion, but did not increase in control-CSF recipients (ΔICP 2.2 ± 7.1 mmHg, peaking at 19 ± 4 hours). **Study 2:** ICP increased 16-24 hours after human stroke-CSF infusion (ΔICP 17.1 and 26.4 mmHg), but there was minimal change in those that received human hydrocephalic (control) CSF (ΔICP 1.7 and 4.6 mmHg).

Conclusions: Our results provide the first evidence that compositional changes in CSF in both humans and animals contribute to the recently identified ICP elevation 24 hours post-stroke. This novel finding has the potential to alter the current views on ICP regulation following stroke and other neurological conditions that involve raised ICP.

759
BRAIN-0279
Poster Session

Molecular Mechanisms

PRETREATMENT BY FIBRATES REDUCED M. SMEGMATIS INFECTION IN HUMAN CELLS THROUGH PPAR INDEPENDENT PATHWAY

M.H. HONG[1], S.Y. KANG[1], M.J. YOU[1], S. YI[2], K.D. SONG[3], H.K. LEE[3], S. KIM[1]
[1]Department of Biotechnology, Hoseo University, Asan, Korea
[2]Department of Biomedical Laboratory Science, Soonchunhyang University, Asan, Korea
[3]The Animal Genomics and Breeding Center, Han-Kyong National University, Anseong, Korea

Tuberculous meningitis, Mycobacterium tuberculosis infection in the meninges, which is the most common form of tuberculosis in the central nervous systmem. Mycobacterium tuberculosis exploits immune privilege to grow and divide in pleural macrophages. Fibrates are associated with immune response and control lipid metabolism through glycolysis with β–oxidation of fatty acids. In this study, we investigated the effect of pretreatment using fibrates on the immune response during M.

Smegmatis infection in U937 cells, a human leukemic monocyte lymphoma cell line. The protein expression of tumor necrosis factor α (TNFα), an inflammatory marker, and myeloid differentiation primary response gene 88 (MyD88), a toll like receptor (TLR) adaptor molecule, in the infected group increased at 1 h and 6 h after M. smegmatis infection into U937 cells. Acetyl coenzyme A acetyl transferase-1 (ACAT-1), Peroxisome proliferatoractivated receptor α (PPAR α), TNF α, and MyD88 were observed to be decreased in U937 cells treated with fibrates at 12 and 24 h after treatment. More than 24 h pretreatment with fibrate exhibited similar expression levels of ACAT-1 and PPAR α between infected vehicle control and infected groups which were pretreated with fibrate for 24h. However, upon exposure with M. smegmatis, the cellular expression of the TNF α and MyD88 in infected groups pretreated with fibrate for 24h was shown to be significantly decreased, compared to the infected vehicle group. Thus, we suggested that fibrate pretreatement reduced the occurrence of M. smegmatis infection in U937 cells through PPAR α independent pathway. Further studies need to be done to confirm the findings on pathophysiology and immune depense mechanism of U937 with fibrates during M. tuberculosis infection. This work was carried out with the support of 'Cooperative Research Program for Agriculture Science & Technology Development (Project No. PJ01104601)" Rural Development Administration, Republic of Korea.

760
BRAIN-0632
Poster Session

Molecular Mechanisms

PRIOR EXPOSURE OF DIABETIC RATS TO RECURRENT HYPOGLYCEMIA EXACERBATES CEREBRAL ISCHEMIC DAMAGE VIA INCREASED INTRA-ISCHEMIC ACIDOSIS.

A. Rehni[1], V. Shukla[1], K.R. Dave[1]
[1]Neurology, University of Miami Miller School of Medicine, Miami, USA

Objectives: Stroke and heart disease are the most serious complications of diabetes. Intensive therapy to control blood glucose not only delays the onset and progression of secondary complications of diabetes but also results in recurrent hypoglycemia (RH). Earlier, we observed increased cerebral ischemic damage in insulin-treated diabetic rats exposed to RH prior to ischemia[1]. Because exposure to hypoglycemia results in increased levels of glucose and monocarboxylic acid transporters, we tested the hypothesis that increased cerebral ischemic damage in diabetic rats exposed to RH is due to increased intra-ischemic acidosis[2,3].

Methods: Streptozotocin-induced diabetic rats were used as an animal model. Three experimental groups were examined: 1) Naïve (non-diabetic), 2) Insulin-treated diabetic (ITD), and 3) ITD + RH (diabetics on insulin therapy experiencing RH). RH was induced once a day for five days with target blood glucose level of 55 to 65 mg/dL during hypoglycemia. Global cerebral ischemia was induced by tightening carotid ligatures bilaterally following hypotension (50 mmHg) for eight minutes on the day after the last hypoglycemia treatment. pH and lactate in CA1 hippocampus were measured before, during and after global cerebral ischemia. pH was measured using a microfiber optic pH meter and lactate in microdialysate using a lactate plus meter.

Results: Ischemia resulted in increased lactate levels (n=6) and lower pH (n=5) in hippocampus of naïve rats (Fig. A-B). Percent changes in lactate concentration in animals belonging to the naïve group, when assessed 4 and 8 min after the induction of ischemia, were significantly lower at respective time points (4 min: 981% and 8 min: 334%) in ITD + RH rats (n=6). Lactate level in the ITD group (n=5) were significantly lower than in ITD + RH group. Lactate level remained higher in the ITD + RH group compared to naïve and ITD groups between 20-75 min post-ischemia (Fig. A). The drop in pH during ischemia in animals belonging to naïve (n=5) and ITD groups (n=5) was

significantly lower when compared to ITD + RH group (n=5) from 7 minutes after induction of ischemia to 38 minutes after the onset of reperfusion (Fig. B).

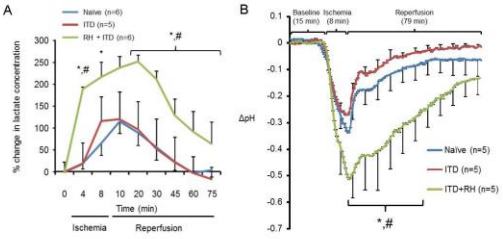

Figure 1: The effect of ischemia on hippocampal (CA1) lactate (A) and pH (B) in ITD+RH rats. Hippocampal (CA1) pH (Δ pH) versus time curve of rats belonging to three experimental groups. *, p<0.05 vs naive + ischemia; #, p<0.05 vs ITD + ischemia.

Conclusions: These results suggest that increased lactate production and larger drop in extracellular pH during and after ischemia may be responsible for increased cerebral ischemic damage in ITD + RH rats. Understanding the mechanism by which RH exposure increases cerebral ischemic damage may help lower the severity of ischemic damage in diabetic patients.

References: 1) Stroke. 2011; 42(5): 1404-11; 2) J Neurochem, 1999. 72(1): p. 238-47; 3) J Mol Neurosci. 2007;31(1):37-46.

Acknowledgement: This study was supported by NIH (NS073779).

761
BRAIN-0661
Poster Session

Molecular Mechanisms

TARGETING PROTEIN INTERACTIONS LINKING NEURONAL ENERGY METABOLISM AND ACUTE AND CHRONIC NEURODEGENERATION

P. Mergenthaler[1], *D.W. Andrews*[1]
[1]*Biological Sciences,*
Sunnybrook Research Institute University of Toron to, Toronto, Canada

Neurons are intolerant of inadequate energy supply in either an acutely or chronically disturbed metabolic environment. The high energy demand of the brain predisposes it to a variety of diseases if energy supplies are interrupted. Here, we investigate the intricate connection of glucose metabolism and the regulation of cell death pathways for neuronal viability or neuronal degeneration.

We have developed a novel biophysical cell-based imaging tool to study biochemistry in live neurons to expedite research on acute and chronic neurodegenerative diseases that is amenable to combined chemical biology screening and RNAi mediated protein knock-down analyses in neurons.

We have previously characterized the glucose phosphorylating enzyme hexokinase II (HKII) as a crucial regulator of neuronal fate after metabolic disturbances. As a prototypic mechanistic example of the interdependence of these major cellular pathways, we hypothesize that disturbed regulation of the protein interaction network of HKII promotes neurodegeneration. Thus, we investigate the molecular pathophysiology of neuronal cell death after metabolic impairment.

This research will permit mechanistic insight into the role of HKII in controlling neuronal survival and death in acute and chronic neurodegeneration. At the same time, we envision that this specific mechanism will provide paradigmatic insight into the regulation of neuronal fate through disturbed glucose metabolism, thus allowing exploitation of the glucose metabolism pathways for novel treatment approaches of stroke and neurodegenerative diseases.

762
BRAIN-0538
Poster Session

Molecular Mechanisms

INVESTIGATING METAL BINDING AND THE RESULTING CONFORMATIONAL CHANGES AND AGGREGATION OF MONOMERIC WILD-TYPE ALPHA-SYNUCLEIN AND A PHOSPHORYLATION MIMIC

A.R. Paskins[1], *C.F. Dalton*[1], *C.J. Duckett*[1], *D.P. Smith*[1]
[1]*Biomedical Research Centre, Sheffield Hallam University, Sheffield, United Kingdom*

Objectives: Alpha-synuclein is a 14.5 kDa intrinsically disordered protein, whose oligomerisation and fibrillisation into amyloid-like aggregates has been implicated in the development of Parkinson's disease and other so-called synucleinopathies. In Parkinson's disease, aggregated α-synuclein forms deposits termed Lewy bodies in the *substantia nigra pars compacta* which are heavily phosphorylated and have been demonstrated to be metal rich in Cu, Zn and Fe[1]. Phosphorylation is increased in synaptic enriched areas of the frontal cortex in the absence of Lewy bodies in early stage disease, suggesting this occurs before the formation of the amyloid aggregates. Structurally α-synuclein is known to populate both extended and more collapsed conformational states, and these states can be observed using Electrospray-ionisation-Ion Mobility Spectrometry-Mass Spectrometry (ESI-IMS-MS). Population of the more collapsed state has been linked to increased amyloid formation. Environmental conditions, such as the presence of cofactors including polyvalent metal ions, are known to increase the population of this collapsed state and hence modulate fibril formation[2]. Little is known however, as to how post-translational modifications affects the interaction of α-synuclein with these modulators and the subsequent conformation state of the full length protein.

Methods: Native and mutant α-synuclein was produced recombinantly in *E.coli*. Post-translational modification mimics (Ser87 to Asp and Ser129 to Asp) were introduced by site directed mutagenesis. ESI-IMS-MS was performed to determine the conformation of the monomeric state through determination of collisional cross sectional areas. These states were then compared with known model structures, and relative populations of the conformational states both apo and metal-bound determined. Immunocytochemistry was performed on untreated and metal-treated SHSY5Y and SHSY5Y (A53T) cell lines using antibodies to both native and phosphorylated α-synuclein to determine both the extent of phosphorylation and the effect of polyvalent metal ions on localisation and aggregation of α-synuclein *in vitro*.

Results: We demonstrate that apo wild-type and mutant α-synuclein co-populates expanded conformational states in conjunction with a range of more collapsed conformations. Binding of divalent metal ions such as Cu^{2+} and Fe^{2+} ions to the protein shifted the conformational equilibrium towards the more collapsed conformational states. Wild-type α-synuclein bound 1 Cu^{2+} ion to the expanded state whereas the compact states bound to 2 ions. In the presence of Fe^{2+}, both the expanded and compact conformations bound a single ion. Preliminary investigations into S129D mutant α-synuclein suggest that metal binding is unaltered, with the same number of metal ions binding to the same conformational states. *In vitro*, the presence of polyvalent metal ions induces aggregation of native α-synuclein, with preliminary results suggesting intracellular aggregated proteins are not phosphorylated.

Conclusions: Native and phospho-mimicked α-synuclein monomers bind a single Cu^{2+} or Fe^{2+} ion to extended conformations and a bind further Cu^{2+} ion to more compact conformations. Mimics of phosphorlayion do not appear to affect the ability of the protein to bind metal ions. *In vitro* results suggest that phosphorylation is not

required for intracellular aggregation in the presence of high metal concentrations.

References:

1. Lee *et al.,* (2014) *Nat Rev Neurol* **10**,92-98

2. Wright & Brown.,(2008) *J. Neurosci. Res* **86**,496-503

763
BRAIN-0057
Poster Session

Molecular Mechanisms

TRANSMISSION ELECTRON MICROSCOPY OF RETINAL PIGMENT EPITHELIUM IN VIGABATRIN-TREATED MICE: ENHANCED MITOCHONDRIAL NUMBERS ASSOCIATED WITH GABA-ELEVATION AND HOMOCARNOSINE-DEPLETION

K. Vogel[1], E.W. Jansen[2], G.S. Salomons[2], K.M. Gibson[1]
[1]Experimental and Systems Pharmacology, Washington State University, Spokane, USA
[2]Clinical Chemistry, VU University Medical Center, Amsterdam, Netherlands

Objectives

The antiepileptic drug (AED) vigabatrin (VGB, g-vinyl GABA; Sabril[R]; LundbeckCorp.) elevates central nervous system gamma-aminobutyric acid (GABA) viairreversible inhibition of GABA-transaminase, the enzyme penultimate to succinicsemialdehyde dehydrogenase (SSADH) in GABA metabolism. VGB is employed as monotherapy for infantilespasms and adjuvant therapy for secondary generalized and complex partialseizures, and it is historically employed in patients with inherited SSADHdeficiency. Unfortunately, VGB has awell-defined retinal toxicity that significantly impacts its long-termuse. In recent work we documented that rapamycin(sirolimus; an mTor inhibitor) alleviated anomalies of mitophagy in the SSADH-deficientmouse, the latter manifesting elevation of GABA (Lakhani et al 2014). In the current study we investigated whether asimilar pathophysiological mechanism between VGB-induced GABA elevations and mitochondrialabnormalities exist and whether mTor inhibition can alleviate these abnormalities.

Methods

We administered VGB (35 and 250 mg/kg/d) and VGB plus Torin1 (5 mg/kg/d) to mice for 7 days collecting tissues for biochemical andtransmission electron microscopy (TEM) analysis. GABA and homocarnosine were quantified byisotope dilution mass spectrometry, and redox parameters (malondialdehyde(MDA), glutathione (GSH)) determined using spectrometric assays. TEM micrographs taken at 5.0K magnificationwere analyzed to quantify mitochondrial abundance in the retina, liver,parietal cortex, and hippocampus.

Results

VGB induced a dose-dependent increase in GABA in the brainand eye, and brain homocarnosine analysis revealed that VGB-relatedGABA-elevation inversely correlated with the level of homocarnosine (Pearsonr=-0.73, $p<0.0001$; Figure 1). TEMmicrographs (5.0K resolution) revealed significantly increased mitochondrialabundance along the retinal pigmented epithelium (vehicle 60 $\pm$ 20 mitochondria/micrograph;VGB (35 mg/kg) 73$\pm$18; $p<0.01$; Figure 2). Mitochondria were also significantly elevated in hippocampus and liverof VGB-treated subjects. MDA levels were3.1-fold elevated with VGB intervention ($p<0.05$) and total GSH levels showeda trend toward depletion in eye, indicative of oxidative stress associated withenhanced mitochondrial number.

Conclusion

We addressed the hypothesis that rapalog intervention (mTorinhibition) would counteract GABA-associated mitochondrial elevations throughapplication of torin 1 (5 mg/kg) concomitantly with VGB (35 mg/kg) for 7days. Although torin 1 did not improvemitochondrial accumulation in the eye or

liver, it corrected this accumulationin the hippocampus. Our data highlightthe potential of adjuvant rapalog intervention with VGB that couldsignificantly mitigate the retinal toxicity of this AED and significantlyimprove its safety and utility profile.

References

Lakhani R,Vogel KR, Till A, Liu J, Burnett SF, Gibson KM, Subramani S. Defects in GABAmetabolism affect selective autophagy pathways and are alleviated by mTORinhibition.EMBO Mol Med. 2014 Apr;6(4):551-66. doi: 10.1002/emmm.201303356.Epub 2014 Feb 27.

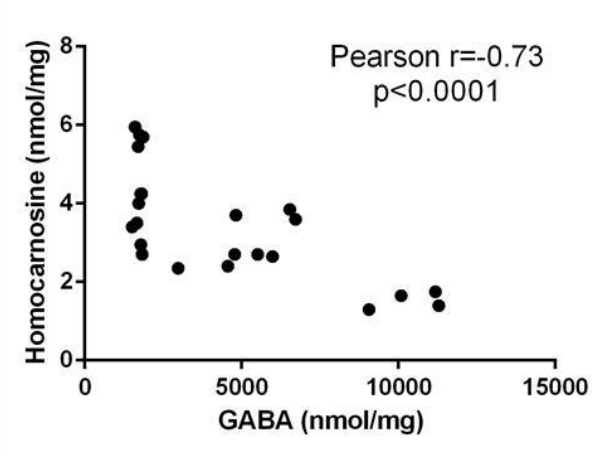

Figure 1. Correlation between GABA and homocarnosine in total brain extracts of VGB-treated mice

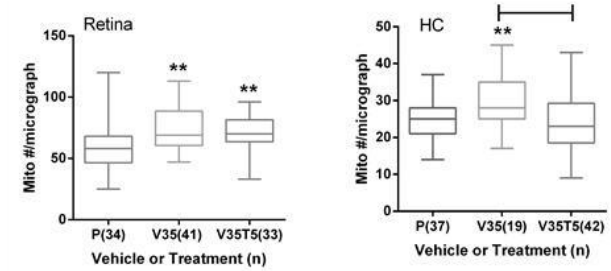

Figure 2. Average mitochondrial number in 5.0K micrographs for vehicle, VGB 35 mg/kg/d, and VGB and Torin 5 mg/kg/d groups in the retina and hippocampus (number of micrographs counted in parentheses)

764
BRAIN-0089
Poster Session

Pharmacology and Therapeutics

PHARMACOKINETIC EVALUATION AND METABOLITE IDENTIFICATION OF THE GHB RECEPTOR ANTAGONIST NCS-382 IN MOUSE AND HUMAN: TOWARDS A NOVEL THERAPY FOR SUCCINIC SEMIALDEHYDE DEHYDROGENASE DEFICIENCY.

G.R. Ainslie[1], *K.R. Vogel*[1], *K.M. Gibson*[1]
[1]*Experimental and Systems Pharmacology, Washinton State University, Spokane, USA*

Objectives. Gamma hydroxybutyric acid (GHB), anendogenous metabolite formed from gamma-aminobutyric acid (GABA), is an agonisttowards both GHB and $GABA_B$ receptors. GHB is elevated during illicitdrug use and in patients with heritable succinic semialdehyde dehydrogenase(SSADH) deficiency, a disorder of GABA metabolism. NCS-382 (6,7,8,9-tetrahydro-5-hydroxy-5H-benzo-cyclohept-6-ylideneaceticacid) is a known GHB receptor antagonist and candidate treatment for SSADHdeficiency, however little is known about NCS-382 pharmacokinetics and metabolism.The goal of the present work was to obtain*in vivo* pharmacokinetic data in a murine model and to identify NCS-382metabolites formed by rodents and humans.

Methods. NCS-382 (100 mg/kg) was administeredintraperitoneally **(i.p.) to mice** (n=3 per time point). Mice were sacrificed from 0-24 hand serum, liver, kidney and brain were harvested. Serum and tissues werequantified for NCS-382 using a robust UPLC-MS/MS assay, and pharmacokineticoutcomes were obtained. Incubations of NCS-382 (20 µM) were conducted in livermicrosomes derived from human (HLM), rat (RLM) and mouse (MLM). Theidentification of NCS-382 metabolites detected in mouse serum and *in vitro* incubations was conducted on anAB

Sciex 6500 QTrap mass spectrometer controlled with LightSight® software(v2.3).

Results. NCS-382 wasquantifiable in liver (0.5-2 h), kidney (0.5-4 h), brain (0.5-8 h) and serum(0.5-2 h) following i.p. administration (100 mg/kg), although the lower limitof quantification varied slightly for each matrix. The maximal observed serumconcentration (C_{max}) was 52 µg/ml. Tissue to serum concentrationratios were determined for brain (B:S=0.11), kidney (K:S=0.22), and liver(L:S=3.16) using the observed C_{max} of each tissue relative to serum.Several key oxidative and conjugated metabolites were identified in mouse serum,including two oxidative (m/z, 233.1) and dehydrogenated (m/z, 215.1) speciesand at least one glucuronide conjugate (m/z, 393.1) indicating diverse mechanismsof metabolic clearance.

Conclusions. In wild-typemice, NCS-382 is absorbed and eliminated within 8 hours following a 100 mg/kgi.p. dose and, importantly, is readily measurable in the brain indicating itdoes cross the blood brain barrier. Several metabolites were identified inrodent and human systems which will facilitate future toxicological evaluationof NCS-382.

References.

CastelliMP, Pibiri F, Carboni G, Piras AP. A review of pharmacology of NCS-382, aputative antagonist of gamma-hydroxybutyric acid (GHB) receptor. *CNS Drug Reviews*. 10(3): 243-260.

Acknowledgement: The general financial support of the SSADHAssociation (www.ssadh.net) is gratefully acknowledged

765
BRAIN-0403
Poster Session

Pharmacology and Therapeutics

TARGETED TEMPERATURE MANAGEMENT WITH A1 ADENOSINE AGONISTS IN CONJUNCTION WITH AMBIENT TEMPERATURE CONTROL IN RATS

I. Bailey[1], C. Murphy[1], K. Drew[1], L. Bogren[2]

[1]Institute of Arctic Biology & Department of Chemistry,
University of Alaska Fairbanks, Fairbanks, USA
[2]SOM-Cell and Devopmental Bio,
University of Colorado Denver - Anschutz Medical Campus, Fairbanks, USA

Objective: The decreased metabolism and body temperature (T_b) of hibernating mammals may offer increased protection from ischemia/reperfusion injury. Through A_1 adenosine receptor (A_1AR) agonists, targeted temperature management may offer similar injury resistance in non-hibernating species. N^6-cyclohexyladenosine (CHA) induces a torpor-like state in rats, but gives variable responses when rats are fed ad lib and carries cardiovascular risks. Capadenoson (CAP), a partial A_1AR agonist carries lower cardiovascular risks and is anticipated to elicit similar effects as CHA. This study focuses on applying surface temperature modulation in conjunction with these adenosine agonists to test the hypothesis that therapeutic hypothermia temperature targets will be obtained rapidly in rats. Metabolites are examined in the liver & brain to determine metabolite profile during or after torpor response.

Methods: IACUC approved procedures were used to instrument adult, male Sprague-Dawley rats (n=10), with IP iButton dataloggers (Maxim Integrated, San Jose, CA). T_b was monitored at 10min intervals, Heart rate was monitored every 2h using a Littmann© Model 4000 electronic stethoscope (3M, St. Paul, MN) and Beat Counter app (http://vetapps.co.uk). Treatments (vehicles, 1mg/kg CHA; 1 and 2 mg/kg CAP, IP) were administered per a balanced block design with 1 week between tests.

Results: A single injection of CHA decreased T_b by 1°C to 17°C below physiological temperatures and Heart rate drops by 12 to 80% with effects lasting from 1 to 24h. Capadenoson gave more consistent responses at the cost of magnitude of response with T_b and HR drops of 1.3 and 1.6°C and 24 and 30% for 1 and 2mg/kg doses. All rats returned to baseline levels without evidence of

stress indicated by porphyrin accumulation around the eyes.

Conclusions: The rapid drop of body temperature upon treatment with CHA indicates that activation of A_1 adenosine receptors could be an alternative method of administering therapeutic hypothermia to invasive cooling methods. However in contrast to expectations, full and partial A_1AR agonist's affects differed in terms duration and magnitude on T_b in rats. The variation in response to CHA indicates additional factors are involved in adenosine A1 receptor activation.

766
BRAIN-0304
Poster Session

Pharmacology and Therapeutics

MONOACYLGLYCEROL LIPASE INHIBITORS REDUCE INFARCT VOLUME AND IMPROVE FUNCTIONAL OUTCOME IN A RAT MODEL OF FOCAL CEREBRAL ISCHEMIA

S.H. Choi[1], A. Arai[2], A.C. Silva[1]
[1]Laboratory of Functional and Molecular Imaging, National Institute of Neurological Disorders and Stroke, Bethesda, USA
[2]School of Medicine, University of Maryland, Baltimore, USA

Objectives: Preclinical stroke studies have led to the development of neuroprotective approaches aimed at decreasing lesion volume and improving functional outcome. Monoacylglycerol lipase (MAGL) is a primary enzyme responsible for hydrolyzing the endocannabinoid 2-arachidonoylglycerol to arachidonic acid and glycerol. Here, we have studied the effects of selective MAGL inhibitors in a rodent model of focal cerebral ischemia.

Methods: The right sensorimotor cortex of adult male spontaneously hypertensive rats (SHR) and their normotensive Wistar-Kyoto (WKY) controls was lesioned by a local intracortical injection of endothelin-1 (ET-1, 2 µg), a potent vasoconstrictor peptide. JZL184 (40 mg/kg, i.p.) or MJN110 (20 mg/kg, i.p.) was administered either 60 min before (n = 8) or 60 min after (n = 6) ET-1 application. Infarct volume, hemispheric swelling, and functional outcomes were assessed between day 1 to day 28 by magnetic resonance imaging and behavioral tests. Neuronal loss and inflammatory response were studied using histology, real-time PCR, and ELISA.

Results: ET-1 induced a reproducible and pronounced ischemic lesion, extending from the primary sensorimotor cortex to as far back as the primary visual cortex, and caused significant functional deficits in the contralateral forelimb. Both pre- and post-treatment of MAGL significantly attenuated infarct volume and hemispheric swelling. MAGL inhibition also ameliorated sensorimotor deficits, suppressed inflammatory response, and decreased degenerating neurons.

Conclusions: Our results suggest that MAGL, which regulates endocannabinoid signaling and prostaglandin production, contributes to neuropathology of cerebral ischemia, and thus is a promising therapeutic target for the treatment of ischemic stroke. We are currently working on determining the molecular mechanisms underlying these beneficial effects of MAGL inhibitors.

References: Long JZ et al (2009) Nat Chem Biol 5:37-44; Nomura DK et al (2011) Science 334: 809-813; Niphakis MJ et al (2013) ACS Chem Neurosci 4:1322-1332.

767
BRAIN-0138
Poster Session

Pharmacology and Therapeutics

NARINGIN REVERSES MEMORY DEFICITS AND RESTORES DECREASED PHOSPHO-GSK3B IN THE HIPPOCAMPUS IN INTRACEREBROVENTRICULAR STREPTOZOTOCIN INDUCED ALZHEIMER'S DISEASE MODEL.

M. Golechha[1], J. Bhatia[1], U. Chaudhry[2], D. Saluja[2], D. Arya[1]
[1]Pharmacology,
All India Institute of Medical Sciences, New Delhi, India
[2]Department of Biomedical Sciences,
University of Delhi, New Delhi, India

Introduction: Intracerebroventricular streptozotocin (ICV-STZ) treated rats have been described as a suitable model for sporadic Alzheimer's disease (AD). Central application of STZ has been demonstrated to induce behavioral and neurochemical features that resemble those found in human AD.

Objectives: Chronic treatments with antioxidants, acetylcholinesterase (AChE) inhibitors, or glucose utilization improving drugs have shown beneficial effects in ICV-STZ treated rats. Therefore, the present study was undertaken to investigate the effects of naringin, a bioflavonoid with potent antioxidant and anti-inflammatory activities on memory functions, brain insulin receptors (IRs), AChE activity, and oxidative stress in intracerebroventricular (ICV) administered streptozotocin (STZ) induced dementia in rats. In these animals, the phosphorylated GSK3β (p-GSK3β) and total GSK3β levels were determined. GSK3β regulates the tau phosphorylation responsible for neurofibrillary tangle formation in AD.

Methods: Wistar rats received ICV-STZ application (3mg/kg twice), and naringin administered for 2 weeks, and after that short- (STM) and long-term memories (LTM) were assessed in an autoshaping learning task. Animals were sacrificed immediately following the last autoshaping session, their brains removed and dissected. The enzymes and IR protein levels were measured in the hippocampus and prefrontal cortex (PFC) by western blotting.

Results: ICV-STZ treated rats showed a memory deficit and significantly decreased p-GSK3β levels and IR protein levels in both the hippocampus and PFC, while total GSK3β did not change, in either the hippocampus or PFC. Memory impairment was reversed by naringin (40 and 80 mg/kg). The p-GSK3β and IR protein levels were restored by naringin in the hippocampus and PFC. Total GSK3β levels did not change with naringin treatment. Furthermore, STZ (ICV) resulted in enhanced AChE activity and MDA levels accompanied with decrease in GSH levels in the hippocampus and PFC, which were normalized by naringin.

Conclusion: Altogether, these results show the beneficial effects of naringin via different mechanisms of action on memory impairment induced by ICV-STZ. The results suggest that besides its anticholinesterase and antioxidant activity, its effects on brain IR and p-GSK3β levels, a kinase key signaling cascade of insulin receptors, may also be important factors in the protective effect of naringin on STZ induced dementia.

768
BRAIN-0333
Poster Session

Pharmacology and Therapeutics

RAPAMYCIN RESTORES CEREBRAL BLOOD FLOW AND BLOOD BRAIN BARRIER INTEGRITY IN COGNITIVELY HEALTHY APOE4 CARRIERS

A. Lin[1], V. Galvan[2], A. Richardson[3]
[1]Sanders-Brown Center on Aging,
University of Kentucky, Lexington, USA
[2]Physiology,
University of Texas Health Science Center at San A ntonio, San Antonio, USA
[3]Geriatric Medicine,
University of Oklahoma Health Science Center, Oklahoma City, USA

Objectives:

The ε4 allele of the apolipoprotein E gene (APOE4) is the major genetic risk factor for Alzheimer's Disease (AD). Cross sectional studies in healthy APOE4 carriers show that cerebrovascular dysfunction was observed in carriers years before any clinical changes in memory occur, suggesting that cerebrovascular dysfunction is an initial event in AD. Restoration of cerebrovascular integrity is thus critical to slow down the progression of AD. We have recently showed that rapamycin, an anti-aging intervention, can restore cerebral blood flow (CBF), vascular density and memory in rodents modeling human AD (1). In the study, we will determine whether rapamycin administered before memory decline will restore cerebrovascular functions in mice expressing the human APOE4 gene.

Methods:

One month old of female wild-type (WT, C57BL/6, N= 6) and Tg APOE4 mice (N= 12) were purchased from the Jackson Laboratory. All WT and six of the APOE4 mice were fed with control diet, whereas the other six APOE4 mice were fed with 14 ppm rapamycin (APOE4-Rapa). Diet was given for 6 months. MR experiments were performed on a Bruker 7T magnet. CBF MRI was acquired using a continues arterial spin labeling technique and was measured longitudinally on each mouse at 1 (baseline), 2, 4, and 7 month of age. We used manganese (Mn)-enhanced MRI to determine blood brain barrier (BBB) integrity at final time point (7 mo) as Mn would not penetrate BBB in normal condition. Manganese (II) chloride tetrahydrate from Sigma-Aldrich was dissolved in saline and injected intraperitoneally. BBB integrity was determined be comparing the impaired and normal area (ratio) of certain brain region. We used Morris Water Maze to test the mice's memory (N = 15 per group) at 7 months of age. We used one-way, repeated measures ANOVA to determine the difference of the measured indices between the three groups. Post-hoc testing was performed by Newman-Keuls test.

Results:

One month old of APOE4 mice showed significant reduction (20%) in CBF compared to the WT (baseline measurement). With rapamycin treatment, however, APOE4 mice began to show restored CBF in one month. The treatment efficacy was more prominent over time - the CBF in APOE4-Rapa were significantly higher than those of APOE4 controls, but had no difference compared to that of WT after 6 months of treatment. Without rapamycin, APOE4 mice showed BBB impairment in temporal lobe, the area highly associated with AD pathology. The BBB integrity has also been restored by rapamycin, with 45% reduction of impairment area relative to the non-treated group. Despite the cerebrovascular dysfunctions found in the young control APOE4 mice, they did not show significant cognitive impairments at 7 months of age, compared with WT and APOE4-Rapa groups.

Conclusion:

We used multi-metric MRI Methods to demonstrate that rapamycin can restore vascular integrity in transgenic APOE4 mice before they had cognitive impairment. Preserved cerebrovascular functions are crucial for cognitively healthy APOE4 carriers to

prevent/slow down the onset of AD. Rapamycin shows promise for future prevention and treatment of AD.

References:

(1) Lin et al., JCBFM, (2013) 33:1412-21

769
BRAIN-0402
Poster Session

Pharmacology and Therapeutics

ANGIOTENSIN RECEPTOR BLOCKER CANDESARTAN AS A POTENTIAL THERAPEUTIC TREATMENT IN A MOUSE MODEL OF ALZHEIMER'S DISEASE

L.J. Trigiani[1], L. Zhang[1], X.K. Tong[1], Y. Papadopoulos[1], J. Royea[1], E. Hamel[1]
[1]Montreal Neurological Institute, McGill University, Montreal QC, Canada

Background: Current pharmacological treatments improve symptoms of Alzheimer's disease (AD) yet lack disease-modifying effects. Accumulating evidence supports the association between vascular disease and AD (1, 2), making the renin-angiotensin system a therapeutic pathway of interest. Given the success of the angiotensin receptor blocker (ARB) losartan (3) in rescuing cerebrovascular and cognitive deficits in an AD mouse model, we investigated whether other ARBs reap the same benefits to establish if losartan has a drug-specific effect or if it is a therapeutic property of this family of compounds.

Objective: We examined the potential therapeutic benefits of the ARB candesartan in an AD mouse model that carries the Swedish and Indiana familial mutations of the human amyloid precursor protein (APP mice, line 20).

Methods: APP mice and wild-type (WT) littermate controls (4-5 months) were implanted subcutaneously with osmotic minipumps that delivered vehicle or candesartan (0.3mg/kg/day) for 2 months. Spatial learning and memory were assessed in a Morris water maze (MWM) (4) following each month of treatment. After the second MWM, one group was used for measuring the cerebral blood flow (CBF) response evoked by whisker stimulation using laser Doppler flowmetry. Subsequently, vascular reactivity was tested in isolated and pressurized segments of the posterior cerebral artery using online videomicroscopy. Mice from the second group were perfused, and their brains were processed for quantitative histo- and immunohistochemical analyses of astrogliosis and amyloid β (Aβ) plaque load.

Results: Candesartan-treated APP mice performed similarly to WT controls on the last day of learning, and there was a small trend towards improved performance in the probe trial of the second MWM. These mild cognitive benefits in candesartan-treated APP mice were not accompanied by rescue of the evoked CBF response, or by normalized endothelium-dependent dilation to acetylcholine. Similarly, the basal vascular production of nitric oxide was not restored. As seen with losartan, candesartan failed to reduce Aβ plaque load in the cortex and hippocampus as measured by Thioflavin S and 6E10 immunohistochemistry. Cortical astrogliosis measured by immunostaining for glial fibrillary acidic protein was significantly attenuated by candesartan. Furthermore, there was a decrease in levels of the antioxidant enzyme manganese superoxide dismutase, a marker for oxidative stress, albeit non-significantly.

Conclusions: Although there were slight cognitive improvements, and reduced neuroinflammation and oxidative stress in brain tissue, cerebrovascular function was not restored after 2 months of candesartan administration. Despite both drugs being selective angiotensin II type 1 receptor antagonists, our findings suggest either a need for longer treatment time or candesartan may not be as promising a therapeutic avenue as losartan for patients with vascular diseases at high risk of developing AD.

References: (1) Lee C W. et al., (2014). ***Current Alzheimer Research,*** *11*, 4; (2) de la Torre JC (2010). ***Ageing Res*** *Rev 9* (3), 218; (3) Ongali B. et

al., (2014). ***Neurobiology of Disease**, 68*, 126; (**4**) DeIpolyi A R et al., ***Neurobiology of Aging**. 29, 253.*

Acknowledgements: Supported by grants from the Canadian Institutes of Health research (CIHR, MOP-126001) and the Heart and Stroke Foundation of Québec.

770
BRAIN-0072
Poster Session

Pharmacology and Therapeutics

SYNERGISTIC USE OF GENIPOSIDE AND GINSENOSIDE RG1 BALANCE MICROGLIAL TNF-A AND TGF-B1 FOLLOWING ISCHEMIC INJURY

J. wang[1], H. lei[2], H.U.I. zhao[3]
[1]experiment center,
Institute of Basic Theory China Academy of Chines e Medical Sciences, Beijing, China
[2]morphology,
The Experimental Research Center China Academy of Chinese Medical Sciences, Beijing, China
[3]Research Department,
China Academy of Chinese Medical Sciences, Beijing, China

Objectives

Ischemia-activated microglia are like a double-edged sword, characterized by both neurotoxic and neuroprotective effects. Activated microglia can threaten the survival of neural cells through release of proinflammatory and cytotoxic factors, including tumor necrosis factor (TNF)-α, interleukin (IL)-1β and IL-6 [1,2]. Activated microglia have also been reported to possess neuroprotective/neurotrophic by the production of anti-inflammatory cytokines such as IL-10 and transforming growth factor (TGF)-β, which have neuroprotective effects in traumatic injury and stroke [3,4]. Microglial cells are the major source of TNF-α and TGF-β1. In this paper, we compared the single pair of proinflammatory cytokine (TNF-α) and anti-inflammatory cytokine (TGF-β1) changes in microglia treated in combination or individually with geniposide and ginsenoside Rg1. We also detected the whole genome-wide mRNA of OGD-injured microglia to explore the synergic effect of geniposide and ginsenoside Rg1.

Methods

BV2 microglial cells were divided into 5 groups: control, oxygen–glucose deprivation, geniposide-treated, ginsenoside-Rg1-treated, and combination-treated. A series of assays was used to detect the effects of geniposide and ginsenoside Rg1 on: (i) cell viability via the Cell Counting Kit-8; (ii) NO content by Griess Reagent; (iii) expression (content) of TNF-α and TGF-β1 by western blotting (ELISA); and (iv) gene expression profiles by next-generation sequencing technology.

Results

Compared with the model group, we observed an obvious improvement in cell viability after co-treatment with geniposide and ginsenoside Rg1, which was prior to ginsenoside Rg1 or geniposide monotherapy. Compared with the model group, there was a marked reduction in NO release after combination of geniposide and ginsenoside Rg1 ($p < 0.01$), which was prior to geniposide or ginsenoside Rg1 monotherapy ($p < 0.05$).(Figure 1)

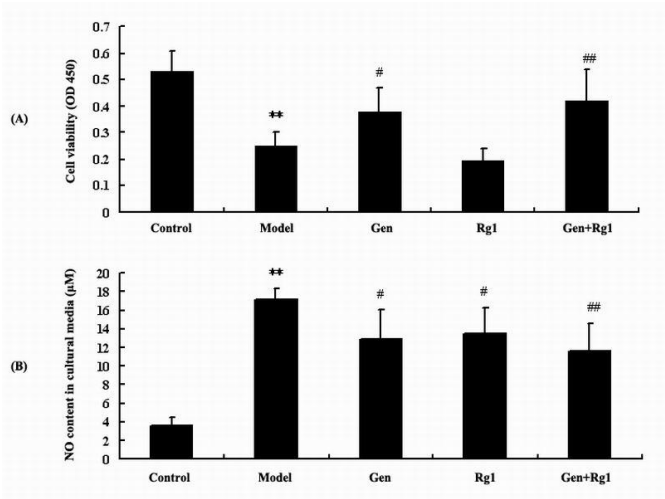

TNF-α content was markedly reduced in the culture media after co-treatment with geniposide and ginsenoside Rg1 ($p < 0.01$), which was prior to geniposide or ginsenoside Rg1 treatment alone ($p < 0.05$). As for TNF-α expression, the effect of co-

treatment with geniposide and ginsenoside Rg1 was the same as geniposide treatment alone, with an obvious reduction. The protein level and expression of TGF-β1 in the geniposide group were unaffected relative to the model group. However, ginsenoside Rg1 monotherapy increased TGF-β1 expression and content significantly ($p < 0.05$), with the same effect as combination of geniposide and ginsenoside Rg1. (Figure 2)

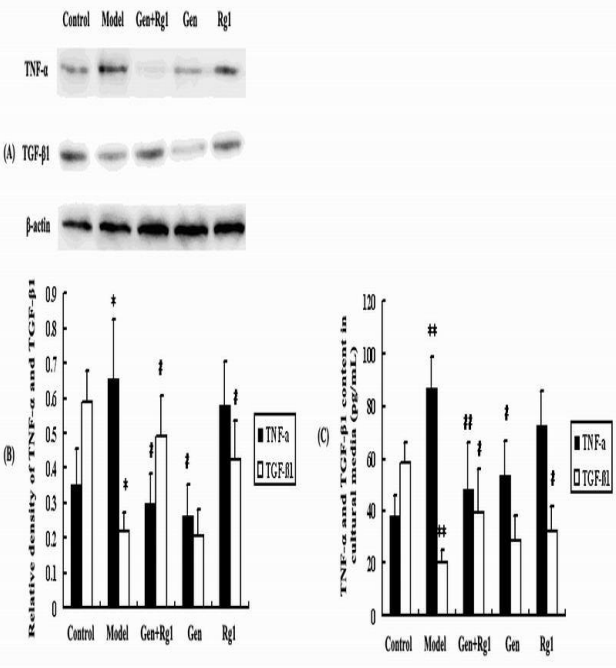

Most of the genes in the TNF-α pathway in the control and geniposide individual group were clustered, which indicated that the expression patterns of the 2 groups were similar to a certain extent. In the TGF-β pathway, the expression pattern of the ginsenoside Rg1 individual group was more similar to that of the control group. Next-generation sequencing also showed that the Fcg-receptor-mediated phagocytosis pathway played a key regulatory role in the balance of TNF-α and TGF-β1 when co-treated with geniposide and ginsenoside Rg1. (Figure 3)

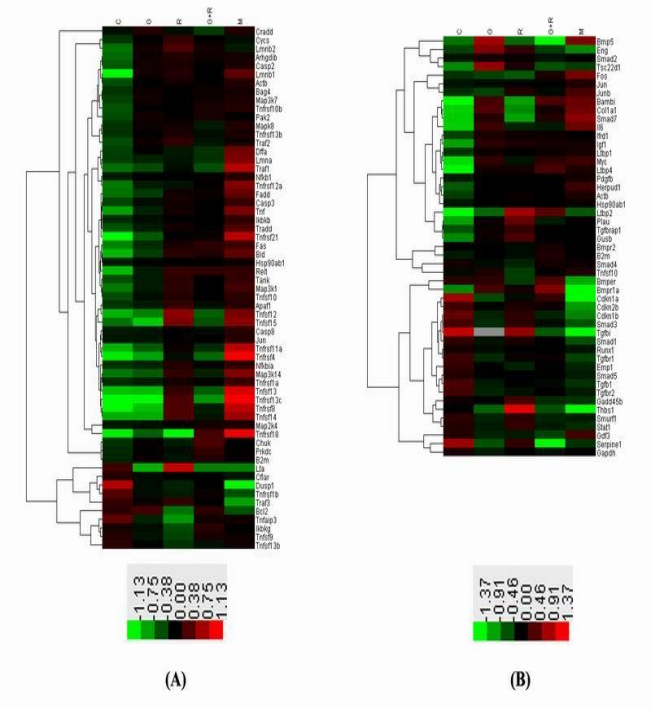

Conclusions

Our findings indicate that combined use of geniposide and ginsenoside Rg1 has a synergistic effect, which is mainly characterized by the balance of proinflammatory cytokine TNF-α and anti-inflammatory cytokine TGF-β1. This synergistic effect may correlate with the most clearly changed genes and the FcgR-mediated phagocytosis pathway.

771
BRAIN-0282
Poster Session

Stem cells and Cell Therapy

RELATIONSHIP BETWEEN INTRA-ARTERIAL ADMINISTRATION OF STEM CELLS, BIODISTRIBUTION AND ANIMAL SURVIVAL

F. Campos[1], B. Argibay[1], M. Pérez-Mato[1], I. López-Loureiro[1], R. Iglesias[1], M. Santamaría[1], T. Sobrino[1], J. Castillo[1]
[1]Neurology, Hospital Clínico Universitario-Clinical Neurosciences Research Laboratory, A Coruña-Santiago de Compostel, Spain

Objective: Stem cell therapy in ischemic stroke has lately shown promising results of functional recovery in preclinical studies; however specific parameters as administration route and cell dose are still under discussion. In this way, intra-arterial delivery (i.a.) has the potential advantage of reach the ischemic brain region more efficiently than intra-venous (i.v.) administrations where most of the cells remain trapped in peripheral organs. However, several preclinical studies have already reported the high mortality associated to this route. Thus, the main goal of this work was to find out the optimal cell dose and the most efficient and the safest protocol for i.a. delivery of mesenchymal stem cells in an animal model of ischemic stroke by studying the *in vivo* distribution of superparamagnetic nanoparticles labeled cells.

Methods: Mesenchymal Stem Cells (MSCs) were purchased from Cultrex, Trevigen and labeled with home-made dextran coated superparamagnetic nanoparticles. Animal model of ischemic stroke was induced by a transitory intraluminal occlusion of the middle cerebral artery (tMCAO) in rats. Different doses ($0.25x10^6$ and $1x10^6$) of labeled MSCs were tested with different combinations of i.a. administration through the ipsilateral carotid (**Table 1**). Cells were administered at 4 hours after ischemic onset. Magnetic resonance imaging (9.4T horizontal bore magnet Bruker BioSpin, Ettlingen, Germany) was performed to assess the territory affected by the occlusion and to study the cell biodistribution by T2* weighted images.

Results: We have observed that doses higher to $0.25x10^6$ cells induce multifocal injuries in brain that can interfere with the beneficial effect of the cell treatment. Administration of cells, following the protocol *d* (see **Table 1**) allows a uniform cell distribution along the brain after i.a. delivery (**Figure 1**). All animals survived after the injection following this procedure (n=14). Meanwhile other configurations of arteries occlusions led to the localization of labeled cells in the cerebellum, several multifocal ischemias or low efficiency of brain targeting (**Figure 2**).

Conclusions: Intra-arterial (i.a.) delivery has the potential advantage of selectively targeting cell therapies to the ischemic brain tissue. However we have observed that i.a. injection of cells carries some risk of reduction in cerebral blood flow and microstrokes. In this study we have elucidated the main pitfalls of the i.a. delivery of stem cells by labeling the injected cells with superparamagnetic nanoparticles and tracking them in MRI. We have described the safest and most efficient model of ischemic stroke combined with i.a. administration of MSCs in rat.

Table 1

Conditions	Con-CC closed during tMCAO	Ip-CC is opened from MCA reperfusion till the injection	Ip-CC is opened during the injection	Ip-CC remains opened after the injection
a	Yes	No	No	No
b	Yes	No	Yes	Yes
c	Yes	Yes	Yes	Yes
d	No	Yes	Yes	Yes

Con-CC: Contralateral Common Carotid Artery

Ip-CC: Ipsilateral Common Carotid Artery

tMCAO: transient Middle Cerebral Artery Occlusion

Figure 1: MR T2* weighted images of 3 brain slices 4h after intraarterial delivery of MSCs labeled with dextran coated superparamagnetic nanoparticles.

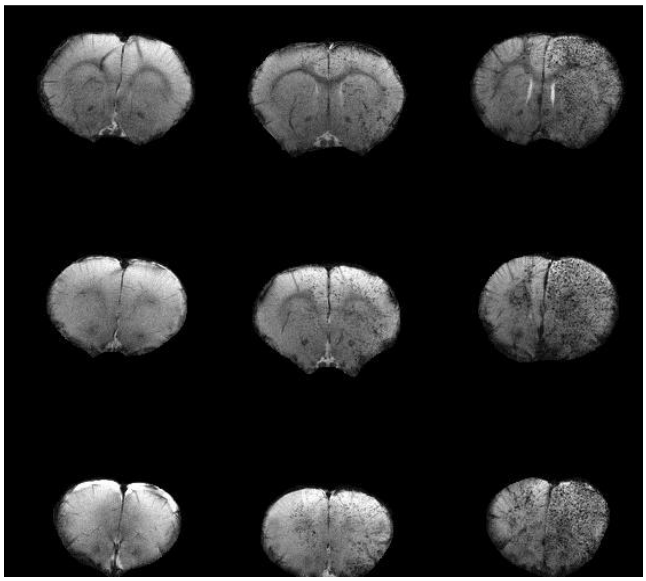

Figure 2: MR T2 weighted images of several brain slices 24h after the cell delivery with microstrokes

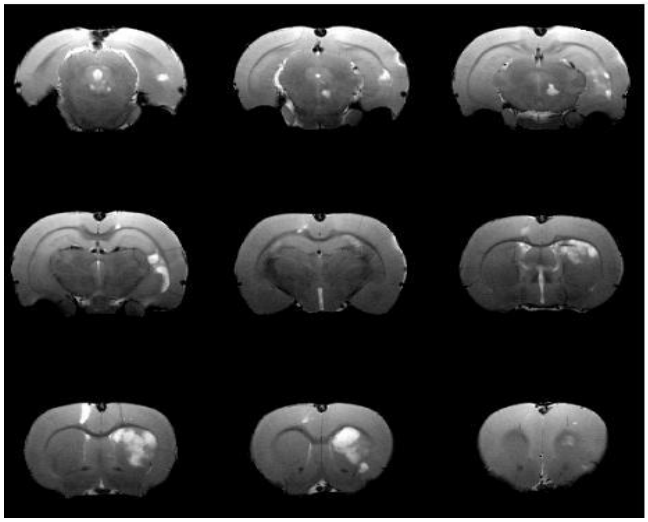

772
BRAIN-0760
Poster Session

Stem cells and Cell Therapy

HUMAN AMNION EPITHELIAL CELLS REDUCE INFARCT VOLUME, SPLENIC ATROPHY AND LUNG INFLAMMATION FOLLOWING ISCHEMIC STROKE IN MICE.

M.A. Evans[1], C.V. Gardiner-Mann[1], R. Lim[2], E.M. Wallace[2], G.R. Drummond[1], C.G. Sobey[1], B.R.S. Broughton[1]
[1]Department of Pharmacology, Monash University, Clayton, Australia
[2]The Ritchie Centre, Monash Institute of Medical Research, Clayton, Australia

Objectives: Outcome following ischemic stroke can be greatly influenced by the extent of brain injury and the occurrence of bacterial infections. These infections occur most frequently in the lungs and are promoted by a phenomenon known as post-stroke immunosuppression. Stem cells offer great therapeutic potential for stroke patients as they can target multiple injury mechanisms and cell types with appropriate timing and mediator concentrations. Human amnion epithelial cells (hAECs), which are a placental-derived stem cell, have been shown to have regenerative and reparative properties and thus the aim of this study was to examine the effect of hAECs on both brain injury and systemic immunosuppression following stroke.

Methods: Ischemic stroke was induced by 1 h middle cerebral artery occlusion-reperfusion in male C57BL6/J mice (7-12 weeks). Mice were injected with $1x10^6$ hAECs or saline (vehicle) i.v. at 0.5 h after reperfusion. Hanging grip and parallel rod tests assessed motor function and coordination at 24 h (n = 8-10 per group) or 72 h (n = 9 per group) after stroke. Mice were subsequently euthanized and cerebral infarct volume, splenic atrophy, splenocyte apoptosis and lung inflammation were assessed. Sham-operated mice served as controls.

Results: After 24 h, mice treated with hAECs had a smaller infarct volume than vehicle-treated mice (hAECs: 27±6 mm^3 vs. vehicle: 47±7 mm^3, $p<0.05$), improved coordination (sham: 7±1, vehicle: 208±98, hAECs: 125±40 foot slips/m traveled) and hanging grip time (hAECs: 46±16 s vs. vehicle: 9±3 s). After 72 h, mice treated with hAECs also had decreased infarct volume (hAECs: 26±5 mm^3 vs. vehicle: 51±9 mm^3, $p<0.05$), less foot slips (sham: 8±1, vehicle: 62±28, hAECs: 8±5 /m) as well 50 % less mortality. In addition, hAEC treatment blunted the stroke-induced reduction

in spleen weight:body weight ratio which occurred only 72 h post-stroke. Despite no change in spleen weight at 24 h post-stroke, the number of cleaved caspase-3 (apoptotic marker) immunoreactive splenocytes was 3-fold higher than sham, but similar to sham in mice treated with hAECs. Furthermore, histological examination indicated markedly less lung inflammation at 72 h in mice treated with hAECs compared to vehicle.

Conclusions: These data indicate that hAEC treatment improves outcome following ischemic stroke by limiting both brain injury and stroke-induced systemic immunosuppression. Thus, hAECs may be a viable therapy for neuroprotection and for promoting recovery of the immune system following ischemic stroke.

773
BRAIN-0063
Poster Session

Stem cells and Cell Therapy

MYOBLAST-MEDIATED CO-DELIVERY OF VEGF AND PDGF AFTER EXPERIMENTAL ENCEPHALOMYOSYNANGIOSIS IMPROVES COLLATERALIZATION AND FUNCTIONAL OUTCOME IN A MODEL OF CHRONIC CEREBRAL HYPOPERFUSION

N. Hecht[1], A. Marushima[1], J. Woitzik[1], R.G. Barrera[2], A. Banfi[2], G. von Degenfeld[3], P. Vajkoczy[1]
[1]Neurosurgery, Charité Berlin, Berlin, Germany
[2]Institute for Surgical Research and Gene Therapy Group, University Hospital Basel, Basel, Switzerland
[3]Baxter Laboratory for Stem Cell Technology, Stanford University, Stanford, USA

Objectives

The myoblast-mediated transfer of angiogenic genes is a cell-based approach for induction of therapeutic collateralization.[1] In chronic cerebral hypoperfusion, we recently demonstrated successful implantation and fusion of primary monoclonal mouse-myoblasts in the non-ischemic temporal muscle of an experimental encephalomyosynangiosis (EMS)[2] with hemodynamic rescue and improved collateralization through myoblast-mediated supplementation of vascular endothelial growth factor-A (VEGF).[3] However, blood vessel stability depends on the coordinated and balanced interaction of multiple signaling pathways in the endothelial and perivascular cells. In the present study, we therefore investigated the effect of myoblast-mediated co-delivery of platelet derived growth factor-BB (PDGF) in addition to VEGF supplementation in an EMS mouse model of chronic cerebral hypoperfusion.

Methods

Monoclonal mouse myoblasts expressing a reporter gene alone (control) or in combination with VEGF, PDGF or VEGF/PDGF were implanted into the temporal muscle of an EMS before permanent ipsilateral ICAO in C57/BL6 mice. Exogenous gene factor expression was confirmed by real-time PCR and western blot analysis. Hemodynamic impairment was quantified by laser speckle imaging and cerebrovascular reserve capacity (CVRC) measurements throughout the observation period of 84 days. On days 21, 42 and 84, transpial collateralization, vessel density and vessel maturity at the muscle/brain interface of the EMS were assessed by in-vivo FITC-lectin perfusion and immunohistochemical staining. Further, cortical stroke volume and neuronal cell death after 60-minute MCAO and 23-hour reperfusion were determined by MRI and immunohistochemical analysis.

Results

By day 21, co-expression of VEGF/PDGF resulted in an improved CVRC (VEGF/PDGF 37±15%; PDGF 27±8%; VEGF 30±11%; control 24±10%; $p<0.05$ for VEGF/PDGF vs. day 0), which was paralleled by significantly improved microvascular remodeling and higher pericyte coverage (VEGF/PDGF 68±11%; PDGF 63±9%; VEGF 47±6%; control 50±5%; $p<0.05$ for VEGF/PDGF vs. VEGF and control) of the collateral and parenchymal vasculature at the target site of VEGF/PDGF

supplementation. Functional and morphological findings were in line with an attenuated cortical stroke volume (VEGF/PDGF 34±12%; PDGF 47±13%; VEGF 41±12%; control 50±10%; $p<0.05$ for VEGF/PDGF vs. control) and decreased neuronal cell death (NeuN cells: VEGF/PDGF 391±145/mm^2; PDGF 239±88/mm^2; VEGF 189±119/mm^2; control 181±95mm^2; $p<0.05$ for VEGF/PDGF vs. all groups).

Conclusions

The myoblast-mediated co-delivery of VEGF and PDGF after indirect experimental revascularization improved morphological and functional outcome compared to delivery of VEGF alone. In the future, an appropriate translational approach could facilitate indirect revascularization procedures in patients suffering from chronic cerebral hypoperfusion with better protection from ischemic stroke.

References

1. Ozawa CR, Banfi A, Glazer NL, Thurston G, Springer ML, Kraft PE, et al. Microenvironmental VEGF concentration, not total dose, determines a threshold between normal and aberrant angiogenesis. J Clin Invest. 2004 Feb;113(4):516–27.

2. Hecht N, Peña-Tapia P, Vinci M, Degenfeld von G, Woitzik J, Vajkoczy P. Myoblast-mediated gene therapy via encephalomyosynangiosis--a novel strategy for local delivery of gene products to the brain surface. J Neurosci Methods. 2011 ed. 2011 Sep 30;201(1):61–6.

3. Hecht N, Marushima A, Nieminen M, Kremenetskaia I, Degenfeld von G, Woitzik J, et al. Myoblast-mediated gene therapy improves functional collateralization in chronic cerebral hypoperfusion. Stroke. 2015 Jan;46(1):203–11.

774
BRAIN-0150
Poster Session

Stem cells and Cell Therapy

STEREOTACTIC TRANSPLANTATION OF STROMAL CELL-DERIVED FACTOR-1 GENE MODIFIED ENDOTHELIAL PROGENITOR CELL EFFECTIVELY ATTENUATED ISCHEMIC BRAIN INJURY IN MOUSE MODEL

Y. Li[1], G. Tang[1], Y. Liu[2], S. Chang[1], G.Y. Yang[1], Y. Wang[1]
[1]Med-X Research Institute, Shanghai Jiao Tong University, Shanghai, China
[2]Department of Neurology Ruijin Hospital, Shanghai Jiao Tong University, Shanghai, China

Objectives: Our previous work showed that post-acute gene therapy with chemokine stromal cell-derived factor 1 (SDF-1, also known as CXCL12) promoted both neurogenesis and angiogenesis after ischemic stroke.[1] Transplantation of endothelial progenitor cells (EPC) alone was also beneficial for ischemic stroke recovery.[2] In this work we used SDF-1 gene modified EPC (EPC-SDF-1) to further explore the benefit of this stem cell-combined gene therapy strategy in treating ischemic stroke.

Methods: Thirty-eight adult ICR male mice received EPC-SDF-1, EPC-GFP, LV-SDF-1, or PBS through stereotactic injection into the peri-infarct area one week after MCAO. Brain atrophy, neurobehavioral scores and immunohistochemistry properties were examined to evaluate the effects of EPC-SDF-1 on angiogenesis, neurogenesis, and neurological function, comparing to EPC cell or SDF-1 gene therapy alone.

Results: Brain atrophy was significantly reduced in both gene and cell therapy groups 5 weeks after ischemia ($p<0.05$; vs. PBS; n=6), with a further reduced brain atrophy in EPC-SDF-1 group ($p<0.01$; vs. LV-SDF-1; vs. EPC-GFP). The results of neurobehavioral tests including modified neurological severity score (mNSS) and rotarod test were consistent with the result of brain

atrophy, with neurological function improved in all therapeutic groups (p<0.001; vs. PBS; n=8-11), and with the best outcome observed in EPC-SDF-1 group (p<0.05; vs. LV-SDF-1; vs. EPC-GFP). The number of $CD31^+$ and $CD31^+/BrdU^+$ blood vessels in peri-infarct area was significantly increased in all therapeutic groups (p<0.05; vs. PBS; n=4), with more $CD31^+$ blood vessels in EPC-SDF-1 group (p<0.01; vs. LV-SDF-1; vs. EPC-GFP; n=4) and more $CD31^+/BrdU^+$ blood vessels in EPC-SDF-1 group comparing to EPC-GFP group (p<0.05; n=4). The number of $DCX^+/BrdU^+$ neural progenitor cells was also enhanced in all groups both in the subventricular zone (SVZ) and peri-infarct area (p<0.05; vs. PBS; n=4), with significantly more $DCX^+/BrdU^+$ cells in the SVZ in EPC-SDF-1 group (p<0.05; vs. LV-SDF-1; vs. EPC-GFP; n=4). The number of $NeuN^+/BrdU^+$ neurons was also significantly increased in all therapeutic groups (p<0.05; vs. PBS; n=4). *In vitro* data also showed that EPC-SDF-1 cells exhibited higher ability for tube-formation (p<0.01; vs. EPC-GFP; vs. EPC; n=3) and proliferation (p<0.001; vs. EPC-GFP; vs. EPC; n=3). Western blot data also showed that EPC-SDF-1 cells also secreted more VEGF.

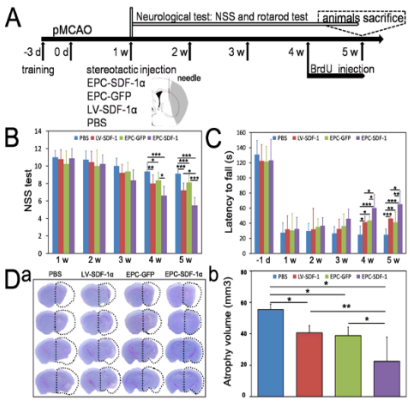

Figure 1: EPC-SDF-1α transplantation improved neurobehavioral outcomes and reduced ischemia-induced brain atrophy. (**A**) Experimental design. Bar graphs summarized the result of mNSS evaluation (**B**) and rotarod test (**C**) in PBS, LV-SDF-1α, EPC-GFP, and EPC-SDF-1α groups (n = 8-11/group). (**D**) Representative photomicrographs of coronal sections stained by cresyl violet (**a**) and quantification of brain atrophy (**b**) (n = 6/group). Data were presented as mean ± SD, *p<0.05, **p<0.01, and ***p<0.001.

Conclusions: Our results demonstrated that transplantation EPC-SDF-1 significantly increased angiogenesis and neurogenesis, reduced brain atrophy, and improved the neurological outcomes of experimental mice after ischemic stroke. Moreover, EPC-SDF-1 enhanced tube-formation, proliferation and VEGF secretion in cell model, suggesting that SDF-1 gene modification of EPC can further promote the therapeutic efficacy in the treatment of ischemic stroke.

References：

1. Li Y, *et al. Stroke* 2014; 45(6)**:** 1822-9.
2. Fan Y, *et al. Ann Neurol* 2010; 67(4)**:** 488-97.

775
BRAIN-0327
Poster Session

Stem cells and Cell Therapy

WHITE MATTER REPAIR AFTER ADIPOSE TISSUE-DERIVED MESENCHYMAL STEM CELL ADMINISTRATION IN SUBCORTICAL ISCHEMIC STROKE

M. Gutierrez-Fernandez[1], L. Otero-Ortega[1], J. Ramos-Cejudo[1], B. Rodríguez-Frutos[1], B. Fuentes[1], M.T. Vallejo-Cremades[1], T. Sobrino[2], T. Navarro-Hernanz[3], F. Campos[2], E. Medina[1], E. Díez-Tejedor[1]

[1]Department of Neurology and Stroke Center Neuroscience and Cerebrovascular Research Laboratory, La Paz University Hospital Neuroscience Area of IdiPAZ Health Research Institute Autónoma University of Madrid, Madrid, Spain

[2]Department of Neurology Clinical Neurosciences Research Laboratory, Hospital Clínico Universitario Health Research Insti

tute of Santiago de Compostela (IDIS) University o f Santiago de Compostela,
Santiago de Compostela, Spain
[3]Laboratory for Imaging and Spectroscopy by Mag netic Resonance,
Institute of Biomedical Research Alberto Sols, Madrid, Spain

Objectives: Stem cell therapy has demonstrated itsefficacy in cortical ischemic stroke and may have a positive effect onsubcortical lesions with white matter injury (axon and myelin damage). The aimof this study was to investigate white matter repair after adipose tissue-derivedmesenchymal stem cell (ADMSC) administration in an experimental model of ischemicsubcortical stroke.

Methods: An animal model of subcortical ischemic stroke with white matteraffectation was induced in 48 male Sprague-Dawley rats (200-250 g) by injectionof Endothelin-1. At 24h, $2x10^6$ ADMSC were administered (IV) by thetail vein to the treatment group. ADMSC migration and implantation to the brainwere analyzed. Functional evaluation, lesion size, fiber tract integrity, celldeath, cellular proliferation, white matter markers implicated in brain repair[Oligodendrocyte Transcription factor (Olig-2), Neurofilament (NF), Myelinbasic protein (MBP)] and NogoA were studied at 7d and 28d.

Results: Neither ADMSC migration nor implantation to the brain were observedafter IV ADMSC administration. On the other hand, ADMSC implantation wasdetected in peripheral organs such us liver, lung and spleen. Treated groupshowed a smaller functional deficit and lesion area, less cell death, moreoligodendrocyte proliferation as well as higher amount of myelin formation and morewhite matter connectivity. The treated animals also showed higher levels ofwhite matter-associated markers in the lesion area than the controls.

Conclusion: The conclusion of this study was that ADMSCtreatment improved functional recovery associated with white matter integrity mediatedby brain repair mechanisms (remyelination, axonal sprouting andoligodendrogenesis) after subcortical ischemic stroke.

This study was supported by research grants PS12/01754, INVICTUS SpanishNeurovascular Network RD12/0014/0006 and Research Institute Carlos III,Ministry of Science and Innovation of Spain.

776
BRAIN-0418
Poster Session

Stem cells and Cell Therapy

SPATIOTEMPORAL RESPONSE OF NEURAL PROGENITORS IN THE ADULT SUBVENTRICULAR ZONE TO EXOGENOUS GROWTH FACTOR STIMULI.

T. OCHI[1], H. NAKATOMI[1], A. ITO[1], N. SAITO[1], S. OKABE[2], M. NAKAFUKU[3]
[1]Neurosurgery,
Graduate School of Medicine The University of Tok yo, Tokyo, Japan
[2]Cellular Neurobiology,
Graduate School of Medicine The University of Tok yo, Tokyo, Japan
[3]Developmental Biology,
Cincinnati Children's Hospital Research Foundatio n, Cincinnati, USA

Objectives
We have previously demonstrated anatomical and functional neuroregeneration in the ischemic brain by recruitment of endogenous neural progenitors with the intraventricular infusion of growth factors (GFs). Now, there is cumulative evidence that this approach is feasible as a method of brain repair. However, outcomes of studies of GF treatment are often divergent and sometimes disappointing. Then optimizing conditions to induce the maximal response of endogenous progenitors by exogenous GF stimuli is an important issue.

Methods
We performed time-course analysis to investigate the changes in the cell profile of the subventricular zone (SVZ) in intact adult male C57/BL6J mice administered an intraventricular

infusion of high-dose growth factor (EGF) and fibroblast growth factor-2 (FGF2) for different durations. First, we treated animals with GF for 0-14 days and investigated the response of SVZ progenitors and neuroblasts soon after the therapy. For that purpose, we used the following antibodies: Tuj1, Ki67, Pax6, Sox2. Second, we treated animals with GF for 7 or 14 days. Then, animals were allowed to survive 2, 6, 10 and 28 days after the end of the therapy and were investigated in the same manner. Finally, we labeled progenitors with BrdU and tracked them in the olfactory bulb and SVZ.

Results

EGF/FGF2 therapy promoted proliferation of SVZ progenitors up to 200% of the control level. Interestingly GF therapy arrested neuroblast production, an effect that was sustained as long as EGF/FGF2 therapy was continued. Withdrawal of EGF/FGF2 led to differentiation of the proliferated SVZ progenitors into neuroblasts with a transient but significant increase up to 150% of the control level.

Conclusions

Our study revealed the mechanism of action underlying the effects of GF treatment. Our findings can help to achieve the maximal response of endogenous progenitors to in vivo GF treatment.

777
BRAIN-0191
Poster Session

Stem cells and Cell Therapy

TRANSPLANTATION OF NEURAL STEM CELLS THAT OVEREXPRESS SOD1 ENHANCES AMELIORATION OF NEURONAL DAMAGE FROM INTRACEREBRAL HEMORRHAGE IN MICE

T. Wakai[1], H. Sakata[2], P. Narasimhan[2], H. Yoshioka[1], Y. Fukumoto[1], K. Kanemaru[1], T. Yagi[1], H. Kinouchi[1], P. Chan[2]
[1]Neurosurgery, Yamanashi University, Chuo, Japan
[2]Neurosurgery, Stanford University, Stanford, USA

Objectives- Previous studies have shown that intraparenchymal transplantation of neural stem cells (NSCs) ameliorates neurological deficits in animals with intracerebral hemorrhage (ICH). However, massive grafted cell death following transplantation, possibly caused by a hostile host brain environment, lessens the effectiveness of this approach. We focused on the effect of oxidative stress against grafted NSCs and hypothesized that conferring antioxidant properties to transplanted NSCs may overcome their death and enhance neuroprotection after ICH. Copper/zinc-superoxide dismutase (SOD1) is a specific antioxidant enzyme that counteracts superoxide anions. We investigated whether genetic manipulation to overexpress SOD1 enhances survival of grafted NSCs and accelerates amelioration of ICH.

Methods - To assess whether SOD1 enhances NSCs survival when exposed to hemoglobin (Hb), NSCs were obtained from fetal mouse striata and exposed different doses of Hb to induce cell death. Cytotoxicity was estimated by measurements of mitochondrial viability (WST-1 assay) and assed with calcein acetoxymethyl and ethidium homodimer-1 staining (LIVE/DEAD assay). The oxidative stress was assessed with *in situ* detection of oxidized hydroethidine (HEt). To study the effectiveness of SOD1 overexpress in NSCs, NSCs with SOD1 overexpression or wild-type stem cells were grafted into the parenchyma 3 days after ICH (induced by autologous blood injection). To observe the carbonyl proteins as indicators of oxidative protein damage in grafted NSCs, 2,4-dinitrophenylhydrazone, and 2,4-dinitrophenyl (DNP) derivatized carbonyl proteins were detected by immunostaining with an anti-DNP biotinylated antibody staining 2 days after transplantation. Striatum size was measured to evaluate atrophy, and surviving neurons in the striatum were counted 35 days after hemorrhagic insult. Neurological evaluation was performed 1, 3, 7, 14, 21, 28 and 35 days after hemorrhagic insult.

Results- Cell viability was significantly higher in the SOD1 NSCs compared with the wild-type NSCs after exposure to Hb ($n = 6$, $p < 0.05$). This cytoprotective effect in the SOD1 NSCs was confirmed by LIVE/DEAD assay, where there was a significant decrease in death (11.9 ± 7.0%)

compared with the wild-type NSCs (32.9 ± 5.9%) (n = 5, p < 0.001). After exposure to Hb, wild-type NSCs showed a significant increase in HEt staining, which indicates production of superoxide anions. This signal was significantly reduced in the SOD1 NSCs (n = 5, p < 0.001). When the wild-type NSCs were transplanted, fluorescence intensity of DNP drastically increased 2 days afterwards compared with NSCs transplanted into intact brains. SOD1 NSCs significantly diminished this increase (n = 5, p < 0.01). SOD1 NSCs transplantation showed a significant reduction in striatum atrophy (86±3% vs 82±4%, n=7, p<0.05) and showed an increase in surviving neurons in the striatum (73±12% vs 57±12%, n=6, p<0.05) compared with wild-type NSCs transplantation. In the SOD1 group, progressive improvement was observed 35 days after hemorrhagic insult compared with the wild-type group in behavioral recovery (n=9, p<0.05).

Conclusion- Our results suggest that enhanced antioxidative activity in NSCs improves efficacy of stem cell therapy for the hemorrhagic stroke brain.

778
BRAIN-0858
Poster Session

Stem cells and Cell Therapy

IINTRA-ARTERIAL STEM CELL TREATMENT REDUCES INJURY IN A REPRODUCTIVELY SENESCENT RAT MODEL OF STROKE

D. Yavagal[1], P. Bhattacharya[1], W. Zhao[1], A. Khan[2], J. Hare[3], M. Perez-Pinzon[4], A. Raval[4]
[1]Neurology, University of Miami, Miami, USA
[2]Interdisciplinary Stem Cell Institute, University of Miami, Miami, USA
[3]Interdisciplinary Stem Cell Institute Department o f Medicine, University of Miami, Miami, USA
[4]Cerebral Vascular Disease Research Laboratories Department of Neurology, University of Miami, Miami, USA

Objective: Stroke remains a leading cause of disability worldwide and needs new therapy. Cell therapy is emerging as a promising treatment for stroke. The intra-arterial (IA) mesenchymal stem cells (MSCs) delivery for the treatment of ischemic stroke has a high potential for clinical translation. However, studies using rat model of stroke have demonstrated that IA MSCs delivery can decrease middle cerebral artery flow, which may limit its clinical translation (*1*). Recently, our study demonstrated that the intra-arterial delivery of mesenchymal stem cell (IA MSCs) at 24h after a reversible middle-cerebral artery occlusion (MCAo) reduces the infarct volume and improves neurological score in female rats at one month post-treatment (*2*). However, an optimal time window for IA MSC therapy for stroke remains unknown. Additionally, majority of ischemic strokes in women occur after onset of menopause therefore, it is crucial that we test the efficacy of IA MSCs in reproductively senescent females consistent with STAIR recommendations. Therefore, we aimed to identify an optimum time window of IA MSCs and validate the efficacy of IA MSCs in reproductively senescent female rats.

Methods: Female Sprague–Dawley rats were exposed to MCAo for 90 min. Rats were treated with IA MSCs ($5x10^5$ cells) or phosphate-buffered saline (PBS) either at 1, 2 or 4 days after MCAo. MSCs or PBS treated rats were sacrificed at 28-30 days for infarct volume measurement using histology. To test motor function, the rotarod test was performed. Rats were trained for 3 consecutive days for the rotarod test before undergoing the MCAo procedure. The mean duration (in seconds) on the device was recorded from 3 rotarod measurements 1 day before surgery. The rats were tested at 1, 7, 15 and 28-30 days after MCAo. In a subsequent experiment retired breeder female (9–11 months) rats showing estrous acyclicity were exposed to MCAo and a day later treated with MSCs or PBS. The rats were tested for neurological and motor function as described for previous experiment and rats were sacrificed at 28-30 days for histopathological analysis.

Results: We observed significant reduction in infarct volume and improved neurological score in rats treated at 1 and 2 days, suggest that IA MSCs

is efficacious at 2-day time window. In case of reproductively senescent rats, we observed significantly lower mean infarct volume in the MSC-treated group (12 ± 3 mm^3; n=6) compared to the PBS-treated group (29 ± 7 mm^3; Mean ± SEM; n=4, p<0.05). Treatment at 1 day after MCAO with MSCs significantly improved functional recovery, as evidenced by improved rotarod test results and neurological scores at 7, 15 and 30 days (P<0.05) compared with the PBS-treated group.

Conclusions: Intra-arterial stem cell treatment reduces ischemic brain injury in reproductively senescent female rats. Validating the efficacy of IA MSC treatment using a reproductively senescent animal stroke model has a high potential for future clinical translation.

References:

1. P. Walczak *et al.*, *Stroke* 39, 1569 (May, 2008).

2. D. R. Yavagal *et al.*, *PloS one* 9, e93735 (2014).

779
BRAIN-0395
Poster Session

Stem cells and Cell Therapy

COMPARISON OF NEURAL DIFFERENTIATION BY NOGGIN ALONE OR NOGGIN PLUS SB431542

L. Ye[1]
[1]*Stroke Division,*
The Florey Institute of Neuroscience and Mental H ealth-Austin Campus, Melbourne, Australia

Objectives: Many studies focus on the pathways that specify the final neural sub-types that can be derived from human embryonic stem cells (hESC). However, few studies now compare the viability and fate of the intermediates and final cellular products produced by different initial induction methods. We compared two of the most commonly used induction methods-- Noggin and Noggin plus SB431542 (Noggin+SB). The cell growth condition, lineage differentiation, and survival rate were compared at different time points.

Methods: hESC was treated with either Noggin for 14 days, or Noggin+SB for 11 days as previously described. After one week (1w) or two weeks (2w) of proliferation as neurospheres, the cells were dissociated into single cells and seeded on 48 well plates. Neural differentiation was then induced as described previously. The cells were grown for up to 21 days. Cell samples were collected at 7, 14, 21 days *in vitro* (DIV) for immunohistochemical staining using Nestin and MAP2. Cell death was determined by propidium iodide staining. HCA-vision software was used to perform the quantification of immunohistochemical staining.

Results: hESC induced by Noggin+SB appeared to differentiate at a faster rate than the cells induced by Noggin alone. Mature clusters appeared at 4 DIV in 1w neurosphere, and 8 Div in 2w neurosphere, comparing to the Noggin, in which they appeared at 14 Div in 1w, and 21 Div in 2w. However, in the dual induction there were significantly higher cell loss, almost double, compared to the Noggin alone induction.

Regardless of which induction method was used, 2w neurospheres gave rise to a lower percentage of Nestin positive cells compared to 1w neurospheres. 2w neurospheres induction by Noggin alone generated a greater percentage of Nestin positive cells than the Noggin+SB method (6.48% vs. 0.05% respectively) did. The same trend was observed in the 1w neurospheres under the two induction methods (7.85% and 3.61% Nestin expression, respectively).

The percentage of Nestin positive cells in the 2w Noggin group decreased at a much slower rate, with 4.58% of neurons still expressing Nestin at 21 DIV. 2w neurospheres gave rise to a relatively low proportion of MAP2 positive neurons using both induction methods. Noggin+SB induction showed slightly lower expression of MAP2 (32.73%) compared to Noggin alone (40.26%) in 2w neurospheres, but a greater MAP2 expression

(62.56% compared to 48.01%) in 1w neurospheres.

Conclusions: 2w neurosphere showed a slower but steadier differentiation than 1w neurospheres in both induction methods. Noggin in combination with SB431542 caused a faster differentiation, quickly losing Nestin positive cells and forming mature cell networks at an earlier stage. However, not all of these cells contribute to MAP positive cells population. Moreover, this faster differentiation appears to lead to greater cell death following the dual induction method, suggesting Noggin alone may be the preferred induction method.

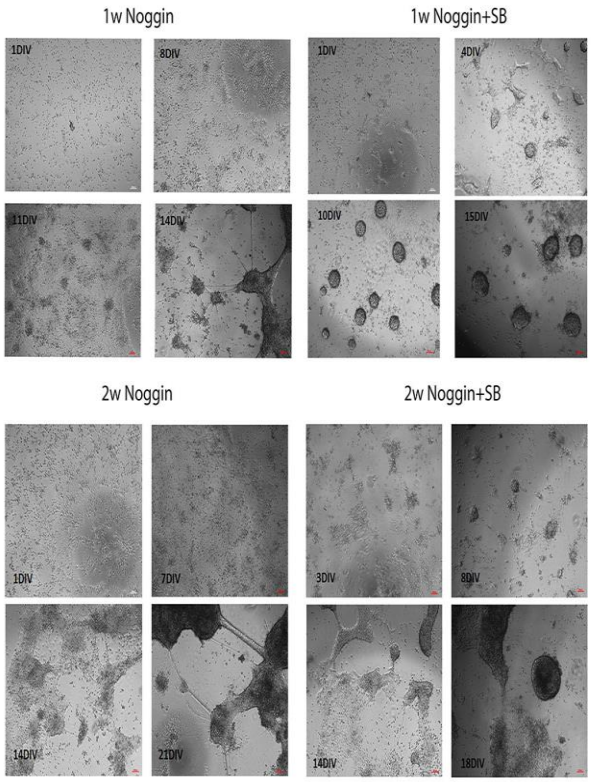

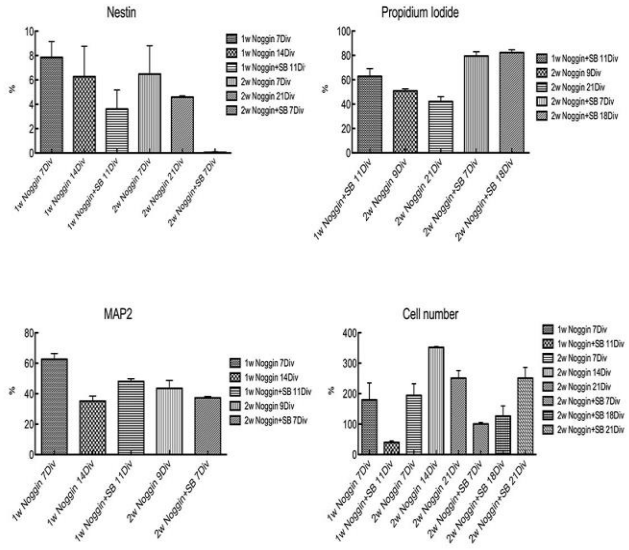

780
BRAIN-0484
Poster Session

BrainPET: Novel Radiotracers

EVALUATION AND QUANTIFICATION OF 18F-FPEB AS RADIOLIGAND FOR PET IMAGING OF THE METABOTROPIC GLUTAMATE RECEPTOR 5 IN RAT BRAIN.

B. de Laat[1], M. Koole[1], S. Celen[2], G. Leurquin-Sterk[1], G. Bormans[2], K. Van Laere[1], C. Casteels[1]
[1]Pathology and Imaging: Division of Nucleaur Medicine & Molecular Imaging, KU Leuven, Leuven, Belgium
[2]Pathology and Imaging: Laboratory for Radiopharmacy, KU Leuven, Leuven, Belgium

Objective:

^{18}F-FPEB is a negative allosteric modulator for the metabotropic glutamate receptor 5 (mGluR5), a high interest target for PET imaging in, among others, addiction and depression. We characterized the pharmacokinetics of ^{18}F-FPEB and evaluated its ability to quantify mGluR5 in rat brain.

Methods:

Nine male Wistar rats (281±18.5 g) were scanned on a FOCUS-220 system for 120 min, following a bolus injection of ^{18}F-FPEB (37.6±5.6 MBq, Specific activity > 35.0 GBq/µmol). Arterial blood samples were collected and parent intact fraction measured by HPLC to obtain the metabolite-corrected plasma input function. Blocking experiments were performed using MTEP to assess specificity (n=3). Time-activity curves were extracted for the striatum, nucleus accumbens, hippocampus, cortex, thalamus, and cerebellum. BP_{ND} ($V_T/V_{T,Ref}$ - 1) of ^{18}F-FPEB was used as outcome measure and compared to simplified methods of quantification using the cerebellum as reference region. Metabolite formation was also evaluated *in vitro* by incubation with blood, plasma and brain homogenate (n=3/condition). Additionally, *ex vivo* brain metabolite formation was assessed in perfused brain homogenates at 10, 30, 60, and 120 minutes post-injection using HPLC.

Results:

Intact ^{18}F-FPEB comprised 68 ± 7 % at 3 minutes after injection, declining to 44±9 % at 10 min, 26±6 % at 40 min, 19±5 % at 60 min, and 16±5 % at 120 min after tracer injection. ^{18}F-FPEB was metabolized into two polar radiometabolite fractions in vivo. However, metabolites were not found in neither the *ex vivo* perfused brain homogenates at any time point, nor in the *in vitro* samples of blood, plasma or brain.

PET images showed an ^{18}F-FPEB activity distribution consistent with mGluR5 localization in rat brain, including no uptake in the cerebellum (1). *In vivo* blocking studies with 20 mg/kg MTEP showed that more than 96±3% of brain activity was mGluR5 specific. A two tissue compartment model was used to determine the BP_{ND} for the striatum (11.7±1.5), nucleus accumbens (10.6±2.0), hippocampus (9.0±1.2), cortex (7.2±1.0) and thalamus (4.0±0.9). SRTM, Logan Non-Invasive, and MRTM0 were tested as reference models with BP_{ND} as outcome parameter. Time stability was evaluated for 3 scan-durations: 60, 90, and 120 minutes. Each reference model showed high correlation with the 2TC BP_{ND} (Spearman r >0.90). This was maintained for shorter scans (Figure A). For the 120 minutes data there was a significant mean underestimation of the BP_{ND} by MRTM0 (0.77), SRTM (0.66), and Logan NI (0.86), but this bias became insignificant for the shorter scan-durations. Bland-Altman analysis showed a coefficient of repeatability of 24.2 percent difference, independent of scan duration (Figure B). Test-retest studies (n=6) showed good reproducibility for MRTM0 (ICC = 0.83), SRTM (ICC = 0.86) and Logan NI (ICC = 0.81).

Conclusions:

Due to its favorable reversible kinetics, high specificity and absence of brain radiometabolites ^{18}F-FPEB seems a highly useful tracer for *in vivo* visualization of the mGluR5 in rat brain. Moreover, reference tissue models allow non-invasive rapid scanning with acceptable test-retest.

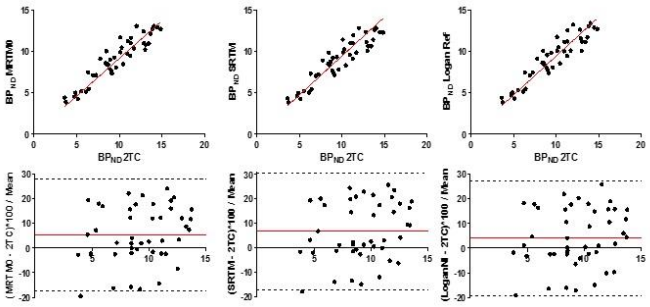

A) Correlation plot for BP_{ND} determined with a 2TC and RTMs. **B)** Bland-Altman plots showing percent difference between 2TC and reference methods.

781
BRAIN-0416
Poster Session

BrainPET: Novel Radiotracers

EFFECT OF LIGAND SIZE ON UPTAKE AND WASHOUT OF EPHA2 TARGETED THERANOSTICS FROM GLIOBLASTOMAS USING 64CU-PET

S. Puttick[1], N. Dowson[2], M. Fay[3], C. Bell[2], J. Martin[4], S. Rose[2]
[1]Australian Institute for Bioengineering and Nanot echnology, University of Queensland, Brisbane, Australia
[2]Digital Productivity, CSIRO, Brisbane, Australia
[3]Radiation Oncology,
Genesis Cancer Care Lake Macquarie Private Hosp ital, Newcastle, Australia
[4]Dept. Pharmacology, University of Newcastle, Newcastle, Australia

Objectives: The ideal theranostic would be highly specific, potent and have rapid uptake but slow diffusion from the target tissue, with the reverse for non-target tissue. Advancements with highly specific biomolecules e.g. monoclonal antibodies, have expedited development of such 'ideal' targeted theranostics. However, the large molecular weight of monoclonal antibodies presents a barrier to effective therapy as movement through selectively permeable barriers and passive transport through the extracellular matrix is reduced. Hence, new biomolecules such as recombinant proteins and peptides are being investigated. To assess the efficacy of these platforms, pharmacokinetics should be examined in vivo. In this context, three newly engineered EphA2 ligands are evaluated in terms of uptake and washout using dynamic PET imaging.
Methods: Three biomolecules that bind specifically to the EphA2 receptor (Wykosky et al. 2005) were radiolabeled with 64Cu; a monoclonal antibody (mAb, molecular weight ≈ 150 kDa) (Sliwkowski, Melman 2013), a short chain variable fragment (scFv, Mn ≈ 28 kDa) (Knowles, Wu 2012) and a peptide (YSA, Mn ≈ 2 kDa) (Koolpe, Dail, Pasquale, 2002). Each tracer was evaluated by simultaneous PET/MRI in an orthotopic mouse model of glioblastoma using the U87 cell line (Clark et al. 2010). A 60-minute dynamic PET acquisition was initiated prior to injection of the tracer. Regions of interest (ROIs) were drawn in the left ventricle of the heart, cerebrum and tumour, on an MR image and propagated to the co-registered PET image (Riveste-Henault et al. 2014). The image derived blood input function (BIF) extracted from the left ventricle was used in a voxel-wise kinetic analysis with a one-compartment model. Within each ROI voxel, the k2 parameter from the kinetic model was used to parameterise washout, and mean activity was used to parameterise uptake. Uptake and washout were compared across tissue (brain versus tumour) and ligand (YSA, scFv and mAb).
Results: The log of uptake and washout are plotted in Fig. 1. Uptake reveals that each EphA2 tracer has a higher affinity for tumour than brain and the separation increases with decreasing molecular weight, with t-values of 17 (mAb), 22 (scFV) and 31 (YSA). Rapidity of washout significantly increases as molecule size decreases (t=5.1 for YSA/scFv and t=6.0 scFv/mAb).
Conclusions: Larger molecules are expected to perfuse less easily into the tumour due to increased resistance by biological barriers in the brain, and to take longer to internalise and be processed by cells on which they bind, slowing the washout. Both mean uptake and washout of the tracers follow anticipated trends: the largest molecule (mAb) shows the lowest uptake within the first hour and the slowest washout, while the smaller molecules (YSA and scFv) show higher

uptake and faster washout. Such data is important in estimating the radiation dose potentially delivered by a theranostic. Future work will aim to increase the statistical significance of these findings through repeated experiments and to investigate the internalisation kinetics of each tracer through confocal microscopy techniques.

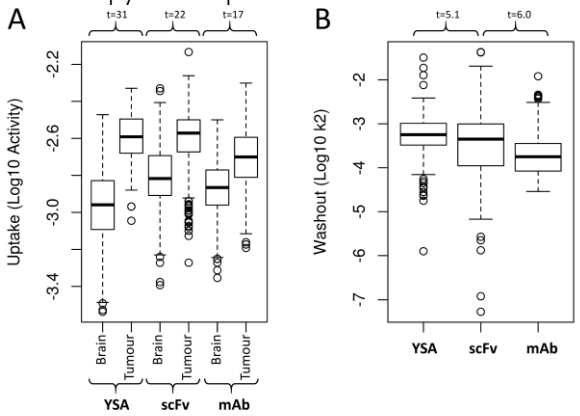

Fig. 1. Box plots of (A) uptake in brain and tumour, and (B) washout in tumour for YSA, scFv and mAb tracers.

782
BRAIN-0316
Poster Session

BrainPET: Novel Radiotracers

MAPPING MAO-B WITH FLUORINE-18 LABELED DEUTERATED FLUORODEPRENYL (18F-FLUORODEPRENYL-D2). DEVELOPMENT, IN VITRO AUTORADIOGRAPHY AND IN VIVO EVALUATION IN NON-HUMAN PRIMATES.

S. Nag[1], P. Fazio[1], M. Svedberg[1], N. Amini[1], L. Lehmann[2], G. Kettschau[2], T. Heinrich[2], S. Leesch[3], A. Catafau[3], A. Varrone[1], C. Halldin[1]
[1]Clinical Neuroscience, Karolinska Institutet, Stockholm, Sweden
[2]Global Drug Discovery, Bayer HealthCare AG, Berlin, Germany
[3]Clinical R&D Neurosciences, Piramal Imaging GmbH, Berlin, Germany

Introduction: Monoamine oxidases (MAO) are involved in the metabolismof monoaminergic neurotransmitters in the brain. Several studies reportedincreased activities of MAO-B during neurodegenerative processes such asAlzheimer and Parkinson's disease (1). Pharmacological MAO inhibition receivedrenewed attention as potential therapeutic target (2). PET biomarkers withfavorable metabolism targeting selectively and reversibly MAO-B could be ofinterest. Deuterium-substituted (D2) ^{11}C-L-deprenyl has beenintroduced to reduce the rate of radiotracer trapping (3) in the human brain. Sofar no successful fluorine-18 labeled PET radioligand have been validated forclinical use. The aim of this study was to validate pre-clinically the recentlydeveloped ^{18}F-labeled analogue of L-deprenyl, ^{18}F-fluorodeprenyl-D2, by examining i) *in vitro* it's specificity to MAO-B withautoradiography on post-mortem human brain and ii) *in vivo* the quantification of the binding to MAO-B with PET innon-human primates.

Method: The radiolabeling was accomplished by a one-step substitution reaction(**Fig 1a**). *In vitro* MAO inhibition was determined based on therate of kynuramine oxidation after block with MAO-B andMAO-A inhibitors. In vitro autoradiography binding was conducted in wholehemisphere postmortem human brain tissue. The specific inhibitors MAO-B(L-Deprenyl) and MAO-A (Pirlindol) were used to block specific binding (**Fig 1b**). *In vivo* PET imaging was performed with the HRRT system in three cynomolgusmonkeys for a total of three baselines and two pretreatment studies with 1mg/kg Deprenyl (**Fig 1c**). Regions ofInterest (ROIs) were manually delineated on coregisteredMRI and arterial input function was measured for kinetic analysis withcompartmental modeling. Models evaluation was performed with Akaike informationcriterion, Schwartz and F-Test methods. Occupancy was calculated with theLassen Plot method. Radiometabolites were measured in plasma using gradient HPLC.

Results anddiscussion: Radiolabeling was accomplishedsuccessfully. The in vitro inhibition of fluorodeprenyl-D_2 gave anIC50 of 227 ± 36.8 nM for MAO-B and >2000 nM for MAO-A activity. The autoradiographyshowed that ^{18}F-fluorodeprenyl-D2 bindingwas inhibited by saturating concentrations (10 µM) of L-Deprenyl

but not withPirlindol. In *vivo* ^{18}F-fluorodeprenyl-D2showed favorable kinetic properties with relatively fast wash-out from thebrain. Regional time activity curves were better described by the 2 TissueCompartments Model and 4 rate constants (K_1,k_2, k_3, and k_4)in all baseline conditions and in 1 pretreatment experiment (***p<0.01*** F-TEST).The MAO-B occupancy after 1 mg/Kg L-Deprenyl was 70%. Metabolite studies demonstrated 20%unchanged radioligand at 120 min post injection. A radiometabolite lesslipophilic than the parent was identified by using a reference compound. Noradiometabolites more lipohilic than the parent were observed.

Conclusion: ^{18}F-Fluorodeprenyl-D_2 binds specifically to MAO-B both *invitro* and *in vivo*. In comparisonwith previously reported MAO-B radioligands, ^{18}F-fluorodeprenyl-D2 showeda less irreversible kinetic behavior. The *invitro* and *in vivo* results suggest that ^{18}F-fluorodeprenyl-$D_2$is a suitable ^{18}F-labelled PET radioligand for visualizationof MAO-B activity in human subjects.

References:

(1) Gulyás, B et al; *Neurochem Int.* **2011**;58(1):60-8.

(2) ZhengH et al; *J Alzheimers Dis*. **2012**;30(1):1-16.

(3) Fowler,J. S. et al; *Journal of Nuclear Medicine***1995**, *36*, 1255-1262.

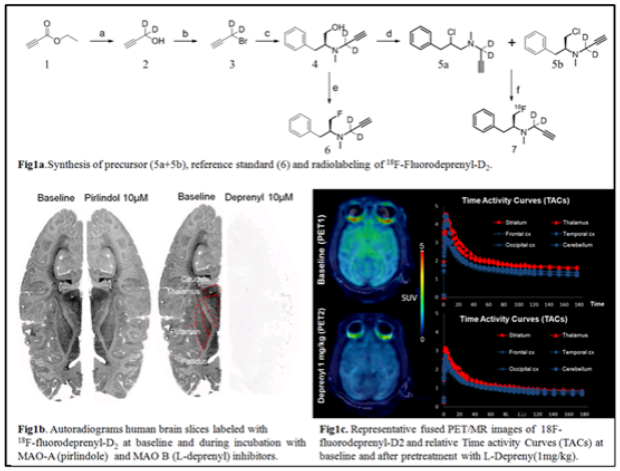

Fig1a.Synthesis of precursor (5a+5b), reference standard (6) and radiolabeling of ^{18}F-Fluorodeprenyl-D_2.

Fig1b. Autoradiograms human brain slices labeled with ^{18}F-fluorodeprenyl-D_2 at baseline and during incubation with MAO-A (pirlindole) and MAO B (L-deprenyl) inhibitors.

Fig1c. Representative fused PET/MR images of 18F-fluorodeprenyl-D2 and relative Time activity Curves (TACs) at baseline and after pretreatment with L-Depreny(1mg/kg).

783
BRAIN-0749
Poster Session

BrainPET: Novel Radiotracers

[18F]NIFENE NICOTINIC ACETYLCHOLINE RECEPTOR BINDING IN HUMANS

P. Lao[1], T.J. Betthauser[1], A.T. Hillmer[1], S.A. Kuruvilla[2], A.T. Higgins[3], T.E. Barnhart[1], C.K. Stone[4], J. Mukherjee[2], B.T. Christian[1]
[1]Medical Physics, University of Wisconsin-Madison, Madison, USA
[2]Radiological Sciences, University of California-Irvine, Irvine, USA
[3]Waisman Center, University of Wisconsin-Madison, Madison, USA
[4]Cardiovascular Medicine, University of Wisconsin-Madison, Madison, USA

Objectives: Imaging of the nicotinic acetylcholine receptor (nAChR) system can elucidate its role in numerous disease processes, such as addiction and Alzheimer's disease. Previous α4β2* nAChR radiotracers, such as [^{18}F]2-FA, are hindered by slow imaging kinetics resulting in long scan times (>5 hrs). We have previously demonstrated in animal models that [^{18}F]nifene exhibits fast kinetics and favorable in vivo imaging properties. The goal of this work was to translate the use of [^{18}F]nifene for first-in-human studies to examine its utility for in vivo imaging and to characterize regional binding in the human brain.

Methods: Three subjects (1M,2F) underwent a 90 min dynamic PET scan (5.4±0.1mCi) using an ECAT EXACT HR+ scanner. Gross anatomical structures were segmented using FreeSurfer in native space and normalized to standard MNI space, while subregions were defined manually in MNI space. MRTM0 and a time frame of 10 to 50 min post-injection were used to calculate the distribution volume ratio (DVR) images. The corpus callosum served as the reference region as previously implemented for the α4β2* system using [^{18}F]2-FA[1]. Peak DVR was calculated as the mean of DVR values above 80% of the maximum DVR to avoid reporting a single voxel intensity.

Results: Our group previously reported DVRs in the rhesus macaque using cerebellum as the reference region. While there was no evidence of cerebellar binding in the nonhuman primate model, the time activity curves extracted from the cerebellum in the human model were similar in magnitude to cortical regions, suggesting elevated levels of specific binding. The thalamus exhibited the highest DVR in all three subjects (mean=2.65±0.17, $peak_{80\%}$=3.47±0.40), with the medial thalamus exceeding the lateral and anterior thalamic regions. The lateral geniculate within the thalamus also revealed elevated binding (1.81±0.16, 2.45±0.29). In the brainstem, the substantia nigra (1.72±0.23, 1.83±0.26) exceeded the pons (1.66±0.08, 1.70±0.09). DVRs were similar in the cortical regions: frontal (1.47±0.24, 1.79±0.34), parietal (1.47±0.29, 1.72±0.37), anterior cingulate (1.44±0.06, 1.69±0.23). Slightly lower in binding was the nucleus accumbens (1.29±0.28, 1.37±.33). The hippocampus DVR values were highest in the subiculum (1.46±0.04, 1.70±0.24), followed by the dentate gyrus and the entorhinal cortex and lower binding in the amygdala (1.26±0.09, 1.44±0.23). In the striatum (1.41±0.03, 2.01±0.14), binding in the putamen exceeded the caudate. The temporal cortex (1.42±0.24, 1.73±0.30) DVRs were higher in the superior temporal cortex compared to the medial and inferior temporal cortices.

Conclusions: [^{18}F]Nifene uptake in the human brain corresponds closely with known α4β2* nAChR distributions measured by [^{18}F]2-FA binding patterns and in situ hybridization studies. Variability between subjects was highest in cortical regions. The favorable kinetics and imaging properties of [^{18}F]nifene support a role for its use in investigations of the human nAChR system.

Research Support: NIH AG029479

References: [1]Kimes AS, Chefer SI, Matochik JA, et al. Quantification of nicotinic acetylcholine receptors in the human brain with PET: Bolus plus infusion administration of 2-[18F]F-A85380. Neuroimage 2008, 39: 717-727.

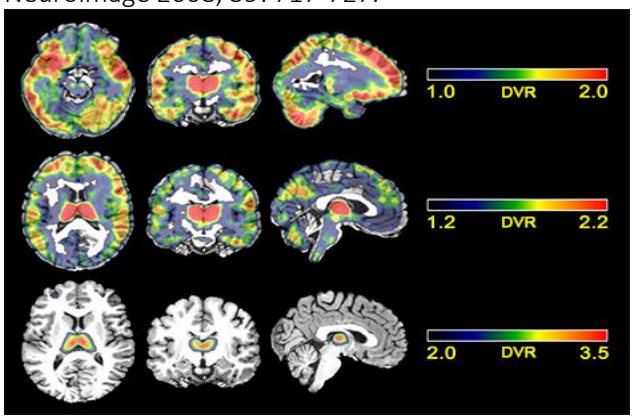

Figure1: [^{18}F]Nifene binding distribution. Each row has been selectively thresholded to highlight regional uptake in DVR images: (top row) midbrain, (middle row) cortex, (bottom row) thalamus.

784
BRAIN-0541
Poster Session

BrainPET: Novel Radiotracers

QUANTIFICATION OF INCREASED CEREBRAL 64CU UPTAKE IN TAU-P301L TRANSGENIC MOUSE MODEL OF ALZHEIMER'S DISEASE WITH 64CUCL2-PET/CT

F. Peng[1], *O. Muzik*[2]
[1]*Radiology,*
University of Texas Southwestern Medical Center, Dallas, USA
[2]*Pediatrics and Radiology, Wayne State University, Detroit, USA*

Objectives: Copper is a transitional metal essential for physiology of human brains, but copper in excess is neurotoxic. Emerging body of evidence suggests the role of copper in pathophysiology of Alzheimer's disease (AD). The aim of this study was to explore changes of copper metabolism in AD and determine feasibility and use of altered copper metabolism as a biomarker for early diagnosis of AD with positron emission tomography/computed tomography (PET/CT) using copper-64 chloride ($^{64}CuCl_2$) as a radioactive tracer ($^{64}CuCl_2$-PET/CT).

Methods: The homozygous Tau-P301L mutant transgenic mice (N=3, F, 18 weeks old), a mouse model of Alzheimer's disease which carries the transgene for the human P301L mutation of the microtubule-associated protein tau (MAPT), were subjected to PET/CT for quantification of cerebral ^{64}Cu uptake after oral administration of $^{64}CuCl_2$ as a radioactive tracer, using a small animal PET/CT scanner. A group of age-matched C57BL/6 mice (N=5, 3 F and 2 M) were used as control. PET quantitative analysis was performed to compare ^{64}Cu uptake in the brains of the Tau-P301L transgenic mice with ^{64}Cu uptake in the brains of C57BL/6 mice of control group.

Results: Increased ^{64}Cu uptake was detected in the brains of Tau-P301L mutant transgenic mice, compared to that in the brains of age-matched C57BL/6 mice. At 24 hr post oral administration of the tracer, ^{64}Cu uptake in the cortex of the Tau-P301L transgenic mice (SUV 0.035 $\pm$ 0.025) was significantly higher than that in the cortex of C57BL/6 mice (SUV 0.0003 $\pm$ 0.0004, $p < 0.001$).

Conclusion: Increased ^{64}Cu uptake was detected in the brains of Tau-P301L mutant transgenic mice, compared with ^{64}Cu uptake in the brains of C57BL/6 mice. The findings support further investigation of alteration of copper metabolism in AD associated with taupathology and potential use of altered copper metabolism as a biomarker for early diagnosis of AD with $^{64}CuCl_2$–PET/CT.

785
BRAIN-0728
Poster Session

BrainPET: Novel Radiotracers

HIGH FAT DIET DECREASES BINDING OF N-11C-METHYL-JNJ-31020028 TO NEUROPEPTIDE Y2 RECEPTORS

M. Winterdahl[1], H. Audrain[1], A. Møller[1], A.K.O. Alstrup[1], J. Scheel-Krüger[2], M.L. Kringelbach[3], A.M. Landau[1]
[1]Department of Nuclear Medicine & PET-Centre, Aarhus University and Hospital, Århus C, Denmark
[2]Center of Functionally Integrative Neuroscience, Aarhus University, Århus C, Denmark
[3]Department of Psychiatry, Oxford University, Oxford, United Kingdom

Objectives:

Neuropeptide Y (NPY) is a potent orexigenic agent expressed in both the central and peripheral nervous system. In the brain, NPY increases food intake and body weight leading to metabolic changes promoting energy storage. The activation of NPY2 receptors, the most prominent NPY receptor in the CNS, has been linked to the induction of satiety, and polymorphisms in this gene have been implicated in human obesity. We have recently developed a novel positron-emitting radioligand based on the NPY2 receptor antagonist, JNJ-31020028, and have used the radiotracer for positron emission tomography brain imaging in pigs. Here we examine changes in the binding potential (BP_{ND}) of NPY2 receptors in response to diet-induced obesity.

Methods:

Four average weight (25kg) adult female Gottingen minipigs were anesthetized and scanned at baseline with N-[11C]methyl-JNJ-31020028 in a Siemens PET/CT scanner. Minipigs were then fed an unlimited, high-fat, palatable diet for 10-12 weeks which resulted in doubling of their body weight (51kg), prior to rescanning with N-[11C]methyl-JNJ-31020028. PET data were registered to an average minipig MRI atlas and processed using Pmod software package 3.6. The BP_{ND} was obtained using the Logan graphical analysis, with corpus callosum as a region of non-displaceable binding.

Results:

On average in the four pigs, JNJ-31020028 BP_{ND} was significantly reduced in the striatum, thalamus and amygdala as a result of the high-fat diet.

Conclusions:

Data demonstrate the use of this novel tracer in longitudinally examining physiological processes

and reinforce the idea of NPY2 antagonism as a potential beneficial treatment of obesity.

786
BRAIN-0476
Poster Session

BrainPET: Novel Radiotracers

CHARACTERIZATION OF [11C]LU AE92686 AS A PHOSPHODIESTERASE 10A PET RADIOLIGAND IN THE MONKEY BRAIN

K.C. Yang[1], V. Stepanov[1], N. Amini[1], S. Martinsson[1], A. Takano[1], J. Nielsen[2], B. Bang-Andersen[3], S. Grimwood[4], C. Halldin[1], L. Farde[1], S.J. Finnema[1]
[1]Department of Clinical Neuroscience, Karolinska Institutet, Stockholm, Sweden
[2]Division of Synaptic Transmission, H. Lundbeck A/S, Valby, Denmark
[3]Division of Discovery Chemistry and DMPK, H. Lundbeck A/S, Valby, Denmark
[4]Neuroscience Research Unit, Pfizer Inc., Cambridge MA, USA

Objectives: The enzyme phosphodiesterase 10A (PDE10A) has received significant attention as a potential therapeutic drug target for neuropsychiatric diseases. In the primate brain the distribution of PDE10A includes high densities in the striatum, globus pallidus (GP) and substantia nigra (SN) [1]. [^{11}C]Lu AE92686 is a novel radioligand with high affinity for PDE10A and has recently been validated in humans [2]. We here characterized [^{11}C]Lu AE92686 as a PDE10A PET radioligand in monkeys.

Methods: A total of 7 HRRT PET measurements were performed in 5 cynomolgus monkeys. All subjects underwent baseline PET measurements and 2 subjects underwent a subsequent PET measurement after pretreatment with the PDE10A inhibitor MP-10 (1.5 mg/kg, i.v.). Arterial blood was collected to determine the metabolite-corrected arterial input function and plasma free fraction (f_P). Five target regions: putamen, caudate nucleus, ventral striatum, GP and SN and 3 candidate reference regions: thalamus, cerebellum (CB) and occipital cortex were delineated on MRI. Volumes of distribution (V_T) were estimated using 1- and 2-tissue compartment models (1TCM & 2TCM) and Logan plot analyses. Binding potential (BP_{ND}) values were determined by indirect methods (DVR-1) and the simplified reference tissue model (SRTM). Lassen plots were applied for validation of reference region selection. PET data were truncated to 93 min and 63 min to evaluate the effect of acquisition duration on quantification of outcome parameters.

Results: Blood analysis indicated that [^{11}C]Lu AE92686 metabolized fairly quickly, with parent fraction in plasma of 20±2.4% at 60 min post injection. The f_P was 5.4±0.81% during baseline and 14% and 9.0% after MP-10 pretreatment. Regional time-activity curves (TACs) were better described with the 2TCM in most regions (except some high binding areas) but V_T values could not be reliably identified by 2TCM in candidate reference regions. Logan plot analyses provided reliable V_T estimates for all regions, with a fair linear relationship to the subset of reliable V_T values from 2TCM (R^2>0.99). Administration of MP-10 reduced V_T/f_P significantly in target regions (46-87%) and modified cerebellum V_T/f_P by 11% and 27%. Occupancy of MP-10 derived by Lassen plots was around 90%. Shortening of the acquisition time to 63 min reduced V_T values of reference regions but did not affect V_T values of target regions. The V_T/f_P of cerebellum agreed with V_{ND}/f_P from Lassen plots and SRTM fitted the regional TACs well when using 63 min of PET data. There was a good linear association between BP_{ND} by DVR-1 and SRTM for 63 min of PET data (R^2=0.94).

Conclusions: Logan plot analyses provided reliable quantification of [^{11}C]Lu AE92686 binding and SRTM may be applied when using 63 min of PET acquisition data. These results are consistent with a previous human study [2] and indicate that [^{11}C]Lu AE92686 can be used to quantify PDE10A in the striatum and substantia nigra of the monkey brain.

References: [1] Nishi et al. 2011, [2] Kehler et al. 2014.

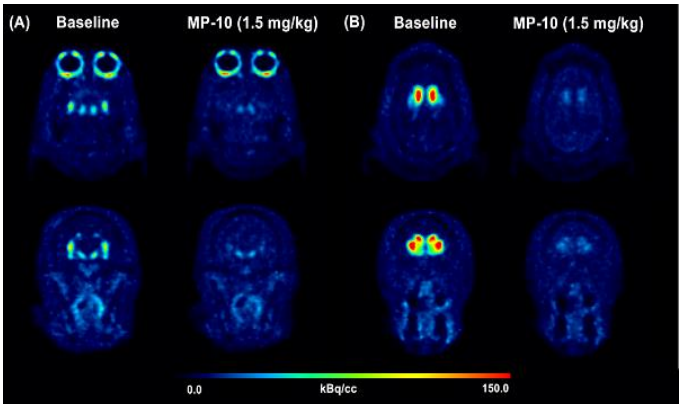

Figure: PET summation images (0-123 min) for (A) substantia nigra and (B) striatum before and after MP-10 pretreatment.

787
BRAIN-0467
Poster Session

BrainPET: Novel Modeling and Methods

UNIFIED THEORY OF SOKOLOFF'S MODEL AND RENKIN-CRONE'S MODEL

M. Kameyama[1], *Y. Kimura*[2]
[1]*Division of Nuclear Medicine, National Center for Global Health and Medicine, Tokyo, Japan*
[2]*Department of Computational Systems and Biology Faculty of Biology-Oriented Science and Technology, Kinki Univiersity, Kinokawa, Japan*

k^*_1 of deoxyglucose (DG) model developed by Sokoloff et al.[1] does not include cerebral blood flow (F), although influx rate constant from arterial plasma into brain tissue (K_1) is a product of the value of F and first-pass extraction (E =1-exp(-PS/F))[2,3].

Some people might think that K_1 of DG is independent of F, because DG goes through transporter competing with glucose. However, it is natural that k^*_1 of Sokoloff's model does not include F, because the model itself does not consider F from first to last. Their model represents that tissue acquires deoxyglucose from the silent blood pool of capillary.

We have corrected their DG model considering flowing blood in capillaries.

Our model show here that k^*_1 of Sokoloff's model is identical as the permeability surface area product (PS). Certainly K_1 of DG can be approximated to PS ,because *E of DG is low.* However, our proposed model predicts that K_1 of DG should be around 15% accurate than the conventional model under the normal condition [4].

Although K_1 is less dependent on flow, we would like to emphasize the fact that K_1 of DG is flow-dependent in principle and a product of E and F, like all the other tracers.

[1] Sokoloff L, Reivich M, Rosies MHD, Patlak CS, Pettigreow KD, Sakurada O *et al.* The [^{14}C]deoxyglucose method for the measurement of local cerebral glucose utilization: Theory, procedure, and normal values in the conscious and anesthetized albino rat. *J Neurochem* 1977;**28**: 897–916.
[2] Renkin EM. Transport of potassium-42 from blood to tissue in isolated mammalian skeletal muscles. *Am J Physiol* 1959;**197**: 1205–1210.
[3] Crone C. The permeability of capillaries in various organs as determined by use of the 'indicator diffusion' method. *Acta Physiol Scand* 1963;**58**: 292–305.
[4] Hasselbalch SG, Knudsen GM, Holm S, Hageman LP, Capaldo B, Paulson OB. Transport of n-Glucose and 2-Fluorodeoxyglucose Across the Blood-Brain Barrier in Humans. *J Cereb Blood Flow Metab* 1996;**16**:659-666

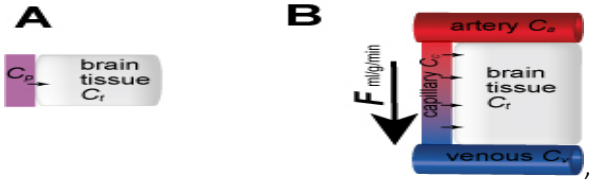

788
BRAIN-0737
Poster Session

BrainPET: Novel Modeling and Methods

UNCOVERING HIDDEN PHYSIOLOGICAL PARAMETERS BASED ON THE REALISTIC TISSUE SIMULATION

T. Ku[1], D. Lee[2], J. Lee[1], C. Choi[1]
[1]Department of Bio and Brain Engineering, Korea Advanced Institute of Science and Technology, Daejeon, Korea
[2]Graduate School of Medical Science and Engineering, Korea Advanced Institute of Science and Technology, Daejeon, Korea

Objectives: Measurement of physiological parameters combined with functional imaging techniques such as metabolic rate (MR) using FDG-PET facilitates understanding physiology and diagnosing diseases. However, the complexity of biological tissues has made identifying such parameters largely depend on theoretical predictions accompanied by simplifications and assumptions, hindering validation and further development. Here we propose an approach for validating and uncovering physiological parameters based on the realistic simulation of molecular kinetics in tissue.

Methods: We prepared a three-dimensional virtual tissue by modeling a cerebral microvasculature obtained with multi-photon microscopy, and simulated the distribution of glucose and FDG based on the current knowledge and enzyme models for glucose metabolism in the brain [1]. We obtained rate constants with two-compartment modeling, calculated physiological parameters including MR, and compared the parameters with the true values in the virtual tissue. We tuned the tissue conditions including MR, plasma glucose level, blood flow, enzyme (glucose transporters and hexokinases) concentration, enzyme efficiency, cellularity and water content. We calculated the physiological parameters for normal subjects and Alzheimer's disease patients using the rate constants reported with FDG-PET in the literatures.

Results: Applying current MR calculation methods resulted in incorrect quantification due to the FDG's different behavior from glucose. The lumped constant varied with tissue conditions, and even the FDG-to-glucose K_1 ratio was not proportional to the ratio of glucose transporter efficiencies. We found a conserved relationship between MR and tissue glucose level, which enabled us to uncover hidden parameters regarding the balance between glucose supply and utilization. The relationship also provided a solution for correcting the MR calculation with evading the influence by tissue conditions. The new parameters in addition to the corrected MR showed heterogeneous region-wise patterns in the progress of cognitive impairment.

Conclusions: The *in silico* implementation of a complex biological tissue with fully accessible information helps uncovering hidden physiological rules and parameters. Our new multifunctional parameters ready for use by single dynamic PET imaging have various potential applications including assessment of cerebrovascular risk, differential diagnosis of brain tumors, and mechanism study of neurodegenerative disorders.

References: [1] Barros LF *et al*.A quantitative overview of glucose dynamics in the gliovascular unit. *Glia* 2007;55:1222-1237.

789
BRAIN-0242
Poster Session

BrainPET: Novel Modeling and Methods

COMPUTATION OF FULL PARAMETRIC IMAGES FOR REVERSIBLE TRACER OF FLT WITHIN REASONABLE TIME

N. Kudomi[1], Y. Maeda[2], T. Hatakeyama[3], Y. Yamamoto[4], N. Yoshihiro[4]
[1]Medical Physics, Kagawa University, Kitagun, Japan
[2]Clinical Radiology, Kagawa University Hospital, Kitagun, Japan
[3]Neurological Surgery, Kagawa University, Kitagun, Japan
[4]Radiology, Kagawa University, Kitagun, Japan

Objectives: PET enables to quantify biomedical functional images such as rate constants of uptake (K_1), washout (k_2), phosphorylation (k_3) and dephosphorylation (k_4), by applying the two tissue compartment model. However there are, so far, no feasible computational strategies for imaging all rate constants within reasonable computation time. We proposed a new method to compute all those rates within a reasonable time, namely, < 1 min.

Methods: A set of differential equations for the reversible two tissue compartment model was converted to one formula expressed as tissue and plasma curve terms involving convolution integral and derivative terms. Applicability was tested by applying clinical data with ^{18}F-FLT PET (ECAT HR+) for patients with glioma (n=15). Then the images of those rates were obtained. To test validity, regions of interest (ROI) were placed on regions with glioma on a summed image. Parametric values were extracted from the obtained rate images. Also, time activity curve was extracted from the placed ROIs and those rate values were computed by the non-linear fitting method (Gauss-Newton method). The obtained rate values were compared between the methods.

Results: Computation time was around 30 s and quality of generated images was reasonably acceptable (Figure). Obtained values for K_1 were 0.16±0.04 and 0.17±0.05 ml/min/g for image and ROI based methods, respectively. Those were 0.15±0.08 and 0.16±0.08 min^{-1} for k_2, 0.050±0.034 and 0.043±0.026 min^{-1} for k_3, 0.019±0.010 and 0.014±0.007 min^{-1} for k_4, respectively. Paired t-test showed no significant difference between the methods. Regression analysis showed correlations as: r=0.75, 0.66, 0.85 and 0.64 for K_1, k_2, k_3 and k_4, respectively.

Conclusion: The present results suggested that all the parametric images tested can be calculated within reasonable time, accuracy and quality.

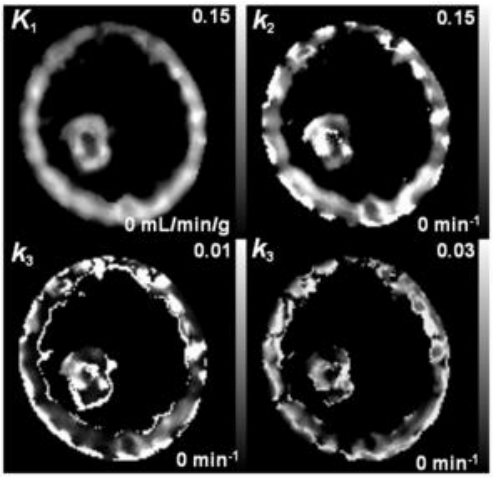

790
BRAIN-0374
Poster Session

BrainPET: Novel Modeling and Methods

REFERENCE TISSUE DUAL TIME POINT QUANTIFICATION OF IRREVERSIBLE TRACER KINETICS APPLIED TO [18F]FDOPA

I. Lopes Alves[1], S. Meles[2], G. Stormezand[2], K.L. Leenders[2], R.A. Dierckx[1], A.M. Marques da Silva[3], M. Koole[4]
[1]NGMB, University Medical Center Groningen, Groningen, Netherlands
[2]Neurology, University Medical Center Groningen, Groningen, Netherlands
[3]Medical Physics, PUCRS, Porto Alegre, Brazil
[4]Nuclear Medicine, KULeuven, Leuven, Belgium

Objectives

Imaging with PET and [^{18}F]FDOPA is a commonly used method for the diagnosis and assessment of Parkinson's disease (PD) progression. Two well established quantitative endpoints for its quantification are the influx constant K_i^{occ}, which requires a full dynamic scan, and the striatal-to-occipital ratio (SOR), which can give information on the disease severity with a short static scan. Aim of this study was to develop a method for quantification of irreversible tracer kinetics using two time points and a reference tissue as input function and validate it for [^{18}F]FDOPA.

Methods

Starting from the Patlak equation with a reference tissue as input function, an approximation can be deduced in which the influx constant can be obtained from only two time points instead of a full dynamic scan. To validate the approximation, a total of 21 subjects were included in the study, divided into three groups, 5 healthy controls, 5 confirmed PD patients and 11 subjects with probable PD. Subjects fasted for at least 4h before the start of the scan and were given 2.5mg/kg of carbidopa orally on arrival. One hour after the carbidopa dose, subjects underwent a 2h dynamic 3D PET scan. Dynamic PET data were spatially normalized to MNI space and TACs of the caudate, putamen and occipital cortex were obtained using the Hammers atlas. The K_i^{occ} was estimated by a Patlak graphical analysis over the 40 to 120 min time interval using the non-specific uptake in the occipital region as input function and considered as gold standard. Next to the Patlak graphical analysis, K_i^{occ} was estimated with a dual time point reference (DTP_{ref}) approach using two PET frames, a 10min frame starting at 40 min post injection and a 15min frame starting 105min post injection (DTP_{ref}40-120). SORs were obtained for each striatal structure using the last 15 min time frame of the dynamic PET scans.

Results

As shown in the graph, linear regression between the DTP approximation for K_i^{occ} and the values obtained from the Patlak graphical analysis yielded a regression slope of 1.014 with R2 = 0.98. Linear regression between Patlak derived K_i^{occ} and SOR yielded an R2 = 0.69.

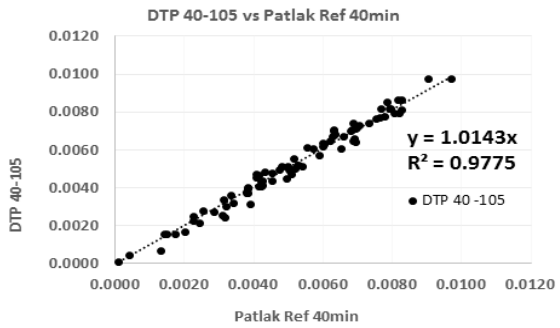

Conclusions

We validated a reference tissue dual time point quantification method for [^{18}F]FDOPA which demonstrated excellent correlation with a Patlak analysis using a reference tissue. These findings suggest the usefulness of the DTP approach for determining the same quantitative endpoint as a graphical Patlak analysis of a full dynamic scan. Therefore, DTP imaging of [^{18}F]FDOPA is able to give the same information for both diagnosis and disease progression while significantly reducing acquisition time, thus increasing patient throughput and comfort.

References

[1] J. van den Hoff, F. Hofheinz, L. Oehme, G. Schramm, J. Langner, B. Beuthien-Baumann, J. Steinbach, and J. Kotzerke. Dual time point based quantification of metabolic uptake rates in 18F-FDG PET. EJNMMI Res., vol. 3, no. 1, p. 16, Mar. 2013.

791
BRAIN-0435
Poster Session

BrainPET: Novel Modeling and Methods

EVALUATION OF PERINIDAL CEREBRAL BLOOD FLOW AND METABOLISM USING A NOVEL QUANTITATIVE 15O-PET METHOD IN PATIENTS WITH ARTERIOVENOUS MALFORMATION

D. Maruyama[1], J. Nakagawara[1], H. Iida[2], K. Koshino[2], N. Morita[3], Y. Abekura[1], E. Hamano[1], T. Satow[1], H. Kataoka[1], K. Iihara[4], J. Takahashi[1]
[1]Neurosurgery,
National Cerebral and Cardiovascular Center, Osaka-Suita, Japan
[2]Investigative Radiology,
National Cerebral and Cardiovascular Center, Osaka-Suita, Japan
[3]Radiology,
National Cerebral and Cardiovascular Center, Osaka-Suita, Japan
[4]Neurosurgery,
Faculty of Medicine Fukuoka University, Fukuoka, Japan

Objectives

We describe a dual-tracer basis function method (DBFM) to avoid the need to assume a fixed fractionation of blood volume as being arterial and venous, a common assumption in dual-tracer autoradiography (DARG) and other three-step approaches[1] [2] [3]. Assuming a fixed fractionation may introduce systematic errors when imaging pathologic tissues, such as in patients with arteriovenous malformation (AVM), a disorder often characterized by increased arterial blood volume. In AVM patients, we compared the quantitative values of ^{15}O-PET parameters derived using the present DBFM and those derived using the previously proposed DARG methods.

Methods

Seven patients with cerebral AVM were examined using ^{15}O-PET scans based on findings of both DBFM and DARG methods, and three patients also underwent ^{123}I-IMP SPECT imaging to obtain cerebral blood flow (CBF) baseline/control values. These three sets of images were calibrated using MR images. Two sets of region-of-interest circles (ROI) were established: (1) within 20 mm of the nidus, which we refer to as perinidal ROI (ROI-p), and (2) more than 20 mm away from the nidus, which we refer to as the remote ROI (ROI-r). A quantitative value of the regional CBF (rCBF), cerebral metabolic rate of oxygen ($rCMRO_2$), and oxygen extraction fraction (rOEF) were obtained and were analyzed using linear regression analysis.

Results

We observed a higher positive correlation between the DBFM method and DARG method in ROI-r (rCBF: r=0.97, $rCMRO_2$: r=0.96, and rOEF: r=0.78) than in ROI-p (rCBF: r=0.63, $rCMRO_2$: r=0.32, and rOEF: r=0.56). In ROI-p, quantitative values of rCBF and $rCMRO_2$ tended to be overestimated more when using DARG than when using DBFM. In ROI-r, significant positive correlations were also observed in values of rCBF between the ^{123}I-IMP SPECT method and DBFM method (r=0.70), or in values of between the ^{123}I-IMP SPECT method and the DARG method (r=0.67), but these correlations were lower for ROI-p values, although relatively remarkable in the DARG method (^{123}I-IMP SPECT and DBFM: r=0.49, and ^{123}I-IMP SPECT and DARG: r=0.33).

Conclusions

Our findings demonstrate the validity of the present DBFM method as a possible way to more accurately evaluate perinidal regions in AVM patients using not only CBF but also $CMRO_2$ and OEF.

References

[1] Kudomi N, et al., J Cereb Blood Flow Metab 2013; 33: 440-8.
[2] Kudomi N, et al., J Cereb Blood Flow Metab 2005; 25: 1209-24.
[3] Subramanyam R, et al., J Nucl Med 1978; 19: 48-53.

792
BRAIN-0568
Poster Session

BrainPET: Novel Modeling and Methods

QUANTIFICATION OF [11C]RO15-4513 SPECIFIC BINDING AND SELECTIVITY IN VIVO.

J. Myers[1], R. Comley[2], R. Gunn[3]
[1]Centre for Neuropsychopharmacology, Imperial College London, London, United Kingdom
[2]Pharma Research and Early Development, Roche, Basel, Switzerland
[3]Centre for Imaging Sciences, Imanova Ltd, Londond, United Kingdom

Objectives: [^{11}C]Ro15-4513 is a partially-selective inverse-agonist radioligand at the GABAAR-α5 receptor subtype with lower but significant affinity for α1, and to a lesser extent α2 and α3 (Myers et al. 2012). As such, the proportion of the [^{11}C]Ro15-4513 specific signal *in vivo* in humans that corresponds to α5 remains an open question. In this work data obtained using a GABAAR-α5-selective blocking agent (RG1662) is used to enable partitioning of the specific [^{11}C]Ro15-4513 signal across different brain regions.

Methods: Previously acquired [^{11}C]Ro15-4513 PET data from 8 healthy male volunteers were provided, at baseline and after administration of 4 separate doses of the α5-selective negative allosteric modulator RG1662. Plasma concentrations of RG1662 were acquired at the start of each scan, as well as full arterial plasma sampling of radioactivity and metabolites for [^{11}C]Ro15-4513. A two-tissue compartmental model (2TCM) was identified as the most appropriate kinetic model and was used to estimate V_T in pre-specified regions of interest (ROIs) in the brain. V_T data were fitted on a regional basis to a single site competition model which also included an α1 term across all subjects and allowed for the estimate of the specific α5 component of the signal:

$$V_T\left(C_P^{RG1662}\right) = \frac{V^{\alpha 5}.EC_{50}^{RG1662}}{EC_{50}^{RG1662} + C_P^{RG1662}} + V'$$

where $V' = V_T + V^{\alpha 1}$.

V_{ND} and $V^{\alpha 1}$were then estimated by employing regional estimates of α1 density from previous studies using [^{11}C]flumazenil (Lassen et al. 1995) and determining the maximal regional correspondence between [^{11}C]Ro15-4513 $V^{\alpha 1}$ and [^{11}C]flumazenil BP_{ND}.

These data also allowed for an evaluation of reference tissue methods and kinetic partitioning of the specific binding with spectral analysis.

Results: The 2TCM provided good fits for time-activity curves in each ROI with baseline V_T estimates ranging from about 1 in the pons to 10 in the nucleus accumbens. The competition binding model produced good fits to the V_T data (Figure 1a) and gave an RG1662 EC_{50} estimate of 427 ng.ml^{-1} with corresponding estimates of occupancy of between 22% and 79% in the dose interval 15-1250 mg. Regional levels of the specific α5 component of the signal were also determined ($V^{\alpha 5}$ ranged from 0.11 to 6.58). Estimation of the V_{ND} by maximising the relationship of $V^{\alpha 1}$ with α1 literature estimates (see Figure 1b) indicated a V_{ND} of 0.78. The individual $V^{\alpha 5}$, $V^{\alpha 1}$and V_{ND} components of the total volume of distribution were then calculated in all ROIs (see Figure 1c). This demonstrates that for cortical regions approximately 80% of the specific signal corresponds to α5 whilst for subcortical regions the proportion is higher.

Strong relationships were seen between 2TCM outcome measures and those derived from the simplified reference tissue model and spectral analysis, though biases were introduced using both methods.

Conclusions: Analysis of the *in vivo* selectivity of [^{11}C]Ro15-4513 specific binding using competition data provides an important characterisation of this ligand and enables assessment of the strengths of different analysis methods.

References: Myers JFM. et al. (2012) JCBFM 32, 731-744

Lassen NA. et al. (1995) JCBFM 15, 152-165

Figure 1:

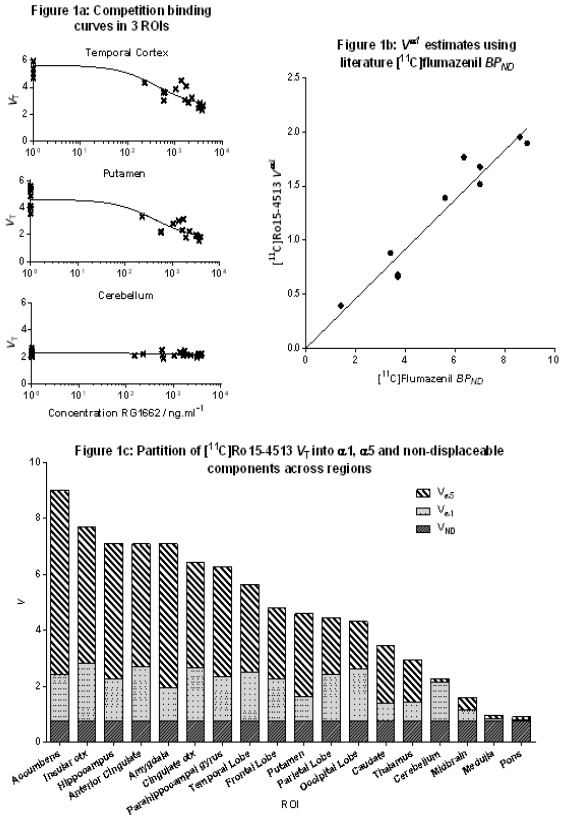

793
BRAIN-0345
Poster Session

BrainPET: Novel Modeling and Methods

VOXEL-WISE QUANTIFICATION OF [11C]CURB IN HUMAN BRAIN WITH THE HIGH RESOLUTION RESEARCH TOMOGRAPH (HRRT)

P. Rusjan[1], I. Boileau[1], J. Tong[1], R. Mizrahi[1], A. Wilson[1], S. Houle[1]
[1]RIC, Centre for Addiction and Mental Health, Toronto, Canada

Objectives: Time-activity curves (TACs) of [^{11}C]CURB, a novel radioligand for Fatty Acid Amide Hydrolase (FAAH), can be fitted by an irreversible two-tissue compartment model (2-TCMi)[1]. However, the creation of voxel-wise parametric maps from high resolution brain tomograph (such as the HRRT) is challenging due to the higher noise level in their smaller voxels. Recently, the Basis Function Method was adapted for 2-TCMi (BAFPIC[2]). In the present work we sought to validate the use of BAFPIC to create brain voxel-wise parametric maps of the net uptake rate constant (K_i) of [^{11}C]CURB using a 2-TCMi with data acquired with the HRRT.

Methods: Five thousand simulations of decay-corrected TACs with increasing levels of Gaussian noise were performed for the mean values of the regional rate constants and for variations including changes in FAAH activities, regional CBF and non displaceable distribution volume (λ). The elements of the function subspace needed, each one characterized by the exponent θ, and the inclusion of the tissue vascular fraction (V_b) as a variable were investigated. Six real data PET scans were used to confront the simulation results.
Results: At the HRRT voxel noise level, shape and mean of the distribution of K_i and λk_3 strongly depend on the function subspace considered. When the model includes V_b as a variable, V_b does not present identifiability and induces an increment in the variability of K_i. Bias in K_i. can be constrained using basis functions with θ between 0.06 and 0.2 min^{-1}. When V_b is fixed, K_i for the standard healthy brain is underestimated for any reasonable values of θ_{min} (the slower member of the basis). The bias depends on the magnitude of K_i. A basis function set with θ between 0.06 and 3 min^{-1} produces approximately normal distribution for K_i and constraints the bias in the range of -5±5% when FAAH activities change by ±65%. K_i estimations are robust (-5±5%) to extreme changes in CBF and λ. The results do not change when the number of basis functions is increased beyond 50. BAFPIC reduces the variability of Patlak's K_i by a factor of 3. Application of the method to real images produces the expected results: in a homogenous ROI, distribution shapes depend on ranges of θ. When the optimum range of θ is chosen, K_i presents a normal distribution, minimal bias (average across ROIs <1%) and excellent correlations with regional estimations (r^2=0.98). However a Bland-Altman analysis shows a minor bias depending of the magnitude (±3% for K_i ±30% of a healthy average brain value).

Conclusions: BAFPIC can be reliably used to obtain parametric images of K_i of [^{11}C]CURB from images acquired with the HRRT. Using variable V_b or adjusting the selection of a subset of basis functions can be decided depending on the range of change of FAAH activities expected or when vascular differences are known. Images with lower resolution (less noise) should be less sensitive to the selection of the limits for the basis functions.

References:
[1] Rusjan PM, JCBFM 2013
[1] Hong YT, JCBFM 2011

794
BRAIN-0527
Poster Session

BrainPET: Novel Modeling and Methods

EARLY DETECTION OF PRE-SYMPTOMATIC AD IN A COGNITIVELY HEALTHY POPULATION

S. Shokouhi[1], W.R. Riddle[1], H. Kang[2], B.P. Rogers[1]
[1]Radiology and Radiological Sciences, Vanderbilt University Medical Center, Nashville, USA
[2]Biostatistics, Vanderbilt University Medical Center, Nashville, USA

Objectives: It is now established that the pathophysiological processes of Alzheimer's disease (AD) begin decades before clinical symptoms present, and there is currently great interest in characterizing the pre-symptomatic stage of AD where the disease has begun but people do not meet the criteria for mild cognitive impairment (MCI). The objective of this study was to identify cognitively normal people that show the earliest metabolic and pathological abnormalities of AD, by combining a novel FDG-PET analysis, the regional FDG time correlation coefficient (rFTC), with cerebrospinal fluid (CSF) measures, cognitive scores, and medical history. The rFTC method (Shokouhi 2013) captures within-subject temporal changes in the regional spatial pattern of FDG distribution. Implementing this method on cognitively normal subjects with from the ADNI (Alzheimer's Disease Neuroimaging Initiative) database, we aimed to identify individuals with faster rFTC decline than other normal subjects and determine whether their rFTC decline correlated with subtle abnormalities in CSF measures or cognitive scores.

Methods: We studied 33 people with multiple followup scans who were classified as "normal" in ADNI database. T1-weighted MRI scans were used to identify 12-24 regions of interest. The regional masks were applied to FDG-PET images to extract a vector of regional activity measurements (FDG vector). For each followup scan in an individual's data, we computed the correlation between the followup scan's FDG vector and the baseline FDG vector, or the rFTC, which reflects the change in spatial patterns of metabolic activity over time (Fig 1). We used linear regression to model the rFTC outcomes as a function of gender, age, CSF-ptau/Aβ, APOE-ε4, and cognitive status (ADAS_cog, MMSE and FAQ) to search for factors that predicted rFTC decline.

Results: The rFTC calculates the correlation coefficient of regional FDG distributions between baseline and follow-up scans. Some individuals showed very high similarity between serial FDG scans (correlation > 97 %, blue lines in Fig.1); others showed changes over time (reduced correlation with baseline, red solid lines in Fig.1). The rFTC of APOE-ε4 allele carriers declined faster than that of non-carriers. Also, rFTC declines faster in those with lower CSF-Aβ.

Conclusion: Early metabolic abnormalities can be followed with the regional FDG time correlation coefficient. This technique does not require normalization of FDG activity to a reference region. It also eliminates the comparison to a control group by monitoring within-subject changes, which makes it less sensitive to metabolic heterogeneities across the population and potentially more useful in clinical practice.

Reference: Shokouhi S, Claassen D, Kang H, Ding Z, Rogers B, Mishra A, Riddle WR; Alzheimer's Disease Neuroimaging Initiative.J Nucl Med. 2013;54 (9):1564-9.

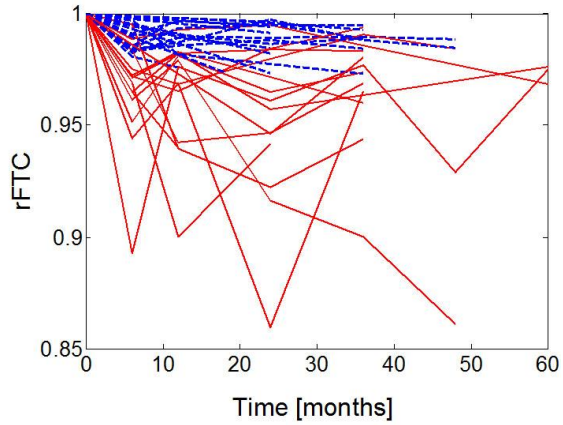

795
BRAIN-0367
Poster Session

BrainPET: Novel Modeling and Methods

HYBRID DECONVOLUTION APPROACH FOR MODEL-FREE ESTIMATION OF NON-SPECIFIC BINDING IN PET STUDIES WITHOUT REQUIRING A REFERENCE REGION

F. Zanderigo[1], *R.T. Ogden*[2], *J.J. Mann*[1]
[1]*Molecular Imaging and Neuropathology, New York State Psychiatric Institute and Columbia University, New York, USA*
[2]*Biostatistics, Columbia University, New York, USA*

Objectives. Estimating *in vivo* Positron Emission Tomography (PET) radiotracer non-specific binding is crucial for accurate quantification of the target specific binding and its occupancy levels. Non-specific binding across the brain is usually quantified using a reference region that is devoid of the target of interest [1]. Such a region often does not exist, for example when targeted receptors are expressed throughout the brain. In the absence of such region, a blocking study with radiotracer injections before and after a pharmaceutical blocking agent [2] can be used to determine non-specific binding. Here quantification generally relies on parametric models to describe the radiotracer kinetics. Model-free quantification is possible by exploiting the extended intravascular indicator dilution theory [3], which describes the PET signal as a convolution between a metabolite-corrected input function and a scaled residue function characterizing the radiotracer molecules "times of residence" in the region. Within this framework, nonparametric deconvolution computes binding estimates that are both close to those by parametric models when the model is valid, and can also show superior test-retest performance [4]. Our goal is to develop a hybrid deconvolution approach (HYDECA) that estimates non-specific binding in a model-free manner when blood data are available and a reference region is not.

Methods. HYDECA combines deconvolution and simultaneous search across regions [5] by: 1) estimating each region's residue function and corresponding radiotracer volume of distribution; 2) decomposing each residue function into non-specific and specific binding components; 3) estimating a common non-specific component across regions by minimizing a cost function that is built on mathematical constraints relating non-specific and specific components to the total residue function. We generated 100 PET signals for each of five regions (cerebellar grey matter, hippocampus, temporal and occipital lobe, cingulate) using kinetic rates estimated from a [^{11}C]CUMI-101 study [6] and adding Gaussian noise with a data-derived variance-covariance matrix. We ran HYDECA and calculated BP_P and BP_{ND} in each region using the estimates of radiotracer volume of distribution in each region and the estimated common non-specific component.

Results. Figure 1 shows the 100 cost functions that express (across regions and non-specific binding values) both the distance between the non-specific component and the total residue function in the first 2 minutes after radiotracer injection, and the total negative area of the corresponding specific component.

Conclusions. HYDECA can provide model-free estimates of PET specific and non-specific binding when a valid reference region is not available, without requiring a blocking study. We are currently assessing HYDECA using data simulations and available blocking studies.

References. [1] Slifstein M et al., Nucl Med Biol, 2001, 28(5): 595-608 [2] Lassen NA et al., J Cereb Blood Flow Metab, 1995, 15(1): 152-165 [3] O'Sullivan F et al., J Am Stat Assoc, 2009, 104(486): 556-571 [4] Zanderigo F et al. Neuroreceptor Mapping of the Living Brain, 2014 [5] Ogden RT et al., Neuroimage, 2014 Dec 24,108C: 234-242 [6] Milak MS et al., J Nucl Med, 2010, 51(12): 1892-1900.

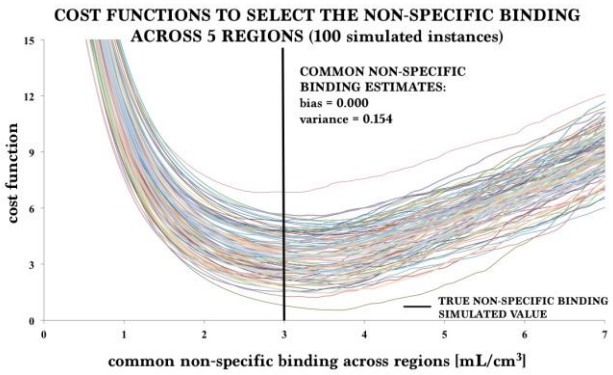

796
BRAIN-0270
Poster Session

BrainPET: Data Acquisition and Analysis

MODEL SELECTION CRITERIA FOR DYNAMIC PET STUDIES

S. Adriaanse[1], S.V.S. Golla[1], M. Yaqub[1], A.D. Windhorst[1], A.A. Lammertsma[1], B.N.M. van Berckel[1], R. Boellaard[1]
[1]Radiology and Nuclear Medicine, VU University Medical Center, Amsterdam, Netherlands

Objectives: Several criteria exist to identify the optimal kinetic model for quantification of tracer uptake or binding. These criteria are all based on the squared difference between observed (measured) and fitted data, the number of fit parameters, the number of frames, and weighting factors applied to residuals. Despite similarities between these criteria, the best criterion for kinetic model selection is under debate and different criteria are being used in the literature. Therefore, the purpose of the present study was to evaluate several commonly used criteria, such as Akaike Information Criteria (AIC), AIC unbiased (AICunb), model selection criteria (MSC), Schwartz Criterion (SC) and the F-Test for 4 different tracers.
Methods: Four tracers with different kinetic properties were evaluated: [11C]flumazenil (FMZ), [18F]DPA-714, [11C]GMOM and [11C]phenytoin (PHT). Previously, different plasma input tracer kinetic models have been selected for these 4 radiotracers. For each tracer, PET data from 5 subjects were included, randomly selecting patients and healthy controls. Time activity curves (TACs) were extracted using PVElab and Hammers template. TACs were then analysed using six plasma input models: single-tissue reversible plasma input model (1T2K), two-tissue irreversible plasma input model (2T3K), two-tissue reversible plasma input model (2T4K) with and without blood volume fraction correction (VB). Parameter boundaries were applied based on previously estimated values. Preferred models across TACs and subjects were then obtained using the various model selection criteria. The F-test requires direct comparison of two models. Therefore, for each subject, the AIC preferred model was compared with the other models using the F-test. The percentage of TACs disagreeing with AIC was calculated per radiotracer.
Results: For all 4 radiotracers strong agreement was seen across the different model selection criteria (Figure 1). The F-Test confirmed the AIC preferred model in 90% of all cases. The poorest regional agreement was found when comparing AIC with AICunb for [11C]PHT, with a 16% difference in model preference. [1¬1C]PHT also showed the poorest agreement between AIC and SC (9%). Despite these regional disagreements, for [11C]PHT, the 1T2K_VB model was selected as the preferred model by all model selection criteria. For all tracers AIC and MSC gave exactly the same model preferences.

Conclusion: AIC and MSC yielded identical results. AICunb showed some regional disagreement when compared with AIC. AICunb has a stronger penalty for number of fit parameters and might therefore favour models with a smaller number of fit parameter more frequently in case of 'noisy' TACs (small VOIs). Overall, the 5 tested model selection criteria preferred the same model across all subjects. In conclusion, all model selection criteria tested performed similarly with only minor, non-relevant differences in practice.

Figure 1: Model preference (percentage of all TACs) per selection criterion for the 4 brain PET radiotracers.

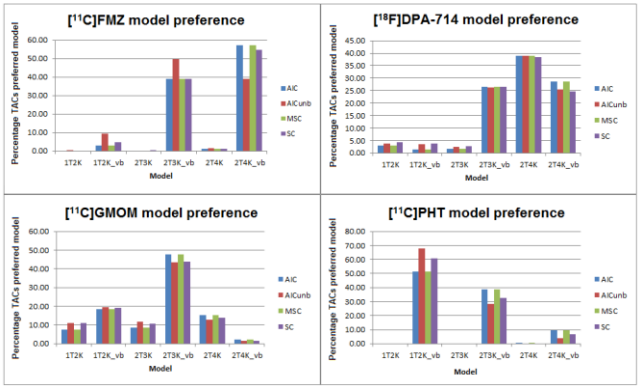

797
BRAIN-0535
Poster Session

BrainPET: Data Acquisition and Analysis

[18F]DPA-714 BRAIN UPTAKE OVER A TWO YEARS PERIOD: STABILITY IN HEALTHY CONTROL AND EVOLUTION IN THE EARLY STAGE OF ALZHEIMER'S DISEASE

C. Leroy[1], L. Hamelin[2], J. Lagarde[3], M.A. Peyronneau[1], C. Baron[1], H. Corne[3], B. Kuhnast[1], P. Gervais[1], J.F. Mangin[4], M. Sarazin[3], M. Bottlaender[1]
[1]Laboratoire Imagerie Moléculaire In Vivo (IMIV) U MR 1023 Inserm/CEA/Université Paris Sud - ERL 9 218 CNRS CEA/I2BM/Service Hospitalier Frédéric J oliot, CEA, Orsay, France
[2]CEA/I2BM/Service Hospitalier Frédéric Joliot, Sainte Anne Hospital Paris, Orsay, France
[3]Langage and Memory Neurology Unit, Sainte Anne Hospital Paris, Paris, France
[4]Neurospin I2BM DSV CEA, CATI Multicenter Neuroimaging Platform, Gif sur Yvette, France

Neuroinflammation is thought to play a crucial role in the early stages of AD. 18 kDa Translocator Protein is expressed at a low level in healthy brain and is up-regulated during inflammatory processes that may occur in neurodegenerative diseases. It is considered as a promising target for the early imaging of microglial activation and can be measured by PET imaging using [18F]DPA-714 radioligand. It has been shown that TSPO ligand uptake was highly dependent on their affinity status based on a genetic polymorphism.

Our goal was to quantify the stability of [18F]DPA-714 brain uptake in healthy volunteers and its evolution in AD patients over a two years period, according to their TSPO-affinity status

Nine subjects were analyzed including : 4 AD patients at the Mild Cognitive Impairment stage (MCI), as defined by a typical progressive amnesic deficit of the hippocampal type and a positive amyloid PET imaging ([11C]-PiB), and 5 healthy controls, with negative amyloid PET imaging. All subjects underwent a first [18F]DPA-714 PET imaging at baseline and after two-years follow up. PET scans were acquired on a HRRT scanner (Siemens) for 90 minutes. Dynamic scans were corrected for head motion and co-registered with3D T1-weighted MRI. Relative [18F]DPA-714 brain uptake was measured, using cerebellum as pseudo reference region, in 76 anatomical regions previously segmented on MRI

Analyses of the TSPO polymorphism showed that 4 controls and 3 AD patients were mixed or high binders (TSPO+ groups), and 1 control and 1 AD patient were low binders (TSPO- group-). At baseline, AD-TSPO+ patients showed a higher [18F]DPA-714 uptake than controls-TSPO+ subjects, with standardized global cortical uptake of 1.40 and 1.22, respectively.

At follow up, [18F]DPA-714 uptake remained stable in the control-TSPO+ group (mean change

over all regions of 6.4%) whereas it increased in all AD-TSPO+ patients (+ 20% on average).

In AD patients, the highest increase was found in the parietal region (mean increase of +26%). No difference at baseline and no longitudinal change was found in the AD and the control TSPO- groups.

[^{18}F]DPA-714 brain uptake did not change significantly over 2 years in healthy volunteers. AD patients at the MCI stage showed a higher [^{18}F]DPA-714 standard uptake at baseline and during follow up, suggesting an early inflammatory involvement in AD pathogenesis

798
BRAIN-0701
Poster Session

BrainPET: Data Acquisition and Analysis

QUANTIFICATION OF ACETYLCHOLINESTERASE USING 11C-PMP PET IN NORMALS: COMPARISON OF 3 DIFFERENT STRATEGIES

C. Evenepoel[1], S.S.V. Golla[2], J. Schaeverbeke[1], N. Nelissen[3], M. Vandenbulcke[4], M.S. Mohlapholi[5], G. Bormans[6], T. de Groot[7], R. Boellaard[2], R. Vandenberghe[1], K. Van Laere[7], P. Dupont[1]
[1]Laboratory for cognitive neurology, KU Leuven, Leuven, Belgium
[2]Dept. Radiology and Nuclear Medicine, VU University Medical Centre (VUMC), Amsterdam, Netherlands
[3]Dept. Of experimental psychology, University of Oxford, Oxford, United Kingdom
[4]Psychiatry, KU Leuven, Leuven, Belgium
[5]Medical Imaging and Clinical Oncology, University of Stellenbosch, Cape Town, South Africa
[6]Radiopharmacy, KU Leuven, Leuven, Belgium
[7]Nuclear Medicine and Molecular Imaging, KU Leuven, Leuven, Belgium

Objectives: To compare different strategies to quantify AChE in cortical regions using ^{11}C-PMP PET.
Methods: Dynamic PET was performed in normal elderly subjects (study approved by the ethical committee) using a HR+ PET in 3D mode after injection of 300MBq ^{11}C-PMP (N-[^{11}C]-methylpiperidin-4-yl-propionate). Images were reconstructed using 3D-filtered back-projection with correction for scatter and attenuation. Dynamic images were processed using an automatic pipeline that includes realignment, coregistration with a structural MRI and the corresponding GM segmentation, warping to MNI and the use of an atlas to define VOIS (AAL atlas). Time-activity curves were extracted in each cortical VOI intersected with the subject-specific GM map. We applied 3 different strategies to determine k_3 as measure for AChE: (1) using an irreversible 2-tissue compartment model including a blood volume component and with arterial blood sampling to determine the metabolite corrected plasma input function (2T3k_Vb) [1]; (2) using a reference region with a high rate of ACh hydrolysis (REF) [2] and (3) using shape analysis (SA) [1]. The last two approaches do not require blood sampling.
Comparisons were performed using a Bland-Altman approach and variability in cortical regions was assessed. Test-retest values for each method were determined based on the subjects who received a repeat scan.
Results: Eight subjects were included (age: 64.2 +/- 5.2 years; 5M/3F) of which 5 had a repeat scan after 2 years (619-812 days). VOIS, which showed estimates considered as outliers in one of the three methods were excluded from the analysis (baseline and follow-up scans were pooled). The putamen was taken as reference region for REF. The analysis was limited to cortical VOIS.
Comparing REF and 2T3k_Vb, we found that both methods weakly correlated ($r=0.32$, $p<10^{-6}$) while REF showed larger bias for larger values of k_3. The comparison between 2T3k_Vb and SA showed a weaker correlation ($r=0.04$, $p>0.1$) but the bias for higher values was smaller. The variability of k_3 values for each method is shown in Figure 1A: 2T3k_Vb showed the smallest variability (interquartile range (IQR) = [0.0197; 0.0238]/min) and the values of k_3 were significantly lower compared to the other methods (ANOVA, $p < 0.05$). The method 2T3k_Vb also showed the lowest amplitudes of the test-retest values (IQR =

[-4.75; 9.45]%) (Figure 1C) and the test-retest values were significantly smaller compared to the other two methods (ANOVA, $p < 0.05$). If we limit our analysis to the baseline scans, the variability of the methods is similar as taking all scans together (Figure 1A and 1B).

Conclusions: Although methods without blood sampling are attractive to use in patients, we found that these methods showed more variability among cortical regions and a weak relation with the values obtained by the irreversible 2-tissue compartment model. Test-retest values were lower in the latter model. Therefore, an irreversible 2-tissue compartment model including arterial blood sampling is required to determine AChE using ^{11}C-PMP in humans.

References

[1] Koeppe et al. JCBFM 1999
[2] Zűndorf et al. Brain Imaging Using PET (eds. Senda et al.) 2002

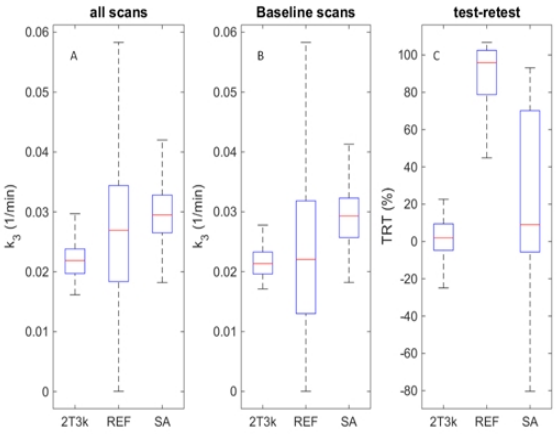

799
BRAIN-0677
Poster Session

BrainPET: Data Acquisition and Analysis

TEST-RETEST VARIABILITY OF [123I]CLINDE-SPECT BINDING IN HEALTHY HUMAN SUBJECTS

L. Feng[1], P. Jensen[1], A. Dyssegaard[1], G. Thomsen[1], K. Møller[2], D. Guilloteau[3], C. Thomsen[4], J.D. Mikkelsen[1], C. Svarer[1], G.M. Knudsen[1], L.H. Pinborg[1]
[1]Neurobiology Research Unit and Center for Integrated Molecular Brain Imaging, Rigshospitalet, Copenhagen, Denmark
[2]Department of Neuroanaesthesiology, Rigshospitalet, Copenhagen, Denmark
[3]UFR de Médecine, Université François Rabelais de Tours, Tours, France
[4]Department of Radiology, Rigshospitalet, Copenhagen, Denmark

Objectives

Neuroimaging of translocator protein (TSPO) unveils neuroinflammation and is a potential marker of immunotherapy in neurological disorders. [^{123}I]CLINDE-SPECT has shown a strong regional TSPO expression within stroke and glioma patients [1] and both cortical and subcortical increase of TSPO binding in anti-NMDA receptor encephalitis [2]. Here we report the results of test-retest [^{123}I]CLINDE-SPECT studies in healthy subjects.

Methods

Ten healthy volunteers (4 females) were scanned twice with [^{123}I]CLINDE-SPECT, with an interval of 49±39 days. The rs6971 TSPO polymorphism was genotyped from genomic DNA using TaqMan® SNP Genotyping Assay (Applied Biosystems, USA, C_2512465_20). Structural MRI was acquired with a 3T Siemens Prisma scanner. Dynamic SPECT (Philips IRIX triple head scanner) images were acquired 90 min post [^{123}I]CLINDE bolus injection. Arterial blood samples were obtained during scanning, and were corrected for metabolites using HPLC. SPECT and MRI were co-registered using interactive image overlay, and 11 anatomical VOIs were automatically delineated using probability maps [3]. The mean standard uptake value (mSUV) weighted by frame length was calculated as an outcome measurement of [^{123}I]CLINDE both in plasma and the brain. The SUV was defined as the time activity curve normalized by injected dose per kg body weight. Within-subject Mean sum of Squares (MSW) to measure reproducibility, Intra-class Correlation Coefficient (ICC) to measure reliability, Coefficient of Variance (COV), and Percentage Difference

(PD=2*(test-retest)/(test+retest)*100%)) across 11 VOIs were calculated.

Results

Large PD was observed in plasma measurements between test and retest: -17.9%±26.5% of the mSUV in plasma; 16.1%±19.4% of the mSUV in parent fraction; and -1.6%±29.9% of mSUV in plasma parent compound. For mSUV of 11 brain VOIs Pearson's correlation coefficients between test and retest of each subject were 0.936±0.04 (0.8617-0.9861). Test-retest outcome of brain binding is shown in Table 1. These matrices were also calculated separately for each genotype group: mixed-affinity binders (MAB) (*n*=4), and high-affinity binders (HAB) (*n*=6), and no significant difference was observed for MSW, ICC (paired-sample t-test) and PD (two-sample t-test). However, COV of MAB was 23.7% higher compared to HAB ($p<<0.001$, paired-sample t-test), indicating lower brain uptake (mSUV) for MAB. An approximately 1.4 fold difference of CLINDE binding was observed between HAB and MAB in the cerebellum ($p<<0.001$), which was the VOI with the highest ICC value, see Figure 1.

Table 1. Test-retest variability in [123I]CLINDE brain binding in ten healthy volunteers

Regions	PD (%)	MSW (g/ml)	ICC
Thalamus	-0.08±13.69	0.009	0.85
Parietal Cortex	-0.32±9.64	0.002	0.93
Neocortex	0.62±8.97	0.003	0.92
Pallidostriatum	1.47±13.66	0.008	0.81
Insular Cortex	1.65±11.48	0.007	0.88
Midbrain	-1.75±11.26	0.009	0.85
Cerebellum	-2.06±7.12	0.002	0.94
White Matter	-2.16±13.45	0.006	0.63
Occipital Cortex	-2.71±10.60	0.004	0.88
Frontal Cortex	2.94±9.30	0.003	0.90

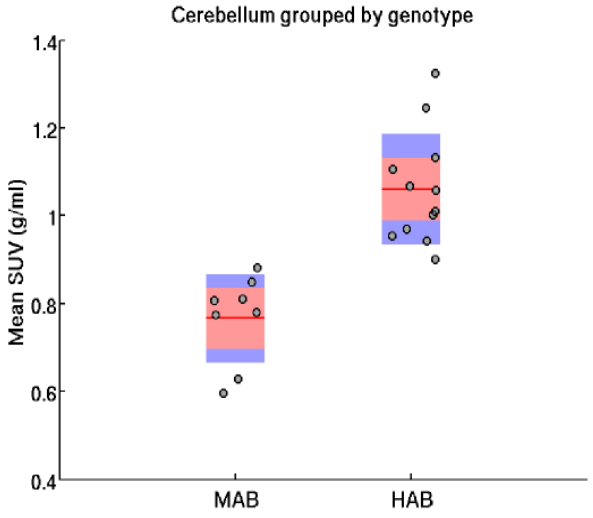

Figure 1. Mean SUV of cerebellum grouped by genotype, MAB: mixed-affinity binder; HAB: high-affinity binder.

Conclusions

Like other second-generation TSPO ligands, [^{123}I]CLINDE binding is influenced by the TSPO polymorphism. The test-retest percentage difference was lower than that of the first-generation TSPO ligand [^{11}C]PK11195-PET [4]. The ICC measurements were also much better than [^{11}C]PK11195 [4] and comparable to [^{11}C]DPA-713 [5]. The instability of plasma measurement will be further investigated; more data are to be acquired in healthy individuals to further validate the use of [^{123}I]CLINDE.

References

[1] Feng et al. *J. Nucl. Med.* 55. (2014) 1966-1972.
[2] Jensen et al. Neurology In press (2015).
[3] Svarer et al. *Neuroimage* 24. (2005) 969-979.
[4] Jucaite et al. *EJNMMI Research* 2. (2012) 15.
[5] Coughlin and Wang, et al. *J. Neurovirol.* 20. (2014) 219-232.

800
BRAIN-0608
Poster Session

BrainPET: Data Acquisition and Analysis

SURFACE-BASED MODELLING OF MOLECULAR IMAGING MARKERS IN PERI-INFARCT CORTEX

T. Funck[1], M. Al-Kuwaiti[2], P. Zepper[3], C. Lepage[4], A. Evans[4], A. Thiel[5]
[1]Department Neurology and Neurosurgery, Montreal Neurological Institute, Montreal, Canada
[2]Department of Neurology and Neurosurgery, Montreal Neurological Institute, Montreal, Canada
[3]Department of Neurology, Technical University Munich, Munich, Germany
[4]McConnell Brain Imaging Center, Montreal Neurological Institute, Montreal, Canada
[5]Department of Neurology, Jewish General Hospital, Montreal, Canada

Objectives

Assessing molecular imaging markers like GABA-A receptor density in peri-infarct cortex is of interest for acute stroke treatment and stroke recovery studies alike (Heiss, 2010). Traditional analysis methods of the peri-infarct region, are based on volumetric dilations, which cut-across cortical regions with distinct vascular territories. We developed a surface-based automatic analysis method which respects the individual sulcal anatomy and vascular territories and compared it to a volumetric approach in 18F-FMZ data from patients with ischemic stroke.

Methods

9 patients with cortical ischemic stroke underwent PET and MR imaging within two weeks after the stroke and again at 6 month follow-up. T1 and flair MR images were acquired on a Siemens Sonata 1.5 Tesla Scanner (Siemens MedicalSolutions, Erlangen, Germany) using a 3D fast-field echo scan and MPRAGE sequences. Surface mesh representations of the cortical gray matter were extracted from the T1 images using CIVET, version 2.0 (Kim, et al. 2005).

PET images were acquired with [18-F]-flumazenil on the ECAT HRRT PET scanner in list mode and reconstructed with filtered back-projection. PET images were partial-volume corrected using the idSURF algorithm (Funck, et al. 2014). Parametric non-displaceable binding (BPnd) images were created using the Logan plot method (Logan et al., 1996).

Infarct masks were drawn on the individual flair MR images for each subject for initial and follow-up scans (Fig.1.A). Surface infarct masks were produced by interpolating the volumetric infarct masks with the surface representations from CIVET (Fig.1.B). Geodesic distances from the infarct masks were calculated on the surfaces (Fig.1.C) and segmented into 3mm rings, from 0 to 21mm from the infarct (Fig.1.D, example of one ring).

In addition, volumetric distance rings were created using a series of 1mm voxel-wise dilations of the original, volumetric infarct mask.

Parametric BPnd images were then analyzed, once using surface-based and then volumetric rings in the affected and at the mirror positions of the non-affected hemisphere. A two-way repeated measures ANOVA was used to analyze the BPnd values observed with the surface-based and volumetric methods, respectively. A second two-way repeated measures ANOVA was used to test the difference between the two methods, once for the initial and once for follow-up scans Fig.1)

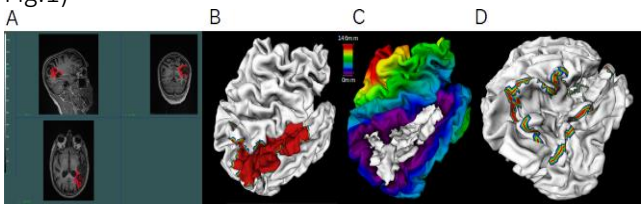

Results

BPnd was significantly different between the peri-infarct regions in the affected hemisphere and

the non-affected hemisphere both when using the surface-based ($p<0.01$) and volumetric ($p<0.05$) methods. The two methods were significantly different at the follow-up ($p<0.01$) (Fig.2). Pariwise multiple comparisons revealed that the significant difference was due to distance rings between 9mm to 21mm away from the infarct (all $p<0.01$).

Fig. 2) Difference between non-affected and affected scans, at initial and follow-up for volumetric and surface-based methods. Surface and volumetric methods were significantly different at follow-up.

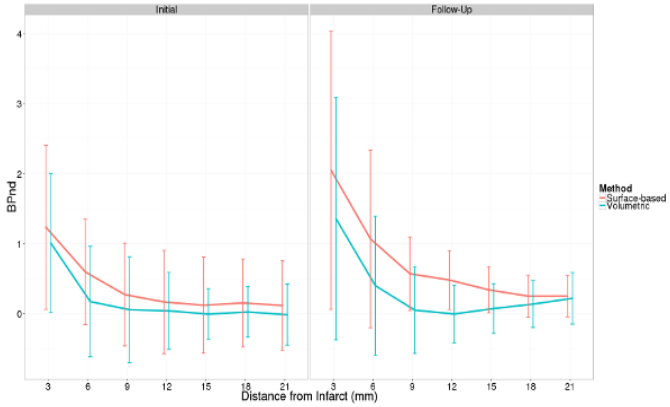

Conclusions

The sensitivity of BPnd measurements in the peri-infarct region can be increased by using a surface based analysis method, which respects anatomical and vascular territories rather than volume-based methods.

References

Heiss, WD, 2010. International Journal of Stroke,5,p.290.

Kim, J.S. et al., 2005. Neuroimage,27,p.210.

Funck T. et al., 2014. Neuroimage,102,p.674.

Logan, J., 1996. Blood Flow Metab,16,p.834.

801
BRAIN-0598
Poster Session

BrainPET: Data Acquisition and Analysis

PREDICTION OF THE LIKELIHOOD FOR SUBSEQUENT PHENOCONVERSION IN RBD PATIENTS WITH METABOLIC NETWORK ACTIVITIES: AN EXPLORATORY STUDY WITH FDG PET

S. Peng[1], J. Ge[2], P. Wu[2], J. Wang[3], V. Dhawan[1], D. Eidelberg[1], C. Zuo[2], Y. Ma[1]
[1]Center for Neurosciences, Feinstein Institute for Medical Research, Manhasset, USA
[2]PET Center, Huashan Hospital, Shanghai, China
[3]Department of Neurology, Huashan Hospital, Shanghai, China

Objectives:
Idiopathic rapid eye movement behavior disorder (RBD) represents a significant risk factor for the development of Parkinson's disease (PD), dementia with Lewy bodies (DLB) and multiple system atrophy (MSA). It has been shown recently that elevated baseline activity of PD-related brain network (PDRP) in RBD patients is predictive of eventual onset of PD and DLB after 4.6 years of clinical follow-up [1]. In this study we evaluated whether it is possible to predict the status of phenoconversion in RBD patients from baseline activities of both metabolic brain networks associated with PD and MSA (i.e. PDRP and MSARP) described previously.
Methods:
We used FDG PET images acquired in China on a Siemens Biography PET/CT scanner in two cohorts of patients with a diagnosis of idiopathic RBD confirmed by polysomnography [2]. The study was approved by the IRB for which the subjects had signed written informed consent. Network scores were computed in all subjects using PDRP and MSARP validated previously [3-4]. The combined sample of 27 independent patients from the two RBD cohorts were classified into three different subgroups using the subject scores of PDRP and MSARP. Group membership was estimated empirically using either the strict criteria (PD: PDRP > 1.5 and MSARP < 0.0; MSA:

by MSARP > 1.5 and PDRP < 0.0) or the liberal criteria (PD: PDRP > 1.5 and MSARP < 1.5; MSA: MSARP > 1.5 and PDRP < 1.5).
Results:
PDRP scores were higher than MSARP scores (P < 0.005) and correlated negatively with each other (R > 0.54, P < 0.01) in each of the two RBD cohorts. Analysis in the 27 patients showed that 9-10 (33-37%) and 1-2 (4-7%) subjects would convert to PD/DLB and MSA respectively over a period of 3-5 years from baseline. These findings were in agreement with previous reports based on prospective clinical follow-up over similar periods [5-6].
Conclusions:
We demonstrated the feasibility of predicting the rates of phenoconversion in RBD subjects by analyzing bivariate distribution of both brain network activities associated with parkinsonism. The accuracy of this prediction model needs be confirmed in this cohort with longer follow-up by clinicians blinded to the imaging outcomes.

Figure 1. Predicting the onset of PD or MSA in RBD patients by two network activities

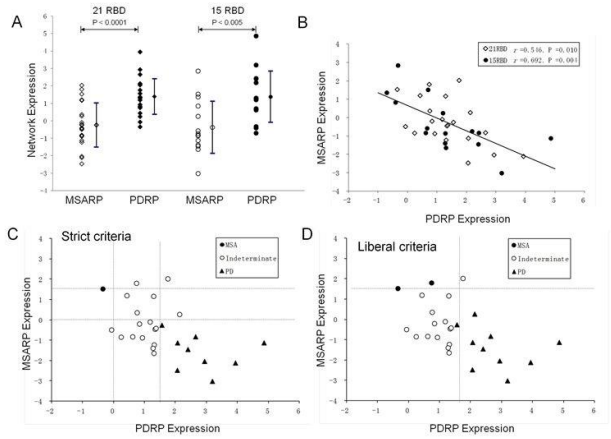

References:
1 Holtbernd F, Gagnon JF, Postuma RB, et al. Abnormal metabolic network activity in REM sleep behavior disorder. Neurology 2014; 82: 620-7.

2. Wu P, Yu H, Peng S, et al. Consistent abnormalities in metabolic network activity in idiopathic rapid eye movement sleep behaviour disorder. Brain 2014; 137:3122-3128.

3. Ma Y, Tang C, Spetsieris PG, et al. Abnormal metabolic network activity in Parkinson's disease: test-retest reproducibility. J Cereb Blood Flow Metab 2007; 27: 597-605.

4. Eckert T, Tang C, Ma Y, et al. Abnormal metabolic networks in atypical parkinsonism. Mov Disord 2008; 23: 727-33.

5. Iranzo A, Molinuevo JL, Santamaria J, et al. Rapid-eye-movement sleep behaviour disorder as an early marker for a neurodegenerative disorder: a descriptive study. Lancet Neurol 2006; 5: 572-7.

6. Postuma RB, Gagnon JF, Montplaisir JY. REM sleep behavior disorder: from dreams to neurodegeneration. Neurobiol Dis 2012; 46: 553-8.

802
BRAIN-0650
Poster Session

BrainPET: Data Acquisition and Analysis

PARKINSON'S DISEASE-RELATED SPATIAL COVARIANCE PATTERNS FROM A RESTING STATE FDG AND O15-WATER PET: COMPARISONS OF NETWORK ACTIVITY MEASURED WITH FDG PET AND ASL MRI

S. Peng[1], Y. Ma[1], P. Spetsieris[1], A. Ulug[1], V. Dhawan[1], D. Eidelberg[1]
[1]Center for Neurosciences, Feinstein Institute for Medical Research, Manhasset, USA

Objectives

Previous studies with FDG PET and multivariate network analysis have consistently demonstrated that Parkinson's disease (PD) is associated with a specific disease-related spatial covariance pattern (PDRP) of regional glucose metabolism [1]. PDRP network activity correlates with disease severity ratings and is modulated by experimental therapies. The expression of PDRP can be assessed by imaging regional cerebral blood flow (rCBF) with PET/SPECT and perfusion MRI (2-3). Analogous PDRP network has also been generated by using resting-state $H_2{}^{15}O$ PET [4]. In this work we evaluated the comparability in

network activity of these PDRPs using dual-modality FDG PET and arterial spin label (ASL) MRI.

Methods

Imaging studies were performed concurrently in 15 PD patients (58.2 ± 7.3 y; Hoehn and Yahr stage I-II) on a PET camera and a separate 3T MRI scanner. Maps of relative metabolism and rCBF were analyzed as described previously [1, 4]. Network scores of the two PDRPs were computed and z-transformed with respect to the same set of healthy controls. The scores from FDG and ASL MRI were compared in the healthy controls and in the PD patients to evaluate their reproducibility.

Results

The PD-related spatial covariance pattern (PDRP-$H_2{}^{15}O$) was characterized by increased activity in the sensorimotor cortex, thalamus, pons and cerebellum, and decreased activity in the premotor areas and occipito-parietal cortices. PDRP-$H_2{}^{15}O$ expression was elevated ($P_2{}^{15}O$ and PDRP-FDG.

Conclusions

We have established that rCBF images can be used for identifying disease-related covariance patterns to discriminate PD patients from controls at an individual-case basis. Subject scores from ASL MRI and FDG PET correlate equally for PDRP-FDG and PDRP-$H_2{}^{15}O$, further demonstrating the similarity of both topographies that are comparable to those from ASL MRI [5]. More study is needed to test the reproducibility of PDRP with rCBF in larger samples, and assess its clinical correlation and therapeutic responses. This method supports the development of a biomarker for PD with the increasing availability of simpler and non-invasive ASL MRI.

Figure 1: PDRP brain networks from FDG and H2O

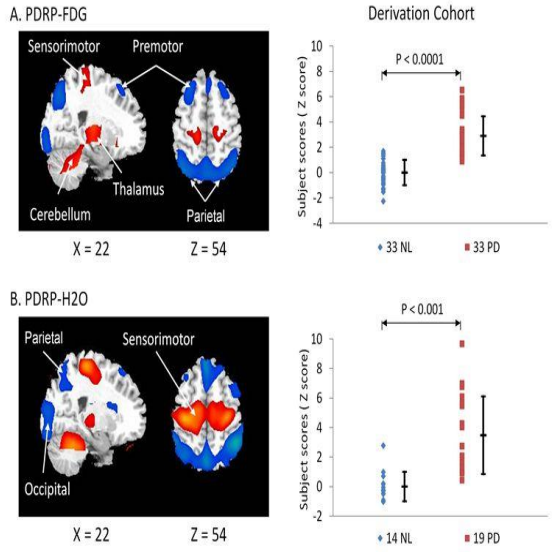

Figure 2: Correlation between PDRP-FDG and PDRP-H2O

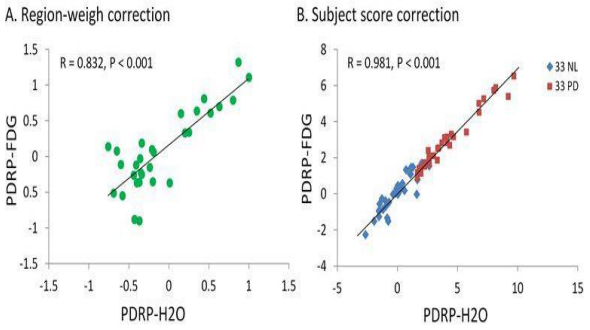

Figure 3: Comparison of PDRP expressions from ASL MRI and FDG PET using two PDRPs

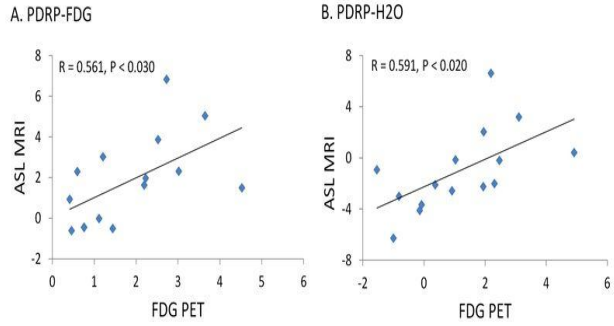

References:

1. Ma, Y, et al. Abnormal metabolic network activity in Parkinson's disease: Test-retest reproducibility. *J Cereb Blood Flow Metab* 2007; 27: 597-605.

2. Hirano, S, et al. Dissociation of metabolic and neurovascular responses to levodopa in the

treatment of Parkinson's disease. *J Neurosci* 2008; 28: 4201-9.
3. Ma, Y, et al. Parkinson's disease spatial covariance pattern: Non-invasive quantification with perfusion MRI. *J Cereb Blood Flow Metab* 2010; 30: 505-9
4. Ma Y, et al. Parkinson's disease-related spatial covariance pattern: a resting-state H2O PET study. 20th OHBM Annual Meeting, Hamburg, Germany, June 8-12, 2014
5. Melzer, TR, et al. Watts R, MacAskill MR, et al. Arterial spin labelling reveals an abnormal cerebral perfusion pattern in Parkinson's disease. *Brain* 2011;134: 845-855.

803
BRAIN-0289
Poster Session

BrainPET: Data Acquisition and Analysis

IMPACT OF NEW SCATTER CORRECTION STRATEGIES ON HIGH-RESOLUTION RESEARCH TOMOGRAPH PET STUDIES

M. Mansor[1], R. Boellaard[1], M.C. Huisman[1], B.N.M. van Berckel[1], A.A. Lammertsma[1], F.H.P. van Velden[1]
[1]Radiology and Nuclear Medicine, VU University Medical Center, Amsterdam, Netherlands

Objectives: Misalignment between transmission and emission data as a result of patient motion may cause scatter scaling artefacts, which in turn can lead to inaccurate quantification, especially for high-resolution scanners such as the High-Resolution Research Tomograph (HRRT) (1). This study was performed to evaluate the impact of μ-map dilation and 3D versus 2D scatter correction on quantification of HRRT data for three tracers covering a wide range in uptake and kinetic profiles.

Methods: A total of fifteen healthy subjects received dynamic HRRT scans with arterial sampling using either *(R)*-[^{11}C]verapamil (n=5), [^{11}C]raclopride (n=5) or [^{11}C]flumazenil (n=5). All data were corrected for attenuation, decay, scatter and random events, and reconstructed using resolution-modelled ordinary-Poisson ordered-subsets expectation maximization (12 iterations, 16 subsets). In order to reduce the effect of patient motion on scatter scaling factors, μ-maps were dilated (up to 17 mm) prior to scatter correction. Scatter correction was performed using either 2D or 3D single scatter simulations (SSS). Volumes of interest (VOI) were generated using PVElab (2). For several VOI, including those that were prominently affected by artefacts, volumes of distribution (V_T) were obtained.

Results: Three out of five *(R)*-[^{11}C]verapamil studies showed prominent artefacts in the lower part of the brain with a reduction of V_T up to 50%. With a μ-map dilation of 9.6 mm or more, artefacts were no longer visible (Figure 1). Use of 3D SSS showed a statistically significantly increase in V_T of, on average, 6% compared with 2D SSS ($p<0.05$, Wilcoxon Signed Rank test). For [^{11}C]raclopride and [^{11}C]flumazenil studies, μ-map dilations did not result in a statistically significant changes in V_T ($p>0.05$). In addition, [^{11}C]flumazenil and [^{11}C]raclopride studies also did not show a significant change in V_T with an average increase of 2% when using 3D versus 2D SSS.

Conclusions: The effect of μ-map dilation seems to be tracer dependent. For tracers such as *(R)*-[^{11}C]verapamil, where uptake is prominent in skin tissue (near the outer contour of the patient), it resulted in more reliable scatter scaling factors, but did not change (and/or deteriorate) quantification for the other tracers. 3D SSS resulted in significant changes for *(R)*-[^{11}C]verapamil only. Application of both μ-map dilation and 3D SSS results in improved quantitative accuracy of HRRT studies. This method might be applicable to other PET systems that use the same scatter scaling method.

References:
[1] Anton-Rodriguez et al, IEEE NSS Conf. Rec. 2010:2935-40
[2] Svarer et al, Neuroimage 2005, 969-79

Figure 1 Coronal (A and C) and sagittal (B and D) images, summed over the last 58 minutes frames, of an (R)-[11C]verapamil scan that was affected by subject motion. A and B are images reconstructed without dilation of the μ-map, C and D those with a 9.6-mm dilation of the μ-map. For all the images, 3D SSS was applied. Red arrows show artefacts, while white arrows show the prominent reduction of artefacts when μ-map dilation was applied.

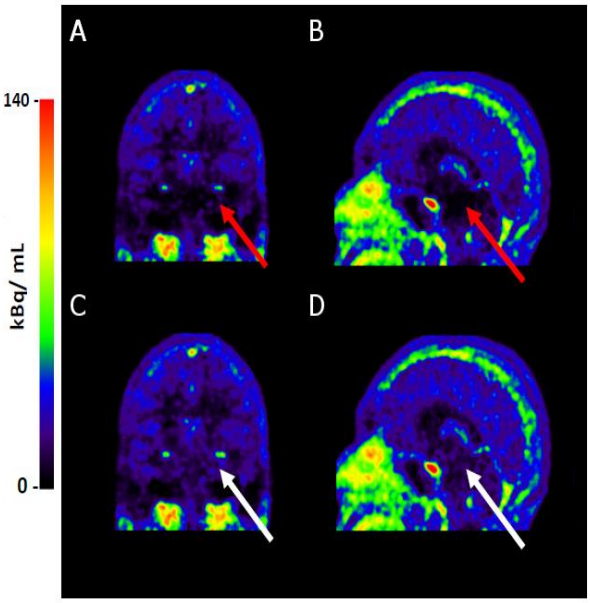

804
BRAIN-0525
Poster Session

BrainPET: Data Acquisition and Analysis

REFERENCE TISSUE METHODS FOR PET NUROIMAGING STUDIES REVISITED

M. Nakano[1], H. Kuwabara[1], A.S. Guarda[2], L. Oswald[3], M.E. McCaul[2], G.S. Wand[4], D.F. Wong[1]
[1]Radiology and Nuclear Medicine, Johns Hopkins University, Baltimore, USA
[2]Psychiatry and Behavioral Sciences, Johns Hopkins University, Baltimore, USA
[3]Department of Family and Community Health, University of Maryland School of Nursing, Baltimore, USA
[4]Department of Medicine, Johns Hopkins University, Baltimore, USA

Background: The simplified and multilinear reference tissue method (SRTM2 [Lammertsma et al., 1996; Wu et al., 2002], and MRTM2 [Ichise et al., 2003], respectively) which utilize the scan's global estimate of k2R, the brain-to-blood clearance rate constant of the reference region, and reference tissue graphical analysis (RTGA [Logan et al., 1996]) which employs population mean values of k2R are widely used in analysis of PET neuroimaging studies of reversible radioligands. The three methods were examined to determine if they yielded acceptably identical regional BP_{ND} values, and causes were identified, if this was not the case.

Methods: Historical human studies (n=165) of 8 radioligands were analyzed with SRTM2, MRTM2, and RTGA to obtain BP_{ND} of regions. Tracers (abbreviations; target systems) were as follows (see also Table 1): [^{11}C]Raclopride (Rac; Dopamine D_2/D_3), [^{11}C]Methylphenidate (MP; Dopamine transporter, DAT), [^{11}C]MDL-100,907 (MDL; $5HT_{2A}$), [^{11}C]Carfentanil (CFN; mu-opioid), [^{11}C]Flumazenil (FMZ; $GABA_A$), [^{11}C]OMAR (CB_1), [^{18}F]FPEB ($mGluR_5$), and [^{11}C]Doxepin (DXPN; histamine H_1) receptors or transporters.

Results: In the BP_{ND} data of SRTM2(=y) vs. MRTM2, none of the tracers showed acceptable correlations (criteria in Table 1; % intercept = intercept over the mean of x). SRTM2 overestimated k2R in all scans that showed obvious (> ±10%) deviations of scatter plots of k2R from y=x. All three criteria were met for all tracers when k2R was fixed across scans. In BP_{ND} plots MRTM2 or SRTM2 vs. RTGA, CFN and FMZ alone showed acceptable correlations, despite generous criteria were employed due to different y-variables. Deviations from y=x of BP_{ND} plots of individual scans correlated with k2R estimates of MRTM2 or SRTM2.

Conclusion: This study showed that variations in k2R estimates were primarily responsible for differences of BP_{ND} values between MRTM2 and SRTM2. The analysis of k2R supported MRTM2 over SRTM2. RTGA yielded almost indistinguishable BP_{ND} values to MRTM2 for CFN and FMZ alone. Thus, cautious should be

employed when to compare published results between MRTM2 or SRTM2 and RTGA.

Table 1.

PET Tracers Target systems	Rac D_2/D_3	MP DAT	MDL $5HT_2$ A	CFN mOR	FMZ $GABA_A$	OMA R CB_1	FPEB $mGluR_5$	DXP N H_1
k2R (min^{-1}) (Reference region)	0.163 (Cb)	0.051 (Cb)	0.038 (Cb)	0.104 (Oc)	0.21 (CW)	0.070 (Po)	0.086 (CW)	0.164 (Cb)
Total scans	108	25	8	60	9	13	28	10
Total regions	1080	250	320	480	378	533	2240	410
MRTM2 vs. SRTM2 (o if 0.99 < slope < 1.01, |% intercept| < 1%, R^2 > 0.999 in this order. Otherwise ×.)								
k2R estimated	×o×	oo×	×××	×oo	oo×	×××	oo×	×××
k2R fixed	ooo	ooo	ooo	ooo	ooo	ooo	ooo	ooo
vs. RTGA (o if 0.97 < slope < 1.03, |% intercept| < 3%, R^2 > 0.995 in this order. Otherwise ×.)								
RTGA vs. MRTM2	o××	o××	o×o	ooo	ooo	o××	oo×	×××
RTGA vs. SRTM2	×××	×××	×××	×oo	ooo	×××	oo×	×××

Cb: Cerebellum; Oc: Occipital cortex; CW: Cerebellum white matter; Po: Pons

805
BRAIN-0347
Poster Session

BrainPET: Data Acquisition and Analysis

INDIVIDUALIZED MAP OF 18F-FDG METABOLISM VARIATION: COMPARISON OF ON AND OFF DEEP BRAIN STIMULATION CONDITIONS IN SEVERE BRAIN INJURED PATIENTS.

B. ROCHE[1], J.J. LEMAIRE[1], J.J. LEMAIRE[2], A. SONTHEIMER[1], A. SONTHEIMER[2], A. KELLY[3], F. FESCHET[1]
[1]Image Guided Clinical Neurosciences and Connect omics (EA 7282), Université Clermont Auvergne, Clermont-Ferrand, France
[2]Neurochirurgie A, CHU de Clermont-Ferrand - Hôpital Gabriel Montpied, Clermont-Ferrand, France
[3]Centre Jean Perrin - Service de Médecine Nucléair e, Université Clermont Auvergne, Clermont-Ferrand, France

Purposes: ^{18}F-fluorodesoxyglucose (^{18}F-FDG) Positron Emission Tomography (Pet-Scan) has been proposed to explore brain metabolism conditions following deep brain stimulation (DBS), prior and after DBS[1], using group comparison analysis (e.g. SPM). We developed an original individual comparison of FDG Pet-Scan, in severe brain injured patients with extensive brain tissue lesions making statistical parametric approach useless.
Materials: Image data sets of 3 severe brain injured patients[2] were used: patient 1, male, 32 yr. old, post-traumatic vegetative state; patient 2, female, 62 yr. old, post-hemorrhage minimally conscious state (MCS); patient 3, male, 24 yr. old, post-traumatic MCS; all suffering of extended brain tissue lesions. Imaging data of each patient were: one T1- weighted MRI on 1.5 tesla machine, 0.47 × 0.47 × 0.7mm^3; two FDG Pet-Scans, DBS On and Off, 2.34 × 2.34 × 3.27mm^3.
Methods: Individualized manual contouring of the whole brain tissue (skull and cerebrospinal spaces removed) was realized from T1-weighted slices, T1-mask, (Iplan, BrainLab, Germany). DBS-On and DBS-Off FDG-Pet scans were co-registered with T1-weighted MRI and re-sliced (Slicer, USA; automatic rigid co-registration, 6 degrees of freedom). FDG Pet-Scans were normalized by the cerebral global mean[3] (CGM) computed using T1-mask; individual metabolism, above and below CGM, maps were generated (in-house development; Insight Segmentation and Registration Toolkit). From On and Off metabolism maps of each patient we computed (voxel based approach) an individualized map of metabolism variations, comparing the two conditions: On versus Off, using a logarithmic function to identify increase (red) or decrease (blue) metabolism. Analysis of maps of metabolism variations were performed (clinical expert) based on visual interpretation according to clinical parameters, and further inferred with connectomic concepts of long term severe

consciousness disorders.

Results: Individual T1-masks, metabolism maps and maps of metabolism variations, were generated for the three patients. Maps of metabolism variations revealed pertinent pathophysiologic mechanisms on consciousness disorders.

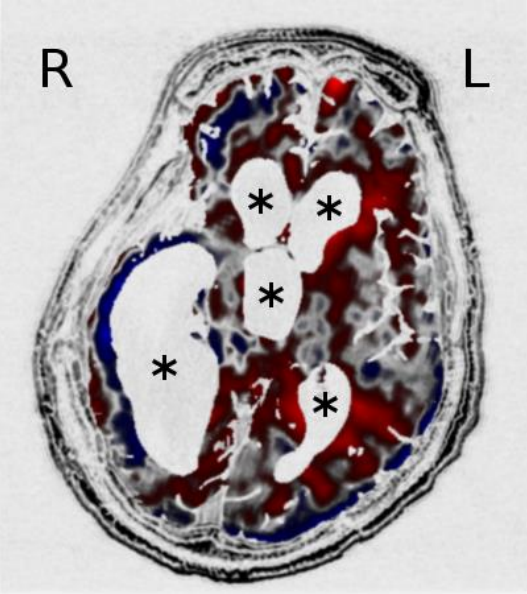

Figure: *Individualized map of metabolism variation (Patient 3) overlaid on horizontal (axial) slice (inverted T1-weighted MRI) going through basal ganglia and thalamus: note the severe brain atrophy and ventricular enlargement*; left (L) hemisphere metabolism increased in DBS On (vs Off).*

Conclusion: The proposed automatic method to compute individualized maps of metabolism variations between DBS On and Off conditions, for severe brain injured patients, harvested results meaningful with pathophysiologic mechanisms of consciousness disorders. It is still mandatory to perform manual mask contouring because of extensive brain tissue lesions.

References:

[1] Garraux G. *et al.* Brain energization in response to deep brain stimulation of subthalamic nuclei in Parkinson's disease, *Journal of Cerebral Blood Flow & Metabolism*, **31**[7], 1612- 1622 (2011).

[2] ClinicalTrials.gov, NCT01718249: Study of Conscious Behavior Under Low-frequency Deep Brain Stimulation in Chronic and Severe Post-coma Disorders of Consciousness. (Post-coma DBS).

[3] Yakushev I. *et al.* SPM-Based Count Normalization Provides Excellent Discrimination of Mild Alzheimers Disease and Amnestic Mild Cognitive Impairment from Healthy Aging, *NeuroImage* **44**[1], 43-50 (2009).

806
BRAIN-0334
Poster Session

BrainPET: Data Acquisition and Analysis

TOWARDS LESS-INVASIVE QUANTIFICATION OF [11C]PBR28: IMAGE-DERIVED AND POPULATION-BASED INPUT FUNCTIONS

N. Kanegawa[1], M. Schain[1], K. Collste[1], N. Amini[1], A. Takano[1], C. Halldin[1], S. Cervenka[1], L. Farde[1], A. Varrone[1]

[1]Department of clinical neuroscience, Karolinska Institutet, Stockholm, Sweden

Objective

[^{11}C]PBR28 is a radioligand for imaging the 18kDa Translocator Protein (TSPO), a protein expressed in microglia. Since microglia is present throughout the brain, it is not possible to designate a reference region free from specific binding. Therefore, quantification of [^{11}C]PBR28 PET data currently requires an arterial input function (AIF) obtained from arterial cannulation. The goal of this study was to evaluate population-based and image-derived input functions (IDIFs, PBIFs) obtained using only a few arterial or venous samples, for the analysis of [^{11}C]PBR28 data.

Method

Fifteen control subjects (8 High affinity binders (HABs) and 7 Mixed affinity binders (MABs)) were examined using [^{11}C]PBR28 and the HRRT PET system. AIFs were acquired for each subject. For 4 of the subjects (2 HABs, 2 MABs), whole blood radioactivity, blood-to-plasma radioactivity ratio (B/P), and radioactive metabolites were also measured in venous blood. Three different less-invasive techniques to estimate the input functions were evaluated; PBIFs (1), IDIFs

obtained with arterial samples (2), and IDIFs obtained with venous samples (3). For objectives (2) and (3), a population-based blood-to-plasma ratio (B/P) was used.

A PBIF was generated for each subject by averaging the AIFs for the remaining subjects (HABs and MABs pooled), and scaled with the measured AIF 20 and 50 min post injection. For the IDIFs, the whole blood radioactivity was estimated using the *pairwise correlation approach* (pwc)[1], and B/Ps were estimated as the population average. Here, HABs and MABs were regarded as different populations, and each subject was omitted when calculating the corresponding average. Both whole blood radioactivity and the population-based B/P were scaled for each individual, using arterial samples for objective (2), and venous samples for objective (3). For objective (2), parent fractions were estimated from arterial samples, whereas venous samples were used for (3).

Using these three different types of input functions, the distribution volumes (V_T) in temporal cortex, thalamus, putamen, cerebellum and white matter were calculated using the Logan Plot(t^*=30 min), and compared to corresponding values obtained using AIF.

Results

V_T values obtained using IDIF and PBIF were in good agreement to those obtained with AIF (figure 1). For the temporal cortex (representative ROI), the average percent deviation from V_T obtained with AIF were -0.2±7.3% for PBIF, 2.7±10.4 % for IDIF with arterial samples, and -0.4±8.2% for IDIF with venous samples.

Conclusion

Overall, this study shows that IDIFs obtained with population-based B/P, as well as PBIFs, can successfully replace AIFs when estimating V_T of [^{11}C]PBR28. Further, although the sample size is small (N=4), this study suggests that venous samples can, in combination with image-derived blood curves, be used to substitute arterial sampling for the analysis of [^{11}C]PBR28.

References

[1]Schain et. al., *J Cereb Blood Flow Metab*, 2013.

This study was supported by the European Union's Seventh Framework Programme (FP7/2007-2013) under grant agreement n° HEALTH-F2-2011-278850 (INMiND). The calculations for the pwc method were performed on resources provided by the Swedish National Infrastructure for Computing (SNIC) at PDC Center for High Performance Computing (PDC-HPC). Drs Kanegawa and Schain provided equal contribution.

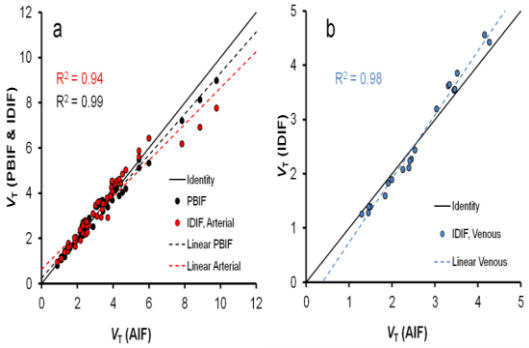

807
BRAIN-0335
Poster Session

BrainPET: Data Acquisition and Analysis

VALIDATION OF PARTIAL VOLUME EFFECT CORRECTION BASED ON FREESURFER AND AAL SEGMENTATION

M. Schain[1], *Z. Cselényi*[1], *R. Arakawa*[1], *G. Rosenqvist*[1], *C. Halldin*[1], *L. Farde*[1], *A. Varrone*[1]
[1]*Department of clinical neuroscience, Karolinska Institutet, Stockholm, Sweden*

Objectives

A consequence of the moderate spatial resolution of PET is loss and contamination of signals obtained from adjacent brain regions. This phenomenon, called *partial volume effect* (PVE), can be corrected for if the anatomical boundaries

and the resolution of the PET system are known. The objective of the present study was to validate a recently implemented PVE-correction (PVEc) scheme based on MR segmentation provided by either FreeSurfer or the Automatic Anatomic Labeling (AAL) template[1].

Methods

To estimate the *effective resolutions* of two PET systems (ECAT EXACT HR and HRRT), a NEMA phantom was filled with solutions providing a radioactivity ratio of 4:1 between spheres and background. In addition, a digital version of the NEMA phantom was created and repeatedly smoothed using varying FWHMs until the recovery coefficient for the spheres matched those obtained from the phantom measurements. The PVEc scheme is based on the geometric transfer matrix approach[2], and uses the *effective resolution* of the PET system and the segmentation of the MRI to estimate the extent of signal contamination occurring between each ROI pair, and correct the measured radioactivity values accordingly.

The PVEc scheme was applied to data from six control subjects examined twice with [^{11}C]raclopride on the same day, using the HRRT (resolution in air ~2mm FWHM) and the HR (~5mm FWHM). ROIs were defined using FreeSurfer and AAL. Time-activity curves were extracted for the caudate, putamen, pallidum, thalamus, and cerebellum, and binding potentials (BP_{ND}) were calculated using SRTM with cerebellum as reference region. Following PVEc, the resolution-dependent measurement errors should be reduced, and the corrected BP_{ND} values expected to be similar for the two PET systems.

Results

The *effective resolutions* were estimated to 7.2mm in plane and 8.9mm transaxially for the HR system, and 4.4mm and 4.8mm for the HRRT. Using FreeSurfer ROIs for striatum, PVEc reduced the difference between the BP_{ND} estimated for the two systems (from 26.9±8.7% (*ppp*BP_{ND}-values, but not increased agreement. The overall improved agreement between the systems was illustrated by regression analysis (figure 1).

Conclusion

The improved agreement observed in the high density regions (from where spill-out of activity is expected) indicate that PVEc compensates for signal loss. For thalamus, PVEc had little effect, likely due to the low density of D2 receptors. In pallidum, the reduction of BP_{ND} caused by PVEc reflects that a proportion of the measured signal originates from nearby structures, such as putamen. The findings support that the proposed PVEc scheme provides detailed correction across brain regions, and may be particularly useful when studying neurodegenerative disorders where volumetric changes are expected.

References

[1]Schain et al., *Neuroinformatics* (2014)
[2]Rousset et al., *J Nucl Med* (1998)

This work was partially supported by CHDI Foundation Inc.

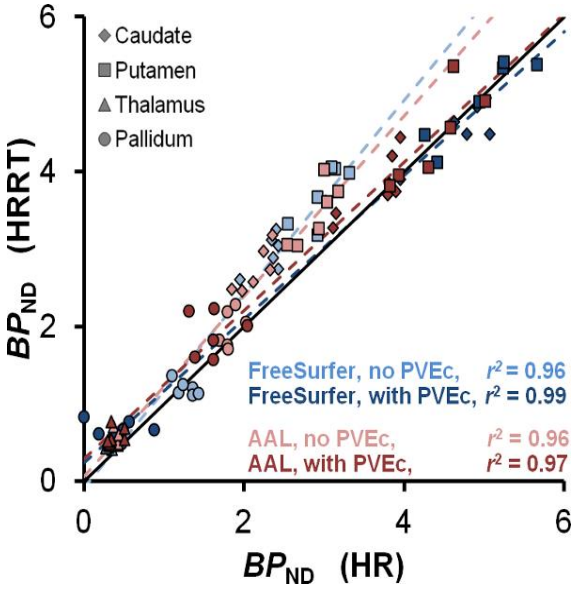

808
BRAIN-0338
Poster Session

BrainPET: Data Acquisition and Analysis

IMPROVED ACCURACY IN THE ESTIMATION OF THE DISTRIBUTION VOLUME OF [18F]MNI-659 IN CEREBELLUM

M. Schain[1], P. Fazio[1], L. Mrzljak[2], N. Amini[1], N. Al-Tawil[3], C. Fitzer-Attas[2], J. Bronzova[2], B. Landwehrmeyer[2], C. Sampaio[2], C. Halldin[1], A. Varrone[1]
[1]Department of clinical neuroscience, Karolinska Institutet, Stockholm, Sweden
[2]CHDI Foundation Inc, Princeton, USA
[3]Karolinska Trial Alliance, Karolinska University Hospital, Stockholm, Sweden

Objectives

Our previous analysis of PET data acquired using the phosphodiesterase 10A radioligand [^{18}F]MNI-659 has revealed that the cerebellar time-activity curve (TAC) cannot be adequately explained by the two-tissue compartment model (2TCM). More precisely, 2TCM consistently underestimates the TAC in the late part of the measurement. In addition, poor agreement between cerebellar distribution volumes (V_T) estimated with 2TCM and those obtained with Logan plot has been observed. A potential reason for this is underestimation of signal contribution from vasculature, which has been observed to be high from parametric images. The objective of this study was to establish a reliable procedure to calculate V_T in cerebellum.

Methods

15 control subjects were measured with [^{18}F]MNI-659 and the HRRT. Regions of interests were defined using FreeSurfer processing of T1-weighted MR images, and arterial input functions were obtained. The cerebellar TACs were fitted with the 2TCM using blood volume factions (*vB*) estimated from fitting the whole brain (WB) TAC, and with *vB* fitted together with the other model parameters. χ^2-test, model selection criteria test (MSC), and an F-test were performed to investigate which of these approaches resulted in a better model fit. Cerebellar V_T values were also estimated using Logan plot (t^*=33 min), and their correlation with V_T derived with 2TCM was investigated.

The slope of the Logan plot is given by $(K_1/k_2)(1+k_3/k_4+vB)$[1], whereas V_T from the 2TCM is given by $(K_1/k_2)(1+k_3/k_4)$[2]. To obtain Logan plot-derived V_T values that were comparable to those obtained with 2TCM, the slopes of the Logan plot were corrected for blood contribution by subtracting $vB(K_1/k_2)$, estimated with 2TCM.

Results

Using a cerebellar specific *vB* resulted in a significantly better model fit as compared to the fit obtained using WB *vB,* as reflected by 61±27% lower χ^2 values ($p<10^{-4}$) and 31±19% higher MSC scores ($p<10^{-4}$), and confirmed by the F-test ($p<10^{-8}$). This procedure increased the estimates of V_T from 0.37±0.12 to 0.56±0.11ml/cm^3($p<10^{-6}$) and *vB* from 0.05±0.00 to 0.08±0.01 ($p<10^{-8}$), and reduced the difference between V_T obtained with 2TCM and Logan plot from 71±36% to 8±18%. In both cases, the correlation between V_T obtained with 2TCM and Logan plot was low (r^2=0.21). Correcting the V_T estimated with Logan plot for *vB* resulted in an improved correlation with V_T obtained with 2TCM (r^2=0.82), and in an average difference of 11±9%.

Conclusions

Significantly improved fitting of the cerebellar TAC is obtained if *vB* is estimated using the 2TCM model curve, compared with the use of *vB* estimated from the WB TAC. This procedure results in higher V_T, which is likely closer to the true values considering the improved fit. Correcting V_T obtained from Logan plot for blood volume improved the correlation with V_T obtained from 2TCM (using *vB* from cerebellum). Therefore, Logan plot can be used to reliably quantify radioligand binding in cerebellum if the outcome measures are corrected accordingly.

References

[1]Logan, J., et al., J Cereb Blood Flow Metab,1990:10(5):p.740-7.

[2]Innis, R.B., et al., J Cereb Blood Flow Metab,2007:27(9):p.1533-9.

This study has been supported by CHDI Foundation Inc.

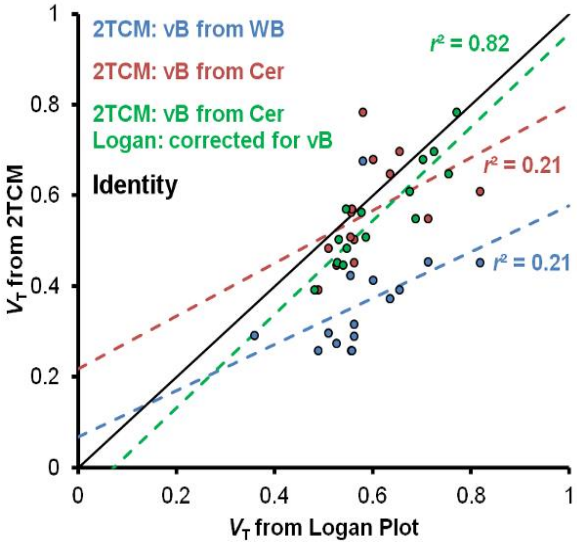

809
BRAIN-0615
Poster Session

BrainPET: Data Acquisition and Analysis

EFFECT OF IMAGE RECONSTRUCTION ALGORITHMS IN PET ON THE EXPRESSION OF CHARACTERISTIC METABOLIC BRAIN NETWORK FOR PARKINSON DISEASE

P. Tomse[1], M. Grmek[1], Z. Pirtosek[2], Y. Ma[3], V. Dhawan[3], D. Eidelberg[3], M. Trost[2]
[1]Department of Nuclear Medicine, University Medical Centre Ljubljana, Ljubljana, Slovenia
[2]Department of Neurology, University Medical Centre Ljubljana, Ljubljana, Slovenia
[3]Center for Neurosciences, Feinstein Institute for Medical Research, Manhasset NY, USA

Objective:

Characteristic metabolic brain network associated with Parkinson Disease (PD) – Parkinson Disease Related Pattern (PDRP) has been consistently reported (Refs 1-3). Our objective was to identify an analogous pattern in a Slovenian cohort of PD patients (PDRP-SLOV) at University Medical Center Ljubljana (UMCL), and to study the effect of various positron emission tomography (PET) reconstruction algorithms on its expression in PD and normal control (NC) images.

Methods:

18F-flourodeoxyglucose (FDG) PET brain images were acquired using Siemens Biograph mCT in two groups of participants. Group A comprised of 27 PD patients whose antiparkinsonian medications had been discontinued for 12 - 24 hours (age 70 ± 7 yrs, disease duration 4 ± 4 yrs, MDS-UPDRS-III 39 ± 15) and 20 age matched normal controls (NC). Group B comprised of 56 PD patients (age 71 ± 9 yrs, disease duration 5 ± 3 yrs) and 12 NC. Images were spatially normalized using SPM5.

To identify PDRP-SLOV network, Scaled Subprofile Model/Principle Component Analysis (SSM/PCA) was performed using customized neuroimaging software scanvp [Ref 4], on Group A images, reconstructed with TRUEX-TOF algorithm which incorporates Point-Spread-Function correction and Time-Of-Flight information. PDRP-SLOV was tested by ability to discriminate between PD and NC participants, and by correlating its expression in PD images with corresponding MDS-UPDRS-III score.

Group B images were reconstructed using Filtered Back Projection (FBP), Ordered Subsets Expectation Maximization (OSEM) (6 iterations, 24 subsets), TRUEX (4 iterations, 21 subsets); FBP-TOF, OSEM-TOF and TRUEX-TOF algorithms. The expressions of PDRP-SLOV were calculated for each image using Topographic Profile Rating (TPR) in scanvp and compared among different reconstruction algorithms.

Results:

The SSM/PCA on images in Group A revealed one principal component, accounting for 16% of subject-voxel variance. This was selected as PDRP-SLOV metabolic brain network (Figure 1), showing hypermetabolism in pallidum, thalamus, brain stem and cerebellum associated with hypometabolism in posterior parietal cortex. PDRP-SLOV was topographically identical to that published in American patient cohorts (Refs 1, 3). The expression of PDRP-SLOV in individual subjects discriminated PD patients from NC (p=2,99E-07) and correlated with MDS-UPDRS-III score (p<0.05) (Figure 2).

PDRP-SLOV subject scores correlated between the reference TRUEX-TOF and FBP, FBP-TOF, OSEM, OSEM-TOF and TRUEX reconstruction algorithms for PD and NC images in Group B (r≥0.999, p<0.00001 for all). Differences in individual subject scores from the reference TRUEX-TOF were 0.03 ± 0.11, 0.02 ± 0.09, 0.01 ± 0.08, 0.04 ± 0.10 and -0.05 ± 0.04 for FBP, FBP-TOF, OSEM, OSEM-TOF and TRUEX respectively (Figure 3).

Conclusion:

We have identified an analogous PDRP-SLOV using FDG/PET brain images acquired on Biograph mCT in UMCL.

Expression of PDRP-SLOV accurately discriminates between PD patients and NC and correlates with MDS-UPDRS-III score.

Different types of PET reconstruction algorithms have no significant effect on the expression of PDRP-SLOV. This study further proves that PDRP provides a reproducible imaging biomarker independent of patient population and PET scanners.

References

Ma Y, et. al.: Cereb Blood Flow Metab 2007;27:597-605.

Teune LK, et. al.: Mov Disord 2013;28:547-551.

Peng S, et. al.: Human Brain Mapping 2014;35:1801–1814.

Spetsieris PG, et. al.: Neuroimage 2011;54:2899-914.

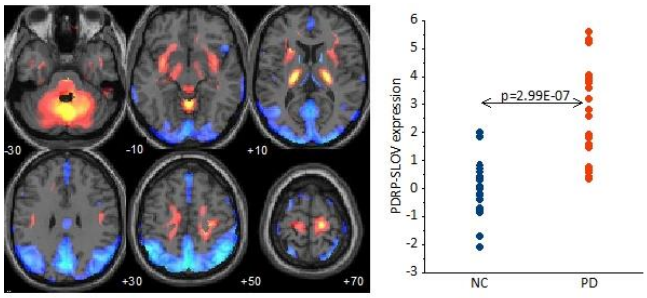

Figure 1: PDRP-SLOV (left), and its expression in derivation Group A (right)

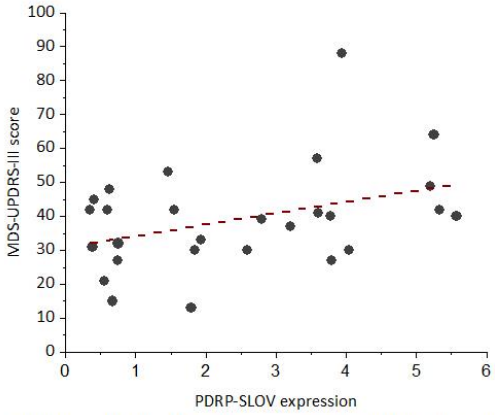

Figure 2: Correlation of PDRP-SLOV expression and MDS-UPDRS-III score (p<0.05)

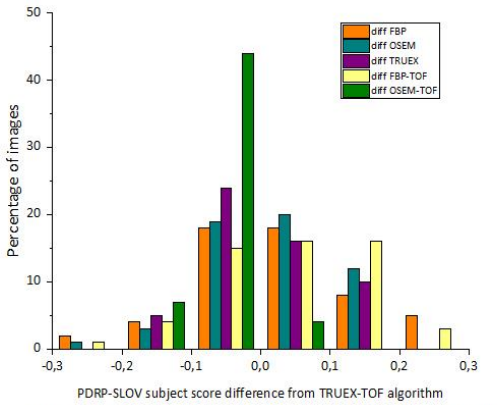

Figure 3: Frequency distribution of PDRP-SLOV expression (subject score) differences from values calculated in TRUEX-TOF images

810
BRAIN-0664
Poster Session

BrainPET: Data Acquisition and Analysis

PREDICTION OF ALZHEIMER'S DISEASE FROM AMYLOID-ß PROFILE IN BRAIN AND CEREBROSPINAL FLUID WITH COMBINED MULTIVARIATE ANALYSIS AND SUPPORT VECTOR MACHINE

P.J. Toussaint[1], *Y. Iturria-Medina*[1], *A.C. Evans*[1]
[1]*McGill University,*
McConnell Brain Imaging Centre Montreal Neurological Institute, Montreal, Canada

Introduction

Accurate measures of amyloid-ß (Aß) burden in the brain are essential to develop disease modifying drugs aimed at delaying or stopping the progression of Alzheimer's disease (AD). At present, a number of measures of Aß pathology are being investigated, and there is great interest in determining which are best related to cognitive assessments and which can optimally predict future cognitive decline and AD progression [1]. Aß protein metabolism in CSF has been proposed as the most promising predictor of AD progression as it provides an early indication of impairment (or failure) in Aß deposition and/or clearance [2]. Nevertheless, this sensitive single point biomarker does not predict the full amount of Aß deposition, nor does it reflect the distribution pattern of Aß plaques that is characteristic of the disease susceptible brain and that is observed with PET measurements of Aß or post-mortem investigation. CSF and PET measures of Aß are complementary but in general only PET is available in centres studying AD, as lumbar puncture for sampling CSF is an invasive and often painful procedure that requires a skilled professional. In this work, we investigate the relationship between CSF and PET Aß to predict the CSF measure from the PET Aß concentration and deposition patterns, in a quest for a minimally invasive and complete Aß profile for early detection of AD.

Methods

A subset population (N = 299) of the Alzheimer's Disease Neuroimaging Initiative (ADNI) database (www.adni-info.org) comprising subjects with both Aß measured in CSF samples and determined by ^{18}F-AV-45 PET at baseline was used. A canonical regression analysis (CCA) was performed to describe the relationships between CSF metabolites (Aß concentration, and levels of total and phosphorylated tau proteins) and PET regional Aß values in 78 predefined regions, with one or more co-variables amongst age, gender, Mini-Mental State Examination (MMSE) score, Apolipoprotein E (ApoE) alleles, and years of education. The most influential variables were then used as features in a support vector classification (SVC) scheme.

Results and discussion

Tests of dimensionality for the CCA indicated that only the first canonical dimension was statistically significant at the 0.05 level ($p < 1e-7$), with a canonical correlation of 0.20 between the sets of variables when all were considered. This dimension was mostly influenced by PET Aß concentrations in the left inferior, superior and transverse temporal gyri, as well as nucleus accumbens bilaterally (standardised canonical coefficient (SCC) > 0.70). These regions are known sites of amyloid deposition in degenerative diseases [3]. For CSF metabolites, the dominating influence within the first dimension was exerted by Aß (SCC > 0.70). Using these variables as features for SVC we could differentiate subjects at later stages of mild cognitive impairment from AD patients with 79% accuracy. Our approach gives a simple means to reliably predict CSF Aß from PET Aß concentrations and could be used for early detection of impairment in Aß metabolism.

References

1. Cummings JL (2010) Neurobiol of Aging, 31:1481-1492
2. Jack CR Jr, et al. (2010) Lancet Neurol 9(1): 119-128
3. Brilliant MJ et al. (1997). Neuropathol Applied Neurobiol, 23(4): 322-325

811
BRAIN-0668
Poster Session

BrainPET: Data Acquisition and Analysis

A COMPARISON OF [18F]PBR111 BINDING POTENTIAL ESTIMATION METHODS IN THE RAT BRAIN FOLLOWING ACUTE ORGANOPHOSPHATE INTOXICATION

Y. Ouyang[1], D.J. Rowland[2], D.A. Bruun[3], B.A. Hobson[3], S. Sisó[4], D.J. Tancredi[5], D.L. Kukis[2], C. Boosalis[3], P.J. Lein[3], S.R. Cherry[6]
[1]Dept. of Biomedical Engineering, University of California, Davis, USA
[2]Center for Molecular & Genomic Imaging, University of California, Davis, USA
[3]Dept. of Molecular Biosciences, University of California, Davis, USA
[4]Dept. of Pathology, Microbiology, and Immunology, University of California, Davis, USA
[5]Dept. of Pediatrics, UCDMC Center for Healthcare Policy and Research, University of California, Sacramento, USA
[6]Dept. of Biomedical Engineering, CMGI, and Dept. of Radiology, University of California, Davis, USA

Objectives: Imaging of the 18-kDa translocator protein (TSPO) has been used for clinical and preclinical assessment of neuroinflammation [1]. Quantification of radioligand binding by estimation of binding potential of the non-displaceable compartment (BP_{ND}) is potentially valuable for evaluating the neuroinflammatory response following organophosphate (OP) exposure. TSPO radioligands have been previously evaluated in other animal models of neuroinflammation using two-tissue compartment and reference tissue modeling [2]. However, the use of contralateral brain regions as a reference tissue in this and other studies [3] is not, in general, applicable to OP exposure models where there is global brain exposure and thus typically bilateral injury. We hypothesize that, in an animal model of diisopropyl fluorophosphate (DFP) exposure we have developed, the cerebellum provides a suitable reference tissue for estimation of *in vivo* binding parameters in the brain, and that the use of reference tissues from automated clustering provides correlated estimates.

Methods: Male Sprague-Dawley rats (280-320 g) were injected subcutaneously with 4 mg/kg DFP and their brains imaged with diffusion-weighted MRI (DWI), T2-weighted MRI (Bruker Biospec 7T/30), and [^{18}F]PBR111 PET (Siemens Inveon DPET). Animals were imaged prior to exposure and at one additional or two consecutive time points on Days 3, 7, 14, 21, or 28, and sacrificed for histopathology after imaging. Pathological subregions (amygdala, hippocampus, piriform cortex, and thalamus) were identified by DWI and histopathology. A separate group underwent PET with real-time blood sampling to obtain an input function. We compared the reversible two-tissue compartment model (2T4k) with the simplified reference tissue method [5] using reference tissues based on cerebellum (SRTM-CB) and supervised cluster analysis [6] with three kinetic classes (SRTM-SVCA3) in the whole brain (excluding cerebellum) and in the identified subregions.

Results: Example PET, MRI, and histology are shown in Figure 1A. Model comparisons appeared to favor reference tissue methods over 2T4k. The mean % standard error in the BP_{ND} estimate for SRTM-CB (1.93% ± 0.70%) was significantly lower (one-tail paired *t*-test $p = 0.002$, $n = 7$) than for 2T4k (10.83% ± 5.08%). BP_{ND} estimates from SRTM-CB and SRTM-SVCA3 were correlated ($R = 0.9$, Figure 1B), the latter having a smaller dynamic range and less sensitivity to longitudinal changes. Additionally, the ratio of brain (excluding cerebellum) to cerebellum uptake was found to be correlated with BP_{ND} from SRTM-CB and SRTM-SVCA3 ($R = 0.98$ and $R = 0.92$, Figures 1C and 1D, respectively). Correlations were weaker in pathological subregions ($R < 0.83$).

Conclusion: We have compared modeling approached for estimating BP_{ND} of [^{18}F]PBR111 in the DFP-exposed rat brain. Both SRTM-CB and SRTM-SVCA3 are viable alternatives to 2T4k in this animal model.

References: [1] Liu, G.-J. et al., *Brain Pathology* (2014). [2] Callaghan P.D. et al., *EJNMMI* (2015). [3] Martín A. et al., *JCBFM* (2009). [4] Flannery B.M. et al., *Tox Sci* (2015) – in preparation. [5] Lammertsma A.A. et al., *Neuroimage* (1996). [6] Turkheimer F.E. et al., *JNM* (2007).

Figure 1

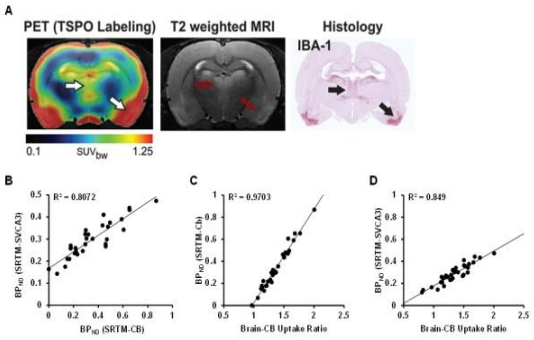

812
BRAIN-0736
Poster Session

BrainPET: Preclinical Imaging

EFFECT OF NORMOBARIC HYPEROXIA (NBO) ON HYPOXIC VOLUME AND INFARCT VOLUME FOLLOWING MIDDLE CEREBRAL ARTERY OCCLUSION (MCAO): AN 18F-FLUORO-MISONIDAZOLE (F-MISO) PET, MR AND TTC STUDY

T.D. Fryer[1], S. Ejaz[2], D.J. Williamson[2], U. Jensen-Kondering[2], S.J. Sawiak[1], F.I. Aigbirhio[1], Y.T. Hong[1], J.C. Baron[2]
[1]Wolfson Brain Imaging Centre, University of Cambridge, Cambridge, United Kingdom
[2]Stroke Research Group Dept of Clinical Neurosciences, University of Cambridge, Cambridge, United Kingdom

Objectives

Whether NBO is effective in reducing infarct volume in ischemic stroke remains inconclusive. NBO modestly increases arterial oxygen content, which in turn may not significantly alleviate tissue hypoxia. In vivo hypoxia markers such as FMISO now make it possible to directly address this issue. We determined the impact of NBO in two rat strains with different leptomeningeal collaterals: well-developed affording natural partial protection (Wistar), and poorly-developed causing marked vulnerability (spontaneously hypertensive rats; SHRs).

Methods

Under isoflurane, 6 Wistars and 7 SHRs underwent distal permanent MCAo (pMCAo) under either normoxic (30% O_2/70% N_2O; n=3 or 4/strain) or hyperoxic (100% O_2; n=3/strain) conditions. Both FMISO PET and NBO commenced ~5min after occlusion. Dynamic PET data were acquired with a microPET P4 for 3hrs. Hypoxic volumes were defined on $SUV_{2\text{-}3hrs}$ maps based on a p1]. A two-compartment irreversible kinetic model was applied to the mean hypoxic volume signal and a mirror ROI [2]. Lesion volume was defined on T2w-MR acquired immediately after PET. Immediately after MR, the infarct was mapped by TTC. Additional rats were used to measure arterial PO_2 (PaO_2) and MCA cortex PO_2 (PtO_2) using an O_2 probe during 2x30min cycles of normoxia/NBO.

Results

In SHRs, NBO increased PaO_2 ~4-fold from normoxia; non-ischemic cortex PtO_2 rose from mean 24 to 50mmHg in SHRs (n=5; p=0.04), and from 46 to 78mmHg in Wistars (n=4; p=0.001). During MCAo, in SHRs compared to Wistars PtO_2 was lower in normoxia (2.5 vs 15mmHg) and increased less with NBO: 6mmHg (p=0.08) vs 26mmHg (p=0.09), respectively. FMISO hypoxic volume was much larger in SHRs than Wistars, but was not significantly different between normoxia and NBO in either strain (mean 207 vs 349mm^3 in SHRs, and 11 vs 9mm^3 in Wistars). FMISO influx rate (K_i) was significantly increased (p_3) also increased in SHRs (p_i and k_3 in the hypoxic volume were not significantly different between normoxia and NBO in either strain. A similar pattern was found for TTC (mean 136 vs 179mm^3, and 18 vs 11mm^3, respectively) and MR (mean 91 vs

103mm^3, and 7 vs 3mm^3, respectively) lesion volumes. There were strong (p

Conclusions

Regardless of strain, there was no protective effect of NBO against tissue hypoxia and infarction. The latter is consistent with previous pMCAo studies, all in Sprague-Dawleys. However, here we directly show no effect on FMISO lesion volume and only mild effects on tissue PtO_2. Early reperfusion is probably necessary for NBO to show benefit, even with good collaterals. The worse tissue hypoxia during MCAo in SHRs is consistent with their intrinsically poorer vascular architecture, apparent already from their lower non-ischemic hemisphere PtO_2 under normoxia.

References

[1] M. Takasawa et al, Exp Neurol, 229 (2011): 251-8.
[2] YT. Hong et al, JCBFM, 31 (2011): 648-57.

813
BRAIN-0741
Poster Session

BrainPET: Preclinical Imaging

AMYLOID AND TAU DEPOSITION IN ALZHEIMER'S DISEASE PROGRESSION USING [C-11]PIB AND [F-18]THK-5117

T. Betthauser[1], P. Lao[1], D. Murali[1], A. Higgins[1], T. Barnhart[1], S. Furumoto[2], N. Okamura[2], C. Stone[3], S. Johnson[4], B. Christian[1]
[1]Medical Physics, University of Wisconsin-Madison, Madison, USA
[2]Pharmacology, Tohoku University, Sendai, Japan
[3]Medicine, University of Wisconsin-Madison, Madison, USA
[4]Alzheimer's Disease Research Center, University of Wisconsin-Madison, Madison, USA

Objectives:

Deposition of beta-amyloid (Aβ42) and tau proteins (τ) are hallmarks of Alzheimer's Disease (AD). Ongoing investigations have shown that amyloid deposition is evident prior to cognitive symptoms, and tau deposition correlates with cognitive decline. The goal of this work is to observe the regional distribution of amyloid and tau deposition during various stages of AD progression via [^{11}C]PIB and [^{18}F]THK-5117 PET, respectively.

Methods:

Three subjects from the Wisconsin Registry for Alzheimer's Prevention and the ADRC with varying levels of AD risk and cognitive decline underwent T1-weighted MRI, [^{11}C]PIB and [^{18}F]THK-5117 PET scans. MRI scans were performed on a GE SIGNA 750, and PET scans on a Siemens ECAT EXACT HR+. The PET time series were motion corrected, denoised, and coregistered to MRI. Parametric distribution volume ratio (DVR) images were created using the Logan Reference Tissue Model with a t* of 35 min and 40 min, and a k_{2bar} of 0.15/min and with the k_{2bar} term removed for PIB and THK, respectively. DVR images were coregistered to MRI by applying the transformation matrix from the PET coregistration. Mean DVR values for PIB were obtained from DVR images using FreeSurfer generated volumes of interest (VOIs). A global VOI composed of the anterior cingulate, precuneus, striatum, and frontal, parietal, and temporal cortical regions was used as an index of amyloid load. Due to highly specific regional distributions of THK, DVR values were obtained using VOIs in the lateral temporal cortex (LTC) and high focal binding regions of the temporal cortex and mesial temporal lobe (MTL) using the DVR PET images. To suppress the levels of THK uptake in the white matter, all VOIs were restricted to gray matter voxels using a SPM12 generated gray matter probability mask with a threshold of 0.3. Cerebellar gray matter was used as the reference region for both PIB and THK scans.

Results:

The subjects were characterized as a stable normal (SN), a cognitive decliner (CD) and AD. The SN (DVR=1.36) and AD subjects (DVR=1.44) were classified as PiB positive (assuming a threshold of 1.25) and the CD subject

revealed a slightly elevated value (DVR=1.14). For tau, all subjects revealed regions of elevated focal THK binding in the LTC (DVR>1.3), with patterns of AD > CD > SN in spatial extent. Specific THK binding could be detected in the MTL for CD (DVR=1.28) but not in SN, and slightly elevated in AD (DVR=1.07) although atrophy was evident.

Conclusions:

These preliminary data reveal THK and PIB have distinct distributions in cortical regions for subjects with varying degrees of presymptomatic and symptomatic AD progression, with tau (THK) binding in the perirhinal cortex only present with symptoms of cognitive decline. Additional studies of paired amyloid/tau PET imaging will be needed to better characterize a potential relationship of pathology with AD progression.

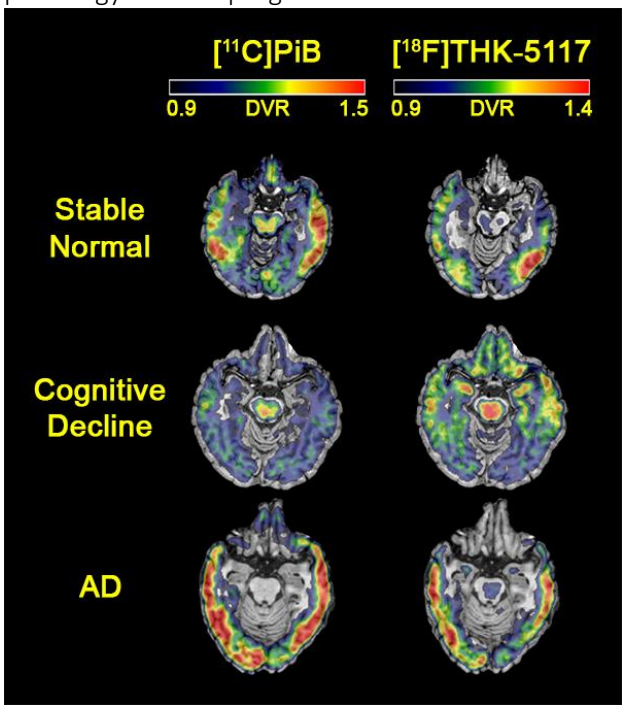

Figure 1: Regional distribution of PIB and THK in SN, CD, and AD subjects. DVR ranges from 0.9 to 1.5 for PIB and 0.9 to 1.4 for THK.

814
BRAIN-0354
Poster Session

BrainPET: Preclinical Imaging

CHANGES IN CEREBRAL METABOLISM IN A PRECLINICAL MODEL OF BLAST-INDUCED TRAUMATIC BRAIN INJURY

A. Divani[1], Y. Wang[2], A. Talan[3], A. Murphy[3], X. Zhu[4], W. Chen[4], J. Froelich[4], M. Pomper[2]
[1]Neurology, University of Minnesota, Minneapolis, USA
[2]Radiology, Johns Hopkins University, Baltimore, USA
[3]Neurology, University of Minnesota, Minneaplis, USA
[4]Radiology, University of Minnesota, Minneaplis, USA

Objectives: Incidence of blast-induced traumatic brain injury (bTBI) has recently increased due to exposure of soldiers to explosive devices in Iraq and Afghanistan. There are very few published studies looking at metabolic changes in bTBI. Accordingly, further research on post-bTBI brain metabolic changes is needed to better understand the pathophysiology of the injury. The objective of this study was to assess changes in brain metabolism over time as a consequence of bTBI using an animal model developed in-house.[1] We conducted PET studies with [^{18}F]fluorodeoxyglucose (FDG).

Methods: We divided 12 rats equally across two bTBI severity groups: 1) bTBI with 5 shockwave (SW) pulses and 2) bTBI with 10 SW pulses. To induce bTBI, anesthetized rats were placed on a lithotripsy machine to deliver 5 or 10 SW pulses to the right side of the frontal cortex. SW pulses of 24kV with 60 Hz frequency were directed to the right frontal cortex of each rat's brain. To assess the level of metabolic activity in the brain, each animal was scanned at baseline, 3 hours post-injury, and 3 days post-injury to compare metabolic changes in acute and sub-acute phases of the injury. We administrated an average (±SD) of 2.30±0.27, 2.57±0.33, and 2.74±0.5 mCi of the FDG ratio tracer for baseline, 3 hours post-injury,

and 3 days post-injury, respectively. Animals were injected in their home cage after fasting, after which they were permitted to move freely for the duration of radiotracer uptake (45-60 min in this case). After radiotracer uptake, anesthesia was administered by IP injection. Once anesthetized, animals were placed in a prone position in a microPET scanner for 10 min static scan. PET and CT images obtained from the scans were analyzed for changes in cerebral glucose uptake in different regions of interest (ROI). Specifically, the ROI standardized uptake value ratios (SUVR) between the blast side (right) and the control side (left) of the rat brains were calculated and compared.

Results: A trend of lower SUVRs were observed from all post-blast FDG-PET studies of the rat brains, particularly in the motor cortex and retrosplenial regions. While those rats receiving 5 SW pulses showed stable or recovering SUVR from acute (3 hours) to the sub-acute (3 days) phase, those receiving 10 pulses demonstrated even lower SUVRs at the sub-acute phase. PET image examples from a rat receiving 10 pulses were shown in Figure 1, together with a plot comparing the trend in different groups at the different imaging time points.

Conclusions: Our study suggests that bTBI might cause hypo-metabolism on the impact side of the rat brains. Different bTBI impact location and severity may result in differing affected brain regions and degree/duration of hypo-metabolism in these regions.

References: 1. Divani AA, Murphy AJ, Meince J, Sadeghi-Bzargain H, Nordberg J, Monga M, Low WC, Bhatia PM, Beilman GJ, SanatCruz K. A Novel Preclinical Model of Moderate Primary Blast-Induced Traumatic Brain Injury. J Neurotrauma. 2015 Jan 13. [Epub ahead of print]

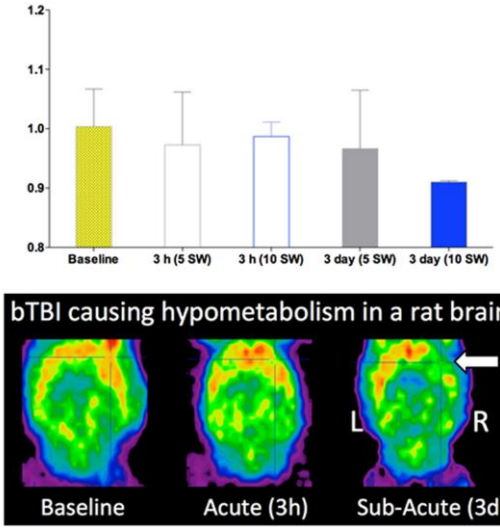

815
BRAIN-0835
Poster Session

BrainPET: Preclinical Imaging

THE STRIATAL BINDING OF YOHIMBINE REFLECTS A PROPORTION OF ALPHA 2C ADRENERGIC RECEPTORS

D.J. Doudet[1], K. Dinelle[2], V. Sossi[2], S. Jakobsen[3]
[1]Medicine/Neurology,
University of British Columbia, Vancouver, Canada
[2]Physics and Astronomy,
University of British Columbia, Vancouver, Canada
[3]Nuclear Medicine, PET Center, Aarhus C, Denmark

Objectives: To determine thedistribution of alpha 2C adrenoceptors versus other subtypes in the cortical,thalamic and striatal regions of the rhesus monkey brain. The striatum (caudate nucleus and putamen) receives limited noradrenergic innervation as shown by in vivo PET studies ofthe noradrenergic transporter. Yet,significant striatal binding of alpha 2 adrenoceptors ligands has been shown in vivo by PET and in vitro by post-mortem autoradiography in both human,non-human primates and rodents. A recent study [1] demonstrated the binding of a selective alpha 2C antagonist ligand in striatum and its displacement by pharmacological challenges. We have validated the use of [^{11}C]-yohimbine as a

tracer of the alpha 2 receptors[2], [3]. In the current pilot study, we evaluated the bindingof yohimbine in cortical, striatal and thalamic regions of the non human primate brain and the contribution of alpha 2C binding to the measuredsignal.

Methods: Four rhesus monkeys were scanned under isofluraneanesthesia in a HRRT scanner. Each animal received a 90 min baseline scanfollowed by a second scan 10 min after a pharmacological dose of ORM-13070(gift of Orion Pharmaceuticals), a selective alpha 2C adrenoceptor antagonist: to date, three doses were tested, 0.1 (N=1), 0.5 (N=2) and 1 (N=1) mg/kg. The PET images were registered to a rhesusmonkey brain atlas and the volume of distribution V_T was measured incortex (frontal, motor, sensory, temporal and occipital cortices), striatum (caudateand putamen) and thalamus using an arterial metabolite corrected plasma curve asinput. The VT was then corrected for the tracer plasma free fraction f_p and the data were subsequently analyzed as V_T/f_p

Results: The plasma freefraction f_p increased in ORM challenge studies. The low doses of ORM13070 (0.1 and 0.5 mg/kg) induceddecreases in yohimbine binding, more pronounced in striatum (10% and 37%) compared to the equal decline in cortex and thalamus (4% and 30% at the same doses). The dose of 1 mg/kg ofalpha 2C antagonist induced a similar decrease in all regions (65%), similar to pharmacological doses of yohimbine (0.02mg/kg).

Conclusions: This small study confirms that the striatal binding of yohimbine is due in part to binding to alpha 2C receptors. Several studies suggest that the preferred ligand of the alpha 2C receptors is dopamine. Our earlier studies with amphetamine challenge and microdialysis strongly support that yohimbine may be used as a surrogate marker of NA release in cortex and thalamus. This initial study suggests that the changes in the striatal binding of yohimbine during challenge studies however, mayalso be affected by DA.

1. Lehto J,Hirvonen MM, Johansson J, et al. Validation of [(11) C]ORM-13070 as a PETtracer for alpha2c -adrenoceptors in the human brain. Synapse 2015;69:172-81.

2. Jakobsen S, Pedersen K, SmithDF, Jensen SB, Munk O, Cumming P. Detection of alpha2 adrenergic receptors inbrain of living pig with 11 C-yohimbine.Journal of Nuclear Medicine 2006;47:2008-15.

3. Landau A, Doudet D, JakobsenS. Amphetamine challenge decreases yohimbine binding to α2 adrenoceptors inLandrace pig brain. Psychopharmacology 2012;222:156-63.

816
BRAIN-0853
Poster Session

BrainPET: Preclinical Imaging

INTERPRETING DIHYDROTETRABENAZINE BINDING DATA IN RODENT MODELS OF PARKINSONISM

M. Mejias[1], K. Dinelle[2], V. Sossi[2], D. Doudet[1]
[1]Medicine/Neurology,
University of British Columbia, Vancouver, Canada
[2]Physics and Astronomy,
University of British Columbia, Vancouver, Canada

Objective: In vivo evaluation of dopaminergic (DA) function in rats and mice is often performed with the use of microPET imaging and the vesicular monoamine transporter ligand, ^{11}C-dihydro-tetrabenazine(DTBZ). Unilateral models of nigro-striatal lesion have been extensively used to study the behavioural and pharmacological consequencesof DA loss. DTBZ is routinely used to evaluate longitudinally the effects of DAlesions, genetic manipulations, resulting compensatory mechanisms and therapeutic responses. Yet, despite the use of well characterized, purposely bred animals,there remains large variability in data. In this study, we evaluated causes in the variability of the published binding data in rodent striatum: role of the animal's origin on baseline binding values and importance of baseline values in interpretation.

Methods: Sprague Dawley (SD) rats (N=6; UBC South Campus: SC) receiveda unilateral lesion of the nigro-striatal pathway with 6-OHDA. Another group of SD rats (N=8; Charles River: CR) received a unilateral lesion of nigro-striatal pathway with lactacystin, a UPS inhibitor. All the animals were scanned at baseline, before lesion and 2 and 8 weeks post lesion. DTBZ scan were performed as previously described [1] [2] in a Siemens microPET Focus120. The striatal binding potentials BP_{ND} were calculated from a Logan graphical analysis using the cerebellum as the non-specific input. The effect of unilateral lesion on DTBZ binding in the contralateral, non–lesioned striatum was evaluated by comparing baseline and post lesion data in each lesion group independently. The effect of animal's origin was measured by comparing the baseline binding data in the SCand CR groups.

Results: Two-tailed paired t-tests were used for all comparisons. There was a significant difference (P= 0.006) in baseline DTBZ binding in SC (3.7±0.24) vs CR rats(4.22±0.32). There was a significant difference (P<0.04) in the DTBZ binding in the unlesioned side of the 6OHDA group (4.21±0.32 versus 4.7±0.3 and 4.6±0.2 at 2 and 8 weeks after lesion) and in the DTBZ binding in the unlesioned striatum of the UPS lesioned group (3.77±0.3 versus 4.37±0.3 and 4.32±0.25 at 2 and 8weeks post lesion). In both lesion models, there was a 11-15% increase in DTBZbinding post lesion compared to respective baseline.

Conclusions: Adequate interpretation of in vivo PET data requires careful attention to study design. While the influence of animal origin on behavioural testing is well established, it is to the best of our knowledge the first time that significant differences in DA innervation has been shown in vivo. Furthermore, our study demonstrates clearly that the use of the non-lesioned hemisphere as control (as opposed to pre-lesionbaseline data) may lead to mis-estimation of the effects of a unilateralintervention.

1. Strome EM,Cepeda IL, Sossi V, Doudet DJ. Evaluation of the Integrity of the DopamineSystem in a Rodent Model of PD: Small Animal Positron EmissionTomography Compared to Behavioral Assessment and Autoradiography. MIB 2006:1-8.

2. Mackeys S, Jing Y, Flores J,Dinelle K, Doudet DJ. Intranigral Administration of an UPS Inhibitor in Rat: Behavior, PET,Immuno-histochemistry. Experimental Neurology 2013;247:19-24.

817
BRAIN-0235
Poster Session

BrainPET: Preclinical Imaging

EVALUATION OF [18F]PBR111 BINDING IN YOUNG AND AGED NON-HUMAN PRIMATE BRAINS WITH AND WITHOUT PHARMACOLOGICAL MODULATION

R. Rajagovindan[1], A. Giamis[1], J. Wang[1], D. Reuter[1], M. Voorbach[1], A. Tovcimak[1], A. Basso[1], P. Jacobson[1], J. Beaver[1]
[1]iSAT, AbbVie Inc., North Chicago, USA

Objective: One of the hallmarks of neuroinflammation is increased microglia activation, characterized by overexpression of mitochondrial 18kDa Translocator Protein (TSPO). Increased microglial activation and TSPO expression have been reported with aging and wide range of neurological and psychiatric disorders [1,2]. Further, previous reports of treatment with minocycline in rodent models of brain injury have demonstrated reduction in microglia activation and binding of TSPO radioligands in pathological tissue [3] which were attributed to the brain-penetrant and anti-inflammatory properties of minocycline. This study examined whether the level of TSPO expression (a) is increased in aged relative to young non-human primates and (b) is reduced following minocycline treatment in aged non-human primates using [18F]PBR111 a second generation radioligand for TSPO.

Methods: [18F]PBR111 dynamic data were collected in young (7-8yrs) and aged (19-21yrs) cynomologus monkeys (n=4 each) with arterial sampling. Whole blood activity, plasma activity

and parent fraction were determined at multiple time points over 120 minutes. All animals received test-retest scans separated by 1-3 weeks. Following the test-retest baseline scans, the aged cohort received minocycline treatment (8mg/kg daily dose) over a period of 10-14 days followed by post-treatment PET scans. Subject-space atlas based on anatomical MRI was coregistered to PET images of each animal to derive regional time activity curves. Volumes of distribution (VT) in predefined regions of the brain (thalamus, midbrain and cortex) were used as the outcome measures and were quantified using Logan and 2TCM+Vb methods. The test-retest variability of VT in each cohort and the changes in VT pre and post minocycline treatment in the aged cohort will be determined.

Results: [18F]PBR111 exhibited deflourination demonstrated by relatively high magnitude of activity in the skull. The Logan and 2TCM+Vb models were able to fit the data well. The VT ranged between 8-30 ml/cm3 across all the young animals. However, the inter-regional variation of VT within each animal was small (%CoV<17%). The test-retest variability of VT in predefined regions of interest was modest ranging between 10-40% across the young animals. Analysis of dynamic PET data from the aged animals with and without minocycline treatment is ongoing.

Conclusion: Logan and 2TCM+Vb models performed well with [18F]-PBR111 data in primates. Analysis of the test-retest variability of VT in the aged cohort and the effect of minocycline treatment is ongoing and will test whether [18F]PBR111 VT is reduced following treatment with minocycline.

References:
1. Kumar et al., Journal of Neuroinflammation (2012) 9:232-241
2. Guo Q et al., Journal of Nuclear Medicine (2013) 54:1-9
3. Converse KA et al., Journal of Nuclear Medicine (2011) 52:257-262

Disclosures: All authors are employees of AbbVie. The design, study conduct, and financial support for this research were provided by AbbVie. AbbVie participated in the interpretation of data, review, and approval of the publication.

818
BRAIN-0528
Poster Session

BrainPET: Preclinical Imaging

PET-FDG EVALUATION OF THE BRAIN GLUCOSE METABOLISM IN QUINPIROLE SENSITISED RATS AS A MODEL FOR OBSESSIVE-COMPULSIVE DISORDER

S. Servaes[1], D. Glorie[1], J. Verhaeghe[1], S. Stroobants[2], S. Staelens[1]
[1]Department of Nuclear Medicine, Molecular Imaging Center Antwerp, Antwerp, Belgium
[2]Department of Nuclear Medicine, University Hospital Antwerp, Antwerp, Belgium

Objectives: A commonly used model for obsessive-compulsive disorder (OCD) is the quinpirole sensitisation rat-model[1]. Despite extensive behavioural evaluation of this model[2], the underlying pathological mechanism remains unknown. Here we describe the first *in vivo* evaluation of the glucose metabolism in this model with 2-deoxy-2-18F-fluoro-β-D-glucose (^{18F}FDG) PET/CT.

Methods: Baseline ^{18F}FDG-scans of the animals (n=14) were done prior to setup of the model. Animals were injected twice a week (for a total of 15 injections) with either quinpirole (0.5 mg/kg in saline) or saline. Paired with each injection, animals were subjected to a 30-minutes open-field test (OF) with 4 objects, videotracking their movement and frequency of visits per object. The most-visited object was referred to as the homebase. After the OF paired with injection 10 and 15, both groups were scanned again with ^{18F}FDG to visualize changes in glucose metabolism. Images were corrected for injected dose and plasma glucose values while the pons as the reference region for quantification. Volume-of-interest (VOI)-based analysis and voxel-based statistical parametric mapping were performed.

Results: After 15 injections, the quinpirole group displayed a strong increase in locomotor activity (31840 ± 3818 cm vs 4435 ± 2010 cm, i.e. +718%) and higher visiting frequencies of the homebase (175 ± 29.1 vs 12 ± 7.51, i.e. +1458%), compared to the saline group. Voxel-based analysis displayed significantly lower ($p<0.01$) levels of ^{18F}FDG-uptake in animals treated with quinpirole compared to the saline group (figure 1).

VOI-based analysis revealed that, when compared to the saline group, average decreases were most notable in the striatum (11.77% ± 7.36%), nucleus accumbens (NAcc; 11.10% ± 8.94%), cingulate gyrus (Cg; 12.47% ± 6.28%), orbitofrontal cortex (OFC; 8.27% ± 5.44%) and medial prefrontal cortex (mPFC; 14.11% ± 8.27%).

Conclusions: This study describes the first *in vivo* evaluation of the brain glucose metabolism in quinpirole-sensitised rats as a model for OCD. Consistent with previous findings, quinpirole induces a decrease in the brain glucose metabolism[3]. Strong significant deficiencies were found in the striatum, NAcc, Cg, OFC and mPFC, which might explain the pathological compulsive behaviour the animals show.

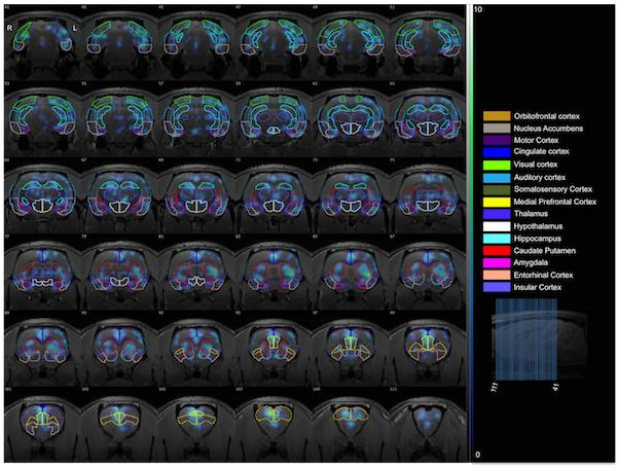

Figure 1: Coronal sections from the posterior to the anterior part of the brain, comparing the quinpirole group to the saline group, displaying T-maps (cluster size > 50 voxels) with significant hypometabolism ($p < 0.01$) overlaid on an MR template.

References:

1. Szechtman, H., Sulis, W. & Eilam, D. Quinpirole induces compulsive checking behavior in rats: a potential animal model of obsessive-compulsive disorder (OCD). *Behavioral Neuroscience* **112,** 1475–1485 (1998).

2. Eagle, D. *et al.* The dopamine D2/D3 receptor agonist quinpirole increases checking-like behaviour in an operant observing response task with uncertain reinforcement: a novel possible model of OCD. *Behavioural Brain Research* **264,** 207–229 (2014).

3. Richards, T. L., Pazdernik, T. L. & Levant, B. Altered quinpirole-induced local cerebral glucose utilization in anterior cortical regions in rats after sensitization to quinpirole. *Brain Res.* **1042,** 53–61 (2005).

819
BRAIN-0296
Poster Session

BrainPET: Preclinical Imaging

CUMI-101 BINDS TO A1 ADRENOCEPTORS IN HUMAN CEREBELLUM AND IS NOT A SUITABLE REFERENCE REGION.

S. Shrestha[1], K.J. Jenko[1], J.S. Liow[1], M. Ikawa[1], S.S. Zoghbi[1], R.B. Innis[1]
[1]Molecular Imaging Branch, National Institute of Mental Health, Bethesda, USA

CUMI-101 binds to α1 adrenoceptors in human cerebellum and is not a suitable reference region.

Stal S. Shrestha, Kimberly J. Jenko, Jeih-San Liow, Masamichi Ikawa, Sami S. Zoghbi, and Robert B. Innis

Molecular Imaging Branch, National Institute of Mental Health, Bethesda, Maryland, USA

Objectives: Previously, we reported that the positron emission tomography (PET) radioligand [^{11}C]CUMI-101 suggested to be selective for the 5-HT_{1A} receptor also binds to α1 adrenoceptors in several brain regions, including cortex, thalamus,

and striatum in monkey and rat brain (Shrestha et al., 2014[1]). *In vitro*, similar results were found in human brain. Furthermore, in monkeys, pre-blocking α1 adrenoceptors by Prazosin displaced [^{11}C]CUMI-101 from cerebellum. In our current study, we examined, *in vitro*, whether CUMI-101 also binds to α1 adrenoceptors in human cerebellum.

Methods: *In vitro* homogenate binding assays were done in the cerebellum of human, monkey, and rat. [^{3}H]Prazosin was used to determine B_{max} as well as K_D of Prazosin, and K_i of CUMI-101. [^{3}H]CUMI-101 was used to directly measure per cent cross-reactivity to α1 adrenoceptors. All studies were done at 37 °C.

Results: CUMI-101 showed similar affinities to α1 adrenoceptors in cerebellum across species. Cerebellar binding potential (B_{max}/K_i) were 24 (human), 23 (monkey), and 34 (rat); the ratio of the affinities of CUMI to that of Prazosin for α1 adrenoceptors in cerebellum (K_i / K_D) were 5 (human), 10 (monkey), and 15 (rat) (Table 1). One-point assay using [^{3}H]CUMI and 50 nM Prazosin displaced α1 adrenoceptors by 30% in human, 60% in monkey, and 70% in rat.

Conclusion: Together, our *in vitro* results suggest that CUMI-101 binds to α1 adrenoceptors in the human cerebellum. As such, cerebellum is not a suitable reference region for [^{11}C]CUMI-101 to measure binding potential.

Reference:

[1]Shrestha, S.S., Liow, J.S., Lu, S., Jenko, K., Gladding, R.L., Svenningsson, P., Morse, C.L., Zoghbi, S.S., Pike, V.W., Innis, R.B., 2014. ^{11}C-CUMI-101, a PET radioligand, behaves as a serotonin 1A receptor antagonist and also binds to alpha(1) adrenoceptors in brain. J Nucl Med 55, 141-46.

Table 1. Binding Potential (BP) and K_i/K_d in human, monkey, and rat

Species	B_{max} (fmol/mg)		Prazosin K_D (nM)		CUMI K_i (nM)		BP B_{max} / K_i		K_i / K_D	
	37 °C	23 °C	37 °C	23 °C	37 °C	23 °C	37 °C	23 °C	37 °C	23 °C
human	104	50	0.93	0.04	4.30	0.64	24	78	5	
monkey	81		0.34	0.34	3.50	3.5	23		10	10
rat	172	74	0.34		5		34		15	

820
BRAIN-0807
Poster Session

BrainPET: Preclinical Imaging

EVALUATION OF [11C]PBR28 PET IMAGING TO DETECT CHANGES IN MICROGLIAL ACTIVATION IN MOUSE MODELS OF ALZHEIMER'S DISEASE

S.P. Tang[1], N. Mirzaei[2], C. Coello[1], S. Ashworth[1], A. Weekes[1], C. Plisson[1], J. Passchier[1], R.J. Tyacke[2], D. Nutt[2], M. Sastre[2]
[1]Imanova, Imanova Limited, London, United Kingdom
[2]Division of brain sciences, Imperial College, London, United Kingdom

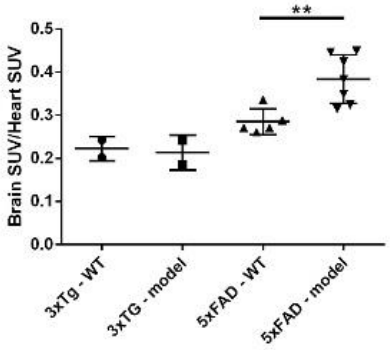

Objectives: Inflammatory changes have been linked with deficits in neuronal function and synaptic plasticity in Alzheimer's disease (AD). It seems that inflammation is an early event, preceding inclusion formation in a number of AD experimental models and in AD patients [1]. In particular, the role of microglia in the pathogenesis of AD has become a major focus of

AD research. TSPO is a mitochondrial translocator protein which is overexpressed in activated microglia and astrocytes. We evaluated the utility of [^{11}C]PBR28 to detect alterations in TSPO levels, as a measure of microglial activation, in the 3xTG mouse model of amyloid and tau pathology and 5xFAD model of amyloidosis at early ages.

Methods: 15 months old 3xTg (n=2) and 6 months old 5xFAD (n=4) female mice and corresponding control wild-type (WT) mice (Hybrid B6;129 n=2 and C57BL6 n=4), were investigated. Dynamic PET-CT scans (60 min, using Siemens INVEON DPET/MM scanner) were acquired under isoflurane anaesthesia following intravenous administration of [^{11}C]PBR28 (4.0 ± 2.3 (0.7 - 8.2) MBq, specific activities 93 ± 54 (8 - 165) GBq/µmol). Four mice underwent a second PET-CT scan (on different days) to assess the test-retest variability. Regions of interest derived time-activity curves (TACs) were obtained for the brain and heart. The average standard uptake value (SUV) between 30 and 60 min was calculated and the brain SUV was normalized to the heart SUV to account for changes in the radioligand delivery to the brain. In addition, immunohistochemistry (IHC) was performed on the mouse brains to detect Aβ plaques and/or tau tangles or co-localization of microglia and TSPO.

Results: The normalized brain SUV showed good test-retest variability (range: 6-15%). There was no significant difference between the brain SUV of [^{11}C]PBR28 in the 3xTg mice compared to the control WT mice (see Figure). IHC also showed very few plaques and tangles in the 3xTg mice brain. The brain SUV of [^{11}C]PBR28 in the 5xFAD mice was higher compared to the corresponding control WT mice (unpaired t-test, P<0.01) and compared to the 3XTg mice. IHC demonstrated co-localization of microglia with the TSPO signal in the 5xFAD mice.

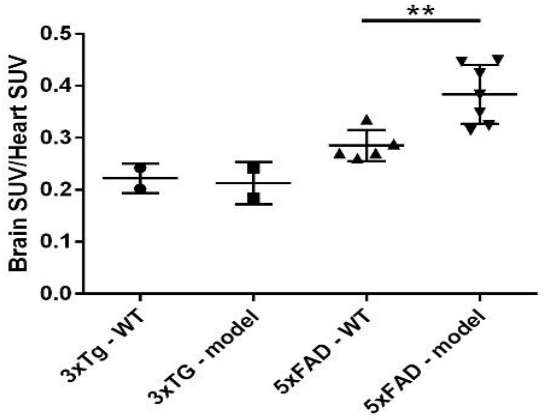

Conclusions: The 5xFAD but not the 3xTg AD mouse model produced significant increases in microglial activation detected with [^{11}C]PBR28 PET imaging. These findings were confirmed by IHC highlighting the suitability of [^{11}C]PBR28 to investigate changes in microglial activation in this pre-clinical model of AD.

References:

[1] Kreisl et al., Brain, 2013, 136 (7), 2228-2238

821
BRAIN-0438
Poster Session

BrainPET: Preclinical Imaging

LONGITUDINAL PET IMAGING OF ZQ175, A MOUSE MODEL OF HUNTINGTON´S DISEASE

J. Häggkvist[1], M. Tóth[1], L. Tari[1], K. Varnäs[1], C. Dominguez[2], I. Munoz-Sanjuan[2], A. Varrone[1], C. Halldin[1], L. Mrzljak[3]
[1]Department of Clinical Neuroscience, Karolinska Institutet, Stockholm, Sweden
[2]Inc. Los Angeles, CHDI Foundation, Los Angeles, USA
[3]Inc. Princeton, CHDI Foundation, Princeton, USA

Objectives: Huntington's disease is a neurodegenerative disorder, characterized by progressive loss of medium spiny neurons in the striatum. The loss of neurons leads to development of motor dysfunction, emotional

disturbances, psychiatric symptoms and cognitive deficits. Huntington´s disease is caused by expansion of the CAG-repeat within the 5´end of the IT15 coding gene for the protein Huntingtin (Htt) [1]. Several animal models have been developed to study the progression of disease as well as to evaluate potential new therapeutics. The zQ175 knock-in mouse model is considered to show high face validity for the human condition [2]. In the present study, we have used small animal positron emission tomography (PET) in order to examine the molecular phenotype of the zQ175 mouse model. We focused on subcortical and cortical markers, including the dopamine D_2 and D_1 receptors, the phosphodiesterase 10A (PDE10A) enzyme and the serotonin (5-HT_{2A}) receptor.

Methods: Male heterozygous zQ175 and wild-type (WT) animals were imaged with the dopamine D_2-receptor radioligand [^{11}C]raclopride, the PDE10A radioligand [^{18}F]MNI-659, the dopamine D_1-receptor radioligand [^{11}C]NNC 112 and the 5-HT_{2A} radioligand [^{11}C]MDL 100907 at 6 and 9 months of age using the nanoScan® PET/MRI and nanoScan® PET/CT scanners (Mediso Ltd, Hungary). The main outcome measure was binding potential (BP_{ND}), estimated using the cerebellum as reference region. We have selected the striatum for all radioligands and the rostral cortex, dorsal cortex and hippocampus for [^{11}C]NNC 112 and [^{11}C]MDL 100907 as regions of interests.

Results: At 6 months of age, the BP_{ND} in the striatum was lower in zQ175 animals compared with WT animals by 40% in the case of [^{11}C]raclopride ($p<0.0001$), by 52% in the case of [^{18}F]MNI-659 ($p<0.001$), by 29% in the case of [^{11}C]NNC 112 ($p<0.001$) and 12% in the case of [^{11}C]MDL 100907 ($p<0.01$). In the rostral cortex, D1-receptor binding was 24% lower in zQ175 compared to WT. In the hippocampus, the BP_{ND} of [^{11}C]MDL 100907 in zQ175 was 12% lower compared to WT. At 9 months there was a slight reduction of D1, D2 and 5-HT2A in the striatum (with a 4-7 % further decrease in zQ175 compared to WT), whereas PDE10A reached a plateau. Cortical markers were also slightly further decreased at 9 months in zQ175 animals.

Conclusions: The present study shows a marked loss of D_1- and D_2- receptors as well as a loss of PDE10A enzyme in the striatum of zQ175 mice, which is in agreement with data obtained in clinical PET studies. The 5-HT_{2A} receptors seemed to be less affected. zQ175 mice represent a suitable model for understanding the pathophysiology of Huntington's disease and for evaluating new therapeutic strategies aimed to interfere with the progression of the disease.

References: 1. The Huntington's Disease Collaborative Research Group (1993) A novel gene containing a trinucleotide repeat that is expanded and unstable on Huntington's disease chromosomes. Cell 72: 971–983

2. Menalled et al. (2012) Comprehensive behavioral and molecular characterization of a new knock-in mouse model of Huntington's disease: zQ175. PLoS One 7(12): e49838

822
BRAIN-0474
Poster Session

BrainPET: Preclinical Imaging

PET IMAGE QUANTIFICATION IN RODENTS: UP TO NON-INVASIVE, STANDARDIZED IMAGING PROTOCOLS ALLOWING LONGITUDINAL STUDIES.

N. Van Camp[1], M. Guerif[2], D. Chéramy[2], M. Guillermier[1], L. Eymin[1], D. Houitte[1], E. Diguet[2], G. Bonvento[1], P. Hantraye[1]
[1]Commissariat à l'Energie Atomique et aux Energies Alternatives (CEA) Département des Sciences du Vivant (DSV), Institut d'Imagerie Biomédicale (I2BM) Molecular Research Center (MIRCen) Centre National de la Recherche Scientifique (CNRS) Université Paris-Sud Université Paris-Saclay UMR 9199 Neurodegenerative Diseases Laboratory, Fontenay aux Roses, France
[2]Institut de Recherches Servier, DRD-RDNPS, Croissy sur Seine, France

Introduction-PET image analysis of the rat brain is often limited to semi-quantitative measurements of SUV or SUV-R, as proper quantification requires a metabolite-corrected arterial input function (AIF). This is an important burden for the animal due to its invasiveness, which might even require the sacrifice of the animal. Additionally, an excess of blood withdrawal during the image acquisition might disturb the animal physiology and bias the outcome. Previously, a method has been published to measure the whole blood AIF using a femoral arteriovenous shunt (Weber et al. 2002) circumventing the problem of the blood volume loss.

Objectives-To adapt the setup published by Weber et al. to non-invasive caudal arteriovenous shunt. We first compared the caudal with the femoral input function and its influence on the graphical quantification of CMR_{glu}. Next we performed repetitive ^{18}F-FDG acquisitions with at least 14 days interval to demonstrate complete recovery of the tail artery.

Methods- ^{18}F-FDG PET imaging was performed on the FOCUS220 PET scanner under isoflurane gas anesthesia. Glucose measurements were performed by One Touch and by GM9 glucose-oxidase measurements (Imlab, Analox Instruments) at the start of the experiment and at 20, 40 and 60 minutes. In a *first* set of experiments, 5 rats underwent double AIF sampling through caudal and femoral arteriovenous shunts using two twilite (Swisstrace) systems in parallel. In a *second* set of experiments, 6 rats underwent AIF measurement through only a caudal arteriovenous shunt, and the same animals were rescanned at least two weeks after the first experiment. In this setup, rats were ventilated and all physiological parameters were kept constant between the test-retest measurements. CMRglu parametric images were calculated according the graphical method of Patlak using PMOD software routines and coregistered to the MRI template of Schiffer et al. (2006). For the first experiment CMRglu was calculated for the caudal and femoral AIF, and the variability on the outcome was compared. For the second experiment Test-Retest covariability was measured between two consecutive experiments.

Results-One touch measurements systematically underestimated glycaemia values up to 30% and thus for quantification of CMRglu only glucose-oxidase measurements were used. Caudal input functions showed a reduction of the AIF peak height by 20% and a maximum peak delay of 30-40 sec as compared to femoral input functions, though no dispersion of the caudal AIF was observed. Quantification of CMRglu by the graphical method of Patlak did not show any significant difference in any brain region, dependent if the caudal or femoral AIF was used ($p>0.05$, paired t-test). The variability between CMRglu calculated with caudal or femoral AIF was less than 5%. In the Test-Retest study, no significant differences of CMRglu were measured in any brain region ($p>0.05$, paired t-test). Test-Retest variability for CMRglu data for the repeated measures was less than 10%.

Conclusion-A standardized method for non-invasive AIF measurements in rats was validated

allowing reliable graphical quantification of PET data with low test-retest variability. The impact on the AIF however was not negligible and further studies need to validate the bias on non-graphical models.

823
BRAIN-0500
Poster Session

BrainPET: Preclinical Imaging

IN VIVO COMPARISON OF TAU-SPECIFIC RADIOLIGANDS IN THE NORMAL RAT BRAIN AND IN VARIOUS RAT MODELS OF SPORADIC AND FAMILIAL TAUOPATHY USING PET IMAGING

N. Van Camp[1], M. Guillermier[1], K. Cambon[1], M. d'Orange[1], Y. Bramoullé[1], L. Eymin[1], G. Auregan[1], M. Guerif[2], D. Chéramy[2], C. Josephine[1], N. Dufour[1], M.C. Gaillard[1], A.M. Chollet[2], E. Diguet[2], M. Colin[3], L. Buée[3], A. Bemelmans[1], P. Hantraye[1]
[1]Commissariat à l'Energie Atomique et aux Energies Alternatives (CEA) Département des Sciences du Vivant (DSV), Institut d'Imagerie Biomédicale (I2BM) MIRCen Centre National de la Recherche Scientifique (CNRS) Université Paris-Sud Université Paris-Saclay UMR 9199 Neurodegenerative Diseases Laboratory, Fontenay-aux-Roses, France
[2]Institut de Recherches Servier, DRD-RDNPS, Croissy sur Seine, France
[3]Inserm UMR-S 1172, Université Lille 2 Faculté de Médecine IMPRT JPARC CMRR CHR, Lille, France

Introduction: Positron emission tomography (PET) imaging of early tau-pathology would be a major asset for the diagnosis and follow up of new therapeutic strategies in Alzheimer's disease and parented disorders. However, validation of radioligands specifically interacting with pathological tau-proteins is challenging due to the existence of different isoforms and, in Alzheimer's disease, the co-existence of tau aggregates with amyloid-β deposits requiring a high *in vivo* specificity of the ligands for tau over amyloid aggregates.

Objectives: *(1) In healthy rat brain:* To investigate the regional cerebral distribution and kinetics of various tau-specific radioligands (^{18}F-THK523, ^{18}F-T808 and ^{18}F-T807) in comparison with ^{18}F-AV45, a specific amyloid marker; and to evaluate the incidence of various reference regions on the estimation of *in vivo* binding. *(2) In rat models of local tau-pathology:* To characterize the regional brain distribution; to examine the specific binding in the presence of abnormal tau species; to validate these results using an *in vivo/ex vivo* 3-dimensional co-registration strategy.

Material&Methods: Tau protein was overexpressed bilaterally in the hippocampus using stereotactic injections of AAV-vectors encoding either the mutant h1N4R-P301L-Tau, or a construct co-expressing equimolarly a pro-aggregating peptide and the human WT h1N4R. PET imaging was performed on healthy controls and 2 months after viral vector injections, using a FOCUS220 preclinical PET scanner. Images were first co-registered to corresponding T_2-weighted MR-images, acquired on a Varian 7T scanner, and then normalized to a T_2-weighted MRI template and corresponding atlas (Schiffer, JNeurosciMethods, 2006) allowing automated segmentation of the entire brain. Finally, brains were immunostained for the detection of early (AT8), and late (AT100) tau pathology and amyloid-b deposition. A 3D-reconstruction of the histological data is ongoing for correlation analysis between *in vivo/ex vivo* data.

Results: In the healthy brain, the regional distribution of ^{18}F-THK523 was very similar to that of ^{18}F-AV45 with a tendency for higher retention in myelin-rich regions. ^{18}F-T808 suffered from an important defluorination *in vivo* that could only temporarily be blocked by high dose of fluconazole pretreatment. ^{18}F-T807 showed a homogeneous brain distribution with extremely low retention and fast clearance from the cerebellum. As a consequence, relative SUVs ($SUV\text{-}R=SUV_{ROI}/SUV_{REF}$) for ^{18}F-T807/^{18}F-T808 were globally superior to 1 in most brain regions when the cerebellum and not the occipital cortex was used as a reference. In the rat models of tau-pathology developing an important and

progressive AT8 immunoreactivity in the injected regions, no obvious uptake of any of the tested ligands was observed. However, a more detailed correlation analysis using 3D histology on sections stained for AT8, AT100 and amyloid is still ongoing.

Discussion&Conclusion: In healthy controls, the binding pattern of ^{18}F-THK523 and ^{18}F-AV45 using the cerebellum as a reference showed higher uptake in regions enriched with β-sheet structures such as myelin. In the case of 18F-T807/18F-T808, the choice of the cerebellum as reference introduced a strong bias in the SUV-R results whereas the occipital cortex generated consistent SUV-R values around 1. Correlative PET-histological analyses are still ongoing to assess the ability of these ligands to detect post-translational and conformational changes in tau protein species.

824
BRAIN-0790
Poster Session

BrainPET: Preclinical Imaging

CHRONIC ETHANOL EXPOSURE AND WITHDRAWAL UPREGULATES TSPO, A MARKER OF NEUROINFLAMMATION

P. Georgiou[1], M. Sklirou[2], N. Kalk[3], A. Lingford-Hughes[3], S.M.O. Hourani[1], I. Kitchen[1], A. Bailey[1], L. Wells[2]
[1]Department of Biochemistry & Physiology, University of Surrey, Surrey, United Kingdom
[2]Radiochemical Sciences, Imanova Centre for Imaging Sciences, London, United Kingdom
[3]Department of Medicine, Imperial College London, London, United Kingdom

Objectives

Recent evidence suggests a role for neuroinflammation underlining alcohol addiction, although the mechanism remains unclear. 18kDa translocator protein (TSPO) is sparsely expressed in the brain parenchyma, and resting glia, but richly expressed in activated glial cells. TSPO PET has been used to detect neuroinflammation *in vivo* in humans in inflammatory conditions. The aim of this study was to investigate the change in TSPO binding sites, using [^{3}H]PBR28, during a model of chronic alcohol consumption and withdrawal to help elucidate the role of neuroinflammation in alcohol addiction.

Methods

Mice (C57Bl/6J) were treated with an ethanol-containing diet or isocaloric control diet up to 10 days, with the following escalating paradigm: 2.3%v/v for 2days, 4.7%v/v for 2days and 7%v/v for 6days. After 10 days of treatment, mice were withdrawn from ethanol. Five cohorts of ethanol-treated groups together with their respective controls (n=5-6) underwent behavioural assessments of memory and motor coordination, (novel object recognition (NOR) and Rota-Rod respectively) on either days 4 (D4), 10 (D10) or post-withdrawal days 1 (WD1), 4 (WD4) and 7 (WD7). At the end of the behavioural tests, brains were removed and coronal brain sections (20um) were taken from the level of the olfactory tubercle to the cerebellum. Total binding was determined by incubating sections with 6nM [^{3}H]PBR28; non-specific binding was determined by the addition of 10uM PK11195. Slides were apposed to film for 8weeks and the specific binding (fmol/mg) determined in the regions of interest.

Results

A decrease in the latency to fall was observed following the 10-day alcohol treatment which persisted 1 day post-withdrawal suggesting impaired motor coordination; no differences were observed 4 and 7 days post-withdrawal. Chronic ethanol treatment did not have a significant effect on memory as evaluated by NOR; however, ethanol-withdrawal resulted in memory impairment on WD1 and WD7.

Chronic ethanol treatment (D10) led to a significant increase in [^{3}H]PBR28 binding in the motor cortex regions compared with control tissue (Bmax, fmol/mg tissue: $M1_{region}$,147±11 vs

95±14; $M2_{region}$ 162±14 vs 106±16 respectively, *P*<0.05). This increase in TSPO binding sites was transient and no significant differences in [^{3}H]PBR28 binding were observed at treatment D4 or withdrawal days 4 and 10. Chronic ethanol treatment did not lead to an increase in TSPO binding sites in other brain regions of interest. A significant increase in [^{3}H]PBR28 binding was observed one day post-ethanol withdrawal in the motor cortex, caudate putamen, nucleus accumbens, hippocampus, amgydala, and cerebellum compared with control tissue (**Table 1**). This increase in TSPO was transient; no difference in [^{3}H]PBR28 binding was observed 4 and 7 days post-withdrawal where the binding sites between ethanol-withdrawn and control subjects were equivalent.

Conclusions

Chronic ethanol treatment and withdrawal leads to regionally specific and time dependent increases in central TSPO binding sites. Ethanol-induced neuroinflammation may be a contributing factor to motor and cognitive impairments. This data supports the use of TSPO PET to monitor these changes *in vivo*.

Table 1	[^{3}H]PBR28 Specific binding (fmol/mg tissue, mean±SEM)		
Brain region (*P<0.05)	Control	1 day post-ethanol withdrawal	Δ change (%)
Motor cortex 1	121 ± 11	160 ± 11*	32%
Caudate Putamen	105 ± 5	142 ± 13*	35%
Nucleus Accumbens	111 ± 7	153 ± 12*	38%
Hippocampus CA1	143 ± 13	209 ± 40*	46%
Hippocampus CA3	112 ± 7	158 ± 17*	41%
Dentate Gyrus	190 ± 8	263 ± 35*	38%
Amygdala	114 ± 7	157 ± 10*	38%
Cerebellum	162 ± 4	232 ± 21*	43%

825
BRAIN-0793
Poster Session

BrainPET: Preclinical Imaging

IMAGING DOPAMINE SYNTHESIS CAPACITY IN THE MALE RAT- A [18F]FDOPA POSITRON EMISSION TOMOGRAPHY STUDY

M. Kokkinou[1], O. Howes[1], M. Veronese[1], A. Romiti[2], N. Keat[2], C. Coello[2], L. Wells[2]

[1]Psychosis Studies, Institute of Psychiatry Kings College London, London, United Kingdom
[2]Radiochemical Sciences, Imanova Centre for Imaging Sciences, London, United Kingdom

Objectives: Dopamine synthesis capacity is thought to be disrupted in a number of neuropsychiatric disorders and potentially provides a translational neurobiological marker for preclinical models of these disorders[1]. In this study we aimed to measure striatal presynaptic dopaminergic function following the repeated administration of saline in the rat, to assess whether these animals could be used as an appropriate control for a preclinical model of schizophrenia.

Methods: Four male Sprague-Dawley rats received once daily 0.9% saline i.p injections for 5 consecutive days and were scanned the following week; three rats did not receive any injections prior to the scanning day. All subjects received a combination of benserazide hydrochloride (10mg/kg i.p.,30min) and tolcapone (40mg/kg i.p., 90min), inhibitors of peripheral aromatic L-amino acid decarboxylase (AADC) and catechol-O-methyl transferase (COMT) respectively, on the scanning day. Following an i.v bolus administration of 7.45±4.79MBq of [^{18}F]FDOPA ([^{18}f]fluoro-3,4-dihydroxyphenyl-*l*-alanine), the seven rats underwent a dynamic PET:CT scan (180min, Inveon PET:CT). The average Standardized Uptake Values (SUV) for [^{18}F]FDOPA were calculated between 75min and 150min. The pharmacokinetics of the tracer were analysed by a modified Patlak method which retrieved the striatal [^{18}F]FDOPA influx rate constants (Ki) to index dopamine synthesis capacity in relation to the uptake in the cerebellum reference region. Data from treated and untreated subjects were compared by independent t-tests with an alpha level of 0.05.

Results: In all 7 rats there was a clear [^{18}F]FDOPA uptake in the bilateral striatum compared to other regions such as the cerebellum **(Image 1)**. In both groups the [^{18}F]FDOPA kinetics in striatum

compared to cerebellum initially showed an irreversible uptake (≤90min) with a slow reversible component seen thereafter. The mean Ki values ± SD for saline treated group and for the naïve group were 0.015±0.003 and 0.014±0.002 respectively.The mean $SUV_{75\text{-}150\ min}$ values ± SD were 1.95 ± 0.17 and 1.94 ± 0.28 for the saline treated and naïve groups respectively. There was no significant difference in the Ki values nor the $SUV_{75\text{-}150min}$ values between the saline treated rats and treatment naïve rats (P>0.05).

Conclusion: These results support the use of [^{18}F]FDOPA PET preclinically to measure [^{18}F]FDOPA uptake in the striatum of male Sprague Dawley rats. Stress induced by the repeated saline administration did not alter the dopamine synthesis capacity. This enables the use of an optimised scanning protocol to investigate the effect of preclinical models of neuropsychiatric disorders impacting on the dopaminergic system.

Reference:[1]Demjaha A., Murray RM, McGuire PK, Kapur S, Howes OD.Dopamine synthesis capacity in patients with treatment-resistantschizophrenia. Am J Psychiatry. 2012 Nov1;169(11):1203-10.

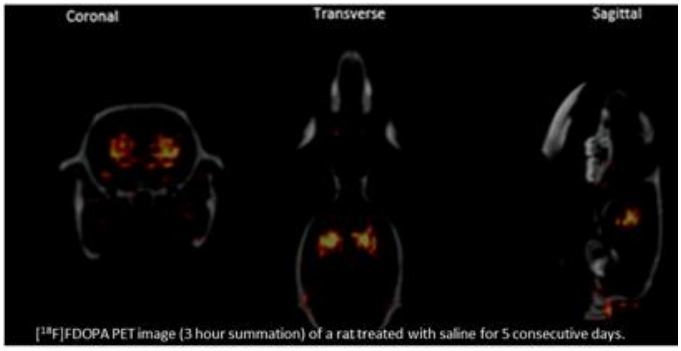

826
BRAIN-0088
Poster Session

BrainPET: Neurotransmitter System Evaluation

IN VIVO POSITRON EMISSION TOMOGRAPHY (PET) EVALUATION OF TARGET OCCUPANCY OF ABT-419, A GLYCINE TRANSPORTER-1 (GLYT1) INHIBITOR, USING [18F]CFPYPB IN NON-HUMAN PRIMATES (NHP) AND HUMAN VOLUNTEERS

A.M. Basso[1], E. Bain[2], A.A. Othman[3], R. Rajagovindan[1], J.Q. Wang[1], A. Tovcimak[1], M.J. Voorbach[1], A. Giamis[1], D. Reuter[1], C. Kalvass[4], P. Jacobson[1], E. van der Kam[5], B. Behl[5], B. Rendenbach-Mueller[2], S. Dutta[3], G.B. Fox[1], J. Beaver[1]
[1]Translational Sciences-Imaging, AbbVie, North Chicago, USA
[2]Neuroscience Clinical Development, AbbVie, North Chicago, USA
[3]Clinical Pharmacology and Pharmacometrics, AbbVie, North Chicago, USA
[4]DMPK-BA, AbbVie, North Chicago, USA
[5]Neuroscience Discovery, AbbVie, Ludwigshafen, Germany

Hypofunction of the NMDA receptor-mediated neurotransmission is thought to be involved in the pathology of schizophrenia. GlyT1 regulates extracellular levels of glycine, a co-agonist at the NMDA receptor. GlyT1 inhibition increases synaptic glycine, and is proposed as potential treatment to reverse NMDA hypofunction in schizophrenia. ABT-419 is a novel potent, selective and competitive GlyT1 inhibitor.

Objective: To evaluate the *in vivo* relationship between ABT-419 plasma concentrations and the brain GlyT1 occupancy in baboons, cynomolgus macaques and healthy human volunteers.

Methods: GlyT1 occupancy was assessed by dynamic PET with arterial sampling in NHP and healthy individuals using [^{18}F]CFPyPB (1, 2, 3). PET imaging was conducted at baseline and following a blockade protocol with ABT-419. In NHP, ABT-419 doses were infused intravenously over a 3-h infusion protocol. [^{18}F]CFPyPB was administered

by intravenous bolus 1-h after the start of ABT-419 infusion, followed by 2-h dynamic scans. The human PET study was conducted following single-oral doses of ABT-419. [^{18}F]-CFPyPB was administered intravenously and followed by 90 min of dynamic PET scans. The temporal relationship between ABT-419 plasma concentrations and GlyT1 occupancy was investigated by injecting [^{18}F]CFPyPB at different times relative to ABT-419 administration up to 22-h (NHP) or 30-h post dose (human). PET images were coregistered with NHP/human MRI to apply a volume of interest template and generate regional time activity curves. Tracer kinetic analysis at baseline and post-dosing, showed that a two-tissue compartment model (2TCM) with a blood volume term is the appropriate plasma input model to calculate the regional equilibrium partition coefficient (V_T). V_T and occupancy plot analysis (4), indicated there was no reference region and SRTM would not be appropriate.

Results: The highest uptake of [^{18}F]CFPyPB and GlyT1 occupancy by ABT-419 was observed in brainstem, pons, midbrain, cerebellum and thalamus. Dose-dependent target occupancy was achieved in NHPs reaching full occupancy (>90%) at high doses. In humans, a dose-dependent target occupancy was observed, but, full occupancy was not achieved due to dose-limiting tolerability issues. There was a disconnect between ABT-419 plasma pharmacokinetic profile and the brain GlyT1 target occupancy, with time dependent EC_{50} values and lower EC_{50} at the later scan time points; suggesting prolonged GlyT1 occupancy and indirect kinetics. Results are discussed in terms of kinetic modeling, PK-target occupancy relationship and translatability value among different species.

Conclusion: ABT-419 penetrated the brain and engaged the GlyT1 target achieving dose dependent occupancy in the brain. Use of a direct relationship between ABT-419 plasma levels and target occupancy is not appropriate for the occupancy analysis and further indirect kinetic modeling or biophase model is needed. Characterization of GlyT1 occupancy and ABT-419 plasma concentrations in NHP supported preliminary prediction of pharmacologically active doses in humans and initial planning for first-in-human study. The human PET data were critical for decisions on further clinical development of ABT-419. These data confirm strongly support the use of brain PET target occupancy studies for translational purpose.

References:
1. Hamill et al., Synapse 65:261-270(2011)
2. Sanabria-Bohorquez et al., NeuroImage 59:2589-2599(2012)
3. Martin-Facklam et al., Neuropsychopharmacology 38:504-512(2013)
4. Cunningham et al., JCBFM 30:46-50(2010)

827
BRAIN-0606
Poster Session

BrainPET: Neurotransmitter System Evaluation

CHARACTERIZATION OF MGLUR5 AVAILABILITY MEASURED BY HIGH-RESOLUTION [11C]ABP688 PET IN HEALTHY CONTROLS

J.M. DuBois[1], O.G. Rousset[2], J. Rowley[3], M. Porras-Betancourt[1], A.J. Reader[4], A. Labbe[5], G. Massarweh[1], J.P. Soucy[1], P. Rosa-Neto[1], E. Kobayashi[1]
[1]Department of Neurology and Neurosurgery, Montreal Neurological Institute McGill University, Montreal, Canada
[2]The Russell H. Morgan Department of Radiology and Radiological Science, Johns Hopkins University, Baltimore, USA
[3]McGill Center for Studies in Aging, Douglas Mental Health University Institute McGill University, Montral, Canada
[4]PET Unit McConnell Brain Imaging Center, Montreal Neurological Institute McGill University, Montral, Canada
[5]Department of Epidemiology Biostatistics and Occupational health, McGill University, Montral, Canada

Objectives: Metabotropic glutamate receptor type 5 (mGluR5) is a G-protein coupled receptor that has been implicated in several psychiatric and neurological diseases[1]. The radiopharmaceutical

[^{11}C]ABP688 allows for *in vivo* quantification of mGluR5 availability using positron emission tomography (PET)[2]. Previous studies of [^{11}C]ABP688 in healthy individuals have shown conflicting age and gender effects, with the caveat that most have used a small number of subjects with a narrow age range, limited to the male population[3-5]. In this study, we aimed to detail the regional distribution of [^{11}C]ABP688 binding potential (BP_{ND}) and the existence of age/gender effects in healthy individuals.

Methods: We studied 31 healthy individuals aged from 20-77 y.o. (males, n=18, 45.3 ± 18.2 y.o; females, n=13, 41.5 ± 19.6 y.o) using the high-resolution research tomograph (HRRT). We developed an advanced partial volume correction method using surface-based analysis to accurately estimate the regional variation of radioactivity. Partial volume corrected $BP_{ND,}$ estimated through the simplified reference tissue model with the cerebellum as a reference region, was obtained using a surface-based analysis. We characterized the distribution of BP_{ND} using vertex-wise analysis and a detail cortical atlas with 34 regions per hemisphere.

Results: Our results show that a high degree of variation exists in [^{11}C]ABP688 BP_{ND} across cortical and subcortical brain regions, with the highest [^{11}C]ABP688 BP_{ND} in the prefrontal and anterior cingulate cortices. The lowest [^{11}C]ABP688 BP_{ND} were observed in the pre- and post-central gyri as well as the occipital lobes and the thalami. While previous studies reported higher BP_{ND} in temporal lobe as compared to the frontal lobe, using more refined regions of interest we found that most frontal cortical regions showed higher [^{11}C]ABP688 BP_{ND} than most temporal cortical regions [6, 7]. Associations between age and [^{11}C]ABP688 BP_{ND} were observed in the right amygdala and left putamen, but did not survive multiple comparisons, using a false discovery rate method, or partial volume correction. In addition, no gender differences were observed.

Conclusions: In conclusion, we show that high–resolution imaging and detailed analysis of cortical regions better describe the complex mGluR5 chemoarchitectural features of humans than previously used approaches. Our results contrast with data from MR spectroscopy showing age-related adaptations on brain concentrations of glutamate but supports a growing conceptual framework in which normal aging is characterized by stable global and regional mGluR5 availability[8].

References

1. Benarroch EE. *Neurol.* 2008; 70(12): 964-8.
2. Ametamey SM. *J. Nucl. Med.* 2006; 47(4): 698–705.
3. Akkus F, *et al. PNAS* 2013; 110(2): 737-42.
4. Deschwanden A, *et al*. *Am J Psychiatry* 2011; 168(7): 727-34.
5. Hulka LM, *et al. Mol. Psychiatry* 2014; 19(5): 625-32.
6. Ametamey SM, *et al. J. Nucl. Med.* 2007; 48(2): 247-52.
7. DeLorenzo C, *et al*. *J. Cereb. Blood Flow Metab.* 2011; 31(11): 2169-80.
8. Hadel S, *et al*. *JMRI* 2013; 38(6): 1480-7.

828
BRAIN-0548
Poster Session

BrainPET: Neurotransmitter System Evaluation

PET EVALUATION OF GABA SENSITIVITY OF BENZODIAZEPINE (BZD) SITE AGONIST [11C]RO6899880 IN THE MONKEY BRAIN

S.J. Finnema[1], V. Stepanov[1], N. Amini[1], S. Martinsson[1], E. Borroni[2], M. Honer[2], L. Gobbi[2], S. Grimwood[3], L. Farde[1], C. Halldin[1]
[1]Department of Clinical Neuroscience, Karolinska Institutet, Stockholm, Sweden
[2]Research and Early Development Roche Innovatio n Center, Roche Pharma, Basel, Switzerland
[3]Neuroscience Research Unit, Pfizer Inc., Cambridge, USA

Objectives: Frankle et al. (2009), previously demonstrated that the GABA transporter I (GAT I) inhibitor tiagabine enhances the binding of [^{11}C]flumazenil in human subjects [1]. This increase in binding has been proposed to be related to tiagabine-enhanced GABA levels

increasing the affinity of $GABA_A$ receptors for benzodiazepine (BZD) site ligands, the so called 'GABA shift' [2]. *In vitro* receptor binding studies have demonstrated that ^{3}H-labeled agonist radioligands for the BZD site are more sensitive to changes in GABA concentration than weak partial agonists, e.g. [^{11}C]flumazenil, or partial inverse agonists, e.g. [^{11}C]Ro 15-4513 [3]. We recently developed a novel full agonist PET radioligand for the $GABA_A$ receptor BZD site, [^{11}C]RO6899880 [4]. We here evaluated the effect of tiagabine on [^{11}C]RO6899880 binding in anesthetized non-human primates.

Methods: A total of 22 PET measurements were performed after bolus injections of [^{11}C]RO6899880 in four rhesus monkeys. Monkeys were anaesthetized using intravenous ketamine/xylazine infusion. PET measurements were performed for 93 min in an HRRT PET system. On each day a baseline PET measurement was followed by a pretreatment PET measurement after intravenous administration of tiagabine (1.0 mg/kg) (n=7) or vehicle (n=4). Arterial blood was obtained for measurement of the metabolite-corrected arterial input function. Regional V_T values were calculated using Logan graphical analysis. Statistical analysis was performed using two-tailed t-tests.

Results: Mean cortical V_T values were 5.8±2.2 mL/cm^3 during baseline conditions. Administration of vehicle or tiagabine increased V_T values across all examined brain regions. Tiagabine increased cortical V_T values to 10.2±4.9 mL/cm^3 (p<0.01), while vehicle administration increased cortical V_T values to 7.5±1.2 mL/cm^3 (p<0.01). V_T values obtained after tiagabine or vehicle administration were not significantly different (p=0.31). The mean increase in cortical V_T was 74±27% and 64±10% after tiagabine and vehicle administration, respectively.

Conclusions: Tiagabine and vehicle both increased V_T of [^{11}C]RO6899880. This apparent lack of tiagabine effect may be due to an interaction with the anesthesia. Future studies evaluating the effect of tiagabine and vehicle on different days are required to control for anesthesia. Follow up studies in awake animals or in human subjects may also facilitate understanding of the here reported results.

References: [1] Frankle et al, 2009, Neuropsychopharmacology 624-33; [2] Kemp et al, 1987, Br J Pharmacol 601-8; [3] Braestup et al, 1982, Science 1241-3; [4] Stepanov et al, 2013, JLCRP P-224.

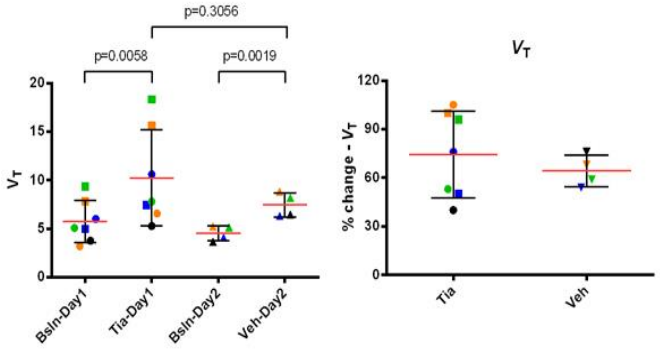

Figure: (Left) Cortical V_T values after intravenous injection of [^{11}C]RO6899880 in cynomolgus monkeys during baseline conditions or after pretreatment with tiagabine (Tia) or vehicle (Veh). (Right) Relative change in cortical V_T after pretreatment with tiagabine (Tia) or vehicle (Veh).

829
BRAIN-0767
Poster Session

BrainPET: Neurotransmitter System Evaluation

BRAIN SEROTONIN TRANSPORTER BINDING IN A MINIPIG MODEL OF PARKINSON'S DISEASE

T. Pinholt Lillethorup[1], A. N. Glud[2], S. Jakobsen[1], A. K. O. Alstrup[1], A. Møller[1], J.C. Sørensen[2], D.J. Doudet[3], A.M. Landau[1]
[1]Department of Nuclear Medicine and PET-Centre, Aarhus University and Hospital, Aarhus C, Denmark
[2]Department of Neurosurgery, Aarhus University Hospital, Aarhus C, Denmark
[3]Department of Medicine/Neurology, University of British Columbia, Vancouver, Denmark

Objectives: Some of the debilitating non-motor aspects of Parkinson's disease (PD) are related to the serotonin system[1]. To investigate the involvement of the brain serotonergic system in a PD animal model, we measured the in vivo binding of [^{11}C]-DASB to the serotonin transporter (SERT) as a marker of serotonergic neurons. In this study, we use the *in vivo* capabilities of positron emission tomography (PET) imaging to study serotonin neurotransmission in a minipig model of PD induced by the intracerebroventricular injection of lactacystin, an inhibitor of the ubiquitin proteasome system.

Methods: This study was done in accordance with a protocol approved by the Danish Animal Inspectorate. Five female Göttingen minipigs were implanted in the cisterna magna with a catheter connected to a subcutaneous titanium injection port under sterile conditions. Six-eight weeks after recovery from the catheter implant, and after injections of sterile saline alone to verify patency, minipigs were scanned at baseline with [^{11}C]-3-amino-4-(2-dimethylaminomethyl-phenylsulfanyl)-benzonitrile (^{11}C-DASB), a label of SERT availability. Four pigs then received eight weekly injections of lactacystin dissolved in sterile saline, and one pig received saline alone, directly into the cerebrospinal fluid through the access port. They were scanned with DASB again after a cumulative dose of 200mg lactacystin. PET data were registered to an average minipig MRI atlas and processed using PMOD software. The binding potential (BP_{ND}) of DASB was obtained with the Logan graphical analysis and cerebellum activity as a region of non-displaceable binding.

Results: Lactacystin administration induced behavioural symptoms including weakness of hindlimbs and decreased motor activity. SERT binding potential was decreased by 35-40% in striatal brain regions and by 20% in thalamic regions compared to the baseline scans.

Conclusions: Our imaging data suggests a loss of brain serotonergic innervation in response to protein aggregation. The decreased striatal binding of DASB observed in this minipig model of PD is to some extend consistent with previous studies done in PD patients[2]. The proteasome inhibition model may therefore be useful in the investigation of non-motor deficits in PD and LDOPA-induced dyskinesia.

References: 1. Politis, M. & Loane, C. Serotonergic dysfunction in Parkinson's disease and its relevance to disability. *TheScientificWorldJournal* **11**, 1726-1734 (2011).
2. Politis, M.*, et al.* Staging of serotonergic dysfunction in Parkinson's disease: an in vivo 11C-DASB PET study. *Neurobiology of disease* **40**, 216-221 (2010).

830
BRAIN-0234
Poster Session

BrainPET: Neurotransmitter System Evaluation

CHARACTERIZING THE RELATIONSHIP BETWEEN DOPAMINE D2 RECEPTOR OCCUPANCY AND PLASMA LEVELS OF HALOPERIDOL IN NON-HUMAN PRIMATES USING [18F]-FALLYPRIDE

R. Rajagovindan[1], J. Wang[1], A. Tovcimak[1], M. Voorbach[1], D. Reuter[1], A. Giamis[1], A. Basso[1], P. Jacobson[1], J. Beaver[1]
[1]iSAT, AbbVie Inc., North Chicago, USA

Objective: [18F]-Fallypride has been used to evaluate the receptor occupancy of antipsychotic drugs and the endogenous dopamine release in both preclinical species and humans. Prior studies [1,2] have evaluated the occupancy of haloperidol using [11C]-Raclopride in humans and determined EC50 to be 320 and 510ug/ml respectively. While prior studies have evaluated the relationship between dopamine D2 receptor occupancy and plasma drug levels in humans, similar work in non-human primates is lacking. The purpose of this study was to determine the relationship between dopamine D2 receptor occupancy and plasma haloperidol levels in non-human primates and compare it to that in humans.

Methods: [18F]-Fallypride dynamic positron emission tomography (PET) data were collected in 6 cynomologus monkeys without arterial sampling. 3 animals received test-retest scans separated by 4-6 weeks and 3 other animals received scans prior to and post haloperidol (3-55ug/kg) administration. The dynamic scans were of 150-180 mins in duration. Subject-space atlas based on anatomical MRI was coregistered to PET images of each animal to derive regional time activity curves. Binding potential (BPND) was used as the outcome measure using Cerebellum as the reference region and was quantified using both simplified reference tissue model (SRTM) and Logan reference method. Sensitivity analysis for t* and the choice of k2 for Logan reference method and time stability analysis for both methods were also performed. The changes in BPND pre and post pharmacological challenge were estimated and the ED50 and EC50 of haloperidol were calculated.

Results: Logan reference method was able to fit the data well and generate reproducible binding potentials in striatal regions. SRTM was only able to fit 30% of the total scans well. The highest binding potential was found in caudate-putamen (BPND=20.51±2.82) followed by globus pallidus (BPND=7.96±2.35), insula (BPND=4.06±1.45), substantia nigra (BPND=1.72±0.44) and the lowest binding potential was found in thalamus (BPND=0.68±0.22) and cortical regions (BPND=0.55±0.19) consistent with prior reports [3]. Test-retest variability of BPND estimated from Logan method was relatively low in striatal regions (%VAR25%), which might be due to the low target density in these regions. Dose dependent receptor occupancy was observed following different doses of haloperidol, however, at the lowest doses the occupancy measured in the extrastriatal region were variable and differed from the measurement in striatal regions. Therefore, when calculating the ED50 and EC50, only occupancy estimated in caudate-putamen was used. ED50 and EC50 were estimated to be 8.3 (95% CI: 5.5-12.5) ug/kg and 287.4 (95% CI: 131.1-629.8) ug/ml respectively and were comparable to estimates in human [2].

Conclusion: Dose dependent receptor occupancy was successfully measured in striatal regions following differing doses of haloperidol. When arterial sampling is not available, the Logan reference method can be used to estimate binding potential of [18F]-Fallypride in nonhuman primate brain.

References:

1. Kapur S et al., Psychopharmacology (1997) 131:148-152

2. Fitzgerald PB et al., Psychopharmacology (2000) 149:1-5

3. Christian BT et al., Synapse (2000) 38:71-79

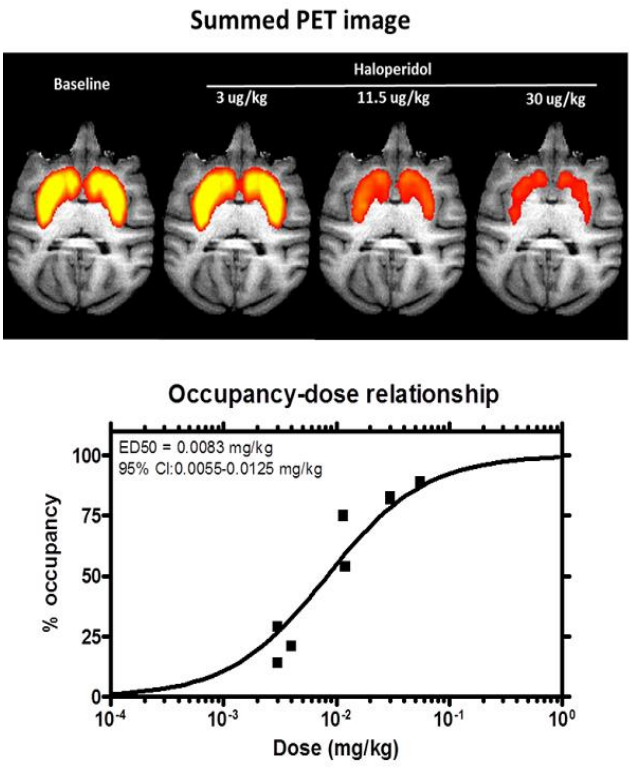

Disclosures: All authors are employees of AbbVie. The design, study conduct, and financial support for this research were provided by AbbVie. AbbVie participated in the interpretation of data, review, and approval of the publication.

831
BRAIN-0667
Poster Session

BrainPET: Neurotransmitter System Evaluation

IN VIVO GLUTAMATE FLUCTUATIONS: A GLT-1 CHALLENGE WITH CEFTRIAXONE AND [11C]ABP688

E. Zimmer[1], M. Parent[1], M. Shin[1], A. Aliaga[1], A. Aliaga[1], M. Luc[1], J. Soucy[1], A. Gratton[1], P. Rosa-Neto[1]
[1]Neurology and Neurosurgery, Douglas Mental Health University institute, Montreal, Canada

Molecular imaging of glutamate neurotransmission offers unprecedented opportunities for investigating mechanisms underlying neuropsychiatric conditions. Here, we evaluated whether [^{11}C]ABP688, a PET ligand that binds to the allosteric site of the metabotropic glutamate 5 receptor (mGlur5), is sensitive to glutamate fluctuations after a pharmacological challenge. For this, we used ceftriaxone (CEF) administration in rats, an activator of the GLT-1 transporter (EAAT2), which is known to decrease extracellular levels of glutamate. MicroPET [^{11}C]ABP688 dynamic acquisitions were conducted in rats following a venous injection of saline (baseline) and after CEF 200 mg/kg. Binding potentials (BP_{ND}) were obtained using the simplified reference tissue method. Between-conditions statistical parametric maps indicating brain regions showing the highest CEF effects (Figure 1) guided placement of microdialysis probes, for subsequent assessment of extracellular levels of glutamate. CEF administration increased [^{11}C]ABP688 BP_{ND} in the thalamic ventral nucleus (VA). Subsequent microdialysis assessment in VA revealed declines in extracellular glutamate concentrations. The present results support the concept that mGluR5 allosteric binding sites availability is sensitive to extracellular concentrations of glutamate. This interesting property of mGluR5 allosteric binding sites has potential applications for interrogating the role of glutamate in the diathesis of neuropsychiatric conditions, which may ultimately boost the development of glutamatergic imaging signatures and allow for the evaluation of glutamatergic-focused therapeutic approaches.

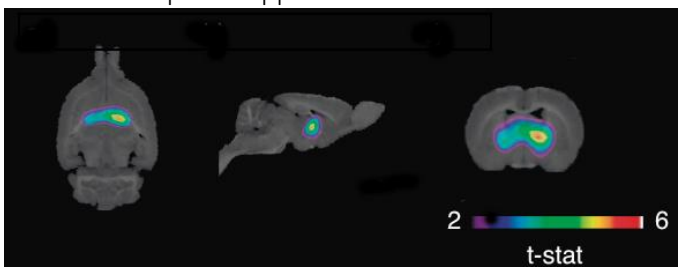

Figure 1. Statistical images projected on the rat brain structural imaging showing t-stat contrast mGluR5 BP_{ND} [baseline < ceftriaxone]

832
BRAIN-0332

Poster Session

BrainPET: Neurotransmitter System Evaluation

MAPPING HUMAN BRAIN FATTY ACID AMIDE HYDROLASE ACTIVITY WITH PET – EFFECT OF C385A GENETIC POLYMORPHISM ON [11C]CURB BINDING

I. Boileau[1], R.F. Tyndale[2], B. Williams[1], E. Mansouri[1], Q. Zhou[2], V. De Luca[3], D. Westwood[1], P. Rusjan[1], R. Mizrahi[1], R. Bazinet[4], A.A. Wilson[5], S. Houle[5], S.J. Kish[5], J. Tong[5]
[1]Research Imaging Centre, Centre for Addiction and Mental Health, Toronto, Canada
[2]Pharmacology and Toxicology, University of Toronto, Toronto, Canada
[3]Psychiatry, University of Toronto, Toronto, Canada
[4]Nutrition, University of Toronto, Toronto, Canada
[5]Research Imaging Centre , Centre for Addiction and Mental Health, Toronto, Canada

Background: rs324420 (C385A) a single nucleotide polymorphism of the endocannabinoid inactivating enzyme Fatty Acid Amide Hydrolase (FAAH) has been associated with drug addiction and related behavioral phenotype. Here, we tested whether the functional polymorphism of FAAH (rs324420, C385A) was related to binding of the FAAH PET probe [^{11}C]CURB. We hypothesized that carriers of the A-allele (a mutation leading to lower peripheral FAAH protein levels and activity) would be associated with diminished [^{11}C]CURB binding.

Methods: 24 healthy controls (12 males, 12 females) with an average age of 34.1 ± 10.5 years completed one [^{11}C]CURB/PET scan with arterial sampling. TaqMan allelic discrimination assay for rs324420 polymorphism (Life Technologies C_1897306_10) was performed using DNA extracted from blood by high salt extraction to determine the genotype. FAAH levels (λk_3) were assessed using an irreversible 2-tissue compartment model in MRI delineated regions of interest.

Results: 15 (62%), 8 (33%) and 1 (4%) subject respectively had C/C, A/C and A/A genotype. Relative to C/C, carriers of the A-allele had a 20% lower [^{11}C]CURB binding (λk_3) across all regions tested.

Conclusion: We report preliminary evidence that genetic variance in FAAH activity (rs324420 (C385A) SNP) is associated with measurable difference in brain FAAH binding as per PET [^{11}C]CURB measurement (λk_3).

833
BRAIN-0771
Poster Session

BrainPET: Neurotransmitter System Evaluation

CHANGES OF METABOTROPIC GLUTAMATE RECEPTOR TYPE 1 BINDING OF [11C]ITMM BY AGING

M. Sakata[1], J. Toyohara[1], K. Wagatsuma[1], K. Ishibashi[1], K. Ishii[1], M.R. Zhang[2], K. Ishiwata[1]
[1]Research Team for Neuroimaging, Tokyo Metropolitan Institute of Gerontology, Tokyo, Japan
[2]Molecular Imaging Center, National Institute of Radiological Sciences, Chiba, Japan

Objectives: Metabotropic glutamate receptor type 1 (mGluR1) has been reported to be a candidate of a drug target for the treatment of the central nervous system diseases, including cerebellar ataxia, and Parkinson's disease. This study examines possible age-related mGluR1 changes in living human brains by PET and the mGluR1 ligand *N*-[4-[6-(isopropylamino)pyrimidin-4-yl]-1,3-thiazol-2-yl]-4-[^{11}C]methoxy-*N*-methylbenzamide ([^{11}C]ITMM)[1].

Methods: Dynamic [^{11}C]ITMM PET scans (90-min) were performed in 14 young (eight males and six females; 26 ± 3 y.o.) and 23 aged (12 males and 11 females; 70 ± 7 y.o.) healthy volunteers using D710 PET/CT scanner (GE Healthcare). The injected dose was 561 ± 81 MBq and the specific activity was 79 ± 38 MBq/nmol. During the scan, arterial blood was sampled at various time

intervals, and the fraction of the parent compound in plasma was determined by HPLC analysis. ROIs were placed on the cerebellar (as a target region) and occipital (as a candidate of the reference region) cortices. Total distribution volume (V_T) for each ROI was estimated by the one- and two-tissue compartment (1T, 2T) model and Logan graphical analysis (LGA; t^* = 30 min), and distribution volume ratio (DVR) for cerebellar cortex was estimated by Logan reference tissue method (LGAR).

Results: The 2T model did not provide stable estimates of V_T. LGA was chosen for the estimation of V_T, because the V_T estimated by the 1T model and LGA were well matched (V_T(1T) = 0.96 × V_T(LGA) – 0.02, R^2=1.00). The V_Ts in occipital cortex and cerebellum and DVR in cerebellum of aged subjects were significantly higher than those of young subjects, and no gender effects were found in this experiment (two-way ANOVA; $p < 0.01$).

Conclusions: The results showed increased binding of the [^{11}C]ITMM in cerebellum of aged subjects. The increase of the mGluR1 density and/or the age-related decline of the endogenous glutamate release might cause of the increased binding of [^{11}C]ITMM. The significant change of V_T in occipital cortex suggests the region is not quite suitable for the reference region. However, the region still has the possibility to be a practical candidate of the reference region because the significant increase could be observed in DVR.

References:

[1] Toyohara J, et al., *J. Nucl. Med.*, 2013; 54:1302–1307.

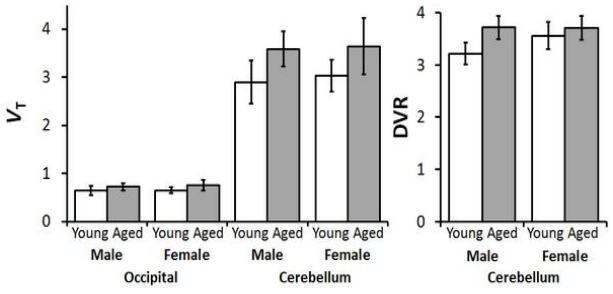

Figure: Total distribution volume (V_T) and distribution volume ratio (DVR) of the [^{11}C]ITMM in young and aged human subjects.

834
BRAIN-0391
Poster Session

BrainPET: Neurotransmitter System Evaluation

PRELIMINARY RESULTS SUGGEST POSITIVE CORRELATION ACROSS SUBJECTS BETWEEN PEAK HEIGHT OF DA RESPONSE TO CIGARETTE SMOKING AND SATISFACTION OF CRAVING IN FEMALE SMOKERS

S. Wang[1], *K.P. Cosgrove*[2], *E.D. Morris*[3]
[1]*Biomedical Engineering, Yale University, New Haven, USA*
[2]*Psychiatry, Yale University, New Haven, USA*
[3]*Diagnostic Radiology, Yale University, New Haven, USA*

Objectives: Our group developed lp-ntPET in recent years to characterize the temporal patterns of transient DA release induced by smoking[1]. We have previously detected sex differences in DA response to cigarette smoking in PET data with voxel-wise lp-ntPET[2]. In this research we investigated the correlation across subjects between DA parameters from PET data and behavioral measures from subjective ratings of the smoking experience.

Methods: 16 healthy human smokers (8 M, 8 F) received either one or two bolus-plus-constant-infusion (B/I) [^{11}C]raclopride scans that included smoking one or two cigarettes while inside the HRRT PET scanner. Smoking began 35 or 45 minutes after the initial tracer bolus. Data were collected for 90 min and subject head motion was recorded using an optical tracking system. Dynamic data were reconstructed iteratively with MOLAR, including all standard corrections. The lp-ntPET model was fitted to time activity curve (TAC) at each voxel in a precommissural striatal mask. Temporal parameters characterized by lp-ntPET including "peak height" of DA release, "Latency" (the "take-off" time of DA release relative to start of smoking), and "Rise Time" (the

"peak time" of DA curve relative to "take-off" time) were calculated for each subject at each voxel. Correlation coefficients were calculated between these DA parameters from PET data and "Satisfaction of Craving" based on the difference in subjective reports of craving before and after smoking. The same procedure was applied to parametric maps from simulated null data. The correlation maps were thresholded to retain correlation coefficients greater than 0.4. A cluster size threshold was determined from the correlation map of null data and applied to the human data to eliminate false positives.

Results: The thresholded correlation map showed 4 big clusters in female striatum where DA peak height was positively correlated with satisfaction of craving. The cluster size threshold was set to be greater than 25 voxels so that any cluster in the simulated null data was eliminated to exclude false positive clusters (Fig. 1). No cluster in the male data survived this cluster size threshold.

Conclusions: Our preliminary data suggest that in female smokers, the higher the peak height of DA release in striatum, the greater the satisfaction (reduction) of craving.

References: [1] Kim SJ, Sullivan JM, Wang S et al., Hum Brain Mapp 2014 [2] Cosgrove KP, Wang S, Kim SJ et al., J Neurosci 2014

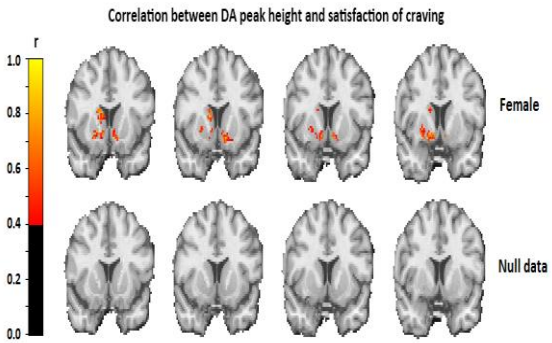

Figure 1. Positive correlations across subjects were observed in the striatum between peak height of DA release induced by cigarette smoking and subjective rating of satisfaction of craving in female smokers (N=8).

835
BRAIN-0726
Poster Session

BrainPET: Neurotransmitter System Evaluation

DOPAMINE D1 LIGANDS SCH23390 AND NNC112 EXHIBIT PARTIAL AGONISTIC PROPERTIES AS MEASURED IN VIVO

D. Wooten[1], J. Mandeville[2], J. Hooker[2], G. El Fakhri[1], N. Alpert[1], M. Normandin[1]
[1]CAMIS/Radiology, Massachusetts General Hospital Harvard Medical School, Boston, USA
[2]Martinos Center, Massachusetts General Hospital Harvard Medical School, Boston, USA

Objectives: We previously presented on the excitatory effects of dopamine D_1-like receptors using simultaneous PET/fMRI to estimate receptor occupancy (R-occ) and functional response to D_1 agonist and antagonist drugs. The agonist resulted in strong excitatory effects measured by fMRI as increases in cerebral blood volume (CBV) even at low receptor occupancies measured with PET. Unexpectedly, the antagonists also provoked excitatory responses across a range of occupancies, calling into question their true antagonist properties. D_1 antagonists should bind to D_1 receptors without a direct response, but instead block access of dopamine to D_1 receptors thereby attenuating endogenous excitation for an overall inhibitory effect and indirect reduction in CBV. Therefore, the goal of this work was to explore the properties of two dopamine D_1 antagonists, SCH23390 and NNC112, under conditions when dopamine residence at the D_1 receptor site will have maximum effects, i.e. when dopamine levels are elevated.

Methods: Two rhesus macaques underwent a total of 16 scans on the simultaneous PET/MR scanner (Siemens Trio with BrainPET insert). Contrast-enhanced fMRI was used to assess striatal D_1 receptor response from antagonists under baseline (b-DA) and high dopamine (h-DA) levels using amphetamine to increase

endogenous dopamine. For the b-DA studies, first a control scan ([^{11}C]NNC112 only) was acquired followed by a competition scan ([^{11}C]NNC112 + 25 µg/kg NNC112 or SCH23390) using the lp-ntPET method to estimate peak R-occ due to the antagonist competition. For the h-DA scans, either NNC112 or SCH23390 was given 40 min after amphetamine injection (~0.5 mg/kg). Due to the complex CBV response resulting from amphetamine, in both animals an amphetamine-only scan was acquired for comparison with h-DA scans having antagonist challenge. Because of NNC112 and SCH23390's affinity for 5-HT$_{2A}$ receptors, b-DA studies were performed using the selective 5-HT$_{2A}$-antagonist MDL100907 (10 mg/kg) as a competitor with concurrent [^{11}C]MDL100907 PET to verify R-occ.

Results: Under b-DA conditions, both antagonists produced moderate increases in CBV (5% at peak for NNC, 6% for SCH) at high peak receptor occupancies (NNC: 85%; SCH: 79%). Under h-DA conditions, both antagonists decreased CBV (NNC: -15%; SCH: -8%) after normalizing against the amphetamine-only response. The 5-HT$_{2A}$ selective antagonist MDL100907 resulted in no significant increase in CBV at peak cortical 5-HT$_{2A}$ R-occ of 95% (average occupancy over the scan measured by MRTM=90%).

Conclusions: These results imply that NNC112 and SCH23390 are not antagonists as widely assumed, but D$_1$ partial agonists as suggested by Sugamori et al. (1998). The partial agonistic properties of SCH23390 redefine the prototypical 'D$_1$ antagonist' and casts new light on the potential of D$_1$ as a therapeutic target. In addition, the lack of an excitatory response from the selective 5-HT$_{2A}$ antagonist indicate the excitatory responses of NNC112 and SCH23390 are not artifacts of their affinity for the 5-HT$_{2A}$ receptor.

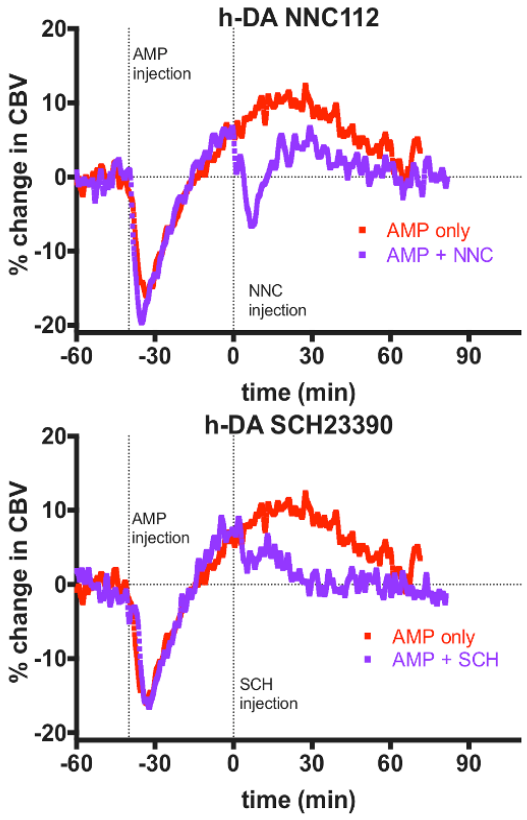

Figure 1: CBV curves for h-DA conditions illustrating decrease in CBV following either NNC (top) or SCH (bottom) injection.

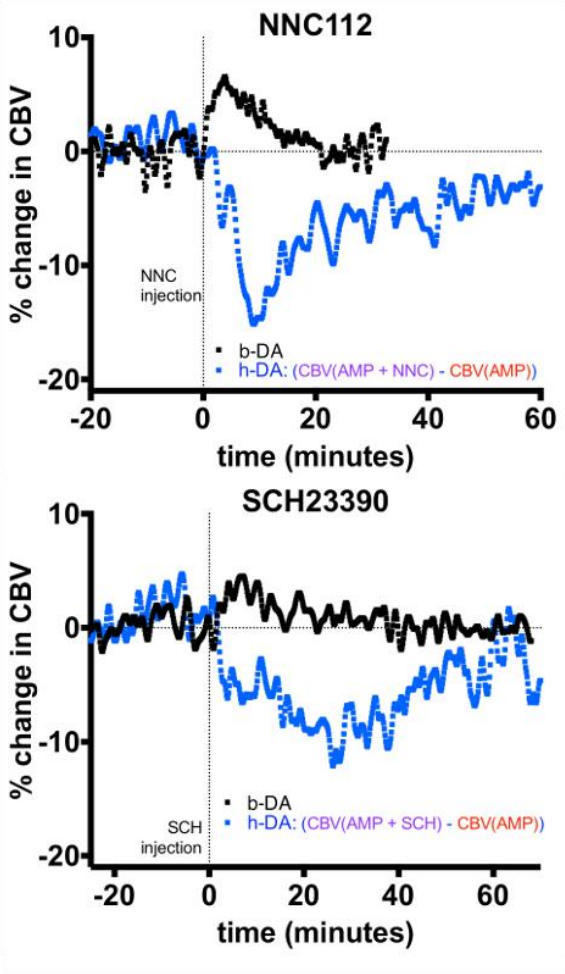

Figure 2: Comparison of b-DA and h-DA CBV curves (h-DA CBV curves were found by subtracting AMP only curves from AMP + antagonist curves).

Research Support: NIH-R01MH100350, NIH-R21NS072148, NIH-T32EB013180

836
BRAIN-0027
Poster Session

Psychiatric Disorders & Addictions

GESTATIONAL AND POSTNATAL ETHANOL CONSUMPTION MODIFIES CART PEPTIDE SYSTEM IN RAT BRAIN: CORRELATES WITH ANXIETY, DEPRESSION AND MEMORY DEFICITS IN OFFSPRING

M. DANDEKAR[1], A. Bharne[1], P. Borkar[1], D. Kokare[1], N. Subhedar[2]
[1]Pharmacology, Department of Pharmaceutical Sciences R.T.M. Nagpur University Nagpur India, NAGPUR, India
[2]Neuroscience, Indian Institute of Science Education and Research Pune India, Pune, India

Objective: Cocaine- and amphetamine-regulated transcript peptide (CART) plays a vital role in brain development and ethanol-mediated behavioral abnormalities. Herein, we attempted to evaluate the role of CART in the brain of offspring obtained form alcoholic female rats and its correlation with anxiety, depression and memory phenotype.

Methods: Female rats were fed with ethanol-containing, or ethanol-free nutritionally balanced liquid diet from 8 days prior of conception and continued till 25 days post parturition to coincide with weaning. We examined the adolescent (day 30) and adult (day 90) offspring for anxiety, depression and memory by using elevated plus maze (EPM), forced swim test (FST) and novel object recognition test (NORT), respectively. Furthermore, half of the pups from each litter were killed at day 30 and others at 90, for profiling of CART using immunocytochemistry.

Results: Offspring of alcoholic mothers at both age groups spent significantly more time in closed arms of EPM, showed more immobility time in FST and failed to recognize novel object versus familiar object in NORT. This indicates presence of anxiety, depression and amnesia. Thirty days old pups showed significant augmentation in the CART-immunoreactivity in the cells of dorsal hypothalamus (DA), while a dramatic reduction was noticed in the perifornical area (Pef). We found no changes in the lateral hypothalamus (LH) and paraventricular nucleus (PVN) at this age of pups compared with control. In adult offspring, the CART-immunoreactivity was significantly increased in the cells of PeF and LH and decreased in the DA and PVN.

Conclusions: We suggest that, the endogenous CART system in discrete brain areas, in a

temporally specific manner, may be involved in the behavioral abnormalities in the offspring following ethanol ingestion by the mother.

837
BRAIN-0819
Poster Session

Psychiatric Disorders & Addictions

DYNAMIC MAGNETISATION TRANSFER MRI IN MAJOR DEPRESSION DISORDER: DELAYED TISSUE RESPONSE TO CARDIAC PULSATION IN THE BASAL GANGLIA.

D. López[1], L. Tozzi[1], S. Joseph[1], V. O'Keane[1], T. Frodl[1], C.M. Kerskens[1]
[1]Lloyds Institute of Neuroscience, Trinity College Dublin, Dublin, Ireland

Objectives: In Major Depressive Disorder (MDD), several brain regions, such as the prefrontal cortex or the basal ganglia, are affected by a loss of glial cells, and in particular of astrocytes [1, 2]. Astrocytes are known to mediate between the brain parenchyma and its vasculature. Therefore, patients suffering from depression possess an abnormal blood circulation and metabolism in those regions [2]. Here, we want to study how those structural changes may affect the tissue pulsation which is related to blood circulation. Using a new method that we have developed, it is possible to measure the sudden change of intracellular water concentration evoked by the cardiac pressure wave [3].

Methods: The MRI sequence consists of a magnetisation transfer (MT) preparation phase followed by single-slice echo-planar imaging sequence across the basal ganglia. MT effect was introduced by a negative (-5236.8 ± 894.18 Hz) and a positive off frequency (6982.5 ± 894.18 Hz) RF pulse. Imaging parameters were voxel size of 3.5 x 3.5 x 3 mm, TR = 60 ms, TE = 12 ms, FA = 35° and 3000 repetitions.

4 depressed patients (between 25 and 42 years old) and 4 control subjects (between 27 and 44 years old) were scanned with the protocols approved by the local ethics committee.

Results: For each subject, ROI's from the basal ganglia and the visual cortex were averaged to showcase the difference between both brain regions and groups. For the control group, only strong cardiac frequencies are resolved in the basal ganglia as well as the cortex. However, the spectra for the depressed patients show lower cardiac response in general but also different behavior in the basal ganglia, where we found a direct cardiac response from the tissue as well as a second response at around half of the cardiac circle. This results in an apparent shorting by the detected frequency by a factor 2, which can be seen in frequency spectrum in the figure.

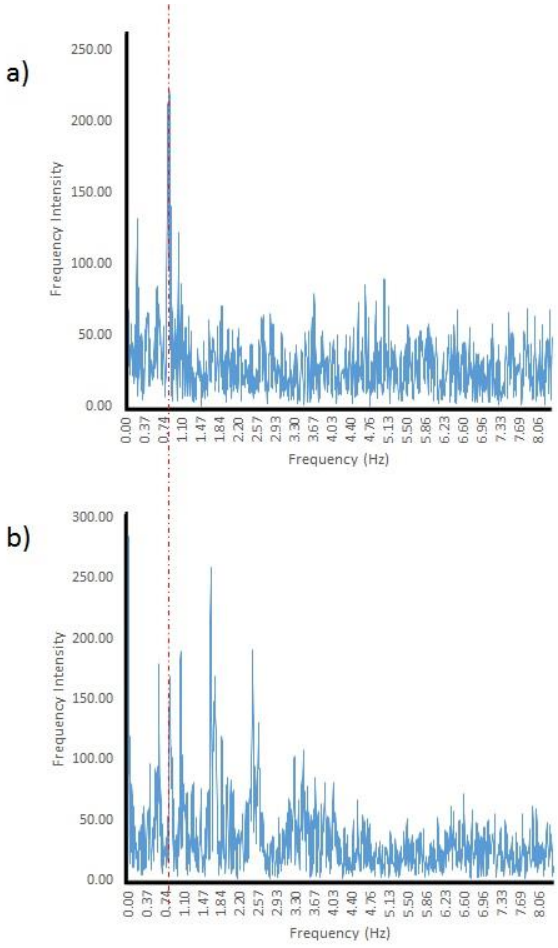

Conclusions:To our knowledge, the observation of a cardiac related MT change and its variation in

MDD patients has not yet been reported. The delayed response is unexpected. Most likely, the suppression of astrocytes in the depressed brain hinders the response of the tissue or the brain tissue uses another mechanism to compensate water dislocation due to the pressure wave. This could be explained with the decrease in astrocytes, which is linked to a decrease in aquaporin-4 (AQP4) water channels, which work as a regulator of blood flow, glucose and metabolism among other functions [1]. At present, we can only hypothesize about the mechanisms, but we strongly believe that we have found a new imaging biomarker for MDD.

References:

[1] Rajkowska, G., et al. *Biol. Psych.* 2013, 73(7):613-21.

[2] Lafer, B., et al *Psych. Clinics of North America* 1997, 20(4):885-896.

[3] López, D. et al. BRAIN and BRAINPET2015.

838
BRAIN-0225
Poster Session

Psychiatric Disorders & Addictions

SELF-TRANSCENDENCE TRAIT AND ITS RELATIONSHIP WITH IN VIVO SEROTONIN TRANSPORTER AVAILABILITY: A HIGH-RESOLUTION PET-MRI STUDY

J.H. Kim[1], Y.D. Son[2], J.H. Kim[2], S.Y. Lee[2], Z.H. Cho[2]
[1]Psychiatry/Neuroscience Research Institute, Gachon University Gil Medical center, Incheon, Korea
[2]Neuroscience Research Institute, Gachon University Gil Medical center, Incheon, Korea

Objectives: Self-transcendence is an inherent personality trait relating to the experience of spiritual aspects of the self. We examined the relationship between self-transcendence and serotonin transporter (SERT) availability in brainstem and thalamus, which are known to contain high SERT density, using high-resolution magnetic resonance imaging (MRI) and positron emission tomography (PET) *with* [^{11}C]DASB to elucidate potential roles of serotonergic innervation in this trait.

Methods: Sixteen healthy subjects completed 7.0-Tesla MRI and high-resolution PET. The regions of interest included midline raphe nucleus groups and thalamic subdivisions. For the estimation of the SERT availability, the binding potential (BP_{ND}) was derived using the simplified reference tissue model (SRTM2). The Temperament and Character Inventory was used to measure self-transcendence.

Results: The self-transcendence total score had significant negative correlations with the [^{11}C]DASB BP_{ND} in the left pulvinar and the caudal raphe. The subscale score for self-forgetful experiences correlated negatively with the [^{11}C]DASB BP_{ND} in both pulvinar nuclei. The spiritual acceptance subscale score correlated negatively with the [^{11}C]DASB BP_{ND} in the median raphe.

Conclusions: These results indicate that self-transcendence trait is associated with SERT availability in specific subregions of raphe nuclei and thalamus, suggesting that the serotonin system may serve as an important biological basis for human self-transcendence and spiritual experiences. The functional activity of these nuclei and their related neural circuitry may have a crucial role in the manifestation of self-transcendence.

References:

Borg J, Andrée B, Soderstrom H, Farde L. The serotonin system and spiritual experiences. *Am J Psychiatry* 2003;160:1965-1969.

Karlsson H, Hirvonen J, Salminen JK, Hietala J. No association between serotonin 5-HT 1A receptors and spirituality among patients with major depressive disorders or healthy volunteers. *Mol Psychiatry* 2011;16:282-285.

839
BRAIN-0394

Poster Session

Psychiatric Disorders & Addictions

STUDIES ON THE ANIMAL MODEL OF POST-STROKE DEPRESSION WITH HIGH VALIDITY AND APPLICATION OF ATYPICAL ANTIPSYCHOTIC ARIPIPRAZOLE

Y.R. Kim[1], H.N. Kim[1], S.M. Ahn[1], J.U. Baek[1], H.K. Shin[1], B.T. Choi[1]
[1]School of Korean Medicine, Pusan National University, Yangsan-si Gyeongnam, Korea

Objectives: The existence of a causal relationship between depression and vascular deficits has been hypothesized clinically as a post-stroke depression. We investigated whether cerebrovascular abnormalities such as ischemic stroke develop to ideal animal model of post-stroke depression by additional chronic mild stress (CMS) procedure. And atypical antipsychotic aripiprazole (ARZ) applied to this model.

Methods: Behavioral, histopathological and immunohistochemical analysis were performed for examination of the depressive disorders and therapeutic effect of aripiprazole in CMS, left middle cerebral artery occlusion (MCAO) and CMS after MCAO (MCAO+CMS) mice.

Results: In all depression-related behavioral tests involving open filed test, sucrose preference test, forced swim test and Morris water maze test, MCAO+CMS group showed significant depressive behaviors compared to MCAO group. MCAO+CMS mice also displayed distinct deficits in forced swim test and Morris water maze test compared with CMS group. In the morphological and immunohistochemical analysis, MCAO+CMS group showed a significant decrease of proliferative cells in the striatum and hippocampus with dopaminergic neuronal injuries in the midbrain as compared with CMS and MCAO mice. When we treated aripiprazole in MCAO+CMS to validate therapeutic effects on the neuroprotection and neurogenesis, treatment with aripiprazole reduced all depressive behaviors examined, especially in a marked shorter time in Morris water maze test. Recovered tyrosine hydroxylase-positive cells in the midbrain and enhanced neurogenesis in the hippocampus also demonstrated in aripiprazole-treated MCAO+CMS mice.

Conclusions: Our results suggest that chronic mild stress after ischemic stroke leads to severe depressive-like behavior than each CMS or MCAO treated mice via extrafocal neurodegeneration and degradation of neurogenesis, and these behavioral and histopathological changes are reversed by treatment of atypical antipsychotic aripiprazole.

840
BRAIN-0207
Poster Session

Psychiatric Disorders & Addictions

MECP2 SUMOYLATION AT LYS-412 RESCUES MECP2 MUTANT-INDUCED BEHAVIORAL DEFICITS IN A MOUSE MODEL OF RETT SYNDROME

H.Y. Lee[1], D. Tai[1], Y.C. Liu[1], W.L. Hsu[1], Y.L. Ma[1]
[1]Neuroscience, Academia Sinica, Taipei, Taiwan

Objectives:

The methyl-CpG-binding protein 2 (MeCP2) gene, *Mecp2*, is an X-linked gene encoding the MeCP2 protein and mutations of *Mecp2* cause Rett syndrome (RTT). But the molecular mechanism of *Mecp2* mutation-caused RTT is less well known. The aim of the present study was to investigate the molecular mechanism of *Mecp2* mutant-induced behavioral deficits using a mouse model of RTT.

Methods:

The major methods adopted for the present study include: *in vitro* SUMOylation assay for MeCP2, oligo pull-down assay for MeCP2 methyl-DNA binding, co-immunoprecipitation, western blot, CREB DNA binding in brain tissue, quantitative real-time PCR for *Bdnf* mRNA expression, *Mecp2* plasmid transfection and Lentiviral vector transduction to animal's brain, recombinase Cre injection to mouse basolateral amygdala,

immunohistochemistry, adoption of loxP-*Mecp2*-loxP conditional knockout mice for behavioral assays including social interaction and cued fear conditioning learning.

Results:
We have found that MeCP2 could be SUMO-modified by the E3 ligase PIAS1 at Lys-412 and MeCP2 SUMOylation is MeCP2 phosphorylation (at Ser-421 and Thr-308)-dependent. MeCP2 SUMOylation is increased by N-methyl-D-aspartate and IGF-1 treatments. Further, most of the *Mecp2* mutations identified in RTT patients showed decreased level of MeCP2 SUMOylation. Moreover, MeCP2K412R sumo-mutant transfection did not alter MeCP2 methyl-DNA binding, but it increased its association with CREB. On the other hand, MeCP2-SUMO1 fusion plasmid transfection decreased its association with CREB and HDAC1 in a dose-dependent manner, suggesting release of CREB from the repressor complex. Enhanced MeCP2 SUMOylation also increased CREB DNA binding to gene promoter and brain-derived neurotrophic factor mRNA expression in the rat brain. Meanwhile, it rescues the behavioral deficits, including social interaction and cued fear conditioning memory, in *Mecp2* conditional knockout mice.

Conclusions:
MeCP2 could be SUMO-modified by the SUMO E3 ligase PIAS1 both *in vitro* and in rat brain and MeCP2 SUMOylation is MeCP2 phosphorylation (at Ser-421 and Thr-308)-dependent. Decreased MeCP2 SUMOylation is observed in most of the *Mecp2* mutations identified in RTT patients. Transduction of Lenti-MeCP2-SUMO1 fusion vector to basolateral amygdala rescues the behavioral deficits in *Mecp2* conditional knockout mice. Drugs that enhance MeCP2 SUMOylation without altering the expression level of MeCP2 may have therapeutic potential against RTT and other autism-like syndrome. Here, we have identified a novel molecular mechanism for RTT.

This work was supported by a Grant (MOST 103-2320-B-001-004-MY3) from the Minister of Science and Technology in Taiwan.

References (selected):
1. Amir RE, Van den Veyver, Wan M et al. Rett syndrome is caused by mutations in X-linked MECP2, encoding methyl-CpG-binding protein 2. *Nat Genet* 1999; 23: 85-188.
2. Castro J, Garcia RI, Kwok S et al. Functional recovery with recombinant human IGF1 treatment in a mouse model of Rett syndrome. *PNAS USA* 2014; 111: 9941-9946.
3. Guy J, Cheval H, Selfridge J, Bird A. The role of MeCP2 in the brain. *Annu Rev Cell Dev Biol* 2011; 27: 631-652.
4. Zhou Z, Hong EJ, Cohen S et al. Brain-specific phosphorylation of MeCP2 regulates activity-dependent *Bdnf* transcription, dendritic growth, and spine maturation. *Neuron* 2006; 52: 255-269.

841
BRAIN-0466
Poster Session

Psychiatric Disorders & Addictions

ASSESSING THE DOPAMINERGIC BASIS OF DELUSIONAL IDEATION: THE RELATIONSHIP BETWEEN D1 AND D2 RECEPTOR AVAILABILITY AND DELUSIONAL BELIEFS IN HEALTHY SUBJECTS

G.J. Matheson[1], A. Louzolo[1], P. Plavén-Sigray[1], P. Stenkrona[1], L. Farde[1], M. Ingvar[1], P. Petrovic[1], S. Cervenka[1]
[1]Department of Clinical Neuroscience, Karolinska Institutet, Stockholm, Sweden

Objectives: Delusions are false beliefs which constitute one of the core symptoms of psychotic disorders. Delusional beliefs are not only observed in patients, but are also present in the general population (*1*), among whom they are more frequent in relatives of psychosis patients (*2*), and may comprise an important risk factor for the development of psychosis (*3*). Delusions have been hypothesized to arise as a result of alterations of salience processing, which, in turn, may be related to changes in dopaminergic transmission (*4*). While disturbances in the dopamine system are well-documented in psychosis, the biochemical underpinnings of delusional ideation remain to be confirmed. In

this study, we aimed to measure the relationship between delusional ideation and the availability of dopamine D1 (D1R) and D2 receptors (D2R) in a large cohort of healthy subjects.

Methods: Healthy young males previously measured using PET with [^{11}C]SCH-23390 for D1R, and [^{11}C]raclopride for D2R, completed the 21-item Peters Delusion Inventory (PDI) scale (*1*). The study was approved by the Regional Ethics Committee in Stockholm and the Radiation Safety Committee of the Karolinska Hospital, and all subjects provided informed consent prior to their participation. In a sample of 84 participants, of whom 40 were measured with [^{11}C]SCH-23390 and 66 were measured with [^{11}C]raclopride, we generated normalized parametric BP_{ND} images using wavelet-aided parametric imaging, applying the non-invasive Logan plot with manually-delineated cerebellar grey matter as reference. Voxel-wise multiple regression analyses were performed to test for relationships between dopamine receptor availability and PDI scores, correcting for age at the time of PET. As this was an exploratory analysis, we utilized a liberal threshold of p

Results: PDI scores ranged from 0 to 14 (mean 3.5). A negative relationship was observed between PDI scores and D1R BP_{ND} in a region within the right orbitofrontal cortex ([20 42 -22], Z=3.36). Similar results were obtained for the PDI conviction scale ([18 44 -24], Z=3.25). We observed no relationship between D2R BP_{ND} and PDI scores or PDI conviction scores.

Conclusions: Our results suggest that individual differences in delusional ideation among healthy participants may be associated with differences in the availability of orbitofrontal D1R. The observed relationships between PDI scores and the availability of D1R and D2R correspond with comparisons of schizophrenia patients and healthy controls; finding differences in frontal D1R, and little or no difference in striatal D2R (*5*). The results support the view that differences in dopamine function underlie the psychosis continuum between health and psychopathology.

References

1. E. Peters, S. Joseph, S. Day, P. Garety, *Schizophr. Bull.* **30**, 1005 (2004).

2. F. Schürhoff *et al.*, *Am. J. Psychiatry* **160**, 1313 (2003).

3. J. van Os, R. Linscott, I. Myin-Germeys, P. Delespaul, L. Krabbendam, *Psychol. Med.* **39**, 179 (2009).

4. S. Kapur, *Am. J. Psychiatry* **160**, 13 (2003).

5. O. D. Howes *et al.*, *Arch. Gen. Psychiatry* **69**, 776 (2012).

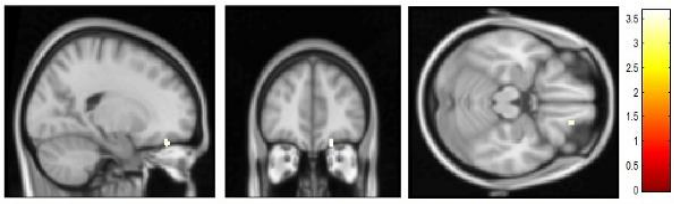

Figure: D1R BP_{ND} in a region of the right orbitofrontal cortex was found to be significantly negatively related to delusional ideation measured using the PDI in healthy control subjects (n=40). T values are indicated by the scale bar on the right.

842
BRAIN-0471
Poster Session

Psychiatric Disorders & Addictions

DIURNAL AND SEASONAL VARIATION OF THE BRAIN SEROTONIN SYSTEM IN HEALTHY MALE SUBJECTS

G.J. Matheson[1], M. Schain[1], R. Almeida[2], J. Lundberg[1], Z. Cselényi[1], J. Borg[1], A. Varrone[1], L. Farde[1], S. Cervenka[1]
[1]Department of Clinical Neuroscience, Karolinska Institutet, Stockholm, Sweden
[2]Department of Neuroscience, Karolinska Institutet, Stockholm, Sweden

Objectives: The mammalian circadian clock underlies both diurnal and seasonal changes in physiology, and its function is thought to be disturbed in both seasonal and non-seasonal depression (*1*). In humans, molecular imaging studies have reported seasonal changes in the

serotonin system (*2-4*). Despite the role of the circadian clock in generating seasonal physiological changes, however, diurnal variation of serotonin receptors and transporters have never been directly studied in humans. The objective of this study was to investigate whether the availability of serotonin 1A receptors and transporters differ across the day and year.

Methods: Using positron emission tomography, 56 subjects were measured with [^{11}C]WAY-100635 and 40 subjects were measured with [^{11}C]MADAM, for the serotonin 1A receptor (5-HT_{1A}R) and the serotonin transporter (5-HTT) respectively. Diurnal and seasonal changes in these proteins were examined, employing a cross-sectional design. Quantification was performed using the simplified reference tissue model for serotonin projection regions, and wavelet-aided parametric imaging, applying the non-invasive Logan plot, for the dorsal raphe nucleus (DRN). Cerebellar grey matter was used as reference. Regions of interest were delineated using FreeSurfer for serotonin projection regions, a semi-automated method for the DRN (*5*), and manual delineation for the cerebellum. We performed multiple linear regressions with daylength and day course, including age as a covariate.

Results: We observed increases in the availability of 5-HT_{1A}R in the cortex, and decreases in the availability of 5-HTT in the DRN across the day. We also found seasonal changes in the 5-HT_{1A}R in serotonin projection regions, with higher availability on days with a longer duration of daylight.

Conclusions: Our observation that serotonin receptor and transporter levels may change across the day in humans is corroborated by experimental research in rodents (*6, 7*). These findings have important implications for understanding the relationship between the circadian and serotonin systems in both the healthy brain and in affective disorders, as well as for the design of future molecular imaging studies.

References

1. A. Wirz-Justice, *Int. Clin. Psychopharmacol.* **21**, S11 (2006).
2. J. Kalbitzer *et al.*, *Biol. Psychiatry* **67**, 1033 (2010).
3. N. Praschak-Rieder, M. Willeit, A. A. Wilson, S. Houle, J. H. Meyer, *Arch. Gen. Psychiatry* **65**, 1072 (2008).
4. C. Spindelegger *et al.*, *World J. Biol. Psychia.* **13**, 413 (2012).
5. M. Schain *et al.*, *Eur. J. Nucl. Med. Mol. Imag.*, 1 (2013).
6. J. Akiyoshi, H. Kuranaga, K. Tsuchiyama, H. Nagayama, *Pharmacol. Biochem. Behav.* **32**, 491 (1989).
7. K. Ushijima *et al.*, *Mol. Pharmacol.* **82**, 264 (2012).

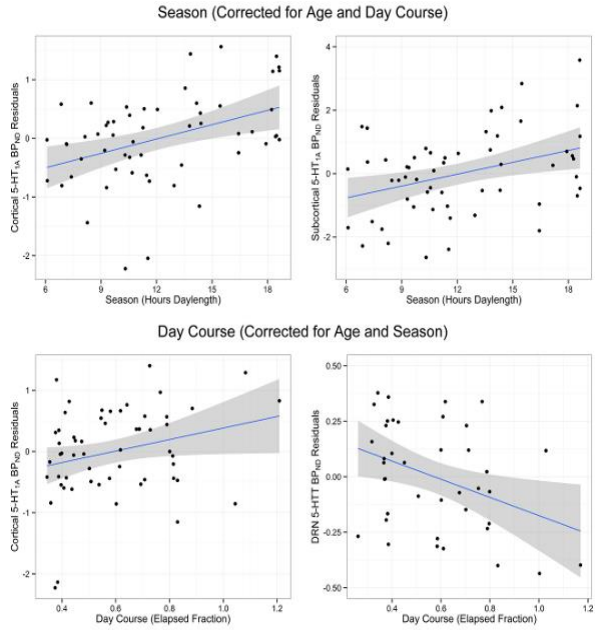

Partial correlation plots of season and day course with unstandardised binding potential residuals after accounting for the remaining variables. Cortical (top left) and subcortical (top right) [^{11}C]WAY-100635 BP_{ND} was significantly related to seasonal changes. Cortical [^{11}C]WAY-100635 BP_{ND} (bottom left) and DRN [^{11}C]MADAM BP_{ND} (bottom right) exhibited opposite directional relationships with day course. The grey shaded regions represent 95% confidence intervals of the fitted regression lines.

843
BRAIN-0337
Poster Session

Psychiatric Disorders & Addictions

PET STUDY OF THALAMIC DOPAMINE D2-RECEPTORS IN DRUG-NAIVE PATIENTS WITH SCHIZOPHRENIA

P. Ikonen[1], S. Cervenka[1], K. Collste[1], H. Fatouros-Bergman[1], G. Matheson[1], P. Plavén Sigray[1], A. Varrone[1], C. Halldin[1], L. Flyckt[1], L. Farde[1]
[1]Clinical Neuroscience, Karolinska Institutet, Stockholm, Sweden

Objective: Positron Emission Tomography (PET) studies have provided support for the dopamine hypothesis of schizophrenia. With regard to postsynaptic markers, such as the D2-dopamine receptor (D2-R), early studies focused on the striatum, a region with a high density of D2-R, for which the results have been inconsistent. A more recent line of research has demonstrated lower levels of D2-R in the thalamus, i.e an extrastriatal region. At a functional level, the thalamic complex is a component of several neurocircuits. However the resolution of previous PET-systems have not allowed for a more detailed anatomical analysis. The aim of the current study was to use high resolution PET to examine D2-R binding in thalamic subregions in first-onset patients with schizophreniform psychosis.

Method: The high-affinity radioligand [^{11}C]FLB 457 and a high resolution research tomography (HRRT) was used to examine D2-R availability in thirteen drug-naive patients with schizophreniform psychosis (DSM-IV) and twelve comparison subjects matched for age, gender and handedness. Five thalamic subregions were manually delineated on T1-weighted MRI according to previously published guidelines. Binding potential (BP_{ND}) was calculated using the simplified reference tissue model with cerebellum as reference region. Partial Volume Effect Correction (PVEC) was performed using established MRI-based method described by Meltzer. Symptoms were rated with the Positive and Negative Syndrome Scale, PANSS. The study was a part of the Karolinska Schizophrenia Project (KaSP). The study was approved by the Regional Ethical Review Board in Stockholm.

Results: When compared with controls the D2-R BP_{ND} in patients with schizophrenia was lower in the right centromedial thalamus (4.95 ± 0.90 and 3.90 ± 0.99; p=0.012) and right posterior thalamus (4.02 ± 1.53 and 2.76 ± 1.20; p = 0.037). There were no significant correlations between D2-R BP_{ND} and PANSS scores.

Conclusions: The present study using high resolution molecular imaging corroborates previous findings of aberrant D2-R availability in thalamic subregions in patients with schizophrenia. Since thalamus has a gating function, filtering sensory inputs to the cortex, it can be speculated that altered dopaminergic neurotransmission in right centromedial and posterior thalamus may be related to perceptual disturbances in schizophrenia.

844
BRAIN-0518
Poster Session

Psychiatric Disorders & Addictions

ELEVATED LEVELS OF ORBITOFRONTAL DOPAMINE D2-RECEPTORS IN PATIENTS WITH SOCIAL ANXIETY DISORDER

P. Plavén Sigray[1], E. Hedman[1], P. Ikonen[1], G. Matheson[1], A. Forsberg[1], D. Djurfeldt[1], C. Rück[1], C. Halldin[1], N. Lindefors[1], S. Cervenka[1]
[1]Department of Clinical Neuroscience, Karolinska Institutet, Stockholm, Sweden

Objectives: Previous molecular imaging studies have investigated striatal dopamine D2-receptors (D2-R) in patients with social anxiety disorder (SAD) with conflicting results (*1, 2*). Extrastriatal brain regions have been proposed to play an important role in SAD, based on blood flow and activation studies (*3*). In a previous study, including only patients, we showed a correlation between change in extrastriatal D2-R and SAD symptoms before and after psychotherapy

treatment (*4*). The objective of the present study was, for the first time, to investigate differences in D2-R between SAD patients and controls in extrastriatal regions.

Methods: Twelve SAD patients and 18 healthy control subjects were examined using HRRT PET and the high-affinity D2-R radioligand [^{11}C]FLB457. Parametric images of D2-R binding potential (BP_{ND}) values were created using the wavelet approach (*5*) with manually delineated cerebellum as reference region. Regions of interest (ROIs) were defined using Freesurfer software and included subdivisions of frontal cortex and the limbic system. Firstly, independent t-test analyses were performed to examine differences in ROI BP_{ND}. Secondly, a more detailed voxel-by-voxel analysis using Statistical Parametric Mapping (SPM) was performed using the ROIs as a mask. The study was approved by the Regional Ethics Review Board and the Karolinska Hospital Radiation Safety Committee, and all subjects gave written informed consent prior to participating.

Results: In the ROI analyses, patients showed elevated levels of D2-R BP_{ND} in the orbitofrontal cortex (mean [SD]=0.99 [0.28]) compared to healthy controls (0.76 [0.26], p=0.03), however this finding did not survive correction for multiple comparisons. In the SPM voxel-by-voxel analysis, a cluster in the right lateral orbitofrontal cortex showed a significant difference between patients and controls, after correction for multiple comparisons. Significant differences were also found in voxels in the left orbitofrontal cortex (Fig 1).

Conclusions: Whereas previous studies have shown a reduction or no difference in striatal D2-R levels in SAD patients (*1, 2*), we found higher levels of D2-R BP_{ND} among patients in the lateral orbitofrontal cortex. This region is central in self-monitoring, processing of negative emotions, and integration of social perception (*6-8*), and has repeatedly been shown to be implicated in SAD in activation studies (*3*). The present findings suggest that deviant dopaminergic neurotransmission could underlie these observations. Future studies should address the relationship between striatal and extrastriatal dopaminergic function and aberrant psychological processes in SAD.

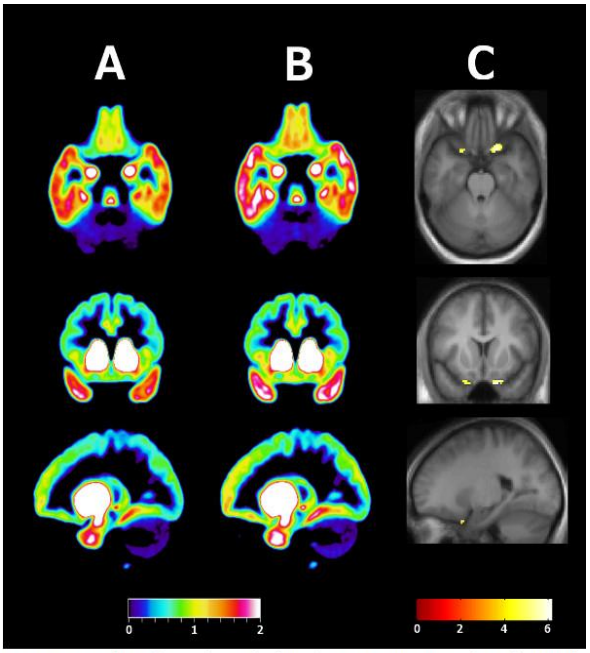

Fig 1. From top to bottom: horizontal, coronal and sagittal D2-R BP_{ND} images averaged over all A) control subjects and B) SAD patients. The scale bar indicates BP_{ND} values. C) Significant differences in voxels (T > 4.44, p<.05, FDR-corrected) between patients and controls in BP_{ND} in the lateral orbitofrontal cortex (right cluster: k_E=63, $p_{corrected}$=.03; left cluster: k_E=10, $p_{corrected}$=.098). The scale bar indicates t-values.

References

1. F. R. Schneier et al., Am. J. Psychiatry 157, 457 (2000).
2. F. R. Schneier et al., Depress. Anxiety 26, 411 (2009).
3. M. Freitas-Ferrari et al., Prog. Neuropsychopharmacol. Biol. Psychiatry 34, 565 (2010).
4. S. Cervenka et al., Transl. Psychiatry. 2, e120 (2012).
5. Z. Cselényi, H. Olsson, L. Farde, B. Gulyás, Neuroimage 17, 47 (2002).
6. M. R. Milad, S. L. Rauch, Ann. N. Y. Acad. Sci. 1121, 546 (2007).
7. J. S. Beer, O. P. John, D. Scabini, R. T. Knight, J. Cogn. Neurosci. 18, 871 (2006).
8. T. Allison, A. Puce, G. McCarthy, Trends Cogn. Sci. 4, 267 (2000).

845
BRAIN-0617
Poster Session

Psychiatric Disorders & Addictions

NEURO-ANATOMY PERSPECTIVE AND FUNCTION IN CLASSIC HYSTERICAL PSYCHOSIS

S. Trifu[1], E.G. Carp[2], A. Gutt[2], D. Braileanu[3]
[1]Psychiatry, UMF Carol Davila, Bucharest, Romania
[2]Psychiatry, Sapunari Psychiatric Hospital, Calarasi, Romania
[3]Psychology, Sapunari Psychiatric Hospital, Calarasi, Romania

The actuality of the research topic: Hysterical psychosis classic issue is known since Charcot without being existed then explanations of functional neuro-sensory area.

Objective: The present paper is a presentation of the case of a patient aged 61 years, admitted to the Sapunari Psychiatric Hospital for major depressive symptoms accompanied by psychotic phenomena (auditory hallucinations).

Hypothisis: Evolution of initial symptoms of type major depressive episode psychotic phenomena in a few weeks went by classical pathology hysterical psychosis, but by modern imaging neuro investigations (CT, MRI, computerized EEG, sleep EEG) can be explained in functional anatomy neuro dynamics.

Results:

*******debut of psychopathological disorders: at 55, symptoms prolonged for two years.

******** A second psychiatric hospitalization: at 57 years of age six weeks

*** Current hospitalization: Early treatment instituted, but regressive evolution type, with disorganization in the thinking and behavior, delusional ideation negative type and guilt.

**** Presentation of neurological investigations, the differential diagnoses neurological and metabolic (meningo-encephalitis, dementia Jacobs Kreutzfeld).

*** EEG: presence of theta, post psychiatric treatment, without any other markers epileptic disorders. During the entire period of hospitalization, patient has not had a fever and leukocytes and leukocytes were not changed. Viral markers, ionogram, T3, T4, ATPO: within normal limits. There never experienced hypertension and headache

*** CT a moderate degree of cortical atrophy. MRI Cerebral: areas of demyelination / gliosis supratentorial unspecified, probably micro-vascular substrate. Gaps sequelae Ponto right midbrain minimal (less than 0.5 cm). We asked two checkups during hospitalization neurological and advice infective diseases, all refuting need for lumbar puncture.

*** CT: un grad de atrofie corticală moderată. RMN cerebral: zone de demielinizare / gliozã

Psychiatric evolution went to disorganization of thought and behavior, not SK type, but dissociative: dietary and verbal negativity, sketch of catalepsy / catatonia, waxy flexibility, stereotypes, posts. The patient presented Answers "alongside", "The will of not knowing", suggestibility, regression going to urinary incontinence. Auditory hallucinations denies, but asserts complex visual hallucinations, type scenes and presents delusional ideation cotardoid negative type, with immortality, enormous guilt and shame for concern.

Conclusions: Evolutions of symptoms (particularity evolution of this psychiatric case) raises modern explanations on neural lesion anatomic substrate.

846
BRAIN-0251
Poster Session

Psychiatric Disorders & Addictions

A NEW METHOD FOR EVALUATION OF REGIONAL PERFUSION ABNORMALITIES OF MILD TRAUMATIC BRAIN INJURY WITH NEUROPSYCHOLOGICAL IMPAIRMENT USING STATISTICAL IMAGING ANALYSIS FOR TC-ECD SPECT

G. Uruma[1], K. Hashimoto[2], M. Abo[1]
[1]Department of Rehabilitation Medicine, The Jikei University School of Medicine, Tokyo, Japan
[2]Division of Rehabilitation Medicine, National Center for Child Health and Development , Tokyo, Japan

Objective: The objective of this study was to identify specific brain lesions with regional perfusion abnormalities possibly associated with neuropsychological impairments (NPI), as sequela after mild traumatic brain injury (MTBI), using Tc-ECD SPECT and its novel analytic software.

Methods: We studied 23 patients with diffuse axonal injury with NPI group (Impaired-DAI), 26 with MTBI with NPI group (Impaired-MTBI) and 24 with MTBI without NPI group (Healthy-MTBI). In each subject, Tc-ECD SPECT images were analyzed by easy Z-score imaging system (eZIS) and voxel-based stereotactic extraction estimation (vbSEE). Segmented into lobule levels, ROIs were set in 140 areas in whole brain, and relative regional low Tc-ECD uptake was computed as ‘‘extent’’ (rate of coordinates with Z score >2.0 in the ROI). ROC analysis was performed using ”extent’’ to discriminate the three groups.

Results: The highest area under the curve (AUC) value for data of Impaired-DAI and Healthy-MTBI groups was obtained in ROI on the left anterior cingulate gyrus (LtACG), with AUC of 0.93, optimal ‘‘extent’’ cutoff value of 10.9 %, sensitivity 87.0 %, specificity 83.3 %. The highest AUC value for data of Impaired-MTBI and Healthy-MTBI groups was also in the LtACG, with AUC of 0.87, optimal ‘‘extent’’ cutoff value of 9.2 %, sensitivity 73.1 %, specificity 83.3 %.

Conclusions: Using two analytic software packages, eZIS and vbSEE, we were able to identify specific areas with low regional Tc-ECD uptake, which were possibly associated with NPIs after MTBI. This trend was most marked in the left anterior cingulated gyrus in MTBI patients with NPIs and those with DAI. The optimal ‘‘extent’’ cutoff value, as a criterion for SPECT abnormality, might help the diagnosis of NPIs after MTBI.

847
BRAIN-0037
Poster Session

Dementia and Neurological Disorders

CHARACTERIZATION OF CEREBROVASCULAR FUNCTION IN MICE WITH CEREBRAL SMALL VESSEL DISEASE

M. Balbi[1], P. Hanecker[1], M. Dichgans[1], N. Plesnila[1]
[1]Institute for stroke and dementia (ISD), LMU, Munich, Germany

Objectives: CADASIL – cerebral autosomal dominant arteriopathy with subcortical infarcts and leukoencephalopathy – is the most common form of hereditary small vessel disease. It is caused by mutations of the Notch 3 gene, located on chromosome 19[1]. Transgenic mice overexpressing mutated Notch3 ($TgNotch^{R169C}$) replicate the diseaseand are therefore the only available model for small vessel disease. This study aims to identify early microvascular dysfunctions in the CADASIL model in order to facilitate the development of therapeutic strategies.

Methods: Pial microvascular reactivity to CO_2 (5 and 10%) was investigated in 7.5(n=21) and 11 (n=16) month old $TgNotch^{R169C}$ and control mice using intravital fluorescence microscopy. Cerebral blood flow (CBF) was measured with a laser Doppler probe over the territory of the middle cerebral artery. Neurovascular coupling (NVC) was investigated in a second group of 8.5 (n=25)

and 12.5 (n=15) month old mice, via stimulation of the forepaw and simultaneous recording of CBF over the associated somatosensory cortex.

Results:Vessels of 20 to 30 micrometers in diameter were selected for analysis. All groups show an increase in vessel diameter in response to CO_2. Estimating the cumulative increase in vessel diameter and CBF, significant differences were found: at 11 months, TgNotch^{R169C} mice show increased vessel dilation at 5% CO_2, and decreased CBF response at 10%. In the second group, NVC was analyzed sorting the first four and last six stimuli separately. While there was no significant difference in NVC between TgNotch^{R169C} and control mice, older mice –8 and 11.5 months old – exhibited a significant decrease in NVC over time compared to younger controls (n=7) – 6 weeks old.

Conclusion: TgNotch^{R169C}mice 11 months old show significant differences in vessel dilation and CBF response to CO_2. While NVC is not altered in CADASIL mice, the animals show a significant change in CO_2 reactivity indicating alteration in the NOS signaling. Therefore, targeting the NOS system could represent a novel therapeutic strategy for CADASIL and small vessel disease in general.

[1]Joutel A, Corpechot C, Ducros A, *et al.* (October 1996). "Notch3 mutations in CADASIL, ahereditary adult-onset condition causing stroke and dementia". *Nature*383 (6602): 707–10

848
BRAIN-0098
Poster Session

Dementia and Neurological Disorders

MTRNR2L12: A CANDIDATE BLOOD MARKER OF EARLY ALZHEIMER'S DISEASE-LIKE DEMENTIA

M. Bik-Multanowski[1], J.J. Pietrzyk[1], A. Madetko-Talowska[1], A. Grabowska[1]
[1]Department of Medical Genetics, Jagiellonian University, Krakow, Poland

Objectives: Histological changes typical for Alzheimer's disease (AD) are constantly reported in autopsied brain tissue of deceased individuals with Down syndrome (trisomy 21) aged above 30-40 years. Interestingly, significant variability of cognitive profiles can be observed in adult persons with Down syndrome. On the one hand symptoms of AD-like dementia develop in them frequently in the fourth or fifth decade of life, but on the other hand several seniors remain not affected. This phenomenon suggests presence of genetic variability influencing metabolic pathways crucial for development of AD-like dementia in Down syndrome.

Recent studies suggest that several genes playing central role in metabolic pathways follow similar expression patterns in brain and in blood. Consequently, alteration of genome expression in brain in case of AD development might be partially detectable in blood.

Considering the above facts we aimed at seeking of potential genomic blood markers of AD-like dementia development in adults with Down syndrome.

Methods: A cohort of 48 adults with Down syndrome aged >35 years who were institutionalized or attended day-care centers was recruited for the study.

To allow for detection of potential markers of early dementia, the participants were divided into two age groups: younger persons (<55 years) and older persons (>55 years).

The cognitive function of each study participant was assessed with use of the Prudhoe Cognitive Function Test (PCFT). The cognitive status was defined as good/acceptable (PCFT score >25%) or as severe cognitive disability (PCFT score up to 25%).

Whole genome expression in blood mononuclear cells was compared between subgroups of younger and of older persons with various cognitive statuses. SurePrint Human Gene

Expression 8x60K v2 Microarrays (Agilent) were used for this purpose.

The study was accepted by the Jagiellonian University Ethics Committee.

Results: The PCFT scores in the subgroups of persons with good/acceptable cognitive function ranged 50-100% in the younger and 57-97% in the older patients. In patients with severe cognitive disability the PCFT could be administered only in three cases (administration of the test in other patients was not possible due to poor contact).

Comparison of the groups of younger and of older persons by means of microarrays revealed significant differences with regard to three transcripts (ESPNL, XLOC_007536 and USP27X-AS1). However, these transcripts do not seem to be involved in pathogenesis of dementia. No significant differences were detected when comparing the group with good/acceptable cognitive status against the group with severe cognitive disability. However, subgroups of younger participants with severe cognitive disability differed significantly when compared with older patients with good/acceptable cognitive status (corrected p=0.00026; Fold Change=17.76) with regard to expression of a single gene: *MTRNR2L12*, an isoform of humanin, considered to be a protective factor in familial AD.

Conclusions: Expression of MTRNR2L12 might be an easy to measure blood marker of severe cognitive disability and, possibly, of early dementia in patients with Down syndrome. Further studies should be performed to evaluate potential usefulness of measurement of *MTRNR2L12* transcript in patients with Alzheimer's disease.
The study was sponsored by the Polish National Science Centre (DEC-2011/03/B/NZ5/01328).

849
BRAIN-0423
Poster Session

Dementia and Neurological Disorders

GLOBAL GENE EXPRESSION PROFILING OF NEW ANIMAL MODEL FOR COGNITIVE DYSFUNCTION

H. Lee[1], S. Choi[1], S. Lee[2], S. Cha[3], K. Yi[3], T. Kim[1], K. Chang[2]
[1]Biomedical Research Institute, Chung Ang University College of Medicine, Seoul, Korea
[2]National Primate Research Center, Korea Research Institute of Bioscience and Biotechnology, Cheongju, Korea
[3]Department of Radiology, Chungbuk National University College of Medicine, Cheongju, Korea

Alzheimer's disease (AD) is a neurodegenerative disorder which observed amyloid plaques and neurofibrillary tangles. Appropriated medicine is not available so far. There are many animal models to imitate AD using mutant genes of presenilin and APP. However, these animal models which used mutant genes are based to familial dementia to developed young age. We proposed new animal model for AD using ibotenic acid (Ibo) and amyloid beta (Aβ) to induce neuronal cell loss. We injected ibotenic acid and Aβ into bilateral hippocampus of mouse at 6 week age. Animal behavioral test and histological analysis were shown to decline of learning, memory, neuronal cell loss and deposits of amyloid plaque in hippocampus regions. Total RNAs were used for global gene network. These results suggested that new animal model may be a useful tool to study as AD-like disease.

850
BRAIN-0092
Poster Session

Dementia and Neurological Disorders

NO RELATIONSHIP BETWEEN CORTICAL BETA-AMYLOID DEPOSITION AND CURRENT DEPRESSIVE SYMPTOMS IN ALZHEIMER'S DISEASE AND MILD COGNITIVE IMPAIRMENT

J.K. Chung[1], E. Plitman[1], S. Nakajima[2], M. Chakravarty[3], F. Caravaggio[1], P. Gerretsen[2], Y. Iwata[2], A. Strafella[1], A. Graff-Guerrero[1]
[1]Institute of Medical Science, University of Toronto, Toronto, Canada
[2]Multimodal Imaging group, Centre for Addiction and Mental Health, Toronto, Canada
[3]Cerebral Imaging Centre, Douglas Mental Health Institute, Montreal, Canada

Abstract: Depressive symptoms are frequently seen in patients with dementia and mild cognitive impairment (MCI). Evidence suggests that there may be a link between depressive symptoms and Alzheimer's disease (AD)-associated pathological changes, such as an increase in cortical beta-amyloid (Aβ). However, limited in-vivo studies have explored the relationship between current depressive symptoms and cortical Aβ accumulation in patients with MCI and AD. Our study, using a large sample consisting of 455 patients with MCI and 153 patients with AD from the Alzheimer's disease Neuroimaging Initiatives databases, investigated whether current depressive symptoms predict cortical Aβ deposition. Depressive symptoms were assessed using Geriatric Depression Scale and Neuropsychiatric Inventory-Depression/Dysphoria. Cortical Aβ deposition was quantified using Positron Emission Tomography with the Aβ probe ^{18}F-Florbetapir. Standardized uptake value ratio (AV-45 SUVR) from the frontal, cingulate, parietal and temporal regions were estimated. In addition, a global AV-45 SUVR defined as the average of frontal, cingulate, precuneus, and parietal cortex regions, was also used. Through correlation analyses, we observed that current depressive symptoms were not related to cortical Aβ deposition, after controlling for potential confounds that may affect Aβ accumulation, including history of previous major depression. We also observed that there was no difference in cortical Aβ deposition between matched subjects with high and low depressive symptoms, as well as no difference between matched subjects with presence and absence of depressive symptoms. In conclusion, we found no relationship between current depressive symptoms and cortical Aβ deposition in patients with MCI and AD. This finding is consistent with the Aβ hypothesis of AD, which suggests that cortical Aβ accumulation occurs early in the illness, prior to the emergence of clinical symptoms.

851
BRAIN-0183
Poster Session

Dementia and Neurological Disorders

PROTECTIVE POTENTIAL OF METFORMIN ON MEMBRANE LINKED FUNCTIONS IN DIABETIC AGING FEMALE RATS.

P. Kumar[1], R. Kale[1], N. Baquer[1]
[1]School of Life Sciences, Jawaharlal Nehru University, New Delhi, India

Objective: The objective of this study was to investigate protective potential of metformin on membrane linked functions and glucose transporter in diabetic aging female rats.
Background: The emerging view is that diabetic brain features many symptoms that are best described as accelerated brain aging. Diabetes is considered to be a kind of 'accelerated aging" by increasing susceptibility to degenerative condition, including kidney disease, retinopathy, hypertension, coronary artery disease, stroke and atherosclerosis. Diabetes mellitus leads to functional and structural changes in the brain which appear to be most pronounced in the elderly.

Methods: Young (3 months) adult (12 months) and aged (24 months) rats will be diabetic by

using alloxan monohydrate. After metformin was given i.p dose 200mg/Kg for one months to both control and diabetic aging rats. Learning was tested in a Morris water maze. A detailed study was carried on membrane linked enzymes, membrane fluidity, lipofuscin, antioxidant enzymes, glucose transporter, bcl-2 and DNA degradation to identify the antidiabetic and antiaging role of metformin using biochemical ,molecular and histiochemical study.

Results: Present study shows that there was a similar pattern of increased lipid peroxidation, neurolipofuscin, DNA degradation and monoamine oxidase activity and a decrease in membrane fluidity, Na+ K+ ATPse, Ca2+ ATPase, sueroxidase dismutase and glutathione S-transferases activities, glucose transporter-4 (GLUT4) in both aging and diabetes. Metformin was found to be an effective treatment in stabilizing and normalizing the membrane functions; therefore this therapy can be considered an alternative to be explored further as a means of diabetic and aged related disorders control. Metformin treatment also helped to reverse the age related changes studied, to normal levels, elucidating an anti-aging, antidiabetic and neuroprotective action.

Conclusions: The cumulative deficits in learning and membrane functions in aged diabetic rats indicate that the effects of diabetes and ageing on the brain could interact. The results of this study will be useful for pharmacological modification of the aging process and applying new strategies for control of age related disorders including metabolic syndrome.

852
BRAIN-0302
Poster Session

Dementia and Neurological Disorders

ASTROCYTE-DERIVED LIPOCALIN-2 MEDIATES HIPPOCAMPAL NEURONAL LOSS IN THE GLOBAL ISCHEMIC MODEL OF VASCULAR DEMENTIA

K. Suk[1], J. Kim[1]
[1]Dept of Pharmacology, Kyungpook National Univsersity School of Medicine, Daegu, Korea

Objectives: Lipocalin-2 (LCN2) is a secreted protein of the lipocalin familyhaving diverse functions in multiple pathophysiological conditions. However,its precise functional role in the central nervous system is ill understood.Likewise, the pathogenic mechanism of vascular dementia, which is accompaniedby cognitive impairment and neuronal loss, is still to be outlined clearly.

Methods: Here, we investigated the role of LCN2 in vascular dementiaemploying a rodent model of transient global cerebral ischemia with cognitiveimpairment and neuroinflammation. Mice subjected to transient bilateral commoncarotid artery occlusion (tBCCAO) for 50 minutes showed neuronal death andgliosis in the hippocampus at 7 days post-tBCCAo.

Results: LCN2 expression was dominantly induced in hippocampal CA1astrocytes, whereas its receptor (24p3R) was mainly detected in neurons andmicroglia. Furthermore, Lcn2-deficient mice showed significantly reduced CA1neuronal loss, cognitive decline, glial activation and pro-inflammatorycytokine (TNF-a, IL-1b and IL-6) production in the hippocampus after tBCCAo compared withwild-type animals. Intracerebroventricular injection of recombinant LCN2protein elicited CA1 neuronal death.

Conclusions: These results indicate that cognitive impairment and hippocampalCA1 neuronal death may be mediated by LCN2 protein secreted from reactiveastrocytes. Taken together, our findings suggest that LCN2 can be a therapeutictarget for the vascular dementia.

853
BRAIN-0054
Poster Session

Dementia and Neurological Disorders

CORRELATION OF DOPAMINERGIC AND SEROTONERGIC DYSFUNCTION IN A RAT MODEL OF PARKINSON'S DISEASE

J.Y. Choi[1], M.K. Lee[2], W.G. Cho[3], C.H. Lyoo[4], K.C. Lee[5], Y.H. Ryu[1]
[1]Department of Nuclear Medicine, Gangnam Severance Hospital, Seoul, Korea
[2]Department of Nuclear Medicine, Inha University Hospital, Incheon, Korea
[3]Department of Anatomy, Yonsei University Wonju College of Medicine, Wonju, Korea
[4]Department of Neurology, Gangnam Severance Hospital, Seoul, Korea
[5]Department of Molecular Imaging, Korea Institute of Radiological & Medical Sciences, Seoul, Korea

Objectives: The purpose of this study is to evaluate the effect of dopaminergic destruction on the serotonergic system in the same subject by using consecutive PET imaging. The interconnection between motor symptoms and depression was also examined.

Method: [^{18}F]FP-CIT was applied to assess dopamine transporters and serotonin 1A (5-HT_{1A}) receptors were evaluated by [^{18}F]Mefway in unilateral 6-hydroxydopamine (6-OHDA) lesioned and sham operated rats. Behavioral tests were used to evaluate the severity of symptoms: rotational number for motor impairment and immobility time, acquired from the forced swim test for depression. Region-of-interests (ROIs) were drawn in the striatum and cerebellum for the dopamine system and hippocampus and cerebellum for the 5-HT system. Non-displaceable binding potential in the striatum and hippocampus were compared between 6-OHDA and sham groups.

Results: Unilateral 6-OHDA-lesioned rats exhibited significant bilateral reduction of hippocampal BP_{ND} for 5-HT_{1A} receptors compared with the sham group and there was a positive correlation between striatal BP_{ND} for DAT. The severity of motor symptoms was also closely related to the depression.

Conclusion: Taken together, the data demonstrate that destruction of the dopaminergic system causes the reduction of the serotonergic system and that the degrees of change in these neurotransmitter systems are also related with behavioral impairment in PD.

References:

Hesse S, Meyer PM, Strecker K, Barthel H, Wegner F, Oehlwein C, Isaias IU, Schwarz J, Sabri O. 2009. Monoamine transporter availability in Parkinson's disease patients with or without depression. Eur J Nucl Mol Imaging 36:428-435.

Politis M, Wu K, Loane C, Turkheimer FE, Molloy S, Brooks DJ, Piccini P. 2010. Depressive symptoms in PD correlate with higher 5-HTT binding in raphe and limbic structures. Neurology 75:1920-1927.

Ravina B, Camicioli R, Como PG, Marsh L, Jankovic J, Weintraub D, Elm J. 2007. The impact of depressive symptoms in early Parkinson disease. Neurology 69:342-347

854
BRAIN-0422
Poster Session

Dementia and Neurological Disorders

ASSOCIATION OF WHITE MATTER HYPERINTENSITIES AND COGNITION WITH AMBULATORY BLOOD PRESSURE MONITORING (ABPM).

H. OHBA[1], F. YAMASHITA[2], M. KIN[1], Y. ISHIBASHI[1], H. YONEZAWA[1], H. OIKAWA[1], K. WATANABE[1], H. SAKASHITA[1], M. SASAKI[2], Y. TERAYAMA[1]
[1]Department of Neurology and Gerontology, Iwate Medical University, Morioka Iwate, Japan
[2]Division of Ultrahigh Field MRI Institute for Biomedical Sciences, Iwate Medical University, Morioka Iwate, Japan

Objectives

White matter hyperintensities (WMH) are a common finding on MRI. Associations of WMH with aging, hypertension and cognitive impairment have been reported. The circadian blood pressure abnormality is reported as a risk factor of cerebrovascular disease. We assessed the circadian blood pressure and associations with the severity of WMH and cognitive impairment in hypertensive patients.

Methods

From March 2013 to November 2014, 101 consecutive hypertensive patients (69+/-8 years of age, 65% men) were recruited from our outpatient department. Ambulatory blood pressures monitoring (ABPM) parameter included BP level, variability during waking and sleep hours, and circadian blood pressure type. We assessed severity of WMH by Fazekas score and volumetric of WMH using 3T MRI and cognitive impairment by Mini-Mental State Examination (MMSE max score 30, cut off <20). Statistical analyses were performed to identify the association between WMH, cognitive impairment, and ABPM parameters.

Results

There was significant association between WMH Fazekas score total, WMH volume, high age, 24h systolic blood pressure (SBP), 24h daytime SBP, nighttime SBP, and MMSE score (27+/-3) ($p<0.05$). No significant relationship was found between circadian blood pressure type, WMH severity, and MMSE score.

Conclusions

Elevated blood pressure by ABPM is a risk factor for WMH independent of the circadian variability. WMH is associated with low cognitive scores.

References

Sierra C et al. J Hypertens. 2002 Mar;20(3):519-24.

855
BRAIN-0870
Poster Session

Dementia and Neurological Disorders

Brain hypometabolism coincides with or precedes cortical thinning in patients with ALS-FTD

V. Rajagopalan[1,2], E.P. Pioro[3]
[1]Department of Electrical and Electronics Engineering ,Institute of Technology and Science, Pilani, Hyderabad Campus, Hyderabad, India
[2]Department of Biomedical Engineering, Lerner Research Institute, Cleveland Clinic, Cleveland, Ohio, USA
[3]Department of Neurology, Neuromuscular Center, Neurological Institute, Department of Neurosciences, Lerner Research Institute, Cleveland Clinic, Cleveland, Ohio, USA

Objectives:
We previously used voxel based morphometry (VBM) to show decreased motor and extramotor grey matter (GM) volume in brains of patients with amyotrophic lateral sclerosis (ALS) and frontotemporal dementia (ALS-FTD) when compared to neurologic controls1. However, VBM

analysis can potentially result in erroneously high GM values because it includes both cortical thickness and cortical foldings (gyri and sulci) as a single GM region. The relationship between structural and functional changes is also unknown. Therefore, we examined whether GM volumetric changes in ALS-FTD patients resulted from changes in cortical thickness, area or both, and compared these structural changes with metabolic changes as revealed by positron emission tomography (PET).
Methods:
High-resolution 3D T1-weighted MRIs were obtained at 1.5T in 18 patients with ALS-FTD and in 15 unaffected neurologic controls during routine clinical scanning. ALS-FTD patients also underwent fluorine-18-2-fluoro-2-deoxy-D-glucose (18F-FDG) PET imaging on a hybrid PET/CT Siemens Biograph TruePoint scanner within 0 to 14 days of MRI. Brain GM structural changes were assessed using VBM and cortical thickness, whereas metabolic changes were assessed using cerebral glucose metabolic rate (CMRglc) obtained from PET images.
Results:
GM volume and cortical thickness were significantly decreased ($p<0.05$) in motor and extramotor regions of ALS-FTD patients compared to controls. Cortical area showed no significant difference in any brain region. In addition, cerebral glucose metabolism rate was significantly reduced ($p<0.05$) in brain regions where structural changes were also observed but sometimes not.
Conclusions:
Significant reductions mostly in cortical thickness seemed to account for GM volume decreases detected by VBM in ALS-FTD. Metabolic changes corresponded well with structural changes in most motor and extramotor areas and occurred even in the absence of GM volume decrease in at least one region. Concurrent changes in GM structure and function suggest that neurodegeneration in ALS-FTD patients may occur as a “neuronopathy”.

References:
1. Rajagopalan V, Pioro EP. Distinct patterns of cortical atrophy in ALS patients with or without dementia: an MRI VBM study. Amyotroph Lateral Scler Frontotemporal Degener 2014;15:216–25.

856
BRAIN-0108
Poster Session

Dementia and Neurological Disorders

STRONG IMPROVEMENT OF APOE/LDL-R SIGNALS AND AMYLOIDGENESIS BY TELMISARTAN IN POST-STROKE SHR-SR

T. Yamashita[1], Y. Zhai[1], S. Kono[1], Y. Nakano[1], R. Morihara[1], K. Deguchi[1], K. Abe[1]
[1]Department of Neurology, Okayama University, Okayama, Japan

Recent studiessuggested that stroke and a factor of metabolic syndrome such as hypertensionand dyslipidemia is an important risk factor of Alzheimer’s disease (AD) viapromoting inflammatory responses. Telmisartan, an angiotensin receptor blocker(ARB), is expected to reduce not only the level of blood pressure (BP) but alsoneuroinflammation and neurotoxicity, then we examined the effects oftelmisartan on both cholesterol transport-related proteins (ApoE/LDL-R) and AD pathologyin spontaneously hypertensive rat stroke resistant (SHR-SR) after transientmiddle cerebral artery occlusion (tMCAO).

SHR-SR received tMCAO for 90 min at 12 weeksof age, and then were divided into 3 experiment groups including a vehicle,low-dose telmisartan (0.3 mg/kg/day), and high-dose telmisartan (3 mg/kg/day).The low dose served to improve the metabolic syndrome of SHR-SR withoutlowering the BP while the high dose was used to improve metabolic syndromewhile lowering BP.

Immunohistologicalanalysis showed that ApoE expression of cortical neurons was strong in thevehicle group at 6, 12 and 18 months of age, and that this ApoE expression patternwas very similar between the ipsilateral and contralateral sides of cerebral ischemia.LDL-R expression of cortical neurons was transiently increased at 6

months ofage only on the ipsilateral side. However, telmisartan dramatically suppressedthe expression of ApoE/LDL-R at both doses. Meanwhile, the numbers of amyloid β(Aβ)-positive neurons and senile plaque (SP) in the ipsilateral cerebral cortexprogressively increased with age until 18 M in the SHR-SR after tMCAO. To our surprise,low-dose/ high-dose telmisartan significantly reduced the number of Aβ-positiveneuron as well as SP at 6, 12, and 18 M.

These findings suggest that both low and highdoses of telmisartan prevented the activation of ApoE/LDL-R in SHR-SR aftertMCAO, reducing both intracellular Aβ and extracellular SP accumulations aftertMCAO in SHR-SR, with a further improvement by combined BP lowering. Such astrong effect of telmisartan could provide a preventative approach for AD inpost-stroke patients with hypertension.

857
BRAIN-0121
Poster Session

Dementia and Neurological Disorders

PROTECTIVE EFFECT OF TELMISARTAN AGAINST PROGRESSIVE OXIDATIVE BRAIN DAMAGE AND SYNUCLEIN PHOSPHORYLATION IN STROKE-RESISTANT SPONTANEOUSLY HYPERTENSIVE RATS

A. Koji[1], Y. Fukui[1], T. Yamashita[1], Y. Nakano[1], R. Morihara[1], K. Deguchi[1]
[1]Department of Neurology, Okayama University, Okayama, Japan

Objective: We previously reported that reactive oxygen species and signaling molecules of angiotensinII produced lipid peroxides, degenerated proteins, and injured DNA aftercerebral ischemia in normotensive Wistar rats. Here, we investigated thelong-term effect of the angiotensin II type I receptor blocker telmisartan onoxidative stress and hyperphosphorylated α-synuclein accumulation instroke-resistant spontaneously hypertensive rats (SHR-SR).

Methods: At the age of 3 months, SHR-SR were dividedinto 3 treatment groups: SHR-SR vehicle (SHR/Ve), SHR-SR low-dose telmisartan(.3 mg/kg/day) (SHR/low), and SHR-SR high-dose telmisartan (3 mg/kg/day)(SHR/high). Immunohistologic analyses were conducted in these groups and Wistarrats at the age of 6, 12, and 18 months.

Results: The SHR/Vegroup demonstrated more progressive increase in advanced glycation end product(AGE)-, 4-hydroxy-2-nonenal (4-HNE)-, and phosphorylated α-synuclein(pSyn)-positive cells in the cerebral cortex and hippocampus compared with theWistar group at 18 months. These expressions were reduced in the SHR/lowgroup even without lowering blood pressure (BP), and expressions weredramatically suppressed in the SHR/high group with lowering of BP.

Conclusion: These data suggest that persistenthypertension in SHR-SR strongly potentiate the markers of oxidative damage(AGEs and 4-HNE) and abnormal accumulation of pSyn, which were greatlysuppressed by telmisartan in a dose-dependent manner without and with loweringof BP.

858
BRAIN-0419
Poster Session

Dementia and Neurological Disorders

CLINICAL FEATURES OF PATIENTS WITH SUSPECTED NON-ALZHEIMER PATHOLOGY (SNAP)

M. YOSHITA[1], S. TUJI[2], K. YOKOYAMA[2], H. SAKAMOTO[3]
[1]Neurology, Hokuriku National Hospital, Nanto, Japan
[2]Nuclear Medicine, Public Central Hospital of Matto Ishikawa, Hakusan, Japan
[3]Psychiatry, Hokuriku National Hospital, Nanto, Japan

Objective: The present study was designed to analyze the clinical features of patients with

suspected non–Alzheimer disease pathology (SNAP) and cognitive impairment in detail.
Methods: We measured markers of amyloid pathology ([11C}-Pittsburgh compound B (PiB)-PET) and neurodegeneration (hippocampal volume on MRI and cortical metabolism on [18F]-fluorodeoxyglucose (FDG)–PET) in 189 consecutive patients who visit our memory clinic. We categorized patients as SNAP based on absence of amyloid pathology and presence neurodegeneration pattern of Alzheimer disease.
Results: In 50 cases with negative PiB-PET, 24 cases showed both Alzheimer-like cortical hypometabolism with FDG-PET and medial temporal atrophy on MRI. Clinical diagnosis were Dementia with Lewy bodies (DLB) in 5 cases, mild cognitive impairment (MCI) with SNAP in 9 case, and dementia with SNAP in 10 cases. The proportion of APOE e4 carriers in DLB, MCI and dementia with SNAP was 20%, 22% and 24%, respectively.
Conclusion: DLB showed similar pattern of brain imaging in patients with SNAP. There might be not a few possibilities that patients with SNAP are diagnosed as AD without using PiB-PET in a memory clinic.

859
BRAIN-0336
Poster Session

BrainPET: Other

INFLUENCE OF TSPO AFFINITY-BINDING ON [18F]DPA-714 WHOLEBODY BIODISTRIBUTION: A PET STUDY IN HEALTHY SUBJECTS AND ALZHEIMER PATIENTS

G. Sayet[1], M.A. Peyronneau[1], P. Gervais[1], C. Baron[1], B. Kuhnast[1], M. Sarazin[2], M. Bottlaender[1]
[1]SHFJ I2BM DSV, CEA, Orsay, France
[2]Sainte Anne Hospital, Neurology department, Paris, France

Neuroinflammation is thought to play a crucial role in the early stages of AD. 18 kDa-Translocator Protein (TSPO) is expressed at a low level in healthy brain and is up-regulated during inflammatory processes that may occur in neurodegenerative diseases. It is considered as a promising target for microglial activation early imaging and can be measured by PET using [^{18}F]DPA-714 radioligand. TSPO ligand uptake was reported to be highly dependent on radioligand binding affinity status based on a genetic polymorphism.

We aimed to quantify the uptake of [^{18}F]DPA-714 in several organs depending on the genetic status of the subject, in healthy volunteers and AD patients.

55 subjects (27 males and 28 females) including 30 healthy subjects and 25 Alzheimer patients (AD; 17 at early, 8 at dementia stage) biologically confirmed (episodic memory deficits associated with an AD-CSF profile and/or positive amyloid PET) were analyzed. All subjects underwent a [^{18}F]DPA-714 static wholebody PET imaging starting 100 min after radioligand injection (102±8 min; five minutes acquisition per bed position). The unchanged [^{18}F]DPA-714 concentration was determined in venous blood samples. [^{18}F]DPA-714 uptake was determined in spleen, myocardium, liver, gastric wall, kidneys, salivary glands, vertebra bodies, and lungs. All subjects were genotyped for the TSPO polymorphism defining three populations: high (HAB; n=28); mixed (MAB; n=24) and low (LAB; n=3) affinity-binders.

No statistical difference was observed in the uptake of [^{18}F]DPA-714 (SUV), between healthy subjects and patients, whatever the binding-affinity group. The distribution pattern of [^{18}F]DPA-714 in organs was similar in each group with slightly lower values in MAB (-18% mean) and significant lower values in LAB subjects (-40%) compared to HAB subjects, excluding the liver where the uptake was significantly higher in LAB (+66% compared to HAB). The highest uptake was found in the gastric wall (6.5±1.8 in HAB; 5.9±1.9 in MAB and 2.7±0.2, in LAB), intermediate in the myocardium, vertebral bodies and parotids (4.2±1.0; 3.7±1.0 and 2.2±0.3) followed by the spleen and the kidney cortical (3.0±0.5 and 2.5±0.7 and 1.6±0.3). The lowest uptake was

observed in lungs (1.0±0.3; 0.7±0.4 and 0.5±0.2). Liver activity was 3.3±0.9; 3.3±0.9 and 4.9±0.6.[^{18}F]DPA-714 (unchanged) concentrations in venous plasma exhibited a four time increase in LAB subjects compared to HAB and MAB (SUV= 0.60±0.09 *vs* 0.13±0.06 and 0.18±0.11).

When correcting the activity measured in the organs by the plasma concentration, the differences between the affinity-binding groups appeared higher: compared to HAB, the uptake in MAB was 30% lower and was dramatically decreased in LAB subjects (-70%; but only -45% in liver). These results reflected the specific uptake of the radiotracer in the organs depending on the affinity status, and showed that liver uptake is partly due to the metabolism.

The biodistribution of [^{18}F]DPA-714 was similar in healthy controls and in AD patients. Plasma concentrations were highly increased in LAB compared to HAB and MAB probably due to a lower binding in the TSPO containing organs. The [^{18}F]DPA-714 activity in the organs have to be corrected by the unchanged radioligand concentrations in plasma for an accurate estimation of the specific uptake

860
BRAIN-0610
Poster Session

BrainPET: Other

IMAGING NEUROINFLAMMATION IN THE EARLY STAGE OF ALZHEIMER'S DISEASE: A PET STUDY USING [18F]DPA-714

C. Leroy[1], L. Hamelin[2], J. Lagarde[3], M.A. Peyronneau[1], H. Corne[3], M. Labit[4], P. Gervais[1], B. Kuhnast[1], C. Oppenhein[5], J.F. Mangin[4], M. Sarazin[3], M. Bottlaender[1]
[1]Laboratoire Imagerie Moléculaire In Vivo (IMIV) U MR 1023 Inserm/CEA/Université Paris Sud - ERL 9 218 CNRS CEA/I2BM/Service Hospitalier Frédéric J oliot, CEA, Orsay, France
[2]Sainte Anne Hospital Paris, SHFJ I2BM DSV CEA, Orsay, France
[3]Langage and Memory Neurology Unit, Sainte Anne Hospital, Paris, France
[4]Neurospin I2BM DSV CATI multicenter Neuroimag ing, CEA, Gif sur Yvette, France
[5]NeuroRadiology, Sainte Anne Hospital, Paris, France

Neuroinflammation is thought to play a crucial role in the early stages of Alzheimer's Disease (AD). 18 kDa Translocator Protein (TSPO) is up-regulated during inflammatory processes that may occur in neurodegenerative diseases.

Our goal was to compare the [^{18}F]DPA-714 binding in AD patients and healthy controls.

Twenty AD patients, as defined by a typical progressive amnesic deficit of the hippocampal type and a positive amyloid PET imaging ([^{11}C]-PiB PET) (13 at an early stage and 7 at dementia stages) were compared to 19 healthy controls with negative amyloid PiB-PET imaging. All subjects underwent a [^{18}F]DPA-714 PET imaging. PET scans were acquired on a HRRT scanner (Siemens) for 90 minutes. Dynamic scans were corrected for head motion and co-registered with 3D T1-weighted MRI. Relative [^{18}F]DPA-714 brain uptake was measured using cerebellum as pseudo reference region, in 76 anatomical regions previously segmented on MRI.
Analyses of the TSPO polymorphism showed that 34 subjects were high (HAB) or mixed (MAB) binders, forming the TSPO+ group (HAB: 6 controls, 8 AD; MAB: 9 controls, 11 AD) while 5 were low binders (TSPO-: 4 controls, 1 AD). Compared to normal controls, TSPO+ AD patients showed increased [^{18}F]DPA-714 uptake: the global cortical uptake was 1.44±0.20 in HAB-AD patients versus 1.24±0.15 in HAB-controls ($p<0.0001$) and 1.41±0.25 in MAB-AD versus 1.35±0.28 in MAB-controls. The highest increase was found in the parietal, precuneus and posterior cingular regions (mean increase of +20 and +8% in both HAB and MAB). The [^{18}F]DPA-714 uptake of the AD patients at the early stage was intermediate between controls and dementia-AD groups, reaching significant difference between the three groups for the HAB-subjects. No differences were found in the AD and controls TSPO low binders.

Neuroinflammation changes associated with AD could be detected using [^{18}F]DPA-714 PET, even at the early stage of the disease. Using a simple quantification approach, the detection sensitivity depended on the affinity status of the subjects. [^{18}F]DPA-714 in PET imaging might become a relevant biomarkers for monitoring AD.

861
BRAIN-0076
Poster Session

BrainPET: Other

EXPLORING THE REWARD VALUE OF SOCIAL RELATIONSHIPS AND DOPAMINE D2/3 RECEPTOR AVAILABILITY IN THE VENTRAL STRIATUM OF HUMANS WITH [11C]-(+)-PHNO

F. Caravaggio[1], J.K. Chung[1], P. Gerretsen[1], G. Fervaha[1], S. Nakajima[1], E. Plitman[1], Y. Iwata[1], A. Wilson[1], A. Graff-Guerrero[1]
[1]Research Imaging Centre, Centre for Addiction and Mental Health, Toronto, Canada

Objectives: As a social species, engaging in social relationships is fundamental to human well-being (Bowlby, 1988). Differences in striatal dopamine (DA) function may be related to both the rewarding value of relationships and drugs of abuse (Nader and Czoty, 2005). As measured with positron emission tomography (PET) both socially detached persons and persons with substance use disorders demonstrate reduced DA $D_{2/3}$ receptor ($D_{2/3}$R) availability in the striatum (Breier et al., 1998; Farde et al., 1997; Martinez et al., 2009). However, previous PET studies have not examined the relationship between social attachment and $D_{2/3}$R availability in the ventral striatum (VS). This is pertinent given the integral role of the VS in the formation of social bonds and drug addiction (Aragona et al., 2006; Dalley et al., 2007).

Methods: Using the agonist radiotracer [^{11}C]-(+)-PHNO we investigated the relationship between self-reported attachment in thirty-two healthy persons and DA $D_{2/3}$R availability in the VS. Participants provided written informed consent. The study was approved by the Research Ethics Board of the Centre for Addiction and Mental Health (CAMH), Toronto.

Results: Surprisingly, more social attachment was related to less [^{11}C]-(+)-PHNO binding in the VS, as measured with the attachment subscale of the temperament and character inventory (r(30)=-.43, p=.01). This relationship held in a subsample who also completed the detachment subscale of the karolinska scales of personality (r(10)=.62, p=.03). However, no relationships were observed between attachment or detachment and BP_{ND} in the dorsal striatum or the D_3R-specific ROIs.

Conclusions: One potential explanation for these findings is that persons who are more socially detached have less endogenous DA occupying $D_{2/3}$R in the VS; an interpretation which warrants investigation by future research. These findings have important implications for better understanding the neurochemical systems involved in attachment, and how these systems may be overridden by drugs of abuse (Insel, 2003; Verdejo-Garcia, 2014).

References:

Aragona BJ, Liu Y, Yu YJ, Curtis JT*, et al.* (2006). Nucleus accumbens dopamine differentially mediates the formation and maintenance of monogamous pair bonds. *Nat Neurosci,* **9**(1): 133-139.

Bowlby J (1988). *A secure base: Clinical applications of attachment theory.* London: Routledge.

Breier A, Kestler L, Adler C, Elman I*, et al.* (1998). Dopamine D2 receptor density and personal detachment in healthy subjects. *Am J Psychiatry,* **155**(10): 1440-1442.

Dalley JW, Fryer TD, Brichard L, Robinson ES*, et al.* (2007). Nucleus accumbens D2/3 receptors predict trait impulsivity and cocaine reinforcement. *Science,* **315**(5816): 1267-1270.

Farde L, Gustavsson JP, Jonsson E (1997). D2 dopamine receptors and personality traits. *Nature,* **385**(6617): 590.

Insel TR (2003). Is social attachment an addictive disorder? *Physiol Behav,* **79**(3): 351-357.

Martinez D, Greene K, Broft A, Kumar D, *et al.* (2009). Lower level of endogenous dopamine in patients with cocaine dependence: findings from PET imaging of D(2)/D(3) receptors following acute dopamine depletion. *Am J Psychiatry,* **166**(10): 1170-1177.

Nader MA, Czoty PW (2005). PET imaging of dopamine D2 receptors in monkey models of cocaine abuse: genetic predisposition versus environmental modulation. *Am J Psychiatry,* **162**(8): 1473-1482.

Verdejo-Garcia A (2014). Social cognition in cocaine addiction. *Proc Natl Acad Sci U S A,* **111**(7): 2406-2407.

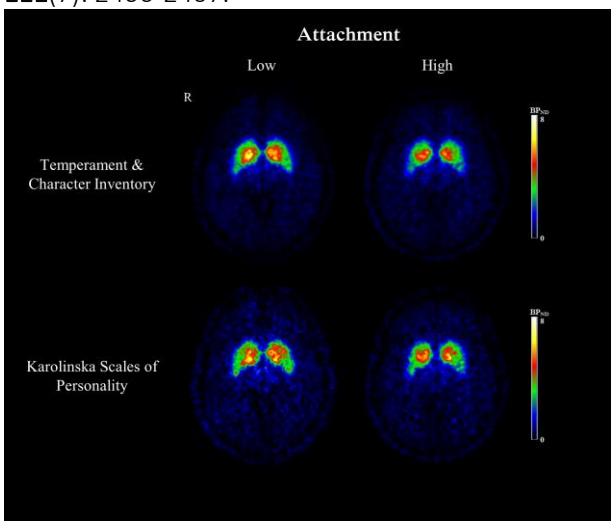

862
BRAIN-0055
Poster Session

BrainPET: Other

PARTIAL VOLUME CORRECTION OF BRAIN PET STUDIES USING ITERATIVE DECONVOLUTION IN COMBINATION WITH HYPR DENOISING

S.V.S. Golla[1], M. Lubberink[2], A.A. Lammertsma[1], R. Boellaard[1]
[1]Department of Radiology and Nuclear Medicine, VU University Medical Center, Amsterdam, Netherlands
[2]Department of Radiology Oncology and Radiation science, Uppsala University, Uppsala, Sweden

Introduction: Quantification of PET studies may be hampered by the limited spatial resolution of PET resulting in partial volume effects (PVE). Iterative deconvolution methods (IDM) have been proposed to correct for PVE. IDM improves the spatial resolution of PET without using structural information, such as MR scans. This is of particular interest when MR data is not available or of insufficient quality, or when PET tracer distributions are not aligned with structural information. Unfortunately, IDM also increases noise, resulting in poor signal to noise ratios (SNR). The primary aim of this study was to implement a partial volume correction (PVC) method based on iterative deconvolution in combination with HighlY constrained back-PRojection (HYPR[1]) denoising to mitigate poor SNR properties of conventional IDM.

Methods: An anthropomorphic brain Hoffman phantom was filled with an [^{18}F]FDG solution of ~25 kBq·mL^{-1} and scanned for 30 min on a Gemini PET/CT (Philips, Cleveland, USA) using a dynamic brain protocol with various frame durations ranging from 10 to 300 s. Both Van Cittert and Lucy Richardson based IDMs were used for PVC of the scans. In addition, HYPR was used to improve SNR of the dynamic PET images, applying it both before and/or after use of IDM. The Hoffman phantom dataset was used to optimize parameters of both IDM and HYPR (number of iterations, type of algorithm, with/without HYPR) based on best average agreement of PET based and actual activity concentrations in grey matter regions. Next, clinical evaluations were performed using dynamic [^{11}C]Flumazenil (n=5) and [^{11}C]PIB (4 healthy subjects and 4 AD patient) studies to assess the impact of IDM with and without HYPR on plasma input derived V_T across various regions of the brain.

Results: Figure 1 illustrates obtained recovery relative to actual activity concentrations after IDM with/without HYPR for the Hoffman phantom scans. IDM improved quantitative accuracy of measured activity concentrations however use of IDM in combination with HYPR (IDM-HYPR) was able to correct for PVE without increasing noise. For the clinical cases IDM-HYPR showed a 5% to 20% increase in the regional distribution volumes (V_T) when compared to the respective V_T from the PVE uncorrected [^{11}C]Flumazenil scan whereas a 0% to 10% increase or decrease was seen in case of [^{11}C]PIB depending on the region of interest or type of subject (healthy or patient)

Conclusion: PVC based on IDM in combination with HYPR improves quantitative accuracy of dynamic PET studies without affecting SNR.

Reference List

(1) Christian BT, Vandehey NT, Floberg JM, Mistretta CA. Dynamic PET denoising with HYPR processing. J Nucl Med 2010 Jul;51(7):1147-1154.

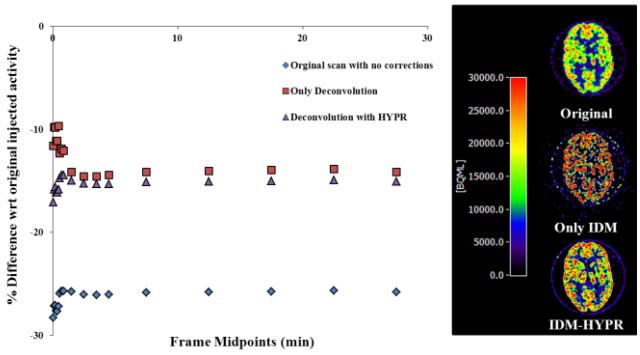

Figure 1: Recovery of measured activity concentrations in grey matter regions of the Hoffman phantom for different implementations of IDM with and without HYPR.

863
BRAIN-0805
Poster Session

BrainPET: Other

DECREASED REGIONAL CEREBRAL BLOOD FLOW EVOKED BY DYNAMIC EXERCISE: A POSITRON EMISSION TOMOGRAPHY STUDY

M. Hiura[1], T. Nariai[2], K. Ishii[3], M. Sakata[3], K. Oda[4], J. Toyohara[3], K. Ishiwata[3]
[1]Faculty of Sports and Health Studies, Hosei University, Tokyo, Japan
[2]Department of Neurosurgery, Tokyo Medical and Dental University, Tokyo, Japan
[3]Research Team for Neuroimaging, Tokyo Metropolitan Institute of Gerontology, Tokyo, Japan
[4]Department of Radiological Technology, Hokkaido University of Science, Sapporo, Japan

【Objectives】 Changes in cerebral blood flow (CBF) followed by dynamic exercise has been investigate in conjunction with postexercise hypotension (PEH) using single photon emission computed tomography[1, 2] and transcranial Doppler ultrasound[3]. However, no previous study examined CBF quantitatively with regards to PEH using positron emission tomography (PET). This study investigated changes in regional CBF (rCBF) that occur after a steady-state cycling exercise. Although underlying central mechanism for PEH has been investigated using animal model, paucity data are available in human brain. The aim of the present study is to examine changes in rCBF during PEH and investigate the possible roles of regions where alteration in rCBF occur. **【Methods】** Nine healthy young males performed a bout of the constant work rate cycling exercise for 20 min. rCBF were measured using oxygen-15-labeled water ($H_2{}^{15}O$) and PET (SET2400W, Shimadzu, Kyoto, Japan) at the baseline (Rest) and 10 minute after the exercise (post-Ex). Heart rate (HR) and mean blood pressure (MBP) were monitored during the procedures. With the accumulated image and the measured arterial input function, the rCBF was calculated on a pixel-by-pixel basis using the autoradiographic

method[4]. For an anatomical reference, individual brain MRI scans were acquired and the image data were analyzed using SPM software (SPM 8, Welcome Department, London, UK). The quantitative analysis of rCBF was performed using Dr. View software (Infocom, Tokyo, Japan) based on the results from the SPM analysis. 【Results】 The average workload for the cycle ergometer exercise was 71 ± 11 watts. During exercise HR increased from 60 ± 5 to 104 ± 9 bpm, and decreased to 68 ± 6 at post-Ex. At post-Ex MBP significantly decreased compared to Rest, from 103 ± 12 to 96 ± 13 mmHg ($P < 0.05$). There were significant decreases in rCBF in the anterior and posterior cingulate cortex, right inferior posterior insular cortex, left hippocampus and pons (P<0.005, uncorrected). Quantitative data for the regions of interest are determined using the results of SPM analysis and we used regions of interest with 8mm square for the calculation. In those areas, rCBF was 8.5-14.1 % lower than Rest. 【Conclusions】 The results of the present study suggest that decreases in rCBF in several regions at post-Ex were in accordance with the earlier studies[1, 2]. As light intensity exercise evoked PEH in the present study, our results are relevant to autonomic function which is regulated via connection between brainstem regions and cardiovascular structures, the central baroreflex network[5]. A finding that rCBF in insular and cingulated cortices decreased in the present study might support that these regions are higher centers for autonomic function. In order to elucidate central mechanism for PEH, further investigation for neural network among the regions where rCBF was identified is mandatory.

. 【References】

1. Williamson et al. *Medicine and science in sports and exercise* 2009; 41(3): 574-80
2. Williamson et al. *J Appl Physiol* 2004; 96(2): 719-24.
3. Willie CK et al. *European journal of applied physiology* 2013; 113(6): 1597-604.
4. Herscovitch et al. *J Nucl Med* 1983; 24(9): 782-9.
5. Chen et al. *Exercise and sport sciences reviews* 2010; 38(3): 122-7.

864
BRAIN-0683
Poster Session

BrainPET: Other

[18F]FCWAY, A SEROTONIN 1A RECEPTOR RADIOLIGAND, IS A WEAK SUBSTRATE FOR EFFLUX TRANSPORTERS AT THE HUMAN BLOOD-BRAIN BARRIER

J.S. Liow[1], S. Hu[2], M.D. Hall[3], C.S. Hines[4], S.S. Zoghbi[1], H.U. Shetty[1], V.W. Pike[1], W.C. Kreisl[5], P. Herscovitch[6], M.M. Gottesman[3], W.H. Theodore[7], R.B. Innis[1]
[1]Molecular Imaging Branch, National Institute of Mental Health, Bethesda, USA
[2]Nuclear Medicine, XiangYa Hospital/Central South University, Changsha, China
[3]Laboratory of Cell Biology, National Cancer Institute, Bethesda, USA
[4]Psychiatry, University of Texas Health Sciences Center San Antonio, San Antonio, USA
[5]Neurology, Columbia University, New York, USA
[6]Clinical Center PET, National Institute of Health, Bethesda, USA
[7]Clinical Epilepsy Section, National Institute of Neurological Disorders and Stroke, Bethesda, USA

Objectives: Avid substrates for efflux transporters at the blood-brain barrier are insensitive to increased transport function, as their uptake into brain is already completely blocked at baseline. In contrast, less avid substrates are sensitive to both decreased and increased efflux function as they have measureable brain uptake at baseline. In this study, we sought to determine whether [^{18}F]FCWAY, a 5-HT$_{1A}$ receptor radioligand, is a weak substrate for P-gp and BCRP, the two most prevalent efflux transporters at the blood-brain barrier.

Methods: For the *in vitro* studies, transporter interactions were assessed indirectly by the ability of FCWAY (50 mM) to inhibit the efflux of fluorescent substrates from cells expressing P-gp

(rhodamine-123) or BCRP (mitoxantrone) using flow cytometry. For the *in vivo* studies, three healthy subjects (all male, age 28-31) had two [^{18}F]FCWAY scans: at baseline and at about 30 min after starting a continuous intravenous infusion of tariquidar (2-4 mg/kg), a potent and selective inhibitor of P-gp. Dynamic PET scans were acquired with a GE Advance scanner after [^{18}F]FCWAY injection (~ 10 mCi) accompanied by arterial blood sampling. The three-tissue compartment model included correction for a brain-penetrating radiometabolite [1].

Results: For the *in vitro* studies with human cancer cells, accumulation of P-gp and BCRP substrates was increased modestly in the presence of FCWAY (4% and 9% respectively), suggesting it is a weak substrate of the transporters. For the *in vivo* PET studies, tariquidar increased brain uptake of [^{18}F]FCWAY in five centrally-located regions by 32% – 99% for V_T and by 14% - 64% for V_T/f_P with moderate variability among the three subjects (Figure 1).

Conclusions: In this on-going study, [^{18}F]FCWAY appears to be a weak substrate for P-gp and/or BCRP at the human blood-brain barrier, based on *in vitro* studies using human cancer cells and on *in vivo* imaging in humans. [^{18}F]FCWAY is a poor candidate to selectively measure efflux function, as its uptake also reflects binding to brain 5-HT1A receptors, but an analog that lacks receptor affinity may be quite useful. Weak substrates for efflux transport would be sensitive to not only decreased transporter function but also increased transporter function which is thought to occur in several forms of drug resistance.

Reference: [1] R.E. Carson, Y. Wu, L. Lang, Y. Ma, M.G. Der, P. Herscovitch and W.C. Eckelman, Brain uptake of the acid metabolites of F-18-labeled WAY 100635 analogs, J Cereb Blood Flow Metab, 23: 249-260, 2003.

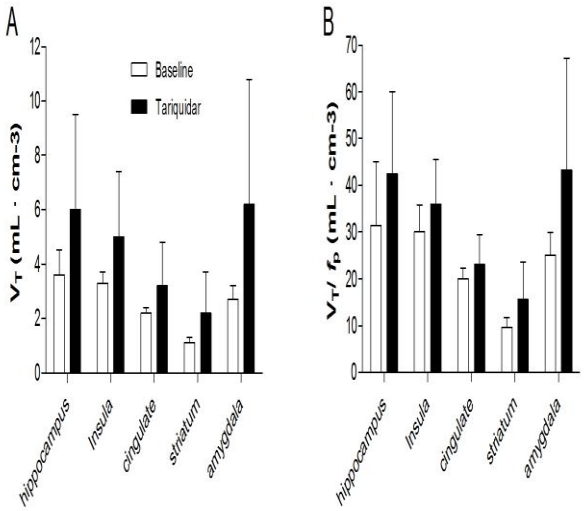

Figure 1. Intravenous tariquidar infusion increased (A) total distribution volume (V_T) and (B) V_T with correction for plasma free fraction (V_T / f_P) of [^{18}F]FCWAY in five centrally-located brain regions of three healthy subjects (mean ± SD).

865
BRAIN-0614
Poster Session

BrainPET: Other

[18F]T807 PET AND DIFFUSION TENSOR IMAGING REVEAL ASSOCIATION BETWEEN TAU PATHOLOGY AND NEURONAL FIBER INTEGRITY IN TRAUMATIC BRAIN INJURY

M.D. Normandin[1], D.W. Wooten[1], X. Zhang[1], B. Ebrahimi[1], C. Huang[1], N. Atassi[2], K.A. Johnson[3], N. Zubcevik[4], R.D. Zafonte[4], G. El Fakhri[1]
[1]Center for Advanced Medical Imaging Sciences & Department of Radiology, Massachusetts General Hospital & Harvard Medical School, Boston, USA
[2]Department of Neurology, Massachusetts General Hospital & Harvard Medical School, Boston, USA
[3]Department of Radiology, Massachusetts General Hospital & Harvard Medical School, Boston, USA
[4]Department of Physical Medicine and Rehabilitation, Spaulding Rehabilitation Hospital & Harvard Medical School, Boston, USA

Objectives: The recently developed radiotracer [^{18}F]T807 exhibits promise for imaging tau protein aggregates, which are implicated in neuropathologies including traumatic brain injury (TBI). Tractographic analysis of data from diffusion tensor imaging (DTI), a magnetic resonance imaging technique, permits measurement of white matter fiber integrity. We sought to evaluate whether tau pathology relates to microarchitectural damage in TBI.

Methods: Participants included 5 healthy men absent head injury and neurological disease matched to 5 men with TBI: 4 with history of multiple mild concussions from past profession in contact sports (1 with concurrent amyotrophic lateral sclerosis) and 1 with isolated severe head injury from an automotive accident 13 years prior. Dynamic [^{18}F]T807 PET data were acquired for 120 minutes on an ECAT HR+. Distribution volume ratio (DVR) was estimated voxel-by-voxel using Logan graphical analysis with cerebellum as reference region input function. DTI data (TR/TE=8800/84 ms, 2.5 mm isotropic resolution, 60 directional encodings with b-value=700 s/mm^2) and T1-weighted MPRAGE anatomical images were acquired on a 3T Siemens Trio with 32 channel head coil. Tractograms were generated using Diffusion Toolkit; the companion software TrackVis was used to visualize the resulting data and perform fiber track counting.

Results: [^{18}F]T807 cerebellar curves normalized by dose and body weight did not differ between groups. Cortical brain regions with elevated [^{18}F]T807 uptake generally had comparatively low DTI track density. The TBI subject with severe injury had high [^{18}F]T807 binding in corpus callosum and posterior cingulate (DVR=1.9 vs. 0.9 in controls) accompanied by low density of white matter fibers (813 tracks passing through the region vs. 2419 through same volume in a matched control). A former professional football player had high [^{18}F]T807 uptake (DVR=1.6) in the left lateral occipital/temporal cortex that corresponded to a reduced fiber count (23 tracks) relative to the contralateral side (DVR=1.1, 169 tracks). Comparable findings were observed in two more former professional athletes: one with thinning of track density and focally elevated [^{18}F]T807 DVR in the posterior cingulate, the other with enhanced [^{18}F]T807 uptake throughout the anterior-superior portion of the left hemisphere (DVR=1.3) with accompanying loss of track density (1998 tracks penetrating left gray matter vs. 2645 contralaterally). The last TBI subject lacked evidence of abnormalities on [^{18}F]T807 and DTI images. Of note, MPRAGE anatomical images showed no discernible macrostructural changes in TBI subjects where [^{18}F]T807 and DTI abnormalities were clearly observed.

Conclusions: Regional reductions in DTI track density accompanied focal [^{18}F]T807 uptake in subjects with TBI stemming from multiple mild concussions or isolated severe injury. The combined measurement of tau deposition and white matter fiber damage may together improve our understanding of microstructural and

molecular pathologies associated with different types of brain injury and aid the development of clinical interventions.

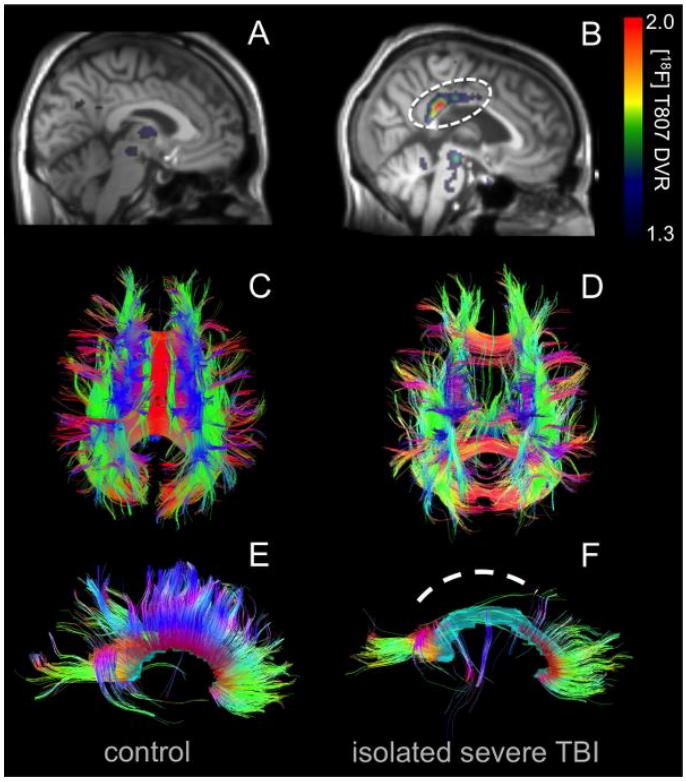

Figure 1. [18F]T807 (A,B) and tractography (C-F) compared between a subject with severe TBI (B,D,F) and matched control (A,C,E). Tau pathology (B) corresponded with reduced neuronal bundles in callosum (D) and dorsal projections of corona radiata (F).

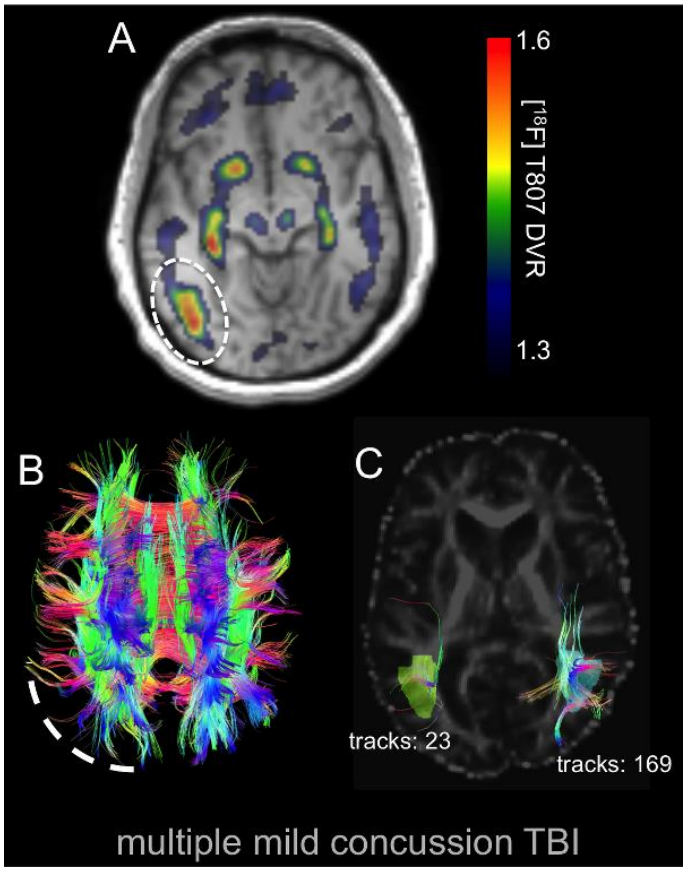

Figure 2. Cortical [18F]T807 (A) in a former professional athlete corresponds with loss of white matter tracks which were preserved contralaterally (B,C).

866
BRAIN-0102
Poster Session

BrainPET: Other

[18F]-RADIOLABELLING OF BASE SENSITIVE O-ARYLCARBAMATES USING A MOM PROTECTING GROUP; APPLICATION TO FAAH RADIOTRACERS

A.A. Wilson[1], J. Hicks[1], J. Parkes[1], O. Sadovski[1], S. Houle[1]
[1]Research Imaging Centre, Centre for Addiction and Mental Health, Toronto, Canada

Objectives.

Direct [18F]-radiolabelling of O-arylcarbamates has proven intractable because of their inherent sensitivity to even the mildest of bases. Thus multi-step synthetic strategies have been

required to prepare [^{18}F]-radiotracers which incorporate this functionality. Such radiotracers have become important in the area of targeting the extensive family of serine hydrolases such as FAAH and MAGL. While carbamates are often used as protecting groups for amines methods of protection of carbamate functionalities themselves are scarce. We report here a novel method using the MOM group to protect the O-arylcarbamate moeity during the [^{18}F]-radiolabelling procedure. This approach greatly simplifies the preparation of [^{18}F]-radiolabelled O-arylcarbamates.

Methods.

N-Alkyl-O-arylcarbamates, containing a tosylate ester suitable for introduction of the [^{18}F]-fluoride were treated with trimethylsilyl chloride and paraformaldehyde under anhydrous conditions, then quenched with methanol, to give MOM-protected carbamates. Conditions for radiolabelling of the protected precursor and deprotection were then explored. The optimised method was applied to the radiosynthesis of a potential radotracer suitable for PET imaging of the serine hydrolase, FAAH.

Results.

The MOM-group was readily incorporated into a variety of O-arylcarbamates. Anhydrous solvents were required for reproducible yields. Model reactions demonstrated that the parent unprotected O-arylcarbamate was generated upon warming with aqueous acid. Standard [^{18}F]-radiolabelling conditions (e.g. K_2CO_3, 2.2.2.K, CH_3CN, 80 °C) gave high (>85%) incorporation of [^{18}F]-fluoride. The MOM-group was easily removed (>95%) by quenching the reaction mixture in either aqueous hydrochloric or sulphuric acid at 80 °C for 5 mins. The synthetic sequences were automated on a commercial module (Synthra), including HPLC purifications and formulations. Using this method a radiolabelled FAAH inhibitor was prepared in 49% radiochemical yield after formulation (uncorrected) and used successfully in rodent experiments as a potential FAAH radiotracer.

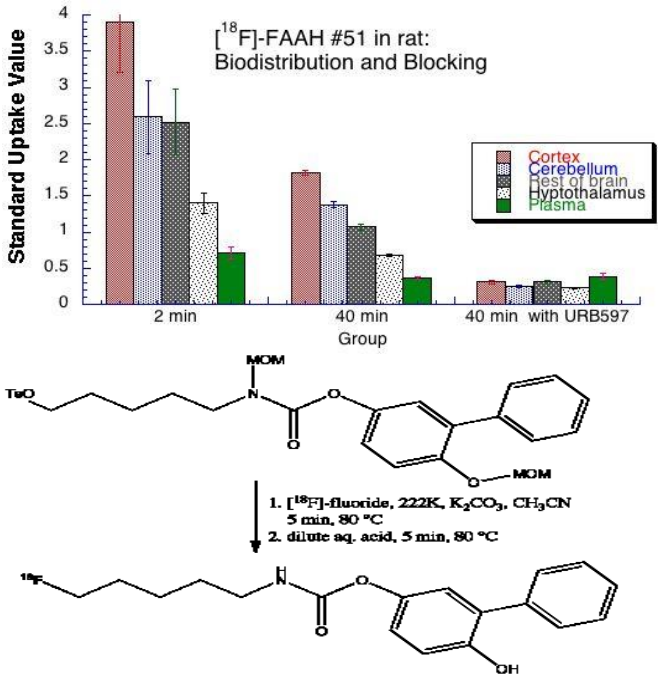

Conclusions.

MOM-protection of O-arylcarbamates is a viable technique to enable facile radiolabelling of these base sensitive substrates. The method greatly simplifies existing methods and provides higher yields and reliability. A practical example of an [^{18}F]-FAAH radiotracer is demonstrated.

867
BRAIN-0886
Poster Session

Late Breaking Abstracts

MODELING THE HYPOXIC/ISCHEMIC BLOOD-BRAIN BARRIER USING INDUCED PLURIPOTENT STEM CELL SOURCE

R. Patel[1], S. Page[1], L. Cucullo[1], A. Alahmad[1]
[1]Pharmaceutical Sciences,
Texas Tech University Health Sciences Center, Amarillo, USA

Objectives: Stroke constitutes the fourth cause of death worldwide and a high morbidity rate in surviving patients. Despite the important effort to find novel therapeutical targets and treatment to alleviate stroke injury, we are still lacking a clinically relevant therapy capable to restore neuronal function and promote brain recovery in patients. The objective of this study is to assess

and validate a novel in vitro model of cerebral hypoxia/ischemia using human brain microvascular endothelial cells (BMECs) and neurons derived from induced pluripotent stem cells (iPSCs).

Methods: In this study, we used the human iPSC IMR90-c4 cell line [1] and induced the differentiation of these cells into brain microvascular endothelial cells (BMECs) and neurons following established differentiation protocols [2, 3]. In addition, immortalized human brain microvascular endothelial cells (hCMEC/D3) were used to compare our BMECs to an established human *in vitro* model. Hypoxia was obtained either by chemical activation (CoCl2) or by incubation into an hypoxic chamber (1%O_2). Ischemic condition was obtained by exposing BMECs monolayers to oxygen-glucose deprivation (OGD). Changes in the barrier function were assessed by measurement of transendothelial electrical resistance (TEER) and permeability to sodium fluorescein (NaF), whereas changes in cell junctions' complexes were measured by immunocytochemistry. In addition, changes in cell viability were assessed by Trypan Blue exclusion and by MTT assays.

Results: We firstly investigated the ability of our BMECs monolayers to respond to CoCl2, a treatment known to disruption rat BMECs monolayers [4, 5]. Interestingly, after 24h of treatment, we noted a significant decrease in barrier function at 30uM and 100uM. In contrast, hCMEC/D3 monolayers failed to respond to such hypoxic stimulus, as we noted no changes in barrier function even at 100uM. Furthermore, we noted a significant decrease in barrier function during either hypoxic stress after 24 hours; such effect was accentuated by OGD stress. Notably, such decrease in barrier function was occurring earlier than previous studies suggesting a high susceptibility to OGD than established models. Our data also the ability to model an "ischemic/reperfusion" injury, as BMECs showed a decrease at 6 hours OGD stress followed by a recovery at 24 hours of "reperfusion".

Conclusions: In this study, we demonstrate the ability of iPSC-derived BMECs monolayers to respond to hypoxic/ischemic stress in a more susceptible fashion than previous in vitro models. Furthermore such model response to OGD showed a temporal pattern similar to cerebral ischemia *in vivo*, as we showed the ability of our model to mimic ischemic/reperfusion injury. Our next goal is to assess the response of iPSC-derived neurons to OGD stress and to better understand how hypoxia inducible factor (HIF-1) activation correlates with the onset of barrier disruption in our model.

References:

1. Yu J et al. *Science* 2007; 318(5858)**:** 1917-20.
2. Lippmann ES et al. *Nature biotechnology* 2012; 30(8)**:** 783-91.
3. Malik N et al. *Neurotoxicology* 2014; 45C**:** 192-200.
4. Al Ahmad A et al. *Journal of cellular physiology* 2009; 218(3)**:** 612-22.
5. Engelhardt S et al. *Journal of cellular physiology* 2014; 229(8)**:** 1096-105.

868
BRAIN-0935
Poster Session

Late Breaking Abstracts

USE IT OR LOSE IT: THE EFFECTS OF DETRAINING ON CEREBRAL BLOOD FLOW IN MASTER ATHLETES.

A.J. Alfini[1], H. Oh[2], L.R. Weiss[1], T.S. Smith[1], B.P. Leitner[1], R. Toledo[1], S. Saheb[1], L.M. Guth[3], R.Q. Landers-Ramos[3], K. Corrigan[3], E.E. Spangenburg[3], J.M. Hagberg[3], J.C. Smith[1]
[1]Kinesiology Exercise for Brain Health, University of Maryland, College Park, USA
[2]Neuroscience and Cognitive Science, University of Maryland, College Park, USA
[3]Kinesiology, University of Maryland, College Park, USA

Objective: While exercise is known to improve cerebrovascular health, it is not known how a short-term cessation of regular exercise training may impact brain health. Our aim was to use

pseudo-continuous arterial spin labeling (pCASL) to measure changes in resting cerebral blood flow (CBF) after a 10-day cessation of exercise training in healthy physically fit older adults.

Methods: Ten master athletes (men=7), defined as 50 years of age or older with a 15-year history of endurance exercise training, were recruited from local running clubs. Criteria for endurance exercise training included four training sessions, and at least four hours of high intensity exercise, per week. Before and immediately after the 10-day cessation of exercise training, CBF was measured with single delay perfusion weighted magnetic resonance imaging. Data were acquired with a Siemens 3.0 Tesla MR system (Magnetom Trio Tim Syngo). The pCASL sequence parameters were the following: single-shot gradient echo planar images, FOV = 210 mm, matrix = 64 x 64, voxel size = 3.3 x 3.3 x 5.0 mm, slices = 20 (axial, acquired in ascending order), slice thickness = 5.0 mm, label duration = 1500 ms, post-label delay = 1000 ms, TI = 2500 ms, TR/TE = 4000/19 ms, volumes = 140, number of label/control pairs = 70, flip angle = 90˚, RF duration = 18.4 ms, pause between pulses = 360 µs, bandwidth = 3004 Hz/Px, RF train length = 80, and sequence duration = 9:28 min. Both the ASL and calibration image time series were motion corrected with AFNI 3dVolreg. Pair-wise subtraction, adaptive spatial smoothing, partial volume correction, and CBF quantification were performed using the FSL v5.0 BASIL toolbox. Perfusion maps were then spatially transformed using the SPM8 unified segmentation normalization function. A gray matter mask was applied to individual perfusion maps and paired T-tests were used to assess CBF changes over time.

Results: We found that a 10-day cessation of exercise training in health physically fit older adults decreased CBF in several brain areas. Significant activation clusters were found using AFNI 3dClustsim to control for false positive perfusion signal (family-wise error (FWE) corrected). FWE correction was dependent on the gray matter mask voxel dimensions, matrix size, and effective smoothness (6.8 mm FWHM). Using a FWE corrected threshold of $p<0.05$, significantly decreased CBF was found in the left temporal gyrus, fusiform gyrus, insula, claustrum and parahippocampal gyrus.

Conclusions: The cessation of exercise training for a period of 10-days in healthy physically fit older adults resulted in decreased resting parenchymal blood flow in several brain regions. This suggests that the cerebrovascular system may be very responsive to the effects of exercise, and that even short-term decreases in exercise training in healthy older adults may reverse these effects.

869
BRAIN-0887
Poster Session

Late Breaking Abstracts

INCREASED PHASIC RELEASE OF DOPAMINE IN THE RIGHT CAUDATE OF ADHD VOLUNTEERS

R. Badgaiyan[1], S. Sinha[1], M. Sajjad[2], D.S. Wack[2]
[1]Psychiatry, University of Minnesota, Minneapolis, USA
[2]Nuclear Medicine, University at Buffalo, Buffalo, USA

Objectives: It is unclear whether dopamine is hyperactive or hypoactive in attention deficit hyperactivity disorder (ADHD). Indirect methods used to study dopaminergic activity have arrived at conflicting conclusions (1). To reconcile these conclusions we estimated the tonic and phasic release of dopamine in separate experiments. We found reduced tonic release in the right caudate of ADHD volunteers in another experiment (2) and in this experiment the single scan dynamic molecular imaging technique (3-5) was used to study the phasic release.

Methods: We estimated the phasic release in adult ADHD (n=10) and healthy control (n=12) volunteers of either sex. In the experiment after volunteers were positioned in the positron emission tomography (PET) camera, they received an intravenous bolus of a radiolabeled dopamine receptor ligand ^{11}C-raclopride. Immediately after the ligand administration PET data were acquired dynamically in list mode and volunteers were

asked to perform the Eriksen's flanker task under congruent (control) and incongruent conditions (6). They performed the task in the scanner for 40 min. Volunteers had to inhibit unwanted responses in the incongruent but not in the congruent condition. The PET data were analyzed using linear extension of simplified reference tissue model (7) and the extended simplified reference tissue model (8). Using these models values of the receptor kinetic parameters were estimated in the congruent and incongruent condition separately by comparing the values of the ligand binding potential (BP) and the rate of ligand displacement measured during each condition.

Results: In the healthy control volunteers we observed significant reduction in the ligand BP and increase in the rate of ligand displacement in the putamen and in the left caudate during task performance (incongruent condition) (4). It indicates phasic release of dopamine in these areas. In ADHD volunteers the BP reduced and the dissociation rate increased in the putamen and in the caudate bilaterally (Figure 1). Comparison of the BP reductions observed in the two groups revealed significantly lower BP and higher rate of ligand displacement in the right caudate of ADHD volunteers, suggesting increased phasic release in this area (Figure 1).

Conclusions: Results indicate that dopamine neurotransmission is dysregulated in the right caudate of ADHD and that the dysregulation involves reduced tonic and enhanced phasic release in this area.

References:

1. Genro JP, Kieling C, Rohde LA, et al. Expert Rev Neurother. 2010;10(4):587-601.
2. Badgaiyan RD, Sinha S, Sajjad M, et al. Under Review.
3. Badgaiyan RD. Frontiers in neuroscience. 2013;7:125.
4. Badgaiyan RD, Wack D. PLoS One. 2011;6(12):e28075.
5. Badgaiyan RD. Current Medical Imaging Reviews. 2011;7:98-103.
6. Eriksen BA, Eriksen CW. Perception and Psychophysics. 1974;16:143-9.
7. Alpert NM, Badgaiyan RD, Livini E, et al. NeuroImage. 2003;19(3):1049-60.
8. Zhou Y, Chen M, Endres C, et al. Neuroimage. 2006;33(2):550-63.

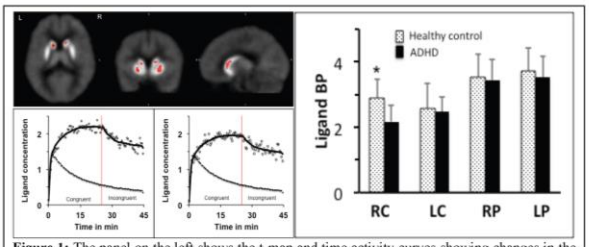

Figure 1: The panel on the left shows the t-map and time activity curves showing changes in the rate of ligand displacement during task performance (incongruent >congruent). The curves on the top shows the data (circles) and model fit (solid line) from the right and left caudate and the lower curves show data from the reference region (cerebellum). The right panel shows the ligand BP in ADHD and healthy control volunteers during task performance (incongruent condition). ADHD volunteers had significantly lower BP (p=0.004) in the right caudate. RC=right caudate,

870
BRAIN-0888
Poster Session

Late Breaking Abstracts

REDUCED TONIC RELEASE OF DOPAMINE IN THE RIGHT CAUDATE OF ADHD VOLUNTEERS

R. Badgaiyan[1], S. Sinha[1], M. Sajjad[2], D.S. Wack[2]
[1]Psychiatry, University of Minnesota, Minneapolis, USA
[2]Nuclear Medicine, University at Buffalo, Buffalo, USA

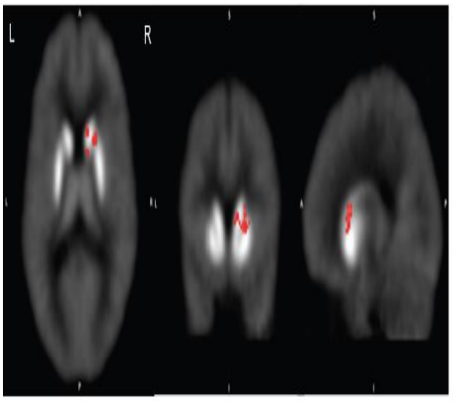

Objectives: Dopamine neurotransmission is dysregulated in most psychiatric conditions but the nature of dysregulation remains unclear because of the use of indirect methods to study dopamine neurotransmission in the human brain. Thus, different sets of data suggest that dopamine is either hyperactive or hypoactive (1) in attention deficit hyperactivity disorder (ADHD). To reconcile contradictory data we used dynamic molecular imaging technique (2-9) to study phasic and tonic release of dopamine in ADHD. In a recent experiment we observed increased phasic release in the right caudate (10) and in this experiment we estimated the tonic release.
Methods: We studied the tonic release in adult ADHD (n=11) and healthy control (n=11) volunteers of either sex. In this experiment after volunteers were positioned in the positron emission tomography (PET) camera, an intravenous bolus of a radiolabeled dopamine receptor ligand ^{11}C-raclopride was administered intravenously. Immediately after the ligand administration PET data were acquired dynamically in list mode and volunteers were asked to stay still in the scanner for 45 min. The PET data were acquired for 45 min and analyzed using simplified reference tissue model (SRTM) (11) to estimate values of a number of receptor kinetic parameters in each voxel and also in the regions of interest. These parameters included the ligand binding potential (BP). Results: Since ligand BP changes in proportion to the amount of endogenously released dopamine (11, 12), we compared the ligand BP in ADHD and healthy control volunteers. The mean BP in ADHD volunteers was 3.21±1.30, which was 27% higher than the mean BP measured in the healthy control volunteers (2.53±0.85). The difference however was not significant statistically. Comparison of the BP in different striatal regions revealed significant difference in the right caudate (Figure 1) where the mean ligand BP in ADHD volunteers (3.19±0.23) was higher (p=0.003) than that in the healthy control volunteers (2.86±0.26).

Conclusions: Results suggest that the reduced tonic release in the right could be the primary deficit of dopamine neurotransmission. Because the tonic and phasic release have reciprocal relationship, the reduced tonic release leads to an increase in the phasic release we observed in another experiment (10). The data indicate that the deficit of dopamine neurotransmission in ADHD is limited to the right caudate and is characterized by reduced tonic and increased phasic release (10) of dopamine.

References

1. Genro JP, Kieling C, Rohde LA, et al. Expert Rev Neurother. 2010;10(4):587-601.
2. Badgaiyan RD. Frontiers in neuroscience. 2013;7:125.
3. Badgaiyan RD, Wack D. PLoS One. 2011;6(12):e28075.
4. Badgaiyan RD. Current Medical Imaging Reviews. 2011;7:98-103.
5. Badgaiyan RD. Prog Brain Res. 2014;211:165-82.
6. Badgaiyan RD. NeuroReport. 2010;21:1172-6.
7. Badgaiyan RD, Fischman AJ, Alpert NM. Neuroimage. 2009;47(4):2041-5.
8. Badgaiyan RD, Fischman AJ, Alpert NM. NeuroReport. 2008;19(4):409-12.
9. Badgaiyan RD, Fischman AJ, Alpert NM. NeuroImage. 2007;38(3):549-56.
10. Badgaiyan RD, Sinha S, Sajjad M, et al. Under Review.
11. Lammertsma A, Hume S. Neuroimage. 1996;4(3 Pt 1):153-8.
12. Alpert NM, Badgaiyan RD, Livini E, et al. NeuroImage. 2003;19(3):1049-60.

871
BRAIN-0893
Poster Session

Late Breaking Abstracts

D-CYCLOSERINE TREATMENT IN A RAT STROKE MODEL INCREASES NMDA RECEPTOR AND BDMF LEVELS IN HIPPOCAMPUS

A. Biegon[1], J. Dhawan[1]
[1]Neurology, Stony Brook Medicine, Stony Brook, USA

Objectives: Ischemic stroke triggers a massive but transient glutamate efflux and activation of

NMDA receptors, followed by long lasting loss of NMDA receptor function. We have recently reported that D-cycloserine (DCS), a partial NMDA agonist improves neurological and cognitive outcome in transient focal ischemia; although the mechanisms mediating these effects are not entirely clear. The present studies were designed to examine the effects of DCS on neuroinflammation, NMDA receptor density, BDNF and aromatase levels following transient focal ischemia in rats.

Methods: Rats subjected to a transient (90 min) Middle Cerebral Artery Occlusion (MCAO) were administered DCS (10 mg/kg, N=14) or vehicle (PBS, N=14) 24 hours post reperfusion. Eight rats were included as non-ischemic controls. Animals were killed more than 4 weeks after MCAO. Consecutive coronal cryosections were processed for quantitative autoradiography with the neuroinflammation marker [^{3}H]PK11195 and the NMDAR antagonist [^{3}H]MK801; and quantitative immunohistochemistry was used to assess BDNF and aromatase expression in the same brains.

Results: As expected, MCAO resulted in a long lasting decrease in NMDA receptor density and a concomitant increase in the neuroinflammation marker TSPO in the hippocampus relative to non-ischemic controls. DCS treatment reversed the decrease in NMDA receptor density and increased hippocampal BDNF, with no effect on neuroinflammation. Aromatase expression in cortical and striatal regions was increased by MCAO and reduced by DCS.

Conclusions*:* A Single administration of DCS given 24 hrs after ischemia normalized NMDAR density and increased BDNF in hippocampus of ischemic rats, suggesting that BDNF contributes to beneficial effects of DCS in stroke acting via a neuro-restorative rather than a neuroprotective mechanism.

872
BRAIN-0924
Poster Session

Late Breaking Abstracts

AROMATASE AVAILABILITY IN AMYGDALA LINKED TO OBESITY AND SELF-CONTROL: PET STUDIES IN HEALTHY MEN AND WOMEN

A. Biegon[1], T. Hidelbrandt[2], A. Nelly[2], S.W. Kim[3], J. Logan[4], D. Pareto[5], D. Schlyer[6], G.J. wang[7], J. Fowler[8]
[1]Neurology, Stony Brook Medicine, Stony Brook, USA
[2]Psychiatry, Mount Sinai School of Medicne, New York, USA
[3]Imaging, NIAAA, Bethesda, USA
[4]Imaging, NYU Med Ctr, New York, USA
[5]Neurlogy, Universitat Autonoma de Barcelona, Barcelona, Spain
[6]Medicine, Brookhaven National Lab, Upton, Spain
[7]Imaging, NIAAA, Behthesda, USA
[8]Medicine, Brookhaven National Lab, Upton, USA

Objectives: Aromatase, the Cyp19A gene product, is the last enzyme in estrogen biosynthesis from androgenic precursors. The aromatase gene is locally expressed and differentially regulated in many organs and tissues, including fat cells and brain. Aromatase expression is reportedly increased in fat tissue of subjects with a high body mass index (BMI), but the relationship between BMI and brain aromatase availability has not been investigated to date. Here we use [^{11}C]vorozole, an aromatase inhibitor radiotracer to assess aromatase availability in brains of normal weight, overweight and obese individuals with PET to test the hypothesis that brain aromatase, specifically in amygdala, is inversely correlated with BMI and positively correlated with personality traits related to inhibitory control of behavior.

Methods: Forty eight otherwise-healthy individuals, divided among normal weight (BMI 18-25, N=14), overweight (25<BMI$\leq$30, N=16) and obese (BMI>30, N=12) were scanned following administration of [^{11}C]vorozole. PET data were acquired over a 90 min session and regions of interest placed bilaterally over the amygdala.

Brain and plasma time activity data were used to calculate the total distribution volume (V_T) from a two-compartment model as well as model free graphical analysis (Logan plot). A subgroup of the subjects (N=29) were administered the multidimensional personality questionnaire (MPQ). The results were analyzed by ANOVA and Pearson's regression analysis.

Results: High BMI was associated with a significant decrease in V_T in the amygdala. Thus, ANOVA revealed highly significant main effect of BMI ($F=9.68$, $p=0.0004$); with both the overweight ($p=0.005$) and obese ($p=0.0001$) groups significantly lower than the normal weight group (Fisher's PLSD posthoc test). In addition, There was a highly significant, inverse correlation ($R^2=0.38$, $p<0.0001$), between BMI and V_T in amygdala, which was evident in both men ($R^2=0.32$, $p=0.001$) and women ($R^2=0.42$, $p=0.0006$). Analysis of the MPQ scores revealed a significant positive correlation between scores on trait constraint (composed of harm avoidance, control and traditionalism) and BMI ($R^2=0.25$, $p=0.01$).

Conclusions*:* Reduced availability of aromatase in the brain of overweight and obese subjects implies reduced conversion of androgens to estrogens in the brain of these individuals; and is correlated with increased BMI and reduced ability to constrain behavior.

873
BRAIN-0920
Poster Session

Late Breaking Abstracts

APPL2 ATTENUATES ADULT NEUROGENESIS IN OLFACTORY BULB

X. Chen[1], T. Yan[1], A. Xu[2], J. Shen[1]
[1]School of Chinese Medicine,
The University of Hong Kong, Hong Kong,
Hong Kong China
[2]Department of Medicine,
The University of Hong Kong, Hong Kong,
Hong Kong China

Objectives： The continuous integration of newborn neurons in olfactory bulb (OB) is important for the odor sensory of mammalians during the lifetime. Neural stem cells (NSCs) in the subventricular zone (SVZ) generate neuroblasts that migrate along the rostral migratory stream (RMS) and integrate into OB circuitry. The molecular signals governing NSCs differentiation still remain undefined. In this study, we aim to explore the roles of adaptor protein, phosphotyrosine interaction, PH domain and leucine zipper containing 2 (APPL2) in modulating SVZ-OB neurogenesis.

Methods： Both in vivo and in vitro experiments were conducted. For *in vitro* experiments, neural Stem/progenitor cells (NSCs) were applied to explore its differentiation directions by immunostaining with different biomarkers for identifying neuron or astrocyte. APPL2 level was manipulated through knockdown with SiRNA transfection and overexpression with adenovirus transfection respectfully. For *in vivo* study, APPL2 transgenic （Tg） mice were used to detect both the neurogenesis status in SVZ, RMS and OB by BrdU incorporation and co-immunstained with neuron biomarkers. Moreover, olfactory discrimination tests (ODT) were performed by a cotton stick presentation based task to detect its odor discrimination ability.

Results： We found that APPL2 expression was increased during the process of NSCs differentiation *in vitro*. APPL2 positive staining was mostly localized in the $GFAP^+$ cells. Overexpression of APPL2 revealed to orient NSCs into astrocytes while knockdown of APPL2 enhanced neuronal differentiation in cultured NSCs. Furthermore, APPL2 Tg mice had more $GFAP^+$ cells in the corpus callosum (CC) while fewer newborn neurons in OB, RMS and SVZ than wild type mice. As a result of suppressed adult neurogenesis in OB, adult APPL2 transgenic mice perform less sensitive in the olfactory discrimination tests compared with wild type mice.

Conclusions : APPL2 might suppress adult neurogenesis in SVZ-OB axis.

References:

1) Breton-Provencher V, Lemasson M, Peralta MR, 3rd, Saghatelyan A (2009) Interneurons produced in adulthood are required for the normal functioning of the olfactory bulb network and for the execution of selected olfactory behaviors. J Neurosci 29:15245-15257.

2) Gheusi G, Cremer H, McLean H, Chazal G, Vincent JD, Lledo PM (2000) Importance of newly generated neurons in the adult olfactory bulb for odor discrimination. Proc Natl Acad Sci U S A 97:1823-1828.

874
BRAIN-0941
Poster Session

Late Breaking Abstracts

CHARACTERIZATION OF A MELANOTRANSFERRIN DERIVED PEPTIDE CAPABLE OF DELIVERING THERAPEUTICS ACROSS THE BLOOD-BRAIN BARRIER.

B.A. Eyford[1], M.M. Tian[2], M. Okon[3], L. McIntosh[3], T. Vitalis[4], R. Gabathuler[2], W.A. Jefferies[1]
[1]Michael Smith Laboratories, University of British Columbia, Vancouver, Canada
[2]R&D, biOasis Technologies Inc, Richmond, Canada
[3]Dept of Chemistry, University of British Columbia, Vancouver, Canada
[4]R&D, biO, Richmond, Canada

The Blood-Brain Barrier (BBB) restricts the passive entrance of most molecules. However, mechanisms must exist to allow entry of desirable compounds (e.g. vitamins and minerals). The well known iron transport protein, transferrin (Tf), does not efficiency cross the BBB but another transferrin family member, melanotransferrin (MTf), is readily able to transcytose the BBB[1]. We also wished to explore the differences between Tf and MTf that allow that later to cross the BBB. To this end, a twelve amino acid peptide derived from MTf (MTfpep) has been identified which is able to cross the BBB, via receptor mediated transcytosis, as well as or better than the entire protein. Studies of MTfpep, through bioinformatics guided NMR experiments have suggested this peptide has the propensity to adopt a conformation, in solution, similar to the shape it adopts as part of the parent protein. This structural characteristic, coupled with key primary sequence differences suggests why MTf is able to cross the BBB but Tf is not. Furthermore, identification of MTfpep and the motif required for BBB transcytosis has lead to the identification of a novel candidate transcytosis receptor found on the surface of the BBB. The MTf and MTfpep platform is also being explored as a vector for the delivery of therapeutic compounds across the BBB for treatment of central nervous system disease. Most recently, MTfpep conjugated to siRNA was shown to prevent or ameliorate damage associated with stroke in a mouse model.

1 Moroo, I. *et al.* Identification of a novel route of iron transcytosis across the mammalian blood-brain barrier. *Microcirculation* 10, 457-462 (2003).

875
BRAIN-0883
Poster Session

Late Breaking Abstracts

CAUDATIN INHIBITS HUMAN GLIOMA CELLS GROWTH THROUGH TRIGGERING DNA DAMAGE-MEDIATED CELL CYCLE ARREST

X. Fu[1], K.U.N. Wang[2], S. Zhang[1], Y. Hou[1], M. Yang[1], J. Sun[1], C. Fan[1], B. Sun[1]
[1]Key Lab of Cerebral Microcirculation in Universitie s of Shandong Taishan Medical University Taian S handong 271000 China, Taishan Medical University, Taian, China
[2]Taishan Vocational College of Nursing Taian Shan dong Province 271000 China, Taishan Vocational College of Nursing, Taian, China

Objectives: Caudatin, one of the species of C-21 steroidal glycosides mainly isolated from the root of Cynanchum bungei Decne, exhibits potent anticancer activities. However, the mechanism

remains poorly defined. In the present study, the growth inhibitory effect and mechanism of caudatin on human glioma cells were evaluated in vitro.

Methods: Several methods of cell biology and molecular biology *in vitro* were employed.

Results: The results revealed that caudatin time- and dose-dependently inhibited U251 and U87 cells growth. Flow cytometry analysis indicated that caudatin-induced growth inhibition against U251 and U87 cells was mainly achieved by induction of G0/G1 and S phase cell cycle arrest through triggering DNA damage, as convinced by the up-regulation of p53, p21 and histone phosphorylation, as well as the down-regulation of cyclin D1. Moreover, caudatin treatment also triggered the activation of ERK and inactivation of AKT pathway. LY294002 (an AKT inhibitor) addition enhanced caudation-induced AKT inhibition, indicating that caudatin inhibited U251 cells growth with an AKT-dependent manner.

Conclusions: Our findings indicate that caudatin may act as a novel cytostatic reagent against human glioma cells through induction of DNA damage-mediated cell cycle arrest with involvement of modulating MAPKs and AKT pathways.

References:

1. Fei HR, Cui LY, Zhang ZR, Zhao Y, Wang FZ (2012) Caudatin inhibits carcinomic human alveolar basal epithelial cell growth and angiogenesis through modulating GSK3beta/beta-catenin pathway. J Cell Biochem 113:3403-3410

2. Ho PJ, Chou CK, Yeh SF (2012) Role of JNK and p38 MAPK in Taiwanin A-induced cell death. Life Sci 91:1358-1365

3. Li X, Zhang X, Liu X, Tan Z, Yang C, Ding X, Hu X, Zhou J, Xiang S, Zhou C, Zhang J (2013) Caudatin induces cell apoptosis in gastric cancer cells through modulation of Wnt/beta-catenin signaling. Oncol Rep 30:677-684

4. Luo Y, Sun Z, Li Y, Liu L, Cai X, Li Z (2013) Caudatin inhibits human hepatoma cell growth and metastasis through modulation of the Wnt/beta-catenin pathway. Oncol Rep 30:2923-2928

The study was supported by the National Natural Science Foundation of China No.81471212, 81271275, 81070947, 30770759 to B.-L. Sun; Natural Science Foundation of Shandong No. ZR2012HZ006 to B.-L. Sun.

*Corresponding author: Cun-dong Fan, Bao-liang Sun, Tel: +86-538-6230027, E-mail: tsmc_nks@tsmc.edu.cn; blsun@tsmc.edu.cn

876
BRAIN-0884
Poster Session

Late Breaking Abstracts

ENHANCED NEUROPROTECTION OF MINIMALLY INVASIVE SURGERY JOINT LOCAL COOLING LAVAGE AGAINST ICH-INDUCED INFLAMMATION INJURY AND APOPTOSIS IN RATS

Y. Hou[1], K.U.N. Wang[1], S. Zhang[2], M. Yang[2], J. Sun[2], X. Fu[2], C. Fan[2], B. Sun[2]
[1]Taishan Vocational College of Nursing Taian Shan dong Province 271000 China,
Taishan Vocational College of Nursing, Taian, China
[2]Key Lab of Cerebral Microcirculation in Universitie s of Shandong Taishan Medical University Taian S handong 271000 China,
Taishan Medical University, Taian, China

Objectives: Hypothermia treatment is one of the neuroprotective strategies that improve neurological outcomes effectively after brain damage. Minimally invasive surgery (MIS) has been a more and more important treatment of intracerebral hemorrhage (ICH). Herein we evaluated the neuroprotective effect and mechanism of MIS joint local cooling lavage (LCL) treatment on intracerebral hemorrhage (ICH) via detecting the inflammatory responses, oxidative injury and neuronal apoptosis around the hematoma cavity in rats.

Methods: ICH model was established by type IV collagenase caudatum infusion. The rats were treated with MIS 6 h after injection then were lavaged by normothermic (37℃) and hypothermic (33℃) normal saline (NS) in brain separately.

Results: The results showed that the MIS joint LCL treatment significantly suppressed IHC-induced inflammation injury and apoptosis in Rats, as convinced by the decline of active-caspase-3 and TUNEL-positive cells, followed by the decrese of IL-1β and LDH and increase of IL-10 and SOD.

Conclusions: This study demonstrated that the strategy of using MIS joint LCL may achieve enhanced neuroprotection against ICH-induced inflammation injury and apoptosis in Rats with potential clinic application.

References:

1. Broderick JP, Brott T, Tomsick T, et al. The risk of subarachnoid and intracerebral hemorrhages in blacks as compared with whites. N Engl J Med 1992;326:733–736

2. Zhou X, Chen J, Li Q, et al. Minimally invasive surgery for spontaneous supratentorial intracerebral hemorrhage: a meta-analysis of randomized controlled trials. Stroke 2012;43:2923–2930.

3. Elliott, J., Smith, M., 2010. The acute management of intracerebral hemorrhage: a clinical review. Anesth. Analg. 110, 1419–1427.

was supported by the National Natural Science Foundation of China No.81471212, 81271275, 81070947, 30770759 to B.-L. Sun; Natural Science Foundation of Shandong No. ZR2012HZ006 to B.-L. Sun.

***Corresponding author**: Cun-dong Fan, Xiao-yan Fu, Bao-liang Sun, Tel: +86-538-6230027, E-mail: tsmc_nks@tsmc.edu.cn; xyfu@tsmc.edu.cn; blsun@tsmc.edu.cn

877
BRAIN-0925

Poster Session

Late Breaking Abstracts

SELENOCYSTINE INDUCES S-PHASE ARREST IN HUMAN GLIOMA CELLS BY TRIGGERING ROS-MEDIATED DNA DAMAGE AND MODULATING ERK AND AKT PHOSPHORYLATION

H. Yuan[1], K. Wang[2], S. Zhang[3], Y. Hou[3], M. Yang[3], C. Fan[3], B. Sun[3]
[1]Neurology,
Affiliated Hospital of Taishan Medical University T aian Shandong 271000 China, Taian, China
[2]Neurology,
Taishan Vocational College of Nursing Taian Shan dong Province 271000 China, Taian, China
[3]Neurology,
Key Lab of Cerebral Microcirculation in Universitie s of Shandong Taishan Medical University Taian S handong 271000 China, Taian, China

Objectives: To evaluate the growth suppressive effect and mechanism of selenocystine (SeC) on human glioma cell lines.

Methods: MTT, flow cytometry and western blotting were all employed to investigate the anticancer mechanism.

Results: The results suggest that SeC inhibited cell growth against several human glioma cell lines in a time- and dose-dependent manner, through the induction of cell cycle arrest, which was associated with a marked decrease in the protein expression of cyclins A, D1, and D3 and cyclin-dependent kinases (CDKs) 4 and 6, with concomitant induction of p21waf1/Cip1, p27Kip1, and p53. Exposure of glioma cells to SeC resulted in apparently DNA damage through ROS overproduction. Moreover, SeC treatment also triggered the activation of JNK, p38 MAPK, ERK, and Akt. Inhibitors of ERK (U0126) and Akt (LY294002), but not JNK (SP600125) and p38 MAPK (SB203580), suppressed SeC-induced S-phase arrest in human glioma cells.

Conclusions: The findings revealed that SeC could act as novel agent in tumor chemotherapies and chemoprevention with potential clinic application.

878
BRAIN-0907
Poster Session

Late Breaking Abstracts

NARINGIN, A NATURAL COMPOUND PROTECTS AGAINST CEREBRAL ISCHEMIA-REPERFUSION INJURY THROUGH REDUCING PEROXYNITRITE

J. FENG[1], J. SHEN[1], X. CHEN[1], H. CHEN[1], H. WU[1]
[1]School of Chinese Medicine,
The University of Hong Kong, Hong Kong,
Hong Kong China

Objectives: Thrombolytic therapy is essential therapeutic strategy for ischemic stroke to quickly restore blood and oxygen supply[1]. However, recanalization causes cerebral ischemia-reperfusion (I/R) injury by producing free radicals including superoxide, nitric oxide (NO), peroxynitrite ($ONOO^-$), etc. $ONOO^-$ is a representative reactive oxygen species (RNS) triggering a series of molecules cascades to further induce brain damage[2]. In this study, we tested the hypothesis that naringin, a non-toxic plant bioflavonoid, could reduce $ONOO^-$ and attenuate neuronal damage during cerebral I/R injury in *vivo* and in *vitro*.

Methods: In the in *vivo* study, male Sprague-Dawley rats weighed 260-280g were subjected to middle cerebral artery occlusion (MCAO) for 2 hours followed by reperfusion for 22 hours to induce cerebral I/R injury. Naringin was intravenously administrated at the onset of reperfusion respectively at 80 mg/kg, 120mg/kg, 160mg/kg. FeTMPyP, a peroxynitrite decomposition catalyst, was used as positive control at 3mg/kg. Neurological deficits score was calculated by mNSS scale and infarct volume was evaluated by TTC staining. Pathological morphology was detected by Hematoxylin-Eosin staining and TUNEL staining for apoptotic cell death. Western blot analysis was used to detect iNOS, NADPH oxidase subunits and cleaved caspase 3 expressions. In the in *vitro* study, SH-SY5Y cells were subjected to oxygen-glucose-deprivation for 10hours and reoxygenation for 14hours (OGD/R). Cell viability was evaluated by MTT. Superoxide anion radical ($O_2.^-$) and NO were detected by HEt and DAF-2DA staining respectively with fluorescent microscopy and 3-nitrotyrosine expression, a footprint of $ONOO^-$, was detected by western blot.

Results: (1) Naringin dose-dependently reduced the neurological deficit score, decreased the infarct volume and attenuated pathological morphological changes by compared with MCAO model group in *vivo*; (2) Naringin reduced apoptotic cell death by inhibiting cleaved caspase 3 activation in ischemia-reperfused brains in *vivo*; (3) Naringin inhibited the expressions of iNOS and NADPH oxidase subunits-$p47^{phox}$ and $p67^{phox}$ and 3-nitrotyrosine level in the ischemic brains and decreased NO level in serum in the rats after cerebral I/R injury in *vivo*; (4) Naringin reduced the level of $O_2.^-$ and NO and down-regulated the expression of 3-nitrotyrosine and attenuated apoptotic cell death in SH-SY5Y cells under OGD/R condition in *vitro*. Naringin revealed similar effects to FeTMPyP.

Conclusions: Naringin might be a promising neuroprotective agent against cerebral I/R injury and its mechanisms could be attributed to its capacity of reducing NADPH oxidase subunits and iNOS expression level and inhibiting peroxynitrite-mediated cell death.

References:

1. Leys D, Cordonnier C. rt-PA for ischaemic stroke: what will the next question be?[J]. Lancet. 2012,379(9834):2320-1

2. Chen XM, Chen HS, Xu MJ, Shen JG. Targeting reactive nitrogen species: a promising therapeutic strategy for cerebral ischemia-reperfusion injury[J]. Acta Pharmacologica Sinica 2013,34(1):67-77

3. Bharti S, Rani N, Krishnamurthy B, Arya DS. Preclinical evidence for the pharmacological actions of naringin: a review[J]. Planta Med. 2014,80(6):437-51.

879
BRAIN-0895
Poster Session

Late Breaking Abstracts

NEUROPROTECTIVE ROLE OF TRANSTHYRETIN THROUGH MEGALIN IN ISCHEMIC BRAIN INJURY

J. Gomes[1], R. Nogueira[1], M. Vieira[1], M.J. Saraiva[1]
[1]Molecular Neurobiology,
Instituto de Biologia Molecular e Celular (IBMC), Porto, Portugal

Objectives:

Transthyretin (TTR) is a protein involved in the transport of thyroxin and retinol, also associated to nerve regeneration in the peripheral nervous system. Recently in our lab, TTR was shown to have a neuroprotective role in focal cerebral ischemia (J. Neurochemistry, (2010) 115, 1434), using a permanent MCAO stroke model. Several studies pointed, in the last years, to the neuroprotective role of TTR in the central nervous system: (i) individuals heterozygous for TTR T119M, a non-pathological mutation of TTR associated with increased levels of the protein in the plasma, show a reduced risk of cerebrovascular disease, and increased life expectancy compared with non-carriers; (ii) TTR can be a good predictor for young strokes, since patients have a worse clinical outcome if they have decreased levels of serum TTR at the time of stroke; (iii) smaller incidence of stroke in women, due to the neuroprotective role of sex steroids (which upregulate TTR in CSF); (iv); in *C.elegans* model, a transthyretin-like protein was determinant in the recognition of apoptotic cells by phagocytes. These effects triggered by TTR might involve transducing receptors, such as megalin, that binds TTR. The goal of this work is to unveil the molecular mechanisms involved in TTR-induced neuroprotection in cerebral ischemia, namely through its interaction with megalin, using in vitro ischemia models.

Methods:

Cultured hippocampal neurons from Wt, TTR KO and Megalin TTR KO mice were subjected to glutamate excitotoxic insults. Protein levels were determined by Immunoblot, and gene expression was analyzed by qPCR. Protein distribution in neurons was also assessed by immunocytochemistry, including neurite outgrowth quantification. Cell death was assessed by nuclear condensation with Hoechst 33342.

Results:

We found that cultured hippocampal neurons from TTR KO mice are more sensitive to an glutamate excitotoxic insult than neurons from Wt mice, as neurite proteins MAP2 and Tau are significantly more affected in TTR KO mice neurons. Moreover, if TTR is administered in a therapeutic way, after the excitotoxic stimulus, a clear neuroprotection in the number and lenght of neurites in neurons from TTR KO cultures is observed. This neuroprotective effect of TTR seems to occur mainly in dendrites rather than in axons. More important when TTR is added to Megalin(+/-) TTR KO cultures after the excitotoxic insult, the neuroprotective effect is lost. Administration of TTR post glutamate stimulation does not prevent the nuclear condensation of apoptotic neurons. However, if TTR is given to cultured hippocampal neurons from TTR KO mice 6h before the glutamate stimulus, as a preventive strategy, a decrease in apoptotic neurons is observed. By opposition in megalin deficient cultures (Megalin(+/-) TTR KO) this soma neuroprotection is lost, indicating that TTR neurite and soma neuroprotection is Megalin dependent.

Conclusions:

Taken together, our results show that TTR should be explored as a potential therapeutic/neuroprotective protein or even used as an indicator of risk factor in stroke outcome. Further studies to characterize the signaling pathways in in-vitro/in-vivo ischemia models behind this neuroprotection are underway.

880
BRAIN-0936
Poster Session

Late Breaking Abstracts

COMPLEX CEREBRAL ANGIOARCHITURE AND NEURONAL METABOLISM LEAD TO WIDE VARIATIONS OF HEMATOCRIT, RBC SATURATION IN THE CAPILLARY BED

I. Gould[1], *P. Tsai*[2], *D. Kleinfeld*[2], *A. Linninger*[1]
[1]*Bioengineering, University at Illinois at Chicago, Chicago, USA*
[2]*Physics, University of California San Diego, La Jolla, USA*

Objective

A quantitative understanding of themulti-scale neurovascular coupling between microcirculatory blood flow andneuronal metabolism would improve the treatment of neurodegenerative diseases. Previousattempts to computationally model cerebral metabolic regulation at the cellularlevel are hampered by the complex microcirculatory structure of the brain,limiting studies to thin subsections of cortical gray matter. To overcome thisobstacle, a 3D computational model was constructed from high-resolutiontwo-photon images which encompass both the cerebral angioarchitecture and relativepositions of neuronal and non-neuronal cells in the primary somatosensorycortex of four mouse brains. This mechanistic computer model predicts thehemodynamic states of blood pressure, hematocrit, and RBC velocity, as well asred blood saturation, the oxygen transport across the blood brain barrier, andthe oxygen tension within individual brain cells.

Methods

The cerebral angioarchitecture of theprimary somatosensory cortex was obtained from high-resolution two-photon microscopyimages. Vessels were assigned as either surface pial arterioles, penetratingarterioles capillaries, draining venules or surface pial venules based on theirsize, orientation, positon, and connectivity. The non-linear biphasickinematics of plasma skimming was computed throughout the blood vessel network.Metabolic activity was assigned to each brain cell, and oxygen tension wascomputed for each brain cell and throughout the extracellular space. Oxygentension in subcellular organelles was also computed for each cell.Additionally, the oxygen saturation of the red blood cells (RBCs) and theplasma oxygen tension in each vessel was determined, as well as the oxygenextraction of each vessel through the microvessel angioarchitecture.

Results

Hemodynamic parameters of bloodflow, pressure, hematocrit, RBC velocity, RBC saturation and intracellularoxygen tension are validated against mouse measurements using *in vivo* models. The effects of oxygenperfusion in response to vasodilation of different arterial group is computed.The change in oxygen perfusion to brain cells in each cortical layer and thevenous oxygen saturation is measured following vasodilation of the surfacearterioles and penetrating arteriole groups. The effects of pial andpenetrating arteriole occlusions on brain tissue oxygen tension is measuredusing the computational model. We found that the occlusion of smaller diameter6.4um vessel cut off the supply of oxygen to cells more severely than theocclusion of a larger 10um vessel.

Conclusions

The complex hierarchy of thecerebral microcirculatory angioarchitecture leads to non-uniform distributionsin hemodynamic parameters, including hematocrit, blood pressure and RBC saturation.Our 3D computational model of the mouse primary somatosensory cortex revealsthat there are wide variations in these hemodynamic parameters, especially inthe capillary bed. Our model quantitates the increase in oxygen perfusion tobrain cells in response to vasodilatory events. Additionally, we can identifyvessel hierarchies that supply large section of the primary somatosensorycortex by simulating the decrease in blood flow following a micro-occlusionevent. This work at steady state gives a baseline for future large-scaledynamical models of oxygen n supply to the brain tissue.

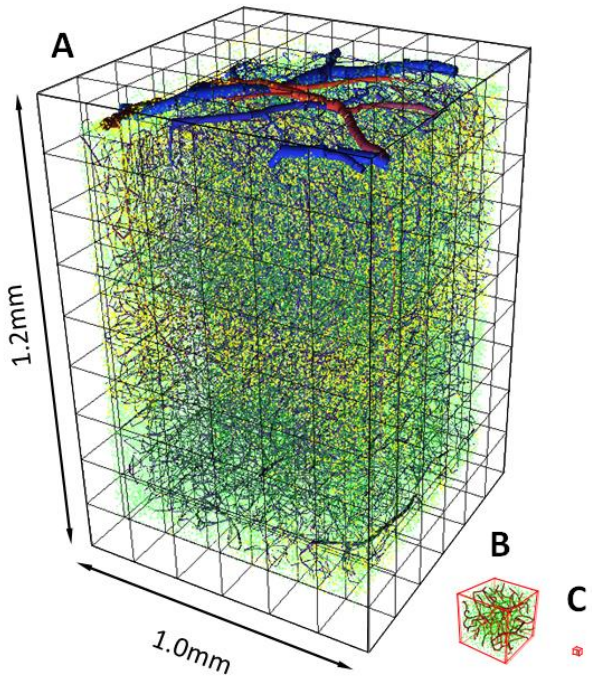

881
BRAIN-0914
Poster Session

Late Breaking Abstracts

CORRELATION ANALYSIS OF MOLECULAR BLOOD BRAIN BARRIER DISRUPTION MARKERS AND STROKE SEVERITY

B. GUAN[1], *J. SHEN*[1]
[1]*School of Chinese medicine, The University of Hong Kong, hong kong, Hong Kong China*

Early prediction of stroke severity is important. During stroke, the blood–brain barrier (BBB) is compromised by endothelial cell death, and cytosolic contents released from injured brain tissues have the potential to cross the BBB. This suggests that the measurement of brain-derived proteins in plasma could be used to monitor stroke onset and severity. In our clinical observational study, we recruited 120 ischemic stroke patients and detect Caveolin-1, AQP-4, MMP-9, HMGB1, ONOO concentrations in ischemic stroke patients' plasma, cerebral spinal fluid and analyze the correlations with BBB permeability and edema degree by MRI method. Caveolin-1 level in ischemic stroke patients plasma had significantly decreased compared to th healthy control group ($p<0.05$); CSF caveolin-1 level showed an increase comparing to the control group ($p<0.05$). ONOO level in plasma of ischemic stroke patients was higher than that of healthy control group ($p<0.05$). There was no significant ONOO change in CSF.

882
BRAIN-0898
Poster Session

Late Breaking Abstracts

THE DOUBLE MODELS STUDY OF REGION BLOOD PERFUSION AND GLUCOSE METABOLISM OF THE PREFRONTAL LOBES IN DEPRESSED PATIENTS WITH FIRST-EPISODE

X. Junling[1], *F. Chang*[1], *G. Yongju*[1], *S. Dapeng*[1]
[1]*Radiology, Henan Provincial People's Hospital, Zhengzhou, China*

Objective: To explore changes of region blood perfusion and glucose metabolism of the prefrontal lobes in patients with depression disorder and, the relationships between these changes and patients'symptoms. **Method** 17 patients with depressive disorder and 16 normal controls accepted magnetic resonance imaging (MRI) scan and positron emission tomography (PET) / computed tomography (CT) scan in the resting state, patients' clinical symptoms were evaluated by Hamilton depression rating scale (HAMD). Data were analyzed by SPM8 and SPSS17.0 software. **Result:** The cerebral metabolism and cerebral blood flow of prefrontal lobes in patients with depression disorder were lower than the those in the controls ($p < 0.005$), the SUV values of bilateral middle frontal gyrus and CBF values of right middle frontal gyrus were positively correlated with cognitive impairment factor of HAMD scores ($r = 0.55, 0.52, p < 0.05$) (0.59, $p<0.05$); the SUV values of right inferior frontal gyrus and CBF values of left middle frontal gryus were positively correlated with anxiety

factor of HAMD scores (-0.71, p<0.05）(-0.69, p<0.05）; the SUV values of left middle frontal gyrus and right inferior frontal gyrus were positively correlated with tardy factor of HAMD(-0.67,-0.64, p<0.05）; the SUV values and CBF values of left middle frontal gyrus were both positively correlated with the total depression scale scores of HAMD (0.58, 0.62, p<0.05), （r=0.51,0.54,p<0.05）.**Conclusion**: The decrease of region blood perfusion and glucose metabolism of the prefrontal lobes in patients with depression disorder was closely correlated clinical symptoms of depressed patients, the left middle frontal gyrus may be the key cerebral region of the prefrontal lobes function decrease in patients with depression disorder.

883
BRAIN-0899
Poster Session

Late Breaking Abstracts

PRELIMINARY STUDY OF BRAIN GLUCOSE METABOLISM CHANGES IN PATIENTS WITH LUNG CANCER OF DIFFERENT HISTOLOGICAL TYPES

G. Yongju[1], X. Junling[1], F. Chang[1], S. Dapeng[1]
[1]Radiology, Henan Provincial People's Hospital, Zhengzhou, China

Background Cerebral glucose metabolism changes are always observed in patients suffering from malignant tumors .This preliminary study is aimed at investigating the brain glucose metabolism changes in patients with lung cancer of different histological types.

Methods One hundred and twenty patients with primary untreated lung cancer who visited Zhengzhou University People's Hospital from February 2012 to July 2013 were divided into three groups based on histological types confirmed by biopsy or surgical pathology, which included adenocarcinoma (52 cases), squamous cell carcinoma (43 cases) and small-cell carcinoma (25 cases). The whole body 18F-fluorodeoxyglucose (18F-FDG) positron emission tomography (PET) / computed tomography (CT) of these cases were retrospectively studied. The brain PET data of the three groups was analyzed individually using statistical parametric maps (SPM) software, with 50 age and gender-matched healthy controls for comparison.

Results The brain resting glucose metabolism in all three lung cancer groups showed regional cerebral metabolic reduction. The hypometabolic cerebral regions were mainly distributed at the left superior and middle frontal, bilateral superior and middle temporal and inferior and middle temporal gyrus. Besides, the hypometabolic regions were also found in the right inferior parietal lobule and hippocampus in the small-cell carcinoma group. The area of the total hypometabolic cerebral regions in the small-cell carcinoma group (total voxel value 3255) was larger than those in the adenocarcinoma group (total voxel value 1217) and squamous cell carcinoma group (total voxel value 1292).

Conclusions The brain resting glucose metabolism in patients with lung cancer shows regional cerebral metabolic reduction and the brain hypometabolic changes are related to the histological types of lung cancer.

884
BRAIN-0937
Poster Session

Late Breaking Abstracts

BRAIN T2-WEIGHTED SIGNAL INTENSITY RATIO IN CHILDREN WITH SICKLE CELL DISEASE WITH AND WITHOUT STROKE

F.J. Kirkham[1], S. Sahota[1], J. McSwiggan[1], J. Collinson[1]
[1]Neurosciences Unit, UCL Institute of Child Health, London, United Kingdom

BACKGROUND
Iron is paramagnetic, accumulates with age, is higher in the deep gray matter in neurodegeneration and if increased in tissues, shortens MRI T1 and T2. There are few data in children with sickle cell disease (SCD). Our aims were to measure T2-weighted signal intensity

ratio (T2SIR), a ratio comparing regional T2 with CSF T2, as a proxy for brain iron status in children with SCD and controls and to compare T2SIR with serum Ferritin, with transcranial Doppler as a measure of cerebral blood flow and with overnight oximetry studies as a measure of exposure to hypoxia.
METHODS
Using ImageJ, 2 masked observers (coefficient variation <5%) measured T2 in regions of interest, excluding visible infarction where necessary, from archived 1.5T MRI data (Siemens Vision; TR=3,458 ms, TE=96 ms) in controls and children with haemoglobin (Hb) SS and SC and generated T2SIR and Pearson correlations with serum ferritin. Controls (n=21) and children with HbSC (HbSC; n=7) or HbSS with no (HbSS-NL; n=23), covert (HbSS-CL, n=19) or overt lesions (HbSS-OL; n=7) and children with overt stroke without SCD (HbAA; n=8) were compared (one way analysis of variance; post hoc Dunnett's test). In the HbSS patients, correlations were computed for T2SIR in the various regions and velocities in the right and left middle, anterior and posterior cerebral and the basilar arteries as well as degree of hypoxic exposure computed as mean and minimum overnight hemoglobin oxygen saturation and the percentage of the night spent with hemoglobin oxygen saturation <90%. T2SIR in the same regions was also obtained in 8 HbSS-CL children randomised to 3 years of blood transfusion or standard care in the Silent Infarct Transfusion Trial.
RESULTS
Serum ferritin significantly correlated (p<.05) with T2SIR in right (R) and left (L) caudate and putamen. Compared with controls and children with overt stroke without SCD of similar age, T2SIR for R/L caudate, R putamen, R/L globus pallidus, and R/L red nucleus was lower in HbSS-OL (p<.01**) and in R/L globus pallidus and R/L red nucleus in HbSS-CL (p<.05). Left posterior cerebral artery velocity was positively correlated with T2SIR in the right caudate, right globus pallidus, left putamen and left red nucleus. For the left red nucleus, there was also a significant negative correlation with the percentage of the night spent with an oxygen saturation <90% during the overnight oximetry study. Compared to those randomised to standard care, there was a reduction in T2SIR in most brain areas in those who were chronically transfused for 3 years in the Silent Infarct Transfusion Trial
DISCUSSION
The significant correlations with serum Ferritin suggest that T2SIR is a proxy measure of brain iron. The most obvious reason for brain iron accumulation in SCD is regular blood transfusions. However, neurodegeneration may play a role, perhaps related in part to ischemic and hypoxic exposure. Studies quantitating and comparing brain T2 measurements with measures of CBF and exposure to hypoxia are warranted.

885
BRAIN-0930
Poster Session

Late Breaking Abstracts

PERICYTE REGULATION OF NEUROVASCULAR COUPLING AND OXYGEN SUPPLY TO THE BRAIN

K. Kisler[1], S.V. Rege[1], A.R. Nelson[1], A. Ramanathan[1], A. Ahuja[1], P.S. Tsai[2], D.A. Boas[3], S. Sakadžić[3], B.Z. Zlokovic[1]
[1]Department of Physiology and Biophysics and the Zilkha Neurogenetic Insitute, University of Southern California, Los Angeles, USA
[2]Department of Physics, University of California San Diego, La Jolla, USA
[3]Optics Division Athinoula A. Martinos Center for Biomedical Imaging Department of Radiology, Massachusetts General Hospital and Harvard Medical School, Charlestown, USA

Objective: Neurovascular coupling, the regulation of cerebral blood flow (CBF) and oxygen supply to match neuronal functional activity, is regulated by synchronous action of different cell types comprising the neurovascular unit[1–3]. Perivascular cells, or pericytes, line capillary walls and play a crucial role in maintaining the blood-brain barrier (BBB)[4-6] and stability of capillary walls[7,8]. It has been recently shown that pericytes also play a

role in the regulation of capillary diameter *in vitro* and *in vivo*, and initiation of the vascular response to stimulus *in vivo*.[9,10]. However, their role in regulation of neurovascular coupling remains debatable[3,11].

Methods: *In vivo* two-photon laser scanning microscopy (TPLSM) was used to study vessel diameter and RBC flow velocity changes in response to stimulus. TPLSM as well as *in vivo* intrinsic optical signaling revealed tissue oxygenation changes. Measurements via *ex vivo* fluorescence imaging and immunohistochemistry corroborated TPLSM observations. Procedures were approved by the respective institutions animal care committees.

Results: Experiments with pericyte-deficient mice[5,6] revealed delayed capillary dilation in response to neuronal stimulus, and reduced red blood cell flow velocity in capillaries carrying oxygen to activated brain areas. Furthermore, we observe decreased local oxygen supply to cortex upon stimulus in pericyte-deficient mice in spite of an unaltered arteriolar response and tone.

Conclusions: Together, these data suggest that pericytes play a role in neurovascular coupling and oxygen supply to brain, and that pericyte degeneration contributes to neurovascular uncoupling. Degeneration of pericytes, as is seen in neurological disorders including Alzheimer's, likely contributes to neurovascular dysregulation of the cerebral blood supply, leading to chronic poor neurovascular health and eventual neurodegeneration.

References:

1. Attwell, D. *et al. Nature* **468,** 232–243 (2010).
2. Zlokovic, B. V. *Nat. Rev. Neurosci.* **12,** 723–738 (2011).
3. Iadecola, C. *Neuron* **80,** 844–866 (2013).
4. Armulik, A. *et al. Nature* **468,** 557–561 (2010).
5. Daneman, R. *et al. Nature* **468,** 562–566 (2010).
6. Bell, R. D. *et al. Neuron* **68,** 409–427 (2010).
7. Armulik, A. *et al. Dev. Cell* **21,** 193–215 (2011).
8. Winkler, E. A. *et al. Nat. Neurosci.* **14,** 1398–1405 (2011).
9. Peppiatt, C. M., *et al*. *Nature* **443,** 700–704 (2006).
10. Hall, C. N. *et al. Nature* **508,** 55–60 (2014).
11. Fernández-Klett, F., *et al*. *PNAS.* **107,** 22290–22295 (2010).

886
BRAIN-0926
Poster Session

Late Breaking Abstracts

ACUTE KETAMINE INFUSION IN RAT DOES NOT AFFECT IN VIVO [11C]ABP688 BINDING TO METABOTROPIC GLUTAMATE RECEPTOR SUBTYPE 5

L. Kosten[1], D. Thomae[2], J. Verhaeghe[1], L. wyffels[2], S. Stroobants[2], S. Staelens[1]
[1]Molecular Imaging Center Antwerp, University of Antwerp, Antwerp, Belgium
[2]University hospital Antwerp Department of nuclear medicine, Molecular Imaging Center Antwerp University of Antwerp, Antwerp, Belgium

Objective: Detecting changes in receptor binding at the metabotropic glutamate receptor 5 (mGluR5) with the positron emission tomography (PET) allosteric antagonist, [^{11}C]ABP688, is valuable for studying dysfunctional glutamate transmission associated with psychiatric illnesses such as schizophrenia and OCD. We imaged the acute effect on rat brain mGluR5 of subanesthetic doses of ketamine, an NMDA receptor antagonist known to increase glutamate release(Moghaddam et al. 1997), with a high-affinity PET ligand [^{11}C]ABP688, a negative allosteric modulator of mGluR5.

Methods: Male Sprague Dawley rats (n=8; 385-525g) underwent a baseline scan and a scan with ketamine administration on the same day. For ketamine, a concentration of 30 mg/kg was chosen(Duncan et al. 1998; Dedeurwaerdere et al. 2011) and was continuously infused via the tail vein during the scan. The final dose of 30mg/kg is reached at the middle of the last frame from a 60 min dynamic acquisition of [^{11}C]ABP688

(0.995±0.286mCi;<3nmol/kg,iv). The nondisplaceable binding potential (BP_{ND}) was calculated using the simplified reference tissue model (SRTM) versus the cerebellum.

Results: BP_{ND} did not change significantly from baseline to ketamine in any region: 4.45±5.48% in the cingulate cortex (CG), 3.79±10.02% in the frontal cortex (FC), 2.00±8.40% in the medial prefrontal cortex (mPFC), 1.35±4.43% in the parietal cortex (PC), 8.40±11.86% in the hippocampus (HC) and 4.67±5.13% in the caudate putamen (CP). These non-significant increases may be due to the test-retest paradigm as decribed by Sandiego *et al*. (Sandiego et al. 2013) and is therefore not attributable to the effects of ketamine. Hence, we confirm previous results of Wyckhuys *et al*. (Wyckhuys et al. 2013) and Sandiego *et al*. (Sandiego et al. 2013) who also showed that [^{11}C]ABP688 BP_{ND} did not reflect changes in acute endogenous glutamate fluctuations in rat and rhesus monkey respectively with other NMDA antagonists. In contrast, a small-scale study of baboons (Miyake et al. 2011) indicated that [^{11}C]ABP688 was able to visualize acute fluctuations in endogenous glutamate levels induced by NAc. Our results on the net effect of ketamine on [^{11}C]ABP688 BP_{ND} in rats also does not reflect the findings of DeLorenzo *et al.* in a human setup (DeLorenzo et al. 2014) showing high variation in the [^{11}C]ABP688 BP_{ND} after bolus of 0.23 mg/kg followed by infusion of 0.58mg/kg ketamine, with seven subjects experiencing <20% change in average V_T after ketamine infusion, and three subjects experienced >40% change. Species differences may have contributed to the different findings in the present study of rats and the studies of baboons and human subjects

Conclusions: We could not confirm in rats that endogenous glutamate changes by ketamine infusion are reflected in [^{11}C]ABP688 BP_{ND} changes as was previously shown for humans (DeLorenzo et al. 2014).

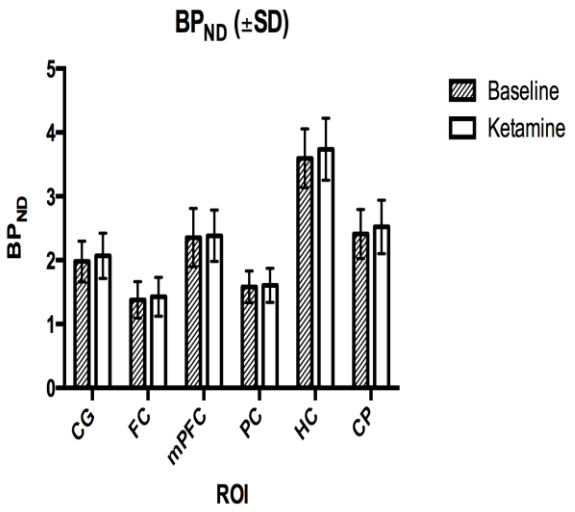

887
BRAIN-0927
Poster Session

Late Breaking Abstracts

A NEW METHOD TO CALCULATE BLOOD-BRAIN BARRIER PERMEABILITY ON A SINGLE CAPILLARY LEVEL IN LIVING MICE USING TWO-PHOTON MICROSCOPY

N.P. Kutuzov[1], *M. Lauritzen*[1]
[1]*Neuroscience and Pharmacology, University of Copenhagen, Copenhagen, Denmark*

Objectives: Our aim was to develop a robust procedure to measure BBB permeability of a single capillary using the two-photon microscopy.

Methods: Measurements were performed on anesthetized C57bl6/j mice. Sodium Fluorescein, a low molecular weight fluorescent dye, was injected into the bloodstream intravenously and visualized using an Olympus two-photon microscope FVMPE-RS FLUOVIEW. Fast scanning mode was employed to collect images yielding a high temporal resolution.

Results: To be able to calculate capillary permeability it is necessary to know the concentration of a diffusive compound inside and outside a capillary. This issue comprise one of the main challenges and usually leads to the

excessively simplificated or complicated experimental setups.

Here we established an image acquisition protocol as well as data analysis algorithm that allows to obtain different types of images, including those which correspond to either extravascular or overall dye signal. Filtering them from other images (reflecting the average distribution of a dye) it is further possible to extract the fluorescent intensity values (proportional to dye concentration) inside and outside a capillary which can be directly used to calculate permeability.

The method requires the use of only one fluorescent tracer and doesn't require comprehensive image processing tools, which makes it handy and robust for the current task.

Conclusions: We provide an example of a two-photon microscopy based approach to study single brain capillaries permeability of living mice in real time.

The method will potentially allow to study BBB pathological conditions as well as test fluorescently labeled drugs or nanocarriers on their ability to cross BBB.

References:

1) Hall, C.N. et al. Capillary pericytes regulate cerebral blood flow in health and disease. Nature 508, 55-60 (2014).
2) Patlak,C.S., Blasberg,R.G., & Fenstermacher,J.D. Graphical evaluation of blood-to-brain transfer constants from multiple-time uptake data. J. Cereb. Blood Flow Metab 3, 1-7 (1983).
3) Abbott,N.J., Patabendige,A.A., Dolman,D.E., Yusof,S.R., & Begley,D.J. Structure and function of the blood-brain barrier. Neurobiol. Dis. 37, 13-25 (2010).

888
BRAIN-0890
Poster Session

Late Breaking Abstracts

DOES BRAIN ISCHAEMIA INDUCE CHANGES IN THE VASCULAR EFFECTS OF PROTEASE ACTIVATED RECEPTORS?

F.F.Y. Lam[1], X. Zhen[1], E.S.K. Ng[1]
[1]School of Biomedical Sciences, Chinese University of Hong Kong, Shatin, Hong Kong China

Objectives: Vascular responses and brain diseases such as ischaemic stroke are inter-related. Many studies have demonstrated altered vascular responses following brain injury (Hansen-Schwarts et al., 2003, Ansar et al., 2010). Four types of protease activated receptors are known; PAR1 to PAR4. They are suggested to have both neuroprotective and neurodegenerative effects in the brain under pathological conditions (Luo et al., 2007). The impact of brain ischaemia on the vascular effects of PARs has not been investigated. Using activating peptides of the four PARs, this study aims to determine whether their vascular effects could be different in middle cerebral arteries (MCA) isolated from normal and ischaemic rat brains.

Methods: MCA were isolated from normal rats and from rats subjected to 45min occlusion of MCA 24h previously. Two 2mm vessel rings were obtained from each MCA and mounted to a myograph system for tension recording. Activating peptides of the four PARs (PAR APs) were tested on the precontracted tone produced by 100nM U46619. Involvement of nitric oxide (NO) in their vascular effects was tested by addition of 100μM of the nitric oxide synthase inhibitor L-NAME prior to cumulative additions of PAR APs.

Results: In MCA isolated from normal rat brains, PAR-1 AP (SFLLRN-NH_2) and PAR-4AP (AYPGKF-NH_2) had no effect, whereas, PAR-2 AP (SLIGRL-NH_2) produced 38% relaxation and PAR-3 AP (SFNGGP-NH_2) produced 46% contraction on the

U46619-precontracted tone. In MCA isolated from ischaemic rat brains, PAR-4 AP remained ineffective, but PAR-1 AP produced a significant 17% relaxation, and PAR-2 AP produced 47% relaxation, whereas, PAR-3 AP produced 102% contraction on the U46619-precontracted tone. Pretreatment with L-NAME completely inhibited the vasodilator effects of PAR-1 AP and PAR-2 AP in both types of MCA.

Conclusions: The present findings have demonstrated that PAR-1 AP possesses vasodilator effect only in MCA isolated from ischaemic rat brains. On the other hand, PAR-2 AP produced vasodilatation in MCA isolated from both normal and ischaemic rat brains. All the vasodilator effects of these two peptides were abolished by L-NAME; indicating involvement of NO. In contrast, PAR-3 AP is a vasoconstrictor, and PAR-4 AP is not vasoactive in both types of blood vessels. Compared to MCA from normal rats, MCA from ischaemic rats showed slightly better vasodilator responses to PAR-1 AP and PAR-2 AP, but greatly augmented vasoconstriction to PAR-3 AP. The latter exaggerated vasoconstrictor effect could potentially worsen ischaemia-induced injuries in the brain.

References: Ansar, S, Larsen, C, Maddahi, A & Edvinsson, L (2010). Subarachnoid hemorrhage induces enhanced expression of thromboxane A2 receptors in rat cerebral arteries. *Brain Res* 1316:163-72.

Hansen-Schwartz, J, Hoel, NL, Xu, CB, Svendgaard, NA & Edvinsson, L (2003). Subarachnoid hemorrhage-induced upregulation of the 5-HT1B receptor in cerebral arteries in rats. *J Neurosurg* 99: 115-20.

Luo, W, Wang, Y & Reiser, G (2007). Protease-activated receptors in the brain: receptor expression, activation, and functions in neurodegeneration and neuroprotection. *Brain Res Rev* 56: 331-45.

889
BRAIN-0877
Poster Session

Late Breaking Abstracts

HIGH DOSE OF ATORVASTATIN INDUCES CEREBRAL HEMORRHAGE BY DAMAGING BLOOD VESSEL STABILITY VIA SMALL GTPASES MEDIATED SRC/VE-CADHERIN/CATENINS PATHWAYS IN HUMAN ENDOTHELIAL CELL

S. Li[1], P.M. Hoi[1], S.M.Y. LEE[1]
[1]State Key Laboratory of Quality Research in Chine se Medicine, Institute of Chinese Medical Sciences, Macau, Macau

Objectives: Statins are a class of drugs used to lower high cholesterol levels and to prevent its complications such as cardiovascular diseases by inhibiting the enzyme HMG-CoA reductase. However, clinical trials showed that statins appear to increase the risk of intracerebral hemorrhage (ICH). Previously studies indicated that statins induced-rupture vessel integrity mediated bleeding could be reproduced in zebrafish larvae. Loss of junctions of the vascular endothelium can result in the rupture of vessels and bleeding into interstitial spaces.

Methods: In view of this, we employed human endothelial cells *in vitro* and zebrafish *in vivo* to study the mechanisms of change of vascular integrity and endothelium permeability underlying the atorvastatin-induced cerebral bleeding process.

Results: Our present study showed that atorvastatin-induced cerebral hemorrhage in zebrafish could be completely rescued by exposure of embryos to mevalonic acid (MVA) and isoprenoids (i.e. IPP, FPP, GGPP) but not cholesterol. Moreover, atorvastatin induced loss of cell-cell junctions by derangement of the actin cytoskeleton and impairment of VE-cadherin (VEC) distribution. Nevertheless, MVA and isoprenoids completely recovered the actin cytoskeleton derangement and VEC loss. Further studies showed that atorvastatin inhibited the post-translation isoprenylation of small GTPases

and disrupted the regulation on Src/ VEC/catenins associated with cell junction and actin cytoskeleton. In addition, inhibition of Src kinase prevents the VEC loss and disruption of cell-cell junctions caused by atorvastatin.

Conclusions: Taken together, we have mapped the mechanism of this disruption to the regulation of small GTPases on VEC/catenins mediated adheren junctions, as well as the actin cytoskeleton. More importantly, we have presented results highlighting the inhibition of Src signaling might be beneficial for the management of cerebral hemorrhage.

References: Eisa-Beygi S, Hatch G, Noble S, Ekker M, Moon TW. The 3-hydroxy-3-methylglutaryl-CoA reductase (HMGCR) pathway regulates developmental cerebral-vascular stability via prenylation-dependent signalling pathway. *Dev Biol* 373, 258-266 (2013).

Adam AP, Sharenko AL, Pumiglia K, Vincent PA. Src-induced tyrosine phosphorylation of VE-cadherin is not sufficient to decrease barrier function of endothelial monolayers. *The Journal of biological chemistry* 285, 7045-7055 (2010).

Huisa BN, Stemer AB, Zivin JA. Atorvastatin in stroke: a review of SPARCL and subgroup analysis. *Vascular health and risk management* 6, 229-236 (2010).

890
BRAIN-0932
Poster Session

Late Breaking Abstracts

NEURAL STEM CELL (NSC)-ENCODED HYPOXIA-INDUCIBLE FACTOR-1ALPHA(HIF-1ALPHA) PROMOTES THE ENDOGENOUS REGENERATIVE RESPONSE TO STROKE

L. Li[1], L. Cunningham[1]
[1]Neurosciences, University of New Mexico, Albuquerque, USA

Focal cerebral ischemia induced by middle cerebral artery occlusion (MCAO) stimulates a multilineage cytogenic response from NSCs within adult subventricular zone (SVZ), which includes production of both glial and neuronal lineages (Li *et al.*, 2010). HIF-1a is a key mediator of the adaptive cellular responses to hypoxia through direct transcriptional regulation of cell and molecular processes, including those involved in angiogenesis, stem cell maintenance and differentiation. Our previous studies have shown that stabilized HIF-1a protein is constitutively expressed within NSCs of the adult SVZ (Roitbak *et al.*, 2011). Using conditional, tamoxifen-inducible HIF-1a knockout (HIF-1a iKO) mice in which tamoxifen administration resulted in concomitant expression of yellow fluorescent protein (YFP) and bi-allelic *Hif1a* exon 2 gene deletion in nestin^{+} NSCs and their progeny (*nestin*-CreER^{T2}:R26R-YFP:*Hif1a*$^{fl/fl}$), we have demonstrated that induced *Hif1α* gene deletion in adult NSCs results in their gradual loss, which is preceded by regression of the SVZ vasculature under non-pathologic condition(Li *et al.*, 2014). To investigate whether NSC-encoded HIF-1a regulates the regenerative response to stroke and vascular recovery in the area of stroke damage, tamoxifen was administered to adult male HIF-1a iKO and wild type mice 14 days prior to 60 minutes transient occlusion of the middle cerebral artery (MCAO), and the mice were sacrificed at two weeks after stroke. YFP positive cells were observed throughout the injured striatal parenchyma in stroke mice. *Hif1α* gene deletion resulted in fewer YFP+ cells within the injured striatum 2 weeks post-MCAO, but caused a 1.8-fold increase in the percentage of doublecortin+/YFP+ cells within the ischemic striatum (21.9 ± 1.7% vs 12.3 ± 0.8%, HIF-1a KO vs. WT, $p<0.01$, n=5/group), indicating a switch toward the neuronal lineage fate. Blood vessel density was decreased by 29% in the injured striatum in HIF-1a iKO mice compared with that of wild type mice ($1.2 \times 10^{-5} \pm 1.7 \times 10^{-6}$ vs. $1.7 \times 10^{-5} \pm 5.4 \times 10^{-7}$ blood vessel number/micron^3, respectively, $p<0.05$ n=5/group). These studies suggest that NSC-encoded HIF-1a promotes the SVZ regenerative response, vascular recovery, and NSC cell fate following stroke injury.

Li et al., 2010 Glia 58:1610.
Li et al., 2014 Journal of Neuroscience 34(50): 16713
Roitbak et al., 2011 Cell Mol Neurobiol. Jan; 31(1): 119

Supported by the American Heart Association Grant-in-Aid 09GRNT2290178

891
BRAIN-0940
Poster Session

Late Breaking Abstracts

FEEDING SUPPORT ALLOWS C57BL/6 MICE TO SURVIVE FILAMENT MCA OCCLUSION LONG-TERM

A. Lourbopoulos[1], U. Mamrak[1], F. Hellal[1], S. Roth[2], M. Balbi[1], A. Liesz[2], N. Plesnila[1]
[1]Laboratory of Experimental Stroke Research, Institute for Stroke and Dementia Research, München, Germany
[2]Stroke-Immunology Group, Institute for Stroke and Dementia Research, München, Germany

Objectives: Long-term behavioral deficits after experimental stroke are difficult to investigate in some of the most commonly used mouse strains because infarcts, large enough to cause neurological deficits, are associated with massive body weight loss and lack of long-term survival. The aim of the current study was to establish an experimental protocol which allows C57BL/6 mice to survive fMCAo long-term.

Methods: Male C57BL/6 mice (8-10 weeks old, n=88) were subjected to one hour fMCAo and fed with three different feeding protocols starting 48 hours after ischemia: ad libitum pellet food (control), medium feeding support (MFS: forced oral feeding with 1ml of gel-food, 3 times per day for 7 days) and high feeding support (HFS: prolonged MFS until reaching the 85% of their initial body weight plus ad libitum provision of gel-food on their cage floor). The gel-food was produced fresh by mixture of 1/3 powder of control pellet-food with 2/3 of water. Animals were observed for 14 days and evaluated in a randomized and blinded fashion for mortality, body weight, body temperature, neurological function, food and water consumption, infarct volume, and brain atrophy. Data are reported as mean±s.e.

Results: The HFS protocol reduced fMCAo-related mortality by 75%, i.e. from 59% (control) to 15% ($p=0.001$) and prolonged the mean survival from 4.2±0.3 to 9.3±1.7 days ($p=0.012$). MFS protocol only prolonged survival (to 8.5±0.6 days, $p=0.001$). Since also animals with large infarcts survived fMCAo in the HFS group, infarct volumes and cortical atrophy almost doubled in this group as compared to controls (32±4% vs. 16±4% and -20±3% vs. -10±2% of the contralateral hemisphere, respectively, $p<0.05$). Accordingly, behavioral deficits were also more prominent in the HFS group ($p<0.05$). Interestingly, the HFS protocol did not prevent the characteristic post-ischemic loss of body weight and reduction of body temperature. Eventually, the HFS protocol partially counterbalanced the reduced food and water consumption that is evident in control group (-39±13% vs. -70±7% and -41±10% vs. -87±5% respectively on day 3, $p<0.05$) and precedes mortality.

Conclusion: The high mortality following filament MCAo in C57BL/6 mice is reduced to only 15% by intensive feeding support (HFS). This suggests that mortality in this model is not primarily caused by the severity of the ischemic brain injury, but secondary by reduced food and water intake. The currently suggested feeding protocol allows using the fMCAo model in C57BL/6 mice for studying the long-term consequences of cerebral ischemia.

Acknowledgements: A. Lourbopoulos is supported by an Intra European (IEF) Marie-Curie Fellowship.

892
BRAIN-0928
Poster Session

Late Breaking Abstracts

DERAILMENT IN NITRIC OXIDE-DEPENDENT NEUROVASCULAR AND NEUROMETABOLIC COUPLING IN AGING

C.F. Lourenço[1], A. Ledo[1], R.M. Barbosa[1], J. Laranjinha[1]
[1]Faculty of Medicine Polo I Piso I, Center for Neuroscience and Cell Biology, Coimbra, Portugal

Introduction: The functional and structural integrity of the brain relies on its ability to locally adjust blood flow and the delivery of metabolic substrates to meet the metabolic demands imposed by neuronal activation. This process – neurovascular coupling – and ensued alterations on glucose and O_2 metabolism - neurometabolic coupling - are accomplished by complex and concerted communication between neural and vascular cells[1]. Recently, direct evidences critically supported the key role of nitric oxide ($^{\cdot}NO$) in the neurovascular coupling, acting in hippocampus as the direct mediator of the process[2]. In addition, $^{\cdot}NO$ is be involved in the regulation of ensued processes, including energy metabolism/cellular respiration by interfering with mitochondrial respiratory complexes, as well as bioenergetic signaling pathways[3,4]. While some evidences support the notion that neurovascular and neurometabolic coupling are perturbed during brain aging, the topic is still controversial [5] Supported by the simultaneous measures of $^{\cdot}NO$, O_2 and CBF dynamics in hippocampus *in vivo* we aimed to address the neurovascular and neurometabolic coupling mediated by neuronal-$^{\bullet}NO$ in aging.

Methods: The experiments were conducted in Fischer F344 inbred rats at two different ages 3-6 months of age (young group) and 23 months of age (old aged group). The animals were evaluated in terms of behavioral and cognitive performance using several behavior tests. The simultaneous measurements of $^{\bullet}NO$, O_2 and CBF were achieved by home-made arrays consisting of $^{\bullet}NO$ and O_2 microelectrodes, micropipette and a laser Doppler probe positioned in the hippocampus of isoflurane-anesthetized animals essentially as previously described [2]. Neuronal activation was elicited by a localized stimulation with glutamate solution.

Results and Discussion: Aging was accompanied by a gradual and significant decrease in locomotion and exploratory behavior, as well as by a decreased cognitive performance. Glutamatergic activation in hippocampus promoted transient increases in $^{\cdot}NO$ concentration levels, followed by transient CBF elevation from a background and biphasic fluctuation of O_2 tension. The latter reflects both, the early increase in tissue O_2 consumption and the blood-dependent O_2 delivery. Quantitatively, it was observed that while $^{\bullet}NO$ production was not significantly affected during aging in this model, the coupled CBF change and the variations of O_2 tension were impaired. In brief, the CBF changes were diminished in terms of amplitude and increased onset delay. Also, although CBF changes were decreased along the age, the O_2 component associated with the hyperemic response was increased in older animals, while no significant alterations occurred in the component associated to O_2 consumption.

Conclusions: Overall, the results points towards an imbalance in the regulation of both $^{\cdot}NO$-mediated neurovascular and neurometabolic coupling during normal aging, in close correlation with a compromised cognitive function.

References

[1] Attwell *et al.* (2010) Nature, 468(7321), 232-43
[2] Lourenço *et al.* (2014) Free Radic Biol Med, 73, 421-9
[3] Antunes and Cadenas (2007). Front Biosci 12, 975-985.
[4] Almeida *et al.* (2005). J Neurosci Res 79, 166-171.
[5] Aanerud et al (2012) J Cereb Blood Flow Metab 32, 1177–1187

Acknowledgments
Work supported by *Fundação para a Ciência e a Tecnologia (*PTDC/BBB-BQB/3217/2012 and *Pest-C/SAU/LA0001/2013-2014).* CFL acknowledges fellowship SFRH/BPD/82436/2011
893
BRAIN-0934
Poster Session

Late Breaking Abstracts

OXIDASE-BASED MICROBIOSENSOR FOR REAL TIME MONITORING OF GLUCOSE AND NEURONAL ACTIVITY IN AWAKE BEHAVING ANIMALS

C.F. Lourenço[1], A. Ledo[1], G.A. Gerhardt[2], J. Laranjinha[1], R.B. Barbosa[1]
[1]Faculty of Medicine Polo I Piso I, Center for Neuroscience and Cell Biology, Coimbra, Portugal
[2]Department of Anatomy and Neurobiology, Center for Microelectrode Technology University o f Kentucky, Lexington, USA

Introduction: The brain is a high energy demanding organ: despite accounting for only 2% of the total body mass, it consumes up to 25% of the total glucose budget. It´s adequate function is critically dependent on the tight coupling between neuronal activity and the continuous delivery of energy substrates from blood stream, which implies that changes in blood supply and glucose and oxygen metabolism must be attuned, with temporal and regional precision, to the physiological demands imposed by neural activation. Both phenomena - neurovascular and neurometabolic coupling - underpin modern neuroimaging techniques, and yet are not fully understood. Our understanding of such complex mechanisms is critically dependent on the availability of suitable tools that allow the dynamical probing, with high temporal and spatial resolutions, of the functional and coordinated interaction between neurons, astrocytes and the vasculature *in situ*. Enzyme-based amperometric microbiosensors are attractive tools for real time monitoring *in vivo* the dynamics of neurotransmitters and metabolism-related biomarkers, such as glucose. In this work we describe the development and characterization of a glucose oxidase based microbiosensor for in vivo real-time continuous monitoring of glucose in awake-behaving rodents using mass-fabricated multisite microelectrode array (MEAs).

Methods: Glucose oxidase (GOx)-modified MEAs were used as microelectrode platforms for in vivo measurements of glucose. The MEA-based GOx biosensors were tested *in vitro* for their general analytical properties towards glucose measurement in brain extracellular space. *In vivo* measurements were performed both in anesthetized and in awake rats using the FAST-16 electrochemical system (Quanteon, LLC, USA). The self-referencing technique was used to address basal levels of glucose and fluctuations along 24-h periods in behaving animals in different brain regions, and in response to arousal status. The data recorded at high frequency was analyzed off-line to extract local field potential (LFP)-related currents allowing to measure changes metabolic markers in together with ongoing neuronal network activity (inferred from LFP features).

Results and Discussion: MEA-based GOx microbiosensor presented suitable analytical toward glucose measurement *in vivo*, as evidenced by the good sensitivity, response time, linear range and selectivity against major interferents. While some dependency on oxygen was observed, the Km was low, allowing the use of these biosensors for studies involving physiological fluctuations of oxygen. Preliminary data support the feasibility of glucose measurements in both anesthetized and freely moving animals with the MEA-based GOx biosensors. Spontaneous fluctuations in glucose levels were detected as a function of animal activity, awareness and sleep-awake cycle. In hippocampus, the basal levels were estimated to range from 0.5 to 1.5 mM.

Conclusions: This work shows the successful use of glucose oxidase_based microbiosensor to direct study tonic and phasic glucose dynamic fluctuations in awake-behaving rodents.

Acknowledgments: This work was supported by *Fundação para a Ciência e a Tecnologia (*PTDC/BBB-BQB/3217/2012 and *Pest-C/SAU/LA0001/2013-2014).* CFL acknowledges FCT post-doctoral fellowship SFRH/BPD/82436/2011

894
BRAIN-0911
Poster Session

Late Breaking Abstracts

NEUROVASCULAR COUPLING AND HEMODYNAMIC RESPONSES IN RAT: A SIMULTANEOUS ECOG-FNIRS STUDY

M. Mahmoudzadeh[1], *G. Dehaene-Lambertz*[2], *F. Wallois*[1]
[1]*Medicine, Centre Hospitalier Universitaire, Amiens, France*
[2]*CEA, Neurospin, Gif/Yvette, France*

The nature of the coupling between the hemodynamic signal and electrical activity of the brain is still under debate. However, optical imaging does not measure neural activity per se; rather, it measures the changes in concentration of blood oxygen in the tissue which is associated with changes in brain neural activity. This complementary method with higher temporal resolution (rather than fMRI) has been used to investigate the hemodynamic basis of neuronal activity in human and animals in more detail. We used a multichannel frequency-domain-based optical spectroscopy imaging system (Imagent®, ISS Inc.) and electrocorticogram (ECoG, A.N.T®) to acquire oxygenated hemoglobin (HbO) and deoxygenated hemoglobin (Hb) concentration changes and electrophysiological responses to somatosensory and auditory stimuli in fourteen adult male Sprague–Dawley rats (mean body weight: 350–450 g). We used electrical forepaw and auditory stimuli which is two robust paradigms for studying neurovascular coupling. For probing the somatosensory and auditory cortex, a special electroptode® was designed to hold the emitter/detector fibers and electrodes to fit to the small skull of the rat (n=14). The hemodynamic responses are characterized by an *initial dip* followed by an increase in total hemoglobin (tHb), an increase in oxyhemoglobin (HbO) concentration with a peak latency of 5 to 6.5 sec after stimulus onset. A decrease in deoxyhemoglobin (Hb) occurred simultaneously. Studying the neurovascular coupling in humans by EEG and optical imaging faced some limitation due to the vascularization of the skin, the presence of the bone and the artifacts due to movements. To overcome these problems, in the present animal study we developed a multimodal electrical and optical approach to investigate directly on the cortex the neurovascular coupling in response to electrical somatosensory and auditory syllabic stimuli. Such multimodal analysis allows characterizing the temporo-spatial specificity of the auditory and somatosensory cerebral responses of both the neuronal and vascular functional systems in rats.

895
BRAIN-0909
Poster Session

Late Breaking Abstracts

DECREASED MU-OPIOD RECEPTOR BINDING IN PATHOLOGICAL GAMBLING: A PET STUDY WITH [11C]CARFENTANIL

J. Majuri[1], *J. Joutsa*[1], *J. Johansson*[1], *K. Alakurtti*[1], *R. Parkkola*[2], *T. Lahti*[3], *H. Alho*[3], *E. Arponen*[1], *V. Kaasinen*[4]
[1]*Turku PET Centre, University of Turku, Turku, Finland*
[2]*Department of Radiology, Turku University Hospital, Turku, Finland*
[3]*Department of Mental Health and Substance Abu se services, National Institute for Health and Welfare, Helsinki, Finland*
[4]*Division of Clinical Neurosciences, Turku University Hospital and University of Turku, Turku, Finland*

Objectives: Pathological gambling (PG) is a behavioral addiction with an estimated life-time prevalence of 0.6% in the United States. Brain neurotransmitter unbalance may trigger the disorder and it may provide options for

pharmacotherapy. Previous studies have shown that substance abuse disorders are associated with increased mu-opioid activity and opioid antagonists show efficacy in the treatment of alcohol addiction. In behavioral addictions, the role of the brain opioid system is unclear. The aim of this study was to investigate possible changes in the brain opioid system in patients with PG.

Methods: Fifteen patients with PG (DSM-IV) and 16 healthy age- and sex-matched volunteers were scanned with [^{11}C]carfentanil PET using a Siemens high-resolution research tomograph (HRRT). Binding potentials (BP_{ND}) were calculated using the simplified reference tissue model with occipital cortex as the reference region. Parametric images were normalized to the Montreal Neurological Institute (MNI) space and analyzed voxel-by-voxel over the entire brain using general linear model with gender, age and nicotine use as covariates. Cluster-level family-wise error (FWE) corrected P-value less than 0.05 was considered statistically significant. The study protocol was approved by the local ethical committee and all subjects signed written informed consent.

Results: Patients with PG had lower [^{11}C]carfentanil BP_{ND} in the anterior cingulate cortex (cluster size 6612mm^3, peak at -6 -51 19 mm, t_{max} = 6.70, P_{FWE} = 0.048) and in the posterior cingulate cortex (cluster size 4523 mm^3, peak at 14 8 37 mm, t_{max} = 7.93, P_{FWE} = 0.009). Bilateral clusters followed anatomical boundaries of the cingulate cortex (Figure). There were no regions that showed higher BP_{ND} in PG compared to controls.

Conclusions: Mu-opioid receptor binding in the cingulate cortex is decreased in PG as compared to healthy subjects. This finding is in contrast with the previous findings in substance abuse as mu-opioid binding has been reported to be elevated in several brain regions, including the cingulate cortex, in patients with alcohol dependence. Our results therefore suggest that PG and substance abuse may modulate cingulate opioid function to opposite directions although the two disorders frequently co-exist. The finding may be associated with the functional significance of the cingulate cortex in the modulation of detecting errors and making reward-based decisions. Our findings provide no neurobiological support for opioid antagonist pharmacotherapy in the treatment of PG.

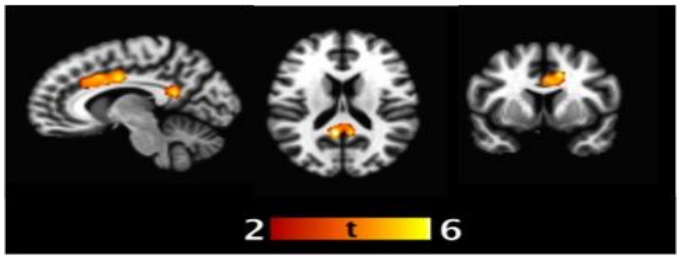

896
BRAIN-0879
Poster Session

Late Breaking Abstracts

ON THE RELATIONSHIP BETWEEN INTRACRANIAL PRESSURE, BLOOD FLOW VELOCITY AND ARTERIAL BLOOD PRESSURE FOR PATIENTS WITH CLOSED TBI

C. marzban[1], *S. Yuan*[1], *P. Mourad*[2]
[1]*Statistics, University of Washington, Seattle, USA*
[2]*Engineering and Mathematics, University of Washington, Bothell, USA*

Objectives: Autoregulation of cerebral blood flow can be assayed by observing blood Flow Velocity (FV) in the middle cerebral artery. FV, however, has a complex relationship with Arterial Blood Pressure (ABP) and Intracranial Pressure (ICP), both of which can also be observed directly. Although it is believed that autoregulation assures relatively constant flow into the brain, here we ask if there exists a specific linear combination of FV, ABP, and ICP that is held constant not only in time (more specifically, with minimum variance across time), but also across patients?

Methods: Data on FV, ABP, and ICP for 109 closed TBI patients from several hospitals in England and USA are examined. A statistical method is developed to infer the linear combination, Q, of these variables that minimizes the variance

(across time) of Q for each patient. The analysis is performed at various frequency categories: ventilation (v), cardiac (c), and other frequencies below, between, and above v and c. Ventilation and cardiac frequencies are selected because the cerebrovascular system can be considered to be an "externally driven" dynamic system (driven by the ventilator and the heart, respectively). By contrast, the remaining frequencies capture the behavior of the system when it is not driven externally, and therefore, allow for comparison of the results.

Results: It is found that the optimum linear combination of ABP, FV, and ICP that minimizes the variance of Q depends on the frequency category. At ventilation frequency, Q is primarily a combination of FV and ICP, mostly of the latter, and with almost no contribution from ABP. The same pattern exists at cardiac frequency but to a lesser degree, and to an even lesser degree at the intermediate frequencies. Moreover, the variance of Q, i.e., the quantity that the cerebrovascular system seeks to hold constant, is mostly the same across patients. More specifically, the variance of Q between patients (i.e., across the 109 patients) is significantly smaller than the variance of Q within each patient.

Conclusions: Ventilation (and to a lesser degree, the heart) acts as an external driving force on the cerebrovascular system. If that system is gauged in terms of ICP, FV, and ABP, then it appears that at ventilation frequency, the body holds a certain combination of the three quantities relatively constant in time. This notion generalizes the concept of the autoregulation of blood flow to the situation wherein a combination of several quantities is regulated.

897
BRAIN-0885
Poster Session

Late Breaking Abstracts

ECM HYDROGEL INJECTION FOR THE TREATMENT OF STROKE: CHARACTERIZATION OF ACUTE HOST CELL INVASION.

H. Ghuman[1], A. Massensini[1], T. Kim[1], C. Medberry[2], F. Nicholls[1], S. Badylak[3], M. Modo[1]
[1]Radiology, University of Pittsburgh, Pittsburgh, USA
[2]Bioengineering, University of Pittsburgh, Pittsburgh, USA
[3]Surgery, University of Pittsburgh, Pittsburgh, USA

Stroke is a severe cerebrovascular accident that results in a localized brain tissue loss, affecting nearly 800,000 Americans each year. Extracellular matrix (ECM) derived from urinary bladder lamina propria and basement membrane has shown therapeutic potential in rats following intracerebral injection for experimentally produced traumatic brain injury in rats. ECM can be prepared in liquid form at room temperature and dependent on concentration creates a hydrogel under physiologic conditions providing ideal material properties for intracerebral injection through a thin needle. To determine an appropriate concentration of ECM (0, 1, 2, 3, 4, 8 mg/ml) for injection and retention of material in the stroke cavity, ECM was injected in liquid form with injection parameters (coordinates and volume) determined by MRI 12 days post-middle cerebral artery occlusion, while simultaneously draining necrotic liquefied brain tissue. Retention of ECM, as well as host cell invasion and their phenotypes were assessed 24 hours post-injection using immunohistochemistry. ECM concentrations <3mg/ml did not gel and were not retained in the cavity. A significant host cell invasion was observed with 20-30% of these being putative microglia/macrophages (Iba1+) across all concentration groups. The number of astrocytes (GFAP+) cells invading the ECM acutely was negligible and there was no evidence of neuronal progenitor invasion. This characterization demonstrates that an ECM

hydrogel can be readily injected and retained within a lesion cavity, while attracting host cells into the damaged region. Further time points and behavioral studies will be required to further evaluate the therapeutic potential of this approach.

898
BRAIN-0921
Poster Session

Late Breaking Abstracts

IS SUSCEPTIBILITY TO SILENT CEREBRAL INFARCTION IN RELATIVES, AKIN TO "SODIUM SENSITIVITY" IN NORMOTENSIVE SUBJECTS, MEDIATED THROUGH CAPILLARY ENDOTHELIAL DYSFUNCTION AND CELLULAR MECHANISMS?

J.B. Myers[1]
[1]*Clinical Research,*
Wellspring's Universal Environment P/L,
Melbourne, Australia

Introduction: Risk stratification using the Framingham Stroke Risk Profile (FSRP) is enhanced when markers of endothelial dysfunction, plasma homocysteine and urinary albumin:creatinine ratio are added. Carotid and internal carotid intima:wall ratio added while serum cholesterol did not add to this. The authors indicated that silent infarcts do not necessarily correlate with side of intimal plaque, which raises questions as to the pathogenesis of silent infarcts and strokes, unrelated to large vessel findings.

Aim: To understand the pathophysiological basis of subclinical infarcts in asymptomatic relatives by comparing results in normotensive "sodium-sensitive" subjects.

Methods: 117/172 subjects aged 3-72y were studied(1) using a two week period cross over design, NaCl tablets or placebo.

Results: Sodium intake resulted in weight gain and rise in hematocrit in 43/117 subjects associated with a rise in diastolic blood pressure (DBP), in whom fluid distribution altered. Systolic blood pressure (SBP) also rose (corr. DBP, 0.44, $p<0.01$) but different factors determined SBP response, which was related to age (or initial systolic BP). Creatinine clearance on the reduced sodium diet was inversely related to change in SBP and to change in DBP response, indicating "sodium sensitivity" of SBP, which is age related, as well as DBP response, are associated with capillary involvement.

Conclusion: Implicating capillary dysfunction in asymptomatic relatives with silent infarcts and stroke, as in normotensive subjects who are "sodium sensitive", helps to unravel the pathophysiological mechanisms that relate to the increased stratification of risk of silent infarcts and strokes that are not explained by larger vessel involvement.

References:

Pikula A, Beiser AS, DeCarli C, Himali JJ, Debette S, Au R, Selhub J, Toffler GH, Wang TJ, Meigs JB, Kelly-Hayes M, Kase CS, Wolf PA, Vasan RS, Seshadri S. Multiple biomarkers and risk of clinical and subclinical vascular brain injury: the Framingham Offspring Study. Circulation. 2012 May 1;125(17):2100-7. doi: 10.1161/CIRCULATIONAHA.110.989145. Epub 2012 Mar 28.

Myers JB. "Sodium Sensitivity" in Man. Medical Hypotheses. 1987; 23: 265-276.

Myers JB. Sodium sensitivity and the microcirculation in man. Evidence for a new microcirculation hypothesis? In: Microcirculation - an update, Vol 2, M. Tsuchiya et al. editors. Elsevier Science Publishers B, V. (Biochemical Division). 1987: 669-670.

Myers JB. The role of capillary integrity, fluid distribution and thus atrial filling pressure and forgotten red cells in sodium sensitive (diastolic blood pressure responsive) subjects. International Society of Hypertension, Sydney 30 Sept-4 October 2012.

Myers JB. The cardiovascular system as a system of "organs" in series. Cardiovascular components and

the Balance Equation of Blood Pressure Regulation. 60Th International Conference of the Israel Heart Society in Association with the Israel Society of Cardio-thoracic Surgery. Jerusalem April 22-23, 2013/5773.

Myers JB. PT216 Capillaries are involved in the systolic and the diastolic blood pressure response to changes in sodium chloride intake in normotensive subjects. Global Heart, Volume 9, Issue 1, Supplement, March 2014, Page e209

Myers JB. Interaction of cardio-renal and bone marrow-renal mechanisms and the Micro-circulation (capillary) Theory of Hypertension. XXVIth World Congress of the International Union of Angiology (IUA). Sydney, Australia. 2014 10-14 August. pages 57-65. http://filesformailing.minervamedica.it/volumi/IUA2014.pdf,

899
BRAIN-0943
Poster Session

Late Breaking Abstracts

REGULATION OF NEUROPROTECTION-ASSOCIATED TRANSCRIPTION FACTOR NPAS4 IN NEUROINFLAMMATION

K.M. Othonos[1], A. Leung[2], J. Quandt[2]
[1]Graduate Program in Neuroscience, University of British Columbia, Vancouver, Canada
[2]Pathology and Laboratory Medicine, University of British Columbia, Vancouver, Canada

Background/Objectives: Multiple Sclerosis (MS) is the most common central nervous system (CNS) neurodegenerative disorder affecting young Canadian adults. The cause of MS remains unknown; however, demyelination and axonal loss associated with disability are believed to be driven by inflammation and infiltration of various immune cells and their mediators (1). Thus, developing therapies that reduce inflammation or provide neuroprotection are most promising to limit disease progression. Neuronal Per Arnt Sim 4 (NPAS4) is a brain-specific, activity-dependent, basic helix-loop-helix (bHLH)-PAS transcription factor that regulates genes important for neuronal and axonal survival, inhibitory synapse development and synaptic plasticity (2). NPAS4 is not constitutively expressed in the CNS, and its upregulation is associated with neuroprotection against disease and neurodegenerative cell-stress inducers (3). We have recently documented its dysregulation during autoimmune demyelination in a model of MS. The objective of this study is to examine the functional relevance of NPAS4 expression patterns in MS disease development and under the influence of inflammatory cells and mediators. We hypothesize that changes in NPAS4 expression levels influence MS disease development and progression.

Methods: Embryonic primary cortical-enriched neuronal cultures were exposed to excitatory stimuli, oxidative stress mediators, glutamate or co-cultured with splenocytes. NPAS4 expression levels were determined via western blotting and immunocytochemistry, while cell viability was assessed through morphological cellular characteristics and lactate dehydrogenase assay.

Results: As previously reported, primary neuronal cultures demonstrate negligible levels of NPAS4, and upregulation with excitatory stimuli such as 4-aminopyridine (4AP), potassium chloride (KCl) and bicuculline was confirmed (2). Protein expression is typically quite rapid, peaking within 2-4hrs following exposure to 4AP and bicuculline before dropping off, whereas KCl maintains high NPAS4 levels for up to 8 hours following exposure. Consistent with immune cell involvement, we observed an early upregulation of NPAS4 expression in primary neuronal cultures following co-culture with splenocytes, which was significantly reduced by a cocktail of inhibitors targeting NMDA and glutamate receptors. In view of these results, immune cell mediators generated by splenocytes, such as glutamate and oxidative stressors were further investigated. Exposure to low levels of glutamate and an oxidative stress mediator, hydrogen peroxide, were found to rapidly increase NPAS4 expression, in a dose and time dependent manner. The direct contributions of NPAS4 to survival in these settings are under investigation.

Conclusions: Understanding the role of processes that govern CNS inflammation and neurodegeneration is an important first step in developing more efficient therapies for MS that focus on limiting disease progression through neuroprotection. Our study describes novel findings related to NPAS4 regulation under inflammatory settings, and suggests an important role for NPAS4 in protecting neurons through initial disease development and progression.

References:

1. Zindler, E. et al., *Neuronal injury in chronic CNS inflammation.* Best Pract Res Clin Anaesthesiol, 2010. **24**(4): p. 551-62.
2. Lin, Y., et al., *Activity-dependent regulation of inhibitory synapse development by NPAS4.* Nature, 2008. **455**(7217): p. 1198-204.
3. Ooe, N., et al., *Functional characterization of basic helix-loop-helix-PAS type transcription ffactor NXF in vivo: putative involvement in an 'on demand" neuroprotection system.* J Biol Chem, 2009. **284**(2): p.1057-63.

900
BRAIN-0891
Poster Session

Late Breaking Abstracts

IDENTIFICATION OF DYSFUNCTIONAL STRESS RESPONSE PATHWAYS IN POST-ISCHEMIC BRAINS OF OLD MICE: IMPLICATIONS FOR IMPAIRED FUNCTIONAL RECOVERY FROM ISCHEMIC STRESS

W. Paschen[1], S. Liu[1], H. Sheng[1], W. Yang[1]
[1]Department of Anesthesiology,
Duke University Medical Center, Durham, USA

Introduction: Aging is associated with increased risk for stroke and impaired functional recovery from transient ischemia. This suggests that the brain's ability to respond to an ischemic challenge declines with age. To comprehensively analyze the effects of age on the response of brains to a transient interruption of blood supply, we subjected young and old mice to transient forebrain ischemia, and analyzed a variety of stress response pathways. These included the heat shock response (HSR), the unfolded protein response (UPR), and ubiquitin, small ubiquitin-like modifier (SUMO) and O-linked β-N-acetylglucosamine (O-GlcNAc) modification of proteins. We chose a transient forebrain ischemia model to guarantee that results would not be confounded by unrelated factors such as size of infarcts.

Methods: Transient forebrain ischemia experiments were performed on male 2 months and 22 months old mice. Animals were anesthetized with isoflurane, temperature-controlled, and subjected to 10 minutes common carotid artery occlusion and blood withdrawal to reduce mean arterial pressure to 30 mm Hg. After 60 minutes of reperfusion, brains were quickly removed, and dissected into cortex and hippocampus. Changes in mRNA and protein levels were analyzed by qPCR and Western blot, respectively, and corrected for β-actin levels. Data are presented as means ± SD (n=4/group). Statistical analysis was performed by ANOVA followed by Tukey's *post hoc* test.

Results: Hsp70 expression, Xbp1 splicing, and eIF2a phosphorylation were activated in young and old mice to a similar extent after ischemia, indicating induction of HSR and UPR. The post-ischemic increase in global ubiquitin (Figure 1; cortex), SUMO1, and SUMO2/3 (Figure 2; cortex) conjugation was significantly less pronounced in aged compared to young mice. Transient ischemia triggered a global increase in levels of O-GlcNAc-modified proteins in young mice that was completely absent in old animals (Figure 3; cortex). Analysis of hippocampus samples showed similar patterns.

Conclusions: We have reported earlier that SUMO2/3 conjugation is dramatically activated after ischemia [1], and provided evidence that this is a neuroprotective stress response [2]. SUMO proteomics analysis identified SUMOylation-dependent ubiquitin conjugation as a putative neuroprotective pathway [3] that plays a key role in DNA damage repair. This pathway may be impaired in old mice since activation of both SUMO2/3 and ubiquitin conjugation was markedly less compared to young animals. O-

GlcNAc modification of proteins has not yet been studied in models of brain ischemia, but ample evidence supports the notion that activation of O-GlcNAc modification protects hearts from ischemic damage [4]. In the brain, levels of O-GlcNAc-modified proteins are particularly enriched at synapses, and are involved in synaptic plasticity [5]. We, therefore, conclude that the inability of aged mice to activate O-GlcNAc modification of proteins in response to transient ischemia could be a critical factor that limits functional recovery from a period of non-sufficient blood supply.

References: [1] Yang et al., J Cereb Blood Flow Metabol 2008;28:269-279; [2] Datwyler et al., J Cereb Blood Flow Metabol 2011;31:2152-2159; [3] Yang et al., Stroke 2014;45:1115-1122; [4] Chatham JC and Marchase RB, Biochim Biophys Acta 2010;1800:57-66; [5] Tallent et al., J Biol Chem 2009;284:174-181.

Figure 1

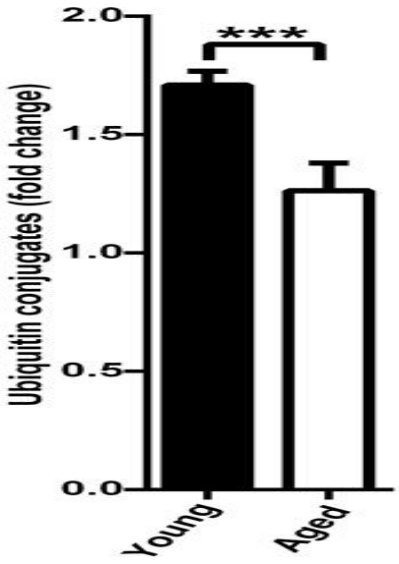

Figure 2

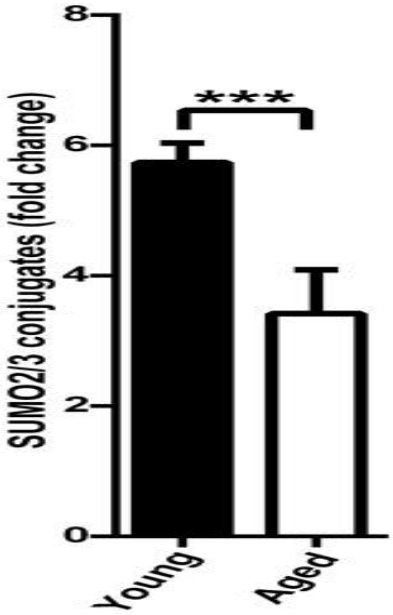

Figure 3

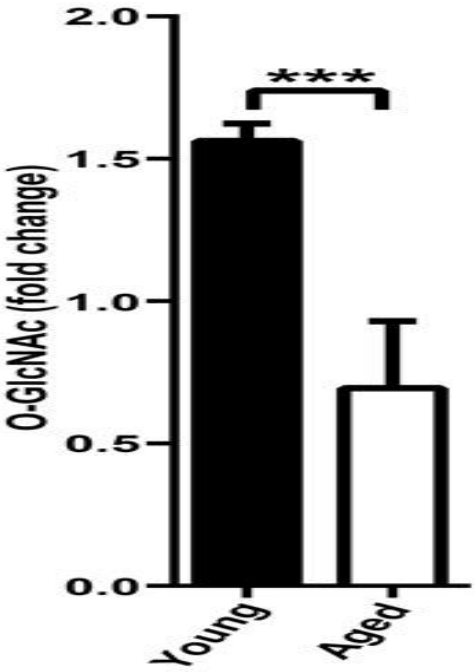

901
BRAIN-0931
Poster Session

Late Breaking Abstracts

ROLE OF THE TYROSINE PHOSPHATASE STEP IN REGULATING POST-ISCHEMIC NEUROINFLAMMATION

S. Rajagopal[1], C. Yang[2], R. Poddar[1], E. Candelario-Jalil[2], S. Paul[1]
[1]Neurology, University of New Mexico, Albuquerque, USA
[2]Neurosciences, University of Florida, Gainesville, USA

Objective - Cerebral ischemia induced brain damage begins as oxygen-glucose deprivation from the loss of blood supply result in the excessive release of the excitatory neurotransmitter glutamate, over-activation of N-methyl-D-aspartate-subtype of glutamate receptors and intracellular Ca^{2+} overload. Emerging evidence indicates that an ischemic insult not only activates multiple cytotoxic pathways, but also triggers some endogenous protective responses capable of limiting injury. The neuron-specific tyrosine phosphatase, STEP is one such protein whose rapid activation provides initial neuroprotection during an ischemic insult. Degradation of active STEP over time leads to loss of its neuroprotective effects, thus allowing the activation of deleterious processes. Maintaining STEP availability with intravenous administration of a degradation resistant STEP-derived peptide effectively reduces ischemic brain damage. Conversely, genetic deletion of STEP in mice exacerbates brain damage following ischemia (Deb et al., 2013). The objective of this study is to elucidate the molecular basis of exacerbated ischemic brain damage caused by the loss of endogenous STEP, and to further determine whether restoring STEP signaling can target multiple components of the ischemic cascade to confer neuroprotection.

Methods – Mild ischemic insult was induced by MCAO (30 min) in both wild-type and STEP KO mice followed by reperfusion (0, 3, 6, 12, 24h). The temporal profile of p38-MAPK phosphorylation, expression of cyclo-oxygenase-2, cleavage of tight-junction proteins and extravasation of IgG in the ipsilateral hemisphere were assessed by immunoblot analysis. Microglial phenotype and activation were assessed using immunohistochemistry and enzyme assay. Fluorojade staining was performed to assess the progression of brain damage. In a subset of STEP KO mice, the STEP-derived peptide was administered intravenously to determine whether restoration of STEP signaling could attenuate these deleterious pathways. (Animal care and protocols approved by IACUC, UNM, following NIH guidelines).

Results – Our findings show that both in the striatum and cortex, the phosphorylation of the stress-activated kinase p38-MAPK and level of the pro-inflammatory enzyme cyclo-oxygenase-2 are elevated in the STEP KO mice within 30 min of the ischemic insult. Both p38-MAPK activity and cyclo-oxygenase-2 level remain elevated in the STEP KO mice even 24h after the onset of the insult. Additional mechanistic studies show transformation of microglial morphology to the reactive amoeboid form, activation of MMP-9 and -3, cleavage of tight junction protein zona occludens-1 and extravasation of IgG in the STEP KO mice brain. Consistent with these findings, accelerated ischemic brain damage is also observed in the STEP KO mice. Intravenous administration of the STEP-derived peptide attenuates p38-MAPK activation, reduces cyclo-oxygenase-2 expression, MMP-9 and -3 activity as well as prevents hemorrhagic transformation.

Conclusions – These findings show that in the absence of STEP, enhanced inflammatory alteration involving microglial activation leads to the exacerbation of ischemic brain injury. The study provides the first evidence for the role of a tyrosine phosphatase in the modulation of neuroinflammatory pathways and raises the possibility that a STEP-based approach could be of significant benefit for stroke treatment.

References – Deb et al., (2013) Neuroprotective role of a brain-enriched tyrosine phosphatase,

STEP, in focal cerebral ischemia. J. Neurosci. 33:17814-17826.

902
BRAIN-0892
Poster Session

Late Breaking Abstracts

REVERSIBLE INACTIVATION MAPPING OF CORTICAL SITES REQUIRED FOR VOLUNTARY FORELIMB MOVEMENTS IN VGAT-CHR2 TRANSGENIC MICE.

R. Katreddi[1], G. Silasi[1], J. Boyd[1], J. Le Due[1], S. Scott[2], T. Murphy[1]
[1]Psychiatry, University of British Columbia, Vancouver, Canada
[2]Center for neuroscience studies, Queens Univeristy, Kingston, Canada

Objectives: The aim of the study is to understand the sensory-motor interactions of the cortical regions that are required to execute a voluntary forelimb movement. Methods: Awake water restricted VGAT-ChR2 mice with transcranial windows were head-fixed and trained to pull a robotic lever to get water rewards. A blue laser was targeted to contralateral and ipsilateral points of the cortex to cause reversible local inhibition (by activation of the GABAergic neurons) while the mouse pulls the lever repeatedly over a 1 min sampling epoch. The total number of pulls done by the mouse at each cortical point was compared with the control point which was out of the cranial windows to probe their role in directed movements. Results: Different frequencies (10, 50, 100Hz) of the blue laser light at different laser power (1, 3, 6mW) were targeted to the regions of interest. Our preliminary results show a 6mW train of 5ms pulses delivered at 100Hz to the contralateral primary motor cortex(M1) reduced the number of rewarded lever pulls by 90±16.8% relative to a control site, while 50 and 10 Hz were less effective. This extent of inhibition was not seen while photo-activating other contralateral points such as M2, visual, retrosplenial cotex, parietal association area and even ipsilateral M1. Moreover, M1 inhibition was fully reversible as the mouse started pulling the lever within seconds once the laser was off the contralateral M1 site. Conclusions: As expected contralateral M1 is required for the execution of voluntary movement and M2, putative hubs such as the retrosplenial cortex, parietal association area were not required to initiate pulling. Future experiments will be done to look at the behavioral recovery of lever pulling after making focal strokes at the forelimb motor cortex in these transgenic mice using photo thrombotic lesion model.

903
BRAIN-0894
Poster Session

Late Breaking Abstracts

A 4 DAY-CLINICAL MICRODIALYSIS MONITORING IN A PATIENT WITH TRAUMATIC BRAIN INJURY (TBI) SUGGESTS A POSSIBLE LINK BETWEEN BRAIN SEROTONIN AND CEREBRAL ENERGY METABOLISM

B. Renaud[1], S. Parrot[2], D. Goncalves[1], M. Algoud[1], M. Gallet[2], F. Dailler[3], L. Denoroy[2]
[1]Neurobiology, Hospices Civils de Lyon, Bron, France
[2]NeuroDialytics, Centre de Recherche en Neuroscience de Lyon, Lyon, France
[3]Neuro Intensive Care Unit, Hospices Civils de Lyon, Bron, France

Objectives

While the continuous microdialysis monitoring of cerebral biomarkers of energy metabolism is frequently used in neurocritical care, very few data on monoamine neurotransmitters, such as serotonin (5-HT), have been reported using clinical microdialysis. Consequently, taking the opportunity of a feasibility study for a project on TBI, we sought to determine 5-HT levels in the brain microdialysis samples obtained from a TBI patient, concomitantly with biomarkers of energy metabolism.

Methods

The probes i) for cerebral microdialysis (CMA 70, flow rate, 0.3 µL/min), for PtO2 (LICOX) and ii) for intracranial pressure were placed into the cortical region containing the traumatic injury of a 23 year-old male patient. The dialysates were collected every hour and the brain extracellular concentrations of glucose, lactate and pyruvate were bedside analyzed on an ISCUSFlex microdialysis analyzer. In addition, the remaining volumes of dialysates were used for 5-HT analysis using a recently developed highly sensitive UHPLC-ED method.[1]

Results

The novelty of this study is the continuous monitoring of extracellular 5-HT in the human cerebral cortex using UHPLC-ED. Microdialysis samples collected between the 5th and the 9th day after TBI exhibited 5-HT concentrations varying between 0.13 and 6.12 nmol/L. Such a high variability in 5-HT concentration led us to determine whether the changes in cerebral 5-HT could be associated with variations in other biomarkers or events related to the patient's management. For instance, on the second day of monitoring, a marked fall in averaged 5-HT concentration (from 2.5 to 1.1 nmole/L, $p< 0.07$) occurred when insulin was administered to control hyperglycemia. This fall was associated with a bigger drop in microdialysate glucose concentration (from 3.7 to 1.1 mmol/L, $p<0.001$) concomitant with a fall in blood glucose concentration (from 13.7 to 7.2 mmol/L). As a consequence, brain/blood glucose ratio varied from 0.27 to 0.15, a decrease which may be linked to a reduction in brain glucose uptake. Brain lactate exhibited a decrease at the time of insulin therapy (from 6.4 to 5.7 mmol/L; $p<0.05$) as pyruvate did (from 248 to 211 µmol/L), leaving the lactate to pyruvate ratio unaltered. However, the decrease in lactate level was modest as compared to the fall in glucose (-11% vs –64%), leading to a 2.6 fold increase in lactate to glucose ratio. Finally, a series of correlation analyses showed that brain 5-HT concentrations were correlated to brain lactate concentrations during the 10-hour hyperglycemic episode ($r2 = 0.4798$, $p<0.05$), but that correlation was totally lost when glycemia was normalized after insulin administration.

Conclusions

These data obtained while performing the probably first monitoring of extracellular 5-HT concentration in the human cerebral cortex allow hypothesizing a possible link between 5-HT and energy metabolism in the human brain, as previously suggested by animal studies. However, further studies performed on cohorts of patients are needed to investigate this possible link, particularly in extreme conditions, i.e. in TBI or subarachnoid hemorrhage.

References

[1] Ferry, B.; Gifu, E. P.; Sandu, I.; Denoroy, L.; Parrot, S. 2014 J Chromatogr B 951-952, 52-57.

904
BRAIN-0901
Poster Session

Late Breaking Abstracts

CLINICAL NEUROCHEMISTRY OF SUBARACHNOID HEMORRHAGE (SAH)-OUTCOME PREDICTION BY MONITORING ENERGY BIOMARKERS: BRAIN ARTERIO-VENOUS VERSUS MICRODIALYSIS INVESTIGATIONS OF 18 PATIENTS WITH SEVERE SAH

B. Renaud[1], Y. Tholance[2], G.K. Barcelos[3], F. Dailler[4], A. Perret-Liaudet[5]
[1]Neurobiology, Hospices Civils de Lyon, Bron, France
[2]Centre Hospitalier Universitaire de Limoges Biochemistry and Molecular Genetics, University of Limoges Medical School, Limoges, France
[3]Pharmacology and Intensive care, Geneva University Hospitals, Geneva, Switzerland
[4]Neuro-intensive Care Unit Neurological Hospital, Hospices Civils de Lyon, Lyon, France

[5]*Neurobiology, Hospices Civils de Lyon, Lyon, France*

Objectives

In order to improve outcome prediction with biomarkers, in subarachnoid hemorrhage (SAH), we sought to evaluate the respective interest of the two main biochemical approaches available, which are either local (cerebral microdialysis, cMD), or global (retrograde jugular vein catheterization, RJVC).

Methods

In this observational prospective study of 18 patients with severe aneurysmal subarachnoid hemorrhage (aSAH), The probes i) for cerebral microdialysis (CMA 70, flow rate, 0.3 µL/min), for PtO2 (LICOX) and ii) for intracranial pressure, were placed into the cortical region containing the aneurysm. The dialysates were collected every hour and the brain extracellular concentrations of glucose, lactate and pyruvate were bedside analyzed on an ISCUSFlex microdialysis analyzer.

Results

According to their neurological outcome, evaluated at 12 months with the Glasgow Outcome Scale (GOS), the patients were divided into two groups of outcome, either favorable (GOS 4- 5), or unfavorable (GOS 1 - 3). This study included 400 sets of paired arterial and jugular venous samples and 8138 brain microdialysates. The microdialysis lactate/pyruvate ratio, exhibited the best sensitivity (90%) for predicting an unfavorable outcome, although its specificity was much less satisfactory. On the other hand, the frequency of increased lactate microdialysis hypoxic events as well as the frequency of reduced RJVC metabolic ratio events were found to predict an unfavorable outcome with an 86% specificity.

Conclusions

This observational prospective study of 18 severe aSAH patients shows that these two methods of investigation, either local (cMD) or global (RJVC) are complementary and that their combination, taking into account the above mentioned three biomarkers, , allows to increases the accuracy of outcome prediction, to reach a 90% sensitivity and a 71% specificity.

Reference

[1] Tholance Y. , Barcelos G. K., Dailler F., Renaud B., Marinesco S., Perret-Liaudet A., : Biochemical Neuromonitoring of poor-grade aneurysmal subarachnoid hemorrhage : comparative analysis of metabolic events detected by cerebral microdialysis and by retrograde jugular vein catheterization. Neurol.ogical Research, 2015, in press.

905
BRAIN-0876
Poster Session

Late Breaking Abstracts

PLANT NATURAL PRODUCT PUERARIN SUPPRESSED 6-HYDROXYDOPAMINE (6-OHDA)-INDUCED NEUROTOXICITY VIA INDUCING MITOCHONDRIAL ENZYME ARGINASE-2

J. Zhao[1], L. Lao[1], J. Rong[1]
[1]School of Chinese Medicine, The University of Hong Kong, Hong Kong, Hong Kong China

Aberrant production of nitric oxide (NO) isimplicated in the progression of neurodegenerative diseases. The aim of the presentstudy was to explore whether plant natural product puerarin could attenuatenitric oxide (NO)-mediated neurotoxicity via modulating the enzymes in theL-arginine-NO pathway. Neurotoxin 6-hydroxydopamine (6-OHDA) is well known toinduce neurodegeneration via a NO-dependent mechanism. We first validated thatpuerarin protected rat

dopamingeric PC12 cells against 6-OHDA-inducedneurotoxicity in a concentration-dependent manner. We subsequently profiled thecellular responses to puerarin by a proteomic response fingerprinting approach.A total of sixteen protein spots with > 1.5-fold change of intensity wereselected and identified by mass spectrometry. As one of puerarin-upregulatedproteins, mitochondrial arginase-2 hydrolyzes L-arginine to L-ornithine,thereby competing with neuronal NOS for substrate L-arginine in mitochondria.Thus, we hypothesize that puerain may attenuate nitric oxide (NO)-mediatedmitochondrial injury via increasing arginase-2 expression. Western blot andRT-PCR analyses confirmed that puerarin increased arginase-2 expression in aconcentration- and time-dependent manner. Accordingly, puerarin suppressed6-OHDA-induced NO production and neurotoxicity in PC12 cells and primary ratmidbrain neurons. Arginase inhibitor BEC diminished the effect of puerarin on6-OHDA-induced NO production and neurotoxicity. The activation of arginase-2 bypuerarin represents an endogenous mechanism for specific control of NO-mediatedmitochondrial damage. Thus, puerarin is useful lead for suppressing NO-mediatedneurotoxicity in neurodegenerative diseases.

906
BRAIN-0875
Poster Session

Late Breaking Abstracts

FACILITATING THE ADOPTION OF OXYGEN PARTIAL PRESSURE IMAGING WITH TWO-PHOTON MICROSCOPY

S. Sakadžić[1], S.A. Vinogradov[2], D.A. Boas[1]
[1]Optics Division,
Athinoula A. Martinos Center for Biomedical Imaging,
Massachusetts General Hospital and Harvard Medical School, Charlestown, Massachusetts 02129, USA
[2]Department of Biochemistry and Biophysics, University of Pennsylvania, Philadelphia, Pennsylvania 19104

Objectives: The assessment of brain oxygenation on the microscopic level has the potential to transform our understanding of important clinical problems, such as stroke, Alzheimer's disease, dementia, chronic hypertension, and brain cancer, facilitating the development of new therapies and helping to improve clinical imaging and treatment protocols. Until now, no technology has been capable of microscopic oxygen imaging in the brain with high spatial and temporal resolution. Over the past several years we have developed a method, termed two-photon phosphorescence lifetime microscopy of oxygen (2PLM), which has the unique capability of fulfilling this niche. This is the only imaging method that allows high resolution mapping of brain oxygenation in real time.

2PLM of oxygen is a combination of state-of-the-art two-photon enhanced phosphorescent probes and a unique variant of two-photon laser scanning microscopy - both of which are not presently available commercially. The transformative power of 2PLM of oxygen has been demonstrated and described in several high-impact publications (Sakadžić et al., 2010; Devor et al., 2011; Lecoq et al., 2011; Parpaleix et al., 2013; Spencer et al., 2014; Sakadžić et al., 2014; Gagnon et al., 2015), producing great interest in the neuroscience community. Consequently, we have been receiving requests from laboratories in the US and across the world to provide the probes and to assist in implementing this new technology. We are aiming to set up a self-sustaining resource that will promote widespread use of the two-photon oxygen imaging technology, making this new powerful method available to a broad group of neuroscience researchers.

References: Devor, A., Sakadžić, S., Saisan, P.A., Yaseen, M.A., Roussakis, E., et al. “Overshoot” of O2 Is Required to Maintain Baseline Tissue

Oxygenation at Locations Distal to Blood Vessels. J. Neurosci. 31, 13676–13681 (2011). Gagnon, L., Sakadžić, S., Lesage, F., Musacchia, J.J., Lefebvre et al. Quantifying the Microvascular Origin of BOLD-fMRI from First Principles with Two-Photon Microscopy and an Oxygen-Sensitive Nanoprobe. J. Neurosci. 35, 3663–3675 (2015). Lecoq, J., Parpaleix, A., Roussakis, E., Ducros, M., Houssen et al. Simultaneous two-photon imaging of oxygen and blood flow in deep cerebral vessels. Nat. Med. 17, 893–898 (2011). Parpaleix, A., Houssen, Y.G., Charpak, S. Imaging local neuronal activity by monitoring PO2 transients in capillaries. Nat. Med. 19, 241–246 (2013). Sakadžić, S., Mandeville, E.T., Gagnon, L., Musacchia, J.J., Yaseen, M.A. et al. Large arteriolar component of oxygen delivery implies a safe margin of oxygen supply to cerebral tissue. Nat. Commun. 5, 5734 (2014). Sakadžić, S., Roussakis, E., Yaseen, M.A., Mandeville, E.T., Srinivasan, V.J. et al. Two-photon high-resolution measurement of partial pressure of oxygen in cerebral vasculature and tissue. Nat. Methods 7, 755–759 (2010). Spencer, J.A., Ferraro, F., Roussakis, E., Klein, A., Wu, et al. Direct measurement of local oxygen concentration in the bone marrow of live animals. Nature 508, 269-273 (2014).

907
BRAIN-0896
Poster Session

Late Breaking Abstracts

CONTRIBUTION OF THE K63-DEUBIQUITINASE CYLINDROMATOSIS (CYLD) TO NEURONAL CELL DEATH AFTER FOCAL CEREBRAL ISCHEMIA

P. Scheffler[1], C. Schwicht[1], L. Meissner[1], F. Hellal[1], N. Plesnila[1]
[1]Experimental Stroke Research, Institut für Schlaganfall- und Demenzforschung (ISD), München, Germany

Objectives

After ischemic stroke, the affected tissue splits up into two different zones: the ischemic core, in which cells die quickly and are not accessible to treatment and the surrounding penumbra in which cells die with a delay of several hours. The precise molecular mechanisms which mediate delayed neuronal cell death are, however, not fully understood yet. The K63-deubiquitinating enzyme Cylindromatosis (CYLD) has been recently identified as key regulator of necroptosis, a form of regulated necrotic cell death. Necroptosis depends on the receptor interacting protein kinase 3 (RIP3) and seems to be responsible for cell death under physiological and several pathological conditions including stroke (Linkermann and Green 2014). Since the role of CYLD for delayed neuronal cell death after stroke is not known, we aimed to evaluate its contribution to ischemic brain damage.

Methods

Focal cerebral ischemia was induced by 1 hour occlusion of the Middle Cerebral Artery in CYLD-knock-out mice and their wild-type littermates. 24 hours after reperfusion the brains were harvested and processed for immunohistochemistry and Western blot to characterize the spatial and temporal expression of CYLD, respectively. Infarct volumes were evaluated by cresyl violet staining, neuronal cell death by TUNEL and NeuN co-labeling. Brain edema was quantified using the wet-dry method and neurological deficits were evaluated at 1h and 24h after reperfusion by the modified Bederson score.

Results

CYLD was mainly expressed in cortical and hippocampal neurons. Cerebral ischemia induced a decrease of CYLD expression in the affected hemisphere. In CYLD-deficient animals the ischemic lesion was significantly smaller than in WT littermates (27.3 ± 17.1% vs. 44.4 ± 13.7%, respectively; P=0.02) 24 hours after stroke. Co-labeling of TUNEL/NeuN revealed that deletion of CYLD increased survival of cortical neurons by more than 30% (74 ± 13% in CYLD-/- vs. 40 ± 13% in WT, P = 0.01) and CYLD-/- animals had a significantly better functional outcome (1.2 ± 0.7, 1.7 ± 0.5 in CYLD-/- *vs* WT, P=0.05). Brain edema formation was not affected by deletion of CYLD.

Conclusion

Our study shows that CYLD is expressed in the brain, that it is present in cortical and hippocampal neurons, and that it is down-regulated after cerebral ischemia. Most importantly deletion of CYLD reduces lesion size and the number of damaged neurons and improves functional outcome after experimental stroke. These findings suggest that CYLD may represent a novel molecular switch responsible for neuronal cell death after ischemic stroke.

Reference

Linkermann, A. and D. R. Green (2014). "Necroptosis." N Engl J Med **370**(5): 455-465.

908
BRAIN-0944
Poster Session

Late Breaking Abstracts

FEASIBILITY OF DIFFUSE CORRELATION SPECTROSCOPY FOR PROLONGED MONITORING OF CEREBRAL AUTOREGULATION DURING NEUROCRITICAL CARE

J. Selb[1], J. Sutin[1], P.I. Lin[1], S.C. Bechek[2], D.A. Boas[1], M.A. Franceschini[1], E.S. Rosenthal[2]
[1]Radiology, Massachusetts General Hospital, Charlestown, USA
[2]Neurology, Massachusetts General Hospital, Charlestown, USA

OBJECTIVES. Cerebral autoregulation (CA) is a protective mechanism that maintains adequate cerebral perfusion in response to varying cerebral perfusion pressure (CPP) [1]. CA can be impaired in a number of brain injuries [2], increasing the risk of secondary ischemic insults. Monitoring of cerebral blood flow (CBF) and assessment of CA are therefore essential components of neurocritical care. Continuous assessment of CA can be derived from 'reactivity indices', computed as moving correlation coefficients between CBF and the slow waves of CPP, or alternatively arterial blood pressure (ABP) [4]. Impaired autoregulation is characterized by CBF passively following CPP fluctuations, with high reactivity indices (>0.2-0.4). The most common CBF surrogate is CBF velocity in the large cerebral arteries assessed by transcranial Doppler [4], but TCD may be unstable over long monitoring epochs. Cerebral oximeters afford non-invasive monitoring of cerebral oxygenation (SO_2). The correlation between CPP and SO_2 [6] has shown clinical promise as a continuous index of autoregulation during surgery [7]. However, SO_2 is difficult to interpret without a measure of cerebral perfusion [8]. Diffuse correlation spectroscopy (DCS) is an emerging non-invasive optics modality that measures a CBF index (CBFi) by monitoring the rapid fluctuations of near-infrared light diffusing through moving red blood cells [9]. Here, we present initial data demonstrating the potential of DCS in cerebral perfusion and autoregulation monitoring among patients in the Neurosciences Intensive Care Unit (NeuroICU).

METHODS. Three patients with aneurysmal SAH were recruited from the Massachusetts General Hospital NeuroICU. After the patient's legal representative provided informed consent, DCS emitters and detectors were attached on the patient's scalp with a clinical adhesive. Data were acquired continuously for up to 20 hours, synchronously with invasive ABP and CPP. A static autoregulation curve was obtained by plotting the DCS-derived absolute CBFi vs. CPP over the whole duration of the recording. By analogy with the 'reactivity indices' previously defined [3], a continuous index of blood flow autoregulation BFAx was computed as the Pearson correlation coefficient, over a moving 5 min window, between the CBFi and the CPP time series down-sampled at 0.5Hz.

RESULTS. Figure 1 presents the dependence of CBFi and BFAx as a function of CPP for one patient over 2 hours. The static autoregulation curve on Fig.1a displays evidence of impaired autoregulation, as the autoregulatory plateau of CBF is only maintained for high CPP values above approximately 70 mmHg. At lower values, CBFi drops linearly with CPP. Using a threshold on BFAx of 0.3, Fig.1b presents indication of impaired

autoregulation for CPP<57 mmHg. The large error bars reflect the fact that instances of impaired autoregulation occurred at varying CPP over the course of the monitoring, suggesting the dynamic nature of the autoregulation disruption and the importance of continuous real-time monitoring.

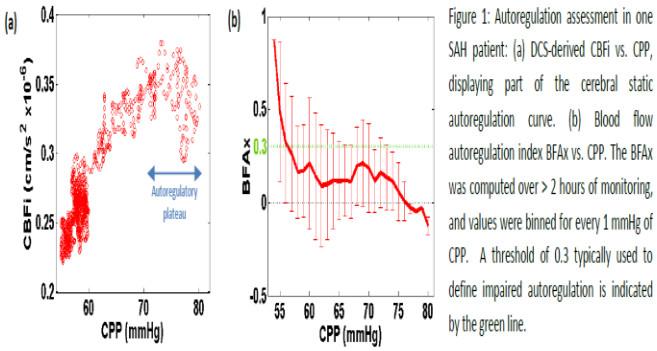

Figure 1: Autoregulation assessment in one SAH patient: (a) DCS-derived CBFi vs. CPP, displaying part of the cerebral static autoregulation curve. (b) Blood flow autoregulation index BFAx vs. CPP. The BFAx was computed over > 2 hours of monitoring, and values were binned for every 1 mmHg of CPP. A threshold of 0.3 typically used to define impaired autoregulation is indicated by the green line.

CONCLUSIONS. DCS is a promising modality for direct, non-invasive monitoring of CBF and continuous assessment of autoregulation in the NeuroICU.

REFERENCES.
[1] Czosnyka, *Neurocrit.Care* (2009)
[2] Diedler, *Stroke* (2009)
[3] Zweifel *Med.Eng.Phys.* (2014)
[4] Czosnyka, *Stroke* (1996)
[5] Lang, *Crit.Care Med.* (2003)
[6] Brady, *Stroke* (2007)
[7] Ono, *Anesth.Analg.* (2013)
[8] Boas, *Philos.Trans.R.Soc.* (2011)
[9] Durduran, *Neuroimage* (2014)

909
BRAIN-0945
Poster Session

Late Breaking Abstracts

MODULATION OF CEREBRAL ANGIOGENESIS: A THERAPEUTIC INTERVENTION TOWARDS ALZHEIMER'S DISEASE

C. Singh[1]
[1]*Medical Genetics, University of British Columbia, Vancouver, Canada*

The widely studied mechanism of pathogenesis of Alzheimer's Disease (AD), the Amyloid cascade hypothesis, states that the accumulation of Amyloid β (Aβ) in vasculature, caused by its impaired clearing, leads to the cognitive decline. The therapeutics based on this hypothesis have proven to be unsuccessful. Though Aβ accumulation is central for this hypothesis, it has been observed to be accumulated in the brain without AD symptoms. Vascular dysfunction is shown as a crucial pathological hallmark of AD, giving way to the alternative Angiogenesis hypothesis according to which the defective neurovasculature and impaired cerebral blood flow compromise the clearance of Aβ.

Our objectives are to establish hypervascularization via neoangiogenesis as a mechanistic explanation for amyloid associated Tight Junction pathology and to look for therapeutic interventions that modulate angiogenesis to restore the Blood Brain Barrier (BBB). We assumed that the BBB leakiness is due to amyloid triggered angiogenesis and not by vascular deterioration and apoptosis induced by hypoxia and neuroinflammation. We have validated this by using techniques like immunostaining and confocal imaging of brain tissues, quantification by western-blot analysis and microvessel density quantification with stereological analysis. Expression of tight junction proteins along with markers of apoptosis and angiogenesis demonstrated that the BBB integrity was compromised in aged Tg2576 mice when compared to age matched wild types. A significant increase in the incidence of disrupted

tight junction proteins was seen directly linked to the increased microvessel density but not to apoptosis[1]. This suggests that Aβ itself is vasculotropic and agrees with our assumption. We have shown that immunization with Aβ peptide not only resolved amyloid triggered neoangiogenesis but also reduced hypervascularity by 50% from diseased to normal state[2]. This provides scope for clinically approved anti-cancer drugs with anti angiogenic properties to modulate cerebral angiogenesis in order to ameliorate Aβ load, vasculature damage, hypervasularization and neuronal loss. Hence the facilitation of new therapeutic intervention for not only AD but also vascular diseases like Parkinson's disease, macular degeneration, hypotension and hypertension.

1. Biron, Kaan E., et al. "Amyloid triggers extensive cerebral angiogenesis causing blood brain barrier permeability and hypervascularity in Alzheimer's disease." *PloS one* 6.8 (2011): e23789.

2. Dickstein, Dara L., et al. "Aβ peptide immunization restores blood-brain barrier integrity in Alzheimer disease." *The FASEB journal* 20.3 (2006): 426-433.

910
BRAIN-0923
Poster Session

Late Breaking Abstracts

ASSESSMENT OF REORGANIZATION OF CEREBRAL ACTIVATION DURING WALKING ALONG A COMPLEX PATHWAY AFTER A SUB-CORTICAL STROKE USING DYNAMIC UPTAKE OF 18F-FDG

J.P. Soucy[1], C. Paquette[2]
[1]McConnell Brain Imaging Centre, Montreal Neurological Institute, Montreal, Canada
[2]Centre for Interdisciplinary Research in Rehabilitation of Greater Montreal, McGill University, Montreal, Canada

There is a higher incidence of falls in stroke victims than in the general population. Such events especially occur when patients are turning or performing wait transfer, and are a major source of injury in a generally older and frailer population. Brain imaging during prolonged, large-scale motion in humans is technically difficult, as it cannot be performed inside a scanner. There is therefore limited information of cerebral activity patterns during ambulation both in normal subjects and in stroke patients. Here, we have assessed whether ^{18}F-FDG PET imaging was capable of showing changes in cerebral activity linked to different ambulatory conditions in post-stroke patients as compared to normal controls.

In this preliminary study, four post-stroke subjects (all with lower limb involvement on the Chedoke-McMaster Scale; average time post-stroke: 25,8 months) and four matched controls were submitted on different days to 2 different locomotion tasks, one involving long segments of walking in a straight line with occasional 180° turns in-between segments, and the other with an irregular pattern involving multiple turns around circulation cones. Immediately before they started walking, subjects received an IV injection of on average 185 MBq of ^{18}F-FDG . They then walked for 40 minutes (allowing full uptake of the tracer). Within 10 minutes, they were brought to the imaging suite and imaged (20 minute emission scan followed by a 10 minutes transmission scan) on a Siemens HR+ PET system. Straight-walking activity was subtracted from that in the multiple-turns task to generate Z-score maps. This project was approved by the MNI REB.

Patterns of activation were much more asymmetrical in stroke subjects than in controls in the superior parietal lobules and somato-motor cortices, with more activity changes between the 2 conditions on the side of the stroke in those with a better functional outcome, and contralateral to the lesion in those with more functional limitations. Also, whereas controls showed increased activity in the vermis during the turning task, stroke subjects showed increased activity in cerebellar hemispheres.

It is therefore possible to study cerebral activation during sustained and complex motor sequences

using ^{18}F-FDG PET imaging, and to use this approach to evaluate normal and impaired gait. Our results show differences in the way stroke patients handle complex ambulatory patterns as compared to controls, with significant reorganization of activation patterns not only at the cerebral but also at the cerebellar level. We are continuing acquisition of data to confirm the present findings, qhich could help better understand the mechanisms leading to falls in such patients.

911
BRAIN-0942
Poster Session

Late Breaking Abstracts

INFLUENCE OF APOE E4 ON CSF BIOMARKERS OF THE NEUROVASCULAR UNIT DURING MILD DEMENTIA AND ALZHEIMER'S DISEASE

M.D. Sweeney[1], A.P. Sagare[1], D.A. Nation[2], M.R. Halliday[1], A.M. Fagan[3], J.C. Morris[4], B.V. Zlokovic[1]
[1]Department of Physiology and Biophysics, Zilkha Neurogenetic Insitute Keck School of Medicine University of Southern California, Los Angeles, USA
[2]Department of Psychology, University of Southern California, Los Angeles, USA
[3]Department of Neurology, The Hope Center for Neurodegenerative Disorders The Knight Alzheimer's Disease Research Center Washington University School of Medicine, St. Louis, USA
[4]Department of Neurology, The Hope Center for Neurodegenerative Disorders Washington University School of Medicine, St. Louis, USA

OBJECTIVES: Alzheimer's disease (AD) is characterized by amyloid-β (Aβ) plaques, tau tangles, gliosis, and neuronal injury and loss. The influence of vascular dysfunction in the etiology of AD is becoming increasingly apparent [1-2]. In sporadic AD, the major genetic risk factor is apolipoprotein E (*APOE*) ε4 allele which has been shown to modulate both vascular integrity [3] and Aβ clearance from the brain [4]. A clinical need exists to identify reliable biomarkers for early AD diagnosis and for evaluating the effectiveness of therapeutics in clinical trials [5]. Cerebrospinal fluid (CSF) biomarkers of blood-brain barrier (BBB) breakdown associate with hippocampal BBB permeability in mild dementia [6] and are increased in preclinical *APOE* ε4 carriers [7]. The present study aimed to assess the impact of *APOE* ε4 allele on neurovascular biomarker concentrations as related to early cognitive impairment.

METHODS: Multiple biomarkers of injury to the neurovascular unit were investigated in a population of 91 subjects. Subjects were stratified by cognitive status (cognitively normal, mild cognitive impairment, and mild AD) and *APOE* genotype (ε3/ε3 and ε3/ε4). Protein concentrations of CSF biomarkers reflecting vascular injury, inflammation, neuronal injury, and Aβ peptides were detected via enzyme-linked immunosorbent assays (ELISA), multiplex assays, or quantitative immunoblots. This study was approved by the Institutional Review Board and subjects have signed written informed consent.

RESULTS: Biomarkers of BBB breakdown, namely blood-derived molecules albumin and fibrinogen, show an age-dependent increase in *APOE* ε4 carriers that increases during early cognitive impairment. Adhesion molecules are biomarkers of endothelial vascular injury, and soluble vascular cell adhesion molecule 1 (sVCAM-1) and soluble intracellular adhesion molecule 1 (sICAM-1) associate with BBB breakdown in only *APOE* ε4 carriers. During mild AD, inflammatory cytokines and neuronal injury biomarkers are not altered regardless of *APOE* genotype, and Aβ42 levels are lower in *APOE* ε4 carriers. These data reveal that vascular injury CSF biomarkers are altered in *APOE* ε4 carriers prior to non-carriers, and they precede astrocyte, inflammatory, neuronal, and Aβ biomarkers.

CONCLUSIONS: Biomarkers of BBB breakdown and vascular injury are changed in CSF during early cognitive impairment, accelerated in *APOE* ε4 carriers. These data show that biomarkers of the neurovascular unit are differentially and

temporally altered during mild dementia, beginning with changes in vascular injury biomarkers, which suggests that a molecular algorithm can define stages of cognitive impairment due to AD.

REFERENCES: [1] Zlokovic. *Nat Rev Neurosci* 2011; 12:723-738. [2] Montine et al. *Neurology* 2014; 83:851-860. [3] Bell et al. *Nature* 2012; 485:512-516. [4] Deane et al. *J Clin Invest* 2008; 118:4002-4013. [5] Sweeney et al. *J Cereb Blood Flow Metab*; in press. [6] Montagne et al. *Neuron* 2015; 85:296-302. [7] Halliday et al. *JAMA Neurol* 2013; 70:1198-1200.

912
BRAIN-0900
Poster Session

Late Breaking Abstracts

IMAGING GLUCOSE ASSIMILATION IN MICE BRAIN WITH SUBCELLULAR RESOLUTION

Y. Takado[1], G. Knott[2], B. Humbel[3], M. Masoodi[4], S. Escrig[1], A. Meibom[1], A. Comment[5]
[1]Laboratory for Biological Geochemistry, École polytechnique fédérale de Lausanne, Lausanne, Switzerland
[2]Centre Interdisciplinaire de Microscopie Electroni que, École polytechnique fédérale de Lausanne, Lausanne, Switzerland
[3]Electron Microscopy Facility, Université de Lausanne, Lausanne, Switzerland
[4]Nestlé Institute of Health Science, École polytechnique fédérale de Lausanne, Lausanne, Switzerland
[5]Institute of Physics of Biological Systems, École polytechnique fédérale de Lausanne, Lausanne, Switzerland

Objectives: In addition to being the brain's primary source of energy, glucose is also used in the anabolic processes maintaining its cellular structures [1]. Little is known, however, about the spatial distribution of assimilated glucose at the cellular level. To investigate this, we correlated electron microscopy (EM) and Nano Secondary ion mass spectroscopy (NanoSIMS) images of thin brain tissue sections from mice injected with ^{13}C-labelled glucose. Importantly, the use of stable isotopes does not impair glucose metabolism.

Methods: Adult mice were injected [U-^{13}C]glucose aqueous solutions (i.p.) at different time intervals (1-3 h). For longer labelling periods (up to 48 h), fasted mice were exclusively fed with a 20% w/v [U-^{13}C]glucose solution ad libitum. At the end of the labeling period, the mice were deeply anaesthetized and perfused via the heart with chemical fixatives. Part of the motor cortex was embedded in resin [2]. EM images spanning over the entire cortex were acquired using a scanning electron microscope. The same areas were imaged by NanoSIMS to reveal the ^{13}C distribution with subcellular resolution [3].

Results: Correlative EM-NanoSIMS images of the mouse brain revealed: 1) differences in ^{13}C-enrichment level among the various cell types identified in the cortical layer, with neurons significantly more enriched than astrocytes, 2) different ^{13}C-enrichment dynamics in neurons and astrocytes, 3) that ^{13}C-enrichment in RNA containing structures is significantly higher than in DNA containing structures, 4) a significant amount of ^{13}C-enrichment in dendrites and synapses.

Conclusions: We have developed an imaging method for investigating glucose assimilation at the single cell level in the mouse brain. High-resolution images demonstrate the capability to differentiate glucose assimilation across different regions of the brain with subcellular resolution (i.e. distinguishing individual sub-cellular compartments, such as nucleolus, dendrites, and synapses). Correlated EM-NanoSIMS imaging combined with injections of [U-^{13}C]glucose is a promising method for further understanding the biosynthetic role of glucose, and the fate of many other metabolic substrates in the brain.

References:

1) Vrba R (1964) UTILIZATION OF GLUCOSE CARBON IN VIVO IN THE MOUSE. Nature 202:247-249
2) Knott GW, Quairiaux C, Genoud C, Welker E (2002) Formation of Dendritic Spines with

GABAergic Synapses Induced by Whisker Stimulation in Adult Mice. Neuron 34:265-273
3) Takado Y, Knott G, Humbel BM, Escrig S, Masoodi M, Meibom A, Comment A (2015) Imaging liver and brain glycogen metabolism at the nanometer scale. Nanomedicine: Nanotechnology, Biology and Medicine 11:239-245

913
BRAIN-0908
Poster Session

Late Breaking Abstracts

NEONATAL DOMOIC ACID DECREASES IN VIVO BINDING OF [11C]YOHIMBINE TO ALPHA-2 ADRENOCEPTORS IN ADULT RAT BRAIN

M.B. Thomsen[1], T.P. Lillethorup[1], S. Jakobsen[1], E.H. Nielsen[1], M. Simonsen[1], G. Wegener[2], R.A. Tasker[3], A.M. Landau[1]
[1]Department of Nuclear Medicine and PET Center, Aarhus University and Hospital, Aarhus C, Denmark
[2]Translational Neuropsychiatry Unit, Aarhus University, Risskov, Denmark
[3]Department of Biomedical Sciences, University of PEI, Charlottetown, Canada

Objectives: Noradrenaline reduces neuronal excitability [1], has anticonvulsant effects [2] and is protective against seizure onset. We investigated the role of alpha-2 adrenoceptors in a neonatal domoic acid (DOM) rat model of epilepsy and studied the effects of neuroinflammation.

Methods: Male Sprague-Dawley rats (n=6-7 per group) were injected (s.c.) daily from postnatal day 8-14 with saline or one of two low sub-convulsive doses, 20µg/kg [DOM20] or 60µg/kg [DOM60] of DOM, an AMPA/kainate receptor agonist. The behaviour of the rats was observed in an open field test, a social interaction test and the forced swim test at day 50, 75 and 98, respectively. At ~120 days of age 3-4 rats per group were injected with [^{11}C]yohimbine, an alpha-2 adrenergic receptor antagonist, and scanned in a Mediso micro positron emission tomography (PET) scanner, to measure alpha-2 adrenoceptor binding. The volume of distribution (V_T) was obtained by Logan plot, using the arterial plasma curve from the rat as the input curve. The rats (n=1-3 per group) were later scanned with [^{11}C]PK11195, a tracer of activated microglia, and standardized uptake values, corrected for injected dose and body weight, were used for simple semi-quantitative analysis. MicroPET images were analyzed using PMOD software and registered to an average Sprague-Dawley rat MRI brain atlas to acquire data in limbic and cortical regions of interest.

Results: In behavioural testing DOM60, and to a lesser extent DOM20 rats, spent more time in the periphery during the open field test and less time struggling in the forced swim test compared to the saline treated rats. Analysis of the microPET data revealed that relative to saline treated rats, DOM60 rats had a 40-47 % reduction in [^{11}C]yohimbine binding in the hypothalamus, amygdala, hippocampus, cingulate cortex and medial and orbital prefrontal cortex. Preliminary data further suggest that DOM60 rats may have a marked increase in [^{11}C]PK11195 retention in the whole brain.

Conclusion: We conclude that neonatal administration of DOM combined with the potential stress associated with behavioural testing results in a significant decrease in [^{11}C]yohimbine binding in limbic and cortical brain regions. We suggest that the observed downregulation of alpha-2 adrenoceptors is a result of elevated extracellular noradrenaline which may represent a form of preconditioning to decrease seizure susceptibility of the brain.

References:

1. Barry, D.I., et al., *Grafted noradrenergic neurons suppress seizure development in kindling-induced epilepsy.* Proc Natl Acad Sci U S A, 1987. **84**(23): p. 8712-5.

2. Loscher, W. and S.J. Czuczwar, *Comparison of drugs with different selectivity for central alpha 1-and alpha 2-adrenoceptors in*

animal models of epilepsy. Epilepsy Res, 1987. **1**(3): p. 165-72.

914
BRAIN-0902
Poster Session

Late Breaking Abstracts

LONGITUDINAL [11C]PBR28 IMAGING OF ACUTE NEUROINFLAMMATION IN A CLINICALLY RELEVANT ISCHEMIC STROKE RAT MODEL

M. Tóth[1], P. Little[1], F. Arnberg[1], J. Häggkvist[1], J. Mulder[2], A. Varrone[1], C. Halldin[1], B. Gulyás[1], S. Holmin[1]
[1]Department of Clinical Neuroscience, Karolinska Institutet, Stockholm, Sweden
[2]Department of Neuroscience, Karolinska Institutet, Stockholm, Sweden

Objectives
Adequate estimation of neuroinflammatory processes following ischemic stroke is essential for better understanding of disease mechanisms, and for the development of treatment strategies. With [^{11}C]PBR28 (radioligand for the 18 kDa Translocator Protein(TSPO)), we monitored longitudinally the inflammatory response after transient cerebral ischemia in rats, using a recently developed rat stroke model which produces isolated focal cortical infarcts with clinical relevance in size and pathophysiology [1].

Methods
Six Sprague-Dawley rats (300-400g) were anaesthetized with isoflurane in 100% O_2. Occlusion of the M2 segment of the middle cerebral artery (M2CAO) was maintained for 90 min, and animals were imaged at 1, 4, 7 and 14 days after reperfusion (one animal missing day 14) with a bolus injection of [^{11}C]PBR28 through tail vein cannulation in nanoScan® PET/MRI and PET/CT systems (Mediso Ltd, Budapest Hungary). PET scans were co-registered to individual T1-weighted MRI images in PMOD 3.3 (Zurich, Switzerland). As a primary outcome BP_{ND} was estimated with SRTM, using the contralateral cortex as reference region.

Results
[^{11}C]PBR28 showed high uptake in the Infarct region from day 4 with gradual decrease at later time points. At day 4, 7 and 14 there was a significantly increased uptake of [^{11}C]PBR28 in the Infarct region compared to the Contralateral Cortex on the same day and the Infarct region at day 1. No significant increase was detected in the Contralateral Cortex during the 14 days of imaging. BP_{ND} in the Infarct region was 0.22 ± 0.19 (n = 6) on day 1 and there was a significant increase in BP_{ND} on day 4: 1.73 ± 0.78 (n = 6), day 7: 1.59 ± 0.96 (n = 6) and day 14: 0.86 ± 0.64 (n = 5) compared to day 1 ($p < 0.05$).

Conclusions
The longitudinal follow up of inflammatory response with the TSPO radioligand [^{11}C]PBR28 in rats after cerebral ischemia showed significantly up-regulated TSPO binding in the Infarct region from day 4, indicating activation of microglia. This activation gradually decreased between day 4 and day 14. The present M2CAO model appears to be well suited for studies on neuroinflammation with a more rapid response compared to the MCAO model [2].

References
[1] Arnberg et al. (2012) Stroke 43 (9):2437-2443.
[2] Martín et al. (2010) J Cereb Blood Flow Metab 30(1):230–241

Acknowledgements
The research leading to these results has received funding from the European Union's Seventh Framework Programme (FP7/2007-2013, GA 278850, INMiND), Uppdrag Besegra Stroke (supported by the Swedish Heart–Lung Foundation, Karolinska Institutet, Friends of Karolinska Institutet USA and the Swedish order of St John), Söderbergska Stiftelsen and COST Action TD1007 ('Bimodal PET-MRI molecular imaging technologies and applications for in vivo monitoring of disease and biological processes").

915
BRAIN-0903
Poster Session

Late Breaking Abstracts

CEREBRAL DYSGEMIA OF CHILDREN AND TEENAGERS

A. Tsokolov[1], V.N. Starykov[1]
[1]Federal State Agency,
«1409 Naval hospital of the Baltic Sea fleet»,
Kaliningrad, Russia

The problem of venousbrain circulation disorder in childhood is of high priority at present.

Research objective: Assessment of cerebral venous hemodynamics inchildren and teenagers having cranialgia with updating cause-effect relationsof venous discirculation.

According to the data ofUltra Sonic Testing (in C- and PW- modes) 109 patients (at the age from 2 to18) it was found that discirculation in thesystem of vertebral veins is linked with apparent extravasal effects onbloodstream in internal jugular vein (with vessel compression on the side ofvasoconstriction registration) (r = +0.67; p<0.05), spasmsof posterior cerebral artery (r =+0.63; p<0.05), coiling of internal carotid artery andvertebral artery (r = +0.20 - +0.32, p<0.05). In case of discirculation in the system of internal jugular vein, the changesmentioned are interrelated with extravasal compression on the level of internaljugular vein sorrunding soft tissues or compression in the bone canal (r=+0.76; p<0.05), anterior cerebralartery spasms, hyperperfusion of vertebral artery and posterior cerebral artery (p<0.05).Intracranial venous discirculation depends on the straightness of vertebralartery in the bone canal (for left vertebral artery r= +0.33; p<0.05), discirculation intensity onthe level of vertebral vein (for Vmax right vertebral vein r= +0.73, p>0.05).

Vasoconstriction inthe vein of Galen is accompanied by ipsilateral hypersthenia of vertebralartery, internal carotid artery and middle cerebral artery (effect ofreflectory changes), and is also interrelated with flexures, sigmoid coiling ofinternal carotid artery.

The link of “headachesyndrome” with accelerated venous blood flow along the veins of Galen turnedout to be quite low (r = +0,22, p<0,05).

Conclusion. Main causes of children’s vasoconstriction are either congenitalpathology of cervical spine (with arcuation and tortuosity of bone canal), or “birthinjuries with pseudo-luxation of cervical vertebrae”.

916
BRAIN-0933
Poster Session

Late Breaking Abstracts

AMPHETAMINE INDUCED PSYCHOMOTOR IMPROVEMENT IN RELATION TO STRIATAL DOPAMINE RELEASE IN HEALTHY SUBJECTS

J. Van der Aart[1], H. Van Gorsel[1], M. De Kam[1], M. Yaqub[2], A.A. Lammertsma[2], B.N.M. Van Berckel[2], M. Timmers[3], P. De Boer[3], J.M. Van Gerven[1]
[1]Centre for Human Drug Research, Centre for Human Drug Research, Leiden, Netherlands
[2]Radiology & Nuclear Medicine, VU University Medical Centre, Amsterdam, Netherlands
[3]Janssen Pharmaceutica N.V, Janssen Research and Development, Beerse, Belgium

Objectives. PET with dopaminergic tracers such as [^{11}C]raclopride have been used to measure psychostimulant induced dopamine release in humans since the early 1990s. Preclinical and clinical results show a large variability in behavioural and neurochemical responses to amphetamine. In this study, we investigated the relationship between d-amphetamine induced striatal dopamine release and psychomotor performance enhancement within subjects.
Methods. 15 healthy male volunteers (mean age 32.9 ±5.6) completed two 60 minute [^{11}C]raclopride PET scans on separate days; at

baseline and 1 hour after oral administration of 20mg d-amphetamine. PET timing post d-amphetamine was replicated from Boileau et al. (2006) [1]. PET scans were co-registered to the corresponding individual MRI acquired on a Philips Ingenuity TF combined PET/MR scanner. Regions of interest (ROIs) were defined using PVE-lab, a software program using a probability map of 35 delineated ROIs. Time activity curves were analysed using a basis function SRTM method with the cerebellum as reference tissue. Dopamine D_2/D_3 receptor occupancy was derived from change in BP_{ND} pre- and post d-amphetamine. All subjects completed multiple runs of the NeuroCart® test battery, which included tests of psychomotor performance such as adaptive tracking, body sway, saccadic and smooth pursuit eye movements, finger tapping and the stop signal task (SST). Pre-dose NeuroCart® scores were averaged over 5 runs following 2 training runs. Post d-amphetamine scores were averaged over 3 runs that were completed after the PET scan. Serum d-amphetamine levels were measured after the PET scan at the start of each NeuroCart® run (3, 4 and 6hrs post-dose).

Results. Subjects showed statistically significant ($p<0.0001$) improvement in all psychomotor tasks after d-amphetamine (Table 1). SST Stop Signal RT was not different between treatment days. Statistically significant [^{11}C]raclopride BP_{ND} reductions ($p<0.05$, single-sided paired T-test) were observed in the caudate nucleus (2.6% ± 5.7), putamen (5.5% ± 9.8%), and pallidum (5.5% ± 8.5%) following d-amphetamine administration. However, up to 7 subjects (depending on the ROI) showed negligible or negative occupancy. Mean serum d-amphetamine C_{max} was 40 ±4.1 ng/mL at 3.9 ±1.1 hours post-dose. On the SST, the number of missed Go-trials correlated negatively with D_2/D_3 receptor occupancy in the caudate (Spearman's ρ=-0.61, p=0.01). Correlations of NeuroCart® performance and occupancy in other ROIs did not reach statistical significance.

Conclusions. 20 mg d-amphetamine led to significant increase in striatal dopamine levels and performance improvement in the NeuroCart® tasks. Striatal occupancy values showed a high variability between subjects, possibly due to the timing of the PET scan in relation to the dosing of d-amphetamine. This study provides preliminary evidence of a positive relationship between psychomotor performance and d-amphetamine induced elevated brain dopamine levels.

References [1]. Boileau, I., Dagher, A., Leyton, M., Gunn, R., Baker, G., & Diksic , M., et al. (2006). Modeling Sensitization to Stimulants in Humans: A [11C]Raclopride/Positron Emission Tomography Study in Healthy Men, Arch Gen Psychiatry, 63, 1386-1395.

NeuroCart® test	Score (drug - baseline)	Score P-value (paired T-test)	Correlation with caudate D_2/D_3 occupancy (Spearman's ρ, *p=0.01)
Adaptive tracking (%)	4.30	p=<.0001	-0.17
Saccadic Peak Velocity (deg/s)	51.78	p=<.0001	-0.01
Saccadic Reaction Time (ms)	-15.0	p=<.0001	-0.13
Smooth Pursuit (%)	-3.62	p=<.0001	-0.23
Body sway (mm)	-30.8	p=<.0001	0.01
Tapping: Mean of 5 trials (taps/10 s)	2.74	p=<.0001	0.16
SST: Total missed Go-trials	-4.13	p=<.0001	-0.61*
SST: Mean RT Go-trials (ms)	31.58	p=0.022	-0.31
SST: Stop Signal RT (ms)	-5.27	p=0.508	0.14
SST: Total correct Stop-trials	0.64	p=0.039	0.03
SST: Mean RT Stop-trials (ms)	26.38	p=0.058	-0.34

917
BRAIN-0919
Poster Session

Late Breaking Abstracts

A COST EFFICIENT APPROACH TO CLARITY

M. Vanagel[1], *C. Frare*[2], *B. Rasley*[1]
[1]*Chemistry and Biochemistry, University of Alaska Fairbanks, Fairbanks, USA*
[2]*Institute of Arctic Biology, University of Alaska Fairbanks, Fairbanks, USA*

Objective: The CLARITY technique, developed in 2014 by Chung et al. [1], provides a new and efficient way to visualize long range cellular projections and neuronal circuit wiring in intact, un-sectioned tissue. The costs associated with the original procedure can make CLARITY prohibitively expensive to perform. Here, aspects from other immersion based imaging techniques are combined with an adaption of the CLARITY tissue clearing protocol to create a more cost effective method for clearing and imaging thick tissue samples.

Methods: Brain samples up to 3cm thick were immersed in an acrylamide rich hydrogel (40% acrylamide, 2% Bis-acrylamide, 16% PFA). Polymerization was initiated by VA-044 (10% wt, Wacko, Japan) Once a solid state indicated polymerization was complete, light scattering lipids were passively removed from the tissue by incubating the brain at 50°C in a solution containing sodium dodecyl sulfate (SDS, 15%). Cleared brains were immersed in a sorbitol based refractive-index matching solution (70% w/v sorbitol in 0.02M PB) described in Yang et al. [2]

Results: 4 brain samples (1-3cm thick from a 3 month old rat) became transparent within 4 weeks while retaining structural integrity. Methods are currently being developed for the staining and immunolabeling of these thick brain sections. The sorbitol based mounting solution was shown to have a refractive index of 1.44, less than 1% different than that of FocusClear – the costly mounting solution used in Chung et al. [1] Overall cost of chemicals was 100 to 400 times less than the cost of chemicals used in the electrophoretic method described in Chung et al. [1]

Conclusions: We have shown that passive clearing can be achieved at significantly lower cost than the electrophoretic method described in Chung et al.[1] A sorbitol based alternative to FocusClear, the mounting solution most commonly used to image CLARITY samples, can be prepared at a total cost that is 400 times cheaper than FocusClear and has been shown to give comparable imaging depths. [2] With passive clearing by the CLARITY technique and an alternative mounting solution that can be prepared for a total cost of about $0.2 per mL, tissue clearing and whole brain imaging and molecular phenotyping is now affordable for practically any lab. This cost optimized approach to the CLARITY technique is now being optimized for staining and immunocytochemistry.

Reference:

[1] Chung et al. (2013) Structural and molecular interrogation of intact biological systems. Nature 497:332–337.

[2] Yang et al. (2014) Single-Cell Phenotyping within Transparent Intact Tissue through Whole-Body Clearing. Cell 158:945-958.

918

BRAIN-0915

Poster Session

Late Breaking Abstracts

PRELIMINARY FINDINGS OF DIFFUSION KURTOSIS IMAGING IN COMATOSE CARDIAC ARREST PATIENTS

O. Wu[1], K. Mott[1], M. Villien[1], W.A. Copen[2], M.B. Westover[3], B.L. Edlow[3], J.L. Januzzi[4], J.T. Giacino[5], P.W. Schaefer[2], D.M. Greer[6], E.S. Rosenthal[3]

[1]Athinoula A. Martinos Center for Biomedical Imaging, Massachusetts General Hospital, Charlestown, USA

[2]Dept of Radiology, Massachusetts General Hospital, Boston, USA

[3]Dept of Neurology, Massachusetts General Hospital, Boston, USA

[4]Dept of Cardiology, Massachusetts General Hospital, Boston, USA

[5]Dept of Psychiatry, Spaulding Rehabilitation Hospital, Charlestown, USA

[6]Dept of Neurology, Yale School of Medicine, New Haven, USA

Objectives:

Once circulation has been reestablished in cardiac arrest (CA) patients, the likelihood of neurologic recovery is the key determinant in decisions regarding withdrawal vs. continuation of life-sustaining treatment. Diffusion-weighted MRI (DWI) has proven to be sensitive to brain injury after CA; however, DWI's specificity in predicting neurologic outcome is questioned. Changes in diffusional heterogeneity measured by diffusion kurtosis MRI (DKI[1]) have been proposed as a more sensitive and specific marker for microstructural injury than fractional anisotropy (FA). We examined whether DKI may provide further insight into tissue integrity and potential for recovery of consciousness in comatose cardiac arrest patients.

Methods:

DKI from 6 CA patients and one 26-year-old female healthy control were analyzed. The CA patients were comatose at admission and were treated with therapeutic hypothermia. All subjects were imaged on a 3T scanner. DKI was acquired using 30 diffusion-encoding directions with b-values=1000 s/mm^2, and 2000 s/mm^2 (3×3×3 mm^3) and 10 b-value=0 s/mm^2 images. Mean kurtosis (MK), axial kurtosis (AK), radial kurtosis (RK), mean diffusivity (MD), axial diffusivity (AD), radial diffusivity (RD) and FA maps were calculated using the Diffusion Kurtosis Estimator.[2] Median whole-brain values in patients with poor outcomes (failure to regain consciousness before discharge) were compared with those from patients who regained consciousness (two-tailed t-test). Average values from the healthy control were calculated for comparison.

Results:

Patients' mean±SD age was 39±19, and 83% were male. Duration of arrest was 45±19 min, with one patient's onset time unclear. 50% were conscious by discharge and 50% were dead due to withdrawal of life-sustaining treatment. Figure 1 shows examples of FA, MD, and AK in the healthy control and two coma patients, one with good and one with poor outcome. There was a significant difference in time-to-MRI between good and poor outcome groups (10±1.7 vs 3±0 days, P=0.02). Significant differences across all metrics were found between good and poor outcome groups except for FA (Figure 2). Greatest differences were found axially, with a 46% increase in AK and a 28% decrease in AD.

Conclusion:

DKI metrics are more sensitive to brain injury post-cardiac arrest than FA. Patients who failed to regain consciousness demonstrated higher values for all kurtosis metrics, particularly axially, consistent with findings from stroke patients.[3] Differences in timing of MRI acquisition and potential bias from self-fulfilling prophecy are limitations of these preliminary findings. Nonetheless, this is the first report investigating acute diffusional heterogeneity changes in post-cardiac arrest patients. Whether kurtosis metrics add further prognostic power to diffusivity metrics remains to be determined.

References:

1. Jensen JH. MRM. 2005; 53, 1432-40.
2. Tabesh A. MRM. 2011; 65, 823-36.
3. Jensen JH. NMR Biomed. 2011; 24, 452-7.

Figure 1: Example FA, MD and AK images from a healthy control and two CA patients .

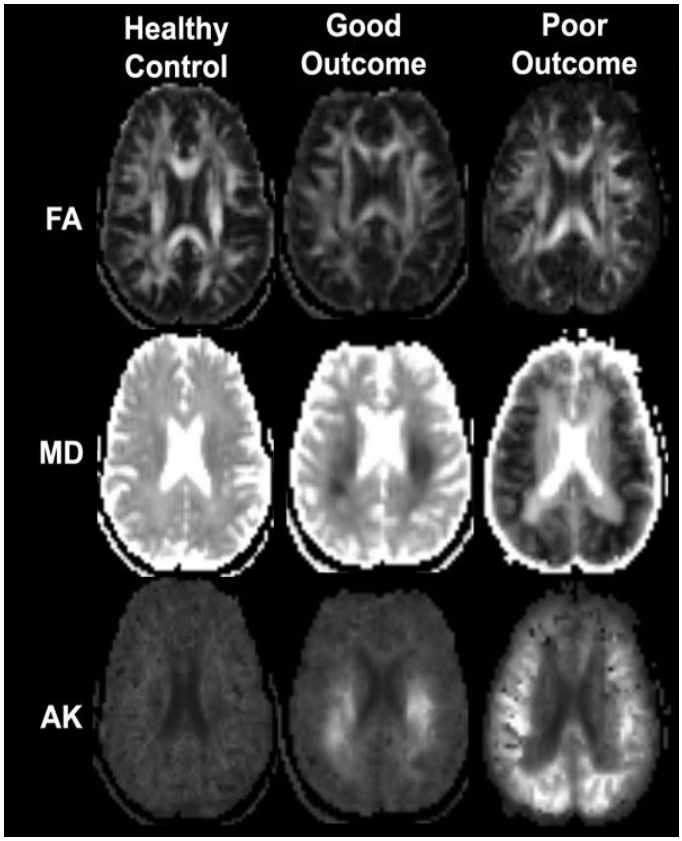

Figure 2: Differences between whole-brain diffusivity and kurtosis metrics in a healthy control and in patients with good and poor outcome. *P=0.01; †P =0.02 good vs poor outcome.

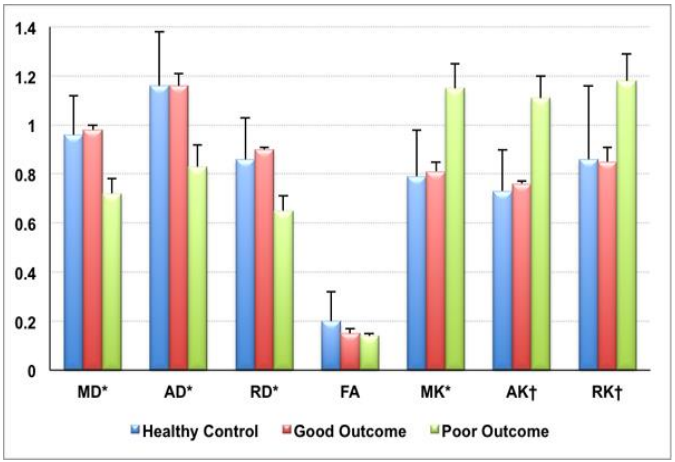

919
BRAIN-0789
Non-Registered Abstracts

STROKE RISK FACTORS AND THEIR INFLUENCE ON SURVIVAL OF PATIENTS DURING 28 POSTSTROKE DAYS

S. Agaev[1], M. Azermacheva[1], O. Antuchova[2], V. Alifirova[1]
[1]Neurology and Neurosurgery, Siberian state medical university, Tomsk, Russia
[2]Neurology, FGBU SibFNKTs FMBA Med Center № 2, Seversk, Russia

The problem of a stroke is the focus the medical community that is caused high rates of morbidity, mortality and disability of the survived patients (85%). The purpose of research is studying of risk factors (RF) of stroke.

Methods

Prevalence of risk factors and their influence on development of a fatal outcome in 853 patients with a stroke is studied. The outcome of a stroke was estimated for the 28th day from the beginning of a disease. All available sources of information were used: data of interview and examination of the patients, interview to relatives, patient's records, cards of the outpatient, cards of calls of ambulance and the medical death certificates.

Results

The rate of stroke in men was 45,5%, women – 54,5%. The prevalence of arterial hypertension was 79,4% (women>men). AH of stage I met more often at the survived patients while AH of stage II and III prevailed in group of the dead. The most of patients with AH didn't receive regular hypotensive therapy (72,97%). It was noticed that patients were treated more often sporadically or not treated absolutely in group of the dead. The prevalence of smoking was 30,4% in the studied group (men>women). Prevalence of cardiovascular diseases was 44,2% (women>men). The obliterating atherosclerosis of the lower extremities takes a leading place among vascular diseases, and ischemic heart disease (IHD) - among heart diseases which main form is angina pectoris. IHD is associated more often with a fatal outcome. Prevalence of atrial fibrillation was 16,8% in the studied group (women>men). The myocardial infarction was observed in 13.3% among the examined patients. This indicator was much higher at men, than at women. Diabetes mellitus was revealed at 14,4%, prevalence was much higher at women. When comparing the groups which survived and died it is established that diabetes mellitus is associated with a fatal stroke more often.

Frequency of all RF was higher in the group of the died patients. It is established that one RF is observed at 20,98% examined. The most of patients had a combination of two (33,2%), three (25,2%), four (12,7%), five and more (3,9%) RF.

Conclusion

AH (79,4%), heart diseases (44,2%) and smoking (30,4%) are the most significant RF of a stroke in the studied population. The prevalence of smoking is 7 times higher, of myocardial infarction is twice higher in group of men. AH, heart diseases meet in group of women more often, prevalence of diabetes mellitus is 3 times higher. AH stage II and III, absence or an irregularity of reception the antihypertensive drugs, existence of angina pectoris, atrial fibrillation, diabetes mellitus were the adverse factors influencing a stroke outcome. Results of the analysis of material give the chance to

develop reasonable recommendations about prevention and the organization of medical care by the patient with acute cerebrovascular disease.

920
BRAIN-0656
Non-Registered Abstracts

PEDIATRIC STRIATAL WHITE MATTER IS RESISTANT TO ISCHEMIA-INDUCED DAMAGE

J. Ahrendsen[1], S. Hickey[1], H. Grewal[2], R. Traystman[3], P. Herson[2], W. Macklin[1]
[1]Cell and Developmental Biology, University of Colorado School of Medicine, Aurora, USA
[2]Anesthesiology, University of Colorado School of Medicine, Aurora, USA
[3]Pharmacology, University of Colorado School of Medicine, Aurora, USA

Introduction: White matter injury following ischemic stroke is a major cause of functional disability. In experimental models of ischemic stroke, in addition to significant neuronal death, oligodendrocytes, the myelin producing cells in the central nervous system, and myelinated axons are also injured. Age-related changes in white matter vulnerability to ischemia have been extensively studied and these studies suggest that both the perinatal and the aged periods are times of increased white matter vulnerability. However, sensitivity of white matter following stroke in the pediatric brain has not been evaluated. Interestingly, the late pediatric period is an important developmental stage, as it is the time of maximal myelination. Due to the high metabolic activity of myelinating oligodendrocytes, we hypothesized that pediatric white matter would be particularly sensitive to ischemia.

Methods: We have developed a middle cerebral artery occlusion (MCAO) mouse model of pediatric stroke in order to understand the cellular responses unique to the juvenile developmental time period. Postnatal day 20-25 or adult (8-12 weeks old) male mice were subjected to 45 minutes of reversible MCAO with an intraluminal filament. Animals were analyzed at 24 hr, 3, 7 and 30 days of recovery.

Results: Neurons in pediatric striatum were vulnerable to ischemic damage, and neuronal death was comparable in pediatric and adult mice following ischemia. By contrast, actively myelinating striatal oligodendrocytes in the pediatric brain were highly resistant to ischemia, whereas adult oligodendrocytes were quite sensitive. As a result, myelin sheaths remained remarkably intact and axons survived well in the injured striatum of pediatric mice, while significant axon damage and tissue loss was observed in adult striatum. In addition to relative resistance of pediatric white matter, we observe very different glial responses in pediatric and adult mice after MCAO, including differences in astrogliosis, fibrosis, NG2-cell reactivity, and vascular integrity.

Conclusions: Together, these results demonstrate that white matter in the pediatric mouse brain is quite resistant to ischemia. Overall, the current study indicates the likelihood that equivalent ischemic insults will result in a tissue environment more conducive to long-term recovery, and potentially less functional deficits in children compared to adults.

921
BRAIN-0103
Non-Registered Abstracts

EFFECT OF DIETARY INCLUSION OF TWO GINGER VARIETIES ON ECTONUCLEOTIDASES AND ACETYLCHOLINESTERASE ACTIVITIES IN SYNAPTOSOMES FROM THE CEREBRAL CORTEX OF HYPERTENSIVE RATS

A. Akinyemi[1], G. Oboh[2], M.R.C. Schetinger[3]
[1]Biochemistry, Afe Babalola University, Ado-Ekiti, Nigeria
[2]Biochemistry,
Federal University of Technology Akure P.M.B. 704 Akure 340001 Nigeria, Akure, Nigeria
[3]Biochemistry,
Universidade Federal de Santa Maria Campus Uni versitário Camobi 97105-
900 Santa Maria RS Brazil, Santa Maria, Brazil

Ginger and its varieties have been reportedly used in folk medicine for the treatment of several cerebrovascular diseases such as stroke and demetia with little/or no scientific basis for their mechanism of action. Hence, the aim of the present study was to investigate the effects of two ginger varieties on activities of ectonucleotidase and acetylcholinesterase (AChE) activities in cerebral cortex synaptosomes from Nx-nitro-L-arginine methyl ester hydrochloride (L-NAME)-induced hypertensive rats. The animals were divided into seven groups (n = 7): normotensive control rats; hypertensive L-NAME rats; hypertensive control rats treated with Atenolol (10 mg/kg body weight/day); normotensive and hypertensive rats treated with 4% supplementation of red ginger respectively, and normotensive and hypertensive rats treated with 4% supplementation of white ginger respectively. After 14days of pre-treatment with red and white ginger, the animals were induced with hypertension by oral administration of L-NAME 40 mg/kg body weight for 10 days. Then the animals were sacrificed and the cerebral cortex was removed for synaptosomes preparation and enzymatic assays. The results revealed an increase in ATP and adenosine hydrolysis in hypertensive rats when compared with the normotensive control. Also, an increase in AChE activity in the cerebral cortex synaptosomes of L-NAME hypertensive rats was observed. However, dietary supplementation of both ginger varieties was efficient in preventing these alterations in L-NAME hypertensive groups by increasing the levels of ATP and ACh (two important neurotransmitters) in synaptic cleft of cerebral cortex. In conclusion, this study demonstrated that the both ginger rhizomes interfere with the purinergic and cholinergic neurotransmission. Therefore, we can suggest that these activities could provide some possible mechanism of action to justify their use in traditional medicine for the treatment of several cerebrovascular diseases.

922
BRAIN-0407
Non-Registered Abstracts

CREATINE MONOHYDRATE SUPPLEMENTATION FOR 10 WEEKS HAS A POTENTIAL TO IMPROVE LEARNING AND MEMORY IN FEMALE ALBINO MICE FOLLOWING NEONATAL HYPOXIA ISCHEMIA ENCEPHALOPATHY

R. Allah Yar[1], F. Iqbal[1], A. Akbar[2]
[1]Institute of Pure and Applied Biology,
Bahauddin Zakariya University Multan, Multan, Pakistan
[2]Department of Statistics,
Bahauddin Zakariya University Multan, Multan, Pakistan

Currently thereare no uniform standard treatments for newborn suffering from cerebralhypoxia-ischemia (HI) and to find new and effective strategies for treating theHI injury remains a key direction for future research. Protective effects of Cragainst ischemic brain injury in animal models remained a subject of interest inseveral studies (Berger et al., 2004[1]; Prass et al., 2007[2], Beard and Braissant, 2010[3]). Thedetermination of optimal Cr dosage that can be applied following HI injury iscrucial to reduce the brain damage. This is particularly true for humans forwhom no meaningful dose-response data is currently available (Wyss and

Schulze,2002[4]). Therefore, present study was designed to demonstrate theeffect of two different doses of Creatine monohydrate (1 and 3%) on behaviourand brain infarct volume in female albino mice following neonatal hypoxicischemic encephalopathy.

On postnatal day10, animals were subjected to left carotid artery ligation followed by 8%hypoxia for 25 minutes. Following weaning on postnatal day 20, mice weredivided into three treatments on the basis of diet supplementation (Normalrodent diet, 1% and 3% creatine supplemented diet) for 10 week. A battery ofneurological tests (Rota rod, open field and Morris water maze) was used todemonstrate effect of Cr supplementation on neurofunction and infarct sizefollowing HI.

Open field testresults indicated that Cr supplementation had significantly improved locomotoryand exploratory behaviour in subjects. It was observed that Cr treated miceshowed better neuromuscular coordination (rota rod) and improved spatial memory(Morris Water Maze test). A significant affect of creatine supplementation inreducing infarct size was also observed. It was also observed that the micesupplemented with 3% Cr for 10 weeks performed better than those on 1% Cr diet indicatingthat this dose has the potential to improve the neurofunction followingneonatal brain damage.

References:

1. Berger, R., Middelanis, J., Vaihinger, H.M., Mies, G., Wilken, B., Jensen, A., 2004. Creatine protects the immature brain from hypoxic-ischemic injury. J. Soc. Gynecol. Invest. 11, 9-15.
2. Prass, K., Royl, G., Lindauer U., Freyer, D., Megow D., Ulrich, D., Stöckler-Ipsiroglu, G., Wallimann, T., Priller J., 2007. Improved reperfusion and neuroprotection by creatine in a mouse model of stroke. J. Cereb. Blood Flow Metabol. 27, 452-459.
3. Beard, E., Braissant, O., 2010. Synthesis and transport of creatine in the CNS: important for cerebral functions. J. Neurochem. 115, 297-313.
4. Wyss, M., Schulze, A., 2002. Health implications of creatine: can oral creatine supplementation protect against neurological and atherosclerotic disease? Neurosci. 112, 243-260.

923
BRAIN-0022
Non-Registered Abstracts

COMPARATIVE STUDY OF RAPID-CYCLING IN BIPOLAR PATIENTS DEPENDENT ON AMPHETAMINE AND INDEPENDENT OF AMPHETAMINE REFERRED TO PSYCHIATRY CLINIC,KERMANSHAH,IRAN,2012-2014

J. shakeri[1], H. shakeri[2], F. arman[2], M. shakeri[2]
[1]psychiatry department,
Behavioral sciences research center, Kermanshah, Iran
[2]Kermanshah university of medical sciences, Behavioral sciences research center, Kermanshah, Iran

Introduction: BMD is a mental disease that is called manic depressive disorder.It is associated with mood changes from low of depression to high of mania. There is same rate in affected male and female. The average age of onset is approximately 21 years .It's called the rapid-cycling if it has at least 4 mood episodes in 12 months.

Aim: This study was designed to evaluate probable causes of rapid-cycling in patients dependent on amphetamine and independent of amphetamine in BMD patients.

Methods: We incorporated a qualitative design that contains one-hundred and ninety four BMD outpatients who fulfilled DSMV-TR criteria. Patients were divided to two groups of dependent on amphetamine and independent of amphetamines .A self-developed and

demographic questionnaire was employed. Data was analyzed by SPSS16 software.

Results: In this study 96(49.5%) of patients were dependent on amphetamine and 98 (50.5%) of patients were independent of amphetamine.144 patients (74%) were male and 50 patients (26%) were female. Most prevalent age group were 22 to 40 years old.140 patients (72.16%) patients lived in urban areas and 54 (27.83%) lived in country side. 128 patients (65.97%)were single and 66 patient(34.2%) were married.148 patients (76.28%)had high school education or below and 46 patients(23.71%)had high school diploma or higher education.

The incidence of rapid-cycling in patient's dependent on amphetamine was 23% in contrast to 6% in patients independent of amphetamines, which was statistically significant. (fourfold)

Conclusion: Our study suggests higher incidence of rapid-cycling in amphetamine dependency.We suggest that:

1- Amphetamine dependency should be considered as a possible cause for rapid-cycling in bipolar patients.

2- Treatment of amphetamine dependency should be considered along with treatment of bipolar disorder.

3-It may be possible to prevent rapid-cycling by means of prevention of amphetamine dependency in bipolar patients.

924
BRAIN-0073
Non-Registered Abstracts

SERUM AMYOLID A PLASMA LEVELS AS A PREDICTOR OF INFECTION IN ANEURYSMAL SUBARACHNOID HAEMORRHAGE

L. Azurmendi[1], V. Degos[2], N. Tiberti[1], N. Kapandji[2], P. Sanchez[2], A. Sarrafzadeh[3], L. Puybasset[2], N. Turck[1], J.C. Sanchez[1]
[1]Human Protein Sciences, Geneva University Hospitals, Geneva, Switzerland
[2]Department of Anaesthesiology, Pitié-Salpêtrière University, Paris, France
[3]Department of Neurosurgery, Charité-Universitätsmedizin Berlin, Berlin, Germany

Introduction: Aneurysmal subarachnoid haemorrhage (aSAH) is associated with high rates of mortality and morbidity[1]. Approximately 40% of the patients die in the first 24 hours after the initial haemorrhage and among the survivors many of them remain hospitalized in the ICU service[2, 3]. Nosocomial infections such as pneumonia, urinary tract infection, bloodstream infection or meningitis are one of the main causes of outcome worsening and death[4]. Until now, no efficient blood biomarker is available for the early detection and prevention of this complication. The aim of this study was to use proteomics strategies to discover biomarkers for infection prediction in aSAH patients.

Material and methods: The plasma proteome of infected (n=4) and non-infected (n=4) patients was compared using the 10-plex tandem mass tag (TMT) isobaric labelling quantitative mass spectrometry. Among the differentially expressed proteins the most interesting one was selected for further ELISA verification in 54 infected and 27 no infected patients. The predictive performances were established using Mann-Whitney U tests and ROC curves[5]. The combination of the selected molecule with clinical parameters was established using PanelomiX[6].

Results: At the day of infection, proteomic results gave rise to 17 significantly regulated proteins. Among those, SAA was selected for further studies; its levels were significantly higher in infected patients than in no infected ones (ratio: 15.86). At the admission to the hospital the concentrations of SAA were already significantly higher in patients that will develop an infection during hospitalisation (p=0.002), reaching a performance of 75.3% (80% SP, 71.8% SE) for a cut-off value of 90.9 µg/mL. Combining SAA with three clinical parameters (white blood cells, WFNS, age) improved its performance to an AUC of 94.4% (100%SP, 83%SE).

Conclusion: Our data suggested that the combination of SAA, an acute phase molecule, with white blood cells, WFNS and age could be an efficient tool for infection determination in aSAH patients. Their prediction capacity could lead to an earlier antibiotherapy and thereby improvement of aSAH patient long-term outcome. In order to evaluate its clinical utility, these results should be validated in a larger multicentric study.

References:

1. Suarez JI, Tarr RW, Selman WR, (2006) Aneurysmal Subarachnoid Hemorrhage. New England Journal of Medicine 354: 387-396
2. de Rooij NK, Linn FH, van der Plas JA, Algra A, Rinkel GJ, (2007) Incidence of subarachnoid haemorrhage: a systematic review with emphasis on region, age, gender and time trends. J Neurol Neurosurg Psychiatry 78: 1365-1372
3. Schievink WI, (1997) Intracranial Aneurysms. New England Journal of Medicine 336: 28-40
4. Frontera JA, Fernandez A, Schmidt JM, Claassen J, Wartenberg KE, Badjatia N, Parra A, Connolly ES, Mayer SA, (2008) Impact of nosocomial infectious complications after subarachnoid hemorrhage. Neurosurgery 62: 80-87
5. Robin X, Turck N, Hainard A, Tiberti N, Lisacek F, Sanchez JC, Muller M, (2011) pROC: an open-source package for R and S+ to analyze and compare ROC curves. BMC Bioinformatics 12: 1471-2105
6. Robin X, Turck N, Hainard A, Tiberti N, Lisacek F, Sanchez J-C, Müller M, (2013) PanelomiX: A threshold-based algorithm to create panels of biomarkers. Translational Proteomics 1: 57-64

925

BRAIN-0649

Non-Registered Abstracts

PERSISTENCE OF LEAD NEUROTOXICITY IN ADULT MALE WISTAR RAT: BEHAVIORAL AND HISTOLOGICAL ASPECTS

F.Z. Azzaoui[1], H. Hami[2], A. Ahami[2], S. Boughribil[3], S. Boulbaroud[2], H. Bouamama[4], M. Najimi[5], F. Chigr[5]

[1]Department of Biology, Faculty of Science Ben M'sik, Casablanca, Morocco

[2]Department of Biology, Faculty of Science, Kenitra, Morocco

[3]Department of Biology, Faculty of Sciences and Technology, Mohammedia, Morocco

[4]Department of Biology, Faculty of Sciences and Technology, Marrakech, Morocco

[5]Department of Biology, Faculty of Sciences and Technology, Beni Mellal, Morocco

Objectives: To investigate the effect of lead persistence on memory and some nervous structures (hippocampus and entorhinal cortex) responsible for the memorization process among adult's male Wistar rats.

Methods: Two main groups of adult Wistar rats are used; intoxicated rats (n= 12) received 50mg/L of lead nitrate diluted in tap water, while control ones (n= 12) received tap water only. The intoxication lasted 6 months and the stopping of treatment was for 4 months. Novel Object Recognition memory test and histological study of different cited brain structures are conducted.

Results: The results show that significant decrease is shown in the index of short and long-term recognition memory ($p<0.05$) of intoxicated rats, compared to the control ones. Indeed, the hippocampus and the entorhinal cortex of intoxicated rats are too affected even the administration of toxic was stopped; the histological study demonstrate the presence of nuclear pyknosis, cell shrinkage and eosinophilic cytoplasm, in both structures of these groups of rats compared to the control ones.

Conclusion: Lead toxicity remains harmful to nervous system structures and to behavioral performances, even the exposure is stopped.

926
BRAIN-0041
Non-Registered Abstracts

NEUROPROTECTIVE EFFECT OF NEVIRAPINE ON CEREBRAL ISCHEMIC STROKE IN WISTAR RATS

V. Bakshi[1], *M. Raam*[1]
[1]*Department of Pharmacology and Toxicology, School of Pharmacy Anurag Group of Institutions, Hyderabad, India*

Objectives: Nevirapine (NVP) is antiretroviral drugs belonging to potent class of non-nucleoside reverse transcriptase inhibitors (NNRTIs) widely used for the treatment human immunodeficiency virus (HIV) infection. The present study was investigated to study the neuroprotective effect of Nevirapine on middle cerebral artery occlusion (MCAO) induced cerebral ischemia in rats and by determining behavioral and biochemical parameters.

Methods: The right middle cerebral artery (MCA) of wistar rats was occluded for 2 h using intraluminal 4-0 monofilament and 22 h reperfusion was allowed. Nevirapine was investigated for its neuroprotective property in cerebral ischemia induced wistar rats at oral dose of 5 and 10 mg kg^{-1}. Nevirapine was administered orally for 14 days prior induction of ischemia.Rats were divided into 5 groups: sham operation, cerebral ischemia-reperfusion untreated (CIRU) group, vehicle treated group (CMC,p.o), Nevirapine low dose group (NVP 5 mg/kg/d), and Nevirapine high dose group (NVP 10 mg/kg/d).

Results: Middle cerebral artery (MCA) occlusion caused significant increase in the glutamate neurotransmitter and also acetylcholinesterase in brain. The neurobehavioral activities were also decreased significantly in MCA occlusion groups. All the alternations induced by ischemia were significantly attenuated by 14 days pretreatment of NVP (5, 10 mg/kg p.o.,) and also exhibited a statistically significant ($p < 0.05$) depletion of glutamate levels as compared to the negative control group. Additionally Nevirapine also exhibited antioxidant activity by increasing the levels of enzymes like superoxide dismutase, catalase, GSH levels which are statistically significant ($p < 0.05$) as compared to negative control.

Conclusion: The present study confirms the protective effect of Nevirapine in cerebral ischemia induced by MCAO and improves the behavioral pattern of memory. Pretreatment with nevirapine restored the antioxidant levels and protected the neuronal damage induced by cerebral ischemia.

References:

Longa E.Z., Weinstein, P.R., Carlson S., and Cummins, R. (1989). 'Reversible middle cerebral artery occlusion without craniectomy in rats,' *Stroke*, 20, 84–91.

Enting, R.H., Hoetelmans, R.M.W. and Lange, J.M.A. (1998). Antiretroviral drugs and the Central Nervous System. *AIDS* , 12, 1941-1955.

Nair,D., Kumar,K.R., Srikumar,B.N., Raju, T.R., Rao, S.B.(2004). Estimation of neurotransmitters n the brain by chromaograhic method. *Brain Behav*, 134-141.

Olufunsho A, Sunday O Olayemi, Joseph A Nwite, Titilope A Adeyemo. (2012) . Investigation of the levels of oxidative stress parameters in HIV and HIV-TB co-infected patients. *Journal of infection in developing countries* 6, 79-85.

Table no: 1: Effect of Nevirepine on exploratory behavior and y- maze

GROUPS	LINE CROSSING	Y-MAZE
Group I (vehicle)	92.18 ± 3.38	44.61 ± 1.931
Group II (MCAO)	22.17^{***} ± 3.038	19.39*** ± 1.300
Group III (MCAO + nev 5 mg/kg)	$66.50^{\#}$ ± 7.343	$33.01^{\#\#\#}$ ± 2.148
Group IV (MCAO + nev10mg/kg)	$87.17^{\$\$}$ ± 8.623	$41.08^{\$\$\$}$ ± 1.848

Group V(sham)	55.83 ± 3.413	32.02 ± 1.738

Values are expressed as mean ± SEM of 6 animals. Superscript letters represent the statistical significance done by ANOVA, followed by Tukey's multiple comparison tests.

***p<0.001 indicates comparision of negative control group with control group

###p<0.001 indicates comparision of low dose group with negative control group

$$$p<0.001,$$p<0.01 indicates comparision of high dose with negative control group.

927
BRAIN-0046
Non-Registered Abstracts

ENDOTHELIAL-GLIA ACTIVATION AND NEURODEGENERATION INDUCED BY CYANIDE TOXICITY AND GLOBAL VASCULAR OCCLUSION; A COMPARATIVE STUDY OF TWO RAT MODELS OF ISCHEMIA

W.G. Balogun[1], O.M. Ogundele[2], P.A.O. Adeniyi[2], A.E. Cobham[3], A.O. Ishola[2], A. Amin[4]
[1]Department of anatomy, University of Ilorin, Ilorin, Nigeria
[2]Department of anatomy, Afe Babalola university, Ado-Ekiti, Nigeria
[3]Department of anatomy, University of Calabar, Calabar, Nigeria
[4]Department of Physiology, university of Ilorin, ilorin, Nigeria

Background: The role of the endothelium of cerebral blood vessels in forming an electrical and physical barrier in the brain has long been described as an important filter for the sensitive cells of the central nervous system. The specialised barrier is composed of the endothelial cells of the cerebral arteries, neurons, foot process of ependymal astrocytes, macrophages and microglia cells. In ischemic injury, the alteration of this structural arrangement leads to compromising of the barrier which is further aggravated by oxygen radical production, inflammation and defective metabolism.
Aim: This study compares the changes in the component cells of the blood brain barrier units in global vascular occlusion (GVO) and cyanide toxicity (CN); 2 models of ischemia in rats. This is to differentiate the effect of GVO and cyanide toxicity on endothelial cell proliferation, glia activation, neurodegeneration, neurogenesis and angiogenesis in the cause and progression of ischemic brain injury.
Method: Adult Wistar rats (N=30) were divided into three groups; VO (n=12), CN (n=12) and Control-CO (n=6). The CN was treated with 30mg/Kg of KCN; VO was subjected to global vascular occlusion- both for duration of 10 days. The control (CO) was fed on normal rat chow and water for the same duration. At day 10, six animals each were separated into withdrawal groups and renamed (CN-I: n=6) and VO-I: n=6). The test groups CN and VO were sacrificed at day 10, while the withdrawal groups CN-I and VO-I were sacrificed at day 20. The brain was excised by dissection and fixed in formolcalcium for antigen retrieval immunohistochemistry (IHC). The following proteins were stained via IHC in the rat brain and blood vessel sections; Neuron (anti-NSE), Astrocytes (anti-GFAP), Endthotelial cells (anti-CD31), Microglia-Monocyte (phagocytic anti-CD45), Neuronal cytoskeleton (anti-NF) and Neurogenesis (anti-NSE, anti-Ki-67). The IHC staining were stereological quantified using image analysis and cell counting techniques.
Result/Discussion: Degenerative changes in CN was rapid compared to VO in the PC, PVZ and the blood vessels. Nitric oxide (NO) over production in cyanide played an important part in the endothelial thickening in the blood vessels in CN (CD31+++) when compared against reduced CD31 expression in CN-I (CD31--). The endothelial activation in CN treatment was linked with a decreased cell proliferation in the neurogenic cells of the PVZ (Ki-67) and monocytes (CD45). The induction of oxidative stress in both VO and CN caused glia activation, although glia was significantly activated in CN than in VO treatment. The GFAP/NSE index shows that glia activation is

higher in the PC than PVZ, and higher in cyanide toxicity than vascular occlusion. Cytoskeletal degradation was higher in cyanide treatment (NF-/+) and improved very little in the withdrawal (NF++). In vascular occlusion, the cytoskeletal degeradation was less (NF++) and improved greatly in the withdrawal (NF++++).

928
BRAIN-0869
Non-Registered Abstracts

Cerebral small vessel disease-related protease HtrA1 processes latent TGF-β binding protein 1 and facilitates TGF-β signalling

N. Beaufort[1], E. Scharrer[1], E. Kremmer[2], V. Lux[3], M. Ehrmann[3], R. Huber[4], H. Houlden[5], D. Werring[6], C. Haffner[1], M. Dichgans[7]
[1]Institute for Stroke and Dementia Research, Klinikum der Universität München, Ludwig Maximilians University, Munich, Germany
[2]Institute of Molecular Immunology, Helmholtz-Zentrum München, Munich, Germany
[3]Centre for Medical Biotechnology, Faculty of Biology, University of Duisburg-Essen, Essen, Germany
[4]Centre for Medical Biotechnology, Faculty of Biology, University of Duisburg-Essen, Essen, Germany
Emeritus Group Structure Research, Max Planck Institute of Biochemistry, Martinsried, Germany
Center for Integrated Protein Science at the Depar tment of Chemistry, Lehrstuhl für Biochemie, Technische Unversität München, Garching, Germany
School of Biosciences, Cardiff University, Cardiff, Wales, United Kingdom
[5]Department of Molecular Neuroscience and Neur ogenetics Laboratory, University College London, Institute of Neurology and The National Hospital f or Neurology and Neurosurgery, London, United Kingdom
[6]Stroke Research Group, Department of Brain Repair and Rehabilitation, UCL Institute of Neurology and The National Hospi tal for Neurology and Neurosurgery, London, United Kingdom
[7]Institute for Stroke and Dementia Research, Klinikum der Universität München, Ludwig Maximilians University, Munich, Germany Munich Cluster for Systems Neurology-SyNergy, Munich, Germany

Objectives. CARASIL is an inherited form of cerebral small vessel disease caused by loss-of-function mutations in the high temperature requirement protease HtrA1. HtrA1 is involved in a variety of cellular processes including transforming growth factor β (TGF-β) signalling, and dysregulated TGF-β signaling is considered to promote CARASIL pathogenesis (Hara et al. 2009), but the underlying molecular mechanisms are incompletely understood.

Methods. We analysed the TGF-β pathway in brain tissue and embryonic fibroblasts from HtrA1-deficient mice, as well as in CARASIL patient skin fibroblasts by qPCR, immunoblot and/or immunohistochemisty. We also investigated the proteolytic processing of latent TGF-β binding protein 1 (LTBP-1) by purified, overexpressed or endogenous HtrA1 and characterized the structural and functional consequences of this cleavage using truncated LTBP-1 variants, aminoterminal microsequencing, as well as matrix binding and incorporation assays.

Results. We present evidence for a facilitating role of HtrA1 in TGF-β pathway activation in HtrA1-defficient tissues and cells, and in CARASIL fibroblasts. We identify latent LTBP-1, an extracellular matrix protein and key regulator of TGF-β bioavailability, as a novel HtrA1 target. Cleavage occurs at physiological protease concentrations, is prevented under HtrA1-deficient conditions as well as by CARASIL mutations and disrupts both LTBP-1 binding to fibronectin and its incorporation into the extracellular matrix.

Conclusions. Our results suggest an attenuation of TGF-β signaling caused by a lack of HtrA1-mediated LTBP-1 processing as mechanism underlying CARASIL pathogenesis.

References. Hara K, Shiga A, Fukutake T (2009) Association of HTRA1 Mutations and Familial Ischemic Cerebral Small-Vessel Disease. N Engl J Med; 360:1729-1739. Beaufort N, Scharrer E, Kremmer E, Lux V, Ehrmann M, Huber R, Houlden H, Werring D, Haffner C, Dichgans M (2014) Cerebral small vessel disease-related protease HtrA1 processes latent TGF-β binding protein 1 and facilitates TGF-β signaling. Proc Natl Acad Sci; 111(46):16496-501.

929
BRAIN-0179
Non-Registered Abstracts

IMPLICATION OF C4D IN PROGRESSION OF ISCHEMIC STROKE ON PATIENTS WITH LUPUS ERYTHEMATOSUS.

S. Bebitov[1], K. Mirzaeva[1], G. Rakhimbaeva[1]
[1]Neurology department,
Tashkent Medical Academy, Tashkent, Uzbekistan

Introduction. Systemic lupus erythematosus (SLE) is one of theuncommon causes of ischemic stroke. According to literature, protein'sconcentrate of complement system (PCS) can be decreased in blood of SLEpatients, but the role of PCS C4d has not been studied completely in ischemicstroke.

Purpose: Aimof our study was to definethe role of PCS C4d inpatients with ischemic stroke, caused by SLE.

Patients and methods: Westudied 42 SLE patients during five years (middle age 45,56 ±4,23). As an indicator of SLE, all patients, which observedischemic stroke, underwent to magnetic resonance image (MRI). Inaddition, Enzyme – linkedimmunosorbent – Assay(ELISA) wasused for determination of concentrate of PCS C4d in blood.

Results: Concentration of PCS C4d was 0,9 – 0,12 g/l in 54,76% SLE patients with multifocal ischemic stroke on MRI.35,7% of SLE patients had 0,7 – 0,1 g/l PCS C4d concentration with lacunarischemic stroke on MRI. 9,5% SLE patients had 0,4 – 0,6 g/l PCS C4d level withoutischemic stroke signs on MRI.

Conclusions: It should be noted that relatively high concentrationof PCS C4d during a long time might be used as a prognostic marker for ischemicstroke in patients with SLE.

930
BRAIN-0180
Non-Registered Abstracts

AGE AND GENDER FEATURES OF ENCEPHALOPATHY IN LUPUS ERYTHEMATOSUS

S. Bebitov[1], K. Mirzaeva[1], N. Vahobova[1]
[1]Neurology department,
Tashkent Medical Academy, Tashkent, Uzbekistan

Objective: We know that encephalopathy is observed as a chroniccomplication in lupus erythematosus (LE). Aim of our study was to establish correlationof encephalopathy in LE with age and gender.

Materials and methods: We studied 38 patients (13 male (M) and 25 female (F)with middle age 31,23±5,32 years) at the neurology and rheumatology departmentof Tashkent Medical Academy. As an indicator of LE, all patients underwent to acutephase reactions (C - reactive protein, gamma globulin and sialic acid). Also duplexscanning of brain vessel carried out for encephalopathy identification.

Results: Acute phase reactions were positive at 72% patients, 88%patients had 0,9-1,1mm intima mediate complex (IMC). 40% patientsof F had determined cortical dementia, 32% patients were with subcorticaldementia and 28% patients of F with established other local syndromes. In acase of M, these indicators had following numbers: 46,2% - subcorticaldementia, 30,8% - cortical dementia and 23% - other local syndromes.

Conclusion:From theseresults, it can be concluded that, women are more resistant to internal andexternal depressing factors physically and psychologically than men, that iswhy women suffering from erythematosus observed to have

more subcorticaldementia while men observed to have more cortical dementia. This study has beencontinuing for confirm accuracy of these results.

931
BRAIN-0181
Non-Registered Abstracts

IMMUNOLOGICAL CHARACTERISTICS AND ANTIGENS OF HLA-SYSTEM IN NEURORHEUMATISM IN UZBEK POPULATION.

S. Aslanova[1], S. Bebitov[1], F. Yunusov[1]
[1]Neurology department,
Tashkent Medical Academy, Tashkent, Uzbekistan

Introduction. Rheumatic fever(RF) and rheumatic heart disease are still remaining an important public healthproblem. The purpose of the study was determination of immunological parametersand analysis of antigens HLA-class system for RF in a case of neurorheumatism inUzbek population.

Materialsand Methods. We examined 44 patients Uzbek nationality with RF - 26 (59%) women and18 (41%) men at 15-59 years (mean age - 31,9 ± 2,0 years). The control group composed245 healthy individuals of the same nationality. Immunoanalysis performed inperipheral blood of patients.

Resultsand discussion. RF patients showed a significant decrease in the peripheral blood of T-cellpool and immunoregulatory subpopulation (1.4 times), B cells (1.7 times) of thenumber of phagocytic neutrophils, increase of zero lymphocytes and the level ofCircular Immune Complex (3 times). It should be noted that the decrease in T-suppressor was more pronounced than that of T-helper cells, which resulted inincrease in the ratio Th / Ts (3,30 ± 0,15 in the control group and 4,10 ± 0,20- patients) .

Occurrence of antigens of HLA-systemwas observed only at loci A and B. Thus, a locus A in 2 times more commonantigen was HLA-A10 (RR = 2,70), in a locus - the greatest risk of developing RFwas for antigen B7 (RR = 2,55), B8 (RR = 2,12), B27 (RR = 5,29), B40 (RR =2,61).

Conclusion. Neurorheumatismaccompanied by disturbances in the immune system. Genetic markers ofpredisposition to RF in Uzbek people were HLA-A10, B7, B8, B27, B40.

932
BRAIN-0881
Non-Registered Abstracts

INFLUENCE OF ANGIOLIN ON NEUROAPOPTOSIS, CAUSED BY AN IMBALANCE OF REDOX POTENTIAL

I.F. Belenichev[1], L.I. Kucherenko[2], N.V. Bukhtiyarova[1]
[1]Pharmacology and Medical Formulation, Zaporozhye State Medical University, Zaporozhye, Ukraine
[2]Pharmaceutical Chemistry, Zaporozhye State Medical University, Zaporozhye, Ukraine

It is shown that an imbalance of redox potential caused by displacement of thiol-disulfide balance and the accumulation of oxidized forms of thiol-containing molecules under conditions of cerebral pathology can cause neuronal apoptosis. Our studies have shown high neuroprotective activity of Angiolin ((S)-2,6 diaminohexane acid 3-methyl-1,2,4-triazolyl-5-thioacetate) on various models of cerebral pathology and in experiments in vitro. Experiments on cerebral cortex neurons of 14-days-old Wistar rats showed that introduction of oxidized glutathione in 1-5mM concentration into suspension of neurons results in the activation of caspase-3 and expression of p53. After processing of neurons with ethidium bromide the increase of the number of *apoptotically changed cells was noted*. The experimental data on dynamics of neuronal apoptosis allow us indirectly connect the action of oxidized glutathione with cascade of reactions of Ras-signaling pathway, as Ras-mediated apoptosis may develop from the level of the protein p53. Pre-processing of neurons with Angiolin (10^{-5} M) resulted in a significant reduction of the number of *apoptotically changed cells*. At the same time in the samples with cerebrocurine significant decrease of p53

expression was found. Pronounced antiapoptotic effect of Angiolin takes place indirectly through reduction of p53 protein, which is involved in Ras-mediated apoptosis and causes increase of oxidative stress. Processing of Ras-protein and several other members of this family of proteins of apoptosis intracellular regulation depends on the status of glutathione pool in the cell. Our experiments suggest that Angiolin can increase the ratio reduced / oxidized glutathione, and thus affect the Ras-signaling cascade.

933
BRAIN-0053
Non-Registered Abstracts

PREDICTIVE VALUE OF CIRCULATING VASCULAR ENDOTHELIAL GROWTH FACTOR-1 IN HYPERTENSIVE PATIENTS AFTER ACUTE ISCHEMIC STROKE

A. Berezin[1], O. Lisovaya[2]
[1]Internal Medicine Department, State Medical University, Zaporozhye, Ukraine
[2]Cardiology Department, City hospital #6, Zaporozhye, Ukraine

Objective: To evaluate value for 6 months survival of vascular endothelial growth factor-1 (VEGF-1) plasma level in hypertensive patients after ischemic stroke.
Design and Methods: 72 mild-to-moderate arterial hypertension patients (47 male, 56-68 aged) within 1-2 weeks after ischemic stroke were enrolled to the scrutiny at baseline and then they were studied prospectively for 6 months period regarding survival rate. All enrolled subjects were similar accordingly clinical status, hemodynamic, Rankin score index, and severity of hypertension. Both VEGF-1 and MMP-9 plasma levels were measured at the study entry and in 6 months after baseline by ELISA. We has been assessed all new cardiovascular events including myocardial infarction (MI), unstable angina (UA), recurrence stroke (RS), TIA, advance heart failure (HF) during study period.
Results. Analysis of obtained outcomes have been shown that all cases (n=28) of new cardiovascular events identified during first 4 weeks after start of observation are correlated well with VEGF-1 plasma levels (r=-0.58; P<0.001) measured at baseline. On the other hand, 4-weeks survival rate was 87.0 % and 68.6% respectively for group subjects (P<0.01) with top and low quartile of VEGF-1 plasma level at baseline. However, lack of tightly interrelationship between cardiovascular outcomes and VEGF-1 (r=0.2; P=0.16) in 6 months after study entry. New events associated with RS and TIA incidences independently study period are correlated well with VEGF-1 (r=-0.63; P<0.05 and r=-0.58; P<0.02 respectively) only.

Conclusions: We has been proposed that circulating VEGF-1 might have more predicting value in comparison with MMP-9 concentration among hypertensive patients during early ischemic stroke period. The predisposed value of VEGF-1 plasma level toward both RS and TIA incidents during 6 month after stroke could be interesting. The role of circulating VEGF-1 as a prognostic indicator for new cardiovascular events in subjects after ischemic stroke can be discussed

934
BRAIN-0929
Non-Registered Abstracts

LACTATE TRANSPORT AND RECEPTOR ACTIONS IN RETINA

L. Bergersen[1], M. Kolko[2]
[1]Oral Biology The Brain and Muscle Energy Group, University of Oslo, Oslo, Norway
[2]Institute of Neuroscience and Pharmacology, University of Copenhagen, Copenhagen, Denmark

In retina, like in brain, lactate equilibrates across cell membranes via monocarboxylate transporters as well as in the extracellular space, forming a basis for the action of lactate as a volume transmitter of metabolic signals. In addition, a lactate permeable depolarization activated anion channel, recently described in brain astroglia, may cause lactate release in response to neural activity. In the present paper, we argue that the lactate receptor GPR81, also known as HCAR1, may contribute importantly to the control of retinal cell functions in health and disease. GPR81, a G-protein coupled receptor, is

known to downregulate cAMP both in adipose tissue and in brain, and acts also through other down-stream mechanisms to control functions such as excitability, metabolism and inflammation. Recent publications predict effects of the lactate receptor on neurodegeneration. Neurodegenerative diseases in retina where the retinal ganglion cells die, such as glaucoma and diabetic retinopathy, may be linked to disturbed lactate homeostasis. Pilot studies reveal high GPR81 mRNA in retina and indicate GPR81 localization in Müller cells and retinal ganglion cells . Monocarboxylate transporters are previously known to be expressed in retinal cells. We envision that lactate receptors, channnels and transporters could be useful future targets of novel therapeutic strategies to protect neurons and prevent or counteract glaucoma as well as

935
BRAIN-0686
Non-Registered Abstracts

OPTIMIZING CNS-DELIVERY BY LACTYL STEARATE-COUPLED LIPOSOMES

M. Bhargava[1], S. Bhargava[2], V. Bhargava[3]
[1]Pharmacy, ICFAI University Dehradun, Kanpur, India
[2]Department of Pharmacy, Manav Bharti University, Kanpur, India
[3]R&D, KRV Hospitals Pvt. Ltd., Kanpur, India

Brain drug targeting brings a healthy skepticism to the study of the BBB, which is the most frustrating obstacle for pharmacologists wishing to find treatments for brain disorders. The BBB restricts the brain uptake of many valuable hydrophilic drugs and limits their efficacy in the treatment of brain diseases because of the presence of tight junctions, high metabolic capacity, low pinocytic vesicular traffic and efficient efflux mechanisms.

Purpose. Meningitis is the inflammation of tissues which covers brain & spinal cord. The drug of choice is rifampicin which is highly lipophilic in nature. Thus lactyl stearate coupled liposomes bearing rifampicin for effective management of meningitis.

Methods. Lactyl stearate was synthesized from stearic acid and lactic acid. Lactyl stearate coupled and uncoupled liposomes bearing rifampicin were prepared by Lipid cast film method using phosphatidyl choline, cholesterol. Formulations were characterized for vesicle shape by Transmission Electron Microscopy (TEM), average vesicle size, drug entrapment efficiency, *in-vitro* drug release. The *in-vivo* studies the drug distribution in various organs and blood of albino rats was assessed after I.V. administration of formulations. The quantitative uptake of the formulations by the brain in albino rats was assessed by fluorescent microscopy. On the basis of in-vitro characteristics formulations LIPO-3 and LIPO-3-III-c were taken for in-vivo performance evaluation.

Results & Discussion: The average particle size was found in the range of 2.33 to 1.0 mm for uncoupled and coupled liposomes. The percentage encapsulation efficiency of liposomes was found to be 41% & 34% in uncoupled & coupled liposomes. Brain uptake was increased about 2-3 times in case of uncoupled liposomes as compared to plain drug. Accumulation was increased about 6-8 times with coupled liposomes in comparison to uncoupled liposomes and about 10-12 times higher compared to plain drug solution.

Conclusion: Higher uptake of lactyl stearate coupled liposomes can be explained as, that mono carboxylic acid transporters present on brain endothelial cells and cross the BBB through carrier mediated transport mechanism. Fluorescence study clearly indicates that the preparation is crossing the basal carotid system and accessing to the nervous system. 6-CF was distributed in blood vessels and accumulated in cerebellum and cerebrum. This delivery system not only increased the brain uptake of the drug but it also reduces the administered dose and toxic effect of the drug. Hence it proves great potential in the delivery of the drug into brain for the treatment of the diseases associated with the brain where very limited drug are available for those diseases. Thus, Lactyl stearate coupled

liposomes effectively delivers the drug to the brain and has great potential for brain targeting.

936
BRAIN-0687
Non-Registered Abstracts

SURFACE MODIFIED SOLID LIPID NANOPARTICLES FOR THE TARGETED DELIVERY TO BRAIN: MANAGEMENT OF HIV-1 ASSOCIATED DEMENTIA

M. Bhargava[1], S. Bhargava[2], V. Bhargava[3]
[1]Pharmacy, ICFAI University Dehradun, Kanpur, India
[2]Department of Pharmacy,
Manav Bharti University, Kanpur, India
[3]R&D, KRV Hospitals Pvt. Ltd., Kanpur, India

Background: HIV-Associated Dementia (HAD) is a significant neurological complication which occurs years after the acute viral sero-conversion reaction responsible for progressive Immuno-suppression and high viral loads. Many patients infected with HIV-1 suffer cognitive impairment ranging from mild to severe HAD which may result from neuronal death in the basal ganglia, cerebral cortex, and hippocampus. With Present available treatment system, there is no satisfactory treatment for HAD available, despite of advancement in the therapeutics.

In this study, nifedipine loaded solid lipid nanoparticles (SLN) were developed for targeting drug into the central nervous system, the site of action of drug to block the apoptosis by HIV-1 virus. This would decrease the process of neurodegeneration and increase the survival time of neuronal cells. Also, this targeted delivery to brain will minimize the systemic effect of nifedipine, avoiding its delivery peripherally.

Method: The uncoated SLN were prepared by Solvent Injection Method & then coated with tween 80 and Lyophylized. Shape & surface morphological studies were done by Scanning Electron Microscopy (SEM) & Transmission Electron Microscopy (TEM). The *in-vitro* release profile of entrapped drug was studied using dialysis membrane. The Ex-vivo studies consisted of DNA fragmentation followed by in-vivo studies on albino rats.

Results: The SEM & TEM images show the smooth & spherical surface of SLN. The *in-vitro* release profile of drug shows more than 90% of drug release in 48hrs. DNA fragmentation was determined in presence and in absence of gp120 mimicking agent which shows no DNA fragmentation thus the developed carrier system works properly in releasing the drug and blocking apoptosis in the cortical cells. The fluorescence microscopy shows the qualitative uptake and localization pattern of the coated SLNs in brain.

Conclusion: *In-vitro* & *in-vivo* studies results shows more specific delivery of the Nifedipine to the Brain. The DNA Fragmentation & Cell Viability studies shows dementia blocking activity on brain cells. Brain specific delivery of Nifedipine could reduce the dose and potential systemic side effects, thus providing site specific delivery to brain. Thus, CNS delivery of these Nifedipine loaded SLNs via Intra Venous delivery will also open new opportunities for other Anti-Retroviral drug delivery to brain.

937
BRAIN-0822
Non-Registered Abstracts

THE NEUROPROTECTIVE EFFECT OF LEPIDIUM MEYENII (MACA) IN ANIMAL MODEL OF MCAO.

K. Taboada-Rosell[1], K.J. Vera-Lopez[2], B.S. Sousa[1], A.C. Tejeda-Sebastiani[1], L.B. Torres[1], L.M. Quaglio[3], B.H.S. Araújo[1], L.R. Oliveira[1], T. Maher[4], A. Pino-Figueroa[4], F.R. Cabral[1]
[1]Brain Institute, Hospital Israelita Albert Einstein, São Paulo, Brazil
[2]Pharmacology, Universidad Catolica de Santa Maria, Arequipa, Peru
[3]Phisiology, Faculdade de Ciências Médicas da Santa Casa de São Paulo, São Paulo, Brazil
[4]Pharmaceutical Sciences, Massachusetts College of Pharmacy and Health Science University, Boston, USA

Stroke is the third leading cause of death and the major cause of adult disability in the world. Any intervention that could reverse or limit the effects of a stroke would have directly benefits in treatment, rehabilitation and public health. The discovery of new substances for the treatment or prevention of stroke is something extremely promising. In this way, *Lepidium meyenii* an herbaceous plant belonging to the Brassicaceae family, known as Maca, has been shown to have a great potential for neuroprotection after brain injury. Our study was conducted to evaluate if Maca has potential to be a neuroprotective agent to stand as a new therapeutic drug for stroke. Futhermore, we also evaluated which is the optimal dose and the best therapeutic window for temporary middle cerebral artery occlusion in rats. The experiments were performed on 22 male Wistar rats weighing between 280 and 320g. The rats were housed in an AAALAC-accredited animal care facility at the Brain Institute of Albert Einstein Hospital. All experimental procedures were approved by the Animal Care and Use Committees of the Albert Einstein Hospital. The animals received twice tail vein injection, the first when anesthetized before surgery (30 min prior to stroke), and the second when the common carotid arteries were reperfused, 1 hour after stroke. The control group received the same treatment as the experimental group, with exception of Maca, which was replaced to aqueous PVP solution. The experimental Maca-group, were treated with different doses of the Maca extract (2,5mg/kg - n=6 and 5mg/kg – n=8). The effect of Maca on infarction size was evaluated by TTC staining. The brain of the control group did not show any detectable lesion or non-viable tissue damage. However, the brain from the stroke groups showed detectable lesions as white patches in areas that are supplied by the middle cerebral artery. The lesions were present in the lateral striatum and the overlying cortex. Our results show that Maca treatment significantly decreased the lesion (5mg/kg - P=0,0002 and 2,5mg/kg - P=0,003) in the striatum and cortex of Maca+Stroke groups as compared to control. Whereas the laboratory evidence supports that Maca administration during a time window for produce neuroprotection, extending this treatment at post-stroke period maybe increase its clinical relevance. In Addition, this work provides scientific evidence that Maca may afford neuroprotection for stroke.

938
BRAIN-0889
Non-Registered Abstracts

HEMODYNAMIC CHANGES WITHIN THE DOME OF HUMAN CEREBRAL ANEURYSMS IN RESPONSE TO ARTIFICIALLY-INDUCED INCREASES IN SYSTEMIC BLOOD PRESSURE

H. Hasan[1], N. Chalouhi[2], B. Hindman[1], M. Todd[1]
[1]Neurosurgery, University of Iowa, Iowa city, USA
[2]Neurosurgery, University of Iowa, Philadelphia, USA

Introduction: The formation and rupture of cerebral aneurysms have been associated with hypertension and inflammation. The effect of transient increases in systemic systolic blood pressure (SBP) and its correlation with intra-aneurysmal hemodynamic parameters have not been studied before. The current study is the first to investigate in vivo the effects of transient elevations in systemic SBP on different

hemodynamic parameters inside the aneurysm sac and corresponding parent arteries using invasive technology.

Methods: Nine patients with unruptured cerebral aneurysms undergoing coiling were recruited. Dual sensor microwires (0.4mm diameter) with the capacity to simultaneously measure flow velocity and pressure were used to measure systolic, diastolic and mean pressure inside the aneurysm sac. Additionally, the microwires provided measurement of pressures and peak/mean flow velocities in the parent vessel just outside the aneurysm. The measurements were obtained at baseline and after transient (<10 minutes) incremental increases in systemic SBP up to 25 mm Hg above baseline with a phenylephrine infusion. Systemic hemodynamic parameters (radial arterial catheter) were correlated to intra-aneurysmal and parent arteries parameters.

Results: Eight females and one male (mean age, 54 years; range, 33-74 years) were enrolled. All aneurysms were located in the anterior circulation. The average maximal dose of phenylephrine needed to achieve the required increase in systemic SBP was 0.8 ug/kg/min (range 0.5-1.0). In 8 of 9 patients, acute changes in systemic arterial pressure resulted in simultaneous and at least equal changes in intra-aneurysmal pressures. Three patterns emerged when comparing intra-aneurysmal hemodynamics to changes in systemic hemodynamic parameters: 1) significantly higher increases in aneurysmal compared with systemic pressures; 2) similar variations in aneurysmal and systemic pressures; 3) significantly lower increases in aneurysmal compared with systemic pressures. Peak and mean flow velocities in the parent arteries were decreased after reaching target pressure using phenylephrine infusion without angiographic change in vessel diameter.

Conclusion: These preliminary data suggest that acute increases in systemic pressures are likely to be the underlying mechanism for aneurysm rupture. There may be a subpopulation of aneurysms with exaggerated pressure responses that would be particularly prone to rupture.

939
BRAIN-0393
Non-Registered Abstracts

ACTIVATION OF NMDA RECEPTORS CAUSES DISRUPTION OF MOUSE CEREBRAL ENDOTHELIAL CELLS-CONSTRUCTING TIGHT JUNCTION BARRIERS VIA MEK-/ERK1/2-MEDIATED ACTIVATION OF MMP-2/9

R. Chen[1], J. Chen[1], Y. Chang[2]
[1]Graduate Institute of Medical Sciences, Taipei Medical University, Taipei city, Taiwan
[2]Brain Disease Research Center, Taipei Medical University-Wan Fang Hospital, Taipei city, Taiwan

Objectives: The blood-brain barrier (BBB) strictly regulates the brain traversal of immune cells from the bloodstream. Under pathological conditions, neurotransmitter glutamate levels increase dramatically and results in excitotoxic neuronal loss, inflammatory response, and subsequent brain edema. The N-methyl-D-aspartate receptor (NMDAR) is calcium permeable channel gated by glutamate. Roles of NMDARs in the BBB are known little. This study is aimed to evaluate the effects of NMDAR activation on maintenance of the BBB and the possible mechanisms.

Methods: Mouse cerebrovascular endothelial cells (MCECs) were prepared from cerebral microvessels. Expressions of NMDAR mRNA and protein in MCECs were verified. Function of NMDARs was assay using confocal microscopy to analyze intracellular calcium mobilization. Transendothelial electrical resistance (TEER), occluding tight junction, and occludin levels were determined to evaluate the effects of NMDAR activation on the integrity of the MCEC-constructing tight junction barrier. Levels of matrix metalloproteinase (MMP)-2, MMP-9, and phosphorylated and non-phosphorylated (ERK) 1/2 and MEK-1 were analyzed to determine the mechanisms of NMDAR activation-induced disruption of the tight junction barrier.

Results: Protein and RNA analyses revealed the expressions of NMDAR subunits GluN1 and GLUN2B protein or mRNA in MCECs. Confocal microscopic examination further showed GLUN1 could be detected in MCECs and the BBB of mouse brains. Exposure of MCECs to NMDA increased calcium influx in a time-dependent manner. In parallel, treatment with NMDA resulted in significant reductions in the TEER due to disruption of the occludin tight junction and diminishing of occludin synthesis. As to the mechanism, NMDA increased amounts of MMP-2 and MMP-9 in MCECs. Sequentially, exposure to NMDA augmented MEK and ERK1/2 phosphorylations.

Conclusions: This study has shown the functional presence of NMDARs in MCECs, and activation of NMDAR can lead to disruption of MCEC-constructed tight junction barrier via MEK/ERK-induced activation of MMP-2 and MMP-9.

940
BRAIN-0743
Non-Registered Abstracts

BLOOD VOLUME MEASUREMENTS BY DUAL T1 AND T2 MRI ACQUISITIONS WITH SINGLE T2 AGENT IN ACUTE ISCHEMIC RAT BRAIN

J.Y. Suh[1], H. Jung[2], H.J. Cho[2], Y.R. Kim[3], J.K. Kim[4], G. Cho[1]
[1]Magnetic Resonance, Korea Basic Science Institute, Cheongju, Korea
[2]Nano-Bioscience and Chemical Engineering, Ulsan National Institute of Science & Technology, Ulsan, Korea
[3]Radiology, Martinos Center for Biomedical Imaging Massach usetts General Hospital, Charlestown, USA
[4]Radiology, Asan Medical Center University of Ulsan college of Medicine, Seoul, Korea

OBJECTIVES: Blood volume changes duringthe acute phase of brain ischemia are not wellunderstood but presumably linked to other neuronal degenerations. In this study, using theroutinely synthesizable superparamagnetic iron oxide(SPION) as a dual contrast agent, we aimed to quantifyMRI-derived vascular blood volumeparameters in rat ischemicbrain models progressed 24hrs reperfusion following 1hr middle cerebral arteryobstruction (MCAO), and compared these parameters with contralesional of the stroke and normal rat brain. We posit that simultaneous acquisitions of both positive and negative contrast-enhancedimages offer complementary information, increasing the certainty and accuracy onthe measurements of blood volumes.

METHODS: MRI experiments wereperformed on 3T magnet system (Philips) using rat brains following 24 hrs afterreperfusion submitted to middle cerebral artery occlusion for 60 min (n=7) andnormal rat brains (n=5). A kind of 3D T1 MRI signalintensity, ultra-short TE (UTE)sequence was used to quantify absolute cerebral blood volume (aCBV) before and after intravenous administration of superparamagnetic iron oxide nanoparticles (SPION, 6.7mg/kg).aCBV was calculated using signal changes in brain tissue as compared torelative signal changes in vessel, after creation of subtractionimages (i.e., SI_{post_SPION}–SI_{pre_SPION}) at 90 flip angle.Additionally, T2- and T2*-weightedimages were acquired before and after SPION injection to obtain relative cerebralvascular blood volume (rCBV, $R2^*_{postSPION}$-$R2^*_{preSPION}$), relative microvascular volume (rMVV, $R2_{postSPION}$-$R2_{preSPION}$). Regionsof interests (ROIs) for stroke lesions were drawn by manual contouring on everyslice: the abnormal bright area on the T2 images.

RESULTS: Positive enhancement of signal change in UTE andnegative diminution signal changes in T2(*) images were observed after SPIONinjections due to itsconcurrent T1-T2 effects. From the hemodynamic perspectives, acute phase ofischemic brain seems to be governed by both protective (via flow compensation)and vascular degenerative (disruption of microenvironment) mechanisms. aCBV(measured from UTE) and rCBV (measured from T2*) were increased whereas rMVVmeasured in the ipsilesional subcortex regions were significantly less than thosein the contralesional stroke and normal subcortex areas.

CONCLUSION: Coupledrelationship between the ischemic tissue damage and increased CBV may suggestthe autoregulatory vasodilation dedicated to therapid normalization of blood oxygen and glucose levels. On the other hand, rMVV decrease in the ipsi-lesion may indicatethe ischemia-induceddefect for the effectiveperfusion reserve that may be used for accurately delineating the true perfusion and neurovascular status.

REFERENCES:[1] Lee HB et al., Blood volume in the rat. Nucl. Med. 1985;26:72-76. [2] DennieJ et al., NMRimaging of changes in vascular morphology due to tumor angiogenesis. *Magn Reson Med* 1998; 40: 793-799. [3] Huang S et al., Cerebral blood volume affects blood-brainbarrier integrity in an acute transient stroke model. J Cereb Blood Flow Metab. 2013 Jun;33(6):898-905.

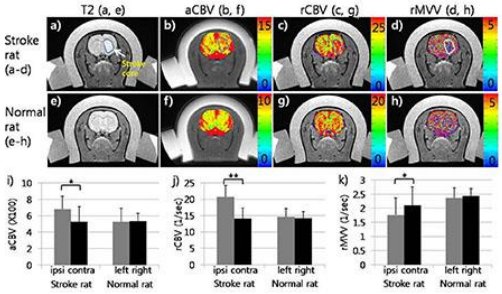

Representative T2, aCBV, rCBV, and rMVV maps (a-h) and their comparisons between ischemia and normal rat subcortical brains (i-k). Note the increased absolute and relative CBV and declined rMVV in the ipsilesional subcortical regions compared to the contralesional (stroke brain) and normal subcortical brains.

941
BRAIN-0592
Non-Registered Abstracts

THE RELEVANCE OF SOME MEMORY DEFICITS IN A VALPROIC ACID-INDUCED RAT MODEL OF AUTISM

A. Ciobica[1], R. Lefter[2], M. Paulet[2], Z. Olteanu[1]
[1]Molecular Biology,
Alexandru Ioan Cuza University Iasi, Iasi, Romania
[2]SOP HRD/159/1.5/S/133675 Project,
Romanian Academy, Iasi, Romania

Background: Autism is a complex disorder characterized by repetitive behavior and impaired social communication. Still, apart from these main manifestations, a significant number of cases display impaired emotional learning and memory functions.

Methods: We tried to better understand the memory functions in an environmentally induced rat animal model of autism, based on the administration of valproic acid (VPA) during gestation (500 mg/kg or saline on day 12.5 of gestation) and examined the resultant progeny on specific memory tests, such as the Y maze task and the 8-arms radial maze.

Results: Our data indicated that animals perinatally exposed to VPA are showing, besides specific social interaction deficiencies, significant behavioral alterations in Y maze task, as expressed in decreased spontaneous alternations percentage, suggesting affected immediate working memory and in the radial arm maze, as expressed to an increased number of both reference and working memory errors.

Conclusions: In conclusion, we showed significant memory deficits in a VPA-induced rat model of autism, demonstrating also the relevance of the memory processes in autism, apart from the social deficiencies.

942
BRAIN-0597
Non-Registered Abstracts

PHYSICAL EXERCISING IS REDUCING ANXIETY, DEPRESSION AND MEMORY DEFICITS ASSOCIATED WITH A MPTP-INDUCED RAT MODEL OF PARKINSON'S DISEASE

A. Ciobica[1], M. Paulet[2], R. Lefter[2], D. Timofte[3]
[1]Molecular Biology,
Alexandru Ioan Cuza University Iasi, Iasi, Romania
[2]SOP HRD/159/1.5/S/133675 Project,
Romanian Academy, Iasi, Romania
[3]Medicine, "Gr.T.Popa" University, Iasi, Romania

Background

It is well known that in Parkinson's disease (PD), individuals have greater reduction in physical activity levels. Also, inactivity is considered an important factor in accelerating the degenerative process of PD. In addition, PD is known for its cognitive impairments, as well as for depression and anxiety disorders, which may be important causes of morbidity (40% prevalence in PD).

Also, one of the most used animal models of PD is generated by the administration of 1-methyl-4-phenyl-1,2,3,6-tetrahydropyridine (MPTP).

Methods:

We want it to see if induced physical exercising in an MPTP-induced rat model of PD (20 mg/kg i.p.), will result in any changes in memory (as tested in Y maze), anxiety (as tested in elevated-plus-maze) and depression-like behaviour (forced-swim-test), as compared to a non-exercised control group of rats which also received MPTP.

The exercising was performed on an adapted treadmill, for 2 weeks (3 series of 5 minutes/day).

Results

In the group of exercised MPTP group we could observe an increased time spent by the rats in the open arms of the elevated-plus-maze, together with a significant decrease of stretching behaviour and increased head dipping, as compared to non-exercised MPTP group, factors with are suggesting an anxiolytic-like manifestation. In addition, spontaneous alternation in Y maze (index for immediate memory), and swim time (anti-depressive index) in forced swim test were increased in the exercised rats with an MPTP-induced model of PD.

Conclusions

Physical exercising seems to reduce anxiety, depression and memory deficits associated with a MPTP-induced rat model of PD.

943
BRAIN-0600
Non-Registered Abstracts

THE INTERACTION BETWEEN DECREASED SHORT-TERM SPATIAL MEMORY AND INCREASED OXIDATIVE STRESS IN A SCOPOLAMINE-INDUCED RAT MODEL OF ALZHEIMER'S DISEASE

A. Ciobica[1], L. Hritcu[1], R. Lefter[2], B. Stoica[3], D. Timofte[3]
[1]Molecular Biology, Alexandru Ioan Cuza University Iasi, Iasi, Romania
[2]SOP HRD/159/1.5/S/133675 Project, Romanian Academy, Iasi, Romania
[3]Medicine, "Gr.T.Popa" University, Iasi, Romania

Objectives

Scopolamine is a well known muscarinic cholinergic competitive antagonist involved in human and animal memory processes, particularly in the processes of learning acquisition and short-term memory and it has been one of the most used drugs to induce animal models of Alzheimer disease (AD). Also, there is an increased awareness regarding the relevance of the oxidative stress in the progression of AD.

· Methods

In this context, we were interested in studying the effects that scopolamine induction of a rat model of AD has on oxidative stress, as expressed by the Total Antioxidant Status (TAS) from the temporal lobe, the most sensitive brain area to the effects of the oxidative stress status.

· Results

The cognitive deficits of scopolamine were confirmed in the Y maze task, as expressed through a significant decrease of the spontaneous alternation. Also, our data indicated that the administration of scopolamine has a significant prooxidant effect, which is manifested by a decrease in the TAS of the temporal lobe, as compared to the controls. Moreover, a significant Pearson correlation was observed between the

levels of the behavioural tasks and the values of the TAs in the temporal lobe.

· Conclusions

In this study we have demonstrated the presence of increased oxidative stress in a rat model of Alzheimer's disease obtained through the administration of scopolamine. Moreover, there is a significant correlation between the behavioral markers in the Y maze and the levels of TAS, as a result of scopolamine administration.

944
BRAIN-0601
Non-Registered Abstracts

MEMORY DEFICITS IN A KETAMINE-INDUCED RAT MODEL OF SCHIZOPHRENIA

A. Ciobica[1], M. Paulet[2], R. Lefter[2], L. Hritcu[1], Z. Olteanu[1], D. Timofte[3]
[1]Molecular Biology, Alexandru Ioan Cuza University Iasi, Iasi, Romania
[2]SOP HRD/159/1.5/S/133675 Project, Romanian Academy, Iasi, Romania
[3]Medicine, "Gr.T.Popa" University, Iasi, Romania

Background

Significant cognitive impairment is common in schizophrenia, affecting up to 75% of patients. In this way, it seems that a wide range of cognitive functions are affected, and particularly memory. Moreover, it seems that the cognitive impairment often pre-dates the illness onset.

Also, it is now generally accepted that a subchronic administration of 30 mg/kg ketamine induces reliable changes in behaviour of rat and parameters of dopaminergic, glutamatergic, and serotonergic neurotransmissions, which could resemble to schizophrenia manifestations.

Methods:

In this way, in the present experiment, we want it to test if there are any memory deficits in a ketamine-induced rat model of schizophrenia, as tested in the Y maze and radial arm maze tasks. To test this, rats were injected with 30 mg/kg ip ketamine or saline daily for seven consecutive days, while the behavioral experiments were performed 2 weeks after ketamine treatment.

Results:

Our data suggested significant memory deficits in this ketamine-induced rat model of schizophrenia in rat, as demonstrated by an increased number of reference memory errors in 8-radial arm maze. Also, the time necessary to finish this test was increased in the ketamine group, as compared to saline. Moreover, the spontaneous alternation percentage was significantly decreased, suggesting deficiencies in the immediate working memory.

Conclusions:

Our results presented here suggest that subchronic treatment with subanaesthetic doses of ketamine are inducing significant memory deficits, as tested in the Y maze and radial arm maze tasks.

945
BRAIN-0603
Non-Registered Abstracts

STUDYING PAIN MANIFESTATIONS IN AN MPTP-INDUCED RAT MODEL OF PARKINSON'S DISEASE

A. Ciobica[1], R. Lefter[2], M. Paulet[2], V. Bild[3], D. Timofte[3]
[1]Molecular Biology, Alexandru Ioan Cuza University Iasi, Iasi, Romania
[2]SOP HRD/159/1.5/S/133675 Project, Romanian Academy, Iasi, Romania
[3]Medicine, "Gr.T.Popa" University, Iasi, Romania

Background

Generally, Parkinson's disease (PD) is less widely appreciated as a disease causing pain syndromes, although pain is found in 40-80 % of PD patients, as described by the very few reports in this area of research. Moreover, in some PD patients, pain is so severe and intractable that it overshadows

the motor symptoms of the disorder. Still, pain in PD frequently goes underacknowledged and undertreated. Also, the studies regarding pain perception in the existing animal models of PD are very few.

Methods

We experimentally induced the PD model in rats by injecting subcutaneously one dose of 1-methyl-4-phenyl-1,2,3,6-tetrahydropyridine (MPTP), 20mg/kg, while the control group received saline. The behavioral testing for pain included the hot-plate task and was performed 7 days after MPTP injection.

Results

In this way, our rat model resulted from the acute treatment with a low dose of MPTP, exhibited an increased sensitivity to pain perception, as demonstrated by the significant decrease in the values of the latency time in hot-plate for rats treated with MPTP, as compared to the controls. The latency time is expressed in seconds and is referring to the reaction time to two different types of behavior: licking the paw and jumping (11.33 ± 2.1 in controls vs. 52.2 % ± 4.1 in MPTP group).

Conclusions

Our data is suggesting, for the first time in our best of knowledge, an increased sensitivity to pain in a MPTP-induced rat model of PD. In this way, further studies in this area of research seem warranted.

946
BRAIN-0607
Non-Registered Abstracts

ONE SINGLE ADMINISTRATION OF MPTP IS ENOUGH TO PRODUCE MEMORY DEFICITS IN A RAT MODEL OF PARKINSON'S DISEASE

A. Ciobica[1], R. Lefter[2], M. Paulet[2], D. Timofte[3]
[1]Molecular Biology,
Alexandru Ioan Cuza University Iasi, Iasi, Romania
[2]SOP HRD/159/1.5/S/133675 Project,
Romanian Academy, Iasi, Romania
[3]Medicine, "Gr.T.Popa" University, Iasi, Romania

Background: Besides the well known locomotory aspects, the various neuropsychological investigations of patients with Parkinson's disease (PD) have shown specific cognitive impairments, ranging from minor disturbances in memory to intellectual function or even dementia.

Also, one of the most used animal models of PD in rats in referring to the administration of 1-methyl-4-phenyl-1,2,3,6-tetrahydropyridine (MPTP).

Methods: In this way, while most of the administration patterns are including several different intraperitoneally (i.p.) injections of MPTP (e.g. 4 injections X·20mg/kg, 2 h apart; 1–2 daily injections of MPTP, 20–30mg/kg, 5 days), here we were interested, for the first time in our best of knowledge, to see if just one acute administration of a single injection of MPTP 20mg/kg i.p. will result in any cognitive deficits in rats, as studies in the Y maze task. The behavioral testing was performed one week after the MPTP administration, while the control group received saline.

Results: In this way, the administration of single i.p. MPTP dose resulted in a significant decrease of the spontaneous alternation percentage in the Y maze task (77.5± 6.2% in controls vs. 52.2± 4.1% in MPTP group), suggesting deficits in the immediate working memory. Moreover, these results were not generated by some locomotor deficiencies, considering that there was no significant difference in the number of arm entries between the two groups of rats.

Conclusions: One single i.p. administration of MPTP 20 mg/kg is enough to produce memory deficits in a rat model of PD, as studies in the Y maze task.

947
BRAIN-0586
Non-Registered Abstracts

THE EFFECT OF MUSIC TRAINING PROGRAM ON DEVELOPMENT OF LANGUAGE, COGNITIVE AND MOTOR SKILLS IN CHILDREN USING COCHLEAR IMPLANTS; A RANDOMIZED CONTROL TRIAL

S. Dastgheib[1], M. Riasi[2], M. Anvari[2], M.M. Ghasemi[2], M. Rajati[2]
[1]Neuroscience,
Shefa Neuroscience Research Center, Tehran, Iran
[2]Otolaryngology,
Sinus and Surgical Endoscopic Research Center, Mashhad, Iran

Objectives: The purpose of this study was to determine whether cochlear-implant (CI) children can gain benefit from music training. Recent studies have shown the role of music training in enhancing language and learning abilities. Our main goals were to provide an opportunity for (CI) children to have access to music training and to determine whether music can improve their language, communication, and cognitive skills rapidly and efficiently.

Study Design*:* A group of 73 CI children were included in the study and classified into three levels; A, B and C, according to their chronological and hearing age. Children in every level were randomly classified into two groups; music and control. The Newsha Developmental Scale, an integrated test for Persian-speaking CI children, was completed three times by the children's teachers: before administration of the music program and after the third and sixth month of intervention.

Results: Before the intervention there was no significant difference between the music and control group in any level (P>0.05). However, after six months of music training program, the mean difference of scores in the music group was significant (P<0.05) in comparison with the control group in four developmental dimensions: hearing, social contact, cognition, and motor skills.

Conclusions: Although music training program may not significantly improve all language skills in cochlear-implanted children over a short period of time, it can direct deaf children along the path to follow and provide an appropriate platform for CI children to fine tune their language, communication, and cognitive skills.

948
BRAIN-0590
Non-Registered Abstracts

THE EFFECTS OF MOZART'S MUSIC ON INTERICTAL ACTIVITY IN EPILEPTIC PATIENTS: SYSTEMATIC REVIEW AND META-ANALYSIS OF THE LITERATURE

S. Dastgheib[1], P. Layegh[2], R. Sadeghi[3], M. Foroughipur[4], A. Shoeibi[4], A. Gorji[4]
[1]Neuroscience,
Shefa Neuroscience Research Center, Tehran, Iran
[2]Radiology,
Mashhad University of Medical Sciences, Mashhad, Iran
[3]Nuclear Medicine,
Mashhad University of Medical Sciences, Mashhad, Iran
[4]Neurology,
Mashhad University of Medical Sciences, Mashhad, Iran

Mozart's music has been shown to have promising effects on nervous system functions. In general, music therapy has been employed as an adjuvant therapy in different neurologic and psychiatric disorders . The impact of Mozart's music on epilepsy is intriguing. In this study, the effects of Mozart's work on epilepsy were systematically reviewed. Articles dated up to January 11th, 2013 were obtained from a variety of resources, including Google Scholar, Scopus, MEDLINE, ISI Web of Knowledge and Science Direct. The results of eleven studies addressing Mozart's music and epilepsy were extracted by two authors who were blinded to each other. Four studies were considered eligible for the meta-analysis. Data analysis indicated that 76.7% of patients listening to Mozart K. 448 showed a significant decrease in epileptic discharges. A noteworthy response to music therapy in patients with a higher intelligence quotient, generalized or

central discharges as well as idiopathic epilepsy was demonstrated. Possible mechanisms of effects of music therapy on epilepsy, such as the release of dopamine and modulation of neural network plasticity, were discussed. In conclusion, the effect of Mozart's music on epilepsy seems to be significant. However, more randomized control studies are needed to determine its clinical efficacy.

949
BRAIN-0882
Non-Registered Abstracts

EVENT-RELATED HIGH FREQUENCY OSCILLATIONS IN THE AGING BRAIN

M. Christov[1], *J. Dushanova*[1]
[1]*Sensory Neurobiology,*
Institute of neurobiology Bulgarian Academy of Sci ences, Sofia, Bulgaria

Background: The brain as a system with gradually decreasing resources by age maximizes its performance by neural networks reorganization for greater efficiency of neuronal oscillations in a given frequency band. Event-related high frequency-band responses, however, have not enough been investigated in the sensory/cognitive mechanisms accompanying aging. *Method*: The aged effect on the brain electrical activitywas studied in auditory discrimination task (low–frequency and high–frequency tone) at particular cortical locations in beta (β1:12.5–20; β2:20.5–30 Hz) and gamma frequency bands (γ1:30.5–49; γ2:52–70 Hz) during sensory (post–stimulus interval 0–250 ms) and cognitive processing (250–600ms). *Results*: The beta1 activity less affected by age (only at temporal and parietal area) during sensory processing. The reduced beta1 was more widespread during cognitive processing. This difference increased in fronto–parietal direction more expressed after a high-frequency tone. Beta2 and gamma activity are more pronounced with a progressive age during sensory processing. They reduced by age on cognitive processes. Reducing regional-process specificity with progressing age characterized age-related and tone-dependent beta2 changes during sensory processing. Only the elderly showed higher frontal gamma1 activity during sensory processing. The centres of gamma2 shifted from posterior to anterior brain regions with advancing age. *Conclusion*: With increasing age, the frontal brain areas become more sensitive to high-tone discrimination and hand reaction choice. The aged influence was higher on the cognitive processes than on the perceptual ones.

References:

1. Dushanova J, Christov M: Auditory event-related brain potentials for an early discrimination between normal and pathological brain aging, Neural Regeneration Research 2013; 8:1390-1399.
2. Dushanova J, Christov M: The effect of aging on EEG brain oscillations related to sensory and sensorimotor functions, Advances in Medical Sciences 2014; 59:61-67.
3. Dushanova J, Philipova D, Nikolova G: Beta and gamma frequency-range abnormalities in parkinsonian patients under cognitive sensorimotor task. Journal of the Neurological Sciences 2010; 293:51-58.

950
BRAIN-0051
Non-Registered Abstracts

GABAERGIC /GLUTAMATERGIC IMBALANCE RELATIVE TO NEUROINFLAMMATION AND DYSREGULATED REDOX STATUS IN AUTISM SPECTRUM DISORDERS

A. El-Ansary[1], *L. Al-Ayadhi*[1]
[1]*Biochemistry, King Saud University, Riyadh, Saudi Arabia*

GABAergic /glutamatergic imbalance relative to neuroinflammation and dysregulated redox status in autism Spectrum Disorders

Background

Autism spectrum disorder (ASD) is characterized by three core behavioural domains: social deficits, impaired communication, and repetitive behaviours. Glutamatergic / GABAergic imbalance has been found in various preclinical models of ASD. Additionally, autoimmunity immune dysfunction, neuroinflammation , and dysregulated redox status are also considered as etiological mechanisms of this disorder. This study aimed to elucidate the relationship between glutamatergic/ GABAergic imbalance, impaired detoxification, and neuroinflammation as recently-discovered autism-related etiological mechanisms.

Methods

Twenty autistic patients aged 3 to 15 years and 19 age- and gender-matched healthy controls were included in this study. The plasma levels of glutamate, GABA and glutamate/GABA ratio as markers of excitotoxicity, glutathione status , thioredoxin, glutathione-s-transferase as markers of redox status or detoxification, and TNF-α, IL-6, IFN-γ and IFI16 as markers of neuroinflammation were determined in both groups.

Results

Autistic patients exhibited glutamate excitotoxicity based on a much higher glutamate compared to control subjects. Unexpectedly higher GABA and lower glutamate/GABA levels were recorded in autistic patients. While TNF-α and IL-6 were significantly lower, IFN-γ and IFI16 were remarkably higher in the autistic patients than in the control subjects. Poor detoxification ability in autistics was demonstrated and presented as lower GSH/GSSG, higher thioredoxin and less active glutathione-s-transferase.

Conclusion

Multiple regression analysis revealed associations between reduced GABA level, neuroinflammation and glutamate excitotoxicity. This study indicates that autism is a developmental synaptic disorder showing imbalance in GABAergic/ glutamatergic synapses as a consequence of neuroinflammation. Additionally, elevated glutamate was associated with the lower GSH/GSSG and glutathione-s-transferase. This could suggest glutamate signaling as target to treat autism.

951
BRAIN-0052
Non-Registered Abstracts

VITAMIN D STATUS ASSOCIATED WITH NEUROINFLAMMATION AND OXIDATIVE STRESS MARKERS IN AUTISTIC PATIENTS WITH VARYING COGNITIVE AND SOCIAL RESPONSIVENESS SCALES

A. El-Ansary[1], *L. Al-Ayadhi*[1]
[1]*Biochemistry, King Saud University, Riyadh, Saudi Arabia*

Objective

Vitamin D deficiency affects 1 billion people worldwide. It has an important role in bone homeostasis, brain development and modulation of the immune system and yet the role of vitamin D deficiency in the etiology of autism is not ascertained. We assessed the levels of 25-hydroxyl vitamin D levels (*25(OH) D_3*) in relation to C-reactive protein (CRP), cytochrome P450 (Cyt P450) and 8 hydroxy deoxyguanine (8-OHdG) in plasma of Saudi autistic patients compared to age and gender matching healthy control participants.

Design and Methods

C reactive protein,Cyt P450and 8-OHdGas biochemical parameters related to inflammation and oxidative stress together with *25(OH) D_3*, were determined in the plasma of 28 Saudi autistic male patients, categorized as mild-moderate and severe as indicated by their Childhood Autism Rating Scale (CARS) or social responsiveness scale (SRS), and compared to 27 age- and gender-matched control samples.

Results

The data indicated that Saudi patients with autism have remarkably lower plasma levels of 25*(OH) D_3* and Cyt P450 and a significant higher levels of CRP and 8-OHdG compared to age and gender-matched controls. While CRP and 8-OHdG did not correlated with the severity in social and cognitive dysfunction, 25*(OH) D_3* and Cyt P450 were remarkably associated with the severity of CARS but not SRS.

Conclusions

The relationship between the selected parameters confirms the role of vitamin D deficiency in the etiology of autism and the possibility of using25*(OH) D_3*, Cyt P450, CRP and 8-OHdG as markers of this disorder. Receiver operating characteristic analysis together with predictiveness diagrams proved that the measured parameters could be used as predictive markers of preclinical presentation of autism and can serve as guide for future therapeutic or protective strategies through vitamin D.

952
BRAIN-0021
Non-Registered Abstracts

DOES CANDESARTAN REDUCE BLOOD- BRAIN BARRIER PERMEABILITY IN TRAUMATIC BRAIN INJURY?

M. eslami[1], S. khosravi koubanani[1], S. shafa[1], M. khaksari[1], Z. soltani[1]
[1]neuropharmacology research center, Kerman University of Medical Sciences, kerman, Iran

Objectives: Traumatic brain injury (TBI) results in complex pathophysiological reactions by secondary cascades including blood–brain barrier dysfunction and edema formation. Angiotensin II (Ang II) is produced in the brain and Ang II receptor type 1 (AT1R) overstimulation links to cerebrovascular remodeling and inflammation leading to neuronal injury. Ang II receptor blockers (ARBs) are neuroprotective in models of stroke. We therefore evaluated effect of candesartan on TBI induced- blood–brain barrier dysfunction.

Methods: The male Albino N-Mary rats were divided to four groups of sham, TBI, vehicle, and candesartan (n= 6 in each group). The diffuse and moderate TBI was induced by Marmarou method. Candesartan (0.3 mg/ kg) or vehicle was administered i.p. The disruption of Blood brain-barrier (BBB) was evaluated by determining brain content of Evans blue, 5 h post- TBI.

Results: The Evans blue dye significantly was higher in TBI and vehicle groups vs. sham group. But that was no different between TBI and vehicle groups. The reduction of TBI- induced BBB disruption was shown with administration of candesartan. The permeability of BBB was significantly different between sham and candesartan groups.

Conclusion: Our data suggest that ARBs may have therapeutic value in treating TBI- induced brain edema by decreasing disruption of BBB.

Key Words: Brain Injury; Blood- Brain Barrier; neuroprotective; Angiotensin II receptor blocker

953
BRAIN-0382
Non-Registered Abstracts

EARLY REPERFUSION AFTER ISCHEMIC STROKE CONDITIONS BRAIN VASCULAR RESPONSES RELATED TO GLIAL SCAR FORMATION

D. Fernández-López[1], J. González-Hijón[1], I. García-Yébenes[1], A. Moraga[1], S. Palma[1], A. García-Culebras[1], P. Homar[1], V. Durán[1], A. Vega[1], I. Lizasoain[1], M.A. Moro[1]
[1]Pharmacology, Complutense University, Madrid, Spain

Background: an important fraction (60-65%) of stroke patients undergo early reperfusion spontaneously by dissolution of the thrombus in the absence of thrombolytic therapy, and several studies have agreed that early (<24h) spontaneous reperfusion results in improved patient outcome. The impact of early reperfusion on the vascular brain component, however, is largely unexplored in both the acute and the chronic phase of stroke. A better understanding of such effects may provide guiding criteria for prediction of patient recovery during the chronic phase based on the presence and timing of early reperfusion and thus help to design more personalized physical and/or pharmacological therapies to promote functional recovery.

Aim: we aimed to explore the effect of early reperfusion on the responses of the brain vascular component (in terms of blood-brain barrier permeability, vascular perfusion, capillary atrophy and stroke-induced angiogenesis) in the ischemic and peri-ischemic brain regions, covering several time points in the acute and chronic phase after experimental stroke.

Methods: distal middle cerebral artery occlusion (MCAO) was performed either permanently (pMCAO) or transiently (60 min occlusion + reperfusion, tMCAO) on C57bl mice. Mice were injected with BrdU in different dose regimes to characterize the time profile of endothelial cell proliferation induced by stroke in both models, and sacrificed at 48h, 72h, 5 days, 14 days or 28 days after MCAO. Ten minutes before the sacrifice, mice were administered fluorescently-labeled tomato lectin by tail vein injection in order to monitor vascular perfusion and blood-brain barrier leakage. A different set of mice was used for collection of brain tissue samples for western blot analysis at 14 and 28 days. Vascular density, vessel perfusion, blood-brain barrier permeability, endothelial cell death and proliferation were quantified volumetrically on z-stacks obtained by confocal microscopy, and different parameters related to the glial scar were characterized by microscopy and western blot analysis.

Results : both pMCAO and tMCAO induced a sustained degeneration of the vascular plexus in the ischemic regions, as measured by a decrease in vascular density. Although endothelial cell proliferation in those regions was observed in both models between 24 and 72 hours after MCAO, such acute angiogenic responses to stroke were counteracted by endothelial cell death mostly associated to non-perfused vessels. While the glial scar progressed, a secondary angiogenic response was initiated in the ischemic boundaries, leading to the formation of aberrant and tortuous vessels with a dysfunctional blood-brain barrier. In the mice with early reperfusion this response was exacerbated ($p<0.05$, n=7-8), leading to a higher coverage with blood vessels and enhanced endothelial proliferation. While in both models a clearly defined glial scar was present, the molecular composition of the scar was radically different, suggesting that scar composition may determine long-term stroke-induced angiogenesis.

Conclusions: early reperfusion leads to the formation of a differentiated glial scar after stroke, conditioning endogenous vascular remodeling in the ischemic boundaries. Identifying the molecules involved in astrocyte-endothelial communication would provide novel therapeutic approaches for promotion of vascular remodeling and neural plasticity during the chronic recovery phase after stroke.
Funding source: CONSOLIDER-INGENIO Program, MINECO

954
BRAIN-0513
Non-Registered Abstracts

EFFECT OF POST-FIXATION ON DIFFUSION TENSOR MRI AND IMMUNOISTOCHEMICAL STAININGS IN THE INFARCTED MOUSE BRAIN

L. Fontana[1], P. Gelosa[2], A. Montini[1], U. Guerrini[1], E. Tremoli[2], M. Abbracchio[1], L. Sironi[1]
[1]Pharmacological and Biomolecular Sciences, Università degli Studi di Milano, Milano, Italy
[2]Unit of Experimental Thrombosis and Imaging in vivo, Centro Cardiologico Monzino, Milano, Italy

Objectives: Diffusion Tensor Imaging (DTI) has been used for studying animal models of neurodegenerative diseases, both in-vivo and ex-vivo [1]. Ex-vivo DTI allows higher imaging resolution than in vivo DTI and is free of motion artefacts [2]. A currently unsolved issue is whether in-vivo and ex-vivo DTIs are comparable in terms of detecting white matter alteration under pathological conditions.

Aim of the study was, thus, to identify - in a murine brain ischemia model - a fixation protocol with shorter post-fixation time that allows long scan times and multiple acquisitions, concomitantly preserving tissue from over-fixation.

Methods: Nine adult male C57BL/6J mice, five weeks after permanent middle cerebral artery occlusion (pMCAo), were imaged in-vivo (2D EPI and T2w scans). Mice were subsequently divided in 3 groups and perfused with 10% formalin/PBS. Excised skulls were soaked in 10% formalin for 1h, 4h, or 24h at 4 °C, stored in fomblin (a medium that prevents MRI susceptibility artefacts) and finally subjected to at least two ex-vivo acquisitions (3D spin-echo).

Images were processed to extract fractional anisotropy (FA) and diffusivities maps and perform statistical calculations. Quantitative analyses of DTI parameters in two areas of grey matter (somatosensory cortex and striatum) and two of white matter (corpus callosum and main body of corpus callosum) were performed.

After ex-vivo MRI acquisition, the brains were cryopreserved in 30% sucrose and stored at -80 °C. Twenty µm cerebral slices were then challenged with specific antigens for astrocytes (GFAP), oligodendrocytes (NG-2, olig2, MBP and GSTpi), macrophages/microglia (Iba1 and CD68), neurons (SMI31) and neuronal precursors cells (DCX).

Results: In healthy hemisphere, diffusivities [Tr(D)=trace, ADC=apparent diffusion coefficient, AD=axial diffusivity, RD=radial diffusivity] are, according to previous data, 25-50% greater in living specimens, as compared with ex-vivo, and substantially homogeneous among different post-fixation times. FA, $D_{\parallel}$ (trace-normalised axial diffusivity) and $D_{\perp}$ (trace-normalised radial diffusivity) parameters show no significant differences between in-vivo and ex-vivo values. In ischemic hemisphere, % variations of FA, AD, and RD are reduced in ex-vivo specimens in comparison with healthy ones, suggesting a differential effect of fixation on sensitivity of DTI in detecting ischemic damage, without any difference between post-fixation times.

The immunofluorescence analyses for MBP, SMI31, Iba-1, and DCX were not influenced by fixation protocols, whereas for other markers post-fixation time appears to determine the output of immunofluorescence analysis. In our experimental conditions the NG2 antigen was not detectable.

Conclusions: We demonstrated that shorter post-fixation times and storage in fomblin do not affect normalised MRI parameters in healthy tissues, but they still reduce the sensitivity of all DTI parameters in ischemic regions.

The evidence that the immunofluorescence detection of several markers is influenced by fixation protocol should be taken into account when designing ex-vivo MRI analysis coupled with immunofluorescence staining.

References:

[1] Jiang Q et al., NeuroImage 32 (2006) 1080-1089.
[2] Zhang J et al., MRM 67 (2012) 750-759.

955
BRAIN-0832
Non-Registered Abstracts

EXPERIMENTAL CEREBRAL MALARIA INDUCES CEREBRAL VASCULAR DYSFUNCTION AND COGNITIVE IMPAIRMENT VIA ENDOTHELIN A RECEPTOR SIGNALING

B. Freeman[1], Y.C. Martins[1], F.P. Bruno[1], D.C. Spray[2], M.S. Desruisseaux[1]
[1]Pathology, Albert Einstein College of Medicine, Bronx, USA
[2]Neuroscience, Albert Einstein College of Medicine, Bronx, USA

Cerebral malaria (CM) is a serious complication of *P. falciparum* infection associated with cerebral vasculopathy, high mortality, and adverse neurological sequelae. The vasoactive peptide, endothelin-1 (ET-1), has been shown to mediate blood-brain barrier (BBB) permeability, inflammation, and vascular tone, and may be important in CM pathogenesis. We previously reported that ET-1 was associated with brain microvascular hemorrhage, reduced cerebral blood flow, and mortality in our experimental CM (ECM) model. We predict that these actions were mediated by ET-1 activation of the endothelin A (ET_A) receptor. To test the hypothesis that ET-1 is involved in the pathological process of ECM, we investigated ET_A receptor mediated signaling in mice infected with *P. berghei* ANKA (PbA). ET_A receptor blockers (ET_ARB) significantly improved cognitive outcome in mice with ECM. In addition, ET_ARB enhanced vascular integrity during PbA infection. Intravital microscopy was performed and demonstrated that ET_ARB treatment prevented cerebral vasoconstriction induced by PbA-infection. BBB permeability, and protein levels of angiopoietin-2 and VCAM-1 were significantly lower in ECM mice treated with an ET_ARB than in mice treated with saline. Furthermore, ET_ARB prevented the ECM-induced decrease in angiopoietin-1 in the brains of PbA-infected mice. CM is associated with astrogliosis in both human disease and in experimental models. Our preliminary data indicate that astrogliosis is associated with abnormal protein levels of connexin 43 (Cx43), a gap junction protein critical in gliosis and BBB integrity. ET_ARB prevented the PbA-induced dysregulation of Cx43. We hypothesized that ET-1 mediated vascular dysfunction in ECM potentially by regulating neuroinflammation and Cx43 expression. In this regard, we observed a significant increase in the activation of JNK in the brains of mice with ECM. JNK, a downstream substrate of ET-1, has been demonstrated to regulate Cx43 expression and function, and is important in CM. Our data indicate that ET-1 may mediate the vascular pathology and neuroinflammation in ECM via regulation of JNK signaling and subsequent Cx43 dysregulation. The ET-1 pathway may thus be a potential therapeutic target as an adjunct therapy in the treatment of human CM.

956
BRAIN-0472
Non-Registered Abstracts

THE POTENTIAL ROLE OF SULFONYLUREA RECEPTOR 1 IN DEVELOPMENT AND THERAPY OF NEONATAL HEMORRHAGIC STROKE

A. Gekalyuk[1], O.V. Semyachkina-Glushkovskaya[1], A. Shirokov[2], O.A. Sindeeva[1]
[1]Biology, Saratov State University, Saratov, Russia
[2]Immunochemistry, Institute of Biochemistry and Physiology of Plants and Microorganisms, Saratov, Russia

Objectives: During the last decade, several studies point to a beneficial effect of glibenclamide to treat stroke[1]. However, the role of Sur1 in neonatal stroke is unclear; the studies in this area are extremely limited. In our previous study, we showed that glibenclamide improves hemorrhagic stroke (HS)-injures of the brain in adult rats but not in newborn rats[2]. To determine potential role of Sur1 in development and therapy of neonatal HS we studied expression of

sulfonylurea receptor 1 (Sur1) in the brain tissues of neonates with HS in human and rats as well as we assessed penetration of glibenclamide into brain.

Methods: To study of expression of Sur1 in the brain tissue of neonates with HS in human and rats we used immunofluorescence and immunoblotting. The brain of human neonates extracted in babies (n=5) who died from HS, the brain newborns who died from severe infection but with the normal brain tissues served as a control group (n=7). To analyze time-depended changes in expression of Sur1 during HS development we used our model of stress-induced HS (pre-stroke, n=17; incidence of HS, n=25). The control group (n=15) included intact newborn rats. To determine whether glibenclamde penetrate into brain before and after HS in newborn rats, we used glibenclamide injection (BODIPY FL, green fluorescence, 10 µg/kg, iv) in groups: 1) intact rats (the control, n=10); 2) rats 4h after stress (pre-stroke, n=25); 3) rats 24h after stress (HS, n=22).

Results: In five died newborns we found subarachnoid hemorrhages, severe edema and hypoxia, congestion of excessive blood in dilated cerebral veins and in vessels of microcirculatory network of pia mater. Sur1 identified in neurons and cerebral capillaries in the HS-injured brain of all studied subjects but not in the control group.

The expression of Sur1 observed in stressed rats 4h after stress that associated with development of cerebral insufficiency and decreased blood outflow from the brain. The higher expression of Sur1 we found in rats with HS that accompanied by critical changes in the brain such as cerebral hypotention, perivascular edema and severe hypoxia. Sur1 didn't identify in the brain of healthy rats.

The glibenclamide labeling was present in endothelial cells of cerebral vessels and neurons pre-stroke
but not 24h after stress.

Conclusion: The upregulation of Sur1 is an important mechanism underlying critical changes on the brain tissues that precede neonatal HS and are associated with HS-injures of brain. These results confirm a beneficial effect of glibenclamide in the treatment of stroke. However, penetration of glibenclamide progressively is reduced in newborn rats with HS and is presented only before HS. Our data suggest that detailed study of effects of glibenclamide for prevention of HS risk in newborns is essential.

References:

1)Woo, S.K.; Kwon, M.S.; Ivanov, A. The sulfonylurea receptor 1 (Sur1)-transient receptor potential melastatin 4 (Trpm4) channel. *J. Biol. Chem.* 2013, *288*, 3655–3667

2)The Simard, J.M.; Geng, Z.; Woo, S.K.; Ivanova, S. Glibenclamide reduces inflammation, vasogenic edema, and caspase-3 activation after subarachnoid hemorrhage. *J. Cereb. Blood Flow Metab.* 2009, *29*, 317–330.

957
BRAIN-0838
Non-Registered Abstracts

CEREBRAL HEMODYNAMIC RESPONSES TO HYPOCAPNIA AND HYPERCAPNIA: MULTI-WAVELENGTH TIME-RESOLVED STUDIES

A. Gerega[1], W. Weigl[2], D. Janusek[1], M. Kacprzak[1], A. Liebert[1]
[1]Department for Biophysical Measurements and I maging,
Institute of Biocybernetics and Biomedical Enginee ring Polish Academy of Science, Warsaw, Poland
[2]Anaesthesiology and Intensive Care Department of Surgical Sciences, Uppsala University, Uppsala, Sweden

Objectives: Recently, near-infrared spectroscopy (NIRS) [1] has a good potential of application at the bedside for assessment of cerebral perfusion and brain oxygenation [2]. We have proposed method of time-resolved diffuse reflectance NIRS with detection of the optical signal at 16 wavelengths. In our study, we investigate the

cerebral hemodynamic changes (HbO_2 and Hb) during controlled hypo- and hypercapnia. Earlier, the cerebral hemodynamic responses were studied with continuous wave NIRS [3], but extracerebral layers, such as scalp and scull, influence the results of the measurements. Application of the proposed by authors method may allow to improve the depth selectivity of the method.

Methods: A time-resolved NIRS instrument allowing the diffuse reflectance measurements simultaneously at multiple wavelengths on the forehead of a healthy volunteer was used [4]. Measurements of were performed by using of a "supercontinuum" source of light and multichannel time-resolved system based on a time-correlated single-photon counting electronics. The instrument was used to record distributions of times of flight of photons (DTOF's) at single source–detector separation of 3 cm during normocapnia, hypocapnia (-15mmHg) and hypercapnia (+15mmHg). The recorded DTOF's were analyzed by calculating the statistical moments (the number of diffusely reflected photons, the mean time of flight of photons and the variance of DTOF) for 16 wavelengths from near-infrared region (from 650 to 850nm with the step of 12.5 nm). The changes of the optical spectra over all detected wavelengths were clearly distinguished due to absorption changes related to changes of hemoglobins concentration during controlled hypocapnia and hypercapnia tests.

Results: In the hypercapnia test, after a 1-minute normocapnia period, a dynamic decrease in the number of photons was observed. However, in the signals of higher-order moments, the changes were observed only at the moment when the CO_2 concentration reached its maximum value. This may indicate the effect of autoregulation which under the influence of increased CO_2 concentration, leads to weak change in cerebral blood flow (until the ΔCO_2 reaches 15 mmHg), while the blood flow in the skin increases.

The polarity of the changes in moments of the DTOF's in both tests are wavelength-dependent because of the behavior of the hemoglobins during controlled cerebral perfusion changes test. Estimating the concentration changes of HbO_2 and Hb was carried out using the algorithm based on estimation of the optical properties from the statistical moments of the measured DTOFs [5] during normocapnia, hypocapnia and hypercapnia. The changes of the HbO_2, Hb as well as ΔHb_{tot} are appropriate to its expected behavior.

Conclusions: The method of the multiple wavelength detection may allow for more precise estimation of hemodynamic parameters (ΔHbO_2 and ΔHb). The multiwavelength measurement was successfully carried out during hyper- and hypocapnic tests.

The study financed by the Project DOBR/0052/R/ID1/2012/03.

References:

1. Villringer, A., Trends in Neuroscience, 1997.
2 Obrig, H., J Cereb Blood Flow Metab, 2003.
3. Rupp, T., J Cereb Blood Flow Metab, 2014.
4. Gerega, A. in *Biomedical Optics and 3-D Imaging*. 2012. Miami, USA.
5. Arridge, S.R., Phys Med Biol, 1992.

958
BRAIN-0346
Non-Registered Abstracts

THE ROLE OF TOXIC PROINFLAMMATORY MEDIATOR-CYTOKINES IN CARDIOCEREBRAL SYNDROME

E.I. Giyazitdinova[1], A.T. Azimov[1], Y.A. Musaeva[1], G.S. Rakhimbaeva[1], S. Musaev[2]
[1]Neurology, Tashkent Medical Academy, Tashkent, Uzbekistan
[2]Neurology, Tashkent Medical Academy, Tashkent, Afghanistan

BACKGROUND AND PURPOSE: The aim is our to study the pathological state of microglial cells, which are not recovered to the condition of functional rest and continued to support phlogosis reactions, producing one of toxic proinflammatory mediator-cytokines in

cardiocerebral syndrome (CCS) at different times of the acute period of the disease.

METHODS: In our observation were 35 patients with CCS, and aged were 34 to 94 years. Spontaneous produce of cytokines in the cerebrospinal fluid from patients determined using monoclonal antibodies.

RESULTS: In patients with CCS on the first day of the disease (7-20 hours after the first symptoms of the disease) showed a significant increase in tumor necrosis factor (TNF-α) to 39.6 ± 6,1 pg / ml, which is 375% of the benchmark. By the third day of illness content TNF-α decreases slightly, amounting to 28,5 ± 3,7 pg / ml (less than the first day of 31.7%). By the tenth day of the disease the content of TNF-α is somewhat reduced, but still has not reached the level of individuals in the control group-19,6 ± 2,5 pg / ml. In 5 patients with CCS the third day of the disease level of TNF-α remained at the same level, and by the tenth day declined slightly.

CONCLUSION: Thus, the study of cytokines CCS showed the prevalence of the disease in the first day of the inflammatory cytokine TNF-α, which indicates the presence of an inflammatory response in the brain ischemic injury. Dynamic increase in proinflammatory cytokines indicates an increase in neurological deficit and worsening prognosis.

959
BRAIN-0353
Non-Registered Abstracts

ONE OF THE MAIN DIAGNOSTIC CRITERIA OF SMALL VESSELS DISEASE OF THE BRAIN

E.I. Giyazitdinova[1], A.T. Azimov[1], S. Musaev[1], Y.A. Musaeva[1], G.S. Rakhimbaeva[1]
[1]Neurology, Tashkent Medical Academy, Tashkent, Uzbekistan

BACKGROUND AND PURPOSE: Dilatation of the Virchow-Robin space (VRS) is constantly characterized as markers of cerebrovascular disease, and it is predictor of vascular dementia. The aim of our study was to observe differences in magnetic resonance imaging of dilatation of VRS between subjects with the subcortical ischemic vascular dementia (SIVD), ill-defined cognitively impaired patients and cognitively normal healthy control subjects, as well as the association between the dilatation of VRS and degree of development the subcortical ischemic vascular dementia .

METHODS: Thirty five subjects with SIVD, twenty five Ill-defined cognitively impaired patients and twenty healthy volunteers of comparable age and sex were studied. We made out deep white matter , periventricular hyperintensities and the VRS dilatation, as figures of magnetic resonance images. Magnetic resonance imaging of VRS dilatation was compared across groups and examined by VRS dilatation's location and size.

RESULTS: White matter lesions were more common in patients with SIVD than in those with Ill-defined cognitively impaired or healthy volunteers ($P < 0.01$). VRS dilatations figures were significantly higher in patients with vascular dementia and SVR were more dilated and prevalenced than in with Ill-defined cognitively impaired patients ($P <0.001$). Magnetic resonance images of VRS were normal of healthy volunteers ($P <0.001$).

Discussion: Dilatation of the Virchow-Robin Space is one of manifestations in small vessels diseases and can be used as the diagnostic criteria for prognostication ischemic vascular dementia.

960
BRAIN-0370
Non-Registered Abstracts

ELIMINATION OF HYPOKINESIA INDUCED CEREBRAL BLOOD FLOW AND MOTOR COORDINATION DISTURBANCES BY CITICOLINE

T. Grigoryan[1], *M. Balasanyan*[2], *K. Alikhanyan*[3]
[1]*Clinical pharmacology, Yerevan State Medical University, Yerevan, Armenia*
[2]*Pharmacology, Yerevan State Medical University, Yerevan, Armenia*
[3]*Clinical Pharmacology, Yerevan State Medical University, Yerevan, Armenia*

Movement restriction- main problem of modern lifestyle, is one of the important risk factors in a lot of pathologies, including cerebral blood flow (CBF) disorders and stroke. Hypokinesia (HK) leads to development of neurochemical, behavioral and morphological changes of brain, typical for chronic ischemisation [1]. So, the purpose of our study is to investigate the influence of citicoline on CBF disturbances and motor coordination changes under the condition of HK. As a natural endogenous compound, citicoline (cytidine-5´-diphosphocholine; CDP-choline) is an essential intermediate in the synthesis of cell membrane structural phospholipids and its formation is the rate-limiting step in phosphatidylcholine synthesis, which appears beneficial effects in a number of CNS injury models and pathological conditions of the brain.

White inbred male rats weighing 180-220g were used. For HK rats were kept individually in narrow cages for 15 and 30 days [2]. Motor coordination of rats was investigated in Rota-Rod Treadmill (RRT) test [3]. Animals were anesthetized by intraperitoneal (i/p) injection of nembutal (40mg/kg). CBF was measured by Laser-Doppler-Flowmeter. During measurement animals were fixed in the stereotaxic apparatus. In the experiments where used animals with high locomotor activity chosen in 'Open field' test. Hypokinetic animals which didn't receive any drugs were considered as control group. Experimental group of rats received citicoline at dose of 12,5mg/kg, i/p twice a day. Paired student's t-test was used to assess to changes of regional CBF and motor coordination parameters. $P < 0.05$ was selected for statistical significance.

The data obtained have shown that after 15 days of HK citicoline leads to increase of CBF. After the injection of the investigated drug rising of the CBF in 5 minutes have been observed, which reaches its maximum value in the 90th minute (about 28%). The effect of citicoline on CBF after 30-day HK was more prominent: on 90th minute 62% increase of CBF was demonstrated (see table).

CBF changes in % after citicoline administration (12,5mg/kg, i/p)

	10 min	20 min	40 min	60 min	90 min
HK 15 day	11,85±8,7	16,0±9,8	20,1±8,9 *	25,4±5,3 *	28,4±3,1 *
HK 30 day	13,6±4,5	20,0±5,5 *	28,5±6,8 *	41,1±7,5	62,2±9,1

*- P<0,05

Assessment of motor coordination demonstrated citicoline ability to improve it: time spent on the drum by 15-day control group was 29,5±11,5, meanwhile administration of citicoline leaded to the increase of time spending on the drum about 50% (47,5±15,5). HK for 30 days resulted in the significant impairment of motor coordination. Administration of citicoline to the experimental group of rats after 30 days of HK was characterized by increasing of motor coordination more than 5 time compare with 30-day control group.

Thus, our results evident, that citicoline could be used as an effective agent for prevention of cerebral blood flow and motor coordination

disturbances in patients with restricted movement activity.

1. Akopyan V.P. et al., Hypokinesia and cerebral blood flow, Med., 1999:p.120-151.

2. Fedorov I.V. et al., Metabolism during hypokinesia, Med., 1982:p.17-25.

3. Yang Y.R. et al., Motor performance improved by exercises in cerebral ischemic rats, J. Mot Behav., 2012;44(2):97-103.

961
BRAIN-0550
Non-Registered Abstracts

FREE RADICAL DEPENDENT NEUROVASCULAR DE-COUPLING IN AN IN VITRO MODEL OF STATUS EPILEPTICUS

L. Hasam Henderson[1], I. Papageorgiou[2], J. Swolinsky[3], V. Muoio[4], A. Friedman[5], R. Kovacs[1]
[1]Institute for Neurophysiology, Charite University Medicine Berlin, Berlin, Germany
[2]Neuroradiology, Universitätsmedizin Göttingen, Göttingen, Germany
[3]Charite, Charite University Medicine Berlin, Berlin, Germany
[4]Neurosurgery, Hospital Sirio-Libanes, Sao Paulo, Brazil
[5]Medical Neurosciences, Delhousie University, Nova Scotia, Canada

Free radical dependent neurovascular de-coupling in an in vitro model of status epilepticus

Luisa A. Hasam, Ismini Papageorgiou, Jutta Swolinsky, Valeria Muoio, Alon Friedman, Richard Kovács

Objectives

Determine the formation of oxygen centered free radicals during epileptiform activity and their effect on neurovascular coupling and blood brain barrier (BBB) function.

Methods

We used organotypic hippocampal slice cultures (OHSCs) to study the neurovascular coupling and the BBB function during induced epileptiform activity.

In order to assess mitochondrial super oxide production and BBB integrity, OHSCs were stained with MitoSOX/calcein-AM. Peroxide levels were determined by staining dihydrodichlorofluorescein-DA. Fluorescence was monitored in selected vessels in stratum radiatum by using a spinning disk confocal microscope while local field potentials and pO_2 recordings were obtained from the CA3 pyramidal layer.

Epileptiform activity was induced by perfusion with modified Mg^{2+} -free ACSF.

Laminin, NG2 and Hoechst staining was performed to assess pericyte location and alterations of the vascularization following epileptiform activity.

Results

BBB integrity and vascular motility was preserved in OHSCs. Vasoconstriction was elicited by mechanical stimulation of the pericytes, increased intraluminal pressure or by exposure to the thromboxane analogue (U46619). Changes in pericyte length corresponded to changes in vessel diameter.

Pre-constricted vessels dilated following the onset seizure-like events (SLEs) indicating functional neurovascular coupling in OHSCs. However, SLE-associated vasodilatation became smaller during the course of recurrent SLEs.

We observed a terminal vasoconstriction which was associated with the opening of the vessel lumen and with the release of intraluminally accumulated dichlorofluorescein. Remarkably, as revealed by MitoSOX fluorescence, free radical formation was also enhanced in pericytes.

Oxidative metabolism increased during SLEs, as revealed by monitoring tissue pO_2. At the same time peroxide formation was enhanced as

suggested by oxidation of dihydrodichlorofluorescein. Capillary network disturbances were observed in OHSCs after 12 hours of SLEs cessation.

Conclusion

Overly reduced electron transport chain complexes in presence of high mitochondrial [Ca^{2+}] might facilitate mitochondrial superoxide formation and hydrogen peroxide release.

Free radical formation during epileptiform activity might be sufficient to disturb neurovascular coupling and increase permeability of BBB.

References

Kovács, Richard, Papageorgiou, I., & Heinemann, U.: *Slice cultures as a model to study neurovascular coupling and blood brain barrier in vitro*. Cardiovascular psychiatry and neurology, vol. *2011*, pp. 646958, 2011.

Malinska, D., Kulawiak, B., Kudin, A. P., Kovacs, R., Huchzermeyer, C., Kann, O., … Kunz, W. S.: *Complex III-dependent superoxide production of brain mitochondria contributes to seizure-related ROS formation*. Biochimica et Biophysica Acta (BBA) - Bioenergetics, vol. *1797*, pp. 1163–1170, 2010.

Peppiatt, C. M., Howarth, C., Mobbs, P., & Attwell, D.: *Bidirectional control of CNS capillary diameter by pericytes*. Nature, vol. *443*, pp. 700–704, 2006.

Yemisci, M., Gursoy-Ozdemir, Y., Vural, A., Can, A., Topalkara, K., & Dalkara, T.: *Pericyte contraction induced by oxidative-nitrative stress impairs capillary reflow despite successful opening of an occluded cerebral artery*. Nature medicine, vol. *15*, pp. 1031–1037, 2009.

962
BRAIN-0211
Non-Registered Abstracts

INFLUENCE OF FISETIN AGAINST HYPERHOMOCYSTEINEMIA INDUCED VASCULAR DEMENTIA AND POSSIBLE ROLE OF FOLIC ACID

B. Hemanth kumar[1], A. Padmanabha Rao[1], P.V. Diwan[1]
[1]Department of pharmacology, School of Pharmacy Anurag Group of Institutions, HYDERABAD, India

Objectives: Fisetin (3, 7, 3′, 4′-tetrahydroxyflavone) belongs to the flavonoid group of polyphenols found in many fruits and vegetables. Folic acid or folate deficiency is well reported in many behavioral disorders and can also lead to hyperhomocystenemia (Hhcy). The main objective of present study is to evaluate therapeutic potential of fisetin perse and in combination with folic acid against hyperhomocystenemia induced vascular dementia.

Methods: Male rats of Wistar type were used in this study. They were treated with homocysteine (Hcy), 0.3-0.6 µmol/g, subcutaneously, twice daily,folic acid , 5mg/kg, intraperitoneally, fisetin,15 mg/kg, orally, donepezil, 0.5mg/kg, intraperitoneally and combination of fisetin with folic acid in the stated doses daily after the second dose of Hcy for one month. Control animals received saline in the same volume as Hcy.Rats were trained on Morris water maze (MWM) and Y-maze and tested for learning and memory tasks using video tracking e-Maze software system. Then, animals were sacrificed by cervical dislocation and blood samples were taken to determine plasma Hcy levels, neutrophill count, serum nitrite and lipid profile (triglycerides, total cholesterol, LDL and HDL).Thoracic aorta was isolated for testing vascular endothelial function and brain tissue was homogenized for determination of acetylcholinesterase activity, glutamate, super oxide dismutase, catalase, reduced glutathione, thiobarbituric acid reactive species.Finally brain histopathology was performed to support the

data obtained from behavioural and biochemical estimations.

Results: The results show that the administration of Hcy produced Hhcy and endothelial dysfunction as reflected by significant ($P < 0.001$) increase in plasma Hcy levels and decrease in serum nitrite concentration.Hcy treated rats have shown impairment in spatial learning and memory tested by MWM and Y-maze. Furthermore, HHcy also induced statistically significant increase ($P < 0.001$) in brain antioxidant levels, AChE activity,glutamate and serum lipid parameters. fisetin per se and folic acid combination significantly ($P < 0.01$) attenuated Hcy induced endothelial dysfunction and cognitive impairment. This intervention also significantly ($P < 0.001$, $P < 0.01$) lowered the neutrophil count and attenuated all the biomarkers of Hhcy. Furthermore, both fisetin perse and combination with folic acid synergistically attenuated all histological alterations induced by Hhcy.

Conclusions: This study reveals the antioxidant potential of fisetin in Hhcy and vascular dementia and also highlights the possible role of Folic acid in synergizing the effects of fisetin. Further studies are in progress to clarify the mechanisms underlying the synergistic effect of fisetin with folic acid and their relevance as an adjuvant therapy in Hhcy.

References:

1. Bazzano LA .No effect of folic acid supplementation on cardiovascular events, cancer or mortality after 5 years in people at increased cardiovascular risk, although homocysteine levels are reduced. Evid Based Med2011; 16 (4): 117–8.

2. Maher P, Akaishi T, Abe K. Flavonoid fisetin promotes ERK-dependent long-term potentiation and enhances memory. Proceedings of the National Academy of Sciences of the United States of America USA 2006; 103:16568–16573.

3. Cristiane M, et al.Concurrent folate treatment prevents Na+,K+-ATPase activity inhibition and memory impairments caused by chronic hyperhomocysteinemia during rat development. Int. J. Devl Neuroscience 2007;25: 545–552.

Fig-1: Effect of Fisetin and Folic acid on Acetylcholine Induced Endothelium Dependent Relaxation Using Aortic Ring Preparation

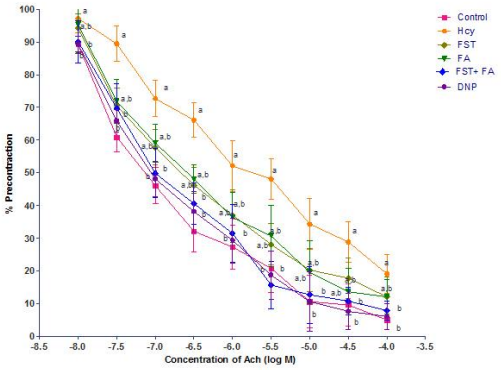

Responses are expressed as percentage of pre -contraction induced by 3×10 $^{-6}$ M phenylephrine. Results are mean ± standard error of means; Repeated measure ANOVA followed by Newman K eul's test. a= P < 0.001 when compared with vehicle control; b=p< 0.001 when compared with Hcy treated group. Ach —acetylcholine; DNP -Donepezil ; FST -Fisetin; FA -Folic acid .

Fig-2: Effect of Fisetin and Folic acid on Sodium Nitroprusside Induced Endothelium Independent Relaxation Using Aortic Ring Preparation

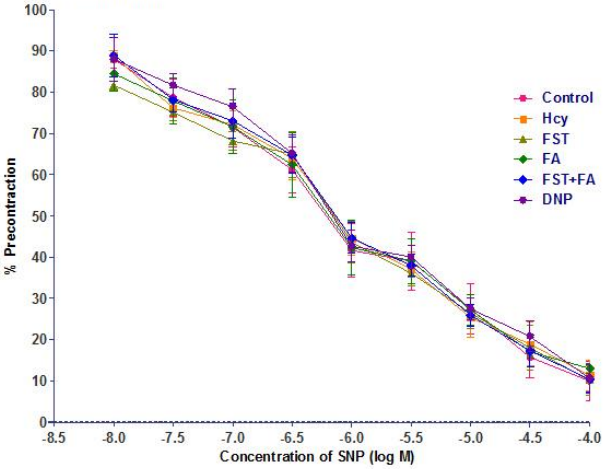

Responses are expressed as percentage of precontraction induced by 3× 10 $^{-6}$ M phenylephrine. n =6 Results are mean ± standard error of means; Repeated measures of ANOVA followed by Newman –Keul's test. SNP —sodium nitroprusside.

963
BRAIN-0042
Non-Registered Abstracts

ACCIDENTAL CHILDREN POISONING WITH METHADONE

N. jafari[1], F. Farnaghi[2], F. Mehregan[2]
[1]Neurology, Mofid Hospital, Tehran, Iran
[2]pediatric, Loghman Hospital, Tehran, Iran

Accidental Children Poisoning With Methadone: An Iranian Pediatric Sectional Study

Abstract

Objective

Toxic poisoning with methadone is common in children in Iran. Our study was carried out due to the changing pattern of methadone poisoning in recent years and increasing methadone toxicity.

Materials & Methods

In this descriptive-sectional study, all of the methadone poisoned children younger than 12 years who were admitted to the Loghman Hakim Hospital in 2012, were assessed. Clinical symptoms and signs, para-clinical findings, and treatment were evaluated.

Results

In this study, 16 boys and 15 girls who had been poisoned by methadone were enrolled. The mean age of patients was 55 months. All patients had been poisoned randomly or due to parent's mistakes. The mean time of symptoms onset after methadone consumption was 1 hour and 30 Min, indicating a relatively long time after onset of symptoms.

Clinical findings were drowsiness (75%), miotic pupil (68 %), vomiting (61%), rapid shallow breathing (57%) and apnea (40%). In paraclinical tests, respiratory acidosis (69%) and leukocytosis (55.2%) were seen. The most important finding was increase in distance of QT in ECG (23.8%). The mean time of treatment with naloxone infusion was 51 hours. Three percent of patients had a return of symptoms after discontinuation of methadone. In patients with apnea, a longer course of treatment was required, and this difference was significant. Also, 17% of patients with apnea had aspiration pneumonia, which was statistically significant.

Conclusion

We suggest long time treatment with naloxone and considering the probability of return of symptoms after discontinuation of methadone.

References

1. Goldfrank L, Flomenbaum N, Lewin N. Goldfrank's Toxicologic Emergencies. 7th ed. McGraw–Hill 2002; p. 590-607.
2. Schelble DT. Phosgene and phosphine. In: Haddad LM, Shannon MW, Winchester J, eds. Clinical Management of Poisoning and Drug Overdose. 3rd ed. Philadelphia: WB Saunders; 2007. p. 640-7.
3. Jennifer C, Gibson A. Accidental methadone poisoning in children: A call for Canadian research action. Child Abuse Negl;2010;34(8):553-4.
4. Binchy JM, Molyneux E, Manning J. Accidental ingestion of methadone by children in Merseyside. BMJ 1994;308(6940:1335-6.
5. Zamani N, Sanaei-Zadeh H, Mostafazadeh B. Hallmarks of opium poisoning in infants and toddlers. Trop Doct 2010;40(4):220-2.
6. LoVecchio F, Pizon A, Riley B, Sami A, D'Incognito C. Onset of symptoms after methadone overdose. Am J Emerg Med 2007;25(1):57-9.
7. Thanavaro KL, Thanavaro JL. Methadone-induced torsades de pointes: a twist of fate. Heart Lung 2011;40(5):448-53.
8. Gaalen FA, Compier EA, Fogteloo AJ. Sudden hearing loss after a methadone overdose. Eur Arch Otorhinolaryngol 2009;266(5):773-4.
9. Lynch RE, Hack RA. Methadone-induced rigid-chest syndrome after substantial overdose.Pediatrics. 2010; 126(1):232-4.
10. Sidlo J, Valuch J, Ocko P, Bauerová J. Fatal methadone intoxication in a 11-month-old male infant. Soud Lek 2009;54(2):23-5.

Keywords
Children; Opium; Methadone; Poisoning
964
BRAIN-0712
Non-Registered Abstracts

MRI-BASED, PREDICTABLE OPENING OF BLOOD BRAIN BARRIER USING HYPEROSMOLAR AGENT FOR PRECISE INTRA-ARTERIAL DRUG DELIVERY

M. Janowski[1], *M. Pearl*[1], *P. Walczak*[1]
[1]*Radiology, Johns Hopkins University, Baltimore, USA*

Purpose

Hyperosmolar opening of BBB for effective delivery of drugs to the central nervous system has been attempted for years, but variability of results prohibited wide clinical acceptance. Here, we used MRI guidance to overcome that limitation and to target desired brain area in a highly predictable fashion.

Methods

After catheter placement in cerebral arteries under x-ray guidance, eight 4-kg New Zealand white rabbits under general anesthesia were transported to a 3T MRI (Magnetom Trio, Siemens) and underwent baseline T2 (TR/TE 1500/105) and T1 (TR/TE 300/9.1) weighted images of the brain. The horizontal plane best displayed the brainstem in its entirety and was chosen as the working view for dynamic susceptibility contrast (DSC) enhanced trans-catheter perfusion. IA Feraheme (dissolved in saline at 1:100; 0.3mgFe/ml) was infused between 0.001 ml/sec to 0.1 ml/sec for 30 seconds to assess the trans-catheter parenchymal perfusion territory at specific speeds. Real-time GE-EPI images (TE=36 ms, TR=3000 ms, FOV=1080, matrix=128, and temporal resolution=3 s) were obtained for DSC. Immediately after the Feraheme injection, 25% IA mannitol was administered at the optimal rate previously determined by the Feraheme injection to produce targeted BBBO. The duration of the mannitol infusion was determined by the infusion speed. Five minutes after IA mannitol, 1.5 ml of gadolinium (Magnevist, 0.125 mmol/kg) and Evans Blue (EB) 2% (2 mg/kg) were injected intravenously. T1-weighted images were acquired post gadolinium. To demonstrate the effect of the microcatheter tip placement, the microcatheter was withdrawn more proximally within basilar artery inside the MR scanner, after which the Feraheme and mannitol infusions were repeated.

Results

DSC MRI of IA Feraheme boluses allowed real-time assessment of local parenchymal perfusion, manifested as MRI signal reduction (hypointensity). Rapid Feraheme washout with clearance of the hypointensities immediately after the bolus allowed for repetitive boluses at different speeds with subsequent DSC imaging to optimize injection rate and microcatheter location to achieve the desired perfusion territory.

The rate of injection greatly affected the perfusion area with slower rates producing a smaller, localized region and faster speeds resulting in a larger, more diffuse territory. Notably, a given injection rate resulted in different ranges of perfusion territories in different rabbits, necessitating personalized titration of injection speed to achieve the desired targeted area for each rabbit.

The microcatheter tip position in the vertebro-basilar circulation also greatly affected the perfusion area with distribution to the medulla, cervical spinal cord, and adjacent paraspinal muscles when in the V4 segment, whereas a position in the mid basilar artery resulted in supply to the pons, medulla and cerebellum. Importantly, even small changes in the microcatheter tip position within the basilar artery resulted in differential perfusion of the brainstem based on the tortuosity and direction of flow within the basilar artery. The territory of BBB opening depicted *in vivo* by gadolinium-enhancement and post mortem Evans Blue staining closely matched the perfusion area.

Conclusions

DSC perfusion imaging, allows for the dynamic depiction of transcatheter parenchymal flow, which in turn enables the prediction and titration the area of BBBO.

965
BRAIN-0754
Non-Registered Abstracts

LONG-TERM SURVIVAL AND DIFFERENTIATION OF HUMAN NEURAL STEM CELLS IN THE ISCHEMIC STROKE BRAIN OF RHESUS MONKEY WITHOUT IMMUNOSUPPRESSION

Y. Jin[1], S. Lee[1], H. Lee[2], Y. Lee[1], K. Yi[3], K. Jeong[1], C. Jeon[1], H. Yeo[1], S. Cha[3], K. Chang[1]
[1]National Primate Research Center, Korea Research Institute of Bioscience & Biotechnology, Cheongju-si, Korea
[2]Medical Research Institute, Chung-Ang University College of Medicine, Seoul, Korea
[3]Department of Radiology, Chungbuk National University College of Medicine, Cheongju-si, Korea

Globally, Stroke was one of the third largest causes of human death in 2012. Also, life lost rates for stroke increased by 12% between 2000 and 2012. Ischemic stroke accounts for approximately 70~80% of stroke. However, ischemic stroke therapies are limited, the majority of ischemic stroke patients are needed alternative treatment. Stem cell transplantation therapy may have great potential to therapeutic strategy in ischemic stroke. In the present study, we inoculated human neural stem cells (hNSCs) in ischemic stroke model of two non-human primate rhesus monkeys brain via the middle cerebral artery and femoral vein without immunosuppression. During 24 months after hNSCs xenograft, we evaluated of hNSCs's survival, differentiation, potential tumorigenesis via magnetic resonance imaging (MRI), histopathological and immunohistochemical analyses. In conclusion, xenografted hNSCs in ischemic stroke model of two monkeys survived successfully for 24 months in the absence of immunosuppression and also were differentiated into neurons and astrocytes. Their long term survival was identifiable with the use of fluorescent magnetic nanoparticles s by MRI follow-up. MRI, histopathological, and immunohistochemical analyses at 24 months post inoculation showed no evidence of tumor formation by the grafted hNSCs. When compared to the results in injection of hNSCs by the middle cerebral artery and femoral vein two kinds of paths, the path of middle cerebral artery was identified as methods to deliver a large number of hNSCs in the brain than in the paths of femoral vein.

966
BRAIN-0028
Non-Registered Abstracts

TRANSCRANIAL DOPPLER ULTRASONOGRAPHY: A METHOD OF EVALUATING COGNITIVELY IMPAIRED AND NON-COGNITIVELY IMPAIRED ELDERLY

M. Kalbi[1], J. Catindig[1], S. Marasigan[1], J. Navarro[1]
[1]Neurology, Jose R. Reyes Memorial Medical Center, Metro Manila, Philippines

Introduction: Aging and dementia are associated with changes in cerebrovascular structure and function which contribute to cognitive decline. Research investigating functional cerebrovascular have employed techniques such as functional magnetic resonance imaging, positron emission tomography or single photon emission computed tomography but these techniques are expensive and are not available in tertiary government hospitals in the Philippines. Transcranial Doppler Ultrasonography (TCD) is a non-invasive, inexpensive and portable technique that can successfully assessed the intracranial hemodynamics of an aging brain.

Objective: The purpose of this study was to investigate and compare the cerebral hemodynamic status (blood flow velocity and pulsatility index) of cognitively impaired and non-cognitively impaired elderly using Transcranial Doppler.

Methods: This is a cross sectional study conducted in Jose R. Reyes Memorial Medical

Center (JRRMMC) from January to August 2013. Forty patients were selected using convenience sampling and were screened using the Montreal Cognitive Assessment-Philippines (MoCA-P). Scores more than or equal to 21 were grouped under non-cognitively impaired elderly while scores lower than 21 were under cognitively impaired elderly. Transcranial ultrasound basal examination were performed using a 2-MHz power motion probe (M-mode) to study the middle cerebral artery (MCA), the anterior circulation artery (ACA) and posterior cerebral artery (PCA).

Results: Our findings showed that patients with cognitive impairment have lower mean flow velocity (p value=0.0001) and higher pulsatility index (p value=0.0001) when compared to non-cognitively impaired elderly.

Conclusion: Our findings are congruent with previous observations that abnormalities in cerebral hemodynamic status are present in cognitively impaired elderly and may be related to microvessel damage secondary to vascular risk factors.

967
BRAIN-0029
Non-Registered Abstracts

PREVALENCE OF INTRACRANIAL STENOSIS USING TRANSCRANIAL DOPPLER AND ITS DIAGNOSTIC ACCURACY IN VERTEBROBASILAR INFARCTION

M. Kalbi[1], *J. Navarro*[1]
[1]*Neurology,*
Jose R. Reyes Memorial Medical Center,
Metro Manila, Philippines

Introduction: Posterior circulation ischemia is an important cause of acute neurological disease. Therefore, emergent non assessment of posterior circulation is critical not only for rapid confirmation of but also for identification of patients at higher risk of poor outcome as candidates for interventional treatment. Transcranial Doppler (TCD) is a fast, non invasive, widely available diagnostic tool that can detect, localize and grade the severity of intracranial arterial obstruction in the setting of acute ischemic stroke.

Objective: The objectives of this study were to determine the prevalence rate of intracranial stenosis using Transcranial Doppler (TCD) among patients with vertebrobasilar ischemia and to evaluate the diagnostic accuracy of TCD compared with brain Magnetic Resonance Angiography (MRA) in the detection of intracranial stenosis.

Methods: This is a prospective study conducted in Jose R. Reyes Memorial Medical Center (JRRMMC) Neurology Ward from January 2012 to December 2012. Consecutive patients admitted to the ward with definite clinical diagnosis of acute vertebrobasilar ischemia underwent TCD and brain MRI with MRA done 48 hours after admission. A second TCD was done one week after admission. SONIA criteria for mean flow velocity (MFV) cutoffs on TCD were used for identification of > 50 % stenosis.

Results: Twenty patients were included in the study. Results showed that 75 % (15 out of 20) of patients with vertebrobasilar infarctions have intracranial stenosis in MRA. Out of the 15 patients with vertebrobasilar stenosis detected by MRA, 6 of them registered high mean flow velocity on TCD. TCD showed high specificity (100%) but less sensitivity (40%) in the detection of vertebrobasilar stenosis

Conclusion: TCD can be suggested as a screening tool in detecting intracranial stenosis in patients with acute vertebrobasilar infarctions.

968
BRAIN-0814
Non-Registered Abstracts

NEURAL CORRELATES OF UNFAMILIAR VERSUS SELF-SELECTED MUSIC GENRES INVESTIGATED WITH FMRI TOWARDS DEVELOPING AN OPTIMIZED PARADIGM FOR MUSIC THERAPY

C. Karmonik[1], F. Brooks[2], J. Anderson[3], A. Brandt[4], S. Fung[5], J.T. Frazier[2]
[1]MRI Core, Houston Methodist Research Institute, Houston, USA
[2]Center for Performing Arts Medicine, Houston Methodist Hospital, Houston, USA
[3]MRI Core, Houston Methodist Hospital Research Institute, Houston, USA
[4]Shepard School of Music, Rice University, Houston, USA
[5]Radiology, Houston Methodist Hospital, Houston, USA

Purpose: To investigate if differences in brain activation when listening to unfamiliar music pieces compared self-selected music with emotional attachment can be utilized to develop a personalized music therapy paradigm.

Methods: fMRI BOLD activation using the generalized linear model (GLM) was quantified in 12 healthy subjects (4 male) listening to 3 music pieces and 3 control spoken-word sections (each 6 minutes, alternating 30 seconds off/on, 3T Philips Ingenia, TR=2.4 seconds) while simultaneously undergoing recording of EEG brain signals (Brainvision, 16 bipolar electrodes). Subjects were instructed to bring one music piece to the session with strong emotional attachment. Unfamiliar pieces included Bach invention #1 and traditional Japanese court music ('Gagaku'). As controls, sonorous African click language ('Click'), emotional speech ('The Great Dictator', Charlie 'Chaplin') and a collection of audio news casts of non-emotional speech ('Cronkite') was included. Bach invention #1 was repeated with visual guidance by a moving cursor through the score sheet.

Results: Brain waves recorded with EEG indicated awareness in all subjects for all paradigms. In addition to sensory areas, self-selected music showed statistical significant (p

Conclusion: Varying degrees of familiarity and emotional attachment when listening to music results in distinct variations in brain activation. Visual guidance increased activation during listening. These individual differences in music processing may be of importance when selecting music for use in therapy to optimize outcome.

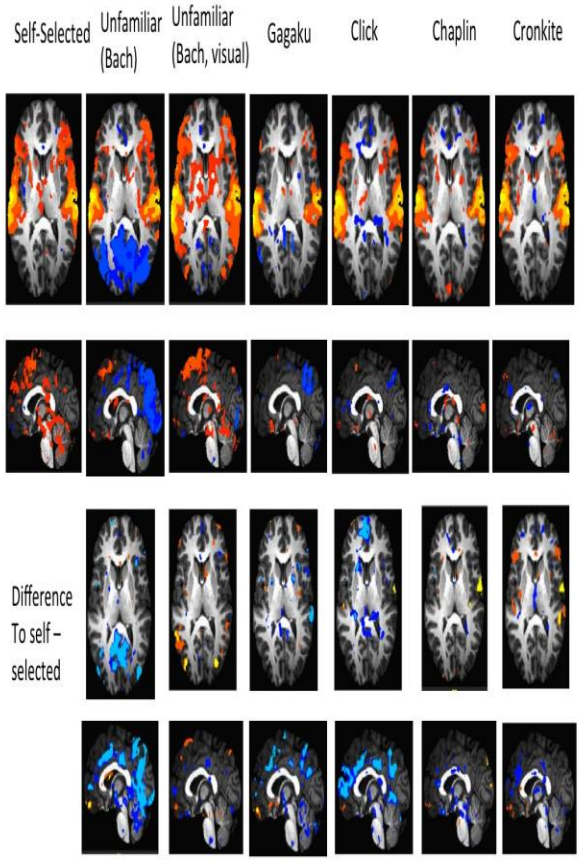

Figure 1: To rows: axial and sagittal fMRI BOLD average activation maps (p<0.05) transferred into Talairach space (yellow-orange: BOLD increase during listening, blue: BOLD increase during rest). Bottom rows: difference in BOLD activation relative to the self-selected music. Variations in activation patterns can be appreciated with emotional centers active for the self-selected music piece and the visually guided Bach piece. Delayed processing in the precuneus are noted in varying degrees for the unfamiliar pieces.

969
BRAIN-0905
Non-Registered Abstracts

CALCIUM CHANNEL BLOCKER ENHANCES BENEFICIAL EFFECTS OF AN ANGIOTENSIN II AT1 RECEPTOR BLOCKER AGAINST CEREBROVASCULAR-RENAL INJURY IN TYPE 2 DIABETIC MICE

R. kazi[1]
[1]*Pharmacology,*
Bangladesh Agricultural University, Mymensingh, Bangladesh

Recentclinical trials have demonstrated that combination therapy with renin-angiotensin system inhibitors plus calciumchannel blockers (CCBs) elicits beneficial effects on cardiovascular and renalevents in hypertensive patients with high cardiovascular risks. In the presentstudy, we hypothesized that CCB enhances the protective effects of anangiotensin II type 1 receptor blocker (ARB) against diabetic cerebrovascular-renalinjury. Saline-drinking type 2 diabetic KK-A^y mice developedhypertension and exhibited impaired cognitive function, blood-brain barrier(BBB) disruption, albuminuria, glomerular sclerosis and podocyte injury. Thesebrain and renal injuries were associated with increased expression of NADPHoxidase components and oxidative stress. Treatment with the ARB, olmesartan (10mg/kg/day) and hydralazine (25 mg/kg/day) similarly reduced blood pressure insaline-drinking KK-A^y mice. However, treatment with olmesartan, butnot with hydralazine, attenuated cognitive decline, BBB disruption, glomerularinjury and albuminuria, which were associated with a reduction in oxidativestress in brain and kidney tissues. Furthermore, a suppressive dose ofazelnidipine (3 mg/kg/day) exaggerated these beneficial effects of olmesartan.These data support the hypothesis that a CCB enhances ARB-associatedcerebrovascular-renal protective effects, independent of blood pressurereduction in type 2 diabetes.

970
BRAIN-0706
Non-Registered Abstracts

FUNCTIONAL ULTRASOUND (FUS) IMAGING OF BRAIN HEMODYNAMICS IN A RAT MIDDLE-CEREBRAL ARTERY OCCLUSION (MCAO) MODEL OF SELECTIVE NEURONAL LOSS (SNL) MIMICKING TRANSIENT ISCHEMIC ATTACK (TIA)

C. Dussaux[1], *C. Brunner*[1], *C. Isabel*[1], *A. Martin*[2], *A. Savoye*[1], *G. Montaldo*[1], *J.C. Baron*[1], *A. Urban*[1]
[1]*Psychiatry and Neurosciences Center - Team Optogenetics and Brain Imaging INSERM U894, Sainte- Anne Hospital, Paris, France*
[2]*Molecular Imaging Unit, CICbiomaGUNE, San Sebastian, Spain*

Objectives: SNL is a known outcome of brief MCAo in rodents, affecting mainly the striatum or cortex with proximal and distal MCAo, respectively[1]. SNL is important as it might also occur after TIAs, potentially impacting the cognitive and plastic 'reserve'. However, both the behavioral and tissue perfusion changes underlying SNL remain only partly understood. In the present study, we assessed SNL and behavior in rodents in conjunction with fUS, a new imaging method for longitudinal whole-brain mapping of cerebral blood volume (CBV) with high spatiotemporal resolution[2].

Methods: Eight adult Sprague-Dawley rats were subjected to 45min MCAo under 1.5% isoflurane and 100% oxygen. Four sham rats were used as controls. fUS data were acquired through previously thinned skull, serially before, during and at 3 and 6 days after reperfusion. Ipsilateral/contralateral CBV ratios (CBVr) were computed for a template of atlas-based cytoarchitectonic ROIs modified from previous work[3]. The Neuroscore and subtle sensorimotor functions (modified Sticky Label test and Beam Walking test) were assessed before and serially after tMCAo. Brains were collected at day 21 for immunofluorescence (IF) using NeuN, Iba1 and GFAP.

Results: We observed a marked (>50%) reduction in CBVr in the MCA territory during occlusion in 7/8 rats (one rat with no CBVr decrease was excluded from further analysis). Maximal CBVr

reduction affected the somatosensory cortex (79±13% relative to baseline; p<0.0001). CBVr had returned to near-baseline 15mins after reperfusion, and to normal levels subsequently (p<0.05, ANOVA). No statistically significant behavioral effects emerged across the group at any time point. No changes in CBVr or behavior were present in sham rats. There was marked striatal SNL (associated with moderate microglial activation and marked astrocytosis) in 5/7 MCAo rats vs 0/4 sham (p<0.05), and mild cortical SNL was present in 4/7 MCAo rats (and 1/4 shams). There was no correlation among CBV, behavioral scores and IF lesion volumes.

Conclusions: This study shows the feasibility of fUS to serially map CBV during and over days following MCAo. Mild and less consistent cortical SNL occurred despite marked initial rCBV reductions. The lack of behavioral correlates with mainly striatal SNL contrasts with cortical SNL[4] and is consistent with previous reports regarding striatal infarcts[5]. Overall, SNL is a frequent sequelae of brief MCAo in rodents and likely also occurs after TIAs, and as such has potential clinical and therapeutic relevance.

[1] J.C. Baron et al, JCBFM, 34 (2014) 2-18.
[2] A. Urban et al, Neuroimage, 101 (2014) 138-49.
[3] J.L. Hughes et al, Neuroimage, 49 (2010) 19-31.
[4] Ejaz S. et al, Stroke (in press)
[5] S. Wegener et al, J Magn Reson Imaging, 21 (2005) 340-6.

971
BRAIN-0176
Non-Registered Abstracts

CROSS-TALK BETWEEN GONADAL STEROID HORMONES SIGNALING AND CYTOKINE SIGNALING AFTER EXPERIMENTAL TRAUMATIC BRAIN INJURY

M. Khaksari Haddad[1], F. Frahani[2], S. Dabiri[3], M. Nikpour[4], R. Khaksari Haddad[4]
[1]Physilogy Research Center,
Kerman University of Medical Sciences, kerman, Iran
[2]Neurosciences Research CenterInstitute of Neuro pharmacology,
Kerman University of Medical Sciences, kerman, Iran
[3]Department of Pathology,
Kerman University of Medical Sciences, kerman, Iran
[4]Physiology Research Center,
Kerman University of Medical Sciences, kerman, Iran

Objectives:The neuroprotectiveand anti-inflammatory effects of female steroid hormones on traumatic brain injury (TBI)are mediated, in part, by inhibitory effects on cytokines (Sarkaki et al., 2013,Khaksari et al., 2011)levels after TBI.In addition to the above mechanism,where it is reported that these steroids may affect the cytokine signaling pathway (Liu et al.,2014), to determine this mechanism by which steroids regulates this signaling pathway, here we investigated the effects of administration of exogenous estrogen /progesteroneon brain STAT3/SOCS3 in female rats after TBI.Methods: In this study, ovariectomized female rats were randomly divided into 7groups: (1) sham, (2) TBI group,(3) vehicle, (4) estrogen low concentrations (E_1), (5) estrogenhighconcentrations (E_2), (6) progesteronelow concentration(P_1), and (7) progesteronehigh concentration(P_2). The TBI model was established using a Marmarou 'sweight-dropping model. Brain samples were extracted 24 h following TBI. The expression levels of STAT3and SOCS3were examined using immunohistochemistry, and brain edema was determined using brain water content (BWC).Results:This model consistently resulted in increased BWC .Both steroid hormones attenuated post injury brain edema. In TBIgroup, theSOCS-3 positive cells,compared toshamdecreased and inallgroups thattreated withestrogenor progesterone, these SOCS-3 positive cells were increased; but this increaseinE1, E2, and P2groups compared to vehicle groupwas statistically significant. Although comparisons between treatment groups showed that E2 effectcompared with E1 and P2 groups was significant. The p-STAT3 positive cells significantly decreased after TBI.However, only

E_2increased p-STAT3 activation,That a greater inhibitory effect of E2 on neuronscompared with astrocytes or microglia. **Conclusion.**These results suggest that exogenous estrogen /progesteroneincrease brainSOCS3 activation and decreasep-STAT3 level after TBI. This represents the initial demonstration offemale steroid hormones crosstalk with cytokines signaling in post injury brain.

References:

Sarkaki AR,Khaksari Haddad M, Shahrokhi N.Time- and Dose-Dependent Neuroprotective Effects of Sex Steroid Hormones on Inflammatory Cytokinesafter a Traumatic Brain Injury. J. Neurotrauma,2013.,30:47–54.

Khaksari M, Shahrokhi N, Moshtaghi G, Asadikaram G.The role of estrogen and progesterone, administered alone and in combination, in modulating cytokine concentration following traumatic brain injury.Can J PhysiolPharmacol. 2011;89(1):31-40

Liu CJ, Kuo FC, Hu HM, Chen CY, Huang YB, Cheng KH, Yokoyama KK, Wu DC, Hsieh S, Kuo CH.17β-Estradiol inhibition of IL-6-Src and Cas and paxillin pathway suppresses human mesenchymal stem cells-mediated gastric cancer cell motility.Transl Res. 2014;164(3):232-43.

972
BRAIN-0015
Non-Registered Abstracts

Non-Registered Abstracts

FOCAL TRIPHASIC SHARP WAVES AND SPIKES IN THE ELECTROENCEPHALOGRAM.

A. Janati[1], N. Alghassab[2], U. Khan[3]
[1]Neurology, Center for Neurology, Fairfax, USA
[2]Neurology, King Khalid Hospital, Ha'il, Saudi Arabia
[3]Neurology, Dow University of Health Sciences, Karachi, Pakistan

OBJECTIVE:There is a plethora of data in the EEG literature on the characteristics of the most prominent component of interictal epileptiform discharges (IED), namely the negative (fast) phase. Surprisingly, however, little attention has been drawn to the after-coming slow wave (ASW), and its pathological as well as clinical significance. In this paper, we will address the significance of prominent (high amplitude) ASW, giving rise to a triphasic morphology of the IED (focal triphasic sharp waves and spikes-FTSW). We will discuss this EEG pattern with respect to its clinical, neurophysiological, and neuropathological significance.
METHOD:This investigation was conducted on a heterogeneous group of patients at KKH, Ha'il, KSA.
RESULT:Our data revealed that FTSW were rare EEG events occurring primarily in the first two decades of life. Ninety percent of the patients with FTSW had epilepsy, presenting clinically with generalized convulsive seizures, often without partial onset. The majority of these patients responded favorably to anticonvulsant monotherapy. We were surprised to find that half of the patients with FTSW had chronic and/or static CNS pathology, particularly congenital CNS anomalies. Even though more than one mechanism may be involved in the pathogenesis of FTSW, we believe a deeply seated pacemaker as the source of this EEG pattern is the most compelling theory.
CONCLUSION:The presence of FTSW should alert clinicians to the possibility of an underlying chronic and/or static CNS pathology, in particular congenital CNS anomalies, underscoring the significance of neuroimaging in the work-up of this population. Moreover, it is conceivable that the prominent ASW may contribute to the interictal intellectual dysfunction of these patients, justifying aggressive anticonvulsant therapy.

REFRENCES:

1. Amer Clin Neurophysiology Society (2006) Guideline 8: guidelines for recording clinical EEG and digital media. J Clin Neurophysiol 23(2):122–124
2. Blume WT (2001) Pathogenesis of Lennox–Gastaut syndrome:

considerations and hypotheses. Epileptic Disord 3(4):183–196
3. Blumenfeld H (2005) Cellular and network mechanisms of spike-wave discharges. Epilepsia 46(Suppl. 9):21–33
4. Cambier DM, Kantarci K, Worrell GA et al (2003) Lateralized and focal clinical, EEG and FLAIR MRI abnormalities in Jacob–Creutzfelt disease. Clin Neurophysiol 114(9):1724–1728
5. Chatrian GE, Bergamini L, Dondey M et al (1974) A glossary of terms most commonly used by clinical electroencephalographers. Electroencephalogr Clin Neurophysiol 37:538–548
6. Daube JR, Stead SM (2009) Basics of neurophysiology. In: Daube JR, Rubin DI (eds) Textbook of clinical neurophysiology, 3rd edn, Oxford, pp 69–96
7. Ebersole JS (1997) Defining epileptogenic foci: past, present, future. J Clin Neurophysiol 14(6):470–483
8. Fisch FJ (2003) Interictal epileptiform activity: diagnostic and behavioral implications. J Clin Neurophys 20(3):155–162
9. Foley JM, Watson CW, Adams RD (1950) Significance of the electroencephalographic changes in hepatic coma. Trans Am Neurol Assoc 75:161–165
10. Golensohn ES, Purpura DP (1963) Intracellular potentials of cortical neurons during focal epileptogenic discharges. Science 139:840–842
11. Janati A, Erba G (1982) Electroencephalographic correlates of near-drowning encephalopathy in children. Electroencephalogr Clin Neurophyiol 53(2):182–191
12. Janati A, Husain MM, Moore DB et al (1986) Suppression-burst pattern associated with generalized epileptiform discharges and alpha-theta pattern coma. Clin Electroencephalogr 17:82–88
13. Kabat J, Kral P (2012) Focal cortical dysplasia. Pol. J Radiol 77(2):35–43

973
BRAIN-0016
Non-Registered Abstracts

POSITIVE SHARP WAVES IN THE EEG OF CHILDREN AND ADULTS.

A. Janati[1], U. Khan[2], N. Alghassab[3], K. Alshurtan[3]
[1]Neurology, Center for Neurology, Fairfax, USA
[2]Neurology, Dow University of Health Sciences, Karachi, Pakistan
[3]Neurology, King Khalid Hospital, Ha'il, Saudi Arabia

Objective: Interictal epileptiform discharges (IEDs) with negative polarity have been extensively studied in the EEG literature. However, little attention has been drawn to IED with positive polarity [positive sharp waves (PSWs)]. In this paper, we discuss pathophysiological, neuroimaging, and clinical correlates of this pattern in a heterogeneous group of children and adults who demonstrated PSW in their scalp EEG.
Method:We prospectively reviewed the EEGs of 1,250 patients from a heterogeneous population over a period of 1 year.
Results:Thirty-one patients had PSW in their EEG. We documented EEG parameters as well as demographic, clinical, and neuroimaging data. Statistical analysis was performed to correlate the aforementioned data. The analysis showed that PSW is an epileptogenic pattern with localizing significance, occurring primarily in the younger age groups. Furthermore, there was a strong association of PSW with chronic and/or static CNS pathology, in particular, congenital CNS anomalies, often accompanied by psychomotor retardation. Patients with "multifocal'' PSW invariably exhibited severe intellectual and motor deficits associated consistently with a variety of congenital CNS insults.
Conclusion:PSW is a rare and under-reported EEG abnormality which, similar to negative IED, signifies focal epileptogenecity. The presence of PSW should prompt neuroimaging studies to investigate an associated chronic/static CNS pathology, in particular, congenital CNS anomalies. This association is particularly strong when PSW is multifocal in which case patients

present with severe intellectual and motor deficits.

Refrences:

1. American Clinical Neurophysiological Society (2006) Guideline 8: guidelines for recording clinical EEG and digital media. J Clin Neurophysiol 23(2):122–124
2. Blume WT (2001) Pathogenesis of Lennox–Gastaut syndrome: considerations and hypotheses. Epileptic Disord 3(4):183–196
3. Brazier MBA (1951) A study of the electrical fields at the surface of the head. Electroencephalogr Clin Neurophysiol: 38–52
4. Chatrian GE, Bergamini L, Dondey M et al (1974) A glossary of terms most commonly used by clinical electroencephalographers. Electroencephalogr Clin Neurophysiol 37:538–548
5. Ebersole JS (1997) Defining epileptogenic foci: past, present, future. J Clin Neurophysiol 14(6):470–483
6. Goldensohn ES, Purpura DP (1963) Intracellular potentials of cortical neurons during focal epileptogenic discharges. Science 139:840–842
7. Kabat J, Kral P (2012) Focal cortical dysplasia. Pol J Radiol 77(2):35–43
8. Kellaway P, Hrachovy RA. Electroencephalography. In: Swaiman KF, Wright FS (eds) The practice of pediatric neurology, 2nd edn, pp 96–114
9. Lombroso CT (1981) Intracranial hemorrhage in the newborn. A prospective clinical and electrophysiological study of 37 cases. In: Proceedings of the IYDP commemorative International Symposium on developmental disabilities. Elsevier, Tokyo, pp 251–56
10. Lombroso CT (1985) Neonatal polygraphy in full term and premature infants: a review of normal and abnormal findings. J Clin Neurophysiol 2:105–155
11. McCulloch W (1972) Mechanisms for the spread of epileptic activation of the brain. Electroencephalogr Clin Neurophysiol 32:529–544
12. Maulsby RL (1971) Some guidelines for assessment of spikes and sharp waves in EEG tracings. Am J EEG Technol 11:3–16
13. Matsuo F, Knott JR (1977) Focal positive spikes in electroencephalography. Electroencephalogr Clin Neurophysiol 42:15–25
14. Nowack WJ, Janati A, Antuago T (1987) Positive temporal sharp waves in the neonate. J Clin Neurophysiol 4:315–317
15. Nowack WJ, Janati A (1990) Positive sharp waves in neonatal EEG. Am J EEG Technol 30:211–221

974
BRAIN-0946
Non-Registered Abstracts

THE EFFECTS OF EXPOSURE TO 915 MHZ RADIOFREQUENCY IDENTIFICATION ON CEREBRAL GLUCOSE METABOLISM IN RAT: A [F-18] FDG MICRO-PET STUDY.

H. Kim[1], Y. LEE[2], Y. An[3], M. Paik[4], H. Choi[5], J. Pack[6], N. Kim[7], Y. Ahn[1]
[1]Department of Neurosurgery, Ajou University School of Medicine, Suwon, Korea
[2]Division of Life Science and Pharmaceuticals College of Pharmacy, Ewha Woman's University, Seoul, Korea
[3]Department of Nuclear Medicine, Ajou University School of Medicine, Suwon, Korea
[4]College of Pharmacy, Sunchon National University, Sunchon, Korea
[5]Department of Nuclear Medicine, Electronics and Telecommunications Research Institute, Daejeon, Korea
[6]Department of Radio Sciences and Engineering College of Engineering, Chungnam National University, Daejeon, Korea
[7]School of Electrical and Computer Engineering, Chungbuk National University, Cheongju, Korea

PURPOSE: We investigated the effect of whole-body exposure to 915-MHz radiofrequency identification (RFID) on rat cortical glucose metabolism by using (18)F-deoxyglucose positron emission tomography (FDG-PET).

MATERIALS AND METHODS: Male Sprague-Dawley rats were divided into three groups: Cage-control, sham-exposed and RFID-exposed groups. Rats were exposed to the 915-MHz RFID for 8 h daily, 5 days per week, for 2 or 16 weeks. The whole-body average specific absorption rate (SAR) was 4 W/kg for the field of the 915 MHz RFID signal. FDG-PET images were obtained the day after RFID exposure, using micro-PET with a FDG tracer. With a Xeleris functional imaging workstation, absolute values in regions of interest (ROI) in the frontal, temporal and parietal cortexes and cerebellum were measured. Cortical ROI values were normalized to the cerebellar value and compared.

RESULTS: The data showed that the relative cerebral glucose metabolic rate was unchanged in the frontal, temporal and parietal cortexes of the 915 MHz RFID-exposed rats, compared with rats in cage-control and sham-exposed groups.

CONCLUSION: Our results suggest that 915 MHz RFID radiation exposure did not cause a significant long lasting effect on glucose metabolism in the rat brain.

975
BRAIN-0214
Non-Registered Abstracts

NEUROTOXICITY OF CASSAVA CYANOGENS: RELEVANCE TO THE PATHOGENESIS OF KONZO, A MOTOR NEURON DISEASE PREVALENT IN SUB-SAHARAN AFRICA

S. Kimani[1], S. Kipruto[2], F.R.E.D. Bukachi[3], V. Monterroso[4], C. Maitai[5], D. Tshala-Katumbay[6]
[1]Nursing, University of Nairobi, Nairobi, Kenya
[2]Pharmacology and Pharmacognosy, University of Nairobi, Nairobi, Kenya
[3]Medical Physiology, University of Nairobi, Nairobi, Kenya
[4]Laboratory animal services, Georgia Regents University, Georgia, USA
[5]Pharmacology and Pharmacognosy, University Of nairobi, Nairobi, Kenya
[6]CROET, Oregon Health and Science University, Portland, USA

Background: Cassava is staple food toover half a billion people globally. Consumption of insufficiently processedcassava and dietary sulfur amino acid (SAA) deficiency has been implicated inthe pathogenesis of Konzo, a paralytic condition prevalent in Sub-Saharancountries. Recently cyanogenic cassava has been associated with cognitivedeficits in humans. The probable

candidates for such neurodegeneration and/ordisability include cyanide, or cyanate, sulfur deficiency, or their respectivecombinations. The susceptibility factors and mechanisms underlying the toxicityof cyanogenic cassava have remained poorly understood.

Objectives: To elucidate themolecular neuro-targets of cassava cyanogens (cyanide or cyanate) toxicityunder SAA-deficient diet in rodents

Methods: Young adult male rats(Crl: NIH-Fox1 rnu/Fox 1+, 6-8 weeks old) were fed either a diet rich in allamino acids (AAA) or 75%-deficient in SAA and treated intraperitoneally witheither 2.5 mg/kg/body weight (bw) NaCN, or 50 mg/kg/bw NaOCN, or 1µl/g/bwsaline, for up to 6 weeks. Behavioral activity and protein carbamoylation wereassessed. Carbamoylation of albumin and spinal cord proteins was analyzed byliquid chromatography mass spectrometry (LC-MS/MS).

Results: Rats treated with NaCN showed acute seizures whereas NaOCN induced limb paralysisunder SAA-restricted diet. Additionally, NaOCN induced high levels ofcarbamoylation relative to NaCN and vehicle ($P<0.001$). At Day 14, adiet-treatment interaction effect on albumin carbamoylation ($p=0.07$) was found,however there was no effect attributed to diet ($p=0.71$) at day 28. The meannumber of NaCN-associated carbamoylated sites on albumin became 47.4%significantly higher relative to vehicle (95% CI:16.7-86.4%) at day 28. Spinalcord proteins were only carbamoylated by NaOCN prominently under theSAA-restricted diet. Differentially carbamoylated proteins included myelinbasic protein, myelin proteolipid protein, neurofilament light polypeptide,glial fibrillary acidic protein, and 2', 3' cyclic-nucleotide3'-phosphodiesterase.

Conclusion: The nervous systemsusceptibility to food (cassava) cyanogenesis and neurotoxic insults seen inkonzo subjects may result from a “multiple hit” process including cyanide,cyanate toxicity, deficiency in sulfane sulfur, and cyanate-induced carbamoylation.The multiple hit processes may combine direct mitochondrial insults, proteincarbamoylation and a thiol-redox derangement. This level of pathogenetic complexity should be considered in biomarkerstudies and efforts to prevent neurotoxicity effects of cassava.

976
BRAIN-0113
Non-Registered Abstracts

PROPHYLACTIC AND PROLONGED HYPOTHERMIA IN POOR-GRADE-SAH REDUCES DEGREE OF VASOSPASM AND RATE OF DELAYED CEREBRAL INFARCTIONS

J.B. Kuramatsu[1], R. Kollmar[1], D. Staykov[1], S.P. Kloska[2], A. Doerfler[2], I.Y. Eyüpoglu[3], S. Schwab[1], H.B. Huttner[1]
[1]Department of Neurology, University Hospital Erlangen, Erlangen, Germany
[2]Department of Neuroradiology, University Hospital Erlangen, Erlangen, Germany
[3]Department of Neurosurgery, University Hospital Erlangen, Erlangen, Germany

Background: Therapeutic hypothermia (TH) is an established neuroprotective approach after cardiac arrest and growing evidence supports TH as supportive treatment in stroke. In subarachnoid haemorrhage (SAH) only few data exists comprising heterogeneous TH-strategies. We evaluated a novel approach of prophylactic and prolonged TH and its influence on key complications in poor-grade SAH - vasospasm and delayed cerebral infarction (DCI).

Methods: This observational matched-controlled study included 36 poor-grade (Hunt&Hess-Scale>3,WFNS-Scale>3) SAH patients. Twelve patients received prophylactic TH (<48h after ictus), mild (35°C), prolonged (7±1days), and were matched to 24 patients from prospective SAH-database. Vasospasm was diagnosed by angiography, serially evaluated by Doppler-sonography and DCI was defined as new infarction on follow-up-CT. Functional outcome was assessed at 6-months by modified-Rankin-Scale and categorized as favorable (mRS=0-2) *versus* unfavorable (mRS=3-6) outcome.

Results: Vasospasm was present in 71.0% of patients. TH neither influenced occurrence nor duration, but the degree of vasospasm as well as peak-spastic velocities were significantly reduced ($p<0.05$). Frequency of DCI was 87.5% in non-TH *versus* 50% in TH-treated patients, translating into a relative risk reduction of 43% with an risk-ratio of 0.33 (CI(0.14-0.77);p=0.036). Favorable functional outcome was twice as frequent in TH-treated patients 66.7% *versus* 33.3% of non-TH (p=0.06).

Conclusion: Prophylactic and prolonged TH seems to influence degree of vasospasm and significantly decreased occurrence of DCI, possibly ameliorating functional outcome. TH may represent a promising therapy targeting the multiple pathways of DCI development, notably vasospasm, which strongly warrants further evaluation of its clinical impact.

977
BRAIN-0038
Non-Registered Abstracts

PREDICTION OF PROGRESSIVE SECONDARY BRAIN DAMAGE FOLLOWING TRAUMATIC INTRACRANIAL HEMORRHAGE.

J. Kuzibaev[1], K. Makhkamov[1]
[1]Neurosurgery,
Republican Research Center of emergency medicin e, Tashkent, Uzbekistan

Introduction: Traumatic intracranial hemorrhage (TIH) represents a challenge for neurosurgeons due to its high mortality and morbidity rates. The most severe lesion associated with TIH is secondary brain damage. Thus, the purpose was to investigate the CT parameters for predicting of progressive secondary brain damage (PSBD) associated with TIH.

Method: We reviewed the records of 252 patients suffering from TIH whose first CT scan was Obtained within 24 h of the injury. The repeat CT examinations were routinely Obtained within 24 h of admission as well as when suggested by clinical worsening. The patients were divided into two groups: PSBD group (124 patients) and non- PSBD group (128 patients). All patients in two groups were comparable due to the level of consciousness and ages of patients and severity of secondary brain injury.

Results: The differences between PSBD and non-PSBD were significant in the initial CT scans showing type, volume and location of TIH, brain swelling and midline shift as well as the associated brain contusion ($P<0.01$). Logistic regression analysis showed that early predictors of PSBD were: intracerebral type of hemorrhage, temporal localization of hematoma, volume of hematoma more than 40 cm3, midline shift more than 5mm, brain swelling and contusion volume more than 20 cm3 ($P<0.01$).

Conclusions: Thus, if the initial CT scan of patients with TIH shows intracerebral hemorrhage, temporal localization of hematoma, volume of hematoma more than 40 cm3, midline shift more than 5mm, brain swelling and contusion volume more than 20 cm3, an earlier CT scan should be performed for detection of PSBD.

978
BRAIN-0039
Non-Registered Abstracts

TREATMENT OF SECONDARY BRAIN DAMAGE IN PATIENTS WITH TRAUMATIC INTRACRANIAL HEMATOMAS USING DECOMPRESSIVE CRANIECTOMY.

J. Kuzibaev[1], K. Makhkamov[1]
[1]Neurosurgery,
Republican Research Center of emergency medicin e, Tashkent, Uzbekistan

INTRODUCTION - OBJECTIVE: Traumatic intracranial hematomas represent a challenge for neurosurgeons due to their high mortality and morbidity. Secondary brain damage is an important factor that influences the outcome of traumatic intracranial hematomas. We compared the effect of early decompressive craniectomy with that of non- decompressive craniectomy on the outcome of patients with secondary brain damage following severe traumatic brain injury.

METHOD: A retrospective review was conducted of 127 consecutive patients who presented with secondary brain damage following isolated severe head injury with intracranial hematomas. Early decompressive craniectomy after hematoma removal (mean time from injury: 5.8±2.5 h) was carried out in 82 patients (mean age: 45.7±5.6 years), whereas 45 patients (mean age: 43.4±4.1 years) were underwent only hematoma removal without decompressive craniectomy (mean time from injury: 6.1±3.1 h). All patients in two groups were comparable due to the level of consciousness of patients, volume and localization of hematoma, severity of secondary brain injury and axial dislocation of middle brain structures.

RESULTS: Due to postoperative CT results volume of secondary brain injury zone was reduced 2.4 times more in patients who underwent early decompressive craniectomy compared with the patients without decompressive craniectomy. Axial dislocation of middle brain structures was decreased from 11.4±3.7 mm to 1.8±0.8 mm in the early decompressive craniectomy group, and from 8.9±4.5 mm to 4.4±2.5 mm in non-decompressive craniectomy group.

CONCLUSIONS: Early decompressive craniectomy, employed prior to the onset of irreversible ischemic changes, may be an effective method of treating the secondary deterioration from secondary brain damage following severe head injury with intracranial hematomas.

979
BRAIN-0324
Non-Registered Abstracts

A BIOMARKER PANEL TO RULE-OUT UNNECESSARY CT-SCANS IN MILD TRAUMATIC BRAIN INJURY (MTBI)

L. Lagerstedt[1], N. Tiberti[2], N. Turck[1], E. Andereggen[3], A. Bulla[4], L. Rinaldi[3], A. Sarrafzadeh-Khorassani[5], K. Schaller[5], J.C. Sanchez[1]
[1]Human Protein Sciences, University of Geneva, Geneva, Switzerland
[2]Pathology, University of Sydney, Sydney, Australia
[3]Emergency Center, Geneva University Hospitals, Geneva, Switzerland
[4]Genetic and Laboratory Medicine, Geneva University Hospitals, Geneva, Switzerland
[5]Clinical Neurosciences, Geneva University Hospitals, Geneva, Switzerland

Background. CT-scans are used to detect brain lesions due to a mild traumatic brain injury (mTBI). However, CT-scans are harmful to the patients and the majority of mTBI patients are CT negative. Despite several years of research, no blood biomarker has yet been found to drastically reduce the number of CT-scans. The protein S100b, with approximatively 30% specificity and almost 100% sensitivity, remains the most promising biomarker. The proteins GSTP1 (glutathione S-transferas pi), NDKA (nucleoside diphosphate kinase A) and H-FABP (heart-type fatty acid binding protein) have previously been discovered in brain injury models. Here, we investigated if these proteins individually or together as a panel could perform better than the S100b to rule-out unnecessary CT-scans.
Methods. mTBI patients (n=87) were recruited within 6h after trauma and their plasma levels of S100b, GSTP1, NDKA and H-FABP were measured using ELISAs. Statistical analyses, on patients dichotomized into CT-positive and CT-negative groups, were performed using Mann-Whitney U test, ROC curves and Panelomix.
Results. GSTP and S100b were significantly increased in CT positive patients ($p<0.05$). The S100b had the best individual performance (sensitivity: 100% and specificity 34%). However, when S100b, GSTP and H-FABP were assembled together in a panel they were capable of reaching 58% specificity and 100% sensitivity.
Conclusions. This study demonstrated that S100b, GSTP and H-FABP combined in a panel could be a useful tool to rule-out unnecessary and harmful CT-scans.

980
BRAIN-0373
Non-Registered Abstracts

ADENOSINE 1AR TARGETED TEMPERATURE MANAGEMENT IN RATS AND RESULTANT PHYSIOLOGICAL EFFECTS OF A PHARMACOLOGICAL INDUCED HYPOMETABOLIC STATE.

B. Laughlin[1], K. Drew[1], I. Bailey[1], K. Dowell[1]
[1]Institute of Arctic Biology,
University of Alaska Fairbanks, Fairbanks, USA

Objectives: Both hype and hope has been generated by promises of inducing suspended animation or a hypometabolic state. Biased reporting of positive results underestimates complications that ultimately limit translation to the clinic. In this study we apply the Adenosine 1A receptor (A1AR) agonist N6-Cycolhexyladenosine (CHA) in a manner similar to prior work in this lab found to induce a hibernation-like state in rats for therapeutic hypothermia. We report worse case scenarios and steps taken to avoid or manage these scenarios.

Methods: Male and female sprague-dawley rats are administered CHA via IV infusion to inhibit thermogenesis. Core body and brain temperatures, oxygen consumption, heart rate, rhythm and blood pressure are monitored throughout the experiment. Core body temperature is maintained between 30-34°C for 24-48hrs by adjusting the dose of CHA and/or adjusting the surface temperature of the cage via a thermoelectric cooling device we built. Side effects of bradycardia and hypotension are managed with administration of 8-SPT and norepinephrine respectively.

Results: Preliminary results indicate a pronounced individual variation in response to the CHA. Low doses of CHA resulted in bradycardia but had little to no effect on the inhibition of thermogenesis. Administration at a starting dose of 0.1mg/kg while doubling the concentration every 4 hours resulted in the development of tolerance to the drug's effect on thermogenesis but not bradycardia. Brain temperature follows core body temperature closely during the cooling and rewarming phases. Oxygen consumption requirements decreased after CHA administration.

Conclusion: CHA is a potent inhibitor of thermogenesis and metabolism at doses greater than 0.4mg/kg. Variations in response and tolerance necessities close monitoring of core body temperature and administration of a loading dose. Changes in core body temperature during targeted temperature management treatment closely resemble changes in brain temperature.

References:
H_2S, Blackstone E, Morrison M, Roth MB. Science. 2005
5'AMP (AMP), Zhang J, Kaasik K, Blackburn MR, Lee CC. Nature 2006
A_1 adenosine agonist, *CHA*, Tupone D, Madden CJ, Morrison SF J. Neurosci. 2013
Inhibiting central pathways for thermoregulatory cold defense, Cerri et al., J Neurosci. 2013
Inhibiting the peripheral cold sensing pathway (TRPM8), Almeida et al., J Neurosci. 2012

981
BRAIN-0913
Non-Registered Abstracts

PRO-ANGIOGENIC FUNCTIONS OF ARGININE-GLYCINE-ASPARTATE-CONTAINING OSTEOPONTIN ICOSAMER PEPTIDE VIA INTERACTING WITH AVB3 INTEGRIN

J. Lee[1], Y. Jin[1], H. Lee[1], H. Lee[1], L. Luo[1], P. Han[2]
[1]Department of Anatomy,
Inha University School of Medicine, Incheon, Korea
[2]Department of Brain and Cognitive Science,
Ewha Womans University, Seoul, Korea

Objectives: Osteopontin (OPN) is a phosphorylated glycoprotein that is secreted into body fluid after being synthesized in various cells and tissues. OPN contains arginine, glycine, aspartate (RGD)-motif, through which it binds to several cell surface integrins, that mediates a wide range of cellular processes, such as, the adhesion, migration, and survival of a variety of cell types. In the present study, authors examined

the pro-angiogenic effects of a RGD-containing 20 amino acids OPN peptide (OPNpt20).

Methods: Pro-angiogenic effects of OPN icosame (OPNpt20) was examined in HUVECs and in a rat model of focal cerebral ischemia, induced by middle cerebral artery occlusion (MCAO). In HUVECs, endothelial cell proliferation, migration, and tube formation were examined in the presence or absence of OPNpt20 and pro-angiogenic processes in the postischemic brain were examined by measuring RECA-1 immunoreactivity and angiogenesis-associated proteins levels.

Results: We found that OPNpt20 exerts a robust pro-angiogenic effect in HUVECs, including proliferation, migration, and tube formation. OPNpt20 also induced blood vessel formation in a Matrigel plug assay in mice. However, a mutant peptide (OPNpt20-RAA), in which RGD was replaced by RAA, failed to activate all of pro-angiogenic processes, indicating that the RGD motif is required for its pro-angiogenic effect. In OPNpt20-treated HUVECs, PI3K/AKT signaling was activated. Moreover, blocking avb_3 integrin by antibody or treating OPNpt20 after pre-incubating it with avb_3 integrin suppressed OPNpt20-mediated pro-angiogenic function, indicating that OPNpt20 stimulates angiogenesis via avb_3/PI3K/AKT signaling pathway in HUVECs. Pro-angiogenic function of OPNpt20 was further confirmed in the postischemic brain, wherein significant inductions of RECA-1 immunoreactivity as well as angiogenesis-associated proteins, such as, VEGF, MMP-9, and smooth muscle actin, were also observed in cortex penumbras of OPNpt20-administered animals.

Conclusion: Together these results demonstrate that RGD-containing OPN peptide has a robust pro-angiogenic effects and it might contribute to a robust neuroprotective effects in the postischemic brain.

982
BRAIN-0424
Non-Registered Abstracts

RELATIONSHIP BETWEEN MYELINATION AND CORTICAL FOLDING IN DEEP SULCAL LANDMARKS

J.M. Lee[1], *H.J. Yun*[1]
[1]*Department of Biomedical Engineering, Hanyang Univ., Seoul, Korea*

Objective

Sulcal pits, known as deep sulcal landmarks, are thought to be regions of cortical growth and first folded area under genetic control. Furthermore, sulcal pits have close relations to cytoarchitectonic areas and retain their identity during development. In neuroimaging studies, gray matter (GM) and white matter (WM) show age-related trajectory with myelin levels and neuronal density. Especially in GM development, cortical folding is dependent on tension of connected tracks in WM. Many researchers employ the diffusion parameters which are assessed for WM tracks and cortical thickness known as a quantitative measure of GM structure to proof the correlation between them. However, most previous studies have not concentrated on deep sulcal regions.

In this study, we investigate that brain morphological features are affected by diffusion parameters in deep sulcal landmarks. Furthermore, we examine age-related changes in cortical folding and WM integrity young healthy subjects.

Methods

Image processing

The WM and GM cortical surfaces were extracted from structural MRIs using the Constrained Laplacian-Based Automated Segmentation with Proximities algorithm. The sulcal pits are identified by watershed algorithm on WM depth map. Cortical thickness, sulcal depth, absolute mean curvature and surface area were extracted from GM surfaces and regional averaged in sulcal

pits. The mean diffusivity (MD) value is measured in diffusion images which are co-registered to their structural MRIs, and calculated in WM regions around sulcal pits with 5mm distance threshold.

Statistical analysis

Linear effects of age on each morphology and diffusion features in deep sulcal regions are calculated for both hemispheres by general linear models (GLMs). To investigate the correlations between GM and WM parameters, we also employ GLMs regressing for effects of gender and age.

Results

The linear models with age are significant for MD ($t = -5.16$; $p < 0.001$) and absolute mean curvature ($t = -2.62$; $p = 0.011$). However, the MD and absolute mean curvature show a positive relationship trend ($t = 1.81$; $p = 0.075$) instead of significant relationship. Cortical thickness ($t = 2.10$; $p = 0.039$) and sulcal depth ($t = 2.12$; $p = 0.038$) correlate positively with MD, although the linear effects of age on them are not significant. Surface area is not any significant results in both GLMs.

Conclusion

We found age-related changes in MD and curvature which indicate myelination and deformation in deep sulcal regions. The results of the relationship between diffusion parameter and morphological features further demonstrate possibility that cortical growth in the first folded area could be associated with WM integrity.

983
BRAIN-0253
Non-Registered Abstracts

EFFECT OF A BROAD SPECIFICITY CHEMOKINE BINDING PROTEIN ON BRAIN LEUKOCYTE INFILTRATION AND INFARCT DEVELOPMENT

S. Lee[1], H.X. Chu[1], H.A. Kim[1], N.C. Real[2], S. Sharif[2], S.B. Fleming[2], A.A. Mercer[2], L.M. Wise[2], G.R. Drummond[1], C.G. Sobey[1]
[1]Department of Pharmacology, Monash University, Clayton, Australia
[2]Department of Microbiology and Immunology, University of Otago, Dunedin, New Zealand

Objectives: Expression of numerous chemokine-related genes is increased in the brain following ischemic stroke. Here, we tested whether post-stroke administration of a chemokine binding protein (CBP), derived from the parapoxvirus bovine papular stomatitis virus, might reduce infiltration of leukocytes into the brain and consequently limit infarct development.

Methods: The binding spectrum of the CBP was evaluated in chemokine ELISAs and binding affinity was determined using surface plasmon resonance. Focal stroke was induced in C57Bl/6 mice by middle cerebral artery occlusion for 1 h, followed by reperfusion for 23 or 47 h. Mice were treated intravenously with either bovine serum albumin (BSA, 10 μg) or CBP (10 μg) at the commencement of reperfusion. At 24 or 48 h, we assessed plasma levels of the chemokines CCL2/MCP-1 and CXCL2/MIP-2, as well as neurological deficit, brain leukocyte infiltration, and infarct volume.

Results: The CBP interacted with a broad spectrum of CC, CXC and XC chemokines, and bound CCL2/MCP-1 and CXCL2/MIP-2 with high affinity (pM range). Stroke markedly increased plasma levels of CCL2/MCP-1 and CXCL2/MIP-2, as well as numbers of microglia and infiltrating leukocytes in the brain. Increases in plasma chemokines were blocked in mice treated with CBP, in which there was reduced neurological deficit, fewer brain-infiltrating leukocytes and ~50% smaller infarcts at 24 h compared with BSA-treated mice. However, CBP treatment was no longer protective at 48 h.

Conclusions: Post-stroke administration of CBP can reduce plasma chemokine levels in association with temporary attenuation of brain inflammation and infarct volume development.

984
BRAIN-0751
Non-Registered Abstracts

CHARACTERIZATION OF CEREBRAL DAMAGE IN A MONKEY MODEL OF ALZHEIMER'S DISEASE INDUCED BY INTRACEREBROVENTRICULAR INJECTION OF STREPTOZOTOCIN

Y. Lee[1], H. Yeo[1], C. Jeon[1], Y. Jin[1], K. Jeong[1], S. Lee[1], K. Chang[1]
[1]National Primate Research Center, Korea Research Institute of Bioscience & Biotechnology, Cheongju-si, Korea

In line with recent findings showing Alzheimer's disease (AD) as an insulin-resistant brain state, a non-transgenic animal model with intracerebroventricular streptozotocin (icv-STZ) administration has been proposed as a representative experimental model of AD. Although icv-STZ rodent models of AD have been increasingly researched, studies in non-human primate models are very limited. In this study, we aimed to characterize the cerebral damage caused by icv-STZ in non-human primates; to achieve this, three cynomolgus monkeys (Macaca fascicularis) were administered four dosages of STZ (2 mg/kg) dissolved in artificial cerebrospinal fluid and another three controls were injected with only artificial cerebrospinal fluid at the cerebellomedullary cistern. In vivo neuroimaging was performed with clinical 3.0 T MRI, followed by quantitative analysis with FSL for evaluation of structural changes. Immunohistochemistry was performed to evaluate histopathology. We showed that icv-STZ caused severe ventricular enlargement and parenchymal atrophy accompanying accumulation of beta-amyloid and phosphorylated tau proteins in the parenchyma of the insula or temporal cortex. Hippocampal cell loss, disintegration of the neurovascular unit, neuroinflammation with microglial activation, and ependymal cell loss, which are observed in human aged or AD brain, also occurred. The findings suggest that the icv-STZ monkey model would be a valuable resource to study the mechanisms and consequences of a variety of pathologies such as ventriculomegaly and amyloidopathy. Furthermore, the study of icv-STZ monkeys could contribute to the development of treatments for age- or AD-associated pathologies.

985
BRAIN-0752
Non-Registered Abstracts

A BLOOD-BASED TRANSCRIPTIONAL PROFILING IN A NONHUMAN PRIMATE MODEL OF ALZHEIMER'S DISEASE INDUCED BY INTRACEREBROVENTRICULAR INJECTION OF STREPTOZOTOCIN

Y. Lee[1], H. Yeo[1], C. Jeon[1], Y. Jin[1], K. Jeong[1], S. Lee[1], K. Chang[1]
[1]National Primate Research Center, Korea Research Institute of Bioscience & Biotechnology, Cheongju-si, Korea

As nonhuman primates share significant genetic, anatomical, physiological, and behavioral traits with humans, they are critical experimental model to investigate human neurodegenerative disease including Alzheimer's disease (AD). In line with recent findings showing AD as an insulin-resistant brain state, an animal model with intracerebroventricular streptozotocin (icv-STZ) administration has been proposed as a representative experimental model of AD, showing AD-like features. However, the effect of icv-STZ on the blood-based transcriptional profiling has not been investigated in nonhuman primates. In this study, we performed a whole genome screen using oligonucleotide microarray analysis on bloods from icv-STZ-treated or normal control cynomolgus monkeys (*Macaca fascicularis*) as a pilot study. Blood samples for total RNA extraction were collected in PAXgene tubes, and gene expression analysis performed on the Agilent's Rhesus Macaque Gene Expression Microarray. The PANTHER website was used to search for the biological significance. 2166 genes were up-regulated and 830 genes were down-regulated in the icv-STZ blood, compared with control (more than 2-fold, $p<0.05$). In the up-regulated genes, 23 biological processes were significantly overrepresented ($p<0.05$) in the signature: cellular process, cell communication, developmental process, multicellular organismal process, single-multicellular organism process,

system process, system development, cell adhesion, biological adhesion, response to stimulus, immune system process, neurological system process, nervous system development, mesoderm development, ectoderm development, localization, cell-cell signaling, transport, response to external stimulus, synaptic transmission, cell-cell adhesion, angiogenesis, reproduction. On the other hand, in the down-regulated genes, only translation was significantly overrepresented ($p<0.01$). Our findings implicate the systemic nature of gene dysregulation in icv-STZ monkey.

986
BRAIN-0880
Non-Registered Abstracts

INFLUENCE OF 3-METHYLXANTHINE DERIVATIVE ON THE MORPHOLOGICAL AND FUNCTIONAL CHARACTERISTICS OF NEURONS OF SENSORIMOTOR CORTEX OF RATS WITH EXPERIMENTAL INTRACEREBRAL HEMORRHAGE

I. Belenichev[1], K. Aleksandrova[2], A. Shkoda[2], S. Levich[2], S. Nosach[1]
[1]Pharmacology and Medical Formulation, Zaporozhye State Medical University, Zaporozhye, Ukraine
[2]Biochemistry and Laboratory Diagnostics, Zaporozhye State Medical University, Zaporozhye, Ukraine

The modern concept of neuroprotection during intracerebral hemorrhage includes sequential administration of primary and secondary neuroprotectors. In the article are represented results of in-depth study of a novel xanthine derivative – hydrazide of 1,3-dimethyl-8-N-benzylaminoxanthinyl-7-acetic acid (compound C-3), which previously showed high neuroprotective, antioxidant and energotropic activity.
The aim of the research was to study the effect of compound C-3 on morphofunctional parameters of neurons of the sensorimotor cortex of rats with experimental intracerebral hemorrhage.
We studied effect of compound C-3 on such morphofunctional parameters of neurons of IV-V layers of the sensorimotor cortex of rats with experimental intracerebral hemorrhage - neuronal density (number of cells per $1mm^2$ area of slice of cerebral cortex), the cellular content in the IV-V layers of the cortex in percentage; area of bodies of neurons (mm^2), RNA content in neurons.
Intracerebral hemorrhage was modeled in albino rats of both sexes weighing 140-160 g (90 animals) by injection into the region of the internal capsule and striatopallidal cores of the brain autologous blood, which was taken from the tail vein. Compound C-3 was injected at a dose of 100 mg / kg / day intragastrically as a suspension stabilized by Tween-80 during 4 or 18 days. As reference drugs were used mexidol and piracetam at doses of 100 mg / kg and 500 mg / kg, respectively.
It was shown that the course administration of hydrazide 1,3-dimethyl-8-N-benzylaminoxanthinyl-7-acetic acid (C-3) at dose 100 mg / kg intragastrically to rats with experimental intracerebral hemorrhage caused a significant neuroprotective effect.
Neuroprotective action of compound C-3 was implemented in the acute period of experimental pathology and manifested in a positive influence on the morphological and functional parameters of neurons of IV-V layers of the sensorimotor cortex. a significant increase in neuronal density and an increase in RNA content in the neurons of both the 4th (the most pronounced effect) and on the 18th day after intracerebral hemorrhage. This fact indicates that the injection of the C-3 reduced neuronal damage and improved the processes of transcription and translation in the cells. The level of influence on the morphological and functional parameters of neurons in experimental intracerebral hemorrhage of novel xanthine derivative C-3 significantly superior on the 4th day of the experiment piracetam and mexidol, and on the 18th day - piracetam.
Thus, the neuroprotective effect of compound C-3, in contrast to the reference drugs, realized in the acute phase of experimental pathology and had a positive effect on the functional activity of neurons.

987
BRAIN-0938
Non-Registered Abstracts

COMPUTATIONAL FLUID DYNAMICS FOR FLOW ASSESSMENT IN DIGITAL SUBTRACTION ANGIOGRAPHY

C.Y. Hsu[1], M. Ghaffari[1], A. Alaraj[2], A. Linninger[1]
[1]Bioengineering, University of Illinois at Chicago, Chicago, USA
[2]Neurosurgery, University of Illinois at Chicago, Chicago, USA

Objectives. In this study, we introduce a novel inversion-based method to quantify blood flow from digital subtraction angiography intensity profiles. Neuro-interventional surgery is at the forefront of fast-response assessment of patients' health. Unfortunately, cerebral blood flow cannot be reliably measured with digital subtraction angiography during intervention. We propose to combine image processing for patient-specific anatomical data, and computational modeling with flow physics for flow quantification in digital subtraction angiography. By providing flow quantification in digital subtraction angiography, we wish to facilitate clinical diagnosis for cerebral vascular diseases.

Methods. We processed 3D rotational angiography to create a network representation of the main cerebral arteries. We extracted from the 2D digital subtraction angiography the intensity profiles along the vessel centerlines. We feed the intensity into a fluid mechanic equations that allow us to infer blood flow based on equations of blood motion and dye convection. The automation of the procedure has several innovative elements. (1) The automatic image reconstruction of the arterial tree. (2) The fully automatic coregistration of intensity data with vascular segments in the simulation. (3) The dynamic generation of an inversion problem, the computation of the flow and the display of a flow map for all visible blood vessels for a specific patient.

Results. We collected medical images from six patients including 3D rotational angiography, 2D digital subtraction angiography, and quantitative magnetic resonance angiography for comparison. We show in six patients that the flow rates are as accurate as quantitative magnetic resonance angiography. We also validated the accuracy of the method using a 3D realistic blood flow phantom with known flow.

Conclusions. By combining image processing and computational modeling, we developed an algorithm that estimates volumetric flow rates from 2D digital subtraction angiography and 3D rotational angiography. Our algorithm provides neurosurgeons with quantitative flow measurements within an hour, which can be improved to minutes by incorporating parallel processing [1].

References.

1. Asano, S.; Maruyama, T.; Yamaguchi, Y. Performance comparison of FPGA, GPU and CPU in image processing. In *International Conference on Field Programmable Logic and Applications, 2009. FPL 2009*; 2009; pp. 126–131.

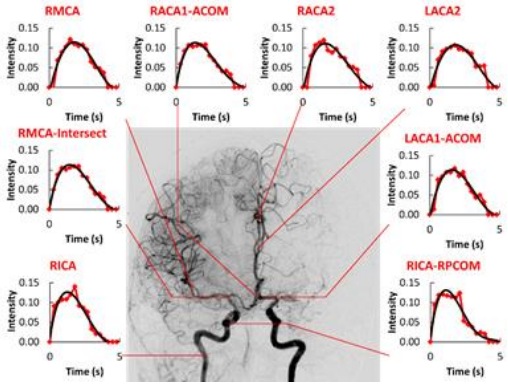

Figure 1. 2D-DSA contrast agent intensity vs. time curves for selected vessels in the Circle of Willis (post-intervention, Patient 2). For each arterial point of interest (RICA, MCA, etc.), the red dots show the intensity values on the y-axis acquired from DSA for the first 5 seconds after bolus injection. The smooth black curve represents the best fit of the red dots using the inversion technique. The best fit solution also precisely determines the flow in all visible blood vessels.

988
BRAIN-0939
Non-Registered Abstracts

HEMODYNAMIC SIMULATION OF THE PATIENT SPECIFIC CEREBRAL BLOOD FLOW TOWARDS A PERSONALIZED SURGICAL PLANNING FOR VASCULAR DISORDERS

M. Ghaffari[1], C.Y. Hsu[1], A. Alaraj[2], A. Linninger[2]
[1]Bioengineering, University of Illinois at Chicago, Chicago, USA
[2]Neurosurgery, University of Illinois at Chicago, Chicago, USA

Objectives

The aim of this work is to generate a patient-specific surgical planning tool for cerebrovascular disease. We performed patient-specific hemodynamic simulations in all main visible vessels to better assess normal and disease states of cerebral blood flow. Hemodynamic simulation of cerebral blood flow requires reconstruction of human angioarchitecture. We acquired patient-specific medical images and reconstructed an anatomically accurate blood flow network counting hundreds to thousands of vessels using an automatic mesh generation algorithm.

Methods

Magnetic resonance imaging was acquired for one healthy volunteer. A vessel filter was applied to suppress signals from other tissues and enhance the vessels (Fig. 1A). The filtered image was process to acquire centerlines and diameter information [1-2], as shown in Fig. 1B.

For hemodynamic simulations, we developed a parametric meshing algorithm to automatically generate surface and volumetric meshes for extracted centerline and radius information (Fig. 1C). Parametric meshes allow for a massive reduction in mesh size, while maintaining meshes quality especially close to the vessels wall where the wall shear stresses are highest. Parametric meshing allows us to control vessel lumen and wall thickness for accurate representation of cerebral angioarchitecture

We used phase contrast magnetic resonance imaging (pcMRI), guided by NOVA software (VasSol Inc., Chicago, IL) to quantify blood flow in large portions of the main cerebroarterial trees. The NOVA software was used for the determination of volumetric blood flow rates using planes perpendicular to the vessel axis (Fig. 1D-E). Based on the parametric meshes the hemodynamic simulations were carried out using ANSYS Fluent 15.0 (ANSYS Inc., Canonsburg, PA).

Results

The quantitative analysis blood flow rate showed good agreement between the simulation and NOVA results. Our 3D simulation of a complete Circle of Willis (CoW) demonstrates velocity field, pressure gradient, with a pulsatile blood flow (Fig. 1F). Dynamic contrast agent distribution for three time frames 0.25s, 0.45s, 0.65s after injection of a contrast agent is shown in Fig. 1G

The simulation results demonstrate the use of our image processing, and meshing techniques with simulation to aid clinical diagnosis. The patient-specific simulations allow quantifying angiographic dye perfusion to illustrate the blood perfusion patterns in the normal subjects and patients with neurovascular diseases such as aneurysms, atherosclerotic and stroke.

Conclusion

These results are encouraging and point to the huge potential of patient-specific simulations to quantify hemodynamic of cerebral vessels to assist in making clinical decisions in surgery. This study can be used for personalized therapy for vascular disorders such as optimization of intracranial aneurysm clipping.

Reference

[1] L. Antiga, M.Piccinelli, L. Botti, B. Ene-Iordache, A. Remuzzi, D. A. Steinman, 2008, An image-based modeling framework for patient specific computationla hemodynamics. Medical

and Biological Engineering and computering, 46, 1097-1112.

[2] M. Ghaffari, C.Y. Hsu, A.A. Linninger, 2015, Automatic Reconstruction and Generation of Structured Hexahedral Mesh for Non-planar Bifurcations in Vascular Networks, Computer Aided Chemical Engineering, volume 37.

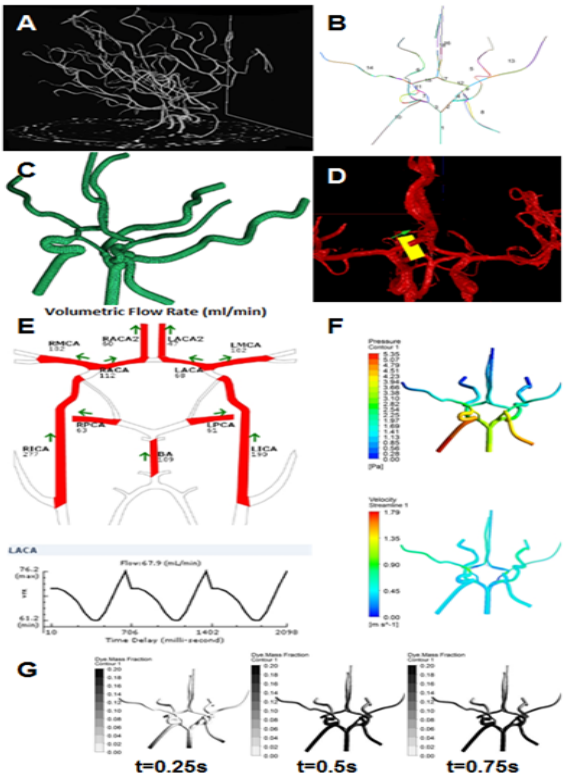

Figure 1. 3D patient-specific hemodynamic simulation of the Circle of Willis (CoW). A) Vessel segmentation after image filtering for cerebral vasculature. B) Vascular centerlines are extracted from the medical images and categorized in different branches. C) Parametric meshes of the Circle of Willis besides the magnified cross section of the segmented CoW. D) The 3D model created by the NOVA system of the cerebral vasculature using pcMRI. The yellow plane illustrate a scan plane for recording the blood flow. E) recorded volumetric flow rates (ml/min) are shown for CoW vessels with the sample of extracted dynamic blood flow rate is shown. F) 3D hemodynamic simulation of the CoW with pulsatile boundary conditions showing velocity fields and pressure fields. G) Dynamic contrast agent distribution for three time frames 0.25s, 0.5s, 0.75s after injection of a contrast agent.

989
BRAIN-0133
Non-Registered Abstracts

MONITOR GENE THERAPY IN VIVO USING TARGET-GUIDED MRI: A PRECLINICAL PLATFORM

P. Liu[1], *Y.I. Chen*[1], *J. Wu*[2]
[1]*Radiology, Massachusetts General Hospital, Charlestown MA, USA*
[2]*Biomedical Science, Florida Atlantic University, Boca Raton FL, USA*

Objectives: Therapy usingexogenous gene has been used to treat neurological disorders. However, itsvalidation of delivery and expression depends on necropsy samples, which is notapplicable clinically. Such deficiency can be addressed using target-guidedmagnetic resonance imaging (MRI) in vivo.

Granulocytecolony-stimulating factor (G-CSF) is a cytokine that stimulates growth anddifferentiation of myeloid precursors. In addition, G-CSF has neuroprotectiveproperties in animal models of Parkinson disorder, stroke, Alzheimer dementiaand other neurodegenerative diseases. Protein therapy using G-CSF is attractivebecause G-CSF is well tolerated after systemic delivery and its receptor isexpressed in neurons. However, its plasma half-life is about 4 hours; moreover,there is potential for chronically elevating white blood cells during repeatedprotein delivery. One alternative is to administer human G-CSF (hG-CSF) encodedby a viral vector (gene therapy)–namely a replication deficientadeno-associated virus (AAV).

Our objectives are to(1) delivery hG-CSF cDNA in AAV-CMV vector, (2) direct monitor the expressionof G-CSF from AAV-CMV-hG-CSF in vivo and (3) neuroprotection in vivo usinghG-CSG-targeting magnetic resonance imaging (MRI) in living brains aftercerebral ischemia models by bilateral carotid artery occlusion (BCAO) ofC57black6 mice.

Methods: Brain damage was inducedusing bilateral carotid artery occlusion (BCAO) for 60 min in C57black6 mice. Wedelivered AAV-CMV-

hG-CSF or AAV-CMV-GFP (placebo) to mice immediately after therelease of BCAO (4 x 10^9 fpu in 2 ul, eye drops) and at 1, 7, and 14days thereafter. We made sODN with antisense sequence for hG-CSF mRNA. Our sODNtargets hG-CSF mRNA, but not rodent G-CSF mRNA. We linked the sODN to superparamagnetic ironoxide nanoparticles (SPION, a T2 susceptibility agent, 4mg Fe per kg) orgadolinium (1 ug), all delivered by non-invasive intraperitoneal injection threedays after the last AAV-CMV-hG-CSF vector application. We acquired MRI 16 hourslater.

Results: The survival rateof C57black6 mice by 60 min of BCAO is 5 out of 38 mice in two experiments. Genetherapy using AAV-CMV-hG-CSF improves survival rate (5 of 6 in two trails). Micetreated with AAV-CMV-hG-CSF after BCAO show less brain damage by ventriculomegalyusing MRI, and corner turn test shows improved bilateral turns from unilateralturns. We observed expression of hG-CSF mRNA in vivo using SPION-hG-CSF and targetguided MRI. The region of hG-CSF expression was validated using anti-h-G-CSFIgG and expression of neural progenitor cells in necropsy samples. Brain repairwas absent in the placebo group with BCAO and AAV-CMV-GFP.

Conclusion: We demonstratedgene tracking using hG-CSF-targeting MRI in vivo. The significance of thisproject is in correlating gene delivery and the accompanied neuroprotection.This is the first step in translating longitudinal MRI of brain repair withoutbiopsy during therapy throughout the life time of patients afflicted withneurodegenerative disorders.

Acknowledgement: Supported by the Boston Area Diabetes EndocrinologyResearch Center [P30DK057521-14 (J Avruch)], DA029889 and EB013768 (PKL). TheMRI system was funded in part by NIH (S10RR025563) to the Martinos Center forBiomedical Imaging, MGH.

990
BRAIN-0025
Non-Registered Abstracts

TRAUMATIC EXPERIENCE AND MENTAL EFFECTS AMONG RWANDAN YOUTHS, 17 YEARS AFTER THE GENOCIDE

L. Lugema[1], I. Mogren[2], J. Ntaganira[3], G. Krantz[4]
[1]Community Health,
College of medicine and Health Sciences - School o f Public Health, kigali, Rwanda
[2]Clinical Sciences Obstetrics and Gynecology, Umeå University., Umeå, Sweden
[3]Biostatistics and Epidemiology,
College of medicine and Health Sciences - School o f Public Health, kigali, Rwanda
[4]Public Health and Community medicine The Sahlg renska Academy,
Gothenburg University Public Health and Commun ity medicine The Sahlgrenska Academy, Gothenburg, Sweden

Background: Common mental disorders (CMD) contribute toapproximately 14% of the global burden of disease. Despite this CMDs have failed to attract the attentionof researchers and planners in low and middle income countries (LMCs) andsubsequently there is little detection and treatment of CMDs. This studyinvestigated the mental health effects associated with trauma exposure inRwanda during the 1994 genocide period and over the life time in Rwandan menand women, aged 20-35 years.

Methods: This cross-sectional population-based study was conducted among 440 menand 477 women, residing in the Southern province of Rwanda. The data collectionincluded individual interviewing followed by a structured questionnaire. Prevalencerates were calculated and multivariable logistic regression was employed forrisk factor analyses of common mental disorders with traumatic exposure as themain risk factor of interest.

Results:Women to ahigher extent than men suffered from major depressive episodes (MDE), suicide risk,post-traumatic stress syndrome (PTSD) and generalized anxiety disorder

(GAD).MDE current was twice as prevalent in women as men. Traumatic episodesexperienced in the genocide period severely affected men's current mental healthstatus with OR 3.35 (CI 95% 1.64-6.84) for MDE past and OR 2.36 (95% CI 1.23-4.54)for suicide risk. Women's mental health was also affected by trauma experiencedin the genocide period but to a higher extent by similar trauma experienced inthe life time with OR 2.16 (95% CI 1.03-4.53) for suicide risk and OR 3.05 (95%CI 1.56-5.93) for GAD, taking spousal physical/sexual violence intoconsideration.

Conclusion: Impact of the genocide is still evident in today'speoples living circumstances. It has made a huge contribution to CMDs among Rwandan youths.

991
BRAIN-0704
Non-Registered Abstracts

GALECTIN-1 IS NEUROPROTECTIVE AND REVERSES METHAMPHETAMINE INDUCED BLOOD BRAIN BARRIER BREAKDOWN.

N.U. Parikh[1], S. Mahajan[1], R. Aalinkeel[1], J.L. Reynolds[1], B.N. Nair[1], D.E. Sykes[1], M.J. Mammen[1], S.A. Schwartz[1]
[1]MEDICINE, SUNY at Buffalo, Buffalo, USA

Methamphetamine (Meth) abuse can lead to the breakdown of the blood-brain-barrier (BBB) integrity leading to compromised CNS function. The role of Galectins in the angiogenesis process in tumor-associated endothelial cells (EC) is well established; however no data are available on the expression of Galectins in normal human brain microvascular endothelial cells and their potential role in maintaining BBB integrity. We evaluated the basal gene/protein expression levels of Galectin-1, -3 and -9 in normal primary human brain microvascular endothelial cells (BMVEC) that constitute the BBB and examined whether Meth altered Galectin-1 expression in these cells, and if Galectin-1 treatment impacted the integrity of an in-vitro BBB. Our results showed that BMVEC expressed significantly higher levels of Galectin-1 as compared to Galectin-3 and -9. Meth treatment increased Galectin-1 expression in BMVEC. Meth induced decrease in TJ proteins ZO-1, Claudin-3 and adhesion molecule ICAM-1 was reversed by Galectin-1. Treatment with 50nM Meth treatment decreased Claudin-3 gene expression by 37% (p

Figure 1

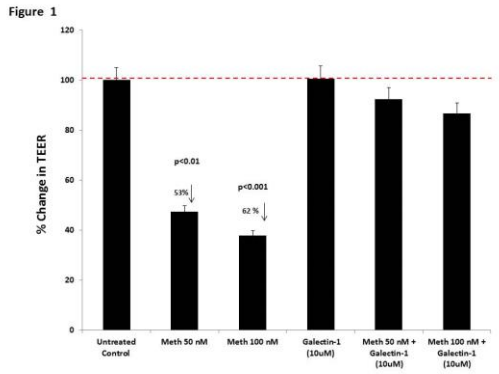

Figure 2

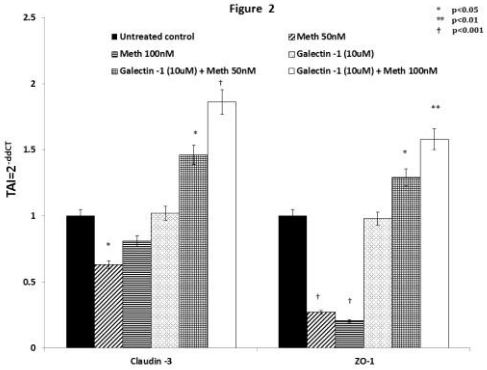

Figure 3

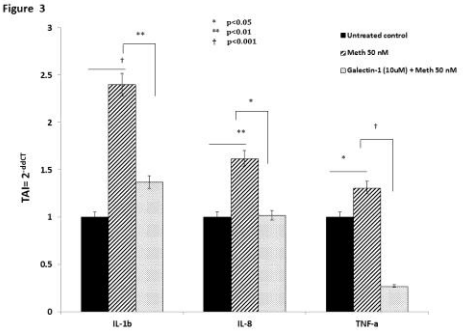

992
BRAIN-0916
Non-Registered Abstracts

DEEP VEIN THROMBOSIS IN PATIENTS WITH SEVERE TRAUMATIC BRAIN INJURIES

P. Mendez[1], A. Chavez[1], L. Avila[1], A. Seifi[1]
[1]Neurosurgery, UTHSCSA, San Antonio, USA

Objectives: Deep venous thrombosis (DVT), often prodromal for pulmonary embolism, is known to

cause significant morbidity and mortality.[1] The use of postoperative chemoprophylaxis is still controversial among clinicians who care for severe traumatic brain injury patients due to concern of intracranial hemorrhage (ICH) and its pernicious effects. In the present study, we evaluated the incidence of DVT in severe traumatic brain injury (TBI), as well as the impact of chemoprophylaxis on development of DVT.

Methods: We conducted a retrospective case control study with patients admitted to University Hospital neurosurgical ICU in San Antonio, Texas from 2011 - 2013. Severe TBI was defined as patients who required intracranial pressure monitoring within 48 hours of admission. Patients who were less than 18 years of age, DVT on admission, pre-existing filter, pregnancy, chronic anticoagulation, and death within 72 hours after TBI were excluded.

Demographic data, etiology of TBI, complications, hospital length of stay (LOS), start date of chemoprophylaxis were gathered. Progression of ICH was defined as lesion expansion or development of a new ICH as documented by radiologist report on a repeat CT scan. Fisher's exact test was utilized to determine incidence and mortality of DVT with and without chemoprophylaxis. The Mann-Whitney U test was utilized to determine hospital LOS.

Results: There were 396 qualifying records, 155 records entered the study group after exclusion criteria. The cohort was mostly composed of white (71.6%), male (76.8%) with a median age of 41. The majority types of TBIs were subdural hemorrhage (62.6%) & subarachnoid hemorrhage (60%).

A total of 122 patients received chemoprophylaxis, the average number of days post admission to begin prophylaxis being 5.04 ±3.95. The mean number of days post stable head CT being 6.69. Meaning some patients received chemoprophylaxis prior to stable CT. The incidence of DVT was 12.26% and PE 2.58%. We found 30.3% of patients who did not receive chemoprophylaxis developed a DVT vs. 7.38% of patients who received chemoprophylaxis developed a DVT. *See Figure 1*.

We observed 9.35 days longer LOS in those who developed a DVT, and did not receive chemoprophylaxis. Our study mortality rate was 18%. The incidence of ICH progression after chemoprophylaxis was 7.74%.

Conclusions: Our data suggests a lower incidence of DVT in patients who received chemoprophylaxis and longer hospital LOS than the group did not. We found improved mortality in patients who received chemoprophylaxis at any point of their hospital stay. Thus, consider starting chemoprophylaxis to reduce patient complications of DVT, hospital length of stay, and hospital costs. Additional larger prospective studies should be undertaken to confirm the best time to begin chemoprophylaxis in severe TBI patients.

References: 1.Farooqui A, Hiser B, Barnes S, et al: Safety and efficacy of early thromboembolism chemoprophylaxis after intracranial traumatic brain injury. Journal of Neurosurgery 2013; 1

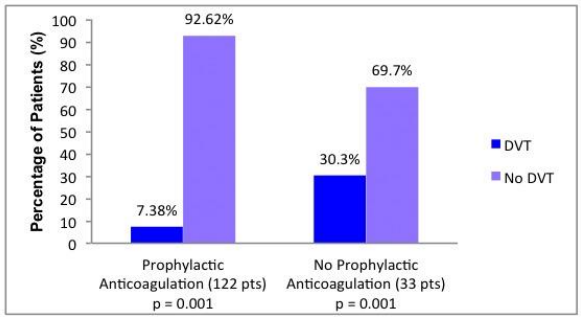

Figure 1. Incidence of DVT in study group

993
BRAIN-0714
Non-Registered Abstracts

CEREBRAL BLOOD CIRCULATION AT EXPERIMENTAL CAROTID-JUGULAR FISTULA

V. Musienko[1]
[1]*Department of pathophysiology, Lugansk medical university, Lugansk, Russia*

Objectives: Cerebral circulatorydisorders at extracranial arteriovenous fistulas and aneurysms arethe main pathogenic factor of the brain damage and therefore requiredetailed study.

Methods: Carotid-jugular fistula was modeled on 40dogs. Physiological and morphological methods of investigation were used.

Results: Morphological changes of the cerebral venoussystem within acute period were characteristic for venous plethora. Diameter ofthe superficial and intracerebral branches of the cerebral arteries wasincreased. Total expansion of the cerebral microcirculatory bed was found.

Further reconstruction was accompanied by formation ofthe vascular system of arteriovenous fistula, collateralarterial circulation and collateral venous one. Collateral arterial cerebralcirculation included dilated carotid and vertebral arteries, extracranialcommunications between them, brain arterial circle, cerebral arteries and theirintracerebral branches and superficial arterial net with anastomoses here. The waysof collateral venous outflow included transformed superficial venous networksof the brain, dural sinuses, additional ways of venous outflow from skullcavity.

Drainage system of arteriovenous fistula includedextracranial veins, dural transversal sinuses and their connections withvertebral venous pool providing mainly extracranial redistribution of theshunted blood. This system developed expansively in result of involving ofincreasing number of arterial branches in blood shunting and also veins intofistula drainage system.

Conclusion: Extracranial arteriovenous fistulas resultin noncompensative disturbances of the cerebral blood circulation. Involving intact arteries, including intracranial ones,in supply of the arteriovenous fistula accompanies by "robbery" ofthe cerebral arterial circulation. Increased disproportion of the arterialinflow ways to the brain and the ways of collateral venous outflow formspredispositions for relative arterial stenosis syndrome. Cerebralmicrocirculatory bed transformation forms the ways for intracerebralarteriovenous blood shunting and pathological acceleration("centralizations") of the cerebral blood flow.

994
BRAIN-0243
Non-Registered Abstracts

PLACEBO EFFECT OF AESTHETIC PACKAGING DESIGN IN TREATMENT OF HEADACHES

Z. OUAZZANI TOUHAMI[1], *A. CHAKOR*[2], *H.O. EL MALKI*[3], *A. BENOMAR*[4]
[1]*Medico-social Department, Hight Institut of Nursing and Health Techniques, RABAT, Morocco*
[2]*Management Department, Faculty of Juridical Economic and Social Sciences U niversity Mohammed Vth, RABAT, Morocco*
[3]*Anatomy Department, Medical School University Mohammed Vth, RABAT, Morocco*
[4]*Neurology Department, Abulkasis International University of Health Scienc es, RABAT, Morocco*

Introduction

Packaging is an extrinsic part of the product. Many studies examine the influence of packaging design on consumer behavior. Our study tests the influence of pharmaceutical packaging design on preference and satisfaction.

Methods

The effect of aesthetic packaging design of two brands of analgesic used to treat headaches was

studied in a sample of women and men when they suffer from headaches. We first conducted a pretest to identify two brand's packaging: the most attractive and the least attractive. The two brands of analgesic contain an active formulation. The sample was randomly into two groups in which subjects received the brand to have an attractive packaging design (Group 1), or that which is have an unattractive packaging design (Group 2). Data were collected by the subjects themselves when they suffered from headaches through a numerical scale of pain assessment. Subjects evaluated their pain before taking an effervescent tablet 500 mg, then 20 min, 2h and 4h after taking it.

Results

The two groups have respectively at the evaluation times t0=5,96; t1= 3,83; t2=2,38; t3=1,85 for the Group 1and t0=5,86; t1=4,3; t2=2,19; t3=1,05 for the Group 2.

We found no significant differences ($p > 0,05$, $p = 0,736$) between the potency of the attractive brand packaging analgesic and the unattractive one.

Conclusion

The findings showed that pharmaceutical packaging has no additional marketing placebo effect. Our results suggest that an attractive brand of analgesic has the same potency than an unattractive brand in relieving headaches.

995
BRAIN-0059
Non-Registered Abstracts

BLOOD–BRAIN BARRIER DYSFUNCTION IN PATIENTS WITH CEREBRAL MICROBLEEDS

T. Poliakova[1], O. Levin[1], N. Trusova[1], P. Hermann[2], M. Schmitz[2], I. Zerr[2]
[1]neurology,
Russian Medical Academy of Postgraduate Educat ion, Moscow, Russia
[2]neurology,
Nationales Referenzzentrum für TSE Klinik für Neu rologie Universitätsmedizin Göttingen, Gottingen, Germany

Background. We hypothesize that cerebral microbleeds (CMB) might be associated with endothelial dysfunction and blood–brain barrier (BBB) damage in patients with different neuropsychological MCI (mild cognitive impairment) profile. Both molecular biomarkers in the CSF and imaging techniques are suggested to be useful to identify AD and VaD at early stages. CMB are small rounded hypointense lesions found with gradient-echo (GRE) T2*-weighted or SWI of MRI sequences and are characterized histologically by the presence of haemosiderin deposits around small blood vessels with a diameter <200 mm.

Methods. MCI patients were diagnosed as following: amnestic with CMB (n=28) and without CMB (n=33), non-amnestic with CMB (n=33) and without CMB (n=42). We analyzed CSF profiles (Aβ42, 40, tau, Ptau, Aß1-40/42, QAlb, cytokines), ApoE genotype and cognitive decline in MCI patients with respect to CMB load and profile in MRI. MRI was performed at 3.0 Tesla scanner using a susceptibility-weighted protocol. Neuropsychological assessment comprised MMSE, MoCA, ACE-R, CAMCOG (part 3).

Results. Sixty-one patients (45%) with a diagnosis of MCI had at least 1 CMB. Most of them were observed in amnestic MCI (67%). No significant differences between the groups stratified by CMB presence were found for Aβ42, 40, tau, Ptau and cytokines, but the ratio of Aß1-40/42 in non-amnestic MCI patients with CMB was significantly lower (mean 0.6) than in patients without CMB (mean 1.2). We found four patients clinically diagnosed as a non-amnestic MCI with reduction Aβ-amyloid Q-coefficient (0.46; 0.40; 0.58; 0.67) as well as multiple cortical MBs (11;21;6;15). A relevant difference in albumin ratio as an indicator of the (BBB)- QAlb- was observed between groups with and without CMB (picture 1). The regression results demonstrated that age, WMHs score and albumin ratio were important predictors of CMBs presence ($\beta=-0,258$, $p = 0,029$, $R2 = -0,093$; $\beta= 0,365$, $p = 0,036$, $R2 = 0,093$;

β=0,158, p = 0,077, R2 = 0,027; β= 0,103, p = 0,036, R2 = 0,043; respectively).

Conclusions. Our data revealed that patients with CMB have more features of BBB dysfunction, which is demonstrated by CSF albumin ratio. Cases of subcortical CMB in non-amnestic MCI patients and increase Q-albumin in CSF might indicate VaD. It might be associated with the progression of ischemic vascular lesions (Wallin A. 1990). Many authors explain the prevalence of CMB largest number of vascular risk factors, inflammatory and BBB disturbance (Charidimou A.Werring DJ. 2014, Miwa K 2014). But number of studies concerning inflammation and BBB disturbance in CMB is currently very small. Previous study is provided no evidence for P-glycoprotein dysfunction, which indicated about decrease BBB disturbance in AD with CMB (Danielle ME van Assema, 2012). It might indicate that amyloid in cerebrovascular and neurodegenerative diseases are different. A β42 is retained in cerebrovascular of AD patients with CMB, while in contrast, VaD patients may possibly drain amyloid (Goos 2012). Further studies are needed to explain the potential link between BBB dysfunction and CMB.

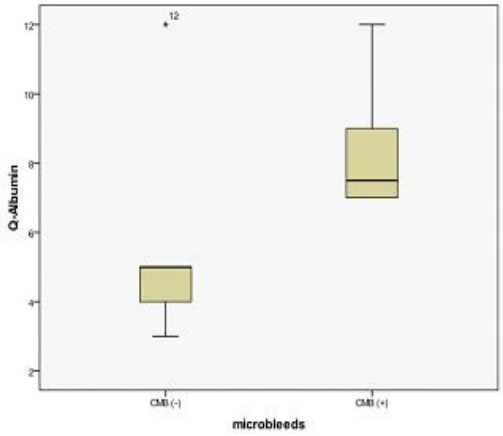

Picture 1 QAlb ratio in CSF depends on CMB

996
BRAIN-0125
Non-Registered Abstracts

FORCED LIMB-USE ENHANCES BRAIN PLASTICITY THROUGH THE CAMP/PKA/CREB SIGNAL TRANSDUCTION PATHWAY AFTER STROKE IN ADULT RATS

H. Qu[1], *C. Zhao*[1]
[1]*Neurology,*
The first hospital of China Medical University, Shenyang, China

Purpose: The mechanism underlying forced limb-use -induced structural plasticity remains to be studied. We examined whether the cyclic adenosine monophosphate (cAMP)–mediated signal transduction pathway was involved in brain plasticity and promoted behavioral recovery induced by forced limb-use after stroke.

Methods: Adult rats were divided into a sham group, an ischemia group, an ischemia group with forced limb-use, and an ischemia group with forced limb-use and infusion of N-[2-(p-bromocinnamylamino)ethyl]-5-isoquinoline-sulfonamide (H89). Forced limb-use began on post-stroke day 7. Biotinylated dextran amine (BDA) was injected into the sensorimotor cortex on post-stroke day 14. Behavioral recovery was evaluated on post-stroke days 29 to 32, and the levels of cAMP, PKA C-α, phosphorylated CREB (pCREB), synaptophysin, PSD-95, BDA, and BrdU/NeuN were measured.

Results: The number of midline-crossing axons and the expression levels of synaptophysin and PSD-95 were increased after forced limb-use. Forced limb-use enhanced the survival of the newborn neurons and increased the levels of cAMP, PKA C-α and pCREB. These were significantly suppressed by H89. Behavioral performance improved with forced limb-use and was reversed with H89.

Conclusions: Enhanced structural plasticity and the behavioral recovery promoted by post-stroke forced limb-use are suggested to be mediated

through the cAMP/PKA/CREB signal transduction pathway.

997
BRAIN-0033
Non-Registered Abstracts

NEUROPROTECTIVE EFFECT OF HYDROXYSAFFLOR YELLOW A AGAINST ISCHEMIA-REPERFUSION INJURY BY INHIBITING MITOCHONDRIAL PERMEABILITY TRANSITION PORE OPENING

S. Ramagiri[1], T. Rajeev[1]
[1]Pharmacy,
Birla Institue of Technology and Sciences, pilani, India

Aim The present study was designed to investigate the neuroprotective effects of hydroxy safflor yellow A (HSYA), an active ingredients of the Chinese herb *Carthamus tinctorius L,* and its molecular mechani sms against cerebral-ischemia reperfusion injury.

Methods Cerebral ischemia reperfusion (I/R) injury was induced by middle cerebral artery occlusion (MCAO) for 30 min in Wistar male rats followed by 24 hrs reperfusion. Cerebral blood flow (CBF) was monitored by Laser-Doppler Perfusion and Temperature Monitor (moor VMF – LDF2, UK) using a flexible probe over the skull.

Key findings I/R injury resulted severe deficits in cognition, sensorimotor and skilled motor functions, as assessed by neurological scoring, rotarod, photoactometer and Y maze. Moreover, it also resulted in elevated oxidative stress and Tumor Necrosis Factor (TNF- α) levels along with higher infarct size. HSYA treatment (8 mg/kg, i.v.) attenuated infract size, oxidative stress, neuro-inflammation along with improvement in motor and cognitive performance. However, administration of carboxyatractyloside (1 mg/kg, i.p.), an opener of mPTP, attenuated the protective effect of HSYA against cerebral I/R-injury.

Conclusion Thus based on above observations, it may be suggested that HSYA possess neuro-protective effects possibly mediated via mPTP closing during reperfusion. Hence, HSYA can be considered a promising approach against cerebral ischemic reperfusion injury.

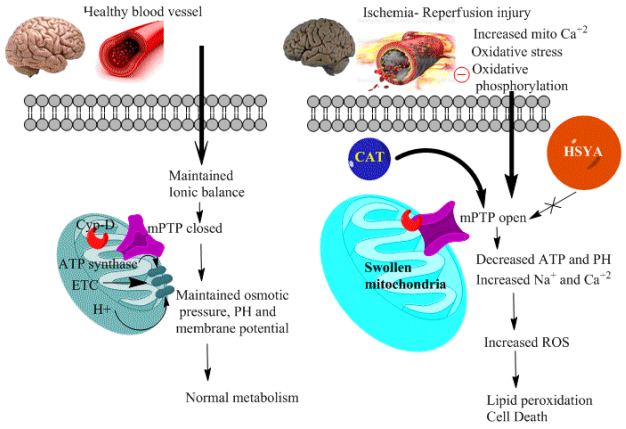

998
BRAIN-0044
Non-Registered Abstracts

MICROGLIAL INHIBITORY EFFECT OF GINSENG AMELIORATES COGNITIVE DEFICITS AND NEUROINFLAMMATION FOLLOWING TRAUMATIC HEAD INJURY IN RATS

P. Rinwa[1], H. Dhar[1], A. Kumar[1]
[1]University Institute of Pharmaceutical Sciences, Panjab University, Chandigarh, India

Traumatic brain injury produces several neuropathological alterations some of them are analogous to patients suffering from memory disorders. Role of neuroinflammation and oxidative stress has been suggested in the pathophysiology of brain injury induced-cognitive dysfunction. Therefore, the present study was designed to explore the possible role of ginseng and its interaction with minocycline (microglial inhibitor) against experimental brain trauma induced behavioral, biochemical and molecular alterations. Wistar rats were exposed to brain traumatic injury using weight-drop method. Following injury and a post-injury rehabilitation period of two weeks, animals were administered vehicle/drugs for another two weeks. Brain injury caused significant memory impairment in Morris water maze task as evident from increase in

escape latency and total distance travelled to reach the hidden platform. This was followed by a significant decrease in time spent in target quadrant and frequency of appearance in target quadrant. Further, there was a significant increase in oxidative stress markers, neuroinflammation (Tissue Necrosis Factor-alpha and Interlukins-6) and acetylcholinesterase levels in both cortex and hippocampal regions of traumatized rat brain. Ginseng (100 and 200 mg/kg) and minocycline (50 mg/kg) treatment for two weeks significantly attenuated all these behavioral, biochemical and molecular alterations. Further, combination of sub effective doses of ginseng (50 and 100 mg/kg) and minocycline (25 mg/kg) potentiated their protective effects which was significant as compared to their effects alone. The results of the present study suggest that the therapeutic effects of ginseng might involve inhibition of microglial pathway against head trauma-induced cognitive impairment and neuroinflammation in rats.

999
BRAIN-0421
Non-Registered Abstracts

IMPACT OF ANEMIA ON OUTCOME IN PATIENTS WITH SEVERE TRAUMATIC BRAIN INJURY

M. Rodriquez[1], A. Ottesen[1], K. Carr[2], A. Seifi[2]
[1]School of Medicine,
University of Texas Health Science Center,
San Antonio, USA
[2]Department of Neurosurgery,
University of Texas Health Science Center,
San Antonio, USA

Objectives

The blood transfusion threshold for severe traumatic brain injury (TBI) patients has been a subject of much discussion. However, no consensus has been reached on the most beneficial transfusion threshold. We sought to further examining the impact of various hemoglobin (Hgb) threshold levels on outcomes in severe TBI patients.

Methods

We reviewed the records of patients admitted with severe TBI to University Hospital in San Antonio, Texas from 2011 to 2013. Severe TBI was defined as patients with TBI who required intracranial pressure monitoring within 48 hours of admission. Patients who were less than 18 years of age, pregnant, non-traumatic brain injuries, expired within 72 hours of admission, or received an operating room procedure for a non-TBI injury or a blood transfusion within 24 hours of admission were excluded.

Demographic data, the lowest Hgb level, and transfusion status were queried. The outcome measures were mortality, change in Glasgow Coma Scale (GCS) score, hospital length of stay (LOS), and intensive care unit length of stay (ICU LOS). Fisher's exact test was utilized to compare the outcomes in the transfused and non-transfused groups using four different Hgb thresholds: 7, 8, 9, and 10 g/dL.

Results

During the study period, there were 407 qualifying records. After exclusion criteria were applied, 89 patients were enrolled in the study. The median age of cohort was 45, of which 82% were male and 56% received transfusions. The mortality rate of the cohort was 17%.

A Hgb greater than 8 g/dL was associated with a shorter ICU LOS [11 vs 15 days, p=0.02] and a shorter hospital LOS [17 vs 32 days, p=0.01]. (*See Figure 1*). We found no association between Hgb level and improvement in GCS. Of patients with Hgb less than 8 g/dL who were transfused, 8.5% died. Whereas, the mortality rate for those not transfused was 35.7% (p=0.01).

Conclusions

Our data suggests that, in severe TBI patients, maintaining Hgb over 8 g/dL may shorten ICU and hospital lengths of stay. Although our data supports that liberal transfusion strategies do not positively impact measured outcomes in patients

with severe TBI, it did suggest an association between blood transfusions and decreased mortality rates for patients with Hgb levels less than 8 g/dL. Additional prospective studies should be undertaken to determine the best transfusion threshold for severe TBI patients.

References

George M, et al. "Aggressive red blood cell transfusion: no association with improved outcomes for victims of isolated traumatic brain injury." (2008) 8:337-343.

Roberts D, Zygun D. "Anemia, red blood cell transfusion, and outcomes after severe traumatic brain injury." *Critical Care* (2012) 16:154.

Sekhon M, et al. "Association of hemoglobin concentration and mortality in critically ill patients with severe brain injury." *Critical Care* (2012) 16:R128.

Warner M, et al. "Transfusions and long-term functional outcomes in traumatic brain injury." *J. Neurosurg* (2010) 113: 539-546.

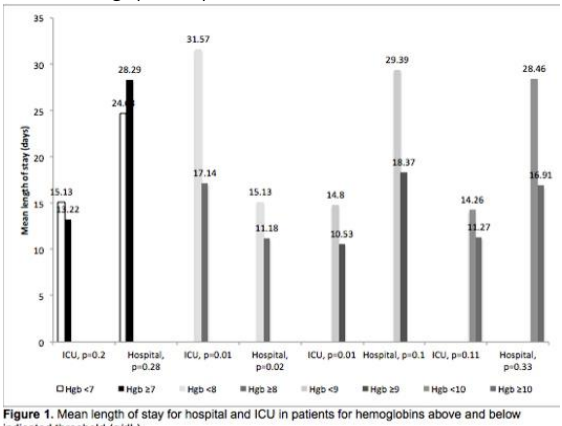

Figure 1. Mean length of stay for hospital and ICU in patients for hemoglobins above and below indicated threshold (g/dL)

1000
BRAIN-0519
Non-Registered Abstracts

MICRORNAS (MIRNA), LET-7/MIR-98, DECREASE INFLAMMATION AND IMPROVE TIGHTNESS OF THE BLOOD BRAIN BARRIER (BBB)

S. Rom[1], H. Dykstra[1], V. Zuluaga-Ramirez[1], N. Reichenbach[1], Y. Persidsky[1]
[1]Pathology, Temple University School of Medicine, Philadelphia, USA

Objectives: Diseases of the central nervous system (CNS) cause a significant challenge, but regardless of their multiplicity, they share many universal features and mechanisms. For example, endothelial dysfunction is perhaps the earliest event in the initiation of vascular disease, caused by inflammation due to stroke, atherosclerosis, trauma or brain infection[1]. Increased blood-brain barrier (BBB) permeability represents a hallmark of CNS inflammation that occurs in variety of neuropathological conditions. Microvasculature endothelial cells are very active participants and regulators of inflammatory processes at a site of inflammation. Immune mediators and engagement of primary human microvascular endothelial cells (BMVEC) with leukocytes contribute to BBB impairment during neuroinflammation. Glycogen synthase kinase (GSK)-3b has been implicated as a key regulator of the inflammatory response. The anti-inflammatory effects of GSK3b inhibition have been shown *in vitro* and in several *in vivo* models of acute and chronic inflammation[2, 3]. Recently, miRNAs have emerged as a class of gene expression regulators. The relationship between inflammation and miRNA expression remains largely unexplored.

Methods: We used microarray technology (miR Base version 16 screening of 1212 miRNAs) to identify miRNAs induced in human primary BMVEC after exposure to the pro-inflammatory cytokine, TNFa, with or without a GSK3b inhibitor. Selected miRNAs were overexpressed in BMVEC, an *in vitro* BBB model, and in an *in vivo* model. All animal studies were approval by the Institutional Animal Care and Use Committee and the animal care and handling were in accord with National Institutes of Health guidelines.

Results: miRNA array showed that 123 microRNAs were downregulated (1-fold) in cells treated with TNFa/GSK3b inhibitor. 14 miRNAs were common to the two groups. Among the highly modified miRNAs, let-7 and miR-98, were predicted by a bioinformatics approach to target several inflammatory molecules such as VCAM-1, CD99, L1CAM, IL8, IL6, CXCL1 and IP-10. Overexpression of let-7 and miR-98 in BMVEC decreased leukocyte adhesion to and migration across BMVEC monolayers and improved transendothelial resistance (TEER). Pretreatment

of mice with let-7/miR-98 diminished leukocyte adhesion to and migration across BBB *in vivo,* and led to a reduction in BBB leakiness.

Conclusions: Overexpression of let-7 and miR-98 in endothelium reduced expression of selected cytokines and improved BBB function both *in vitro* and *in vivo*. In this work we explored use of GSK3b-regulated miRNAs as therapeutic tools to prevent deleterious effects of endothelial dysfunction on neuroinflammation.

References:

1. Faraci FM. Protecting against vascular disease in brain. *Am J Physiol Heart Circ Physiol* 2011; 300(5): H1566-82.

2. Woodgett JR, Ohashi PS. GSK3: an in-Toll-erant protein kinase? *Nat Immunol* 2005; 6(8): 751-2.

3. Ramirez SH, Fan S, Dykstra H, Rom S, Mercer A, Reichenbach NL *et al.* Inhibition of Glycogen Synthase Kinase 3beta Promotes Tight Junction Stability in Brain Endothelial Cells by Half-Life Extension of Occludin and Claudin-5. *PLoS One* 2013; 8(2): e55972.

1001
BRAIN-0489
Non-Registered Abstracts

IL-1A ENHANCES ANGIOGENIC NEUROREPAIR AFTER EXPERIMENTAL ISCHEMIC STROKE

K. Salmeron[1], E. Pinteaux[2], G. Bix[1]
[1]Sanders Brown Center on Aging, University of Kentucky, Lexington, USA
[2]Department of Life Sciences, University of Manchester, Manchester, United Kingdom

Objective:

Stroke is a major cause of death and disability worldwide. Unfortunately, all clinical trials that have targeted the primary cerebral ischemia (CI) injury mechanisms of oxidative stress and excitotoxicity have failed. However, CI also induces a potent local inflammatory response that leads to damage in the ischemic penumbra but may also, less acutely, initiate and sustain post-stroke repair processes such as angiogenesis. We hypothesize that the pro-inflammatory cytokine IL-1α promotes angiogenesis after stroke via generation of pro-angiogenic perlecan laminin globular domain 3 (LG3) protein fragments from the brain extracellular matrix. This is based on our previous observations that LG3 is rapidly and persistently generated after CI in vivo, and that IL-1α causes cells of the neuromuscular unit to generate LG3 *in vitro.* Importantly, the potential role of IL-1α in brain angiogenesis has not been previously studied.

Methods:

Adult male C57/Bl6 mice underwent distal transient middle cerebral artery occlusion (MCAO) for 1 hour. IL-1α levels were measured at PSD 3, 7 and 21. *In vitro* angiogenesis assays were performed in 12, 24, and 96 well plates with brain endothelial cells isolated from C57/Bl6 mice. Cell lysates were obtained to determine levels of VCAM-1, ICAM-1 and iNOS by qPCR and Western Blot respectively. MTS Assays were performed using a spectrophotometric plate reader. Migration experiments were done using Scratch/Wound and Boyden Chamber modalities. Finally, capillary morphogenesis assays were performed on growth factor reduced Matrigel.

Results:

IL-1α activates primary endothelial cells (BECs) *in vitro* and significantly enhances several stages of BEC angiogenesis including proliferation, migration and capillary tube-like structure morphogenesis. IL-1α levels are chronically (21 days) elevated (measured by qPCR and ELISA) suggesting that IL-1α persists beyond the acute stroke phase to affect post-stroke angiogenic repair. Finally, IL-1α deficient mice have diminished post-stroke penumbral angiogenesis.

Conclusions:

Our results collectively suggest that inflammatory mediators such as IL-1α, in addition to their acute deleterious effects, may play an important and previously unrecognized role in post-stroke angiogenic neurorepair that could be therapeutically exploited.

1002
BRAIN-0023
Non-Registered Abstracts

THE CORRELATION BETWEEN BULIMIA NERVOSA AND BIPOLAR PATIENTS REFERRED TO PSYCHIATRY CLINIC .KERMANSHAH,IRAN,2012-2014

J. Shakeri[1], H. Shakeri[1], F. Arman[1], M. Shakeri[1]
[1]Psychiatry,
Kermanshah University of Medical Sciences, Kermanshah, Iran

Introduction:

Bulimia nervosa(BN) is an eating disorder characterized by binge eating large amounts of food and then purge.Although the incidence rate is still a matter of debate,the prevalence rate has been increasing all over the world.
BMD is a mental disorder characterized by abnormal and elated or irritable mood possibly with depressive episodes at times.

Objective:

The aim of this study was to investigate any possible relationship between bipolar disorder and Bulimia nervosa in order to improve the standard of living among these patients.

Methods:

130 known cases of BMD were interviewed and the data was gathered with demographic and Bulimia self-report questionnaire.The data was analyzed with SPSS 21 software.

Results:

Of 130 patients,85 patients (65.38%) were female and 45 patients (34.61%) were male.Most prevalent age group was between 20-40 years (M=28.7, S.D=3.4). The mean BMI of patients was 27.82 kg/m^2 with SD equal to 9.54. 72 (55.38%) of patients were single while 58 (44.61%) were married .76 patients (58.46%) lived in city and 54 of them (41.53%) lived in countryside. 80 patients (61.53%) had high school education or below and 50 (38.46%) had high school diploma or higher. 45 patients were diagnosed with bulimia .40 patients were female with an incidence rate of 88.88% and 12.22% between male.32 patients had history of drug abuse and 5 of them had a history of suicide attempt.We compared these results in these two groups of patients .Patients with BMD had a significantly higher prevalence of bulimia.Patients with co-morbidity of bulimia and BMD had double suicide attempts and their drug dependency was 3 times more than BMD without bulimia.

Discussion:

Although prevalence of bulimia in normal population maybe higher than our current knowledge due to the nature of the disorder which tends to go under-recognized, our study showed that there is significantly higher incidence of bulimia in bipolar patients. We suggest that:

1. The possibility of co-morbidity of BMD and Bulimia should be considered in resistant cases of both disorders.

2. Clinician should pay close attention to possible drug and non-drug interactions of treatment of both diseases.

1003
BRAIN-0131
Non-Registered Abstracts

NON-INVASIVE BRAIN AND KIDNEY COOLING IN SEVERE MULTISYSTEM BRAIN INJURY COMPLICATED BY SEPTIC SHOCK

V. Avakov[1], I. Shakhova[1]
[1]Anaesthesiology Resuscitation and Intensive Care , Tashkent MAdical Academy, Tashkent, Uzbekistan

Background. The worldwide burden of sepsis is high and is increasing (Stehr SN et al., 2013). Brain dysfunction is a severe complication of sepsis with an incidence ranging from 9% to 71% that is associated with increased morbidity and mortality (Siami S et al., 2008). Our understanding of sepsis-associated acute kidney injury pathophysiology is shifting from renal vasoconstriction, ischemia,

and acute tubular necrosis to heterogeneous vasodilation, hyperemia, and acute tubular apoptosis (Koçkara A et al., 2013). Regarding pathogenesis, rates of morbidity and mortality are aimed to be reduced through the new methods of therapy that have been studied (Koçkara A et al., 2013). Various drugs acting on sepsis-induced blood-brain barrier dysfunction, brain oxidative stress and inflammation have been tested in septic animals but not yet in patients (Adam N et al., 2013).

The aim of our study was to optimize prevention and treatment of acute kidney injury and toxic encephalopathy in patients with severe traumatic brain injury combined with an acute surgical abdominal pathology and complicated by septic shock.

Materials and Methods. During the period from 2011 to 2014 18 patients were admitted to our hospital urgently because of injury due to accidents, falls, fights. All patients were subjected to emergency surgery - midline laparotomy (ML), 10 of them (55%) cases of simultaneous operations: removal of intracranial hematoma (hydroma) with ML. ML accompanied nephrectomy (3 patients), nephrectomy with splenectomy (3 patients), nephrectomy with resection of the liver (2), splenectomy (3), resection of liver and intestine (4) and bowel resection (3). After ML laparostomy set (Fig. 1) to the disappearance of signs of sepsis.

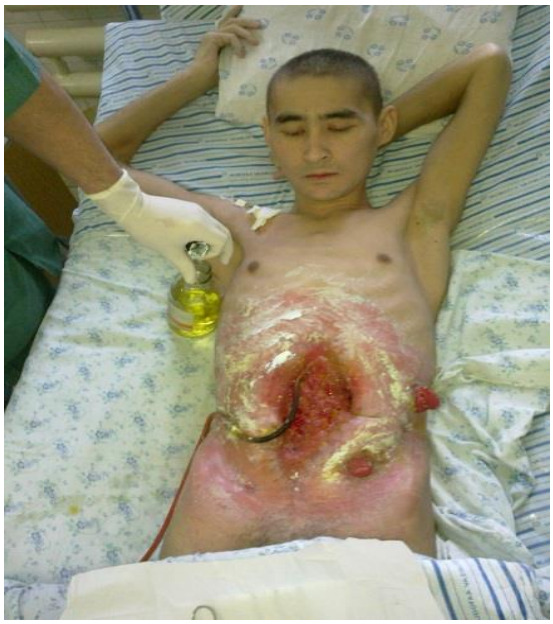

Fig.1. Photo of patient with severe multisystem traumatic brain and abdominal injury complicated by septic shock (Day 83 in the ICU)

3-5 days in 12 patients showed signs of toxic encephalopathy, 5-8 days - liver failure (6 patients), 7-11 - renal failure (7), 6-12 - septic shock (18), 8 - refractory septic shock, 18 - hyperthermic syndrome. Malignant fever was observed in 9 patients.

Due to the above, for 2-4 days in all patients on the basic therapy with prophylactic or therapeutic purposes began brain (Fig. 2) and kidney (Fig. 3) cooling in accordance with the method developed by us.

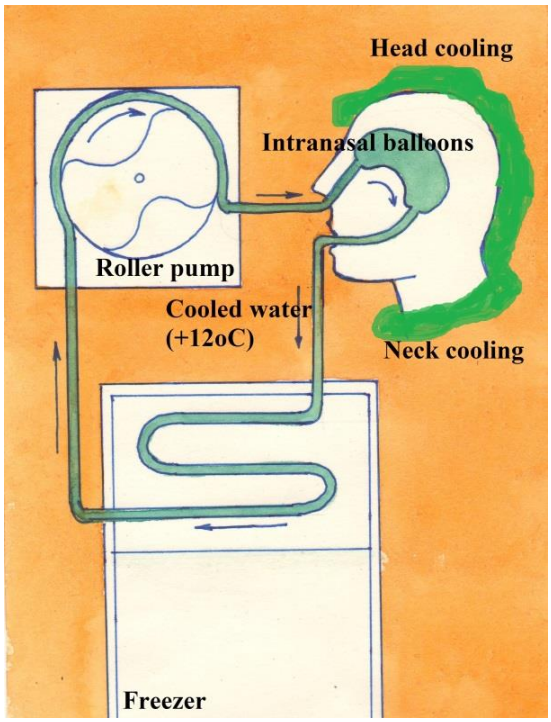

Fig.2. Method of brain cooling (schematic view)

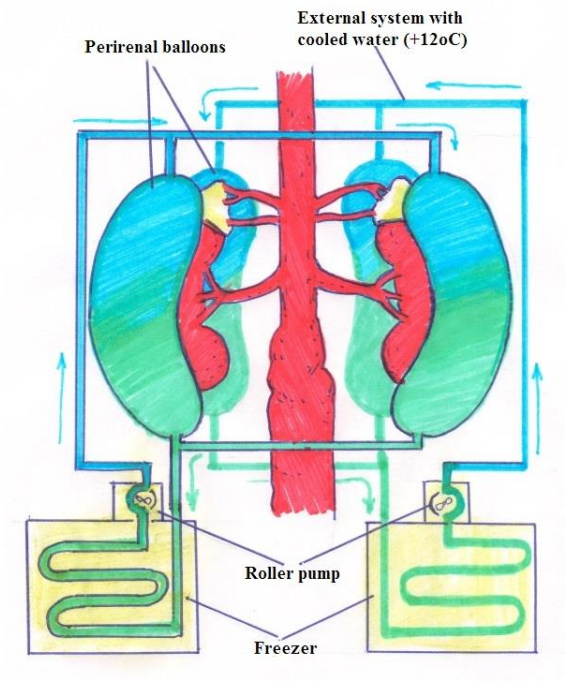

Fig.3. Method of kidney cooling (schematic view)

Nasopharyngeal cooling (Fig. 2) can block the activity of the thermoregulatory center, located in the hypothalamus, which is especially relevant in our febrile septic patients.

Results. Brain and kidney cooling for 24-72 hours contributed to the complete disappearance/prevent symptoms of toxic encephalopathy and renal failure, as well as hyperthermia syndrome and malignant fever. This will reduce the length of stay of patients in ICU and greatly reduce the costs associated with the treatment of septic patients. There was no case of death. All patients fully recovered and returned to normal activities.

Conclusions. Brain and kidney cooling in according to our method allowed to obtain good results in the treatment of patients with toxic encephalopathy, malignant hyperthermia, septic shock.

Конец формы

1004
BRAIN-0056
Non-Registered Abstracts

GINSENOSIDE-RD IS EFFICACIOUS AGAINST ACUTE ISCHEMIC STROKE BY SUPPRESSING MICROGLIAL PROTEASOME-MEDIATED INFLAMMATION

M. Shi[1], *X. Liu*[1]
[1]*Department of Neurology, Xijing Hospital The Fourth Military Medical University, Xi'an, China*

Background and Purpose—A great deal of attention has been paid to neuroprotective therapies for stroke. Our recent TWO clinical trials showed that ginsenoside-Rd (Rd), a monomeric compound from Chinese herbs, *Panax ginseng* and *Panax notoginseng*, was safe and efficacious in the treatment of ischemic stroke. To better understand the advantage of Rd, here we conducted a pooled analysis of these two trials and further explored possible neuroprotective mechanisms of Rd.

Methods—To increase the statistical power, data from 199 patients with acute ischemic stroke in the first trial and 390 in the second were pooled and reanalyzed to assess the efficacy and safety of Rd. Animal stroke models were used for studying the underlying mechanisms.

Results—. The pooled analysis showed that compared with placebo group, Rd was associated with a reduction of patients' disability at day 90 assessed by mRS score and reduced neurologic deficits at day 15 assessed by NIHSS score and at days 15 and 90 by BI score. On animal ischemic stroke models, late administration of Rd (4 h after stroke) was found to inhibit ischemia-induced microglial activation. Rd could decrease the expression levels of various proinflammatory cytokines and suppress IκBα phosphorylation and NF-κB nuclear translocation. An in vitro proteasome activity assay showed a significant inhibitory effect of Rd on proteasome activity in microglia. Interestingly, Rd was revealed to have less side effects than glucocorticoid.

*Conclusions—*Our study demonstrated that Rd could safely improve the outcome of patients with ischemic stroke, and this therapeutic effect may result from its capability of suppressing microglial proteasome activity and sequential inflammation.

1005
BRAIN-0591
Non-Registered Abstracts

MECHANISMS UNDERLYING IMPAIREMENT OF CEREBRAL AUTOREGULATION IN HYPERTENSIVE RATS

S.S. Sindeev[1], O.A. Sindeeva[1], E.M. Zinchenko[1]
[1]Biology, Saratov State University, Saratov, Russia

Objectives: Well known, that cerebral blood flow (CBF) is weakly depends on peripherial blood pressure. That fact caused by cerebral autoregulation [1], but it also known that in some pathological states (Alzheimer desease, cerebral hemorrhages, etc.) autoregulation became insufficient [2]. Until now it is undiscovered how peripheral blood pressure affects on CBF in normal and hypertension states [3]. To better understanding relationship between peripheral and cerebral circulation we studied here changes in CBF in acute and chronic hypertensive states.

Methods: To induce acute increase in peripheral mean blood pressure (MAP) we administered phenylephrine (PE) in different doses (0.25 – 0.5 – 1 μg/kg, iv) to normotensive (n=10) and hypertensive rats (n=10). To induce two kidney, one clip (2K1C) hypertension rats were clipped at the left renal artery with a silver clip. The rats were instrumented with polyethylene catheters for monitoring MAP using PowerLab system. CBF changes evaluated using laser speckle imaging system. To assessment of expression of structural elements of brain blood barrier we used immunofluorescence and immunoblotting.

Results: PE administration caused the dose-depended increase in MAP in both normotensive and hypertensive rats but the magnitude of pressure response was greater in normotensive rats compared with hypertensive animals. The recovery after phenylephrine-induced increase in MAP was longer in hypertensive rats than in normotensive ones.

CBF remain unchanged in normotensive rats despite significant dose-depended increase in MAP by 15%-27%-52%, respectively. In contrast to normotensive rats, hypertensive rats demonstrated essential CBF response related to MAP changes. So, small dose of PE is accompanied by moderate MAP response (12%, $p<0.05$) and, in parallel, increase in CBF by 17% ($p<0.05$). The high dose of PE caused significant increase in MAP (32%, $p<0.05$) that was associated with increase in CBF (24%, $p<0.05$).

We found less expression of structural elements of BBB such as clauding-5, occluding, collagen IV, laminin and increase in permeability of BBB to small (3kDa) but not large albumins (70kDa) in hypertensive rats compared with normotensive rats.

Conclusion: Hypertension is accompanied by increase in permeability of BBB with decrease in expression of tight junction's and basal lamina proteins of BBB. Interruption of BBB in hypertensive rats is associated with impairment of cerebral autoregulation: even moderate peripheral pressure responses cause pronounced increase in CBF. These results allow to conclude that hypertension-induced interruption of BBB

can be one of important mechanism underlying impairment of cerebral autoregulation.

References:
1. Lassen N A. Cerebral blood flow and oxygen consumption in man. // Physiological Reviews. - 1959, Vol. 39(2). - P. 183–238.
2. Bruder N., Pellessier D., Grillot P. Cerebral Hyperemia During Recoveryfrom General Anesthesia in Neurosurgical Patients // Anesthesia &Analgesia. – 2002. Vol. 94. - no. 3. P. 650-654
3. Lucas S.J., Tzeng Yu.C., Galvin S.D. et al. Influence of Changes in Blood Pressure on Cerebral Perfusion and Oxygenation // Hypertension. – 2010. - Vol. 55. - P. 698-705.

Aknowledgements:
This work supported by grant of President of Russian Federation, agreement MD-2216.2014.4; RFBR grant 14-02-00526-a

1006
BRAIN-0192
Non-Registered Abstracts

ROLE OF THE CLINIC SCALE, FOR THE IDENTIFICATION STAGE OF THE COGNITIVE DYSFUNCTION IN PATIENTS WITH POST-TRAUMATIC ENCEPHALOPATHY.

N. Sokhibnazarov[1], F. Muratov[1]
[1]Neurology, Tashkent Medical Academy, Tashkent, Uzbekistan

Objective: To study the value of various clinical scales to determine the degree of cognitive dysfunction in patients with post-traumatic encephalopathy, during the neuroprotective therapy.

Material methods: The study included 30 patients (21 male and 9 female) who are hospitalized in the neurology department of TMA from the (2013-2014), aged 30 to 55 years (middle age 43,2 ± 7,4 years) suffering with post-traumatic encephalopathy. To assessment neurological status used brief scale to assessment cognitive status (MMSE), the Monreal Assessment Scale (MAS). Patients were divided into 2 groups: the main group consisted of 15 patients with traditional therapy was appointed «Gliatilin» during the 2 weeks. The control group consisted of 15 patients who received only conventional therapy without «Gliatilin». .

Results: In the study group patients, who take «Gliatilin» cognitive function are improved (memory, thinking, comprehension) to 38 % than in the control group. It was found that prior to treatment, patients in the study group took 20.8 on the MMSE, and 20.9 point from the MAS. Patients in the control group, respectively, 20.5 and 20.6. After treatment, the patients of the main group on the MMSE score increased to 28.3 points, patients in the control group score been 24.2 points. By «MAS» the study group scored 25.6 points, patients in the control group 22.4 points.

Conclusions:
1. The use of scales to determine the cognitive dysfunctions enables to improved identification degree of cognitive dysfunctions.

2. The use of a neuroprotective drug «Gliatilin» in patients with post-traumatic encephalopathy to improved the condition of patients and reduce the severity of the degree of cognitive impairment, frequent in this pathology.

References:
1. Ibodullaev Z.R. Nervous diseases. Uzbekistan: FAN VA TEXNOLOGIYA UNIT ENTERPRISE, 2014.
2. Majidova Y.N. Samigova D.A. Neurology journal. Treatment for childs with traumatic encephalopathy by perinatal affect of nervous system. Uzbekistan. 2014(1) 4-5 pp.

1007
BRAIN-0091
Non-Registered Abstracts

SALUTARY EFFECT OF PROGESTERONE IN TRAUMATIC BRAIN INJURY

Z. soltani[1], B. Mofid[2], N. Shahrokhi[1], M. Khaksari[3], S. Karamouzian[2], N. Nakhaee[4], M. Ahmadinejad[5]
[1]Neuroscience Research Center, Institute of Neuropharmacology Kerman University of Medical Sciences, kerman, Iran
[2]Dept. of Neurosurgery, Kerman Hospital of Shahid Bahonar, kerman, Iran
[3]Physiology Research Center, Institute of Neuropharmacology Kerman University of Medical Sciences, kerman, Iran
[4]Dept. of Social Medicine, Medical School of Afzalipour Kerman University of Medical Sciences, kerman, Iran
[5]Dept. of Intensive Care Unit, Kerman Hospital of Shahid Bahonar, kerman, Iran

Objective: The sex hormone progesterone has been shown to improve outcomes in animal models with traumatic brain injury (TBI). The aim of this clinical study was to assess the effect of progesterone on the improvement of neurologic outcome in patients with diffuse and acute TBI.

Methods: A prospective, randomized, double-blind trial of progesterone was conducted in our teaching hospital. A total of 50 patients with diffuse acute TBI who arrived within 4 hours of injury with a Glasgow Coma Score ≤ 12 were enrolled in the study, when their family consented. In a randomized style 25 received progesterone (1 mg/kg per 12 h for 5 days) and 25 did not. The primary efficacy endpoint was the Glasgow Outcome Scale score 3 months after brain injury. Secondary efficacy endpoint included the mortality.

Results: The demographic characteristics, and the mechanism of injury were similar for the two groups. After 3 months of treatment, the Glasgow Outcome Scale score analysis exhibited more favorable outcome among the patients who were given progesterone compared with the control individuals (P = 0.056). The mortality rate of the control group was 20.8%, whereas any of patients in progesterone group did not die. Instances of complications and adverse events associated with the administration of progesterone were not found in any of patients.

Conclusion: Our data suggest that the administration of progesterone for TBI patients improved neurologic outcome for up to 3 months and reduced mortality. These results indicate that progesterone can considered as a promising neuroprotective drug.

1008
BRAIN-0692
Non-Registered Abstracts

NEUROLOGICAL COMPLICATIONS IN ICU AFTER ON-PUMP CARDIAC SURGERY: A CHINESE STUDY

T. Sosorburam[1], L. Yao[1], P. Xiao[2]
[1]Anesthesiology, Tongji Medical College, Wuhan, China
[2]ICU, Tongji Medical College, Wuhan, China

Objectives: Despite having advanced medical care and surgical techniques, neurological complications remain significant causes of postoperative mortality and morbidity in patients underwent cardiac surgery. Whether anesthetic drugs influence the outcome or not is still unclear. Therefore, we conduct the research to determine effects of different anesthetic drugs.
Method: The study was conducted at Union Hospital, China from May 2013 to December 2014. Total 120 patients, who are undergoing on-pump cardiac surgeries without any history of cerebrovascular diseases are recruited. The subjects randomly selected into two most commonly used anesthetic agents groups: volatile anesthetic/VA/ or total intravenous anesthetic/TIVA/ groups. Evaluation of major neurological and physiological dysfunctions were recorded until the patient discharged from the hospital. Comparisons between the groups were analyzed using the t-Student test, and P values of less than 0.05 were considered statistically significant.
Results: There was no significant difference found between the demographics data, intraoperative

monitoring and cerebral protective measures between the groups. The incidence of postoperative stroke and postoperative delirium were 2.5% and 5.8% in TIVA group and 3.7% and 6.4% in VA group. Early mortality was higher in VA (4.3% vs 3.5%). Multivariate analysis revealed that postoperative cognitive disorder was associated with longer duration of cardiopulmonary bypass (mean time 132±2.4min in VA vs 118±4.8min in TIVA). Another significant difference was transient ischemic attack, which was 7.1% in VA and 6.5% in TIVA. The hospital length of stay and ICU stay were longer in VA group (14.1 and 5.2 days vs 12.3 and 6.2 days).
Conclusion: TIVA associated with lower postoperative mortality and morbidity than VA. The advantage of TIVA over VA is evident regarding interference with neurological and cognitive disorders. However, all the potential neuroprotective effect of TIVA cannot be measured by single anesthetic drug or technique, TIVA appears to be the first choice for on-pump cardiac surgery. We suggest further systemic and multi-centered study should be conducted to implement guidelines regarding the neuroprotective anesthesia.

1009
BRAIN-0918
Non-Registered Abstracts

SNORING AS A RISK FACTOR OF STROKE AMONG FILIPINOS: A CASE CONTROL STUDY

A. Tan[1], J. Navarro[1], A. Baroque[1], I. David[1]
[1]Neurology & Psychiatry,
University of Santo Tomas Hospital, Manila, Philippines

Objective: The study described the association between stroke and snoring among Filipinos.

Methodology: This case-control study included 109 cases with first-ever stroke and 109 matched control subjects for age, sex and at least two stroke risk factors. A structured interview was done using the validated Berlin Questionnaire in Filipino to identify snoring, daytime sleepiness and stroke risk factors. Univariate odds ratios (OR) for stroke associated with snoring were calculated and significance was assessed.

Results: The case and control groups were matched for age (±2 years), sex and at least two stroke risk factors, which showed no significant difference among groups. There was a significant association between stroke patients who snore compared to controls [OR 31, CI 95% (10.66-90.05)]. The Berlin questionnaire stratified the risk of having sleep apnea among snorers in both groups [OR 3, CI 95% (1.72-5.99].

Conclusion: The study validated that snoring alone is a significant risk factor for stroke.

1010
BRAIN-0099
Non-Registered Abstracts

THERAPEUTIC HYPOTHERMIA IN SEVERE TRAUMATIC BRAIN INJURY

A. Tomar[1], C. Thomas[1], R. Talukder[1], K. Carr[1], A. Parra[1], A. Seifi[1]
[1]Neurosurgery,
The University of Texas Health Science Center at S an Antonio, San Antonio, USA

Background:

Traumatic brain injury (TBI) is a common and often devastating injury leading to high intracranial pressure (ICP). Therapeutic hypothermia (TH) is one of the few possible therapeutic options in refractory high ICP. We sought to determine the efficacy of TH in controlling high ICP and to find predictors of functional outcome in severe TBI.

Materials and Methods:

Retrospective study conducted at University Hospital in San Antonio, TX from 2011-2014. All severe TBI patients were assessed via an imaging TBI score. The primary outcome measure was ICP control and modified Rankin Scale (mRS) at discharge.

Results:

During the study period, 77 patients met inclusion criteria, 19 underwent TH and 58 did not. There was no significant difference for age, gender, and ethnicity (P>0.5). Patients in TH group had significantly higher imaging TBI score, specifically more brain edema (P=0.001), SDH (P=0.006) and IVH (P=0.001), and higher duration of intractable ICP (P=0.011). There was no significant difference in hospital length of stay (P=0.541), mRS at discharge (P=0.082), and mortality (P=0.139). In multivariate analysis a “TBI scale” using the 24hr GCS, age>40, presence of SAH, EDH, and edema on imaging score were the best combination to predict mRS at discharge and ICP control (>80% sensitivity and specificity). Higher “TBI scale” was significantly associated with mRS<3 at discharge (P=0.028) and ICP control (P=0.001). Hypothermia was not significantly associated with mRS<3 at discharge (P=0.892), but associated with higher intractable ICP (P=0.003).

Conclusions:

Our study showed that patients with severe TBI who underwent TH usually had higher imaging TBI score. Although TH doesn't show a direct improvement in the outcome of severe TBI, a mixture of parameters including 24hr GCS, age>40, EDH, SAH and brain edema can predict severe TBI outcome.

1011
BRAIN-0910
Non-Registered Abstracts

INTRACRANIAL VENOUS HEMODYNAMICS AND RUPTURE OF CEREBRAL ANEURYSM.

F. Tsai[1], K.W. Lee[2], W.L. Chen[2], C.K. Liu[2], C.L. Ku[2], S. Chen[1]
[1]Imaging Research Center, Taipei Medical University, Taipei, Taiwan
[2]Imaging Research Center, Chang-Hua Christian Hospital, TaipeChang-Hua, Taiwan

Objectives:

Many uncertainty and inconsistent etiologies of cerebral aneurysmal rupture even wide spectra of factors being reported. Our observation elucidate the potential new factor of cerebral aneurysmal rupture with cerebral venous pressure gradient.

Material and Methods:

Retrospectively reviewed 52 were treated with coil embolization with or without cerebral aneurysmal rupture. seventeen male and thirty female were recruited in this study. Color coded quantitative cerebral angiography were performed during coil therapeutic procedure. Cerebral venous circulation were measured with this quantitative cerebral angiography.

Result:

Ruptured cases had shorter and symmetrical cerebral venous circulation time (p

Conclusion:

Symmetry and shorter cerebral venous circulation in dysplasia venous outlet may play a potential new factor for cerebral aneurysmal rupture.

Table:

Right Circulation: CCT Standard deviation Standard error

Symmetry(mm) 18 10.885 2.493 0.487

Asymmetry(mm) 34 12.102 2.452 0.577

Left circulation:

Symmetry(mm) 18 10.680 2.818 0.445

Asymmetry(mm) 34 10.831 2.151 0.507

Diameter of Jugular Vein:

Symmetry(mm) Right 9.13 Left 8.08

Asymmetry(mm) Right 8.81 Left 6.11

CCT :Cerebral Circulation Time

1012
BRAIN-0276
Non-Registered Abstracts

METABOLIC SHIFTS IN NORMAL-APPEARING CHILDREN BRAIN CORTEX IN ACUTE PERIOD OF SEVERE TBI.

N.A. Semenova[1], M.V. Ublinskiy[1], T.A. Akhadov[1], I.A. Melnikov[1]
[1]radiology,
Children's Clinical and Research Institute Emergency Surgery and Trauma, Moscow, Russia

Background: The aim of this study is to reveal and characterize compensatory processes in normal-appearing cortex in acute and subacute period of traumatic brain injury (TBI)

Methods: 34 patients were studied in age from 5 to 16 years (mean age – 12.7 y.). Group of patients consisted of 18 children with severe brain injury (volume of injured tissue was 30-50 ml). 16 age-matched healthy volunteers comprised control group. Phillips Achieva 3.0T scanner was used. MRS-studies were conducted in acute and subacute period of trauma. The area of interest in intact frontal - parietal cortex (volume = 3 cm^3) was studied using PRESS (TE = 35 ms, TR = 2000 ms, NSA = 32). The intensities of resonances in each spectrum were normalized to the signal of unsuppressed water. Statistical processing of spectral data was performed using software package Statistica 6.0.

Results: In comparison with control group significant decrease of NAA, increase of Cho, mI and Cr+PCr was found in patients. A direct statistically significant correlation ($p<0,05$) between NAA, Cr+PCr and Cho was revealed in both groups: in control group - $R_{NAA-Cr} = 0.65$, $R_{NAA-Cho} = 0.64$, $R_{Cr-Cho} = 0.61$; in patients group - $R_{NAA-Cr} = 0.82$, $R_{NAA-Cho} = 0.53$, $R_{Cr-Cho} = 0.66$

Discussion: Increase of Cr+Pcr, Cho signal intensities (in absence of changes in its relaxation characteristics) indicates activation of compensatory processes of choline and creatine synthesis in brain cells. At the same time NAA level is reduced. Existing of NAA-Cr and NAA-Cho correlations and Cr and Cho increase could mean that activation of Cr and Cho synthesis causes the NAA decrease. The scheme of metabolism which is implemented in neurons and explains NAA, Cr, Cho level changes in TBI is proposed. It follows from the scheme that enhancement of compensatory processes activity requires activation of Krebs cycle.

1013
BRAIN-0280
Non-Registered Abstracts

DYNAMICS OF NAA IN MOTOR CORTEX OF NORMAL INDIVIDUALS IN THE PERIOD OF BOLD RESPONSE ON MILISECOND STIMULUS.

M. Ublinskiy[1], N.A. Semenova[1], I.A. Melnikov[1], T.A. Akhadov[1]
[1]radiology,
Children's Clinical and Research Institute Emergency Surgery and Trauma, Moscow, Russia

The aim of this study was the analysis of dynamics of N-acetylaspartate in motor cortex of normal brain after short single stimulus.

Patients and methods. The patients group consisted of 9 healthy mails of 16 – 28 years old in initial stage of schizophrenia and in remission. Phillips Achieva 3.0T scanner was used for the study. Volume of interest in motor cortex was localized on the base of fMRI (EPI BOLD, TR = 3000, TE = 30) as the zone of activation caused by bottom push at the response to single auditory stimuli transmitted with the period of 18 s. The BOLD signal was measured with time resolution of 3 s. 1H MR spectra were run using synchronization of FID signals acquisition (PRESS, TE = 30 ms TR = 3000 ms) with dynamics of BOLD response after the stimulation at the same paradigm. Auditory stimulus was repeated 98 times and 98 × 7 FID signals were collected. The same method was applied for spectra accumulation in resting state. The signals obtained at time points t = 0, 3, 6, 9, 12, 15, 18 c. after stimulus were summarized. For FID processing homemade program was used. After

apodization filtering (LB = 20, GB = -5) FT and manual phase correction amplitudes of resonances were measured. NAA, Cho, Cr signal intensities at the time point *t* were normalized to the corresponding values at *t* = 0 and to the volume of activated cells containing in the voxel (measured manually).

Results and conclusions. The BOLD signal demonstrated maximum at the 6th s after target stimulus. The stable values of [NAA], [Cr] and [Cho] were observed in dynamic of resting state. [NAA] significantly decreased at the 12th s after stimulus and returned to initial value at the 15th s. Thus [NAA] minimum delayed relative to maximum of BOLD by 6 s.

Reversible decrease of [NAA] after stimulus presentation might be associated with activation of ASPA reaction. ASPA hydrolyzes NAA into acetate and aspartate. Substantial number of axons express ASPA and AceCS1(the enzyme catalyzing synthesis of acetyl CoA)[Moffet J. et al. Glia. 2011. 59(10) 1414]. NAA-derived acetate can be converted to acetyl CoA for further metabolism in axons.

Thus the stimulation might lead to NAA hydrolysis to compensate increased metabolic demands.

1014
BRAIN-0621
Non-Registered Abstracts

STRESS-RELATED PATHOLOGICAL CHANGES IN CEREBRAL VENOUS BLOOD FLOW IN NEWBORN RATS ASSESSED BY DOCT

M. Ulanova[1], V.L.A.D. Lichagov[2], A. Abdurashitov[2], M. Kassim[1], F. Ali[1], L. Hassani[1]
[1]Biology, Saratov State University, Saratov, Russia
[2]Physics, Saratov State University, Saratov, Russia

Objectives: Intracranial hemorrhage (ICH) is a major problem of neonatal intensive care. The incidence of ICH is typically asymptomatic and cannot be effectively detected by standard diagnostic methods. The lack of effective diagnostic technologies for early determination and criteria of ICH risk in newborns explains the high rate of neonatal death and less optimistic neurologic prognosis in infants after ICH. The mechanisms underlying ICH are unknown but there is evidence that stress-related alterations of cerebral venous blood flow (CVBF) may contribute to the pathogenesis of ICH. Therefore, quantitative assessment of CVBF may significantly advance understanding of nature of ICH. The aim of this study was determine the prognostic criteria for pathological changes in pattern of CVBF using Doppler optical coherence tomography (DOCT) in newborn rats with model of stress-induced ICH.
Methods: To induce development of ICH the newborn rats underwent influence of severe sound stress (120 dB, 10 Hz – infrasound, during 2 h). The monitor of CVBF (superior sagittal vein) was performed in anesthetized rats with fixed head using a commercially available Thorlabs swept source optical coherence tomography system OCS1300SS in the masked period of ICH (4 hours after stress) and during ICH (24 hours after stress), the control group included healthy rats.
Results: The results have shown that on latent stage of ICH in stressed rats without ICH the diameter of sagittal vein was in 2.1-fold higher compared with one before stress. The dilation of superior sagittal vein was accompanied by decrease in the speed of blood flow. In rats with ICH these pathological changes in CVBF were greater than in stressed rats on masked period of ICH and especial compared with healthy animals. Adrenaline infusion (10 μg/kg, iv) in healthy rats induced the decrease in diameter of sagittal vein and the increase in speed of blood flow. Note, adrenaline treatment of stressed rats on different stages of ICH was not accompanied by any changes in CVBF.
Conclusion: In summary, in experiments on newborn rats with stress-related ICH using DOCT we have shown that latent stage of ICH (4h after stress) is characterized by decrease of venous blood outflow and the loss of sensitivity of sagittal vein to vasoconstrictor effect of adrenaline. The incidence of ICH (24 h after stress) was accompanied by progression of early pathological changes in CVBF and development of venous insufficiency. Taking into consideration of this

fact, we suggest that the suppression of CVBF related to the severity to the deleterious effect of stress on the brain hemodynamics in newborn rats. These facts allow us to conclude that the venous insufficiency with the loss of vasoconstrictor response to adrenaline is an informative and sensitive component of pattern of CVBF that can be important diagnostic criteria of risk of ICH development in newborns.
Grants: 14.Z56.14.2216-MD, RFBR14-02-00526-14-a, RNF 14-15-00128

1015
BRAIN-0348
Non-Registered Abstracts

A ROLE OF PERFUSION CT IN PATIENTS WITH ACUTE INTERNAL CAROTID ARTERY OCCLUSION FOR EC-IC BYPASS PERFORMANCE.

E. Varaksina[1], P. Chechulov[1], V. Savello[1], I. Voznuk[1], A. Kostenikov[1]
[1]Neurosurgery,
Scientific and Research Institute of Emergency Hel p n.a. I.I. Dzhanelidze, St-Petersburg, Russia

BACKGROUND: Up to date there are no specific data on indications to EC-IC bypass in patients with acute symptomatic internal carotid artery (ICA) occlusion.
PURPOSE: Studying a role of perfusion CT (PCT) for EC-IC bypass indications definition in patients with acute ICA occlusion.
MATERIALS AND METHODS: EC-IC bypass was performed on 43 patients with acute symptomatic ICA occlusion. Middle age was 57 years (38-71). Average time from hospitalization to surgery – 8,9 days. PCT was performed on 25 patients during 4-6 days from receipt. Control group – 9 patients of comparable age with asymptomatic isolated ICA occlusion.
RESULTS: There were statisticaly significant distinctions in brain perfusion indicators between two groups of investigated. Selection criteria for surgical revascularisation (EC-IC bypass) in patients with acute ICA occlusion were defined: asymmetric increasing of mean transit time (MTT), decreasing of cerebral blood flow (CBF) in combination with relative increase of cerebral blood volume (CBV) on the side of occlusion.
CONCLUSIONS: PCT is recommended to be used in selection algorithm for EC-IC bypass in patients with acute symptomatic ICA occlusion. Indicators of brain blood flow velocity decreasing in patients with acute symptomatic ICA occlusion according to PCT data has to be considered as additional criterion of surgical treatment.

1016
BRAIN-0140
Non-Registered Abstracts

A NOVAL NEUROPROTECTIVE AGENT AND ENHANCES COGNITION TREATMENT WITH MANASAMITRA VATAKAM(MMV) DIAGNOSED BY PETCT.

V. Thirunavukkarasu[1], S. Venkataraman[1]
[1]Dept. of Medical Cyclotron, HCG Enterprise LTD, Chennai, India

Background: *Manasamitra vatakam* (*MMV*) as pivotal role against Aluminium induced neuronal apoptosis. Herbo-mineral formulation of *MMV* prepared by Indian system of Ayurvedic medicine and used to improve cognitive functions against Aluminium induced dysfunction of rats.

Objectives: The study focused *MMV* as an alternative Ayurvedic medicine against neuronal cell death caused cognitive dysfunction induced by Aluminium treated rats.

Materials and Methods: The study consists of five groups, six animals in each. Male healthy Swiss albino rats (200–220 gm) were used and housed in clean polypropylene cages and maintained the room temperature 23°C - 25°C with alternating 12 h light and dark cycles. The animals were treated Aluminium orally and fed with standard pellet diet and clean drinking water. The study was assessed cognitive functions of behavioral parameters like active avoidance and radial arm maze. The whole experimental studies were conducted for 90 days. The biochemical and molecular studies (Western blot, RT-PCR and Immunohistology) were carried out by standard methods.

Results: The results shown that *MMV* treated animals significantly improved neurotransmitters

such as 5-HT and Acetyl Choline as well as cognitive functions of rats and restrain expression of oxidative stress (HSP70) & pro-apoptotic genes like *Bcl-2, Bcl-xL* and *Caspas-3* against Aluminium induced hippocampus region of rat's brain. In aluminium induced animals were observed pro-apoptosis genes like *Bcl-2, Bcl-xL* and *caspas-3* were significantly expressed high in hippocampus and cerebral cortex of brain regions. Whereas *MMV* treated animals were observed normal brain with the help of PETCT scan and behavioral activities as on control.

Conclusion: The present study reveals that Herbo-mineral formulation of *Manasamitra vatakam* (*MMV)* potentially improved memory function and inhibited oxidative stress, neuronal apoptosis against Aluminium induced neurodegenerative disorder rats.

1017
BRAIN-0715
Non-Registered Abstracts

REGIONAL CORRELATION BETWEEN PCASL PERFUSION AND PIB-PET IN FAMILIAL ALZHEIMER'S DISEASE

D.J.J. Wang[1], L. Yan[1], C. Liu[2], K.P. Wong[1], S.C. Huang[1], D. Wharton[1], J. Ringman[1]
[1]Neurology, UCLA School of Medicine, Los Angeles, USA
[2]Neurology, University of Southern California, Los Angeles, USA

OBJECTIVE: [^{11}C]Pittsburgh compound B ([^{11}C]PiB) PET amyloid imaging has been widely used for monitoring amyloid-β deposition, and for evaluating anti-amyloid therapies of Alzheimer's disease (AD). Tracer kinetic modeling of PiB-PET can yield multiple parameters including R1 (related to tracer delivery or relative perfusion), binding potential (BP) and distribution volume ratio (DVR=BP+1) of PiB[1]. Arterial spin labeling (ASL) is a noninvasive MRI technique to measure cerebral blood flow (CBF), and has shown promises as an imaging marker of AD[2]. The purpose of the present study was to systematically compare ASL perfusion MRI with PiB PET in a cohort of familial AD (fAD) related subjects who are either carriers of *PSEN1*, *PSEN2*, or *APP* mutations or their non-mutation carrying family members.

Methods: Twenty-five fAD related subjects (age 38±12 years, 15F) underwent dynamic ^{11}C-PIB PET/CT scans in list-mode for 70 mins. Raw PET data were reconstructed using ordered subset expectation maximization algorithm. A retrospective image-based movement correction procedure was applied to correct for possible misalignment between CT and PET scans and between PET image frames. All subjects also underwent MRI scans on a Siemens Tim Trio 3T scanner. Pseudo-continuous ASL (pCASL) with 3D background suppressed GRASE sequence was applied for perfusion measurement. Both ASL and PET images were coregistered to the subject's structural MRI, which were warped to MNI brain template. Tissue time-activity curve was generated for cerebellar gray matter (reference region) and parametric images of relative perfusion (R1) and distribution volume ratio (DVR) were constructed by simplified reference tissue model (SRTM) and Logan graphical method, respectively.

Results: Figure 1 shows the mean rCBF, R1 and DVR images averaged across 25 subjects. R1 and rCBF images show high consistency with each other with high contrast between gray and white matter. DVR images show more uniform spatial distribution between gray and white matter. Voxel-by-voxel correlations between the mean rCBF and mean R1 maps of 25 subjects were calculated for 9 ROIs. Significant correlations between rCBF and R1 were observed in each ROI with an overall mean correlation coefficient of r=0.65. A reduced correlation with the mean correlation coefficient of 0.4 was acquired between rCBF and DVR. The correlation between the mean rCBF and R1 values across 25 subjects in the 9 ROIs was also calculated. The overall correlation was intermediate (mean r=0.19). The cross-subject correlation between the mean rCBF and DVR values showed negative correlations

with the mean correlation coefficient of r=-0.18.

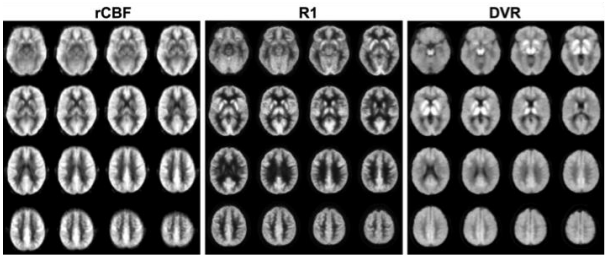

Discussion: To the best our knowledge, this is the first study to systematically compare ASL perfusion with PiB PET. The similar spatial pattern and significant voxel-wise correlations between rCBF and R1 are expected since both parameters estimate brain perfusion. The negative cross-subject correlation between rCBF and DVR suggest that brain regions with high DVR values may be associated with hypoperfusion. Our data suggest that both ASL and PiB PET can provide valuable imaging markers for AD.

References: 1.Zhou et al Neuroimage. 2007; 36(2):298-312. 2. Alsop et al J Alzheimers Dis. 2010;20(3):871-80.

1018
BRAIN-0784
Non-Registered Abstracts

NEUROPROTECTIVE EFFECTS AND MECHANISM OF POMALIDOMIDE AGAINST TRAUMATIC BRAIN INJURY

J. WANG[1], J. Wang[1], L. Yang[1], N. Greig[2]
[1]Graduate Institute of Med Sci,
Taipei Medical University, Taipei city, Taiwan
[2]Drug Design & Development Section,
National Institute on Aging, Baltimore, USA

Traumatic brain injury (TBI) is a risk factor for neurodegenerative disease and death worldwide. In response to acute brain trauma, glial cells become activated and secrete pro-inflammatory cytokines such as tumour necrosis factor-α (TNF-α), interleukin-6 (IL-6), interleukin-1β (IL-1β). This neuroinflammation plays a crucial role in the secondary tissue damage. Thalidomide has anti-inflammatory property. Its analog Pomalidomide (Pom) has been shown more potent as a TNF-α inhibitor than Thalidomide. The aim of our study is to investigate the effect and window of Pomalidomide (Pom) and 3,6'-dithiothalidomide (3,6'-DT) on functional and histological outcomes and inflammatory cytokine expression after TBI.

We have previously established the rat model of TBI using adult Sprague-Dawley rats subjected to controlled cortical impact (CCI). Five hours or seven hours after TBI, Pom (0.5mg/kg, i.v.), 3,6'-DT (28mg/kg, i.p.) or vehicle was administered. Neurological functions were evaluated using swing test, adhesive removal, modified neurological severity scores and beam walking. Contusion volume and neuronal degeneration were measured using cresyl violet and FluoroJade C staining. Levels of TNF-α, IL-1β and IL-6 mRNA were measured by real-time quantitative reverse transcriptase-PCR, protein were estimated by enzyme-linked immunosorbent assay and immunohistochemistry from TBI with or without drug treatment. In vitro, primary rat cortical cultures were treated with H_2O_2 (300μM) in the presence or absence of various concentration of Pom to investigate whether the drug protects cells from oxidative stress. Cell death was estimated by LDH assays. Neurons, microglia and astrocytes were identified by ICC with specific markers.

Post-injury treatment with Pom significantly improved functional recovery and decreased contusion volume at 24 hours post-injury. The time window is between 5 and 7 hours, and the dose window is between 0.1 and 0.5mg/kg (i.v.). Pom treatment also reduced the number of degenerating neurons at the contusion site. Pom (50μM) enhanced cell viability against H_2O_2-induced oxidative stress and reduced microglia activation.

Our data suggest that post-treatment of Pom improves histological and functional outcomes after experimental TBI and reduces inflammatory responses. The pre-clinical results with Pom has a potential for further clinical trial.

1019
BRAIN-0855
Non-Registered Abstracts

MODERATE AND SEVERE HYPOGLYCAEMIA ASSOCIATED METABOLIC CHANGES IN CORTEX AND HIPPOCAMPUS OF MICE

V. Pitchaimani[1], S. Arumugam[1], V. Karuppagounder[1], R. Sreedhar[1], R. Afrin[1], M. Harima[1], H. Suzuki[1], M. Nomoto[1], S. Miyashita[1], T. Nakamura[1], K. Suzuki[2], M. Nakamura[3], K. Watanabe[1]
[1]Clinical Pharmacology, Niigata University of Pharmacy and Applied Life Sciences, Niigata, Japan
[2]Gastroenterology, Niigata University of Graduate School of Medicine and Dental Sciences, Niigata, Japan
[3]Cardiology, Yamanashi Prefectural Central Hospital Kofu, Yamanashi, Japan

Fasting or starvation (moderate hypoglycaemia) decrease glucose utilization and metabolism in brain. During severe hypoglycemic emergency, the dextrose administration is the first choice and it preserve neuronal metabolism associated with NADPH dependent oxidative stress.

This raises two questions. 1) How the brain decreases glucose metabolism and uptake in moderate hypoglycemia and how it regain glucose metabolism in severe hypoglycemia 2) what mechanism could contribute to oxidative stress.

In this study we investigated the insulin signalling kinases (AKT, Ps6K, and ERK),glycolytic markers (PFK1 and BADser^{155}), glucose transporters (GLUT1and GLUT3) and glutamate reuptake markers (Excitatory amino acid transporter (EAAT2) and Na+K+ATPase) by western blot analysis in moderate hypoglycemic (24hr. fasting and 2 IU insulin induced hypoglycemia (IIH) at 10 and 30 min) and severe hypoglycemia (IIH at 90 min after experienced seizure like behaviour).

Fasting hypoglycemia (BGL 58.2 mg/dl) decrease insulin signalling kinases and glycolysis and may shifts to HMP shunt to synthesize antioxidant glutathione(GSH). The glucose uptake in neurons may get slightly decreased by GLUT3 and nochange was observed in astrocytic GLUT1.

IIH after 10 min (BGL 67.8 mg/dl) decrease AKT expression and glycolysis and nochange was observed in glucose transporter expression. This raises a question that how the AKT decreases at 10 min. Other reports suggesting that insulin phosphorylate AKT first and then Ps6K in a time dependant manner. We observed a significant increase in Ps6k in hippocampus but not in cortex suggesting that insulin crosses the blood brain barrier first in cortex and phosphorylate AKT and then hippocampus nearly 5 min. Due to the hypoglycemia mediated effect, AKT andglycolysis decrease at 10 min.

IIH after 30 min (BGL 54.80 mg/dl) regained AKT expression and glycolysis and therewas more decrease in GLUT 3 but not significant and no change was observed inGLUT1. Previous reports suggesting that IIH decrease glutamate and restored with other fuels like lactate. NMDA receptor activation increase GLUT3 expression. This indirectly suggesting that IIH at 30 min after decrease GLUT3 expression in neuron by possibly decreasing glutamate.

IIH after 90 min (BGL below 20 mg/dl) has increased insulin signalling but decreased glycolysis and may shifts to HMP shunt but unable to synthesizeglutathione and it restored GLUT 3. The glutathione synthesis require cysteinefrom astrocytes by an ATP dependent mechanism. Other reports suggesting that severe hypoglycemia decreases ATP and thismay increase NADPH dependent oxidative stress during glucose reperfusion. Numerousreports suggesting that severe hypoglycemia increase glutamate. The restored GLUT 3 possibly associated with the increased glutamate mediated NMDA receptoractivation.

This raises another question how the decreased glutamate in 30 min after INS increasedat 90 min after INS. The extracellular glutamate is mainly removed by EAAT2 which functionally associated

Na+K+ATPase. We checked the EAAT2 and Na+K+ATPase Ty[10]and no change was observed. This suggesting that Na+K+ATPase may get phosphorylated at other residue or excess glutamate accumulated by reversed glutamate transport.

1020
BRAIN-0447
Non-Registered Abstracts

DISRUPTED WHITE MATTER INTEGRITY IN PARKINSON'S DISEASE WITH DEPRESSION

J.Y. Wu[1], Y. Zhang[1], W.B. Wu[1], Y. Xu[1]
[1]Neurology,
Affiliated Drum Tower Hospital of Nanjing Universi ty Medical School, Nanjing, China

Depression is one ofthe most commonnon-motor symptoms in Parkinson's disease (PD) which can causefunctional impairment and further reduce the quality of life. But thepathophysiological relationship between PD and depression is still remainsunclear. Increasing evidence suggest that depression in PD is closely relatedto the white matter abnormalities. In this study we investigated whole brainwhite matter integrity in 24 depressed PD patients and 32 non-depressed PDpatients. There was no difference in age, gender, education, disease duration,Hoehn–Yahr stages, Unified Parkinson's Disease Rating Scale scores and Mini-MentalState Examination scores between the two groups. The only difference was the HamiltonRating Scale for Depression score (HDRS). The depressed PD patients groupshowed reduced fractional anisotropy (FA) value in the left superiorlongitudinal fasciculus, inferior longitudinal fasciculus, superior andposteriorof corona radiate, posterior thalamic radiation, sagittal stratum(include inferiorlongitudinal fasciculus and inferior fronto-occipitalfasciculus), stria terminalis, and superior fronto-occipital fasciculus. Inpatients with PD, the HDRS was negativelycorrelated with the FA value in theleft superior fronto-occipital fasciculus (r=−0.691, p= 0.028). This studysuggested that PD patients with depression arecharacterised by decreasedfunctional integration in the left hemisphere. Thesefindings may be helpful forfurther understanding the potential mechanisms underlying depression in PD.

1021
BRAIN-0897
Non-Registered Abstracts

RAPID MESOSCALE TRANSCRANIAL CORTICAL IMAGING WITH GENETIC-ENCODED GLUTAMATE SENSOR – IGLUSNFR

Y. Xie[1], A. Chan[1], A. McGirr[1], S. Xue[1], D. Xiao[1], T. Murphy[1]
[1]Psychiatry, University of British Columbia, Vancouver, Canada

Wide field of view mesoscopic cortical imaging with genetic encoded sensors enables decoding regional activity and connectivity in anesthetized and behaving mice. However, the temporal kinetics of most genetically-encoded sensors can be suboptimal for *in vivo* characterization of frequency bands higher than 1 Hz. Furthermore, existing sensors in particular those which measure calcium (genetically encoded calcium indicators; GECIs), can be affected by non-linearities associated with spiking or calcium binding. Here, we demonstrate using in vivo mesoscopic imaging the rapid and robust kinetics of virally transduced (AAV1-synapsin-iGluSnFR) and transgenically expressed glutamate-sensing fluorescent reporter (EMX1:tTA-CamkII: iGluSnFR). In both awake and anesthetized mice we imaged a 8 x8 mm field of view through an intact transparent skull preparation. iGluSnFR demonstrates rapid and robust kinetics during cortical representation of sensory stimulation, that is then paralleled in spontaneous cortical activity with maps recovered up to alpha frequencies (8-12 Hz). iGluSnFR also resolved other features of sensory processing such as an intracortical re-bound during the processing visual stimuli that was not seen with other GECIs. The regional cortical kinetics of iGluSnFR were more rapid than EMX-GCaMP3, and comparable to the temporal responses seen with RH1692 voltage sensitive dye (VSD), with similar signal amplitude. Regional cortical connectivity detected by iGluSnFR in spontaneous brain activity identified functional circuits consistent

with maps generated from EMX-GCaMP3 mice and VSD sensors. The iGluSnFR sensor is a fast genetic-encoded sensor of extracellular glutamate, with potential utility in normal physiology, as well as neurologic and psychiatric pathologies in which glutamatergic abnormalities are recognized.

1022
BRAIN-0047
Non-Registered Abstracts

CONTRIBUTION OF PREOPTIC AREA THERMO TRANSIENT RECEPTOR POTENTIAL VANILLOID TYPE IV (TRPV4) CHANNEL IN THERMOREGULATION IN RATS

R. Yadav[1], H. Mallick[1], A. Jaryal[1], K. Kumari[1]
[1]Physiology, All India Institute of Medical Science, Delhi, India

Method

The study was conducted in six male Wistar rats. Under thiopentone sodium anesthesia (fourty miligramg/kilogram BodyWeight) a bilateral guide cannula with indwelling styli was implanted with their tips aimed at two mm above the preoptic area as per De Groot's atlas. A radio transmitter (Data Science International, USA) for the telemetric recording of body temperature was implanted in the abdomen. A K- type thermocouple wire was inserted near the hypothalamus to measure the brain temperature . Brain temperature was recorded at fifteen second interval through a fluke digital thermometer. Tb was recorded telemetrically at fifteen second interval. The temperature was measured from 10.00 to 16.00 h and injection was given at 12.00 h. Temperature data was averaged at fifteen minute epochs. TRPV4 agonist,(GSK1016790A),injection was given bilaterally at the Preoptic area at a rate of 0.1 micro liter /minute using an injector cannula. The site of injection was confirmed histologically. The statistical comparison was made between pre and post injection record at every fifteen minutes using paired t-test.

Result

TRPV4 agonist cause hypothermia in rats

Conclusion

The TRPV4 channel agonist injection in the preoptic area brings about fall in body and brain temperature by stimulating warm sensitive neurons.

1023
BRAIN-0473
Non-Registered Abstracts

EFFECTS OF ALOGLIPTIN ON THE METABOLISM OF NITRIC OXIDE (NO) AND HYDROXY RADICALS IN BRAIN DURING BRAIN ISCHEMIA-REPERFUSION

M. yamazato[1], M. yamazato[2], M. Hirayama[3], Y. Ito[3], R. Nishioka[3], R. Nishioka[3], N. Araki[3]
[1]neurology, Saitama Medical Center, Saitama, Japan
[2]neurology, Higashimatsuyama Medical Association Hospital, Saitama, Japan
[3]neurology, Saitama Medical University, Saitama, Japan

Purpose: The metabolism of nitric oxide (NO) and hydroxy radicals in the brain of C57BL during brain ischemia-reperfusion is investigated under treatment with alogliptin, an innovative drug and one of the DPP4 inhibitors for controlling incretin levels in blood glucose metabolism.
Methods: (1) C57BL treated with alogliptin 45mg/kg/day (n=5) for 4 weeks and and the control group (n=8) were used. Both NO production and hydroxyl radical metabolism were continuously monitored by *in vivo* microdialysis. Microdialysis probes were inserted into the bilateral striatum. A Laser Doppler probe was placed on the skull surface. Blood pressure, blood gases and temperature were monitored and maintained within normal ranges throughout the procedure. Forebrain cerebral ischemia was produced by occlusion of both common carotid arteries for 10 minutes. Levels of nitric oxide metabolites, nitrite (NO_2^-) and nitrate (NO_3^-), in the dialysate were determined using the Griess reaction. Right side is for 2,3-dihydroxybenzoic acid (2,3-DHBA) and 2,5-dihydroxybenzoic acid (2,5-DHBA). Samples were measured by the salicylic rate trapping method.Three days thereafter, we removed the brain and made the

slide, and divided the extent of ischemia injury into three "stages" ("severe ischemia group", "moderate ischemia group" and 'survive group"), according to the nucleus' degree of transformation and degree of staining. Considering as the survival rate the rate of the "survive group" that represents the percentage of the sum, we carried out a comparative examination among the three groups.
Results:(1) BloodPressure:Alogliptin group (73.2±10.6mmHg; mean±SD) showed significantly lower than those of the control group (88.3±7.35).20 minutes after the start of reperfusion ($p<0.05$).
(2) Cerebral Blood Flow (CBF): There were no significant differences between the groups.
(3) Nitric oxide metabolites: 1) NO_2^- ; Alogliptin group (0.86±0.2, 0.73±0.2, 0.7±0.2 mol/L) showed significantly lower level than those of the control group(1.17±0.1, 0.99±0.2, 1.1±0.2) pre-ischemia, ischemia and 50 minutes after the start of reperfusion ($p<0.05$) (Figure 1).
2) NO_3^- ; There were no significant differences between the groups.
(4) Hydroxyl radical; Alogliptin group (96.3±3.3, 87.6±9.0, 84.8±7.2, 84.3±7.2 %) showed significantly lower level than those of the control group (100±1.1, 98.7±2.6, 98.8±3.4, 98.2±4.6) ischemia and 80-120 minutes after the start of reperfusion ($p<0.05$) (Figure 2).
(5) Pathology; There were almost significant differences between the groups ($P=0.051$).
Conclusion: It has been suggested that Alogliptin can affect the nitric oxide metabolism in the brain after cerebral ischemia-reperfusion in the C57BL mice.

1024
BRAIN-0050
Non-Registered Abstracts

CT PERFUSION IMAGING IN PATIENTS WITH TRANSIENT ISCHEMIC ATTACKS: A PROSPECTIVE CLINICAL STUDY

L. Yuxia[1], Y.Q. Li[2], Y. Han[3]
[1]Department of Neurology,
Xuanwu Hospital Capital Medical University,
Beijing, China
[2]Department of Neurology,
Tangshan Worker's Hospital Clinical Medical College of Hebei Medical University, Tangshan, China
[3]Department of Neurology,
Xuan Wu Hospital Capital Medical University,
Beijing, China

Objective: Transient ischemic attacks (TIA) are an emergency in neurology, and it can be progressed to ischemic stroke promptly if not timely diagnosis and treatment. There are no positive findings in routine computerized tomography (CT)/magnetic resonance imaging, and is there really any abnormality at the TIA interphase in radiologic imaging? A prospective clinical study was performed to evaluate the cerebral blood flow in patients with TIA using cerebral CT perfusion imagine (CTP), and investigating the risk factor of CTP abnormality. **Methods:** CTP and CT angiography (CTA) were performed on all 69 cases of TIA patients, and got parameters of cerebral blood flow (CBF), cerebral blood volume (CBV), mean transit time (MTT), time to peak (TTP) and the cerebral artery stenosis. Compared the affected lateral with the contra lateral to get information of cerebral ischemia, and analysis of the relationship between parameters of CTP and the clinical symptoms, investigate the risk factor of CTP abnormality. **Results:** Persisting abnormal perfusion changes corresponding to clinical symptoms were found in 52 cases with prolonged TTP and MTT, CBF and CBV drop was not statistically significant between both groups. Cerebral hypoperfusion correlated with increased NIHSS score of TIA onset, the duration of TIA onset, and the cerebral artery stenosis in TIA patients. **Conclusion:** TTP, MTT maps in CTP had a high sensitivity on showing cerebral perfusion abnormalities. The more serious of TIA onsets in clinical, the higher ratio of CT perfusion abnormality.

References

1 Eliasziw M, Kennedy J, Hill MD, etal. Early risk of stroke after a transient ischemic attack in patients with internal carotid artery disease [J].CMAJ, 2004, 170:1105-1109.

2 中华神经科学会.各类脑血管疾病诊断要点.中华神经科杂志[J], 1996,29(6):379-380.

3 Lev MH, Romero JM, Goodman DN, etal. Total occlusion versus hairline residual lumen of the internal carotid arteries: accuracy of single section helical CT angiography [J].AJNR Am J Neuroradio, 2003, 24:1123-1129.

4 Sparacia G，Laia A，Assadi B，et al. Perfusion CT acute stroke: predictive value of perfusion parameters in assessing tissue viability versus infarction[J]. Radiol Med，2007，112(1) : 113-122.

5 王维治.神经病学[M].第5版.北京:人民卫生出版社,2004,7:131 –141.

6 M iles KA. Measurement of tissue perfusion by dynamic computed tomography[J]. B r J Radiol, 1991, 64 (5):409-412.

7 Flohr TG, Schaller S, Stierstorfer K, etal. Multi-detector row CT systems and imaging-reconstruction techniques[J]. Radiology, 2005, 235(3): 756-773.

8 Lee TY, Belesky V, Kalapos P, etal. CT perfusion imaging in cerebral ischemia[J]. Stroke, 2005,36(1):1-3.

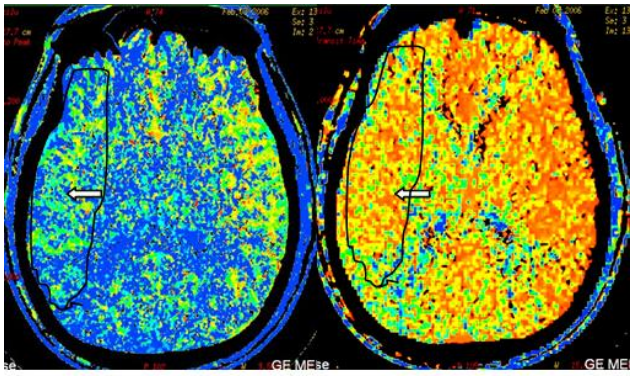

TTP MTT

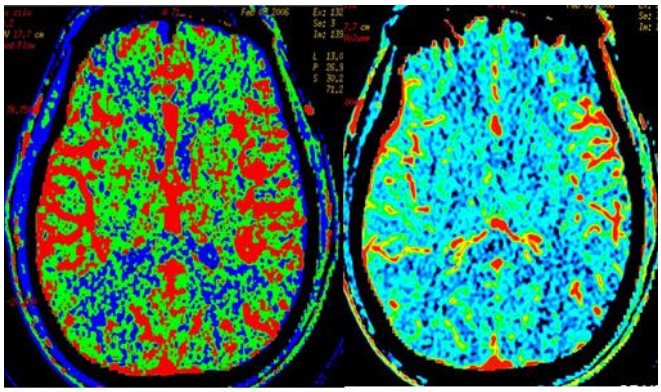

CBF CBV

1025
BRAIN-0917
Non-Registered Abstracts

BRAIN MAPPING OF THE METABOLISM CHANGES: A PET/CT STUDY IN THE PATIENTS WITH NON-SMALL CELL LUNG CANCER BEFORE TREATMENT

W. Zhang[1], N. Ning[2], X. Li[3], J. Ma[1], Y. Guo[1], J. Yang[1]
[1]Radiology Department, The First Affiliated Hospital of Xi'an Jiaotong University, Xi'an, China
[2]Nuclear Medicine Department, The Second Affiliated Hospital of Xi'an Jiaotong University, Xi'an, China
[3]Department of Biomedical Engineering, The Key Laboratory of Biomedical Information Engineering of the Ministry of EducationThe School of Life Science and Technology of Xi'an Jiaotong University, Xi'an, China

Objective: Cancer research has largely focused on neurobiology [1]. The neurobiological view of cancer aetiopathogenesis suggests that cancer information is conveyed by neural and humoral pathways to the special brain structures, and that brain might consequently modulate the neuroendocrine-immune system to regulate tumor growth [1-5]. The present study aimed to observe brain glucose metabolism pattern in non-small cell lung cancer (NSCLC) patients and to explore the changes of the brain metabolism caused by the lung cancer.

Methods: ^{18}F-FDG PET/CT of 83 NSCLC patients (35 to 69 years, mean = 53.65±7.81 years old, male/female=58/25) and 76 healthy controls (age from 33 to 67 years, mean = 51.83±8.01 years old, male/female=51/25) were performed in a resting state. The malignant group consisted of histopathologically proven cases with NSCLC by pneumocentesis, surgery or thoracoscope (clinical stage 1 [n =16], 2 [n=15], 3 [n=28], or 4 [n=24]). The pathological types were 51 adenocarcinoma, 27 squamous carcinoma and 5 bronchioloalveolar carcinoma. Images were registered to the atlas by using the statistical parametric mapping (SPM) software. The brain normalized metabolic differences between groups (patients versus controls, clinical stages, adenocarcinoma group versus squamous carcinoma group) were analyzed by two samples t-test and multivariate-test with SPSS 13.0 software.

Results: Significant differences were found in brain glucose metabolisms between patients and controls ($p<0.01$). The hypermetabolism regions included the orbital part of right inferior frontal gyrus, insular, basal ganglia, thalamus, hippocampus, amygdala and cerebellum, while the hypometabolism regions included left superior parietal lobule, bilateral inferior parietal lobule, and left fusiform gyrus (figure 1). The multivariate-test showed no significant differences among clinical stages or between adenocarcinoma and squamous carcinoma groups.

Conclusions: There were abnormal glucose uptakes in brain regions in NSCLC patients, and different clinical stages and pathological types (just for adenocarcinoma and squamous carcinoma) were not considerable factors affecting on the brain FDG uptake. The hypermetabolisms in the brain interpret a tumor-to-brain pathway on central neuromodulation of lung malignancy. The brain hypometabolisms associated with visual and spatial orientation functions may be caused by cancer related inflammation.

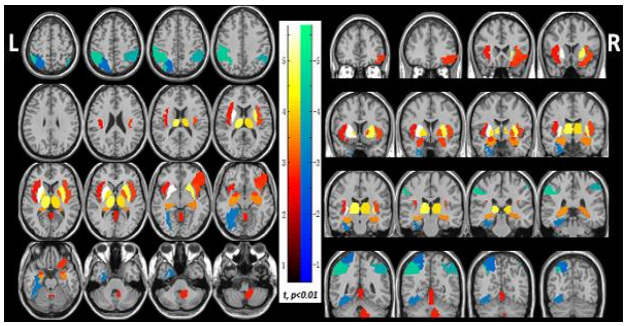

Figure 1. Abnormal glucose metabolisms in the non-small cell lung cancer patients. Both decreased and increased brain glucose uptake are observed ($p<0.01$). Color bar indicates t-values; L: left; R: right.

References:

[1]. Mravec, B., Y. Gidron and I. Hulin, Neurobiology of cancer: Interactions between nervous, endocrine and immune systems as a base for monitoring and modulating the tumorigenesis by the brain. Semin Cancer Biol, 2008. 18(3): p. 150-63.

[2]. Benveniste, H., et al., Brain metabolomic profiles of lung cancer patients prior to treatment characterized by proton magnetic resonance spectroscopy. Int J Clin Exp Med, 2012. 5(2): p. 154-64.

[3]. Ondicova, K. and B. Mravec, Role of nervous system in cancer aetiopathogenesis. Lancet Oncol, 2010. 11(6): p. 596-601.

[4]. Armaiz-Pena, G.N., et al., Neuroendocrine modulation of cancer progression. Brain Behav Immun, 2009. 23(1): p. 10-5.

[5]. Golan, H., et al., Brain mapping of patients with lung cancer and controls: inquiry into tumor-to-brain communication. J Nucl Med, 2009. 50(7): p. 1072-5.

1026
BRAIN-0432
Non-Registered Abstracts

CORRELATIONS OF DEPRESSION WITH OTHER NON-MOTOR SYMPTOMS IN PD

Y. zhang[1], J. wu[1], Y.U.N. xu[1]
[1]Neurology,
Affiliated Drum Tower Hospital of Nanjing University Medical School, Nanjing, China

Depression is a frequent behavioral disorder in patients with Parkinson's disease(PD). Many research of depression has been investigated in PD. Nevertheless, whether depression is related to other non-motor symptoms in PD is unknown. Our objective was to determine the prevalence and features of depression and associated factors in a group of PD patients. Eighty five PD patients participated in the study. Depression, motor symptoms, and other non-motor symptoms were assessed. The presence of the main non-motor symptoms was checked during a detailed clinical interview. Group comparisons were carried out to investigate the association with depression. Thirty seven patients (43.5%) were diagnosed as depression. Depressive patients had significantly more lower cognitive status than non-depressive patients. When considering non-motor symptoms, depression was significantly associated with fatigue and anxiety, both of which were more prevalent in depressive patients than in non-depressive patients. Depression was significantly associated with more severe motor symptoms and a lower cognitive status. After adjustment for these factors, depression appeared to be a relatively isolated, independent symptom because the only other associated non-motor symptoms were fatigue and anxiety.

1027
BRAIN-0049
Non-Registered Abstracts

FORCED LIMB-USE ENHANCED NEUROGENESIS AND BEHAVIORAL RECOVERY AFTER STROKE IN THE AGED RATS

C. Zhao[1], H. Qu[1]
[1]Neurology,
The first hospital of China Medical University, Shenyang, China

Constraint-induced movement therapy (CIMT) after stroke enhances not only functional reorganization but also structural plasticity of the brain in the adult rats. We examined whether forced limb-use which mimicked CIMT could influence ischemia-induced neurogenesis, apoptosis and behavioral recovery in the aged rats. Aged rats were divided into a sham group, an ischemia group, and an ischemia group with forced limb-use. Focal cerebral ischemia was induced by injection of endothelin-1. Forced limb-use began on post-stroke day 7 by fitting a plaster cast around the unimpaired upper limbs of rats for 3 weeks. Behavioral recovery was evaluated by tapered/ledged beam-walking test on postoperative day 32. The expression of doublecortin (DCX), neuronal nuclei (NeuN), glial fibrillary acidic protein (GFAP) and Iba-1 were measured by single or double immunohistochemistry, and apoptosis was measured by TdT-mediated dUTP-biotin nick-end labeling (TUNEL) assay. The production of neuroblasts in the subventricular zone (SVZ) was significantly increased after stroke. Forced limb-use enhanced the proliferation of newborn neurons in the SVZ, as well as increased the long-term survival of newborn neurons. Furthermore, forced limb-use suppressed apoptosis and improved the motor functions after stroke in the aged rats. Forced limb-use exerted few effects on inflammation. Neither the number nor dendritic complexity of newborn granule cells in the hippocampus was affected by forced limb-use. Forced limb-use is effective in enhancing neurogenesis and behavioral recovery after stroke even in the aged rats.

B

C

E

G

I

M

N

O

S

Z